(12) INTERNATIONAL APPLICATION PUBLISHED UNDER THE PATENT COOPERATION TREATY (PCT)

(19) World Intellectual Property Organization
International Bureau

(43) International Publication Date
31 March 2022 (31.03.2022)

WIPO | PCT

(10) International Publication Number
WO 2022/067091 A1

(51) International Patent Classification:
A61K 9/127 (2006.01) *A61K 39/395* (2006.01)
A61K 39/215 (2006.01) *C12N 15/85* (2006.01)

(21) International Application Number:
PCT/US2021/052040

(22) International Filing Date:
24 September 2021 (24.09.2021)

(25) Filing Language: English

(26) Publication Language: English

(30) Priority Data:
63/083,625 25 September 2020 (25.09.2020) US

(71) Applicant: **DNARX** [US/US]; 235 Berry St., #610, San Francisco, California 94158 (US).

(72) Inventors: **DEBS, Robert**; c/o DNARX, 235 Berry St., #610, San Francisco, California 94158 (US). **HANDUMRONGKUL, Chakkrapong**; c/o DNARX, 235 Berry St., #610, San Francisco, California 94158 (US). **HEATH, Timothy**; c/o DNARX, 235 Berry St., #610, San Francisco, California 94158 (US). **YE, Alice**; c/o DNARX, 235 Berry St., #610, San Francisco, California 94158 (US). **MACK, Marissa**; c/o DNARX, 235 Berry St., #610, San Francisco, California 94158 (US). **CHMURA, Stephen**; c/o DNARX, 235 Berry St., #610, San Francisco, California 94158 (US).

(74) Agent: **BOND, Jason R.**; Casimir Jones, S.C., 2275 Deming Way, Suite 310, Middleton, Wisconsin 53562 (US).

(81) Designated States *(unless otherwise indicated, for every kind of national protection available)*: AE, AG, AL, AM, AO, AT, AU, AZ, BA, BB, BG, BH, BN, BR, BW, BY, BZ, CA, CH, CL, CN, CO, CR, CU, CZ, DE, DJ, DK, DM, DO, DZ, EC, EE, EG, ES, FI, GB, GD, GE, GH, GM, GT, HN, HR, HU, ID, IL, IN, IR, IS, IT, JO, JP, KE, KG, KH, KN, KP, KR, KW, KZ, LA, LC, LK, LR, LS, LU, LY, MA, MD, ME, MG, MK, MN, MW, MX, MY, MZ, NA, NG, NI, NO, NZ, OM, PA, PE, PG, PH, PL, PT, QA, RO, RS, RU, RW, SA, SC, SD, SE, SG, SK, SL, ST, SV, SY, TH, TJ, TM, TN, TR, TT, TZ, UA, UG, US, UZ, VC, VN, WS, ZA, ZM, ZW.

(84) Designated States *(unless otherwise indicated, for every kind of regional protection available)*: ARIPO (BW, GH, GM, KE, LR, LS, MW, MZ, NA, RW, SD, SL, ST, SZ, TZ, UG, ZM, ZW), Eurasian (AM, AZ, BY, KG, KZ, RU, TJ, TM), European (AL, AT, BE, BG, CH, CY, CZ, DE, DK, EE, ES, FI, FR, GB, GR, HR, HU, IE, IS, IT, LT, LU, LV, MC, MK, MT, NL, NO, PL, PT, RO, RS, SE, SI, SK, SM, TR), OAPI (BF, BJ, CF, CG, CI, CM, GA, GN, GQ, GW, KM, ML, MR, NE, SN, TD, TG).

Published:
— *with international search report (Art. 21(3))*
— *before the expiration of the time limit for amending the claims and to be republished in the event of receipt of amendments (Rule 48.2(h))*
— *with sequence listing part of description (Rule 5.2(a))*

(54) **Title:** SYSTEMS AND METHODS FOR EXPRESSING BIOMOLECULES IN A SUBJECT

(57) **Abstract:** The present invention provides compositions, systems, kits, and methods for expressing at least one therapeutic protein or biologically active nucleic acid molecule in a subject. In certain embodiments, the subject is first administered a composition comprising poly cationic structures that is free, or essentially free, of nucleic acid molecules, and then (e.g., 1-30 minutes later) is administered a composition comprising a plurality of one or more non-viral expression vectors that encode at least one therapeutic protein (e.g., at least one anti-SARS-CoV-2 antibody, multiple different antibodies, an ACE2 protein, or human growth hormone) or a biologically active nucleic acid molecule.

WO 2022/067091 A1

SYSTEMS AND METHODS FOR EXPRESSING BIOMOLECULES IN A SUBJECT

The present application claims priority to U.S. Provisional application serial number 63/083,625, filed September 25, 2020, which is herein incorporated by reference in its entirety.

SEQUENCE LISTING

The text of the computer readable sequence listing filed herewith, titled "38655-601_SEQUENCE_LISTING_ST25", created September 24, 2021, having a file size of 2,893,042 bytes, is hereby incorporated by reference in its entirety.

FIELD OF THE INVENTION

The present invention provides compositions, systems, kits, and methods for expressing at least one therapeutic protein or biologically active nucleic acid molecule in a subject. In certain embodiments, the subject is first administered a composition comprising polycationic structures that is free, or essentially free, of nucleic acid molecules, and then (e.g., 1-30 minutes later) is administered a composition comprising a plurality of one or more non-viral expression vectors that encode at least one therapeutic protein (e.g., at least one anti-SARS-CoV-2 antibody, multiple different antibodies, one anti-SARS-CoV-2 recombinant ACE2 protein, at least one cytokine, or human growth hormone) or a biologically active nucleic acid molecule.

BACKGROUND

The simplest non-viral gene delivery system uses naked expression vector DNA. Direct injection of free DNA into certain tissues, particularly muscle, has been shown to produce high levels of gene expression, and the simplicity of this approach has led to its adoption in a number of clinical protocols. In particular, this approach has been applied to the gene therapy of cancer where the DNA can be injected either directly into the tumor or can be injected into muscle cells in order to express tumor antigens that might function as a cancer vaccine.

Although direct injection of plasmid DNA has been shown to lead to gene expression, the overall level of expression is much lower than with either viral or liposomal vectors. Naked DNA is also generally thought to be unsuitable for systemic administration due to the presence of serum nucleases. As a result, direct injection of plasmid DNA appears to be limited to only a few applications involving tissues that are easily accessible to direct injection such as skin and muscle cells.

SUMMARY OF THE INVENTION

The present invention provides compositions, systems, kits, and methods for expressing at least one therapeutic protein or biologically active nucleic acid molecule in a subject. In certain embodiments, the subject is first administered a composition comprising polycationic structures that is free, or essentially free, of nucleic acid molecules, and then (e.g., 1-30 minutes later) is administered a composition comprising a plurality of one or more non-viral expression vectors that encode at least one therapeutic protein (e.g., at least one anti-SARS-CoV-2 antibody, multiple different antibodies, or human growth hormone) or a biologically active nucleic acid molecule. In some embodiments, an agent is further administered (e.g., EPA or DHA) that increases the level and/or length of expression in a subject. In particular embodiments, the first and/or second composition is administered via the subject's airway.

In some embodiments, provided herein are methods comprising: a) administering a first composition to a subject, wherein the first composition comprises polycationic structures, and wherein the first composition is free, or essentially free, of nucleic acid molecules; and b) administering a second composition to the subject after administering the first composition, wherein the second composition comprises a plurality of one or more non-viral expression vectors that encode at least one anti-SARS-CoV-2 antibody or antigen-binding portion thereof, and/or recombinant ACE2, and wherein, as a result of the administering the first and second compositions, the at least one anti-SARS-CoV-2 antibody, or antigen-binding portion thereof, and/or said recombinant ACE2, is expressed in the subject.

In certain embodiments, provided herein are systems comprising: a) a first container; b) a first composition inside the first container and comprising polycationic structures, wherein the first composition is free, or essentially free, of nucleic acid molecules; c) a second container; and d) a second composition inside the second container and comprising a plurality of one or more non-viral expression vectors that encode at least one anti-SARS-CoV-2 antibody or antigen-binding portion thereof, or an ACE2 protein.

In some embodiments, the systems further comprise an Agent that: i) increases the level of expression of the at least one anti-SARS-CoV-2 antibody or antigen-binding portion thereof, or the ACE2 protein, when administered to a subject, and/or ii) and/or the length of time of the expression; as compared to when the agent is not administered to the subject. In further embodiments, the Agent is present in the first composition and/or the second composition. In other embodiments, the systems further comprise: a third container, and wherein the agent is present in the third container.

In certain embodiments, the systems further comprise an anti-viral agent (e.g., Remdesivir or a protein comprising at least part of the ACE2 receptor) and/or an anti-inflammatory and/or anticoagulant.

In particular embodiments, wherein: A) the subject is infected with the SARS-CoV-2 virus, and wherein the at least one anti-SARS-CoV-2 antibody, or antigen-binding portion thereof, or recombinant ACE2 is expressed in the subject at an expression level sufficient to reduce: i) the SARS-CoV-2 viral load in the subject, and/or ii) at least one symptom in the subject caused by the SARS-CoV-2 infection; or B) the subject is not infected with the SARS-CoV-2 virus, and wherein the at least one anti-SARS-CoV-2 antibody, or antigen-binding portion thereof, or recombinant ACE2 is expressed in the subject at an expression level sufficient to prevent the subject from being infected by the SARS-CoV-2 virus.

In certain embodiments, the expression level is maintained in the subject for at least two weeks without: i) any further, or only one, two, or three further repeat, of steps a) and b), and ii) any further administration of vectors encoding the at least one anti-SARS-CoV-2 antibody or antigen-binding portion thereof. In other embodiments, the expression level is maintained in the subject for at least one month without: i) any further, or only one, two, or three further repeat, of steps a) and b), and ii) any further administration of vectors encoding the at least one anti-SARS-CoV-2 antibody or antigen-binding portion thereof. In further embodiments, the expression level is maintained in the subject for at least one year, or two years, or for the lifetime of the subject, without: i) any further, or only one, two, or three further repeat, of steps a) and b), and ii) any further administration of vectors encoding the at least one anti-SARS-CoV-2 antibody or antigen-binding portion thereof. In some embodiments, the at least one anti-SARS-CoV-2 antibody, or antigen-binding portion thereof, is expressed in the subject at a level of: i) between 500ng/ml and 50ug/ml, or 10-20ug/ml, for at least 25 days, or ii) at least 250 ng/ml for at least 25 days.

In some embodiments, provided herein are methods of simultaneously expressing at least three different antibodies, or antigen binding portions thereof, in a subject comprising: a) administering a first composition to a subject, wherein the first composition comprises polycationic structures, and wherein the first composition is free, or essentially free, of nucleic acid molecules; and b) administering a second composition to the subject after administering the first composition, wherein the second composition comprises a plurality of one or more non-viral expression vectors that encode at least three different antibodies or antigen-binding portions thereof, and wherein, as a result of the administering the first and second compositions, the at least three different antibodies, or antigen-binding portions thereof, are simultaneously expressed in the subject. In certain embodiments, the at least three different antibodies, or antigen binding portions thereof, are specific for SARS-CoV-2 and/or influenza A, and/or influenza B. In some

embodiments, the at least three different antibodies, or antigen-binding portions thereof, are each fully or substantially neutralizing for SARS-CoV-2. In other embodiments, the at least three different antibodies, or antigen-binding portions thereof, are each fully or substantially neutralizing for a virus selected from the group consisting of: HIV, influenza A, influenza B, and malaria.

In certain embodiments, provided herein are systems comprising: a) a first container; b) a first composition inside the first container and comprising polycationic structures, wherein the first composition is free, or essentially free, of nucleic acid molecules; c) a second container; and d) a second composition inside the second container and comprising a plurality of one or more non-viral expression vectors that encode at least three different antibodies or antigen-binding portions thereof. In certain embodiments, the systems further comprise: an agent that: i) increases the level of expression of at least one of the at least three different antibodies or antigen-binding portions thereof when administered to a subject, and/or ii) and/or the length of time of the expression, as compared to when the agent is not administered to the subject. In other embodiments, the agent is present in the first composition and/or the second composition. In additional embodiments, the systems further comprise a third container, and wherein the agent is present in the third container.

In certain embodiments, the at least three different antibodies or antigen-binding portions thereof, are each expressed in the subject at a level of at least 100 ng/ml (e.g., at least 100 ... 500 ... 900 ng/ml). In other embodiments, the at least three different antibodies or antigen-binding portions thereof, are each expressed in the subject at a level of at least 100 ng/ml for at least 25 days. In other embodiments, the at least three different antibodies or antigen-binding portions thereof, are expressed in the subject at a level of at least 200 ng/ml.

In further embodiments, the at least three different antibodies or antigen-binding portions thereof, are expressed in the subject at a level of at least 200 ng/ml for at least 25 days. In other embodiments, wherein: A) the expression level for each of the three different antibodies, or antigen binding portions thereof, is maintained in the subject for at least two weeks, or at least 3 weeks, without: i) any further, or only one further, repeat of steps a) and b), and ii) any further administration of vectors encoding the at least three different antibodies or antigen binding portions thereof; and/or B)repeating steps a) and b) at least once or at least twice. In particular embodiments, the expression level is maintained in the subject for at least two weeks, or at least 3 weeks, without: i) any further, or only one or two further, repeats of steps a) and b), and ii) any further administration of vectors encoding the at least three different antibodies or antigen binding portions thereof.

In other embodiments, the one or more non-viral expression vectors comprise three non-viral expression vectors. In further embodiments, each of the three non-viral expression vector encodes a different antibody or antigen binding fragment thereof. In further embodiments, the one

or more non-viral expression vectors comprise six non-viral expression vectors. In additional embodiments, each of the six non-viral expression vectors encodes a different antibody light chain variable region, or heavy chain variable region. In further embodiments, the one or more non-viral expression vectors comprise first, second, and third nucleic acid sequences each encoding an antibody light chain variable region, and fourth, fifth, and sixth nucleic acid sequences each encoding an antibody heavy chain variable region. In other embodiments, the antigen-binding portions thereof are selected from the group consisting of: a Fab', F(ab)2, Fab, and a minibody.

In some embodiments, at least one of the at least three different antibodies or antigen-binding portions thereof is an anti-SARS-CoV-2 antibody or antigen binding portion thereof. In other embodiments, the at least one of the at least three different antibodies or antigen-binding portions thereof is an antibody or antigen binding portion thereof selected from Table 4 and/or Table 7. In further embodiments, the at least three different antibodies or antigen-binding portions thereof comprise at least four, five, six, seven, or eight different antibodies or antigen-binding portions thereof. In some embodiments, the administering comprises intravenous administering.

In some embodiments, provided herein are methods comprising: a) administering a first composition to a subject, wherein the first composition comprises polycationic structures, and wherein the first composition is free, or essentially free, of nucleic acid molecules; and b) administering a second composition to the subject after administering the first composition, wherein the second composition comprises a plurality of non-viral expression vectors that encode human growth hormone (hGH) and/or hGH linked to a half-life extending peptide (hGH-ext), and wherein, as a result of the administering the first and second compositions, the hGH is expressed in the subject.

In particular embodiments, the hGH and/or hGH-ext is expressed in the subject at a serum expression level of at least 1 ng/ml (e.g., at least 1 ... 10 ... 100 ... 500 ng/ml). In other embodiments, the expression level is maintained in the subject for at least two weeks without: i) any further, or only one further repeat, of steps a) and b), and ii) any further administration of vectors encoding the hGH or hGH-ext. In other embodiments, the expression level is maintained in the subject for at least one month without: i) any further, or only one further repeat, of steps a) and b), and ii) any further administration of vectors encoding the hGH or hGH-ext. In additional embodiments, the expression level is maintained in the subject for at least one year without: i) any further, or only one further repeat, of steps a) and b), and ii) any further administration of vectors encoding the hGH or hGH-ext. In further embodiments, the plurality of non-viral expression vectors encode the hGH-ext, and wherein the half-life extending peptide is selected from the group consisting of: an Fc region peptide, serum albumin, carboxy terminal peptide of human chorionic gonadotropin b-subunit (CTP), and XTEN (see, Schellenberger et al., Nat Biotechnol. 2009

Dec;27(12):1186-90). In additional embodiments, the methods further comprise: c) administering an agent, in the first and/or second composition, or present in a third composition, wherein the agent: i) increases the level of expression of the hGH and/or hGH-ext, and/or ii) and/or the length of time of the expression compared to when the agent is not administered to the subject.

In some embodiments, provided herein are systems comprising: a) a first container; b) a first composition inside the first container and comprising polycationic structures, wherein the first composition is free, or essentially free, of nucleic acid molecules; c) a second container; and d) a second composition inside the second container and comprising a plurality of non-viral expression vectors that encode human growth hormone (hGH) and/or hGH linked to a half-life extending peptide (hGH-ext). In certain embodiments, systems further comprise: an Agent that: i) increases the level of expression of the hGH and/or the hGH-ext when administered to a subject, and/or ii) and/or the length of time of the expression; as compared to when the agent is not administered to the subject. In other embodiments, the agent is present in the first composition and/or the second composition. In particular embodiments, the systems further comprise: a third container, and wherein the agent is present in the third container.

In some embodiments, provided herein are methods comprising: a) administering a first composition to a subject, wherein the first composition comprises polycationic structures, and wherein the first composition is free, or essentially free, of nucleic acid molecules; b) administering a second composition to the subject after administering the first composition, wherein the second composition comprises a plurality of expression vectors that each comprise a first nucleic acid sequence encoding a first protein and/or a first biologically active nucleic acid molecule; and c) administering an agent, in the first and/or second composition, or present in a third composition, wherein the agent: i) increases the level of expression of the first protein or the first biologically active nucleic acid molecule, and/or ii) and/or the length of time of the expression; and/or iii) decreases toxicity as measured by alanine aminotransferase (ALT) levels; all as compared to when the agent is not administered to the subject; wherein the agent is selected from the group consisting of: docosahexaenoic acid (DHA), eicosapenaenoic acid (EPA), alpha Linolenic acid (ALA), lipoxin A4 (LA4), 15-deoxy-12,14-prostaglandin J2 (15d), arachidonic acid (AA), cocosapentaenoic acid (DPA), retinoic acid (RA), diallyl disulfide (DADS), oleic acid (OA), alpha tocopherol (AT), sphingosine-1-phosphate (S-1-P), palmitoyl sphingomyelin (SPH), an anti-TNFa antibody or antigen binding fragment thereof, a heparinoid, and N-Acetyl-De-O-Sulfated Heparin; and wherein, as a result of the administering the first and second compositions and the agent to the subject, the first protein or the first biologically active nucleic acid molecule is expressed in the subject.

In other embodiments, the first protein or the first biologically active nucleic acid molecule, is expressed in the subject at a serum expression level of at least 10 ng/ml or at least 100 ng/ml. In additional embodiments, the expression level is maintained in the subject for at least two weeks without: i) any further, or only one further repeat, of steps a), b) and c), and ii) any further administration of vectors encoding the first protein or the first biologically active nucleic acid molecule. In further embodiments, the expression level is maintained in the subject for at least one month without: i) any further, or only one further repeat, of steps a), b) and c), and ii) any further administration of vectors encoding the first protein or the first biologically active nucleic acid molecule. In additional embodiments, the expression level is maintained in the subject for at least one year without: i) any further, or only one further repeat, of steps a), b), and c), and ii) any further administration of vectors encoding the first protein or the first biologically active nucleic acid molecule. In other embodiments, the first nucleic acid sequence provides the first protein or the first biologically active nucleic acid molecule, wherein the first biologically active nucleic acid molecule comprises a sequence selected from: an siRNA or shRNA sequence, a miRNA sequence, an antisense sequence, a CRISPR multimerized single guide, and a CRISPR single guide RNA sequence (sgRNA). In other embodiments, each of the expression vectors further comprises a second nucleic acid sequence encoding: i) a second therapeutic protein, and/or ii) a second biologically active nucleic acid molecule.

In some embodiments, the agent is present in the first composition. In particular embodiments, the agent is present in the third composition, and is administered at least one hour prior to the first composition. In additional embodiments, the agent comprises docosahexaenoic Acid (DHA). In further embodiments, the agent comprises eicosapenaenoic Acid (EPA).

In additional embodiments, provided herein are systems comprising: a) a first container; b) a first composition inside the first container and comprising polycationic structures, wherein the first composition is free, or essentially free, of nucleic acid molecules; c) a second container; and d) a second composition inside the second container and comprising a plurality of expression vectors that each comprise a first nucleic acid sequence encoding a first protein and/or a first biologically active nucleic acid molecule; and e) an agent in the first and/or second composition, or present in a third composition in a third container, wherein the agent is selected from the group consisting of: docosahexaenoic acid (DHA), eicosapenaenoic acid (EPA), alpha Linolenic acid (ALA), lipoxin A4 (LA4), 15-deoxy-12,14-prostaglandin J2 (15d), arachidonic acid (AA), cocosapentaenoic acid (DPA), retinoic acid (RA), diallyl disulfide (DADS), oleic acid (OA), alpha tocopherol (AT), sphingosine-1-phosphate (S-1-P), palmitoyl sphingomyelin (SPH), an anti-TNFa antibody or antigen binding fragment thereof, a heparinoid, and N-Acetyl-De-O-Sulfated Heparin.

In further embodiments, the agent, when administered to a subject with the first and second compositions: i) increases the level of expression of the first protein or the first biologically active nucleic acid molecule, and/or ii) and/or the length of time of the expression; and/or iii) decreases toxicity as measured by alanine aminotransferase (ALT) levels; all as compared to when the agent is not administered to the subject. In other embodiments, the agent is present in the first composition and/or the second composition. In further embodiments, the systems further comprise said third container, and wherein the agent is present in the third container.

In some embodiments, provided herein are methods comprising: a) administering a first composition to a subject via the subject's airway, wherein the first composition comprises polycationic structures, and wherein the first composition is free, or essentially free, of nucleic acid molecules; and b) administering a second composition to the subject after administering the first composition, wherein the administering is via the subject's airway, and wherein the second composition comprises a plurality of expression vectors that each comprise a first nucleic acid sequence encoding a first protein and/or a first biologically active nucleic acid molecule; and wherein, as a result of the administering the first and second compositions to the subject, the first protein or the first biologically active nucleic acid molecule is expressed in the subject.

In certain embodiments, the first protein or the first biologically active nucleic acid molecule is expressed in the subject's lungs. In further embodiments, the first composition is an aqueous composition or a freeze-dried composition. In other embodiments, the second composition is an aqueous composition or a freeze-dried composition. In additional embodiments, the polycationic structure comprise lipids selected from the group consisting of: 1,2-dioleoyl-3-trimethylammonium-propane (DOTAP); 1,2-Dimyristoyl-sn-glycero-3-phosphocholine (DMPC); 1,2-dioleoyl-sn-glycero-3-phospho-L-serine (DOPS); and 1-stearoyl-2-oleoyl-sn-glycero-3-phospho-L-serine. In other embodiments, the subject has lung inflammation. In further embodiments, the subject is on a ventilator.

In additional embodiments, provided herein are systems comprising: a) a first container; b) a first composition inside the first container and comprising polycationic structures, wherein the first composition is free, or essentially free, of nucleic acid molecules, and wherein the polycationic structure comprise lipids selected from the group consisting of: 1,2-dioleoyl-sn-glycero-3-phospho-L-serine (DOPS); and 1-stearoyl-2-oleoyl-sn-glycero-3-phospho-L-serine; c) a second container; and d) a second composition inside the second container and comprising a plurality of expression vectors that each comprise a first nucleic acid sequence encoding a first protein and/or a first biologically active nucleic acid molecule.

In some embodiments, provided herein are systems comprising: a) a first container; b) a first composition inside the first container and comprising polycationic structures, wherein the first

composition is free, or essentially free, of nucleic acid molecules; c) a second container; and d) a second composition inside the second container and comprising a plurality of expression vectors that each comprise a first nucleic acid sequence encoding a first protein and/or a first biologically active nucleic acid molecule, wherein the first and/or second composition is a freeze-dried composition.

In some embodiments, provided herein are methods of treating a subject comprising: administering a composition to a subject, wherein the composition comprises: i) an emulsion and/or plurality of liposomes, and ii) an Agent, wherein the subject has: inflammation, an autoimmune disease, an immune-deficiency disease, SARS-CoV-2 infection, and/or is receiving a checkpoint inhibitor, and wherein the Agent selected from the group consisting of: dexamethasone, dexamethasone palmitate, a dexamethasone fatty acid ester, docosahexaenoic Acid (DHA), eicosapenaenoic Acid (EPA), alpha Linolenic Acid (ALA), lipoxin A4 (LA4), 15-deoxy-12,14-Prostaglandin J2 (15d), arachidonic acid (AA), docosapentaenoic acid (DPA), retinoic Acid (RA), diallyl disulfide (DADS), oleic acid (OA), alpha tocopherol (AT), sphingosine-1-phosphate (S-1-P), palmitoyl sphingomyelin (SPH), an anti-TNFa antibody or antigen binding fragment thereof, a heparinoid, and N-Acetyl-De-O-sulfated heparin. In further embodiments, the administration comprises airway administration. In other embodiments, the administration comprises systemic administration. In other embodiments, the composition comprises the liposomes, and wherein Agent is incorporated into the liposomes. In other embodiments, the composition further comprises one or more of the Agents not in the liposomes. In additional embodiments, the composition is free, or essentially free, or nucleic acid molecules. In other embodiments, the subject is infected with SARS-CoV-2, and the method further comprises administering an anti-viral agent to the subject. In further embodiments, the anti-viral agent comprises Remdesivir or a protein comprising at least part of the ACE2 receptor. In other embodiments, the methods further comprise: administering an anti-inflammatory and/or anticoagulant to the subject. In some embodiments, the composition is an aqueous composition or a freeze-dried composition. In additional embodiments, the liposomes comprise lipids selected from the group consisting of: 1,2-dioleoyl-3-trimethylammonium-propane (DOTAP); 1,2-Dimyristoyl-sn-glycero-3-phosphocholine (DMPC); 1,2-dioleoyl-sn-glycero-3-phospho-L-serine (DOPS); and 1-stearoyl-2-oleoyl-sn-glycero-3-phospho-L-serine.

In certain embodiments, provided herein are methods comprising: a) administering a first composition to an animal model, wherein the first composition comprises polycationic structures, and wherein the first composition is free, or essentially free, of nucleic acid molecules, and wherein the animal model is infected with SARS-CoV-2; and b) administering a second composition to the animal model after administering the first composition, wherein the second

composition comprises a plurality of one or more non-viral expression vectors that encode first and second anti-SARS-CoV-2 antibodies or antigen-binding portion thereof, and wherein, as a result of the administering the first and second compositions, the first and second candidate anti-SARS-CoV-2 antibodies or antigen-binding portions thereof, are expressed in the animal model; and c) determining the extent to which the expression of the first and second candidate anti-SARS-CoV-2 antibodies, or antigen-binding portions thereof, i) reduce the SARS-CoV-2 viral load in the animal model, and/or ii) reduce at least one symptom in the animal model caused by the SARS-CoV-2 infection. In particular embodiments, the plurality of one or more non-viral expression vectors further encode third, fourth, fifth, sixth, seventh, eighth, ninth, tenth, or eleventh candidate anti-SARS-CoV-2 antibodies or antigen-binding fragments thereof. In certain embodiments, the animal model is selected from a: mouse, rat, hamster, Guinee pig, primate, monkey, chimpanzee, or rabbit. In further embodiments, first and anti- SARS-CoV2 antibodies, or antigen binding portions thereof, are from Table 7 or Table 5. In additional embodiments, the first and second anti- SARS-CoV2 antibodies, or antigen binding portions thereof, are selected from the group consisting of: REGN10933, REGN10987; VIR-7831; LY-CoV1404; LY3853113; Zost 2355K; CV07-209K; C121L; Zost 2504L; CV38-183L; COVA215K; RBD215; CV07-250L; C144L; COVA118L; C135K; and B38. In certain embodiments, the first and second anti- SARS-CoV2 antibodies, or antigen binding portions thereof, are REGN10933 and REGN10987.

In further embodiments, the polycationic structures comprise cationic lipids. In some embodiments, first composition comprises a plurality of liposomes, wherein at least some of said liposomes comprises said cationic lipids. In other embodiments, at least some of said liposomes comprise neutral lipids. In further embodiments, the ratio of said cationic lipids to said neutral lipids in said liposomes is 95:05 - 80:20 or about 1:1. In other embodiments, the cationic and neutral lipids are selected from the group consisting of: distearoyl phosphatidyl choline (DSPC); hydrogenated or non-hydrogenated soya phosphatidylcholine (HSPC); distearoylphosphatidylethanolamine (DSPE); egg phosphatidylcholine (EPC); 1,2-Distearoyl-sn-glycero-3-phospho-rac-glycerol (DSPG); dimyristoyl phosphatidylcholine (DMPC); 1,2-Dimyristoyl-sn-glycero-3-phosphoglycerol (DMPG); 1,2-Dipalmitoyl-sn-glycero-3-phosphate (DPPA); trimethylammonium propane lipids; DOTIM (1-[2-9(2)-octadecenoylloxy)ethyl]-2-(8(2)-heptadecenyl)-3-(2-hydroxyethyl) midizolinium chloride) lipids; and mixtures of two or more thereof.

In some embodiments, the one or more non-viral expression vectors comprise plasmids, wherein the plasmids are not attached to, or encapsulated in, any delivery agent. In additional embodiments, the one or more non-viral expression vectors comprise a first nucleic acid sequence encoding an antibody light chain variable region, and a second nucleic acid sequence encoding an

antibody heavy chain variable region, and optionally, a third nucleic acid sequence encoding an antibody light chain variable region, and a fourth nucleic acid sequence encoding an antibody heavy chain variable region. In certain embodiments, wherein: A) the antigen-binding portion thereof is selected from the group consisting of: a Fab', F(ab)2, Fab, and a minibody, and/or B) the wherein the at least one anti-SARS-CoV-2 antibody, or antigen-binding portion thereof, is bi-specific for different SARS-CoV-2 antigens. In other embodiments, the anti-SARS-CoV-2 antibody is monoclonal antibody selected from the group consisting of: REGN10933, REGN10987; VIR-7831; LY-CoV1404; LY3853113; Zost 2355K; CV07-209K; C121L; Zost 2504L; CV38-183L; COVA215K; RBD215; CV07-250L; C144L; COVA118L; C135K; and B38. These antibodies are described in the following reference, which are each herein incorporated by reference: Zost et al., Nature Medicine volume 26, pages1422–1427 (2020); Robbiani et al., Nature volume 584, pages437–442 (2020); and Wu et al., Science, 2020 Jun 12;368(6496):1274-1278; and see references in Table 7. Any combination of 2, 3, 4, 5, 6, 7, 8, 9, 10, 11, 12, 13, 14, 15, 16, or all 17 of these antibodies, or antigen binding fragments thereof, may be used in any of the embodiments described herein. In some embodiments, the anti-SARS-CoV-2 antibody, or antigen-binding portion thereof, comprises at least two, three, four, five, six, seven, eight, nine, ten, eleven, twelve, or more of any combination of the following: REGN10933, REGN10987; VIR-7831; LY-CoV1404; LY3853113; Zost 2355K; CV07-209K; C121L; Zost 2504L; CV38-183L; COVA215K; RBD215; CV07-250L; C144L; COVA118L; C135K; and B38 (or any of those shown in Table 7 or Table 5). In additional embodiments, the anti-SARS-CoV-2 antibody, or antigen binding portion thereof, is as described in Table 7.

In some embodiments, the at least one anti-SARS-CoV-2 antibody, or antigen-binding portion thereof, comprises at least two anti-SARS-CoV-2 antibodies, and/or antigen-binding portions thereof, which are expressed in the subject at an expression level sufficient to reduce: i) the SARS-CoV-2 viral load in the subject, and/or ii) at least one symptom in the subject caused by the SARS-CoV-2 infection. In other embodiments, the at least one anti-SARS-CoV-2 antibody, or antigen-binding portion thereof, comprises at least four, or at least eight, or at least eleven, anti-SARS-CoV-2 antibodies and/or antigen-binding portions thereof. In additional embodiments, the at least one anti-SARS-CoV-2 antibody, or antigen-binding portion thereof, comprises at least four, or at least eight, or at least 11, anti-SARS-CoV-2 antibodies and/or antigen-binding portions thereof, and which are expressed in the subject at an expression level sufficient to reduce: i) the SARS-CoV-2 viral load in the subject, and/or ii) at least one symptom in the subject caused by the SARS-CoV-2 infection.

In some embodiments, the administering comprises intravenous administering. In other embodiments, the second composition is administered: i) between 0.5 and 80 minutes after the first

composition, or between about 1 and 20 minutes after the first composition. In particular embodiments, the methods further comprise: c) administering an agent, in the first and/or second composition, or present in a third composition, wherein the agent: i) increases the level of expression of the at least one anti-SARS-CoV-2 antibody or antigen-binding portion thereof, and/or ii) and/or the length of time of the expression compared to when the agent is not administered to the subject. In other embodiments, the agent is present in the first composition. In particular embodiments, the agent is present in the third composition, and is administered at least one hour prior to the first composition. In some embodiments, the agent is selected from the group consisting of: dexamethasone, dexamethasone palmitate, a dexamethasone fatty acid ester, Docosahexaenoic Acid (DHA), Eicosapenaenoic Acid (EPA), Alpha Linolenic Acid (ALA), Lipoxin A4 (LA4), 15-deoxy-12,14-Prostaglandin J2 (15d), Arachidonic Acid (AA), Docosapentaenoic Acid (DPA), Retinoic Acid (RA), Diallyl Disulfide (DADS), Oleic Acid (OA), Alpha Tocopherol (AT), Sphingosine-1-Phosphate (S-1-P), Palmitoyl Sphingomyelin (SPH), an anti-TNFa antibody or antigen binding fragment thereof, a heparinoid, and N-Acetyl-De-O-Sulfated Heparin. In certain embodiments, the dexamethasone fatty acid ester has the following Formula:

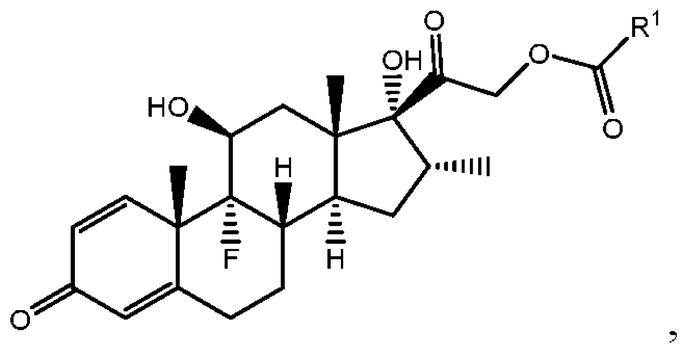

, wherein R^1 is C_5-C_{23} alkyl or C_5-C_{23} alkenyl.

In certain embodiments, the agent (e.g., water soluble dexamethasone, aka dexamethasone cyclodextrin inclusion complex; see Sigma Sku D2915) is present in the first, second, or third composition at a concentration of 0.1-35 mg/ml or 0.001-1.0 mg/ml (e.g., 0.001 ... 0.005 ... 0.01 ... 0.05 ... 0.1 ... 0.5 ... 1.0 mg/ml). In other embodiments, the subject has lung, cardiovascular, and/or multi-organ inflammation. In particular embodiments, the subject is on a ventilator.

In some embodiments, the first and/or second compositions further comprise a physiologically tolerable buffer or intravenous solution. In other embodiments, the first and/or second compositions further comprise lactated Ringer's solution or saline solution.

In additional embodiments, the first compositions comprise liposomes comprising the polycationic structures, wherein the liposomes further comprising one or more macrophage targeting moieties selected from the group consisting of: mannose moieties, maleimide moieties, a folate receptor ligand, folate, folate receptor antibody or fragment thereof, formyl peptide receptor ligands, N-formyl-Met-Leu-Phe, tetrapeptide Thr-Lys-Pro-Arg, galactose, and lactobionic acid.

In other embodiments, the plurality of one or more non-viral expression vectors are not attached to, or encapsulated in, any delivery agent.

In certain embodiments, the subject is a human. In particular embodiments, wherein 0.05-60 mg/mL of the expression vectors are present in the second composition. In other embodiments, the polycationic structures comprise cationic liposomes which are present at a concentration of 0.5-100 mM in the first composition. In further embodiments, the subject is a human, wherein: i) an amount of the first composition is administered such that the human receives a dosage of 2-50 mg/kg of the polycationic structures; and/or ii) an amount of the second composition is administered such that the human receives a dosage of 0.05-60 mg/kg of the expression vectors.

In some embodiments, the polycationic structures comprise cationic liposomes, wherein the cationic liposomes further comprise a lipid bi-layer integrating peptide and/or a target peptide. In certain embodiments, the lipid bi-layer integrating peptide is selected from the group consisting of: surfactant protein D (SPD), surfactant protein C (SPC), surfactant protein B (SPB), and surfactant protein A (SPA), and ii) the target peptide is selected from the group consisting of: microtubule-associated sequence (MTAS), nuclear localization signal (NLS), ER secretion peptide, ER retention peptide, and peroxisome peptide.

In other embodiments, steps a) and b) are repeated between 1 and 60 days after the initial step b). In some embodiments, each of the non-viral expression vectors comprise between 5,500 and 30,000 nucleic acid base pairs. In certain embodiments, the methods further comprise: administering an anti-viral agent to the subject. In some embodiments, the anti-viral agent comprises Remdesivir or a protein comprising at least part of the ACE2 receptor. In additional embodiments, the methods further comprise: administering an anti-inflammatory and/or anticoagulant to the subject. In some embodiments, the one or more non-viral expression vectors are CPG-free or CPG-reduced.

In some embodiments, the Agent herein comprises a dexamethasone fatty acid ester (e.g., as shown in Formula I). For example, dexamethasone palmitate has the following formula (Formula I):

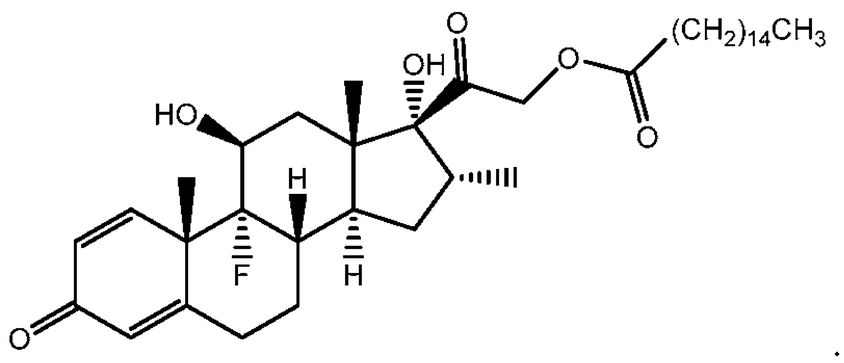

Other fatty acid esters of dexamethasone can also be used, with another fatty acid ester replacing the palmitate group. In some embodiments, the fatty acid ester is a C_6-C_{24} fatty acid ester, such as hexanoate (caproate), heptanoate (enanthate), octanoate (caprylate), nonanoate (pelargonate),

decanoate (caprate), undecanoate, dodecanoate (laurate), tetradecanoate (myristate), octadecenoate (stearate), icosanoate (arachidate), docosanoate (behenate), and tetracosanoate (lignocerate). Accordingly, in some embodiments, the compound is selected from dexamethasone caproate, dexamethasone enanthate, dexamethasone caprylate, dexamethasone pelargonate, dexamethasone caprate, dexamethasone undecanoate, dexamethasone laurate, dexamethasone myristate, dexamethasone palmitate, dexamethasone stearate, dexamethasone arachidate, dexamethasone behenate, and dexamethasone lignocerate.

In certain embodiments, the agent is said dexamethasone fatty acid ester of Formula I, and wherein R^1 is a C_5-C_{23} alkyl. In other embodiments, the agent is said dexamethasone fatty acid ester of Formula I, and wherein R^1 is a C_5-C_{23} straight chain alkyl. In other embodiments, the agent is said dexamethasone fatty acid ester of Formula I, and wherein R^1 is a C_{15} alkyl.

DESCRIPTION OF THE FIGURES

The patent or application file contains at least one drawing executed in color. Copies of this patent or patent application publication with color drawings will be provided by the Office upon request and payment of the necessary fee.

Figure 1 shows results from Example 1, showing expression levels over 36 days for four different antibodies or antibody fragments (anti-IL5; 5J8 anti-flu; anti- SARS-CoV-2; and anti-CD20).

Figure 2 shows results from Example 2, showing expression levels over 43 days for anti-SARS-CoV-2 antibody, as well as expression data for anti-IL5, 5J8 anti-flu, and anti-Sars-Cov2.

Figure 3A shows results from Example 3, which shows expression levels of multiple unique monoclonal antibodies. Figure 3B shows results from Example 3, which shows expression levels of the antibodies at various time points over 29 days after initial injection.

Figure 4 shows results from Example 4, which shows expression levels of antibodies at certain days after injection.

Figure 5A shows results from Example 5, which shows expression levels of various proteins over 15 days. Figure 5B shows the results of Example 5, which shows expression levels of various proteins over 22 days.

Figure 6 shows results from Example 6, which shows expression levels of various antibodies over 22 days.

Figure 7 shows results from Example 7, which shows expression levels of various proteins.

Figures 8A and 8B show results from Example 8, which shows expression levels of cDNA-encoded recombinant ACE2 proteins over 9 days.

Figure 9 shows results from Example 9 which shows expression levels of human ACE2 and a variant thereof.

Figure 10 shows the nucleic acid sequence for plasmid 070120 # 1 : B38-Lambda-BV3 (SEQ ID NO:10).

Figure 11 shows the nucleic acid sequence for plasmid 070120 # 11 : B38H-B38L-BV3 : Dual (SEQ ID NO:11).

Figure 12 shows the nucleic acid sequence for plasmid 070320 # 4 : B38-Kappa-BV3 (SEQ ID NO:12).

Figure 13 shows the nucleic acid sequence for plasmid 071320 # 3 : H4-Kappa-BV3 (SEQ ID NO:13).

Figure 14 shows the nucleic acid sequence for plasmid 080920 # 6 : H4-H4-Kappa-BV3 (SEQ ID NO:14).

Figure 15 shows the nucleic acid sequence for plasmid 072620 # 5A : 4A8- BV3 (SEQ ID NO:15).

Figure 16 shows the nucleic acid sequence for plasmid 081820 # 2 : 4A8- 4A8-BV3 (SEQ ID NO:16).

Figure 17 shows the nucleic acid sequence for plasmid 081820 # 3 : 4A8- B38Kappa-BV3 (SEQ ID NO:17).

Figure 18 shows the nucleic acid sequence for plasmid 081820 # 4 : 4A8- H4-BV3 (SEQ ID NO:18).

Figure 19 shows the nucleic acid sequence for plasmid 081820 # 5 : 4A8- shACE2-BV3 (SEQ ID NO:19).

Figure 20 shows the nucleic acid sequence for plasmid 080420 # 3 : shACE2- BV3 (SEQ ID NO:20).

Figure 21 shows the nucleic acid sequence for plasmid 082020 # 1 : shACE2 TYLTNY-BV3 (SEQ ID NO:21).

Figure 22 shows the nucleic acid sequence for plasmid 081320 # 2A : shACE2-1xL-Fc-BV3 (SEQ ID NO:22).

Figure 23 shows the nucleic acid sequence for plasmid 081320 # 4A : shACE2-1xL-FcLALA- BV3 (SEQ ID NO:23).

Figure 24 shows the nucleic acid sequence for plasmid 082620 # 5A : shACE2 TYLTNY-1xL-FcLALA- BV3 (SEQ ID NO:24).

Figure 25 shows the nucleic acid sequence for plasmid 080420 # 4 : shACE2- shACE2-BV3 (SEQ ID NO:25).

Figure 26 shows the nucleic acid sequence for plasmid 081120 # 1 : B38Kappa- shACE2-BV3 (SEQ ID NO:26).

Figure 27 shows the nucleic acid sequence for plasmid 081120 # 4 : shACE2-B38Kappa - BV3 (SEQ ID NO:27).

Figure 28 shows the nucleic acid sequence for plasmid 081120 # 2 : H4- shACE2-BV3 (SEQ ID NO:28).

Figure 29 shows the nucleic acid sequence of plasmid 081120 # 5 : shACE2-H4 -BV3 (SEQ ID NO:29).

Figure 30 shows the nucleic acid sequence of plasmid 072320 # 2 : H4-aCD20-aIL5-5J8-BV2 (SEQ ID NO:30).

Figure 31 shows the nucleic acid sequence of plasmid 070620 # 2 : B38 Lambda-aCD20(Cys)-BV3 (SEQ ID NO:31).

Figure 32 shows the nucleic acid sequence of plasmid 120717 # 1 : aCD20-aIL5-5J8-BV2 (SEQ ID NO:32).

Figure 33 shows the nucleic acid sequence of plasmid 122019 # 2A: GLA-1xL-hyFc (SEQ ID NO:33).

Figure 34 shows the nucleic acid sequence of plasmid 011215 # 7 : hGCSF-BV3 (SEQ ID NO:34).

Figures 35 shows the nucleic acid sequence of plasmid 071816# 1: (SEQ ID NO:35).

Figure 36 shows the nucleic acid sequence of plasmid 072520 # 4: aCD20-aCD20 (SEQ ID NO:36).

Figure 37 shows the nucleic acid sequence of plasmid 111517 # 1 : 5J8-5J8: Double 2A (SEQ ID NO:37).

Figure 38 shows the nucleic acid sequence of plasmid 111517 # 3 : aIL5-aIL5 : Double 2A (SEQ ID NO:38).

Figure 39 shows the nucleic acid sequence of plasmid 111517 # 19A : 5J8-aIL5 : Daul 2A (SEQ ID NO:39).

Figure 40 shows the nucleic acid sequences of: A) Codon Optimized Human Growth Hormone (hGH1) cDNA (SEQ ID NO:40); B) hGH1-Fc (SEQ ID NO:41); C) Linker GGGGS (SEQ ID NO:42), 1xLinker: GGTGGAGGAGGTAGT (SEQ ID NO:43), 2xLinker: GGTGGAGGAGGTAGTGGGGGTGGAGGTTCA (SEQ ID NO:44), and 3xLinker: GGAGGAGGTGGATCAGGTGGAGGAGGTAGTGGGGGTGGAGGTTCA (SEQ ID NO:45); D) Fc (SEQ ID NO:46); E) Fc chainA (SEQ ID NO:47); and F) Fc chainB (SEQ ID NO:48).

Figure 41 shows the nucleic acid sequences of: A) Fc chainAB (SEQ ID NO:49); B) Fc-IgG4 (SEQ ID NO:50); C) hyFc (SEQ ID NO:51); D) mFc (SEQ ID NO:52); E) GAALIE (SEQ ID NO:53); and F) GAALIE-LS (SEQ ID NO:54).

Figure 42 shows the nucleic acid sequences of: A) hGH1-HSA (SEQ ID NO:55); and B) HSA-K753P-Linker-GH1: (SEQ ID NO:56).

Figure 43 shows the nucleic acid sequences of: A) hGH1-CTP (SEQ ID NO:57); B) CTP-hGH1-CTP (SEQ ID NO:58); C) CTP-hGH1 (SEQ ID NO:59); and D) XTEN1-hGH1 (SEQ ID NO:60).

Figure 44 shows the nucleic acid sequences of: A) XTEN1-hGH1-XTEN2 (SEQ ID NO:61); and B) hGH1-XTEN2 (SEQ ID NO:62).

Figure 45A shows that expression of the wild type hGH cDNA fused to a protein half-life extending DNA sequence, including Fc, serum albumin or Xten can significantly increase serum hGH levels over time in immunocompetent mice. Figure 45B shows that the cDNA-encoded hGH protein produced is fully bioactive, as it appropriately increases the levels of the hGH-regulated, endogenous mouse, IGF-1 protein. Figure 45C shows one injection of a DNA vector in the procedure of Example 10 procedure drives the wild type hGH cDNA but lacking any protein half-life extending DNA sequence can produce durable production of therapeutic hGH serum levels in immunocompetent mice.

Figure 46 shows that the procedures of Example 11 can be used to express wild type hGH cDNA fused to a protein half-life extending DNA sequence, including Fc, serum albumin or Xten to significantly increase serum hGH levels over time in immunocompetent mice.

Figure 47 shows that, using the procedure of Example 12, one re-injection of a DNA vector driving the wild type hGH cDNA into fully immunocompetent mice can significantly and durably further increase serum hGH levels produced by the initial HEDGES hGH DNA vector injection.

Figure 48 show expression levels of hGH fused to an Fc region protein extends the half-life of hGH out to a least 225 days and after a single DNA injection in mice.

Figure 49 shows expression levels of hGH fused to an Fc region protein out 64 days from treatment.

Figure 50A shows that selective site-directed mutagenesis of the Fc region of an DNA vector driving the wild type hGH cDNA fused to an Fc protein half-life extending DNA sequence can selectively either increase or decrease serum hGH levels produced in immunocompetent mice. Figure 50B shows that selective site-directed mutagenesis of the Fc region of a DNA vector driving the wild type hGH cDNA fused to an Fc protein half-life extending DNA sequence can selectively increase serum hGH levels produced over time in immunocompetent mice.

Figure 51 shows that incorporating an optimized molar percentage of dexamethasone palmitate (DexPalm) into cationic liposomes can both further increase gene expression and further decrease toxicity.

Figure 52 shows that incorporating an optimized molar percentage of dexamethasone palmitate into cationic liposomes can both further increase gene expression and further decrease toxicity.

Figure 53 shows that pre-injecting an optimized molar percentage of dexamethasone palmitate in liposomes prior to injecting cationic liposomes can both further increase gene expression and further decrease toxicity.

Figure 54 shows that injecting some AILs incorporated into cationic liposomes can both further increase gene expression and further decrease toxicity (ALT levels).

Figure 55 shows that injecting certain AILs incorporated into cationic liposomes can both further increase gene expression and further decrease toxicity (ALT levels).

Figure 56 shows that incorporating an optimized molar percentage of dexamethasone palmitate into cationic liposomes can further increase peak levels of gene expression following an otherwise ineffective hG-CSF-DNA dose.

Figure 57 shows that by selectively modifying the lipid composition of liposomes administered intranasally, that these liposomes can be selectively targeted to intrapulmonary monocytes and macrophages to different extents, thus selectively immune-modulating the lung.

Figure 58 shows that by selectively modifying a parenteral aqueous soluble pre-dose, and/or the molar percentage of dexamethasone palmitate incorporated into subsequently administered liposomes, that the level of T lymphocyte activation both in lung and in the blood can be selectively immuno-modulated.

Figure 59 shows that by selectively modifying a parenteral aqueous soluble pre-dose, and/or the molar percentage of dexamethasone palmitate incorporated into subsequently administered liposomes, that the level of T lymphocyte activation both in lung and in the blood can be selectively immuno-modulated.

Figure 60 shows that pre-administration of an anti-TNF monoclonal antibody, can both further increase gene expression while further reducing its toxicity.

Figure 61, which shows that either pre- or post-administration of NSH can reduce toxicity.

Figure 62 shows that either pre- or post-administration of NSH can reduce toxicity.

Figure 63 shows that either pre-administration of NSH can both further increase gene expression while further reducing its toxicity.

Figure 64 shows that administration of various formulations of liposomes containing dexamethasone palmitate decreases lymphocyte counts in blood compared to systemic administration of dexamethasone alone.

Figure 65 shows that administration of various formulations of liposomes containing dexamethasone palmitate decreases monocyte counts in blood compared to systemic administration of dexamethasone alone.

Figure 66 shows results of Example 22, which shows that one injection of different single DNA expression plasmids each encoding one of five different SARS-CoV2-specific mAb (C135, C215, COV2-2355, CV07-209, and C121) produces fully neutralizing serum levels of each SARS-CoV2-specific mAb for the full experimental course of at least 134 days following administration, and that these ongoing serum mAb levels functionally and continuously block SARS-CoV2 spike – human ACE2 binding for at least 120 days.

Figure 67 shows results from Example 23, which shows that a single injection results in expression of two SARS-CoV2-specific mAbs from a single plasmid for the course of at least 134 days following this procedure, and that these serum-expressed mAbs sera are functionally capable of blocking SARS-CoV2 spike – human ACE2 interactions for at least 134 days.

Figure 68 shows results from Example 24 where three different approaches were successfully employed to express simultaneously express two anti-SARS-CoV2 mAbs simultaneously by the three approaches tried. All three approaches successfully allow for the expression of two mAbs in serum of animals at levels (Figure 68B shows expression levels) that allow for neutralization of SARS-CoV2 / ACE2 interactions (Figure 68b shows neutralization ability).

Figure 69 shows results from Example 25, which shows that two weekly injections of one or two DNA expression plasmids encoding a total of three different individual SARS-CoV2-specific mAbs produces fully neutralizing serum levels of three different SARS-CoV2-specific mAbs for the course of at least 70 days following administration, and that these ongoing serum mAbs levels functionally and continuously block SARS-CoV2 spike – human ACE2 for at least 70 days.

Figure 70 shows the results from Example 26, which shows the expression levels and neutralizing ability of four anti-SARS-CoV-2 antibodies expressed in mice.

Figure 71 shows the results from Example 27, which shows the expression levels and neutralizing ability of four anti-SARS-CoV-2 antibodies expressed in mice.

Figure 72 shows the results from Example 28, which shows the expression levels and neutralizing ability of four anti-SARS-CoV-2 antibodies expressed in mice.

Figure 73 shows the results from Example 29, which shows the expression levels and neutralizing ability of four anti-SARS-CoV-2 antibodies expressed in mice.

Figure 74 shows the results from Example 30, which shows the expression levels and neutralizing ability of four anti-SARS-CoV-2 antibodies expressed in mice.

Figure 75 shows the results from Example 31, which shows the expression levels and neutralizing ability of five anti-SARS-CoV-2 antibodies expressed in mice.

Figure 76 shows the results from Example 32, which shows the expression levels and neutralizing ability of six anti-SARS-CoV-2 antibodies expressed in mice.

Figure 77 shows the results from Example 33, which shows the expression levels and neutralizing ability of six anti-SARS-CoV-2 antibodies expressed in mice.

Figure 78 shows the results from Example 34, which shows the expression levels and neutralizing ability of six anti-SARS-CoV-2 antibodies expressed in mice.

Figure 79 shows the results from Example 35, which shows the expression levels and neutralizing ability of eight anti-SARS-CoV-2 antibodies expressed in mice.

Figure 80 shows the results from Example 36, which shows the expression levels and neutralizing ability of eight anti-SARS-CoV-2 antibodies expressed in mice.

Figure 81 shows the results from Example 37, which shows the expression levels and neutralizing ability of eight anti-SARS-CoV-2 antibodies expressed in mice.

Figure 82 shows the results from Example 38, which shows the expression levels and neutralizing ability of eight anti-SARS-CoV-2 antibodies expressed in mice.

Figure 83 shows the results from Example 39, which shows the expression levels and neutralizing ability of 10 anti-SARS-CoV-2 antibodies, as well as expression levels of other non-Sars-CoV-2 antibodies and various therapeutic proteins, expressed in mice.

Figure 84 shows the results from Example 40, which shows the expression levels and neutralizing ability of 11 anti-SARS-CoV-2 antibodies, as well as expression levels of other non-Sars-CoV-2 antibodies and various therapeutic proteins, expressed in mice.

Figure 85 shows the results from Example 41, which shows the expression levels and neutralizing ability of 10 anti-SARS-CoV-2 antibodies, as well as expression levels of other non-Sars-CoV-2 antibodies, expressed in mice.

Figure 86A shows the results from Example 42, which shows expression levels of the indicated mAbs over 1-48 hours. Figures 86B shows neutralizing ability of the indicated mAbs over a period of 1-48 hours.

Figure 87 shows the results from Example 43, which describes the simultaneous expression of six different mAb and genes using a single injection.

Figure 88 shows the results from Example 44, which describes the use of various eukaryotic promoters to express a target gene (human growth hormone) over 120 days.

Figure 89 shows the results from Example 45, which describes simultaneously testing 11 different hGLA DNA vectors, showing that they produce a spectrum of serum levels over time.

Figure 90 shows the results from Example 46, which shows Fc-modified GLA can be expressed in heart tissue at therapeutic levels 104 days after injection of vector.

Figure 91 shows the results from Example 47, which compares the expression of various mutated Fc regions for GLA-Fc expression.

Figure 92 shows the results of Example 48, which describes the use of low dose dexamethasone pretreatment does not interfere with the durability of protein expression durability (and acute expression may be augmented).

DEFINITIONS

As used herein, the phrase "CpG-reduced" refers to a nucleic acid sequence or expression vector that has less CpG di-nucleotides than present in the wild-type versions of the sequence or vector. "CpG-free" means the subject nucleic acid sequence or vector does not have any CpG di-nucleotides. An initial sequence, that contains CpG dinucleotides (e.g., wild-type version of an anti-SARS-CoV-2 antibody), may be modified to remove CpG dinucleotides by altering the nucleic acid sequence. Such CpG di-nucleotides can be suitably reduced or eliminated not just in a coding sequence, but also in the non-coding sequences, including, e.g., 5′ and 3′ untranslated regions (UTRs), promoter, enhancer, polyA, ITRs, introns, and any other sequences present in the nucleic acid molecule or vector. In certain embodiments, the nucleic acid sequences employed herein are CpG-reduced or CpG-free.

As used herein, "empty liposomes" refers to liposomes that do not contain nucleic acid molecules but that may contain other bioactive molecules (e.g., liposomes that are only composed of the lipid molecules themselves, or only lipid molecules and a small molecule drug). In certain embodiments, empty liposomes are used with any of the methods or compositions disclosed herein.

As used herein, "empty cationic micelles" refers to cationic micelles that do not contain nucleic acid molecules but that may contain other bioactive molecules (e.g., micelles that are only composed of lipid and surfactant molecules themselves, or only lipid and surfactant molecules and a small molecule drug). In certain embodiments, empty cationic micelles are used with any of the methods or compositions disclosed herein.

As used herein, "empty cationic emulsions" refers to cationic emulsions or micro-emulsions that do not contain nucleic acid molecules but that may contain other bioactive molecules. In certain embodiments, empty cationic emulsions are used with any of the methods or compositions disclosed herein.

As used herein, the term "alkyl" means a straight or branched saturated hydrocarbon chain containing from 1 to 30 carbon atoms, for example 1 to 16 carbon atoms (C_1-C_{16} alkyl), 1 to 14 carbon atoms (C_1-C_{14} alkyl), 1 to 12 carbon atoms (C_1-C_{12} alkyl), 1 to 10 carbon atoms (C_1-C_{10} alkyl), 1 to 8 carbon atoms (C_1-C_8 alkyl), 1 to 6 carbon atoms (C_1-C_6 alkyl), 1 to 4 carbon atoms (C_1-C_4 alkyl), or 5 to 23 carbon atoms (C_5-C_{23} alkyl). Representative examples of alkyl include, but are not limited to, methyl, ethyl, n-propyl, iso-propyl, n-butyl, sec-butyl, iso-butyl, tert-butyl, n-pentyl, isopentyl, neopentyl, n-hexyl, 3-methylhexyl, 2,2-dimethylpentyl, 2,3-dimethylpentyl, n-heptyl, n-octyl, n-nonyl, n-decyl, n-undecyl, and n-dodecyl.

As used herein, the term "alkenyl" refers to a straight or branched hydrocarbon chain containing from 2 to 30 carbon atoms and containing at least one carbon-carbon double bond, for example 2 to 16 carbon atoms (C_2-C_{16} alkyl), 2 to 14 carbon atoms (C_2-C_{14} alkyl), 2 to 12 carbon atoms (C_2-C_{12} alkyl), 2 to 10 carbon atoms (C_2-C_{10} alkyl), 2 to 8 carbon atoms (C_2-C_8 alkyl), 2 to 6 carbon atoms (C_2-C_6 alkyl), 2 to 4 carbon atoms (C_2-C_4 alkyl), or 5 to 23 carbon atoms (C_5-C_{23} alkyl). Representative examples of alkenyl include, but are not limited to, ethenyl, 2-propenyl, 2-methyl-2-propenyl, 3-butenyl, 4-pentenyl, 5-hexenyl, 2-heptenyl, 2-methyl-1-heptenyl, and 3-decenyl.

As used herein, the terms "subject" and "patient" refer to any animal, such as a mammal like a dog, cat, bird, livestock, and preferably a human.

As used herein, the term "administration" refers to the act of giving a composition as described herein to a subject. Exemplary routes of administration to the human body can be through the mouth (oral), skin (transdermal, topical), nose (nasal), lungs (inhalant), oral mucosa (buccal), by injection (e.g., intravenously, subcutaneously, intratumorally, intraocular, intraperitoneally, etc.), and the like.

DETAILED DESCRIPTION

The present invention provides compositions, systems, kits, and methods for expressing at least one therapeutic protein or biologically active nucleic acid molecule in a subject. In certain embodiments, the subject is first administered a composition comprising polycationic structures that is free, or essentially free, of nucleic acid molecules, and then (e.g., 1-30 minutes later) is administered a composition comprising a plurality of one or more non-viral expression vectors that encode at least one therapeutic protein (e.g., at least one anti-SARS-CoV-2 antibody, multiple

different antibodies, at least one recombinant ACE2, or human growth hormone) or a biologically active nucleic acid molecule. In some embodiments, an agent is further administered (e.g., EPA or DHA) that increases the level and/or length of expression in a subject. In particular embodiments, the first and/or second composition is administered via the subject's airway.

The present disclosure provides methods, systems, and compositions, that allow a single injection (e.g., intravenous injection) of cationic liposomes, followed shortly thereafter by injection (e.g., intravenous injection) of vectors encoding at least one protein or biologically active nucleic acid molecule, to produce circulating protein levels many times (e.g., 2-20 times higher) than with other approaches (e.g., allowing for expression for a prolonged period, such at 190 days or over 500 days).

In certain embodiments, the present disclosure employs polycationic structures (e.g., empty cationic liposomes, empty cationic micelles, or empty cationic emulsions) not containing vector DNA, which are administered to a subject prior to vector administration. In certain embodiments, the polycationic structures are cationic lipids and/or are provided as an emulsion. The present disclosure is not limited to the cationic lipids employed, which can be composed, in some embodiments, of one or more of the following: DDAB, dimethyldioctadecyl ammonium bromide; DPTAP (1,2-dipalmitoyl 3-trimethylammonium propane); DHA; prostaglandin, N-[1-(2,3-Dioloyloxy)propyl]-N,N,N-- trimethylammonium methylsulfate; 1,2-diacyl-3-trimethylammonium-propanes, (including but not limited to, dioleoyl (DOTAP), dimyristoyl, dipalmitoyl, disearoyl); 1,2-diacyl-3-dimethylammonium-propanes, (including but not limited to, dioleoyl, dimyristoyl, dipalmitoyl, disearoyl) DOTMA, N-[1-[2,3-bis(oleoyloxy)]propyl]-N,N,N-trimethylammoniu-m chloride; DOGS, dioctadecylamidoglycylspermine; DC-cholesterol, 3.beta.-[N-(N',N'-dimethylaminoethane)carbamoyl]cholesterol; DOSPA, 2,3-dioleoyloxy-N-(2(sperminecarboxamido)-ethyl)-N,N-dimethyl-1-propanami-nium trifluoroacetate; 1,2-diacyl-sn-glycero-3-ethylphosphocholines (including but not limited to dioleoyl (DOEPC), dilauroyl, dimyristoyl, dipalmitoyl, distearoyl, palmitoyl-oleoyl); beta-alanyl cholesterol; CTAB, cetyl trimethyl ammonium bromide; diC14-amidine, N-t-butyl-N'-tetradecyl-3-tetradecylaminopropionamidine; 14Dea2, O,O'-ditetradecanolyl-N-(trimethylammonioacetyl) diethanolamine chloride; DOSPER, 1,3-dioleoyloxy-2-(6-carboxy-spermyl)-propylamide; N,N,N',N'-tetramethyl-N,N'-bis(2-hydroxylethyl)-2,3-dioleoyloxy-1,4-butan- ediammonium iodide; 1-[2-acyloxy)ethyl]2-alkyl (alkenyl)-3-(2-hydroxyethyl-) imidazolinium chloride derivatives such as 1-[2-(9(Z)-octadecenoyloxy)eth- yl]-2-(8(Z)-heptadecenyl-3-(2-hydroxyethyl)imidazolinium chloride (DOTIM), 1-[2-(hexadecanoyloxy)ethyl]-2-pentadecyl-3-(2-hydroxyethyl)imidazolinium chloride (DPTIM); 1-[2-tetradecanoyloxy)ethyl]-2-tridecyl-3-(2-hydroxyeth- yl)imidazolium chloride (DMTIM) (e.g., as described in Solodin et al. (1995)

Biochem. 43:13537-13544, herein incorporated by reference); 2,3-dialkyloxypropyl quaternary ammonium compound derivates, containing a hydroxyalkyl moiety on the quaternary amine, such as 1,2-dioleoyl-3-dimethyl-hydroxyethyl ammonium bromide (DORI); 1,2-dioleyloxypropyl-3-dimethyl-hydroxyethyl ammonium bromide (DORIE); 1,2-dioleyloxypropyl-3-dimethyl-hydroxypropyl ammonium bromide (DORIE-HP), 1,2-dioleyloxypropyl-3-dimethyl-hydroxybutyl ammonium bromide (DORIE-HB); 1,2-dioleyloxypropyl-3-dimethyl-hydroxypentyl ammonium bromide (DORIE-HPe); 1,2-dimyristyloxypropyl-3-dimethyl-hydroxylethyl ammonium bromide (DMRIE); 1,2-dipalmityloxypropyl-3-dimethyl-hydroxyethyl ammonium bromide (DPRIE); 1,2-disteryloxypropyl-3-dimethyl-hydroxyethyl ammonium bromide (DSRIE) (e.g., as described in Felgner et al. (1994) J. Biol. Chem. 269:2550-2561, herein incorporated by reference in its entirety). Many of the above-mentioned lipids are available commercially from, e.g., Avanti Polar Lipids, Inc.; Sigma Chemical Co.; Molecular Probes, Inc.; Northern Lipids, Inc.; Roche Molecular Biochemicals; and Promega Corp.

In certain embodiments, the neutral lipids employed with the methods, compositions, systems, and kits includes diacylglycerophosphorylcholine wherein the acyl chains are generally at least 12 carbons in length (e.g., 12 … 14 … 20 … 24 … or more carbons in length), and may contain one or more cis or trans double bonds. Examples of said compounds include, but are not limited to, distearoyl phosphatidyl choline (DSPC), dimyristoyl phosphatidylcholine (DMPC), dipalmitoyl phosphatidylcholine (DPPC), palmitoyl oleoyl phosphatidylcholine (POPC), palmitoyl stearoyl phosphatidylcholine (PSPC), egg phosphatidylcholine (EPC), hydrogenated or non-hydrogenated soya phosphatidylcholine (HSPC), or sunflower phosphatidylcholine.

In certain embodiments, the neutral lipids include, for example, up to 70 mol diacylglycerophosphorylethanolamine/100 mol phospholipid (e.g., 10/100 mol … 25/100 mol … 50/100 … 70/100 mol). In some embodiments, the diacylglycerophosphorylethanolamine has acyl chains that are generally at least 12 carbons in length (e.g., 12 … 14 … 20 … 24 … or more carbons in length), and may contain one or more cis or trans double bonds. Examples of such compounds include, but are not limited to distearoylphosphatidylethanolamine (DSPE), dimyristoylphosphatidylethanolamine (DMPE), dipalmitoylphosphatidylethanolamine (DPPE), palmitoyloleoylphosphatidylethanolamine (POPE), egg phosphatidylethanolamine (EPE), and transphosphatidylated phosphatidylethanolamine (t-EPE), which can be generated from various natural or semisynthetic phosphatidylcholines using phospholipase D.

In certain embodiments, the present disclosure employs CpG-reduced or CpG-free expression vectors. An initial sequence that contains CpG dinucleotides (e.g., wild-type version of an anti-SARS-CoV-2 antibody), may be modified to remove CpG dinucleotides by altering the nucleic acid sequence. Such CpG di-nucleotides can be suitably reduced or eliminated not just in a

coding sequence, but also in the non-coding sequences, including, e.g., 5′ and 3′ untranslated regions (UTRs), promoter, enhancer, polyA, ITRs, introns, and any other sequences present in the nucleic acid molecule or vector. CpG di-nucleotides may be located within a codon triplet for a selected amino acid. There are five amino acids (serine, proline, threonine, alanine, and arginine) that have one or more codon triplets that contain a CpG di-nucleotide. All five of these amino acids have alternative codons not containing a CpG di-nucleotide that can be changed to, to avoid the CpG but still code for the same amino acid as shown in Table 1 below. Therefore, the CpG di-nucleotides allocated within a codon triplet for a selected amino acid may be changed to a codon triplet for the same amino acid lacking a CpG di-nucleotide.

TABLE 1

	DNA Codons	DNA Codons
Amino Acid	**Containing CpG**	**Lacking CpG**
Serine (Ser or S)	TCG	TCT, TCC, TCA,
		AGT, AGC
Proline (Pro or P)	CCG	CCT, CCC, CCA,
Threonine (Thr or T)	ACG	ACA, ACT, ACC
Alanine (Ala or A)	GCG	GCT, GCC, GCA
Arginine (Arg or R)	CGT, CGC,	AGA, AGG
	CGA, CGG	

In addition, within the coding region, the interface between triplets should be taken into consideration. For example, if an amino acid triplet ends in a C-nucleotide which is then followed by an amino acid triplet which can start only with a G-nucleotide (e.g., Valine, Glycine, Glutamic Acid, Alanine, Aspartic Acid), then the triplet for the first amino acid triplet is changed to one which does not end in a C-nucleotide. Methods for making CpG free sequences are shown, for example, in U.S. Pat. 7,244,609, which is herein incorporated by reference. A commercial service provided by INVIVOGEN is also available to produce CpG free (or reduced) nucleic acid sequences/vectors (plasmids). A commercial service provided by ThermoScientific produces CpG free nucleotide.

Provided below in Table 2 are exemplary promoters and enhancers that may be used in the vectors described herein. Such promoters, and other promoters known in the art, may be used alone or with any of the enhancers, or enhancers, known in the art. Additionally, when multiple proteins or biologically active nucleic acid molecules (e.g., two, three, four, or more) are expressed from the same vector, the same or different promoters may be used in conjunction with the subject nucleic acid sequence. In some embodiments, a promoter selected from the following list is employed to control the expression levels of the protein or nucleic acid: FerL, FerH, Grp78, hREG1B, and cBOX1. Such promoter can be used, for example, to control production of a protein

(e.g., HGH) protein production over a broad temporal range (e.g., without the use of any other modifications including Gene switches).

TABLE 2

Promoter	Enhancer
CMV	human CMV
EF1α	mouse CMV
Ferritin (Heavy/Light) Chain	SV40
GRP94	Ubc
U1	AP1
UbC	hr3
Beta Actin	IE2
PGK1	IE6
GRP78	E2-RS
CAG	MEF2
SV40	C/EBP
TRE	HNF-1

In some embodiments, compositions and systems herein are provided and/or administered in doses selected to elicit a therapeutic and/or prophylactic effect in an appropriate subject (e.g., mouse, human, etc.). In some embodiments, a therapeutic dose is provided. In some embodiments, a prophylactic dose is provided. Dosing and administration regimes are tailored by the clinician, or others skilled in the pharmacological arts, based upon well-known pharmacological and therapeutic/prophylactic considerations including, but not limited to, the desired level of pharmacologic effect, the practical level of pharmacologic effect obtainable, toxicity. Generally, it is advisable to follow well-known pharmacological principles for administrating pharmaceutical agents (e.g., it is generally advisable to not change dosages by more than 50% at time and no more than every 3-4 agent half-lives). For compositions that have relatively little or no dose-related toxicity considerations, and where maximum efficacy is desired, doses in excess of the average required dose are not uncommon. This approach to dosing is commonly referred to as the "maximal dose" strategy. In certain embodiments, a dose (e.g., therapeutic of prophylactic) is about 0.01 mg/kg to about 200 mg/kg (e.g., 0.01 mg/kg, 0.02 mg/kg, 0.05 mg/kg, 0.1 mg/kg, 0.2 mg/kg, 0.5 mg/kg, 1.0 mg/kg, 2.0 mg/kg, 5.0 mg/kg, 10 mg/kg, 20 mg/kg, 50 mg/kg, 100 mg/kg , 200 mg/kg, or any ranges therebetween (e.g., 5.0 mg/kg to 100 mg/kg)). In some embodiments, a subject is between 0.1 kg (e.g., mouse) and 150 kg (e.g., human), for example, 0.1 kg, 0.2 kg, 0.5 kg, 1.0 kg, 2.0 kg, 5.0 kg, 10 kg, 20 kg, 50 kg, 100 kg, 200 kg, or any ranges therebetween (e.g., 40-125 kg). In some embodiments, a dose comprises

between 0.001 mg and 40,000 mg (e.g., 0.001 mg, 0.002 mg, 0.005 mg, 0.01 mg, 0.02 mg, 0.05 mg, 0.1 kg, 0.2 mg, 0.5 mg, 1.0 mg, 2.0 mg, 5.0 mg, 10 mg, 20 mg, 50 mg, 100 mg, 200 mg, 500 mg, 1,000 mg, 2,000 mg, 5,000 mg, 10,000 mg, 20,000 mg, 40,000 mg, or ragnes therebetween.

In certain embodiments, a target peptide is used with the cationic or neutral liposomes in the compositions herein. Exemplary target peptides are shown in Table 3 below. In table 3, "[n]" prefix indicates the N-terminus and a "[c]" suffix indicates the C-terminus; sequences lacking either are found in the middle of the protein.

TABLE 3

Target	Sequence	Source protein or organism
nucleus (NLS)	PKKKRKV (SEQ ID NO:1)	SV40 large T antigen (P03070)
Out of nucleus (NES)	IDMLIDLGLDLSD (SEQ ID NO:2)	HSV transcriptional regulator IE63 P10238
ER, secretion (signal peptide)	[n]MMSFVSLLLVGILFWATEAEQLTKCEVFQ (SEQ ID NO:3)	Lactalbumin (P09462)
ER, retention (KDEL)	KDEL[c] (SEQ ID NO:4)	
Mitochondrial matrix	[n]MLSLRQSIRFFKPATRTLCSSRYLL (SEQ ID NO:5)	*S. cerevisiae* COX4 (P04037)
Plastid	[n]MVAMAMASLQSSMSSLSLSSNSFLGQ PLSPITLSPFLQG (SEQ ID NO:6)	*Pisum sativum* RPL24 (P11893)
Folded secretion (Tat)	(S/T)RRXFLK (SEQ ID NO:7)	Near the N terminus[6]
peroxisome (PTS1)	SKL[c] (SEQ ID NO:8)	
peroxisome (PTS2)	[c]XXXXRLXXXXXHL (SEQ ID NO:9)	

In certain embodiments, one or more (e.g., at least 3, or at least 8 antibodies) are expressed with the systems and methods herein. In some embodiments, this includes the therapeutic

monoclonal antibodies (mAbs), Fabs, F(ab)2s, and scFv's that are shown in Table 4 below, as well as the anti-SARS-CoV2 antibodies and antigen bindings provided at Table 5 and Table 7, which is herein incorporated by reference.

TABLE 4

Antibody Name	Trade name	Type	Source	Target	Use
3F8		mab	mouse	GD2 ganglioside	neuroblastoma
8H9		mab	mouse	B7-H3	neuroblastoma, sarcoma, metastatic brain cancers
Abagovomab		mab	mouse	CA-125 (imitation)	ovarian cancer
Abciximab	ReoPro	Fab	chimeric	CD41 (integrin alpha-IIb)	platelet aggregation inhibitor
Abituzumab		mab	humanized	CD51	cancer
Abrilumab		mab	human	integrin α4β7	inflammatory bowel disease, ulcerative colitis, Crohn's disease
Actoxumab		mab	human	Clostridium difficile	Clostridium difficile colitis
Adalimumab	Humira	mab	human	TNF-α	Rheumatoid arthritis, Crohn's Disease, Plaque Psoriasis, Psoriatic Arthritis, Ankylosing Spondylitis, Juvenile Idiopathic Arthritis, Hemolytic disease of the newborn
Adecatumumab		mab	human	EpCAM	prostate and breast cancer
Aducanumab		mab	human	beta-amyloid	Alzheimer's disease
Afasevikumab		mab	human	IL17A and IL17F	---
Afelimomab		$F(ab')_2$	mouse	TNF-α	sepsis
Afutuzumab		mab	humanized	CD20	lymphoma
Alacizumab pegol		$F(ab')_2$	humanized	VEGFR2	cancer
ALD518		---	humanized	IL-6	rheumatoid arthritis
Alemtuzumab	Lemtrada, Campath	mab	humanized	CD52	Multiple sclerosis
Alirocumab		mab	human	PCSK9	hypercholesterolemia
Altumomab pentetate	Hybri-ceaker	mab	mouse	CEA	colorectal cancer (diagnosis)
Amatuximab		mab	chimeric	mesothelin	cancer
Anatumomab mafenatox		Fab	mouse	TAG-72	non-small cell lung carcinoma
Anetumab ravtansine		mab	human	MSLN	cancer
Anifrolumab		mab	human	interferon α/β receptor	systemic lupus erythematosus
Anrukinzumab (= IMA-638)		mab	humanized	IL-13	asthma
Apolizumab		mab	humanized	HLA-DR ---	hematological cancers
Arcitumomab	CEA-Scan	Fab'	mouse	CEA	gastrointestinal cancers (diagnosis)
Ascrinvacumab		mab	human	activin receptor-like kinase 1	cancer
Aselizumab		mab	humanized	L-selectin (CD62L)	severely injured patients
Atezolizumab		mab	humanized	CD274	cancer
Atinumab		mab	human	RTN4	---
Atlizumab (= tocilizumab)	Actemra, RoActemra	mab	humanized	IL-6 receptor	rheumatoid arthritis
Atorolimumab		mab	human	Rhesus factor	hemolytic disease of the newborn[citation needed]
Avelumab		mab	human	CD274	---

Bapineuzumab		mab	humanized	beta amyloid	Alzheimer's disease
Basiliximab	Simulect	mab	chimeric	CD25 (α chain of IL-2 receptor)	prevention of organ transplant rejections
Bavituximab		mab	chimeric	phosphatidylserine	cancer, viral infections
Bectumomab	LymphoScan	Fab'	mouse	CD22	non-Hodgkin's lymphoma (detection)
Begelomab		mab	mouse	DPP4	---
Belimumab	Benlysta, LymphoStat-B	mab	human	BAFF	non-Hodgkin lymphoma etc.
Benralizumab		mab	humanized	CD125	asthma
Bertilimumab		mab	human	CCL11 (eotaxin-1)	severe allergic disorders
Besilesomab	Scintimun	mab	mouse	CEA-related antigen	inflammatory lesions and metastases (detection)
Bevacizumab	Avastin	mab	humanized	VEGF-A	metastatic cancer, retinopathy of prematurity
Bezlotoxumab		mab	human	Clostridium difficile	Clostridium difficile colitis
Biciromab	FibriScint	Fab'	mouse	fibrin II, beta chain	thromboembolism (diagnosis)
Bimagrumab		mab	human	ACVR2B	myostatin inhibitor
Bimekizumab		mab	humanized	IL 17A and IL 17F	---
Bivatuzumab mertansine		mab	humanized	CD44 v6	squamous cell carcinoma
Bleselumab		mab	human	CD40	---
Blinatumomab		BiTE	mouse	CD19	pre-B ALL (CD19+)
Blontuvetmab	Blontress	mab	veterinary	CD20	---
Blosozumab		mab	humanized	SOST	osteoporosis
Bococizumab		mab	humanized	neural apoptosis-regulated proteinase 1	dyslipidemia
Brazikumab		mab	human	IL23	Crohn's disease
Brentuximab vedotin		mab	chimeric	CD30 (TNFRSF8)	hematologic cancers
Briakinumab		mab	human	IL-12, IL-23	psoriasis, rheumatoid arthritis, inflammatory bowel diseases, multiple sclerosis
Brodalumab		mab	human	IL-17	inflammatory diseases
Brolucizumab		mab	humanized	VEGFA	wet age-related macular degeneration
Brontictuzumab		mab	humanized	Notch 1	cancer
Burosumab		mab	human	FGF 23	X-linked hypophosphatemia
Cabiralizumab		mab	humanized	CSF1R	---
Canakinumab	Ilaris	mab	human	IL-1---	rheumatoid arthritis
Cantuzumab mertansine		mab	humanized	mucin CanAg	colorectal cancer etc.
Cantuzumab ravtansine		mab	humanized	MUC1	cancers
Caplacizumab		mab	humanized	VWF	thrombotic thrombocytopenic purpura, thrombosis
Capromab pendetide	Prostascint	mab	mouse	prostatic carcinoma cells	prostate cancer (detection)
Carlumab		mab	human	MCP-1	oncology/immune indications
Carotuximab		mab	chimeric	endoglin	---
Catumaxomab	Removab	3funct	rat/mouse hybrid	EpCAM, CD3	ovarian cancer, malignant ascites, gastric cancer
cBR96-doxorubicin immunoconjugate		mab	humanized	Lewis-Y antigen	cancer
Cedelizumab		mab	humanized	CD4	prevention of organ transplant rejections, treatment of autoimmune diseases

Cergutuzumab amunaleukin		mab	humanized	IL2	---
Certolizumab pegol	Cimzia	Fab'	humanized	TNF-α	Crohn's disease Rheumatoid arthritis axial spondyloarthritis psoriasis arthritis
Cetuximab	Erbitux	mab	chimeric	EGFR	metastatic colorectal cancer and head and neck cancer
Ch.14.18		mab	chimeric	GD2 ganglioside	neuroblastoma
Citatuzumab bogatox		Fab	humanized	EpCAM	ovarian cancer and other solid tumors
Cixutumumab		mab	human	IGF-1 receptor (CD221)	solid tumors
Clazakizumab		mab	humanized	Oryctolagus cuniculus	rheumatoid arthritis
Clenoliximab		mab	chimeric	CD4	rheumatoid arthritis
Clivatuzumab tetraxetan	hPAM4-Cide	mab	humanized	MUC1	pancreatic cancer
Codrituzumab		mab	humanized	glypican 3	cancer
Coltuximab ravtansine		mab	chimeric	CD19	cancer
Conatumumab		mab	human	TRAIL-R2	cancer
Concizumab		mab	humanized	TFPI	bleeding
CR6261		mab	human	Influenza A hemagglutinin	infectious disease/influenza A
Crenezumab		mab	humanized	1-40-β-amyloid	Alzheimer's disease
Crotedumab		mab	human	GCGR	diabetes
Dacetuzumab		mab	humanized	CD40	hematologic cancers
Daclizumab	Zenapax	mab	humanized	CD25 (α chain of IL-2 receptor)	prevention of organ transplant rejections
Dalotuzumab		mab	humanized	IGF-1 receptor (CD221)	cancer etc.
Dapirolizumab pegol		mab	humanized	CD154 (CD40L)	---
Daratumumab		mab	human	CD38 (cyclic ADP ribose hydrolase)	cancer
Dectrekumab		mab	human	IL-13	---
Demcizumab		mab	humanized	DLL4	cancer
Denintuzumab mafodotin		mab	humanized	CD19	cancer
Denosumab	Prolia	mab	human	RANKL	osteoporosis, bone metastases etc.
Depatuxizumab mafodotin		mab	chimeric/humanized	EGFR	cancer
Derlotuximab biotin		mab	chimeric	histone complex	recurrent glioblastoma multiforme
Detumomab		mab	mouse	B-lymphoma cell	lymphoma
Dinutuximab		mab	chimeric	GD2 ganglioside	neuroblastoma
Diridavumab		mab	human	hemagglutinin	influenza A
Domagrozumab		mab	humanized	GDF-8	Duchenne muscular dystrophy
Dorlimomab aritox		$F(ab')_2$	mouse	---	---
Drozitumab		mab	human	DR5	cancer etc.
Duligotumab		mab	human	ERBB3 (HER3)	testicular cancer
Dupilumab		mab	human	IL4	atopic diseases
Durvalumab		mab	human	CD274	cancer
Dusigitumab		mab	human	ILGF2	cancer
Ecromeximab		mab	chimeric	GD3 ganglioside	malignant melanoma
Eculizumab	Soliris	mab	humanized	C5	paroxysmal nocturnal hemoglobinuria, atypical HUS
Edobacomab		mab	mouse	endotoxin	sepsis caused by Gram-negative bacteria
Edrecolomab	Panorex	mab	mouse	EpCAM	colorectal carcinoma
Efalizumab	Raptiva	mab	humanized	LFA-1 (CD11a)	psoriasis (blocks T-cell migration)
Efungumab	Mycograb	scFv	human	Hsp90	invasive Candida infection
Eldelumab		mab	human	interferon gamma-	Crohn's disease,

				induced protein	ulcerative colitis
Elgemtumab		mab	human	ERBB3 (HER3)	cancer
Elotuzumab		mab	humanized	SLAMF7	multiple myeloma
Elsilimomab		mab	mouse	IL-6	---
Emactuzumab		mab	humanized	CSF1R	cancer
Emibetuzumab		mab	humanized	HHGFR	cancer
Emicizumab		mab	humanized	activated F9, F10	haemophilia A
Enavatuzumab		mab	humanized	TWEAK receptor	cancer etc.
Enfortumab vedotin		mab	human	AGS-22M6	cancer expressing Nectin-4
Enlimomab pegol		mab	mouse	ICAM-1 (CD54)	---
Enoblituzumab		mab	humanized	CD276	cancer
Enokizumab		mab	humanized	IL9	asthma
Enoticumab		mab	human	DLL4	---
Ensituximab		mab	chimeric	5AC	cancer
Epitumomab cituxetan		mab	mouse	episialin	---
Epratuzumab		mab	humanized	CD22	cancer, SLE
Erenumab		mab	human	CGRP	migraine
Erlizumab		$F(ab')_2$	humanized	ITGB2 (CD18)	heart attack, stroke, traumatic shock
Ertumaxomab	Rexomun	3funct	rat/mouse hybrid	HER2/neu, CD3	breast cancer etc.
Etaracizumab	Abegrin	mab	humanized	integrin αvβ3	melanoma, prostate cancer, ovarian cancer etc.
Etrolizumab		mab	humanized	integrin α7 β7	inflammatory bowel disease
Evinacumab		mab	human	angiopoietin 3	dyslipidemia
Evolocumab		mab	human	PCSK9	hypercholesterolemia
Exbivirumab		mab	human	hepatitis B surface antigen	hepatitis B
Fanolesomab	NeutroSpec	mab	mouse	CD15	appendicitis (diagnosis)
Faralimomab		mab	mouse	interferon receptor	---
Farletuzumab		mab	humanized	folate receptor 1	ovarian cancer
Fasinumab		mab	human	HNGF	acute sciatic pain
FBTA05	Lymphomun	3funct	rat/mouse hybrid	CD20	chronic lymphocytic leukaemia
Felvizumab		mab	humanized	respiratory syncytial virus	respiratory syncytial virus infection
Fezakinumab		mab	human	IL-22	rheumatoid arthritis, psoriasis
Fibatuzumab		mab	humanized	ephrin receptor A3	---
Ficlatuzumab		mab	humanized	HGF	cancer etc.
Figitumumab		mab	human	IGF-1 receptor (CD221)	adrenocortical carcinoma, non-small cell lung carcinoma etc.
Firivumab		mab	human	influenza A virus hemagglutinin	---
Flanvotumab		mab	human	TYRP1(glycoprotein 75)	melanoma
Fletikumab		mab	human	IL 20	rheumatoid arthritis
Fontolizumab	HuZAF	mab	humanized	IFN-γ	Crohn's disease etc.
Foralumab		mab	human	CD3 epsilon	---
Foravirumab		mab	human	rabies virus glycoprotein	rabies (prophylaxis)
Fresolimumab		mab	human	TGF-β	idiopathic pulmonary fibrosis, focal segmental glomerulosclerosis, cancer
Fulranumab		mab	human	NGF	pain
Futuximab		mab	chimeric	EGFR	cancer
Galcanezumab		mab	humanized	calcitonin	migraine
Galiximab		mab	chimeric	CD80	B-cell lymphoma
Ganitumab		mab	human	IGF-1 receptor (CD221)	cancer
Gantenerumab		mab	human	beta amyloid	Alzheimer's disease

Gavilimomab		mab	mouse	CD147 (basigin)	graft versus host disease
Gemtuzumab ozogamicin	Mylotarg	mab	humanized	CD33	acute myelogenous leukemia
Gevokizumab		mab	humanized	IL-1β	diabetes etc.
Girentuximab	Rencarex	mab	chimeric	carbonic anhydrase 9 (CA-IX)	clear cell renal cell carcinoma[84]
Glembatumumab vedotin		mab	human	GPNMB	melanoma, breast cancer
Golimumab	Simponi	mab	human	TNF-α	rheumatoid arthritis, psoriatic arthritis, ankylosing spondylitis
Gomiliximab		mab	chimeric	CD23 (IgE receptor)	allergic asthma
Guselkumab		mab	human	IL23	psoriasis
Ibalizumab		mab	humanized	CD4	HIV infection
Ibritumomab tiuxetan	Zevalin	mab	mouse	CD20	non-Hodgkin's lymphoma
Icrucumab		mab	human	VEGFR-1	cancer etc.
Idarucizumab		mab	humanized	dabigatran	reversal of anticoagulant effects of dabigatran
Igovomab	Indimacis-125	$F(ab')_2$	mouse	CA-125	ovarian cancer (diagnosis)
IMAB362		mab	human	CLDN18.2	gastrointestinal adenocarcinomas and pancreatic tumor
Imalumab		mab	human	MIF	cancer
Imciromab	Myoscint	mab	mouse	cardiac myosin	cardiac imaging
Imgatuzumab		mab	humanized	EGFR	cancer
Inclacumab		mab	human	selectin P	cardiovascular disease
Indatuximab ravtansine		mab	chimeric	SDC1	cancer
Indusatumab vedotin		mab	human	GUCY2C	cancer
Inebilizumab		mab	humanized	CD19	cancer, systemic sclerosis, multiple sclerosis
Infliximab	Remicade	mab	chimeric	TNF-α	rheumatoid arthritis, ankylosing spondylitis, psoriatic arthritis, psoriasis, Crohn's disease, ulcerative colitis
Inolimomab		mab	mouse	CD25 (α chain of IL-2 receptor)	graft versus host disease
Inotuzumab ozogamicin		mab	humanized	CD22	ALL
Intetumumab		mab	human	CD51	solid tumors (prostate cancer, melanoma)
Ipilimumab	Yervoy	mab	human	CD152	melanoma
Iratumumab		mab	human	CD30 (TNFRSF8)	Hodgkin's lymphoma
Isatuximab		mab	chimeric	CD38	cancer
Itolizumab		mab	humanized	CD6	---
Ixekizumab		mab	humanized	IL 17A	autoimmune diseases
Keliximab		mab	chimeric	CD4	chronic asthma
Labetuzumab	CEA-Cide	mab	humanized	CEA	colorectal cancer
Lampalizumab		mab	humanized	CFD	geographic atrophy secondary to age-related macular degeneration
Lanadelumab		mab	human	kallikrein	angioedema
Landogrozumab		mab	humanized	GDF-8	muscle wasting disorders
Laprituximab emtansine		mab	chimeric	EGFR	---
Lebrikizumab		mab	humanized	IL-13	asthma
Lemalesomab		mab	mouse	NCA-90 (granulocyte antigen)	diagnostic agent
Lendalizumab		mab	humanized	C5	---

Lenzilumab		mab	human	CSF2	---
Lerdelimumab		mab	human	TGF beta 2	reduction of scarring after glaucoma surgery
Lexatumumab		mab	human	TRAIL-R2	cancer
Libivirumab		mab	human	hepatitis B surface antigen	hepatitis B
Lifastuzumab vedotin		mab	humanized	phosphate-sodium co-transporter	cancer
Ligelizumab		mab	humanized	IGHE	severe asthma and chronic spontaneous urticaria
Lilotomab satetraxetan		mab	mouse	CD37	cancer
Lintuzumab		mab	humanized	CD33	cancer
Lirilumab		mab	human	KIR2D	solid and hematological cancers
Lodelcizumab		mab	humanized	PCSK9	hypercholesterolemia
Lokivetmab		mab	veterinary	Canis lupus familiaris IL31	---
Lorvotuzumab mertansine		mab	humanized	CD56	cancer
Lucatumumab		mab	human	CD40	multiple myeloma, non-Hodgkin's lymphoma, Hodgkin's lymphoma
Lulizumab pegol		mab	humanized	CD28	autoimmune diseases
Lumiliximab		mab	chimeric	CD23 (IgE receptor)	chronic lymphocytic leukemia
Lumretuzumab		mab	humanized	ERBB3 (HER3)	cancer
MABp1	Xilonix	mab	human	IL1A	colorectal cancer
Mapatumumab		mab	human	TRAIL-R1	cancer
Margetuximab		mab	humanized	ch4D5	cancer
Maslimomab		---	mouse	T-cell receptor	---
Matuzumab		mab	humanized	EGFR	colorectal, lung and stomach cancer
Mavrilimumab		mab	human	GMCSF receptor α-chain	rheumatoid arthritis
Mepolizumab	Bosatria	mab	humanized	IL-5	asthma and white blood cell diseases
Metelimumab		mab	human	TGF beta 1	systemic scleroderma
Milatuzumab		mab	humanized	CD74	multiple myeloma and other hematological malignancies
Minretumomab		mab	mouse	TAG-72	tumor detection (and therapy---)
Mirvetuximab soravtansine		mab	chimeric	folate receptor alpha	cancer
Mitumomab		mab	mouse	GD3 ganglioside	small cell lung carcinoma
Mogamulizumab		mab	humanized	CCR4	cancer
Monalizumab		mab	humanized	KLRC1	---
Morolimumab		mab	human	Rhesus factor	---
Motavizumab	Numax	mab	humanized	respiratory syncytial virus	respiratory syncytial virus (prevention)
Moxetumomab pasudotox		mab	mouse	CD22	cancer
Muromonab-CD3	Orthoclone OKT3	mab	mouse	CD3	prevention of organ transplant rejections
Nacolomab tafenatox		Fab	mouse	C242 antigen	colorectal cancer
Namilumab		mab	human	CSF2	---
Naptumomab estafenatox		Fab	mouse	5T4	non-small cell lung carcinoma, renal cell carcinoma
Naratuximab emtansine		mab	chimeric	CD37	---
Narnatumab		mab	human	RON	cancer
Natalizumab	Tysabri	mab	humanized	integrin α4	multiple sclerosis, Crohn's disease
Navicixizumab		mab	chimeric/humanized	DLL4	---

Navivumab		mab	human	influenza A virus hemagglutinin HA	---
Nebacumab		mab	human	endotoxin	sepsis
Necitumumab		mab	human	EGFR	non-small cell lung carcinoma
Nemolizumab		mab	humanized	IL31RA	eczema[106]
Nerelimomab		mab	mouse	TNF-α	---
Nesvacumab		mab	human	angiopoietin 2	cancer
Nimotuzumab	Theracim, Theraloc	mab	humanized	EGFR	squamous cell carcinoma, head and neck cancer, nasopharyngeal cancer, glioma
Nivolumab	Opdivo	mab	human	PD-1	cancer
Nofetumomab merpentan	Verluma	Fab	mouse	---	cancer (diagnosis)
Obiltoxaximab		mab	chimeric	Bacillus anthracis anthrax	Bacillus anthracis spores
Obinutuzumab	Gazyva	mab	humanized	CD20	Chronic lymphatic leukemia
Ocaratuzumab		mab	humanized	CD20	cancer
Ocrelizumab		mab	humanized	CD20	rheumatoid arthritis, lupus erythematosus etc.
Odulimomab		mab	mouse	LFA-1 (CD11a)	prevention of organ transplant rejections, immunological diseases
Ofatumumab	Arzerra	mab	human	CD20	chronic lymphocytic leukemia etc.
Olaratumab		mab	human	PDGF-R α	cancer
Olokizumab		mab	humanized	IL6	---
Omalizumab	Xolair	mab	humanized	IgE Fc region	allergic asthma
Onartuzumab		mab	humanized	human scatter factor receptor kinase	cancer
Ontuxizumab		mab	chimeric/humanized	TEM1	cancer
Opicinumab		mab	human	LINGO-1	multiple sclerosis
Oportuzumab monatox		scFv	humanized	EpCAM	cancer
Oregovomab	OvaRex	mab	mouse	CA-125	ovarian cancer
Orticumab		mab	human	oxLDL	---
Otelixizumab		mab	chimeric/humanized	CD3	diabetes mellitus type 1
Otlertuzumab		mab	humanized	CD37	cancer
Oxelumab		mab	human	OX-40	asthma
Ozanezumab		mab	humanized	NOGO-A	ALS and multiple sclerosis
Ozoralizumab		mab	humanized	TNF-α	inflammation
Pagibaximab		mab	chimeric	lipoteichoic acid	sepsis (Staphylococcus)
Palivizumab	Synagis, Abbosynagis	mab	humanized	F protein of respiratory syncytial virus	respiratory syncytial virus (prevention)
Pamrevlumab		mab	human	CTGF	---
Panitumumab	Vectibix	mab	human	EGFR	colorectal cancer
Pankomab		mab	humanized	tumor specific glycosylation of MUC1	ovarian cancer
Panobacumab		mab	human	Pseudomonas aeruginosa	Pseudomonas aeruginosa infection
Parsatuzumab		mab	human	EGFL7	cancer
Pascolizumab		mab	humanized	IL-4	asthma
Pasotuxizumab		mab	chimeric/humanized	folate hydrolase	cancer
Pateclizumab		mab	humanized	LTA	TNF
Patritumab		mab	human	ERBB3 (HER3)	cancer
Pembrolizumab		mab	humanized	PDCD1	melanoma and other cancers
Pemtumomab	Theragyn	---	mouse	MUC1	cancer

Perakizumab		mab	humanized	IL 17A	arthritis
Pertuzumab	Omnitarg	mab	humanized	HER2/neu	cancer
Pexelizumab		scFv	humanized	C5	reduction of side effects of cardiac surgery
Pidilizumab		mab	humanized	PD-1	cancer and infectious diseases
Pinatuzumab vedotin		mab	humanized	CD22	cancer
Pintumomab		mab	mouse	adenocarcinoma antigen	adenocarcinoma (imaging)
Placulumab		mab	human	human TNF	pain and inflammatory diseases
Plozalizumab		mab	humanized	CCR2	diabetic nephropathy and arteriovenous graft patency
Pogalizumab		mab	humanized	TNFR superfamily member 4	---
Polatuzumab vedotin		mab	humanized	CD79B	cancer
Ponezumab		mab	humanized	human beta-amyloid	Alzheimer's disease
Prezalizumab		mab	humanized	ICOSL	---
Priliximab		mab	chimeric	CD4	Crohn's disease, multiple sclerosis
Pritoxaximab		mab	chimeric	E. coli shiga toxin type-1	---
Pritumumab		mab	human	vimentin	brain cancer
PRO 140		---	humanized	CCR5	HIV infection
Quilizumab		mab	humanized	IGHE	asthma
Racotumomab		mab	mouse	N-glycolylneuraminic acid	cancer
Radretumab		mab	human	fibronectin extra domain-B	cancer
Rafivirumab		mab	human	rabies virus glycoprotein	rabies (prophylaxis)
Ralpancizumab		mab	humanized	neural apoptosis-regulated proteinase 1	dyslipidemia
Ramucirumab	Cyramza	mab	human	VEGFR2	solid tumors
Ranibizumab	Lucentis	Fab	humanized	VEGF-A	macular degeneration (wet form)
Raxibacumab		mab	human	anthrax toxin, protective antigen	anthrax (prophylaxis and treatment)
Refanezumab		mab	humanized	myelin-associated glycoprotein	recovery of motor function after stroke
Regavirumab		mab	human	cytomegalovirus glycoprotein B	cytomegalovirus infection
Reslizumab		mab	humanized	IL-5	inflammations of the airways, skin and gastrointestinal tract
Rilotumumab		mab	human	HGF	solid tumors
Rinucumab		mab	human	platelet-derived growth factor receptor beta	neovascular age-related macular degeneration
Risankizumab		mab	humanized	IL23A	---
Rituximab	MabThera, Rituxan	mab	chimeric	CD20	lymphomas, leukemias, some autoimmune disorders
Rivabazumab pegol		mab	humanized	Pseudomonas aeruginosa type III secretion system	---
Robatumumab		mab	human	IGF-1 receptor (CD221)	cancer
Roledumab		mab	human	RHD	---
Romosozumab		mab	humanized	sclerostin	osteoporosis
Rontalizumab		mab	humanized	IFN-α	systemic lupus erythematosus
Rovalpituzumab tesirine		mab	humanized	DLL3	---

Rovelizumab	LeukArrest	mab	humanized	CD11, CD18	haemorrhagic shock etc.
Ruplizumab	Antova	mab	humanized	CD154 (CD40L)	rheumatic diseases
Sacituzumab govitecan		mab	humanized	tumor-associated calcium signal transducer 2	cancer
Samalizumab		mab	humanized	CD200	cancer
Sapelizumab		mab	humanized	IL6R	---
Sarilumab		mab	human	IL6	rheumatoid arthritis, ankylosing spondylitis
Satumomab pendetide		mab	mouse	TAG-72	cancer (diagnosis)
Secukinumab		mab	human	IL 17A	uveitis, rheumatoid arthritis psoriasis
Seribantumab		mab	human	ERBB3 (HER3)	cancer
Setoxaximab		mab	chimeric	E. coli shiga toxin type-2	---
Sevirumab		---	human	cytomegalovirus	cytomegalovirus infection
SGN-CD19A		mab	humanized	CD19	acute lymphoblastic leukemia and B-cell non-Hodgkin lymphoma
SGN-CD33A		mab	humanized	CD33	Acute myeloid leukemia
Sibrotuzumab		mab	humanized	FAP	cancer
Sifalimumab		mab	humanized	IFN-α	SLE, dermatomyositis, polymyositis
Siltuximab		mab	chimeric	IL-6	cancer
Simtuzumab		mab	humanized	LOXL2	fibrosis
Siplizumab		mab	humanized	CD2	psoriasis, graft-versus-host disease (prevention)
Sirukumab		mab	human	IL-6	rheumatoid arthritis
Sofituzumab vedotin		mab	humanized	CA-125	ovarian cancer
Solanezumab		mab	humanized	beta amyloid	Alzheimer's disease
Solitomab		BiTE	mouse	EpCAM	---
Sonepcizumab		---	humanized	sphingosine-1-phosphate	choroidal and retinal neovascularization
Sontuzumab		mab	humanized	episialin	---
Stamulumab		mab	human	myostatin	muscular dystrophy
Sulesomab	LeukoScan	Fab'	mouse	NCA-90 (granulocyte antigen)	osteomyelitis (imaging)
Suvizumab		mab	humanized	HIV-1	viral infections
Tabalumab		mab	human	BAFF	B-cell cancers
Tacatuzumab tetraxetan	AFP-Cide	mab	humanized	alpha-fetoprotein	cancer
Tadocizumab		Fab	humanized	integrin αIIbβ3	percutaneous coronary intervention
Talizumab		mab	humanized	IgE	allergic reaction
Tamtuvetmab	Tactress	mab	veterinary	CD52	---
Tanezumab		mab	humanized	NGF	pain
Taplitumomab paptox		mab	mouse	CD19	cancer[citation needed]
Tarextumab		mab	human	Notch receptor	cancer
Tefibazumab	Aurexis	mab	humanized	clumping factor A	Staphylococcus aureus infection
Telimomab aritox		Fab	mouse	---	---
Tenatumomab		mab	mouse	tenascin C	cancer
Teneliximab		mab	chimeric	CD40	autoimmune diseases and prevention of organ transplant rejection
Teplizumab		mab	humanized	CD3	diabetes mellitus type 1
Teprotumumab		mab	human	IGF-1 receptor (CD221)	hematologic tumors
Tesidolumab		mab	human	C5	---
Tetulomab		mab	humanized	CD37	cancer[141]
Tezepelumab		mab	human	TSLP	asthma, atopic dermatitis
TGN1412		---	humanized	CD28	chronic lymphocytic

					leukemia, rheumatoid arthritis
Ticilimumab (= tremelimumab)		mab	human	CTLA-4	cancer
Tigatuzumab		mab	humanized	TRAIL-R2	cancer
Tildrakizumab		mab	humanized	IL23	immunologically mediated inflammatory disorders
Timolumab		mab	human	AOC3	---
Tisotumab vedotin		mab	human	coagulation factor III	---
TNX-650		---	humanized	IL-13	Hodgkin's lymphoma
Tocilizumab (= atlizumab)	Actemra, RoActemra	mab	humanized	IL-6 receptor	rheumatoid arthritis
Toralizumab		mab	humanized	CD154 (CD40L)	rheumatoid arthritis, lupus nephritis etc.
Tosatoxumab		mab	human	Staphylococcus aureus	---
Tositumomab	Bexxar	---	mouse	CD20	follicular lymphoma
Tovetumab		mab	human	CD140a	cancer
Tralokinumab		mab	human	IL-13	asthma etc.
Trastuzumab	Herceptin	mab	humanized	HER2/neu	breast cancer
Trastuzumab emtansine	Kadcyla	mab	humanized	HER2/neu	breast cancer
TRBS07	Ektomab	3funct	---	GD2 ganglioside	melanoma
Tregalizumab		mab	humanized	CD4	---
Tremelimumab		mab	human	CTLA-4	cancer
Trevogrumab		mab	human	growth differentiation factor 8	muscle atrophy due to orthopedic disuse and sarcopenia
Tucotuzumab celmoleukin		mab	humanized	EpCAM	cancer
Tuvirumab		---	human	hepatitis B virus	chronic hepatitis B
Ublituximab		mab	chimeric	MS4A1	cancer
Ulocuplumab		mab	human	CXCR4 (CD184)	hematologic malignancies
Urelumab		mab	human	4-1BB (CD137)	cancer etc.
Urtoxazumab		mab	humanized	Escherichia coli	diarrhoea caused by E. coli
Ustekinumab	Stelara	mab	human	IL-12, IL-23	multiple sclerosis, psoriasis, psoriatic arthritis
Utomilumab		mab	human	4-1BB (CD137)	cancer
Vadastuximab talirine		mab	chimeric	CD33	---
Vandortuzumab vedotin		mab	humanized	STEAP1	cancer
Vantictumab		mab	human	Frizzled receptor	cancer
Vanucizumab		mab	humanized	angiopoietin 2	cancer
Vapaliximab		mab	chimeric	AOC3 (VAP-1)	---
Varlilumab		mab	human	CD27	solid tumors and hematologic malignancies
Vatelizumab		mab	humanized	ITGA2 (CD49b)	---
Vedolizumab	Entyvio	mab	humanized	integrin α4β7	Crohn's disease, ulcerative colitis
Veltuzumab		mab	humanized	CD20	non-Hodgkin's lymphoma
Vepalimomab		mab	mouse	AOC3 (VAP-1)	inflammation
Vesencumab		mab	human	NRP1	solid malignancies
Visilizumab	Nuvion	mab	humanized	CD3	Crohn's disease, ulcerative colitis
Vobarilizumab		mab	humanized	IL6R	inflammatory autoimmune diseases
Volociximab		mab	chimeric	integrin α5β1	solid tumors
Vorsetuzumab mafodotin		mab	humanized	CD70	cancer
Votumumab	HumaSPECT	mab	human	tumor antigen CTAA16.88	colorectal tumors

Xentuzumab		mab		IGF1, IGF2	---
Zalutumumab	HuMax-EGFr	mab	human	EGFR	squamous cell carcinoma of the head and neck
Zanolimumab	HuMax-CD4	mab	human	CD4	rheumatoid arthritis, psoriasis, T-cell lymphoma
Zatuximab		mab	chimeric	HER1	cancer
Ziralimumab		mab	human	CD147 (basigin)	---
Zolimomab aritox		mab	mouse	CD5	systemic lupus erythematosus, graft-versus-host disease

TABLE 5

Sponsors	**Drug code**	**Trial IDs**
Celltrion	CT-P63	NCT05017168
Exevir Bio BV	XVR011	NCT04884295
Jemincare Group	JMB2002	**ChiCTR2100042150**
Luye Pharma Group Ltd	LY-CovMab	**NA**
AbbVie	ABBV-47D11	**NCT04644120**
HiFiBiO Therapeutics	HFB30132A	**NCT04590430**
Ology Bioservices	ADM03820	**NCT04592549**
Beigene	DXP604	**NCT04669262**
Zydus Cadila	ZRC-3308	**NA**
Hengenix Biotech Inc	HLX70	**NCT04561076**
CORAT Therapeutics	COR-101	**NCT04674566**
Vir Biotechnol./	VIR-7832	**NCT04746183**
AbCellera / Eli Lilly and Company	LY-CoV1404, LY3853113	**NCT04634409**
Sorrento Therapeutics, Inc.	COVI-AMG (STI-2020)	**NCT04734860**
Beigene	DXP593	**NCT04532294; NCT04551898**
Junshi Biosciences / Eli Lilly and Company	JS016, LY3832479, LY-CoV016	**NCT04441918; NCT04441931; NCT04427501**

Mabwell (Shanghai) Bioscience Co., Ltd.	MW33	**NCT04533048; NCT04627584**
Toscana Life Sciences Sviluppo s.r.l.	MAD0004J08	**NCT04932850; NCT04952805**
Bristol-Myers Squibb, Rockefeller University	C144-LS and C-135-LS	**NCT04700163; Activ-2 study**
Sinocelltech Ltd.	SCTA01	**NCT04483375; NCT04644185**
Adagio Therapeutics	ADG20	**NCT04805671 NCT04859517**
Brii Biosciences	BRII-196	**NCT04479631; Activ-3 study**
Brii Biosciences	BRII-198	**NCT04479644; Activ-3 study**
Tychan Pte. Ltd.	TY027	**NCT04429529; NCT04649515**
AstraZeneca	AZD7442 (AZD8895 + AZD1061)	**NCT04507256; NCT04625725; NCT04625972**
Celltrion	CT-P59	**NCT04525079; NCT04593641**; **NCT04602000**
Vir Biotechnol./ GlaxoSmithKline	VIR-7831/ GSK4182136	**NCT04545060; Activ-3 study**
AbCellera / Eli Lilly and Company	LY-CoV555 (LY3819253); combination of LY-CoV555 with LY-CoV016 (LY3832479)	**NCT04411628** (Phase 1); **NCT04427501** (Phase 2); **NCT04497987** (Phase 3); **NCT04501978** (Activ-3 study); **NCT04518410** (Phase 2/3)
Regeneron	REGN-COV2 (REGN10933 + REGN10987)	**NCT04425629** (Phase 1/2); **NCT04426695** (Phase 1/2); **NCT04452318** (Phase 3)

In certain embodiments, an agent, such as an anti-inflammatory agent or bioactive lipid, is used to increase the expression level and/or duration of any the therapeutic protein (or biologically active nucleic acid molecules) expressed from the non-viral vectors in the methods herein. In work

conducted during the development of embodiments, herein, the anti-inflammatory agents (AILs) and bioactive lipids in Table 6 below were tested, and the ones in black were found to be successful agents.

TABLE 6

AILs and bioactive lipids tested

•	Docosahexaenoic Acid	(DHA)	3/10/15%
•	Eicosapentaenoic Acid	(EPA)	10/15%
•	Alpha Linolenic Acid	(ALA)	3/10/15%
•	Maresin 1	(MAR1)	3%
•	Lipoxin A4	(LA4)	2%
•	15-deoxy-12,14-Prostaglandin J2	(15d)	3%
•	Arachidonic Acid	(AA)	10/15%
•	Eicosatetraynoic Acid	(ETA)	10%
•	Docosapentaenoic Acid	(DPA)	10/15%
•	Stearidonic Acid	(SA)	10%
•	Retinoic Acid	(RA)	10%
•	Trans Retinal	(TA)	10%
•	2-Arachidonoyl Glycerol	(AG)	10%
•	Diallyl Disulfide	(DADS)	10%
•	3,3-Diindolylmethane	(DIM)	10%
•	Prostaglandin E2	(PE2)	10%
•	Oleic Acid	(OA)	5/10/15/30/50%
•	Alpha Tocopherol	(AT)	2.5%
•	Sphingosins-1-Phosphate	(S-1-P)	10%
•	Palmitoyl Sphingomyelin	(SPH)	10%

Red = Unsuccessful in Culture

EXAMPLES

In the Examples below, the dexamethasone is water-soluble dexamethasone which contains dexamethasone complexed to cyclodextrin to make it soluble. The dexamethasone palmitate is dexamethasone 21-palmitate.

EXAMPLE 1

Multiple-MAb Expression

This Example describes in vivo expression of multiple unique monoclonal antibodies following serial treatments in mice over a 4 week treatment course.

Experimental Methods: On day 0, three mice per group were given IP injections of dexamethasone (40 mg/kg) two hours prior to sequential IV injection of lipids (1000nmol DOTAP SUV with 2.5mol% dexamethasone palmitate and 1000nmol DMPC (1,2-Dimyristoyl-SN-glycero-3-phosphocholine) neutral lipid with 5mol% dexamethasone palmitate), followed two hours later

by 75mg of a single plasmid DNA (pDNA) containing 5J8 and anti-IL5 cDNAs ("5J8-IL5"). These mice were again re-treated on days 7, 14, and 21 with IP dexamethasone and IV lipid and sequential pDNA as before, however with pDNA(s) containing the following cDNAs at indicated doses: Day 7: 88mg B38-lambda anti-CoV2 "B38 Lambda", Day 14: 44mg B38-lambda anti-CoV2, and 44mg of a single pDNA containing two copies of anti-IL5 cDNA (IL5-IL5), Day 21: 44mg rituximab (aCD20 dual), and 44mg H4 anti-CoV2 ("H4"). Serum levels of mAb proteins were measured by ELISA 24 hours after each treatment and every 2-3 weeks thereafter. Group mean +/- SEM serum levels of target proteins are shown in the graph. The displayed "Days after injection" time points are all relative to the initial injection of pDNA containing 5J8 and anti-IL5 cDNAs at Day 0.

The results are shown in Figure 1, and demonstrate that serial injection of different DNA mAb vectors on a weekly basis can produce ongoing therapeutic levels of four different intact monoclonal antibodies in individual mice.

EXAMPLE 2

Multiple-MAb Expression

This Example describes in vivo expression of multiple unique monoclonal antibodies following serial treatments in mice over a 6 week treatment course.

Experimental methods: On day 0, three mice per group were given IP injections of dexamethasone (40 mg/kg) two hours prior to sequential IV injection of lipids (1000nmol DOTAP SUV with 2.5mol% dexamethasone palmitate and 1000nmol DMPC (1,2-Dimyristoyl-SN-glycero-3-phosphocholine) neutral lipid with 5mol% dexamethasone palmitate), followed two hours later by 44mg each of pDNA containing anti-IL5 and 5J8 cDNAs ("aIL5 + 5J8"). These same mice were similarly re-treated on days 7, 14, with IP dexamethasone and IV lipid and sequential pDNA as before, however with pDNA(s) containing the following cDNAs at indicated doses: Day 7: 75mg of the anti-Sars-Cov-2 monoclonal antibody B38 Kappa cDNA ("B38-Kappa"), Day 14: 44mg of a single pDNA containing two copies of rituximab cDNA ("aCD20-aCD20"), and 44mg of a single pDNA containing two copies of 5J8 ("5J8-5J8"). Serum levels of mAb proteins were measured by ELISA 24 hours one day following the second treatment (day 8) and every 1-2 weeks thereafter. Group mean +/- SEM serum levels of target proteins are shown in the graph. The indicated time points are all relative to the initial injection of pDNAs-containing anti-IL5 and 5J8 cDNAs at Day 0.

Results are shown in Figure 2, and demonstrate that serial injection of different DNA mAb vectors injected on a weekly basis can produce ongoing therapeutic levels of four different intact monoclonal antibodies in individual mice.

EXAMPLE 3

Multiple-MAb Expression

This Example describes in vivo expression of multiple unique monoclonal antibodies following serial treatments in mice over a 3 week treatment course.

Experimental methods:

With regard to Figure 3A: On day 0, 4 groups of three mice per group were given IP injections of dexamethasone (40 mg/kg) two hours prior to sequential IV injection of lipids (1000nmol DOTAP SUV with 2.5mol% dexamethasone palmitate and 1000nmol DMPC (1,2-Dimyristoyl-SN-glycero-3-phosphocholine) neutral lipid with 5mol% dexamethasone palmitate), followed two hours later by 75mg of one of four separate pDNA containing anti-Sars-Cov-2 monoclonal antibody B38 cDNA as follows: Group 1: B38-Lambda-BV3, Group 2: modSE3-2-mCMV-B38-BV3, Group 3: modSE3-2-hCMV-B38-BV3, and Group 4: B38-Kappa-BV3. Serum levels of anti-CoV2 mAb proteins were measured by ELISA 24 hours after the initial treatment, and are displayed as group mean +/- SEM.

With regard to Figure 3B: These same mice were similarly treated on days 7 and 14 with IP dexamethasone and IV lipid and sequential pDNA as before, however with pDNA(s) containing the following cDNAs at indicated doses: Day 7: 44mg anti-IL5 ("aIL5") and 44mg 5J8 ("5J8"). Day 14: 88mg rituximab ("aCD20 Dual").

Serum levels of anti-CoV2 mAb proteins were measured by ELISA 24 hours after the initial treatment and weekly thereafter. Serum levels of anti-IL5, 5J8, and rituximab were determined on days 22 and 29, and are displayed as group mean +/- SEM. The indicated time points in Figures 3A and 3B are all relative to the initial injection of pDNAs-containing anti-IL5 and 5J8 cDNAs at Day 0.

These results, shown in Figures 3A and 3B, demonstrate: A) that various configurations of pDNA expression vectors result in disparate expression levels of target proteins, and B) that serial injection of pDNA mAb vectors encoding for different mAb clones can produce significant ongoing serum levels of four different intact monoclonal antibodies in individual mice.

EXAMPLE 4

Multiple-MAb Expression

This Example describes in vivo expression of multiple unique monoclonal antibodies following serial treatments in mice over a 3 week Treatment Course.

Experimental methods: On day 0, three groups of mice each containing three mice per group, were similarly given IP injections of dexamethasone (40 mg/kg) two hours prior to sequential IV injection of lipids (1000nmol DOTAP SUV with 2.5mol% dexamethasone palmitate

and 1000nmol DMPC (1,2-Dimyristoyl-SN-glycero-3-phosphocholine) neutral lipid) with 5mol% dexamethasone palmitate, followed by the following pDNA(s) containing the following cDNAs at indicated doses: 44mg of a single pDNA containing two copies of 5J8 cDNA ("5J8-5J8"), and 44mg of a single pDNA containing two copies of anti-IL5 cDNA ("aIL5-aIL5"). These same groups of mice were treated on days 7, 14, with IP dexamethasone and IV lipid and sequential pDNA as before, however with pDNA(s) containing the following cDNAs at indicated doses: Group 1: Day 7 - 44mg of rituximab cDNA ("aCD20-dual") and 44mg of the B38 anti-SARS CoV2 cDNAs ("B38-Tag"), Day 14 - 88mg of the anti-Sars-Cov-2 monoclonal antibody ("H4"). Group 2: Day 7 - 44mg of a single pDNA containing two copies of rituximab cDNAs ("aCD20-aCD20") and 44mg of the anti-Sars-Cov-2 monoclonal antibody B38 Kappa cDNA ("B38-Kappa") cDNAs ("B38-Tag"), Day 14 - 88mg of the anti-Sars-Cov-2 monoclonal antibody H4 cDNA ("H4"). Group 3: Day 7 - 44mg of rituximab cDNA ("aCD20-dual") and 44mg of the B38 anti-SARS CoV2 cDNAs ("B38-Tag"), Day 14 – No Treatment.

Serum levels of mAb proteins were measured by ELISA on days 1, 8, and 15. The indicated time points are all relative to the initial injection of pDNAs containing 5J8 and aIL5 cDNAs. Results are shown in Figure 4, which show that serial injection of different DNA mAb vectors on a weekly basis can produce significant ongoing serum levels of four different intact monoclonal antibodies in individual mice.

EXAMPLE 5

Multiple Protein Expression

This Example describes in vivo expression of multiple unique monoclonal antibodies following serial treatments in Mice over a 3 week Treatment.

Experimental methods:

With regard to Figure 5A: On day 0, eight groups of mice, each containing three mice per group, were given IP injections of dexamethasone (40 mg/kg) two hours prior to sequential IV injection of lipids (1000nmol DOTAP SUV with 2.5mol% dexamethasone palmitate and 1000nmol DMPC (1,2-Dimyristoyl-SN-glycero-3-phosphocholine neutral lipid) with 5mol% dexamethasone palmitate, followed by the following pDNA(s) containing the following cDNAs at indicated doses: Group 1: 88mg of a single pDNA encoding rituximab, anti-IL5 and 5J8 cDNAs ("maCD20-haIL5-m5J8"); Group 2: 88mg of a single pDNA encoding the anti-SARS-Cov-2 monoclonal antibody B38 Lambda cDNA ("B38-Kappa"), rituximab, anti-IL5 and 5J8 cDNAs ("mB38Ld-maCD20-haIL5-m5J8"); Group 3: 88mg of a single pDNA encoding the anti-Sars-Cov-2 monoclonal antibody H4 cDNA ("mH4"), rituximab, anti-IL5 and 5J8 cDNAs ("mH4-

maCD20-haIL5-m5J8"); Group 4: 88mg of a single pDNA encoding the anti-Sars-Cov-2 monoclonal antibody B38 Kappa cDNA ("B38-Kappa") and anti-IL5 cDNAs ("mB38Kp-haIL5"); Group 5: 88mg of a single pDNA encoding the anti-Sars-Cov-2 monoclonal antibody B38 Kappa cDNA ("B38-Kappa") and 5J8 cDNAs ("mB38Kp-m5J8"); Group 6: 88mg of a single pDNA encoding the anti-Sars-Cov-2 monoclonal antibody B38 Lambda cDNA ("B38-Lambda") and anti-IL5 cDNAs ("mB38Ld-maIL5"); Group 7: 88mg of a single pDNA encoding the anti-Sars-Cov-2 monoclonal antibody B38 Lambda cDNA and 5J8 cDNAs ("mB38Ld-m5J8"); Group 8: 88mg of a single pDNA encoding anti-IL5 and B38 Lambda cDNAs ("maIL5-mB38Ld"). Some of these same groups of mice were re-treated on days 7 and/or day 14, with IP dexamethasone and IV lipid and sequential pDNA as before, however with pDNA(s) containing the following cDNAs at indicated doses:

Group 1: Day 7 - 44mg rituximab ("aCD20-dual") and 44mg of a single pDNA containing anti-SARS-CoV2 mAb H4, Day 14 – No Treatment. Group 2: Day 7 – No Treatment, Day 14 – No Treatment. Groups 3, 4: Day 7 - 44mg rituximab ("aCD20-dual") and 44mg of a single pDNA containing two copies of 5J8 cDNAs ("5J8-5J8"), Day 14 - 44mg human G-CSF ("GCSF") and 44mg human alpha-glactosidase A ("GLA") ("hGLA-hyFc"), Day 21 - 44mg human Ace2 ("hACE2") and 44mg human growth hormone ("hGH") ("hGH-Fc"). Groups 5: Day 7 - 44mg rituximab ("aCD20-dual") and 44mg of a single pDNA containing two copies of anti-IL5 cDNAs ("aIL5-aIL5"), Day 14 - 44mg GCSF ("GCSF") and 44mg GLA ("GLA"). Groups 6 and 8: Day 7 - 44mg rituximab ("aCD20-dual") and 44mg of a single pDNA containing two copies of 5J8 cDNAs ("5J8-5J8"), Day 14 – No Treatment. Group 7: Day 7 - 44mg rituximab ("aCD20-dual") and 44mg of a single pDNA containing two copies of anti-IL5 cDNAs ("aIL5-aIL5"), Day 14 – No Treatment. Serum levels of anti-CoV2 mAb proteins were measured by ELISA 24 hours after the initial treatment and weekly thereafter. The indicated time points are all relative to the initial injection of pDNAs. Group mean +/- SEM expression levels are indicated on the graph.

With regard to Figure 5B: Serum from treated mice in treatment group 4 (above) were measured by ELISA for expression of non-monoclonal antibody therapeutic human proteins G-CSF, GLA, GH, and ACE2 in serum at day 15 and day 22 following treatment with GCSF + GLA and ACE2 + GH containing pDNAs as indicated.

These results, shown in Figures 5A and 5B, demonstrate that serial injection of different DNA mAb vectors on a weekly basis can produce significant ongoing serum levels of a total of four different intact monoclonal antibodies and four other non-monoclonal antibody therapeutic proteins (total of eight therapeutic proteins) in individual mice.

EXAMPLE 6

Multiple-MAb Expression

This Example describes the production of three different monoclonal antibody proteins following a single treatment in Mice.

Experimental methods: On day 0, eight groups of mice, each containing three mice per group, were given IP injections of dexamethasone (40 mg/kg) two hours prior to sequential IV injection of lipids (1000nmol DOTAP SUV with 2.5mol% dexamethasone palmitate and 1000nmol DMPC (1,2-Dimyristoyl-SN-glycero-3-phosphocholine neutral lipid with 5mol% dexamethasone palmitate), followed by the following pDNA(s) containing the following cDNAs at indicated doses: Group 1: 88mg of a single pDNA encoding anti-SARS-CoV2 B38 kappa and anti-IL5 ("mB38-haIL5"); Group 2: 88mg of a single pDNA encoding anti-SARS-CoV2 B38 kappa and anti-IL5 ("mB38-maIL5"); Group 3: 88mg of a single pDNA encoding anti-SARS-CoV2 B38 lambda and anti-influenza A 5J8 ("mB38-h5J8"); Group 4: 88mg of a single pDNA encoding anti-SARS-CoV2 B38 lambda and anti-influenza A 5J8 ("mB38-m5J8"); Group 5: 44mg of a single pDNA encoding two copies of anti-IL5 ("aIL5-aIL5") and 44mg of a single pDNA encoding anti-SARS-CoV2 ("H4"); Group 6: 44mg of a single pDNA encoding three copies of anti-IL5 ("aIL5-aIL5-aIL5") and 44mg of a single pDNA encoding anti-SARS-CoV2 ("H4"); Group 7: 88mg of a single pDNA encoding anti-influenza A 5J8 and anti-IL5 ("5J8-aILH-aILL"); Group 8: 88mg of a single pDNA encoding anti-influenza A 5J8 and anti-IL5 ("5J8-aIL5"). Serum levels of expressed mAb proteins were measured by ELISA 1, 14 and 22 days after the initial treatment. Group mean +/- SEM expression levels are indicated in Figure 6.

These results, shown in Figure 6, demonstrate that one dose (e.g., using cationic and neutral lipids) of DNA-encoded mAb vectors, in the form of a single pDNA or composed of multiple pDNAs, can produce sustained expression of a two separate mAbs in mice, and that the structure and composition of the pDNA or pDNAs contribute to mAb expression levels.

EXAMPLE 7

Anti-Sars-CoV2 Protein Expression

This Example describes production of multiple different anti-SARS CoV2 therapeutic proteins separately and in combination following a single treatment in mice.

Experimental methods: On day 0, eight groups of mice, each containing three mice per group, were given IP injections of dexamethasone (40 mg/kg) two hours prior to sequential IV injection of lipids (1000nmol DOTAP SUV with 2.5mol% dexamethasone palmitate and 1000nmol DMPC (1,2-Dimyristoyl-SN-glycero-3-phosphocholine neutral lipid with 5mol% dexamethasone palmitate), followed by injection of 88mg of a single pDNA encoding the

following cDNAs: Group 1: soluble human ACE2 ("hACE2-BV3"), Group 2: two copies of soluble human ACE2 ("hACE2-hACE2"), Group 3: anti-SARS-CoV2 mAb B38 Kappa ("B38Kp"), Group 4: two copies of anti-SARS-CoV2 mAb H4 ("H4-H4"), Group 5: anti-SARS-CoV2 mAb B38 Kappa and soluble human ACE2 ("B38Kp-hACE2"), Group 6: soluble human ACE2 and anti-SARS-CoV2 mAb B38 Kappa ("hACE2-B38Kp"), Group 7: anti-SARS-CoV2 mAb H4 and soluble human ACE2 ("H4-hACE2"), Group 8: soluble human ACE2 and anti-SARS-CoV2 mAb H4 ("hACE2-H4"). Serum expression levels of anti-SARS-CoV2 mAbs were measured by an anti-RBD ELISA using recombinant purified H4 or B38 kappa as standards, or by a non-antigen-specific human IgG or human kappa light chain ELISA. Serum expression levels of soluble human ACE2 were determined by commercial ELISA. Group mean +/- SEM expression levels are indicated in Figure 7.

The results, in Figure 7, demonstrate anti-SARS-CoV2 therapeutics (either soluble human ACE2 protein and/or anti-SARS-CoV-2 mAbs reactive to SARS-CoV2 spike protein alone, or in combination) can be produced in animals following a single treatment with a single pDNA vector.

EXAMPLE 8

Anti-Sars-CoV2 Protein Expression

This Example describes production of Multiple anti-SARS CoV2 therapeutics separately and in combination following liposome and dexamethasone treatment in mice.

Experimental methods: On day 0, four groups of mice, each containing three mice per group, were given IP injections of dexamethasone (40 mg/kg) two hours prior to sequential IV injection of lipids (1000nmol DOTAP SUV with 2.5mol% dexamethasone palmitate and 1000nmol DMPC (1,2-Dimyristoyl-SN-glycero-3-phosphocholine neutral lipid with 5mol% dexamethasone palmitate), followed by injection of 88mg of a single pDNA encoding the following cDNAs: Group 1: soluble human ACE2-Fc fusion ("shACE2-Fc"), Group 2: soluble human ACE2-Fc fusion LALA variant ("shACE2-Fc-LALA") Group 3: anti-SARS-CoV2 mAb 4A8 and soluble human ACE2-Fc fusion ("4A8-shACE2-Fc"), Group 4: two copies of soluble human ACE2-Fc fusion ("shACE2-shACE2").

In Figure 8A, serum expression levels of soluble human ACE2-containing proteins were determined by a SARS-CoV2 RBD-based ELISA on days 1 and 9 following treatment. Group mean +/- SEM expression levels are indicated on the graph.

In Figure 8B, serum expression levels of soluble human ACE2-Fc fusions were determined in groups 1 thru 3 by an Fc-specific ELISA on days 1 and 9 following treatment. Group mean +/- SEM expression levels are indicated on the graph.

The results, shown in Figures 8A and 8B, demonstrate anti-SARS-CoV2 therapeutics (either soluble human ACE2 fusion protein alone, or in combination with the 4A8 mAb reactive against SARS-CoV2 spike protein, may be expressed in vivo following liposome and dexamethasone treatment with a pDNA vector.

EXAMPLE 9

ACE2 Protein Expression

This Example describes production of Human ACE2 and modified variants in mice.

Experimental methods: On day 0, twelve groups of mice, each containing three mice per group, were given IP injections of dexamethasone (40 mg/kg) two hours prior to sequential IV injection of lipids (1000nmol DOTAP SUV with 2.5mol% dexamethasone palmitate and 1000nmol DMPC (1,2-Dimyristoyl-SN-glycero-3-phosphocholine neutral lipid with 5mol% dexamethasone palmitate), followed by injection of 88mg of a single pDNA encoding human ACE2 cDNA (Group 1) or a modified version of ACE2, groups 2 thru 12, as indicated. One day later, serum expression of ACE2 was determined by ELISA using recombinant RBD protein for capture, and either an anti-Fc reagent or anti-ACE2 reagent for detection. Group mean +/- SEM expression levels are indicated in Figure 9, which shows the results.

EXAMPLE 10

Expression of Human Growth Hormone Fused to Half-Life Extending Peptide

This Example describes the in vivo expression of human growth hormone (hGH) fused to a half-life extending peptide.

Methods: Groups of 4 (red) or 3 (other groups) CD-1 mice each were injected with 40mg/kg water-soluble dexamethasone IP. Two hours later, mice were injected IV, first with liposomes followed approximately 2 minutes later with 75ug plasmid DNA encoding human GH (hGH). All liposome mixtures contained 1000nmol DOTAP SUV with 2.5% Dexamethasone 21-Palmitate as well as 1000nmol DMPC with 5% Dexamethasone 21-palmitate. Mice were bled 24 hours after injection, then weekly or every few weeks thereafter to obtain serum. Serum levels of hGH were assessed by ELISA. At day 127 after injection, serum levels of mouse IGF-1, as well as of hGH were coordinately assessed by their respective ELISAs.

The results are shown in Figure 45. Figure 45A shows this procedure drives expression of the wild type hGH cDNA fused to a protein half-life extending DNA sequence, including Fc, serum albumin or Xten, and can significantly increase serum hGH levels over time in immunocompetent mice when compared to hGH serum levels produced by a hGH DNA vector that lack protein half-life extending DNA sequences. Figure 45B shows that the cDNA-encoded

hGH protein produced is fully bioactive, as it appropriately increases the levels of the hGH-regulated, endogenous mouse, IGF-1 protein. Figure 45C shows one injection of a DNA vector in this procedure drives the wild type hGH cDNA but lacking any protein half-life extending DNA sequence can produce durable production of therapeutic hGH serum levels in immunocompetent mice. This is despite the fact that the serum half-life of the hGH protein is less than 20 minutes.

EXAMPLE 11

Expression of Human Growth Hormone Fused to Half-Life Extending Peptide

This Example describes the in vivo expression of human growth hormone (hGH) fused to a half-life extending peptide.

Methods: Groups of 4 CD-1 mice each were injected with 40mg/kg water-soluble dexamethasone IP. Two hours later, mice were injected IV, first with liposomes followed approximately 2 minutes later with 75ug plasmid DNA encoding human GH. All liposome mixtures contained 1000nmol DOTAP SUV with 2.5% Dexamethasone 21-Palmitate as well as 1000nmol DMPC with 5% Dexamethasone 21-palmitate. Mice were bled 24 hours after injection and every 7-21 days thereafter to isolate serum, and serum expression assessed by ELISA.

The results are shown in Figure 46, which demonstrate that this procedure with vectors driving the wild type hGH cDNA fused to a protein half-life extending DNA sequence, including Fc, serum albumin or Xten, can significantly increase serum hGH levels over time in immunocompetent mice when compared to hGH serum levels produced by a hGH DNA vector that lack protein half-life extending DNA sequences.

EXAMPLE 12

Expression of Human Growth Hormone with Reinjection of Plasmid

This Example describes the in vivo expression of human growth hormone (hGH) with reinjection of the plasmid.

Methods: Groups of 4 CD-1 mice each were injected with 40mg/kg water-soluble dexamethasone IP. Two hours later, mice were injected IV, first with liposomes followed approximately 2 minutes later with 75ug plasmid DNA encoding human GH. All liposome mixtures contained 1000nmol DOTAP SUV with 2.5% Dexamethasone 21-Palmitate as well as 1000nmol DMPC with 5% Dexamethasone 21-palmitate. Mice were bled weekly to assess expression. Expression for 43 days after initial injection are shown for pre-reinjection. On day 49, mice were given the same treatment as the initial injection. Mice were bled 24 hours after re-injection to isolate serum and every 7-21 days thereafter, and serum expression assessed by ELISA.

These results are shown in Figure 47 and demonstrate that, using this procedure, one re-injection of a DNA vector driving the wild type hGH cDNA into fully immunocompetent mice can significantly and durably further increase serum hGH levels produced by the initial hGH DNA vector injection.

EXAMPLE 13

Expression of Human Growth Hormone Fused to Half-Life Extending Peptide

This Example describes the in vivo expression of human growth hormone (hGH) fused to a half-life extending peptide.

Methods: Groups of 5 CD-1 mice were used. Mice were injected with 40mg/kg water-soluble dexamethasone IP. Two hours later, mice were injected IV, first with liposomes followed approximately 2 minutes later with 75ug plasmid DNA encoding human GH. All liposome mixtures contained 1000nmol DOTAP SUV with 2.5% Dexamethasone 21-Palmitate as well as 1000nmol DMPC with 5% Dexamethasone 21-palmitate. Mice were bled 24 hours after injection and every 7-28 days thereafter to isolate serum, and serum expression assessed by ELISA.

The results are shown in Figure 48. These results demonstrate that this procedure with DNA vectors driving the wild type hGH cDNA fused to an Fc protein half-life extending DNA sequence can produce serum hGH levels within the 1 to 10 ng/ml hGH therapeutic range for at least the next 225 days (>30% of a normal mouse's lifetime) after a single injection into immunocompetent mice.

EXAMPLE 14

Expression of Human Growth Hormone Fused to Half-Life Extending Peptide

This Example describes the in vivo expression of human growth hormone (hGH) fused to a half-life extending peptide.

Methods: Groups of 3 CD-1 mice each were injected with 40mg/kg water-soluble dexamethasone IP. Two hours later, mice were injected IV, first with liposomes followed approximately 2 minutes later with 75ug plasmid DNA encoding human GH. All liposome mixtures contained 1000nmol DOTAP SUV with 2.5% Dexamethasone 21-Palmitate as well as 1000nmol DMPC with 5% Dexamethasone 21-palmitate. Mice were bled 24 hours after injection and every 7-21 days thereafter to isolate serum, and serum expression assessed by ELISA.

The results are shown in Figure 49. These results demonstrate this procedure with DNA vectors driving the wild type hGH cDNA fused to an Fc protein half-life extending DNA sequence

produce fully bioactive hGH protein in mice, as the cDNA-encoded hGH protein appropriately increases the levels of the hGH-regulated, endogenous mouse, IGF-1 protein.

EXAMPLE 15

Expression of Human Growth Hormone Fused to Half-Life Extending Peptide

This Example describes the in vivo expression of human growth hormone (hGH) fused to a half-life extending peptide.

Methods: Groups of 3 CD-1 mice each were injected with 40mg/kg water-soluble dexamethasone IP. Two hours later, mice were injected IV, first with liposomes followed approximately 2 minutes later with 75ug plasmid DNA encoding human GH. All liposome mixtures contained 1000nmol DOTAP SUV with 2.5% Dexamethasone 21-Palmitate as well as 1000nmol DMPC with 5% Dexamethasone 21-palmitate. Mice were bled day 1 and day 15 after injection to isolate serum, and serum expression assessed by ELISA.

Figure 50 shows the results. Figure 50A shows that selective site-directed mutagenesis of the Fc region of an DNA vector driving the wild type hGH cDNA fused to an Fc protein half-life extending DNA sequence including CTP can selectively either increase or decrease serum hGH levels produced in immunocompetent mice. Figure 50B shows that selective site-directed mutagenesis of the Fc region of a DNA vector driving the wild type hGH cDNA fused to an Fc protein half-life extending DNA sequence can selectively increase serum hGH levels produced over time in immunocompetent mice.

EXAMPLE 16

Immuno-modulation Agents

This Example describes the testing of various immuno-modulating agents.

Part 1

Methods: Groups of 3 CD-1 mice each were injected with 900nmol DOTAP SUV, with or without Dexamethasone 21-palmitate or Cholesteryl palmitate in molar percentages as shown in Figure 51. Two minutes after liposome injection, mice were injected with 70ug plasmid DNA encoding hG-CSF. Mice were bled the following day and serum levels of hG-CSF protein was assessed by ELISA. ALT levels were assessed in sera. Results are shown in Figure 51, which shows that incorporating an optimized molar percentage of dexamethasone palmitate (DexPalm) into cationic liposomes can both further increase gene expression and further decrease toxicity.

Part 2

Methods: Groups of 3 CD-1 mice each were used. One group (+ Dex) was injected IP with 40mg/kg Dexamethasone, one group (+ DexP IP) was injected IP with 900nmol DOTAP liposomes containing 2.5 molar% Dexamethasone 21-palmitate, and one group (Protamine) was injected IP with 5mg/kg Protamine sulfate. Two hours later, mice were first injected with 900nmol DOTAP SUV, with or without Dexamethasone 21-palmitate or Cholesteryl palmitate in molar percentages as shown in Figure 52. Two minutes after liposome injection, mice were injected with 70ug plasmid DNA encoding hG-CSF. Mice were bled the following day and serum levels of hG-CSF protein was assessed by ELISA. ALT levels were assessed in sera. The results are shown in Figure 52, which show that incorporating an optimized molar percentage of dexamethasone palmitate into cationic liposomes can both further increase gene expression and further decrease toxicity.

Part 3

Methods: Groups of 3 CD-1 mice each were used. One group each was injected IP with 900nmol DOTAP liposomes containing 2.5% Dexamethasone 21-palmitate, 5 minutes before, 5 minutes after, or 30 minutes before IV injections. One group was and one group (Protamine) was injected IP with 5mg/kg Protamine sulfate 5 minutes before IV injections. For IV injections, mice were first injected with 900nmol DOTAP SUV with 2.5% Dexamethasone 21-palmitate in the liposomes. Two minutes after liposome injection, mice were injected with 70ug plasmid DNA encoding hG-CSF. Mice were bled the following day and serum levels of hG-CSF protein was assessed by ELISA. ALT levels were assessed in sera. Figure 53 shows the results, which show that pre-injecting an optimized molar percentage of dexamethasone palmitate in liposomes prior to injecting cationic liposomes can both further increase gene expression and further decrease toxicity.

Part 4

Methods: Groups of 3 CD-1 mice each were injected with 900nmol DOTAP SUV, with or without one of a number of different endogenous, anti-inflammatory lipids (AILs) in molar percentages in the liposomes as shown in Figure 54. Two minutes after liposome injection, mice were injected with 70ug plasmid DNA encoding hG-CSF. Mice were bled the following day and serum levels of hG-CSF protein was assessed by ELISA. ALT levels were assessed in sera. The results are shown in Figure 54, which shows that injecting some AILs incorporated into cationic liposomes can both further increase gene expression and further decrease toxicity (ALT levels). In

contrast, injecting selected molar percentages of other AILs incorporated into cationic liposomes can significantly increase ALT.

Part 5

Methods: Groups of 3 CD-1 mice each were injected with 900nmol DOTAP SUV, with or without one of a number of different endogenous, anti-inflammatory lipids (AILs) in molar percentages as shown in Figure 55. Two minutes after liposome injection, mice were injected with 70ug plasmid DNA encoding hG-CSF. Mice were bled the following day and serum levels of hG-CSF protein was assessed by ELISA. ALT levels were assessed in sera. The results, shown in Figure 55, show that injecting certain AILs incorporated into cationic liposomes can both further increase gene expression and further decrease toxicity (ALT levels). In contrast, injecting selected molar percentages of other AILs incorporated into cationic liposomes can significantly increase ALT.

Part 6

Methods: Groups of 3 CD-1 mice each were used. One group (+ Dex) was injected IP with 40mg/kg Dexamethasone, one group. Two hours later, mice were first injected with 900nmol DOTAP SUV, with or without 5 mole percent Dexamethasone 21-palmitate. Two minutes after liposome injection, mice were injected with either 40 or 130 ug plasmid DNA encoding hG-CSF. Mice were bled the following day and serum levels of hG-CSF protein was assessed by ELISA. ALT levels were assessed in sera. The results are shown in Figure 56, and show that incorporating an optimized molar percentage of dexamethasone palmitate into cationic liposomes can further increase peak levels of gene expression following an otherwise ineffective hG-CSF-DNA dose.

EXAMPLE 17

Intranasal Administration and Immunomodulation

This Example describes targeting hematopoietic cells in mouse lungs following Intranasal administration of liposomes.

Experimental Methods: Mice were anesthetized and administered via intranasal route 200nmol of the indicated liposome formulations each containing 1mol% fluorescent phosphatidyl-ethanolamine to track uptake of liposomes or lactated ringers control. One day later, lungs were harvested, digested to single cell suspensions and surface stained with fluorescent antibodies to detect mouse CD45, CD11b and F4/80 markers prior to analysis by flow cytometry. DOPS = 1,2-dioleoyl-sn-glycero-3-phospho-L-serine, mixPS = 1-stearoyl-2-oleoyl-sn-glycero-3-phospho-L-serine. The results are shown in Figure 57, which shows that by selectively modifying the lipid

composition of liposomes administered intranasally, that these liposomes can be selectively targeted to intrapulmonary monocytes and macrophages to different extents, thus selectively immune-modulating the lung.

EXAMPLE 18

Differential T Cell Activation

This Example describes differential T cell activation resulting from administration of particular liposome formulations.

Experimental Methods: On day 0, six groups of mice, each containing three mice per group, were given the following treatments:

Group 1 - IP injection of dexamethasone (40 mg/kg) two hours prior to sequential IV injection of lipids (1000nmol DOTAP SUV with 2.5mol% dexamethasone palmitate and 1000nmol DMPC (1,2-Dimyristoyl-SN-glycero-3-phosphocholine neutral lipid) with 5mol% dexamethasone palmitate), followed by a single pDNA encoding anti-SARS CoV2 H4 kappa mAb, anti-CD20, anti-influenza A 5J8, and anti-human IL-5.

Group 2 – Sequential IV injection of lipids (1000nmol DOTAP SUV with 2.5mol% dexamethasone palmitate and 1000nmol DMPC (1,2-Dimyristoyl-SN-glycero-3-phosphocholine neutral lipid) with 5mol% dexamethasone palmitate), followed by a single pDNA encoding anti-SARS CoV2 H4 kappa mAb, anti-CD20, anti-influenza A 5J8, and anti-human IL-5.

Group 3 – Sequential IV injection of lipids (1000nmol DOTAP SUV and 1000nmol DMPC (1,2-Dimyristoyl-SN-glycero-3-phosphocholine neutral lipid) with 5mol% dexamethasone palmitate), followed by a single pDNA encoding anti-SARS CoV2 H4 kappa mAb, anti-CD20, anti-influenza A 5J8, and anti-human IL-5.

Group 4 – Sequential IV injection of lipids (1000nmol DOTAP SUV with 2.5mol% dexamethasone palmitate and 1000nmol DMPC (1,2-Dimyristoyl-SN-glycero-3-phosphocholine neutral lipid), followed by a single pDNA encoding anti-SARS CoV2 H4 kappa mAb, anti-CD20, anti-influenza A 5J8, and anti-human IL-5.

Group 5 – Sequential IV injection of lipids (1000nmol DOTAP SUV with 2.5mol% dexamethasone palmitate and 1000nmol DMPC (1,2-Dimyristoyl-SN-glycero-3-phosphocholine neutral lipid) with 5mol% dexamethasone palmitate), followed by a single pDNA encoding anti-SARS CoV2 H4 kappa mAb, anti-CD20, anti-influenza A 5J8, and anti-human IL-5.

Group 6 – No Treatment

Figure 58 shows the results and shows that by selectively modifying a parenteral aqueous soluble predose, and/or the molar percentage of dexamethasone palmitate incorporated into

subsequently administered liposomes, that the level of T lymphocyte activation both in lung and in the blood can be selectively immuno-modulated.

EXAMPLE 19

Differential T Cell Activation

This Example describes differential T cell activation resulting from administration of liposome formulations.

Experimental Methods: On day 0, eight groups of mice, each containing three mice per group, were treated as follows:

Group 1 – Untreated

Group 2 - IP injection of dexamethasone (40 mg/kg) two hours prior to sequential IV injection of lipids (1000nmol DOTAP SUV with 2.5mol% dexamethasone palmitate and 1000nmol DMPC (1,2-Dimyristoyl-SN-glycero-3-phosphocholine neutral lipid) with 5mol% dexamethasone palmitate), followed by a single pDNA encoding human PECAM-1.

Group 3 - IP injections of dexamethasone (40 mg/kg) two hours prior to sequential IV injection of lipids (1000nmol DOTAP:cholesterol (85:15) SUV with 2.5mol% dexamethasone palmitate and 1000nmol DMPC (1,2-Dimyristoyl-SN-glycero-3-phosphocholine neutral lipid) with 5mol% dexamethasone palmitate), followed by a single pDNA encoding human PECAM-1.

Group 4 - IP injections of dexamethasone (40 mg/kg) two hours prior to sequential IV injection of lipids (1000nmol DOTAP:DODAP (1:1) SUV with 2.5mol% dexamethasone palmitate and 1000nmol DMPC (1,2-Dimyristoyl-SN-glycero-3-phosphocholine neutral lipid) with 5mol% dexamethasone palmitate), followed by a single pDNA encoding human PECAM-1.

Group 5 - IP injections of dexamethasone (40 mg/kg) two hours prior to sequential IV injection of lipids (1000nmol DOTAP SUV with 2.5mol% dexamethasone palmitate and 1000nmol DMPC (1,2-Dimyristoyl-SN-glycero-3-phosphocholine neutral lipid):cholesterol (1:1) with 5mol% dexamethasone palmitate), followed by a single pDNA encoding human PECAM-1.

Group 6 – Two IP injections of dexamethasone (40 mg/kg) two hours prior and just prior to sequential IV injection of lipids (1000nmol DOTAP SUV with 2.5mol% dexamethasone palmitate and 1000nmol DMPC (1,2-Dimyristoyl-SN-glycero-3-phosphocholine neutral lipid):cholesterol (1:1) with 5mol% dexamethasone palmitate), followed by a single pDNA encoding human PECAM-1.

Group 7 – Two IP injections of 2.5mol% dexamethasone palmitate in phosphatidylserine:cholesterol 2:1 MLV 24 hours and two hours prior to sequential IV injection of lipids (1000nmol DOTAP SUV with 2.5mol% dexamethasone palmitate and 1000nmol DMPC

(1,2-Dimyristoyl-SN-glycero-3-phosphocholine neutral lipid) with 5mol% dexamethasone palmitate), followed by a single pDNA encoding human PECAM-1.

Group 8 – Two IP injections of 2.5mol% dexamethasone palmitate in DOTAP:cholesterol 2:1 MLV 24 hours and two hours prior to sequential IV injection of lipids (1000nmol DOTAP SUV with 2.5mol% dexamethasone palmitate and 1000nmol DMPC (1,2-Dimyristoyl-SN-glycero-3-phosphocholine neutral lipid) with 5mol% dexamethasone palmitate), followed by a single pDNA encoding human PECAM-1.

One day later, lungs and peripheral blood were harvested, digested to single cell suspensions if necessary, and surface stained with fluorescent antibodies to detect mouse CD4, CD8 alpha, CD44, CD69, and human PECAM-1 markers prior to analysis by flow cytometry.

Figure 59 shows the results, which show that by selectively modifying a parenteral aqueous soluble pre-dose, and/or the molar percentage of dexamethasone palmitate incorporated into subsequently administered liposomes, that the level of T lymphocyte activation both in lung and in the blood can be selectively immuno-modulated.

EXAMPLE 20

Anti-TNFa and Heparinoid Agents

This Example describes the use of anti-TNFa monoclonal antibodies and Heparinoid Agents for increasing expressing in in vivo expression methods.

PART 1 - anti-TNFa Monoclonal antibody

Methods: Groups of 3 mice were used. One group was given 100ug each anti-TNFa monoclonal antibody per mouse IP, 2 hours prior to IV injections. Mice were then injected IV with 900nmol DOTAP SUV, followed 2 minutes later by either 70ug or 130ug plasmid DNA encoding hG-CSF. Mice were bled 24 hours after injection, and hG-CSF expression in the sera assessed by ELISA. Serum ALT/AST levels were measured.

Results are shown in Figure 60, which shows that pre-administration of an anti-inflammatory agent, here anti-TNF monoclonal antibody, can both further increase gene expression while further reducing its toxicity.

PART 2 - NSH

Methods: Groups of 3 mice were used. Except for the control group, mice were given NSH (N-Acetyl-De-O-Sulfated Heparin) IP at .25 or 1mg per mouse either 2 hours pre or 2 hours post lipid and DNA injection. Mice were then injected IV with 900nmol DOTAP SUV, followed 2

minutes later by 70ug plasmid DNA encoding hG-CSF. Mice were bled 24 hours after injection, and hG-CSF expression in the sera assessed by ELISA. Serum ALT/AST levels were measured.

Results are shown in Figure 61, which shows that either pre- or post-administration of a NSH can reduce toxicity.

PART 3 - NSH

Methods: Groups of 3 mice were used. Heparinoid-treated mice were given NSH (N-Acetyl-De-O-Sulfated Heparin) IP at .25 or 1mg per mouse either 2 hours pre or 2 hours post lipid and DNA injection. Mice were then injected IV with 900nmol DOTAP SUV, followed 2 minutes later by 70ug plasmid DNA encoding hG-CSF. Mice were bled 24 hours after injection, and hG-CSF expression in the sera assessed by ELISA. Tocopherol-treated mice were given 900nmol DOTAP SUV containing alpha-tocopherol, followed by 70ug plasmid DNA encoding hG-CSF. Serum ALT/AST levels were measured.

The results are shown in Figure 62, which show that either pre- or post-administration of a NSH can reduce toxicity.

PART 4 - NSH

Methods: Groups of 3 mice were used. Heparinoid-treated mice were given NSH (N-Acetyl-De-O-Sulfated Heparin) IP 2 hours prior to lipid and DNA injection. Mice were then injected IV with 900nmol DOTAP SUV, followed 2 minutes later by 70ug plasmid DNA encoding hG-CSF. Mice were bled 24 hours after injection, and hG-CSF expression in the sera assessed by ELISA. Tocopherol mice were given 900nmol DOTAP SUV containing alpha-tocopherol, followed by 70ug plasmid DNA encoding hG-CSF. Serum ALT/AST levels were measured.

Figure 63 shows the results which show that either pre-administration of NSH can both further increase gene expression while further reducing its toxicity.

EXAMPLE 21

Immunomodulation following Liposome Administration

This example describes immunomodulation of the lymphocyte and monocyte cell populations in mice following administration of various liposome formulations containing dexamethasone and/or dexamethasone palmitate.

Experimental Methods: Groups of 2-3 CD-1 mice were used. On day 0, eight groups of mice, were given the following treatments:

Group 1 - IP injection of water-soluble dexamethasone (40 mg/kg) only.

Group 2 - IP injection of dexamethasone (40 mg/kg) two hours prior to IV injection of lipids (1000nmol DOTAP SUV with 2.5mol% dexamethasone palmitate and 1000nmol DMPC (1,2-Dimyristoyl-SN-glycero-3-phosphocholine neutral lipid) with 5mol% dexamethasone palmitate).

Group 3 - IV injection of lipids (1000nmol DOTAP SUV with 2.5mol% dexamethasone palmitate and 1000nmol DMPC (1,2-Dimyristoyl-SN-glycero-3-phosphocholine neutral lipid) with 5mol% dexamethasone palmitate).

Group 4 - IP injection of 1000nmol DMPC (1,2-Dimyristoyl-SN-glycero-3-phosphocholine neutral lipid) with 5mol% dexamethasone palmitate) MLV two hours prior to IV injection of lipids (1000nmol DOTAP SUV with 2.5mol% dexamethasone palmitate and 1000nmol DMPC (1,2-Dimyristoyl-SN-glycero-3-phosphocholine neutral lipid) MLV with 5mol% dexamethasone palmitate.

Group 5 - IP injection of 1000nmol DMPC (1,2-Dimyristoyl-SN-glycero-3-phosphocholine neutral lipid) with 5mol% dexamethasone palmitate) SUV two hours prior to IV injection of lipids (1000nmol DOTAP SUV with 2.5mol% dexamethasone palmitate and 1000nmol DMPC (1,2-Dimyristoyl-SN-glycero-3-phosphocholine neutral lipid) MLV with 5mol% dexamethasone palmitate.

Group 6 - IP injection of 1000nmol DMPC (1,2-Dimyristoyl-SN-glycero-3-phosphocholine neutral lipid) with 5mol% dexamethasone palmitate) MLV two hours prior to IV injection of lipids (1000nmol DOTAP SUV with 2.5mol% dexamethasone palmitate and 1000nmol DMPC (1,2-Dimyristoyl-SN-glycero-3-phosphocholine neutral lipid) MLV with 5mol% dexamethasone palmitate containing MTAS-NLS-SPD peptide.

Group 7 - IP injection of 1000nmol DMPC (1,2-Dimyristoyl-SN-glycero-3-phosphocholine neutral lipid) with 5mol% dexamethasone palmitate) SUV two hours prior to IV injection of lipids (1000nmol DOTAP SUV with 2.5mol% dexamethasone palmitate and 1000nmol DMPC (1,2-Dimyristoyl-SN-glycero-3-phosphocholine neutral lipid) MLV with 5mol% dexamethasone palmitate containing MTAS-NLS-SPD peptide.

Group 8 – No treatment.

Twenty four hours following liposome treatment, peripheral blood was harvested in EDTA containing microtainer tubes and analyzed by CBC apparatus. Group mean values +/- SEM are displayed. Figure 64 shows that administration of various formulations of liposomes containing dexamethasone palmitate decreases lymphocyte counts in blood compared to systemic administration of dexamethasone alone. Figure 65 shows that administration of various formulations of liposomes containing dexamethasone palmitate decreases monocyte counts in blood compared to systemic administration of dexamethasone alone.

EXAMPLE 22

Production of ongoing fully SARS-CoV-2 neutralizing levels of a single anti-SARS-CoV2 mAb following a single HEDGES DNA vector administration

This example describes expression of single SARS-CoV-2 antibodies in mice produces fully neutralizing levels of mAb using the following injection protocol. The five different SARS-CoV-2 antibodies individually expressed in mice were: C135, C215, COV2-2355, CV07-209, and C121 (see Table 7 for sequence information). At day 0, groups of mice were pretreated with 40mg/kg water-soluble dexamethasone i.p. two hours prior to dosing i.v. with liposomes composing 1100nmol each of DOTAP / 2.5mol% dexamethasone palmitate / SUV and DMPC / 5mol% dexamethasone palmitate / MLV. After two minutes, mice were dosed i.v. with about 80ug of a single plasmid DNA containing one expression cassette for one of the five SARS-CoV2-specific mAbs. Mice were bled at days 1, 8, 22, 30, 36, 50, 78, 92, 106, and 120 after treatment and serum mAb protein levels were determined by a human IgG ELISA assay. Results are shown in Figure 66 (left axis, pink bar graphs represent mean + or – SEM shown in ascending order from day 1 to day 120 for each mAb). The functional bioactivity of SARS-CoV2-specific mAb containing sera to inhibit SARS-CoV2 spike – human ACE2 protein interactions was determined by a commercially-available in vitro SARS-CoV2 spike / ACE2 blocking assay (cPASS, right axis, green dots represent mean + or – SEM shown in ascending order from day 1 to day 120 for each mAb clone, Genscript).

This example demonstrates, as shown in Figure 66, that one injection of different single DNA expression plasmids each encoding one of five different SARS-CoV2-specific mAb produces fully neutralizing serum levels of each SARS-CoV2-specific mAb for the full experimental course of at least 120 days following administration, and that these ongoing serum mAb levels functionally and continuously block SARS-CoV2 spike – human ACE2 binding for at least 120 days (which is the human equivalent of greater than 20 years). These results demonstrate that this protocol, which includes a DNA injection encoding a single SARS-CoV2-specific mAb, can produce durable (greater than 20 human years equivalence) of neutralizing anti-SARS-CoV2 serum levels.

EXAMPLE 23

Expression of two anti-SARS-CoV2 mAb from a Single Plasmid

This example describes expression of two SARS-CoV-2 antibodies from a single plasmid (4 different plasmids) in mice produces neutralizing levels of mAb using the following injection protocol. The expressed SARS-CoV-2 antibodies were as follows: first plasmid (C135 + CV07-209); second plasmid (RBD215 LALA + CV07-209); third plasmid (C121 + CV07-209); and

fourth plasmid (CV07-209 + Zost-2355) (see Table 7 for sequence information). At day 0, groups of mice were pretreated with 40mg/kg water-soluble dexamethasone i.p. two hours prior to dosing i.v. with liposomes composing 1100nmol each of DOTAP / 2.5mol% dexamethasone palmitate / SUV and DMPC / 5mol% dexamethasone palmitate / MLV. After two minutes, mice were dosed i.v. with about 80ug of a single plasmid DNA containing two expression cassettes for SARS-CoV2-specific mAbs. Mice were bled at days 1, 8, 22, 30, 36, 50, 78, 92, 106, 120, and 134 after treatment and serum mAb protein levels were determined by a human IgG ELISA assay. The results are shown in Figure 67 (left axis, pink bar graphs represent mean + or – SEM shown in ascending order from day 1 to day 134 for each mAb). The functional bioactivity capacity of SARS-CoV2-specific mAb containing sera to inhibit SARS-CoV2 spike – human ACE2 protein interactions was determined by a commercially-available in vitro SARS-CoV2 spike / ACE2 blocking assay (cPASS, right axis, green dots represent mean + or – SEM shown in ascending order from day 1 to day 134 for each mAb clone, Genscript).

This example demonstrates, as shown in Figure 67, that this procedure with a single injection of a single expression plasmid results in expression of two SARS-CoV2-specific mAbs from a single plasmid for the course of at least 134 days following this procedure, and that these serum-expressed mAbs sera are functionally capable of blocking SARS-CoV2 spike – human ACE2 interactions for at least 134 days.

EXAMPLE 24

Expression of Two anti-SARS-CoV2 mAbs by three approaches

This example describes expression of two anti-SARS-CoV2 mAbs simultaneously by three different approaches: 1) Single injection of a single expression plasmid coding two unique mAbs; 2) Single injection of two unique plasmids simultaneously as a mixture (co-injection); and 3) Two injections of single mAb expression plasmids separated by an amount of time, here 7 days (reinj). The various anti-SARS-CoV2 mAbs expressed are shown in Figure 68 (see Table 7 for sequences).

On day 0, groups of mice were pretreated with 40mg/kg water-soluble dexamethasone i.p. two hours prior to dosing i.v. with liposomes composing 1000nmol each of DOTAP / 2.5mol% dexamethasone palmitate / SUV and DMPC / 5mol% dexamethasone palmitate / MLV. After two minutes, mice were dosed i.v. with either 75ug of a single plasmid DNA containing one or two expression cassettes for SARS-CoV2-specific mAbs, or 38ug each of two plasmids each containing cassettes for one or two mAb clones (co-inject – "coinj"). On day 7, some of these groups of mice underwent an additional injection (re-injection – "reinj") of dexamethasone retreatment, liposomes dosing, and plasmid DNA as on day 0, and were similarly treated with

either 75ug of a single plasmid DNA containing two expression cassettes for SARS-CoV2-specific mAbs. Mice were bled at day 1, 8, and 15, 22 and serum expression of mAbs was analyzed by a human IgG ELISA assay. Results are shown in Figure 68a, where each series of bar graphs indicates mean +/- SEM mAb expression or inhibition amount at days 1, 8, 15, and 22 in order from left to right.

Figure 68b shows the functional capacity of the SARS-CoV2-specific mAb containing sera to inhibit SARS-CoV2 spike – human ACE2 protein interactions determined by a commercially-available in vitro SARS-CoV2 spike / ACE2 blocking assay (cPASS, Genscript).
Each series of bar graphs indicates mean +/- SEM mAb expression or inhibition amount at days 1, 8, 15, and 22 in order from left to right.

This examples shows (results in Figure 68) how this protocol produces two anti-SARS-CoV2 mAbs simultaneously by the three approaches tried. All approaches successfully allow for the expression of two mAbs in serum of animals at levels that allow for neutralization of SARS-CoV2 / ACE2 interactions.

EXAMPLE 25

Expression of three anti-SARS-CoV2 mAbs

This example describes expression of three different anti-SARS-CoV2 mAbs from one or two plasmids based on two weekly injections of the plasmids. This was performed with three different collections of mAbs, as shown in Figure 69 (sequences in Table 7).

At day 0, groups of mice were pretreated with 40mg/kg water-soluble dexamethasone i.p. two hours prior to dosing i.v. with liposomes composing 1000nmol each of DOTAP / 2.5mol% dexamethasone palmitate / SUV and DMPC / 5mol% dexamethasone palmitate / MLV. After two minutes, mice were dosed i.v. with 80ug of a single plasmid DNA containing one expression cassette for SARS-CoV2-specific mAbs. On day 7, these groups of mice underwent an additional injection of dexamethasone pretreatment, liposomes dosing, and plasmid DNA as on day 0. These groups were treated with 80ug of a single plasmid DNA containing two expression cassettes for SARS-CoV2-specific mAbs.

Mice were bled at days 1, 8, 15, 21, 36, 50, 64, 78, 92, 106, 120 following their first treatment, and serum expression levels of mAbs were analyzed by a human IgG ELISA assay. The results are shown in Figure 69, where each series of bar graphs indicates mean +/- SEM mAb expression (left y-axis) at days 1, 8, 15, 21, 36, 50, 64, 78, 92, 106, 120 in order from left to right. In parallel, functional capacities of SARS-CoV2-specific mAb containing sera to inhibit SARS-CoV2 spike – human ACE2 protein interactions were determined by a commercially-available in vitro SARS-CoV2 spike / ACE2 blocking assay across the timecourse (cPASS, Genscript). These

inhibition results are shown in figure 69 in green. Each series of bar graphs indicates mean +/- SEM mAb inhibition (right y-axis) at days 1, 8, 15, 21, 36, 50, 78, 92, 106, 120.

These examples demonstrate that two weekly injections of one or two DNA expression plasmids encoding a total of three different individual SARS-CoV2-specific mAbs produces fully neutralizing serum levels of three different SARS-CoV2-specific mAbs for the course of at least 70 days following administration, and that these ongoing serum mAbs levels functionally and continuously block SARS-CoV2 spike – human ACE2 for at least 70 days, which is the human equivalent of greater than 10 years. These results indicate that two weekly hedges DNA injections encoding three different SARS-CoV2-specific mAbs produce durable (greater than 10 human years equivalence) fully neutralizing anti-SARS-CoV2 mAb serum levels.

EXAMPLE 26

Expression of four anti-SARS-CoV2 mAbs

This example describes expression of four (4) anti-SARS-CoV2 mAbs shown in Figure 70 (see Table 7 for sequence information) using the following protocol. At day 0, groups of mice were pretreated with 40mg/kg water-soluble dexamethasone i.p. two hours prior to dosing i.v. with liposomes composing 1000nmol each of DOTAP / 2.5mol% dexamethasone palmitate / SUV and DMPC / 5mol% dexamethasone palmitate / MLV. After two minutes, mice were dosed i.v. with 40ug each of two plasmids each containing two mAb expression cassettes.

Mice were bled at days 1, 8, 15, 21, 36, 50, 64, 78, 92 and 106 following their first treatment, and serum expression levels of mAbs were analyzed by a human IgG ELISA assay. Results are shown in Figure 70, where each series of bar graphs indicates mean +/- SEM mAb expression (left y-axis) at days 1, 8, 15, 21, 36, 50, 64, 78, 92, and 106 in order from left to right. In parallel, functional capacities of SARS-CoV2-specific mAb containing sera to inhibit SARS-CoV2 spike – human ACE2 protein interactions were determined by a commercially-available in vitro SARS-CoV2 spike / ACE2 blocking assay across the timecourse (cPASS, Genscript). Each series of bar graphs indicates mean +/- SEM mAb inhibition (right y-axis) at days 1, 8, 15, 21, 36, 50, 78, 92 and 106.

EXAMPLE 27

Expression of four anti-SARS-CoV2 mAbs with one injection

This example describes expression of four anti-SARS-CoV2 mAbs shown in Figure 71 (see Table 7 for sequence information) using the following protocol. At day 0, groups of mice were pretreated with 40mg/kg water-soluble dexamethasone i.p. two hours prior to dosing i.v. with liposomes composing 1000nmol each of DOTAP / 2.5mol% dexamethasone palmitate / SUV and

DMPC / 5mol% dexamethasone palmitate / MLV. After two minutes, mice were dosed i.v. with 40ug each of two plasmids each containing two mAb expression cassettes.

Mice were bled at days 1, 8, 15, 21, 36, 50, 64, 78, and 92 following their first treatment, and serum expression levels of SARS-CoV2 mAbs were analyzed by a human IgG ELISA assay. Results are shown in Figure 71, where each series of bar graphs indicates mean +/- SEM mAb expression (left y-axis) at days 1, 8, 15, 21, 36, 50, 64, 78, and 92 in order from left to right. In parallel, functional capacities of SARS-CoV2-specific mAb containing sera to inhibit SARS-CoV2 spike – human ACE2 protein interactions were determined by a commercially-available in vitro SARS-CoV2 spike / ACE2 blocking assay across the timecourse (cPASS, Genscript). Each series of bar graphs (in green in Figure 71) indicates mean +/- SEM mAb inhibition (right y-axis) at days 1, 8, 15, 21, 36, 50, 64, 78 and 92 in order from left to right.

EXAMPLE 28

Expression of four anti-SARS-CoV2 mAbs

This example describes expression of four anti-SARS-CoV2 mAbs shown in Figure 72 (see Table 7 for sequence information) using the following protocol. At day 0, groups of mice were pretreated with 40mg/kg water-soluble dexamethasone i.p. two hours prior to dosing i.v. with liposomes composing 1000nmol each of DOTAP / 2.5mol% dexamethasone palmitate / SUV and DMPC / 5mol% dexamethasone palmitate / MLV. After two minutes, mice were dosed i.v. with 45ug each of two plasmids each containing two mAb expression cassettes.

Mice were bled at days 1, 8, 22, 36, 50, 64, 78, 99 following their first treatment, and serum expression levels of mAbs were analyzed by a human IgG ELISA assay. Results are shown in Figure 72, where each series of bar graphs indicates mean +/- SEM mAb expression (left y-axis) at days 1, 8, 22, 36, 50, 64, 78, 99 in order from left to right. In parallel, functional capacities of SARS-CoV2-specific mAb containing sera to inhibit SARS-CoV2 spike – human ACE2 protein interactions were determined by a commercially-available in vitro SARS-CoV2 spike / ACE2 blocking assay across the timecourse (cPASS, Genscript). These results are shown in green, where each series of bar graphs indicates mean +/- SEM mAb inhibition (right y-axis) at days 1, 8, 22, 36, 50, 64, 78, 99.

These examples demonstrate that a single co-injection of two different single DNA expression plasmids each encoding two different individual SARS-CoV2-specific mAbs (together the co-injection produces a total of four different individual SARS-CoV2-specific mAbs) produces fully neutralizing serum levels of four different SARS-CoV2-specific mAbs for at least 90 days following administration, and that these ongoing serum mAb levels functionally and continuously

blocked SARS-CoV2 spike – human ACE2 binding for at least 90 days, which is the human equivalent of greater than 15 years.

EXAMPLE 29

Expression of four anti-SARS-CoV2 mAbs with two injections

This example describes expression of four anti-SARS-CoV2 mAbs shown in Figure 73 (see Table 7 for sequence information) using the following protocol. At day 0, groups of mice were pretreated with 40mg/kg water-soluble dexamethasone i.p. two hours prior to dosing i.v. with liposomes composing 1000nmol each of DOTAP / 2.5mol% dexamethasone palmitate / SUV and DMPC / 5mol% dexamethasone palmitate / MLV. After two minutes, mice were dosed i.v. with 80ug of a single plasmid DNA containing two expression cassettes for SARS-CoV2-specific mAbs.

On day 7, mice underwent an additional injection of dexamethasone pretreatment, liposomes dosing, and plasmid DNA as on day 0 (indicated by hashed bar). Mice were treated with 80ug of a single plasmid DNA containing two expression cassettes for SARS-CoV2-specific mAbs.

Mice were bled at days 1, 8, 15, 21, 36, 50, 64, 78, 92, 106, 120 following their first treatment, and serum expression levels of mAbs were analyzed by a human IgG ELISA assay. Results are shown in Figure 73, where each series of bar graphs indicates mean +/- SEM mAb expression (left y-axis) at days 1, 8, 15, 21, 36, 50, 64, 78, 92, 106, 120 in order from left to right. In parallel, functional capacities of SARS-CoV2-specific mAb containing sera to inhibit SARS-CoV2 spike – human ACE2 protein interactions were determined by a commercially-available in vitro SARS-CoV2 spike / ACE2 blocking assay across the timecourse (cPASS, Genscript). Each series of bar graphs (in green in Figure 73) indicates mean +/- SEM mAb inhibition (right y-axis) at days 1, 8, 15, 21, 36, 50, 78, 92, 106, 120.

EXAMPLE 30

Expression of four anti-SARS-CoV2 mAbs with two injections

This example describes expression of four anti-SARS-CoV2 mAbs shown in Figure 74 (see Table 7 for sequence information) using the following protocol. At day 0, groups of mice were pretreated with 40mg/kg water-soluble dexamethasone i.p. two hours prior to dosing i.v. with liposomes composing 1000nmol each of DOTAP / 2.5mol% dexamethasone palmitate / SUV and DMPC / 5mol% dexamethasone palmitate / MLV. After two minutes, mice were dosed i.v. with 80ug of a single plasmid DNA containing two expression cassettes for SARS-CoV2-specific mAbs.

On day 7, some of these groups of mice underwent a second round of injection of dexamethasone pretreatment, liposomes dosing, and plasmid DNA as on day 0 (indicated by dot fill pattern). These groups were treated with 40ug each of two plasmids each containing two mAb expression cassettes. Mice were bled at days 1, 8, 15, 21, 36, 50, 64, 78, and 92 following their first treatment, and serum expression levels of SARS-CoV2 mAbs were analyzed by a human IgG ELISA assay. Results are shown in Figure 74, where each series of bar graphs indicates mean +/- SEM mAb expression (left y-axis) at days 1, 8, 15, 21, 36, 50, 64, 78, and 92 in order from left to right. In parallel, functional capacities of SARS-CoV2-specific mAb containing sera to inhibit SARS-CoV2 spike – human ACE2 protein interactions were determined by a commercially-available in vitro SARS-CoV2 spike / ACE2 blocking assay across the timecourse (cPASS, Genscript). Each series of bar graphs (in green) indicates mean +/- SEM mAb inhibition (right y-axis) at days 1, 8, 15, 21, 36, 50, 64, 78 and 92 in order from left to right.

These examples demonstrate that serial, weekly co-injection of two different single DNA expression plasmids each encoding two different individual SARS-CoV2-specific mAbs (together the serial co-injection produces a total of four different individual SARS-CoV2-specific mAbs) produce fully neutralizing serum levels of four different SARS-CoV2-specific mAbs for the course of at least 70 days following administration, and that these ongoing serum mAb levels functionally and continuously blocked SARS-CoV2 spike – human ACE2 binding for at least 70 days, which is the human equivalent of greater than 10 years.

EXAMPLE 31

Expression of five anti-SARS-CoV2 mAbs with two injections

This example describes expression of five anti-SARS-CoV2 mAbs shown in Figure 75 (see Table 7 for sequence information) using the following protocol. At day 0, groups of mice were pretreated with 40mg/kg water-soluble dexamethasone i.p. two hours prior to dosing i.v. with liposomes composing 1000nmol each of DOTAP / 2.5mol% dexamethasone palmitate / SUV and DMPC / 5mol% dexamethasone palmitate / MLV. After two minutes, mice were dosed i.v. with either 80ug of a single plasmid DNA containing one expression cassette for SARS-CoV2-specific mAbs.

On day 7, these groups of mice underwent an additional injection of dexamethasone pretreatment, liposomes dosing, and plasmid DNA as on day 0. Some groups were treated with 40ug each of two plasmids each containing two mAb expression cassettes.

Mice were bled at days 1, 8, 15, 21, 36, 50, 64, 78, 92, 106, 120 following their first treatment, and serum expression levels of mAbs were analyzed by a human IgG ELISA assay. Results are shown in Figure 75, where each series of bar graphs indicates mean +/- SEM mAb

expression (left y-axis) at days 1, 8, 15, 21, 36, 50, 64, 78, 92, 106, 120 in order from left to right. In parallel, functional capacities of SARS-CoV2-specific mAb containing sera to inhibit SARS-CoV2 spike – human ACE2 protein interactions were determined by a commercially-available in vitro SARS-CoV2 spike / ACE2 blocking assay across the timecourse (cPASS, Genscript). Each series of bar graphs (shown in green in Figure 75) indicates mean +/- SEM mAb inhibition (right y-axis) at days 1, 8, 15, 21, 36, 50, 78, 92, 106, 120.

EXAMPLE 32

Expression of six anti-SARS-CoV2 mAbs with single injection

This example describes expression of six anti-SARS-CoV2 mAbs shown in Figure 76 (see Table 7 for sequence information) using the following protocol. At day 0, groups of mice were pretreated with 40mg/kg water-soluble dexamethasone i.p. two hours prior to dosing i.v. with liposomes composing 1000nmol each of DOTAP / 2.5mol% dexamethasone palmitate / SUV and DMPC / 5mol% dexamethasone palmitate / MLV. After two minutes, mice were dosed i.v. with 30ug each of three plasmids each containing two mAb expression cassettes.

Mice were bled at days 1, 8, 22, 36, 50, 64, 78, 99 following their first treatment, and serum expression levels of mAbs were analyzed by a human IgG ELISA assay. Results are shown in Figure 76, where each series of bar graphs indicates mean +/- SEM mAb expression (left y-axis) at days 1, 8, 22, 36, 50, 64, 78, 99 in order from left to right. In parallel, functional capacities of SARS-CoV2-specific mAb containing sera to inhibit SARS-CoV2 spike – human ACE2 protein interactions were determined by a commercially-available in vitro SARS-CoV2 spike / ACE2 blocking assay across the time course (cPASS, Genscript). Each series of bar graphs (in green in Figure 76) indicates mean +/- SEM mAb inhibition (right y-axis) at days 1, 8, 22, 36, 50, 64, 78, 99.

EXAMPLE 33

Expression of six anti-SARS-CoV2 mAbs with two injections

This example describes expression of six anti-SARS-CoV2 mAbs shown in Figure 77 (see Table 7 for sequence information) using the following protocol. At day 0, groups of mice were pretreated with 40mg/kg water-soluble dexamethasone i.p. two hours prior to dosing i.v. with liposomes composing 1000nmol each of DOTAP / 2.5mol% dexamethasone palmitate / SUV and DMPC / 5mol% dexamethasone palmitate / MLV. After two minutes, mice were dosed i.v. with either 80ug of a single plasmid DNA containing two expression cassettes for SARS-CoV2-specific mAbs, or 40ug each of two plasmids each containing one or two mAb expression cassettes.

On day 7, these groups of mice underwent an additional injection of dexamethasone pretreatment, liposomes dosing, and plasmid DNA as on day 0. These groups were treated with either 80ug of a single plasmid DNA containing two expression cassettes for SARS-CoV2-specific mAbs, or 40ug each of two plasmids each containing two mAb expression cassettes.

Mice were bled at days 1, 8, 15, 21, 36, 50, 64, 78, 92, 106, 120 following their first treatment, and serum expression levels of mAbs were analyzed by a human IgG ELISA assay. Results are shown in Figure 77, where each series of bar graphs indicates mean +/- SEM mAb expression (left y-axis) at days 1, 8, 15, 21, 36, 50, 64, 78, 92, 106, 120 in order from left to right. In parallel, functional capacities of SARS-CoV2-specific mAb containing sera to inhibit SARS-CoV2 spike – human ACE2 protein interactions were determined by a commercially-available in vitro SARS-CoV2 spike / ACE2 blocking assay across the time course (cPASS, Genscript). Each series of bar graphs (in green in Figure 77) indicates mean +/- SEM mAb inhibition (right y-axis) at days 1, 8, 15, 21, 36, 50, 78, 92, 106, 120.

EXAMPLE 34

Expression of six anti-SARS-CoV2 mAbs 2 or 3 injections

This example describes expression of six anti-SARS-CoV2 mAbs shown in Figure 78 (see Table 7 for sequence information) using the following protocol. At day 0, groups of mice were pretreated with 40mg/kg water-soluble dexamethasone i.p. two hours prior to dosing i.v. with liposomes composing 1000nmol each of DOTAP / 2.5mol% dexamethasone palmitate / SUV and DMPC / 5mol% dexamethasone palmitate / MLV. After two minutes, mice were dosed i.v. with either 80ug of a single plasmid DNA containing two expression cassettes for SARS-CoV2-specific mAb, or 40ug each of two plasmids each containing one or two mAb expression cassettes.

On day 7, these groups of mice underwent a second round of injection of dexamethasone pretreatment, liposomes dosing, and plasmid DNA as on day 0 (indicated by dot fill pattern). These groups were treated 40ug each of two plasmids each containing two mAb expression cassettes.

On day 14, some of these groups of mice underwent a third round of injection of dexamethasone pretreatment, liposomes dosing, and plasmid DNA as on day 0. These groups were treated with 80ug of a single plasmid DNA containing two expression cassettes for SARS-CoV2-specific mAb.

Mice were bled at days 1, 8, 15, 21, 36, 50, 64, 78, and 92 following their first treatment, and serum expression levels of SARS-CoV2 mAbs were analyzed by a human IgG ELISA assay. Results are shown in Figure 78, where each series of bar graphs indicates mean +/- SEM mAb expression (left y-axis) at days 1, 8, 15, 21, 36, 50, 64, 78, and 92 in order from left to right.

In parallel, functional capacities of SARS-CoV2-specific mAb containing sera to inhibit SARS-CoV2 spike – human ACE2 protein interactions were determined by a commercially-available in vitro SARS-CoV2 spike / ACE2 blocking assay across the timecourse (cPASS, Genscript). Each series of bar graphs (in green in Figure 78) indicates mean +/- SEM mAb inhibition (right y-axis) at days 1, 8, 15, 21, 36, 50, 64, 78 and 92 in order from left to right.

These examples demonstrate that serial co-injection of three different single DNA expression plasmids each encoding two different individual SARS-CoV2-specific mAbs (together the serial injections produce a total of six different individual SARS-CoV2-specific mAbs) each produce fully neutralizing serum levels of six different SARS-CoV2-specific mAbs for the course of at least 90 days following administration, and that these ongoing serum mAbs levels produced functionally block SARS-CoV2 spike – human ACE2 binding and that these functionally and continuously blocked SARS-CoV2 spike – human ACE2 binding for at least 90 days, which is the human equivalent of greater than 15 years.

EXAMPLE 35

Expression of eight anti-SARS-CoV2 mAbs with two injections

This example describes expression of eight anti-SARS-CoV2 mAbs shown in Figure 79 (see Table 7 for sequence information) using the following protocol. At day 0, groups of mice were pretreated with 40mg/kg water-soluble dexamethasone i.p. two hours prior to dosing i.v. with liposomes composing 1000nmol each of DOTAP / 2.5mol% dexamethasone palmitate / SUV and DMPC / 5mol% dexamethasone palmitate / MLV. After two minutes, mice were dosed i.v. with 40ug each of two plasmids each containing two mAb expression cassettes.

On day 7, mice underwent an additional injection of dexamethasone pretreatment, liposome dosing, and plasmid DNA as on day 0. Mice were treated with 40ug each of two plasmids each containing two mAb expression cassettes.

Mice were bled at days 1, 8, 15, 21, 36, 50, 64, 78, 92, 106, 120 following their first treatment, and serum expression levels of mAbs were analyzed by a human IgG ELISA assay. Results are shown in Figure 79, where each series of bar graphs indicates mean +/- SEM mAb expression (left y-axis) at days 1, 8, 15, 21, 36, 50, 64, 78, 92, 106, 120 in order from left to right. In parallel, functional capacities of SARS-CoV2-specific mAb containing sera to inhibit SARS-CoV2 spike – human ACE2 protein interactions were determined by a commercially-available in vitro SARS-CoV2 spike / ACE2 blocking assay across the time course (cPASS, Genscript). Each series of bar graphs (green in Figure 79) indicates mean +/- SEM mAb inhibition (right y-axis) at days 1, 8, 15, 21, 36, 50, 78, 92, 106, 120.

EXAMPLE 36

Expression of eight anti-SARS-CoV2 mAbs with two injections

This example describes expression of eight anti-SARS-CoV2 mAbs shown in Figure 80 (see Table 7 for sequence information) using the following protocol. At day 0, groups of mice were pretreated with 40mg/kg water-soluble dexamethasone i.p. two hours prior to dosing i.v. with liposomes composing 1000nmol each of DOTAP / 2.5mol% dexamethasone palmitate / SUV and DMPC / 5mol% dexamethasone palmitate / MLV. After two minutes, mice were dosed i.v. with 40ug each of two plasmids each containing two mAb expression cassettes.

On day 7, mice underwent a second round of injection of dexamethasone pretreatment, liposomes dosing, and plasmid DNA as on day 0. These mice were treated with 40ug each of two plasmids each containing two mAb expression cassettes.

Mice were bled at days 1, 8, 15, 21, 36, 50, 64, 78, and 92 following their first treatment, and serum expression levels of SARS-CoV2 mAbs were analyzed by a human IgG ELISA assay. Results are shown in Figure 80, where each series of bar graphs indicates mean +/- SEM mAb expression (left y-axis) at days 1, 8, 15, 21, 36, 50, 64, 78, and 92 in order from left to right. In parallel, functional capacities of SARS-CoV2-specific mAb containing sera to inhibit SARS-CoV2 spike – human ACE2 protein interactions were determined by a commercially-available in vitro SARS-CoV2 spike / ACE2 blocking assay across the time course (cPASS, Genscript). Each series of bar graphs (shown in green in Figure 80) indicates mean +/- SEM mAb inhibition (right y-axis) at days 1, 8, 15, 21, 36, 50, 64, 78 and 92 in order from left to right.

EXAMPLE 37

Expression of eight anti-SARS-CoV2 mAbs with three injections

This example describes expression of eight anti-SARS-CoV2 mAbs shown in Figure 81 (see Table 7 for sequence information) using the following protocol. At day 0, groups of mice were pretreated with 40mg/kg water-soluble dexamethasone i.p. two hours prior to dosing i.v. with liposomes composing 1000nmol each of DOTAP / 2.5mol% dexamethasone palmitate / SUV and DMPC / 5mol% dexamethasone palmitate / MLV. After two minutes, mice were dosed i.v. with 40ug each of two plasmids each containing two mAb expression cassettes.

On day 7, mice underwent a second round of injection of dexamethasone pretreatment, liposomes dosing, and plasmid DNA as on day 0. These groups were treated with 80ug of a single plasmid DNA containing two expression cassettes for SARS-CoV2-specific mAbs.

On day 14, mice underwent a third round of injection of dexamethasone pretreatment, liposomes dosing, and plasmid DNA as on day 0 (indicated by hashed bar). These groups were treated with 80ug each of a single plasmid containing two mAb expression cassettes.

Mice were bled at days 1, 8, 15, 21, 36, 50, 64, 78, and 92 following their first treatment, and serum expression levels of SARS-CoV2 mAbs were analyzed by a human IgG ELISA assay. Results are shown in Figure 81, where each series of bar graphs indicates mean +/- SEM mAb expression (left y-axis) at days 1, 8, 15, 21, 36, 50, 64, 78, and 92 in order from left to right. In parallel, functional capacities of SARS-CoV2-specific mAb containing sera to inhibit SARS-CoV2 spike – human ACE2 protein interactions were determined by a commercially-available in vitro SARS-CoV2 spike / ACE2 blocking assay across the time course (cPASS, Genscript). Each series of bar graphs (green in Figure 81) indicates mean +/- SEM mAb inhibition (right y-axis) at days 1, 8, 15, 21, 36, 50, 64, 78 and 92 in order from left to right.

EXAMPLE 38

Expression of eight anti-SARS-CoV2 mAbs

This example describes expression of eight anti-SARS-CoV2 mAbs shown in Figure 82 (see Table 7 for sequence information) using the following protocol. At day 0, groups of mice were pretreated with 40mg/kg water-soluble dexamethasone i.p. two hours prior to dosing i.v. with liposomes composing 1000nmol each of DOTAP / 2.5mol% dexamethasone palmitate / SUV and DMPC / 5mol% dexamethasone palmitate / MLV. After two minutes, mice were dosed i.v. with 40ug each of two plasmids each containing one or two mAb expression cassettes.

On day 7, these groups of mice underwent a second round of injection of dexamethasone pretreatment, liposomes dosing, and plasmid DNA as on day 0. These groups were treated with either 80ug of a single plasmid DNA containing two expression cassettes for SARS-CoV2-specific mAb, or 40ug each of two plasmids each containing two mAb expression cassettes.

On day 14, some of these groups of mice underwent a third round of injection of dexamethasone pretreatment, liposomes dosing, and plasmid DNA as on day 0 (indicated by hashed bar). These groups were treated with 80ug of a single plasmid DNA containing two expression cassettes for SARS-CoV2-specific mAbs.

Mice were bled at days 1, 8, 15, 21, 36, 50, 64, 78, and 92 following their first treatment, and serum expression levels of SARS-CoV2 mAbs were analyzed by a human IgG ELISA assay. Results are shown in Figure 82, where each series of bar graphs indicates mean +/- SEM mAb expression (left y-axis) at days 1, 8, 15, 21, 36, 50, 64, 78, and 92 in order from left to right. In parallel, functional capacities of SARS-CoV2-specific mAb containing sera to inhibit SARS-CoV2 spike – human ACE2 protein interactions were determined by a commercially-available in vitro SARS-CoV2 spike / ACE2 blocking assay across the time course (cPASS, Genscript). Each series of bar graphs (green in Figure 82) indicates mean +/- SEM mAb inhibition (right y-axis) at days 1, 8, 15, 21, 36, 50, 64, 78 and 92 in order from left to right.

EXAMPLE 39

Expression of 10 anti-SARS-CoV2 mAbs with other protein and mAbs

This example describes expression of ten anti-SARS-CoV2 mAbs shown in Figure 83 (see Table 7 for sequence information), and other proteins and mAbs, using the following protocol. At day 0, groups of mice were pretreated with 40mg/kg water-soluble dexamethasone i.p. two hours prior to dosing i.v. with liposomes composing 1000nmol each of DOTAP / 2.5mol% dexamethasone palmitate / SUV and DMPC / 5mol% dexamethasone palmitate / MLV. After two minutes, mice were dosed i.v. with 40ug each of two plasmids each containing one or two mAb expression cassettes.

On day 7, these groups of mice underwent a second round of injection of dexamethasone pretreatment, liposomes dosing, and plasmid DNA as on day 0 (indicated by dot fill pattern). These groups were treated with 40ug each of two plasmids each containing two mAb expression cassettes.

On day 14, these groups of mice underwent a third round of injection of dexamethasone pretreatment, liposomes dosing, and plasmid DNA as on day 0. These groups were treated with 80ug of a single plasmid DNA containing two expression cassettes for SARS-CoV2-specific mAb clones.

On day 21, some of these groups of mice underwent a fourth round of injection of dexamethasone pretreatment, liposomes dosing, and plasmid DNA as on day 0. These groups were treated with 80ug of a single plasmid DNA containing two expression cassettes for non-SARS-CoV2-related proteins. These non-SARS-CoV2-related proteins included mepoluzimab (aIL5), and anti-influenza A hemagglutinin H1 (5J8).

Mice were bled at days 1, 8, 15, 21, 36, 50, 64, 78, and 92 following their first treatment, and serum expression levels of SARS-CoV2 mAbs were analyzed by a human IgG ELISA assay. Results are shown in Figure 83, where each series of bar graphs indicates mean +/- SEM mAb expression (left y-axis) at days 1, 8, 15, 21, 36, 50, 64, 78, and 92 in order from left to right. In parallel, functional capacities of SARS-CoV2-specific mAb containing sera to inhibit SARS-CoV2 spike – human ACE2 protein interactions were determined by a commercially-available in vitro SARS-CoV2 spike / ACE2 blocking assay across the time course (cPASS, Genscript). Each series of bar graphs (green in Figure 83) indicates mean +/- SEM mAb inhibition (right y-axis) at days 1, 8, 15, 21, 36, 50, 64, 78 and 92 in order from left to right.

EXAMPLE 40

Expression of 11 anti-SARS-CoV2 mAbs with other protein and mAbs

This example describes expression of eleven anti-SARS-CoV2 mAbs shown in Figure 84 (see Table 7 for sequence information), and other proteins and mAbs, using the following protocol. At day 0, groups of mice were pretreated with 40mg/kg water-soluble dexamethasone i.p. two hours prior to dosing i.v. with liposomes composing 1000nmol each of DOTAP / 2.5mol% dexamethasone palmitate / SUV and DMPC / 5mol% dexamethasone palmitate / MLV. After two minutes, mice were dosed i.v. with 40ug each of two plasmids each containing two mAb expression cassettes.

On day 7, these groups of mice underwent a second round of injection of dexamethasone pretreatment, liposomes dosing, and plasmid DNA as on day 0. These groups were treated with 40ug each of two plasmids each containing two mAb expression cassettes.

On day 14, these groups of mice underwent a third round of injection of dexamethasone pretreatment, liposomes dosing, and plasmid DNA as on day 0. These groups were treated with 40ug each of two plasmids each containing two mAb expression cassettes.

On day 21, these groups of mice underwent a fourth round of injection of dexamethasone pretreatment, liposomes dosing, and plasmid DNA as on day 0. These groups were treated with either 80ug of a single plasmid DNA containing two or more expression cassettes for non-SARS-CoV2-related proteins, 40ug each of two plasmids each containing two non-SARS-CoV2-related proteins, or 25ug each of three plasmids each containing two non-SARS-CoV2-specific protein expression cassettes. These non-SARS-CoV2-related proteins included human growth hormone (GH), galactosidase alpha (GLA), G-CSF, and mAbs rituximab (aCD20), mepoluzimab (aIL5), and anti-influenza A hemagglutinin H1 (5J8).

Mice were bled at days 1, 8, 15, 21, 36, 50, 64, 78, and 92 following their first treatment, and serum expression levels of SARS-CoV2 mAbs were analyzed by a human IgG ELISA assay. Results are shown in Figure 84, where each series of bar graphs indicates mean +/- SEM mAb expression (left y-axis) at days 1, 8, 15, 21, 36, 50, 64, 78, and 92 in order from left to right. In parallel, functional capacities of SARS-CoV2-specific mAb containing sera to inhibit SARS-CoV2 spike – human ACE2 protein interactions were determined by a commercially-available in vitro SARS-CoV2 spike / ACE2 blocking assay across the time course (cPASS, Genscript). Each series of bar graphs (green in Figure 84) indicates mean +/- SEM mAb inhibition (right y-axis) at days 1, 8, 15, 21, 36, 50, 64, 78 and 92 in order from left to right.

These examples demonstrate that serial co-injection of up to six different single DNA expression plasmids, each plasmid encoding two different individual SARS-CoV2-specific mAbs (together the serial injections produce a total of up to 11 different individual SARS-CoV2-specific

mAbs) produce neutralizing serum levels of up to 11 different SARS-CoV2-specific mAbs for the course of at least 90 days following administration, and that these ongoing serum mAbs levels functionally and continuously blocked SARS-CoV2 spike – human ACE2 binding for at least 90 days, which is the human equivalent of greater than 15 years.

EXAMPLE 41

Expression of 10 anti-SARS-CoV2 mAbs with other protein and mAbs

This example describes expression of ten anti-SARS-CoV-2 mAbs shown in Figure 85 (see Table 7 for sequence information), and other non-Sars-CoV-2 mAbs, using the following protocol. At day 0, groups of mice were pretreated with 40mg/kg water-soluble dexamethasone i.p. two hours prior to dosing i.v. with liposomes composing 1000nmol each of DOTAP / 2.5mol% dexamethasone palmitate / SUV and DMPC / 5mol% dexamethasone palmitate / MLV. After two minutes, mice were dosed i.v. with 40ug each of two plasmids each containing two mAb expression cassettes.

On day 7, mice underwent a second round of injection of dexamethasone pretreatment, liposomes dosing, and plasmid DNA as on day 0 (indicated by dot fill pattern). Mice were treated with 40ug each of two plasmids each containing two mAb expression cassettes.

On day 14, mice underwent a third round of injection of dexamethasone pretreatment, liposomes dosing, and plasmid DNA as on day 0 (indicated by hashed bar). These mice were treated with 80ug of a single plasmid DNA containing two expression cassettes for SARS-CoV2-specific mAbs.

On day 21, mice underwent a fourth round of injection of dexamethasone pretreatment, liposomes dosing, and plasmid DNA as on day 0. These groups were treated with 80ug of a single plasmid DNA containing two expression cassettes for non-SARS-CoV2-related proteins. These non-SARS-CoV2-related proteins included mepoluzimab biosimilar (aIL5), and anti-influenza A hemagglutinin H1 (5J8).

Mice were bled at days 1, 8, 15, 21, 36, 50, 64, 78, and 92 following their first treatment, and serum expression levels of SARS-CoV2 mAbs were analyzed by a human IgG ELISA assay. Results are shown in Figure 85, where each series of bar graphs indicates mean +/- SEM mAb expression (left y-axis) at days 1, 8, 15, 21, 36, 50, 64, 78, and 92 in order from left to right. In parallel, functional capacities of SARS-CoV2-specific mAb containing sera to inhibit SARS-CoV2 spike – human ACE2 protein interactions were determined by a commercially-available in vitro SARS-CoV2 spike / ACE2 blocking assay across the time course (cPASS, Genscript). Each series of bar graphs indicates (green in Figure 85) mean +/- SEM mAb inhibition (right y-axis) at days 1, 8, 15, 21, 36, 50, 64, 78 and 92 in order from left to right.

This example demonstrates that serial co-injection of a total of 6 different single DNA expression plasmids, 5 of which encode two different individual SARS-CoV2-specific mAbs and the sixth encodes the heavy and light chains cDNAs of mAb 5J8, which is directed against the 1918 pandemic influenza virus. Together these serial injections produced neutralizing levels of a total of 10 different individual SARS-CoV2-specific serum mAb proteins together with one 1918 pandemic influenza specific serum mAb protein. These injections produced neutralizing serum levels of all 10 different SARS-CoV2-specific mAbs as well as neutralizing serum levels of the 1918 pandemic influenza-specific mAbs for the course of at least 90 days following administration, and that these ongoing SARS-CoV2-specific mAbs serum levels functionally and continuously blocked SARS-CoV2 spike – human ACE2 binding. In addition, hedges produced anti-pandemic influenza A mAb 5J8 serum levels neutralized the Cal/09 pandemic influenza virus strain for at least 90 days, which is the human equivalent of greater than 15 years. This means that a total of four serial DNA vector administrations can neutralize both the SARS-CoV-2 virus as well as a pandemic influenza virus for decades thereafter.

EXAMPLE 42

SARS-CoV2 Inhibition by 14 hours post-treatment.

This example describes inhibition of SARS-CoV2 by 14 hours post-treatment with the anti-SARS-CoV-2 mAbs shown in Figure 86 (see Table 7 for sequence information). At day 0, groups of mice were pretreated with 40mg/kg water-soluble dexamethasone i.p. two hours prior to dosing i.v. with liposomes composing 1000nmol each of DOTAP / 2.5mol% dexamethasone palmitate / SUV and DMPC / 5mol% dexamethasone palmitate / MLV. After two minutes, mice were dosed i.v. with 80ug of a single plasmid DNA containing one or two expression cassettes for SARS-CoV2-specific mAbs clones.

Mice were bled at 1, 4, 8, 14, 18, 20, 24, and 48 hours following treatment with plasmid DNA, and serum expression levels of mAbs were analyzed by a human IgG ELISA assay. Results are shown in Figure 86A, where each series of bar graphs indicates mean +/- SEM mAb expression at the indicated times (hr). In parallel, functional capacities of SARS-CoV2-specific mAb containing sera to inhibit SARS-CoV2 spike – human ACE2 protein interactions were determined by a commercially-available in vitro SARS-CoV2 spike / ACE2 blocking assay across the time course (cPASS, Genscript). Results are shown in Figure 86B, where each series of bar graphs indicates mean +/- SEM mAb inhibition at the indicted time in hours following treatment.

This example uses assaying a time course of the ability of anti-SARS-CoV-2 mAb serum levels produced over time between one and 24 hours after a single anti-SARS-CoV-2 DNA vector administration encoding either one or two anti-SARS-CoV-2 mAb heavy and light chain cDNAs

to functionally block SARS-CoV2 spike – human ACE2 binding. The results demonstrate that SARS-CoV2 spike – human ACE2 binding is efficiently blocked within 8 hours of one IV hedges DNA vector injection encoding either one or two anti-SARS-CoV-2 mAbs. In contrast, neutralizing protection following two different anti-SARS-CoV-2 vaccine administration generally requires five weeks.

EXAMPLE 43

Simultaneous expression of multiple different mAb and genes

This example describes the simultaneous expression of six different mAb and genes using a single injection. Four mice per group were injected IP with 40mg/kg water-soluble dexamethasone. Two hours later, mice were injected i.v. with cationic liposomes containing 2.5% dexamethasone 21-palmitate, at doses shown in Figure 87, as well as 1000nmol DMPC liposomes containing 5% dex palmitate. Two minutes following the first i.v. injection, mice were injected with 25 ug each, 30ug each, or 34ug each of three DNA plasmids: one encoding anti-IL5 and 5J8, one encoding hGH and hGCSF, and one encoding an anti-SARS-CoV2 and GLA. Mice were bled the following day and sera analyzed for expression of target genes. Expression results are shown in Figure 87. This example demonstrates that a single co-injection of three different DNA vectors, each vector encoding either two or three different human genes, produces significant serum levels of all six different human proteins.

EXAMPLE 44

Controlled Gene Expression with Various Eukaryotic Promoters

This example describes the use of various eukaryotic promoters to express a target gene (human growth hormone). At day 0, groups of mice were pretreated with 40mg/kg water-soluble dexamethasone i.p. two hours prior to dosing i.v. with liposomes composing 1100nmol ea of DOTAP / 2.5mol% dexamethasone palmitate / SUV and DMPC / 5mol% dexamethasone palmitate / MLV. After two minutes, mice were dosed i.v. with 75ug of various single plasmid DNA construct each containing an expression cassette for human growth hormone-Fc fusion driven by the promoters of heterologous genes, shown in Figure 88. Mice were bled at days 1, 8, 22, 29, 43, 50, 84 and 120 after treatment and serum mAb protein levels were determined by a human IgG ELISA assay. Bar graphs shown for each promoter in Figure 88 are in ascending order from day 1 to day 120 for each. Mean hGH-FC expression and SEM are displayed.

This data shows that selected changes in the identity and composition of the DNA vector promoter element within the DNA vector expression cassette allows for longitudinal control over

the magnitude of protein expression and bioactivity without the use of gene switches or any other additional modification.

EXAMPLE 45

Testing of 11 Different hGLA DNA Vectors

This example describes simultaneously testing 11 different hGLA DNA vectors, showing that they produce a spectrum of serum levels over time. This allowed, for example to identify vectors that maintain hGLA levels in the 1-19 ng/ml range. On day 0, groups of mice were pretreated with 40mg/kg water-soluble dexamethasone IP two hours prior to i.v. injection. Liposome injection i.v. contained 1000nmol each of DOTAP SUV with 2.5mol% dexamethasone 21-palmitate and DMPC MLV with 5mol% dexamethasone palmitate / MLV. Two minutes later, 75ug DNA was injected i.v., with constructs encoding GLA as shown in Figure 89. Mice were bled the following day and every 7 or 14 days thereafter and sera assessed for hGLA protein production. Results are shown in Figure 89.

EXAMPLE 46

Fc-Modified Protein Expression

Figure 89a shows that multiple different FC modified human GLA cDNA-encoded hedges DNA vectors produce therapeutic serum hGLA levels (>1ng/ml) at day one after administration. However by day eight (Figure 89b), only the HyFc, and particularly the Hy-Fc 1xL-containing the hGLA DNA vectors remain within the GLA therapeutic range. All other 9, Fc modified DNA vectors have dropped below therapeutic levels by day eight. These results show that optimizing the Fc portion of Fc hybrid DNA vectors can greatly improve serum half-life of modified Fc containing DNA vectors.

Figure 90 demonstrates that this Fc modifications is of clinical importance, as the use of this hyFc hGLA containing DNA vector significantly increases hGLA tissue levels in heart 104 days after a single hedges DNA vector administration. Heart is one of the most damaged target organs in GLA deficient Fabry's patients. For this example that Fc-modified GLA can be expressed in heart tissue at therapeutic levels 104 days after injection of vector: on day 0, groups of mice were pretreated with 40mg/kg water-soluble dexamethasone IP two hours prior to i.v. injection. Liposome injection i.v. contained 1000nmol each of DOTAP SUV with 2.5mol% dexamethasone 21-palmitate and DMPC MLV with 5mol% dexamethasone 21-palmitate. Two minutes later, 75ug DNA was injected i.v., with constructs encoding GLA-Fc with point mutations as shown in Figure 91. Mice were sacrificed at day 104 after injection. Hearts were perfused with PBS and then removed to lysis buffer on ice. Hearts were sonicated and protein quantified by Lowry. 50ug total

protein was loaded into wells and GLA measured by ELISA. Heart tissue expression levels are shown in Figure 92.

EXAMPLE 47

Various Fc protein mutations affect expression

This example compares the expression of various mutated Fc regions (shown in Figure 91) for GLA-Fc expression. On day 0, groups of mice were pretreated with 40mg/kg water-soluble dexamethasone IP two hours prior to i.v. injection. Liposome injection i.v. contained 1000nmol each of DOTAP SUV with 2.5mol% dexamethasone 21-palmitate and DMPC MLV with 5mol% dexamethasone 21-palmitate. Two minutes later, 75ug DNA was injected i.v., with constructs encoding GLA with point mutations as shown in Figure 91. Mice were bled the following day and every 7 or 14 days thereafter and sera assessed for hGLA protein production. Figure 91 demonstrates that targeted single or several DNA base modification of the HyFC-1xL-hGLA DNA vector via site directed mutagenesis allows precisely targeted single base modification of hybrid Fc DNA vector encoded protein function.

EXAMPLE 48

Use of Low Dose of Dexamethasone

This example describes the use of low dose dexamethasone pretreatment does not interfere with the durability of protein expression (and acute expression may be augmented). On day 0, groups of 25gram mice were pretreated with the indicated amounts (in Figure 92) of water-soluble dexamethasone IP two hours prior to i.v. injection. Liposome injection i.v. contained 1000nmol each of DOTAP SUV with 2.5mol% dexamethasone 21-palmitate and DMPC MLV with 5mol% dexamethasone 21-palmitate. Two minutes later, 75ug of rituximab-biosimilar expression DNA plasmid was injected i.v. Mice were bled the following day and at day 8, 15, and 22. Serum expression of rituximab-biosimilar were determined by commercial ELISA, and shown as mean +/- SEM. Results are shown in Figure 92, which shows that free dexamethasone, when pre-dosed in the range of 1 to 40mg/kg dose, each maintains IV DNA vectors already high level, long term protein production, as well as their ability to limit critical toxicity markers at or closely approximating background control levels. In addition, a number of the lowest free dexamethasone doses statistically significantly increased rituximab serum protein levels at day 1 following i.v. treatment.

TABLE 7

Name	Ab or Nb	Binds to	Doesn't Bind to	Neutralising Vs	Not Neutralising Vs	Protein + Epitope	Origin	SEQ ID NO.:	VH or VHH	SEQ ID NO.:	VL	Heavy V Gene	Heavy J Gene	Light V Gene	Light J Gene	SEQ ID NO.:	CDRH3	SEQ ID NO.:	CDRL3	Sources
0304-2F8	Ab	SARS-CoV2 (weak)			SARS-CoV2	S; Unk	B-cells; SARS-CoV2 Human Patient	63	EVQLVQSGAEVSQPGESLKISCKGSGYSF TGYWISWVRQMPGKGLEWMGIIYPGD SDTKYTPSFQGQVTISTDKSINTAYLQWS SLKASDTAMYYCARRGDGLYYYGMDV WGQGTTVTVSS	1145	EIVMTQSHTLLPVTPGEPASITCRSSQS LLHSNGYNYLDWYLQKPGQSPQLLIYL GSNRASGVPDRFSGSGSGTDFTLKISR VEAEDVGVYYCMQALQTPQTFGQGT KVDIK	IGHV5-51 (Human)	IGHJ6 (Human)	IGKV2-28 (Human)	IGKJ3 (Human)	2057	ARRGDGLYYY GMDV	3266	MQALQTP QT	Xiangyang Chi et al., 2020 (https://science.sciencemag.org/content/early/2020/06/19/science.abc6952/tab-pdf)
0304-3H3	Ab	SARS-CoV2		SARS-CoV2		S; S2	B-cells; SARS-CoV2 Human Patient	64	EVQLVESGPGLVKPSETLSLTCTASGGSI STYYWSWIRQPPGKGLEWIGYIYYSGST NYNPSLKSRVTISVDTSKNQFSLKLSSVTA ADTAVYYCARDRIAPVGKFFGWYFDLW GRGTLVTVSS	1146	DIVMTQSPATLSVSPEERATLSCRASQ SVSSNLAWYQQKPGQAPRLLIYGAST RATGIPARFSGSGSGTEFTLTISSLQSE DFAVYYCQQYNKWPPWTFGQGTKV DIK	IGHV4-59 (Human)	IGHJ2 (Human)	IGKV3-15 (Human)	IGKJ1 (Human)	2058	ARDRIAPVGK FFGWYFDL	3267	QQYNKWP PWT	Xiangyang Chi et al., 2020 (https://science.sciencemag.org/content/early/2020/06/19/science.abc6952/tab-pdf)
0304-4A10	Ab	SARS-CoV2			SARS-CoV2	S; S2	B-cells; SARS-CoV2 Human Patient	65	EVQLVESGGGLVQPGGSLRLSCAASGFT FSTYAMHWVRQAPGKGLEYVSGISSNG GSTYYANSVKGRFTISRDNSKNTLYIQM GSLRAEDMAVYYCARSSSRGFDYWGQ GTLVTVSS	1147	EIVLTQSPDSLAVSLGERATINCRSSQS VLYSSNNKNYLAWYQQKPGQPPKVLI YWASTRESGVPDRFSGSGSGTDFTLTI SSLQAEDVAVYYCQQYYSSPYAFGPGT KVDIK	IGHV3-64 (Human)	IGHJ4 (Human)	IGKV4-1 (Human)	IGKJ3 (Human)	2059	ARSSSRGFDY	3268	QQYYSSPY A	Xiangyang Chi et al., 2020 (https://science.sciencemag.org/content/early/2020/06/19/science.abc6952/tab-pdf)
0304-4A2	Ab	SARS-CoV2			SARS-CoV2	S; S1 (non-RBD)	B-cells; SARS-CoV2 Human Patient	66	EVQLVESGPGLVKPSETLSLTCAVSGDST SSSSSYWDWIRQPPGKGLEWIGNIYYTG TTYYNPSLKSRVTISVDTSKDQFSLKLSSV TAADTAVYYCARELFTAVAGKGGIDYW GQGTLVTVSS	1148	EIVLTQSPDSLAVSLGERATINCKSSQS VLYSSNNKNYLAWYQQKPGQPPKLLI YWASTRESGVPDRFSGSGSGTDFTLTI SSLQAEDVAVYYCHQYYNTPRTFGQG TKVEIK	IGHV4-39 (Human)	IGHJ4 (Human)	IGKV4-1 (Human)	IGKJ1 (Human)	2060	ARELFTAVAG KGGIDY	3269	HQYYNTPR T	Xiangyang Chi et al., 2020 (https://science.sciencemag.org/content/early/2020/06/19/science.abc6952/tab-pdf)
0317-A1	Ab	SARS-CoV2			SARS-CoV2	S; S2	B-cells; SARS-CoV2 Human Patient	67	QVQLVQSGGGVVQPGRSLRLSCAAPGF TFSSYGMHWVRQAPGKGLEWVAVISY DGSNKYYADSVKGRFTISRDNSKNTLYL QMNSLRAEDTAVYYCAKDFKGGSSSWY TPEIEYGMDVWGQGTTVTVSS	1149	DIVMTQSPATLSLSPGERATLSCRASQ SVSSYLAWYQQKPGQAPRLLIYDASN RATGIPARFSGSGSGADFTLTISSLEPE DFAVYYCRQRSNWPPTFGGGTKVDIK	IGHV3-30 (Human)	IGHJ6 (Human)	IGKV3-11 (Human)	IGKJ3 (Human)	2061	AKDFKGGSSS WYTPEIEYG MDV	3270	RQRSNWP PT	Xiangyang Chi et al., 2020 (https://science.sciencemag.org/content/early/2020/06/19/science.abc6952/tab-pdf)
0317-A2	Ab	SARS-CoV2			SARS-CoV2	S; S2	B-cells; SARS-CoV2 Human Patient	68	QVQLVQSGSELKKPGASVKVSCKASGYT FTSYAMNWVRQAPGQGLEWMGWINT NTGNPTYAQGFTGRFVFSLDTSVSTAYL QISSLKAEDTAVYYCARLIRHEAHTYCSG GSCYSPDYYYGMDVWGQGTMVTVSS	1150	DIVMTQSPSSLSASVGDRVTITCRASQ SISSYLNWYQQEPGKAPKLLIYAASSLQ SGVPSRFSGSGSGTDFTLTISSLQPEDF ATYYCQQSYSTPPTFGQGTKVDIK	IGHV7-4-1 (Human)	IGHJ6 (Human)	IGKV1-39 (Human)	IGKJ3 (Human)	2062	ARLIRHEAHT YCSGGSCYSP DYYYGMDV	3271	QQSYSTPP T	Xiangyang Chi et al., 2020 (https://science.sciencemag.org/content/early/2020/06/19/science.abc6952/tab-pdf)
0317-A3	Ab	SARS-CoV2 (weak)			SARS-CoV2	S; Unk	B-cells; SARS-CoV2 Human Patient	69	EVQLLQSGGGLVQPGGSLRLSCVASGFT FSSYEMNWVRQAPGKGLEWVSYISTSG STINYADSVKGRFSISRDNAKKSLYLQM NSLRAEDTAVYYCASNPPLGEPYFDIWG QGTMVTVSS	1151	DIQMTHSLILLSASVGDRVTITCRASQS ISSYLNWYQQKPGKAPKLLIYAASSLQS GVPSRFSGSGSGADFTLTISSLQPEDFA TYYCQQTYRPPWTFGQGTKVDIK	IGHV3-48 (Human)	IGHJ3 (Human)	IGKV1-39 (Human)	IGKJ1 (Human)	2063	ASNPPLGEPY FDI	3272	QQTYRPP WT	Xiangyang Chi et al., 2020 (https://science.sciencemag.org/content/early/2020/06/19/science.abc6952/tab-pdf)
0317-A7	Ab	SARS-CoV2			SARS-CoV2	S; S1 (non-RBD)	B-cells; SARS-CoV2 Human Patient	70	EVQLLESGGGVVQPGRSLRLSCAASGFT FSNYAMHWVRQAPGKGLEWVAVISYD GSNKYYADSVKGRFTISRDNSKNTLYLQ MNSLRAEDTAVYYCARWGGGMQYLD VWGQGTTVTVSS	1152	EIVVTQSLLSLPVTPGEPASISCRSSQSL LHSNGYNYLDWYLQKPGQSPQVLIYL GSNRASGVPDRFSGSGSGTDFTLKISR VEAEDVGVYYCMQTLQTPYTFGQGTK VEIK	IGHV3-30-3 (Human)	IGHJ6 (Human)	IGKV2-28 (Human)	IGKJ1 (Human)	2064	ARWGGGMQ YLDV	3273	MQTLQTP YT	Xiangyang Chi et al., 2020 (https://science.sciencemag.org/content/early/2020/06/19/science.abc6952/tab-pdf)
0317-A8	Ab	SARS-CoV2 (weak)			SARS-CoV2	S; S1 (non-RBD)	B-cells; SARS-CoV2 Human Patient	71	EVQLVQSGSELKKPGASVKVSCKASGYT FTSYAMNWVRQAPGQGLEWMGWINT NTGNPTYAQGFTGRFVFSLDTSVSTAYL QISSLKAEDTAVYYCARAGPNYDFWSGY YQTFDYWGQGTMVTVSS	1153	DIQMTQSPSSLSASVGDRVTITCQASQ DISNYLNWYQQKPGKAPKLLIYDASNL ETGVPSRFSGSGSGTDFTFTISSLQPED IATYYCQQYDNLPLTFGGGTKVEIK	IGHV7-4-1 (Human)	IGHJ4 (Human)	IGKV1-33 (Human)	IGKJ4 (Human)	2065	ARAGPNYDF WSGYYQTFD Y	3274	QQYDNLPL T	Xiangyang Chi et al., 2020 (https://science.sciencemag.org/content/early/2020/06/19/science.abc6952/tab-pdf)
0317-A9	Ab	SARS-CoV2 (weak)			SARS-CoV2	S; Unk	B-cells; SARS-CoV2 Human Patient	72	EVQLVQSGAEVKKPGASVKVSCKVSGYT LTELSMHWVRQAPGKGLEWMGGFDP EDGETIYAQKFQGRVTMTEDTSTDTAY MELSSLRSEDTAVYYCATATAMDGYYYY YGMDVWGQGTTVTVSS	1154	EIVMTQSPLSSPVTLGQPASISCRSSQS LVHSDGNTYLSWLQQRPGQPPRLLIY KISNRFSGVPDRFSGSGAGTDFTLKISR VEAEDVGVYYCMQATQFPYTFGQGT KVDIK	IGHV1-24 (Human)	IGHJ6 (Human)	IGKV2-24 (Human)	IGKJ3 (Human)	2066	ATATAMDGY YYYYGMDV	3275	MQATQFP YT	Xiangyang Chi et al., 2020 (https://science.sciencemag.org/content/early/2020/06/19/science.abc6952/tab-pdf)
0317-B1	Ab	SARS-CoV2 (weak)			SARS-CoV2	S; Unk	B-cells; SARS-CoV2 Human Patient	73	EVQLVESGAEVKKPGESLKISCKGSGYSF TSYWIGWVRQMPGEGLEWMGIIYPGD SDTRYSPSFQGQVTISADKSISTAYLQWS SLKASDTAMYYCASAGSSWYGDAFDIW GQGTMVTVSS	1155	DIVMTHSLRLLAVSLGERATINCKSSQS VLYSSNNKNYLAWYQQKPGQPPKLLI YWASTRESGVPDRFSGSGSGTDFTLTI SSLQAEDVAVYYCQQYYSTYGSFGGG TKVDIK	IGHV5-51 (Human)	IGHJ3 (Human)	IGKV4-1 (Human)	IGKJ3 (Human)	2067	ASAGSSWYG DAFDI	3276	QQYYSTYG S	Xiangyang Chi et al., 2020 (https://science.sciencemag.org/content/early/2020/06/19/science.abc6952/tab-pdf)
0317-C4	Ab	SARS-CoV2 (weak)			SARS-CoV2	S; Unk	B-cells; SARS-CoV2 Human Patient	74	QVQLVQSGAEVKKPGASVKVSCKVSGC TLTELSMHWVRQAPGKGLEWMGGFD PEDGETIYAQKFQGRVTMTEDTSTDTAY MELSSLRSEDTAVYYCATATIFGVANNW FDPWGQGTTVTVSS	1156	QAVVTQPPSVSAAPGQKVTISCSGSSS NIGNNYVSWYQQLPGTAPKLLIYDNN KRPSGIPDRFSGSKSGTSATLGITGLQT GDEADYYCGTWDSSLSVVVFGGGTKL TVL	IGHV1-24 (Human)	IGHJ5 (Human)	IGLV1-51 (Human)	IGLJ3 (Human)	2068	ATATIFGVAN NWFDP	3277	GTWDSSLS VVV	Xiangyang Chi et al., 2020 (https://science.sciencemag.org/content/early/2020/06/19/science.abc6952/tab-pdf)

0317-C9	Ab	SARS-CoV2			SARS-CoV2	S; S2	B-cells; SARS-CoV2 Human Patient	75	QVQLVQSGGGVVQPGRSLRLSCAASGF TFSSYGMHWVRQAPGKGLEWVAVISY DGSNKYYADSVKGRFTISRDNSKNTLYL QMNSLRAEDTAVYYCAKDLGYYDILTGQ LGGYYYYYGMDVWGQGTTVTVSS	1157	QAVVTQPPSASGTPGQRVTISCSGSSS NIGSNTVNWYQQLPGTAPKLLIYSNN QRPSGVPDRFSGSKSGTSASLAISGLQ SEDEADYYCAAWDDSLNGVVFGGGT KLTVL	IGHV3-30 (Human)	IGHJ6 (Human)	IGLV1-44 (Human)	IGLJ3 (Human)	2069	AKDLGYYDILT GQLGGYYYYY GMDV	3278	AAWDDSL NGVV	Xiangyang Chi et al., 2020 (https://science.sciencemag.org/content/early/2020/06/19/science.abc6952/tab-pdf)
10C10	Ab	SARS-CoV2			SARS-CoV2	S; Unk	B-cells; SARS-CoV2 Human Patient	76	QVQLVQSGGGLVQPGGSLRLSCAASGF TFSSYWMSWVRQAPGKGLEWVANIN QDGSEKYYVDSVKGRFTISRDNAKNSLY LQMNSLRAEDTAVYYCARDWDYDILTG SWFGAFDIWGQGTMVTVSS	1158	DIQLTQSPSSLSASVRNRVTITCRASQG IKNDLCWYQQKPGKAPKRLIYAASSLQ SGVPSRFSGSGSGTEFTLTISSLQPEDF ATYYCLQHNNYPLTFGGGTNEEIK	IGHV3-7 (Human)	IGHJ3 (Human)	IGKV1-17 (Human)	IGKJ4 (Human)	2070	ARDWDYDILT GSWFGAFDI	3279	LQHNNYPL T	Xiangyang Chi et al., 2020 (https://science.sciencemag.org/content/early/2020/06/19/science.abc6952/tab-pdf)
1A09	Ab	SARS-CoV2	SARS-CoV1		SARS-CoV2	S; RBD	Immunised Mouse	77	QVQLKESGPGLVAPSQSLSITCTVSGFSL TSYAISWVRQPPGKGLEWLGVIWTGGG TNYNSALKSRLSISKDNSKSQVFLKMNSL QTDDTARYYCARKDYYYGSSYAMDYWG QGTSVTVSS	1159	QAVVTQESALTTSPGETVTLTCRSSTG AVTTSNYANWVQEKPDHLFTGLIGGT NNRAPGVPARFSGSLIGDKAALTITGA QTEDEAIYFCALWYSNHWVFGGGTKL TVL	IGHV2-9-1 (Mouse)	IGHJ4 (Mouse)	IGLV1 (Mouse)	IGLJ1 (Mouse)	2071	ARKDYYYGSS YAMDY	3280	ALWYSNH WV	Wafaa Alsoussi et al., 2020 (https://www.jimmunol.org/content/early/2020/06/23/jimmunol.2000583)
1A10	Ab	SARS-CoV2	MERS-CoV, SARS-CoV1		SARS-CoV2	S; RBD	Immunised Mouse	78	EVQLQQSGAELVRPGASVKLSCKASGYT FSDYYINWVKQRPGQGLEWIARIYPGS GNTYYNEKFTGKATLTAEKSSSTAYMQL SSLTSEDSAVYFCARDYGSSYVDYFDYW GQGTTLTVSS	1160	DIQMTQSPSSLSASLGDRVTISCRASQ DISNYLNWYQQKPDGTVKLLIFYTSRL HSGVPSRFSGSGSGTDYSLTISNLEQE DIATYFCQQGNTLPYTFGGGTKLEIK	IGHV1-76 (Mouse)	IGHJ2 (Mouse)	IGKV10-96 (Mouse)	IGKJ2 (Mouse)	2072	ARDYGSSYVD YFDY	3281	QQGNTLP YT	Wafaa Alsoussi et al., 2020 (https://www.jimmunol.org/content/early/2020/06/23/jimmunol.2000583)
1A12	Ab	SARS-CoV2	MERS-CoV, SARS-CoV1	SARS-CoV2 (weak)		S; RBD	Immunised Mouse	79	EVQLQQSGAELVRPGASVKLSCTASGFN IKDDYMHWVKQRPEQGLEWIGWINPE NGDTEYASKFQGKAAITADTSSNTACLQ LSSLTSEDTAVYYCSTGGYGNYVDAMDY WGQGTSVTVSS	1161	DIKMTQSPSSMYASLGERVTITCKASQ DINSFLSWFQQKPGKSPKTLIYRANRL VDGVPSRFSGSGSGQDYSLTISSLEYE DMGIYYCLQYDEFRTFGGGTKLEIK	IGHV14-4 (Mouse)	IGHJ4 (Mouse)	IGKV14-111 (Mouse)	IGKJ1 (Mouse)	2073	STGGYGNYV DAMDY	3282	LQYDEFRT	Wafaa Alsoussi et al., 2020 (https://www.jimmunol.org/content/early/2020/06/23/jimmunol.2000583)
1B07	Ab	SARS-CoV2	MERS-CoV, SARS-CoV1	SARS-CoV2		S; RBD	Immunised Mouse	80	QVQLKESGPGLVAPSQSLSITCTVSGFSL TSYAISWVRQPPGKGLEWLGVIWTGGG TNYNSALKSRLSISKDNSKSQVFLKMNSL QTDDTARYYCARKDYYGSSSNVMDYW GQGTSVTVSS	1162	QAVVTQESALTTSPGETVTLTCRSSTG AVTTSNYANWVQEKPDHLITGLIGGT NNRVPGVPARFSGSLIGDKAALTITGA QTEDEAIYFCALWYSNQFIFGSGTKVT VL	IGHV2-9-1 (Mouse)	IGHJ4 (Mouse)	IGLV1 (Mouse)	IGLJ3 (Mouse)	2074	ARKDYYGSSS NVMDY	3283	ALWYSNQ FI	Wafaa Alsoussi et al., 2020 (https://www.jimmunol.org/content/early/2020/06/23/jimmunol.2000583)
1B10	Ab	SARS-CoV2	MERS-CoV, SARS-CoV1	SARS-CoV2		S; RBD	Immunised Mouse	81	QVQLKESGPGLVAPSQSLSITCTVSGFSL TNYAINWVRQPPGKGLEWLGVIWTGG GTNYNSALRSRLSISKDNSKSQVFLKMN SLHTDDTARYYCARKDYYGSSLAMDYW GQGTSVTVSS	1163	QAVVTQESALTTSPGETVTLTCRSSTG AVTTSNYANWVQEKPDHLFTGLIGGT NNRAPGVPARFSGSLIGDKAALTITGA QTEDEAIYFCALWYSNHWVFGGGTKL TVL	IGHV2-9-1 (Mouse)	IGHJ4 (Mouse)	IGLV1 (Mouse)	IGLJ1 (Mouse)	2075	ARKDYYGSSL AMDY	3284	ALWYSNH WV	Wafaa Alsoussi et al., 2020 (https://www.jimmunol.org/content/early/2020/06/23/jimmunol.2000583)
1C05	Ab	SARS-CoV1, SARS-CoV2	MERS-CoV	SARS-CoV2 (weak)		S; RBD	Immunised Mouse	82	EVQLQQSGPELVKPGASVKISCKASGYS FTDYYMNWVKQSPEKSLEWIGEINPST GGPTYNQKFKAKATVTVDKSSSTAYMQ LKSLTSEDSAVYYCARRNYDLYYYAMDY WGQGTSVTVSS	1164	DIVLTQSPASLAVSLGQRATISCRASES VDSYGTSFMHWYQQKPGQPPKLLIYL ASNLESGVPARFSGSGSRTDFTLTIDPV EADDAATYYCQQNNEDPLTFGAGTKL ELK	IGHV1-42 (Mouse)	IGHJ4 (Mouse)	IGKV3-10 (Mouse)	IGKJ5 (Mouse)	2076	ARRNYDLYYY AMDY	3285	QQNNEDP LT	Wafaa Alsoussi et al., 2020 (https://www.jimmunol.org/content/early/2020/06/23/jimmunol.2000583)
1C06	Ab	SARS-CoV2	MERS-CoV, SARS-CoV1		SARS-CoV2	S; RBD	Immunised Mouse	83	EVQLQQSGAELAKPGASVKLSCKASGYT FTNYWMHWVKQRPGQGLEWIGYINPS SGYTKFNQKFNDKATLTADKSSTTAYMQ LSSPTYEDSAVYYCARSDYYGSSYVGYA MDYWGQGTSVTVSS	1165	DVVMTQTPLSLPVSLGDQASISCRSSQ SIVHSNGNTYLEWYLQKPGQSPKLLIY KVSNRFSGVPDRFSGSGSGTDFTLKIS RVEAEDLGVYYCFQGSHVPPTFGGGT KLEIK	IGHV1-7 (Mouse)	IGHJ4 (Mouse)	IGKV1-117 (Mouse)	IGKJ1 (Mouse)	2077	ARSDYYGSSY VGYAMDY	3286	FQGSHVPP T	Wafaa Alsoussi et al., 2020 (https://www.jimmunol.org/content/early/2020/06/23/jimmunol.2000583)
1C07	Ab	SARS-CoV1, SARS-CoV2	MERS-CoV		SARS-CoV2	S; RBD	Immunised Mouse	84	EVQLQQPGPELVKPGASVKISCKASGYS FTDYYMNWVKQSPEKSLEWIGEINPST GGTSYNQKFKGKATLTVDKSSSTAYMQL KSLTSEDSAVYYCARRNYDLYYYAMDYW GQGTSVTVSS	1166	DIVLTQSPASLAVSLGQRATISCRASEG VDSYGSSFMHWYQQKPGQPPKLLIYL ASNLESGVPARFSGSGSGTDFTLTIDP VEADDAATYYCQQNNEDPLTFGAGTK LELK	IGHV1-42 (Mouse)	IGHJ4 (Mouse)	IGKV3-10 (Mouse)	IGKJ5 (Mouse)	2078	ARRNYDLYYY AMDY	3287	QQNNEDP LT	Wafaa Alsoussi et al., 2020 (https://www.jimmunol.org/content/early/2020/06/23/jimmunol.2000583)
1D04	Ab	SARS-CoV2	MERS-CoV, SARS-CoV1		SARS-CoV2	S; RBD	Immunised Mouse	85	EVQLQQSGAELVRPGASVKLSCTASGFN IKDDYMHWVKQRPEQGLEWIGWINPE NGDTEYASKFQGKAAITADTSSNTACLQ LSSLTSEDTAVYYCSTGGYGNYVDAMDY WGQGTSVTVSS	1167	DIKMTQSPSSMYASLGERVTITCKASQ DINSFLSWFQQKPGKSPKTLIYRANRL VDGVPSRFSGSGSGQDYSLTISSLEYED MGIYYCLQYDEFRTFGGGTKLEIK	IGHV14-4 (Mouse)	IGHJ4 (Mouse)	IGKV14-111 (Mouse)	IGKJ1 (Mouse)	2079	STGGYGNYV DAMDY	3288	LQYDEFRT	Wafaa Alsoussi et al., 2020 (https://www.jimmunol.org/content/early/2020/06/23/jimmunol.2000583)
1D05	Ab	SARS-CoV2	MERS-CoV, SARS-CoV1		SARS-CoV2	S; RBD	Immunised Mouse	86	QVQLKESGPGLVAPSQSLSITCTVSGFSL TSYAISWVRQPPGKGLEWLGVIWTGGG TNYNSALKSRLSISKDNSKSQVFLKMNSL QTDDTARYYCARKDYYGSSSNVMDYW GQGTSVTVSS	1168	QAVVTQESALTTSPGETVTLTCRSSTG AVTTSNYANWVQEKPDHLITGLIGGT NNRVPGVPARFSGSLIGDKAALTITGA QTEDKAIYFCALWYSNQFIFGSGTKVT VL	IGHV2-9-1 (Mouse)	IGHJ4 (Mouse)	IGLV1 (Mouse)	IGLJ3 (Mouse)	2080	ARKDYYGSSS NVMDY	3289	ALWYSNQ FI	Wafaa Alsoussi et al., 2020 (https://www.jimmunol.org/content/early/2020/06/23/jimmunol.2000583)

1E02	Ab	SARS-CoV2	MERS-CoV, SARS-CoV1		SARS-CoV2	S; RBD	Immunised Mouse	87	EVQLQQPGPELVKPGASVKISCKASGYS FTDYYMNWVKQSPEKSLEWIGEINPST GGTSYNQKFKGKATLTVDKSSSTAYMQL KSLTSEDSAVYYCSRRNYDLYYYAMDYW GQGTSVTVSS	1169	DIVLTQSPASLAVSLGQRATISCRASEG VDSYGSSFMHWYQQKPGQAPKLLIYL ASNLESGVPARFSGSGSRTDFTLTIDPV EADDAAIYYCQQNNEDPLTFGAGTKL EIK	IGHV1-42 (Mouse)	IGHJ4 (Mouse)	IGKV3-10 (Mouse)	IGKJ5 (Mouse)	2081	SRRNYDLYYY AMDY	3290	QQNNEDP LT	Wafaa Alsoussi et al., 2020 (https://www.jimmunol .org/content/early/202 0/06/23/jimmunol.2000 583)
1E07	Ab	SARS-CoV2	MERS-CoV, SARS-CoV1	SARS-CoV2		S; RBD	Immunised Mouse	88	EVQLQQSGPELVKPGASVKISCKASGYS FTGYSMNWVKKSPEKSLEWIGEINPSTG GTTYNQKFKAKATLTVDKSSSTAYIQLKS LTSEDSAVYYCARGAGAYWGQGTLVTV SA	1170	DIVLTQSPASLAVSLGQRATISCRASES VEYYGTSLMQWFQQKPGQPPKLLIFA ASNVESGVPARFGGSGSGTDFSLNIHP VEEDDIAMYFCQQSRKVPWTFGGGT KLEIK	IGHV1-42 (Mouse)	IGHJ3 (Mouse)	IGKV3-1 (Mouse)	IGKJ1 (Mouse)	2082	ARGAGAY	3291	QQSRKVP WT	Wafaa Alsoussi et al., 2020 (https://www.jimmunol .org/content/early/202 0/06/23/jimmunol.2000 583)
1E10	Ab	SARS-CoV2	MERS-CoV, SARS-CoV1		SARS-CoV2	S; RBD	Immunised Mouse	89	EVQLQQSGPELVKPGASVKISCKASGYA FSSSWMNWVKQRPGKGLEWIGRIYPG DGDTNYNGKFKGKATLTADKSSSTAYM QLSSLTSEDSAVYFCARDHGPAWFAYRG QGTLVTVSA	1171	QIVLTQSPAIMSASPGEKVTMTCSASS SVSYMHWYQQKSGTSPKRWIYDTSKL ASGVPARFSGSGSGTSYSLTISSMEAE DAATYYCQQWSSNPPTFGSGTKLEIK	IGHV1-82 (Mouse)	IGHJ3 (Mouse)	IGKV4-59 (Mouse)	IGKJ2 (Mouse)	2083	ARDHGPA	3292	QQWSSNP PT	Wafaa Alsoussi et al., 2020 (https://www.jimmunol .org/content/early/202 0/06/23/jimmunol.2000 583)
1H06	Ab	SARS-CoV2	MERS-CoV, SARS-CoV1		SARS-CoV2	S; RBD	Immunised Mouse	90	EVQLQQSGPELVKPGASVKISCKASGYS FTGYSMNWVKKSPEKSLEWIGEINPSTG GTTYNQKFKAKATLTVDKSSSTAYIQLKS LTSEDSAVYYCARGAGAYWGQGTLVTV SA	1172	DIVLTQSPASLAVSLGQRATISCRASES VEYYGTSLMQWFQQKPGQPPKLLIFA ASNVESGVPARFGGSGSGTDFSLNIHP VEEDDIATYFCQQSRKVPWTFGGGTK LEIK	IGHV1-42 (Mouse)	IGHJ3 (Mouse)	IGKV3-1 (Mouse)	IGKJ1 (Mouse)	2084	ARGAGAY	3293	QQSRKVP WT	Wafaa Alsoussi et al., 2020 (https://www.jimmunol .org/content/early/202 0/06/23/jimmunol.2000 583)
1H10	Ab	SARS-CoV2	MERS-CoV, SARS-CoV1	SARS-CoV2 (weak)		S; RBD	Immunised Mouse	91	QVQLKESGPGLVAPSQSLSITCTVSGFSL TNYAISWVRQPPGKGLEWLGVIWTGG GTNYNSALKSRLSISKDNSKSQVFLKMN SLQTDDTARYYCARISYYDYEGVDYWGQ GTTLTVSS	1173	QAVVTQESALTTSPGETVTLTCRSSTG AVTTSNYANWVQEKPDHLFTGLIGGT NNRAPGVPARFSGSLIGDKAALTITGA QTEDEAIYFCALWYSNHWVFGGGTKL TVL	IGHV2-9-1 (Mouse)	IGHJ2 (Mouse)	IGLV1 (Mouse)	IGLJ1 (Mouse)	2085	ARISYYDYEG VDY	3294	ALWYSNH WV	Wafaa Alsoussi et al., 2020 (https://www.jimmunol .org/content/early/202 0/06/23/jimmunol.2000 583)
1M-1D2	Ab	SARS-CoV2		SARS-CoV2		S; RBD	B-cells; SARS-CoV2 Human Patient	92	QVQLVESGGGLVQPGGSLRLSCAASGF TFSSYAMHWVRQAPGKGLEYVSAISGN GGSTYYAKSVKGRFTISRDNSKNTLYLQ MGSLRAEDMAVYYCARGAEYYDFWSG YYSAYFDYWGQGTLVTVSS	1174	QAVVTQPPSASGTPGQRVTISCSGSSS NIGSNYVYWYQQLPGTAPKLLIYNNN QRPSGVPDRFSGSKSGTSASLAISGLRS EDEADYYCAAWDDSLIYVLFGGGTKLT VL	IGHV3-64 (Human)	IGHJ4 (Human)	IGLV1-47 (Human)	IGLJ3 (Human)	2086	ARGAEYYDF WSGYYSAYFD Y	3295	AAWDDSLI YVL	Xiangyang Chi et al., 2020 (https://science.science mag.org/content/early/ 2020/06/19/science.abc 6952/tab-pdf)
2B04	Ab	SARS-CoV2	MERS-CoV, SARS-CoV1	SARS-CoV2		S; RBD	Immunised Mouse	93	QVQLKQSGPGLVAPSQSLSITCTVSGFSL INYAISWVRQPPGKGLEWLGVIWTGGG TNYNSALKSRLSISKDNSKSQVFLKMNSL QTDDTARYYCARKDYYGRYYGMDYWG QGTSVTVSS	1175	QAVVTQESALTTSPGETVTLTCRSSTG AVTTSNYANWVQEKPDHLFTGLIGGT NNRAPGVPARFSGSLIGDKAALTITGA QTEDEAIYFCALWYNNHWVFGGGTK LTVL	IGHV2-9-1 (Mouse)	IGHJ4 (Mouse)	IGLV1 (Mouse)	IGLJ1 (Mouse)	2087	ARKDYYGRYY GMDY	3296	ALWYNNH WV	Wafaa Alsoussi et al., 2020 (https://www.jimmunol .org/content/early/202 0/06/23/jimmunol.2000 583)
2C02	Ab	SARS-CoV1, SARS-CoV2	MERS-CoV		SARS-CoV2	S; RBD	Immunised Mouse	94	EVQLQQPGAELVKPGASVKVSCKASGYI FTNYWMHWVKQRPGQGLEWIGRIHPS DSDTKYNQKFKGKATLTVDKSSSTAYMQ LSSLTSEDSAVYYCAILDSYWYFDVWGT GTTVTVSS	1176	QIVLTQSPAIMSASPGEKVTMTCSASS SVSYMYWYQQKPGSSPRLLIYDTSNLA SGVPIRFSGSGSGTSYSLTISRMEAEDA ATYYCQQWSSYPLTFGAGTKLELK	IGHV1-74 (Mouse)	IGHJ1 (Mouse)	IGKV4-55 (Mouse)	IGKJ5 (Mouse)	2088	AILDSYWYFD V	3297	QQWSSYP LT	Wafaa Alsoussi et al., 2020 (https://www.jimmunol .org/content/early/202 0/06/23/jimmunol.2000 583)
2C03	Ab	SARS-CoV2	MERS-CoV, SARS-CoV1	SARS-CoV2 (weak)		S; RBD	Immunised Mouse	95	EVQLQQSGPELVKPGASVKISCKASGYA FSSSWMNWVKQRPGKGLEWIGRIYPG DGDTNYNGKLKGKATLTADKSSSTAYM QLSSLTSEDSAVYFCARKSYGYWHFDV WGTGTTVTVSS	1177	DVVMTQTPLSLPVSLGDQASISCRSSQ SIVYSNGNTYLEWYLQKPGQSPKLLIYK VSNRFSGVPDRFSGSGSGTDFTLKISG VEAEDLGVYYCFQGSHVPYTFGGGTK LEIK	IGHV1-82 (Mouse)	IGHJ1 (Mouse)	IGKV1-117 (Mouse)	IGKJ2 (Mouse)	2089	ARKSYGYWH FDV	3298	FQGSHVPY T	Wafaa Alsoussi et al., 2020 (https://www.jimmunol .org/content/early/202 0/06/23/jimmunol.2000 583)
2C04	Ab	SARS-CoV2	MERS-CoV, SARS-CoV1		SARS-CoV2	S; RBD	Immunised Mouse	96	EVQLQQPGPELVKPGTSVKISCKASGYT FTDYYMNWVKQSHGKSLEWIGDINPN NGGTNYNQKFKGKATLTVDKSSSTAYM ELRSLTSEDSAVCYCAAGKGDYWGQGT TLTVSS	1178	DIVLTQSQASLAVSLGQRATISCRASES VEYYGTSLMQWYQQKPGQPPKLLIYA ASNVESGVPARFSGSGSGTDFSLNIHP VEEDDIAMYFCQQSRKVPWTFGGGT KLEIK	IGHV1-26 (Mouse)	IGHJ2 (Mouse)	IGKV3-1 (Mouse)	IGKJ1 (Mouse)	2090	AAGKGDY	3299	QQSRKVP WT	Wafaa Alsoussi et al., 2020 (https://www.jimmunol .org/content/early/202 0/06/23/jimmunol.2000 583)
2D01	Ab	SARS-CoV2	MERS-CoV, SARS-CoV1		SARS-CoV2	S; RBD	Immunised Mouse	97	EVQLQQPGAELVKPGASVKVSCKASGYI FTNYWMHWVKQRPGQGLEWIGRIHPS DSDTKYNQKFKGKATLTVDKSSSTAYMQ LSSLTSEDSAVYYCAILDSYWYFDVWGT GTTVTVSS	1179	QIVLTQSPAIMSASPGEKVTMTCSASS SVSYMYWYQQKPGSSPRLLIYDTSNLA SGVPIRFSGSGSGTSYSLTISRMEAEDA ATYYCQQWSSYPLTFGAGTKLELK	IGHV1-74 (Mouse)	IGHJ1 (Mouse)	IGKV4-55 (Mouse)	IGKJ5 (Mouse)	2091	AILDSYWYFD V	3300	QQWSSYP LT	Wafaa Alsoussi et al., 2020 (https://www.jimmunol .org/content/early/202 0/06/23/jimmunol.2000 583)
2D08	Ab	SARS-CoV2	MERS-CoV, SARS-CoV1	SARS-CoV2 (weak)		S; RBD	Immunised Mouse	98	EVQLQQSGPELVKPGTSVKISCKASGYTF TDYYMNWVKQSHGKSLEWIGDINPNN GGTNYNQKFKGKATLTVDKSSSTAYMEL RSLTSEDSAVYYCAAGKGDYWGQGTTL TVSS	1180	DIVLTQSQASLAVSLGQRATISCRASES VEYYGTSLMQWYQQKPGQPPKLLIYA ASNVESGVPARFSGSGSGTDFSLNIHP VEEDDIAMYFCQQSRKVPWTFGGGT KLEIK	IGHV1-26 (Mouse)	IGHJ2 (Mouse)	IGKV3-1 (Mouse)	IGKJ1 (Mouse)	2092	AAGKGDY	3301	QQSRKVP WT	Wafaa Alsoussi et al., 2020 (https://www.jimmunol .org/content/early/202 0/06/23/jimmunol.2000 583)

2D11	Ab	SARS-CoV2	MERS-CoV, SARS-CoV1		SARS-CoV2	S; RBD	Immunised Mouse	99	EVQLQQSGPELVKPGASVKISCKASGYT FTDYYMNWVKQSHGKSLEWIGDINPN NGGTSYNQKFKGKATLTVDKSSSTAYME LRSLTSEDSAVYYCARKGDGYYGGFAYW GQGTLVTVSA	1181	DIVLTQSPASLAVSLGQRATISCRASES VDNYGISFMNWFQQKPGQPPKLLIYA ASNQGSGVPARFSGSGSGTDFSLNIHP MEEDDTAMYFFQQSKEVPWTFGGGT KLEIK	IGHV1-26 (Mouse)	IGHJ3 (Mouse)	IGKV3-2 (Mouse)	IGKJ1 (Mouse)	2093	ARKGDGYYG GFAY	3302	QQSKEVP WT	Wafaa Alsoussi et al., 2020 (https://www.jimmunol .org/content/early/202 0/06/23/jimmunol.2000 583)
2E06	Ab	SARS-CoV1, SARS-CoV2	MERS-CoV	SARS-CoV2 (weak)		S; RBD	Immunised Mouse	100	EVQLQQSVADLVRPGASVKLSCTASGFN IKNTYMHWVKQRPEQGLEWIGRIDPTN GDTKYVSKFQGKATITADTSSNTAYLQLS SLTSEDTAIYYCATGSYYLYYYAMNYWG QGTSVTVSS	1182	DIVLTQSPASLTVSLGQRATISCKASQS VDYGGDRYMNWYQQKPGQPPKLLIF AASNLESGIPARFSGSGSGTDFTLNIHP VEEEDAATYYCQQSNEDPYTFGGGTK LEIK	IGHV14-3 (Mouse)	IGHJ4 (Mouse)	IGKV3-4 (Mouse)	IGKJ2 (Mouse)	2094	ATYGSYYLYYY AMNY	3303	QQSNEDP YT	Wafaa Alsoussi et al., 2020 (https://www.jimmunol .org/content/early/202 0/06/23/jimmunol.2000 583)
2E10	Ab	SARS-CoV1, SARS-CoV2	MERS-CoV		SARS-CoV2	S; RBD	Immunised Mouse	101	EVQLQQPGAELVRPGASVKLSCKASGYT FTDYYINWVKQRPGQGLEWIARIYPGT GTTYYNEKFKGKATLTAEKSSSTAYMQLS SLTSEDSAVYFCARYDGNLYYYAMDYW GQGTSVTVSS	1183	DIVLTQSPASLAVSLGQRATMSCRASE SVDSYGNGFMHWYQQKPGQPPKLLI YLASNLESGVPARFSGSGSRTDFSLTID PVEADDAAIYYCQQNNEDPLTFGAGT KLELK	IGHV1-76 (Mouse)	IGHJ4 (Mouse)	IGKV3-4 (Mouse)	IGKJ5 (Mouse)	2095	ARYDGNLYYY AMDY	3304	QQNNEDP LT	Wafaa Alsoussi et al., 2020 (https://www.jimmunol .org/content/early/202 0/06/23/jimmunol.2000 583)
2F04	Ab	SARS-CoV2	MERS-CoV, SARS-CoV1		SARS-CoV2	S; RBD	Immunised Mouse	102	EVQLQQPGAELVKPGASVKMSCKASGY TFTSYWITWVKQRPGQGLEWIGDIYPG SGSTKYNEKFRSEATLTVDTSSTTAYMQL SSLTSEDSAVYYCARWDFYGSRTFDYWG QGTTLTVSS	1184	DIVLTQSPAILSVSPGERVSFSCRASQN IGTIIHWYQQRTNGSPRLLIKYASESVS GIPSRFSGSGSGTDFTLSINSVESEDIA DYYCQQSSSWPLTFGAGTKLELK	IGHV1-55 (Mouse)	IGHJ2 (Mouse)	IGKV5-48 (Mouse)	IGKJ5 (Mouse)	2096	ARWDFYGSR TFDY	3305	QQSSSWP LT	Wafaa Alsoussi et al., 2020 (https://www.jimmunol .org/content/early/202 0/06/23/jimmunol.2000 583)
2H04	Ab	SARS-CoV2	MERS-CoV, SARS-CoV1	SARS-CoV2		S; RBD	Immunised Mouse	103	EVQLQQSGAELVKPGASVKMSCKASGY TFTSYWITWVKQRPGQGLEWIGDIYPG SGSTKYNEKFRSEATLTVDTSSTTAYMQL SSLTSEDSAVYYCARWDFYGSRTFDYWG QGTTLTVSS	1185	DIVLTQSPAILSVSPGERVSFSCRASQN IGTIIHWYQQRTNGSPRLLIKYASESVS GIPSRFSGSGSGTDFTLSINSVESEDIA DYYCQQSSSWPLTFGAGTKLELK	IGKV5-48 (Mouse)	IGKJ5 (Mouse)	IGHV1-55 (Mouse)	IGHJ2 (Mouse)	2097	ARWDFYGSR TFDY	3306	QQSSSWP LT	Wafaa Alsoussi et al., 2020 (https://www.jimmunol .org/content/early/202 0/06/23/jimmunol.2000 583)
2M-10B11	Ab	SARS-CoV2			SARS-CoV2	S; RBD	B-cells; SARS-CoV2 Human Patient	104	EVQLVESGGGLVQPGGSLRLSCAASGFT VSSNYMSWVRQAPGKGLEWVSVIYSG GSTYYADSVKGRFTISRDNSKNTLYLQM NSLRAEDTAVYYCARATWLRGVMDVW GQGTTVTVSS	1186	QSALTQPHSVSESPGKTVTISCTGSSGS IASNYVQWYQQRPGSAPTTVIYEDNQ RPSGVPDRFSGSIDSSSNSASLTISGLKT EDEADYYCQSYDSSNHWVFGGGTKLT VL	IGHV3-66 (Human)	IGHJ6 (Human)	IGLV6-57 (Human)	IGLJ3 (Human)	2098	ARATWLRGV MDVW	3307	QSYDSSNH WV	Xiangyang Chi et al., 2020 (https://science.science mag.org/content/early/ 2020/06/19/science.abc 6952/tab-pdf)
2M-12D7	Ab	SARS-CoV2			SARS-CoV2	S; S2	B-cells; SARS-CoV2 Human Patient	105	EVQLVESGGGLVQPGRSLRLSCAASGFT FDDYVMHWVRQAPGKGLEWVSGINW NSGSIGYADSVKGRFTISRDNAKNSLYLQ MNSLRAEDTALYYCAKDVRYCSSTSCYFS AFDIWGQGTMVTVSS	1187	AIRMTQSPSSLSASVGDRVTITCRASQ SITGYLNWYQQKPGKAPKLLISAASSL QSGVPSRFSGSGSGTDFTLTISSLQPED FATYYCQQSYSTPRTFGPGTKVEIK	IGHV3-9 (Human)	IGHJ3 (Human)	IGKV1-39 (Human)	IGKJ3 (Human)	2099	AKDVRYCSST SCYFSAFDI	3308	QQSYSTPR T	Xiangyang Chi et al., 2020 (https://science.science mag.org/content/early/ 2020/06/19/science.abc 6952/tab-pdf)
2M-13A3	Ab	SARS-CoV2			SARS-CoV2	S; S2	B-cells; SARS-CoV2 Human Patient	106	EVQLVESGGGVVQPGRSLRLSCAASGFT FSGYAMHWVRQAPGKGLEWVAVISYD GSNKYYADSVKGRFTISRDNSKNTLYLQ MNSLRAEDTAVYYCARGGGSYYYWFDP WGQGTMVTVSS	1188	AIRMTQSPDSLAVSLGERATINCKSSQ SVLYSPNNKNYLAWYQQKPGQPPKLL IYWASTRESGVPDRFSGSGSGTDFTLTI SSLQAEDVAVYYCQQYYSTPFTFGQGT RLEIK	IGHV3-30 (Human)	IGHJ3 (Human)	IGKV4-1 (Human)	IGKJ5 (Human)	2100	ARGGGSYYY WFDP	3309	QQYYSTPF T	Xiangyang Chi et al., 2020 (https://science.science mag.org/content/early/ 2020/06/19/science.abc 6952/tab-pdf)
2M-13D11	Ab	SARS-CoV2			SARS-CoV2	S; S2	B-cells; SARS-CoV2 Human Patient	107	EVQLVQWGAGLLKPSETLSLTCAVYGGS FSGYYWSWIRQPPGKGLEWIGEINHSG STNYNPSLKSRVTISVDTSKNQFSLKLSSV TAADTAVYYCARAGYSSSWYGVRGVDP WGQGTMVTVSS	1189	EIVMTQSPGTLSLSPGERATLSCRASQ SVSSSYLAWYQQKPGQAPRLLIYGASS RATGIPDRFSGSGSGTDFTLTISRLEPE DFAVYYCQQYGSSRSWTFGQGTKVEI K	IGHV4-34 (Human)	IGHJ3 (Human)	IGKV3-20 (Human)	IGKJ1 (Human)	2101	ARAGYSSSWY GVRGVDP	3310	QQYGSSRS WT	Xiangyang Chi et al., 2020 (https://science.science mag.org/content/early/ 2020/06/19/science.abc 6952/tab-pdf)
2M-14B2	Ab	SARS-CoV2			SARS-CoV2	S; S2	B-cells; SARS-CoV2 Human Patient	108	QVQLLQSGGGVVQPGRSLRLSCAASGF TFSTYGMHWVRQAPGKGLEWVAVISY DGSNKYYADSVKGRFTISRDNSKNTLYL QMNSLRAEDTAVYYCAKGSDIVVVPVG NWFDPWGQGTLVTVSS	1190	AIRMTQSPSSLSASVGDRVTITCRASQ SISSYLNWYQQKPGKAPKLLIYAASSLQ SGVPSRFSGSGSGTDFTLTISSLQPEDF ATYYCQQSYSTFTLYTFGQGTKVDIK	IGHV3-30 (Human)	IGHJ5 (Human)	IGKV1-39 (Human)	IGKJ3 (Human)	2102	AKGSDIVVVP VGNWFDP	3311	QQSYSTFT LYT	Xiangyang Chi et al., 2020 (https://science.science mag.org/content/early/ 2020/06/19/science.abc 6952/tab-pdf)
2M-14E4	Ab	SARS-CoV2			SARS-CoV2	S; S2	B-cells; SARS-CoV2 Human Patient	109	QVQLQESGPGLVKPSETLSLACTVSGGS VSSDNSYWSWIRQPPGKGLEWIGYTFH SGSANYNPSLKSRVTISVDTSKNQFSLKL SSVTAADTAVYYCARVQRYYPDSSGFYG RRFDIWGQGTLVTVSS	1191	DIVMTQSPSSLSASVGDRVSITCRASQ NISNYLNWYQQKPGEAPKLLISAASSL QSGVPSRFGGSGSGTGFTLTINSLQPE DFATYYCQQSHSFPFTFGPGTKVDIK	IGHV4-61 (Human)	IGHJ4 (Human)	IGKV1-39 (Human)	IGKJ3 (Human)	2103	ARVQRYYPDS SGFYGRRFDI	3312	QQSHSFPF T	Xiangyang Chi et al., 2020 (https://science.science mag.org/content/early/ 2020/06/19/science.abc 6952/tab-pdf)
2M-14E5	Ab	SARS-CoV2			SARS-CoV2	S; S2	B-cells; SARS-CoV2 Human Patient	110	EVQLVESGGGVVQPGRSLRLSCAASGFT FSTYSMHWVRQAPGKGLEWVAVISYD GSNKYYADSVKGRFTISRDNSKNTLYLQ VNSLRAEDTAVYYCARSGGGSYRGPFDY WGQGTLVTVSS	1192	AIRMTQSPSFLSVSVGDRVTITCRASQ GISSYLAWYQQKPGKAPKLLIYAASTL QSGVPSRFSGSGSGTEFTLTISSLQPED FATYYCQQLNSYVTFGGGTKVEIK	IGHV3-30 (Human)	IGHJ4 (Human)	IGKV1-9 (Human)	IGKJ4 (Human)	2104	ARSGGGSYR GPFDY	3313	QQLNSYVT	Xiangyang Chi et al., 2020 (https://science.science mag.org/content/early/ 2020/06/19/science.abc 6952/tab-pdf)

2M-2D1	Ab	SARS-CoV2			SARS-CoV2	S; S2	B-cells; SARS-CoV2 Human Patient	111	EVQLVESGPGLVKPSETLSLTCTVSGGSI SSSSYYWGWIRQPPGKGLEWIGSIYYSG STYYNPSLKSRVTISVDTSKNQFSLKLSSV TAADTAVYYSARGDRIQLWLLDAFDIW GQGTMVTVSS	1193	QSVLTQLPSASGTPGQTVTISCSGNVF KEKSNYVYWYQQLPGTAPKLLIYRNN HRPSGVPDRFSGSKSGTSPSLAISGLRS EDEADYYCAARDDSLSGWVFSGRTKL TVL	IGHV4-39 (Human)	IGHJ3 (Human)	IGLV1-47 (Human)	IGLJ3 (Human)	2105	ARGDRIQLW LLDAFDI	3314	AARDDSLS GWV	Xiangyang Chi et al., 2020 (https://science.sciencemag.org/content/early/2020/06/19/science.abc6952/tab-pdf)
2M-2D4	Ab	SARS-CoV2			SARS-CoV2	S; S2	B-cells; SARS-CoV2 Human Patient	112	EVQLVESGGGLVQPGGSLRLSCAASGFT FSSYAMSWVRQAPGKGLEWVSAISGSG GSTYYADSVKGRFTISRDNSKNTLYLQM NSLRAEDTAVYYCAKIGLGLGGLLRRYFD YWGQGTLVTVSS	1194	EIVMTQSPATLSLSPGERATLSCRASQS VSTSLAWYQQKPGQAPRLLIYDASNR ATGVPARFSGSGSGTDFTLTISSLEPDD FAVYYCQQRTNWPLFGPGTKVEIK	IGHV3-23 (Human)	IGHJ4 (Human)	IGKV3-11 (Human)	IGKJ3 (Human)	2106	AKIGLGLGGL LRRYFDY	3315	QQRTNWP L	Xiangyang Chi et al., 2020 (https://science.sciencemag.org/content/early/2020/06/19/science.abc6952/tab-pdf)
2M-2G12	Ab	SARS-CoV2			SARS-CoV2	S; S2	B-cells; SARS-CoV2 Human Patient	113	QVQLVESGGGLLKPGETLSLSCAASGFTF SDYYWSWIRQAPGKGLEWIAVINHSGS TIYYPYPVKGVFIFSRDTANNFSLKLMN MMTSDTAVYYCGTRIMITWYSRRGMD GWGKGVTVTVSS	1195	DIQMTQSPSSLSVSAGERATLSCRASQ SVSSYLIWCHQKPGKAPKLLIYDASTLQ TGVPSRFIGGGSGTNFTLTIISLQPEDF AAYYCQQNYSTWTIGQGSRVEMK	IGHV3-11 (Human)	IGHJ6 (Human)	IGKV1-39 (Human)	IGKJ1 (Human)	2107	GTRIMITWYS RRGMDG	3316	QQNYSTW T	Xiangyang Chi et al., 2020 (https://science.sciencemag.org/content/early/2020/06/19/science.abc6952/tab-pdf)
2M-4G4	Ab	SARS-CoV2			SARS-CoV2	S; RBD	B-cells; SARS-CoV2 Human Patient	114	EVQLVESGAEVKKPGASVKVSCKASGYT FTSYYIHWVRQAPGQGLEWMGVINPS GGSTTYAQKFQGRVTVTRDTSTSTVYM ELSSLRSEDTAVYYCARERGDSSGYYEIIT TANRRFGMDVWGQGTTVTVSS	1196	QSVLTQPASVSGSPGQSITISCTGTSSD VGMYNLVSWYQQHPGQAPKLMIYE GSKRPSGVSNRFSGSKSGNTASLTISGL QAEDEAYYYCCSYAVSSTWVFGGGTK LTVL	IGHV1-46 (Human)	IGHJ6 (Human)	IGLV2-23 (Human)	IGLJ3 (Human)	2108	ARERGDSSGY YEIITTANRRF GMDV	3317	CSYAVSST WV	Xiangyang Chi et al., 2020 (https://science.sciencemag.org/content/early/2020/06/19/science.abc6952/tab-pdf)
2M-7E9	Ab	SARS-CoV2			SARS-CoV2	S; S2	B-cells; SARS-CoV2 Human Patient	115	EVQLVESGAEVKKPGSSVKVSCKASGGT FSSFAISWVRQAPGQGLEWMGGIIPIFD TTNYAQKFQGRVTITADESTRTAYMELS SLRSEDTAVYYCARIPGWDRGTDRNWN DDWGQGTTVTVSS	1197	DIVMTQSPATLSLSPGERATLSCRASQ SVSNFLAWYQQKPGQAPRLLIYDASN RATGIPARFSGSGSGTDFTLTISSLEPE DFAVYYCQQRSNWPPAFTFGPGTKVE IK	IGHV1-69 (Human)	IGHJ6 (Human)	IGKV3-11 (Human)	IGKJ3 (Human)	2109	ARIPGWDRG TDRNWNDD	3318	QQRSNWP PAFT	Xiangyang Chi et al., 2020 (https://science.sciencemag.org/content/early/2020/06/19/science.abc6952/tab-pdf)
2M-8E7	Ab	SARS-CoV2			SARS-CoV2	S; S2	B-cells; SARS-CoV2 Human Patient	116	EVQLVESGAEVKKPGSSVKVSCKASGGT FSSYAISWVRQAPGQGLEWMGGIIPIFG TANYAQKFQGRVTVTADESTSTAYMELS SLRSEDTAVYYCARTYSFDSSGYYYDYW GQGTMVTVSS	1198	EIVLTQSPATLSLSPGERATLSCRASQS VSSYLAWYQQKPGQAPRLLIYDASNR ATGIPARFSGSGSGTDFTLTISSLEPEDF AVYYCQQRSNWPPKITFGQGTRLEIK	IGHV1-69 (Human)	IGHJ4 (Human)	IGKV3-11 (Human)	IGKJ5 (Human)	2110	ARTYSFDSSG YYYDY	3319	QQRSNWP PKIT	Xiangyang Chi et al., 2020 (https://science.sciencemag.org/content/early/2020/06/19/science.abc6952/tab-pdf)
2M-8H10	Ab	SARS-CoV2			SARS-CoV2	S; S2	B-cells; SARS-CoV2 Human Patient	117	QVQLVESGGGVVLPGRSLRLSCAASGFT FSTFAMHWVRQAPGKGLEWVAVISDE GSNKYYADSVKGRFTISRDNSRNTLYLQ MNSLRAEDTAVYYCARAFYDSNWSVGS YFDSWGQGTPVTVSS	1199	DIQMTQSPDSLAVSLGERATIKCKSSQ SVLHSSNNKNYLAWYQQKAGQPPSLL LYWASTRESGVPDRFSGSGSGTDFTLT ISSLQAEDVAVYYCQQYYNNQWTFGQ GTKVDIK	IGHV3-30 (Human)	IGHJ5 (Human)	IGKV4-1 (Human)	IGKJ1 (Human)	2111	ARAFYDSNW SVGSYFDS	3320	QQYYNNQ WT	Xiangyang Chi et al., 2020 (https://science.sciencemag.org/content/early/2020/06/19/science.abc6952/tab-pdf)
2M-9F10	Ab	SARS-CoV2			SARS-CoV2	S; S2	B-cells; SARS-CoV2 Human Patient	118	EVQLLQSGGDLIQPGRSLRLSCAASGFSF EDYAMHWVRQAPGQGLEWVSGISYN GGSIDYVDSVKGRFTISRDNAKNALYLE MNSLRPEDTAFYYCAKDSVRREYTHARV PFDNWGLGTLVTVSS	1200	AIRMTQSPSSLSASVGDRVTISCRATQ NINYFLNWYQQKPGRAPKLLIYAASGL QSGVPSRFSGSGTGRVFTLTINSLQPD DFATYYCQQSFVSPRTFGQGTKVDIK	IGHV3-9 (Human)	IGHJ4 (Human)	IGKV1-39 (Human)	IGKJ3 (Human)	2112	AKDSVRREYT HARVPFDN	3321	QQSFVSPR T	Xiangyang Chi et al., 2020 (https://science.sciencemag.org/content/early/2020/06/19/science.abc6952/tab-pdf)
2M-9H1	Ab	SARS-CoV2			SARS-CoV2	S; S2	B-cells; SARS-CoV2 Human Patient	119	EVQLLESGGGVVQPGRSLRLSCVASGFN FNNYGMHWVRQAPGKGLEWLAALSYE GSKEHYADSLKGRFTVSRDYSRATLHLH MNSLEPEDTAVYFCAKSSKIFYLGESREV DYWGRGTLVTVSS	1201	DIVMTQSPSSLSAFVGDRVTITCRASR DIGGDLSWFQQKPGKAPERLIYAASSL ESGVPSRFSGSGSATEFALTITSLQPED FATYYCLQHKSYPLTFGGGTKVDIK	IGHV3-30 (Human)	IGHJ4 (Human)	IGKV1-17 (Human)	IGKJ4 (Human)	2113	AKSSKIFYLGE SREVDY	3322	LQHKSYPL T	Xiangyang Chi et al., 2020 (https://science.sciencemag.org/content/early/2020/06/19/science.abc6952/tab-pdf)
31B5	Ab	SARS-CoV2		SARS-CoV2		S; RBD	B-cells; SARS-CoV2 Human Patient		ND		ND	ND	ND	ND	ND	2114	ARVEYYYGSG SYMPWYFDL		ND	Xiangyu Chen et al., 2020 (https://www.nature.com/articles/s41423-020-0426-7)
31B9	Ab	SARS-CoV2			SARS-CoV2	S; RBD	B-cells; SARS-CoV2 Human Patient		ND		ND	ND	ND	ND	ND	2115	ATYYYDSSGYS YGMDV		ND	Xiangyu Chen et al., 2020 (https://www.nature.com/articles/s41423-020-0426-7)
32D4	Ab	SARS-CoV2		SARS-CoV2		S; RBD	B-cells; SARS-CoV2 Human Patient		ND		ND	ND	ND	ND	ND	2116	TEEGSGSEGP IEFDY		ND	Xiangyu Chen et al., 2020 (https://www.nature.com/articles/s41423-020-0426-7)
413-2	Ab	SARS-CoV2	SARS-CoV1	SARS-CoV2	SARS-CoV1	S; non-RBD	B-cells; SARS-CoV2 Human Patient		ND		ND	ND	ND	ND	ND	2117	ARDNNYRNY YYYMDVW	3323	QQYGSSPP LT	Jinkai Wan et al., 2020 (https://www.sciencedirect.com/science/article/pii/S2211124720308998)

414-1	Ab	SARS-CoV2	SARS-CoV1	SARS-CoV2	SARS-CoV1	S; RBD	B-cells; SARS-CoV2 Human Patient		ND		ND	ND	ND	ND	ND	2118	ARGALGCSSTSCYPNNFDYW	3324	AAWDDSLNGVV	Jinkai Wan et al., 2020 (https://www.sciencedirect.com/science/article/pii/S2211124720308998)
47D11	Ab	SARS-CoV1, SARS-CoV2		SARS-CoV2 and SARS-CoV1		S; RBD	B-cells; SARS-CoV1 Human Patient		ND		ND	ND	ND	ND	ND	2119	ND		ND	Chunyan Wang et al., 2020 (https://www.nature.com/articles/s41467-020-16256-y)
4A8	Ab	SARS-CoV2		SARS-CoV2		S; S1 (non-RBD)	B-cells; SARS-CoV2 Human Patient	120	EVQLVESGAEVKKPGASVKVSCKVSGYTLTELSMHWVRQAPGKGLEWMGGFDPEDGETMYAQKFQGRVTMTEDTSTDTAYMELSSLRSEDTAVYYCATSTAVAGTPDLFDYYYGMDVWGQGTTVTVSS	1202	EIVMTQSPLSSPVTLGQPASISCRSSQSLVHSDGNTYLSWLQQRPGQPPRLLIYKISNRFSGVPDRFSGSGAGTDFTLKISRVEAEDVGVYYCTQATQFPYTFGQGTKVDIK	IGHV1-24 (Human)	IGHJ6 (Human)	IGKV2-24 (Human)	IGKJ3 (Human)	2120	ATSTAVAGTPDLFDYYYGMDV	3325	TQATQFPYT	Xiangyang Chi et al., 2020 (https://science.sciencemag.org/content/early/2020/06/19/science.abc6952/tab-pdf)
505-3	Ab	SARS-CoV2	SARS-CoV1	SARS-CoV2	SARS-CoV1	S; RBD	B-cells; SARS-CoV2 Human Patient		ND		ND	ND	ND	ND	ND	2121	ARDFISRPRGYRW	3326	MQGTHWPPT	Jinkai Wan et al., 2020 (https://www.sciencedirect.com/science/article/pii/S2211124720308998)
505-5	Ab	SARS-CoV2	SARS-CoV1	SARS-CoV2	SARS-CoV1	S; RBD	B-cells; SARS-CoV2 Human Patient		ND		ND	ND	ND	ND	ND	2122	ARDFISRPRGYRW	3327	MQGTHWPPT	Jinkai Wan et al., 2020 (https://www.sciencedirect.com/science/article/pii/S2211124720308998)
505-8	Ab	SARS-CoV2	SARS-CoV1	SARS-CoV2	SARS-CoV1	S; non-RBD	B-cells; SARS-CoV2 Human Patient		ND		ND	ND	ND	ND	ND	2123	ARGQDDFWSMNWFDPW	3328	SSYTSSSIVV	Jinkai Wan et al., 2020 (https://www.sciencedirect.com/science/article/pii/S2211124720308998)
515-1	Ab	SARS-CoV2	SARS-CoV1	SARS-CoV2	SARS-CoV1	S; RBD	B-cells; SARS-CoV2 Human Patient		ND		ND	ND	ND	ND	ND	2124	ARDFISRPRGYRW	3329	MQGTHWPPT	Jinkai Wan et al., 2020 (https://www.sciencedirect.com/science/article/pii/S2211124720308998)
515-5	Ab	SARS-CoV2	SARS-CoV1	SARS-CoV2	SARS-CoV1	S; non-RBD	B-cells; SARS-CoV2 Human Patient		ND		ND	ND	ND	ND	ND	2125	TRGSQWATINDARFDYW	3330	LQHNSYPIT	Jinkai Wan et al., 2020 (https://www.sciencedirect.com/science/article/pii/S2211124720308998)
553-15	Ab	SARS-CoV1, SARS-CoV2		SARS-CoV1, SARS-CoV2		S; RBD	B-cells; SARS-CoV2 Human Patient		ND		ND	ND	ND	ND	ND	2126	ARVWYYYGPRDYW	3331	QSYDGSNHNVV	Jinkai Wan et al., 2020 (https://www.sciencedirect.com/science/article/pii/S2211124720308998)
553-49	Ab	SARS-CoV2	SARS-CoV1	SARS-CoV2	SARS-CoV1	S; RBD	B-cells; SARS-CoV2 Human Patient		ND		ND	ND	ND	ND	ND	2127	AKDSSSWYNYYGMDVW	3332	QSYDSSNHVV	Jinkai Wan et al., 2020 (https://www.sciencedirect.com/science/article/pii/S2211124720308998)
553-60	Ab	SARS-CoV2	SARS-CoV1	SARS-CoV2	SARS-CoV1	S; RBD	B-cells; SARS-CoV2 Human Patient		ND		ND	ND	ND	ND	ND	2128	ARVFRGSQYWFDPW	3333	QQYGSSPPT	Jinkai Wan et al., 2020 (https://www.sciencedirect.com/science/article/pii/S2211124720308998)
553-63	Ab	SARS-CoV2	SARS-CoV1	SARS-CoV2	SARS-CoV1	S; RBD	B-cells; SARS-CoV2 Human Patient		ND		ND	ND	ND	ND	ND	2129	ARMEAPKLTLDPW	3334	QQSYSIPRT	Jinkai Wan et al., 2020 (https://www.sciencedirect.com/science/article/pii/S2211124720308998)
8D2	Ab	SARS-CoV2			SARS-CoV2	S; S2	B-cells; SARS-CoV2 Human Patient	121	EVQLVESGGGLVQPGGSLRLSCAASGFTFSSYWMSWVRQAPGKGLEWVANINQDGSEKYYVDSVKGRFTISRDNAKNSLYLQVNSLRAEDTAVYYCARDWDYDILTGSWFGAFDIWGQGTTVTVSS	1203	DIQMTQSPSSLSASVGDRVTITCRASQGIRNDLGWYQQKPGKAPKRLIYAASSLQSGVPSRFSGSGSGTEFTLTISSLQPEDFATYYCLQHNSYPLTFGGGTKVEIK	IGHV3-7 (Human)	IGHJ3 (Human)	IGKV1-17 (Human)	IGKJ4 (Human)	2130	ARDWDYDILTGSWFGAFDI	3335	LQHNSYPLT	Xiangyang Chi et al., 2020 (https://science.sciencemag.org/content/early/2020/06/19/science.abc6952/tab-pdf)
8D9	Ab	SARS-CoV2			SARS-CoV2	S; S2	B-cells; SARS-CoV2 Human Patient	122	EVQLLESGGGLVQPGGSLRLSCTASGFTFSSYWMSWVRQAPGKGLEWVANIQQDGSEKYYVDSVKGRFTISRDNAKNSLYLQMNSLRAEDTAVYYCARPTIGYSYGSDYWGQGTTVTVSS	1204	SYELTQPPSVSVSPGQTASITCSGDKLGDKYACWYRQKPGQSPVLVIYQDSKRPSGIPERFSGSNSGNTATLTISGTQAMDEADYYCQAWDSSTGVFGGGTKLTVL	IGHV3-7 (Human)	IGHJ4 (Human)	IGLV3-1 (Human)	IGLJ3 (Human)	2131	ARPTIGYSYGSDY	3336	QAWDSSTGV	Xiangyang Chi et al., 2020 (https://science.sciencemag.org/content/early/2020/06/19/science.abc6952/tab-pdf)

9A1	Ab	SARS-CoV2			SARS-CoV2	S; S2	B-cells; SARS-CoV2 Human Patient	123	EVQLLESGGGVVQPGRSLRLSCVVSGFT FNNYGMHWVRQAPGKGLEWVAVISYE GSVKYYGDHVDGRFTISRDPFKNTLYLH MNNLRPDDTAVYYCAKVSAIFWLGQGL SPIDVWGQGTTVTVSS	1205	DIVMTQSPATLSASPGERVTLSCRASQ NIRNNLAWYQQKPGQAPRLLIHGAST RAAGAPARFSGSGSDTQFTLTVSSLQS EDFAVYYCHQYSKWPVTFGGGTKVDI K	IGHV3-30 (Human)	IGHJ6 (Human)	IGKV3-15 (Human)	IGKJ3 (Human)	2132	AKVSAIFWLG QGLSPIDV	3337	HQYSKWP VT	Xiangyang Chi et al., 2020 (https://science.sciencemag.org/content/early/2020/06/19/science.abc6952/tab-pdf)
Ab_510A 4	Ab	SARS-CoV2		SARS-CoV2 (weak)		S; RBD	B-cells; SARS-CoV2 Human Patient		ND		ND	IGHV2-70 (Human)	IGHJ4 (Human)	IGKV2-28 (Human)	IGKJ1 (Human)	2133	ARVQVAAAG SPYDY	3338	MQALQM GT	Xiaojian Han et al., 2020 (https://www.biorxiv.org/content/10.1101/2020.08.19.253369v2.full.pdf+html)
Ab_510A 5	Ab	SARS-CoV2			SARS-CoV2	S; RBD	B-cells; SARS-CoV2 Human Patient		ND		ND	IGHV3-9 (Human)	IGHJ4 (Human)	IGKV1-39 (Human)	IGKJ2 (Human)	2134	AKDRGYEILTP ASFDY	3339	QQSYSTPP YT	Xiaojian Han et al., 2020 (https://www.biorxiv.org/content/10.1101/2020.08.19.253369v2.full.pdf+html)
Ab_510D 7	Ab	SARS-CoV2		SARS-CoV2		S; RBD	B-cells; SARS-CoV2 Human Patient		ND		ND	IGHV1-69 (Human)	IGHJ4 (Human)	IGKV3-20 (Human)	IGKJ2 (Human)	2135	ATGRYTYGYG YYFDY	3340	QQYGSSRT	Xiaojian Han et al., 2020 (https://www.biorxiv.org/content/10.1101/2020.08.19.253369v2.full.pdf+html)
Ab_510G 4	Ab	SARS-CoV2		SARS-CoV2		S; RBD	B-cells; SARS-CoV2 Human Patient		ND		ND	IGHV4-31 (Human)	IGHJ4 (Human)	IGKV1-33 (Human)	IGKJ4 (Human)	2136	ARDYGGNSN YFHY	3341	QQYDTLPL T	Xiaojian Han et al., 2020 (https://www.biorxiv.org/content/10.1101/2020.08.19.253369v2.full.pdf+html)
Ab_510H 10	Ab	SARS-CoV2				S; RBD	B-cells; SARS-CoV2 Human Patient		ND		ND	IGHV2-70 (Human)	IGHJ4 (Human)	IGKV1-39 (Human)	IGKJ2 (Human)	2137	ARIQRGIAAD Y	3342	QQSYSTPR T	Xiaojian Han et al., 2020 (https://www.biorxiv.org/content/10.1101/2020.08.19.253369v2.full.pdf+html)
Ab_510H 2	Ab	SARS-CoV2		SARS-CoV2 (weak)		S; RBD	B-cells; SARS-CoV2 Human Patient		ND		ND	IGHV3-66 (Human)	IGHJ4 (Human)	IGKV1-9 (Human)	IGKJ4 (Human)	2138	ARDKWEGTF DY	3343	QQLNSYPR MT	Xiaojian Han et al., 2020 (https://www.biorxiv.org/content/10.1101/2020.08.19.253369v2.full.pdf+html)
Ab_510H 4	Ab	SARS-CoV2		SARS-CoV2		S; RBD	B-cells; SARS-CoV2 Human Patient		ND		ND	IGHV3-66 (Human)	IGHJ6 (Human)	IGKV3-11 (Human)	IGKJ1 (Human)	2139	AETGWDGM DV	3344	QQRSNWP GT	Xiaojian Han et al., 2020 (https://www.biorxiv.org/content/10.1101/2020.08.19.253369v2.full.pdf+html)
Ab_510H 7	Ab	SARS-CoV2		SARS-CoV2		S; RBD	B-cells; SARS-CoV2 Human Patient		ND		ND	IGHV4-59 (Human)	IGHJ5 (Human)	IGKV1D-13 (Human)	IGKJ4 (Human)	2140	ARHCPWQQL VSNWFDP	3345	QQFNNFLL T	Xiaojian Han et al., 2020 (https://www.biorxiv.org/content/10.1101/2020.08.19.253369v2.full.pdf+html)
Ab_511A 1	Ab	SARS-CoV2				S; RBD	B-cells; SARS-CoV2 Human Patient		ND		ND	IGHV4-31 (Human)	IGHJ6 (Human)	IGKV3-15 (Human)	IGKJ1 (Human)	2141	AREKIRSIAAA GTVYYYGMD V	3346	QQYNNWP PWT	Xiaojian Han et al., 2020 (https://www.biorxiv.org/content/10.1101/2020.08.19.253369v2.full.pdf+html)
Ab_511A 5	Ab	SARS-CoV2		SARS-CoV2		S; RBD	B-cells; SARS-CoV2 Human Patient		ND		ND	IGHV4-31 (Human)	IGHJ2 (Human)	IGLV3-21 (Human)	IGLJ1 (Human)	2142	ARIYRGTMVV VFSDLHWYFD L	3347	QVWDSSA DHYV	Xiaojian Han et al., 2020 (https://www.biorxiv.org/content/10.1101/2020.08.19.253369v2.full.pdf+html)
Ab_511B 11	Ab	SARS-CoV2				S; RBD	B-cells; SARS-CoV2 Human Patient		ND		ND	IGHV3-7 (Human)	IGHJ4 (Human)	IGLV1-40 (Human)	IGLJ1 (Human)	2143	AGLFWYGGY FDY	3348	QSYDRSLS VLYV	Xiaojian Han et al., 2020 (https://www.biorxiv.org/content/10.1101/2020.08.19.253369v2.full.pdf+html)

WO 2022/067091
PCT/US2021/052040

Ab_511B4	Ab	SARS-CoV2		SARS-CoV2		S; RBD	B-cells; SARS-CoV2 Human Patient		ND		ND	IGHV4-59 (Human)	IGHJ5 (Human)	IGKV1D-12 (Human)	IGKJ4 (Human)	2144	ASTYWDSSGYYYGVDY	3349	QQANSFRLT	Xiaojian Han et al., 2020 (https://www.biorxiv.org/content/10.1101/2020.08.19.253369v2.full.pdf+html)
Ab_511D11	Ab	SARS-CoV2				S; RBD	B-cells; SARS-CoV2 Human Patient		ND		ND	IGHV1-18 (Human)	IGHJ6 (Human)	IGKV3-20 (Human)	IGKJ2 (Human)	2145	AVLDYCSGGSSSSGYYNYGMDV	3350	QQYGRSPYT	Xiaojian Han et al., 2020 (https://www.biorxiv.org/content/10.1101/2020.08.19.253369v2.full.pdf+html)
Ab_511E5	Ab	SARS-CoV2				S; RBD	B-cells; SARS-CoV2 Human Patient		ND		ND	IGHV1-2 (Human)	IGHJ2 (Human)	IGLV1-40 (Human)	IGLJ2 (Human)	2146	ARDSLFSRVDWYFDL	3351	NSRDSSGNTVV	Xiaojian Han et al., 2020 (https://www.biorxiv.org/content/10.1101/2020.08.19.253369v2.full.pdf+html)
Ab_511E7	Ab	SARS-CoV2				S; RBD	B-cells; SARS-CoV2 Human Patient		ND		ND	IGHV5-51 (Human)	IGHJ4 (Human)	IGKV1-33 (Human)	IGKJ3 (Human)	2147	ALAVGRGIPTSYFDY	3352	QQYHNLPIT	Xiaojian Han et al., 2020 (https://www.biorxiv.org/content/10.1101/2020.08.19.253369v2.full.pdf+html)
Ab_511E9	Ab	SARS-CoV2				S; RBD	B-cells; SARS-CoV2 Human Patient		ND		ND	IGHV1-18 (Human)	IGHJ4 (Human)	IGKV6-21 (Human)	IGKJ2 (Human)	2148	AREGAGLIIAYDY	3353	HQSSSLPYT	Xiaojian Han et al., 2020 (https://www.biorxiv.org/content/10.1101/2020.08.19.253369v2.full.pdf+html)
Ab_511G5	Ab	SARS-CoV2				S; RBD	B-cells; SARS-CoV2 Human Patient		ND		ND	IGHV1-46 (Human)	IGHJ4 (Human)	IGLV1-47 (Human)	IGLJ3 (Human)	2149	ARDGALYSNPTEFDY	3354	TTWDASRGGWV	Xiaojian Han et al., 2020 (https://www.biorxiv.org/content/10.1101/2020.08.19.253369v2.full.pdf+html)
Ab_511G7	Ab	SARS-CoV2		SARS-CoV2		S; RBD	B-cells; SARS-CoV2 Human Patient		ND		ND	IGHV3-33 (Human)	IGHJ4 (Human)	IGKV1-33 (Human)	IGKJ4 (Human)	2150	AKGGNYGDYLRGFDY	3355	QQYHNVPPA	Xiaojian Han et al., 2020 (https://www.biorxiv.org/content/10.1101/2020.08.19.253369v2.full.pdf+html)
Ab_511H11	Ab	SARS-CoV2				S; RBD	B-cells; SARS-CoV2 Human Patient		ND		ND	IGHV3-33 (Human)	IGHJ6 (Human)	IGKV1-39 (Human)	IGKJ1 (Human)	2151	VRGDHSSGWYGTYYYYMDV	3356	QQSYSSPPWT	Xiaojian Han et al., 2020 (https://www.biorxiv.org/content/10.1101/2020.08.19.253369v2.full.pdf+html)
Ab_511H7	Ab	SARS-CoV2				S; RBD	B-cells; SARS-CoV2 Human Patient		ND		ND	IGHV3-23 (Human)	IGHJ6 (Human)	IGLV1-47 (Human)	IGLJ3 (Human)	2152	ARGLQYYYDTSGYYKDSYYYGVDV	3357	AAWDDSLSGPV	Xiaojian Han et al., 2020 (https://www.biorxiv.org/content/10.1101/2020.08.19.253369v2.full.pdf+html)
Ab_51A1	Ab	SARS-CoV2		SARS-CoV2 (weak)		S; RBD	B-cells; SARS-CoV2 Human Patient		ND		ND	IGHV3-66 (Human)	IGHJ3 (Human)	IGKV1-9 (Human)	IGKJ5 (Human)	2153	ARDLNIAGGFDI	3358	QHLNIDPIT	Xiaojian Han et al., 2020 (https://www.biorxiv.org/content/10.1101/2020.08.19.253369v2.full.pdf+html)
Ab_51A3	Ab	SARS-CoV2				S; RBD	B-cells; SARS-CoV2 Human Patient		ND		ND	IGHV1-18 (Human)	IGHJ4 (Human)	IGKV3-11 (Human)	IGKJ5 (Human)	2154	ARDLAWFGELSESPIEY	3359	QQRGNSIT	Xiaojian Han et al., 2020 (https://www.biorxiv.org/content/10.1101/2020.08.19.253369v2.full.pdf+html)
Ab_51D2	Ab	SARS-CoV2		SARS-CoV2		S; RBD	B-cells; SARS-CoV2 Human Patient		ND		ND	IGHV2-5 (Human)	IGHJ3 (Human)	IGKV1-39 (Human)	IGKJ4 (Human)	2155	AHRLAPDYDFLTGYYNGDDAFDV	3360	QQSYNTLALS	Xiaojian Han et al., 2020 (https://www.biorxiv.org/content/10.1101/2020.08.19.253369v2.full.pdf+html)

Ab_51D3	Ab	SARS-CoV2		SARS-CoV2 (weak)		S; RBD	B-cells; SARS-CoV2 Human Patient		ND		ND	IGHV3-66 (Human)	IGHJ6 (Human)	IGKV1-33 (Human)	IGKJ2 (Human)	2156	AREGLLVGPT GRGLGMDV	3361	QQYADLPY T	Xiaojian Han et al., 2020 (https://www.biorxiv.org/content/10.1101/2020.08.19.253369v2.full.pdf+html)
Ab_51D4	Ab	SARS-CoV2		SARS-CoV2 (weak)		S; RBD	B-cells; SARS-CoV2 Human Patient		ND		ND	IGHV2-70 (Human)	IGHJ4 (Human)	IGKV1-39 (Human)	IGKJ2 (Human)	2157	ARMVVRGV MLDY	3362	QQSYSPPH S	Xiaojian Han et al., 2020 (https://www.biorxiv.org/content/10.1101/2020.08.19.253369v2.full.pdf+html)
Ab_51D7	Ab	SARS-CoV2		SARS-CoV2 (weak)		S; RBD	B-cells; SARS-CoV2 Human Patient		ND		ND	IGHV5-51 (Human)	IGHJ3 (Human)	IGKV1-39 (Human)	IGKJ2 (Human)	2158	ATRTGWTND AFDI	3363	QQSYSTPC T	Xiaojian Han et al., 2020 (https://www.biorxiv.org/content/10.1101/2020.08.19.253369v2.full.pdf+html)
Ab_51E1 0	Ab	SARS-CoV2		SARS-CoV2 (weak)		S; RBD	B-cells; SARS-CoV2 Human Patient		ND		ND	IGHV1-18 (Human)	IGHJ2 (Human)	IGKV4-1 (Human)	IGKJ4 (Human)	2159	ARARQLVLN WYFDL	3364	QQYYITPQ LT	Xiaojian Han et al., 2020 (https://www.biorxiv.org/content/10.1101/2020.08.19.253369v2.full.pdf+html)
Ab_51E1 2	Ab	SARS-CoV2		SARS-CoV2		S; RBD	B-cells; SARS-CoV2 Human Patient		ND		ND	IGHV3-7 (Human)	IGHJ4 (Human)	IGKV1-8 (Human)	IGKJ2 (Human)	2160	ARLMYYYGNF DY	3365	QQYYGYPT	Xiaojian Han et al., 2020 (https://www.biorxiv.org/content/10.1101/2020.08.19.253369v2.full.pdf+html)
Ab_51E7	Ab	SARS-CoV2		SARS-CoV2		S; RBD	B-cells; SARS-CoV2 Human Patient		ND		ND	IGHV3-13 (Human)	IGHJ2 (Human)	IGKV1-39 (Human)	IGKJ1 (Human)	2161	ARVGYYGSGS YPLYWYFDL	3366	QQSYSAPP WT	Xiaojian Han et al., 2020 (https://www.biorxiv.org/content/10.1101/2020.08.19.253369v2.full.pdf+html)
Ab_51F1 1	Ab	SARS-CoV2		SARS-CoV2		S; RBD	B-cells; SARS-CoV2 Human Patient		ND		ND	IGHV1-69 (Human)	IGHJ4 (Human)	IGKV3-20 (Human)	IGKJ2 (Human)	2162	ATGRYTYGYG YYFDY	3367	QQYGSSRT	Xiaojian Han et al., 2020 (https://www.biorxiv.org/content/10.1101/2020.08.19.253369v2.full.pdf+html)
Ab_52C1	Ab	SARS-CoV2				S; RBD	B-cells; SARS-CoV2 Human Patient		ND		ND	IGHV3-66 (Human)	IGHJ4 (Human)	IGLV1-40 (Human)	IGLJ3 (Human)	2163	ARLASDGSGS YLDYFDY	3368	QSYDSSLS GSWV	Xiaojian Han et al., 2020 (https://www.biorxiv.org/content/10.1101/2020.08.19.253369v2.full.pdf+html)
Ab_52C6	Ab	SARS-CoV2		SARS-CoV2		S; RBD	B-cells; SARS-CoV2 Human Patient		ND		ND	IGHV1-69 (Human)	IGHJ6 (Human)	IGLV8-61 (Human)	IGLJ2 (Human)	2164	ATDGGGGSY YYAHYYYGM DV	3369	VLYMGSGI VV	Xiaojian Han et al., 2020 (https://www.biorxiv.org/content/10.1101/2020.08.19.253369v2.full.pdf+html)
Ab_52F7	Ab	SARS-CoV2		SARS-CoV2 (weak)		S; RBD	B-cells; SARS-CoV2 Human Patient		ND		ND	IGHV3-9 (Human)	IGHJ6 (Human)	IGKV2D-30 (Human)	IGKJ2 (Human)	2165	AKDIGVMVP GVTPYGMDV	3370	MQGTHW PPGT	Xiaojian Han et al., 2020 (https://www.biorxiv.org/content/10.1101/2020.08.19.253369v2.full.pdf+html)
Ab_52G9	Ab	SARS-CoV2		SARS-CoV2		S; RBD	B-cells; SARS-CoV2 Human Patient		ND		ND	IGHV3-66 (Human)	IGHJ6 (Human)	IGKV1-33 (Human)	IGKJ1 (Human)	2166	ARDPMRPG MDV	3371	QQYDNLP RT	Xiaojian Han et al., 2020 (https://www.biorxiv.org/content/10.1101/2020.08.19.253369v2.full.pdf+html)
Ab_53C1 0	Ab	SARS-CoV2				S; RBD	B-cells; SARS-CoV2 Human Patient		ND		ND	IGHV3-43 (Human)	IGHJ4 (Human)	IGLV3-21 (Human)	IGLJ1 (Human)	2167	ARESPKLTGY FDY	3372	QVWDSSS DPYV	Xiaojian Han et al., 2020 (https://www.biorxiv.org/content/10.1101/2020.08.19.253369v2.full.pdf+html)

Ab_53C5	Ab	SARS-CoV2				S; RBD	B-cells; SARS-CoV2 Human Patient		ND		ND	IGHV1-69 (Human)	IGHJ4 (Human)	IGKV1-5 (Human)	IGKJ2 (Human)	2168	ARGRYTYGTE GYFDN	3373	QQYNNLYT	Xiaojian Han et al., 2020 (https://www.biorxiv.org/content/10.1101/2020.08.19.253369v2.full.pdf+html)
Ab_53F12	Ab	SARS-CoV2		SARS-CoV2 (weak)		S; RBD	B-cells; SARS-CoV2 Human Patient		ND		ND	IGHV3-66 (Human)	IGHJ6 (Human)	IGKV3-15 (Human)	IGKJ2 (Human)	2169	ARDAVGSYYY GMEV	3374	QHYNNWPLYT	Xiaojian Han et al., 2020 (https://www.biorxiv.org/content/10.1101/2020.08.19.253369v2.full.pdf+html)
Ab_53F9	Ab	SARS-CoV2				S; RBD	B-cells; SARS-CoV2 Human Patient		ND		ND	IGHV3-53 (Human)	IGHJ4 (Human)	IGKV2D-30 (Human)	IGKJ2 (Human)	2170	AREGLVGTTL TFDY	3375	MQGTHW PPGT	Xiaojian Han et al., 2020 (https://www.biorxiv.org/content/10.1101/2020.08.19.253369v2.full.pdf+html)
Ab_53H3	Ab	SARS-CoV2		SARS-CoV2 (weak)		S; RBD	B-cells; SARS-CoV2 Human Patient		ND		ND	IGHV3-66 (Human)	IGHJ3 (Human)	IGKV1-33 (Human)	IGKJ3 (Human)	2171	ARYYGPQGR AFDI	3376	QQYDNLPLT	Xiaojian Han et al., 2020 (https://www.biorxiv.org/content/10.1101/2020.08.19.253369v2.full.pdf+html)
Ab_55A8	Ab	SARS-CoV2		SARS-CoV2 (weak)		S; RBD	B-cells; SARS-CoV2 Human Patient		ND		ND	IGHV1-69 (Human)	IGHJ4 (Human)	IGKV1-5 (Human)	IGKJ2 (Human)	2172	ARGTEYGDYD VSHD	3377	QQYNSYSHT	Xiaojian Han et al., 2020 (https://www.biorxiv.org/content/10.1101/2020.08.19.253369v2.full.pdf+html)
Ab_55C9	Ab	SARS-CoV2		SARS-CoV2 (weak)		S; RBD	B-cells; SARS-CoV2 Human Patient		ND		ND	IGHV3-53 (Human)	IGHJ4 (Human)	IGKV1-39 (Human)	IGKJ2 (Human)	2173	AREGLVGTAL AFDY	3378	QQSYSTPPYT	Xiaojian Han et al., 2020 (https://www.biorxiv.org/content/10.1101/2020.08.19.253369v2.full.pdf+html)
Ab_56C12	Ab	SARS-CoV2		SARS-CoV2		S; RBD	B-cells; SARS-CoV2 Human Patient		ND		ND	IGHV3-30 (Human)	IGHJ5 (Human)	IGKV1-39 (Human)	IGKJ1 (Human)	2174	AKDPTSLYCS GGSCYNNWF DP	3379	QQTYSTPRT	Xiaojian Han et al., 2020 (https://www.biorxiv.org/content/10.1101/2020.08.19.253369v2.full.pdf+html)
Ab_56D7	Ab	SARS-CoV2		SARS-CoV2 (weak)		S; RBD	B-cells; SARS-CoV2 Human Patient		ND		ND	IGHV3-66 (Human)	IGHJ6 (Human)	IGKV1-9 (Human)	IGKJ5 (Human)	2175	ARDLDYYGM DV	3380	QQLNSYPPIT	Xiaojian Han et al., 2020 (https://www.biorxiv.org/content/10.1101/2020.08.19.253369v2.full.pdf+html)
Ab_56E1	Ab	SARS-CoV2		SARS-CoV2		S; RBD	B-cells; SARS-CoV2 Human Patient		ND		ND	IGHV3-30 (Human)	IGHJ3 (Human)	IGLV1-44 (Human)	IGLJ3 (Human)	2176	AGGGVLVTS DPDAFDI	3381	AAWDDSLNGWV	Xiaojian Han et al., 2020 (https://www.biorxiv.org/content/10.1101/2020.08.19.253369v2.full.pdf+html)
Ab_56H11	Ab	SARS-CoV2				S; RBD	B-cells; SARS-CoV2 Human Patient		ND		ND	IGHV4-4 (Human)	IGHJ4 (Human)	IGLV1-44 (Human)	IGLJ3 (Human)	2177	AGEQHIVTTII DY	3382	ATWDDSLNGRV	Xiaojian Han et al., 2020 (https://www.biorxiv.org/content/10.1101/2020.08.19.253369v2.full.pdf+html)
Ab_56H3	Ab	SARS-CoV2		SARS-CoV2		S; RBD	B-cells; SARS-CoV2 Human Patient		ND		ND	IGHV3-66 (Human)	IGHJ4 (Human)	IGKV3-20 (Human)	IGKJ1 (Human)	2178	ARDYGDYYFD Y	3383	QQYGSSPRT	Xiaojian Han et al., 2020 (https://www.biorxiv.org/content/10.1101/2020.08.19.253369v2.full.pdf+html)
Ab_57A6	Ab	SARS-CoV2		SARS-CoV2		S; RBD	B-cells; SARS-CoV2 Human Patient		ND		ND	IGHV5-51 (Human)	IGHJ4 (Human)	IGLV3-19 (Human)	IGLJ3 (Human)	2179	ARQESGWSF DY	3384	NSRDSSGNHWV	Xiaojian Han et al., 2020 (https://www.biorxiv.org/content/10.1101/2020.08.19.253369v2.full.pdf+html)

Ab_57A8	Ab	SARS-CoV2		SARS-CoV2		S; RBD	B-cells; SARS-CoV2 Human Patient		ND		ND	IGHV3-23 (Human)	IGHJ4 (Human)	IGKV1-5 (Human)	IGKJ4 (Human)	2180	AKGQRGSPD FFDY	3385	QQYNSYSP LT	Xiaojian Han et al., 2020 (https://www.biorxiv.org/content/10.1101/2020.08.19.253369v2.full.pdf+html)
Ab_57A9	Ab	SARS-CoV2		SARS-CoV2		S; RBD	B-cells; SARS-CoV2 Human Patient		ND		ND	IGHV1-3 (Human)	IGHJ4 (Human)	IGKV4-1 (Human)	IGKJ1 (Human)	2181	ARAGWELNY	3386	QQYYSFW A	Xiaojian Han et al., 2020 (https://www.biorxiv.org/content/10.1101/2020.08.19.253369v2.full.pdf+html)
Ab_57B8	Ab	SARS-CoV2		SARS-CoV2 (weak)		S; RBD	B-cells; SARS-CoV2 Human Patient		ND		ND	IGHV3-53 (Human)	IGHJ4 (Human)	IGKV1-9 (Human)	IGKJ5 (Human)	2182	ARDLVTWGL DY	3387	QLLNTDPI T	Xiaojian Han et al., 2020 (https://www.biorxiv.org/content/10.1101/2020.08.19.253369v2.full.pdf+html)
Ab_57C4	Ab	SARS-CoV2		SARS-CoV2		S; RBD	B-cells; SARS-CoV2 Human Patient		ND		ND	IGHV3-15 (Human)	IGHJ5 (Human)	IGKV1-39 (Human)	IGKJ4 (Human)	2183	STTNDYGDYS ANY	3388	QQSYSTPL T	Xiaojian Han et al., 2020 (https://www.biorxiv.org/content/10.1101/2020.08.19.253369v2.full.pdf+html)
Ab_57E1 1	Ab	SARS-CoV2		SARS-CoV2		S; RBD	B-cells; SARS-CoV2 Human Patient		ND		ND	IGHV1-8 (Human)	IGHJ5 (Human)	IGLV1-44 (Human)	IGLJ3 (Human)	2184	ARGLWFGDL TRTKYNWFD P	3389	AAWDDSL NGWV	Xiaojian Han et al., 2020 (https://www.biorxiv.org/content/10.1101/2020.08.19.253369v2.full.pdf+html)
Ab_57F7	Ab	SARS-CoV2		SARS-CoV2 (weak)		S; RBD	B-cells; SARS-CoV2 Human Patient		ND		ND	IGHV4-34 (Human)	IGHJ6 (Human)	IGLV1-44 (Human)	IGLJ3 (Human)	2185	ARDDSSSSGV GTGMDV	3390	AVWDDSL NGWV	Xiaojian Han et al., 2020 (https://www.biorxiv.org/content/10.1101/2020.08.19.253369v2.full.pdf+html)
Ab_57G9	Ab	SARS-CoV2		SARS-CoV2		S; RBD	B-cells; SARS-CoV2 Human Patient		ND		ND	IGHV2-70 (Human)	IGHJ4 (Human)	IGKV1-39 (Human)	IGKJ2 (Human)	2186	ARITPHLVYDY	3391	QQSYSIPR T	Xiaojian Han et al., 2020 (https://www.biorxiv.org/content/10.1101/2020.08.19.253369v2.full.pdf+html)
Ab_58A4	Ab	SARS-CoV2				S; RBD	B-cells; SARS-CoV2 Human Patient		ND		ND	IGHV4-59 (Human)	IGHJ5 (Human)	IGKV3-20 (Human)	IGKJ1 (Human)	2187	ARTLGAYYDIL TGFRTPGGW FAP	3392	QQYGSSP WT	Xiaojian Han et al., 2020 (https://www.biorxiv.org/content/10.1101/2020.08.19.253369v2.full.pdf+html)
Ab_58D2	Ab	SARS-CoV2				S; RBD	B-cells; SARS-CoV2 Human Patient		ND		ND	IGHV3-11 (Human)	IGHJ2 (Human)	IGKV3-11 (Human)	IGKJ2 (Human)	2188	ASPLLSHNYG SGSYYNVYWY FEL	3393	QQLGT	Xiaojian Han et al., 2020 (https://www.biorxiv.org/content/10.1101/2020.08.19.253369v2.full.pdf+html)
Ab_58G1	Ab	SARS-CoV2		SARS-CoV2		S; RBD	B-cells; SARS-CoV2 Human Patient		ND		ND	IGHV3-53 (Human)	IGHJ6 (Human)	IGKV1D-12 (Human)	IGKJ4 (Human)	2189	ARDLENGGL DV	3394	QQTNSFPT	Xiaojian Han et al., 2020 (https://www.biorxiv.org/content/10.1101/2020.08.19.253369v2.full.pdf+html)
Ab_58G6	Ab	SARS-CoV2			SARS-CoV2	S; RBD	B-cells; SARS-CoV2 Human Patient		ND		ND	IGHV1-58 (Human)	IGHJ3 (Human)	IGKV3-20 (Human)	IGKJ1 (Human)	2190	AAPNCNSTTC HDGFDI	3395	QQYDNSP WT	Xiaojian Han et al., 2020 (https://www.biorxiv.org/content/10.1101/2020.08.19.253369v2.full.pdf+html)
Ab_59A2	Ab	SARS-CoV2				S; RBD	B-cells; SARS-CoV2 Human Patient		ND		ND	IGHV3-66 (Human)	IGHJ4 (Human)	IGKV1-33 (Human)	IGKJ3 (Human)	2191	ARDLPLHGDY FDY	3396	QQSDNVP VT	Xiaojian Han et al., 2020 (https://www.biorxiv.org/content/10.1101/2020.08.19.253369v2.full.pdf+html)

Ab_59D6	Ab	SARS-CoV2				S; RBD	B-cells; SARS-CoV2 Human Patient		ND		ND	IGHV4-34 (Human)	IGHJ4 (Human)	IGLV1-40 (Human)	IGLJ2 (Human)	2192	ARHRRDYITM IVRPTRLWAF DY	3397	QSYDSALV V	Xiaojian Han et al., 2020 (https://www.biorxiv.org/content/10.1101/2020.08.19.253369v2.full.pdf+html)
Ab_81A11	Ab	SARS-CoV2				S; RBD	B-cells; SARS-CoV2 Human Patient		ND		ND	IGHV1-69 (Human)	IGHJ2 (Human)	IGLV1-40 (Human)	IGLJ2 (Human)	2193	AREAGTTDW YFDL	3398	QSYDSSLS VVV	Xiaojian Han et al., 2020 (https://www.biorxiv.org/content/10.1101/2020.08.19.253369v2.full.pdf+html)
Ab_81C3	Ab	SARS-CoV2		SARS-CoV2 (weak)		S; RBD	B-cells; SARS-CoV2 Human Patient		ND		ND	IGHV4-39 (Human)	IGHJ4 (Human)	IGLV2-14 (Human)	IGLJ1 (Human)	2194	ARHPRFSWR GNDSGYFDY	3399	SSFTSSSTP YV	Xiaojian Han et al., 2020 (https://www.biorxiv.org/content/10.1101/2020.08.19.253369v2.full.pdf+html)
Ab_81C7	Ab	SARS-CoV2				S; RBD	B-cells; SARS-CoV2 Human Patient		ND		ND	IGHV2-5 (Human)	IGHJ4 (Human)	IGLV1-36 (Human)	IGLJ3 (Human)	2195	AHSMVRGVL FGADFDY	3400	AAWDDSL NGPV	Xiaojian Han et al., 2020 (https://www.biorxiv.org/content/10.1101/2020.08.19.253369v2.full.pdf+html)
Ab_81C8	Ab	SARS-CoV2		SARS-CoV2		S; RBD	B-cells; SARS-CoV2 Human Patient		ND		ND	IGHV3-33 (Human)	IGHJ4 (Human)	IGKV1-39 (Human)	IGKJ1 (Human)	2196	ARDGVDFGM VTLFDY	3401	QQSYNTPP WT	Xiaojian Han et al., 2020 (https://www.biorxiv.org/content/10.1101/2020.08.19.253369v2.full.pdf+html)
Ab_81E1	Ab	SARS-CoV2		SARS-CoV2 (weak)		S; RBD	B-cells; SARS-CoV2 Human Patient		ND		ND	IGHV1-24 (Human)	IGHJ4 (Human)	IGLV1-47 (Human)	IGLJ2 (Human)	2197	AITSVARGLR GYFDT	3402	AAWDDSL SRVV	Xiaojian Han et al., 2020 (https://www.biorxiv.org/content/10.1101/2020.08.19.253369v2.full.pdf+html)
Ab_81E10	Ab	SARS-CoV2				S; RBD	B-cells; SARS-CoV2 Human Patient		ND		ND	IGHV1-24 (Human)	IGHJ4 (Human)	IGLV1-47 (Human)	IGLJ2 (Human)	2198	AITSLARGLKG YFDS	3403	AAWDDSL SGVI	Xiaojian Han et al., 2020 (https://www.biorxiv.org/content/10.1101/2020.08.19.253369v2.full.pdf+html)
Ab_81F2	Ab	SARS-CoV2				S; RBD	B-cells; SARS-CoV2 Human Patient		ND		ND	IGHV4-34 (Human)	IGHJ5 (Human)	IGKV2-28 (Human)	IGKJ4 (Human)	2199	ARGWTVPPL WVLNWFDP	3404	MQALQTP RT	Xiaojian Han et al., 2020 (https://www.biorxiv.org/content/10.1101/2020.08.19.253369v2.full.pdf+html)
Ab_82B6	Ab	SARS-CoV2				S; RBD	B-cells; SARS-CoV2 Human Patient		ND		ND	IGHV4-61 (Human)	IGHJ5 (Human)	IGKV2-30 (Human)	IGKJ1 (Human)	2200	AMTYYDYIW GRVDPQFDP	3405	CMQGTH WPPT	Xiaojian Han et al., 2020 (https://www.biorxiv.org/content/10.1101/2020.08.19.253369v2.full.pdf+html)
Ab_82C6	Ab	SARS-CoV2				S; RBD	B-cells; SARS-CoV2 Human Patient		ND		ND	IGHV4-39 (Human)	IGHJ4 (Human)	IGKV2-30 (Human)	IGKJ2 (Human)	2201	ARFITDGYSS GSDS	3406	MQGTHW PMYT	Xiaojian Han et al., 2020 (https://www.biorxiv.org/content/10.1101/2020.08.19.253369v2.full.pdf+html)
Ab_82F6	Ab	SARS-CoV2		SARS-CoV2		S; RBD	B-cells; SARS-CoV2 Human Patient		ND		ND	IGHV3-30 (Human)	IGHJ4 (Human)	IGKV1-33 (Human)	IGKJ4 (Human)	2202	AKQASPYCSG GSCYSGNFDY	3407	QQHDNVP LT	Xiaojian Han et al., 2020 (https://www.biorxiv.org/content/10.1101/2020.08.19.253369v2.full.pdf+html)
Acharya et al., 2020	Ab	HIV Glycans, SARS-CoV2 Glycans				S Glycans	B-cells; HIV Human Patient		Various		Various	Various	Various	Various	Various		Various		Various	Priyamvada Acharya et al., 2020 (https://www.biorxiv.org/content/10.1101/2020.06.30.178897v1);Wilton Williams et al., 2020 (https://www.biorxiv.org/content/10.1101/2020.06.30.178921v1)

B38	Ab	SARS-CoV2		SARS-CoV2		S; RBD	B-cells; SARS-CoV2 Human Patient	124	EVQLVESGGGLVQPGGSLRLSCAASGFIVSSNYMSWVRQAPGKGLEWVSVIYSGGSTYYADSVKGRFTISRHNSKNTLYLQMNSLRAEDTAVYYCAREAYGMDVWGQGTTVTVSS	1206	DIVMTQSPSFLSASVGDRVTITCRASQGISSYLAWYQQKPGKAPKLLIYAASTLQSGVPSRFSGSGSGTEFTLTISSLQPEDFATYYCQQLNSYPPYTFGQGTKLEIK	IGHV3-53 (Human)	IGHJ6 (Human)	IGKV1-9 (Human)	IGKJ2 (Human)	2203	AREAYGMDV	3408	QQLNSYPPYT	Yan Wu et al., 2020 (https://science.sciencemag.org/content/early/2020/05/12/science.abc2241)
BD-236	Ab	SARS-CoV2		SARS-CoV2		S; RBD	B-cells; SARS-CoV2 Human Patient	125	EVQLVESGGGLIQPGGSLRLSCAASGITVSSNYMSWVRQAPGKGLEWVSVIYSGGSTDYADSVKGRFTISRDKSKNTLYLQMNSLRAEDTAVYYCARDLGEAGGMDVWGQGTTVTVSS		ND	IGHV3-53 (Human)	IGHJ6 (Human)	ND	ND	2204	ARDLGEAGGMDV		ND	Shuo Du et al., 2020 (https://www.biorxiv.org/content/10.1101/2020.07.09.195263v1)
BD-368-2	Ab	SARS-CoV2		SARS-CoV2		S; RBD	B-cells; SARS-CoV2 Human Patient		ND		ND	ND	ND	ND	ND		ND		ND	Shuo Du et al., 2020 (https://www.biorxiv.org/content/10.1101/2020.07.09.195263v1)
BD-494	Ab	SARS-CoV2		SARS-CoV2		S; probably RBD (implied by clustering)	Phage Display Library (Antibody, human, immune - CoV2)		ND		ND	IGHV3-53 (Human)	IGHJ6 (Human)	IGKV1-9 (Human)	IGKJ3 (Human)	2205	ARDLVVYGMDV	3409	QQLNSYPFT	Yunlong Cao et al., 2020 (https://www.sciencedirect.com/science/article/pii/S0092867420306206)
BD-498	Ab	SARS-CoV2		SARS-CoV2		S; probably RBD (implied by clustering)	Phage Display Library (Antibody, human, immune - CoV2)		ND		ND	IGHV3-66 (Human)	IGHJ6 (Human)	IGKV1-9 (Human)	IGKJ5 (Human)	2206	ARDLVVYGMDV	3410	QQLNSYPLT	Yunlong Cao et al., 2020 (https://www.sciencedirect.com/science/article/pii/S0092867420306206)
BD-500	Ab	SARS-CoV2		SARS-CoV2		S; probably RBD (implied by clustering)	B-cells; SARS-CoV2 Human Patient		ND		ND	IGHV3-53 (Human)	IGHJ6 (Human)	IGKV1-39 (Human)	IGKJ5 (Human)	2207	ARDAMSYGMDV	3411	QQSYSTPPDT	Yunlong Cao et al., 2020 (https://www.sciencedirect.com/science/article/pii/S0092867420306206)
BD-503	Ab	SARS-CoV2		SARS-CoV2		S; RBD	B-cells; SARS-CoV2 Human Patient		ND		ND	IGHV3-53 (Human)	IGHJ6 (Human)	IGKV1-39 (Human)	IGKJ3 (Human)	2208	ARDAAVYGIDV	3412	QQSYTTPLFT	Yunlong Cao et al., 2020 (https://www.sciencedirect.com/science/article/pii/S0092867420306206)
BD-504	Ab	SARS-CoV2		SARS-CoV2		S; RBD	B-cells; SARS-CoV2 Human Patient		ND		ND	IGHV3-66 (Human)	IGHJ6 (Human)	IGKV1-9 (Human)	IGKJ3 (Human)	2209	ARDLISRGMDV	3413	QQSYTTPLFT	Yunlong Cao et al., 2020 (https://www.sciencedirect.com/science/article/pii/S0092867420306206)
BD-505	Ab	SARS-CoV2		SARS-CoV2		S; RBD	B-cells; SARS-CoV2 Human Patient		ND		ND	IGHV3-53 (Human)	IGHJ6 (Human)	IGKV1-33 (Human)	IGKJ5 (Human)	2210	ARDRVVYGMDV	3414	HQYDNLPPT	Yunlong Cao et al., 2020 (https://www.sciencedirect.com/science/article/pii/S0092867420306206)
BD-506	Ab	SARS-CoV2		SARS-CoV2		S; RBD	B-cells; SARS-CoV2 Human Patient		ND		ND	IGHV3-53 (Human)	IGHJ6 (Human)	IGKV1-9 (Human)	IGKJ4 (Human)	2211	ARDLVSYGMDV	3415	QQLNSYPLT	Yunlong Cao et al., 2020 (https://www.sciencedirect.com/science/article/pii/S0092867420306206)
BD-507	Ab	SARS-CoV2		SARS-CoV2		S; RBD	B-cells; SARS-CoV2 Human Patient		ND		ND	IGHV3-53 (Human)	IGHJ6 (Human)	IGKV1-9 (Human)	IGKJ3 (Human)	2212	ARDLVVYGMDV	3416	QQLNSNPPIT	Yunlong Cao et al., 2020 (https://www.sciencedirect.com/science/article/pii/S0092867420306206)
BD-508	Ab	SARS-CoV2		SARS-CoV2		S; RBD	B-cells; SARS-CoV2 Human Patient		ND		ND	IGHV3-53 (Human)	IGHJ6 (Human)	IGKV1-39 (Human)	IGKJ2 (Human)	2213	ARDAQNYGMDV	3417	QQSYSTPPYT	Yunlong Cao et al., 2020 (https://www.sciencedirect.com/science/article/pii/S0092867420306206)
BD-515	Ab	SARS-CoV2		SARS-CoV2		S; RBD	B-cells; SARS-CoV2 Human Patient		ND		ND	IGHV3-66 (Human)	IGHJ4 (Human)	IGKV1-39 (Human)	IGKJ5 (Human)		ND		ND	Yunlong Cao et al., 2020 (https://www.sciencedirect.com/science/article/pii/S0092867420306206)

BD-604	Ab	SARS-CoV2		SARS-CoV2		S; RBD	B-cells; SARS-CoV2 Human Patient	126	EVQLVESGGGLIQPGGSLRLSCAASGIIV SSNYMTWVRQAPGKGLEWVSVIYSGG STFYADSVKGRFTISRDNSKNTLYLQMSS LRAEDTAVYYCARDLGPYGMDVWGQG TTVTVSS		ND	IGHV3-53 (Human)	IGHJ6 (Human)	IGKV1-9 (Human)	IGKJ2 (Human)	2214	ARDLGPYGM DV		ND	Shuo Du et al., 2020 (https://www.biorxiv.org/content/10.1101/2020.07.09.195263v1)
BD-629	Ab	SARS-CoV2		SARS-CoV2		S; RBD	B-cells; SARS-CoV2 Human Patient	127	EVQLVESGGGLIQPGGSLRLSCAASEFIV SRNYMSWVRQAPGKGLEWVSVIYSGG STYYADSVKGRFTISRDNSKNTLNLQMN SLRAEDTAVYYCARDYGDYYFDYWGQG TLVTVSS		ND	IGHV3-53 (Human)	IGHJ4 (Human)	IGKV3-20 (Human)	IGKJ1 (Human)	2215	ARDYGDYYFD Y		ND	Shuo Du et al., 2020 (https://www.biorxiv.org/content/10.1101/2020.07.09.195263v1)
BD23	Ab	SARS-CoV2		SARS-CoV2		S; RBD	B-cells; SARS-CoV2 Human Patient	128	QVQLVQSGSELKKPGASVKVSCKASGYT FTSYAMNWVRQAPGQGLEWMGWINT NTGNPTYAQGFTGRFVFSLDTSVSTAYL QISSLKAEDTAVYYCARPQGGSSWYRDY YYGMDVWGQGTTVTVSS	1207	DIQMTQSPSTLSASVGDRVTITCRASQ SISSWLAWYQQKPGKAPKLLIYKASSL ESGVPSRFSGSGSGTEFTLTISSLQPDD FATYYCQQYNSYPYTFGQGTKLEIK	IGHV7-4-1 (Human)	IGHJ6 (Human)	IGKV1-5 (Human)	IGKJ2 (Human)	2216	ARPQGGSSW YRDYYYGMD V	3418	QQYNSYPY T	Yunlong Cao et al., 2020 (https://www.sciencedirect.com/science/article/pii/S0092867420306206)
Bertoglio et al., 2020	Ab	SARS-CoV2		SARS-CoV2		S; RBD	Phage Display Library (Antibody, human, non-immune)		17	17	ND	Various	Various	Various	Various		Various		Various	Federico Bertoglio et al., 2020 (https://www.biorxiv.org/content/10.1101/2020.06.05.135921v1)
C002	Ab	SARS-CoV2	SARS-CoV1	SARS-CoV2	SARS-CoV1	S; RBD	B-cells; SARS-CoV2 Human Patient	129	EVQLVESGGGVVQPGRSLRLSCAASGFT FSIYGMHWVRQAPGKGLEWVAVISYD GSNKYYADSVKGRFTISRDNSKNTLYLQ MNSLRAEDTAVYYCAKEGRPSDIVVVVA FDYWGQGTLVTVSS	1208	DIQLTQSPSSLSASVGDRVTITCRASQS ISSYLNWYQQKPGKAPKLLIYAASSLQS GVPSRFSGSGSGTDFTLTISSLQPEDFA TYYCQQSYSTPRTFGQGTKVEIK	IGHV3-30 (Human)	IGHJ4 (Human)	IGKV1-39 (Human)	IGKJ1 (Human)	2217	AKEGRPSDIV VVVAFDY	3419	QQSYSTPR T	Davide Robbiani et al., 2020 (https://www.nature.com/articles/s41586-020-2456-9)
C003	Ab	SARS-CoV2	SARS-CoV1	SARS-CoV2 (weak)	SARS-CoV1	S; RBD	B-cells; SARS-CoV2 Human Patient	130	EVQLVESGGGLIQPGGSLRLSCAASGFT VSSNYMSWVRQAPGKGLEWVSVIYSG GSTYYADSVKGRFTISRDNSKNTLYLQM NSLRAGDTAVYYCARDYGDFYFDYWGQ GTLVTVSS	1209	EIVLTQSPGTLSLSPGERATLSCRASQS VSSTYLAWYQQKPGQAPRLLIYGASSR ATGIPDRFSGSGSGTDFTLTISRLEPED FAVYYCQQYGSSPRTFGQGTKLEIK	IGHV3-53 (Human)	IGHJ4 (Human)	IGKV3-20 (Human)	IGKJ2 (Human)	2218	ARDYGDFYFD Y	3420	QQYGSSPR T	Davide Robbiani et al., 2020 (https://www.nature.com/articles/s41586-020-2456-9)
C004	Ab	SARS-CoV2	SARS-CoV1	SARS-CoV2	SARS-CoV1	S; RBD	B-cells; SARS-CoV2 Human Patient	131	QVQLVQSGAEVKKPGASVKVSCKASGY TFTGYYMHWVRQAPGQGLEWMGWI NPISGGTNYAQKFQGRVTMTRDTSISTA YMELSRLRSDDTAVYYCASPASRGYSGY DHGYYYYMDVWGKGTTVTVSS	1210	AIRMTQSPSSLSASVGDRVTITCQASQ DISNYLNWYQQKPGKAPKLLIYDASNL ETGVPSRFSGSGSGTDFTFTISSLQPED IATYYCQQYDNLPITFGQGTRLEIK	IGHV1-2 (Human)	IGHJ6 (Human)	IGKV1-33 (Human)	IGKJ5 (Human)	2219	ASPASRGYSG YDHGYYYYM DV	3421	QQYDNLPI T	Davide Robbiani et al., 2020 (https://www.nature.com/articles/s41586-020-2456-9)
C005	Ab	SARS-CoV2	SARS-CoV1	SARS-CoV2	SARS-CoV1	S; RBD	B-cells; SARS-CoV2 Human Patient	132	QVQLVQSGPEVKKPGTSVKVSCKASGFT FTSSAVQWVRQARGQRLEWIGWIVVG SGNTNYAQKFQERVTITRDMSTSTAYM ELSSLRSEDTAVYYCAAPHCSGGSCLDAF DIWGQGTMVTVSS	1211	EIVLTQSPGTLSLSPGERATLSCRASQS VRSSYLAWYQQKPGQAPRLLIYGASSR ATGIPDRFSGSGSGTDFTLTISRLEPED FAVYYCQQYGSSPWTFGQGTKVEIK	IGHV1-58 (Human)	IGHJ3 (Human)	IGKV3-20 (Human)	IGKJ1 (Human)	2220	AAPHCSGGSC LDAFDI	3422	QQYGSSP WT	Davide Robbiani et al., 2020 (https://www.nature.com/articles/s41586-020-2456-9)
C006	Ab	SARS-CoV2	SARS-CoV1	SARS-CoV2 (weak)	SARS-CoV1	S; RBD	B-cells; SARS-CoV2 Human Patient	133	QVQLVESGGGLVKPGGSLRLSCAASGFI FSDYCMSWIRRAPGKGLEWLSYISNSGT TRYYADSVKGRFTISRDNGRNSLYLQMD SLSAEDTAVYYCARRGDGSSSIYYYNYM DVWGKGTTVTVSS	1212	QSVLTQPPSASGTPGQRVTVSCSGSSS NIGSNTVNWYQQLPGTAPKLLIYSNN QRPSGVPDRFSGSKSGTSASLAISGLQ SEDEADYFCAAWDDSLNGPVFGGGT KLTVL	IGHV3-11 (Human)	IGHJ6 (Human)	IGLV1-44 (Human)	IGLJ3 (Human)	2221	ARRGDGSSSI YYYNYMDV	3423	AAWDDSL NGPV	Davide Robbiani et al., 2020 (https://www.nature.com/articles/s41586-020-2456-9)
C008	Ab	SARS-CoV2	SARS-CoV1	SARS-CoV2 (weak)	SARS-CoV1	S; RBD	B-cells; SARS-CoV2 Human Patient	134	EVQLVESGGGVVQPGRSLRLSCAASGFT FSSYGMHWVRQAPGKGLEWVTVISYD GRNKYYADSVKGRFTISRDNSKNTLYLQ MNSLRAEDTAVYYCAREFGDPEWYFDY WGQGTLVTVSS	1213	DIQMTQSPSTLSASVGDRVTITCRANQ SISSWLAWYQQKPGKAPKLLIYKASSL ESGVPSRFSGSGSGTEFTLTISSLQPDD FATYYCQQYNSYWTFGQGTKVEIK	IGHV3-30 (Human)	IGHJ4 (Human)	IGKV1-5 (Human)	IGKJ1 (Human)	2222	AREFGDPEW YFDY	3424	QQYNSYW T	Davide Robbiani et al., 2020 (https://www.nature.com/articles/s41586-020-2456-9)
C009	Ab	SARS-CoV2	SARS-CoV1	SARS-CoV2	SARS-CoV1	S; RBD	B-cells; SARS-CoV2 Human Patient	135	QVQLVQSGAEVKKPGASVKVSCMASGY TFTGYYMHWVRQAPGQGLEWMGWI NPNSGGTNYAQKFQGRVTMTRDTSIST AYMELSRLRSDDTAVYYCARDSPFSALG ASNDYWGQGTLVTVSS	1214	QSALTQPPSASGSPGQSVTISCTGTSS DVGGYNYVSWYQQHPGKAPKLMIYE VSKRPSGVPDRFSGSKSGNTASLTVSG LQAEDEAEYYCSSDAGSNNVVFGGGT KLTVL	IGHV1-2 (Human)	IGHJ4 (Human)	IGLV2-8 (Human)	IGLJ3 (Human)	2223	ARDSPFSALG ASNDY	3425	SSDAGSNN VV	Davide Robbiani et al., 2020 (https://www.nature.com/articles/s41586-020-2456-9)
C010	Ab	SARS-CoV2	SARS-CoV1		SARS-CoV1, SARS-CoV2	S; RBD	B-cells; SARS-CoV2 Human Patient	136	EVQLVESGGGVVQPGRSLRLSCAASGFT FSSYAMHWVRQAPAKGLEWVAVILYD GSGKYYADSVKGRFTISRDNSKNTLYLQ MNSLRAEDTAVYYCARDGIVDTALVTW FDYWGQGTLVTVSS	1215	DIQLTQSPSSLSASVGDRVTITCRASQS ISTYLNWYQQKPGKAPKLLIYAASSLQS GVPSRFSGSGSGTDFTLTISSLQPEDFA TYYCQQSYSTPPWTFGQGTKVEIK	IGHV3-30 (Human)	IGHJ4 (Human)	IGKV1-39 (Human)	IGKJ1 (Human)	2224	ARDGIVDTAL VTWFDY	3426	QQSYSTPP WT	Davide Robbiani et al., 2020 (https://www.nature.com/articles/s41586-020-2456-9)
C013	Ab	SARS-CoV2	SARS-CoV1	SARS-CoV2 (weak)	SARS-CoV1	S; RBD	B-cells; SARS-CoV2 Human Patient	137	QVQLVQSGAEVKKPGSSVKVSCKASGG TFSSYAISWVRQAPGQGLEWMGGIIPIF GTANYAQKFQGRVTITADESTSTAYMEL SSLRSEDTAVYYCARGNRLLYCSSTSCYL DAVRQGYYYYYYMDVWGKGTTVTVSS	1216	EIVLTQSPATLSLSPGERATLSCRASQS VSSYLAWYQQKPGQAPRLLIYDASNR ATGIPARFSGSGSGTDFTLTISSLEPEDF AVYYCQQRSNWPLTFGGGTKVEIK	IGHV1-69 (Human)	IGHJ6 (Human)	IGKV3-11 (Human)	IGKJ4 (Human)	2225	ARGNRLLYCS STSCYLDAVR QGYYYYYYM DV	3427	QQRSNWP LT	Davide Robbiani et al., 2020 (https://www.nature.com/articles/s41586-020-2456-9)
C016	Ab	SARS-CoV2	SARS-CoV1		SARS-CoV1, SARS-CoV2	S; RBD	B-cells; SARS-CoV2 Human Patient	138	EVQLVESGGGVVQPGRSLRLSCAASGFT FSRYGMHWVRQAPGKGLEWVAVISYD GSNKYYADSVKGRFTISRDNSKNTLYLQ MNSLRAEDTAVYYCAKVTAPYCSGGSCY GGNFDYWGQGTLVTVSS	1217	AIRMTQSPSSLSASVGDRVTITCQASQ DISNYLNWYQQKPGKAPKLLIYDASNL ETGVPSRFSGSGSGTDFTFTINSLQPED IATYYCQQYDNLPPTFGGGTKVEIK	IGHV3-30 (Human)	IGHJ4 (Human)	IGKV1-33 (Human)	IGKJ4 (Human)	2226	AKVTAPYCSG GSCYGGNFDY	3428	QQYDNLP PT	Davide Robbiani et al., 2020 (https://www.nature.com/articles/s41586-020-2456-9)

C017	Ab	SARS-CoV2	SARS-CoV1	SARS-CoV2	SARS-CoV1	S; RBD	B-cells; SARS-CoV2 Human Patient	139	EVQLVESGGGLVQPGRSLRLSCAASGFT FDDYAMHWVRQAPGKGLEWVSGISW NSGTIGYADSVKGRFTISRDNAKNSLYLQ MNSLRAEDTAFYYCAKAGVRGIAAAGP DLNFDHWGQGTLVTVSS	1218	EIVLTQSPATLSLSPGERATLSCRASQS VSSYLAWYQQKPGQAPRLLIYDASNR ATGIPARFSGSGSGTDFTLTISSLEPEDF AVYYCQQRITFGQGTRLEIK	IGHV3-9 (Human)	IGHJ4 (Human)	IGKV3-11 (Human)	IGKJ5 (Human)	2227	AKAGVRGIAA AGPDLNFDH	3429	QQRIT	Davide Robbiani et al., 2020 (https://www.nature.com/articles/s41586-020-2456-9)
C018	Ab	SARS-CoV2	SARS-CoV1		SARS-CoV1, SARS-CoV2	S; RBD	B-cells; SARS-CoV2 Human Patient	140	EVQLVESGGGVVQPGRSLRLSCAASGFT FSNYAIHWVRQAPGKGLEWVAVISYDG SNKYYADSVKGRFTISRDNSKNTLYLQM NSLRAEDTAVYYCARDFDDSSFWAFDY WGQGTLVTVSS	1219	DIQLTQSPSSLSASVGDRVTITCRASQS IRSYLNWYQQKPGKAPKLLIYAASSLQ SGVPSRFSGSGSGTDFTLTISSLQPDDF ATYYCQQSYSTPPATFGQGTKLEIK	IGHV3-30 (Human)	IGHJ4 (Human)	IGKV1-39 (Human)	IGKJ2 (Human)	2228	ARDFDDSSF WAFDY	3430	QQSYSTPP AT	Davide Robbiani et al., 2020 (https://www.nature.com/articles/s41586-020-2456-9)
C019	Ab	SARS-CoV2	SARS-CoV1		SARS-CoV1, SARS-CoV2	S; RBD	B-cells; SARS-CoV2 Human Patient	141	QVQLVQSGAEVKKPGASVKVSCKASGY TFTSYYMHWVRQAPGQGLEWMGIINP SGGSTSYAQKFQGRVTMTRDTSTSTVY MELSSLRSEDTAVYYCARVPREGTPGFD PWGQGTLVTVSS	1220	SYELTQPPSVSVAPGKTARITCGENNI GSKSVHWYQQKPGQAPVLVIYYDSDR PSGIPERFSGSNSGNTATLTINRVEAG DEADYYCQVWDSSSDHVVFGGGTKL TVL	IGHV1-46 (Human)	IGHJ5 (Human)	IGLV3-21 (Human)	IGLJ3 (Human)	2229	ARVPREGTPG FDP	3431	QVWDSSS DHVV	Davide Robbiani et al., 2020 (https://www.nature.com/articles/s41586-020-2456-9)
C021	Ab	SARS-CoV2	SARS-CoV1		SARS-CoV1, SARS-CoV2	S; RBD	B-cells; SARS-CoV2 Human Patient	142	QVQLQESGPGLVKPSQTLSLTCTVSGGSI SSGGYYWSWIRQHPGKGLEWIGYIYYS GSTYYNPSLKSRVTISVDTSKNQFSLKLSS VTAADTAVYYCARVWQYYDSSGSFDYW GQGTLVTVSS	1221	DIVMTQSPLSLPVTPGEPASISCRSSQS LLHSNGYNYLDWYLQKPGQSPQLLIYL GSNRASGVPDRFSGSGSGTDFTLKISR VEAEDVGVYYCMQALQTPFTFGPGTK VDIK	IGHV4-31 (Human)	IGHJ4 (Human)	IGKV2-28 (Human)	IGKJ3 (Human)	2230	ARVWQYYDS SGSFDY	3432	MQALQTP FT	Davide Robbiani et al., 2020 (https://www.nature.com/articles/s41586-020-2456-9)
C022	Ab	SARS-CoV1, SARS-CoV2		SARS-CoV2		S; RBD	B-cells; SARS-CoV2 Human Patient	143	QVQLQESGPGLVKPSETLSVTCTVSGGSI SSSRYYWGWIRQPPGKGLEWIGSIYYSG STYYNPSLKSRVTISVDTSKNQFSLKLSSV TAADTAVYYCARHAAAYYDRSGYYFIEYF QHWGQGTLVTVSS	1222	DIQMTQSPSTLSASVGDSVTITCRASQ SISSWLAWYQQKPGKAPKLLIYKASSL ESGVPSRFSGSGSGTEFTLTISSLQPDD FATYYCQQYNNYRYTFGQGTKLEIK	IGHV4-39 (Human)	IGHJ1 (Human)	IGKV1-5 (Human)	IGKJ2 (Human)	2231	ARHAAAYYDR SGYYFIEYFQH	3433	QQYNNYR YT	Davide Robbiani et al., 2020 (https://www.nature.com/articles/s41586-020-2456-9)
C027	Ab	SARS-CoV1 (weak), SARS-CoV2			SARS-CoV2	S; RBD	B-cells; SARS-CoV2 Human Patient	144	EVQLVESGGGVVQPGRSLRLSCAASGFT FSSYGMHWVRQAPGKGLEWVAVISYD GSNKYYADSVKGRFTISRDNSKNTLYLQ MNSLRAEDTAVYYCAKASGIYCSGGDCY SYYFDYWGQGTLVTVSS	1223	DIQMTQSPSTLSASVGDRVTITCRASQ SISSWLAWYQQKPGKAPKLLIYKASSL ESGVPSRFSGSGSGTEFTLTISSLQPDD FATYYCQQYNSYSTFGQGTKVEIK	IGHV3-30 (Human)	IGHJ4 (Human)	IGKV1-5 (Human)	IGKJ1 (Human)	2232	AKASGIYCSG GDCYSYYFDY	3434	QQYNSYST	Davide Robbiani et al., 2020 (https://www.nature.com/articles/s41586-020-2456-9)
C029	Ab	SARS-CoV2	SARS-CoV1		SARS-CoV1, SARS-CoV2	S; RBD	B-cells; SARS-CoV2 Human Patient	145	QVQLQESGPGLVKPSQTLSLTCTVSGGSI SSGGYYWSWIRQHPGKGLEWIGYIYYS GSTYYNPSLKSRVTISVDTSKNQFSLKLSS VTAADTAVYYCARTMYYYDSSGSFDYW GQGTLVTVSS	1224	DIVMTQSPLSLPVTPGEPASISCRSSQS LLHSNGYNYLDWYLQKPGQSPQLLIYL GSNRASGVPDRFSGSGSGTDFTLKISR VEAEDVGVYYCMQALQTPHTFGGGT KVEIK	IGHV4-31 (Human)	IGHJ4 (Human)	IGKV2-28 (Human)	IGKJ4 (Human)	2233	ARTMYYYDSS GSFDY	3435	MQALQTP HT	Davide Robbiani et al., 2020 (https://www.nature.com/articles/s41586-020-2456-9)
C030	Ab	SARS-CoV2	SARS-CoV1		SARS-CoV1, SARS-CoV2	S; RBD	B-cells; SARS-CoV2 Human Patient	146	EVQLVESGGGVVQPGRSLRLSCAASGFT FSSYGMHWVRQAPGKGLEWVAVISYD GSNKYYADSVKGRFTISRDNSKNTLYLQ MNSLRAEDTAVYYCAKASGIYCSGGNCY SYYFDYWGQGTLVTVSS	1225	DIQMTQSPSTLSASVGDRVTITCRASQ SISSWLAWYQQKPGKAPKLLIYKASSL ESGVPSRFSGSGSGTEFTLTISSLQPDD FATYYCQQYNSYSTFGQGTKVEIK	IGHV3-30 (Human)	IGHJ4 (Human)	IGKV1-5 (Human)	IGKJ1 (Human)	2234	AKASGIYCSG GNCYSYYFDY	3436	QQYNSYST	Davide Robbiani et al., 2020 (https://www.nature.com/articles/s41586-020-2456-9)
C031	Ab	SARS-CoV2	SARS-CoV1		SARS-CoV1, SARS-CoV2	S; RBD	B-cells; SARS-CoV2 Human Patient	147	EVQLVESGGGLVQPGGSLRLSCAASGFT FSSYDMHWVRQATGKGLEWVSAIGTA GDTYYPGSVKGRFTISRENAKNSLYLQM NSLRAGDTAVYYCARVGYDSSGYSGWY FDLWGRGTLVTVSS	1226	DIQMTQSPSSLSASVGDRVTITCRASQ SISSYLNWYQQKPGKAPKVLIYAASSL QSGVPSRFSGSGSGTDFTLTISSLQPED FATYYCQQSYSTPPLTFGGGTKVEIK	IGHV3-13 (Human)	IGHJ2 (Human)	IGKV1-39 (Human)	IGKJ4 (Human)	2235	ARVGYDSSGY SGWYFDL	3437	QQSYSTPP LT	Davide Robbiani et al., 2020 (https://www.nature.com/articles/s41586-020-2456-9)
C101	Ab	SARS-CoV2	SARS-CoV1	SARS-CoV2	SARS-CoV1	S; RBD	B-cells; SARS-CoV2 Human Patient	148	QVQLVESGGGLIQPGGSLRLSCAASGFI VSSNYMSWVRQAPGKGLEWVSVIYSG GSTFYTDSVKGRFTISRDNSKNTLYLQM NSLRAEDTAVYYCVRDYGDFYFDYWGQ GTLVTVSS	1227	EIVLTQSPGTLSLSPGERATLSCRASQS VSSSYLAWYQQKPGQAPRLLIYGASSR ATGIPDRFSGSGGSETDFTLTISRLEPED CAVYYCQQYGSSPRTFGQGTKVEIK	IGHV3-53 (Human)	IGHJ4 (Human)	IGKV3-20 (Human)	IGKJ1 (Human)	2236	VRDYGDFYFD Y	3438	QQYGSSPR T	Davide Robbiani et al., 2020 (https://www.nature.com/articles/s41586-020-2456-9)
C102	Ab	SARS-CoV2	SARS-CoV1	SARS-CoV2	SARS-CoV1	S; RBD	B-cells; SARS-CoV2 Human Patient	149	QVQLVESGGGLIQPGGSLRLSCAASGFI VSSNYMSWVRQAPGKGLEWVSVIYSG GSTFYADSVKGRFTISRDNSKNTLYLQM NSLRAEDTAVYYCARDYGDYYFDYWGQ GTLVTVSS	1228	EIVLTQSPGTLSLSPGERATLSCRASQS VSSSYLAWYQQKPGQAPRLLIYGASSR ATGIPDRFSGSGSGTDFTLTISRLEPED FAVYYCQQYGSSPRTFGQGTKVEIK	IGHV3-53 (Human)	IGHJ4 (Human)	IGKV3-20 (Human)	IGKJ1 (Human)	2237	ARDYGDYYFD Y	3439	QQYGSSPR T	Davide Robbiani et al., 2020 (https://www.nature.com/articles/s41586-020-2456-9)
C103	Ab	SARS-CoV2	SARS-CoV1	SARS-CoV2	SARS-CoV1	S; RBD	B-cells; SARS-CoV2 Human Patient	150	QVQLQQWGAGLLKPSETLSLTCAVSGG SLSGFYWTWIRQPPGKGLEWIGETNHF GSTGYKPSLKSRVTISVDMSRNQFSLKVT SVTAADTAVYYCARKPLLYSDFSPGAFDI WGQGTMVTVSS	1229	EIVLTQSPGTLSLSPGERATLSCRASQT VTANYLAWYQQKPGQAPRLLIYGASK RATGIPDRFSGSGSGTDFTLSISRLEPE DFAVYYCQQYTTTPRTFGGGTKVEIK	IGHV4-34 (Human)	IGHJ3 (Human)	IGKV3-20 (Human)	IGKJ4 (Human)	2238	ARKPLLYSDFS PGAFDI	3440	QQYTTTPR T	Davide Robbiani et al., 2020 (https://www.nature.com/articles/s41586-020-2456-9)
C104	Ab	SARS-CoV2	SARS-CoV1	SARS-CoV2	SARS-CoV1	S; RBD	B-cells; SARS-CoV2 Human Patient	151	QVQLQQWGAGLLKPSETLSLSCAVYGG SLSGYYWSWIRQPPGKGLEWIGEINHF GSTGYNPSLKSRVTISVDTSKSQFSVKLSS VTAADTAVYYCARKPLLYSNLSPGAFDI WGQGTMVTVSS	1230	EIVLTQSPGTVSLSPGERATLSCWASQ SVSASYLAWYQQKPGQAPRLLIYGASS RATGIPDRFSGSGSGTDFTLTISRLEPE DFAVYYCQQYGTTPRTFGGGTKVEIK	IGHV4-34 (Human)	IGHJ3 (Human)	IGKV3-20 (Human)	IGKJ4 (Human)	2239	ARKPLLYSNLS PGAFDI	3441	QQYGTTPR T	Davide Robbiani et al., 2020 (https://www.nature.com/articles/s41586-020-2456-9)

C105	Ab	SARS-CoV2	SARS-CoV1	SARS-CoV2	SARS-CoV1	S; RBD	B-cells; SARS-CoV2 Human Patient	152	QVQLVESGGGLIQPGGSLRLSCAASGFT VSSNYMSWVRQAPGKGLEWVSVIYSG GSTYYADSVKGRFTISRDNSKNTLYLQM NSLRAEDTAVYYCARGEGWELPYDYWG QGTLVTVSS	1231	QSALTQPPSASGSPGQSVTISCTGTSS DVGGYKYVSWYQQHPGKAPKLMIYE VSKRPSGVPDRFSGSKSGNTASLTVSG LQAEDEADYYCSSYEGSNNFVVFGGG TKLTVL	IGHV3-53 (Human)	IGHJ4 (Human)	IGLV2-8 (Human)	IGLJ3 (Human)	2240	ARGEGWELP YDY	3442	SSYEGSNN FVV	Davide Robbiani et al., 2020 (https://www.nature.com/articles/s41586-020-2456-9);Christopher Barnes et al., 2020 (https://www.sciencedirect.com/science/article/pii/S0092867420307571)
C106	Ab	SARS-CoV1, SARS-CoV2			SARS-CoV2	S; RBD	B-cells; SARS-CoV2 Human Patient	153	QLQLQESGPGLVKPSETLSLTCTVSGASV SSGSYYWSWIRQPPGKGLEWIGYIYYSG STNYNPSLKSRVTISVDTSKNQFSLKLSSV TAADTAVYYCARERPGGTYSNTWYTPT DTNWFDTWGQGTLVTVSS	1232	SYELTQPPSVSVAPGKTARITCGGNNI GSKSVHWYQQKPGQAPVLVIYFDSDR PSGIPERFSGSNSGNTATLTISRVEAGD EADYYCQVWDSSRDHVVFGGGTKLT VL	IGHV4-61 (Human)	IGHJ4 (Human)	IGLV3-21 (Human)	IGLJ3 (Human)	2241	ARERPGGTYS NTWYTPTDT NWFDT	3443	QVWDSSR DHVV	Davide Robbiani et al., 2020 (https://www.nature.com/articles/s41586-020-2456-9)
C107	Ab	SARS-CoV2	SARS-CoV1		SARS-CoV1, SARS-CoV2	S; RBD	B-cells; SARS-CoV2 Human Patient	154	QVQLVQSGAEVKKPGASVRVSCKASGY TFTSYGFSWVRQAPGQGLEWMGWISA YNGNTNFAQKLQGRVTMTTDTSTSTAY MELRSLRSDDTAVYYCARGEAVAGTTGF FDYWGQGTLVTVSS	1233	QSVLTQPPSASGTPGQRVTISCSGSSS NIGSNYVYWYQQLPGTAPKLLIYRNN QRPSGVPDRFSGSKSGTSASLAISGLRS EDEADYYCAAWDDSLSGFVVFGGGTK LTVL	IGHV1-18 (Human)	IGHJ4 (Human)	IGLV1-47 (Human)	IGLJ3 (Human)	2242	ARGEAVAGTT GFFDY	3444	AAWDDSL SGFVV	Davide Robbiani et al., 2020 (https://www.nature.com/articles/s41586-020-2456-9)
C108	Ab	SARS-CoV2	SARS-CoV1	SARS-CoV2 (weak)	SARS-CoV1	S; RBD	B-cells; SARS-CoV2 Human Patient	155	QVQLQESGPGLVKPSGTLSLTCAVSGGS ISSTNWWSWVRQPPGKGLEWIGEIYHT GSTNYNPSLKSRVTISVDKSKNQFSLKLSS VTAADTAVYYCVRDGGRPGDAFDIWG QGTMVTVSS	1234	QSALTQPASVSGSPGQSITISCTGTSSD VGGYNYVSWYQQHPGKAPKLMIYDV SNRPSGVSNRFSGSKSGNTASLTISGL QAEDEADYYCNSYTSSSTRVFGTGTKV TVL	IGHV4-4 (Human)	IGHJ3 (Human)	IGLV2-14 (Human)	IGLJ1 (Human)	2243	VRDGGRPGD AFDI	3445	NSYTSSSTR V	Davide Robbiani et al., 2020 (https://www.nature.com/articles/s41586-020-2456-9)
C109	Ab	SARS-CoV2				S; RBD	B-cells; SARS-CoV2 Human Patient	156	EVQLVESGGGLVQPGGSLRLSCAASGFT FSSYWMSWVRQAPGKGLEWVANIKQ DGSEKYYVDSVKGRFTISGDNAKNSLYL HMNSLRAEDTAVYYCAIQLWLRGGYDY WGQGTLVTVSS	1235	QSALTQPPSASGSPGQSVTISCTGTSS DVGGYNYVSWYQQHPGKAPKLMIYE VTKRPSGVPDRFSGSKSGNTASLTVSG LQAEDEADYYCSSYAGSNNYVVFGGG TKLTVL	IGHV3-7 (Human)	IGHJ4 (Human)	IGLV2-8 (Human)	IGLJ3 (Human)	2244	AIQLWLRGGY DY	3446	SSYAGSNN YVV	Davide Robbiani et al., 2020 (https://www.nature.com/articles/s41586-020-2456-9)
C110	Ab	SARS-CoV2	SARS-CoV1	SARS-CoV2	SARS-CoV1	S; RBD	B-cells; SARS-CoV2 Human Patient	157	QVQLQQSGAEVKKPGESLKISCKGSGYS FTSYWIGWVRQMPGKGLEWMGIIYPG DSDTRYSPSFQGQVTISADKSISTAYMQ WSSLKASDTAMYYCARSFRDDPRIAVA GPADAFDIWGQGTMVTVSS	1236	DIQMTQSPSTLSASVGDRVTITCRASQ SISYWLAWYQQKPGKAPKLLIYQASSL ESGVPSRFSGSESGTEFTLTISSLQPDD FATYYCQQYNSYPYTFGQGTKLEIK	IGHV5-51 (Human)	IGHJ3 (Human)	IGKV1-5 (Human)	IGKJ2 (Human)	2245	ARSFRDDPRI AVAGPADAF DI	3447	QQYNSYPY T	Davide Robbiani et al., 2020 (https://www.nature.com/articles/s41586-020-2456-9)
C111	Ab	SARS-CoV2				S; RBD	B-cells; SARS-CoV2 Human Patient	158	QLQLQESGPGLVKPSETLSLTCTVSGGSI SSYYWSWIRQPPGKGLEWIGYIYYSGST NYNPSLKSRVTISVDTSKNQFSLKLSSVTA ADTAVYYCAARVEDWGYCSSTNCYSGAF DIWGQGTMVTVSS	1237	QSVLTQPPSVSEAPRQRVTISCSGSSS NIGNNAVNWYQQVPGKAPKLLIYDD LLPSGVSDRFSGSKSGTSASLAISGLQS EDEADYYCAAWDDSLNGAWVFGGG TKLTVL	IGHV4-59 (Human)	IGHJ3 (Human)	IGLV1-36 (Human)	IGLJ3 (Human)	2246	ARVEDWGYC SSTNCYSGAF DI	3448	AAWDDSL NGAWV	Davide Robbiani et al., 2020 (https://www.nature.com/articles/s41586-020-2456-9)
C112	Ab	SARS-CoV2	SARS-CoV1	SARS-CoV2 (weak)	SARS-CoV1	S; RBD	B-cells; SARS-CoV2 Human Patient	159	QVQLVESGGGVVQPGRSLRLSCAASGF TFSSHAMHWVRQAPGKGLEWVAVISY DGSNKYYADSVKGRFTISRDNSKNTLYL QMNSLRAEDTAVYYCAREDYYDSSGSF DYWGQGTLVTVSS	1238	QSALTQPASVSGSPGQSITISCTGTSSD VGGYNYVSWYQQHPGKAPKLMIYDV SNRPSGVSNRFSGSKSGNTASLTISGL QAEDEADYYCSSYTSSSTWVFGGGTKL TVL	IGHV3-30 (Human)	IGHJ4 (Human)	IGLV2-14 (Human)	IGLJ3 (Human)	2247	AREDYYDSSG SFDY	3449	SSYTSSST WV	Davide Robbiani et al., 2020 (https://www.nature.com/articles/s41586-020-2456-9)
C113	Ab	SARS-CoV2	SARS-CoV1		SARS-CoV1, SARS-CoV2	S; RBD	B-cells; SARS-CoV2 Human Patient	160	QVQLVESGGGVVQPGRSLRLSCAASGF TFSNFGMHWVRQAPGKGLEWVAVIW YDGSNKYYADSVKGRFTISRDNSKNTLYL QMNSLRAEDTAVYYCARGVNPDDILTG VDAFDIWGQGTMVTVSS	1239	DIQMTQSPSTLSASVGDRVTITCRASQ SMSSWLAWYQQKPGNAPKLLIYKASS LESGVPSRFSGSGSGTEFTLTISSLQPD DFATYYCQQHNSSPLTFGGGTKVEIK	IGHV3-33 (Human)	IGHJ3 (Human)	IGKV1-5 (Human)	IGKJ4 (Human)	2248	ARGVNPDDIL TGVDAFDI	3450	QQHNSSPL T	Davide Robbiani et al., 2020 (https://www.nature.com/articles/s41586-020-2456-9)
C114	Ab	SARS-CoV2	SARS-CoV1		SARS-CoV1, SARS-CoV2	S; RBD	B-cells; SARS-CoV2 Human Patient	161	QVQLVESGGGLIQPGGSLKLSCVVSGFT VSKNYISWVRQAPGKGLEWVSVIFAGG STFYADSVKGRFAISRDNSNNTLFLQMN SLRVEDTAIYYCARGDGELFFDQWGQG TLVTVSS	1240	QSVLTQPPSVSGAPGQRVTISCTGTSS NIGAGYDVHWYQQLPGRAPKVLISGN NIRPSEVPDRFSGSRSGTSASLAITSLQ PEDEAQYYCQSYDSSLYAVFGGGTKLT VL	IGHV3-53 (Human)	IGHJ4 (Human)	IGLV1-40 (Human)	IGLJ3 (Human)	2249	ARGDGELFFD Q	3451	QSYDSSLY AV	Davide Robbiani et al., 2020 (https://www.nature.com/articles/s41586-020-2456-9)
C115	Ab	SARS-CoV2	SARS-CoV1	SARS-CoV2 (weak)	SARS-CoV1	S; RBD	B-cells; SARS-CoV2 Human Patient	162	QVQLVESGGGLIKPGRSLRLSCTASGFTF GDYAMTWFRQAPGKGLEWVGFIRSKA YGGTTGYAASVKYRFTISRDDSKSIAYLQ MDSLKTEDTAVYYCTRWDGWSQHDY WGQGTLVTVSS	1241	DIVMTQSPLSLSVTPGEPASISCRSSQS LLHSNGNNYFDWYLQKPGQSPQLLIY LGSNRASGVPDRFSGSGSGTDFTLKIS RVEAEDVGVYYCMQVLQIPYTFGQGT KLEIK	IGHV3-49 (Human)	IGHJ4 (Human)	IGKV2-28 (Human)	IGKJ2 (Human)	2250	TRWDGWSQ HDY	3452	MQVLQIPY T	Davide Robbiani et al., 2020 (https://www.nature.com/articles/s41586-020-2456-9)
C116	Ab	SARS-CoV2	SARS-CoV1		SARS-CoV1, SARS-CoV2	S; RBD	B-cells; SARS-CoV2 Human Patient	163	QVQLVESGGGVVQPGRSLRLSCAASGF TYSTYAMHWVRQAPGKGLEWVAFISYD GSNKYYADSVKGRFTISRDNSKNTLYLQ MNSLRAEDTAVYYCARDFYHNWFDPW GQGTLVTVSS	1242	NFMLTQPHSVSESPGKTVTISCTGSSG SIASNYVQWYQQRPGSAPTTVIYEDN QRPSGVPDRFSGSIDRSSNSASLTISGL KTEDEADYYCQSYDSGNHWVVFGGG TRLTVL	IGHV3-30 (Human)	IGHJ5 (Human)	IGLV6-57 (Human)	IGLJ3 (Human)	2251	ARDFYHNWF DP	3453	QSYDSGN HWVV	Davide Robbiani et al., 2020 (https://www.nature.com/articles/s41586-020-2456-9)
C117	Ab	SARS-CoV2	SARS-CoV1	SARS-CoV2 (weak)	SARS-CoV1	S; RBD	B-cells; SARS-CoV2 Human Patient	164	QVQLVESGGGVVQPGRSLRLSCAASGF TFSTYAMHWVRQAPGEGLEWVAVISY DGSNTYYADSVKGRFTISRDNSKNTLYL QMNSLRAEDTAVYYCARDPIWFGELLSP PFVHFDYWGQGTLVTVSS	1243	QSVLTQPPSVSAAPGQKVTISCSGSSS NIGNNLVSWYQQLPGTAPKLLIYENN KRPSGIPDRFSGSKSGTSATLGITGLQT GDEADYYCGAWDSSLSAGGVYVFGT GTKVTVL	IGHV3-30 (Human)	IGHJ4 (Human)	IGLV1-51 (Human)	IGLJ1 (Human)	2252	ARDPIWFGEL LSPPFVHFDY	3454	GAWDSSLS AGGVYV	Davide Robbiani et al., 2020 (https://www.nature.com/articles/s41586-020-2456-9)

C118	Ab	SARS-CoV1, SARS-CoV2		SARS-CoV2 (weak)		S; RBD	B-cells; SARS-CoV2 Human Patient	165	QVQLVESGGGVVQPGRSLRLSCAASGF TFSNYAMHWVRQAPGKGLEWVAVISY DGSNKYYADSVKGRFTISRDNSKNTLYL QMNSLRAEDTAIYYCASGYTGYDYFVRG DYYGLDVWGQGTTVTVSS	1244	QPVLTQSPSASASLGASVKLTCTLSSGH SSYAIAWHQQQPEKGPRYLMKLNTD GSHSKGDGIPDRFSGSSSGAERYLTISS LQSEDEADYYCQTWGTGILVFGGGTK LTVL	IGHV3-30 (Human)	IGHJ6 (Human)	IGLV4-69 (Human)	IGLJ3 (Human)	2253	ASGYTGYDYF VRGDYYGLD V	3455	QTWGTGIL V	Davide Robbiani et al., 2020 (https://www.nature.com/articles/s41586-020-2456-9)
C119	Ab	SARS-CoV2	SARS-CoV1	SARS-CoV2	SARS-CoV1	S; RBD	B-cells; SARS-CoV2 Human Patient	166	QVQLVQSGAEVKKPGASVKVSCKASGY TFTSYYMHWVRQAPGQGLEWMGIINP SGGSTSYAQKLQGRVTMTRDTSTSTVY MELSSLRSEDTAVYYCARANHETTMDTY YYYYYMDVWGKGTTVTVSS	1245	QSALTQPASVSGSPGQSITISCTGTSSD VGGYKYVSWYQRHPGKAPKLMIYDV SNRPSGVSNRFSGSKSGNTASLTISGL QAEDEADYYCSSYTSSSTSVVFGGGTQ LTVL	IGHV1-46 (Human)	IGHJ6 (Human)	IGLV2-14 (Human)	IGLJ3 (Human)	2254	ARANHETTM DTYYYYYYMD V	3456	SSYTSSSTS VV	Davide Robbiani et al., 2020 (https://www.nature.com/articles/s41586-020-2456-9)
C120	Ab	SARS-CoV2	SARS-CoV1	SARS-CoV2	SARS-CoV1	S; RBD	B-cells; SARS-CoV2 Human Patient	167	EVQLVESGGGLIQPGGSLRLSCAASGFT VSSNYMTWVRQAPGKGLEWVSLIYPG GSTYYADSVKGRFTISRDNSKNTLYLQM NSLRAEDTAVYYCAREGMGMAAAGTW GQGTLVTVSS	1246	AIRMTQSPSSLSASVGDTVTITCQASQ DISKYLNWYQQKPGKAPKLLIYDASNL ETGVPSRFSGSGSGTDFTFTISSLQPED IATYYCQQYDNLPQTFGGGTKVEIK	IGHV3-53 (Human)	IGHJ4 (Human)	IGKV1-33 (Human)	IGKJ4 (Human)	2255	AREGMGMA AAGT	3457	QQYDNLP QT	Davide Robbiani et al., 2020 (https://www.nature.com/articles/s41586-020-2456-9)
C121	Ab	SARS-CoV2	SARS-CoV1	SARS-CoV2	SARS-CoV1	S; RBD	B-cells; SARS-CoV2 Human Patient	168	QVQLVQSGAEVKKPGASVKVSCKASGY TFTGYYMHWVRQAPGQGLEWMGWIS PVSGGTNYAQKFQGRVTMTRDTSISTAY MELSRLRSDDTAVYYCARAPLFPTGVLA GDYYYYGMDVWGQGTTVTVSS	1247	QSALTQPASVSGSPGQSITISCTGTSSD VGSYNLVSWYQQHPGKAPKLMIYEGS KRPSGVSNRFSGSKSGNTASLTISGLQ AEDEADYYCCSYAGSSTLVFGGGTKLT VL	IGHV1-2 (Human)	IGHJ6 (Human)	IGLV2-23 (Human)	IGLJ3 (Human)	2256	ARAPLFPTGV LAGDYYYYG MDV	3458	CSYAGSSTL V	Davide Robbiani et al., 2020 (https://www.nature.com/articles/s41586-020-2456-9)
C122	Ab	SARS-CoV2	SARS-CoV1	SARS-CoV2	SARS-CoV1	S; RBD	B-cells; SARS-CoV2 Human Patient	169	EVQLVESGGGLIQPGGSLRLSCAASGLT VSSNYMSWVRQAPGKGLEWVSVLYSG GSSFYADSVKGRFTISRDNSKNTLYLQM NSLRAEDTAVYYCARESGDTTMAFDYW GQGTLVTVSS	1248	DIQLTQSPSFLSASVGDRVTITCRASQG ISSYLAWYQQKPGKAPKLLIYAASTLQS GVPSRFSGSGSGTEFTLTISSLQPEDFA TYYCQQLNSDSYTFGQGTKLEIK	IGHV3-53 (Human)	IGHJ4 (Human)	IGKV1-9 (Human)	IGKJ2 (Human)	2257	ARESGDTTM AFDY	3459	QQLNSDSY T	Davide Robbiani et al., 2020 (https://www.nature.com/articles/s41586-020-2456-9)
C123	Ab	SARS-CoV2	SARS-CoV1	SARS-CoV2	SARS-CoV1	S; RBD	B-cells; SARS-CoV2 Human Patient	170	EVQLVESGGGLIQPGGSLRLSCAASGVT VSRNYMSWVRQAPGKGLEWVSVIYSG GSTYYADSVKGRFTISRDNSKNTLYLQM NSLRAEDTAVYYCARDLSAAFDIWGQG TMVTVSS	1249	DIQLTQSPSFLSASVGDRVTITCRASQG ISSYLAWYQQKPGKAPKLLIYAASTLQS GVPSRFSGSGSGTEFTLTISSLQPEDFA TYYCQQLNSYPPAFGQGTRLEIK	IGHV3-53 (Human)	IGHJ3 (Human)	IGKV1-9 (Human)	IGKJ5 (Human)	2258	ARDLSAAFDI	3460	QQLNSYPP A	Davide Robbiani et al., 2020 (https://www.nature.com/articles/s41586-020-2456-9)
C124	Ab	SARS-CoV2	SARS-CoV1	SARS-CoV2 (weak)	SARS-CoV1	S; RBD	B-cells; SARS-CoV2 Human Patient	171	EVQLVESGGGLVQPGGSLRLSCAASGFT FSGYSMNWVRQAPGKGPEWVSYISRSS STIYYADSVKGRFTISRDNAKNSLYLQMN SLRDEDTAVYYCAREGARVGATYDTYYF DYWGQGTLVTVSS	1250	EIVLTQSPATLSLSPGERATLSCRASQSF SSYLAWYQQKPGQAPRLLIYDASNRA TGIPARFSGSGSGTDFTLTISSLEPEDFA VYYCQQRNNWPPEWTFGQGTKVEIK	IGHV3-48 (Human)	IGHJ4 (Human)	IGKV3-11 (Human)	IGKJ1 (Human)	2259	AREGARVGA TYDTYYFDY	3461	QQRNNW PPEWT	Davide Robbiani et al., 2020 (https://www.nature.com/articles/s41586-020-2456-9)
C125	Ab	SARS-CoV2	SARS-CoV1	SARS-CoV2	SARS-CoV1	S; RBD	B-cells; SARS-CoV2 Human Patient	172	QVQLVESGSEVKKPGSSVKVSCKASGG TFSSYAFSWVRQAPGQGLEWMGRIIPIL ALANYAQKFQGRVTITADKSTSTAYMEL SSLRSEDTAVYYCARVNQAVTTPFSMDV WGQGTTVTVSS	1251	EIVMTQSPATLSVSPGERATLSCRASQ SVSSNLAWYQQKPGQAPRLLIYGAST RATGIPARFSGSGSGTEFTLTISSLQSE DFAVYYCQQYNNWPITFGQGTRLEIK	IGHV1-69 (Human)	IGHJ6 (Human)	IGKV3-15 (Human)	IGKJ5 (Human)	2265	ARVNQAVTT PFSMDV	3467	QQYNNWP IT	Davide Robbiani et al., 2020 (https://www.nature.com/articles/s41586-020-2456-9)
C126	Ab	SARS-CoV2	SARS-CoV1		SARS-CoV1, SARS-CoV2	S; RBD	B-cells; SARS-CoV2 Human Patient	173	QVQLQESGPGLVKPSETLSLSCAVSGGSI GSYFWSWIRQPPGKGLEWIGYLHYSGS TNYNPSLKSRVTISVDTSKNQFSLKLSSVT AADTAVYYCARLQWLRGAFDIWGQGT MVTVSS	1252	NFMLTQPHSVSESPGKTVTISCTGSSG SIASNYVQWYQQRPGSAPTTVINEDN QRPSGVPDRFSGSIDSSSNSASLTISGL KTEDEADYYCQSYDSSNLVFGGGTKLT VL	IGHV4-59 (Human)	IGHJ3 (Human)	IGLV6-57 (Human)	IGLJ3 (Human)	2261	ARLQWLRGA FDI	3463	QSYDSSNL V	Davide Robbiani et al., 2020 (https://www.nature.com/articles/s41586-020-2456-9)
C127	Ab	SARS-CoV2	SARS-CoV1	SARS-CoV2	SARS-CoV1	S; RBD	B-cells; SARS-CoV2 Human Patient	174	QVQLVQSGAEVKKPGASVKVSCKASGY TFTGYYMHWVRQAPGQGLEWMGWI NPNSGGTNYAQKFQGRVTMTRDTSIST AYMELSRLRSDDTAVYYCATAHPRRIQG VFFLGPGVWGQGTTVTVSS	1253	QSVLTQPPSASGTPGQRVTISCSGSSS NIGSNTVNWYQQLPGTAPKLLIYSNN QRPSGVPDRFSGSKSGTSASLAISGLQ SEDEADYYCAAWDDSLNGVVFGGGT KLTVL	IGHV1-2 (Human)	IGHJ6 (Human)	IGLV1-44 (Human)	IGLJ3 (Human)	2262	ATAHPRRIQG VFFLGPGV	3464	AAWDDSL NGVV	Davide Robbiani et al., 2020 (https://www.nature.com/articles/s41586-020-2456-9)
C128	Ab	SARS-CoV2	SARS-CoV1	SARS-CoV2	SARS-CoV1	S; RBD	B-cells; SARS-CoV2 Human Patient	175	EVQLLESGGGLVQPGGSLRLSCAASGFT FSTYAMSWVRQAPGKGLEWVSTITGSG RDTYYADSVKGRFTISRDNSKNTLFLQLN SLRAEDAAVYSCANHPLASGDDYYHYY MDVWGKGTTVTVSS	1254	EIVLTQSPGTLSLSPGERATLSCRASQS VNSRQLAWYQQKPGQAPRLLIYGASS RATGIPERFSGSGSGTDFTLTISRLESED FAVYHCQQYGSSRALTFGGGTKVEIK	IGHV3-23 (Human)	IGHJ6 (Human)	IGKV3-20 (Human)	IGKJ4 (Human)	2263	ANHPLASGD DYYHYYMDV	3465	QQYGSSRA LT	Davide Robbiani et al., 2020 (https://www.nature.com/articles/s41586-020-2456-9)
C130	Ab	SARS-CoV2	SARS-CoV1		SARS-CoV1, SARS-CoV2	S; RBD	B-cells; SARS-CoV2 Human Patient	176	QVQLVQSGAEVKKPGASVKVSCKASGY TFTNYYMHWVRQAPGQGLEWMGIINP SGGSTGYAQKFQGRVTMTRDTSTSTVY MELSSLRSEDTAVYYCARSRPTPDWYFD LWGRGTLVTVSS	1255	SYELTQPPSVSVAPGKTARITCGGNNI GSKSVHWYQQKPGQAPVLVIYYDSDR PSGIPERFSGSNSGNTATLTISRVEAGD EADYYCQVWDSSSDHPGVVFGGGTK LTVL	IGHV1-46 (Human)	IGHJ2 (Human)	IGLV3-21 (Human)	IGLJ3 (Human)	2264	ARSRPTPDW YFDL	3466	QVWDSSS DHPGVV	Davide Robbiani et al., 2020 (https://www.nature.com/articles/s41586-020-2456-9)
C131	Ab	SARS-CoV2	SARS-CoV1	SARS-CoV2	SARS-CoV1	S; RBD	B-cells; SARS-CoV2 Human Patient	177	QVQLVQSGSEVKKPGSSVKVSCKASGG TFSSYAFSWVRQAPGQGLEWMGRIIPIL ALANYAQKFQGRVTITADKSTSTAYMEL SSLRSEDTAVYYCARVNQAVTTPFSMDV WGQGTTVTVSS	1256	EIVMTQSPATLSVSPGERATLSCRASQ SVSSNLAWYQQKPGQAPRLLIYGAST RATGIPARFSGSGSGTEFTLTISSLQSE DFAVYYCQQYNNWPITFGQGTRLEIK	IGHV1-69 (Human)	IGHJ6 (Human)	IGKV3-15 (Human)	IGKJ5 (Human)	2265	ARVNQAVTT PFSMDV	3467	QQYNNWP IT	Davide Robbiani et al., 2020 (https://www.nature.com/articles/s41586-020-2456-9)
C132	Ab	SARS-CoV2	SARS-CoV1	SARS-CoV2 (weak)	SARS-CoV1	S; RBD	B-cells; SARS-CoV2 Human Patient	178	QVQLQESGPGLVKPSGTLSLTCAVSGGS ISSNNWWSCVRQPPGKGLEWIGEIYHS GSTNYNPSLKSRVTISVDKSKNQFSLKLSS VTAADTAVYYCARGGDTAMGPEYFDY WGQGTLVTVSS	1257	QSALTQPASVSGSPGQSITISCTGTSSD VGGYNYVSWYQQHPGKAPKLMIYDV SNRPSGVSNRFSGSKSGNTASLTISGL QAEDEADYYCSSYTSSSTLLFGGGTKLT VL	IGHV4-4 (Human)	IGHJ4 (Human)	IGLV2-14 (Human)	IGLJ3 (Human)	2266	ARGGDTAMG PEYFDY	3468	SSYTSSSTL L	Davide Robbiani et al., 2020 (https://www.nature.com/articles/s41586-020-2456-9)

C133	Ab	SARS-CoV2	SARS-CoV1		SARS-CoV1, SARS-CoV2	S; RBD	B-cells; SARS-CoV2 Human Patient	179	QVQLVESGGGVVQPGRSLRLSCAASGF TFSSYAMHWVRQAPGKGLEWVAVILY DGSNKYYADSVKGRFTISRDNSKNTLYL QMNSLRAEDTAVYYCARDSDVDTSMVT WFDYWGQGTLVTVSS	1258	DIQMTQSPSSLSASVGDRVTITCRASQ SISSYLNWYQQKPGKAPKLLIYAASSLQ SGVPSRFSGSGSGTDFTLTISSLQPEDF ATYYCQQSYSTPPWTFGQGTKVEIK	IGHV3-30 (Human)	IGHJ4 (Human)	IGKV1-39 (Human)	IGKJ1 (Human)	2267	ARDSDVDTS MVTWFDY	3469	QQSYSTPP WT	Davide Robbiani et al., 2020 (https://www.nature.com/articles/s41586-020-2456-9)
C134	Ab	SARS-CoV2	SARS-CoV1		SARS-CoV1, SARS-CoV2	S; RBD	B-cells; SARS-CoV2 Human Patient	180	EVQLLESGGGLVQPGGSLRLSCAASGFT FSNYAMSWVRQAPGKGLEWVSAISGS DGSTYYAGSVKGRFTISRDNSKNTLYLQ MNSLRAEDTAVYYCAKDPLITGPTYQYF HYWGQGTLVTVSS	1259	SYELTQPPSVSVAPGKTARITCGGNNI GSKSVHWYQQKPGQAPVLVIYYDSDR PSGIPERFSGSNSGNTATLTISRVEAGD EAEYHCQVWDSSSDRPGVVFGGGTK LTVL	IGHV3-23 (Human)	IGHJ4 (Human)	IGLV3-21 (Human)	IGLJ3 (Human)	2268	AKDPLITGPTY QYFHY	3470	QVWDSSS DRPGVV	Davide Robbiani et al., 2020 (https://www.nature.com/articles/s41586-020-2456-9)
C135	Ab	SARS-CoV2	SARS-CoV1	SARS-CoV2	SARS-CoV1	S; RBD	B-cells; SARS-CoV2 Human Patient	181	QVQLVESGGGVVQPGRSLRLSCAASGF TFSSYAMHWVRQAPGKGLEWVAVIPF DGRNKYYADSVTGRFTISRDNSKNTLYL QMNSLRAEDTAVYYCASSSGYLFHSDY WGQGTLVTVSS	1260	DIQMTQSPSTLSASVGDRVTITCRASQ SISNWLAWFQQKPGKAPKLLIYEASSL ESGVPSRFSGSGSGTEFTLTISSLQPDD FATYYCQQYNSYPWTFGQGTKVEIK	IGHV3-30 (Human)	IGHJ4 (Human)	IGKV1-5 (Human)	IGKJ1 (Human)	2269	ASSSGYLFHS DY	3471	QQYNSYP WT	Davide Robbiani et al., 2020 (https://www.nature.com/articles/s41586-020-2456-9)
C138	Ab	SARS-CoV2	SARS-CoV1		SARS-CoV1, SARS-CoV2	S; RBD	B-cells; SARS-CoV2 Human Patient	182	EVQLVESGGGLVQPGGSLRLSCAASGFT FSTYWMSWVRQPPGKGLEWVANIKQ DGSEKYYVDSVKGRFTISRDNAKNSLYL QMNSLRADDTAVYYCAGGTWLRSSFDY WGQGTLVTVSS	1261	NFMLTQPHSVSESPGKTVTISCTGSSG SIASNYVQWYQQRPGSAPTTVIYEDN QRPSGVPDRFSGSIDSSSNSASLTISGL KTEDEADYYCQSYDSSNWVFGGGTKL TVL	IGHV3-7 (Human)	IGHJ4 (Human)	IGLV6-57 (Human)	IGLJ3 (Human)	2270	AGGTWLRSSF DY	3472	QSYDSSN WV	Davide Robbiani et al., 2020 (https://www.nature.com/articles/s41586-020-2456-9)
C139	Ab	SARS-CoV2	SARS-CoV1		SARS-CoV1, SARS-CoV2	S; RBD	B-cells; SARS-CoV2 Human Patient	183	EVQLVESGGGVVQPGRSLRLSCAASGFT FSSYAMHWVRQAPGKGLEWVAVISYD GSNKYSADSVKGRFTISRDNSKNTLYLQ MNSLRAEDTAVYYCAKGGAYSYYYYMD VWGKGTTVTVSS	1262	DIQMTQSPSSLSASVGDRVTITCQASQ DISNYLNWYQQKPGKAPKLLIYDASNL ETGVPSRFSGSGSGTDFTFTISSLQPED IATYYCQQYDNLPLTFGGGTKVEIK	IGHV3-30-3 (Human)	IGHJ6 (Human)	IGKV1-33 (Human)	IGKJ4 (Human)	2271	AKGGAYSYYY YMDV	3473	QQYDNLPL T	Davide Robbiani et al., 2020 (https://www.nature.com/articles/s41586-020-2456-9)
C140	Ab	SARS-CoV2	SARS-CoV1	SARS-CoV2	SARS-CoV1	S; RBD	B-cells; SARS-CoV2 Human Patient	184	EVQLVESGGGLVQPGGSLRLSCAASGVT VSSNYMSWVRQAPGKGLEWVSLIYSGG STFYADSVKGRFTISRDNSENTLYLQMN TLRAEDTAVYYCARDLYYYGMDVWGQ GTTVTVSS	1263	DIQLTQSPSFLSASVGDRVTITCRASQG ISSYLAWYQQKPGKAPKLLIYAASTLQS GVPSRFSGSGSGTEFTLTISSLQPEDFA TYYCQQLNSYSYTFGQGTKLEIK	IGHV3-66 (Human)	IGHJ6 (Human)	IGKV1-9 (Human)	IGKJ2 (Human)	2272	ARDLYYYGM DV	3474	QQLNSYSY T	Davide Robbiani et al., 2020 (https://www.nature.com/articles/s41586-020-2456-9)
C141	Ab	SARS-CoV2	SARS-CoV1		SARS-CoV1, SARS-CoV2	S; RBD	B-cells; SARS-CoV2 Human Patient	185	EVQLVESGGGVVQPGRSLRLSCAASGFT FSSYAMFWVRQAPGKGLEWVAVISYD GSNKYYADSVKGRFTISRDNSKNTLYLQ MNSLRAEDTAVYYCARADLGYCTNGVC YVDYWGQGTLVTVSS	1264	NFMLTQPHSVSESPGKTVTISCTGSSG SIASNYVQWYQQRPGSAPTTVIYEDN QRPSGVPDRFSGSIDSSSNSASLTISGL KTEDEADYYCQSYDSSNWVFGGGTKL TVL	IGHV3-30 (Human)	IGHJ4 (Human)	IGLV6-57 (Human)	IGLJ3 (Human)	2273	ARADLGYCTN GVCYVDY	3475	QSYDSSN WV	Davide Robbiani et al., 2020 (https://www.nature.com/articles/s41586-020-2456-9)
C143	Ab	SARS-CoV2	SARS-CoV1		SARS-CoV1, SARS-CoV2	S; RBD	B-cells; SARS-CoV2 Human Patient	186	EVQLVESGGGLVQPGGSLRLSCAASGFS VSTKYMTWVRQAPGKGLEWVSVLYSG GSDYYADSVKGRFTISRDNSKNALYLQM NSLRVEDTGVYYCARDSSEVRDHPGHP GRSVGAFDIWGQGTMVTVSS	1265	QSALTQPASVSGSPGQSITISCTGTSND VGSYTLVSWYQQYPGKAPKLLIFEGTK RSSGISNRFSGSKSGNTASLTISGLQGE DEADYYCCSYAGASTFVFGGGTKLTVL	IGHV3-66 (Human)	IGHJ3 (Human)	IGLV2-23 (Human)	IGLJ3 (Human)	2274	ARDSSEVRDH PGHPGRSVG AFDI	3476	CSYAGAST FV	Davide Robbiani et al., 2020 (https://www.nature.com/articles/s41586-020-2456-9)
C144	Ab	SARS-CoV2	SARS-CoV1	SARS-CoV2	SARS-CoV1	S; RBD	B-cells; SARS-CoV2 Human Patient	187	EVQLVESGGGLIQPGGSLRLSCAASGFT VSNNYMSWVRQAPGKGLEWVSVIYSG GSTYYADSVKGRFTISRDKSKNTLYLQM NRLRAEDTAVYYCAREGEVEGYNDFWS GYSRDRYYFDYWGQGTLVTVSS	1266	QSALTQPASVSGSPGQSITISCTGTSSD VGGYNYVSWYQQHPGKAPKLMIYDV SNRPSGVSNRFSGSKSGNTASLTISGL QAEDEADYYCSSYTSSSTRVFGTGTKV TVL	IGHV3-53 (Human)	IGHJ4 (Human)	IGLV2-14 (Human)	IGLJ1 (Human)	2275	AREGEVEGY NDFWSGYSR DRYYFDY	3477	SSYTSSSTR V	Davide Robbiani et al., 2020 (https://www.nature.com/articles/s41586-020-2456-9)
C145	Ab	SARS-CoV2	SARS-CoV1	SARS-CoV2	SARS-CoV1	S; RBD	B-cells; SARS-CoV2 Human Patient	188	EVQLVESGGGLIQPGGSLRLSCAASGFS VSSNYMSWVRQAPGKGLEWVSVIYSG GSTYYADSVKGRFTISRDNSKNTLYLQM NSLRAEDTAVYYCAREGEVEGYYDFWS GYSRDRYYFDYWGQGTLVTVSS	1267	QSALTQPASVSGSPGQSITISCTGTSSD VGGYNYVSWYQQHPGKAPKLMIYDV SNRPSGVSNRFSGSKSGNTASLTISGL QAEDEADYYCSSYTSSTTRVFGTGTRV TVL	IGHV3-53 (Human)	IGHJ4 (Human)	IGLV2-14 (Human)	IGLJ1 (Human)	2276	AREGEVEGYY DFWSGYSRD RYYFDY	3478	SSYTSSTTR V	Davide Robbiani et al., 2020 (https://www.nature.com/articles/s41586-020-2456-9)
C146	Ab	SARS-CoV2	SARS-CoV1		SARS-CoV1, SARS-CoV2	S; non-RBD	B-cells; SARS-CoV2 Human Patient	189	EVQLVESGGLVKPGGSLRLSCAASGLT FTAYRMNWVRQAPGKGLEWLSSISNTN GDIYYADSVKGRFTISRDNAKNSLYLQM NSLRADDTAVYYCARDVASNYAYFDLW GQGTLVTVSS	1268	QSALTQPASVSGSPGQSITISCTGTSSD IGVYNYISWSQQHPGKAPKVMIYDVT NRPSGVSNRFSGSKSGNTASLTISGLQ AEDEADYYCSSYRGSSTPYVFGTGTKV TVL	IGHV3-21 (Human)	IGHJ4 (Human)	IGLV2-14 (Human)	IGLJ1 (Human)	2277	ARDVASNYAY FDL	3479	SSYRGSSTP YV	Davide Robbiani et al., 2020 (https://www.nature.com/articles/s41586-020-2456-9)
C147	Ab	SARS-CoV2	SARS-CoV1		SARS-CoV1, SARS-CoV2	S; non-RBD	B-cells; SARS-CoV2 Human Patient	190	EVQLVQSGAEVKKPGESLKISCKGSGYR FTNYWIGWVRQMPGKGLEWMGIIYPG DSDTRYSPSFQGQVTISADKSITTAYLQW SSLKASDTAMYYCARLSDRWYSPFDPW GQGTLVTVSS	1269	QAVVTQEPSLTVSPGGTVTLTCGSSTG AVTSGHYPYWFQQKSGQAPRTLIYETS IKHSWTPARFSGSLLGGKAALTLSGAQ PEDEADYYCLLSYSGARPVFGGGTKLT VL	IGHV5-51 (Human)	IGHJ5 (Human)	IGLV7-46 (Human)	IGLJ3 (Human)	2278	ARLSDRWYSP FDP	3480	LLSYSGAR PV	Davide Robbiani et al., 2020 (https://www.nature.com/articles/s41586-020-2456-9)
C148	Ab	SARS-CoV2	SARS-CoV1		SARS-CoV1, SARS-CoV2	S; RBD	B-cells; SARS-CoV2 Human Patient	191	EVQLVESGGGLVQPGGSQRLSCAASGF TVSSNYMSWIRQAPGKGLEWVSVIYSG GSAYYVDSVKGRFTISRDNSKNTLYLQM NSLRPEDTAVYYCARIANYMDVWGKGT TVTVSS	1270	EIVMTQSPATLSVSPGERATLSCRASQ SVSSHLAWYQQKPGQAPRLLIYGAST RATGIPTRFSGSGSGTEFTLTISSLQSED FAVYYCQQYNNWPPLTFGGGTKVEIK	IGHV3-66 (Human)	IGHJ6 (Human)	IGKV3-15 (Human)	IGKJ4 (Human)	2279	ARIANYMDV	3481	QQYNNWP PLT	Davide Robbiani et al., 2020 (https://www.nature.com/articles/s41586-020-2456-9)
C150	Ab	SARS-CoV2	SARS-CoV1		SARS-CoV1, SARS-CoV2	S; RBD	B-cells; SARS-CoV2 Human Patient	192	EVQLVESGGGLVQPGGSLRLSCVASGFT FSSYWMHWVRQVPGKGPVWVSHINS EGSSTNYADSVRGRFTISRDNAKDTLYL QMNNLRAEDTAVYYCARPTAVAAAGN YFYYYGMDVWGQGTTVTVSS	1271	QSALTQPASVSGSPGQSITISCTGTSSD VGYYNFVSWYQQHPGKAPKLMIYEVS NRPSGVSNRFSGSKSGNTASLIISGLQA EDEADYYCSSYRSSSTLVFGGGTKLTVL	IGHV3-74 (Human)	IGHJ6 (Human)	IGLV2-14 (Human)	IGLJ3 (Human)	2280	ARPTAVAAA GNYFYYYGM DV	3482	SSYRSSSTL V	Davide Robbiani et al., 2020 (https://www.nature.com/articles/s41586-020-2456-9)

C151	Ab	SARS-CoV2	SARS-CoV1	SARS-CoV2 (weak)	SARS-CoV1	S; RBD	B-cells; SARS-CoV2 Human Patient	193	EVQLVESGGGLVKPGGSLRLSCAASGFT FSSYNMNWVRQAPGKGLEWVSCISSSS SYIYYADSVKGRFTISRDNAKNSLYLQMN SLRAEDTAVYYCARERGYDGGKTPPFLG GQGTLVTVSS	1272	NFMLTQPHSVSESPGKTVTISCTGSSG SIASNYVQWYQQRPGSAPTTVIYEDN QRPSGVPDRFSGSIDSSSNSASLTISGL KTEDEADYYCQSYDSSNYWVFGGGTK LTVL	IGHV3-21 (Human)	IGHJ4 (Human)	IGLV6-57 (Human)	IGLJ3 (Human)	2281	ARERGYDGG KTPP	3483	QSYDSSNY WV	Davide Robbiani et al., 2020 (https://www.nature.com/articles/s41586-020-2456-9)
C153	Ab	SARS-CoV2	SARS-CoV1	SARS-CoV2 (weak)	SARS-CoV1	S; RBD	B-cells; SARS-CoV2 Human Patient	194	EVQLVESGGGLIQPGGSLRLSCAASGFT VSSNYMSWVRQAPGKGLEWVSVIYSGY STYYVDSVKGRFTISRDNSKNTLYLQMN SLRAEDTAVYYCARVGGAHSGYDGSFDY WGQGTLVTVSS	1273	QSALTQPASVSGSPGQSITISCTGTSSD VGSYNLVSWYQQHPGKAPKLMIYEGS KRPSGVSNRFSGSKSGNTASLTISGLQ AEDEADYYCCSYAGSSTWVFGGGTKL TVL	IGHV3-53 (Human)	IGHJ4 (Human)	IGLV2-23 (Human)	IGLJ3 (Human)	2282	ARVGGAHSG YDGSFDY	3484	CSYAGSST WV	Davide Robbiani et al., 2020 (https://www.nature.com/articles/s41586-020-2456-9)
C154	Ab	SARS-CoV1, SARS-CoV2		SARS-CoV2 (weak)		S; RBD	B-cells; SARS-CoV2 Human Patient	195	QVQLVESGGGVVQPGRSLRLSCAASGF TFSRYGMHWVRQAPGKGLEWVAVMS YDGSSKYYADSVKGRFTISRDNSKNTLCL QMNSLRAEDTAVYYCAKQAGPYCSGGS CYSAPFDYWGQGTLVTVSS	1274	DIQMTQSPSSLSASVGDRVTITCQASQ GISNYLNWYQQKPGKAPKLLIYDASNL ETGVPSRFSGSGSGTDFTFTISSLQPED IATYYCQQYDNLPITFGQGTRLEIK	IGHV3-30 (Human)	IGHJ4 (Human)	IGKV1-33 (Human)	IGKJ5 (Human)	2283	AKQAGPYCS GGSCYSAPFD Y	3485	QQYDNLPI T	Davide Robbiani et al., 2020 (https://www.nature.com/articles/s41586-020-2456-9)
C155	Ab	SARS-CoV2	SARS-CoV1	SARS-CoV2	SARS-CoV1	S; RBD	B-cells; SARS-CoV2 Human Patient	196	EVQLVESGGGLIQPGGSLRLSCAASGFIV SSNYMSWVRQAPGKGLEWVSVIYSGG STFYADSVKGRFTISRDNSKNTLYLQMN SLRAEDTAVYYCARDFGEFYFDYWGQG TLVTVSS	1275	EIVMTQSPATLSVSPGERATLSCRASQ SVSSNLAWYQQKPGQAPRLLIYGAST RATAIPARFSGSGSGTEFTLTISSLQSED FAVYYCQQYNNWPRTFGQGTKVEIK	IGHV3-53 (Human)	IGHJ4 (Human)	IGKV3-15 (Human)	IGKJ1 (Human)	2284	ARDFGEFYFD Y	3486	QQYNNWP RT	Davide Robbiani et al., 2020 (https://www.nature.com/articles/s41586-020-2456-9)
C156	Ab	SARS-CoV2	SARS-CoV1		SARS-CoV1, SARS-CoV2	S; RBD	B-cells; SARS-CoV2 Human Patient	197	QVQLVESGGGVVQPGRSLRLSCAASGF TFSNYGMHWVRQAPGKGLEWVAVISY DGNNKYYADSVKGRFTISRDNSKNTLYL QMNSLRAEDTAVYYCAKDPFPLAVAGT GYFDYWGQGTLVTVSS	1276	SYELTQPPSVSVAPGQTARISCGGNNI GSKNVHWYQQKPGQAPVLVVYDDS DRPSGIPERFSGSNSGNTATLTISRVEA GDEADYYCQVWDSSSDPWVFGGGTK LTVL	IGHV3-30 (Human)	IGHJ4 (Human)	IGLV3-21 (Human)	IGLJ3 (Human)	2285	AKDPFPLAVA GTGYFDY	3487	QVWDSSS DPWV	Davide Robbiani et al., 2020 (https://www.nature.com/articles/s41586-020-2456-9)
C164	Ab	SARS-CoV2	SARS-CoV1	SARS-CoV2 (weak)	SARS-CoV1	S; RBD	B-cells; SARS-CoV2 Human Patient	198	EVQLVESGGGLVQPGGSLRLSCAASGFS VSTKYMTWVRQAPGKGLEWVSVLYSG GSDYYADSVKGRFTISRDNSKNALYLQM NSLRVEDTGVYYCARDSSEVRDHPGHP GRSVGAFDIWGQGTMVTVSS	1277	QSALTQPASVSGSPGQSITISCTGTSND VGSYTLVSWYQQYPGKAPKLLIFEVTK RSSGISNRFSGSKSGNTASLTISGLQGE DEADYYCCSYAGASTFVFGGGTKLTVL	IGHV3-66 (Human)	IGHJ3 (Human)	IGLV2-23 (Human)	IGLJ3 (Human)	2286	ARDSSEVRDH PGHPGRSVG AFDI	3488	CSYAGAST FV	Davide Robbiani et al., 2020 (https://www.nature.com/articles/s41586-020-2456-9)
C165	Ab	SARS-CoV2	SARS-CoV1	SARS-CoV2	SARS-CoV1	S; RBD	B-cells; SARS-CoV2 Human Patient	199	QVQLVQSGAEVKKPGSSVKVSCKASGG TFSSYAINWVRQAPGQGLEWMGRIIPI VGIANYAQKFQGRVTITADKSSSTAYME LSSLRSEDTAVYYCARDLLDPQLDDAFDI WGQGTMVTVSS	1278	EIVLTQSPGTLSLSPGERATLSCRASQS VSSTYLAWYQQKPGQAPRLLIYGASSR ATGIPDRFSGSGSGTDFTLTISRLEPED FAVYYCQQYGSSPWTFGQGTKVEIK	IGHV1-69 (Human)	IGHJ3 (Human)	IGKV3-20 (Human)	IGKJ1 (Human)	2287	ARDLLDPQLD DAFDI	3489	QQYGSSP WT	Davide Robbiani et al., 2020 (https://www.biorxiv.org/content/10.1101/2020.05.13.092619v2)
C201	Ab	SARS-CoV2	SARS-CoV1		SARS-CoV1, SARS-CoV2	S; RBD	B-cells; SARS-CoV2 Human Patient	200	EVQLVESGGGLVQPGGSLRLSCAASGFT FDDYAMHWVRQAPGKGLEWVSGISW NSGSIGYADSVKGRFTISRDNAKNSLYLQ MNSLRAEDTALYYCVKGVEYSSSSNFDY WGQGTLVTVSS	1279	IRMTQSPSSVSASVGDRVTITCRASQG ISSWLAWYQQKPGKAPKLLIYVESSLQ SGVPSRFSGSGSGTDFTLTISSLQPEDF ATYYCQQANSFPLTFGGGTKVEIK	IGHV3-9 (Human)	IGHJ4 (Human)	IGKV1-12 (Human)	IGKJ4 (Human)	2288	VKGVEYSSSS NFDY	3490	QQANSFPL T	Davide Robbiani et al., 2020 (https://www.biorxiv.org/content/10.1101/2020.05.13.092619v2)
C202	Ab	SARS-CoV2	SARS-CoV1		SARS-CoV1, SARS-CoV2	S; RBD	B-cells; SARS-CoV2 Human Patient	201	EVQLVESGGGLVQPGGSLRLSCAASGFT VSSNYMSWVRQAPGKGLEWVSLIYSGG STYYADSVKGRFTISRDNSKNTLYLQMN SLRAEDTAVYYCARDTLGRGGDYWGQ GTLVTVSS	1280	DIQLTQSPSSLSASVGDRVTITCQASQ DISNYLNWYQQKPGKAPKLLIYDASNL ETGVPSRFSGSGSGTDFTFTISSLQPED IATYYCQQYDNLPRSFGQGTKLEIK	IGHV3-66 (Human)	IGHJ4 (Human)	IGKV1-33 (Human)	IGKJ2 (Human)	2289	ARDTLGRGG DY	3491	QQYDNLP RS	Davide Robbiani et al., 2020 (https://www.biorxiv.org/content/10.1101/2020.05.13.092619v2)
C204	Ab	SARS-CoV1, SARS-CoV2			SARS-CoV2	S; RBD	B-cells; SARS-CoV2 Human Patient	202	EVQLLESGGGLEQPGGSLRLSCAASGFT FSTYAMSWVRQAPGKGLEWVSAISGSG AGTFYADSVKGRFTISRDNSKNTLYLQM NSLRAEDTAVYYCARESDCGSTSCYQVG WFDPWGQGTLVTVSS	1281	DIQLTQSPSSLSASVGDRVTITCRASQS ISSYLNWYQQKPGKAPKLLIYAASSLQS GVPSRFSGSGSGTDFTLTISSLQPEDFA TYYCQQSYSTPPWTFGQGTKVEIK	IGHV3-23 (Human)	IGHJ5 (Human)	IGKV1-39 (Human)	IGKJ1 (Human)	2290	ARESDCGSTS CYQVGWFDP	3492	QQSYSTPP WT	Davide Robbiani et al., 2020 (https://www.biorxiv.org/content/10.1101/2020.05.13.092619v2)
C205	Ab	SARS-CoV2	SARS-CoV1		SARS-CoV1, SARS-CoV2	S; non-RBD	B-cells; SARS-CoV2 Human Patient	203	QVQLVQSGAEVKKPGASVKVSCKASGH TFTSYYMHWVRQAPGQGLEWMGIINP SGGSTSYAQKFQGRVTMTRDTSTSTVY MELSSLRSEDTAVYYCARGPERGIVGAT DYFDYWGQGTLVTVSS	1282	EIVLTQSPGTLSLSPGERATLSCRASQS VSSSYLAWYQQKPGQAPRLLIYGASSR ATGIPDRFSGSGSGTDFTLTISRLEPED FAVYYCQQYVSSPWTFGQGTKVEIK	IGHV1-46 (Human)	IGHJ4 (Human)	IGKV3-20 (Human)	IGKJ1 (Human)	2291	ARGPERGIVG ATDYFDY	3493	QQYVSSP WT	Davide Robbiani et al., 2020 (https://www.biorxiv.org/content/10.1101/2020.05.13.092619v2)
C207	Ab	SARS-CoV2	SARS-CoV1	SARS-CoV2 (weak)	SARS-CoV1	S; RBD	B-cells; SARS-CoV2 Human Patient	204	EVQLLESGGGLVQPGGSLRLSCAASGFT FSSYAMSWVRQAPGKGLEWVSAISGSG GSTYYADSVKGRFTISRDNSKNTLYLQM NSLRAEDTAVYYCAKEPIGQPLLWWDY WGQGTLVTVSS	1283	EIVLTQSPATLSLSPGERATLSCRASQS VSSYLAWYQQKPGQAPRLLIYDASNR ATGIPARFSGSGSGTDFTLTISSLEPEDF AVYYCQQRSNWPRGFGQGTKVEIK	IGHV3-23 (Human)	IGHJ4 (Human)	IGKV3-11 (Human)	IGKJ1 (Human)	2292	AKEPIGQPLL WWDY	3494	QQRSNWP RG	Davide Robbiani et al., 2020 (https://www.biorxiv.org/content/10.1101/2020.05.13.092619v2)
C208	Ab	SARS-CoV2	SARS-CoV1		SARS-CoV1, SARS-CoV2	S; non-RBD	B-cells; SARS-CoV2 Human Patient	205	EVQLVQSGAEVKKPGESLKISCKGSGYSF TSYWIGWVRQMPGKGLEWMGIIYPGD SDTRYSPSFQGQVTISADKSISTAYLKWS SLKASDSAMYYCARGPNLQNWFDPWG QGTLVTVSS	1284	EIVLTQSPGTLSLSPGERATLSCRASQS VSGSYLAWYQQRPGQAPRLLIYGASS RATGIPDRFSGSGSGTDFTLTISRLEPE DFAVYYCQQYGSSLTFGGGTKVEIK	IGHV5-51 (Human)	IGHJ5 (Human)	IGKV3-20 (Human)	IGKJ4 (Human)	2293	ARGPNLQNW FDP	3495	QQYGSSLT	Davide Robbiani et al., 2020 (https://www.biorxiv.org/content/10.1101/2020.05.13.092619v2)
C210	Ab	SARS-CoV2	SARS-CoV1	SARS-CoV2	SARS-CoV1	S; RBD	B-cells; SARS-CoV2 Human Patient	206	EVQLVESGGGLIQPGGSLRLSCAASGFT VSSNYMSWVRQAPGKGLEWVSVIYSG GSTFYADSVKGRFTFSRDNSKNTLYLQM NSLRAEDTAVYYCARDLMAYGMDVWG QGTTVTVSS	1285	DIQLTQSPSFLSASVGDRVTITCRASQG ISSYLAWYQQKPGKAPKLLIYAASTLQS GVPSRFSGSGSGTEFTLTISSLQPEDFA TYYCQQLNSYPQGTFGQGTKVEIK	IGHV3-53 (Human)	IGHJ6 (Human)	IGKV1-9 (Human)	IGKJ4 (Human)	2294	ARDLMAYGM DV	3496	QQLNSYP QGT	Davide Robbiani et al., 2020 (https://www.biorxiv.org/content/10.1101/2020.05.13.092619v2)

C211	Ab	SARS-CoV2	SARS-CoV1	SARS-CoV2	SARS-CoV1	S; RBD	B-cells; SARS-CoV2 Human Patient	207	EVQLVESGGGLVQPGGSLRLSCAASEFT VSSNYMSWVRQAPGKGLEWVSVIYSG GSTFYADSVKGRFTISRDNSKNTLYLQM NSLRPEDTAVYYCARDYGDFYFDFWGQ GTLVTVSS	1286	EIVMTQSPATLSVSPGERATLSCRASQ SVSSNLAWYQQKPGQGPRLLIYGAST RATGIPARFSGSGSGTEFTLTISSLQSE DFAVYYCQQYNNWPRTFGQGTKVEIK	IGHV3-66 (Human)	IGHJ4 (Human)	IGKV3-15 (Human)	IGKJ1 (Human)	2295	ARDYGDFYFD F	3497	QQYNNWP RT	Davide Robbiani et al., 2020 (https://www.biorxiv.org/content/10.1101/2020.05.13.092619v2)
C212	Ab	SARS-CoV2	SARS-CoV1		SARS-CoV1, SARS-CoV2	S; non-RBD	B-cells; SARS-CoV2 Human Patient	208	QVQLVQSGAEVKKPGASVKVSCKASGY TVTGYYIHWVRQAPGQGLEWMGWISP NSGGTNYAQKFQGWVTMTRDMSITTA YMELSRLRSDDTAVYYCARERYFDLGG MDVWGQGTTVTVSS	1287	LTQPASVSGSPGQSITISCTGTSSDVGS YNLVSWYQQHPGKAPKLMIYEDSKRP SGVSNRFSGSKSGNTASLTISGLQAED EADYYCCSYAGSSTRLFGGGTKLTVL	IGHV1-2 (Human)	IGHJ6 (Human)	IGLV2-23 (Human)	IGLJ3 (Human)	2296	ARERYFDLGG MDV	3498	CSYAGSST RL	Davide Robbiani et al., 2020 (https://www.biorxiv.org/content/10.1101/2020.05.13.092619v2)
C214	Ab	SARS-CoV2	SARS-CoV1		SARS-CoV1, SARS-CoV2	S; RBD	B-cells; SARS-CoV2 Human Patient	209	QVQLVESGGGVVQPGRSLRLSCAASGF TFSSYGMHWVRQAPGKGLEWVAAIWY DGSNKHYADSVKGRFTISRDNSKNTLYL QMNSLRAEDTAVYYCARDVGRVTTWF DPWGQGTLVTVSS	1288	DIQLTQSPSSLSASVGDRVTITCRASQS ISSYLTWYQQKPGKAPKLLIYAASSLQS GVPSRFSGSGSGTDFTLTISSLQPEDFA TYYCQQSYSTPPWTFGQGTKVEIK	IGHV3-33 (Human)	IGHJ5 (Human)	IGKV1-39 (Human)	IGKJ1 (Human)	2297	ARDVGRVTT WFDP	3499	QQSYSTPP WT	Davide Robbiani et al., 2020 (https://www.biorxiv.org/content/10.1101/2020.05.13.092619v2)
C215	Ab	SARS-CoV1, SARS-CoV2			SARS-CoV2	S; RBD	B-cells; SARS-CoV2 Human Patient	210	EVQLLESGGGLVQPGGSLRLSCAASGFT FSSYAMSWVRQAPGKGLEWVSAITDSG DGTFYADSVKGRFTISRDNSKNTLYLQM NSLRAEDTAVYYCASEEDYSNYVGWFD PWGQGTLVTVSS	1289	DIQLTQSPSSLSASVGDRVTITCRASQS ISSYLNWYQQKPGKAPKLLIYAASSLQS GVPSRFSGSGSGTDFTLTISSLQPEDFA TYYCQQSYSTPPWTFGQGTKVEIK	IGHV3-23 (Human)	IGHJ5 (Human)	IGKV1-39 (Human)	IGKJ1 (Human)	2298	ASEEDYSNYV GWFDP	3500	QQSYSTPP WT	Davide Robbiani et al., 2020 (https://www.biorxiv.org/content/10.1101/2020.05.13.092619v2)
C216	Ab	SARS-CoV2	SARS-CoV1		SARS-CoV1, SARS-CoV2	S; RBD	B-cells; SARS-CoV2 Human Patient	211	EVQLVESGGGLVQPGGSLRLSCAASGFT FSSYDMHWVRQATGKGLEWVSAIGTA GDTYYPDSVKGRFTISRENAKNSLYLQM NSLRAGDTAVYYCARDRGSSGWYGWY FDLWGRGTLVTVSS	1290	DIQLTQSPSSLSASVGDRVTITCRASQS ISSYLNWYQQKPGKAPKLLIYVASSLQS GVPSRFSGSGSGTDFTLTISSLQPEDFA TYYCQQSYSTPPITFGQGTRLEIK	IGHV3-13 (Human)	IGHJ2 (Human)	IGKV1-39 (Human)	IGKJ5 (Human)	2299	ARDRGSSGW YGWYFDL	3501	QQSYSTPPI T	Davide Robbiani et al., 2020 (https://www.biorxiv.org/content/10.1101/2020.05.13.092619v2)
CA1	Ab	SARS-CoV2		SARS-CoV2		S; RBD	B-cells; SARS-CoV2 Human Patient	212	EVQLVQSGAEVKKPGASVKVSCKASGYT FTSYGISWVRQAPGQGLEWMGWISAY NGNTNYAQKLQGRVTMTTDTSTSTAY MELRSLRSDDTAVYYCAREGYCSGGSCY SGYYYYYGMDVWGQGTTVTVSS	1291	DIVMTQTPATLSLSPGERATLSCRASQ SVSSYLAWYQQKPGQAPRLLIYDASN RATGIPARFSGSGSGTDFTLTISSLEPE DFAVYYCQQRRNWGTFGPGTKVDIK	IGHV1-18 (Human)	IGHJ6 (Human)	IGKV3-11 (Human)	IGKJ3 (Human)	2300	AREGYCSGGS CYSGYYYYYG MDV	3502	QQRRNW GT	Rui Shi et al., 2020 (https://www.nature.com/articles/s41586-020-2381-y_reference.pdf);NCBI (https://www.ncbi.nlm.nih.gov/nuccore/MT470194);NCBI (https://www.ncbi.nlm.nih.gov/nuccore/MT4701945)
CB6	Ab	SARS-CoV2		SARS-CoV2		S; RBD	B-cells; SARS-CoV2 Human Patient	213	EVQLVESGGGLVQPGGSLRLSCAASGFT VSSNYMSWVRQAPGKGLEWVSVIYSG GSTFYADSVKGRFTISRDNSMNTLFLQM NSLRAEDTAVYYCARVLPMYGDYLDYW GQGTLVTVSS	1292	DIVMTQSPSSLSASVGDRVTITCRASQ SISRYLNWYQQKPGKAPKLLIYAASSL QSGVPSRFSGSGSGTDFTLTISSLQPED FATYYCQQSYSTPPEYTFGQGTKLEIK	IGHV3-66 (Human)	IGHJ4 (Human)	IGKV1-39 (Human)	IGKJ2 (Human)	2301	ARVLPMYGD YLDY	3503	QQSYSTPP EYT	Rui Shi et al., 2020 (https://www.nature.com/articles/s41586-020-2381-y_reference.pdf);NCBI (https://www.ncbi.nlm.nih.gov/nuccore/MT470194);NCBI (https://www.ncbi.nlm.nih.gov/nuccore/MT4701945)
CC12.1	Ab	SARS-CoV2	SARS-CoV1	SARS-CoV2	SARS-CoV1	S; RBD	B-cells; SARS-CoV2 Human Patient	214	EVQLVESGGGLIQPGGSLRLSCAASGLT VSSNYMSWVRQAPGKGLEWVSVIYSG GSTFYADSVKGRFTISRDNSKNTLYLQM NSLRAEDTAVYYCARDLDVYGLDVWGQ GTTVTVSS	1293	DIVMTQSPSFLSASVGDRVTITCRASQ GISSYLAWYQQKPGKAPKLLIYAASTL QSGVPSRFSGSGSGTEFTLTISSLQPED FATYYCQQLNSYPPKFTFGPGTKVEIK	IGHV3-53 (Human)	IGHJ6 (Human)	IGKV1-9 (Human)	IGKJ3 (Human)	2302	ARDLDVYGLD V	3504	QQLNSYPP KFT	Thomas Rogers et al., 2020 (https://science.sciencemag.org/content/early/2020/06/15/science.abc7520);Meng Yuan et al., 2020 (https://www.biorxiv.org/content/10.1101/2020.06.08.141267v1)
CC12.10	Ab	SARS-CoV2	SARS-CoV1	SARS-CoV2	SARS-CoV1	S; RBD	B-cells; SARS-CoV2 Human Patient	215	QVQLVQSGAEVKKPGASVKVSCKASGYI YSGYFMHWVRQAPGQGLEWMGWISP DSGGANYAQTFQGRVTMTRDTSTTTAH MELSRLRSDDTAVYYCARGPRYSGTHFD YWGQGTLVTVSS	1294	QSALTQPASVSGSPGQSLTISCTGTSSD VGGYNYVSWYQQHPDKAPKLMIYDV NNRPSGVSNRFSGSKSGSTASLTISGL QAEDEADYYCSSYAGSSTQVFGGGTK LTVL	IGHV1-2 (Human)	IGHJ4 (Human)	IGLV2-14 (Human)	IGLJ3 (Human)	2303	ARGPRYSGTH FDY	3505	SSYAGSST QV	Thomas Rogers et al., 2020 (https://science.sciencemag.org/content/early/2020/06/15/science.abc7520)
CC12.11	Ab	SARS-CoV2	SARS-CoV1	SARS-CoV2	SARS-CoV1	S; RBD	B-cells; SARS-CoV2 Human Patient	216	QVQLVQSGAEVKKPGASVKVSCKASGYI FSGYYTHWVRQAPGQGLEWMGWISP DSGGTNYAQKFQGRVTMTRDTSITTAY VELSGLRSDDTAVYYCARGPRYSGTYFD YWGQGTLVTVSS	1295	QSVLTQPASVSGSPGQSITISCTGTSSD VGGYNYVSWYQQHPGKVPKLMIYDV SNRPSGVSNRFSGSKSGNTASLTISGL QAEDEADYYCSSYTSSSAQLFGGGTKL TVL	IGHV1-2 (Human)	IGHJ4 (Human)	IGLV2-14 (Human)	IGLJ3 (Human)	2304	ARGPRYSGTY FDY	3506	SSYTSSSAQ L	Thomas Rogers et al., 2020 (https://science.sciencemag.org/content/early/2020/06/15/science.abc7520)
CC12.12	Ab	SARS-CoV2	SARS-CoV1	SARS-CoV2	SARS-CoV1	S; RBD	B-cells; SARS-CoV2 Human Patient	217	QVQLVQSGAEVKKPGASVKVSCKASGYI YSGYYMHWVRQAPGQGLEWMGWISP DSGGTNYAQRFQGRVTMTRDTSTTTAY MELSRLRSDDTAVYYCARGPRYSGTYFD YWGQGTLVTVSS	1296	QSALTQPASVSGSPGQSITISCTGTSSD VGGYNYVSWYQQHPDKAPKLMIYDV SNRPSGVSNRFSGSKSGNTASLTISGL QAEDEADYYCSSYTSGSTQVFGGGTKL TVL	IGHV1-2 (Human)	IGHJ4 (Human)	IGLV2-14 (Human)	IGLJ3 (Human)	2305	ARGPRYSGTY FDY	3507	SSYTSGST QV	Thomas Rogers et al., 2020 (https://science.sciencemag.org/content/early/2020/06/15/science.abc7520)

CC12.13	Ab	SARS-CoV2	SARS-CoV1	SARS-CoV2	SARS-CoV1	S; RBD	B-cells; SARS-CoV2 Human Patient	218	EVQLVESGGGLIQPGGSLRLSCAASGFT VSSNYMSWVRQAPGKGLEWVSVIYSG GSTYYADSVKGRFTISRDNSKNTLYLQM NSLRAEDTAVYYCARDPYGYSSIWDGQ GGHWGQGTLVTVSS	1297	DVVMTQSPSSLSASVGDRVTITCQAS QDISNYLNWYQQKPGKAPKLLIYDAS NFATGVPSRFSGTGSGTDFTFTISSLQP EDIATYYCQQYDNLPITFGQGTRLEIK	IGHV3-53 (Human)	IGHJ4 (Human)	IGKV1-33 (Human)	IGKJ5 (Human)	2306	ARDPYGYSSI WDGQGGH	3508	QQYDNLPI T	Thomas Rogers et al., 2020 (https://science.sciencemag.org/content/early/2020/06/15/science.abc7520)
CC12.14	Ab	SARS-CoV2	SARS-CoV1	SARS-CoV2	SARS-CoV1	S; RBD	B-cells; SARS-CoV2 Human Patient	219	QVQLVESGGGLVKPGGSLRLSCAASGFT FNYYSMNWVRQAPGKGLEWISSISTSSS FVYYADSVKGRFTISRDNAKTSLYLQMN SLRAEDTAVYFCARGGYCSDGSCYVQDR LIYYYSGLDVWGQGTTVTVSS	1298	DVVMTQSPLSLPVTLGQPASISCRSSQ SLVYSDGNTYLNWFQQRPGQSPRRLI YKVSNRDSGVPDRFSGSGSGTDFTLKI SRVEAEDVGVFYCMQGTHWPPTFGQ GTKVDIK	IGHV3-21 (Human)	IGHJ6 (Human)	IGKV2-30 (Human)	IGKJ3 (Human)	2307	ARGGYCSDGS CYVQDRLIYYY SGLDV	3509	MQGTHW PPT	Thomas Rogers et al., 2020 (https://science.sciencemag.org/content/early/2020/06/15/science.abc7520)
CC12.15	Ab	SARS-CoV2	SARS-CoV1	SARS-CoV2	SARS-CoV1	S; RBD	B-cells; SARS-CoV2 Human Patient	220	EVQLVESGGGLVQPGGSLRLSCAASGFT FSTYEMNWVRQAPGKGLEWVSYISSSG STIYYADSVKGRFTISRDNAKNSLYLQMS SLRAEDTAIYYCARDRRRRYCTNGVCYR PEEIDYWGQGTLVTVSS	1299	QAVLTQPPSVSGAPGQRVTISCTGSSS NIEAGYDVHWYQQLPGTAPKLLIYVN SNRPSGVPDRFSGSKSGTSASLAITGL QAEDEADYYCQSYDSSLSGVVFGGGT KLIVL	IGHV3-48 (Human)	IGHJ4 (Human)	IGLV1-40 (Human)	IGLJ3 (Human)	2308	ARDRRRRYCT NGVCYRPEEI DY	3510	QSYDSSLS GVV	Thomas Rogers et al., 2020 (https://science.sciencemag.org/content/early/2020/06/15/science.abc7520)
CC12.16	Ab	SARS-CoV2	SARS-CoV1	SARS-CoV2 (weak)	SARS-CoV1	S; RBD	B-cells; SARS-CoV2 Human Patient	221	QVQLVESGGGVVQPGRSLRLSCAASGF TFSSYGMHWVRQAPGKGLEWVALIWY DGSNKNYADSVKGRFTISRDNSKNTLDL QMNSLRAEDTAVYYCARDPFPGAVAGT GYLQYWGQGTLVTVSS	1300	SYELTQPPSVSVAPGQTARITCGGNNI GSKSVHWYQQKPGQAPVLVVYDDSD RPSGIPERFSGSNSGNTATLTISRVEAG DEADYYCQVWDSSSDPWVFGGGTKL TVL	IGHV3-33 (Human)	IGHJ4 (Human)	IGLV3-21 (Human)	IGLJ3 (Human)	2309	ARDPFPGAV AGTGYLQY	3511	QVWDSSS DPWV	Thomas Rogers et al., 2020 (https://science.sciencemag.org/content/early/2020/06/15/science.abc7520)
CC12.17	Ab	SARS-CoV2	SARS-CoV1	SARS-CoV2 (weak)	SARS-CoV1	S; RBD	B-cells; SARS-CoV2 Human Patient	222	EVQLVESGGGVVQPGRSLRLSCAASGFT FRNYGMHWVRQAPGKGLEGVAVISYD GSNKYYADSVKGRFTISRDNSKNTLYLQ MNSLRAEDTAVYYCAKSSGSYYYYYYGM DVWGQGTTVTVSS	1301	SYELTQPPSVSVAPGKTARITCGGNNI GSKSVHWYQQKPGQAPVLVVYDDTD RPSGIPERFSGSSSGNTATLTISRVEAG DEADYYCQVWDSSSDHPVVFGGGTK LTVL	IGHV3-30 (Human)	IGHJ6 (Human)	IGLV3-21 (Human)	IGLJ3 (Human)	2310	AKSSGSYYYYY YGMDV	3512	QVWDSSS DHPVV	Thomas Rogers et al., 2020 (https://science.sciencemag.org/content/early/2020/06/15/science.abc7520)
CC12.18	Ab	SARS-CoV1, SARS-CoV2		SARS-CoV2 (weak)	SARS-CoV1	S; RBD	B-cells; SARS-CoV2 Human Patient	223	EVQLVQSGAEVKKPGASVKVSCKASGYT FTSYYMHWVRQAPGQGLEWMGIINPS GGSTSYAQKFQGRVTMTRDTSTSTVYM ELSSLRSEDTAVYYCARLHCGGDCYLDY WGQGTLVTVSS	1302	NFMLTQPHSVSESPGKTVTISCTRSSG SIANNYVKWYQQRPGSSPTTVIYEDN QRPSGVPDRFSGSIDSSSNSASLTISGL KTEDEADYYCQSYDSSNHEEIWVFGG GTKLIVL	IGHV1-46 (Human)	IGHJ4 (Human)	IGLV6-57 (Human)	IGLJ3 (Human)	2311	ARLHCGGDC YLDY	3513	QSYDSSNH EEIWV	Thomas Rogers et al., 2020 (https://science.sciencemag.org/content/early/2020/06/15/science.abc7520)
CC12.19	Ab	SARS-CoV2	SARS-CoV1	SARS-CoV2 (weak)	SARS-CoV1	S; RBD	B-cells; SARS-CoV2 Human Patient	224	EVQLLESGGGLVQPGGSLRLSCAASGFT FSSYAMSWVRQAPGKGLEWVSAISGSG GSTYYADSVKGRFTISRDNSKNTLYLQM NSLRAEDTAVYYCAKGSGSGSYPNYYYY YGMDVWGQGTTVTVSS	1303	SYELTQSPSVSVAPGQTARITCGGNNI GSKSVHWYQRKPGQAPVLVVYDDSD RPSGIPERFSGSNSGNTATLTISRVEAG DEADYYCQVWDNNSDHLVFGGGTKL TVL	IGHV3-23 (Human)	IGHJ6 (Human)	IGLV3-21 (Human)	IGLJ3 (Human)	2312	AKGSGSGSYP NYYYYYGMD V	3514	QVWDNNS DHLV	Thomas Rogers et al., 2020 (https://science.sciencemag.org/content/early/2020/06/15/science.abc7520)
CC12.2	Ab	SARS-CoV2	SARS-CoV1	SARS-CoV2	SARS-CoV1	S; RBD	B-cells; SARS-CoV2 Human Patient	225	EVQLVESGGGLIQPGGSLRLSCAASGFT VSSNYMSWVRQAPGKGLEWVSVFYSG GSTYYADSVKGRFTISRDNSKNTLYLQM NSLRAEDTAVYYCARDYGDLYFDYWGQ GTLVTVSS	1304	EIVMTQSPGTLSLSPGERATLSCRASQ SVSSSYLAWYQQKPGQAPRLLIYGVSS RATGIPDRFSGSGSETDFTLTISRLEPEE FAVYYCQQYGSSPRTFGQGTKLEIK	IGHV3-53 (Human)	IGHJ4 (Human)	IGKV3-20 (Human)	IGKJ2 (Human)	2313	ARDYGDLYFD Y	3515	QQYGSSPR T	Thomas Rogers et al., 2020 (https://science.sciencemag.org/content/early/2020/06/15/science.abc7520)
CC12.20	Ab	SARS-CoV2	SARS-CoV1		SARS-CoV1	S; non-RBD	B-cells; SARS-CoV2 Human Patient	226	QVQLVESGGGVVQPGRSLRLSCAASGF TFSSYGMHWVRQAPGKGLEWVAVISY DGSNKYYADSVKGRFTISRDNSKNTLYL QMSSLRGEDTAVYYCAKDQAYYDILTGY LNPPKNYYYYGMDVWGQGTTVTVSS	1305	QSVLTQPPSASSTPGQRVTISCSGSSSN IGSNYVYWYQQLPGTAPKLLIYTNNQR PSGVPDRFSGSKSGTSASLAISGLRSED EADYYCAAWDDSLSGRVVFGGGTKLT VL	IGHV3-30 (Human)	IGHJ6 (Human)	IGLV1-47 (Human)	IGLJ3 (Human)	2314	AKDQAYYDIL TGYLNPPKNY YYYGMDV	3516	AAWDDSL SGRVV	Thomas Rogers et al., 2020 (https://science.sciencemag.org/content/early/2020/06/15/science.abc7520)
CC12.21	Ab	SARS-CoV2	SARS-CoV1		SARS-CoV1	S; non-RBD	B-cells; SARS-CoV2 Human Patient	227	QVQLVQSGAEVKKPGASVKVSCKVSGY TLTELSMHWVRQAPGKGLEWMGGFD PEDGETIYAQKFQGRVTMTEDTSTDTAY MDLSSLRSEDTAVYYCATAFSIFGVVPPD YWGQGTLVTVS	1306	QAVVTQPPSASGTPGQRVTISCSGSSS NIGSNTVNWYQQLPGTAPKLLIYSNN QRPSGVPDRFSGSKSGTSASLAISGLQ SEDEADYYCAAWDDSLNGPVFGGGT KLTVL	IGHV1-24 (Human)	IGHJ4 (Human)	IGLV1-44 (Human)	IGLJ3 (Human)	2315	ATAFSIFGVVP PDY	3517	AAWDDSL NGPV	Thomas Rogers et al., 2020 (https://science.sciencemag.org/content/early/2020/06/15/science.abc7520)
CC12.23	Ab	SARS-CoV2	SARS-CoV1	SARS-CoV2 (weak)	SARS-CoV1	S; non-RBD	B-cells; SARS-CoV2 Human Patient	228	QVQLQESGPGLVKPSETLSLTCTVSGGSI SSSSYYWGWIRQPPGKGLEWIGSIYYSG STYYNPSLKSRVTISVDTSKNQFSLKLSSV TAADTAVYYCARQGDCSTTSCAYDYWG QGTLVTVSS	1307	SYELTQPPSVSVSPGQTARITCSGDALP KQYAYWYQQKPGQAPVLVIYKDSERP SGIPERFSGSSSGTTATLTISGVQAEDE ADYYCQSADSSGTYLVVFGGGTKLAV	IGHV4-39 (Human)	IGHJ4 (Human)	IGLV3-25 (Human)	IGLJ3 (Human)	2316	ARQGDCSTTS CAYDY	3518	QSADSSGT YLVV	Thomas Rogers et al., 2020 (https://science.sciencemag.org/content/early/2020/06/15/science.abc7520)
CC12.24	Ab	SARS-CoV2	SARS-CoV1		SARS-CoV1	S; Unk	B-cells; SARS-CoV2 Human Patient	229	EVQLVESGGGVVQPGRSLRLSCSASGFT FSIYGMHWVRQAPGKGLEWVAVISYD GSNKYYADSVKGRFTISRDNSKNTLYLQ MNSLRAEDTAVYYCAKDRTGNYYYGM DVWGQGTTVTVSS	1308	DIQLTQSPSSLSASVGDRVTITCRASQS ISSYLNWYQQKPGKAPKLLIYAASNLQ SGVPSRFSGSGSGTDFTLTISSLQPEDF ATYYCQQSYSTPWTFGQGTKVEIK	IGHV3-30 (Human)	IGHJ6 (Human)	IGKV1-39 (Human)	IGKJ1 (Human)	2317	AKDRTGNYYY GMDV	3519	QQSYSTP WT	Thomas Rogers et al., 2020 (https://science.sciencemag.org/content/early/2020/06/15/science.abc7520)

CC12.25	Ab	SARS-CoV1, SARS-CoV2			SARS-CoV1	S; non-RBD	B-cells; SARS-CoV2 Human Patient	230	QVQLVESGGGLVQPGGSLRLSCAASGFTFSSYAMSWVRQAPGKGLEWVSAISGSGDSTYYADSVKGRFTISRDNSKNTLYLQMNSLRAEDTAVYYCAKDRYYEFWSGYSNWFDPWGQGTLVTISS	1309	QSALTQPPSASGTPGQRVTISCSGSSSNIGSNTVNWYQQLPGTAPKVLVYSNDQRPSGVPDRFSGSKSGTSASLAISGLQSEDEADYYCAAWDDSLNGPVFGGGTKLTVL	IGHV3-23 (Human)	IGHJ5 (Human)	IGLV1-44 (Human)	IGLJ3 (Human)	2318	AKDRYYEFWSGYSNWFDP	3520	AAWDDSLNGPV	Thomas Rogers et al., 2020 (https://science.sciencemag.org/content/early/2020/06/15/science.abc7520)
CC12.26	Ab	SARS-CoV2	SARS-CoV1		SARS-CoV1	S; non-RBD	B-cells; SARS-CoV2 Human Patient	231	EVQLVQSGAEVKKPGESLKISCKGSGYSFTSYWIGWVRQMPGKGLEWMGIIYPGDSDTRYSPSFQGQVTVSADKSISTAYLQWSSLKASDTAMYYCARVNYYDSSGYPSFHFDYWGQGTLVTVS	1310	QTVVTQEPSLTVSPGGTVTLTCVSSTGAVTSGYYPNWFQQKPGQAPRALIYSTSKKHSWTPARFSGSLLGGKAALTLSGVQPEDEAEYYCLLYYGGAQRWVFGGGTKLTVL	IGHV5-51 (Human)	IGHJ4 (Human)	IGLV7-43 (Human)	IGLJ3 (Human)	2319	ARVNYYDSSGYPSFHFDY	3521	LLYYGGAQRWV	Thomas Rogers et al., 2020 (https://science.sciencemag.org/content/early/2020/06/15/science.abc7520)
CC12.27	Ab	SARS-CoV1, SARS-CoV2			SARS-CoV1	S; non-RBD	B-cells; SARS-CoV2 Human Patient	232	QVQLVQSGAEVKKPGASVKVSCKASGYTFIGYYMHWVRQAPGQGLEWMGWINPNSGGTNYAQKFQGRVTMTRDTSISTVYMELSRLRSDDTAVYYCARMPAAMGYYYYGMDVWGQGTTVTVSS	1311	QSVLTQPASVSGSPGQSITISCTGTSSDVGSYNLVSWYQQHPGKAPKLMIYEGSKRPSGVSNRFSGSKSGNTASLTISGLQAEDEADYYCYSYAGSSTFVFVFGTGTKVIVL	IGHV1-2 (Human)	IGHJ6 (Human)	IGLV3-23 (Human)	IGLJ1 (Human)	2320	AREMPAAMGYYYYGMDV	3522	YSYAGSSTFV	Thomas Rogers et al., 2020 (https://science.sciencemag.org/content/early/2020/06/15/science.abc7520)
CC12.28	Ab	SARS-CoV1, SARS-CoV2		SARS-CoV2 and SARS-CoV1		S; RBD	B-cells; SARS-CoV2 Human Patient	233	EVQLLESGGGLVQPGGSLRLSCAASGFTFSNYAMTWVRQAPGKGLEWVSAISSGSGSTYYADSVKGRFTISRDNSKNTVYLQMNSLRAEDTAIYYCAKANKYSSSEFDFWGQGTLVTISS	1312	QSALTQPPSASGTPGQRVTISCSGSSSNIGSNYVYWYQQLPGAAPKLLIYRNDQRPSGVPDRFSGSKSGTSVSLAISGLRSEDEADYYCAAWDDSLSGWVFGGGTKLTVL	IGHV3-23 (Human)	IGHJ4 (Human)	IGLV1-47 (Human)	IGLJ3 (Human)	2321	AKANKYSSSEFDF	3523	AAWDDSLSGWV	Thomas Rogers et al., 2020 (https://science.sciencemag.org/content/early/2020/06/15/science.abc7520)
CC12.3	Ab	SARS-CoV2	SARS-CoV1	SARS-CoV2	SARS-CoV1	S; RBD	B-cells; SARS-CoV2 Human Patient	234	QVQLVESGGGLIQPGGSLRLSCAASGFTVSSNYMSWVRQAPGKGLEWVSVIYSGGSTFYADSVKGRFTISRDNSKSTLYLQMNSLRVEDTAVYYCARDFGDFYFDYWGQGTLVTVSS	1313	EIVLTQSPGTLSLSPGERATLSCRASQSVSSYLAWYQQKPGQAPRLLIYGASSRATGIPDRFSGSGSGTDFTLTISRLEPEDFAVYYCQQYGSSPRTFGQGTKLEIK	IGHV3-53 (Human)	IGHJ4 (Human)	IGKV3-20 (Human)	IGKJ2 (Human)	2322	ARDFGDFYFDY	3524	QQYGSSPRT	Thomas Rogers et al., 2020 (https://science.sciencemag.org/content/early/2020/06/15/science.abc7520);Meng Yuan et al., 2020 (https://www.biorxiv.org/content/10.1101/2020.06.08.141267v1)
CC12.4	Ab	SARS-CoV2	SARS-CoV1	SARS-CoV2	SARS-CoV1	S; RBD	B-cells; SARS-CoV2 Human Patient	235	QVQLVQSGAEVKKPGASVKVSCKASGYTFTGYYMHWVRQAPGQGLEWMGWISPNSGGTNYAQKFQGWVTMTRDTSVSTAYMELSRLRFDDTAVYYCATESWVYGSGSYSSGAFDIWGQGTMVTVSS	1314	QSVLTQPPSASGSPGQSVTISCTGTSSDVGGGYDYVSWYQQHPGKAPKLMIYEVSKRPSGVPDRFSGSKSGNTASLTVPGLQAEDEADYYCTSYAGSNNFVFGGGTKLIVL	IGHV1-2 (Human)	IGHJ3 (Human)	IGLV2-8 (Human)	IGLJ3 (Human)	2323	ATESWVYGSGSYSSGAFDI	3525	TSYAGSNNFV	Thomas Rogers et al., 2020 (https://science.sciencemag.org/content/early/2020/06/15/science.abc7520)
CC12.5	Ab	SARS-CoV2	SARS-CoV1	SARS-CoV2	SARS-CoV1	S; RBD	B-cells; SARS-CoV2 Human Patient	236	EVQLVQSGAEVKKPGASVKVSCKASGYIYSGYYMHWVRQAPGQGLEWMGWISPDSGGTNYAQRFQGRVTMTRDTSTTTAYMELSRLRSDDTAMYYCARGPRYSGTYFDYWGQGTLVTVSS	1315	QTVVTQPASVSGSPGQSITISCTGTSSDVGGYNYVSWYQQHPDKAPKLIIYDVSNRPSGVSNRFSGSKSGNTASLTISGLQAEDEAAYYCSSYTSSSTQVFGGGTKLTVL	IGHV1-2 (Human)	IGHJ4 (Human)	IGLV2-14 (Human)	IGLJ3 (Human)	2324	ARGPRYSGTYFDY	3526	SSYTSSSTQV	Thomas Rogers et al., 2020 (https://science.sciencemag.org/content/early/2020/06/15/science.abc7520)
CC12.6	Ab	SARS-CoV2	SARS-CoV1	SARS-CoV2	SARS-CoV1	S; RBD	B-cells; SARS-CoV2 Human Patient	237	QVQLVQSGAEVKKPGASVKVSCKASGYIFSGYYMHWVRQAPGQGLEWMGWISPDSGGTNYAQKFQGRVTMTRDTSITTGYMELSGLRSDDTAVYYCARGPRYSGTYFDYWGQGTLVTVSS	1316	QSALTQPTSVSGSPGQSITISCTGTSSDVGGYNYVSWYQQHPGKAPKLIIYDVSNRPSGVSNRFSGSKSGNTASLTISGLQAEDEADYYCSSYTVSSTQVFGGGTKLTVL	IGHV1-2 (Human)	IGHJ4 (Human)	IGLV2-14 (Human)	IGLJ3 (Human)	2325	ARGPRYSGTYFDY	3527	SSYTSSSTQV	Thomas Rogers et al., 2020 (https://science.sciencemag.org/content/early/2020/06/15/science.abc7520)
CC12.7	Ab	SARS-CoV2	SARS-CoV1	SARS-CoV2	SARS-CoV1	S; RBD	B-cells; SARS-CoV2 Human Patient	238	EVQLVQSGAEVKKPGASVKVTCKTSGYIFSGYYMHWVRQVPGQGLEWMGWISPDSGATNYAQKFQGRVTMTRDTSITTSYVELTWLKSDDTAVYYCARGPRYSGTYFDFWGQGTLVTVSS	1317	QPVLTQPASVSGSPGQSLTISCTGTSSDIGGFNYVSWYQQHPGKAPKLMIFDVSKRPSGVPNRFSGSKSGNTASLTISGLQAEDEGDYYCSSYTISSAQVFGGGTKLTVL	IGHV1-2 (Human)	IGHJ4 (Human)	IGLV2-14 (Human)	IGLJ3 (Human)	2326	ARGPRYSGTYFDY	3528	SSYTVSSTQV	Thomas Rogers et al., 2020 (https://science.sciencemag.org/content/early/2020/06/15/science.abc7520)
CC12.8	Ab	SARS-CoV2	SARS-CoV1	SARS-CoV2	SARS-CoV1	S; RBD	B-cells; SARS-CoV2 Human Patient	239	QVQLVQSGAEVKKPGASVKVSCKASGYIFSGYYTHWVRQAPGQGLEWMGWISPDSGGTNYAQKFQGRVTMTRDTSITTAYVELSGLRSDDTAVYYCARGPRYSGTYFDYWGQGTLVTVSS	1318	QSALTQPASVSGSPGQSITISCTGTSSDVGGYNHVSWYQQHPGKAPKLMIYDVSNRPSGVSNRFSGSKSGNTASLTISGLQAEDEADYYCSSYTSSSAQLFGGGTKLTVL	IGHV1-2 (Human)	IGHJ4 (Human)	IGLV2-14 (Human)	IGLJ3 (Human)	2327	ARGPRYSGTYFDY	3529	SSYTSSSAQL	Thomas Rogers et al., 2020 (https://science.sciencemag.org/content/early/2020/06/15/science.abc7520)
CC12.9	Ab	SARS-CoV2 (weak)	SARS-CoV1	SARS-CoV2	SARS-CoV1	S; non-RBD	B-cells; SARS-CoV2 Human Patient	240	EVQLVQSGAEVKKPGASVKVSCKASGYIFSGYYMHWVRQAPGQGLEWMGWISPDSGGTNYAQNFQGRVTMTRDTSISTGYMELSRLRSDDTAMYYCARGPRYSGTYFDYWGQGVLVTVSS	1319	QSVLTQPASVSGSPGQSITISCTGTSSDVGGYNYVSWYQQHPGKVPKLMIYDVSNRPSGVSNRFSGSKSGNTASLTISGLQAEDEADYYCSSYTSSSAQVFGGGTKLTVL	IGHV1-2 (Human)	IGHJ4 (Human)	IGLV2-14 (Human)	IGLJ3 (Human)	2328	ARGPRYSGTYFDY	3530	SSYTSSSAQV	Thomas Rogers et al., 2020 (https://science.sciencemag.org/content/early/2020/06/15/science.abc7520)
CC6.29	Ab	SARS-CoV2		SARS-CoV2		S; RBD	B-cells; SARS-CoV2 Human Patient	241	QVQLVQSGSELKKPGASVKVSCKASGYTFATYALNWVRQAPGQGLEWMGWVNTNTGSPTYAQGFTGRFVFSFDTSVSTAYLQIRTLKAEDTAVYYCAVYYYDSGSPGWFDPWGQGTLVTVSS	1320	DIQLTQSPSSLSASVGDRVTITCRASQTASSYLNWYQQKPGKAPNLLIYAASSLQSGVPSRFSGSGSVTDFTLTISSLQPEDFATYYCQQSYSTPPTFGQGTKVDIK	IGHV7-4-1 (Human)	IGHJ5 (Human)	IGKV1-39 (Human)	IGKJ3 (Human)	2329	AVYYYDSGSPGWFDP	3531	QQSYSTPPT	Thomas Rogers et al., 2020 (https://science.sciencemag.org/content/early/2020/06/15/science.abc7520)

CC6.30	Ab	SARS-CoV2		SARS-CoV2		S; RBD	B-cells; SARS-CoV2 Human Patient	242	QVQLVQSGAEVKKPGSSVKVSCKASGG TFSIYAITWVRQAPGQGLEWMGGIIPII GTANYAQKFQGRVTITADKSTSTAYMEL SSLRSEDTAVYYCARDFRYCSSTRCYFWF DPWGQGTLVTVSS	1321	DIQMTQSPSSLSASVGDRVTITCRASQ NISSYLNWYQQEAGKAPKLLIYAASSL QSGVPSRFSGSGSGTDFTLTISSLQPED FATYYCQQSYSTPRTFGQGTKVDIK	IGHV1-69 (Human)	IGHJ5 (Human)	IGKV1-39 (Human)	IGKJ3 (Human)	2330	ARDFRYCSST RCYFWFDP	3532	QQSYSTPR T	Thomas Rogers et al., 2020 (https://science.sciencemag.org/content/early/2020/06/15/science.abc7520)
CC6.31	Ab	SARS-CoV2		SARS-CoV2		S; RBD	B-cells; SARS-CoV2 Human Patient	243	EVQLVQSGAEVKKPGASVKVSCMASGY TFTSYYMHWVRQAPGQGLEWMGIISP SGGGTSYAQKFQGRVTLTRDTSTSTVYM ELSSLRSEDTAVYYCARWYDSTGSIDYW GQGTLVTVSS	1322	DIQMTQSPSSLSASVGDRVTITCRASQ GIRNDLGWYQQKPGKAPKRLIYAASSL QSGVPSRFSGSGSGTEFTLTISSLQPED FATYYCLQHNSYPILTFGGGTKLEIK	IGHV1-46 (Human)	IGHJ4 (Human)	IGKV1-17 (Human)	IGKJ4 (Human)	2331	ARWYDSTGSI DY	3533	LQHNSYPIL T	Thomas Rogers et al., 2020 (https://science.sciencemag.org/content/early/2020/06/15/science.abc7520)
CC6.32	Ab	SARS-CoV1, SARS-CoV2		SARS-CoV2		S; RBD	B-cells; SARS-CoV2 Human Patient	244	EVQLVESGGGLVQPGRSLRLSCAASGFT FDDYAMHWVRQAPGKGLEWVSGISW NSGSIAFAGSVKGRFTISRDNAKNSLYLQ MNSLRAEDTALYYCAKDQGYSYGNYFD YWGQGTLVTVSS	1323	QLVLTQPPSVSVAPGKTARITCGGNNI GSKSVYWYQQKPGQAPVLVVYDDSD RPSGIPERFSGSNSGNTATLTISRVEAG DEADYYCQVWDSSSDHPYVFGSGTKV TVL	IGHV3-9 (Human)	IGHJ4 (Human)	IGLV3-21 (Human)	IGLJ6 (Human)	2332	AKDQGYSYG NYFDY	3534	QVWDSSS DHPYV	Thomas Rogers et al., 2020 (https://science.sciencemag.org/content/early/2020/06/15/science.abc7520)
CC6.33	Ab	SARS-CoV1, SARS-CoV2		SARS-CoV2 and SARS-CoV1		S; RBD	B-cells; SARS-CoV2 Human Patient	245	QVQLVQSGAEVKKPGSSVKVSCKASGG TFSSSAISWVRQAPGQGLEWMGGIIPIL DITNYAQKFQGRVTITADKSTSTAFMELS SLRSEDTAVYYCALRNQWDLLVYWGQG TLVTVSS	1324	EIVLTQSPGTLSLSPGERATLSCRASQS VSSSYLAWYQQKPGQAPRLLIYGASSR ATGIPDRFSGSGSGTDFTLTISRLEPED FAVYYCQHYGSSLWTFGQGTKLEIK	IGHV1-69 (Human)	IGHJ4 (Human)	IGKV3-20 (Human)	IGKJ1 (Human)	2333	ALRNQWDLL VY	3535	QHYGSSL WT	Thomas Rogers et al., 2020 (https://science.sciencemag.org/content/early/2020/06/15/science.abc7520)
Clone11-9	Ab	SARS-CoV2				S; RBD	Immunised Mouse	246	QVQLQQPGAELVMPGASVKMSCKASG YTFTDYWMHWVKQRPGQGLEWIGAE DTSDSYTSYNQKFKGKATLTVDESSSTAY MQLSSLTSEDSAVYYCARRGYGSSYTWF AYWGQGTLVTVSA	1325	DVLMTQTPLSLPVSLGDQASISCRSSQ SIVHSNGNTYLEWYLQKPGQSPKLLIY KVSNRFSGVPDRFSGSGSGTDFTLKIS RVEAEDLGVYYCFQGSHVPLTFGAGT KLELK	IGHV1-69 (Mouse)	IGHJ3 (Mouse)	IGKV1-117 (Mouse)	IGKJ5 (Mouse)	2334	ARRGYGSSYT WFAY	3536	FQGSHVPL T	Nadezhda Antipova et al., 2020
CnC2t1p1_B10	Ab	SARS-CoV2			SARS-CoV2	S; Unk	B-cells; SARS-CoV2 Human Patient	247	QVQLVQSGAEVKKPGSSVKVSCKASGG TFSSYAISWVRQAPGQGLEWMGGIIPIF GTANYAQKFQGRVTITADKSTSTAYMEL SSLRSEDTAVYYCARVSGYDSSGYWGDY WGQGTLVTVSS	1326	EIVLTQSPATLSLSPGERATLSCRASQS VSSYLAWYQQKPGQAPRLLIYDASNR ATGIPARFSGSGSGTDFTLTISSLEPEDF AVYYCQQRSNWPPALTFGGGTKVEIK	IGHV1-69 (Human)	IGHJ4 (Human)	IGKV3-11 (Human)	IGKJ4 (Human)	2335	ARVSGYDSSG YWGDY	3537	QQRSNWP PALT	Christoph Kreer et al., 2020 (https://doi.org/10.1016/j.cell.2020.06.044)
CnC2t1p1_B4	Ab	SARS-CoV2		SARS-CoV2		S; RBD	B-cells; SARS-CoV2 Human Patient	248	QVQLVQSGAEVKKPGASVKVSCKASGY TFTSYGISWVRQAPGQGLEWMGWISA YNGNTNYAQKLQGRVTMTTDTSTSTAY MELRSLRSDDTAVYYCARDGELLGWFD PWGQGTLVTVSS	1327	QSALTQPASVSGSPGQSITISCTGTSSD VGSYNLVSWYQQHPGKAPKLMIYEGS KRPSGVSNRFSGSKSGNTASLTISGLQ AEDEADYYCCSYAGSSTWVFGGGTKL TVL	IGHV1-18 (Human)	IGHJ5 (Human)	IGLV2-23 (Human)	IGLJ3 (Human)	2336	ARDGELLGW FDP	3538	CSYAGSST WV	Christoph Kreer et al., 2020 (https://doi.org/10.1016/j.cell.2020.06.044)
CnC2t1p1_D6	Ab	SARS-CoV2		SARS-CoV2		S; RBD	B-cells; SARS-CoV2 Human Patient	249	EVQLVESGGGLVQPGRSLRLSCTASGFT FGDYAMSWFRQAPGKGLEWVGFIRSK AYGGTTEYAASVKGRFTISRDDSKSIAYL QMNSLKTEDTAVYYCTRVRRLWFGSYY YGMDVWGQGTTVTVSS	1328	DIVMTQSPLSLPVTPGEPASISCRSSQS LLHSNGYNYLDWYLQKPGQSPQLLIYL GSNRASGVPDRFSGSGSGTDFTLKISR VEAEDVGVYYCMQALQTPGTFGPGT KVDIK	IGHV3-49 (Human)	IGHJ6 (Human)	IGKV2-28 (Human)	IGKJ3 (Human)	2337	TRVRRLWFGS YYYGMDV	3539	MQALQTP GT	Christoph Kreer et al., 2020 (https://doi.org/10.1016/j.cell.2020.06.044)
CnC2t1p1_E12	Ab	SARS-CoV2		SARS-CoV2		S; RBD	B-cells; SARS-CoV2 Human Patient	250	EVQLVESGGGLVQPGRSLRLSCTASGFT FGDYAMSWFRQAPGKGLEWVGFIRSK AYGGTTEYAASVKGRFTISRDDSKSIVYL QMNSLKTEDTAVYYCTRVRRLWFGSYY YGMDVWGQGTTVTVSS	1329	DIVMTQSPLSLPVTPGEPASISCRSSQS LLHSNGYNYLDWYLQKPGQSPQLLIYL GSNRASGVPDRFSGSGSGTDFTLKISR VEAEDVGVYYCMQALQTPGTFGPGT KVDIK	IGHV3-49 (Human)	IGHJ6 (Human)	IGKV2-28 (Human)	IGKJ3 (Human)	2338	TRVRRLWFGS YYYGMDV	3540	MQALQTP GT	Christoph Kreer et al., 2020 (https://doi.org/10.1016/j.cell.2020.06.044)
CnC2t1p1_E8	Ab	SARS-CoV2		SARS-CoV2		S; RBD	B-cells; SARS-CoV2 Human Patient	251	QVQLVQSGAEVKNPGASVKVSCKASGY IFTNYYIHWVRQAPGQGLEWVGWIHSL SGGTSYAQKFQGRVTLTRDASIRTAYME LSRLGSDDTALYYCARASVSTITDFDYWG QGTLVAVSS	1330	QSALTQPASVSGSPGQSITISCTGTSGD VGSYNLVSWYQQHPGKAPKLVIYEAT KRPSGVSNRFFASKSGNTASLTISGLQ AEDEADYYCCSYAGVRTVVFGGGTKL TVL	IGHV1-2 (Human)	IGHJ4 (Human)	IGLV2-23 (Human)	IGLJ3 (Human)	2339	ARASVSTITDF DY	3541	CSYAGVRT VV	Christoph Kreer et al., 2020 (https://doi.org/10.1016/j.cell.2020.06.044)
CnC2t1p1_G6	Ab	SARS-CoV2		SARS-CoV2		S; RBD	B-cells; SARS-CoV2 Human Patient	252	QVQLVQSGAEVKKPGASVKVSCKASGYI FTNYYIHWVRQAPGQGLEWVGWIHSL SGGTSYAQKFQGRVTLTRDAPIRTAYME LSGLGSDDTAVYYCARASVATITDFDYW GQGTLVAVSS	1331	QSALTQPASVSGSPGQSITISCTGTSGD IGSYNLVSWYQQYPGKAPKLIIYEASKR PSGVSNRFFASKSGNTASLTISGLQAE DEADYYCCSYAGVRTVVFGGGTKLTVL	IGHV1-2 (Human)	IGHJ4 (Human)	IGLV2-23 (Human)	IGLJ3 (Human)	2340	ARASVATITDF DY	3542	CSYAGVRT VV	Christoph Kreer et al., 2020 (https://doi.org/10.1016/j.cell.2020.06.044)
COV2-2006	Ab	SARS-CoV1, SARS-CoV2			SARS-CoV2	S; non-RBD	B-cells; SARS-CoV2 Human Patient	253	QVQLVESGGGVVQPGRSLRLSCAASGF TFSYYAILWFRQAPGKGLEWVAIISYDGS NKYYADSVKGRFTISRDNSKNTLYLQMN SLRPEDTAVYYCARPQSGGYYAPLDYW GQGTLVTVSS	1332	EIVLTQSPGTLSLSPGERATLSCRASQS VSSSYLAWYQQKPGQAPRLLIYGASSR ATGIPDRFSGSGSGTDFTLTISRLEPED FAVYYCQQYGSSPWTFGQGTKVEIK	IGHV3-30-3 (Human)	IGHJ4 (Human)	IGKV3-20 (Human)	IGKJ1 (Human)	2341	ARPQSGGYYA PLDY	3543	QQYGSSP WT	Seth Zost et al., 2020 (https://www.nature.com/articles/s41591-020-0998-x)
COV2-2007	Ab	SARS-CoV1, SARS-CoV2			SARS-CoV2	S; RBD	B-cells; SARS-CoV2 Human Patient	254	QVQLVESGGGVVQPGRSLRLSCAASGF TFSRYGMHWVRQAPGKGLEWVGIISYD ASDKTYAESVKGRFTISRDNSKNTLYLQ MNSLRAEDTAVYYCAKVSATYYYYYYG MDVWGQGTTVTVSS	1333	DIQMTQSPSSLSASVGDRVTITCQASQ DISTYLNWYQQKPGKAPKLLIYDASNL ETGVPSRFSGSGSGTDFTFTISSLQPED IATYYCQQYDNLLFTFGPGTKVDVK	IGHV3-30 (Human)	IGHJ6 (Human)	IGKV1-33 (Human)	IGKJ3 (Human)	2342	AKVSATYYYY YGMDV	3544	QQYDNLLF T	Seth Zost et al., 2020 (https://www.nature.com/articles/s41591-020-0998-x)
COV2-2009	Ab	SARS-CoV1, SARS-CoV2			SARS-CoV2	S; non-RBD	B-cells; SARS-CoV2 Human Patient	255	QVQLVESGGGVVQPGRSLRLSCAASGF TFSTYAMHWVRQAPGKGLEWVAVISY DGSNKYYADSVKGRFTISRDNPKNTLYL QMNSLRAEDTAVYYCARDTATYVLLWS GDFNLDYWGQGTLVTVSS	1334	QSALTQPASVSGSPGQSITISCTGTSGD VGAYNYVSWYQQHPVKAPKLMIYDV SKRPSGVSNRFSGSKSGNTASLTISGLQ TEDEADYYCSSYTSSSTLWVFGGGTKL TVL	IGHV3-30 (Human)	IGHJ4 (Human)	IGLV2-14 (Human)	IGLJ3 (Human)	2343	ARDTATYVLL WSGDFNLDY	3545	SSYTSSSTL WV	Seth Zost et al., 2020 (https://www.nature.com/articles/s41591-020-0998-x)

COV2-2011	Ab	SARS-CoV1, SARS-CoV2			SARS-CoV2	S; non-RBD	B-cells; SARS-CoV2 Human Patient	256	QVQLVESGGGVVQPGRSLRLSCAASGFTFSTYAMHWVRQAPGKGLEWVTLISYDGGNKYYADSVKGRFTISRDNSKNTLYLQMNSLRAEDAAVYFCARGHTGNYYYGMDVWGQGTTVTVSS	1335	ITCRASQSISSYLNWYQQKPGKAPKLLIYAASSLQSGVPSRFGGSASGTDFTLTISSLQPEDFATYYCQQSYSTFTFGPGTKVDIK	IGHV3-30-3 (Human)	IGHJ6 (Human)	IGKV1-39 (Human)	IGKJ3 (Human)	2344	ARGHTGNYYYGMDV	3546	QQSYSTFT	Seth Zost et al., 2020 (https://www.nature.com/articles/s41591-020-0998-x)
COV2-2013	Ab	SARS-CoV1, SARS-CoV2			SARS-CoV2	S; non-RBD	B-cells; SARS-CoV2 Human Patient	257	QVHLVESGGGVVQPGRSLRLSCAASGFTFSNYGMHWVRQAPGKGLEWVAVISGDENNKFYANSVKGRFTISRDNSKNTLSLQMNSLRPEDTARYYCAKGGDSSGWAWDGDNPPTDYWGQGTLVIVSS	1336	DIVMTQSPDFLAVSLGERATINCKSSQSVLHTPKNKNYLAWYKQKPGQPPKVLIYWASTRESGVPERFSGSGSGTDFTLIISSLQAEDAAVYYCQQYYTAPLTFGGGTKVEIK	IGHV3-30 (Human)	IGHJ4 (Human)	IGKV4-1 (Human)	IGKJ4 (Human)	2345	AKGGDSSGWAWDGDNPPTDY	3547	QQYYTAPLT	Seth Zost et al., 2020 (https://www.nature.com/articles/s41591-020-0998-x)
COV2-2015	Ab	SARS-CoV1, SARS-CoV2		SARS-CoV2 (weak)		S; RBD	B-cells; SARS-CoV2 Human Patient	258	EVQLVESGGGLVQPGRSLRLSCAASGFTFDDYAMHWVRQAPGKGLEWVSGISWNSGSIGYADSVKGRFTISRDNAKNSLYLQMNSLRTEDTALYYCAMGPFGELLPYYFDYWGQGTLVTVSS	1337	EIVLTQSPATLSLSPGERATLSCRASQSVSSYLAWYQQKPGQAPRLLIYDTSNRATGIPARFSGSGSGTDFTLTISSLEPEDFAVYYCQQRSNWPPYTFGQGTKLEIK	IGHV3-9 (Human)	IGHJ4 (Human)	IGKV3-11 (Human)	IGKJ2 (Human)	2346	AMGPFGELLPYYFDY	3548	QQRSNWPPYT	Seth Zost et al., 2020 (https://www.nature.com/articles/s41591-020-0998-x)
COV2-2016	Ab	SARS-CoV1, SARS-CoV2			SARS-CoV2	S; RBD	B-cells; SARS-CoV2 Human Patient	259	QVQLVQSGAEVKKPGASVKVSCKVSGYTLTELSIHWVRQAPGKGLEWMGGFDPEDAETIYAQNFQGRVTMTEDTSTDTAYMELSSLRSEDTALYYCAAAPAVMTAGWFDPWGQGTLVSVSS	1338	QSALTQPASVSGSPGQSITISCTGTSSDVGGYHYVSWYQHHPGKAPKLIIYDVIKRPSGVSNRFSGSKSGNTASLTISGLQAEDEAYYYCSSYTSSTTWVFGGGTRLTVL	IGHV1-24 (Human)	IGHJ5 (Human)	IGLV2-14 (Human)	IGLJ3 (Human)	2347	AAAPAVMTAGWFDP	3549	SSYTSSTTWV	Seth Zost et al., 2020 (https://www.nature.com/articles/s41591-020-0998-x)
COV2-2017	Ab	SARS-CoV1, SARS-CoV2			SARS-CoV2	S; non-RBD	B-cells; SARS-CoV2 Human Patient	260	QVQLEESGPGLVKPSETLSLTCTVSGGSISSHYWSWIRQPPGKGLEWIGYIQDSGSTNYNPSLKSRVTISVDTSKNQFSLRLSSVTTADTAVYYCVRGAMAWFDPWGQGTLVTVSS	1339	QSVLTQPPSVSGAPGQRVTISCTGSSSNIGAGYNVHWYQQLPGTAPKLLIYGNNNRPSGVPDRFSGSKSGTSASLAITGLQAEDEADYYCQSFDSSLSGSDVFGTGTKVSVL	IGHV4-59 (Human)	IGHJ5 (Human)	IGLV1-40 (Human)	IGLJ1 (Human)	2348	VRGAMAWFDP	3550	QSFDSSLSGSDV	Seth Zost et al., 2020 (https://www.nature.com/articles/s41591-020-0998-x)
COV2-2021	Ab	SARS-CoV2	SARS-CoV1		SARS-CoV1, SARS-CoV2	S; NTD	B-cells; SARS-CoV2 Human Patient	261	QVQLVQSGAEVKKPGASVKVSCKVSGYTLIELSIHWVRQAPGKGLEWMGGFDPEDVETIYAQKFQGRVTMTEDTSTDTAYMELSSLTSEDRAVYYCATQPAAIGGTPPYYWGQGTLVTVSS	1340	QSVLTQPPSASGTPGQRVTISCSGSSSNIGSNYVYWYQQLPGTAPKLLIYRNNQRPSGVPDRFSGSKSGTSASLAISGLRSEDEADYYCAAWDASLSGHVVFGGGTKLTVL	IGHV1-24 (Human)	IGHJ4 (Human)	IGLV1-47 (Human)	IGLJ2 (Human)	2349	ATQPAAIGGTPPYY	3551	AAWDASLSGHVV	Seth Zost et al., 2020 (https://www.nature.com/articles/s41591-020-0998-x)
COV2-2022	Ab	SARS-CoV2	SARS-CoV1		SARS-CoV1, SARS-CoV2	S; non-RBD	B-cells; SARS-CoV2 Human Patient	262	QVQLVQSGAEVKKPGASVKVSCKASGYTFTSYVISWVRQAPGQGLEWMGWISAYNGNTNYAQKLQGRVTMTTDTSTSTAYMELRSLRSDDTAVYYCARDQGPTYYYGSGSPHYGMDVWGQGTTVTVSS	1341	DIVMAQTPLSLPVTPGEPASISCRSSQSLLDSDDGNTYFDWYLQKPGQSPQLLIYTLSYRASGVPDRFSGSGSGTDFTLKINRVEAEDVGVYYCMQRIEFPWTFGQGTKLEIK	IGHV1-18 (Human)	IGHJ6 (Human)	IGKV2-40 (Human)	IGKJ2 (Human)	2350	ARDQGPTYYYGSGSPHYGMDV	3552	MQRIEFPWT	Seth Zost et al., 2020 (https://www.nature.com/articles/s41591-020-0998-x)
COV2-2025	Ab	SARS-CoV1, SARS-CoV2			SARS-CoV2	S; non-RBD	B-cells; SARS-CoV2 Human Patient	263	QVHLVESGGGVVQPGRSLRLSCAASGFTFSNYGMHWVRQAPGKGLEWVAVISGDENNKFYANSVKGRFTISRDNSKNTLSLQMNSLRPEDTARYYCAKGGDSSGWAWDGDNPPTDYWGQGTLVIVSS	1342	DIVMTQSPDFLAVSLGERATINCKSSQSVLHTPKNKNYLAWYKQKPGQPPKVLIYWASTRESGVPERFSGSGSGTDFTLIISSLQAEDAAVYYCQQYYTAPLTFGGGTKVEIK	IGHV3-30 (Human)	IGHJ4 (Human)	IGKV4-1 (Human)	IGKJ4 (Human)	2351	AKGGDSSGWAWDGDNPPTDY	3553	QQYYTAPLT	Seth Zost et al., 2020 (https://www.nature.com/articles/s41591-020-0998-x)
COV2-2026	Ab	SARS-CoV2	SARS-CoV1		SARS-CoV1, SARS-CoV2	S; NTD	B-cells; SARS-CoV2 Human Patient	264	QVQLVQSGAEVKKPGASVKVSCKVSGYTLTELSIHWVRQAPGKGLEWMGGFDPEDGETVYAQKFQGRVTMTEDTSSDTAYMELSSLRSEDTAVYYCATSFPIRGDPSYYYYYGMDVWGQGTTVTVSS	1343	DIQMTQSPSSLSASVGDRVTITCRASQGITNYLAWFQQKPGKAPKSLIYAVSSLQSGVPSKFSGSGSGTDFTLTISSLQPEDFATYYCQQYNSYPWTFGQGTKVEIK	IGHV1-24 (Human)	IGHJ6 (Human)	IGKV1-16 (Human)	IGKJ1 (Human)	2352	ATSFPIRGDPSYYYYYYGMDV	3554	QQYNSYPWT	Seth Zost et al., 2020 (https://www.nature.com/articles/s41591-020-0998-x)
COV2-2027	Ab	SARS-CoV2	SARS-CoV1		SARS-CoV1, SARS-CoV2	S; non-RBD	B-cells; SARS-CoV2 Human Patient	265	QVQLVESGGGVVQPGRSLRLSCAASGFIFSTYGMHWVRQAPGKGLEWVAVISYDGSNKYNADSVKGRFTISRDNSKNTLYLQMNSLRVEDTAVYYCAIYGYYYYGLDVWGQGTTVTVSS	1344	SYELTQPPSVSVSPGQTARITCSGDALPKQYAYWYQQKPGQAPVLVIYKDSERPSGIPERFSGSSSGTTVTLTISGVQAEDEADYYCQSADSSGTYFWVFGGGTKLTVL	IGHV3-30 (Human)	IGHJ6 (Human)	IGLV3-25 (Human)	IGLJ3 (Human)	2353	AIYGYYYYGLDV	3555	QSADSSGTYFWV	Seth Zost et al., 2020 (https://www.nature.com/articles/s41591-020-0998-x)
COV2-2028	Ab	SARS-CoV1, SARS-CoV2			SARS-CoV2	S; non-RBD	B-cells; SARS-CoV2 Human Patient	266	QVHLVESGGGVVQPGRSLRLSCAASGFSFRNYGMHWVRQAPGKGLEWVAVISGDENNKFYANSVKGRFTISRDNSKNTLSLQMNSLRPEDTARYYCAKGGDSSGWAWDGDNPPTDYWGQGTLVIVSS	1345	DIVMTQSPDFLAVSLGERATINCKSSQSVLHTPKNKNYLAWYKQKPGQPPKVLIYWASTRESGVPERFSGSGSGTDFTLIISSLQAEDAAVYYCQQYYTAPLTFGGGTKVEIK	IGHV3-30 (Human)	IGHJ4 (Human)	IGKV4-1 (Human)	IGKJ4 (Human)	2354	AKGGDSSGWAWDGDNPPTDY	3556	QQYYTAPLT	Seth Zost et al., 2020 (https://www.nature.com/articles/s41591-020-0998-x)
COV2-2029	Ab	SARS-CoV1, SARS-CoV2			SARS-CoV2	S; non-RBD	B-cells; SARS-CoV2 Human Patient	267	QVQLQESGPGLVKPSGTLSLTCVVSGGSISSSNWGWVRQPPGKGLEWIGEIYLSGTTNYNPSLTSRVTISVDKSKNQFSLKLNSVTAADTAIYYCARPTAGAGGAFDIWGQGTVVTVSS	1346	QSVLTQPPSVSGTPGQRVTISCSGSNSKIGSYSVNWYQQLPGTAPKLLIYRNNQRPSGVPDRFFGSKSGTSASLAISGLQSEDEADYYCSVWDDSLNGPLFGGGTKLTFV	IGHV4-4 (Human)	IGHJ3 (Human)	IGLV1-44 (Human)	IGLJ3 (Human)	2355	ARPTAGAGGAFDI	3557	SVWDDSLNGPL	Seth Zost et al., 2020 (https://www.nature.com/articles/s41591-020-0998-x)
COV2-2031	Ab	SARS-CoV1, SARS-CoV2			SARS-CoV2	S; RBD	B-cells; SARS-CoV2 Human Patient	268	QVTLKESGPVLVKPTETLTLTCTVSGFSLSNARMGVSWIRQPPGKALEWLAHIFWNDENSYSTSLKTRLTISKDTSKSQVVLNMTNMDPVDTATYYCARTEWLLSDNWFDSWGQGTLVTVSS	1347	SYELTQPPSVSVSPGQTARITCSGDAWPNQYAYWYQQKPGQAPVLVIYKDTERPSGIPERFSGSSSGTTVTLTISGVQAEDEADYFCQSSDSSGVVFGGGTKLTVL	IGHV2-26 (Human)	IGHJ5 (Human)	IGLV3-25 (Human)	IGLJ3 (Human)	2356	ARTEWLLSDNWFDS	3558	QSSDSSGVV	Seth Zost et al., 2020 (https://www.nature.com/articles/s41591-020-0998-x)
COV2-2032	Ab	SARS-CoV1, SARS-CoV2			SARS-CoV2	S; RBD	B-cells; SARS-CoV2 Human Patient	269	QVQLVQSGAEVKKPGASVKVSCKASGDTFSSYYLHWVRQAPGQGLQWMGISNPSGGSTTYAQKFQGRVTMTGDTSTSTVYMELSSLRSEDTAVYYCARGGLVPAARNAFDIWGQGTMVTVSS	1348	DIQMTQSPSTLSASVGDRVTITCRASQSISSWLAWYQQKPGKAPKLLIYKASSLESGVPSRFSGSGSGTEFTLTISSLQPDDFATYYCQQYNSYSWTFGQGTKVEIK	IGHV1-46 (Human)	IGHJ3 (Human)	IGKV1-5 (Human)	IGKJ1 (Human)	2357	ARGGLVPAARNAFDI	3559	QQYNSYSWT	Seth Zost et al., 2020 (https://www.nature.com/articles/s41591-020-0998-x)

COV2-2033	Ab	SARS-CoV1, SARS-CoV2			SARS-CoV2	S; non-RBD	B-cells; SARS-CoV2 Human Patient	270	QVQLQESGPGLVKPSGTLSLTCVVSGGSISSSNWGWVRQPPGKGLEWIGEIYHSGTTNYNPSLRSRVTISVDKSKNQLSLKLNSVTAADTAIYYCARPTAGAGGAFDTWGQGTMVTVSA	1349	QSVLTQPPSASGTPGQRVTISCSGSNSKIGSYSVNWYQQLPGTAPKLLIYRNNQRPSGVPDRFSGSKSGTSASLAISGLQSEDEADYYCSVWDDSLNGPLFGGGTKLTFL	IGHV4-4 (Human)	IGHJ3 (Human)	IGLV1-44 (Human)	IGLJ3 (Human)	2358	ARPTAGAGGAFDT	3560	SVWDDSLNGPL	Seth Zost et al., 2020 (https://www.nature.com/articles/s41591-020-0998-x)
COV2-2034	Ab	SARS-CoV1, SARS-CoV2			SARS-CoV2	S; non-RBD	B-cells; SARS-CoV2 Human Patient	271	QVQLVQSGAEVKKPGASVKVSCKASGYTFTTYGISWVRQAPGQGLEWMGWISAYNGNSNYGKKFQGRVTMTADTSTSTAYMELRSLRSDDTAVYYCARDLPIKVVVPAADYNWFDPWGQGTLVTVSS	1350	DIQMTQSPSSLSASVGDRVTITCRASQSISSYLNWYQQKPGKAPKLLIYAASSLQSGVPSRFSGSGSGTDFTLTISSLQPEDFATYYCQQSYSTPPTFGGGTKVQIK	IGHV1-18 (Human)	IGHJ5 (Human)	IGKV1-39 (Human)	IGKJ4 (Human)	2359	ARDLPIKVVVPAADYNWFDP	3561	QQSYSTPPT	Seth Zost et al., 2020 (https://www.nature.com/articles/s41591-020-0998-x)
COV2-2035	Ab	SARS-CoV2	SARS-CoV1		SARS-CoV1, SARS-CoV2	S; non-RBD	B-cells; SARS-CoV2 Human Patient	272	QITLKESGPTLVKPTQTLTLTCTFSGFSLNTNGVAVGWIRQPPGKALEWLALIYWDDDKRYSPSLKSRLTITKDTSKNQVVLTMTNMDPVDTATYYCAHRRGILTEDAFDIWGQGTMVTVSS	1351	DIQMTQSPSSLSASVGDRVTITCRASQSISSYLNWYQQRPGKAPKLLIYAASSLQSGVPSRFSGSGYGTDFTLTISSLQPEDFATYYCQQSYNTPRTFGQGTKVEIK	IGHV2-5 (Human)	IGHJ3 (Human)	IGKV1-39 (Human)	IGKJ1 (Human)	2360	AHRRGILTEDAFDI	3562	QQSYNTPRT	Seth Zost et al., 2020 (https://www.nature.com/articles/s41591-020-0998-x)
COV2-2037	Ab	SARS-CoV2	SARS-CoV1	SARS-CoV2		S; RBD	B-cells; SARS-CoV2 Human Patient	273	EVQLVESGGGLVQPGESLRLSCAASGITVSSNYMSWVRQAPGKGLEWVSVIYSGGSTFYADSVKGRFIISRHNSKNTLYLQMNSLRAEDTAVYYCARDLNEHGLDVWGQGTTVSVSS	1352	DIQMTQSPSSVSASVGDRVTITCRASQGISSWLAWYQQKPGKAPKLLIYAASSLQSGVPSRFSGSGSGTDFTLTISSLQPEDFATYYCQQTNSFPTFGQGTRLEIR	IGHV3-53 (Human)	IGHJ6 (Human)	IGKV1-12 (Human)	IGKJ5 (Human)	2361	ARDLNEHGLDV	3563	QQTNSFPT	Seth Zost et al., 2020 (https://www.nature.com/articles/s41591-020-0998-x)
COV2-2039	Ab	SARS-CoV2	SARS-CoV1		SARS-CoV1, SARS-CoV2	S; RBD	B-cells; SARS-CoV2 Human Patient	274	QVQLVQSGAEVKKPGASVKVSCKASGYTFTSYYMHWVRQAPGQGLEWMGIINPSAGSTSYAQKFQGRVTMTRDTSTSTVYMELSSLRSEDTAVYYCARGTLIPAHRGAFDIWGQGTMVTVSS	1353	EIVLTQSPGTLSLSPGERATLSCRASQSVSSSFLAWYQQKPGQAPRLLIYGASNRATGIPDRFSGSGSGTDFTLTISRLEPEDFAVYYCQQYGNSPQFGPGTKVDIK	IGHV1-46 (Human)	IGHJ3 (Human)	IGKV3-20 (Human)	IGKJ3 (Human)	2362	ARGTLIPAHRGAFDI	3564	QQYGNSPQ	Seth Zost et al., 2020 (https://www.nature.com/articles/s41591-020-0998-x)
COV2-2041	Ab	SARS-CoV1, SARS-CoV2			SARS-CoV2	S; non-RBD	B-cells; SARS-CoV2 Human Patient	275	QVQLQESGPGLVKPSQTLSLTCTVSGGSISSGTYYWSWIRQPAGKGLEWIGRFYTSGSTNYNPSLKSRVTISVDASKNQFSLKLSSVTAADTAVYYCARARPDYYYYYAMDVWGQGTTVTVSS	1354	DIQMTQSPSSLSASVGDRVTITCRASQSISNWLAWYQQKPGKAPKLLIYKASSLESGVPSRFSGSGSGTEFTLTISSLQPDDFATYYCQQYNSYSTWTFGQGTKVEIK	IGHV4-61 (Human)	IGHJ6 (Human)	IGKV1-5 (Human)	IGKJ1 (Human)	2363	ARARPDYYYYAMDV	3565	QQYNSYSTWT	Seth Zost et al., 2020 (https://www.nature.com/articles/s41591-020-0998-x)
COV2-2046	Ab	SARS-CoV2	SARS-CoV1	SARS-CoV2		S; RBD	B-cells; SARS-CoV2 Human Patient	276	EVQLVESGGGLVQPGRSLRLSCAASGFTFDDYAMHWVRQAPGKGLEWVSGISWNSGSIAYTDSVKGRFTISRDNAKNSLYLQMNSLRAEDTALYYCAKAHSTGHQYYYGMDVWGQGTTVTVSS	1355	DIQMTQSPSSLSASVGDRVTITCRASQSISSFLNWYQQKPGKAPKLLIYAAFNLQSGVPSRFSGSGSGTDFTLTISSLQSEDFATYYCQQSYNTPYTFGQGTKLEIK	IGHV3-9 (Human)	IGHJ6 (Human)	IGKV1-39 (Human)	IGKJ2 (Human)	2364	AKAHSTGHQYYYGMDV	3566	QQSYNTPYT	Seth Zost et al., 2020 (https://www.nature.com/articles/s41591-020-0998-x)
COV2-2050	Ab	SARS-CoV2	SARS-CoV1	SARS-CoV2		S; RBD	B-cells; SARS-CoV2 Human Patient	277	QVQLVQSGAEVKKPGASVKVSCKASGYTFTDYYMHWVRQAPGQGLEWMGWINPNSRGTNYAQKFQGRVTMTRDTSISTVYMELSRLTSDDTAVYYCARVVVLGYGRPNNYYDGRNVWDYWGQGTLVTVSS	1356	QSVLTQPPSASGTPGQRVIISCSGSSSNIGSNTVKWYHQLPGTAPKLLICSNNQRPSGVPDRFSGSKSDTSASLAISGLQSEDEADYYCAAWDDSLNALVFGGGTKLTVL	IGHV1-2 (Human)	IGHJ4 (Human)	IGLV1-44 (Human)	IGLJ2 (Human)	2365	ARVVVLGYGRPNNYYDGRNVWDY	3567	AAWDDSLNALV	Seth Zost et al., 2020 (https://www.nature.com/articles/s41591-020-0998-x)
COV2-2051	Ab	SARS-CoV2	SARS-CoV1		SARS-CoV1, SARS-CoV2	S; RBD	B-cells; SARS-CoV2 Human Patient	278	QVTLRESGPALVKPTQTLSLTCTFSGFSLGTSGMCVSWIRQPPGKALEWLARIDWDDDKYYSTSLKTRLTISKDTSKNQVVLTMTNMDPVDTATYYCARGVVTYDYWGQGTLVTVSS	1357	DIQMTQSPSSLSASVGDRVTITCRASQSIAGYLNWYQQKPGKAPKLLIYGTTSLQSGVPVRFSGSGSGTDFTLTISSLQPEDFATYYCQQSYSTPGTFGQGTRLEIK	IGHV2-70 (Human)	IGHJ4 (Human)	IGKV1-39 (Human)	IGKJ5 (Human)	2366	ARGVVTYDY	3568	QQSYSTPGT	Seth Zost et al., 2020 (https://www.nature.com/articles/s41591-020-0998-x)
COV2-2054	Ab	SARS-CoV2	SARS-CoV1		SARS-CoV1, SARS-CoV2	S; non-RBD	B-cells; SARS-CoV2 Human Patient	279	QVQLVQSGAEVKKPGSSVKVSCKASGDTFSSYTINWVRQAPGQGLEWMGRIIPILGIPNYAQKFQGRVTITADKSTSTAFMELSSLRSEDTAVYYCARGRGYSNYGASYYMDVWGKGTTVTVSS	1358	DIQMTQSPSSLSASVGDRVTITCQASQDINHYLNWYQQKPGKAPKLLIYDASNLETGVPSRFSGSGSGTDFTFTISSLQPEDVATYYCQQSDNLPMYTFGQGTKLEIK	IGHV1-69 (Human)	IGHJ6 (Human)	IGKV1-33 (Human)	IGKJ2 (Human)	2367	ARGRGYSNYGASYYMDV	3569	QQSDNLPMYT	Seth Zost et al., 2020 (https://www.nature.com/articles/s41591-020-0998-x)
COV2-2055	Ab	SARS-CoV1, SARS-CoV2			SARS-CoV2	S; RBD	B-cells; SARS-CoV2 Human Patient	280	EVQLVESGGGLVQPGRSLRLSCAASGFTFDDYAMNWVRQPPGKGLEWVSGISWNSDSIGYADSVKGRFTISRDNAKNSLYLQMNSLRAEDTAMYYCAKGRGAGYTSYMDVWGKGTTVTVSS	1359	SYVLTQPPSVSVAPGKTARITCEGNNIGSKSVHWYQQKPGQAPVLVVYDDSGRPSGIPERFSGSNSGNTATLTISRVEAGDEADYFCQVWDSSSDHHVVFGGGTKLTVL	IGHV3-9 (Human)	IGHJ6 (Human)	IGLV3-21 (Human)	IGLJ2 (Human)	2368	AKGRGAGYTSYMDV	3570	QVWDSSSDHHVV	Seth Zost et al., 2020 (https://www.nature.com/articles/s41591-020-0998-x)
COV2-2064	Ab	SARS-CoV2	SARS-CoV1	SARS-CoV2		S; RBD	B-cells; SARS-CoV2 Human Patient	281	QVQLAQSGAEVKKPGASVKVSCKAAGYTFTSYDINWVRQATGQGLEWMGWMNSNSGNAGYAQKFQGRVTMTRDTSTSTAYMELSSLTSDDTAVYYCARMRTGWPTHGRPDDFWGRGTLVTVSS	1360	QSVLTQPPSASGTPGQRVTISCSGSNSNIGSYTVNWYQQFPGTAPKLLIYDNNQRTSGVPDRFSGSKSGTSASLAISGLQSEDEANYYCLVWDDSLNGLVFGGGTKLTVL	IGHV1-8 (Human)	IGHJ4 (Human)	IGLV1-44 (Human)	IGLJ2 (Human)	2369	ARMRTGWPTHGRPDDF	3571	LVWDDSLNGLV	Seth Zost et al., 2020 (https://www.nature.com/articles/s41591-020-0998-x)
COV2-2068	Ab	SARS-CoV2	SARS-CoV1	SARS-CoV2		S; RBD	B-cells; SARS-CoV2 Human Patient	282	EVQLVESGGGLVQPGGSLRLSCAASGFTVSSNYMSWVRQAPGKGLEWVSVIYPGGSAFYADSVKGRFTISRHNSNNTLCLQMNSLRTEDTAVYYCARSYDILTGYRDAFDIWGQGTMVTVSS	1361	QSVLTQPPSVSGAPGQRVTISCTGSSSNIGSGSDVHWYQQLPGTAPKLLIYGNTNRPSGVPDRFSGSKSGTSASLAITGLQAEDEADYYCQSYDSRLSGFVVFGGGTKLTVL	IGHV3-53 (Human)	IGHJ3 (Human)	IGLV1-40 (Human)	IGLJ2 (Human)	2370	ARSYDILTGYRDAFDI	3572	QSYDSRLSGFVV	Seth Zost et al., 2020 (https://www.nature.com/articles/s41591-020-0998-x)
COV2-2070	Ab	SARS-CoV2	SARS-CoV1		SARS-CoV1, SARS-CoV2	S; RBD	B-cells; SARS-CoV2 Human Patient	283	QVQLQQWGAGLLKPSETLSLTCAVSGGSFSAYYWSWIRQPPGKGLEWIGEINHSGSTNYNPSLRSRVTISVDTSKNQFSLKLSSVTAADTAVYYCARVGYSQGYYYYYMDVWGKGTTVTVSS	1362	DIQMTQSPSSLSASVGDRVTITCRASQSISNYLNWYQQKPGKAPKLLIYAASSLQSGVPSRFSGSGSGTDFSLTISSLQPEDFATYSCQQSYTTLLTFGGGTKVEIK	IGHV4-34 (Human)	IGHJ6 (Human)	IGKV1-39 (Human)	IGKJ4 (Human)	2371	ARVGYSQGYYYYYMDV	3573	QQSYTTLLT	Seth Zost et al., 2020 (https://www.nature.com/articles/s41591-020-0998-x)

COV2-2072	Ab	SARS-CoV2	SARS-CoV1	SARS-CoV2		S; RBD	B-cells; SARS-CoV2 Human Patient	284	QMQLVQSGPEVKKPGTSVKVSCKTSGFTFTSSAIQWVRQARGQRLEWIGWIVVGSGNTNYAQKFQERVTITRDMSTSTAYMELSSLRSEDTAVYYCAAPHCNRTSCYDAFDLWGQGTMVTVSS	1363	EIVLTQSPGTLSLSPGERATLSCRASQSVSSSYLGWYQQKPGQAPRLLIYGASSRATGIPDRFSGSGSGTDFTLTISRLEPEDFAVYYCQQYGSSPWTFGQGTKVEIK	IGHV1-58 (Human)	IGHJ3 (Human)	IGKV3-20 (Human)	IGKJ1 (Human)	2372	AAPHCNRTSCYDAFDL	3574	QQYGSSPWT	Seth Zost et al., 2020 (https://www.nature.com/articles/s41591-020-0998-x)
COV2-2078	Ab	SARS-CoV2	SARS-CoV1		SARS-CoV1, SARS-CoV2	S; RBD	B-cells; SARS-CoV2 Human Patient	285	QVQLVQSGAEVKKPGSSVKVSCKASGGTFSSYSITWVRQAPGQGLEWMGRIIPVLGIANYAQKFQDRVTITADKSTSTAYMELSSLRSEDTAVYYCARVGVSGFKSGSNWYFDLWGRGTLVTVSS	1364	QSVLTQPPSVSGAPGQRVTLSCTGSNSNIGAGYDVHWYQQLPGTAPKLLIYGNSNRPSGVPDRFSGSKSGTSASLAITGLQAEDEADYYCQSYDSSLSDSVFGGGTKVTVL	IGHV1-69 (Human)	IGHJ2 (Human)	IGLV1-40 (Human)	IGLJ3 (Human)	2373	ARVGVSGFKSGSNWYFDL	3575	QSYDSSLSDSV	Seth Zost et al., 2020 (https://www.nature.com/articles/s41591-020-0998-x)
COV2-2080	Ab	SARS-CoV2	SARS-CoV1		SARS-CoV1, SARS-CoV2	S; RBD	B-cells; SARS-CoV2 Human Patient	286	EVQLVESGGGLVQPGGSLRLSCAASGLTVRSNYMTWVRQTPGKGLEWVSVIYSGGSTFYADSVKGRFTISRDNSKNTVYLQMNSLRAEDTAVYYCARDLVTYGLDVWGQGTTVTVSS	1365	DIQLTQSPSFLSASVGDRVTITCRASQGISNYLAWYQQKPGTAPNLLIYAASTLQSGVPSRFSGSGSGTEFTLTISSLQPEDFATYYCQLLNSHPLTFGQGTRLEIK	IGHV3-66 (Human)	IGHJ6 (Human)	IGKV1-9 (Human)	IGKJ5 (Human)	2374	ARDLVTYGLDV	3576	QLLNSHPLT	Seth Zost et al., 2020 (https://www.nature.com/articles/s41591-020-0998-x)
COV2-2082	Ab	SARS-CoV1, SARS-CoV2			SARS-CoV2	S; RBD	B-cells; SARS-CoV2 Human Patient	287	EVQLVESGGGVVRPGGSLRLSCAASGFIFDDYDMTWVRQAPGKGLEWVSGISWNGGNTGYADSVKGRFTISRDNAKNSLYLQMNSLRAEDTALYHCAVIMSPIPRYSGYDWAGGAFDIWGQGTMVTVSS	1366	SSELTQDPAVSVALGQTVRITCQGDSLRSYYASWYQQKPGQVPILVIYDKNNRPSGIPDRFSGSSSGNTASLTITGAQAEDEADYYCNSRDSSGNAVVFGGGTKLTVL	IGHV3-20 (Human)	IGHJ3 (Human)	IGLV3-19 (Human)	IGLJ3 (Human)	2375	AVIMSPIPRYSGYDWAGGAFDI	3577	NSRDSSGNAVV	Seth Zost et al., 2020 (https://www.nature.com/articles/s41591-020-0998-x)
COV2-2083	Ab	SARS-CoV1, SARS-CoV2			SARS-CoV2	S; RBD	B-cells; SARS-CoV2 Human Patient	288	QVQLVESGGGVVQPGRSLRLSCAASGFTFSNYGMHWVRQAPGKGLEWVAVMSYDGSNKYYADSVKGRFTISRDNSKNTLYLQMNSLRAEDTAVYYCAKNLGPYCSGGTCYSLVGDYWGQGTLVTVSS	1367	DIQMTQSPSSLSASVGDRVTITCQASQDISNYLNWYQQKPGKAPKLLIYDASNLETGVPSRFSGSGSGTDFTFTISSLQPEDIATYYCQQYANLPFTFGPGTKVDIK	IGHV3-30 (Human)	IGHJ4 (Human)	IGKV1-33 (Human)	IGKJ3 (Human)	2376	AKNLGPYCSGGTCYSLVGDY	3578	QQYANLPFT	Seth Zost et al., 2020 (https://www.nature.com/articles/s41591-020-0998-x)
COV2-2094	Ab	SARS-CoV1, SARS-CoV2			SARS-CoV2	S; RBD	B-cells; SARS-CoV2 Human Patient	289	EVQLVESGGGVVRPGGSLRLSCAASGFIFDDYDMTWVRQAPGKGLEWVSGINWNGGSTGYADSVKGRFTISRDNAKNSLYLQMNSLRAEDTALYHCAVIMSPIPRYSGYDWAGDAFDIWGQGTMVTVSS	1368	SSELTQDPAVSVALGQTVRITCQGDSLRSYYASWYQQKPGQVPILVIYDKNNRPSGIPDRFSGSSSGNTASLTITGAQAEDEADYYCNSRDSSGNAVVFGGGTKLTVL	IGHV3-20 (Human)	IGHJ3 (Human)	IGLV3-19 (Human)	IGLJ2 (Human)	2377	AVIMSPIPRYSGYDWAGDAFDI	3579	NSRDSSGNAVV	Seth Zost et al., 2020 (https://www.nature.com/articles/s41591-020-0998-x)
COV2-2096	Ab	SARS-CoV2	SARS-CoV1	SARS-CoV2		S; RBD	B-cells; SARS-CoV2 Human Patient	290	QVQLVQSGAEVKKPGASVKVSCKASGYTFGSFDINWVRQATGQGLEWMGRMNSNSGNTAYAQKFQGRVTMTRDTSTNTAYMELSSLRSEDTAMYYCARMRSGWPTHGRPDDFWGRGTLVTVSS	1369	QSVLTQAPSASGTPGQRVTISCSGSNSNIGSYTINWYQQLPGTAPKLLIYGNDQRTSGVPDRFSGSKFGTSASLAISGLQSEDENNYYCAVWDDSLNGLVFGGGTKLTVL	IGHV1-8 (Human)	IGHJ4 (Human)	IGLV1-44 (Human)	IGLJ2 (Human)	2378	ARMRSGWPTHGRPDDF	3580	AVWDDSLNGLV	Seth Zost et al., 2020 (https://www.nature.com/articles/s41591-020-0998-x)
COV2-2097	Ab	SARS-CoV2	SARS-CoV1	SARS-CoV2		S; RBD	B-cells; SARS-CoV2 Human Patient	291	EVQLVESGGGLVQPGRSLRLSCAASGFTFDDYAMHWVRQAPGKGLEWVSGISWNSGTIGYADSVKGRFTISRDNAKNSLYLQMNSLRPEDTALYYCAKDIIRQGEDGMDVWGQGTTVTVSS	1370	DIQMTQSPSSLSASVGDRVTITCRASQNIASYLNWYQQKPGKAPKLLIYAASSLQSGVPSRFSGSGSGTDFTLTISSLQPEEFATYYCQQSYSTPWTFGQGTKVEIK	IGHV3-9 (Human)	IGHJ6 (Human)	IGKV1-39 (Human)	IGKJ1 (Human)	2379	AKDIIRQGEDGMDV	3581	QQSYSTPWT	Seth Zost et al., 2020 (https://www.nature.com/articles/s41591-020-0998-x)
COV2-2098	Ab	SARS-CoV2	SARS-CoV1	SARS-CoV2		S; RBD	B-cells; SARS-CoV2 Human Patient	292	EVQLLESGGGLIQPGGSLRLSCAASGFTFSNYAMSWVRQAPGKGLEWVSGIISTSGGATYNADSVRGRFTTSRDNSKNILYLQMNSLRGEDTAVYYCVKGLFDWFPLWGQGTMVTVSS	1371	DIVMTQSPATLSVSPGERAILSCRASQSVRSNLAWYQQKPGQAPRLLISGASTRATAIPARFSGSGSGTEFTLTITSLQSEDCAVYYCHQYNNWPQTFGQGTKVEIK	IGHV3-23 (Human)	IGHJ3 (Human)	IGKV3-15 (Human)	IGKJ1 (Human)	2380	VKGLFDWFPL	3582	HQYNNWPQT	Seth Zost et al., 2020 (https://www.nature.com/articles/s41591-020-0998-x)
COV2-2103	Ab	SARS-CoV1, SARS-CoV2		SARS-CoV2		S; RBD	B-cells; SARS-CoV2 Human Patient	293	EVQLVESGGGLVQPGGSLRLSCAASGFTFSRHWMTWVRQAPGKGLEWVANIKQDGSEKYYVDSVKGRLTISRDNAKNSLYLQMNSLRAEDTAVYYCARLGFYYGGADYWGQGTLVTVSS	1372	NFMLTQPHSVSESPGKTVTISCTGSSGSIASNYVQWYQQRPGSAPTTVISEDNQRPSGVPDRFSGSIDSSSNSASLTISGLKTEDEADYYCQSYDGINRAWVFGGGTKLTVL	IGHV3-7 (Human)	IGHJ4 (Human)	IGLV6-57 (Human)	IGLJ3 (Human)	2381	ARLGFYYGGADY	3583	QSYDGINRAWV	Seth Zost et al., 2020 (https://www.nature.com/articles/s41591-020-0998-x)
COV2-2108	Ab	SARS-CoV2	SARS-CoV1		SARS-CoV1, SARS-CoV2	S; RBD	B-cells; SARS-CoV2 Human Patient	294	NVQLVESGGGLVQPGGSLRLSCAASGFTFHHYAMHWVRQAPGKGLEWVSGISGSSDYRAYADSLKGRFTISRDYAKNSLWLQMNSLTSEDTAFYYCAKGVDYGGKLAYFDSWGQGTLVTVSS	1373	DIVMTQSPLSLPVTPGEPASISCRSSQSLLHSLGYNSLSWYLQKPGQSPHLLIYLGSNRASGVPDRFSGSGSATDFTLKISRLEAEDVGVYYCMQALQTPLTFGQGTRLEIK	IGHV3-9 (Human)	IGHJ4 (Human)	IGKV2-28 (Human)	IGKJ5 (Human)	2382	AKGVDYGGKLAYFDS	3584	MQALQTPLT	Seth Zost et al., 2020 (https://www.nature.com/articles/s41591-020-0998-x)
COV2-2110	Ab	SARS-CoV2	SARS-CoV1		SARS-CoV1, SARS-CoV2	S; RBD	B-cells; SARS-CoV2 Human Patient	295	QVQLVESGGGVVQPGRSLRLSCAASGFSFSSYVMNWVRQAPGKGqLEWVAVISYDGSSKYYADSVKGRFTISRDNSKNTLYLQMNSLRAEDTAVYYCARDIDSGYDPTPVFDYWGQGTLVTVSS	1374	DIQMTQSPSSLSACVGDRVTITCRASQSISSYLNWYQQKPGKAPKLLIYAASSLQSGVPSRFSGSGSGTDFTLTISSLQPEDFATYYCQQSYSSLSITFGQGTRLEIK	IGHV3-30-3 (Human)	IGHJ4 (Human)	IGKV1-39 (Human)	IGKJ5 (Human)	2383	ARDIDSGYDPTPVFDY	3585	QQSYSSLSIT	Seth Zost et al., 2020 (https://www.nature.com/articles/s41591-020-0998-x)
COV2-2111	Ab	SARS-CoV1, SARS-CoV2			SARS-CoV2	S; RBD	B-cells; SARS-CoV2 Human Patient	296	EVQLVESGGGLVQPGGSLRLSCAASGFTFSSYDLHWVRQGTGKRLEWVSAIGTAGDTYYLGSVKGRFTISRENAKNSLYLQMNSLRAGDTAVYYCARVLYDSSGFYNWFDPWGQGTLVTVSS	1375	DIQMTQSPSSLSASVGDRVTITCRASQSISSYLNWYQQKPGKAPKLLIYAASSLSGVPSRFSGSGSGTDFTLTISSLQPEDFATYYCQQSYEIPPWTFGQGTKVEIK	IGHV3-13 (Human)	IGHJ5 (Human)	IGKV1-39 (Human)	IGKJ1 (Human)	2384	ARVLYDSSGFYNWFDP	3586	QQSYEIPPWT	Seth Zost et al., 2020 (https://www.nature.com/articles/s41591-020-0998-x)
COV2-2113	Ab	SARS-CoV2	SARS-CoV1	SARS-CoV2		S; RBD	B-cells; SARS-CoV2 Human Patient	297	EVQLVESGGGLIQPGGSLRLSCAASEVTVSSNYMSWVRQAPGKGLEWVSLIYSGGTTYYADSVKGRFTISRDNSKNTLYLQMNSLRAEDTAVYYCARDFLRWHDLWGQGTLVTVSS	1376	DIQMTQSPSSLSASVGDRVTITCQASQDINNYLNWYQQKPGKAPKLLIYDASNLETGVPLRFSGSGSGTDFIFTISSLQPEDIATYYCQQYDNLPPVFGGGTKVEIK	IGHV3-53 (Human)	IGHJ5 (Human)	IGKV1-33 (Human)	IGKJ4 (Human)	2385	ARDFLRWHDL	3587	QQYDNLPPV	Seth Zost et al., 2020 (https://www.nature.com/articles/s41591-020-0998-x)

COV2-2114	Ab	SARS-CoV2	SARS-CoV1		SARS-CoV1, SARS-CoV2	S; RBD	B-cells; SARS-CoV2 Human Patient	298	QVQLVQSGAEVKKPGSSVKVSCKASGDTFSSYTINWVRQAPGQGLEWMGRIIPILGIPNYAQKFQGRVTITADKSTSTAFMELSSLRSEDTAVYYCARGRGYSNYGASYYMDVWGKGTTVTVSS	1377	QSVLTQPPSVSGAPGQRVTISCTGSSSNIGAGYDVHWYQQLPETAPKLLIYANSNRPSGVPDRFSGSKSGTSASLAITGLQAEDEADYYCQSYDSSLSGSVFGGGTKLTVL	IGHV1-69 (Human)	IGHJ6 (Human)	IGLV1-40 (Human)	IGLJ2 (Human)	2386	ARGRGYSNYGASYYMDV	3588	QSYDSSLSGSV	Seth Zost et al., 2020 (https://www.nature.com/articles/s41591-020-0998-x)
COV2-2128	Ab	SARS-CoV1, SARS-CoV2			SARS-CoV2	S; RBD	B-cells; SARS-CoV2 Human Patient	299	QLQLQESGPGLVKPSETLSLTCTVSGGSISSSSYYWGWIRQPPGNGLEWIGSIYYSGSTYYNPSLKGRVSISVDTSKNQFSLKLSSVTAADTAVYYCARILVIFTLNWFDPWGQGTLVTVSS	1378	NFMLTQPHSVSESPGKTVTISCTGSSGSIASNYVQWYQQRPGSAPTTVIYEDNQRPSGVPDRFSGSIDSSSNSASLTISGLKTEDEADYYCQSYDSGNPIFGGGTKLTVL	IGHV4-39 (Human)	IGHJ5 (Human)	IGLV6-57 (Human)	IGLJ2 (Human)	2387	ARILVIFTLNWFDP	3589	QSYDSGNPI	Seth Zost et al., 2020 (https://www.nature.com/articles/s41591-020-0998-x)
COV2-2130	Ab	SARS-CoV2	SARS-CoV1	SARS-CoV2		S; RBD	B-cells; SARS-CoV2 Human Patient	300	EVQLVESGGGLVKPGGSLRLSCAASGFTFRDVWMSWVRQAPGKGLEWVGRIKSKIDGGTTDYAAPVKGRFTISRDDSKNTLYLQMNSLKTEDTAVYYCTTAGSYYYDTVGPGLPEGKFDYWGQGTLVTVSS	1379	DIVMTQSPDSLAVSLGERATINCKSSQSVLYSSNNKNYLAWYQQKPGQPPKLLMYWASTRESGVPDRFSGSGSGAEFTLTISSLQAEDVAIYYCQQYYSTLTFGGGTKVEIK	IGHV3-15 (Human)	IGHJ4 (Human)	IGKV4-1 (Human)	IGKJ4 (Human)	2388	TTAGSYYYDTVGPGLPEGKFDY	3590	QQYYSTLT	Seth Zost et al., 2020 (https://www.nature.com/articles/s41591-020-0998-x)
COV2-2132	Ab	SARS-CoV2	SARS-CoV1	SARS-CoV2		S; RBD	B-cells; SARS-CoV2 Human Patient	301	EVQLVESGGGLIQPGGSLRLSCAASEVTVSSNYMSWVRQAPGKGLEWVSLIYSGGTTYYADSVKGRFTISRDNSKNTLYLQMNSLRAEDTAVYYCARDFLRWHDLWGQGTLVTVSS	1380	DIQMTQSPSSLSASVGDRVTITCQASQDINNYLNWYQQKPGKAPKLLIYDASNLETGVPLRFSGSGSGTDFTFTISSLQPEDIATYYCQQYDNLPPVFGGGTKVEIK	IGHV3-53 (Human)	IGHJ5 (Human)	IGKV1-33 (Human)	IGKJ4 (Human)	2389	ARDFLRWHDL	3591	QQYDNLPPV	Seth Zost et al., 2020 (https://www.nature.com/articles/s41591-020-0998-x)
COV2-2137	Ab	SARS-CoV2	SARS-CoV1		SARS-CoV1, SARS-CoV2	S; RBD	B-cells; SARS-CoV2 Human Patient	302	QVQLQESGPGLVKPSETLSLTCTVSGGSVSSGSYYWSWIRQPPGKGLECIGYIYYSGSSNYNPSLKSRVTISVDTSKNQFSLKMSSVTAADTAVYYCAGSPVPPTIVGASYWGQGTLVTVSS	1381	NFMLTQPHSVSESPGKTVTFSCTGSSGSIASNYVQWYQQRPGSAPTTVIYEDNQRPSGVPDRFSGSIDSSSNSASLTISGLKTEDEADYYCQSYDGINRWLVFGGGTKLTVL	IGHV4-61 (Human)	IGHJ4 (Human)	IGLV6-57 (Human)	IGLJ2 (Human)	2390	AGSPVPPTIVGASY	3592	QSYDGINRWLV	Seth Zost et al., 2020 (https://www.nature.com/articles/s41591-020-0998-x)
COV2-2142	Ab	SARS-CoV2	SARS-CoV1		SARS-CoV1, SARS-CoV2	S; non-RBD	B-cells; SARS-CoV2 Human Patient	303	EVQLVQSGAEVKKPGESLKISCKGSGYSFTSYWIDWVRQMPGKGLEWMGIIYPGDSDTRYSPSFQGQVTISADKSTSTAYLQWSSLKASDTAMYYCARRGEAAGIWYFDLWGRGTLVTVSS	1382	QPVLTQPPSASASLGASVTLTCTLSSGYSNYKVDWYQQRPGKGPRFVMRVGTGGIVGSKGDGIPDRFSVLGSGLNRYLTIKNIQEEDESDYHCGADHGSGSNFEYVVFGGGTKLTVL	IGHV5-51 (Human)	IGHJ2 (Human)	IGLV9-49 (Human)	IGLJ2 (Human)	2391	ARRGEAAGIWYFDL	3593	GADHGSGSNFEYVV	Seth Zost et al., 2020 (https://www.nature.com/articles/s41591-020-0998-x)
COV2-2143	Ab	SARS-CoV2	SARS-CoV1		SARS-CoV1, SARS-CoV2	S; non-RBD	B-cells; SARS-CoV2 Human Patient	304	EVQLVESGGGLVQPGGSLRLSCAASGFTVSSNYMSWVRQAPGKGLEWVSVIYSAGSTYYADSVKGRFSISRDKSKNTLYLQMNSLRAEDTAVYYCAKEGGSGSLRYYYYGMDVWGQGTTVTVSS	1383	QSVVTQPPSASGTPGQRVTISCSGSSSNIGYNIVNWYQQLPGTAPKLLIYSNNQRPSGVPDRFSGSKSGTSASLSISGLQSEDEADYYCAAWDDSLNGYVFGTGTKVTVL	IGHV3-66 (Human)	IGHJ6 (Human)	IGLV1-44 (Human)	IGLJ1 (Human)	2392	AKEGGSGSLRYYYYGMDV	3594	AAWDDSLNGYV	Seth Zost et al., 2020 (https://www.nature.com/articles/s41591-020-0998-x)
COV2-2146	Ab	SARS-CoV2	SARS-CoV1		SARS-CoV1, SARS-CoV2	S; NTD	B-cells; SARS-CoV2 Human Patient	305	EVQLVESGGGLVQPGGSLRLSCEASGFTFSSSEINWVRQAPGKGLEWVSHISSSGSIIYYADSVKGRFTISRDNAKNSLYLQMNSLRAEDTAVYYCARRSYRSSWYYYYGMDVWGQGTTVTVSS	1384	DIQLTQSPSFLSASVGDRVTITCRASQGISSYLAWYQQKPGKAPKLLIYAASTLQSGVPSRFSGSGSGTEFTLTISSLQPEDFATYYCQQLNSYPVTFGQGTKVEIK	IGHV3-48 (Human)	IGHJ6 (Human)	IGKV1-9 (Human)	IGKJ1 (Human)	2393	ARRSYRSSWYYYYGMDV	3595	QQLNSYPVT	Seth Zost et al., 2020 (https://www.nature.com/articles/s41591-020-0998-x)
COV2-2147	Ab	SARS-CoV2	SARS-CoV1		SARS-CoV1, SARS-CoV2	S; non-RBD	B-cells; SARS-CoV2 Human Patient	306	QVQLAESGGGVVQPGRSLRLSCAASGFTFSSYAMHWVRQAPGKGLEWVAVISYDGSNKYYADSVKGRFTISRDNSKNTLYLQMNSLRAEDTAVYYCARSTSGSYYYGMDVWGQGTTVTVSS	1385	QSALTQPASVSGSPGQSITISCTGTSSDVGDYNYVSWYQQHPGKAPKLMIYDVSNRPSGVSNRFSGSKSGNTASLTISGLQAEDEAEYYCSSYTSSSTLLYVFGTGTKVTVL	IGHV3-30-3 (Human)	IGHJ6 (Human)	IGLV2-14 (Human)	IGLJ1 (Human)	2394	ARSTSGSYYYGMDV	3596	SSYTSSSTLLYV	Seth Zost et al., 2020 (https://www.nature.com/articles/s41591-020-0998-x)
COV2-2150	Ab	SARS-CoV2	SARS-CoV1		SARS-CoV1, SARS-CoV2	S; NTD	B-cells; SARS-CoV2 Human Patient	307	QVQLVESGGGVVQPGRSLRLSCAASGFTFSTYAMHWVRQAPGKGLEWVAVISYDGSNKYYADSVKGRFTISRDNSKNTLYLQMIGLRAEDTAVYYCARDWAPTYYDMPSAFDIWGQGTMVTVSS	1386	SYVLTQPPSVSVAPGKTARITCGGNNIGNKGVHWYQQKPGQAPVLVVDDDSDRPSGIPERFSGSNSGNTATLIISSVEVGDEADFYCQVWDSSSDHPGVFGGGTKLTVL	IGHV3-30-3 (Human)	IGHJ3 (Human)	IGLV3-21 (Human)	IGLJ3 (Human)	2395	ARDWAPTYYDMPSAFDI	3597	QVWDSSSDHPGV	Seth Zost et al., 2020 (https://www.nature.com/articles/s41591-020-0998-x)
COV2-2151	Ab	SARS-CoV1, SARS-CoV2			SARS-CoV2	S; non-RBD	B-cells; SARS-CoV2 Human Patient	308	QVQLVQSGAEVRKPGSSVKVSCKASGGTFSSYAISWVRQAPGQGLEWMGGIIPVFGTANYAQKFQGRVTITADKSTSTAFMELNSLRSEDTAVYYCARIGSYPEYFQHWGQGTLVTVSS	1387	EIVLTQSPATLSLSPGERATLSCRASQSVSSFLAWYQQKPGQAPRLLIYDASNRATGIPARFSGSGSGTDFTLTISSLEPEDFAVYYCHYRSNWPPVLTFGGGTKVEIE	IGHV1-69 (Human)	IGHJ1 (Human)	IGKV3-11 (Human)	IGKJ4 (Human)	2396	ARIGSYPEYFQH	3598	HYRSNWPPVLT	Seth Zost et al., 2020 (https://www.nature.com/articles/s41591-020-0998-x)
COV2-2158	Ab	SARS-CoV1, SARS-CoV2			SARS-CoV2	S; RBD	B-cells; SARS-CoV2 Human Patient	309	QVQLQESGPGLVKPSQTLSLTCTVSGGSISSGGYFWSWIRQHPGKGLEWIGSIYYSGSTYYNPSLRSRITISVDTSKNQFSLKLSSVTAADTAVYYCARGGSGSYSLFDYWGQGTLVTVSS	1388	DIQMTQSPSSLSASVGDRVTITCQASQDITNYLNWYQQKPGKAPKLLIYDASNLETGVPSRFSGSGSGTDFTFTISSLQPEDFATYYCQQYDNLYSVHFGQGTKLEIK	IGHV4-31 (Human)	IGHJ4 (Human)	IGKV1-33 (Human)	IGKJ2 (Human)	2397	ARGGSGSYSLFDY	3599	QQYDNLYSVH	Seth Zost et al., 2020 (https://www.nature.com/articles/s41591-020-0998-x)
COV2-2159	Ab	SARS-CoV1, SARS-CoV2			SARS-CoV2	S; non-RBD	B-cells; SARS-CoV2 Human Patient	310	QVQLAESGGGVVQPGRSLRLSCAASGFTFSSYAMHWVRQAPGKGLEWVAVISYDGSNKYYADSVKGRFTISRDNSKNTLYLQMNSLRAEDTAVYYCARSTSGSYYYGMDVWGQGTTVTVSS	1389	QSALTQPASVSGSPGQSITISCTGTSSDVGDYNYVSWYQQHPGKAPKLMIYDVSNRPSGVSNRFSGSKSGNTASLTISGLQAEDEAEYYCSSYTSSSTLLYVFGTGTKVTVL	IGHV3-30-3 (Human)	IGHJ6 (Human)	IGLV2-14 (Human)	IGLJ1 (Human)	2398	ARSTSGSYYYGMDV	3600	SSYTSSSTLLYV	Seth Zost et al., 2020 (https://www.nature.com/articles/s41591-020-0998-x)
COV2-2160	Ab	SARS-CoV1, SARS-CoV2			SARS-CoV2	S; non-RBD	B-cells; SARS-CoV2 Human Patient	311	QVQLAESGGGVVQPGRSLRLSCAASGFTFSSYAMHWVRQAPGKGLEWVAVISYDGSNKYYADSVKGRFTISRDNSKNTLYLQMNSLRAEDTAVYYCARSTSGSYYYGMDVWGQGTTVTVSS	1390	QSALTQPASVSGSPGQSITISCTGTSSDVGDYNYVSWYQQHPGKAPKLMIYDVSNRPSGVSNRFSGSKSGNTASLTISGLQAEDEAEYYCSSYTSSSTLLYVFGTGTKVTVL	IGHV3-30-3 (Human)	IGHJ6 (Human)	IGLV2-14 (Human)	IGLJ1 (Human)	2399	ARSTSGSYYYGMDV	3601	SSYTSSSTLLYV	Seth Zost et al., 2020 (https://www.nature.com/articles/s41591-020-0998-x)
COV2-2165	Ab	SARS-CoV2	SARS-CoV1	SARS-CoV2		S; RBD	B-cells; SARS-CoV2 Human Patient	312	EVQLVESGGGLVQPGGSLRLSCAASGLTVRSNYMTWVRQTPGKGLEWVSVIYSGGSTFYADSVKGRFTISRDNSKNTVYLQMNSLRAEDTAVYYCARDLVTYGLDVWGQGTTVTVSS	1391	DIQLTQSPSFLSASVGDRVTITCRASQGISNYLAWYQQKPGTAPNLLIYAASTLQSGVPSRFSGSGSGTEFTLTISSLQPEDFATYYCQLLNSHPLTFGQGTRLEIK	IGHV3-66 (Human)	IGHJ6 (Human)	IGKV1-9 (Human)	IGKJ5 (Human)	2400	ARDLVTYGLDV	3602	QLLNSHPLT	Seth Zost et al., 2020 (https://www.nature.com/articles/s41591-020-0998-x)

COV2-2166	Ab	SARS-CoV1, SARS-CoV2			SARS-CoV2	S; non-RBD	B-cells; SARS-CoV2 Human Patient	313	QVQLVQSGAEVKKPGSSVKVSCKASGGTFSSYAIIWVRQAPGQGLEWMGGIIPIFGTTNYAQKFQGRVTITADESTSTAYVELSSLRSEDTAVYYCARIGHFDSSGYYLDYWGQGTLVTVSS	1392	EIVLTQSPATLSLSPGERATLSCRASQSVSSFLAWYQQKPGQAPRLLIYDASNRPTGIPARFTGSGSGTDFTLTISSLEPEDFAVYYCQHRTNWPPLFTFGPGTKVDIK	IGHV1-69 (Human)	IGHJ4 (Human)	IGKV3-11 (Human)	IGKJ3 (Human)	2401	ARIGHFDSSGYYLDY	3603	QHRTNWPPLFT	Seth Zost et al., 2020 (https://www.nature.com/articles/s41591-020-0998-x)
COV2-2171	Ab	SARS-CoV1, SARS-CoV2			SARS-CoV2	S; non-RBD	B-cells; SARS-CoV2 Human Patient	314	EVQLVESGGGLVQPGGSLRLSCVASGFTFSFYWMSWVRQAPGKGLEWVANIKQDGGEKYYVDSVKGRFTISRDNAKNSLYLQMNSLRAEDTAVYYCARLSGSSWDFDYWGQGTLVTVSS	1393	SYELTQPPSVSVSPGQTASITCSGDKLGDKYACWYQQRPGQSPVLVIYQDSKRPSGIPERFSGSNSGNTATLTISGTQAMDEADYYCQAWDSSTGVFGTGTKVTVL	IGHV3-7 (Human)	IGHJ4 (Human)	IGLV3-1 (Human)	IGLJ1 (Human)	2402	ARLSGSSWDFDY	3604	QAWDSSTGV	Seth Zost et al., 2020 (https://www.nature.com/articles/s41591-020-0998-x)
COV2-2173	Ab	SARS-CoV2	SARS-CoV1		SARS-CoV1, SARS-CoV2	S; non-RBD	B-cells; SARS-CoV2 Human Patient	315	EVQLVESGGGVVRPGGSLRLSCAASGFTFDDYGMSWVRQAPGKGLEWVSAINWNGGSTGYADSVKGRFTISRDNAKNSLYLQMNSLRAEDTALYHCARRRSSSRYSSGWYMYYYYMDVWGKGTTVTVSS	1394	DIQMTQSPSTLSASVGDRVTITCRASQSVSTWLAWYQQKPGKAPNLLIYEASSLESGVPSRFSGSGSGTEFTLTISSLQPDDFATYYCQQYNTYSGTFGQGTKVEIK	IGHV3-20 (Human)	IGHJ6 (Human)	IGKV1-5 (Human)	IGKJ1 (Human)	2403	ARRRSSSRYSSGWYMYYYYMDV	3605	QQYNTYSGT	Seth Zost et al., 2020 (https://www.nature.com/articles/s41591-020-0998-x)
COV2-2175	Ab	SARS-CoV1, SARS-CoV2			SARS-CoV2	S; non-RBD	B-cells; SARS-CoV2 Human Patient	316	EVQLVESGGGLVQPGGSLRLSCVASGFTFSFYWMSWVRQAPGKGLEWVANIKQDGGEKYYVDSVKGRFTISRDNAKNSLYLQMNSLRAEDTAVYYCARLSGSSWDFDYWGQGTLVTVSS	1395	SYELTQPPSVSVSPGQTASITCSGDKLGDKYACWYQQRPGQSPVLVIYQDSKRPSGIPERFSGSNSGNTATLTISGTQAMDEADYYCQAWDSSTGVFGTGTKVTVL	IGHV3-7 (Human)	IGHJ4 (Human)	IGLV3-1 (Human)	IGLJ1 (Human)	2404	ARLSGSSWDFDY	3606	QAWDSSTGV	Seth Zost et al., 2020 (https://www.nature.com/articles/s41591-020-0998-x)
COV2-2177	Ab	SARS-CoV2	SARS-CoV1		SARS-CoV1, SARS-CoV2	S; non-RBD	B-cells; SARS-CoV2 Human Patient	317	QITFKESGPTLVKPTETLTLTCTFSGFSVSTSGEGVGWIRQPPGKALEWLAVIYWDDDKRYSPSLKSRLTITRDTSKNQVVLTMTNMDPVDTATYYCAHRLWFRDAFDIWGQGTTVTVSS	1396	DIQMTQSPSSLSASVGDRVTITCRARQSISNYLNWYQQKPGKAPKLLIYAASSLHSGVPSRFSGSGSGTDFTLTISSLQPEDFATYYCQQTYSTFWTFGQGTNVEIK	IGHV2-5 (Human)	IGHJ3 (Human)	IGKV1-39 (Human)	IGKJ1 (Human)	2405	AHRLWFRDAFDI	3607	QQTYSTFWT	Seth Zost et al., 2020 (https://www.nature.com/articles/s41591-020-0998-x)
COV2-2178	Ab	SARS-CoV1, SARS-CoV2			SARS-CoV2	S; non-RBD	B-cells; SARS-CoV2 Human Patient	318	EVQLVESGGGLVQPGGSLRLSCAASGFTFSTYWMTWVRQAPGKGLEWVANIKQDGSEKYYVDSVKYRFTISRDNAKNSLYLQMNSLRAEDTAVYYCARVGSSSWYFDYWGQGTLVTVSS	1397	SYELTQPPSVSVSPGQTASITCSGDKLGDKYACWYQQKPGQSPVVVIYQDSKRPSGIPERFSGSNSGNTATLTISGTQAMDEADYYCQAWDSSTAVFGGGTKLTVL	IGHV3-7 (Human)	IGHJ4 (Human)	IGLV3-1 (Human)	IGLJ2 (Human)	2406	ARVGSSSWYFDY	3608	QAWDSSTAV	Seth Zost et al., 2020 (https://www.nature.com/articles/s41591-020-0998-x)
COV2-2183	Ab	SARS-CoV1, SARS-CoV2			SARS-CoV2	S; non-RBD	B-cells; SARS-CoV2 Human Patient	319	QVQLVESGGGVVQPGRSLRLSCAASGFTFSSYAMHWVRQAPGKGLEWVAGISYDGSNKYYADSVKGRFTISRDNSKNTLYLQMNSLRAEDTAVYYCARADTMVRGTYFEYWGQGTLVTVSS	1398	QSALTQPASVSGSPGQSITISCTGTSSDVGGYNYVSWYQQHPGKAPKLMIYDVSNRPSGVSNRFSGSKSGNTASLTISGLQAEDEADYCCSSYTSSRAVLFGGGTKLTVL	IGHV3-30-3 (Human)	IGHJ4 (Human)	IGLV2-14 (Human)	IGLJ2 (Human)	2407	ARADTMVRGTYFEY	3609	SSYTSSRAVL	Seth Zost et al., 2020 (https://www.nature.com/articles/s41591-020-0998-x)
COV2-2187	Ab	SARS-CoV1, SARS-CoV2			SARS-CoV2	S; non-RBD	B-cells; SARS-CoV2 Human Patient	320	QVQLVESGGGVVQPGRSLRLSCAASGFTFSYYPMHWLWVRQAPGKGLEWVAVTSYDGTNKYYADSVKGRFTISRDNSKNTLYLQMNSLRAEDTAVYYCARGGATNFDYWGQGTLVTVSS	1399	SYVLTQPPSVSVAPGKTANITCGGNNIGRKSVHWYQQKSGQAPVLVVYDDSDRPSGIPERFSGSNSGNTATLTISRVEAGDEADYYCQVWDSSSDHPEWVFGGGTKLTVL	IGHV3-30-3 (Human)	IGHJ4 (Human)	IGLV3-21 (Human)	IGLJ3 (Human)	2408	ARGGATNFDY	3610	QVWDSSSDHPEWV	Seth Zost et al., 2020 (https://www.nature.com/articles/s41591-020-0998-x)
COV2-2189	Ab	SARS-CoV1, SARS-CoV2			SARS-CoV2	S; non-RBD	B-cells; SARS-CoV2 Human Patient	321	EAQLVESGGGLVQPGRSLRLSCAASGFTFDDSAMHWVRQAPGKGLEWVSGISWNSGNVGYADSVKGRFTISRDNAKNSLYLQMNSLRAEDTALYYCTKASRYCSSTICWNWFDPWGQGTLVTVSS	1400	DIQMTQSPSSLSASVGDRVTITCRASQSISSYLNWYQQKPGKAPKLLIYGASSLQTGVPSRFSGSGSGTDFTLTIRSLQPEDFASYYCQQSYSTPTFGGGTKVEIK	IGHV3-9 (Human)	IGHJ5 (Human)	IGKV1-39 (Human)	IGKJ4 (Human)	2409	TKASRYCSSTICYWNWFDP	3611	QQSYSTPT	Seth Zost et al., 2020 (https://www.nature.com/articles/s41591-020-0998-x)
COV2-2190	Ab	SARS-CoV2	SARS-CoV1		SARS-CoV1, SARS-CoV2	S; NTD	B-cells; SARS-CoV2 Human Patient	322	EVQLVESGGGLVQPGGSLRLSCAASGFTFSSYEMNWVRQAPGKGLEWVSYISSSGSAIYYADSVKGRFTISRDNAKNSLYLQMNSLRVEDTAVYYCAREARSRYFDWLPSYYFDYWGQGTLVTVSS	1401	QSALTQPASVSGSPGQSITISCTGTSSDIGGYNYVSWYQQHPGKAPKLLIYDVSNRPSGVSTRFSGSKSGNTASLTISGLQAEDEADYYCSSYTSSSTHVVFGGGTKLTVL	IGHV3-48 (Human)	IGHJ4 (Human)	IGLV2-14 (Human)	IGLJ2 (Human)	2410	AREARSRYFDWLPSYYFDY	3612	SSYTSSSTHVV	Seth Zost et al., 2020 (https://www.nature.com/articles/s41591-020-0998-x)
COV2-2191	Ab	SARS-CoV2	SARS-CoV1		SARS-CoV1, SARS-CoV2	S; non-RBD	B-cells; SARS-CoV2 Human Patient	323	EVQLVESGGGVVRPGGSLRLSCAASGFTFDDYGMSWVRQAPGKGLEWVSAINWNGGSTGYADSVKGRFTISRDNAKNSLYLQMNSLRAEDTALYHCARRRSSSRYSSGWYMYYYYMDVWGKGTTVTVSS	1402	DIQMTQSPSTLSASVGDRVTITCRASQSVSTWLAWYQQKPGKAPNLLIYEASSLESGVPSRFSGSGSGTEFTLTISSLQPDDFATYYCQQYNTYSGTFGQGTKVEIK	IGHV3-20 (Human)	IGHJ6 (Human)	IGKV1-5 (Human)	IGKJ1 (Human)	2411	ARRRSSSRYSSGWYMYYYYMDV	3613	QQYNTYSGT	Seth Zost et al., 2020 (https://www.nature.com/articles/s41591-020-0998-x)
COV2-2195	Ab	SARS-CoV2	SARS-CoV1		SARS-CoV1, SARS-CoV2	S; non-RBD	B-cells; SARS-CoV2 Human Patient	324	QVHLVESGGGVVQPGRSLRLSCAASGFTFSNYGMHWVRQAPGKGLEWVAVISNDEFNKFYANSVKGRFTISRDNSKNTVYLQLNSLRTEDTARYYCAKGGDGSGWAWDGDNPPTDYWGQGTLVIVSS	1403	DIVMTQSPDFLAVSLGERATISCKSSQSVLYTPKNKNYLAWYKQKPGQPPKVLIYWASTRESGVPDRFSGSGSGTDFTLIISSLQAEDAAVYYCQQYYTAPLTFGGGTRVEIK	IGHV3-30 (Human)	IGHJ4 (Human)	IGKV4-1 (Human)	IGKJ4 (Human)	2412	AKGGDGSGWAWDGDNPPTDY	3614	QQYYTAPLT	Seth Zost et al., 2020 (https://www.nature.com/articles/s41591-020-0998-x)
COV2-2196	Ab	SARS-CoV2	SARS-CoV1	SARS-CoV2		S; RBD	B-cells; SARS-CoV2 Human Patient	325	QMQLVQSGPEVKKPGTSVKVSCKASGFTFMSSAVQWVRQARGQRLEWIGWIVIGSGNTNYAQKFQERVTITRDMSTSTAYMELSSLRSEDTAVYYCAAPYCSSISCNDGFDIWGQGTMVTVSS	1404	EIVLTQSPGTLSLSPGERATLSCRASQSVSSSYLAWYQQKPGQAPRLLIYGASSRATGIPDRFSGSGSGTDFTLTISRLEPEDFAVYYCQHYGSSRGWTFGQGTKVEIK	IGHV1-58 (Human)	IGHJ3 (Human)	IGKV3-20 (Human)	IGKJ1 (Human)	2413	AAPYCSSISCNDGFDI	3615	QHYGSSRGWT	Seth Zost et al., 2020 (https://www.nature.com/articles/s41591-020-0998-x)
COV2-2197	Ab	SARS-CoV2	SARS-CoV1		SARS-CoV1, SARS-CoV2	S; non-RBD	B-cells; SARS-CoV2 Human Patient	326	EVQLVQSGAEVKKPGESLKISCKGSGYSFTSYWIGWVRQMPGKGLEWMGIIYPGDSDTRYSPSFQGQVTISADKSISTAYLQWSSLKASDTAMYYCARPDYSSGWFSYWYFDLWGRGTLVTVSS	1405	EIVLTQSPGTLSLSPGERATLSCRASQSVSSNFLAWYQQKPGQAPRLLIYGASSRATGIPDRFSGSGSGTDFTLTISRLEPEDFAVYYCQQYGRSPITFGQGTRLEIK	IGHV5-51 (Human)	IGHJ2 (Human)	IGKV3-20 (Human)	IGKJ5 (Human)	2414	ARPDYSSGWFSYWYFDL	3616	QQYGRSPIT	Seth Zost et al., 2020 (https://www.nature.com/articles/s41591-020-0998-x)

COV2-2199	Ab	SARS-CoV2	SARS-CoV1		SARS-CoV1, SARS-CoV2	S; NTD	B-cells; SARS-CoV2 Human Patient	327	QVQLVQSGAEVKKPGASVKVSCKVSGY TLTELSIHWVRQAPGKGLEWMGGFDP EDAETIYAQQFQGRVTMTEDTSTDTAY MELSSLKSEDTALYYCATGFAVFGRAAV PYWGQGTLVTVSS	1406	SYELTQPPSVSVSPGQTASITCFGDKLG DKYACWFQQKPGQSPVLIIYQGAKRP SGIPERFSGSNSGNTATLTISGTQAMD EADYYCQAWDSSTVVFGGGTKLTVL	IGHV1-24 (Human)	IGHJ4 (Human)	IGLV3-1 (Human)	IGLJ2 (Human)	2415	ATGFAVFGRA AVPY	3617	QAWDSST VV	Seth Zost et al., 2020 (https://www.nature.com/articles/s41591-020-0998-x)
COV2-2203	Ab	SARS-CoV1, SARS-CoV2			SARS-CoV2	S; non-RBD	B-cells; SARS-CoV2 Human Patient	328	QVQLVESGGGVVQPGRSLRLSCAASGF TFSTYAMHWVRQAPGKGLAWVALISYD GYNKYYADSVRGRFTISRINSKNTLSLQM NSLRAEDTAVYYCARGSAGNYYYGMDV WGQGTTVTVSS	1407	DIQMTQSPSSLSASVGDRVTITCRASQ TITNYLNWYQLKSGRAPKLLIYAASSLQ SGVPSRFSGSGSGTDFTLTISSLQPEDF ATYYCQQSYSTPYTFGQGTKLEIK	IGHV3-30 (Human)	IGHJ6 (Human)	IGKV1-39 (Human)	IGKJ2 (Human)	2416	ARGSAGNYYY GMDV	3618	QQSYSTPY T	Seth Zost et al., 2020 (https://www.nature.com/articles/s41591-020-0998-x)
COV2-2207	Ab	SARS-CoV2	SARS-CoV1		SARS-CoV1, SARS-CoV2	S; non-RBD	B-cells; SARS-CoV2 Human Patient	329	EVQLVQSGAEVKKPGESLKISCKGSGYSF TSHWIGWVRQMPGKGLEWMGIIYPG DSDTRYSPSFQGQVTISADKSISTAYLQW SSLKASDTAMYYCASALRERGVQLWSV WGQGTLVTVSS	1408	QSVLTQPPSVSGAPGQRVTISCTGSSS NIGAGYDVHWYQQLPGTAPKLLIFINS NRPSGVPDRFSGSKSGTSASLAITGLQ AEDEADYYCQSYDSSLGALFGGGTKLT VL	IGHV5-51 (Human)	IGHJ4 (Human)	IGLV1-40 (Human)	IGLJ3 (Human)	2417	ASALRERGVQ LWSV	3619	QSYDSSLG AL	Seth Zost et al., 2020 (https://www.nature.com/articles/s41591-020-0998-x)
COV2-2210	Ab	SARS-CoV2	SARS-CoV1		SARS-CoV1, SARS-CoV2	S; NTD	B-cells; SARS-CoV2 Human Patient	330	QVQLVESGGGVVQPGRSLRLSCAASGF TFSSYAMHWVRQAPGKGLEWVAVISY DGSNKYYADSVKGRFTISRDNSKNTLYL QMNSLRVEDTAVYYCARDQEWFRELFL FDYWGQGTLVTVSS	1409	DIQMTQSPSSVSASVGDRVTITCRASQ GISSWLAWYQQKPGKAPKLLIYDASSL QSGVPSRFSGSGSGTDFTLTISSLQPED FATYYCQQANSFPPTFGPGTKVDIK	IGHV3-30-3 (Human)	IGHJ4 (Human)	IGKV1-12 (Human)	IGKJ3 (Human)	2418	ARDQEWFRE LFLFDY	3620	QQANSFPP T	Seth Zost et al., 2020 (https://www.nature.com/articles/s41591-020-0998-x)
COV2-2212	Ab	SARS-CoV2	SARS-CoV1		SARS-CoV1, SARS-CoV2	S; NTD	B-cells; SARS-CoV2 Human Patient	331	EVQLVESGGGLVKPGGSLRLSCAASGFT FSSYSMNWVRQAPGKGLEWVSSISNSN SFIYYADSMKGRFTISRDNAKNSLYLQM NSLRAEDTAVYYCARVNGNSNWNFGSY YYYYMDVWGKGTTVTVSS	1410	EIVLTQSPAILSLSPGERATLSCRASQSV SSYLAWYQQKPGQAPRLLIYDTSNRAT GIPARFSGSGSGTDFTLTISSLEPEDFAF YYCQQRGNWWTFAQGTKVEIK	IGHV3-21 (Human)	IGHJ6 (Human)	IGKV3-11 (Human)	IGKJ1 (Human)	2419	ARVNGNSN WNFGSYYYYY MDV	3621	QQRGNW WT	Seth Zost et al., 2020 (https://www.nature.com/articles/s41591-020-0998-x)
COV2-2214	Ab	SARS-CoV1, SARS-CoV2			SARS-CoV2	S; non-RBD	B-cells; SARS-CoV2 Human Patient	332	QVQLVQSGAEVKKPGSSVKVSCKASGG TFSSYAIIWVRQAPGQGLEWMGGIIPIF GTTNYAQKFQGRVTITADESTSTAYVELS SLRSEDTAVYYCARIGHFDSSGYYLDYW GQGTLVTVSS	1411	EIVLTQSPATLSLSPGERATLSCRASQS VSSFLAWYQQKPGQAPRLLIYDASNR PTGIPARFTGSGSGTDFTLTISSLEPEDF AVYYCQHRTNWPPLFTFGPGTKVDIK	IGHV1-69 (Human)	IGHJ4 (Human)	IGKV3-11 (Human)	IGKJ3 (Human)	2420	ARIGHFDSSG YYLDY	3622	QHRTNWP PLFT	Seth Zost et al., 2020 (https://www.nature.com/articles/s41591-020-0998-x)
COV2-2215	Ab	SARS-CoV2	SARS-CoV1		SARS-CoV1, SARS-CoV2	S; NTD	B-cells; SARS-CoV2 Human Patient	333	EVQLVESGGGLVKPGGSLRLSCAASGFT FSGYSMNWVRQAPGKGLEWVSSISSSS SYIYYADSVKGRFTISRDNAKNSLYLQMN SLRAEDTAVYYCARWLQLRSDYYYFGM DVWGQGTTVTVSS	1412	EIVMTQSPATLSVSPGERATLSCRASQ SVSNNLAWYQHKPGQAPRLLIYGAST RATGIPARFSGSGSGTEFTLTISSLQSE DFAVYFCQQCYNWPPWTFGQGTKVE IK	IGHV3-21 (Human)	IGHJ6 (Human)	IGKV3-15 (Human)	IGKJ1 (Human)	2421	ARWLQLRSD YYYFGMDV	3623	QQCYNWP PWT	Seth Zost et al., 2020 (https://www.nature.com/articles/s41591-020-0998-x)
COV2-2216	Ab	SARS-CoV1, SARS-CoV2			SARS-CoV2	S; non-RBD	B-cells; SARS-CoV2 Human Patient	334	QVQLVQSGAEVKKPGSSVKVSCKASGG TFSSYAISWVRQAPGQGLEWMGGIIPIF GAANYAQNFQGRVTITADESTSTGYMQ LSSLRFEDTAVYYCARTSHYDSSGSYFEY WGQGTLVTVSS	1413	EIVLTQSPATLSLSPGERATLSCRASQS VSSYLAWYQQKPGQAPRLLIYDASNR ATGIPARFSGSGSGTDFTLTISSLDPED FAVYYCHKRSNWPPSLTFGGGTKVEIK	IGHV1-69 (Human)	IGHJ4 (Human)	IGKV3-11 (Human)	IGKJ4 (Human)	2422	ARTSHYDSSG SYFEY	3624	HKRSNWP PSLT	Seth Zost et al., 2020 (https://www.nature.com/articles/s41591-020-0998-x)
COV2-2218	Ab	SARS-CoV1, SARS-CoV2			SARS-CoV2	S; non-RBD	B-cells; SARS-CoV2 Human Patient	335	QVQLVESGGGVVQPGRSLRLSCAASGF TFSSYALFWVRQAPGKGLEWVAVISYD GNNKYYADSVRGRFTISRDNSKNTLYLQ MNSLRPEDTAVYYCARPYTGSYKSYMD VWGKGTTVTVSS	1414	DIVMTQSPDSLAVSLGERATINCKSSQ SVLYSSNNKNSLAWYQQKPGQPPKLLI YWASTRESGVPDRFSGSGSGTDFTLTI SSLQAEDVAVYYCQQYYSISWTFGQG TKVEIK	IGHV3-30 (Human)	IGHJ6 (Human)	IGKV4-1 (Human)	IGKJ1 (Human)	2423	ARPYTGSYKS YMDV	3625	QQYYSISW T	Seth Zost et al., 2020 (https://www.nature.com/articles/s41591-020-0998-x)
COV2-2222	Ab	SARS-CoV2	SARS-CoV1		SARS-CoV1, SARS-CoV2	S; NTD	B-cells; SARS-CoV2 Human Patient	336	QVQLQESGPGLVKPSETLSLTCTVSGGSI SSYYWSWIRQPPGKGLEWIGYIYYSGST NYNPSLKSRVTISVDMSKNQFSLKLRSVT AADTAVYYCARAPRERLQWGEYYFDYW GQGTLVTVSS	1415	QSALTQPASVSGSPGQSITISCTGTSSD VGSYNLVSWYQQHAGKAPKLMIYEVI KRPSGVSNRFSGSKSGNTASLTISGLQ AEDEADYYCCSYAVSTTYVIFGGGTKLT VL	IGHV4-59 (Human)	IGHJ4 (Human)	IGLV2-23 (Human)	IGLJ2 (Human)	2424	ARAPRERLQ WGEYYFDY	3626	CSYAVSTTY VI	Seth Zost et al., 2020 (https://www.nature.com/articles/s41591-020-0998-x)
COV2-2224	Ab	SARS-CoV1, SARS-CoV2			SARS-CoV2	S; non-RBD	B-cells; SARS-CoV2 Human Patient	337	QVQLVESGGGVVQPGRSLRLSCAASGF TFSTYGMHWVRQAPGKGLEWVAVISY DGSNKYYADSVKGRFTISRDNSKNTLYL QMNSLRAEDTAMYYCAKDGSIAAADY WGQGTLVTVSS	1416	DIVMTQSPDSLAVSLGERATINCKSSQ SVLHSSNNKDSLVWYQQKPGQPPKLL IYWASSRESGVPDRFSGSGSGTDFTLTI SSLQAEDVAVYYCQQYYSTPWTFGQG TKVEIK	IGHV3-30 (Human)	IGHJ4 (Human)	IGKV4-1 (Human)	IGKJ1 (Human)	2425	AKDGSIAAAD Y	3627	QQYYSTP WT	Seth Zost et al., 2020 (https://www.nature.com/articles/s41591-020-0998-x)
COV2-2226	Ab	SARS-CoV2	SARS-CoV1		SARS-CoV1, SARS-CoV2	S; non-RBD	B-cells; SARS-CoV2 Human Patient	338	EVQLVQSGAEVKKPGESLKISCKGSGYSF TNSWIGWVRQMPGKGLEWMGIIYPG DSDTRYSPSFQGQVTISADKSISTAYLQW SSLKASDTAIYYCATHRCSGGFCYLAYWG QGTLVTVSS	1417	QPVLTQPPSASASLGASVTLTCTLSSGY SNYKVDWYQQRPGKGPRFVMRVGT GGIVGSKGDGIPDRFSVLGSGLNRYLTI KNIQEEDESDYHCGADHGSGSNFVFV VFGGGTKLTVL	IGHV5-51 (Human)	IGHJ4 (Human)	IGLV9-49 (Human)	IGLJ2 (Human)	2426	ATHRCSGGFC YLAY	3628	GADHGSG SNFVFVV	Seth Zost et al., 2020 (https://www.nature.com/articles/s41591-020-0998-x)
COV2-2227	Ab	SARS-CoV1, SARS-CoV2			SARS-CoV2	S; non-RBD	B-cells; SARS-CoV2 Human Patient	339	QVQLVESGGGVVQPGRSLRLSCAASGF TFSSYGMHWVRQAPGKGLEWVAVIWY DGSKKDYADSVKGRFTISRDNSKNTLYL QMNSLRAEDTAVYYCARDQSQGAYILT GYRGYGMDVWGQGTTVTVSS	1418	DIVMTQSPLSLPVTPGEPASISCRSSQS LLHSNGYNYLDWYLQKPGQSPQFLIYL GSNRASGVPDRFSGSGSGTDFILKISR VEAEDVGVYYCMQALQTPFTFGPGTK VDIK	IGHV3-33 (Human)	IGHJ6 (Human)	IGKV2-28 (Human)	IGKJ3 (Human)	2427	ARDQSQGAYI LTGYRGYGM DV	3629	MQALQTP FT	Seth Zost et al., 2020 (https://www.nature.com/articles/s41591-020-0998-x)
COV2-2228	Ab	SARS-CoV2	SARS-CoV1		SARS-CoV1, SARS-CoV2	S; NTD	B-cells; SARS-CoV2 Human Patient	340	QVQLQQWGAGLLKPSETLSLTCAVYGG SFSGHYWSWIRQPPGKGLEWIGEINHS GSTNYNPSLKSRVTISVDTSKNQFSLKLSS VTAADTAVYYCARPPQAARIHYYYYMD VWGKGTTVTVSS	1419	EIVMTQSPATLSVSPGERATLSCRASQ SVSSNLAWYQQKPGQAPRLLIYGAST RATGIPARFSGSGSGTEFTLTISSLQSE DFAVYYCQQYNYWPPLTFGGGTKVEI K	IGHV4-34 (Human)	IGHJ6 (Human)	IGKV3-15 (Human)	IGKJ4 (Human)	2428	ARPPQAARIH YYYYMDV	3630	QQYNYWP PLT	Seth Zost et al., 2020 (https://www.nature.com/articles/s41591-020-0998-x)
COV2-2231	Ab	SARS-CoV1, SARS-CoV2			SARS-CoV2	S; RBD	B-cells; SARS-CoV2 Human Patient	341	EVQLVESGGGLVQPGRSLRLSCAASGFT FDDYAMNWVRQPPGKGLEWVSGISW NSDSIGYADSVKGRFTISRDNAKNSLYLQ MNSLRAEDTAMYYCAKGRGAGYTSYM DVWGKGTTVTVSS	1420	SYVLTQPPSVSVAPGKTARITCEGNNI GSKSVHWYQQKPGQAPVLVVYDDSG RPSGIPERFSGSNSGNTATLTISRVEAG DEADYFCQVWDSSSDHHVVFGGGTK LTVL	IGHV3-9 (Human)	IGHJ6 (Human)	IGLV3-21 (Human)	IGLJ2 (Human)	2429	AKGRGAGYTS YMDV	3631	QVWDSSS DHHVV	Seth Zost et al., 2020 (https://www.nature.com/articles/s41591-020-0998-x)

COV2-2235	Ab	SARS-CoV1, SARS-CoV2			SARS-CoV2	S; non-RBD	B-cells; SARS-CoV2 Human Patient	342	EVQLVESGGGLIQPGGSLRLSCAASGFIVSSNYMSWVRQAPGKGLEWVSVIYSGGSTYYADSVKGRFTISRDNSKNTLYLQMNSLRAEDTAVYYCARESTQWGQGTLVTVSS	1421	DIQMTQSPSTLSASVGDRVTITCRASHSISSWLAWYQQKPGKAPKLLIYKASSLESGVPSRFSGSGSGTEFTLTISSLQPDDFATYYCQQYNTYSQTFGQGTKVEIK	IGHV3-53 (Human)	IGHJ4 (Human)	IGKV1-5 (Human)	IGKJ1 (Human)	2430	ARESTQ	3632	QQYNTYSQT	Seth Zost et al., 2020 (https://www.nature.com/articles/s41591-020-0998-x)
COV2-2238	Ab	SARS-CoV2	SARS-CoV1		SARS-CoV1, SARS-CoV2	S; non-RBD	B-cells; SARS-CoV2 Human Patient	343	QITLKESGPPLVEPKQTLTLTCTFSGFSLTTSGEAVGWIRQPPGKALEWLALIYWDDDKHYSPSLRNRLTITRDTSKNQVVLTLTNVDPADTGTYYCAHRAVILNFDHWGQGFLVTVSS	1422	FYELTQPPSVSVSPGQTAGITCSGDKLGHKYAYWYQQKPGQSPILLIYQDDKRPSGIPERFSGSNSGTIATLTISGTQPVDEADYYCQAWDNDAGVVFGGGTKLTVL	IGHV2-5 (Human)	IGHJ4 (Human)	IGLV3-1 (Human)	IGLJ3 (Human)	2431	AHRAVILNFDH	3633	QAWDNDAGVV	Seth Zost et al., 2020 (https://www.nature.com/articles/s41591-020-0998-x)
COV2-2239	Ab	SARS-CoV1, SARS-CoV2			SARS-CoV2	S; non-RBD	B-cells; SARS-CoV2 Human Patient	344	QVQLVESGGGVVQPGRSLRLSCAASGFTFSSYAMHWVRQAPGKGLEWVAVISYDGINKYYADAVKGRFTISRDNSKNTLYLQMNSLRAEDTAVYYCARPRSGSYYAYFDYWGQGTLVTVSS	1423	DIQMTQSPSSLSASVGDRVTITCRASQGISNYLAWFQQKPGKAPKSLIYAASSLQSGVPSKFSGSGSGTDFTLTISSLQPEDVATYYCQQYNSHPPTFGGGTKVEIK	IGHV3-30-3 (Human)	IGHJ4 (Human)	IGKV1-16 (Human)	IGKJ4 (Human)	2432	ARPRSGSYYAYFDY	3634	QQYNSHPPT	Seth Zost et al., 2020 (https://www.nature.com/articles/s41591-020-0998-x)
COV2-2240	Ab	SARS-CoV2	SARS-CoV1		SARS-CoV1, SARS-CoV2	S; RBD	B-cells; SARS-CoV2 Human Patient	345	EVQLVESGGGLVQPGRSLRLSCAASGFTFDDYAMHWVRQAPGKGLEWVSGISWNSGSIGYADSVKGRFTISRDNAKNSLYLQMNSLRAEDTALYYCAKVGYTISRQWLVGEFDYWGQGTLVTVSS	1424	QSALTQPPSASGSPGQSVTISCTGTSSDVGTYNYVSWYQQHPGKAPKLMIYEVSKRPSGVPDRFSGSKSGNTASLTVSGLQAEDEAEYYCSAYAGSNNLVFGGGTKLTVL	IGHV3-9 (Human)	IGHJ4 (Human)	IGLV2-8 (Human)	IGLJ2 (Human)	2433	AKVGYTISRQWLVGEFDY	3635	SAYAGSNNLV	Seth Zost et al., 2020 (https://www.nature.com/articles/s41591-020-0998-x)
COV2-2241	Ab	SARS-CoV2	SARS-CoV1		SARS-CoV1, SARS-CoV2	S; non-RBD	B-cells; SARS-CoV2 Human Patient	346	EVQLVQSGAEVKKPGESLKISCKGSGYSFTSYWIDWVRQMPGKGLEWMGIIYPGDSDTRYSPSFQGQVTISADKSTSTAYLQWSSLKASDTAMYYCARRGEAAGIWYFDLWGRGTLVTVSS	1425	QPVLTQPPSASASLGASVTLTCTLSSGYSNYKVDWYQQRPGKGPRFVMRVGTGGIVGSKGDGIPDRFSVLGSGLNRYLTIKNIQEEDESDYHCGADHGSGSNFEYVVFGGGTKLTVL	IGHV5-51 (Human)	IGHJ2 (Human)	IGLV9-49 (Human)	IGLJ2 (Human)	2434	ARRGEAAGIWYFDL	3636	GADHGSGSNFEYVV	Seth Zost et al., 2020 (https://www.nature.com/articles/s41591-020-0998-x)
COV2-2243	Ab	SARS-CoV2	SARS-CoV1		SARS-CoV1, SARS-CoV2	S; RBD	B-cells; SARS-CoV2 Human Patient	347	QLQLQESGPGLVKPSETLPLTCTVSGGSISSSSYYWGWIRQPPGKGLQWIGNIYYSGSTYYNSSLKSRVTISVDTSKNQFSLKLSSVTAADTAVYYCARQSRGYSYAWSFDYWGQGTLVTVSS	1426	QSALTQPASVSGSHGQSITISCTGTSSDVGSYNLVSWYQQHPGKAPKLMIYEVSKRPSGVSNRFSGSTSGNTASLTISGLQAEDEADYYCCSYAGIVLFGGGTKVTVL	IGHV4-39 (Human)	IGHJ4 (Human)	IGLV2-23 (Human)	IGLJ2 (Human)	2435	ARQSRGYSYAWSFDY	3637	CSYAGIVL	Seth Zost et al., 2020 (https://www.nature.com/articles/s41591-020-0998-x)
COV2-2245	Ab	SARS-CoV2	SARS-CoV1		SARS-CoV1, SARS-CoV2	S; non-RBD	B-cells; SARS-CoV2 Human Patient	348	QVQLVESGGGVVQPGRSLRLSCAASGFTFSNYGIHWVRQAPGQGLEWVAGIWYDGSNKYYVDSVKGRFTISRDNSKNTLYLQMNSLRAEDTAVYYCAGSSGEGGLYYYYGMDVWGQGTTVTVSS	1427	SYELTQPPSVSVSPGQTTRITCSGDALPKQYGYWYQQKAGQAPILVIYKDSERPSGIPERFSGSSSGTTVTLTISGVQAEDEAHYYCQSGDSSGTYVVFGGGTKLTVL	IGHV3-33 (Human)	IGHJ6 (Human)	IGLV3-25 (Human)	IGLJ3 (Human)	2436	AGSSGEGGLYYYYGMDV	3638	QSGDSSGTYVV	Seth Zost et al., 2020 (https://www.nature.com/articles/s41591-020-0998-x)
COV2-2248	Ab	SARS-CoV2	SARS-CoV1		SARS-CoV1, SARS-CoV2	S; non-RBD	B-cells; SARS-CoV2 Human Patient	349	QVQLVESGGGVVQPGRSLRLSCAASGFTFDSYGVHWVRQAPGKGLEWVAVISYDGSNKHYADSVKGRFTISRDNSKNTLYVQMNSLRTEDTAVYYCARDSGGNYGDSYFDYWGQGTLVTVSS	1428	SYELTQPPSVSVSPGQTARITCSGDALSKQYAYWYQQKPGQAPVLVIYKDSERPSGIPERFSGSSSGTTVTLTISGVQAEDEADYYCQSVDRSGTYFNWVFGGGTKLTVL	IGHV3-30 (Human)	IGHJ4 (Human)	IGLV3-25 (Human)	IGLJ3 (Human)	2437	ARDSGGNYGDSYFDY	3639	QSVDRSGTYFNWV	Seth Zost et al., 2020 (https://www.nature.com/articles/s41591-020-0998-x)
COV2-2251	Ab	SARS-CoV2	SARS-CoV1		SARS-CoV1, SARS-CoV2	S; NTD	B-cells; SARS-CoV2 Human Patient	351	QVQLVESGGGVVQPGRSLRLSCAASGFTFSTYAMHWVRQAPGKGLAWVALISYDGSNAKMGVSWIRQPPGKALEWLAHIFSNDEKAYSTSLKTRLTISKDTSKSQVVLTVTNMDPVDTATYYCARIVLGASGTYPSPGFDPWGQGTLVTVSS	1430	QTVVTQEPSLTVSPGGTVTLTCASSAGAVTSGYYPNWFQQKPGQAPRALIYSTANKHSWTLARFSGSLLGGKAALTLSGVQPEDEAEYYCLLYYGGAWVFGGGTKLTVL	IGHV2-26 (Human)	IGHJ5 (Human)	IGLV7-43 (Human)	IGLJ3 (Human)	2439	ARIVLGASGTYPSPGFDP	3641	LLYYGGAWV	Seth Zost et al., 2020 (https://www.nature.com/articles/s41591-020-0998-x)
COV2-2253	Ab	SARS-CoV2	SARS-CoV1		SARS-CoV1, SARS-CoV2	S; RBD	B-cells; SARS-CoV2 Human Patient	352	EVQLVESGGGLVQPGGSLRLSCAASGFTFSSYWMHWVRQVPGKGLVWVSRINSDGSSTSYADSVKGRFTISRDNAKNTLYLEMNSLRAQDTAVYYCAGSPWLRGDIDYWGQGTLVTVSS	1431	NFMLTQPHSVSESPGKTVTISCTGSSGSIASNYVQWYQQRPGSAPTTVIYEDNQRPSGVPDRFSGSIDSSSNSASLTISGLMTEDEADYYCQSYDGSNHAVVFGGGTKLTVL	IGHV3-74 (Human)	IGHJ4 (Human)	IGLV6-57 (Human)	IGLJ2 (Human)	2440	AGSPWLRGDIDY	3642	QSYDGSNHAVV	Seth Zost et al., 2020 (https://www.nature.com/articles/s41591-020-0998-x)
COV2-2256	Ab	SARS-CoV1, SARS-CoV2			SARS-CoV2	S; RBD	B-cells; SARS-CoV2 Human Patient	353	QVQLVQSGSELTKPGASVKVSCKASGYTFTSYAMNWVRQAPGQGLEWMGWINTDTGNPTYAQGFTGRFVFSLDTSVSTAYLQISSLKAEDTAVYYCARDPSYCSSTRCYTVGWFDPWGQGTLVTVSS	1432	SYVLTQPPSVSVAPGKTARITCGGNNIGSKNVHWYQQKPGQAPVVVVYDDSDRPSGIPERFSGSNSGNTATLTISRVEAGDEADYYCQVWDSSSDPVVFGGGTKLTVL	IGHV7-4-1 (Human)	IGHJ5 (Human)	IGLV3-21 (Human)	IGLJ2 (Human)	2441	ARDPSYCSSTRCYTVGWFDP	3643	QVWDSSSDPVV	Seth Zost et al., 2020 (https://www.nature.com/articles/s41591-020-0998-x)
COV2-2257	Ab	SARS-CoV2	SARS-CoV1		SARS-CoV1, SARS-CoV2	S; NTD	B-cells; SARS-CoV2 Human Patient	354	QVQLQESGPGLVKPSQTLSLTCTVSGDSINSGNYYWSWIRQPAGKGLEWIGRMFTSGSTNYNPSLTSRVTMSIDTSKNQFSLNLNSVTAADTAMYYCARGHVAAWESCYYWGQGILVTVSS	1433	NIVMTQSPLSLPVTPGEPASISCRSSQSLLNSNGLTYLDWYLQKPGQSPQLLIYFVSNRASGVSDRFSGSGSGADFTLTISRVEAEDVGVYYCMQALQTPQTFGQGTKVEIK	IGHV4-61 (Human)	IGHJ4 (Human)	IGKV2-28 (Human)	IGKJ1 (Human)	2442	ARGHVAAWESCYY	3644	MQALQTPQT	Seth Zost et al., 2020 (https://www.nature.com/articles/s41591-020-0998-x)
COV2-2258	Ab	SARS-CoV1, SARS-CoV2		SARS-CoV2		S; RBD	B-cells; SARS-CoV2 Human Patient	355	EVQLVESGGGVVRPGGSLRLSCAASGFTLDDYGLSWVRHAPGKGLEWVSGINWNGGRTAYADSVKGRFTISRDNAKNSLYLQMNSLRAEDTALYHCARARGPSEQTYYDLLTGYYDAFDIWGQGTMVTVSS	1434	EIVLTQSPGTLSLSPGERATLSCGASQSISSSYLAWYQQKPGQAPRLLIYGASSRAAGIPDRFSGSGSGTDFTLTISRLEPEDFAVYFCQQYGGSLTFGGGTKVEIK	IGHV3-20 (Human)	IGHJ3 (Human)	IGKV3-20 (Human)	IGKJ4 (Human)	2443	ARARGPSEQTYYDLLTGYYDAFDI	3645	QQYGGSLT	Seth Zost et al., 2020 (https://www.nature.com/articles/s41591-020-0998-x)

COV2-2260	Ab	SARS-CoV2	SARS-CoV1		SARS-CoV1, SARS-CoV2	S; NTD	B-cells; SARS-CoV2 Human Patient	356	EVQLLESGGGLVHPGGSLRLSCAASGFTFSSYALSWVRQAPGKGLEWVSAISGSGGSTYYADSVKGRFTISRDNSKNTLYLQMNRLRAEDTAVYYCAQMGPLGSTSSAADYWGQGTLVTVSS	1435	SYELTQPPSVSVSPGQTASITCSGDKMGDKYACWYQQKPGQSPVVVIYEDNKRPSGIPERFSGSNSGNTATLTISGTQAMDEADYYCQAWDSSLVVFGGGTKLTVL	IGHV3-23 (Human)	IGHJ4 (Human)	IGLV3-1 (Human)	IGLJ2 (Human)	2444	AQMGPLGSTSSAADY	3646	QAWDSSLVV	Seth Zost et al., 2020 (https://www.nature.com/articles/s41591-020-0998-x)
COV2-2262	Ab	SARS-CoV2	SARS-CoV1	SARS-CoV2 (weak)		S; non-RBD	B-cells; SARS-CoV2 Human Patient	357	QVQLVQSGAEVKKPGASVKVSCKASGYTFTSYDINWVRQATGQGLEWMGWMNPNSGNTGYAQKFQGRVTMTRNTSISTAYMELSSLRSEDTALYYCAREARYFDWIFEGSDYYYYGMDVWGQGTTVTVSS	1436	QSALTQPPSVSGSPGQSVTISCTGTSSDVGSYNRVSWYQQPPGTAPKLMIYEVSNRPSGVPDRFSGSKSGNTASLTISGLQAEDEADYYCSSYTSSSLRVFGGGTKLTVL	IGHV1-8 (Human)	IGHJ6 (Human)	IGLV2-18 (Human)	IGLJ3 (Human)	2445	AREARYFDWIFEGSDYYYYGMDV	3647	SSYTSSSLRV	Seth Zost et al., 2020 (https://www.nature.com/articles/s41591-020-0998-x)
COV2-2263	Ab	SARS-CoV2	SARS-CoV1		SARS-CoV1, SARS-CoV2	S; NTD	B-cells; SARS-CoV2 Human Patient	358	EVQLVESGGGLVQPGGSLRLSCEASGFTFSSSEINWVRQAPGKGLEWVSHISSSGSIIYYADSVKGRFTISRDNAKNSLYLQMNSLRAEDTAVYYCARRSYRSSWYYYYGMDVWGQGTTVTVSS	1437	DIQLTQSPSFLSASVGDRVTITCRASQGISSYLAWYQQKPGKAPKLLIYAASTLQSGVPSRFSGSGSGTEFTLTISSLQPEDFATYYCQQLNSYPVTFGQGTKVEIK	IGHV3-48 (Human)	IGHJ6 (Human)	IGKV1-9 (Human)	IGKJ1 (Human)	2446	ARRSYRSSWYYYYGMDV	3648	QQLNSYPVT	Seth Zost et al., 2020 (https://www.nature.com/articles/s41591-020-0998-x)
COV2-2266	Ab	SARS-CoV1, SARS-CoV2			SARS-CoV2	S; non-RBD	B-cells; SARS-CoV2 Human Patient	359	EVQLVESGGGLVQPGRSLRLSCTASGFIFGDYAMGWVRQAPGKGLEWVGFIRGKAYDGTTEYAASVKGRFTISRDDSKYIAHLQMNSLKTEDTAVYYCIRDYDFWGGYYYHPLRAFDIWGRGTMVTVSS	1438	QSALTQPRSVSGSPGQSVTISCTGTSSDVGGYNYVSWYQQHPGKAPKLMIYDVTKRPSGVPERFSGSKSGNTASLTISGLQAEDEADYSCCSYAGSYTYVFGTGTKVTVL	IGHV3-49 (Human)	IGHJ3 (Human)	IGLV2-11 (Human)	IGLJ1 (Human)	2447	IRDYDFWGGYYYHPLRAFDI	3649	CSYAGSYTYV	Seth Zost et al., 2020 (https://www.nature.com/articles/s41591-020-0998-x)
COV2-2268	Ab	SARS-CoV2	SARS-CoV1	SARS-CoV2		S; RBD	B-cells; SARS-CoV2 Human Patient	360	QITLKESGPTLVKPTQTLTLTCTFSGFSLSTSGVGVGWIRQPPGKALEWLALIYWDDDKRYSPSLKSRLSITKDTSKNQVVLTMTNMDPVDTGTYYCARHQIVVLFDMWGQGTRVTVSS	1439	QSALTQPASVSGSPGQSITISCTGTGSDVGGSNYVSWYQQHPGKAPKLMIYDVSNRPSGVSNRFSGSKSGNTASLTISGLQAEDEADYYCSSYTSSSTLVLFGGGTKLSVL	IGHV2-5 (Human)	IGHJ3 (Human)	IGLV2-14 (Human)	IGLJ2 (Human)	2448	ARHQIVVLFDM	3650	SSYTSSSTLVL	Seth Zost et al., 2020 (https://www.nature.com/articles/s41591-020-0998-x)
COV2-2270	Ab	SARS-CoV1, SARS-CoV2			SARS-CoV2	S; non-RBD	B-cells; SARS-CoV2 Human Patient	361	QVQLVQSGAEVKKPGSSVKVSCKASGGTFSSYAISWVRQAPGQGLEWMGGIIPIFGTANYAQKFQGRVTITADESTSTAYMELSSLRSEDTAVYYCAITYYYDSSGYWWDDWGQGTLVTVSS	1440	EIVLTQSPATLSLSPGERATLSCRASQSVSSFLAWYQQKPGQAPRLLIYDASNRATGIPARFSGSGSGTDFTLTISSLEPEDFAVYYCQQRSNWPPSYTFGQGTKLEIK	IGHV1-69 (Human)	IGHJ4 (Human)	IGKV3-11 (Human)	IGKJ2 (Human)	2449	AITYYYDSSGYWWDD	3651	QQRSNWPPSYT	Seth Zost et al., 2020 (https://www.nature.com/articles/s41591-020-0998-x)
COV2-2273	Ab	SARS-CoV1, SARS-CoV2			SARS-CoV2	S; non-RBD	B-cells; SARS-CoV2 Human Patient	362	QLQLQESGPGLVKPSETLSLTCTVSGGSISSSSYYWGWIRQPPGKGLEWIGTIYYSGSTYYNPSLKSRVTISVDTSKKQFSLKLSSVTAADTAVYYCAGEEVRGVKLYYYYAMDVWGQGTTVTVSS	1441	QSALTQPASVSGSPGQSITISCTGTSSDIGGYNYVSWYQQHPGKAPKLMIYDVSNRPSGVSNRFSGSKSGNTASLTISGLQAEDEADYYCSSYTSISTWVFGGGTKVTVL	IGHV4-39 (Human)	IGHJ6 (Human)	IGLV2-14 (Human)	IGLJ3 (Human)	2450	AGEEVRGVKLYYYYAMDV	3652	SSYTSISTWV	Seth Zost et al., 2020 (https://www.nature.com/articles/s41591-020-0998-x)
COV2-2274	Ab	SARS-CoV1, SARS-CoV2			SARS-CoV2	S; non-RBD	B-cells; SARS-CoV2 Human Patient	363	EVQLVESGGRLVLPGGSLRLSCAASGFTFSVYEMNWVRQAPGKGLEWLSYIGTSGSPIYYADSVKGRFTVSRDNAKNSLYLQMNSLRVEDTALYYCARDRGWNYGLDYWGQGTLVTVSS	1442	SYELTQPSSVSVSPGQTARITCSGDALPKRYAYWYRQKSGQAPVLVIHEDSKRPSGIPERFSGSTSGTMATLTITGAQLEDEADYYCFSMDSSGDLRVFGGGTKLTVL	IGHV3-48 (Human)	IGHJ4 (Human)	IGLV3-10 (Human)	IGLJ2 (Human)	2451	ARDRGWNYGLDY	3653	FSMDSSGDLRV	Seth Zost et al., 2020 (https://www.nature.com/articles/s41591-020-0998-x)
COV2-2277	Ab	SARS-CoV2	SARS-CoV1		SARS-CoV1, SARS-CoV2	S; RBD	B-cells; SARS-CoV2 Human Patient	364	QVQLVESGGGVVQPGRSLRLSCAASGFTFSSYAIHWVRQAPGKGLEWVALISSDGGNKFYADSVKGRFTISRDNSKNTLYLQMNSLRAEDTAVYYCARDVPTTVTAFTVFTYWGQGTLVTVSS	1443	DIQMTQSPSSLSASVGDRVTITCRASQSISTYLNWYQQKPGKAPKLLIYAASSLQSGVPSRFSGSGSGTDFTLTISSLQPEDYATYYCQQSYSTPGLTFGGGTKVEIK	IGHV3-30 (Human)	IGHJ4 (Human)	IGKV1-39 (Human)	IGKJ4 (Human)	2452	ARDVPTTVTAFTVFTY	3654	QQSYSTPGLT	Seth Zost et al., 2020 (https://www.nature.com/articles/s41591-020-0998-x)
COV2-2281	Ab	SARS-CoV1, SARS-CoV2			SARS-CoV2	S; non-RBD	B-cells; SARS-CoV2 Human Patient	365	QVQLVESGGGVVQPGRSLRLSCAASGFAFSNYAIHWVRQAPGKGLEWVAVISYDGNNKDYADSVKGRFTISRDNSKNTLYLQMNSLRAEDTAVYYCARVPVMVRGVYFDYWGQGTLVTVSS	1444	QSALTQPASVSGSPGQSITISCTGTSSDVVGYNYVSWYQQHPGKAPKLMIYDVRNRPSGVSNRFSGSKSGNTASLTISGLQAEDEADYFCISYTSSRTLVFGGGTKLTVL	IGHV3-30-3 (Human)	IGHJ4 (Human)	IGLV2-14 (Human)	IGLJ2 (Human)	2453	ARVPVMVRGVYFDY	3655	ISYTSSRTLV	Seth Zost et al., 2020 (https://www.nature.com/articles/s41591-020-0998-x)
COV2-2287	Ab	SARS-CoV1, SARS-CoV2			SARS-CoV2	S; RBD	B-cells; SARS-CoV2 Human Patient	366	QVQLVQSGAEVKKPGASVKVSCKVSGYTFTSYDINWVRQATGQGLEWMGWMNPNSGHTGYAQKFQGRVTMTRNTSISTAYMELSSLRYEDTAVYYCARGYGLTYYMDVWGKGTTVTVSS	1445	SYVLTQPPSVSVAPGKTARITCGGNNIGSKNVHWYQQKPGQAPVLVVYDDSDRPSGIPERFSGSNSGNTATLTISRVEAGDEADYYCQVWDSSYYHPVVFGGGTKLTVL	IGHV1-8 (Human)	IGHJ6 (Human)	IGLV3-21 (Human)	IGLJ2 (Human)	2454	ARGYGLTYYMDV	3656	QVWDSSYYHPVV	Seth Zost et al., 2020 (https://www.nature.com/articles/s41591-020-0998-x)
COV2-2290	Ab	SARS-CoV2	SARS-CoV1	SARS-CoV2 (weak)		S; RBD	B-cells; SARS-CoV2 Human Patient	367	QVQLAQSGAEVKKPGASVKVSCKAAGYTFTSYDINWVRQATGQGLEWMGWMNPNSGNAGYAQKFQGRVTMTRDTSISTAYMELSSLRSEDTAVYYCARMRSGWPTHGRPDDFWGRGTLVTVSS	1446	QSVLTQPPSASGTPGQRVTISCSGSNSNIGSYTVNWYQQFPGTAPKLLIYDNNQRTSGVPDRFSGSKSGTSASLAISGLQSEDEANYYCLVWDDSLNGLVFGGGTKLTVL	IGHV1-8 (Human)	IGHJ4 (Human)	IGLV1-44 (Human)	IGLJ2 (Human)	2455	ARMRSGWPTHGRPDDF	3657	LVWDDSLNGLV	Seth Zost et al., 2020 (https://www.nature.com/articles/s41591-020-0998-x)
COV2-2293	Ab	SARS-CoV2	SARS-CoV1		SARS-CoV1, SARS-CoV2	S; NTD	B-cells; SARS-CoV2 Human Patient	368	EVQLLQSGGGLVQPGGSLRLSCAASGFTFRNYAMSWVRQAPGKGLEWVSAISGSGGTTYYADSVKGRFTISRDNSKNTLYLQMNSLRAEDTAVYYCAKNERITMLVVVTLFDYWGQGTLVTVSS	1447	QSVLTQPPSVSAAPGQKVTISCSGSSSNIGNNYISWYQQLPGTAPKLLIYDNNKRPSGIPDRFSGSKSGTSATLGITGLQTGDEADYYCGTWDSSLSAVVFGGGTKLTVL	IGHV3-23 (Human)	IGHJ4 (Human)	IGLV1-51 (Human)	IGLJ2 (Human)	2456	AKNERITMLVVVTLFDY	3658	GTWDSSLSAVV	Seth Zost et al., 2020 (https://www.nature.com/articles/s41591-020-0998-x)
COV2-2296	Ab	SARS-CoV2	SARS-CoV1		SARS-CoV1, SARS-CoV2	S; non-RBD	B-cells; SARS-CoV2 Human Patient	369	EVQLVESGGGLVQPGGSLRLSCAASGFTVSGNYMSWVRQAPGKGLEWVSVIYSGGSTYYADSVKGRFTISRDNSKNTLYLQMNSPRAEDTAVYYCARDPSAYYDILTGYSGDVWGKGTTVTVSS	1448	DIQMTQSPSTLSASVGDRVTITCRASQSINSWLAWYQQKPGKAPKLLIYKASSLESGVPSRFSGSGSGTEFTLTISSLQPDDFATYYCQQYSIYSWTFGQGTKVEIK	IGHV3-66 (Human)	IGHJ6 (Human)	IGKV1-5 (Human)	IGKJ1 (Human)	2457	ARDPSAYYDILTGYSGDV	3659	QQYSIYSWT	Seth Zost et al., 2020 (https://www.nature.com/articles/s41591-020-0998-x)

COV2-2299	Ab	SARS-CoV2	SARS-CoV1		SARS-CoV1, SARS-CoV2	S; RBD	B-cells; SARS-CoV2 Human Patient	370	QVQLVESGGGVVQPGRSLRLSCAASGFSFSSYVMNWVRQAPGKGLEWVAVISYDGSSKYYADSVKGRFTISRDNSKNTLYLQMNSLRAEDTAVYYCARDIDSGYDPTPVFDYWGQGTLVTVSS	1449	DIQMTQSPSSLSACVGDRVTITCRASQSISSYLNWYQQKPGKGPKLLIYAASSLQSGVPSRFSGSGSGTDFTLTISSLQPEDFATYYCQQSYSTPWTFGQGTKVEIK	IGHV3-30-3 (Human)	IGHJ4 (Human)	IGKV1-39 (Human)	IGKJ1 (Human)	2458	ARDIDSGYDPTPVFDY	3660	QQSYSTPWT	Seth Zost et al., 2020 (https://www.nature.com/articles/s41591-020-0998-x)
COV2-2300	Ab	SARS-CoV2	SARS-CoV1		SARS-CoV1, SARS-CoV2	S; non-RBD	B-cells; SARS-CoV2 Human Patient	371	QVQLQESGPGLVKPSGTLSLTCAVSGGSISSSNWWTWVRQPPGKGLEWIGEIYHSGSTNYNPSLKSRVTISVDKSKNQFSLKLSSVTAADTAVYYCASRWGDYFDSSGAYDSWGQGTLVTVSS	1450	DIQMTQSPSSVSASVGDRVTITCRASQGISSWLAWYQQKPGKAPKLLIYAASSLQRGVPSRFSGSGSGTDFTLTISSLQPEDFATYYCQQANSLPLTFGGGTKVEVK	IGHV4-4 (Human)	IGHJ4 (Human)	IGKV1-12 (Human)	IGKJ4 (Human)	2459	ASRWGDYFDSSGAYDS	3661	QQANSLPLT	Seth Zost et al., 2020 (https://www.nature.com/articles/s41591-020-0998-x)
COV2-2304	Ab	SARS-CoV2	SARS-CoV1		SARS-CoV1, SARS-CoV2	S; RBD	B-cells; SARS-CoV2 Human Patient	372	EVQLVESGGGLVKPGGSLRLSCAASGFTFSSYSMNWVRQAPGKGLEWVSCISSSSSFIYYADSVKGRFTISRDNAKNSLYLQMNSLRAEDTAVYYCARDPVWVDGELLSGGIPFDYWGQGTLVTVSS	1451	QSVLTQPPSASGTPGQRVTISCSGSSSNIESNSVNWYQQLPGTAPKLLIYSNNQRPSGVPDRFSGSKSGTSASLAISGLQSEDEADYYCAAWDDSLNGVVFGGGTKLTVL	IGHV3-21 (Human)	IGHJ4 (Human)	IGLV1-44 (Human)	IGLJ2 (Human)	2460	ARDPVWVDGELLSGGIPFDY	3662	AAWDDSLNGVV	Seth Zost et al., 2020 (https://www.nature.com/articles/s41591-020-0998-x)
COV2-2305	Ab	SARS-CoV2	SARS-CoV1		SARS-CoV1, SARS-CoV2	S; NTD	B-cells; SARS-CoV2 Human Patient	373	QLQLQESGPGLVKPSETLSLTCTVSGGSIRSSSYYWGWIRQPPGKGLEWIASIYYSGSTYYNSSLKSRVTISVDTSKNQFSLKVNSMTAADTAVYYCAILWRGSSWADRHYYYYSMDVWGQGTTVTVSS	1452	QSVLTQPPSASGTPGQRVTISCSGSTSNIGSNTVNWYQQLPGTAPKLLIYSNNQRPSGVPDRFSGSKSGPSASLAISGLQSVDEADYYCAAWDDSLNGWVFGGGTKLTVL	IGHV4-39 (Human)	IGHJ6 (Human)	IGLV1-44 (Human)	IGLJ3 (Human)	2461	AILWRGSSWADRHYYYYSMDV	3663	AAWDDSLNGWV	Seth Zost et al., 2020 (https://www.nature.com/articles/s41591-020-0998-x)
COV2-2307	Ab	SARS-CoV2	SARS-CoV1		SARS-CoV1, SARS-CoV2	S; NTD	B-cells; SARS-CoV2 Human Patient	374	QVQLVESGGGVVQPGRSLRLSCTASGFTFSSYAMHWVRQAPGKGLEWVALISYDGNNKYYADSAKGRFTISRDNSKNTLYLQMNSLRSEDTAVYYCARDLGRGLDPWGQGTLVTVSS	1453	SYELTQSPSVSVSPGQTASITCSGDKLGDKYACWYQQRPGQSPVLVIYQDSQRPSGIPERFSGSNSGNTATLTISGTQAMDEADYYCQAWDSSTAVFGGGTKLTVL	IGHV3-30-3 (Human)	IGHJ5 (Human)	IGLV3-1 (Human)	IGLJ3 (Human)	2462	ARDLGRGLDP	3664	QAWDSSTAV	Seth Zost et al., 2020 (https://www.nature.com/articles/s41591-020-0998-x)
COV2-2308	Ab	SARS-CoV2	SARS-CoV1	SARS-CoV2		S; RBD	B-cells; SARS-CoV2 Human Patient	375	EVQLLESGGGLIQPGGSLRLSCAASGFTFSNYAMSWVRQAPGKGLEWVSGIISSSGGATYNADSVRGRFTTSRDNSKNILYLQMNSLRGEDTAVYYCVKGLFDWFPLWGQGTMVTVSS	1454	DIVMTQSPATLSVSPGERAILSCRASQSVRSNLAWYQQKPGQAPRLLISGASTRATAIPARFSGSGSGTEFTLTITSLQSEDCAVYYCHQYNNWPQTFGQGTKVEIK	IGHV3-23 (Human)	IGHJ3 (Human)	IGKV3-15 (Human)	IGKJ1 (Human)	2463	VKGLFDWFPL	3665	HQYNNWPQT	Seth Zost et al., 2020 (https://www.nature.com/articles/s41591-020-0998-x)
COV2-2310	Ab	SARS-CoV1, SARS-CoV2			SARS-CoV2	S; non-RBD	B-cells; SARS-CoV2 Human Patient	376	QVQLQESGPGLVKPSQTLSLTCAVSGASISSGSYYWSWIRQPAGKGLEWIGRIYTSGNTNYNPSLKSRVTISVDTSKNQFSLKLSSVTAADTAVYYCATGYIGTYYYYMDVWGKGTTVTVSS	1455	DIQMTQSPSSLSASVGDRVTITCRASQSISTYLNWYQQKPGKAPKLLIYAASSLQSGVPSRFSGSGSGTDFTLTISSLQPEDFATYHCQQSYSTLTFGGGTKVEIK	IGHV4-61 (Human)	IGHJ6 (Human)	IGKV1-39 (Human)	IGKJ4 (Human)	2464	ATGYIGTYYYYMDV	3666	QQSYSTLT	Seth Zost et al., 2020 (https://www.nature.com/articles/s41591-020-0998-x)
COV2-2313	Ab	SARS-CoV1, SARS-CoV2			SARS-CoV2	S; RBD	B-cells; SARS-CoV2 Human Patient	377	EVQLVESGGGLVQPGRSLRLSCAASGFTFDDYAMHWVRQAPGKGLEWVSGISWNSGSIGYADSVKGRFTISRDNAKNSLYLQMNSLRAEDTALYYCAKVSSITSLLGYYFDSWGQGTLVTVSS	1456	EIVLTQSPATLSLSPGERATLSCRASQSVSSYLAWYQQKPGQAPRLLIYDASNRATGIPARFSGSGSGTDFTLTISSLEPEDFAVYYCQHRSNWPPRLTFGGGTKVEIK	IGHV3-9 (Human)	IGHJ4 (Human)	IGKV3-11 (Human)	IGKJ4 (Human)	2465	AKVSSITSLLGYYFDS	3667	QHRSNWPPRLT	Seth Zost et al., 2020 (https://www.nature.com/articles/s41591-020-0998-x)
COV2-2318	Ab	SARS-CoV2	SARS-CoV1		SARS-CoV1, SARS-CoV2	S; RBD	B-cells; SARS-CoV2 Human Patient	378	QVTLRESGPALVKPTQTLSLTCTFSGFSLGTSGMCVSWIRQPPGKALEWLARIDWDDDKYYSTSLKTRLTISKDTSKNQVVLTMTNMDPVDTATYYCARGVVTYDYWGQGTLVTVSS	1457	DIQMTQSPSSLSASVGDRVTITCRASQSIAGYLNWYQQKPGKAPKLLIYGTTSLQSGVPVRFSGSGSGTDFTLTISSLQPEDFATYYCQQSYSTPGTFGQGTRLEIK	IGHV2-70 (Human)	IGHJ4 (Human)	IGKV1-39 (Human)	IGKJ5 (Human)	2466	ARGVVTYDY	3668	QQSYSTPGT	Seth Zost et al., 2020 (https://www.nature.com/articles/s41591-020-0998-x)
COV2-2322	Ab	SARS-CoV2			SARS-CoV2	S; non-RBD	B-cells; SARS-CoV2 Human Patient	379	QVQLVESGGGVVQPGRSLRLSCAASGFTFSNYAMHWVRQAPGKGLDWVAVISYDGSNRYYAASVKGRFTISRDNSKNTLYLQMNSLRTEDTAVYFCARGDGYRSQFDPWGQGTLVTVSS	1458	EIVLTQSPGTLSLSPGERATLSCRASQSVSSSYLAWYQQKPGQAPRLLIYGASSRATGIPDRFSGSGSGTDFTLTISRLEPEDFAVYYCQQYGSSYTFGQGTKLEIK	IGHV3-30 (Human)	IGHJ5 (Human)	IGKV3-20 (Human)	IGKJ2 (Human)	2467	ARGDGYRSQFDP	3669	QQYGSSYT	Seth Zost et al., 2020 (https://www.nature.com/articles/s41591-020-0998-x)
COV2-2325	Ab	SARS-CoV2			SARS-CoV2	S; non-RBD	B-cells; SARS-CoV2 Human Patient	380	QITFKESGPTLVKPTETLTLTCTFSGFSVSTSGEGVGWIRQPPGKALEWLAVIYWDDDKRYSPSLKSRLTITRDTSKNQVVLTMTNMDPVDTATYYCAHRLWFRDAFDIWGQGTTVTVSS	1459	DIQMTQSPSSLSASVGDRVTITCRARQSISNYLNWYQQKPGKAPKLLIYAASSLHSGVPSRFSGSGSGTDFTLTISSLQPEDFATYYCQQTYSTFWTFGQGTNVEIK	IGHV2-5 (Human)	IGHJ3 (Human)	IGKV1-39 (Human)	IGKJ1 (Human)	2468	AHRLWFRDAFDI	3670	QQTYSTFWT	Seth Zost et al., 2020 (https://www.nature.com/articles/s41591-020-0998-x)
COV2-2329	Ab	SARS-CoV2			SARS-CoV2	S; RBD	B-cells; SARS-CoV2 Human Patient	381	EVQLLESGGGLVQPGGSLRLSCAASGFTFNNYAMSWVRQAPGKGLEWVSAIGGSGGSTYYADSVKGRFTVSRDNSENTLYLQMSSLRAEDTAVYYCARVEGDWLLGGPYYHYYGMDVWGQGTTVTVSS	1460	QSVLTQPPSASGTPGQRVTISCSGSSSNIGSNYVYWYQQLPGTAPKLLISRNNQRPSGVPDRFSGSKSGTSASLAISGLRSEDEADYYCAAWDDSLSSWVFGGGTKLTVL	IGHV3-23 (Human)	IGHJ6 (Human)	IGLV1-47 (Human)	IGLJ3 (Human)	2469	ARVEGDWLLGGPYYHYYGMDV	3671	AAWDDSLSSWV	Seth Zost et al., 2020 (https://www.nature.com/articles/s41591-020-0998-x)
COV2-2331	Ab	SARS-CoV1, SARS-CoV2			SARS-CoV2	S; RBD	B-cells; SARS-CoV2 Human Patient	382	QLQLQESGPGLVKPSETLSLTCTVSGGSISSSSYYWGWIRQPPGNGLEWIGSIYYSGSTYYNPSLKGRVSISVDTSKNQFSLKLSSVTAADTAVYYCARILVIFTLNWFDPWGQGTLVTVSS	1461	NFMLTQPHSVSESPGKTVTISCTGSSGSIASNYVQWYQQRPGSAPTTVIYEDNQRPSGVPDRFSGSIDSSSNSASLTISGLKTEDEADYYCQSYDSGNPIFGGGTKLTVL	IGHV4-39 (Human)	IGHJ5 (Human)	IGLV6-57 (Human)	IGLJ2 (Human)	2470	ARILVIFTLNWFDP	3672	QSYDSGNPI	Seth Zost et al., 2020 (https://www.nature.com/articles/s41591-020-0998-x)
COV2-2333	Ab	SARS-CoV1, SARS-CoV2			SARS-CoV2	S; non-RBD	B-cells; SARS-CoV2 Human Patient	383	EVQLVESGGGLVQPGGSLRLSCAASGFTFSIYWMSWVRQAPGKGLQWVANIKQDASEKYYVDSVKGRFTISRDNAKNSLYLQMNSLRAEDTAVYYCARLGGSSWHFDYWGQGTLVTVSS	1462	SYELTQPPSVSVSPGQTASITCSGDKLGDKYSSWYQQKPGQSPVLVIYEDTKRPSGIPERFSGSNSGNTATLTISGTQAMDEADYYCQAWSSTAVFGGGTKLTVL	IGHV3-7 (Human)	IGHJ4 (Human)	IGLV3-1 (Human)	IGLJ3 (Human)	2471	ARLGGSSWHFDY	3673	QAWSSSTAV	Seth Zost et al., 2020 (https://www.nature.com/articles/s41591-020-0998-x)

COV2-2335	Ab	SARS-CoV2	SARS-CoV1		SARS-CoV1, SARS-CoV2	S; NTD	B-cells; SARS-CoV2 Human Patient	384	QLQLQESGPGLVKPSETLSLTCTVSGGPI SSSRYYWGWIRQPPGKGLEWIGSIYYSG STYYNPSLKSRVTISVDTSKNQFSLKLNSV TAADTAVYYCARHDGSGEMDTITWGPI YYYMDVWGKGTTVTVSS	1463	QSALTQPASVSGSPGQSITISCTGTSSD VGGYNYVSWYQQHPGKAPKLMIYYV SNRPSGVSNRFSGSKSGNTASLTISGL QAEDEADYYCSSYTSSTLNVLFGGGTK LTVL	IGHV4-39 (Human)	IGHJ6 (Human)	IGLV2-14 (Human)	IGLJ2 (Human)	2472	ARHDGSGEM DTITWGPIYYY MDV	3674	SSYTSSTLN VL	Seth Zost et al., 2020 (https://www.nature.com/articles/s41591-020-0998-x)
COV2-2337	Ab	SARS-CoV1, SARS-CoV2			SARS-CoV2	S; non-RBD	B-cells; SARS-CoV2 Human Patient	385	QITFKESGPTLVKPTETLTLTCTFSGFSVS TSGEGVGWIRQPPGKALEWLAVIYWD DDKRYSPSLKSRLTITRDTSKNQVVLTMT NMDPVDTATYYCAHRLWFRDAFDIWG QGTTVTVSS	1464	DIQMTQSPSSLSASVGDRVTITCRARQ SISNYLNWYQQKPGKAPKLLIYAASSL HSGVPSRFSGSGSGTDFTLTISSLQPED FATYYCQQSYSTPGTFGQGTRLEIK	IGHV2-5 (Human)	IGHJ3 (Human)	IGKV1-39 (Human)	IGKJ5 (Human)	2473	AHRLWFRDA FDI	3675	QQSYSTPG T	Seth Zost et al., 2020 (https://www.nature.com/articles/s41591-020-0998-x)
COV2-2340	Ab	SARS-CoV1, SARS-CoV2			SARS-CoV2	S; non-RBD	B-cells; SARS-CoV2 Human Patient	386	QVQLVQSGAEVKKPGASVKVSCKASGY TFTSYGMHWVRQAPGQRLEWMGWIN VGNGNTKYSQRFQGRVTITRDTSASTAY MELSSLRSEDTAVYYCAMGPSAFSWLD PWGQGTLVTVSS	1465	QSVLTQPPSVSGAPGQRVTISCTGSSS NIGAGYDVHWYQHLPGTAPKLLIYGN SNRPSGVPDRFSGSKSGTSASLAITGL QAEDEADYYCQSYDSSLSGWSVFGTG TKVTVL	IGHV1-3 (Human)	IGHJ5 (Human)	IGLV1-40 (Human)	IGLJ1 (Human)	2474	AMGPSAFSW LDP	3676	QSYDSSLS GWSV	Seth Zost et al., 2020 (https://www.nature.com/articles/s41591-020-0998-x)
COV2-2341	Ab	SARS-CoV1, SARS-CoV2			SARS-CoV2	S; non-RBD	B-cells; SARS-CoV2 Human Patient	387	QVQLAESGGGVVQPGRSLRLSCAASGF TFSSYAMHWVRQAPGKGLEWVAVISY DGSNKYYADSVKGRFTISRDNSKNTLYL QMNSLRAEDTAVYYCARSTSGSYYYGM DVWGQGTTVTVSS	1466	QSALTQPASVSGSPGQSITISCTGTSSD VGDYNYVSWYQQHPGKAPKLMIYDV SNRPSGVSNRFSGSKSGNTASLTISGL QAEDEAEYYCSSYTSSSTLLYVFGTGTK VTVL	IGHV3-30-3 (Human)	IGHJ6 (Human)	IGLV2-14 (Human)	IGLJ1 (Human)	2475	ARSTSGSYYY GMDV	3677	SSYTSSSTL LYV	Seth Zost et al., 2020 (https://www.nature.com/articles/s41591-020-0998-x)
COV2-2342	Ab	SARS-CoV1, SARS-CoV2			SARS-CoV2	S; RBD	B-cells; SARS-CoV2 Human Patient	388	QITLKESGPTLVKPTQTLTLTCTFSGFSLN TSGVGVGWIRQPPGKALEWLALIYWD DDKRYNPSLKSRLTITKDTSKNQVVLTM TNMDPVDTATYYCAHRPPSYHGWCYF DYWGQGNLVTVSS	1467	DIQMTQSPSSLSASVGDRVTITCRASQ SISIYLNWYQQKPGKAPKLLIYAASTLQ SGVPSRFSGSGSGTDFTLTISSLQPEDF ATYYCQQSYSTHMSTFGQGTKLEIK	IGHV2-5 (Human)	IGHJ4 (Human)	IGKV1-39 (Human)	IGKJ2 (Human)	2476	AHRPPSYHG WCYFDY	3678	QQSYSTH MST	Seth Zost et al., 2020 (https://www.nature.com/articles/s41591-020-0998-x)
COV2-2343	Ab	SARS-CoV1, SARS-CoV2			SARS-CoV2	S; non-RBD	B-cells; SARS-CoV2 Human Patient	389	QVQVVQSGAEVKKPGASVKVSCKASGY TFKNYGISWVRQAPGQGLEWMGWISA YTGNTNYAQKFQGRMTMTTDTSTGTG YMELRSLRSDDTAVYYCARVQRRRLDY WGQGTLVIVSS	1468	DIVVTQTPLSLSVTPGQPASISCKSSETL LHSDGKTYLSWYLQKPGQPPQLLIYEV SNRFSGVPDRFSGSGSGTDFTLKIGRV EAEDVGLYYCMQSIQLAFGQGTRLEIE	IGHV1-18 (Human)	IGHJ4 (Human)	IGKV2D-29 (Human)	IGKJ5 (Human)	2477	ARVQRRRLDY	3679	MQSIQLA	Seth Zost et al., 2020 (https://www.nature.com/articles/s41591-020-0998-x)
COV2-2346	Ab	SARS-CoV2	SARS-CoV1		SARS-CoV1, SARS-CoV2	S; NTD	B-cells; SARS-CoV2 Human Patient	390	QVQLQQWGAGLLKPSETLSLTCAVYGG SFSGHYWSWIRQPPGKGLEWIGEINHS GSTNYNPSLKSRVTISVDTSKNQFSLKLSS VTAADTAVYYCARPPQAARIHYYYYMD VWGKGTTVTVSS	1469	EIVMTQSPATLSVSPGERATLSCRASQ SVSSNLAWYQQKPGQAPRLLIYGAST RATGIPARFSGSGSGTEFTLTISSLQSE DFAVYYCQQYNYWPPLTFGGGTKVEI K	IGHV4-34 (Human)	IGHJ6 (Human)	IGKV3-15 (Human)	IGKJ4 (Human)	2478	ARPPQAARIH YYYYMDV	3680	QQYNYWP PLT	Seth Zost et al., 2020 (https://www.nature.com/articles/s41591-020-0998-x)
COV2-2351	Ab	SARS-CoV2	SARS-CoV1		SARS-CoV1, SARS-CoV2	S; RBD	B-cells; SARS-CoV2 Human Patient	391	EVQLVQSGAEVKKPGESLKISCKGSGYSF TSYWIGWVRQMPGKGLEWMGIIYPGD SDTTYNPSFQGQVTISADKSLTTAFLHW SSLKASDTAIYYCARRFYGPSSFDYWGQ GTLVIVSS	1470	SSELTQDPAVSVALGQTVTITCQGDSL RSHYASWYKVKPGQAPLLVIYGRNNR PSGIPDRFSGSRSGNTASLTITGAQVD DEADYYCSSGDSSTDHHVVFAGGTKL AVV	IGHV5-51 (Human)	IGHJ4 (Human)	IGLV3-19 (Human)	IGLJ2 (Human)	2479	ARRFYGPSSF DY	3681	SSGDSSTD HHVV	Seth Zost et al., 2020 (https://www.nature.com/articles/s41591-020-0998-x)
COV2-2352	Ab	SARS-CoV2	SARS-CoV1		SARS-CoV1, SARS-CoV2	S; RBD	B-cells; SARS-CoV2 Human Patient	392	QVQLVQSGAEVKRPGASMNISCKASGY NFNNNYIYWVRQAPGQGLEWMGVVN PTGGGTAYAQGFQDRVTITSDTPRNTVY LGVTGLHSEDTAVYFCARGGEWRIVPG GRDYFDYWGQGTLVTVSA	1471	DMEVTQFPSSLSASIGDRVTITCRATQ SISTYLNWYQQKPGKAPNLLIYSASHL QRGVPARFSGSGSGTEFTLTITSLQPE DVGTYYCHQSYGVPITFGGGTKVDIK	IGHV1-46 (Human)	IGHJ4 (Human)	IGKV1-39 (Human)	IGKJ4 (Human)	2480	ARGGEWRIV PGGRDYFDY	3682	HQSYGVPI T	Seth Zost et al., 2020 (https://www.nature.com/articles/s41591-020-0998-x)
COV2-2353	Ab	SARS-CoV2	SARS-CoV1	SARS-CoV2		S; RBD	B-cells; SARS-CoV2 Human Patient	393	EVQLVQSGAEVKKPGESLKISCKGFGYN FTNYWIGWVRQMPGKGLEWMGIIYPG DSETRNSPSFQGQVTISADKSMSTAYLQ WSSLKASDTAMYYCARLGVSKYCSGGR CLSGGSNWFDPWGQGTLVTVSS	1472	EIVMTQSPATLSVSPGERATLSCRASQ SVSSNLAWYQQKPGQAPRLLIYGAST RATGIPARFSGSGSGTEFTLTISSLQSE DFAVYYCQQYNNWPPMYTFGQGTKL EIK	IGHV5-51 (Human)	IGHJ5 (Human)	IGKV3-15 (Human)	IGKJ2 (Human)	2481	ARLGVSKYCS GGRCLSGGS NWFDP	3683	QQYNNWP PMYT	Seth Zost et al., 2020 (https://www.nature.com/articles/s41591-020-0998-x)
COV2-2354	Ab	SARS-CoV1, SARS-CoV2		SARS-CoV2		S; RBD	B-cells; SARS-CoV2 Human Patient	394	EVHLVGSGGGLIQPGGSLRLSCAASGFT VSSNFMSWVRQAPGKGLEWVSIIHNG GDSYYTDSVKGRFTISRDNSKNTLYLQM NNLRAEDTAVYYCASSSWLRGAFDIWG QGTMVTVSS	1473	NFMLTQPHSVSESPGKTVTISCTGSSG SIASNYVQWYQQRPGSAPTTVIYEDN QRPSGVPDRFSGSIDSSSNSASLTISGL KTEDEADYYCQSYDSSKYVVFGGGTKL TVL	IGHV3-53 (Human)	IGHJ3 (Human)	IGLV6-57 (Human)	IGLJ2 (Human)	2482	ASSSWLRGAF DI	3684	QSYDSSKY VV	Seth Zost et al., 2020 (https://www.nature.com/articles/s41591-020-0998-x)
COV2-2355	Ab	SARS-CoV2	SARS-CoV1	SARS-CoV2		S; RBD	B-cells; SARS-CoV2 Human Patient	395	QMQLVQSGPEVKKPGTSVKVSCKTSGF TFTSSAIQWVRQARGQRLEWIGWIVVG SGNTNYAQKFQERVTITRDMSTSTAYM ELSSLRSEDTAVYYCAAPHCNRTSCYDAF DLWGQGTMVTVSS	1474	EIVLTQSPGTLSLSPGERATLSCRASQS VSSSYLGWYQQKPGQAPRLLIYGASSR ATGIPDRFSGSGSGTDFTLTISRLEPED FAVYYCQQYGSSPWTFGQGTKVEIK	IGHV1-58 (Human)	IGHJ3 (Human)	IGKV3-20 (Human)	IGKJ1 (Human)	2483	AAPHCNRTSC YDAFDL	3685	QQYGSSP WT	Seth Zost et al., 2020 (https://www.nature.com/articles/s41591-020-0998-x)
COV2-2357	Ab	SARS-CoV1, SARS-CoV2			SARS-CoV2	S; RBD	B-cells; SARS-CoV2 Human Patient	396	EVQLVESGGDLVKPGRSLRLSCSASGFTF GDYTMSWFRQAPGKGLEWVAFIRSKAY GGTTEYAASVIGRFTISRDDSKSIAYLQM NSLKSEDTAVYYCSRVRGSFYGSVGKNY GMDVWGQGTTVTVSS	1475	DIVMTQSPLSLPVTPGEPASISCRSSQS LLHSNGYNYLDWYLQKPGQSPQLLIYL GSTRASGVPDRFSGSGSGTDFTLKISR VEAEDVGVYYCMQALQTPLYTFGQGT KLEIK	IGHV3-49 (Human)	IGHJ6 (Human)	IGKV2-28 (Human)	IGKJ2 (Human)	2484	SRVRGSFYGS VGKNYGMDV	3686	MQALQTP LYT	Seth Zost et al., 2020 (https://www.nature.com/articles/s41591-020-0998-x)
COV2-2358	Ab	SARS-CoV1, SARS-CoV2			SARS-CoV2	S; RBD	B-cells; SARS-CoV2 Human Patient	397	QVQLVESGGGVVQPGRSLRLSCAASGF SFSSYVMNWVRQAPGKGLEWVAVISY DGSSKYYADSVKGRFTISRDNSKNTLYLQ MNSLRAEDTAVYYCARDIDSGYDPTPVF DYWGQGTLVTVSS	1476	DIQMTQSPSSLSACVGDRVTITCRASQ SISSYLNWYQQKPGKGPKLLIYAASSLQ SGVPSRFSGSGSGTDFTLTISSLQPEDF ATYYCQQSYSSLSITFGQGTRLEIK	IGHV3-30-3 (Human)	IGHJ4 (Human)	IGKV1-39 (Human)	IGKJ5 (Human)	2485	ARDIDSGYDP TPVFDY	3687	QQSYSSLSI T	Seth Zost et al., 2020 (https://www.nature.com/articles/s41591-020-0998-x)

COV2-2367	Ab	SARS-CoV1, SARS-CoV2			SARS-CoV2	S; non-RBD	B-cells; SARS-CoV2 Human Patient	398	QVQLVQSGAEVKKPGSSVKVSCKASGGTFSSYAISWVRQAPGQGLEWMGGIIPIFGAANYAQNFQGRVTITADESTSTGYMQLSSLRFEDTAVYYCARTSHYDSSGSYFEYWGQGTLVTVSS	1477	EIVLTQSPATLSLSPGERATLSCRASQSVSSYLAWYQQKPGQAPRLLIYDASNRATGIPARFSGSGSGTDFTLTISSLDPEDFAVYYCHKRSNWPPSLTFGGGTKVEIK	IGHV1-69 (Human)	IGHJ4 (Human)	IGKV3-11 (Human)	IGKJ4 (Human)	2486	ARTSHYDSSGSYFEY	3688	HKRSNWPPSLT	Seth Zost et al., 2020 (https://www.nature.com/articles/s41591-020-0998-x)
COV2-2368	Ab	SARS-CoV2	SARS-CoV1		SARS-CoV1, SARS-CoV2	S; non-RBD	B-cells; SARS-CoV2 Human Patient	399	EVQLVQSGAEVKKPGESLKISCKGSGYSFTTYWIGWVRQMPGKGLEWMGIIYPGDSDTRYSPSFQGQVTISADKSISTAYLQWSSLKASDTAMYYCARRRGGIGIEYGMDVWGQGTTVTVSS	1478	SNELTQPPSVSVSPGQTARITCSGDALPKQYAYWYQQKPGQAPVLVIYKDTERPSGIPERFSGSSSGTTVTLTISGVQAEDEADYYCQSTASSGTYVVFGGGTKLTVL	IGHV5-51 (Human)	IGHJ6 (Human)	IGLV3-25 (Human)	IGLJ2 (Human)	2487	ARRRGGIGIEYGMDV	3689	QSTASSGTYVV	Seth Zost et al., 2020 (https://www.nature.com/articles/s41591-020-0998-x)
COV2-2369	Ab	SARS-CoV2	SARS-CoV1		SARS-CoV1, SARS-CoV2	S; non-RBD	B-cells; SARS-CoV2 Human Patient	400	QVQLVESGGGVVQPGRSLRLSCAASGFTFSSYAMHWVRQAPGKGLEWVADISYDGSEKYYADSVKGRFTIYRDNSKNTLYLQMNSLRAEDTAVYYCAKDFGGDNTAMVEYFFDFWGQGTLVTVSS	1479	DIQMTQSPSTLSASVGDRVTITCRASQSISSWLAWYQQKPGKAPKLLIYKASSLESGVPSRFSGSGSGTEFTLTISSLQPDDFATYYCQQYNSYSPTFGQGTKVEIK	IGHV3-30 (Human)	IGHJ4 (Human)	IGKV1-5 (Human)	IGKJ1 (Human)	2488	AKDFGGDNTAMVEYFFDF	3690	QQYNSYSPT	Seth Zost et al., 2020 (https://www.nature.com/articles/s41591-020-0998-x)
COV2-2370	Ab	SARS-CoV2	SARS-CoV1		SARS-CoV1, SARS-CoV2	S; RBD	B-cells; SARS-CoV2 Human Patient	401	QVQLQESGPGLVKPSETLSLTCTVSGGSVSSGSYYWSWIRQPPGKGLECIGYIYYSGSSNYNPSLKSRVTISVDTSKNQFSLKMSSVTAADTAVYYCAGSPVPPTIVGASYWGQGTLVTDSS	1480	NFMLTQPHSVSESPGKTVTFSCTGSSGSIASNYVQWYQQRPGSAPTTVIYEDNQRPSGVPDRFSGSIDSSSNSASLTISGLKTEDEADYYCQSYDGINRWLVFGGGTKLTVL	IGHV4-61 (Human)	IGHJ4 (Human)	IGLV6-57 (Human)	IGLJ2 (Human)	2489	AGSPVPPTIVGASY	3691	QSYDGINRWLV	Seth Zost et al., 2020 (https://www.nature.com/articles/s41591-020-0998-x)
COV2-2371	Ab	SARS-CoV1, SARS-CoV2			SARS-CoV2	S; non-RBD	B-cells; SARS-CoV2 Human Patient	402	QVQLVESGGGVVQPGRSLRLSCAASGFTFSNYGMHWVRQAPGKGLEWVAVISYDGTNKYYADSVKGRFTISRDNSKNTLYLQMNSLRADDTAVYYCAKGRGNYLTFFDSWGQGTLVTVSS	1481	EIVMTQSPATLSVSPGERATLSCRASQSVSSNLAWYQQKPGQAPRLLIYGASTRATGIPARFSGSGSGTEFTLTISSLQSEDFAVYYCQQYNNWPGTFGQGTKVEIK	IGHV3-30 (Human)	IGHJ4 (Human)	IGKV3-15 (Human)	IGKJ1 (Human)	2490	AKGRGNYLTFFDS	3692	QQYNNWPGT	Seth Zost et al., 2020 (https://www.nature.com/articles/s41591-020-0998-x)
COV2-2373	Ab	SARS-CoV2	SARS-CoV1		SARS-CoV1, SARS-CoV2	S; non-RBD	B-cells; SARS-CoV2 Human Patient	403	EVQLVESGGGLVQPGGSLRLSCAASGLTVSSNYMSWVRQAPGKGLEWVSVIYSGGSTYYADSVKGRFTISGDNSKNTLYLQMNSLRVDDTAVYYCARDPGSRYSGGWYDYYYAMDVWGQGTTVTVSS	1482	EIVLTQSPGTLSLSPGERATLSCRASQSVSSSYLAWYQQKPGQAPRLLIYGASSRATGIPDRFSGSGSGTDFTLTISRLEPEDFAVYYCQQYGSSPPYTFGQGTKLEIK	IGHV3-66 (Human)	IGHJ6 (Human)	IGKV3-20 (Human)	IGKJ2 (Human)	2491	ARDPGSRYSGGWYDYYYAMDV	3693	QQYGSSPPYT	Seth Zost et al., 2020 (https://www.nature.com/articles/s41591-020-0998-x)
COV2-2378	Ab	SARS-CoV2	SARS-CoV1		SARS-CoV1, SARS-CoV2	S; non-RBD	B-cells; SARS-CoV2 Human Patient	404	EVQLVQSGAEVKKPGESLKISCKGSGYSFPTYWIGWVRQMPGKGLEWMGIIYPGDSDTRYGPSFQGQVTISADKSISTAYLQWSSLKASDTAMYYCARRDTDFDYWGQGTLVTVSS	1483	QPVLTQPPSASASLGASVTLTCTLSSGYSNYKVDWFQQRPGKGPRFVMRVGTGGIVGSKGDGIPDRFSVLGSGLNRYLTIKNIQEEDESDYHCGADHGSGSNFVYVVFGGGTKLTVL	IGHV5-51 (Human)	IGHJ4 (Human)	IGLV9-49 (Human)	IGLJ2 (Human)	2492	ARRDTDFDY	3694	GADHGSGSNFVYVV	Seth Zost et al., 2020 (https://www.nature.com/articles/s41591-020-0998-x)
COV2-2381	Ab	SARS-CoV2	SARS-CoV1	SARS-CoV2		S; RBD	B-cells; SARS-CoV2 Human Patient	405	QMQLVQSGPEVKKPGTSVKVSCKASGFTFTSSAVQWVRQARGQRLEWIGWIAVGSGNTNYAQKFQERVSITRDMSTSTAYMELSSLRSEDTAVYYCAAPYCSRTSCHDAFDIWGQGTKVTVSS	1484	EVVLTQSPGTLSLSPGERATLSCRASQSVSSSYLAWYQQKPGQAPRLLIYGASSRATGIPDRFSGSGSGTDFTLTISRLEPEDFAVYHCQHFGSSSQWTFGQGTKVEIK	IGHV1-58 (Human)	IGHJ3 (Human)	IGKV3-20 (Human)	IGKJ1 (Human)	2493	AAPYCSRTSCHDAFDI	3695	QHFGSSSQWT	Seth Zost et al., 2020 (https://www.nature.com/articles/s41591-020-0998-x)
COV2-2382	Ab	SARS-CoV1, SARS-CoV2			SARS-CoV2	S; RBD	B-cells; SARS-CoV2 Human Patient	406	QVQLVESGGGVVQPGRSLRLSCVASGFTFSSYGMHWVRQAPGKGLEWVAVISFDGSNKYYADSVKGRFTISRDNSKNTLYLQMNSLRAEDTAVFYCAKDLPPYASGWYEGGFDYWGRGTQVTVSS	1485	QTVVTQEPSLTVSPGGTVTLTCASSTGAVTSGYFPNWFQQKPGQAPRALIFSTNNRHSWTPARFSGSLLGDKAALTLSGVQPEDEAEYYCLLYYGGPWVFGGGTKLTVL	IGHV3-30 (Human)	IGHJ4 (Human)	IGLV7-43 (Human)	IGLJ3 (Human)	2494	AKDLPPYASGWYEGGFDY	3696	LLYYGGPWV	Seth Zost et al., 2020 (https://www.nature.com/articles/s41591-020-0998-x)
COV2-2383	Ab	SARS-CoV2	SARS-CoV1		SARS-CoV1, SARS-CoV2	S; non-RBD	B-cells; SARS-CoV2 Human Patient	407	QVQLVESGGGVVQPGRSLRLSCAASGFTFSSYGMHWVRQAPGKGLEWVAVVSYDGSNKYYTDSVKGRFTISRDNSKNTLFLQMIGLREEDTAVYYCAQGRGGYYSPFDDWGQGTLVTVSS	1486	EIVMTQSPGTLSVSPGERATLSCRASQTLSSNLAWYQQKPGQAPRLLIYGASTRATGIPARFSGSGSGTEFTLTISSLQSEDFAVYHCQQYNNWPLAFGQGTKVEIK	IGHV3-30 (Human)	IGHJ4 (Human)	IGKV3-15 (Human)	IGKJ1 (Human)	2495	AQGRGGYYSPFDD	3697	QQYNNWPLA	Seth Zost et al., 2020 (https://www.nature.com/articles/s41591-020-0998-x)
COV2-2384	Ab	SARS-CoV2	SARS-CoV1		SARS-CoV1, SARS-CoV2	S; NTD	B-cells; SARS-CoV2 Human Patient	408	QVTLKESGPVLVKPTETLTLTCTVSGFSLSNARMGVSWIRQPPGKALEWLAHIFSGDEKSYSTSLKSRLTISKDTSKSQVVLTMTNMDPLDTATYYCARTTWGTWIQAWYFDIWGRGTLVTVSS	1487	QSALTQPASVSGSPGQSITISCTGTSSDIGSYNLVSWYQQYPGKAPKLMIYEVSKRPSGVSNRFSGSKSGNTASLTISGLQAEDEADYYCCSYAGGNTFVVFGGGTKLTVL	IGHV2-26 (Human)	IGHJ2 (Human)	IGLV2-23 (Human)	IGLJ2 (Human)	2496	ARTTWGTWIQAWYFDI	3698	CSYAGGNTFVV	Seth Zost et al., 2020 (https://www.nature.com/articles/s41591-020-0998-x)
COV2-2386	Ab	SARS-CoV2	SARS-CoV1		SARS-CoV1, SARS-CoV2	S; non-RBD	B-cells; SARS-CoV2 Human Patient	409	QVQLVESGGGVVQPGRSLRLSCAASGFTFSSYGMHWVRQAPGKGLEWVAVIWFDGSNKHYADSVKGRFTISRDNSKNTLYLQMNSLRAEDTAVYYCAREGDFWSGYYTGWFDPWGQGTLVTVSS	1488	EIVMTQSPATLSVSPGERATLSCRASQSVSSNLAWYQQKPGQAPRLLIYGASTRATGIPARFSGSGSGTEFTLTISSLQSEDFAVYYCQQYNNWPRTFGQGNRVEIN	IGHV3-33 (Human)	IGHJ5 (Human)	IGKV3-15 (Human)	IGKJ1 (Human)	2497	AREGDFWSGYYTGWFDP	3699	QQYNNWPRT	Seth Zost et al., 2020 (https://www.nature.com/articles/s41591-020-0998-x)
COV2-2387	Ab	SARS-CoV1, SARS-CoV2			SARS-CoV2	S; non-RBD	B-cells; SARS-CoV2 Human Patient	410	QVQLVESGGGVVQPGRSLRLSCAASGFTFSSYGMHWVRQAPGKGLEWVAVISYDGSNKYYADSVKGRFTISRDNSKNTLYLQMNSLRAEDTAVYYCAKDLTIVVIPAAPNFDYWGQGTLVTVSS	1489	QSALTQPASVSGSPGQSITISCTGTSSDVGGYNYVSWYQQHPGKAPKLMIYDVSNRPSGVSNRFSGSRSGNTASLTISGLQAEDEADYYCSSYTSSSTPVVFGGGTKLTVL	IGHV3-30 (Human)	IGHJ4 (Human)	IGLV2-14 (Human)	IGLJ2 (Human)	2498	AKDLTIVVIPAAPNFDY	3700	SSYTSSSTPVV	Seth Zost et al., 2020 (https://www.nature.com/articles/s41591-020-0998-x)
COV2-2388	Ab	SARS-CoV1, SARS-CoV2			SARS-CoV2	S; non-RBD	B-cells; SARS-CoV2 Human Patient	411	EVQLLESGGGLVQPGGSLRLSCAASGFTFSSYAMSWVRQAPGKGLEWVSFISGTGDSTYYADSVKGRFTISRDNSKNTLYLQMNSLRAEDTAVYYCAKDQARVQDYIWGSYRSYGMDVWGLGTTVTVSS	1490	DIVMTQSPLSLPVTPGEPASISCRSSQSLLHSNGYNYLDWYLQKPGQSPHLLIYLGSNRASGVPDRFSGSGSGTDFTLKISRVEAEDVGVYYCMQALQTPRTFGQGTKVEIK	IGHV3-23 (Human)	IGHJ6 (Human)	IGKV2-28 (Human)	IGKJ1 (Human)	2499	AKDQARVQDYIWGSYRSYGMDV	3701	MQALQTPRT	Seth Zost et al., 2020 (https://www.nature.com/articles/s41591-020-0998-x)

COV2-2389	Ab	SARS-CoV2	SARS-CoV1	SARS-CoV2		S; RBD	B-cells; SARS-CoV2 Human Patient	412	EVQLVESGGGLVQPGRSLRLSCAASGFTFDDYAMHWVRQAPGKGLEWVSGISWNSGTIGYADSVKGRFIISRDNAKNSLYLQMNSLRPEDTALYYCAKDIIRQGEDGMDVWGQGTTVTVSS	1491	DIQMTQSPSSLSASVGDRVTITCRASQNIASYLNWYQQKPGKAPKLLIYAASSLQSGVPSRFSGSGSGTDFTLTISSLQPEDFATYYCQQSYSTPWTFGQGTKVEIK	IGHV3-9 (Human)	IGHJ6 (Human)	IGKV1-39 (Human)	IGKJ1 (Human)	2500	AKDIIRQGEDGMDV	3702	QQSYSTPWT	Seth Zost et al., 2020 (https://www.nature.com/articles/s41591-020-0998-x)
COV2-2391	Ab	SARS-CoV2	SARS-CoV1	SARS-CoV2		S; RBD	B-cells; SARS-CoV2 Human Patient	413	QVQLVQSGAEVKKPGASVKVSCKASGYTFGSFDINWVRQATGQGLEWMGRMNSNSGNTAYAQKFQGRVTMTRDTSTNTAYMELSSLRSEDTAMYYCARMRSGWPTHGRPDDFWGRGTLVTVSS	1492	QSVLTQAPSASGTPGQRVTISCSGSNSNIGSYTINWYQQLPGTAPKLLIYGNDQRTSGVPDRFSGSKFGTSASLAISGLQSEDENNYYCAVWDDSLNGLVFGGGTKLTVL	IGHV1-8 (Human)	IGHJ4 (Human)	IGLV1-44 (Human)	IGLJ2 (Human)	2501	ARMRSGWPTHGRPDDF	3703	AVWDDSLNGLV	Seth Zost et al., 2020 (https://www.nature.com/articles/s41591-020-0998-x)
COV2-2394	Ab	SARS-CoV2	SARS-CoV1		SARS-CoV1, SARS-CoV2	S; NTD	B-cells; SARS-CoV2 Human Patient	414	EVQLVESGGGLVKPGGSLRLSCAASGFTFSGYSMNWVRQAPGKGLEWVSSISSSSSYIYYADSVKGRFTISRDNAKNSLYLQMNSLRAEDTAVYYCARWLQLRSDYYYFGMDVWGQGTTVTVSS	1493	EIVMTQSPATLSVSPGERATLSCRASQSVSNNLAWYQHKPGQAPRLLIYGASTRATGIPARFSGSGSGTEFTLTISSLQSEDFAVYFCQQCYNWPPWTFGQGTKVEIK	IGHV3-21 (Human)	IGHJ6 (Human)	IGKV3-15 (Human)	IGKJ1 (Human)	2502	ARWLQLRSDYYYFGMDV	3704	QQCYNWPPWT	Seth Zost et al., 2020 (https://www.nature.com/articles/s41591-020-0998-x)
COV2-2397	Ab	SARS-CoV1, SARS-CoV2			SARS-CoV2	S; non-RBD	B-cells; SARS-CoV2 Human Patient	415	EVQLVESGGGLVQPGGSLRLSCVASGFTFSFYWMSWVRQAPGKGLEWVANIKQDGGEKYYVDSVKGRFTISRDNAKNSLYLQMNSLRAEDTAVYYCARLSGSSWDFDYWGQGTLVTVSS	1494	SYELTQPPSVSVSPGQTASITCSGDKLGDKYACWYQQRPGQSPVLVIYQDSKRPSGIPERFSGSNSGNTATLTISGTQAMDEADYYCQAWDSSTGVFGTGTKVTVL	IGHV3-7 (Human)	IGHJ4 (Human)	IGLV3-1 (Human)	IGLJ1 (Human)	2503	ARLSGSSWDFDY	3705	QAWDSSTGV	Seth Zost et al., 2020 (https://www.nature.com/articles/s41591-020-0998-x)
COV2-2399	Ab	SARS-CoV2	SARS-CoV1		SARS-CoV1, SARS-CoV2	S; RBD	B-cells; SARS-CoV2 Human Patient	416	EVQLVESGGGLVQPGGSLRLSCAASGFSVSTNYMSWVRQAPGKGLEWVSVIYSGGSTFYADSVKGRFTISRDNSKNTLYLQMNSLRAEDTAVYYCARDYRDWIWGQGTLVTVSS	1495	DIQMTQSPSSLSASVGDRVTITCQASQDISKYLNWYQQKPGKAPKLLIYDASNLERGVPSRFSGSGSGTDFTFTISSLQAEDIATYYCQQYHNLPRTFGQGTKVEIK	IGHV3-66 (Human)	IGHJ4 (Human)	IGKV1-33 (Human)	IGKJ1 (Human)	2504	ARDYRDWI	3706	QQYHNLPRT	Seth Zost et al., 2020 (https://www.nature.com/articles/s41591-020-0998-x)
COV2-2400	Ab	SARS-CoV2	SARS-CoV1		SARS-CoV1, SARS-CoV2	S; non-RBD	B-cells; SARS-CoV2 Human Patient	417	QITLKESGPTLVKPTQTLTLTCTFSGFSLSTSGVGVGWIRQPPGKALEWLALIYWDDDKRYSPSLKSRLTITKDTSKNQVVLTMTNMDPVDTATYYCAHNRFQYCSSTTCYTLLPFDYWGQGTLVTVSS	1496	DIQLTQSPSFLSASVRDRVTITCRASQGISSYLAWYQQKPGKAPKLLIYAASTLQSGVPSRFSGSGSGTEFTLTISSLQPEDFATYYCQQLNSYPFTFGPGTKVDIK	IGHV2-5 (Human)	IGHJ4 (Human)	IGKV1-9 (Human)	IGKJ3 (Human)	2505	AHNRFQYCSSTTCYTLLPFDY	3707	QQLNSYPFT	Seth Zost et al., 2020 (https://www.nature.com/articles/s41591-020-0998-x)
COV2-2401	Ab	SARS-CoV1, SARS-CoV2			SARS-CoV2	S; non-RBD	B-cells; SARS-CoV2 Human Patient	418	QVQLVESGGGVVQPGRSLRLSCAASGFTFSSYALFWVRQAPGKGLEWVAVISYDGNNKYYADSVRGRFTISRDNSKNTLYLQMNSLRPEDTAVYYCARPYTGSYKSYMDVWGKGTTVTVSS	1497	DIVMTQSPDSLAVSLGERATINCKSSQSVLYSSNNKNSLAWYQQKPGQPPKLLIYWASTRESGVPDRFSGSGSGTDFTLTISSLQAEDVAVYYCQQYYSISWTFGQGTKVEIK	IGHV3-30 (Human)	IGHJ6 (Human)	IGKV4-1 (Human)	IGKJ1 (Human)	2506	ARPYTGSYKSYMDV	3708	QQYYSISWT	Seth Zost et al., 2020 (https://www.nature.com/articles/s41591-020-0998-x)
COV2-2403	Ab	SARS-CoV1, SARS-CoV2			SARS-CoV2	S; non-RBD	B-cells; SARS-CoV2 Human Patient	419	QVQLVESGGGVVQPGRSLRLSCAASGFTFSSYAMHWVRQAPGKGLEWVAVISYDGSNKYYADSVKGRFTISRDNSKNTLYLQMSSLRAEDTAVFYCARGDGDVYNFLLVRNWFDPWGQGTLVTVSS	1498	QSALTQPASVSGSPGQSITISCTGTSSDVGGYNYVSWYQQHPGKAPKLMIYDVGNRPSGVSNRFSGSKSGNTASLTISGLQAEDEADYYCSSYTSSSTLYVFGTGTKVTVL	IGHV3-30 (Human)	IGHJ5 (Human)	IGLV2-14 (Human)	IGLJ1 (Human)	2507	ARGDGDVYNFLLVRNWFDP	3709	SSYTSSSTLYV	Seth Zost et al., 2020 (https://www.nature.com/articles/s41591-020-0998-x)
COV2-2405	Ab	SARS-CoV2	SARS-CoV1		SARS-CoV1, SARS-CoV2	S; NTD	B-cells; SARS-CoV2 Human Patient	420	QLQLQESGPGLVKPSETLSLTCTVSGGSISSSSYYWGWIRQPPGKGLEWIGSFYYSGSTYYNPSLKSRVTISVDTSKNQFSLNLSSVTAADTAVYSCASLWFGDLYSFDYWGQGTLVTVSS	1499	DIQMTQSPSSLSASVGDRVTFTCRASQGISNYLAWYQQKPGKVPKLLIYAASTLQSGVPSRFSGIGSGTDFTLTISSLQPEDVATYYCQKYNSAPWTFGQGTKVEIK	IGHV4-39 (Human)	IGHJ4 (Human)	IGKV1-27 (Human)	IGKJ1 (Human)	2508	ASLWFGDLYSFDY	3710	QKYNSAPWT	Seth Zost et al., 2020 (https://www.nature.com/articles/s41591-020-0998-x)
COV2-2406	Ab	SARS-CoV1, SARS-CoV2			SARS-CoV2	S; non-RBD	B-cells; SARS-CoV2 Human Patient	421	EVQLVESGGGLVQPGGSLRLSCADSAFTFSSFWMSWVRQAPGKGLEWVANIKQDGSEKFYLDSVKGRFTISRDNAKNSLYLQMNSLRAEDTAVYYCARLGRSSWNFDYWGQGTLVTVSS	1500	SYELTQPPSVSVSPGQTASITCSGDKLGDKFVCWYQQKPGQSPVLVIYQDNKRPSGIPERFSGSNSGNTATLTISGTQALDEADYYCQAWDSSTGVFGGGTKLTVL	IGHV3-7 (Human)	IGHJ4 (Human)	IGLV3-1 (Human)	IGLJ2 (Human)	2509	ARLGRSSWNFDY	3711	QAWDSSTGV	Seth Zost et al., 2020 (https://www.nature.com/articles/s41591-020-0998-x)
COV2-2408	Ab	SARS-CoV1, SARS-CoV2			SARS-CoV2	S; non-RBD	B-cells; SARS-CoV2 Human Patient	422	QVQLQESGPGLVKPSQTLSLTCTVSGDSISSGSYYWSWIRQPAGKGLEWIGRIYTSGSTTYNPSLKSRVTISVNTSKNQFSLNLSSVTAADTAVYYCARVGGISPYYYYYYMDVWGKGTTVTVSS	1501	DIQLTQSPSFLSASVGDRVTITCRASQGISSYLAWYQQKPGKAPKLLMYAASTLQSGVPSRFSGSGSGTEFTLTINTLQPEDFATYYCQQLNSYPITFGQGTRLEIK	IGHV4-61 (Human)	IGHJ6 (Human)	IGKV1-9 (Human)	IGKJ5 (Human)	2510	ARVGGISPYYYYYMDV	3712	QQLNSYPIT	Seth Zost et al., 2020 (https://www.nature.com/articles/s41591-020-0998-x)
COV2-2413	Ab	SARS-CoV2	SARS-CoV1	SARS-CoV2 (weak)		S; RBD	B-cells; SARS-CoV2 Human Patient	423	QVQLVQSGAEVKKPGASVKVSCKASGYTFTSYDINWVRQATGQGLEWMGWMNPNSGNAGYGQKFQGRVTMTRNTSISTAYMELSSLRSEDTAVYYCARMRSGWPTHGRPDDYWGRGTLVTVSS	1502	QSVLTQPPSASGTPGQRVTFSCSGSNSNIGSYTVNWYQQLPGTAPKLLIYDNNQRPSGVPDRFSGSKSGTSASLAISGLQSEDEADYYCAVWDDSLNGLVFGGGTKLTVL	IGHV1-8 (Human)	IGHJ4 (Human)	IGLV1-44 (Human)	IGLJ3 (Human)	2511	ARMRSGWPTHGRPDDY	3713	AVWDDSLNGLV	Seth Zost et al., 2020 (https://www.nature.com/articles/s41591-020-0998-x)
COV2-2416	Ab	SARS-CoV2	SARS-CoV1		SARS-CoV1, SARS-CoV2	S; RBD	B-cells; SARS-CoV2 Human Patient	424	QVQLQESGPGLVKPSQTLSLTCTVSGGSISSGGYYWSWIRQHPGKGLEWIGYIYYSGSTYYNPSLKSRVTISVDTSKNQFSLKLSSVTAADTAVYYCASAKLVATISYFDYWGQGTLVTVSS	1503	QSVLTQPPSVSEAPRQRVTISCSGSSSNIGNNAVNWYQQLPGKAPKLLIYYDDLLPSGVSDRFSGSKSGTSASLAISGLQSEDEADYYCAAWDDSLNGVVFGGGTKLTVL	IGHV4-31 (Human)	IGHJ4 (Human)	IGLV1-36 (Human)	IGLJ2 (Human)	2512	ASAKLVATISYFDY	3714	AAWDDSLNGVV	Seth Zost et al., 2020 (https://www.nature.com/articles/s41591-020-0998-x)
COV2-2417	Ab	SARS-CoV1, SARS-CoV2			SARS-CoV2	S; RBD	B-cells; SARS-CoV2 Human Patient	425	QVQLQQWGAGLLKPSETLSLTCAVYGGSFSGYYWNWLRQPPGKGLEWIGEINHSGSTNYNPSLKSRVTISVDTSKNQFSLKLSSVTAADTAVYYCARVGGYYYYYMDVWGKGTTVTVSS	1504	DIQMTQSPSSLSASVGDRVTITCRASQSITSYLNWYQQRPGKAPKLLIYAASSLQSGVPSRFSGSGSGTDFTLSISSLQPEDFATYYCQQSYTTLLTFGGGTKVEIK	IGHV4-34 (Human)	IGHJ6 (Human)	IGKV1-39 (Human)	IGKJ4 (Human)	2513	ARVGGYYYYYMDV	3715	QQSYTTLLT	Seth Zost et al., 2020 (https://www.nature.com/articles/s41591-020-0998-x)

COV2-2418	Ab	SARS-CoV2	SARS-CoV1		SARS-CoV1, SARS-CoV2	S; non-RBD	B-cells; SARS-CoV2 Human Patient	426	EVRLLESGGGLVQPGGSLRLSCAASGFTFSDYAMNWVRQAPGKGLEWVSAISATGGSTFYADSVKGRFSISRDNSKNSLVLQMNSLRAEDTAVYYCAKPYGMDVWGQGTTVTVSS	1505	QSALTQPASVSGSPGQSITISCTGTSSDVGGYNFVSWHQQHPGKAPKNMIYDVSKRPSGVSNRFSGSKSGNTASLTISGLHTEDEADYYCSSYTSTSTPWVFGGGTKLTVL	IGHV3-23 (Human)	IGHJ6 (Human)	IGLV2-14 (Human)	IGLJ3 (Human)	2514	AKPYGMDV	3716	SSYTSTSTPWV	Seth Zost et al., 2020 (https://www.nature.com/articles/s41591-020-0998-x)
COV2-2420	Ab	SARS-CoV2	SARS-CoV1		SARS-CoV1, SARS-CoV2	S; non-RBD	B-cells; SARS-CoV2 Human Patient	427	QGQLVQSGGDVVQPGKSLRLSCAASGFTFTNYAMHWVRQAPGKGLEWVAVISNDGSNEKYVDSVKGRFSLSRDNSKNTVYLDMHSLRPEDTAIYYCARDRSNLERLVMTFGGIIAGAFDIWGQGARVTVSS	1506	EIVMTQSPGTLSVSPGERATLSCRASQSLSSHLAWYQQKPGQAPRLLIYGVSTRATGIPARFSGSGSGTEFTLAISSLQSEDSAVYYCQQYHVWPPITFGQGTRLEIK	IGHV3-30 (Human)	IGHJ3 (Human)	IGKV3-15 (Human)	IGKJ5 (Human)	2515	ARDRSNLERLVMTFGGIIAGAFDI	3717	QQYHVWPPIT	Seth Zost et al., 2020 (https://www.nature.com/articles/s41591-020-0998-x)
COV2-2422	Ab	SARS-CoV1, SARS-CoV2			SARS-CoV2	S; non-RBD	B-cells; SARS-CoV2 Human Patient	428	QVQLVESGGGVVQPGRSLRLSCAASGFTFSSYAMYWVRQAPGKGLEWVAVISYDGINKYYADSVKGRFTISRDNSKNTLYLQMNSLRAEDTAVYYCARVNSGSYYSYFDYWGQGTLVTVSS	1507	DIVMTQSPDSLAVSLGERATINCKSSQSVLYSSNNKNYLAWYQQKPGQPPKLLIYWASTRESGVPDRFSGSGSGTDFTLTISSLQAEDVAVYYCQQYYSTPLTFGQGTKVEIK	IGHV3-30 (Human)	IGHJ4 (Human)	IGKV4-1 (Human)	IGKJ1 (Human)	2516	ARVNSGSYYSYFDY	3718	QQYYSTPLT	Seth Zost et al., 2020 (https://www.nature.com/articles/s41591-020-0998-x)
COV2-2427	Ab	SARS-CoV2	SARS-CoV1		SARS-CoV1, SARS-CoV2	S; non-RBD	B-cells; SARS-CoV2 Human Patient	429	QVQLQESGPGLVKPSGTLSLTCAVSGGSISSSNWWSWVRQPPGKGLEWIGEIYHSGSTNYNPSLKSRVTISVDKSKNQFSLKLNSVTAADTAVYYCASRWGDYFDSSGAYDSWGQGTLLTVSS	1508	DIQMTQSPSSVSASVGDRVTITCRASQGISSWLAWYQQKPGKAPKLLIYAASSLQSGVPSRFSGSGSGTDFTLTITSLQPEDFATYYCQQGNSFPLTFGGGTKVEIK	IGHV4-4 (Human)	IGHJ4 (Human)	IGKV1-12 (Human)	IGKJ4 (Human)	2517	ASRWGDYFDSSGAYDS	3719	QQGNSFPLT	Seth Zost et al., 2020 (https://www.nature.com/articles/s41591-020-0998-x)
COV2-2428	Ab	SARS-CoV2	SARS-CoV1		SARS-CoV1, SARS-CoV2	S; non-RBD	B-cells; SARS-CoV2 Human Patient	430	QVQLVESGGGVVQPGKSLRLSCAASGFTFSSYGMHWVRQAPGKGLEWVAVIWYDGNNKFYVDSVKGRFTISRDNSKNTLYMEMNSLRAEDTAVYYCARKGPLWRFDYWGQGTLVTVSS	1509	QSVLTQPPSVSGAPGQRVTISCTGSSSNIGAGYDVHWYQQIPGTAPKLLFYGNNNRPSGVPDRFSDSKSGTSASLAITGLQAEDEADYYCQSYDSSLSAWVFGGGTKLTVL	IGHV3-33 (Human)	IGHJ4 (Human)	IGLV1-40 (Human)	IGLJ3 (Human)	2518	ARKGPLWRFDY	3720	QSYDSSLSAWV	Seth Zost et al., 2020 (https://www.nature.com/articles/s41591-020-0998-x)
COV2-2429	Ab	SARS-CoV1, SARS-CoV2			SARS-CoV2	S; non-RBD	B-cells; SARS-CoV2 Human Patient	431	EVQLVESGGGLIQPGGSLRLSCAASGFIVSSNYMSWVRQAPGKGLEWVSVIYSGGSTYYADSVKGRFTISRDNSKNTLYLQMNSLRAEDTAVYYCARESTQWGQGTLVTVSS	1510	DIQMTQSPSTLSASVGDRVTITCRASHSISSWLAWYQQKPGKAPKLLIYKASSLESGVPSRFSGSGSGTEFTLTISSLQPDDFATYYCQQYNTYSQTFGQGTKVEIK	IGHV3-53 (Human)	IGHJ4 (Human)	IGKV1-5 (Human)	IGKJ1 (Human)	2519	ARESTQ	3721	QQYNTYSQT	Seth Zost et al., 2020 (https://www.nature.com/articles/s41591-020-0998-x)
COV2-2430	Ab	SARS-CoV1, SARS-CoV2			SARS-CoV2	S; non-RBD	B-cells; SARS-CoV2 Human Patient	432	QLQLQESGPGLVKPSETLSLTCTVSGGSISSSSYYWGWIRQPPGKGLEWIGSVYYIGSTYYNPSLKSRVTMSVDTSKNQFSLKLSSVTAADTAVYYCARAPFQLLDKYYFFYYMDVWGKGTTVTVSS	1511	EIVLTQSPATLSLSPGERATLSCRASQSVSSYLAWYQQKPGQAPRLLIYDASNRATGIPARFSGSGSGTDFTLTISSLEPEDFAVYYCQQRSNWPPGVTFGQGTRLEIK	IGHV4-39 (Human)	IGHJ6 (Human)	IGKV3-11 (Human)	IGKJ5 (Human)	2520	ARAPFQLLDKYYFFYYMDV	3722	QQRSNWPPGVT	Seth Zost et al., 2020 (https://www.nature.com/articles/s41591-020-0998-x)
COV2-2434	Ab	SARS-CoV2	SARS-CoV1		SARS-CoV1, SARS-CoV2	S; RBD	B-cells; SARS-CoV2 Human Patient	433	EVQLVESGGDLIQPGGSLRLSCAASGLTVSSNYMSWVRQAPGKGLEWVSIIYSGGSTYYADSVKGRFSISRDNSNNTLYLQMNSLRAEDTAVYFCARHIPAWGYKWGQGTLVTVSS	1512	DIQMTQSPSSLSASVGDRVTITCQASQDIRNYLNWYQQKPGKAPELLIYDASNLETGVPSRFSGSGSGTDFIFTISSLQPEDIATYYCHQYDYLPYTFGQGTKLDIK	IGHV3-53 (Human)	IGHJ4 (Human)	IGKV1-33 (Human)	IGKJ2 (Human)	2521	ARHIPAWGYK	3723	HQYDYLPYT	Seth Zost et al., 2020 (https://www.nature.com/articles/s41591-020-0998-x)
COV2-2438	Ab	SARS-CoV2	SARS-CoV1		SARS-CoV1, SARS-CoV2	S; NTD	B-cells; SARS-CoV2 Human Patient	434	EVQLLESGGGLVQPGGSLRLSCAASGFTFSYGMSWVRQAPGKGLEWVSAISISGGSTYYADSVKGRFTISRDNSKNTLYLQMNSLRAEDTAVYYCAKLLGSGITLDNDAFDIWGQGTMVTVSS	1513	DIQMTQSPSSLSASVGDRVTITCRASQSISSYLNWYQQKPGKAPKLLIYAATSLQSGVPSRFSGSGSGTDFTLTISSLQPEDFATYYCQQTYSTPLYTFGQGTKLEIK	IGHV3-23 (Human)	IGHJ3 (Human)	IGKV1-39 (Human)	IGKJ2 (Human)	2522	AKLLGSGITLDNDAFDI	3724	QQTYSTPLYT	Seth Zost et al., 2020 (https://www.nature.com/articles/s41591-020-0998-x)
COV2-2441	Ab	SARS-CoV1, SARS-CoV2			SARS-CoV2	S; non-RBD	B-cells; SARS-CoV2 Human Patient	435	QVQLVQSGAEVKKPGSSVKVSCKASGGTFSSYAIIWVRQAPGQGLEWMGGIIPIFGTTNYAQKFQGRVTITADESTSTAYVELSSLRSEDTAVYYCARIGHFDSSGTDFTLTISSLEPEDFAVYYCQHRTNWPPLFTFGPGTKVDIK	1514	EIVLTQSPATLSLSPGERATLSCRASQSVSSFLAWYQQKPGQAPRLLIYDASNRPTGIPARFTGSGSGTDFTLTISSLEPEDFAVYYCQHRTNWPPLFTFGPGTKVDIK	IGHV1-69 (Human)	IGHJ4 (Human)	IGKV3-11 (Human)	IGKJ3 (Human)	2523	ARIGHFDSSGYYLDY	3725	QHRTNWPPLFT	Seth Zost et al., 2020 (https://www.nature.com/articles/s41591-020-0998-x)
COV2-2444	Ab	SARS-CoV2	SARS-CoV1		SARS-CoV1, SARS-CoV2	S; NTD	B-cells; SARS-CoV2 Human Patient	436	EVQLLESGGGLVQPGGSLRLSCAASGFTFSYAMNWVRQAPGKGLEWVSAISVSGGSTYYADSVKGRFTISRDNSKNTLYLQMNSLRAEDTAVYYCAKDFGSGIVGATGFDFWGQGTLVTVSS	1515	SYELTQPPSVSVSPGQTARITCSGDALPNQYAYWYQQKPGQAPVLVMCKDSERPSGIPERFSGSSSGTTVTLTISGVQAEDEADYYCQSADSSGTYVVFGGGTKLTVL	IGHV3-23 (Human)	IGHJ4 (Human)	IGLV3-25 (Human)	IGLJ2 (Human)	2524	AKDFGSGIVGATGFDF	3726	QSADSSGTYVV	Seth Zost et al., 2020 (https://www.nature.com/articles/s41591-020-0998-x)
COV2-2445	Ab	SARS-CoV2	SARS-CoV1		SARS-CoV1, SARS-CoV2	S; non-RBD	B-cells; SARS-CoV2 Human Patient	437	EVQLVESGGGVVRPGGSLRLSCAASGFTFDDYGMSWVRQAPGKGLEWVSAINWNGGSTGYADSVKGRFTISRDNAKNSLYLQMNSLRAEDTALYHCARRRSSSRYSSGWYMYYYYMDVWGKGTTVTVSS	1516	DIQMTQSPSTLSASVGDRVTITCRASQSVSTWLAWYQQKPGKAPNLLIYEASSLESGVPSRFSGSGSGTEFTLTISSLQPDDFATYYCQQYNTYSGTFGQGTKVEIK	IGHV3-20 (Human)	IGHJ6 (Human)	IGKV1-5 (Human)	IGKJ1 (Human)	2525	ARRRSSSRYSSGWYMYYYYMDV	3727	QQYNTYSGT	Seth Zost et al., 2020 (https://www.nature.com/articles/s41591-020-0998-x)
COV2-2446	Ab	SARS-CoV2	SARS-CoV1		SARS-CoV1, SARS-CoV2	S; non-RBD	B-cells; SARS-CoV2 Human Patient	438	EVQLVQSGAEVKKPGESLKISCKGSGYSFTNSWIGWVRQMPGKGLEWMGIIYPGDSDTRYSPSFQGQVTISADKSISTAYLQWSSLKASDTAIYYCATHRCSGGFCYLAYWGQGTLVTVSS	1517	QPVLTQPPSASASLGASVTLTCTLSSGYSNYKVDWYQQRPGKGPRFVMRVGTGGIVGSKGDGIPDRFSVLGSGLNRYLTIKNIQEEDESDYHCGADHGSGSNFVFVFGGGTKLTVL	IGHV5-51 (Human)	IGHJ4 (Human)	IGLV9-49 (Human)	IGLJ2 (Human)	2526	ATHRCSGGFCYLAY	3728	GADHGSGSNFVFVV	Seth Zost et al., 2020 (https://www.nature.com/articles/s41591-020-0998-x)
COV2-2449	Ab	SARS-CoV1, SARS-CoV2			SARS-CoV2	S; non-RBD	B-cells; SARS-CoV2 Human Patient	439	QVQLVESGGGVVQPGRSLRLSCATSGFTFSSFALHWVRQAPGKGLEWVTVISDDGNNKYYVDSVKGRFTISRDNSKNTLFLQMNSLRVEDTAIYYCARASYNSNWSIGEYFRDWGQGTLVTVSS	1518	DIVMTQSPDSLAVSLGERATINCKSSQSLLYTSNNKNYLAWYQQKPGQPPKLLIYWASTRESGVPDRFSGSGSGTDFTLTISSLQAEDVAVYYCQQYYSPPWTFGQGTKVEIK	IGHV3-30 (Human)	IGHJ1 (Human)	IGKV4-1 (Human)	IGKJ1 (Human)	2527	ARASYNSNWSIGEYFRD	3729	QQYYSPPWT	Seth Zost et al., 2020 (https://www.nature.com/articles/s41591-020-0998-x)

COV2-2450	Ab	SARS-CoV1, SARS-CoV2			SARS-CoV2	S; RBD	B-cells; SARS-CoV2 Human Patient	440	QVQLVESGGGVVQPGRSLRLSCAASGFTFSTYGMHWVRQAPGKGLEWVAVILYDGSNRYYADSVKGRFTISRDNSKNTLYLQMNSLRAEDTAVYYCAKQGGLYCSGTNCWGGYLDYWGQGTLVTVSS	1519	DIQMTQSPSSLSASVGDRVTITCQASQDISNYLHWYQQKPGKAPKLLIYDASNLETGVPSRFSGSGSGTDFTFTISSLQPEDIATYYCQQYHNLPPITFGQGTRLEIK	IGHV3-30 (Human)	IGHJ4 (Human)	IGKV1-33 (Human)	IGKJ5 (Human)	2528	AKQGGLYCSGTNCWGGYLDY	3730	QQYHNLPPIT	Seth Zost et al., 2020 (https://www.nature.com/articles/s41591-020-0998-x)
COV2-2451	Ab	SARS-CoV2	SARS-CoV1		SARS-CoV1, SARS-CoV2	S; non-RBD	B-cells; SARS-CoV2 Human Patient	441	QITLKESGPTLVKPTQTLTLTCTVSGFSLSTSGVGVGCIRQPPGKALEWLALIYWDDDKRYSPSLKSRLTITRDTSKNQVVLTMTNMDPVDTGTYFCVHRHVSGAFDYWGQGTLVTVSS	1520	SYELTQPPSVSVSPGQTASITCSGDKLGETYVSWYQQKPGQSPVLVIYEDSKRPSGIPERFSGSNSGNTATLTISGTQAMDEADYYCQAWDSSTGGVFGTGTKVTVL	IGHV2-5 (Human)	IGHJ4 (Human)	IGLV3-1 (Human)	IGLJ1 (Human)	2529	VHRHVSGAFDY	3731	QAWDSSTGGV	Seth Zost et al., 2020 (https://www.nature.com/articles/s41591-020-0998-x)
COV2-2453	Ab	SARS-CoV1, SARS-CoV2			SARS-CoV2	S; non-RBD	B-cells; SARS-CoV2 Human Patient	442	QVQLVQSGSELKKPGASVKVSCKASGYTFTSYAMNWVRQAPGQGLEWMGWINTNGNPTYAQGFTGRFVFSLDTSVNTAYLQISSLKAEDTAVYYCARARLLGYCSSTSCYTIGWGAFDIWGQGTMVTVSS	1521	DIQMTQSPSSLSASVGDRVTITCQASLDISKYLNWYQHKPGKAPNLLIYDAFNLERGVPSRFSGSGSGTDFTFTISSLQPEDIATYYCQQYDNLPPGVSTTFGQGTRLEIK	IGHV7-4-1 (Human)	IGHJ3 (Human)	IGKV1-33 (Human)	IGKJ5 (Human)	2530	ARARLLGYCSSTSCYTIGWGAFDI	3732	QQYDNLPPGVSTT	Seth Zost et al., 2020 (https://www.nature.com/articles/s41591-020-0998-x)
COV2-2454	Ab	SARS-CoV2	SARS-CoV1		SARS-CoV1, SARS-CoV2	S; non-RBD	B-cells; SARS-CoV2 Human Patient	443	QVQLVESGGGVVQPGRSLRLSCAASGFTFSSYGMHWVRQAPGKGLEWVAVIWYDGSNKYYADSVKGRFTISRDNSKNTLYLQMNSLRAEDTAVYYCAREGQGTYLDYWGQGTLVTVSS	1522	SYELTQPPSVSVSPGQTARITCSGDALPKKYAHWYQQKSGQAPVLVIYEDSKRPSGIPERFSGSSSGTMATLTISGAQVEDEADYYCCSTDSSGNQRVFGGGTKLTVL	IGHV3-33 (Human)	IGHJ4 (Human)	IGLV3-10 (Human)	IGLJ3 (Human)	2531	AREGQGTYLDY	3733	CSTDSSGNQRV	Seth Zost et al., 2020 (https://www.nature.com/articles/s41591-020-0998-x)
COV2-2455	Ab	SARS-CoV2	SARS-CoV1		SARS-CoV1, SARS-CoV2	S; NTD	B-cells; SARS-CoV2 Human Patient	444	EVQLVESGGGLVQPGGSLRLSCAASGFTFSSYEMNWVRQAPGKGLEWVSYISSSGSAIYYADSVKGRFTISRDNAKNSLYLQMNSLRVEDTAVYYCAREARSRYFDWLPSYYFDYWGQGTLVTVSS	1523	QSALTQPASVSGSPGQSITISCTGTSSDIGGYNYVSWYQQHPGKAPKLLIYDVSNRPSGVSTRFSGSKSGNTASLTISGLQAEDEADYYCSSYTSSSTHVVFGGGTKLTVL	IGHV3-48 (Human)	IGHJ4 (Human)	IGLV2-14 (Human)	IGLJ2 (Human)	2532	AREARSRYFDWLPSYYFDY	3734	SSYTSSSTHVV	Seth Zost et al., 2020 (https://www.nature.com/articles/s41591-020-0998-x)
COV2-2458	Ab	SARS-CoV1, SARS-CoV2			SARS-CoV2	S; non-RBD	B-cells; SARS-CoV2 Human Patient	445	QVQLVESGGGVVQPGRSLRLSCAASGFTFSRHAMHWVRQAPGKGLEWVAVISYDGSNKYYADSVKGRFAISRDNSKNTLYLQMNSLRPEDTAVYYCARDPSPLVLITSIDYWGQGTLVTVSS	1524	SYELTQPPSVSVSPGQTARITCSGDALPRQYTYWYQQKPGQAPVLVIYKDSERPSGIPERFSGSSSGTTVTLTISGVQAEDEADYYCQSADTIGTYWVFGGGTKLTVL	IGHV3-30 (Human)	IGHJ4 (Human)	IGLV3-25 (Human)	IGLJ2 (Human)	2533	ARDPSPLVLITSIDY	3735	QSADTIGTYWV	Seth Zost et al., 2020 (https://www.nature.com/articles/s41591-020-0998-x)
COV2-2459	Ab	SARS-CoV2	SARS-CoV1		SARS-CoV1, SARS-CoV2	S; NTD	B-cells; SARS-CoV2 Human Patient	446	QLQLQESGPGLVKPSETLSLTCTVSGGSISSGTYYCGWIRQPPGKGLEWIGSTYYGGSTLYNPSLRGRVTISVDTSKNQFSLKLSSVTAADTAVYYCARRGNYYDSKNWFDPWGQGTLVTVSS	1525	EIVMTQSPATVSVSPGERATLSCRASQSVSSNLAWYQQKPGQAPRLLIYGASTRATGIPARFSASGSGTEFTLTISSLQSEDFAVYYCQQYNNWPPMYTFGQGTKVEIK	IGHV4-39 (Human)	IGHJ5 (Human)	IGKV3-15 (Human)	IGKJ2 (Human)	2534	ARRGNYYDSKNWFDP	3736	QQYNNWPPMYT	Seth Zost et al., 2020 (https://www.nature.com/articles/s41591-020-0998-x)
COV2-2461	Ab	SARS-CoV1, SARS-CoV2			SARS-CoV2	S; RBD	B-cells; SARS-CoV2 Human Patient	447	QVQLQESGPGLVKPSQTLSLTCTVSGGSISSGGYFWSWIRQHPGKGLEWIGSIYYSGSTYYNPSLRSRITISVDTSKNQFSLKLSSVTAADTAVYYCARGGSGSYSLFDYWGQGTLVTVSS	1526	DIQMTQSPSSLSASVGDRVTITCQASQDITNYLNWYQQKPGKAPKLLIYDASNLETGVPSRFSGSGSGTDFTFTISSLQPEDFATYYCQQYDNLYSVHFGQGTKLEIK	IGHV4-31 (Human)	IGHJ4 (Human)	IGKV1-33 (Human)	IGKJ2 (Human)	2535	ARGGSGSYSLFDY	3737	QQYDNLYSVH	Seth Zost et al., 2020 (https://www.nature.com/articles/s41591-020-0998-x)
COV2-2462	Ab	SARS-CoV1, SARS-CoV2			SARS-CoV2	S; RBD	B-cells; SARS-CoV2 Human Patient	448	EVQLVESGGGLVQPGGSLRLSCAASGFTFSSSDLHWVRQATGKGLEWVSAIGTAGDTYYLGSVKGRFTISRENGKNSLYLQMNSLRAGDTAVYYCARVLYDSSGFYNWFDPWGQGTLVTVSS	1527	DIQMTQSPSSLSASVGDRVTITCRASQSISSYLNWYQQKPGKAPKLLIYAASSLKSGVPSRFGGSGSGTDFTLTISSLQPEDFATYYCQQSYEMPPWTFGQGTKVEIE	IGHV3-13 (Human)	IGHJ5 (Human)	IGKV1-39 (Human)	IGKJ1 (Human)	2536	ARVLYDSSGFYNWFDP	3738	QQSYEMPPWT	Seth Zost et al., 2020 (https://www.nature.com/articles/s41591-020-0998-x)
COV2-2464	Ab	SARS-CoV1, SARS-CoV2			SARS-CoV2	S; RBD	B-cells; SARS-CoV2 Human Patient	449	QVQLQESGPGLVKPSQTLSLTCTVSGGSISSGGYYWSWIRQHPGKGLEWIGYISYSGSTYYNPSLKSRLTISVDTSKNQFSLKLSSVTAADTAVYYCARDLGDGYNLRVPAYFDLWGRGTLVTVSS	1528	SYELTQPPSVSVSPGQTARITCSGDALPNQYAYWYHQKPGQAPVVVIYKDSERPSGIPQRFSGSSSGTTVTLTISGVQAEDEADYYCQSADSSGYEADYYCQSADSSGYVFGTGTKVTVL	IGHV4-31 (Human)	IGHJ2 (Human)	IGLV3-25 (Human)	IGLJ1 (Human)	2537	ARDLGDGYNLRVPAYFDL	3739	QSADSSGYV	Seth Zost et al., 2020 (https://www.nature.com/articles/s41591-020-0998-x)
COV2-2465	Ab	SARS-CoV1, SARS-CoV2			SARS-CoV2	S; RBD	B-cells; SARS-CoV2 Human Patient	450	QVQLQESGPGLVKPSGTLSLTCAVSGGSISSSNWWSWVRQPPGKGLEWIGEIYHGGSTDYNPSLKSRVTISVDKSKNQFSLKLTSVTAADTAVYYCARVDHVNVRDYWGPGTLVTVSS	1529	QSALTQPASVSGSPGQSITISCTGTSSDVGGYNYVSWYQQHPGKAPKLMIYDVSKRPSGVSNRFSGSKSGNTASLTISGLQAEDEADYYCSSYTSSSIPYVFGTGTKVTVL	IGHV4-4 (Human)	IGHJ4 (Human)	IGLV2-14 (Human)	IGLJ1 (Human)	2538	ARVDHVNVRDY	3740	SSYTSSSIPYV	Seth Zost et al., 2020 (https://www.nature.com/articles/s41591-020-0998-x)
COV2-2466	Ab	SARS-CoV2	SARS-CoV1		SARS-CoV1, SARS-CoV2	S; NTD	B-cells; SARS-CoV2 Human Patient	451	EVQLVESGGGLVKPGGSLRLSCAASGFTFSSYSMNWVRQAPGKGLEWVSSISNSNSFIYYADSMKGRFTISRDNAKNSLYLQMNSLRAEDTAVYYCARVNGNSNWNFGSYYYYMDVWGKGTTVTVSS	1530	EIVLTQSPAILSLSPGERATLSCRASQSVSSYLAWYQQKPGQAPRLLIYDTSNRATGIPARFSGSGSGTDFTLTISSLEPEDFAFYYCQQRGNWWTFAQGTKVEIK	IGHV3-21 (Human)	IGHJ6 (Human)	IGKV3-11 (Human)	IGKJ1 (Human)	2539	ARVNGNSNWNFGSYYYYYMDV	3741	QQRGNWWT	Seth Zost et al., 2020 (https://www.nature.com/articles/s41591-020-0998-x)
COV2-2473	Ab	SARS-CoV2	SARS-CoV1		SARS-CoV1, SARS-CoV2	S; non-RBD	B-cells; SARS-CoV2 Human Patient	452	QVQLVESGGGVVQPGRSLRLSCAASGFTFSNYGMHWVRQAPGKGLEWVAVIYYDGSNKYYADSVKGRFTISRDNSKNTLYLQIHSLRAEDTAVYYCAREGQMAATTGIDYWGQGTLVTVSS	1531	SYELTQPPSVSVSPRQTARITCSGDALPKKYAYWYQQKSGQAPVLVIYEDSKRPSGIPERFSGSSSGTMATLTISGAQVEDEADYYCYSTDTSGNHWVFGGGTKLTVL	IGHV3-33 (Human)	IGHJ4 (Human)	IGLV3-10 (Human)	IGLJ3 (Human)	2540	AREGQMAATTGIDY	3742	YSTDTSGNHWV	Seth Zost et al., 2020 (https://www.nature.com/articles/s41591-020-0998-x)
COV2-2474	Ab	SARS-CoV2	SARS-CoV1		SARS-CoV1, SARS-CoV2	S; non-RBD	B-cells; SARS-CoV2 Human Patient	453	EVQLVESGGGLVKPGGSLRLSCAASGFTFSNAWMSWVRQAPGKGLEWVGRIKGKTDGGTTDYAAPVKGRFTISKDDSKNTLYLQMSSLNTEDTAVYWCTTLTYYYDSSAYLNDAFDIWGQGTMVTVSS	1532	SYELTQPPSVSVSPGQTARITCSGDALPKKYAYWYQQKSGQAPVLVISEDSKRPSGIPERFSGSSSGTVATLTISGAQVEDEADYYCYSTDSSGNHRVFGGGTKLTVL	IGHV3-15 (Human)	IGHJ3 (Human)	IGLV3-10 (Human)	IGLJ3 (Human)	2541	TTLTYYYDSSAYLNDAFDI	3743	YSTDSSGNHRV	Seth Zost et al., 2020 (https://www.nature.com/articles/s41591-020-0998-x)

WO 2022/067091
PCT/US2021/052040

COV2-2478	Ab	SARS-CoV1, SARS-CoV2			SARS-CoV2	S; non-RBD	B-cells; SARS-CoV2 Human Patient	454	EVQLVESGGGLVQPGRSLRLSCAASGFTFDDYAMHWVRQAPGKGLEWVSGISWNSDNIGYADSVKGRFTISRDIAKNSLYLQMNSLRAEDTALYYCAKGIYYDIFMPLLDWGRGTLVTVSS	1533	EIVLTQSPGTLSLSPGERATLSCRASQSVSSTFLAWYQQKPGQAPRLLIFGASSRATGIPDRFSGSGSGTDFTLTISRLEPEDFAVYYCHQYGTSPYTFGQGTKLEIK	IGHV3-9 (Human)	IGHJ4 (Human)	IGKV3-20 (Human)	IGKJ2 (Human)	2542	AKGIYYDIFMPLLD	3744	HQYGTSPYT	Seth Zost et al., 2020 (https://www.nature.com/articles/s41591-020-0998-x)
COV2-2479	Ab	SARS-CoV2	SARS-CoV1	SARS-CoV2		S; RBD	B-cells; SARS-CoV2 Human Patient	455	QVQLVQSGAEVKKPGSSVKVSCKTSGDTSSSYTVGWVRQAPGQGLEWMGRIIPILGIAYSAQKFQGRLTITADKSTSTSYMELSSLRSEDTAVYYCARGVVAATPGWFDPWGQGTLVTVSS	1534	EIVMTQSPATLSVSPGERVTLSCRASQSVSSNLAWYQQKPGQAPRLLIYGASTRATGIPARFSGGGSGTEFTLTISSLQSEDFAVYYCQQYNNFLTFGGGTKVEIK	IGHV1-69 (Human)	IGHJ5 (Human)	IGKV3-15 (Human)	IGKJ4 (Human)	2543	ARGVVAATPGWFDP	3745	QQYNNFLT	Seth Zost et al., 2020 (https://www.nature.com/articles/s41591-020-0998-x)
COV2-2481	Ab	SARS-CoV1, SARS-CoV2			SARS-CoV2	S; non-RBD	B-cells; SARS-CoV2 Human Patient	456	QVQLVQSGAEVKKPGSSVKVSCKASGGTFGSYVISWVRQAPGQGLQWMGGIIPIFGKPNYAQKFQGRVTITADESTSTAYMELSSLRSEDTAVYYCARGWFGELLKGTYWFDPWGQGTLVTVSS	1535	DIVMTQSPDSLAVSLGERATINCKSSQSVLYSSNNKNYLAWYQQKPGQPPKLLIYWASTRESGVPDRFSGSGSGTDFTLTISSLQAEDVAVYYCQQYYSTPGFGQGTKLEIK	IGHV1-69 (Human)	IGHJ5 (Human)	IGKV4-1 (Human)	IGKJ2 (Human)	2544	ARGWFGELLKGTYWFDP	3746	QQYYSTPG	Seth Zost et al., 2020 (https://www.nature.com/articles/s41591-020-0998-x)
COV2-2485	Ab	SARS-CoV2	SARS-CoV1	SARS-CoV2 (weak)		S; RBD	B-cells; SARS-CoV2 Human Patient	457	QVQLVQSGAEVKKPGSSVKVSCKASGGTFSSYSITWVRQAPGQGLEWMGRIIPVLGIANYAQKFQDRVTITADKSTSTAYMELSSLRSEDTAVYYCARVGVSGFKSGSNWYFDLWGRGTLVTVSS	1536	QSVLTQPPSVSGAPGQRVTLSCTGSNSNIGAGYDVHWYQQLPGTAPKLLIYGNSNRPSGVPDRFSGSKSGTSASLAITGLQAEDEADYYCQSYDSSLSDSVFGGGTKVTVL	IGHV1-69 (Human)	IGHJ2 (Human)	IGLV1-40 (Human)	IGLJ3 (Human)	2545	ARVGVSGFKSGSNWYFDL	3747	QSYDSSLSDSV	Seth Zost et al., 2020 (https://www.nature.com/articles/s41591-020-0998-x)
COV2-2488	Ab	SARS-CoV2	SARS-CoV1		SARS-CoV1, SARS-CoV2	S; non-RBD	B-cells; SARS-CoV2 Human Patient	458	EVQLVESGGGLVQPGGSLRLSCAVSGFTFSSYWMHWVRQAPGKGLVWVSRINSDGSSTSYADSVKGRFTISRDNAKNTLYLQMNSLRAEDTAVYYCAREVEQLAHMVDYWGQGTLVTVSS	1537	SYELTQPPSVSVSPGQTARITCSGDALPNQYAYWYQQKPGQAPVLVIYKDSERPSGIPERFSGSSSGTTVTLTISGVQAEDEADYYCQSADSSGTSWVFGGGTKLTVL	IGHV3-74 (Human)	IGHJ4 (Human)	IGLV3-25 (Human)	IGLJ3 (Human)	2546	AREVEQLAHMVDY	3748	QSADSSGTSWV	Seth Zost et al., 2020 (https://www.nature.com/articles/s41591-020-0998-x)
COV2-2489	Ab	SARS-CoV2	SARS-CoV1	SARS-CoV2 (weak)		S; NTD	B-cells; SARS-CoV2 Human Patient	459	QLQLQESGPGLVKPSETLSLTCTVSGGSISSSTTYYWGWIRQPPGKGLEWIASIYYSGSTYYNPSLKSRLTVSVDTSKNQFSLKLSSVTAADTAVYYCARQWKWFGEAWYFDLWGRGTLVTVSS	1538	EIVLTQSPGTLSLSPGERASLSCRASQSVSSSYLAWYQQKPGQAPRLLIYGASSRATGIPDRFSGSGSGTDFTLTISRLEPEDFAVYYCQQYGSSPFTFGGGTKVEIK	IGHV4-39 (Human)	IGHJ2 (Human)	IGKV3-20 (Human)	IGKJ4 (Human)	2547	ARQWKWFGEAWYFDL	3749	QQYGSSPFT	Seth Zost et al., 2020 (https://www.nature.com/articles/s41591-020-0998-x)
COV2-2490	Ab	SARS-CoV2	SARS-CoV1		SARS-CoV1, SARS-CoV2	S; NTD	B-cells; SARS-CoV2 Human Patient	460	EVQLVESGGGLVQPGGSLRLSCAASGFTFSSYWMNWVRQAPGKGLEWVANINQDGGEKYYVDSVRGRFTISRDNAKNSLYLQMNSLRAEDTAVYYCARDPYDLYGDYGGTFDYWGQGTLVTVSS	1539	DIQMTQSPSTLSASVGDRVTITCRASQSISSWLAWYQQKPRKAPKLLIYKASTLESGVPSRFSGSGSGTEFTLTISSLQPDDFATYYCQQYNSYSLTFGGGTKVEIK	IGHV3-7 (Human)	IGHJ4 (Human)	IGKV1-5 (Human)	IGKJ4 (Human)	2548	ARDPYDLYGDYGGTFDY	3750	QQYNSYSLT	Seth Zost et al., 2020 (https://www.nature.com/articles/s41591-020-0998-x)
COV2-2495	Ab	SARS-CoV2	SARS-CoV1		SARS-CoV1, SARS-CoV2	S; NTD	B-cells; SARS-CoV2 Human Patient	461	QVQLVQSGAAVKKPGSSVKVSCKASGGTFSSYAISWVRQAPGQGLEWMGGIVPIFGTANYAQKFQGRVTITADESTTAYMELNSLRSEDTAVYYCAREDYYGSGSLVDPYYYYRMDVWGQGTTVTVSS	1540	EIVLTQSPATLSVSPGERATLSCRASQSVSSNLAWYQQKPGQAPRLLIYGASTRATGIPARFSGSGSGTEFTLTISSLQSEDFALYYCQQYNNWWRTFGQGTKVEIN	IGHV1-69 (Human)	IGHJ6 (Human)	IGKV3-15 (Human)	IGKJ1 (Human)	2549	AREDYYGSGSLVDPYYYYRMDV	3751	QQYNNWWRT	Seth Zost et al., 2020 (https://www.nature.com/articles/s41591-020-0998-x)
COV2-2496	Ab	SARS-CoV2	SARS-CoV1		SARS-CoV1, SARS-CoV2	S; non-RBD	B-cells; SARS-CoV2 Human Patient	462	QVQLVESGGGVVQPGRSLRLSCAASGFTFSNYGMHWVRQAPGKGLEWVAVIWYDGSNKYYADSVKGRFTISRDNSKNTLYLQMNSLRAEDTAVYYCVRDLALFEVVIQQGVWGQGTLVTVSS	1541	SYELTQPPSVSVSPGQTARITCSGDALPKKYAYWYQQKSGQAPVLVIYEDSKRPSGIPERFSGSSSGTMATLTISGAQVEDEADYYCYSTDSSGNHWVFGGGTKLTVL	IGHV3-33 (Human)	IGHJ4 (Human)	IGLV3-10 (Human)	IGLJ3 (Human)	2550	VRDLALFEVVIQQGV	3752	YSTDSSGNHWV	Seth Zost et al., 2020 (https://www.nature.com/articles/s41591-020-0998-x)
COV2-2499	Ab	SARS-CoV2	SARS-CoV1	SARS-CoV2		S; RBD	B-cells; SARS-CoV2 Human Patient	463	QLQLQESGPGLVKPSETLSLTCTVSGGSVSSRSYYWGWIRQPPGKGLEWIGSIYYSGSTYYNPSLKSRVTISVDTSKNQFSLKLSSVTAADTAVYYCARHTVDCGGDCFPNDAFDIWGQGTMVTVSS	1542	SSELTQDPAVSVALGQTVRITCQGDSLRSYYASWYQQKPGQAPLVIYGKNNRPSGIPDRFSGSSSGNTPSLTITGAQAEDEADYYCNFRDSSGHHPVFGEGTKLTVL	IGHV4-39 (Human)	IGHJ3 (Human)	IGLV3-19 (Human)	IGLJ2 (Human)	2551	ARHTVDCGGDCFPNDAFDI	3753	NFRDSSGHHPV	Seth Zost et al., 2020 (https://www.nature.com/articles/s41591-020-0998-x)
COV2-2504	Ab	SARS-CoV2	SARS-CoV1	SARS-CoV2		S; RBD	B-cells; SARS-CoV2 Human Patient	464	QVQLVQSGAEVKKPGASVKVSCKASGYTFTDYYMHWVRQAPGQGLEWMGWINPNSRGTNYAQKFQGRVTMTRDTSISTVYMELSRLTSDDTAVYYCARVVLGYGRPNNYYDGRNVWDYWGQGTLVTVSS	1543	QSVLTQPPSASGTPGQRVIISCSGSSSNIGSNTVKWYHQLPGTAPKLLICSNNQRPSGVPDRFSGSKSDTSASLAISGLQSEDEADYYCAAWDDSLNALVFGGGTKLTVL	IGHV1-2 (Human)	IGHJ4 (Human)	IGLV1-44 (Human)	IGLJ2 (Human)	2552	ARVVVLGYGRPNNYYDGRNVWDY	3754	AAWDDSLNALV	Seth Zost et al., 2020 (https://www.nature.com/articles/s41591-020-0998-x)
COV2-2509	Ab	SARS-CoV1, SARS-CoV2			SARS-CoV2	S; non-RBD	B-cells; SARS-CoV2 Human Patient	465	QVQLVESGGGVVQPGRSLRLSCAASGFIFSTYAMHWVRQAPGKGLEWVAVISYDGDNKYYADSVKGRFTISRDNSKNTLYLEMNSLRAEDTAVYYCARPRGGSYQTCFDYWGQGTLVTVSS	1544	EIVMTQSPATLSVSPGERATLSCRASQSVSSNLAWYQQKPGQAPRLLIYGASTRATGIPARFSGSGSGTEFTLTISSLQSEDFAVYYCQQYNNWPGTFGQGTKVEIK	IGHV3-30-3 (Human)	IGHJ4 (Human)	IGKV3-15 (Human)	IGKJ1 (Human)	2553	ARPRGGSYQTCFDY	3755	QQYNNWPGT	Seth Zost et al., 2020 (https://www.nature.com/articles/s41591-020-0998-x)
COV2-2510	Ab	SARS-CoV2	SARS-CoV1		SARS-CoV1, SARS-CoV2	S; RBD	B-cells; SARS-CoV2 Human Patient	466	QVQLVQSGSELKKPGASVKVSCKASGYTFTSHTMNWVRQAPGQGLEWMGWINTNTGNPMYAQGFTGRFVFSLDTSGSTAYLQISSLKAEDTAVYYCARWGPDYGDYASNDYWGQGTLVTVSS	1545	SYELTQPSSVSVSPGQTARITCSGDVLAKNYARWFQQKPGQAPVLVIYKDSERPSGIPKRFSGSSSGTTVTLTISGAQVEDEADYYCYSAADNNRVFGGGTKLTVL	IGHV7-4-1 (Human)	IGHJ4 (Human)	IGLV3-27 (Human)	IGLJ2 (Human)	2554	ARWGPDYGDYASNDY	3756	YSAADNNRV	Seth Zost et al., 2020 (https://www.nature.com/articles/s41591-020-0998-x)
COV2-2514	Ab	SARS-CoV1, SARS-CoV2		SARS-CoV2 (weak)		S; RBD	B-cells; SARS-CoV2 Human Patient	467	EVQLVESGGGVVRPGGSLRLSCAASGFIFDDYDMTWVRQAPGKGLEWVSGINWNGGSTGYADSVKGRFTISRDNAKNSLYLQMNSLRAEDTALYHCAVIMSPIPRYSGYDWAGDAFDIWGQGTMVTVSS	1546	SSELTQDPAVSVALGQTVRITCQGDSLRSYYASWYQQKPGQVPILVIYDKNNRPSGIPDRFSGSSSGNTASLTITGAQAEDEADYYCNSRDSSGNAVVFGGGTKLTVL	IGHV3-20 (Human)	IGHJ3 (Human)	IGLV3-19 (Human)	IGLJ2 (Human)	2555	AVIMSPIPRYSGYDWAGDAFDI	3757	NSRDSSGNAVV	Seth Zost et al., 2020 (https://www.nature.com/articles/s41591-020-0998-x)

COV2-2515	Ab	SARS-CoV1, SARS-CoV2			SARS-CoV2	S; non-RBD	B-cells; SARS-CoV2 Human Patient	468	QVQLVQSGSELKKPGASVKVSCKASGYT FTTYAMNWVRQAPGQGLEWMGWIN TNTGNPTYAQDFTGRFVFSLDTSVSTAYL QISSLKAEDTAVYYCARGLVGRIDPWGQ GTLVTVSS	1547	DIQMTQSPSSLSASVGDRVTITCQASQ DISNSLSWYQQKPGKAPKLLIYDASNL KTGVPSRFSGSGSGTDFTFTISSLQPED IATYYCQQYDNLLLFTFGPGTKVDIK	IGHV7-4-1 (Human)	IGHJ5 (Human)	IGKV1-33 (Human)	IGKJ3 (Human)	2556	ARGLVGRIDP	3758	QQYDNLLLFT	Seth Zost et al., 2020 (https://www.nature.com/articles/s41591-020-0998-x)
COV2-2516	Ab	SARS-CoV1, SARS-CoV2			SARS-CoV2	S; RBD	B-cells; SARS-CoV2 Human Patient	469	QVQLVQSGAEVKKPGASVKVSCKASGY TFTNYYMHWVRQAPGQGLEWMGILN PGAGSTSYAQKFQGRVTMTSDTSTNTV YMQLSSLKSEDTAVYYCARDQQIVPHAD GFDIWGQGTMVTVSS	1548	EIVLTQSPATLSLSPGERATLSCRASQS VSSYLAWYQQKPGQAPRLLIYDASNR ATGIPARFSGSGSGTDFTLTISSLEPEDF AVYYCQQRSNWPPRTWTFGQGTKVE IK	IGHV1-46 (Human)	IGHJ3 (Human)	IGKV3-11 (Human)	IGKJ1 (Human)	2557	ARDQQIVPH ADGFDI	3759	QQRSNWP PRTWT	Seth Zost et al., 2020 (https://www.nature.com/articles/s41591-020-0998-x)
COV2-2517	Ab	SARS-CoV1, SARS-CoV2			SARS-CoV2	S; non-RBD	B-cells; SARS-CoV2 Human Patient	470	QVQLVQSGAEVRKPGSSVKVSCKASGG TFSSYAISWVRQAPGQGLEWMGGIIPV FGTANYAQKFQGRVTITADKSTSTAFME LNSLRSEDTAVYYCARIGSYPEYFQHWG QGTLVTVSS	1549	EIVLTQSPATLSLSPGERATLSCRASQS VSSFLAWYQQKPGQAPRLLIYDASNR ATGIPARFSGSGSGTDFTLTISSLEPEDF AVYYCHYRSNWPPVLTFGGGTKVEIE	IGHV1-69 (Human)	IGHJ1 (Human)	IGKV3-11 (Human)	IGKJ4 (Human)	2558	ARIGSYPEYFQ H	3760	HYRSNWP PVLT	Seth Zost et al., 2020 (https://www.nature.com/articles/s41591-020-0998-x)
COV2-2518	Ab	SARS-CoV2	SARS-CoV1		SARS-CoV1, SARS-CoV2	S; RBD	B-cells; SARS-CoV2 Human Patient	471	EVQLVESGGGLVQPGRSLRLSCAASGFT FDDYAMHWVRQAPGKGLEWVSGISW NSGTIGYADSVKGRFIISRDNAKNSLYLQ MNSLRPEDTALYYCAKDIIRQGEDGMD VWGQGTTVTVSS	1550	SSELTQDPAVSVALGQTVRITCQGDSL RSYYASWYQQKPGQVPILVIYDKNNR PSGIPDRFSGSSSGNTASLTITGAQAED EADYYCNSRDSSGNAVVFGGGTKLTV A	IGHV3-9 (Human)	IGHJ6 (Human)	IGLV3-19 (Human)	IGLJ2 (Human)	2559	AKDIIRQGED GMDV	3761	NSRDSSGN AVV	Seth Zost et al., 2020 (https://www.nature.com/articles/s41591-020-0998-x)
COV2-2520	Ab	SARS-CoV1, SARS-CoV2			SARS-CoV2	S; non-RBD	B-cells; SARS-CoV2 Human Patient	472	EVQLVESGGGLVQPGGSLRLSCAASGFT FSSYWMSWVRQAPGKGLEWVANIKED GSEKYYVDSVKGRFTISRDNAKNSLYLQ MNSLRAEDTAVYYCARDVGGYSGYDLG FDYYYYMDVWGKGTTVTVSS	1551	SSELTQDPAVSVALGQTVRITCQGDSL RSYYANWYQQKPGQAPVVVIFGKNN RPSGIPDRFSGSNSGNTASLTITGAQA EDEADYYCNSRDSSGYIWGWMFGGG TKLTVL	IGHV3-7 (Human)	IGHJ6 (Human)	IGLV3-19 (Human)	IGLJ3 (Human)	2560	ARDVGGYSG YDLGFDYYYY MDV	3762	NSRDSSGY IWGWM	Seth Zost et al., 2020 (https://www.nature.com/articles/s41591-020-0998-x)
COV2-2521	Ab	SARS-CoV2	SARS-CoV1		SARS-CoV1, SARS-CoV2	S; non-RBD	B-cells; SARS-CoV2 Human Patient	473	QVQLVESGGGVVQPGRSLRLACAASGF TFSSYGMHWVRQAPGKGLEWVAVISY DGNNKYYADSLKGRFTISRDDSKNTLYL QMNSLRAEDTAVYYCAKDRTAVFLFFGL GDAFDIWGQGTMVTVSS	1552	SYVLTQPPSVSVAPGKTARITCGGNNI GSKSVHWYQQKPGQAPVVVVYDDSD RPSGLPERFSGSNSGNTATLTISRVEA GDEADYYCQVWDSSSDHWVFGGGT KLTVL	IGHV3-30 (Human)	IGHJ3 (Human)	IGLV3-21 (Human)	IGLJ3 (Human)	2561	AKDRTAVFLF FGLGDAFDI	3763	QVWDSSS DHWV	Seth Zost et al., 2020 (https://www.nature.com/articles/s41591-020-0998-x)
COV2-2524	Ab	SARS-CoV1, SARS-CoV2			SARS-CoV2	S; non-RBD	B-cells; SARS-CoV2 Human Patient	474	EVQLVQSGAEVKKPGESLKISCKGSGYSF TSHWIGWVRQMPGKGLEWMGIIYPG DSDTRYSPSFQGQVTISADKSISTAYLQW SSLKASDTAMYYCASALRERGVQLWSV WGQGTLVTVSS	1553	QSVLTQPPSVSGAPGQRVTISCTGSSS NIGAGYDVHWYQQLPGTAPKLLIFNS NRPSGVPDRFSGSKSGTSASLAITGLQ AEDEADYYCQSYDSSLGALFGGGTKLT VL	IGHV5-51 (Human)	IGHJ4 (Human)	IGLV1-40 (Human)	IGLJ3 (Human)	2562	ASALRERGVQ LWSV	3764	QSYDSSLG AL	Seth Zost et al., 2020 (https://www.nature.com/articles/s41591-020-0998-x)
COV2-2525	Ab	SARS-CoV2	SARS-CoV1		SARS-CoV1, SARS-CoV2	S; NTD	B-cells; SARS-CoV2 Human Patient	475	EVRLLESGGGLVQPGGSLRLSCAASGFT FTSYAMSWVRQAPGKGLQWVSTISVSG GSTYYADSVKGRFTISRDNSKNTLYLQM NSLRAEDTAVYYCAKDPASGIVGPTHFD YWGQGTLVTVSS	1554	QLVLTQSPSASASLGASVKLTCTLSSGH TTYAIAWHQQQPEKGPRYLMKLNSD GSHTRGDGIPDRFSGSSSGAERYLTISS LQSEDEADYYCQSWDTGIGVFGGGTK LTVL	IGHV3-23 (Human)	IGHJ4 (Human)	IGLV4-69 (Human)	IGLJ3 (Human)	2563	AKDPASGIVG PTHFDY	3765	QSWDTGI GV	Seth Zost et al., 2020 (https://www.nature.com/articles/s41591-020-0998-x)
COV2-2526	Ab	SARS-CoV2	SARS-CoV1		SARS-CoV1, SARS-CoV2	S; NTD	B-cells; SARS-CoV2 Human Patient	476	QVQLVQSGAEVKKPGASVKVSCKVSGY TLTELSIHWVRQAPGKGLEWMGGFDP EDAETIYAQQFQGRVTMTEDTSTDTAY MELSSLKSEDTALYYCATGFAVFGRAAV PYWGQGTLVTVSS	1555	SYELTQPPSVSVSPGQTASITCFGDKLG DKYACWFQQKPGQSPVLIIYQGAKRP SGIPERFSGSNSGNTATLTISGTQAMD EADYYCQAWDSSTVVFGGGTKLTVL	IGHV1-24 (Human)	IGHJ4 (Human)	IGLV3-1 (Human)	IGLJ2 (Human)	2564	ATGFAVFGRA AVPY	3766	QAWDSST VV	Seth Zost et al., 2020 (https://www.nature.com/articles/s41591-020-0998-x)
COV2-2527	Ab	SARS-CoV2	SARS-CoV1		SARS-CoV1, SARS-CoV2	S; RBD	B-cells; SARS-CoV2 Human Patient	477	QVQLQESGPGLVKPSQTLSLTCTVSGGSI SSGDYYWSWIRQPPGKGLEWIGYIYYSG STYYNPSLKSRVTISVDTSKNQVSLKLSSV TAADTAVYYCARFRRSYGSGSYYNISFDY WGQGTLVTVSS	1556	QSALTQPASVSGSPGQSITISCTGTSSD VGSYNLVSWYQQHPGKAPKLMIYEVS KRPSGVSNRFSGSKSGNTASLTISGLQ AEDEADYYCCSYVGSSTYVVFGGGTKL TVL	IGHV4-30-4 (Human)	IGHJ4 (Human)	IGLV2-23 (Human)	IGLJ2 (Human)	2565	ARFRRSYGSG SYYNISFDY	3767	CSYVGSST YVV	Seth Zost et al., 2020 (https://www.nature.com/articles/s41591-020-0998-x)
COV2-2529	Ab	SARS-CoV2	SARS-CoV1		SARS-CoV1, SARS-CoV2	S; non-RBD	B-cells; SARS-CoV2 Human Patient	478	QVQLVQSGSELKKPGASVKVSCKASGYT FTRHAMNWVRQAPGQGLEWMGWIN TNTGNPTYAQGFTGRFVFSLDTSVSTAY LQISSLKAEDTAVYYCVREYGSGHPLPIW GQGTLVTVSS	1557	SYELTQPPSVSVSPGQTARITCSADALS KQYAYWYQQKPGQAPVVVIYKDSERP SGIPERFSGSSSGTTVTLTISGVQAEDE ADYYCQSADSSSHWVFGGGTKLTVL	IGHV7-4-1 (Human)	IGHJ4 (Human)	IGLV3-25 (Human)	IGLJ3 (Human)	2566	VREYGSGHPL PI	3768	QSADSSSH WV	Seth Zost et al., 2020 (https://www.nature.com/articles/s41591-020-0998-x)
COV2-2531	Ab	SARS-CoV2	SARS-CoV1	SARS-CoV2		S; RBD	B-cells; SARS-CoV2 Human Patient	479	QVQLQESGPGLVKPSETLSLTCSVSGGSI RSYFWNWVRQPPGKGLEWIGYIYYSGS TNYKPSFKSRVTISLDTSKNQISLKLSSVT AADTAVYYCARATWLRDAFGIWGQGT MVTVSS	1558	NFMLTQPHSVSESPGKTVTISCTGNSG SIASNYVQWYQQRPGSAPTTVIYEDS QRPSGVPDRFSGSIDSSSNSASLTISGL KTEDEADYYCQSFDSGNVVFGGGTKL TVL	IGHV4-59 (Human)	IGHJ3 (Human)	IGLV6-57 (Human)	IGLJ2 (Human)	2567	ARATWLRDA FGI	3769	QSFDSGNV V	Seth Zost et al., 2020 (https://www.nature.com/articles/s41591-020-0998-x)
COV2-2532	Ab	SARS-CoV2	SARS-CoV1		SARS-CoV1, SARS-CoV2	S; RBD	B-cells; SARS-CoV2 Human Patient	480	QVQLVQSGAEVKKPGASVRVSCKAPGY TFTTYYIHWVRQAPGQGLEWMGIINPS AGSTTYAQKFQGRVTMTRDTSTSTVYM ELSSLRSEDTAVYYCARGFHVPAALRNW FDPWGQGTLVTVSS	1559	QSVLTQPPSASGTPGQRVTISCSGSSS NIGSNTVNWYQQLPGTAPKLLIYNNN QRPSGVPDRLSGSKSGTSASLAISGLQ SEDEADYYCVAWDDSRNGLVFGGGT KLTVL	IGHV1-46 (Human)	IGHJ5 (Human)	IGLV1-44 (Human)	IGLJ2 (Human)	2568	ARGFHVPAAL RNWFDP	3770	VAWDDSR NGLV	Seth Zost et al., 2020 (https://www.nature.com/articles/s41591-020-0998-x)
COV2-2533	Ab	SARS-CoV2	SARS-CoV1		SARS-CoV1, SARS-CoV2	S; NTD	B-cells; SARS-CoV2 Human Patient	481	QVQLQESGPGLVKPSQTLSLTCTVSGGSI SSGGYYWSWIRQHPGKGLEWIGYIYYS GSTYYNPSLKSRVTISVDTSKNQFSLKLTS VTAADTAVYYCAREANDSGSFYNGPFDY WGQGTLVTVSS	1560	DIVMTQSPDSLAVSLGERATINCKSSQ SVLYSSNNKNYLAWYQQKPGQPPKLLI YWASTRESGVPDRFSGSGSGTDFTLTI SSLQAEDVAVYYCQQYYSTRTFGQGT KLEIK	IGHV4-31 (Human)	IGHJ4 (Human)	IGKV4-1 (Human)	IGKJ2 (Human)	2569	AREANDSGSF YNGPFDY	3771	QQYYSTRT	Seth Zost et al., 2020 (https://www.nature.com/articles/s41591-020-0998-x)

COV2-2536	Ab	SARS-CoV1, SARS-CoV2			SARS-CoV2	S; non-RBD	B-cells; SARS-CoV2 Human Patient	482	QVQLQESGPGLVKPSQTLSLTCTVSGGSISSGSYYWSWIRQPAGKGLEWIGRIFTSGSTNYNPSLKSRVTISVDTSKNQFSLKLSSVTAADTAVYYCARGGLLWFGGAGNYMDVWGKGTTVTVSS	1561	DIVMTQSPDSLAVSLGERATINCKSSQSVLYSSNNKNYLAWYQQKPGQPPKLLIYWASTRESGVPDRFSGSGSGTDFTLTISSLQAEDVAVYYCQQYYSTPPYTFGQGTKVEIK	IGHV4-61 (Human)	IGHJ6 (Human)	IGKV4-1 (Human)	IGKJ2 (Human)	2570	ARGGLLWFGGAGNYMDV	3772	QQYYSTPPYT	Seth Zost et al., 2020 (https://www.nature.com/articles/s41591-020-0998-x)
COV2-2539	Ab	SARS-CoV2	SARS-CoV1	SARS-CoV2		S; RBD	B-cells; SARS-CoV2 Human Patient	483	QVQLAQSGAEVKKPGASVKVSCKAGGYTFTSYDINWVRQATGQGLEWMGWMNSNSGNAGYAQKFQGRVTMTRDTSISTAYMELSSLRSEDTAVYYCARMRTGWPTHGRPDDFWGRGTLVTVSS	1562	QSVLTQPPSASGTPGQRVTISCSGSNSNIGSYTVNWYQQFPGTAPKLLIYDNNQRTSGVPDRFSGSKSGTSASLAISGLQSEDEASYYCLAWDDSLNGLVFGGGTKLTVL	IGHV1-8 (Human)	IGHJ4 (Human)	IGLV1-44 (Human)	IGLJ3 (Human)	2571	ARMRTGWPTHGRPDDF	3773	LAWDDSLNGLV	Seth Zost et al., 2020 (https://www.nature.com/articles/s41591-020-0998-x)
COV2-2545	Ab	SARS-CoV2	SARS-CoV1		SARS-CoV1, SARS-CoV2	S; non-RBD	B-cells; SARS-CoV2 Human Patient	484	QVQIQQWGAGVLKPSETLSLTCAVYGGSFSGHYWSWIRQPPGKGLEWIGEINHSGSTKYNPSLKSRVTISVDTSKNQFSLKLSSVTAADTAVYYCARGPPVTTFFVFSLLFDPWGQGTLVTVSS	1563	QSVLTQPPSASGTPGQRVTISCSGSSSNIGSNYVYWYQQLPGTAPKLLIYSSNQRPSGVPDRFSGSKSGTSASLAISGLRSEDEADYYCAAWDASLSGWVFGGGTKLTVL	IGHV4-34 (Human)	IGHJ5 (Human)	IGLV1-47 (Human)	IGLJ3 (Human)	2572	ARGPPVTTFFVFSLLFDP	3774	AAWDASLSGWV	Seth Zost et al., 2020 (https://www.nature.com/articles/s41591-020-0998-x)
COV2-2546	Ab	SARS-CoV2	SARS-CoV1		SARS-CoV1, SARS-CoV2	S; non-RBD	B-cells; SARS-CoV2 Human Patient	485	QVQLVESGGGVVQPGRSLRLSCAASGFTFSSYGMHWVRQAPGKGLEWVAVISYDGRNKYYADSVKGRFTISRDNSKNTLYLQMSSLRAEDTAVYYCAKEGEWELRGNALDIWGQGTMVTVSS	1564	SYELTQPPSVSVSPGQTARITCSADALPKHYAYWYQQRPGQAPVLVIYKDIERPSGIPERFSGSSSGTTVTLTITGAQAEDEADYYCQSVDSGSGSSVVFGGGTKLAVL	IGHV3-30 (Human)	IGHJ3 (Human)	IGLV3-25 (Human)	IGLJ3 (Human)	2573	AKEGEWELRGNALDI	3775	QSVDSGSGSSVV	Seth Zost et al., 2020 (https://www.nature.com/articles/s41591-020-0998-x)
COV2-2549	Ab	SARS-CoV2	SARS-CoV1		SARS-CoV1, SARS-CoV2	S; non-RBD	B-cells; SARS-CoV2 Human Patient	486	QVQLVESGGGVVQPGRSLRLSCAASGFTFSSYGMHWVRQAPDKGLEWVAVIWYDGSNKYYADSVKGRFTISRDNSKNTLYLQMNSLRAEDTAVYYCAREGQWPNQAFDIWGQGTMVTVSS	1565	SYELTQPPSVSVSPGQTASITCSGDKLGDKYACWYQQKPGQSPVLVIHQDSQRPSGIPERFSGSNSGNTATLTISGTQAMDEADYYCQAWDSSTHVVFGGGTKLTVL	IGHV3-33 (Human)	IGHJ3 (Human)	IGLV3-1 (Human)	IGLJ2 (Human)	2574	AREGQWPNQAFDI	3776	QAWDSSTHVV	Seth Zost et al., 2020 (https://www.nature.com/articles/s41591-020-0998-x)
COV2-2551	Ab	SARS-CoV1, SARS-CoV2			SARS-CoV2	S; non-RBD	B-cells; SARS-CoV2 Human Patient	487	QVQLQESGPGLVKPSETLSLTCTVSGGSISSSSYYWGWIRQPPGKGLEWIGSIYYSGSSYYSPSLKSRVTISADTSKNQFSLNLRSVTAADTAVYYCASGPPYMATFSYYFDYWGQGTLVTVSS	1566	QSALTQPASVSGSPGQSITISCTGTSSDVGGYNYVSWFQHHPDKAPRLMIYDVSKRPSGVSNRFSGSKSGNTASLTISGLQAEDEADYYCSSYTSSSTPFVFGTGTKVTVL	IGHV4-39 (Human)	IGHJ4 (Human)	IGLV2-14 (Human)	IGLJ1 (Human)	2575	ASGPPYMATFSYYFDY	3777	SSYTSSSTPFV	Seth Zost et al., 2020 (https://www.nature.com/articles/s41591-020-0998-x)
COV2-2552	Ab	SARS-CoV1, SARS-CoV2		SARS-CoV2 (weak)		S; RBD	B-cells; SARS-CoV2 Human Patient	488	QVQLVESGGGLVKPGGSLRLSCAASGFTFSDYYMSWIRQAPGKGLECVSYISSSGSTIYYADSVKGRFTISRDNAKNSLYLQMNSLRAEDTAVYYCARDPIRDGVWGLNENDYWGQGTLVTVSS	1567	QPVLTQSSSASASLGSSVKLTCTLSSGHSSYIIAWHQQQPGKAPRYLMKLEGSGSYNKGSGVPDRFSGSSSGADCYLTISNLQSEDEADYYCETWDSNTRVFAGGTKLTVL	IGHV3-11 (Human)	IGHJ4 (Human)	IGLV4-60 (Human)	IGLJ3 (Human)	2576	ARDPIRDGVWGLNENDY	3778	ETWDSNTRV	Seth Zost et al., 2020 (https://www.nature.com/articles/s41591-020-0998-x)
COV2-2553	Ab	SARS-CoV2	SARS-CoV1		SARS-CoV1, SARS-CoV2	S; non-RBD	B-cells; SARS-CoV2 Human Patient	489	QVQLVESGGGVVQPGRSLRLSCAASGFIFSSYAMHWVRQAPGKGLEWVAVISYDGSNKYYADSVKGRFTISRDNSKNTLYLQMNSLRAEDTAVYYCARSPPASYYNPSTGYFDYWGQGTLVTVSS	1568	DIQMTQSPSSLSASVGDRVTITCRASQSISSYLNWYQQKPGKAPKLLIYAASSLQSGVPSRFSGSGSGTDFTLTISSLQPEDFATFYCQQSYSTPMHTFGQGTKLEIK	IGHV3-30 (Human)	IGHJ4 (Human)	IGKV1-39 (Human)	IGKJ2 (Human)	2577	ARSPPASYYNPSTGYFDY	3779	QQSYSTPMHT	Seth Zost et al., 2020 (https://www.nature.com/articles/s41591-020-0998-x)
COV2-2554	Ab	SARS-CoV1, SARS-CoV2			SARS-CoV2	S; RBD	B-cells; SARS-CoV2 Human Patient	490	QVQLVESGPGLVKPSGAEVKKPGASVKVSCKASGYTFTSHYMHWVRQAPGQGLEWMGIINPSGGSTSYAQKFQGRVTMTSDTSTSTVYMELSSLRSEDTAMYYCARDVFWVPAASSFDYWGQGTLVTVSS	1569	DIQLTQSPSFLSASVGDRVTITCRASQGISSYLAWYQQKPGKAPKLLIYAASTLQSGVPSRFSGSGSGTEFTLTISSLQPEDFATYYCQQLNSYLGTFGQGTKVEIK	IGHV1-46 (Human)	IGHJ4 (Human)	IGKV1-9 (Human)	IGKJ1 (Human)	2578	ARDVFWVPAASSFDY	3780	QQLNSYLGT	Seth Zost et al., 2020 (https://www.nature.com/articles/s41591-020-0998-x)
COV2-2558	Ab	SARS-CoV2	SARS-CoV1		SARS-CoV1, SARS-CoV2	S; NTD	B-cells; SARS-CoV2 Human Patient	491	QVQLVESGGGVVQPGRSLRLSCAASGFTFSSYAMHWVRQAPGKGLEWVAVISYDGSNKYYADSVKGRFTISRDNSKNTLYLQMNSLRVEDTAVYYCARDQEWFRELFLFDYWGQGTLVTVSS	1570	DIQMTQSPSSVSASVGDRVTITCRASQGISSWLAWYQQKPGKAPKLLIYDASSLQSGVPSRFSGSGSGTDFTLTISSLQPEDFATYYCQQANSFPPTFGPGTKVDIK	IGHV3-30-3 (Human)	IGHJ4 (Human)	IGKV1-12 (Human)	IGKJ3 (Human)	2579	ARDQEWFRELFLFDY	3781	QQANSFPPT	Seth Zost et al., 2020 (https://www.nature.com/articles/s41591-020-0998-x)
COV2-2562	Ab	SARS-CoV2	SARS-CoV1	SARS-CoV2		S; RBD	B-cells; SARS-CoV2 Human Patient	492	QVQLAQSGAEVKKPGASVKVSCKAAGYTFTSYDINWVRQATGQGLEWMGWMNSNSGNAGYAQKFQGRVTMTRDTSTSTAYMELSSLTSDDTAVYYCARMRTGWPTHGRPDDFWGRGTLVTVSS	1571	QSVLTQPPSASGTPGQRVTISCSGSNSNIGSYTVNWYQQFPGTAPKLLIYDNNQRTSGVPDRFSGSKSGTSASLAISGLQSEDEANYYCLVWDDSLNGLVFGGGTKLTVL	IGHV1-8 (Human)	IGHJ4 (Human)	IGLV1-44 (Human)	IGLJ2 (Human)	2580	ARMRTGWPTHGRPDDF	3782	LVWDDSLNGLV	Seth Zost et al., 2020 (https://www.nature.com/articles/s41591-020-0998-x)
COV2-2563	Ab	SARS-CoV2	SARS-CoV1		SARS-CoV1, SARS-CoV2	S; NTD	B-cells; SARS-CoV2 Human Patient	493	QVQLQQWGAGLLKPSETLSLTCAVYGGSFSGYYWSWIRQPPGKGLEWIGEINHSGSSNYNPSLKSRVTISVDTSKNQFSLKLSSVTAADTAVYYCARGWGWGAVAGRAEYYFDYWGQGTLVTVSS	1572	QSALTQPASVSGSPGQSITISCTGTSSDVGSYNLVSWYQQHPGKAPKLMIYEVSKRPSGVSNRFSGSKSGNTASLTISGLQAEDEADYYCCSYAGSSTWGFGTGTKVTVL	IGHV4-34 (Human)	IGHJ4 (Human)	IGLV2-23 (Human)	IGLJ1 (Human)	2581	ARGWGWGAVAGRAEYYFDY	3783	CSYAGSSTWG	Seth Zost et al., 2020 (https://www.nature.com/articles/s41591-020-0998-x)
COV2-2564	Ab	SARS-CoV1, SARS-CoV2			SARS-CoV2	S; non-RBD	B-cells; SARS-CoV2 Human Patient	494	QVQLVESGGGVVQPGRSLRLSCAASGFTFSSYAMHWVRQAPGKGLEWVAVISYDGYNKYYADSVKGRFTISRDNSKNTLYLQMNSLRAEDTAVYYCARAQGGNYYYGMDVWGQGTTVTVSS	1573	SYVLTQPPSVSVAPGKTARITCGGNNIGTKGVHWYQQKPGQAPVLVVYDDSDRPSGIPGRFSGSNSGNTATLTISRVEAGDEADYFCQVWDSSSDHHVVFGGGTKLTVL	IGHV3-30-3 (Human)	IGHJ6 (Human)	IGLV3-21 (Human)	IGLJ2 (Human)	2582	ARAQGGNYYYGMDV	3784	QVWDSSSDHHVV	Seth Zost et al., 2020 (https://www.nature.com/articles/s41591-020-0998-x)
COV2-2565	Ab	SARS-CoV1, SARS-CoV2			SARS-CoV2	S; non-RBD	B-cells; SARS-CoV2 Human Patient	495	QVQLQESGPGLVKPSQTLSLTCTVSGGSISSGSYYWSWIRQPAGKGLEWIGRVYIYSSGSTNYNPSLKSRVTISVDTSKNQFSLKLSSVTAADTAVYYCARGAASFDYWGQGTLVTVSS	1574	DIVMTQSPLSLPVTPGEPASISCRSSQSLLHSDGYTYLDWYLQKPGQSPQLLIYLGSKRASGVPDRFSGSGSGTDFTLKISRVEAEDVGVYYCMQALQTPLTFGGGTKVEIK	IGHV4-61 (Human)	IGHJ4 (Human)	IGKV2-28 (Human)	IGKJ4 (Human)	2583	ARGAASFDY	3785	MQALQTPLT	Seth Zost et al., 2020 (https://www.nature.com/articles/s41591-020-0998-x)

COV2-2570	Ab	SARS-CoV2	SARS-CoV1		SARS-CoV1, SARS-CoV2	S; non-RBD	B-cells; SARS-CoV2 Human Patient	496	QLQLQESGPGLVKPSETLSLTCTVSGGSISSSSNYWGWIRQPPGKGLEWIGSIYYSGSTYYNPSLKSRVTISVDTSKNQFSLKLSSVTAADTAVYYCARDPRVVVTARMYNWFDPWGQGTLVTVSS	1575	EIVMTQSPGTLSVSPGERATLSCRASQSVSSNLAWYQQKPGQAPRLLIYGASTRATGVPARFSGSGSGTEFTLTISSLQSEDFAVYYCQQYNNWPPMYTFGQGTKLEIK	IGHV4-39 (Human)	IGHJ5 (Human)	IGKV3-15 (Human)	IGKJ2 (Human)	2584	ARDPRVVVTARMYNWFDP	3786	QQYNNWPPMYT	Seth Zost et al., 2020 (https://www.nature.com/articles/s41591-020-0998-x)
COV2-2571	Ab	SARS-CoV2	SARS-CoV1		SARS-CoV1, SARS-CoV2	S; NTD	B-cells; SARS-CoV2 Human Patient	497	QVQLQESGPGLVKPSETLSLTCTVSGGSLSSYYWSWIRQPPGKGLEWIGYIYDSGGASRSTNYNPSLKSRVTISVDTSRNQLSLKLSSVTAADTAVYYCARDQRQFQLLGRFGWFDPWGQGTLVTVSS	1576	EIVMTQSPATLSVSPGERATLSCRASQSVSSNLAWYQQKPGQAPRLLIYGASTRATGIPARFSGSGSGTEFTLTISSLQSEDFAVYYCQQYNNWPRTFGQGTKVEIK	IGHV4-59 (Human)	IGHJ5 (Human)	IGKV3-15 (Human)	IGKJ1 (Human)	2585	ARDQRQFQLLGRFGWFDP	3787	QQYNNWPRT	Seth Zost et al., 2020 (https://www.nature.com/articles/s41591-020-0998-x)
COV2-2574	Ab	SARS-CoV2	SARS-CoV1		SARS-CoV1, SARS-CoV2	S; non-RBD	B-cells; SARS-CoV2 Human Patient	498	QLQLQESGPGLVKPSETLSLTCTVSGGSISSTTYYWGWIRQPPGKGLEWIASIYYSGSTYYNPSLKSRLTVSVDTSKNQFSLKLSSVTAADTAVYYCARQWKWFGEAWYFDLWGRGTLVTVSS	1577	QPVVTQSPSASASLGASVKLTCTLDSGHRSYAIAWHQQRPEKGPRFLMRITTDGRHTKGDGIPDRFSGSGSGTERYLTISSLQSEDEADYYCQTWGTFGGGTRLTVL	IGHV4-39 (Human)	IGHJ2 (Human)	IGLV4-69 (Human)	IGLJ2 (Human)	2586	ARQWKWFGEAWYFDL	3788	QTWGT	Seth Zost et al., 2020 (https://www.nature.com/articles/s41591-020-0998-x)
COV2-2582	Ab	SARS-CoV2	SARS-CoV1		SARS-CoV1, SARS-CoV2	S; non-RBD	B-cells; SARS-CoV2 Human Patient	499	QVQLVQSGSELKKPGASVKVSCKASGYTFTTYAMNWVRQAPGQGLEWMGWINTNTGNPTYAQGFTGRFVFSLDTSVNTAFLHIGSLKAEDTAVYYCARDQDSGYPTYYYYYMDVWGKGTTVTVSS	1578	DIVMTQTPLSLSVTPGQPASISCKSSQSLLHSDGKTYLYWYLQKPGQSPQLLIYEVSNRFSGVPDRFSGSGSGTDFTLKISRVEAEDVGVYYCMQSIQPPLTFGGGTKVEIK	IGHV7-4-1 (Human)	IGHJ6 (Human)	IGKV2D-29 (Human)	IGKJ4 (Human)	2587	ARDQDSGYPTYYYYYMDV	3789	MQSIQPPLT	Seth Zost et al., 2020 (https://www.nature.com/articles/s41591-020-0998-x)
COV2-2583	Ab	SARS-CoV1, SARS-CoV2			SARS-CoV2	S; non-RBD	B-cells; SARS-CoV2 Human Patient	500	QVQLVQSGAEVKKPGASVKVSCKASGYTFTSYDMNWVRQATGQGLEWMGWMNPNSGNTGYAQKFQGRVTMTRNTSISTAYMELSSLRSEDTAVYYCARGGIYYLVRGFIIGYYGMDVWGQGTTVTVSS	1579	DIVMTQSPDSLAVSLGERATINCKSSQSVLYSSNNKNYLAWYQQKPGQPPKLLIYWASTRESGVPDRFSGSGSGTDFTLTISSLQAEDVAVYYCQQYYSTPLTFGGGTKVEIK	IGHV1-8 (Human)	IGHJ6 (Human)	IGKV4-1 (Human)	IGKJ4 (Human)	2588	ARGGIYYLVRGFIIGYYGMDV	3790	QQYYSTPLT	Seth Zost et al., 2020 (https://www.nature.com/articles/s41591-020-0998-x)
COV2-2584	Ab	SARS-CoV2	SARS-CoV1		SARS-CoV1, SARS-CoV2	S; non-RBD	B-cells; SARS-CoV2 Human Patient	501	EVALVESGGGLVKPGGSLRLSCAASGFIFSNAWMTWVRQAPGKGLEWVGRIKSKSEGGTPEYAAPVKGRFIISRDDSTNSLHLQMNYLRIEDTAVYYCTTGGYSSYAASDYWGQGTLVTVSS	1580	QSALTQPASVSGSPGQLITIFCNGSISDVGGWNYVSWYQQHPDKAPKMMIYDVRHRPSGVSSRFSGSKSGNTASLTISGLQAEDEGDYYCSSFTSRGALVLFGGGTKLTVL	IGHV3-15 (Human)	IGHJ4 (Human)	IGLV2-14 (Human)	IGLJ2 (Human)	2589	TTGGYSSYAASDY	3791	SSFTSRGALVL	Seth Zost et al., 2020 (https://www.nature.com/articles/s41591-020-0998-x)
COV2-2585	Ab	SARS-CoV2	SARS-CoV1		SARS-CoV1, SARS-CoV2	S; RBD	B-cells; SARS-CoV2 Human Patient	502	EVQLVESGGGLVQPGGSLRLSCAASGFTFSSYSMNWVRQAPGKGLEWVSYISSRSSTIKYADSVKGRFTISRDNAKNSLYLQMNSLRDEDTAVYYCARVDYYGSGSVYWYFDLWGRGTLVTVSS	1581	QSALTQPRSVSGSPGQSVTISCTGTSSDVGGYNYVSWYQQHPGKAPKLMIYDVSKRPSGVPDRFSGSKSGNTASLTISGLQAEDEADYYCCSYAGIWVFGGGTKLTVL	IGHV3-48 (Human)	IGHJ2 (Human)	IGLV2-11 (Human)	IGLJ2 (Human)	2590	ARVDYYGSGSVYWYFDL	3792	CSYAGIWV	Seth Zost et al., 2020 (https://www.nature.com/articles/s41591-020-0998-x)
COV2-2586	Ab	SARS-CoV2	SARS-CoV1		SARS-CoV1, SARS-CoV2	S; non-RBD	B-cells; SARS-CoV2 Human Patient	503	EVQLVESGGGLVQPGRSLRLSCAASGFTFDDYAMHWVRQAPGKGLEWVSGISWNSGSIAYADSVKGRFTISRDNAKNSLYLQMNSLRAEDTALYFCAKVGWELSIDAFDLWGQGTMVTVSS	1582	EIVLTQSPGTLSLSPGERATLSCRASQSVSSSYLGWYHQKPGQAPRLLIYGASSRATGIPDRFSGSGSGTDFTLTISRLEPEDFAVYYCQHYGSSRSTFGQGTKLEIK	IGHV3-9 (Human)	IGHJ3 (Human)	IGKV3-20 (Human)	IGKJ2 (Human)	2591	AKVGWELSIDAFDL	3793	QHYGSSRST	Seth Zost et al., 2020 (https://www.nature.com/articles/s41591-020-0998-x)
COV2-2587	Ab	SARS-CoV1, SARS-CoV2			SARS-CoV2	S; non-RBD	B-cells; SARS-CoV2 Human Patient	504	QITFKESGPTLVKPTETLTLTCTFSGFSVSTSGEGVGWIRQPPGKALEWLAVIYWDDDKRYSPSLKSRLTITRDTSKNQVVLTMTNMDPVDTATYYCAHRLWFRDAFDIWGQGTTVTVSS	1583	DIQMTQSPSSLSASVGDRVTITCRARQSISNYLNWYQQKPGKAPKLLIYAASSLHSGVPSRFSGSGSGTDFTLTISSLQPEDFATYYCQQSYSTPTFGGGTKVEIK	IGHV2-5 (Human)	IGHJ3 (Human)	IGKV1-39 (Human)	IGKJ4 (Human)	2592	AHRLWFRDAFDI	3794	QQSYSTPT	Seth Zost et al., 2020 (https://www.nature.com/articles/s41591-020-0998-x)
COV2-2589	Ab	SARS-CoV2	SARS-CoV1	SARS-CoV2 (weak)		S; RBD	B-cells; SARS-CoV2 Human Patient	505	QVTLRESGPALVKPTQTLTLTCTFSGFSLSTSGMCVSWIRQPPGKALEWLARIDWDDDKYYSTSLETRLTISKDTSKNQVVLTMTNMDPVDTATYYCARIQYQLNGMDVWGQGTTVTVSS	1584	DIQMTQSPSSLSASVGDRVTITCRASQSISSYLNWYQQKPGKAPKLLIYAASSLHSGVPSRFSGSGSGTDFTLTISSLQPEDFATYYCQQSYSTPYTFGQGTKLEIK	IGHV2-70 (Human)	IGHJ6 (Human)	IGKV1-39 (Human)	IGKJ2 (Human)	2593	ARIQYQLNGMDV	3795	QQSYSTPYT	Seth Zost et al., 2020 (https://www.nature.com/articles/s41591-020-0998-x)
COV2-2590	Ab	SARS-CoV1, SARS-CoV2			SARS-CoV2	S; non-RBD	B-cells; SARS-CoV2 Human Patient	506	QVQLVQSGAEVKKPGASVKVSCKASGYTFSSYDINWVRQATGQGLEWMGWVNPNSGHTGYAQKFQGRVTMTRNTSVSTAYMELSSLRSEDTAVFYCARGRVGYVGSGSRGYYYYYDMDVWGQGTTVTVSS	1585	SSELTQDPAVSVALGQTVRITCQGDSLRSYYASWYQQKPRQAPVLIISGNNNRPSGIPDRFSGSSSGNTASLTITGAQAEDEADYYCNSRDSSGNHLRVFGGGTKLTVL	IGHV1-8 (Human)	IGHJ6 (Human)	IGLV3-19 (Human)	IGLJ2 (Human)	2594	ARGRVGYVGSGSRGYYYYYDMDV	3796	NSRDSSGNHLRV	Seth Zost et al., 2020 (https://www.nature.com/articles/s41591-020-0998-x)
COV2-2602	Ab	SARS-CoV1, SARS-CoV2			SARS-CoV2	S; non-RBD	B-cells; SARS-CoV2 Human Patient	507	EVQLVQSGAEVKKPGESLKISCKGSGYSFTSYWIGWVRQMPGKGLEWMGIIYPGDSDTRYSPSFQGQVTISADKSISTAYLQWSSLKASDTAMYYCARPDYSSGWFSYWYFDLWGRGTLVTVSS	1586	EIVLTQSPGTLSLSPGERATLSCRASQSVSSNFLAWYQQKPGQAPRLLIYGASSRATGIPDRFSGSGSGTDFTLTISRLEPEDFAVYYCQQYGRSPITFGQGTRLEIK	IGHV5-51 (Human)	IGHJ2 (Human)	IGKV3-20 (Human)	IGKJ5 (Human)	2595	ARPDYSSGWFSYWYFDL	3797	QQYGRSPIT	Seth Zost et al., 2020 (https://www.nature.com/articles/s41591-020-0998-x)
COV2-2610	Ab	SARS-CoV1, SARS-CoV2			SARS-CoV2	S; non-RBD	B-cells; SARS-CoV2 Human Patient	508	QVQLVQSGSALKKPGASVKVSCKASGYTFTSYAMNWVRQAPGQGLEWMGWINTNTGNPTYAQGFTGRFVFSLDTSVSTAYLQISSLKAEDTAVYYCARGRSYGLSLGYWGQGTLVTVSS	1587	DIQMTQSPSSLSASVGDRVTITCQASQDISNYLNWYQQKPGKAPKLLIYAASNLETGVPSRFSGSGSGTDFTFTISSLQPEDIATYYCQQYDNLLQFTFGPGTKVDIK	IGHV7-4-1 (Human)	IGHJ4 (Human)	IGKV1-33 (Human)	IGKJ3 (Human)	2596	ARGRSYGLSLGY	3798	QQYDNLLQFT	Seth Zost et al., 2020 (https://www.nature.com/articles/s41591-020-0998-x)
COV2-2611	Ab	SARS-CoV2	SARS-CoV1		SARS-CoV1, SARS-CoV2	S; non-RBD	B-cells; SARS-CoV2 Human Patient	509	QVQLVESGGGVVQPGRSLRVSCAASGFTFSSHGMHWVRQAPGKGLEWVSVIWYDGSNKYYADSVKGRFTISRDNSKNTLSLQMNSLRAEDTAVYYCARESADISSRLDYWGRGTLVTVSS	1588	SYELTQPPSVSVSPGQTARITCSGDALPTKYAYWYQQKSGQAPVLVIYDDSKRPSGIPERFSGSSSGTMATLTISGAQVEDEADYYCYSTDSSGNVFGTGTKVTVL	IGHV3-33 (Human)	IGHJ4 (Human)	IGLV3-10 (Human)	IGLJ1 (Human)	2597	ARESADISSRLDY	3799	YSTDSSGNV	Seth Zost et al., 2020 (https://www.nature.com/articles/s41591-020-0998-x)

COV2-2614	Ab	SARS-CoV1, SARS-CoV2			SARS-CoV2	S; non-RBD	B-cells; SARS-CoV2 Human Patient	510	QITFKESGPTLVKPTETLTLTCTFSGFSVS TSGEGVGWIRQPPGKALEWLAVIYWD DDKRYSPSLKSRLTITRDTSKNQVVLTMT NMDPVDTATYYCAHRLWFRDAFDIWG QGTTVTVSS	1589	EIVMTQSPATLSVSAGERATLSCRASQ SISSNLAWYHQKPGQAPRLLIYGASTR ATGIPARFSGSGSGTEFTLTISSLQSEDF AVYYCQQYNSYSLTFGGGTKVEIK	IGHV2-5 (Human)	IGHJ3 (Human)	IGKV3-15 (Human)	IGKJ4 (Human)	2598	AHRLWFRDA FDI	3800	QQYNSYSL T	Seth Zost et al., 2020 (https://www.nature.com/articles/s41591-020-0998-x)
COV2-2616	Ab	SARS-CoV1, SARS-CoV2			SARS-CoV2	S; non-RBD	B-cells; SARS-CoV2 Human Patient	511	EVQLVESGGGLVQPGGSLRLSCAASGFI LSDHYMDWVRQAPGKGLEWVGRTRN KANSYTTEYAASVKGRFTISRDDSKNSLY LQMNSLKTEDTAVYYCASVITFGGVIVRS YWGQGTLVTVSS	1590	EIVLTQSPGTLSLSPGERATLSCRASQS VSSSYLAWYQQKPGQAPRLLIYGASSR ATGIPDRFSGSGSGTDFTLTISRLEPED FAVYYCQYYGSSPFGFGPGTKVDIK	IGHV3-72 (Human)	IGHJ4 (Human)	IGKV3-20 (Human)	IGKJ3 (Human)	2599	ASVITFGGVIV RSY	3801	QYYGSSPF G	Seth Zost et al., 2020 (https://www.nature.com/articles/s41591-020-0998-x)
COV2-2617	Ab	SARS-CoV1, SARS-CoV2			SARS-CoV2	S; non-RBD	B-cells; SARS-CoV2 Human Patient	512	QVQLVQSGAEVKKPGSSVKVSCKASGG TFSSYAISWVRQAPGQGLEWMGGIIPV FGTTNYAQKLQGRVTISADESTSTAYME VSSLRSEDTAVYYCARVSGYGDYGAYSD YWGQGTLVTVSS	1591	EIVLTQSPATLSLSPGERATLSCRASQS VSRFLAWYQQKPGQAPRLLIYDASNR ATGIPARFSGSGSGTDFTLTISSLEPEDF AVYYCQQRSNWPPRLTFGGGTKVEIK	IGHV1-69 (Human)	IGHJ4 (Human)	IGKV3-11 (Human)	IGKJ4 (Human)	2600	ARVSGYGDY GAYSDY	3802	QQRSNWP PRLT	Seth Zost et al., 2020 (https://www.nature.com/articles/s41591-020-0998-x)
COV2-2618	Ab	SARS-CoV2	SARS-CoV1		SARS-CoV1, SARS-CoV2	S; RBD	B-cells; SARS-CoV2 Human Patient	513	EVQLVESGGGLVQPGGSLRLSCVASEFT FSSYWMSWFRQAPGKGLEWVSGINW NGGSTGYADSVKGRFTISRDNAKNSLYL QMNSLKTEDTAVYYCASVITFGGVIVRSY WGQGTLVTVSS	1592	QSVLTQPPSASGTPGQRVTISCSGSSS NIGSNTVNWYQQLPGTAPKLLIYSNN QRPSGVPDRFSGSKSGTSASLAISGLQ SEDENNYYCAVWDDSLNGVVFGGGT KLTVL	IGHV3-20 (Human)	IGHJ4 (Human)	IGLV1-44 (Human)	IGLJ2 (Human)	2601	ASVITFGGVIV RSY	3803	AVWDDSL NGVV	Seth Zost et al., 2020 (https://www.nature.com/articles/s41591-020-0998-x)
COV2-2619	Ab	SARS-CoV1, SARS-CoV2			SARS-CoV2	S; non-RBD	B-cells; SARS-CoV2 Human Patient	514	EVQLLESGGGLVQPGGSLRLSCAASGFT FNNYAMSWVRQAPGKGLEWVSAIGGS GGSTYYADSVKGRFTVSRDNSENTLYLQ MSSLRAEDTAVYYCARVEGDWLLGGPY YHYYGMDVWGQGTTVTVSS	1593	QSVLTQPPSASGTPGQRVTISCSGSSS NIGSNYVYWYQQLPGTAPKLLISRNN QRPSGVPDRFSGSKSGTSASLAISGLQ SEDEANYYCLVWDDSLNGLVFGGGTK LTVL	IGHV3-23 (Human)	IGHJ6 (Human)	IGLV1-47 (Human)	IGLJ2 (Human)	2602	ARVEGDWLL GGPYYHYYG MDV	3804	LVWDDSL NGLV	Seth Zost et al., 2020 (https://www.nature.com/articles/s41591-020-0998-x)
COV2-2620	Ab	SARS-CoV1, SARS-CoV2			SARS-CoV2	S; non-RBD	B-cells; SARS-CoV2 Human Patient	515	QVQLVESGGGVVQPGRSLRLSCAASGF TFSSYAMHWVRQAPGKGLEWVAGISY DGSNKYYADSVKGRFTISRDNSKNTLYL QMNSLRAEDTAVYYCARADTMVRGTYF EYWGQGTLVTVSS	1594	QSALTQPASVSGSPGQSITISCTGTSSD VGGYNYVSWYQQHPGKAPKLMIYDV SNRPSGVSNRFSGSKSGNTASLTISGL QAEDEADYCCSSYTSSRAVLFGGGTKL TVL	IGHV3-30-3 (Human)	IGHJ4 (Human)	IGLV2-14 (Human)	IGLJ2 (Human)	2603	ARADTMVRG TYFEY	3805	SSYTSSRAV L	Seth Zost et al., 2020 (https://www.nature.com/articles/s41591-020-0998-x)
COV2-2621	Ab	SARS-CoV2	SARS-CoV1		SARS-CoV1, SARS-CoV2	S; non-RBD	B-cells; SARS-CoV2 Human Patient	516	QVQLVESGGGVVQPGRSLRLSCAASGF TFSSYLMHWVRQAPGKGLEWVAVIWA NGNRYYADSVKGRFTISRDISKNTLYLQ MNSLRAEDTAMYYCARDYCNGVTCNS NYWGQGTLVTVSS	1595	DFVMTQSPGSLAVSLGERATINCRSSQ SVLDNSSNKNHLAWHQQKPGQPPKL LIYWASTRESGVPDRFSGSGSGTDFTL TISSLQAEDVAVYYCQQYYSSHWTFG QGTKVEIK	IGHV3-33 (Human)	IGHJ4 (Human)	IGKV4-1 (Human)	IGKJ1 (Human)	2604	ARDYCNGVT CNSNY	3806	QQYYSSH WT	Seth Zost et al., 2020 (https://www.nature.com/articles/s41591-020-0998-x)
COV2-2622	Ab	SARS-CoV2	SARS-CoV1		SARS-CoV1, SARS-CoV2	S; NTD	B-cells; SARS-CoV2 Human Patient	517	QVQLQESGPGLVKPSGTLSLTCAVSGGS ISSSNWWSWVRQPPGKGLEWIGEIYHS GSTNYNPSLKSRVTISVDKSKNQFSLKLSS VTAADTAVYYCARGWYFDYWGQGTLV TVSA	1596	QSALTQPASVSGSPGQSITISCTGTSSD VGSYNLVSWYQQHPGKAPKLMIYEVS KRPSGVSNRFSGSKSGNTASLTISGLQ AEDEADYYCSYAGSSTWVFGGGTKL TVL	IGHV4-4 (Human)	IGHJ4 (Human)	IGLV2-23 (Human)	IGLJ3 (Human)	2605	ARGWYFDY	3807	YSYAGSST WV	Seth Zost et al., 2020 (https://www.nature.com/articles/s41591-020-0998-x)
COV2-2624	Ab	SARS-CoV2	SARS-CoV1		SARS-CoV1, SARS-CoV2	S; non-RBD	B-cells; SARS-CoV2 Human Patient	518	QVQLVQSGAEVKKPGSSVKVSCKASGG TFHNYAISWVRQAPGQGLEWMGGFIPI LGTTNYAQKFQGRVTITADESTSTAYME LSSLRSEDTAVYYCARVEGEGVDSYYYG MDVWGQGTTVTVSS	1597	SYELTQPPSVSVSPGQTARITCSADALP KQYAYWYQQKPGQAPVLVIYKDSERP SGIPERFSGSSSGTTVTLTISGVQAEDE ADYYCQSTDSSGSYVVFGGGTKLTVL	IGHV1-69 (Human)	IGHJ6 (Human)	IGLV3-25 (Human)	IGLJ2 (Human)	2606	ARVEGEGVD SYYYGMDV	3808	QSTDSSGS YVV	Seth Zost et al., 2020 (https://www.nature.com/articles/s41591-020-0998-x)
COV2-2628	Ab	SARS-CoV2	SARS-CoV1	SARS-CoV2 (weak)		S; RBD	B-cells; SARS-CoV2 Human Patient	519	EVQLVESGGGLVQPGRSLRLSCAASGFT FDDYAMHWVRQAPGKGLEWVSGISW NSGTIGYADSVKGRFIISRDNAKNSLYLQ MNSLRPEDTALYYCAKDIIRQGEDGMD VWGQGTTVTVSS	1598	DIQMTQSPSSLSASVGDRVTITCRASQ NIASYLNWYQQKPGKAPKLLIYAASSL QSGVPSRFSGSGSGTDFTLTISSLQPEE FATYYCHQSYFTPQTFGQGTKLEIK	IGHV3-9 (Human)	IGHJ6 (Human)	IGKV1-39 (Human)	IGKJ2 (Human)	2607	AKDIIRQGED GMDV	3809	HQSYFTPQ T	Seth Zost et al., 2020 (https://www.nature.com/articles/s41591-020-0998-x)
COV2-2631	Ab	SARS-CoV2	SARS-CoV1		SARS-CoV1, SARS-CoV2	S; RBD	B-cells; SARS-CoV2 Human Patient	520	QLQVVQSGPGLVKPSETLSLTCTVSGDP VINTNYYWGWIRQPPGKGLEWIGTLSY SGGTHYNPSLSSRVTIAVDSSKKRFSLTLR SVTAADTAIYYCARHPVDGYNYGYSDL WGQGTLVTVSS	1599	EIVLTQSPATLALSVGERATLSCVASQR VSSDYIAWYQKKPGLAPRLLVYHGSA WATGSSARFSGSGSGTAFTLTISSLEPE DFAVYYCQQYGNSPFTFGPGTKVEFK	IGHV4-39 (Human)	IGHJ5 (Human)	IGKV3D-20 (Human)	IGKJ3 (Human)	2608	ARHPVDGYN YGYSDL	3810	QQYGNSP FT	Seth Zost et al., 2020 (https://www.nature.com/articles/s41591-020-0998-x)
COV2-2632	Ab	SARS-CoV2	SARS-CoV1		SARS-CoV1, SARS-CoV2	S; RBD	B-cells; SARS-CoV2 Human Patient	521	QVQLVQSGAEVKKPGASVKVSCKASGY TFTDYYMHWVRQAPGQGLEWMGWI NPNSRGTNYAQKFQGRVTMTRDTSIST VYMELSRLTSDDTAVYYCARVVVLGYGR PNNYYDGRNVWDYWGQGTLVTVSS	1600	EIVLTQSPGTLSLSPGERATLSCRASQS VSSSYLAWYQEKPGQAPRLLMYSASS RATGIPDRFSGSGSATDFTLTINRLEPE DFAVYYCQQYYVEPPFTFGQGTKLEIK	IGHV1-2 (Human)	IGHJ4 (Human)	IGKV3-20 (Human)	IGKJ2 (Human)	2609	ARVVVLGYGR PNNYYDGRN VWDY	3811	QQYVEPPF T	Seth Zost et al., 2020 (https://www.nature.com/articles/s41591-020-0998-x)
COV2-2639	Ab	SARS-CoV1, SARS-CoV2			SARS-CoV2	S; non-RBD	B-cells; SARS-CoV2 Human Patient	522	QVQLVESGGGVVQPGRSLRLSCAASGF TFSSYAMHWVRQAPGKGLEWVAVISY DEINKYYADSVKGRFTISRDNSKTTLDLQ MNSLRAEDTAVYYCARAGGGSYRGPFD YWGQGTLVTVSS	1601	QSALTQPRSVSGSPGQSVTISCTGTSS DVGGYNYVSWYQQHPGKAPKLMIYD VSKRPSGVPDRFSGSKSGNTASLTVSG LQAEDEAEYYCSAYAGSNNLVFGGGT KLTVL	IGHV3-30 (Human)	IGHJ4 (Human)	IGLV2-11 (Human)	IGLJ2 (Human)	2610	ARAGGGSYR GPFDY	3812	SAYAGSNN LV	Seth Zost et al., 2020 (https://www.nature.com/articles/s41591-020-0998-x)
COV2-2641	Ab	SARS-CoV1, SARS-CoV2			SARS-CoV2	S; non-RBD	B-cells; SARS-CoV2 Human Patient	523	QVQLVESGGGVVQPGRSLRLSCAASGF TFSTYAMHWVRQAPGKGLEWVTVISYD GSNKYYADSVKGRFTISRDNSKNTLYLQ MNSLRAEDTAVYYCAKSYNGNYYDAFDI WGQGTMVTVSS	1602	EIVLTQSPGTLSLSPGERATLSCRAGQT VSSSYLAWYQHKPGQAPRLLIYGASSR ATGIPDRFSGSGSGTDFTLTISRLEPED FAVYYCQQYGSSYTFGQGTKLEIK	IGHV3-30 (Human)	IGHJ3 (Human)	IGKV3-20 (Human)	IGKJ2 (Human)	2611	AKSYNGNYYD AFDI	3813	QQYGSSYT	Seth Zost et al., 2020 (https://www.nature.com/articles/s41591-020-0998-x)

COV2-2643	Ab	SARS-CoV2	SARS-CoV1		SARS-CoV1, SARS-CoV2	S; non-RBD	B-cells; SARS-CoV2 Human Patient	524	QVQLVESGGGVVQPGRSLRLSCAASGFTFSSYGMHWVRQAPGKGLEWVAVISYDGSNKYYADSVKGRFTISRDNAKNSLYLQMNSLRAEDTAVYYCARGSAGNYYYGMDVWGQGTTVTVSS	1603	DIQMTQSPSSLSASVGDRVTITCRASQSISSYLNWYQQKPGKAPKLLIYAASSLQSGVPSRFSGSGSGTDFTLTISSLQPEDYATYYCQQSYSTPGTFGQGTRLEIK	IGHV3-30 (Human)	IGHJ6 (Human)	IGKV1-39 (Human)	IGKJ5 (Human)	2612	ARGSAGNYYYGMDV	3814	QQSYSTPGT	Seth Zost et al., 2020 (https://www.nature.com/articles/s41591-020-0998-x)
COV2-2656	Ab	SARS-CoV2	SARS-CoV1		SARS-CoV1, SARS-CoV2	S; non-RBD	B-cells; SARS-CoV2 Human Patient	525	EVQLVQSGAEVKKPGESLKISCKGSGYSFSDYWIGWVRQMPGKGLEWMGIIYPGDSDTRYSPSFQGQVTISADKSISTAYLQWSSLKASDTAMYYCARLTFGGSGSYYFYYNGMDVWGQGTTVTVSS	1604	EIVLTQSPGTLSLSPGERATLSCRASQSVSSSYLAWYQQKPGQAPRLLIYGASSRATGIPDRFSGSGSGTDFTLTISRLEPEDFAVYYCQQYGRSSGTFGQGTKVEIK	IGHV5-51 (Human)	IGHJ6 (Human)	IGKV3-20 (Human)	IGKJ1 (Human)	2613	ARLTFGGSGSYYFYYNGMDV	3815	QQYGRSSGT	Seth Zost et al., 2020 (https://www.nature.com/articles/s41591-020-0998-x)
COV2-2660	Ab	SARS-CoV2	SARS-CoV1		SARS-CoV1, SARS-CoV2	S; non-RBD	B-cells; SARS-CoV2 Human Patient	526	EVQLVESGGGLVQPGGSLRLSCAASGFTFSSYDMHWVRQATGKGLEWVSAIGTAGDTYYPGSVKGRFTISRENAKNSLYLQMNSLRAGDTAVYYCARADPYQLLGQHYYYGMDVWGQGTTVTVSS	1605	EIVLTQSPGTLSLSPGERATLSCRASQSVSSSYLAWYQQKPGQAPRLLIYGASSRATGIPDRFSGSGSGTDFTLTISRLEPEDFAVYYCQQYGSSPLITFGQGTRLEIK	IGHV3-13 (Human)	IGHJ6 (Human)	IGKV3-20 (Human)	IGKJ5 (Human)	2614	ARADPYQLLGQHYYYGMDV	3816	QQYGSSPLIT	Seth Zost et al., 2020 (https://www.nature.com/articles/s41591-020-0998-x)
COV2-2669	Ab	SARS-CoV1, SARS-CoV2			SARS-CoV2	S; non-RBD	B-cells; SARS-CoV2 Human Patient	527	QVHLVESGGGVVQPGRSLRLSCAASGFTFSNYGMHWVRQAPGKGLEWVAVISNDEFNKFYANSVKGRFTISRDNSKNTVYLQLNSLRTEDTARYYCAKGGDGSGWAWDGDNPPTDYWGQGTLVIVSS	1606	DIVMTQSPDFLAVSLGERATISCKSSQSVLYTPKNKNYLAWYKQKPGQPPKVLIYWASTRESGVPDRFSGSGSGTDFTLIISSLQAEDAAVYYCQQYYTAPLTFGGGTRVEIK	IGHV3-30 (Human)	IGHJ4 (Human)	IGKV4-1 (Human)	IGKJ4 (Human)	2615	AKGGDGSGWAWDGDNPPTDY	3817	QQYYTAPLT	Seth Zost et al., 2020 (https://www.nature.com/articles/s41591-020-0998-x)
COV2-2673	Ab	SARS-CoV2	SARS-CoV1		SARS-CoV1, SARS-CoV2	S; NTD	B-cells; SARS-CoV2 Human Patient	528	QVTLKESGPVLVKPTETLTLTCAVSGFSLSNAKMGVSWIRQPPGKALEWLAHIFSNDEKAYSTSLKTRLTISKDTSKSQVVLTVTNMDPVDTATYYCARIVLGASGTYPSPGFDPWGQGTLVTVSS	1607	QTVVTQEPSLTVSPGGTVTLTCASSAGAVTSGYYPNWFQQKPGQAPRALIYSTANKHSWTPARFSGSLLGGKAALTLSGVQPEDEAEYYCLLYYGGAWVFGGGTKLTVL	IGHV2-26 (Human)	IGHJ5 (Human)	IGLV7-43 (Human)	IGLJ3 (Human)	2616	ARIVLGASGTYPSPGFDP	3818	LLYYGGAWV	Seth Zost et al., 2020 (https://www.nature.com/articles/s41591-020-0998-x)
COV2-2675	Ab	SARS-CoV2	SARS-CoV1		SARS-CoV1, SARS-CoV2	S; non-RBD	B-cells; SARS-CoV2 Human Patient	529	QVQLVESGGGVVQPGRSLRLSCAASGFTFSIYGMHWVRQAPGKGLEWVAVISFDGSNKYYADSVKGRFTISRDNSKNTLYLQMNSLRAEDTAVYYCAKDGSGSYYGWFDPWGQGTLVTVSS	1608	EIVLTQSPDFQSVTPKEKVTITCRASQNIGSSLHWYQQKPDQSPKVIIKYASQSFSGVPSRFSGSGSGTDFTLTINSLEAEDAATYYCHQSSSLPPTFGGGTKVEIK	IGHV3-30 (Human)	IGHJ5 (Human)	IGKV6-21 (Human)	IGKJ4 (Human)	2617	AKDGSGSYYGWFDP	3819	HQSSSLPPT	Seth Zost et al., 2020 (https://www.nature.com/articles/s41591-020-0998-x)
COV2-2676	Ab	SARS-CoV2	SARS-CoV1	SARS-CoV2 (weak)		S; non-RBD	B-cells; SARS-CoV2 Human Patient	530	QVQLVQSGAEVKKPGSSVKVSCKASGGTFSSYAINWVRQAPGQGLEWMGGIIPIFGTANYAQKFQGRVTFTADESTSTAYMEVSSLRSEDTAVYYCARSCGDCYSADLDFWGQGTLVTVSS	1609	EIVLTQSPATLSLSPGERATLSCRASQSISSFLAWYQQKPGQAPRLLIYDASNRATGIPARFSGSGSGTDFTLTISSLEPEDFAVYYCQRRSNWPPFTFGPGTKVDIK	IGHV1-69 (Human)	IGHJ4 (Human)	IGKV3-11 (Human)	IGKJ3 (Human)	2618	ARSCGDCYSADLDF	3820	QRRSNWPPFT	Seth Zost et al., 2020 (https://www.nature.com/articles/s41591-020-0998-x)
COV2-2677	Ab	SARS-CoV1, SARS-CoV2		SARS-CoV2		S; RBD	B-cells; SARS-CoV2 Human Patient	531	QLQLQESGPGLVKPSETLSLTCTVSGGSISSSSYYWGWIRQPPGKGLEWIGSMYYSGSTYYNPSLKSRVTISVDTSKNQFSLKLSSVTAADTAVYYCARLLWLRGHFDYWGQGTLVTVSS	1610	NFMLTQPHSVSESPGKTVTISCTGSSGSIASNYVQWYQQRPGSAPTTVIYEDNQRPSGVPDRFSGSIDSSSNSASLTISGLKTEDEADYYCQSYDSSNYWVFGGGTKLTVL	IGHV4-39 (Human)	IGHJ4 (Human)	IGLV6-57 (Human)	IGLJ3 (Human)	2619	ARLLWLRGHFDY	3821	QSYDSSNYWV	Seth Zost et al., 2020 (https://www.nature.com/articles/s41591-020-0998-x)
COV2-2678	Ab	SARS-CoV1, SARS-CoV2		SARS-CoV2		S; RBD	B-cells; SARS-CoV2 Human Patient	532	EVQLVESGGGVVRPGGSLRLSCAASGFIFDDYDMTWVRQAPGKGLEWVSGISWNGGNTGYADSVKGRFTISRDNAKNSLYLQMNSLRAEDTALYHCAVIMSPIPRYSGYDWAGGAFDIWGQGTMVTVSS	1611	SSELTQDPAVSVALGQTVRITCQGDSLRSYYASWYQQKPGQVPILVIYDKNNRPSGIPDRFSGSSSGNTASLTITGAQAEDEADYYCNSRDSSGNAVVFGGGTKLTVL	IGHV3-20 (Human)	IGHJ3 (Human)	IGLV3-19 (Human)	IGLJ3 (Human)	2620	AVIMSPIPRYSGYDWAGGAFDI	3822	NSRDSSGNAVV	Seth Zost et al., 2020 (https://www.nature.com/articles/s41591-020-0998-x)
COV2-2681	Ab	SARS-CoV1, SARS-CoV2			SARS-CoV2	S; non-RBD	B-cells; SARS-CoV2 Human Patient	533	QVQLVESGGGVVQPGRSLRLSCAASGFTFSFYAIHWVRQAPGQGLEWAAAISSDGTYKYYADSVKGRFTISRDNSKNTSYLQMNSLRAEDTAVYYCARALNKGFDPWGQGTLLTVSS	1612	DIVMTQSPDSLAVSLGERATINCKSSQSVLYSSNNKNYLAWYQQKPGQPPKLLIYWASTRESGVPDRFSGSGSGTDFTLTISSLQAEDVAVYYCQQYYSSPYTFGQGTKLEIK	IGHV3-30 (Human)	IGHJ5 (Human)	IGKV4-1 (Human)	IGKJ2 (Human)	2621	ARALNKGFDP	3823	QQYYSSPYT	Seth Zost et al., 2020 (https://www.nature.com/articles/s41591-020-0998-x)
COV2-2684	Ab	SARS-CoV2	SARS-CoV1	SARS-CoV2 (weak)		S; RBD	B-cells; SARS-CoV2 Human Patient	534	QMQLVQSGPEVKKPGTSVKVSCKTSGFTFTSSAIQWVRQARGQRLEWIGWIVVGSGNTNYAQKFQERVTITRDMSTSTAYMELSSLRSEDTAVYYCAAPHCNRTSCYDAFDLWGQGTMVTVSS	1613	EIVLTQSPGTLSLSPGERATLSCRASQSVSSSYLGWYQQKPGQAPRLLIYGASSRATGIPDRFSGSGSGTDFTLTISRLESEDFALYYCQQYGNWWRTFGQGTKVEIK	IGHV1-58 (Human)	IGHJ3 (Human)	IGKV3-20 (Human)	IGKJ1 (Human)	2622	AAPHCNRTSCYDAFDL	3824	QQYNNWWRT	Seth Zost et al., 2020 (https://www.nature.com/articles/s41591-020-0998-x)
COV2-2685	Ab	SARS-CoV1, SARS-CoV2			SARS-CoV2	S; non-RBD	B-cells; SARS-CoV2 Human Patient	535	QVQLVQSGAEVKKPGASVQVSCEASGYTFTTYYMHWVRQAPGQGLEWMGIINPSGGSTTYAQKFQGRVTMTRDTSTSTVYMDLSSLRSEDTAVYYCARDRLGDGSYLGGGYYGMDVWGQGTTVTVSS	1614	EIVLTQSPGTLSLSPGERATLSCRASQSVSSSYLAWYQQKRGQAPRLLIYGASSRATGIPDRFSGSGSGTDFTLTISRLEPEDFAVYYCQQYGSSPRLTFGGGTKVEIK	IGHV1-46 (Human)	IGHJ6 (Human)	IGKV3-20 (Human)	IGKJ4 (Human)	2623	ARDRLGDGSYLGGGYYGMDV	3825	QQYGSSPRLT	Seth Zost et al., 2020 (https://www.nature.com/articles/s41591-020-0998-x)
COV2-2693	Ab	SARS-CoV2	SARS-CoV1	SARS-CoV2 (weak)		S; RBD	B-cells; SARS-CoV2 Human Patient	536	QVQLVQSGAEVKKPGASVKVSCQASGYTFTSYDINWVRQATGQGLEWMGWMKSNSGNTGYAQKFQGRVTMTRNTSISTAYMELTSLRSEDTAVYYCARMRSGWPTHGRPDDLWGRGTLVTVSS	1615	QSVLTQPPSASGTPGQRVTISCSGSNSNIGSYTVNWYQQLPGTAPKLLIYDNNQRTSGVPDRLSGSKSGTSASLAISGLQSEDEANYYCAVWDDSLNGLVFGGGTKLTVL	IGHV1-8 (Human)	IGHJ5 (Human)	IGLV1-44 (Human)	IGLJ2 (Human)	2624	ARMRSGWPTHGRPDDL	3826	AVWDDSLNGLV	Seth Zost et al., 2020 (https://www.nature.com/articles/s41591-020-0998-x)
COV2-2694	Ab	SARS-CoV2	SARS-CoV1		SARS-CoV1, SARS-CoV2	S; RBD	B-cells; SARS-CoV2 Human Patient	537	QVQLVQSGAEVKRPGSSVKVSCKASGGTFSSYTISWVRQAPGQGLEWMGRIIPILAVANYAQKFQGRVTITADKSTSTAYMELSSLRSEDTAVYYCARDHSGYYDSTSLMSPFFDYWGQGTLVTVSS	1616	QSVLTQPPSVSGAPGQRVTISCTGSSSNIGAGYDVHWYQQLPGTAPKLLIFGNTNRPSGVPDRFSGSKSGTSTSLAITGLQAEDEADYYCQSYDSSLNGDVFGGGTKLTVL	IGHV1-69 (Human)	IGHJ4 (Human)	IGLV1-40 (Human)	IGLJ3 (Human)	2625	ARDHSGYYDSTSLMSPFFDY	3827	QSYDSSLNGDV	Seth Zost et al., 2020 (https://www.nature.com/articles/s41591-020-0998-x)

COV2-2697	Ab	SARS-CoV2	SARS-CoV1		SARS-CoV1, SARS-CoV2	S; non-RBD	B-cells; SARS-CoV2 Human Patient	538	QVQLVQSGAEVKKPGASVKVSCKASGYTFTSHYMHWVRQAPGQGLEWMGIINPSGGSTSYAQKFQGRVTMTGDTSTSTVYMELSSLRSEDTAVYYCARDLAGVPAALGCWFDPWGQGTLVTVSS	1617	EIVLTQSPATLSLSPGERATLSCRASQSVSSYLAWYQQKPGQAPRLLIYDAYKRDTGIPARFSGSGSGTDFTLTISSLEPEDFAVYYCQQRSNWPLIFTFGPGTKVDIK	IGHV1-46 (Human)	IGHJ5 (Human)	IGKV3-11 (Human)	IGKJ3 (Human)	2626	ARDLAGVPA ALGCWFDP	3828	QQRSNWP LIFT	Seth Zost et al., 2020 (https://www.nature.com/articles/s41591-020-0998-x)
COV2-2700	Ab	SARS-CoV2	SARS-CoV1		SARS-CoV1, SARS-CoV2	S; non-RBD	B-cells; SARS-CoV2 Human Patient	539	QVQLVESGGGVVQPGRSLRLSCAASGFTFSTYAMHWVRQAPGKGLEWVAVISYDGGNKYYADSVKGRFTISRDNSKNTLYLQMNSLRAEDTAVYYCAKNLGPYCSGGTCYSLVGDYWGQGTLVTVSS	1618	QSVLTQPPSVSGVPGQRVTVSCTGSSSNIGAGFDVYWYQQFLGTAPKLLIYGNNNRPSGVPDRFSASKSGTSASLAITGLQAEDEADYYCQSYDSSLSGYVFGTGTKVTVL	IGHV3-30-3 (Human)	IGHJ4 (Human)	IGLV1-40 (Human)	IGLJ1 (Human)	2627	AKNLGPYCSG GTCYSLVGDY	3829	QSYDSSLS GYV	Seth Zost et al., 2020 (https://www.nature.com/articles/s41591-020-0998-x)
COV2-2703	Ab	SARS-CoV2	SARS-CoV1		SARS-CoV1, SARS-CoV2	S; RBD	B-cells; SARS-CoV2 Human Patient	540	EVQLVESGGGLVQPGGSLRLSCAASGFTFSSYDMHWVRQATGKGLEWVSAIGTAGDTYYPGSVKGRFTISRENAKNSLYLQMNSLRAGDTAVYYCARARGGYNWNFDYWGQGTLVTVSS	1619	DIQMTQSPSSLSASVGDRVTITCRASQSISSYLNWYQQKPGKAPKLLIYDASSLQSGVPSRFSGSGSGTDFTLTISSLQPEDFATYYCQQSYSTPPITFGQGTRLEIK	IGHV3-13 (Human)	IGHJ4 (Human)	IGKV1-39 (Human)	IGKJ5 (Human)	2628	ARARGGYNW NFDY	3830	QQSYSTPPI T	Seth Zost et al., 2020 (https://www.nature.com/articles/s41591-020-0998-x)
COV2-2705	Ab	SARS-CoV1, SARS-CoV2			SARS-CoV2	S; RBD	B-cells; SARS-CoV2 Human Patient	541	QVQLVESGGGVVQPGRSLRLSCAASGFTFSSYAMHWVRQAPGKGLEWVAVISYDGSYKYFADSVKGRFTISRDNSKNTLYLQMNSLRAEDTAVYYCARDQGTVVTHFDYWGQGTLVTVSS	1620	DIQMTQSPSSLSTSVGDRVTITCRASQSIRSYLNWYQQKPGKAPKLLIYVASSLQSGVPSRFSGSGSGTDFTLTISSLQPEDFATYYCQQSYSTPPWTFGQGTKVEIK	IGHV3-30 (Human)	IGHJ4 (Human)	IGKV1-39 (Human)	IGKJ1 (Human)	2629	ARDQGTVVT HFDY	3831	QQSYSTPP WT	Seth Zost et al., 2020 (https://www.nature.com/articles/s41591-020-0998-x)
COV2-2709	Ab	SARS-CoV1, SARS-CoV2			SARS-CoV2	S; RBD	B-cells; SARS-CoV2 Human Patient	542	QVQLVESGGGVVQPGRSLRLSCAASGFTFSNYGMHWVRQAPGKGLEWVAVMSYDGSNKYYADSVKGRFTISRDNSKNTLYLQMNSLRAEDTAVYYCAKNLGPYCSGGTCYSLVGDYWGQGTLVTVSS	1621	DIQMTQSPSSLSASVGDRVTITCQASQDISNYLNWYQQKPGKAPKLLIYDASNLETGVPSRFSGSGSGTDFTFTISSLQPEDIATYYCQQYANLPFTFGPGTKVDIK	IGHV3-30 (Human)	IGHJ4 (Human)	IGKV1-33 (Human)	IGKJ3 (Human)	2630	AKNLGPYCSG GTCYSLVGDY	3832	QQYANLPF T	Seth Zost et al., 2020 (https://www.nature.com/articles/s41591-020-0998-x)
COV2-2710	Ab	SARS-CoV2	SARS-CoV1		SARS-CoV1, SARS-CoV2	S; RBD	B-cells; SARS-CoV2 Human Patient	543	QVQLVQSGAEVKKPGASVKVSCKASGYTFTSYDINWVRQATGQGLEWMGWMSPNSGNTGYAQKFQGRVTMTRDTSISTAYMELNSLRSEDTAVYYCARMRSGWPTHGRPDDHWGQGTLVTVSS	1622	QSVLTQPPSASGTPGQRVTISCSGSNSNIGSYTVNWYQQLPGTAPKLLIFGNNQRPSGVPDRFSGSKSGTSASLAISGLQSEDEADYYCAAWDDSRNGLVFGGGAKLTVL	IGHV1-8 (Human)	IGHJ4 (Human)	IGLV1-44 (Human)	IGLJ2 (Human)	2631	ARMRSGWPT HGRPDDH	3833	VAWDDSR NGLV	Seth Zost et al., 2020 (https://www.nature.com/articles/s41591-020-0998-x)
COV2-2713	Ab	SARS-CoV1, SARS-CoV2			SARS-CoV2	S; RBD	B-cells; SARS-CoV2 Human Patient	544	EVQLVESGGGVVQPGGSLRLSCAASGFTFDDYAMHWVRQAPGKGLEWVSLISGDGGNTYYADSVKGRFTISRDNSKNSLYLQMNSLRTEDTALYYCAKDEMAYPPSHHYYYYMDVWGKGTTVTVSS	1623	SYELTQPPSVSVSPGQTARITCSTDALPNEYIYWYQQKPGQAPVLVIYKDSERPSGIPERFSGSSSGTTVTLTISGVQAEDEADYYCQSYDSSGTYPHVIFGGGTKLTVL	IGHV3-43 (Human)	IGHJ6 (Human)	IGLV3-25 (Human)	IGLJ2 (Human)	2632	AKDEMAYPP SHHYYYYYMD V	3834	QSVDSSGT YPHVI	Seth Zost et al., 2020 (https://www.nature.com/articles/s41591-020-0998-x)
COV2-2717	Ab	SARS-CoV1, SARS-CoV2			SARS-CoV2	S; RBD	B-cells; SARS-CoV2 Human Patient	545	QVQLVQSGAEVKTPGASVKVSCKASGYTFTSYDINWVRQATGQGPEWMGWMNPNSGNTGYAHKFQGRVTMTRNTSISTAYMELSSLRSEDTAVYYCARGPSILTGFYNPLDYWGQGTLVTVSS	1624	DIQMTQSPSSLSASVGDRVTITCRASQSIISYLNWYHQKPGKAPKLLIYAASSLQSGVPSRFSGSGSGTDFTLTISSLQPEDFATYYCQQSYSTPYTFGQGTKLEIK	IGHV1-8 (Human)	IGHJ4 (Human)	IGKV1-39 (Human)	IGKJ2 (Human)	2633	ARGPSILTGFY NPLDY	3835	QQSYSTPY T	Seth Zost et al., 2020 (https://www.nature.com/articles/s41591-020-0998-x)
COV2-2718	Ab	SARS-CoV2	SARS-CoV1		SARS-CoV1, SARS-CoV2	S; non-RBD	B-cells; SARS-CoV2 Human Patient	546	QLQLQESGPGLVKPSETLSLTCTVSGGSISSSNYYWGWIRQPPGKGLEWIGTIHYSGISYYNPSLKSRVTISVDTSNNKFSLELSSVTAADTAVYFCARRTYYDLWSAYSSTAYYCMDVWGKGTTVTVSS	1625	DIQLTQSPSFLSASVGDRVTITCRASQGISSYLAWYQQKPGKAPKLLIYAASTLQSGVPSRFSGSGSGTEFTLTISSLQPEDFATYYCQQLNSYPLTFGGGTKVEIK	IGHV4-39 (Human)	IGHJ6 (Human)	IGKV1-9 (Human)	IGKJ4 (Human)	2634	ARRTYYDLWS AYSSTAYYCM DV	3836	QQLNSYPL T	Seth Zost et al., 2020 (https://www.nature.com/articles/s41591-020-0998-x)
COV2-2722	Ab	SARS-CoV1, SARS-CoV2		SARS-CoV2		S; RBD	B-cells; SARS-CoV2 Human Patient	547	QVRLVQSGAEVKKPGSSVKVSCKASGGTFSDYAISWVRQAPGQGLEWMGGIIPIFGTANYAQKFQGRVTITADEFTITAYMELSSLRSEDTAVYYCARLSGSGWLGYAMDVWGQGTTVTVSS	1626	QSALTQPASVSGSPGQSITISCTGTSSDVGGYNFVSWYQQHPGKAPKLIIYDVSNRPSGVSNRFSGSKSGNTASLTISGLQAEDEADYYCTSYTSSSTLNVVFGGGTKLTVL	IGHV1-69 (Human)	IGHJ6 (Human)	IGLV2-14 (Human)	IGLJ2 (Human)	2635	ARLSGSGWL GYAMDV	3837	TSYTSSSTL NVV	Seth Zost et al., 2020 (https://www.nature.com/articles/s41591-020-0998-x)
COV2-2726	Ab	SARS-CoV2	SARS-CoV1		SARS-CoV1, SARS-CoV2	S; non-RBD	B-cells; SARS-CoV2 Human Patient	548	QVQLVESGGGVVQPGRSLRLSCAASGFTFSSYAMHWVRQAPGKGLEWVAVISNDGRNKYYADSVKGRLTISRDNSKNTLYLQMNSLRAEDTAVYYCARPSNWYFDLWGRGTLVTVSS	1627	QSALTQPASVSGSPGQSITISCTGTSSDVGSYNLVSWYQQHPGKAPKLMIYEVSKRPSGVSNRFSGSKSGNTASLTISGLQAEDEADYYCCSYASSSIVVFGGGTKLTVL	IGHV3-30 (Human)	IGHJ2 (Human)	IGLV2-23 (Human)	IGLJ2 (Human)	2636	ARPSNWYFD L	3838	CSYASSSIV V	Seth Zost et al., 2020 (https://www.nature.com/articles/s41591-020-0998-x)
COV2-2730	Ab	SARS-CoV2	SARS-CoV1	SARS-CoV2 (weak)		S; RBD	B-cells; SARS-CoV2 Human Patient	549	EVQLVESGGGLVQPGRSLTLSCAASGFTFDDYTMHWVRQAPGKGLEWVSGIDWNGGTIGYADSVKGRFTISRDNAKNSLYLQMNSLRAEDTALYYCAKAGYYAYVWGSYRFEYFDNWGQGTLVTVSS	1628	DIQMTQSPSSLSASVGDRVTITCRASQSISSYLNWYQQKPGKAPKLLLYAASSLQSGVPSRFSGSGSGTDFTLTISSLQPEDFATYYCQQSYSTPPWTFGQGTKVEIK	IGHV3-9 (Human)	IGHJ4 (Human)	IGKV1-39 (Human)	IGKJ1 (Human)	2637	AKAGYYAYV WGSYRFEYFD N	3839	QQSYSTPP WT	Seth Zost et al., 2020 (https://www.nature.com/articles/s41591-020-0998-x)
COV2-2733	Ab	SARS-CoV2	SARS-CoV1	SARS-CoV2		S; RBD	B-cells; SARS-CoV2 Human Patient	550	EVQLVESGGGLVQPGGSLRLSCAASGVTVSSNYMSWVRQAPGKGLEWVSLIYSGGSTFYADSVKGRFTISRHNSKNTLYLQMNSLRPEDTAVYYCARGPEPDAFDIWGQGTMVTVSS	1629	DIQLTQSPSFLSASVGDRVTITCRASQGISSYLAWYQQKPGKAPKLLIYAASTLQSGVPSRFSGSGSGTEFTLTISSLQPEDFATYYCQQLNSYSFETFGPGTKVAIK	IGHV3-53 (Human)	IGHJ3 (Human)	IGKV1-9 (Human)	IGKJ3 (Human)	2638	ARGPEPDAFD I	3840	QQLNSYSF ET	Seth Zost et al., 2020 (https://www.nature.com/articles/s41591-020-0998-x)
COV2-2734	Ab	SARS-CoV1, SARS-CoV2		SARS-CoV2 (weak)		S; RBD	B-cells; SARS-CoV2 Human Patient	551	QVQLQESGPGLVKPSETLSLTCTVSGGSVSSGSYYWSWIRQPPGKGLECIGYIYYSGSSNYNPSLKSRVTISVDTSKNQFSLKMSSVTAADTAVYYCAGSPVPPTIVGASYWGQGTLVTVSS	1630	NFMLTQPHSVSESPGKTVTFSCTGSSGSIASNYVQWYQQRPGSAPTTVIYEDNQRPSGVPDRFSGSIDSSSNSASLTISGLKTEDEADYYCQSYDGINRWLVFGGGTKLTVL	IGHV4-61 (Human)	IGHJ4 (Human)	IGLV6-57 (Human)	IGLJ2 (Human)	2639	AGSPVPPTIV GASY	3841	QSYDGINR WLV	Seth Zost et al., 2020 (https://www.nature.com/articles/s41591-020-0998-x)

COV2-2736	Ab	SARS-CoV1, SARS-CoV2			SARS-CoV2	S; RBD	B-cells; SARS-CoV2 Human Patient	552	QVQLVESGGGVVQPGRSLRLSCAASGFTFSDYAMHWVRQAPGKGLEWVADISFDGSNKYYADSVKGRFTISRDSSENTLYLQMDSLRADDTAVYYCARDLSTTWYLEMWGPDAFDIWGQGTVVTVSS	1631	DIQMTQSPSTLSASIGDRVTITCRASQSISSWLAWYQQIPGKAPKLLIYKASSLESGVPSRFSGSGSGTEFTLTISSLQPDDFATYYCQQYNSYPYTFGQGTKLEIK	IGHV3-30-3 (Human)	IGHJ3 (Human)	IGKV1-5 (Human)	IGKJ2 (Human)	2640	ARDLSTTWYLEMWGPDAFDI	3842	QQYNSYPYT	Seth Zost et al., 2020 (https://www.nature.com/articles/s41591-020-0998-x)
COV2-2740	Ab	SARS-CoV1, SARS-CoV2			SARS-CoV2	S; RBD	B-cells; SARS-CoV2 Human Patient	553	QVQLVESGGGVVQPGRSLRLSCAASGFTFRRYGMYWVRQAPGKGLEWVAVISYDGTDKYYTDSVKGRFTISRDNSKNTLYLQMNSLRAEDTAVYYCAKKGGPYCGGGNCYAGYFDYWGQGTLVTVSS	1632	DIQMTQSPSSLSASIGDRVTITCRASQNIRSYLNWYQHKPGKAPKLLIYAASTLQSGVPSRFSGSESGTDFTLTISSLQPEDFATYYCQQSSSSPITFGQGTKLEIK	IGHV3-30 (Human)	IGHJ4 (Human)	IGKV1-39 (Human)	IGKJ2 (Human)	2641	AKKGGPYCGGGNCYAGYFDY	3843	QQSSSSPIT	Seth Zost et al., 2020 (https://www.nature.com/articles/s41591-020-0998-x)
COV2-2749	Ab	SARS-CoV1, SARS-CoV2			SARS-CoV2	S; RBD	B-cells; SARS-CoV2 Human Patient	554	QVQLQQWGAGLLKPSETLSLTCAVSGGSFSAYYWSWIRQPPGKGLEWIGEINHSGSTNYNPSLRSRVTISVDTSKNQFSLKLSSVTAADTAVYYCARVGYSQGYYYYYMDVWGKGTTVTVSS	1633	DIQMTQSPSSLSASVGDRVTITCRASQSISNYLNWYQQKPGKAPKLLIYAASSLQSGVPSRFSGSGSGTDFSLTISSLQPEDFATYSCQQSYTTLLTFGGGTKVEIK	IGHV4-34 (Human)	IGHJ6 (Human)	IGKV1-39 (Human)	IGKJ4 (Human)	2642	ARVGYSQGYYYYYMDV	3844	QQSYTTLLT	Seth Zost et al., 2020 (https://www.nature.com/articles/s41591-020-0998-x)
COV2-2751	Ab	SARS-CoV2	SARS-CoV1		SARS-CoV1, SARS-CoV2	S; RBD	B-cells; SARS-CoV2 Human Patient	555	EVQVVESGGGLVQPGRSLRLSCVSSGFIFDDYVMHWVRQRPGKGLEWVAGITYNGGILGYGDSVKGRFIIARDNVRGFLSLQMGDLRTEDTALYYCARDYCSSTTCPAETYYYMDVWGKGTAVTVSS	1634	SYELAQPPSVSVAPGETATIFCRATYIGRKNVQWYQQKPGQAPVLVVYDDSDRPSGIPGRFSGSNSGDTATLTISRIEAGDEAAYYCQVWDGINDRVVFGGGTKLTVL	IGHV3-9 (Human)	IGHJ6 (Human)	IGLV3-21 (Human)	IGLJ2 (Human)	2643	ARDYCSSTTCPAETYYYMDV	3845	QVWDGINDRVV	Seth Zost et al., 2020 (https://www.nature.com/articles/s41591-020-0998-x)
COV2-2752	Ab	SARS-CoV2	SARS-CoV1	SARS-CoV2		S; RBD	B-cells; SARS-CoV2 Human Patient	556	EVQLVESGGGLIQPGGSLRLSCAASEVTVSSNYMSWVRQAPGKGLEWVSLIYSGGTTYYADSVKGRFTISRDNSKNTLYLQMNSLRAEDTAVYYCARDFLRWHDLWGQGTLVTVSS	1635	DIQMTQSPSSLSASVGDRVTITCQASQDINNYLNWYQQKPGKAPKLLIYDASNLETGVPLRFSGSGSGTDFTFTISSLQPEDIATYYCQQYDNLPPVFGGGTKVEIK	IGHV3-53 (Human)	IGHJ5 (Human)	IGKV1-33 (Human)	IGKJ4 (Human)	2644	ARDFLRWHDL	3846	QQYDNLPPV	Seth Zost et al., 2020 (https://www.nature.com/articles/s41591-020-0998-x)
COV2-2753	Ab	SARS-CoV1, SARS-CoV2			SARS-CoV2	S; RBD	B-cells; SARS-CoV2 Human Patient	557	EVQLVESGGGLVQPGGSLRLSCAASGFTFSSYDMHWVRQATGKGLEWVSTIGTAGDTYYPDSVKGRFTISRENAKNSLFLQMNSLRAGDTAVYYCARVDFDILTGYYSNWGQGTLVTVSS	1636	DFQMTQSPSSLSASVGDRVTITCRASQSISTYLNWYQQKPGKAPNLLIFAASSLHSGVPSRFSGSGSGTDFTLSISSLQPEDFATYYCQQSYSSEWTFGQGTKVEIK	IGHV3-13 (Human)	IGHJ4 (Human)	IGKV1-39 (Human)	IGKJ1 (Human)	2645	ARVDFDILTGYYSN	3847	QQSYSSEWT	Seth Zost et al., 2020 (https://www.nature.com/articles/s41591-020-0998-x)
COV2-2756	Ab	SARS-CoV2	SARS-CoV1		SARS-CoV1, SARS-CoV2	S; RBD	B-cells; SARS-CoV2 Human Patient	558	EAQLLESGGALVQPGGSLRLSCAASGFTFSCCAMGWVRQAPGRGLEWVSSIHDDGVGTFYAVSVKGRFSISRDNSKNTVYLQMNGLRAEDTGVYYCAKWAGPIVMKYYLQYWGQGALVTVSS	1637	QSLLTQPPSVSGAPGQRVTLSCAGATSNIGAGSDVHWYQQLPGTAPKLLIYYNTNRPSGVPDRFSGSKSATSASLVITGLQTEDEADYYCQSYDISLGGWVFGGGTKLTVL	IGHV3-23 (Human)	IGHJ4 (Human)	IGLV1-40 (Human)	IGLJ3 (Human)	2646	AKWAGPIVMKYYLQY	3848	QSYDISLGGWV	Seth Zost et al., 2020 (https://www.nature.com/articles/s41591-020-0998-x)
COV2-2758	Ab	SARS-CoV1, SARS-CoV2			SARS-CoV2	S; RBD	B-cells; SARS-CoV2 Human Patient	559	EVQLVESGGGLVQPGGSLRLSCAASGFTFSSYDMHWVRQATGKGLEWVSAIGTAGDTYYPDSVKGRFTISRENAKNSLYLQMNSLRAGDTAVYYCARGGDSGYDLGAWYFDLWGRGTLVTVSS	1638	DIQMTQSPSSLSASVGDRVTITCRASQSVSIYLNWYQQKPGKAPKLLIYAASSLQSGVPSRFSGSGSGTDFTLTVSSLQPEDFATYYCQQSYSMPPITFGQGTRLEIK	IGHV3-13 (Human)	IGHJ2 (Human)	IGKV1-39 (Human)	IGKJ5 (Human)	2647	ARGGDSGYDLGAWYFDL	3849	QQSYSMPPIT	Seth Zost et al., 2020 (https://www.nature.com/articles/s41591-020-0998-x)
COV2-2759	Ab	SARS-CoV2	SARS-CoV1		SARS-CoV1, SARS-CoV2	S; RBD	B-cells; SARS-CoV2 Human Patient	560	EVQLVQSGAEVKKPGESLKISCKGSGYSFTNYWIGWVRQMPGKGLEWMGIIYPGDSDTRYSPSFQGQVTISADKSISTAYLQWSSLKASDTAMYYCARTPTLYNWFHPWGQGTPVTVSS	1639	QSVLTQPPSASGTPGQRVTISCSGSSSNIGSNSLNWYQQLPGTAPKLLIYSNNQRPSGVPDRFSGSKSGTSASLAISGLQSEDEADYYCAAWDDSLNGSWVFGGGTKLTVL	IGHV5-51 (Human)	IGHJ5 (Human)	IGLV1-44 (Human)	IGLJ3 (Human)	2648	ARTPTLYNWFHP	3850	AAWDDSLNGSWV	Seth Zost et al., 2020 (https://www.nature.com/articles/s41591-020-0998-x)
COV2-2760	Ab	SARS-CoV2	SARS-CoV1	SARS-CoV2 (weak)		S; RBD	B-cells; SARS-CoV2 Human Patient	561	QVTLRESGPALVKPTQTLTLTCTFSGFSLSTSGLCVSWIRQPPGKALEWLARIDWDDDKYYNTSLRTRLTISKDTSKNQVVLTMTNMDPVDTATYYCARATTFFYGMDVWGQGTTVTVSS	1640	QSVLTQPPSASGTPGQRVTISCSGSRYNIGSNYVYWYQQLPGTAPRLLIYSNNQRPSGVPDRFSGSKSGTSASLAISGLRSEDEADYYCAAWDDSLSGLIFGGGTKLTVQ	IGHV2-70 (Human)	IGHJ6 (Human)	IGLV1-47 (Human)	IGLJ2 (Human)	2649	ARATTFFYGMDV	3851	AAWDDSLSGLI	Seth Zost et al., 2020 (https://www.nature.com/articles/s41591-020-0998-x)
COV2-2762	Ab	SARS-CoV2	SARS-CoV1		SARS-CoV1, SARS-CoV2	S; RBD	B-cells; SARS-CoV2 Human Patient	562	QLQLQESGPGLVKPSETLSLTCTVSGGSISSSSYYWGWIRQPPGKGLEWIGSIYYSGITYYNPSLKSRVTISVDTSKNQFSLKLSSVTAADTAVYYCARHQRYCSSSSCHVWDYWGQGTLVTVSS	1641	QSALTQPASVSGSPGQSITISCTGTSSDVGSYNLVSWYQQHPGKAPKLMIYEGSKRPSGVSNRFSGSKSGNTASLTISGLQAEDEADYYCCSYAGSSTVLFGGGTKLTVL	IGHV4-39 (Human)	IGHJ4 (Human)	IGLV2-23 (Human)	IGLJ3 (Human)	2650	ARHQRYCSSSSCHVWDY	3852	CSYAGSSTWL	Seth Zost et al., 2020 (https://www.nature.com/articles/s41591-020-0998-x)
COV2-2765	Ab	SARS-CoV1, SARS-CoV2			SARS-CoV2	S; RBD	B-cells; SARS-CoV2 Human Patient	563	EVQLVESGGGLVQPGRSLRLSCAASGFTFDDYAMNWVRQPPGKGLEWVSGISWNSDSIGYADSVKGRFTISRDNAKNSLYLQMNSLRAEDTAMYYCAKGRGAGYTSYMDVWGKGTTVTVSS	1642	SYVLTQPPSVSVAPGKTARITCEGNNIGSKSVHWYQQKPGQAPVLVVYDDSGRPSGIPERFSGSNSGNTATLTISRVEAGDEADYFCQVWDSSSDHHVVFGGGTKLTVL	IGHV3-9 (Human)	IGHJ6 (Human)	IGLV3-21 (Human)	IGLJ2 (Human)	2651	AKGRGAGYTSYMDV	3853	QVWDSSSDHHVV	Seth Zost et al., 2020 (https://www.nature.com/articles/s41591-020-0998-x)
COV2-2767	Ab	SARS-CoV2	SARS-CoV1		SARS-CoV1, SARS-CoV2	S; RBD	B-cells; SARS-CoV2 Human Patient	564	EVQLVESGGGLVQPGGSLRLSCAASGFTVSSNYMSWVRQAPGKGLEWVSVIYPGGSAFYADSVKGRFTISRHNSNNTLCLQMNSLRTEDTAVYYCARSYDILTGYRDAFDIWGQGTMVTVSS	1643	QSVLTQPPSVSGAPGQRVTISCTGSSSNIGAGYDVHWYQQLPETAPKLLIYANSNRPSGVPDRFSGSKSGTSASLAISGLQSEAEADYYCVAWDDSRNGLVFGGGAKLTVL	IGHV3-53 (Human)	IGHJ3 (Human)	IGLV1-50 (Human)	IGLJ2 (Human)	2652	ARSYDILTGYRDAFDI	3854	VAWDDSRNGLV	Seth Zost et al., 2020 (https://www.nature.com/articles/s41591-020-0998-x)
COV2-2768	Ab	SARS-CoV2	SARS-CoV1		SARS-CoV1, SARS-CoV2	S; RBD	B-cells; SARS-CoV2 Human Patient	565	QVQLVESGGGVVQPGRSLRLSCAASGFTFSSYAMHWVRQAPGKGLEWVAVISYDGSNKYYADSVKGRFTISRDNSKNTLYLQMNSLRAEDTAVYYCARDDNSPQGSGWYFYYYYAMDVWGQGTTVTVSS	1644	QSVLTQPPSVSAAPGQKVTISCSGSSSNIGNNYVSWYQQLPGTAPKLLIYDNNERPSGIPDRFSGSKSGTSATLGITGLQTGDEADYYCGTWDSSLSAYVFGTGTKVTVL	IGHV3-30-3 (Human)	IGHJ6 (Human)	IGLV1-51 (Human)	IGLJ1 (Human)	2653	ARDDNSPQGSGWYFYYYYAMDV	3855	GTWDSSLSAYV	Seth Zost et al., 2020 (https://www.nature.com/articles/s41591-020-0998-x)

COV2-2769	Ab	SARS-CoV2	SARS-CoV1		SARS-CoV1, SARS-CoV2	S; NTD	B-cells; SARS-CoV2 Human Patient	566	QVQLVESGGGVVQPGRSLRLSCAASGFTFSTYAMHWVRQAPGKGLEWVAVISYDGSNKYYADSVKGRFTISRDNSKNTLYLQMIGLRAEDTAVYYCARDWAPTYYDMPSAFDIWGQGTMVTVSS	1645	SYVLTQPPSVSVAPGKTARITCGGNNIGNKGVHWYQQKPGQAPVLVVDDDSDRPSGIPERFSGSNSGNTATLIISSVEVGDEADFYCQVWDSSSDHPGVFGGGTKLTVL	IGHV3-30-3 (Human)	IGHJ3 (Human)	IGLV3-21 (Human)	IGLJ3 (Human)	2654	ARDWAPTYYDMPSAFDI	3856	QVWDSSSDHPGV	Seth Zost et al., 2020 (https://www.nature.com/articles/s41591-020-0998-x)
COV2-2774	Ab	SARS-CoV1, SARS-CoV2			SARS-CoV2	S; non-RBD	B-cells; SARS-CoV2 Human Patient	567	EVQLVESGGGLVQPGGSLRLSCAASGFTFSSYWMTWVRQAPGKGLEWVANIKQDGSEKYYVDSVKGRFTISRDNAKNSLSLQMNSLRVEDTAVYYCVRLGVSSWYFDYWGQGTLVTVSS	1646	SYELTQPPSVSVSPGQTASITCSGDKLGDKYACWYQQKPGQSPVLVIYQDTKRPSGIPERFSGSNSGNTATLTISGTQAMDEADYYCQAWGSSRGVFGGGTKLTVL	IGHV3-7 (Human)	IGHJ4 (Human)	IGLV3-1 (Human)	IGLJ3 (Human)	2655	VRLGVSSWYFDY	3857	QAWGSSRGV	Seth Zost et al., 2020 (https://www.nature.com/articles/s41591-020-0998-x)
COV2-2776	Ab	SARS-CoV1, SARS-CoV2			SARS-CoV2	S; non-RBD	B-cells; SARS-CoV2 Human Patient	568	EVQLVESGGDLVQPGGSLRLTCAASGFTFSSHWMTWVRQAPGKGLEWVANIKEDGREKYYVDSVKGRLTISRDNAKNSLYLQMNSLRAEDTAVYYCARVVVEVATNKGIHGVDYYYYYYMDVWGKGTTVTVSS	1647	SSELTQDPAVSVALGQTVRITCQGDSLRSYYASWYQQKPGQAPVVVIYGKNNRPSGIPDRFSGSSSGNKASLTITGAQAGDEADYYCNSRDNSGNLNWVFGGGTKLTVL	IGHV3-7 (Human)	IGHJ6 (Human)	IGLV3-19 (Human)	IGLJ3 (Human)	2656	ARVVVEVATNKGIHGVDYYYYYYMDV	3858	NSRDNSGNLNWV	Seth Zost et al., 2020 (https://www.nature.com/articles/s41591-020-0998-x)
COV2-2780	Ab	SARS-CoV2	SARS-CoV1	SARS-CoV2 (weak)		S; RBD	B-cells; SARS-CoV2 Human Patient	569	QVQLQQWGAGLLKPSETLSRTCAVYGASFSNYYWSWIRQPPGKGLEWIGEINHSENTNYNPSLKSRVTISVDTSKNQFSLRLSSVTAADTAVYYCARLRYSSSGGHIFDYWGQGTLVTVSS	1648	DIQMTQSPSSLSASVGDRVTITCQASQDINNYLNWYQQKSGKAPKLLIYDASNLETGVPSRFSGSGSGTDFTFTINSLQPEDIATYYCQQYDNLPYTFGQGTKLEIK	IGHV4-34 (Human)	IGHJ4 (Human)	IGKV1-33 (Human)	IGKJ2 (Human)	2657	ARLRYSSSGGHIFDY	3859	QQYDNLPYT	Seth Zost et al., 2020 (https://www.nature.com/articles/s41591-020-0998-x)
COV2-2783	Ab	SARS-CoV1, SARS-CoV2			SARS-CoV2	S; RBD	B-cells; SARS-CoV2 Human Patient	570	QVQLVQSGAEVKKPGSSVKVSCKASGGTFSSYAISWVRQAPGQGLEWMGGIIPIFGTANYAQKFQGRVTITADESTSTAYMELSSLRSEDTAVYYCARGLTGSSAYKDEIYFDYWGQGTLVTVSS	1649	SYELTQPPSVSVSPGQTARITCSGDALPKQYAYWYQQKPGQAPVLVIYKDTERPSGIPERFSGSSSGTTVTLTISGVQAEDEADYYCQSADSSGSRFGGGTKLTVL	IGHV1-69 (Human)	IGHJ4 (Human)	IGLV3-25 (Human)	IGLJ2 (Human)	2658	ARGLTGSSAYKDEIYFDY	3860	QSADSSGSR	Seth Zost et al., 2020 (https://www.nature.com/articles/s41591-020-0998-x)
COV2-2784	Ab	SARS-CoV2	SARS-CoV1		SARS-CoV1, SARS-CoV2	S; non-RBD	B-cells; SARS-CoV2 Human Patient	571	QVQLQESGPGLVKPSETLSLTCTVSGGSISSYYWSWIRQPPGKGLEWIGYIYYSGSTKYNPSLKSRVTISVDTSKNQFSLKLSSVTAADTAVYYCARDGGNAYSSGWYRYYYHMDVWGKGTTVTVSS	1650	EIVMTQSPATLSVSPGERATLSCRASQSVSSNLAWYQQKPGQAPRLLIYGASTRATVIPARFSGSGSGTEFTLTISSLQSEDFAVYYCQQYNNWPYTFGQGTKLEIK	IGHV4-59 (Human)	IGHJ6 (Human)	IGKV3-15 (Human)	IGKJ2 (Human)	2659	ARDGGNAYSSGWYRYYYHMDV	3861	QQYNNWPYT	Seth Zost et al., 2020 (https://www.nature.com/articles/s41591-020-0998-x)
COV2-2786	Ab	SARS-CoV2	SARS-CoV1		SARS-CoV1, SARS-CoV2	S; RBD	B-cells; SARS-CoV2 Human Patient	572	EVQLVESGGGLVQPGGSLRLSCAASGFTFSSYDLHWVRQGTGKRLEWVSAIGTAGDTYYLGSVKGRFTISRENAKNSLYLQMNSLRAGDTAVYYCARVLYDSSGFYNWFDPWGQGTLVTVSS	1651	DIQMTQSPSSLSASVGDRVTITCRASQSISSYLNWYQQKPGKAPKLLIYAASSLESGVPSRFSGSGSGTDFTLTISSLQPEDFATYYCQQSYEIPPWTFGQGTKVEIK	IGHV3-13 (Human)	IGHJ5 (Human)	IGKV1-39 (Human)	IGKJ1 (Human)	2660	ARVLYDSSGFYNWFDP	3862	QQSYEIPPWT	Seth Zost et al., 2020 (https://www.nature.com/articles/s41591-020-0998-x)
COV2-2789	Ab	SARS-CoV2	SARS-CoV1		SARS-CoV1, SARS-CoV2	S; RBD	B-cells; SARS-CoV2 Human Patient	573	QVQLVQSGAEVKKPGASVRVSCKAPGYTFTTYYIHWVRQAPGQGLEWMGIINPSAGSTTYAQKFQGRVTMTRDTSTSTVYMELSSLRSEDTAVYYCARGFHVPAALRNWFDPWGQGTLVTVSS	1652	QSVLTQPPSASGTPGQRVTISCSGSSSNIGSNTVNWYQQLPGTAPKLLIYNNNQRPSGVPDRLSGSKSGTSASLAISGLQSEDEADYYCATWDDSLNGPVFGGGTKLTVL	IGHV1-46 (Human)	IGHJ5 (Human)	IGLV1-44 (Human)	IGLJ2 (Human)	2661	ARGFHVPAALRNWFDP	3863	ATWDDSLNGPV	Seth Zost et al., 2020 (https://www.nature.com/articles/s41591-020-0998-x)
COV2-2790	Ab	SARS-CoV2	SARS-CoV1	SARS-CoV2		S; RBD	B-cells; SARS-CoV2 Human Patient	574	EVQLVESGGGLVQPGGSLRLSCAASGFTVSSNYMSWVRQAPGKGLEWVSVIYPGGSAFYADSVKGRFTISRHNSNNTLCLQMNSLRTEDTAVYYCARSYDILTGYRDAFDIWGQGTMVTVSS	1653	QSVLTQPPSVSGAPGQRVTISCTGSSSNIGSGSDVHWYQQLPGTAPKLLIYGNTNRPSGVPDRFSGSKSGTSASLAITGLQAEDEADYYCQSYDSRLSGFVVFGGGTKLTVL	IGHV3-53 (Human)	IGHJ3 (Human)	IGLV1-40 (Human)	IGLJ2 (Human)	2662	ARSYDILTGYRDAFDI	3864	QSYDSRLSGFVV	Seth Zost et al., 2020 (https://www.nature.com/articles/s41591-020-0998-x)
COV2-2794	Ab	SARS-CoV1, SARS-CoV2			SARS-CoV2	S; RBD	B-cells; SARS-CoV2 Human Patient	575	EAQLVESGGGLVQPGGSLRLSCEASGFIFSSYWMSWVRQAPGKGLEWVANIKQDGSEKYYVDSVKGRFTISRDNAKNSLYLQMNSLRAEDTAVYYCARVNDGRPNPLEYYFDYWGQGTLVTVSS	1654	SYELTQPPSVSVSPGQTARITCSGDALPKQYAYWYHQKPGQAPVLVIYKDSERPSGIPERFSGSSSGTTVTLTISGVQAEDEADYYCQSADSSGTSVLFGGGTKLTVL	IGHV3-7 (Human)	IGHJ4 (Human)	IGLV3-25 (Human)	IGLJ2 (Human)	2663	ARVNDGRPNPLEYYFDY	3865	QSADSSGTSVL	Seth Zost et al., 2020 (https://www.nature.com/articles/s41591-020-0998-x)
COV2-2796	Ab	SARS-CoV2	SARS-CoV1		SARS-CoV1, SARS-CoV2	S; RBD	B-cells; SARS-CoV2 Human Patient	576	QVQLQESGPGLVKPSQTLSLTCTVSGDSISSGRYYWSWIRQHPGKGLEWIGFVYYSGSTYYNPSLKSRVTISVDTSKNQFSLRLSSVTAADTAVYYCARETYSAYEMPPYFDYWGQGTLVTVSS	1655	QSALTQPASVSGSPGQSITISCTGTSSDVGSYNLVSWYQQHPGKAPKLMIYEGSKRPSGVSNRFSGSKSGNTASLTISGLQAEDEADYYCCSYARSSTRVFGGGTKLTVL	IGHV4-31 (Human)	IGHJ4 (Human)	IGLV2-23 (Human)	IGLJ3 (Human)	2664	ARETYSAYEMPPYFDY	3866	CSYARSSTRV	Seth Zost et al., 2020 (https://www.nature.com/articles/s41591-020-0998-x)
COV2-2797	Ab	SARS-CoV1, SARS-CoV2			SARS-CoV2	S; RBD	B-cells; SARS-CoV2 Human Patient	577	EVQLVQSGAEVKKPGESLKISCKGSGYSFTSYWIGWVRQMPGKGLEWMGIIQPGDSDTRYSPSFQGQVTMSADKSTSTAYLQWSSLKASDTAMYYCARDLIIESTIAARPGYYGMDVWGQGTTVTVSS	1656	SYELTQPPSVSVSPGQTARITCSGDAFPKQYGYWYQQKPGQAPVLVIYKDSERPSGIPERFSGSSSGTTVTLTISGVQAEDEADYYCQSADSRGAVFGSGTKVTVL	IGHV5-51 (Human)	IGHJ6 (Human)	IGLV3-25 (Human)	IGLJ1 (Human)	2665	ARDLIIESTIAARPGYYGMDV	3867	QSADSRGAV	Seth Zost et al., 2020 (https://www.nature.com/articles/s41591-020-0998-x)
COV2-2801	Ab	SARS-CoV2	SARS-CoV1		SARS-CoV1, SARS-CoV2	S; RBD	B-cells; SARS-CoV2 Human Patient	578	QVHLVQSGAEVKKPGASVKLSCKASGYTFTNYLLHWVRQAPGQGLEWMGNVNPSRGTATYPQKLDDRVTMTSDKSASTIYMELSGLRSEDTAIYYCARERSGTYFFDYWGQGTLLTVSS	1657	QSVLTQPPSASGTPGQSVTISCSGSSSNIGNNKVNWYQQLPGTAPKVLIYNSNQRPSGVPDRFSGSKSGTSASLAISGLQSEDEADYYCAVWDDSLHSYVFGTETKVTVL	IGHV1-46 (Human)	IGHJ4 (Human)	IGLV1-44 (Human)	IGLJ1 (Human)	2666	ARERSGTYFFDY	3868	AVWDDSLHSYV	Seth Zost et al., 2020 (https://www.nature.com/articles/s41591-020-0998-x)
COV2-2807	Ab	SARS-CoV2	SARS-CoV1	SARS-CoV2		S; RBD	B-cells; SARS-CoV2 Human Patient	579	QVTLRESGPALVKPTQTLTLTCTFSGFSLTTSGMCVSWIRQPPGKALEWLARIDWDDDKYYSTSLQTRLTISKDTSKNQVVLTMTNMDPVDTATYYCARETPVTAIDYWGQGTLVTVSS	1658	DIQMTQSPSSLSASVGDRVTITCRASQSISRYLNWYQQKPGKAPKLLIYTASSLQSGVPSRFSGSGSGTDFTLTISSLQPEDFATYYCQQSYSTPRTFGQGTKVEIK	IGHV2-70 (Human)	IGHJ4 (Human)	IGKV1-39 (Human)	IGKJ1 (Human)	2667	ARETPVTAIDY	3869	QQSYSTPRT	Seth Zost et al., 2020 (https://www.nature.com/articles/s41591-020-0998-x)

COV2-2808	Ab	SARS-CoV1, SARS-CoV2			SARS-CoV2	S; RBD	B-cells; SARS-CoV2 Human Patient	580	QVQLVQSGAEVKKPGSSVKVSCKASGFTFMSSAVQWVRQARGQRLEWIGWIVIGSGNTNYAQKFQERVTITRDMSTSTAYMELSSLRSEDTAVYYCAAPYCSSISCNDGFDIWGQGTMVTVSS	1659	DIQMTQSPSSLSASVGDRVTITCRASQSISNYLNWYQQKPGKAPKLLIYDASNLETGVPSRFSGSGSGTDFTFTISSLQPDDIATYYCQQYDNLPLAFGPGTKVDIK	IGHV1-58 (Human)	IGHJ3 (Human)	IGKV1-33 (Human)	IGKJ3 (Human)	2668	AAPYCSSISCNDGFDI	3870	QQYDNLPLA	Seth Zost et al., 2020 (https://www.nature.com/articles/s41591-020-0998-x)
COV2-2809	Ab	SARS-CoV2	SARS-CoV1		SARS-CoV1, SARS-CoV2	S; RBD	B-cells; SARS-CoV2 Human Patient	581	QVQLVQSGAEVKKPGASVKVSCKVSGYTFTGYVVHWVRQAPGQDLEWMGWINTGYGNTKYSQKFQGRVTISWDTSATTAYMELSNLKSEDKAVYYCASMTRMSEQTYYGMDVWGQGTTVTVSS	1660	DIQMTQSPSSLSASVGDRVTITCRASQSISNYLNWYQQKPGKAPKLLIYAASSLQSGVPSRFSGSGSGTDFSLTISSLQPEDFATYSCQQSYTTLLTFGGGTKVEIK	IGHV1-3 (Human)	IGHJ6 (Human)	IGKV1-39 (Human)	IGKJ4 (Human)	2669	ASMTRMSEQTYYGMDV	3871	QQSYTTLLT	Seth Zost et al., 2020 (https://www.nature.com/articles/s41591-020-0998-x)
COV2-2811	Ab	SARS-CoV1, SARS-CoV2			SARS-CoV2	S; non-RBD	B-cells; SARS-CoV2 Human Patient	582	QVQLVESGGGVVQPGRSLRLSCAASGFTFSSFAMHWVRQAPGKGLEWVAVISYDGSNKYYADSVKGRFTISRDNSKNTLYLQMNSLRAEDTAAYYCARELMSVGWGQGTLVTVSS	1661	QSVLTQPPSVSGAPGQRVTISCTGSSSNIGARYDVHWYQQLPGTAPKLLMYGNNNRPSGVPDRFSGSKSGTSVSLAITGLQAEDEADYYCQSYDSSLSGWVFGGGTKLTVL	IGHV3-30 (Human)	IGHJ4 (Human)	IGLV1-40 (Human)	IGLJ3 (Human)	2670	ARELMSVG	3872	QSYDSSLSGWV	Seth Zost et al., 2020 (https://www.nature.com/articles/s41591-020-0998-x)
COV2-2812	Ab	SARS-CoV2	SARS-CoV1	SARS-CoV2		S; RBD	B-cells; SARS-CoV2 Human Patient	583	EVQLVESGGGLIQPGGSLRLSCAASGITVSSNYMSWVRQAPGKGLEWVSVIYAGGSTYYADSVKGRFTISRDNSKNTLYLQMNSLRAEDTAVYYCARDALYYNGPGRDGMDVWGQGTTVTVSS	1662	VIQMTQSPSSLSASVGDRVTITCQASQDINKYLNWYQQKPGKAPKLLIYDASNLETGVPSRFSGSGSGTDFTFTISSLQPEDIATYYCQQYANLPFTFGPGTKVDIK	IGHV3-53 (Human)	IGHJ6 (Human)	IGKV1-33 (Human)	IGKJ3 (Human)	2671	ARDALYYNGPGRDGMDV	3873	QQYANLPFT	Seth Zost et al., 2020 (https://www.nature.com/articles/s41591-020-0998-x)
COV2-2813	Ab	SARS-CoV2	SARS-CoV1	SARS-CoV2		S; RBD	B-cells; SARS-CoV2 Human Patient	584	EVQLVESGGGLIQPGGSLRLSCAASGITVSSNYMSWVRQAPGKGLEWVSVIYAGGSTYYADSVKGRFTISRDNSKNTLYLQMNSLRAEDTAVYYCARDALYYNGPGRDGMDVWGQGTTVTVSS	1663	VIQMTQSPSSLSASVGDRVTITCQASQDINKYLNWYQQKPGKAPKLLIYDASNLETGVPSRFSGSGSGTDFTFTISSLQPEDIATYYCQQYDNLPRTFGQGTKLEIK	IGHV3-53 (Human)	IGHJ6 (Human)	IGKV1-33 (Human)	IGKJ2 (Human)	2672	ARDALYYNGPGRDGMDV	3874	QQYDNLPRT	Seth Zost et al., 2020 (https://www.nature.com/articles/s41591-020-0998-x)
COV2-2814	Ab	SARS-CoV1, SARS-CoV2			SARS-CoV2	S; non-RBD	B-cells; SARS-CoV2 Human Patient	585	QVQLVESGGGVVQPGRSLRLSCAASGFTFSSYGMHWVRQAPGKGLEWVAVISSDGSNKYYAGSVKGRFTISRDNSKNTLYLQMNSLRAEDTAVYYCAKDMVEPLFSHYYYYGMDVWGQGTTVTVSS	1664	QSVLTQPPSVSGAPGQRVTISCTGSSSNIGAGYDVHWYQQLPGTAPKLLIYGNSNRPSGVPDRFSGSKSGTSASLAISGLQAEDEADYSCQSYDSSLSGYVFGTGTKVTVL	IGHV3-30 (Human)	IGHJ6 (Human)	IGLV1-40 (Human)	IGLJ1 (Human)	2673	AKDMVEPLFSHYYYYGMDV	3875	QSYDSSLSGYV	Seth Zost et al., 2020 (https://www.nature.com/articles/s41591-020-0998-x)
COV2-2816	Ab	SARS-CoV2	SARS-CoV1		SARS-CoV1, SARS-CoV2	S; NTD	B-cells; SARS-CoV2 Human Patient	586	QVQLQESGPGLVKPSETLSLTCTVSGGSISSYYWSWIRQPPGKGLEWIGYIYYSGSTNYNPSLKSRVTISVDMSKNQFSLKLRSVTAADTAVYYCARAPRERLQWGEYYFDYWGQGTLVTVSS	1665	QSALTQPASVSGSPGQSITISCTGTSSDVGSYNLVSWYQQHAGKAPKLMIYEVIKRPSGVSNRFSGSKSGNTASLTISGLQAEDEADYYCCSYAVSTTYVIFGGGTKLTVL	IGHV4-59 (Human)	IGHJ4 (Human)	IGLV2-23 (Human)	IGLJ2 (Human)	2674	ARAPRERLQWGEYYFDY	3876	CSYAVSTTYVI	Seth Zost et al., 2020 (https://www.nature.com/articles/s41591-020-0998-x)
COV2-2817	Ab	SARS-CoV1, SARS-CoV2			SARS-CoV2	S; RBD	B-cells; SARS-CoV2 Human Patient	587	EVQLVESGGGLVQPGGSLRLSCAASGFTFRSYDMHWVRQVTGKGLEWVSTIGTAGDTYYPGSVKGRFTISRENAKNSLYLQMNSLRAGDTAVYYCARVFETKVIRGGRYYYYYMDVWGKGTTVTVSS	1666	DIQMTQSPSSLSASVGDRVTITCRASQSISSYLNWYQQKPGKAPKLLIYAASSLQSGVPSRFSGSGSGTDFTLTISSLQPEDFATYYCQQSYSNPSYTFGQGTKLEIK	IGHV3-13 (Human)	IGHJ6 (Human)	IGKV1-39 (Human)	IGKJ2 (Human)	2675	ARVFETKVIRGGRYYYYYMDV	3877	QQSYSNPSYT	Seth Zost et al., 2020 (https://www.nature.com/articles/s41591-020-0998-x)
COV2-2818	Ab	SARS-CoV2	SARS-CoV1		SARS-CoV1, SARS-CoV2	S; non-RBD	B-cells; SARS-CoV2 Human Patient	588	QVQLQQWGAGLLKPSETLSLTCAVYGGSFSGYYWSWIRQPPGKGLEWIGEINHSGSTNYNPSLKSRVTISVDTSKNHFSLKMNSVTAADTAVYYCARCRQMGNFYYYYMDVWGKGTTVTVSS	1667	EIVLTQSPGTLSLSPGERATLSCRASQSVASSYLAWYQQKPGQAPRLLIYGASGRATGIPDRFSGSGSGTDFTLTISRLEPEDFAVYYCQQYGSSPPRYTFGQGTKLEIK	IGHV4-34 (Human)	IGHJ6 (Human)	IGKV3-20 (Human)	IGKJ2 (Human)	2676	ARCRQMGNFYYYYMDV	3878	QQYGSSPPRYT	Seth Zost et al., 2020 (https://www.nature.com/articles/s41591-020-0998-x)
COV2-2819	Ab	SARS-CoV2	SARS-CoV1	SARS-CoV2		S; RBD	B-cells; SARS-CoV2 Human Patient	589	QVQLQESGPGLVKPSQTLSLTCTVSGDSISSAGYYWSWIRQHPGKGLEWIGYIYYSGRTYYNPSLKSRVTMSVDTSKNQFSLRLRSVTAADTAVYYCARVVPTRGPVAWFDPWGQGTLVTVSS	1668	DIQMTQSPSSLSASVGDRVTITCRASQSISSYLNWYQQRPGKAPKLLIYAASSLQSGVPSRFSGSGSGTDFTLTISTLQPEDFATYYCQQSYSTLLYTFGQGTKLEIK	IGHV4-31 (Human)	IGHJ5 (Human)	IGKV1-39 (Human)	IGKJ2 (Human)	2677	ARVVPTRGPVAWFDP	3879	QQSYSTLLYT	Seth Zost et al., 2020 (https://www.nature.com/articles/s41591-020-0998-x)
COV2-2820	Ab	SARS-CoV1, SARS-CoV2			SARS-CoV2	S; non-RBD	B-cells; SARS-CoV2 Human Patient	590	QVQLVESGGGVVQPGRSLRLSCAASGFTFSSYGMHWVRQAPGKGLEWVAVIWYDGSKKDYADSVKGRFTISRDNSKNTLYLQMNSLRAEDTAVYYCARDQSQGAYILTGYRGYGMDVWGQGTTVTVSS	1669	DIVMTQSPLSLPVTPGEPASISCRSSQSLLHSNGYNYLDWYLQKPGQSPQFLIYLGSNRASGVPDRFSGSGSGTDFILKISRVEAEDVGVYYCMQALQTPFTFGPGTKVDIK	IGHV3-33 (Human)	IGHJ6 (Human)	IGKV2-28 (Human)	IGKJ3 (Human)	2678	ARDQSQGAYILTGYRGYGMDV	3880	MQALQTPFT	Seth Zost et al., 2020 (https://www.nature.com/articles/s41591-020-0998-x)
COV2-2821	Ab	SARS-CoV1, SARS-CoV2			SARS-CoV2	S; RBD	B-cells; SARS-CoV2 Human Patient	591	QVQLVQSGAEVKKPGSSVKVSCKTAGGTSSSYAISWVRQAPGQGLEWMGRIIPILGVAIYAQKFQGRVTITADKSTSTAYMELNSLRSEDTAVYYCTTTQGGDYGDNLYYLDYWGQGTLVTVSS	1670	SYVLTQPPSVSVAPGKTASITCEGNNIGSKSVHWYQQKPGQAPVLVIYYDSDRPSGIPERFSGSNSGNTATLTISRVEAGDEADYYCQVWDSSSDRLYVFGTGTKVTVL	IGHV1-69 (Human)	IGHJ4 (Human)	IGLV3-21 (Human)	IGLJ1 (Human)	2679	TTTQGGDYGDNLYYLDY	3881	QVWDSSSDRLYV	Seth Zost et al., 2020 (https://www.nature.com/articles/s41591-020-0998-x)
COV2-2822	Ab	SARS-CoV2	SARS-CoV1		SARS-CoV1, SARS-CoV2	S; RBD	B-cells; SARS-CoV2 Human Patient	592	EVQLVESGGGLVQPGGSLRLSCAASGVTVSSNYMSWVRQAPGKGLEWVSLIYSGGSTFYADSVKGRFTISRHNSKNTLYLQMNSLRPEDTAVYYCARGPEPDAFDIWGQGTMVTVSS	1671	DIQLTQSPSFLSASVGDRVTITCRASQGISSYLAWYQQKPGKAPKLLIYAASTLQSGVPSRFSGSGSGTDFTLTISSLQPEDFATYYCQQSYSNPSYTFGQGTKLEIK	IGHV3-53 (Human)	IGHJ3 (Human)	IGKV1-9 (Human)	IGKJ2 (Human)	2680	ARGPEPDAFDI	3882	QQSYSNPSYT	Seth Zost et al., 2020 (https://www.nature.com/articles/s41591-020-0998-x)
COV2-2826	Ab	SARS-CoV2	SARS-CoV1		SARS-CoV1, SARS-CoV2	S; RBD	B-cells; SARS-CoV2 Human Patient	593	QVQLVQSGAEVKKPGASVKVSCKASGDTFTTYYIHWVRQAPGQGLEWMGIINPSGGSRSYAQKFQGRISMTSDTSTSTVYMELSSLRSEDTAVYYCARGYGFVPNVLYYFDYWGQGTLVTVST	1672	QSALTQPASVSGSPGQSITISCTGTSSDVGSYNLVSWYQQHPGKAPKLMIYEGSKRPSGVSNRFSGSKSGITASLTISGLQAEDEADYYCCSYAGSSTWLFGGGTKLTVL	IGHV1-46 (Human)	IGHJ4 (Human)	IGLV2-23 (Human)	IGLJ3 (Human)	2681	ARGYGFVPNVLYYFDY	3883	CSYAGSSTWL	Seth Zost et al., 2020 (https://www.nature.com/articles/s41591-020-0998-x)

COV2-2828	Ab	SARS-CoV1, SARS-CoV2		SARS-CoV2		S; RBD	B-cells; SARS-CoV2 Human Patient	594	EVQLVESGGGLVKPGGSLRLSCAASGFTFRDYSMNWVRQAPGKGLEWVSSISSGGSYIYYADSVKGRFTISRDNAKNSLYLQMNSLRAEDTAVYYCARGGSILWWLIDYWGQGTLVTVSS	1673	NFMLTQPHSVSESPGKTVTISCTGSSGSIASNYVQWYQQRPGSAPTTVIYEDNQRPSGVPDRFSGSIDSSSNSASLTISGLKTEDEADYYCQSYDSTSRVVFGGGTKLTVL	IGHV3-21 (Human)	IGHJ4 (Human)	IGLV6-57 (Human)	IGLJ2 (Human)	2682	ARGGSILWWLIDY	3884	QSYDSTSRVV	Seth Zost et al., 2020 (https://www.nature.com/articles/s41591-020-0998-x)
COV2-2830	Ab	SARS-CoV2	SARS-CoV1		SARS-CoV1, SARS-CoV2	S; NTD	B-cells; SARS-CoV2 Human Patient	595	EVQLLESGGGLVQPGGSLRLSCAASGFTFSYAMSWVRQAPGKGLEWVSGISISGGSTYYAASVKGRFTISRDNSKNTLYLQMNSLRAEDTAVYYCAKDSRSGIAGVDAFDIWGQGTMVTVSS	1674	SYVLTQPPSVSVAPGRTARITCGGNNIGSKSVHWYQQKPGQAPVLVVYDDSDRPSGIPERFSGSKFGNTATLIISRVEAGDEADYSCQVWDSGSDHVVFGGGTKVTVL	IGHV3-23 (Human)	IGHJ3 (Human)	IGLV3-21 (Human)	IGLJ2 (Human)	2683	AKDSRSGIAGVDAFDI	3885	QVWDSGSDHVV	Seth Zost et al., 2020 (https://www.nature.com/articles/s41591-020-0998-x)
COV2-2832	Ab	SARS-CoV2	SARS-CoV1	SARS-CoV2		S; RBD	B-cells; SARS-CoV2 Human Patient	596	EVQLVESGGGLVQPGGSLRLSCAASGLTVSSNYMSWVRQAPGKGLECVSVIYAGGNTYYADSVKGRFTISRDNSKNTLYLQMNSLRAEDTAVYYCARGDGGYYSPFDYWGQGTLVTVSS	1675	DIQMTQSPSSLSASVGDRVTITCRASQSISSYLNWYQQKPGKAPKVLIYAASTMQSGVPSRFRGSGSGTDFTLTISSLQLEDFATYYCQQSYSTPQTFGQGTKVEIK	IGHV3-66 (Human)	IGHJ4 (Human)	IGKV1-39 (Human)	IGKJ1 (Human)	2684	ARGDGGYYSPFDY	3886	QQSYSTPQT	Seth Zost et al., 2020 (https://www.nature.com/articles/s41591-020-0998-x)
COV2-2834	Ab	SARS-CoV1, SARS-CoV2			SARS-CoV2	S; RBD	B-cells; SARS-CoV2 Human Patient	597	QITLKESGPTLVKPTQTLTLTCTFSGFSLSTSGVGVAWIRQPPGKALEWLALIYWDDDKRYSPSLKSRLTITKDTSKNQVVLTMTNMDPVDTATYYCAHRLPTPQLLPSFENWFDPWGQGTLVTVSS	1676	QSVLTQPPSVSEAPRQRVTISCSGGSSNIGNNAVNWYQQLPGKAPKLLIYYDDLLPSGVSDRFSGSKSGTSASLAISGLQSEDEADYYCASWDDSLIGPVFGGGTKLTVL	IGHV2-5 (Human)	IGHJ5 (Human)	IGLV1-36 (Human)	IGLJ2 (Human)	2685	AHRLPTPQLLPSFENWFDP	3887	ASWDDSLIGPV	Seth Zost et al., 2020 (https://www.nature.com/articles/s41591-020-0998-x)
COV2-2835	Ab	SARS-CoV2	SARS-CoV1	SARS-CoV2		S; RBD	B-cells; SARS-CoV2 Human Patient	598	EVQLVESGGGLVQPGGSLRLSCAASGLTVGSNYMNWVRQAPGKGLEWVSVIYSGGSTFYADSVKGRFTISRDNSKNTLYLQLNSLRAEDTAVYYCARFVVGYFDCWGQGTLVTVSS	1677	DIQLTQSPSFLSASVGDRVTITCRASQGISTYLAWYQQKPGKAPKLLIYAASTLQSGVPSRFSGSGSGTEFTLTISSLQPEDFATYYCQQLNSYPGYTFGQGTKLEIK	IGHV3-66 (Human)	IGHJ4 (Human)	IGKV1-9 (Human)	IGKJ2 (Human)	2686	AREVVGYFDC	3888	QQLNSYPGYT	Seth Zost et al., 2020 (https://www.nature.com/articles/s41591-020-0998-x)
COV2-2841	Ab	SARS-CoV2	SARS-CoV1	SARS-CoV2		S; RBD	B-cells; SARS-CoV2 Human Patient	599	QVQLQESGPGLVKPSETLSLTCTVSGGSISSYYWSWIRQPPGKGLEWIGHIYYTGSSYYNPSLKSRVTISLDTSKNQFSLKLNSVTAADTAVYYCARLRWLRGGIDFWGQGTLVIVSS	1678	NLMLTQPHSVSESPGKTVTISCTGSSGSIASNYVQWYQQRPGSAPTTVIYEDNQRPSGVPDRFSGSIDSSSNSASLTISGLKTEDEADYYCQSYDSNNQVFGGGTKLTVL	IGHV4-59 (Human)	IGHJ4 (Human)	IGLV6-57 (Human)	IGLJ3 (Human)	2687	ARLRWLRGGIDF	3889	QSYDSNNQV	Seth Zost et al., 2020 (https://www.nature.com/articles/s41591-020-0998-x)
COV2-2842	Ab	SARS-CoV1, SARS-CoV2			SARS-CoV2	S; RBD	B-cells; SARS-CoV2 Human Patient	600	QVQLVQSGAEVKKPGASVKVSCKASGDTFTTYYIHWVRQAPGQGLEWMGIINPSGGSRSYAQKFQGRISMTSDTSTSTVYMELSSLRSEDTAVYYCARGYGFVPNVLYYFDYWGQGILVTVSS	1679	QVQLVQSGAEVKKPGASVKVSCKASGDTFTTYYIHWVRQAPGQGLEWMGIINPSGGSRSYAQKFQGRISMTSDTSTSTVYMELSSLRSEDTAVYYCARGYGFVPNVLYYFDYWGQGILVTVSS	IGHV1-46 (Human)	IGHJ4 (Human)	IGLV6-57 (Human)	IGLJ2 (Human)	2688	ARGYGFVPNVLYYFDY	3890	QSYDSSDVV	Seth Zost et al., 2020 (https://www.nature.com/articles/s41591-020-0998-x)
COV2-2844	Ab	SARS-CoV1, SARS-CoV2			SARS-CoV2	S; non-RBD	B-cells; SARS-CoV2 Human Patient	601	QVELVESGGGVVQPGRSLRLSCAASGFIFSSYAMHWVRQAPGKGLEWVAVISYDGGNKYYADSVKGRFTISRDNSKNTLYLQMNSLRAEDTAVYYCARAQGGNYYYGMDVWGQGTTVTVSS	1680	SYVLTQPPSVSVAPGKTARITCGGNNIGSKNVHWYQQKPGQAPVKVVYHDGDRPSGIPERFSGSNSGNTATLTINRVEAGDEADYSCQVWDSSSDHHVVFGGGTKLTVL	IGHV3-30-3 (Human)	IGHJ6 (Human)	IGLV3-21 (Human)	IGLJ2 (Human)	2689	ARAQGGNYYYGMDV	3891	QVWDSSSDHHVV	Seth Zost et al., 2020 (https://www.nature.com/articles/s41591-020-0998-x)
COV2-2848	Ab	SARS-CoV1, SARS-CoV2		SARS-CoV2 (weak)		S; RBD	B-cells; SARS-CoV2 Human Patient	602	QVQLVESGGGVVQPGRSLRLSCAASGFTFSRYAMYWVRQAPGKGLEWVALISYDGRNEYYADSVKGRFTISRDNSKNTLYLQMNSLRAGDSAVYYCARDLAYHPYRDYGDDDYYYYGMDVWGQGTTVTVSS	1681	SYELTQPPSVSVSPGQTARITCFGDALPKQYAYWYQQKPGQGPVLVIYKDSERPSGIPERFSGSTSGTTVTLTISGVQAEDEADYYCQSADSSGTYRVFGGGTKLTVL	IGHV3-30 (Human)	IGHJ6 (Human)	IGLV3-25 (Human)	IGLJ3 (Human)	2690	ARDLAYHPYRDYGDDDYYYYGMDV	3892	QSADSSGTYRV	Seth Zost et al., 2020 (https://www.nature.com/articles/s41591-020-0998-x)
COV2-2853	Ab	SARS-CoV2	SARS-CoV1		SARS-CoV1, SARS-CoV2	S; RBD	B-cells; SARS-CoV2 Human Patient	603	QVQLVQSGAEVKKPGASVKVSCKASGYTFTSYYMHWVRQAPGQGLEWMGIINPGGGSTTYAQKFQGRVTMTSDTSTSTVYMELSSLRSEDTAMYYCARGAIPPNSRAEIDYWGQGTLVTVSS	1682	EIVMTQSPATLSVSPGERVTLSCRASQSVSSNLAWCQQKPGQAPRLLIYGASTRATGIPARFSGSGSGTEFTLTISSLQSEDFAVYYCQQYYNWPLTFGGGTKVEIK	IGHV1-46 (Human)	IGHJ4 (Human)	IGKV3-15 (Human)	IGKJ4 (Human)	2691	ARGAIPPNSRAEIDY	3893	QQYYNWPLT	Seth Zost et al., 2020 (https://www.nature.com/articles/s41591-020-0998-x)
COV2-2863	Ab	SARS-CoV1, SARS-CoV2			SARS-CoV2	S; RBD	B-cells; SARS-CoV2 Human Patient	604	QVQLVQSGAEVKKPGASVKVSCKASGYTFTSYYLHWVRQAPGQGLEWMGIINPSGGSTTYAQKFQGRVTMTRDTSTSAVYMELRSLRSEDTAVYYCARENDYGDYVEPRDYYYGMDVWGQGTTVTVSS	1683	SYELTQPPSVSVSPGQTARITCSGDALPKQYAYWYQQKPGQAPVLVIYKDSERPSGIPERFSGSSSGTTVTLTISGVQAEDEADYYCQSADSSAAYVVFGGGTKLTVL	IGHV1-46 (Human)	IGHJ6 (Human)	IGLV3-25 (Human)	IGLJ2 (Human)	2692	ARENDYGDYVEPRDYYYGMDV	3894	QSADSSAAYVV	Seth Zost et al., 2020 (https://www.nature.com/articles/s41591-020-0998-x)
COV2-2872	Ab	SARS-CoV2	SARS-CoV1		SARS-CoV1, SARS-CoV2	S; non-RBD	B-cells; SARS-CoV2 Human Patient	605	QVQLVESGGGVVQPGRSLRLSCAASGFTFSTYGMHWVRQAPGKGLEWVAVIWYDGNKKYCADSVKGRCTISRDNSKNTLYLQMNSLRAEDTAVYYCAREGPFGDREASGAFDVWGQGTMVTVSS	1684	SYELTQPPSVSVSPGQTARITCSGDALPKKYTYWYQQKSGQAPVVVIYEDSKRPSGIPERFSGSSSGTMATLTISGAQVEDEADYYCYSTDSSGKGVFGGGTKLTVL	IGHV3-33 (Human)	IGHJ3 (Human)	IGLV3-10 (Human)	IGLJ3 (Human)	2693	AREGPFGDREASGAFDV	3895	YSTDSSGKGV	Seth Zost et al., 2020 (https://www.nature.com/articles/s41591-020-0998-x)
COV2-2873	Ab	SARS-CoV1, SARS-CoV2			SARS-CoV2	S; RBD	B-cells; SARS-CoV2 Human Patient	606	QVQLVESGGGLVKPGGSLRLSCAASGFTFSDYYMSWIRQAPGKGLEWVSYISSSGITIYYADSVKGRFTISRDNAKNSLYLQMNSLRAEDTAVYYCTGVVAAPAEYFQHWGQGTLVTVSS	1685	SYVLTQPPSVSVAPGKTARITCGGNNIGSKSVHWYQQKPGQAPVLVVYDDSDRPSGIPERFSGSNSGNTATLTISRVEAGDEADYYCQVWDSSSDPFYVFGTGTKVTVL	IGHV3-11 (Human)	IGHJ1 (Human)	IGLV3-21 (Human)	IGLJ1 (Human)	2694	TGVVAAPAEYFQH	3896	QVWDSSSDPFYV	Seth Zost et al., 2020 (https://www.nature.com/articles/s41591-020-0998-x)
COV2-2878	Ab	SARS-CoV1, SARS-CoV2		SARS-CoV2 (weak)		S; RBD	B-cells; SARS-CoV2 Human Patient	607	EVQLVESGGGLVQPGGSLRLSCAASGFTFSRHWMTWVRQAPGKGLEWVANIKQDGSEKYYVDSVKGRLTISRDNAKNSLYLQMNSLRAEDTAVYYCARLGFYYGGADYWGQGTLVTVSS	1686	NFMLTQPHSVSESPGKTVTISCTGSSGSIASNYVQWYQQRPGSAPTTVISEDNQRPSGVPDRFSGSIDSSSNSASLTISGLKTEDEADYYCQSYDGINRAWVFGGGTKLTVL	IGHV3-7 (Human)	IGHJ4 (Human)	IGLV6-57 (Human)	IGLJ3 (Human)	2695	ARLGFYYGGADY	3897	QSYDGINRAWV	Seth Zost et al., 2020 (https://www.nature.com/articles/s41591-020-0998-x)

COV2-2883	Ab	SARS-CoV1, SARS-CoV2			SARS-CoV2	S; non-RBD	B-cells; SARS-CoV2 Human Patient	608	QVQLVESGGGVVQPGRSLRLSCAASGFTFSTYGMHWVRQAPGKGLEWVAVISYDGSNKYYADSVKGRFTISRDNSKNTLYLQMNSLRAEDTAMYYCAKDGSIAAADYWGQGTLVTVSS	1687	DIVMTQSPDSLAVSLGERATINCKSSQSVLHSSNNKDSLVWYQQKPGQPPKLLIYWASSRESGVPDRFSGSGSGTDFTLTISSLQAEDVAVYYCQQYYSTPWTFGQGTKVEIK	IGHV3-30 (Human)	IGHJ4 (Human)	IGKV4-1 (Human)	IGKJ1 (Human)	2696	AKDGSIAAADY	3898	QQYYSTPWT	Seth Zost et al., 2020 (https://www.nature.com/articles/s41591-020-0998-x)
COV2-2891	Ab	SARS-CoV2	SARS-CoV1		SARS-CoV1, SARS-CoV2	S; RBD	B-cells; SARS-CoV2 Human Patient	609	QVQLVQAGAEVKKPGASVKVSCKASGYTFTSYYMHWVRQAPGQGLEWMGIINPSGGSTSYAQKFQGRVTMTRDTSTSTVYMELSSLRSEDTAVYYCARGAAVPAAGEFDYWGQGTLVTVSS	1688	DIQMTQSPSTLSASVGDRVTITCRASQSISSWLAWYQQKPGKAPKLLIYKASSLESGVPSRFSGSGSGTEFTLTISSLQPDDFATYYCQQYNSYSYTFGQGTKLEIK	IGHV1-46 (Human)	IGHJ4 (Human)	IGKV1-5 (Human)	IGKJ2 (Human)	2697	ARGAAVPAAGEFDY	3899	QQYNSYSYT	Seth Zost et al., 2020 (https://www.nature.com/articles/s41591-020-0998-x)
COV2-2894	Ab	SARS-CoV1, SARS-CoV2			SARS-CoV2	S; RBD	B-cells; SARS-CoV2 Human Patient	610	QVQLVESGGGVVQSGGSLRLSCAASGFTFSTYGMHWVRQAPGKGLEWVAIISYDGINKYYADSVKGRFTISRDNSKNTVYLQMNSLRTEDTAMYYCAKGDGSYLMDYFDYWGQGTLVTVSS	1689	EIVMTQSPATLSVSPGERATLSCRASQSVSNNLAWYQQKPGQAPRLLIYGASTRATGIPVRFSGSGSGTEFTLTISSLQSEDFAVYYCQQYDDWPPEVTFGGGTKVEIK	IGHV3-30 (Human)	IGHJ4 (Human)	IGKV3-15 (Human)	IGKJ4 (Human)	2698	AKGDGSYLMDYFDY	3900	QQYDDWPPEVT	Seth Zost et al., 2020 (https://www.nature.com/articles/s41591-020-0998-x)
COV2-2901	Ab	SARS-CoV2	SARS-CoV1		SARS-CoV1, SARS-CoV2	S; RBD	B-cells; SARS-CoV2 Human Patient	611	EVQLVESGGGLVQPGGSLRLSCAASGFTVSSNYMSWVRQAPGKGLEWVSVIYPGGSAFYADSVKGRFTISRHNSNNTLCLQMNSLRTEDTAVYYCARSYDILTGYRDAFDIWGQGTMVTVSS	1690	QSVLTQPPSVSGAPGQRVTISCTGSSSNIGSGSDVHWYQQLPGTAPKLLIYGNTNRPSGVPDRFSGSKSGTSASLAITGLQAEDEADYYCVAWDDSRNGLVFGGGAKLTVL	IGHV3-53 (Human)	IGHJ3 (Human)	IGLV1-40 (Human)	IGLJ2 (Human)	2699	ARSYDILTGYRDAFDI	3901	VAWDDSRNGLV	Seth Zost et al., 2020 (https://www.nature.com/articles/s41591-020-0998-x)
COV2-2904	Ab	SARS-CoV1, SARS-CoV2			SARS-CoV2	S; non-RBD	B-cells; SARS-CoV2 Human Patient	612	QVQLQQWGAGLLKPSETLSLTCAVYGGSFSGYYWSWIRQPPGKGLEWIGEINHSGSTNYNPSLKSRVTISVDTSKNHFSLKMNSVTAADTAVYYCARCRQMGNFYYYYMDVWGKGTTVTVSP	1691	QSVLTQPPSVSGVPGQRVTVSCTGSSSNIGAGFDVYWYQQFLGTAPKLLIYGNNNRPSGVPDRFSASKSGTSASLAITGLQAEDEADYYCQSFDIGRGGWIFGGGTKLTVL	IGHV4-34 (Human)	IGHJ6 (Human)	IGLV1-40 (Human)	IGLJ2 (Human)	2700	ARCRQMGNFYYYYMDV	3902	QSFDIGRGGWI	Seth Zost et al., 2020 (https://www.nature.com/articles/s41591-020-0998-x)
COV2-2906	Ab	SARS-CoV1, SARS-CoV2			SARS-CoV2	S; RBD	B-cells; SARS-CoV2 Human Patient	613	EVQLVQSGAEVKKPGESLKISCKGSGYSFTSYWVGWVRQMPGKGLEWMGIIYPGDSDTRDSPSFQGQVTISADKSISTAYLQWSSLKASDTAMYYCARLGSESKIDYYYYGMDVWGQGTTVTVSS	1692	DIQMTQSPSSLSASVGDRVTITCRPSQSITTYLNWYQQKPGKAPRLLIYAVSSLQSGVPSRFSGSGSGTDFTLTISSLQPEDFATYYCQQSYSTPPTFGQGTRLEIK	IGHV5-51 (Human)	IGHJ6 (Human)	IGKV1-39 (Human)	IGKJ5 (Human)	2701	ARLGSESKIDYYYYGMDV	3903	QQSYSTPPT	Seth Zost et al., 2020 (https://www.nature.com/articles/s41591-020-0998-x)
COV2-2909	Ab	SARS-CoV2	SARS-CoV1		SARS-CoV1, SARS-CoV2	S; RBD	B-cells; SARS-CoV2 Human Patient	614	QVQLVQSGAEVKKPGSSVKVSCKASGDTFSSYTINWVRQAPGQGLEWMGRIIPILGIPNYAQKFQGRVTITADKSTSTAFMELSSLRSEDTAVYYCARGRGYSNYGASYYMDVWGKGTTVTVSS	1693	QSVLTQPPSVSGAPGQRVTISCTGSSSNIGAGYDVHWYQQLPETAPKLLIYANSNRPSGVPDRFSGSKSGTSASLAITGLQAEDEADYYCQSYDSSLSGSVFGGGTKLTVL	IGHV1-69 (Human)	IGHJ6 (Human)	IGLV1-40 (Human)	IGLJ2 (Human)	2702	ARGRGYSNYGASYYMDV	3904	QSYDSSLSGSV	Seth Zost et al., 2020 (https://www.nature.com/articles/s41591-020-0998-x)
COV2-2911	Ab	SARS-CoV2	SARS-CoV1		SARS-CoV1, SARS-CoV2	S; RBD	B-cells; SARS-CoV2 Human Patient	615	QLQLRESGPGLVKPSETLSLTCTVSGGSISSSSYYWGWIRQPPGKGLEWIGSIYYSGSTYYNPSLKSRVTISVDTSKNQFSLKLSSVTAADTAVFYCARMSRGYNYAYTFDIWGQGTMVTVSS	1694	QSALTQPASVSGSPGQSITISCTGTSSDVGSYNLVSWYQQHPGKAPKLKIYEGSKRPSGVSNRFSGSKSGNTASLTISGLQAEDEADYYCCSYAGSVLFGGGTKLTVL	IGHV4-39 (Human)	IGHJ3 (Human)	IGLV2-23 (Human)	IGLJ2 (Human)	2703	ARMSRGYNYAYTFDI	3905	CSYAGSVL	Seth Zost et al., 2020 (https://www.nature.com/articles/s41591-020-0998-x)
COV2-2919	Ab	SARS-CoV2	SARS-CoV1	SARS-CoV2		S; RBD	B-cells; SARS-CoV2 Human Patient	616	QVTLRESGPALVKPTQTLTLTCTFSGFSLSTSGMCLSWIRQPPGKALEWLARIDWDDDKYYSTSLETRLTISKDTSKNQVVLTMTNMDPVDTGTYYCARTMATINAFDIWGQGTMVTVSS	1695	DIQMTQSPSSLSASAGDRVTITCRASQSIRYYLNWYQQKPGKAPKLLIYAASSLQSGVPSRFSGSGSGTDFTLTISSLQPEDFAAYYCQQSFSTPRTFGQGTKLEIK	IGHV2-70 (Human)	IGHJ3 (Human)	IGKV1-39 (Human)	IGKJ2 (Human)	2704	ARTMATINAFDI	3906	QQSFSTPRT	Seth Zost et al., 2020 (https://www.nature.com/articles/s41591-020-0998-x)
COV2-2933	Ab	SARS-CoV1, SARS-CoV2			SARS-CoV2	S; non-RBD	B-cells; SARS-CoV2 Human Patient	617	QVQLVESGGGVVQPGRSLRLSCAASGFTFSYYPMHWLWVRQAPGKGLEWVAVTSYDGTNKYYADSVKGRFTISRDNSKNTLYLQMNSLRAEDTAVYYCARGGATNFDYWGQGTLVTVSS	1696	SYVLTQPPSVSVAPGKTANITCGGNNIGRKSVHWYQQKSGQAPVLVVYDDSDRPSGIPERFSGSNSGNTATLTISRVEAGDEADYYCQVWDSSSDHPEWVFGGGTKLTVL	IGHV3-30-3 (Human)	IGHJ4 (Human)	IGLV3-21 (Human)	IGLJ3 (Human)	2705	ARGGATNFDY	3907	QVWDSSSDHPEWV	Seth Zost et al., 2020 (https://www.nature.com/articles/s41591-020-0998-x)
COV2-2934	Ab	SARS-CoV2	SARS-CoV1		SARS-CoV1, SARS-CoV2	S; non-RBD	B-cells; SARS-CoV2 Human Patient	618	QVQLVQSGSELKKPGASVKVSCKASEYTFTSYAMNWVRQAPGQGLEWMGWINTNTGNPTYAQGFTGRFVFSLDTSVSTAYLQISSLKAEDTAVYYCARPGKAAAFDYWGQGTLVTVSS	1697	DIVMTQSPLSLPVTPGEPASISCRSSQSLLHSNGYNFLDWYLQKPGQSPQLLIYLGSNRASGVPDRFSGSGSGTDFTLKISRVQAEDVGVYYCMQALQTPWTFGQGTKVEIK	IGHV7-4-1 (Human)	IGHJ4 (Human)	IGKV2-28 (Human)	IGKJ1 (Human)	2706	ARPGKAAAFDY	3908	MQALQTPWT	Seth Zost et al., 2020 (https://www.nature.com/articles/s41591-020-0998-x)
COV2-2939	Ab	SARS-CoV2	SARS-CoV1		SARS-CoV1, SARS-CoV2	S; RBD	B-cells; SARS-CoV2 Human Patient	619	QVQLVESGGGVVQPGRSLRLSCAASGFTFSSYGMHWVRQAPGKGLEWVAVIWYDGSNKYYAESVKGRFTISRDNSKNTLYLQMNSLRAEDTAVYYCARDLHQDWVVVVAANVYGMDVWGQGTTVTVSS	1698	SSELTQDPAVSVALGQTVRITCQGDSLRRYYASWYQQKPGQAPVLVIYGKNNRPSGIPDRFSGSSSGNTASLTITGAQAEDEADYYCNSRDSSGNPRWFGGGTKLTVL	IGHV3-33 (Human)	IGHJ6 (Human)	IGLV3-19 (Human)	IGLJ3 (Human)	2707	ARDLHQDWVVVVAANVYGMDV	3909	NSRDSSGNPRW	Seth Zost et al., 2020 (https://www.nature.com/articles/s41591-020-0998-x)
COV2-2941	Ab	SARS-CoV2	SARS-CoV1	SARS-CoV2 (weak)		S; RBD	B-cells; SARS-CoV2 Human Patient	620	QMQLVQSGPEVKKPGTSVKVSCKASGFTFMSSAVQWVRQARGQRLEWIGWIVIGSGNTNYAQKFQERVTITRDMSTSTAYMELSSLRSEDTAVYYCAAPYCSSISCNDGFDIWGQGTMVTVSS	1699	EIVLTQSPGTLSLSPGERATLSCRASQSVSSSYLAWYQQKPGQAPRLLIYGASSRATGIPDRFSGSGSGTDFTLTISRLEPEDFAVYYCQQYGSSPPRYTFGQGTKLEIK	IGHV1-58 (Human)	IGHJ3 (Human)	IGKV3-20 (Human)	IGKJ2 (Human)	2708	AAPYCSSISCNDGFDI	3910	QQYGSSPPRYT	Seth Zost et al., 2020 (https://www.nature.com/articles/s41591-020-0998-x)
COV2-2942	Ab	SARS-CoV2	SARS-CoV1		SARS-CoV1, SARS-CoV2	S; non-RBD	B-cells; SARS-CoV2 Human Patient	621	QVTLRESGPALVKPTQTLTLTCTFSGFSLSTSGLCVSWIRQPPGKALEWLARIDWDDDKYYNTSLRTRLTISKDTSKNQVVLTMTNMDPVDTATYYCARATTFFYGMDVWGQGTTATVSS	1700	SYELTQPPSVSVSPGQTARITCSTDALPNEYIYWYQQKPGQAPVLVIYKDSERPSGIPERFSGSSSGTTVTLTISGVQAEDEADYYCQSVDSSGTYRVFGGGTKLTVL	IGHV2-70 (Human)	IGHJ6 (Human)	IGLV3-25 (Human)	IGLJ3 (Human)	2709	ARATTFFYGMDV	3911	QSVDSSGTYRV	Seth Zost et al., 2020 (https://www.nature.com/articles/s41591-020-0998-x)
COV2-2944	Ab	SARS-CoV1, SARS-CoV2			SARS-CoV2	S; RBD	B-cells; SARS-CoV2 Human Patient	622	QVQLVESGGGVVQPGRSLRLSCAASGFTFRRYGMYWVRQAPGKGLEWVAVISYDGTDKYYTDSVKGRFTISRDNSKNTLYLQMNSLRAEDTAVYYCAKKGGPYCGGGNCYAGYFDYWGQGILVTVSS	1701	DIQMTQSPSSLSASVGDRVTITCQASQDISNYLNWYQQKAGKAPKLLIYDASNLETGVPSRFSGSGSGTDFTFTISSLQPDDIATYYCQQYDNLPLAFGPGT KVDVK	IGHV3-30 (Human)	IGHJ4 (Human)	IGKV1-33 (Human)	IGKJ3 (Human)	2710	AKKGGPYCGGGNCYAGYFDY	3912	QQYDNLPLA	Seth Zost et al., 2020 (https://www.nature.com/articles/s41591-020-0998-x)

COV2-2945	Ab	SARS-CoV1, SARS-CoV2			SARS-CoV2	S; RBD	B-cells; SARS-CoV2 Human Patient	623	EVQVVESGGGLVQPGRSLRLSCAASGFT FEDYAMHWVRQAPGKGLEWVSGVSW NSGIIGYADSVKGRFTISRDNAKNSLYLQ MNSLRAEDTALYYCAKLDVGGYDFVSG HYYAFDIWGQGTMVTVSS	1702	DVVMTQSPLSLPVTLGQPASISCRSSQ SLVYSDGNTYLNWFQQRPGQSPRRLI YKVSSRDSGVPDRFSGSGSGTAFTLKIS RVEAEDVGVYYCMQGTHWPYTFGQ GTKLEIK	IGHV3-9 (Human)	IGHJ3 (Human)	IGKV2-30 (Human)	IGKJ2 (Human)	2711	AKLDVGGYDF VSGHYYAFDI	3913	MQGTHW PYT	Seth Zost et al., 2020 (https://www.nature.com/articles/s41591-020-0998-x)
COV2-2947	Ab	SARS-CoV2	SARS-CoV1		SARS-CoV1, SARS-CoV2	S; non-RBD	B-cells; SARS-CoV2 Human Patient	624	QVQLVQSGSELKKPGASVKVSCKASGYT FSDYAMNWVRQAPGQGLEWMGWIN TNTGNPTYAQGFTGRFVFSLDTSVSTAY LQISSLKAEDTAVYYCARGLISLFRGAIFH YYYGMDVWGQGTTVTVSS	1703	QSALTQPRSVSGSPGQSVTISCTGTSS DVGGYTYVSWYQQHPGKAPKLMIYD VNKRPSGVPDRFSGSKSGITASLTISGL QAEDEADYYCCSYAGRYTWVFGGGTT LTVL	IGHV7-4-1 (Human)	IGHJ6 (Human)	IGLV2-11 (Human)	IGLJ3 (Human)	2712	ARGLISLFRGA IFHYYYGMDV	3914	CSYAGRYT WV	Seth Zost et al., 2020 (https://www.nature.com/articles/s41591-020-0998-x)
COV2-2952	Ab	SARS-CoV2	SARS-CoV1	SARS-CoV2		S; RBD	B-cells; SARS-CoV2 Human Patient	625	EVQLVESGGGLVQPGGSLRLSCAASGLT VRSNYMTWVRQTPGKGLEWVSVIYSG GSTFYADSVKGRFTISRDNSKNTVYLQM NSLRAEDTAVYYCARDLVTYGLDVWGQ GTTVTVSS	1704	DIQLTQSPSFLSASVGDRVTITCRASQG ISNYLAWYQQKPGTAPNLLIYAASTLQ SGVPSRFSGSGSGTEFTLTISSLQPEDF ATYYCQLLNSHPLTFGQGTRLEIK	IGHV3-66 (Human)	IGHJ6 (Human)	IGKV1-9 (Human)	IGKJ5 (Human)	2713	ARDLVTYGLD V	3915	QLLNSHPL T	Seth Zost et al., 2020 (https://www.nature.com/articles/s41591-020-0998-x)
COV2-2953	Ab	SARS-CoV1, SARS-CoV2			SARS-CoV2	S; RBD	B-cells; SARS-CoV2 Human Patient	626	QITLKESGPTLVKPTQTLTLTCTFSGFSLS TKRVGVGWIRQPPGKALEWLALIYWDD DQRYSPSLKSRLTITKDTSKNQVVLTMT NMDPVDTATYYCAHSGPPDLSPVLSQG WFDPWGQGTLVTVSS	1705	SYELTQPPSVSVSPGQTARITCSGDALP KQYAYWYQQKPGQAPVLVIYRDSERP SGIPERFSGSTSGTTVTLTISGVQAEDE ADYYCQSADSTGWVFGGGTKLTVL	IGHV2-5 (Human)	IGHJ5 (Human)	IGLV3-25 (Human)	IGLJ3 (Human)	2714	AHSGPPDLSP VLSQGWFDP	3916	QSADSTG WV	Seth Zost et al., 2020 (https://www.nature.com/articles/s41591-020-0998-x)
COV2-2955	Ab	SARS-CoV2	SARS-CoV1	SARS-CoV2		S; RBD	B-cells; SARS-CoV2 Human Patient	627	QVQLVESGGGVVQPGRSLRLSCAASGF TFVTSGIHWVRQAPGKGLEWVAVISYD GSNKYYADSVKGRFTISRDNSKNTLYLQ MNSLRAEDTAVYYCAKGGPNKEVLYFG ELLDYGMDVWGQGTTVTVSS	1706	DIVMTQTPLSLSVTPGQPASFSCKSSQ SLLHSDGKTYLYWYLQKPGQSPQLLIY AVSNRFSGVPDRFSGSGSGTDFTLKIS RVEAEDVGVYYCMQSIQLPYTFGQGT KLEIK	IGHV3-30 (Human)	IGHJ6 (Human)	IGKV2D-29 (Human)	IGKJ2 (Human)	2715	AKGGPNKEVL YFGELLDYGM DV	3917	MQSIQLPY T	Seth Zost et al., 2020 (https://www.nature.com/articles/s41591-020-0998-x)
COV2-2960	Ab	SARS-CoV1, SARS-CoV2			SARS-CoV2	S; non-RBD	B-cells; SARS-CoV2 Human Patient	628	QVQVVQSGAEVKKPGASVKVSCKASGY TFKNYGISWVRQAPGQGLEWMGWISA YTGNTNYAQKFQGRMTMTTDTSTGTG YMELRSLRSDDTAVYYCARVQRRRLDY WGQGTLVIVSS	1707	DIVVTQTPLSLSVTPGQPASISCKSSETL LHSDGKTYLSWYLQKPGQPPQLLIYEV SNRFSGVPDRFSGSGSGTDFTLKIGRV EAEDVGLYYCMQSIQLAFGQGTRLEIE	IGHV1-18 (Human)	IGHJ4 (Human)	IGKV2D-29 (Human)	IGKJ5 (Human)	2716	ARVQRRRLDY	3918	MQSIQLA	Seth Zost et al., 2020 (https://www.nature.com/articles/s41591-020-0998-x)
COV2-2961	Ab	SARS-CoV2	SARS-CoV1	SARS-CoV2		S; RBD	B-cells; SARS-CoV2 Human Patient	629	QMQLVQSGPEVKKPGTSVKVSCKASGF TFMSSAVQWVRQARGQRLEWIGWIVI GSGNTNYAQKFQERVTITRDMSTSTAY MELSSLRSEDTAVYYCAAPYCSSISCNDG FDIWGQGTMVTVSS	1708	ETVLTQSPGTLSLSPGERATLSCRASQS VSSSYLAWYQQKPGQAPRLLIYGASSR ATGIPDRFSGSGSGTDFTLTISRLEPED FAVYYCQHYGSSRGWTFGQGTKVEIK	IGHV1-58 (Human)	IGHJ3 (Human)	IGKV3-20 (Human)	IGKJ1 (Human)	2717	AAPYCSSISCN DGFDI	3919	QHYGSSRG WT	Seth Zost et al., 2020 (https://www.nature.com/articles/s41591-020-0998-x)
COV2-2997	Ab	SARS-CoV2	SARS-CoV1		SARS-CoV1, SARS-CoV2	S; RBD	B-cells; SARS-CoV2 Human Patient	630	QVQLVQSGAEVKKPGASVKVSCKASGY TFTSYYMHWVRQAPGQGLEWMGIINP GGGSTTYAQKFQGRVTMTSDTSTSTVY MELSSLRSEDTAMYYCARGAIPPNSRAE IDYWGQGTLVTVSS	1709	EIVMTQSPATLSVSPGERVTLSCRASQ SVSSNLAWCQQKPGQAPRLLIYGAST RATGIPARFSGSGSGTEFTLTISSLQSE DFAVYYCQQYYNWPLTFGGGTKVEIK	IGHV1-46 (Human)	IGHJ4 (Human)	IGKV3-15 (Human)	IGKJ4 (Human)	2718	ARGAIPPNSR AEIDY	3920	QQYYNWP LT	Seth Zost et al., 2020 (https://www.nature.com/articles/s41591-020-0998-x)
COV2-3010	Ab	SARS-CoV2	SARS-CoV1		SARS-CoV1, SARS-CoV2	S; RBD	B-cells; SARS-CoV2 Human Patient	631	QVQLVESGGGVVQPGRSLRLSCAASGF TFSDYAMHWVRQAPGKGLEWVADISF DGSNKYYADSVKGRFTISRDSSENTLYLQ MDSLRADDTAVYYCARDLSTTWYLEM WGPDAFDIWGQGTVVTVSS	1710	DIQMTQSPSTLSASIGDRVTITCRASQS ISSWLAWYQQIPGKAPKLLIYKASSLES GVPSRFSGSGSGTEFTLTISSLQPDDFA TYYCQQYNSYPYTFGQGTKLEIK	IGHV3-30-3 (Human)	IGHJ3 (Human)	IGKV1-5 (Human)	IGKJ2 (Human)	2719	ARDLSTTWYL EMWGPDAF DI	3921	QQYNSYPY T	Seth Zost et al., 2020 (https://www.nature.com/articles/s41591-020-0998-x)
COV2-3012	Ab	SARS-CoV2	SARS-CoV1		SARS-CoV1, SARS-CoV2	S; RBD	B-cells; SARS-CoV2 Human Patient	632	EVQLVESGGGLVQPGGSLRLSCAASGFT FSSYDLHWVRQGTGKRLEWVSAIGTAG DTYYLGSVKGRFTISRENAKNSLYLQMN SLRAGDTAVYYCARVLYDSSGFYNWFDP WGQGTLVTVSS	1711	DIQMTQSPSSLSASVGDRVTITCRASQ SISSYLNWYQQKPGKAPKLLIYAASSLE SGVPSRFSGSGSGTDFTLTISSLQPEDF ATYYCQQSYEIPPWTFGQGTKVEIK	IGHV3-13 (Human)	IGHJ5 (Human)	IGKV1-39 (Human)	IGKJ1 (Human)	2720	ARVLYDSSGF YNWFDP	3922	QQSYEIPP WT	Seth Zost et al., 2020 (https://www.nature.com/articles/s41591-020-0998-x)
COV2-3013	Ab	SARS-CoV2	SARS-CoV1		SARS-CoV1, SARS-CoV2	S; RBD	B-cells; SARS-CoV2 Human Patient	633	QVQLVESGGGVVQPGRSLRLSCAASGF TFSNYGMHWVRQAPGKGLEWVAVMS YDGSNKYYADSVKGRFTISRDNSKNTLYL QMNSLRAEDTAVYYCAKNLGPYCSGGT CYSLVGDYWGQGTLVTVSS	1712	DIQMTQSPSSLSASVGDRVTITCQASQ DISNYLNWYQQKPGKAPKLLIYDASNL ETGVPSRFSGSGSGTDFTFTISSLQPED IATYYCQQYANLPFTFGPGTKVDIK	IGHV3-30 (Human)	IGHJ4 (Human)	IGKV1-33 (Human)	IGKJ3 (Human)	2721	AKNLGPYCSG GTCYSLVGDY	3923	QQYANLPF T	Seth Zost et al., 2020 (https://www.nature.com/articles/s41591-020-0998-x)
COV2-3025	Ab	SARS-CoV2	SARS-CoV1	SARS-CoV2		S; RBD	B-cells; SARS-CoV2 Human Patient	634	EVQLVQSGPEVKKPGTSVKVSCKASGFT FMSSAVQWVRQARGQRLEWIGWIVIG SGNTNYAQKFQERVTITRDMSTSTAYM ELSSLRSEDTAVYYCAAPYCSSISCNDGF DIWGQGTMVTVSS	1713	EIVLTQSPGTLSLSPGERATLSCRASQS VSSSYLAWYQQKPGQAPRLLIYGASSR ATGIPDRFSGSGSGTDFTLTISRLEPED FAVYYCQHYGSSRGWTFGQGTKVEIK	IGHV1-58 (Human)	IGHJ3 (Human)	IGKV3-20 (Human)	IGKJ1 (Human)	2722	AAPYCSSISCN DGFDI	3924	QHYGSSRG WT	Seth Zost et al., 2020 (https://www.nature.com/articles/s41591-020-0998-x)
COV2-3029	Ab	SARS-CoV1, SARS-CoV2			SARS-CoV2	S; RBD	B-cells; SARS-CoV2 Human Patient	635	EVQLVESGGGVVQPGGSLRLSCAASGF TFDDYAMHWVRQAPGKGLEWVSLISG DGGNTYYADSVKGRFTISRDNSKNSLYL QMNSLRTEDTALYYCAKDEMAYPPSHH YYYYYMDVWGKGTTVTVSS	1714	SYELTQPPSVSVSPGQTARITCSTDALP NEYIYWYQQKPGQAPVLVIYKDSERPS GIPERFSGSSSGTTVTLTISGVQAEDEA DYYCQSVDSSGTYPHVIFGGGTKLTVL	IGHV3-43 (Human)	IGHJ6 (Human)	IGLV3-25 (Human)	IGLJ2 (Human)	2723	AKDEMAYPP SHHYYYYYMD V	3925	QSVDSSGT YPHVI	Seth Zost et al., 2020 (https://www.nature.com/articles/s41591-020-0998-x)
COV2-3057	Ab	SARS-CoV1, SARS-CoV2			SARS-CoV2	S; non-RBD	B-cells; SARS-CoV2 Human Patient	636	EVQLVESGGGLVQPGGSLRLSCAASGFT FSSYWMSWVRQAPGKGLEWVANIKQ DGSEKYFVDSVKGRFTISRDNAKNSLYL QMNSLRAEDAAVYYCARLVTTVTTANG LYYYSYYYMDVWGKGTTVTVSS	1715	QSVLTQPPSVSGAPGQRVTISCTGSSS NIGAGYDVHWYQQLPGTAPKLLIYGN TNRPSGVPDRFSGSKSGTSASLAITGL QAEDEADYYCQSYASSLSAHVVFGGG TKLTVL	IGHV3-7 (Human)	IGHJ6 (Human)	IGLV1-40 (Human)	IGLJ2 (Human)	2724	ARLVTTVTTA NGLYYYSYYY MDV	3926	QSYASSLS AHVV	Seth Zost et al., 2020 (https://www.nature.com/articles/s41591-020-0998-x)

COV2-3058	Ab	SARS-CoV1, SARS-CoV2			SARS-CoV2	S; non-RBD	B-cells; SARS-CoV2 Human Patient	637	EVQLVESGGGAVQPGRSLRLSCAASGFTFSTYAMYWVRQAPGKGLEWVAVISYDGSNRYYADSVKGRFTISRDNSKNTLYLQMNSLRPEDTAVYYCARDRSGNYRDAFDIWGQGTMVTVSS	1716	DIVMTQSPDSLAVSLGERATINCKSSQSVLYSSNNENYLAWYQQKPGQPPKLLIYWASTRESGVPDRFSGSGSGTDFTLTISSLQAEDVAVYYCQQYYSSYTFGQGTKVEIK	IGHV3-30 (Human)	IGHJ3 (Human)	IGKV4-1 (Human)	IGKJ2 (Human)	2725	ARDRSGNYRDAFDI	3927	QQYYSSYT	Seth Zost et al., 2020 (https://www.nature.com/articles/s41591-020-0998-x)
COVA1-01	Ab	SARS-CoV2	SARS-CoV1		SARS-CoV1, SARS-CoV2	S; non-RBD	B-cells; SARS-CoV2 Human Patient	638	HQHQVEQGPGGVEQSETLFLTCCVSGGFTISSCYKRGGIRQPPRKGEEWAVSSYYSSSTYYTPSLKSRVTISVDKSKNQFSLKMSSVTAADTAVYYCARVSSGYYFTPFDYWGQGTRGHRLF	1717	EIVMTQSPGTLSLSPGERATLSCRASQSVSSSYLAWYQQKPGQAPRLLIYGASSRATGIPDRFSGSGSGTDFTLTISRLEPEDFAVYYCQQYGSSPPPFTFGPGTKVDIK	IGHV4-39 (Human)	IGHJ4 (Human)	IGKV3-20 (Human)	IGKJ3 (Human)	2726	ARVSSGYYFTPFDY	3928	QQYGSSPPPFT	Philip Brouwer et al., 2020 (https://science.sciencemag.org/content/early/2020/06/15/science.abc5902)
COVA1-02	Ab	SARS-CoV2	SARS-CoV1		SARS-CoV1, SARS-CoV2	S; non-RBD	B-cells; SARS-CoV2 Human Patient	639	EVQLVESGGGVVQPGRSLRLSCAASGFTFSIYAMHWVRQAPGKGLEWVAVISYDGSNQYYADSVRGRFTISRGNSKNTLYLQMNSLRPEDTAVYYCARARGGSYNDAFDIWGQGTMVTVSS	1718	NFMLTQPASVSGSPGQSITISCTGASSDVGGYNYVSWYQQHPGKAPKLMIYDVSNRPSGVSNRFSGSKSGNTASLTISGLQAEDEADYYCSSYTSSSTPVVFGGGTELTVL	IGHV3-30 (Human)	IGHJ3 (Human)	IGLV2-14 (Human)	IGLJ3 (Human)	2727	ARARGGSYNDAFDI	3929	SSYTSSSTPVV	Philip Brouwer et al., 2020 (https://science.sciencemag.org/content/early/2020/06/15/science.abc5902)
COVA1-03	Ab	SARS-CoV2	SARS-CoV1	SARS-CoV2	SARS-CoV1	Unk	B-cells; SARS-CoV2 Human Patient	640	EVQLVESGGGVVQPGRSLRLSCAASGFTFSSYGMHWVRQAPGKGLEWVAVISYDGSNKYYADSVKGRFTISRDNSKNTLYLQMNSLRAEDTAVYYCAKDGQYYDFWSGYLGARTNPHYYYYMDVWGKGTMVTVSS	1719	DIVMTQSPSSLSASVGDRVTITCRASQGISNYLAWYQQKPGKVPKLLIYAASTLQSGVPSRFSGSGSGTDFTLTISSLQPEDVATYYCQKYNSAPPAFGQGTKVDIK	IGHV3-30 (Human)	IGHJ6 (Human)	IGKV1-27 (Human)	IGKJ3 (Human)	2728	AKDGQYYDFWSGYLGARTNPHYYYYMDV	3930	QKYNSAPPA	Philip Brouwer et al., 2020 (https://science.sciencemag.org/content/early/2020/06/15/science.abc5902)
COVA1-06	Ab	SARS-CoV2	SARS-CoV1		SARS-CoV1, SARS-CoV2	S; non-RBD	B-cells; SARS-CoV2 Human Patient	641	EVQLVQSGGGLVQPGRSLRLSCAASGFTFGEYAMHWVRQAPGKGLEWVSGISWNSGSIDYADSVKGRFTISRDNAKNSLYLQMNSLRAEDTALYYCAKDMGEAVAGTHYGMDVWGQGTMVTASS	1720	QSALTQPPSVSVSPGQTASIPCSGDKLGDIYACWYQQKPGQSPVLVIYQDTKRPSGIPERFSGSNSGNTATLTISGTQAMDEADYYCQAWGSTTAKVFGGGTKLTVP	IGHV3-9 (Human)	IGHJ6 (Human)	IGLV3-1 (Human)	IGLJ3 (Human)	2729	AKDMGEAVAGTHYGMDV	3931	QAWGSTTAKV	Philip Brouwer et al., 2020 (https://science.sciencemag.org/content/early/2020/06/15/science.abc5902)
COVA1-07	Ab	SARS-CoV1, SARS-CoV2			SARS-CoV1, SARS-CoV2	S; non-RBD	B-cells; SARS-CoV2 Human Patient	642	QVQLVESGAEVKKPGSSVKVSCKASGGTLSSYAITWVRQAPGQGLEWVGGIIPIFGTANYAQKFQGRVTITADESTSTAYMELSSLRSEDTAVYYCARVGAYDSSGYSNDYWGQGTLVTVSS	1721	DIQLTQSPATLSLSPGERATLSCRASQSVSSYLAWYQQKPGQAPRLLIYDASNRATGIPARFSGSGSGTDFTLTISSLEPEDFAVYYCQQRSNWPPRVTFGGGTKVEIK	IGHV1-69 (Human)	IGHJ4 (Human)	IGKV3-11 (Human)	IGKJ4 (Human)	2730	ARVGAYDSSGYSNDY	3932	QQRSNWPPRVT	Philip Brouwer et al., 2020 (https://science.sciencemag.org/content/early/2020/06/15/science.abc5902)
COVA1-08	Ab	SARS-CoV2	SARS-CoV1		SARS-CoV1, SARS-CoV2	S; RBD	B-cells; SARS-CoV2 Human Patient	643	EVQLVESGGGVVQPGGSLRLSCAASGFTFSSYAMHWVRQAPGKGLEWVAVISYDGSNKYYADSVKGRFTISRDNSKNTLYLQMNSLRAEDTAVYYCAREDYYDSSGSFDYWGQGTLVTVSS	1722	QSVLTQPASVSGSPGQSITISCTGTSSDVGGYNYVSWYQQHPGKAPKLMIYDVSNRPSGVSNRFSGSKSGNTASLTISGLQAEDEADYYCSSYTSSSTRHWVFGGGTKLTVL	IGHV3-30 (Human)	IGHJ4 (Human)	IGLV2-14 (Human)	IGLJ3 (Human)	2731	AREDYYDSSGSFDY	3933	SSYTSSSTRHWV	Philip Brouwer et al., 2020 (https://science.sciencemag.org/content/early/2020/06/15/science.abc5902)
COVA1-09	Ab	SARS-CoV2	SARS-CoV1		SARS-CoV1, SARS-CoV2	S; non-RBD	B-cells; SARS-CoV2 Human Patient	644	QLQLVESGPGLVKPSETLSLTCTVSGGSISSYFWSWIRQPPGKGLEWIGYIYYSGSTNYNPSLKSRVTISVDTSKNQFSLKLSSVTAADTAVYYCARHSQGWLQQAVAFDIWGQGTMVTVSS	1723	DIQMTQSPSSLSASVRDRVTITCRASQSITSSLNWYQQKPGKAPKLLIYAASSLQSGVPSRFSGSGSGTDFTLTISSLEPEDFATYYCQQSYSTPYTFGQGTKVEIK	IGHV4-59 (Human)	IGHJ3 (Human)	IGKV1-39 (Human)	IGKJ1 (Human)	2732	ARHSQGWLQQAVAFDI	3934	QQSYSTPYT	Philip Brouwer et al., 2020 (https://science.sciencemag.org/content/early/2020/06/15/science.abc5902)
COVA1-10	Ab	SARS-CoV2	SARS-CoV1		SARS-CoV1, SARS-CoV2	S; RBD	B-cells; SARS-CoV2 Human Patient	645	EVQLVESGGGLVQPGGSLRLSCAASGFTVTSTYMTWVRRAPGKGLEWVSIIYNDDTTYYADSVKDRVTVSRDDSKNTLYLQMNSLRAEDTAIYYCARGGYYYDPSGYYSRSFSFDYWGQGTLVTVSS	1724	NFMLTQPASVSGSPGQSITISCTGSSSDIAPYTFVSWYQQHSGTAPKLIIYDVRNRPSGISDRFSGSRSGNTASLSISGLQAEDEADYYCSAYTTTSTSWVFGGGTKLTVL	IGHV3-66 (Human)	IGHJ4 (Human)	IGLV2-14 (Human)	IGLJ3 (Human)	2733	ARGGYYYDPSGYYSRSFSFDY	3935	SAYTTTSTSWV	Philip Brouwer et al., 2020 (https://science.sciencemag.org/content/early/2020/06/15/science.abc5902)
COVA1-12	Ab	SARS-CoV2	SARS-CoV1	SARS-CoV2	SARS-CoV1	S; RBD	B-cells; SARS-CoV2 Human Patient	646	EVQLVQSGTEVKKPGASVKVSCKASGYTFPGYYIHWVRQAPGQGLEWMGWINPNSGVAKSAQKFQGRVTMTRDSSISTVYLDVTSDDTAVYYCARDLVWATVSGTMDVWGQGTTVTVSS	1725	QSALTQPPSASGSPGQSVTISCTGTSSDIGTYNYVSWYQQHPGKAPKLMIYEVTKRPSGVPDRFSGSKSGNTASLTVSGLQADDEGDYYCSSYVGNNNWVFGGGTKLTVL	IGHV1-2 (Human)	IGHJ6 (Human)	IGLV2-8 (Human)	IGLJ3 (Human)	2734	ARDLVWATVSGTMDV	3936	SSYVGNNNWV	Philip Brouwer et al., 2020 (https://science.sciencemag.org/content/early/2020/06/15/science.abc5902)
COVA1-16	Ab	SARS-CoV1, SARS-CoV2		SARS-CoV1, SARS-CoV2		S; RBD	B-cells; SARS-CoV2 Human Patient	647	QVQLVQSGAEVKKPGASVKVSCKASGYTFTSYYMHWVRQAPGQGLEWMGIINSSGGSTSYAQKFQGRVTMTRDTSTSTVYMELSSLRSEDTAVYYCARPRNYYDRSGYYQRAEYFQHWGQGTLVTVSS	1726	DIQLTQSPSSLSASVGDRVTITCQASQDISNYLNWYQQRPGKAPKLLIYDASNLETGVPSRFSGSGSGTDFTFTISSLQPEDIATYYCQQYDNPPLTFGGGTKLEIK	IGHV1-46 (Human)	IGHJ1 (Human)	IGKV1-33 (Human)	IGKJ4 (Human)	2735	ARPPRNYYDRSGYYQRAEYFQH	3937	QQYDNPPLT	Philip Brouwer et al., 2020 (https://science.sciencemag.org/content/early/2020/06/15/science.abc5902), Hejun Liu et al 2020 (https://www.biorxiv.org/content/10.1101/2020.08.02.233536v1.full.pdf)
COVA1-18	Ab	SARS-CoV2	SARS-CoV1	SARS-CoV2	SARS-CoV1	S; RBD	B-cells; SARS-CoV2 Human Patient	648	EVQLVESGGGLVQPGGSLRLSCAASGFTVSSNYMSWVRQAPGKGLEWVSVIYSGGSTYYADSVKGRFTISRDNSKNTLYLQMNSLRAEDTAVYYCARVEWAAAGTFYWGQGTLVTVSS	1727	QSALTQEPSLTVSPGGTVTLTCGSSTGAVTSGHYPYWFQQKPGQAPRTLIYDTSNKRSWTPARFSGSLLGGKAALTLSGAQPEDEAEYYCLLSYSGVWVFGGGTKLTVL	IGHV3-66 (Human)	IGHJ4 (Human)	IGLV7-46 (Human)	IGLJ3 (Human)	2736	ARVEWAAAGTFY	3938	LLSYSGVWV	Philip Brouwer et al., 2020 (https://science.sciencemag.org/content/early/2020/06/15/science.abc5902)

COVA1-19	Ab	SARS-CoV2	SARS-CoV1		SARS-CoV1, SARS-CoV2	S; non-RBD	B-cells; SARS-CoV2 Human Patient	649	QVQLVESGGGLVKPGGSLRLSCAASGFTFSSYSMNWVRQAPGKGLEWVSSISSSSSFIYYADSVKGRFTISRDNAKNSLYLQMNSLRAEDTAVYYCARWKSDYYDSSGYYPAAFDIWGQRDKWSPSS	1728	EIVMTQSPATLSVSPGERATLSCRASQSVSSNLAWYQQKPGQAPRLLIYGASTRATGIPARFSGSGSGTEFTLTISSLQSEDFAVYYCQQYNNWPPWTFGQGTKVEIK	IGHV3-21 (Human)	IGHJ3 (Human)	IGKV3-15 (Human)	IGKJ1 (Human)	2737	ARWKSDYYDSSGYYPAAFDI	3939	QQYNNWPPWT	Philip Brouwer et al., 2020 (https://science.sciencemag.org/content/early/2020/06/15/science.abc5902)
COVA1-20	Ab	SARS-CoV2	SARS-CoV1		SARS-CoV1, SARS-CoV2	S; non-RBD	B-cells; SARS-CoV2 Human Patient	650	QVQLVESGGGLVKPGGSLRLSCAASGFTFSSYSMNWVRQAPGKGLEWVSSISSSSSYIYYADSVKGRFTISRDDAKNSLFLQMNSLRAEDTAVYYCAGDQNLYCSGDSCYYHYYGMDVWGQGTVVTVSS	1729	NFMLTQPPSVSVAPGKTARITCGGNNIGSKSVHWYQQKPGQAPVLVIYYDSDRPSGIPERFSGSNSGNTATLTISRVEAGDEADYYCQVWDSSSDHWVFGGGTKLTVL	IGHV3-21 (Human)	IGHJ6 (Human)	IGLV3-21 (Human)	IGLJ3 (Human)	2738	AGDQNLYCSGDSCYYHYYGMDV	3940	QVWDSSSDHWV	Philip Brouwer et al., 2020 (https://science.sciencemag.org/content/early/2020/06/15/science.abc5902)
COVA1-21	Ab	SARS-CoV2	SARS-CoV1	SARS-CoV2	SARS-CoV1	S; non-RBD	B-cells; SARS-CoV2 Human Patient	651	EVQLVESGGGVVQPGRSLRLSCAASGFTFSSYAMHWVRQAPGKGLEWVAVISYDGSNKYYADSVKGRFTISRDNTKNTLYLQMNSLRAEDTAVYYCARDSEYYDILTGYLAPTHYYYYYMDVWGKGTTVTVSS	1730	EIVMTQSPATLSVSPGERATLSYRASQSVSSNLAWYQQKPGQAPRLLIYGASTRATGIPARFSGSGSGTEFTLTISSLQSEDFAVYYCQQYNNWPPGTFGQGTKLEIK	IGHV3-30 (Human)	IGHJ6 (Human)	IGKV3-15 (Human)	IGKJ2 (Human)	2739	ARDSEYYDILTGYLAPTHYYYYYMDV	3941	QQYNNWPPGT	Philip Brouwer et al., 2020 (https://science.sciencemag.org/content/early/2020/06/15/science.abc5902)
COVA1-22	Ab	SARS-CoV2	SARS-CoV1		SARS-CoV1, SARS-CoV2	S; non-RBD	B-cells; SARS-CoV2 Human Patient	652	EVQLVESGAEVKKPGASVKVSCKASGYTFTSYGISWVRQAPGQGLEWMGWISAYNGYTNSAQKLQGRVTMTTDTSTSTAYMELRSLRSDDTAVYYCARDLVDTAMVQTLDDYGMDVWGQGTMVTVSS	1731	SYELTQPPSVSVSPGQTASITCSGDKLGDKYACWYQQKPGQSPVLVTYQDNKRPSGIPERFSGSNSGNTATLTISGTQAMDEADYYCQAWDSSTAVFGGGTKLTVL	IGHV1-18 (Human)	IGHJ6 (Human)	IGLV3-1 (Human)	IGLJ3 (Human)	2740	ARDLVDTAMVQTLDDYGMDV	3942	QAWDSSTAV	Philip Brouwer et al., 2020 (https://science.sciencemag.org/content/early/2020/06/15/science.abc5902)
COVA1-23	Ab	SARS-CoV2	SARS-CoV1		SARS-CoV1, SARS-CoV2	S; non-RBD	B-cells; SARS-CoV2 Human Patient	653	QVQLVQSGAEVKKPGESLKISCKGSGYRFTTYWIGWVRQMPGKGLEWMGIIYPGDSDTRYSPSFQGQVTISADKSISTAYLQWSSLTASDTAIYYCARYYYDSRGYTSIDFWGQGTLVTVSS	1732	SYELTQPPSVSVSPGQTARITCSGDALPKQYAYWYQQKPGQAPVLVIYKDSERPSGIPERFSGSSSGTTVTLTISGVQAEDEADYYCQSADSSGTYSVVFGGGTKLTVL	IGHV5-51 (Human)	IGHJ4 (Human)	IGLV3-25 (Human)	IGLJ3 (Human)	2741	ARYYYDSRGYTSIDF	3943	QSADSSGTYSVV	Philip Brouwer et al., 2020 (https://science.sciencemag.org/content/early/2020/06/15/science.abc5902)
COVA1-25	Ab	SARS-CoV2	SARS-CoV1		SARS-CoV1, SARS-CoV2	S; non-RBD	B-cells; SARS-CoV2 Human Patient	654	EVQLVESGPGLVKPSETLSLTCTVSGGSISSTSYYWGWIRQPPGKGLECIGSIYYSGSTYYNPSLKSRVTISVDTSKNQFSLKLSSVTAADTAVYYCARLNYDFWSGYYSYALYYMDVWGKGTMVTVSS	1733	DIQLTQSPSTLSASVGDRVTITCRASQSISSWLAWYQQKPGKAPKLLIYKASSLESGVPSRFSGSGSGTEFTLTISSLQPDDFATYYCQQYNSYSITFGPGTKVDIK	IGHV4-39 (Human)	IGHJ6 (Human)	IGKV1-5 (Human)	IGKJ3 (Human)	2742	ARLNYDFWSGYYSYALYYMDV	3944	QQYNSYSIT	Philip Brouwer et al., 2020 (https://science.sciencemag.org/content/early/2020/06/15/science.abc5902)
COVA1-26	Ab	SARS-CoV2	SARS-CoV1		SARS-CoV1, SARS-CoV2	S; non-RBD	B-cells; SARS-CoV2 Human Patient	655	QLQLQESGPGLVKPSQTLSLTCTVSGGSISSGGYYWSWIRQLPGKGLEWIGYIYYSGSTYYNPSLKSRVTISVDTSKNQFSLNLSSVTAADTAVYYCARQQLDYYDSSGCFDYWGQGTLVTVSS	1734	DIVMTQSPSFLSASVGDRVTITCRASQGISSYLAWYQQKPGKAPKLLIYAASTLQSGVPSRFSGSGSGTEFTLTISSLQPEDFATYYCQQLHSYPLTFGGGTKVDIK	IGHV4-31 (Human)	IGHJ4 (Human)	IGKV1-9 (Human)	IGKJ4 (Human)	2743	ARQQLDYYDSSGCFDY	3945	QQLHSYPLT	Philip Brouwer et al., 2020 (https://science.sciencemag.org/content/early/2020/06/15/science.abc5902)
COVA1-27	Ab	SARS-CoV2	SARS-CoV1		SARS-CoV1, SARS-CoV2	S; non-RBD	B-cells; SARS-CoV2 Human Patient	656	EVQLVESGPGLVKPSETLSLTCTVSGGSISSYYWSWIRQPPGKRLEWIGYIYYSGSTNYNPSLKSRVTISVDTSKNQFSLNLSSVTAADTAAYYCARGFDYWGQGTRVTVSS	1735	DVVMTQSPGTLSLSPGERATLSCRASQNVSSSYLAWYQQKPGQAPRLLIYGASSRATGIPDRFSGSGSGTDFTLTISRLEPEDFAVYYCQQYGSSPLFTFGPGTKVEIK	IGHV4-59 (Human)	IGHJ4 (Human)	IGKV3-20 (Human)	IGKJ3 (Human)	2744	ARAMGSYRSPFDY	3946	QQYGSSPLFT	Philip Brouwer et al., 2020 (https://science.sciencemag.org/content/early/2020/06/15/science.abc5902)
COVA2-01	Ab	SARS-CoV2	SARS-CoV1		SARS-CoV1, SARS-CoV2	S; RBD	B-cells; SARS-CoV2 Human Patient	657	EVQLVESGGGLVQPGGSLRLSCAASGFTFSSYDMHWVRQTTGKGLQWVSAIGTAGDTYYPGSVKGRFTISRENAKNSLYLQMNSLRAGDTAVYYCARGGDRYPVGYFDLWGRGTLVTVSS	1736	DIVMTQSPSSLSASVGDRVTITCRASQSISSYLNWYQQKPGKAPKLLIYAASSLQSGVPSRFSGSGSGTDFTLTISSLQPEDFATYYCQQSYSTPPVTFGGGTKVEIK	IGHV3-13 (Human)	IGHJ2 (Human)	IGKV1-39 (Human)	IGKJ4 (Human)	2745	ARGGDRYPVGYFDL	3947	QQSYSTPPVT	Philip Brouwer et al., 2020 (https://science.sciencemag.org/content/early/2020/06/15/science.abc5902)
COVA2-02	Ab	SARS-CoV1, SARS-CoV2		SARS-CoV1, SARS-CoV2 (weak)		S; RBD	B-cells; SARS-CoV2 Human Patient	658	VQLQQESGPGLVKPSETLSLTCTVSGGSISSSSYYWGWIRQPPGKGLEWIGSIYYSGSTYYNPSLKSRVTISVDTSKNQFSLKLSSVTAADTAVYYCARRSTSRWGYYYMDVWGKGTRVTVSS	1737	DIVMTQSPSSLSASVGDRVTITCRASQSISNYLNWYQQKPGKAPKLLLYAASDLQSGVPSRFSGSGSGTDFTLTISSLQPEDFATYYCQQSYSTHMSTFGQGTKVDIK	IGHV4-39 (Human)	IGHJ6 (Human)	IGKV1-39 (Human)	IGKJ3 (Human)	2746	ARRSTSRWGYYYMDV	3948	QQSYSTHMST	Philip Brouwer et al., 2020 (https://science.sciencemag.org/content/early/2020/06/15/science.abc5902)
COVA2-03	Ab	SARS-CoV2	SARS-CoV1		SARS-CoV1, SARS-CoV2	S; non-RBD	B-cells; SARS-CoV2 Human Patient	659	EVQLVESGGGLVQPGGSLRLSCAASGFTFSSYSMNWVRQAPGKGLEWVSYISSSSSTIYYADSVKGRFTISRDNAKNSLYLQMNSLRAEDTAVYYCAREANSDFWSGYLGYFDYWGQGTLVTVSS	1738	EIVMTQSPATLSLSPGERATLSCRASQSVSSYLAWYQQKPGQAPRLLIYDASNRATGIPARFSGSGSGTDFTLTISSLEPEDFAVYYCQQRSNWPQVTFGQGTRLEIK	IGHV3-48 (Human)	IGHJ4 (Human)	IGKV3-11 (Human)	IGKJ5 (Human)	2747	AREANSDFWSGYLGYFDY	3949	QQRSNWPQVT	Philip Brouwer et al., 2020 (https://science.sciencemag.org/content/early/2020/06/15/science.abc5902)
COVA2-04	Ab	SARS-CoV2	SARS-CoV1	SARS-CoV2	SARS-CoV1	S; RBD	B-cells; SARS-CoV2 Human Patient	660	QVQLVETGGGLIQPGGSLRLSCAASGFTVSSNYMSWVRQAPGKGLEWVSVIYSGGSTFYADSVKGRFTISRDNSKNTLYLQMNSLRAEDTAVYYCARDLERAGGMDVWGQGTMVTVSS	1739	EIVMTQSPGTLSLSPGERATLSCRASQSVSSSYLAWYQQKPGQAPRLLIYGASSRATGIPDRFSGSGSGTDFTLTISRLEPEDFAVYYCQQYGSLYTFGQGTKVDIK	IGHV3-53 (Human)	IGHJ6 (Human)	IGKV3-20 (Human)	IGKJ3 (Human)	2748	ARDLERAGGMDV	3950	QQYGSLYT	Philip Brouwer et al., 2020 (https://science.sciencemag.org/content/early/2020/06/15/science.abc5902);Nicholas Wu (https://www.biorxiv.org/content/10.1101/2020.07.26.222232v1)

COVA2-05	Ab	SARS-CoV2	SARS-CoV1		SARS-CoV1, SARS-CoV2	S; RBD	B-cells; SARS-CoV2 Human Patient	661	EVQLLESGAEVKKPGESLKISCKGSGYSF TSYWIGWVRQMPGKGLEWMGIIYPGD SDTRYSPSFQGQVTISADKSISTAYLQWS SLKASDTAMYYCARHMRPSIAARPGYQ YYMDVWGKGTRVTVSS	1740	DIQMTQSPSSLSASVGDRVTITCQASQ DISNYLNWYQQKPGKAPKLLIYDASNL ETGVPSRFSGSGSGTDFTFTISSLQPED IATYYCQQYDNLPLTFGGGTKLEIK	IGHV5-51 (Human)	IGHJ6 (Human)	IGKV1-33 (Human)	IGKJ4 (Human)	2749	ARHMRPSIAA RPGYQYYMD V	3951	QQYDNLPL T	Philip Brouwer et al., 2020 (https://science.sciencemag.org/content/early/2020/06/15/science.abc5902)
COVA2-07	Ab	SARS-CoV2	SARS-CoV1	SARS-CoV2	SARS-CoV1	S; RBD	B-cells; SARS-CoV2 Human Patient	662	EVQLVETGGGLIQPGGSLRLSCAASGLT VSSNYMNWVRQAPGKGLEWVSVIYSG GSTYYADSVKGRFTISRDNSKNTLYLQM NSLRAEDTAVYYCAREAYGMDVWGQG TMVTVSS	1741	EIVLTQSPGTLSLSPGERATLSCRASQS VSSSYLAWYQQKPGQAPRLLIYGASSR ATGIPDRFSGSWSGTDFTLTISRLEPED FAVYYCQQYGSSPGTFGQGTKVDIK	IGHV3-53 (Human)	IGHJ6 (Human)	IGKV3-20 (Human)	IGKJ3 (Human)	2750	AREAYGMDV	3952	QQYGSSP GT	Philip Brouwer et al., 2020 (https://science.sciencemag.org/content/early/2020/06/15/science.abc5902)
COVA2-10	Ab	SARS-CoV2	SARS-CoV1		SARS-CoV1, SARS-CoV2	S; non-RBD	B-cells; SARS-CoV2 Human Patient	663	EVQLLESGGGLVQPGGSLKLSCAASGFT FSSYAMSWVRQAPGKGLEWVSAISGSG SNTYYADSVKGRFTISRDNSKNTLYLQM NSLRAEDTAVYYCAKGLRGQQLVIPTEY FQHWGQGTLVTVSS	1742	DIVMTQSPGTLSLSPGERATLSCRASQ SVSSSYLAWYQQKPGQAPRLLIYGASS RATGIPDRFSGSGSGTDFTLTISRLEPE DFAVYYCQQYGSSLLTFGGGTKVEIK	IGHV3-23 (Human)	IGHJ1 (Human)	IGKV3-20 (Human)	IGKJ4 (Human)	2751	AKGLRGQQL VIPTEYFQH	3953	QQYGSSLL T	Philip Brouwer et al., 2020 (https://science.sciencemag.org/content/early/2020/06/15/science.abc5902)
COVA2-11	Ab	SARS-CoV2	SARS-CoV1	SARS-CoV2 (weak)	SARS-CoV1	S; RBD	B-cells; SARS-CoV2 Human Patient	664	EVQLVESGAEVKKPGSSVKVSCKASGGT LSSYAISWVRQAPGQGLEWMGGIIPIFG TANYAQKFQGRVTITTDESTSTAYMELSS LRSEDTAVYYCARGPRGCSSTSCYGSYFD YWGQGTLVTVSS	1743	DIQLTQSPGTLSLSPGERATLSCRASQS VSSSYLAWYQQKPGQAPRLLIYGASSR ATGIPDRFSGSGSGTDFTLTISRLEPED FAVYYCQQYGSSPRLTFGGGTKVDIK	IGHV1-69 (Human)	IGHJ4 (Human)	IGKV3-20 (Human)	IGKJ4 (Human)	2752	ARGPRGCSST SCYGSYFDY	3954	QQYGSSPR LT	Philip Brouwer et al., 2020 (https://science.sciencemag.org/content/early/2020/06/15/science.abc5902)
COVA2-12	Ab	SARS-CoV2	SARS-CoV1		SARS-CoV1, SARS-CoV2	S; non-RBD	B-cells; SARS-CoV2 Human Patient	665	EVQLVESGGGLVKPGGSLRLSCAASGFT FGSYSMSWVRQAPGKGLEWVSSISRSS SYIYNADSVRGRLTISRDNAKNSLYLQM NSLRVEDTAVYYCARDQPLPDILTGYYT GPLDYWGQGTLVTVSS	1744	EIVLTQSPATLSVSPGERATLSCRASQS VSSSLAWYQQKPGQAPRLLIYAASTRA TGIPARFSGSGSGTEFTLTISSLQSEDFA VYYCQQYNNWPPWTFGQGTKLEIK	IGHV3-21 (Human)	IGHJ4 (Human)	IGKV3-15 (Human)	IGKJ1 (Human)	2753	ARDQPLPDIL TGYYTGPLDY	3955	QQYNNWP PWT	Philip Brouwer et al., 2020 (https://science.sciencemag.org/content/early/2020/06/15/science.abc5902)
COVA2-13	Ab	SARS-CoV2	SARS-CoV1	SARS-CoV2 (weak)	SARS-CoV1	S; RBD	B-cells; SARS-CoV2 Human Patient	666	QVQLVETGGGLIQPGGSLRLSCAASGFT VSSNYMSWVRQAPGKGLEWVSVIYSG GSTYYADSVKGRFTISRDNSKNTLYLQM NSLRAEDTAVYYCARDLDTMGGMDVW GQGTRVTVSS	1745	EIVMTQSPGTLSLSPGERATLSCRASQ SVSSSYLAWYQQKPGQAPRLLIYGASS RATGIPDRFSGSGSGTDFTLTISRLEPE DFAVYYCQQYGSSPGTFGQGTKVEIK	IGHV3-53 (Human)	IGHJ6 (Human)	IGKV3-20 (Human)	IGKJ1 (Human)	2754	ARDLDTMGG MDV	3956	QQYGSSP GT	Philip Brouwer et al., 2020 (https://science.sciencemag.org/content/early/2020/06/15/science.abc5902)
COVA2-14	Ab	SARS-CoV1, SARS-CoV2			SARS-CoV1, SARS-CoV2	S; non-RBD	B-cells; SARS-CoV2 Human Patient	667	QVQLVQSGAEVKKPGSSVKVSCKASGG TFSSYAIIWVRQAPGQGLEWMGGIIPIF GTANYAQKFQGRVTITTDESTSTAYMEL SSLRSEDTAVYYCARVRYYDSSGYYEDY WGQGTLVTVSS	1746	EIVLTQSPATLSLSPGERATLSCRASQS VSSYLAWYQQEPGQAPRLLIYDASNR ATGIPARFSGSGSGTDFTLTISSLEPEDF AVYYCQQRSNWPPMYTFGQGTKVEI K	IGHV1-69 (Human)	IGHJ4 (Human)	IGKV3-11 (Human)	IGKJ1 (Human)	2755	ARVRYYDSSG YYEDY	3957	QQRSNWP PMYT	Philip Brouwer et al., 2020 (https://science.sciencemag.org/content/early/2020/06/15/science.abc5902)
COVA2-15	Ab	SARS-CoV2	SARS-CoV1	SARS-CoV2	SARS-CoV1	S; RBD	B-cells; SARS-CoV2 Human Patient	668	QVQLLESGGGLVQPGGSLRLSCAASGFT FSSYAMSWVRQAPGKGLEWASAISGSG GSTYYADSVEGRFTISRDNSKNTLYLQM NSLRAEDTAVYYCAKDTGYCGDDCYIKLI RGGPDYWGQGTLVTVSS	1747	DIVMTQSPLSLPVTLGQPASISCRSSQS LVYSDGNTFLNWFQQRPGQSPRRLIY QVSNRDSGVPDRFSGSGSGTDFTLKIS RVEAEDVGVYYCMQGTHWPRTFGQ GTKLEIK	IGHV3-23 (Human)	IGHJ4 (Human)	IGKV2-30 (Human)	IGKJ2 (Human)	2756	AKDTGYCGD DCYIKLIRGGP DY	3958	MQGTHW PRT	Philip Brouwer et al., 2020 (https://science.sciencemag.org/content/early/2020/06/15/science.abc5902)
COVA2-16	Ab	SARS-CoV2	SARS-CoV1		SARS-CoV1, SARS-CoV2	S; RBD	B-cells; SARS-CoV2 Human Patient	669	QVQLVQSGAEVKKPGATVKISCKVSGYT FTDYYMHWVQQAPGKGLEWMGLVDP EDGETIYAEKFQGRVTITADTSTDTAYM ELSSLRSEDTAVYYCASSDSSGFVGSRGF DYWGQGTRVTVSS	1748	DIQLTQSPSSLSASVGDRVTITCRASQG IRNDLGWYQQKPGKAPKRLIYAASSL QSGVPSRFSGSGSGTEFTLTISSLQPED FATYYCLQHNSYPPLFGQGTKVEIK	IGHV1-69 (Human)	IGHJ4 (Human)	IGKV1-17 (Human)	IGKJ1 (Human)	2757	ASSDSSGFVG SRGFDY	3959	LQHNSYPP L	Philip Brouwer et al., 2020 (https://science.sciencemag.org/content/early/2020/06/15/science.abc5902)
COVA2-17	Ab	SARS-CoV2	SARS-CoV1		SARS-CoV1, SARS-CoV2	S; RBD	B-cells; SARS-CoV2 Human Patient	670	QVQLVESGAEVKKPGSSVKVSCKASGGT FSSYGINWVRQAPGQGLEWMGGIIPIF GTANYAQKFQGRVTITTDESTSTAYMEL SSLRSEDTAVYYCASFGDDSGDEGVRW GQGTLVTVSS	1749	EIVMTQSPATLSLSPGERATLSCRASQS VSSSYLAWYQQKPGQAPRLLIYDASNR ATGIPARFSGSGSGTDFTLTISSLEPEDF AVYYCQQRSNWPPYTFGQGTKVEIK	IGHV1-69 (Human)	IGHJ4 (Human)	IGKV3-11 (Human)	IGKJ1 (Human)	2758	ASFGDDSGDE GVR	3960	QQRSNWP PYT	Philip Brouwer et al., 2020 (https://science.sciencemag.org/content/early/2020/06/15/science.abc5902)
COVA2-18	Ab	SARS-CoV1, SARS-CoV2		SARS-CoV2	SARS-CoV1	S; non-RBD	B-cells; SARS-CoV2 Human Patient	671	EVQLVQSGAEVKKPGSSVKVSCKASGGT FSSYAISWVRQAPGQGLEWMGGIIPIFG TTNYAQKFQGRVTITTDESTSTAYMELSS LRSEDTAVYYCARVYSYDSSGYYLEYWG QGTRVTVSS	1750	EIVLTQSPATLSLSPGERATLSCRASQS VSSYLAWYQQKPGQAPRLLIYDASNR ATGIPARFSGSGSGTDFTLTISSLEPEDF AVYYCQQRSNWPPSITFGQGTRLEIK	IGHV1-69 (Human)	IGHJ4 (Human)	IGKV3-11 (Human)	IGKJ5 (Human)	2759	ARVYSYDSSG YYLEY	3961	QQRSNWP PSIT	Philip Brouwer et al., 2020 (https://science.sciencemag.org/content/early/2020/06/15/science.abc5902)
COVA2-20	Ab	SARS-CoV2	SARS-CoV1		SARS-CoV1, SARS-CoV2	S; RBD	B-cells; SARS-CoV2 Human Patient	672	EVQLVESGGGLIQPGGSLRLSCAASGFT VSSNYMSWVRQAPGKGLEWVSVIYSG GSTYYADSVKGRFTISRDNSKNTLYLQM NSLRAEDTAVYYCASPLLLTPPDYYYYMD VWGKGTMVTVSS	1751	DVVMTQSPSSLSVSVGDRVTITCRASQ GIRNDLGWYQQKPGKAPKRLIYAASSL QSGVPSRFSGSGSGTEFTLTISSLQPED FATYYCLQHNSYLWTFGQGTKLEIK	IGHV3-53 (Human)	IGHJ6 (Human)	IGKV1-17 (Human)	IGKJ1 (Human)	2760	ASPLLLTPPDY YYYMDV	3962	LQHNSYL WT	Philip Brouwer et al., 2020 (https://science.sciencemag.org/content/early/2020/06/15/science.abc5902)

COVA2-22	Ab	SARS-CoV2	SARS-CoV1		SARS-CoV1, SARS-CoV2	S; non-RBD	B-cells; SARS-CoV2 Human Patient	673	EVQLVESGPGLVKPSETLSLTCTVSGGSISSYYWSWIRQPAGKGLEWIGRIYTSGSTNYNPSLKSRVTMSVDTSKNQFSLKLSSVTAADTAVYYCARWKYNDRFDYWGQGTRVTVSS	1752	AIRMTQSPSSLSASVGDRVTITCQASQDISNYLNWYQQKPGKAPKLLIYDASNLETGVPSRFSGSGSGTDFTFTISSLQPEDIATYYCQQYDNLPITFGQGTRLEIK	IGHV4-4 (Human)	IGHJ4 (Human)	IGKV1-33 (Human)	IGKJ5 (Human)	2761	ARGPRYCSSTSCYAGVYFDY	3963	QQYDNLPIT	Philip Brouwer et al., 2020 (https://science.sciencemag.org/content/early/2020/06/15/science.abc5902)
COVA2-23	Ab	SARS-CoV2	SARS-CoV1		SARS-CoV1, SARS-CoV2	S; RBD	B-cells; SARS-CoV2 Human Patient	674	EVQLVESGAEVKKPGSSVKVSCKASGGTFSSYAISWVRQAPGQGLEWMGGIIPIFGTANYAQKFQGRVTITTDESTSTAYMELSSLRSEDTAVYYCARGPRYCSSTSCYAGVYFDYWGQGTRVTVSS	1753	EIVLTQSPGTLSLSPGERATLSCRASQSVSSSYLAWYQQKPGQAPRLLIYGASSRATGIPDRFSGSGSGTDFTLTISRLEPEDFAVYYCQQYGSSPGVTFGGGTKLEIK	IGHV1-69 (Human)	IGHJ4 (Human)	IGKV3-20 (Human)	IGKJ4 (Human)	2762	ARDGFGDVEEMATIKDAFDI	3964	QQYGSSPGVT	Philip Brouwer et al., 2020 (https://science.sciencemag.org/content/early/2020/06/15/science.abc5902)
COVA2-24	Ab	SARS-CoV2	SARS-CoV1		SARS-CoV1, SARS-CoV2	S; RBD	B-cells; SARS-CoV2 Human Patient	675	EVQLVQSGAEVKKPGESLRISCKGSGYSFTSYWISWVRQMPGKGLEWMGRIDPSDSYTNYSPSFQGHVTISADKSISTAYLQWSSLKASDTAMYYCARPNPAGGYDSSGWVDAFDIWGQGTRVTVSS	1754	AIRMTQSPSSLSASVGDRVTITCRASQSISSYLNWYQQKPGKAPKLLIYAASSLQSGVPSRFSGSGSGTDFTLTISSLQPEDFATYYCQQSYSTPQTFGQGTKLEIK	IGHV5-10-1 (Human)	IGHJ3 (Human)	IGKV1-39 (Human)	IGKJ2 (Human)	2763	ARPNPAGGYDSSGWVDAFDI	3965	QQSYSTPQT	Philip Brouwer et al., 2020 (https://science.sciencemag.org/content/early/2020/06/15/science.abc5902)
COVA2-25	Ab	SARS-CoV2	SARS-CoV1		SARS-CoV1, SARS-CoV2	S; non-RBD	B-cells; SARS-CoV2 Human Patient	676	EVQLVESGAEVKKPGASVKVSCKVSGYTLPELSMHWVRQTPGKGLEWMGGFDPEDGETIYAQKFQGRVTMTEDTSTDTAYMELSSLRSEDTAVYYCATGPTIAAAATNWFDPGGQGTLVTVSS	1755	QPVLTQPASVSGSPGQSITISCTGTSSDVGGYNYVSWYQQHPGKAPKLMIYDVSNRPSGVSNRFSGSRSGDTASLTISGLQAEDEADYYCSSYTSSSTWVFGGGTKLTVL	IGHV1-24 (Human)	IGHJ5 (Human)	IGLV2-14 (Human)	IGLJ3 (Human)	2764	ATGPTIAAAATNWFDP	3966	SSYTSSSTWV	Philip Brouwer et al., 2020 (https://science.sciencemag.org/content/early/2020/06/15/science.abc5902)
COVA2-26	Ab	SARS-CoV2	SARS-CoV1		SARS-CoV1, SARS-CoV2	S; non-RBD	B-cells; SARS-CoV2 Human Patient	677	EVQLVESGGGLVKPGGSLRLSCAASGFTFSNAWMSWVRQAPGKGLEWVGRIKSKTDGGTTDYAAPVKGRFTISRDDSKNTLYLQMNSLKTEDTAVYYCTTDRGDSYGYYYCMDVWGKGTRVTVSS	1756	QLVLTQPPSVSVSPGQTASITCSGDKLGDKYACWYQQKPGQSPVLVIYQDSKRPSGIPERFSGSNSGNTATLTISGTQAMDEADYYCQAWDSSTAVVFGGGTKLTVL	IGHV3-15 (Human)	IGHJ6 (Human)	IGLV3-1 (Human)	IGLJ3 (Human)	2765	TTDRGDSYGYYYCMDV	3967	QAWDSSTAVV	Philip Brouwer et al., 2020 (https://science.sciencemag.org/content/early/2020/06/15/science.abc5902)
COVA2-28	Ab	SARS-CoV2	SARS-CoV1		SARS-CoV1, SARS-CoV2	S; non-RBD	B-cells; SARS-CoV2 Human Patient	678	EVQLVESGGGVVQPGRSLRLSCAASGFTFSSYGMHWVRQAPGKGLEWVAVIWYDGSNKYYADSVKGRFTISRDNSKNTLYLQMDSLRAEDTAMYYCAKDKAPPCSSGWYYFDYWGQGTLVTVSS	1757	EIVMTQSPATLSVSPGERATLSCRASQSVSSNLAWYQHKPGQAPRLLIYGASTRATGIPARFSGSGSGTEFTLTISSLQSEDFAVYYCQQYNYWPLITFGQGTRLEIK	IGHV3-33 (Human)	IGHJ4 (Human)	IGKV3-15 (Human)	IGKJ5 (Human)	2766	AKDKAPPCSSGWYYFDY	3968	QQYNYWPLIT	Philip Brouwer et al., 2020 (https://science.sciencemag.org/content/early/2020/06/15/science.abc5902)
COVA2-29	Ab	SARS-CoV2	SARS-CoV1	SARS-CoV2	SARS-CoV1	S; RBD	B-cells; SARS-CoV2 Human Patient	679	EVQLVESGGGVVQPGRSLRLSCAASGFTFSSYTMHWVRQAPGKGLEWVAVISYDGSNKYYADSVKGRFTISRDNSKNTLYLQMNSLRAEDTAVYYCASLPVVPAAIGPLPAFDIWGQGTMVTVSS	1758	DIVMTQSPSSLSASVGDRVTITCRASQSISSYLNWYQQKPGKAPKLLIYAASSLQSGVPSRFSGSGSGTDFTLTISSLQPEDFATYYCQQSYSTPRTFGQGTKVEIK	IGHV3-30 (Human)	IGHJ3 (Human)	IGKV1-39 (Human)	IGKJ1 (Human)	2767	ARGVEDPVVPAAIPWCWFDP	3969	QQSYSTPRT	Philip Brouwer et al., 2020 (https://science.sciencemag.org/content/early/2020/06/15/science.abc5902)
COVA2-30	Ab	SARS-CoV2	SARS-CoV1		SARS-CoV1, SARS-CoV2	S; non-RBD	B-cells; SARS-CoV2 Human Patient	680	EVQLVESGPGLVKPSQTLSLTCTVSGGSISSGDYYWSWIRQPPGKGLEWIGYIYYSGSTYYNPSLKSRVTISVDTSKNQFSLKLSSVTAADTAVYYCARGVEDPVVPAAIPWCWFDPWGQGTRVTVSS	1759	QSVLTQPPSVSVAPGQTARITCGGNNIGSKSVHWYQQKPGQAPVLVVYDDSDRPSGIPERFSGSNSGNTATLTISRVEAGDEADYYCQVWASSSVVFGGGTKLTVL	IGHV4-30-4 (Human)	IGHJ5 (Human)	IGLV3-21 (Human)	IGLJ3 (Human)	2768	ASLPVVPAAIGPLPAFDI	3970	QVWASSSVV	Philip Brouwer et al., 2020 (https://science.sciencemag.org/content/early/2020/06/15/science.abc5902)
COVA2-31	Ab	SARS-CoV2	SARS-CoV1		SARS-CoV1, SARS-CoV2	S; RBD	B-cells; SARS-CoV2 Human Patient	681	EVQLVESGVEVKKPGASVKVSCKAFGYTFTGQDMHWVRQAPGQGLEWMGWINPSSAGTNYAQKFQGRVTMTRDTSISTAYMELSRLRSDDTSVYYCRKMLTIFGKVNQTMLLISGAKGQWSPSLQWGQGTMVTVSS	1760	DIVMTQTPLSLSVTPGQPASISCKSGQSLLHSDGKTYLYWYLQKPGQPPQLLIYEVSNRFSGVPDRFSGSGSGTDFTLKISRVEAEDVGVYYCMQSIQLPPTFGQGTKVEIK	IGHV1-2 (Human)	IGHJ3 (Human)	IGKV2D-29 (Human)	IGKJ1 (Human)	2769	RKMLTIFGKVNQTMLLISGAKGQ	3971	MQSIQLPPT	Philip Brouwer et al., 2020 (https://science.sciencemag.org/content/early/2020/06/15/science.abc5902)
COVA2-32	Ab	SARS-CoV1, SARS-CoV2			SARS-CoV1, SARS-CoV2	S; RBD	B-cells; SARS-CoV2 Human Patient	682	EVQLVESGAEVKKPGSSVKVSCKASGGTFSSYAISWVRQAPGQGLEWMGGIIPIFGTANYAQKFQGRATITTDESTSTAYMELSSLGSEDTAVYYCARTHSYDNSGQYFDYWGQGTMVTVSS	1761	DIVMTQSPATLSLSPGERATLSCRASQSVSSFLAWYQQKPGQAPRLLIYDASNRATGIPARFSGSGSGTDFTLTISSLEPEDFAVYYCQQRSNWPPRLTFGGGTKVDIK	IGHV1-69 (Human)	IGHJ4 (Human)	IGKV3-11 (Human)	IGKJ4 (Human)	2770	ARTHSYDNSGQYFDY	3972	QQRSNWPPRLT	Philip Brouwer et al., 2020 (https://science.sciencemag.org/content/early/2020/06/15/science.abc5902)
COVA2-33	Ab	SARS-CoV2	SARS-CoV1		SARS-CoV1, SARS-CoV2	S; non-RBD	B-cells; SARS-CoV2 Human Patient	683	QVQLVQSGAEVKKPGESLRISCKGSGYSFTSHWISWVRQMPGKGLEWMGRIDPSDSYTNYSPSFQGHVTISADKSISTAYLQWSSLKASDTAMYYCARLKVITIFGVVRDDYGMDVWGQGTTVTVSS	1762	QSALTQPASVSGSPGQSITISCTGTSSDVGSYNLVSWYQQHPGKAPKLMIYDSSKRPSGVSNRFSGSKSGNTASLTISGLQAEDEADYYCCSYAGSVFGGGTKLTVL	IGHV5-10-1 (Human)	IGHJ6 (Human)	IGLV2-23 (Human)	IGLJ3 (Human)	2771	ARLKVITIFGVVRDDYGMDV	3973	CSYAGSV	Philip Brouwer et al., 2020 (https://science.sciencemag.org/content/early/2020/06/15/science.abc5902)
COVA2-34	Ab	SARS-CoV2	SARS-CoV1		SARS-CoV1, SARS-CoV2	S; non-RBD	B-cells; SARS-CoV2 Human Patient	684	QVQLVESGGGVVQPGRSLRLSCAASGFTFSSYAMHWVRQAPGKGLEWVAVISYDGSNKYYADSVKGRFTISRDNSKNTLYLQMNSLRAEDTAVYYCARSASGSYYGDYWGQGTLVTVSS	1763	QTVVTQPASVSGSPGQSITISCTGTSSDVGGYNYVSWYQQHPGKAPKLMIYDVSNRPSGVSNRFSGSKSGNTASLTISGLQAEDEADYYCSSYTSSSTLGLYVFGTGTKVTVL	IGHV3-30 (Human)	IGHJ4 (Human)	IGLV2-14 (Human)	IGLJ1 (Human)	2772	ARSASGSYYGAFDY	3974	SSYTSSSTLGLYV	Philip Brouwer et al., 2020 (https://science.sciencemag.org/content/early/2020/06/15/science.abc5902)

COVA2-37	Ab	SARS-CoV2	SARS-CoV1		SARS-CoV1, SARS-CoV2	S; non-RBD	B-cells; SARS-CoV2 Human Patient	685	EVQLVESGAEVKKPGASVKVSCKVSGYT LPELSMHWVRQAPGKGLDWMGGFDP EDGETIYAQKFQGRVTMTEDTSTDTAY MELSSLRSEDTAVYYCATSPAVMSVGW VDPWGQGTLVTVSS	1764	QSVLTQPPSVSGAPGQRVTISCTGSSS NIGAGYDVHWYQQLPGTAPKVLIYDN NNRPSGVPDRFSGSKSGTSASLAITGL QAEDEADYYCQSYDSSLSGSVFGGGT KLTVL	IGHV1-24 (Human)	IGHJ5 (Human)	IGLV1-40 (Human)	IGLJ3 (Human)	2773	ATSPAVMSV GWVDP	3975	QSYDSSLS GSV	Philip Brouwer et al., 2020 (https://science.sciencemag.org/content/early/2020/06/15/science.abc5902)
COVA2-38	Ab	SARS-CoV2	SARS-CoV1		SARS-CoV1, SARS-CoV2	S; non-RBD	B-cells; SARS-CoV2 Human Patient	686	QVQLQQSGPGLVKPSETLPLTCTVSGGS ISSSSYYWGWIRQPPGKGLEWIGSVFYS GSTYYNPSLKSRVTISVDTSKNQLSLKLSS VTAADTAVYYCARQVRQWLEDDAFDI WGQGTMVTVSS	1765	DIQLTQSPSSLSASVGDRVTITCRASQG IRNDLGWYQQKPGKAPKRLIYAASSL QSGVPSRFSGSGSGTEFTLTISSLQPED FATYYCLQHNSYPLTFGGGTKVDIK	IGHV4-39 (Human)	IGHJ3 (Human)	IGKV1-17 (Human)	IGKJ4 (Human)	2774	ARQVRQWLE DDAFDI	3976	LQHNSYPL T	Philip Brouwer et al., 2020 (https://science.sciencemag.org/content/early/2020/06/15/science.abc5902)
COVA2-39	Ab	SARS-CoV2	SARS-CoV1		SARS-CoV1, SARS-CoV2	S; RBD	B-cells; SARS-CoV2 Human Patient	687	QVQLVETGGGLIQPGGSLRLSCAASGFT VSSNYMSWVRQAPGKGLEWVSVIYTG GTTYYADSVKGRFTISRDNSKNTLYLQM NSLRAEDTAVYYCARAHVDTAMVESGA FDIWGQGTRVTVSS	1766	QSALTQPASVSGSPGQSITISCTGTSSD VGSYNLVSWYQQHPGKAPKLMIYEVT KRPSGVSNRFSGSKSGNTASLTISGLQ AEDEADYYCCSYAGSSTWVFGGGTKL TVL	IGHV3-53 (Human)	IGHJ3 (Human)	IGLV2-23 (Human)	IGLJ3 (Human)	2775	ARAHVDTAM VESGAFDI	3977	CSYAGSST WV	Philip Brouwer et al., 2020 (https://science.sciencemag.org/content/early/2020/06/15/science.abc5902);Nicholas Wu (https://www.biorxiv.org/content/10.1101/2020.07.26.222232v1)
COVA2-40	Ab	SARS-CoV2	SARS-CoV1		SARS-CoV1, SARS-CoV2	S; non-RBD	B-cells; SARS-CoV2 Human Patient	688	QVQLQESGPGLVKPSGTLSLTCAVSGGS ISSSNWWSWVRQPPGKGLEWIGEIYHS GSSNYNPSLKSRVTISVDKSKNQFSLKLN SVTAADTAVYYCAGRYCSGGRCGWFDP WGQGTLVTVSS	1767	QSVLTQPASVSGSPGQSITISCTGTSSD VGSYNLVSWYQQHPGKAPKLMIYEAS KRPSGISNRFSGSKSGNTASLTISGLQA EDEADYYCCSYAGSSTWVFGGGTKPT VL	IGHV4-4 (Human)	IGHJ5 (Human)	IGLV2-23 (Human)	IGLJ3 (Human)	2776	AGRYCSGGRC GWFDP	3978	CSYAGSST WV	Philip Brouwer et al., 2020 (https://science.sciencemag.org/content/early/2020/06/15/science.abc5902)
COVA2-41	Ab	SARS-CoV2	SARS-CoV1		SARS-CoV1, SARS-CoV2	S; non-RBD	B-cells; SARS-CoV2 Human Patient	689	EVQLVESGGGLVKPGGSLRLSCSASGFT FSNYNMDWVRQAPGKGLEWVSSISSSS SYIYLADSVKGRFTISRDNAKNSLYLQMN SLRAEDTAVYYCARVQKDIVVVPVALAD YYYYGMDVWGQGTTVTVSS	1768	DIVMTQSPATLSVSPGERATLSCRASQ SVSSNLAWYQQKPGQAPRLLIYGAST RATGIPARFSGSGSGTEFTLTISSLQPE DFAVYYCQQCYNWPPWTFGQGTRVE FK	IGHV3-21 (Human)	IGHJ6 (Human)	IGKV3-15 (Human)	IGKJ1 (Human)	2777	ARVQKDIVVV PVALADYYYY GMDV	3979	QQCYNWP PWT	Philip Brouwer et al., 2020 (https://science.sciencemag.org/content/early/2020/06/15/science.abc5902)
COVA2-43	Ab	SARS-CoV2	SARS-CoV1		SARS-CoV1, SARS-CoV2	S; non-RBD	B-cells; SARS-CoV2 Human Patient	690	QVQLVQPGAEVKKPGASVKVSCKASGY TFTSYGISWVRQAPGQGLEWMGWISA YNGDTNYAQKLQGRVTMTTDTSTSTAY MELRSLKSDDTAVYYCARFDYGYPYSSW SVLSIDYWGQGTLVTVSS	1769	DIVMTQSPSSLSASVGDRVTITCRASQ GIRNDLGWYQQKPGKAPKRLIYAASSL QSGVPSRFSGSGSGTEFTLTISSLQPED FATYYCLQHNSYPLTFGGGTKLEIK	IGHV1-18 (Human)	IGHJ4 (Human)	IGKV1-17 (Human)	IGKJ4 (Human)	2778	ARFDYGYPYS SWSVLSIDY	3980	LQHNSYPL T	Philip Brouwer et al., 2020 (https://science.sciencemag.org/content/early/2020/06/15/science.abc5902)
COVA2-44	Ab	SARS-CoV1, SARS-CoV2			SARS-CoV1, SARS-CoV2	S; RBD	B-cells; SARS-CoV2 Human Patient	691	EVQLVESGGGVVQPGRSLRLSCAASGFT FSSYAMHWVRQAPGKGLEWVAVISYD GSYKYYADSVKGRFTISRDNSKNTLYLQ MNSLTAEDTAVYYCAREGSRQWLVIYF DYWGQGTLVTVSS	1770	AIRMTQSPSSLSASVGDRVTITCRASQ SISSYLNWYQQKPGKAPKLLIYAASSLQ SGVPSRFSGSGSGTDFTLTISSLQPEDF ATYYCQQSYTTFIYTFGQGTKLEIK	IGHV3-30 (Human)	IGHJ4 (Human)	IGKV1-39 (Human)	IGKJ2 (Human)	2779	AREGSRQWL VIYFDY	3981	QQSYTTFIY T	Philip Brouwer et al., 2020 (https://science.sciencemag.org/content/early/2020/06/15/science.abc5902)
COVA2-45	Ab	SARS-CoV2			SARS-CoV1, SARS-CoV2	S; RBD	B-cells; SARS-CoV2 Human Patient	692	EVQLLESGAEVKKPGASVKISCKASGYTF TGYYMHWVRQAPGQGLEWMGWINP NSGGTNYAQKFQGRVTMTRDTSISTAY MELSRLRSDDTAVYYCARGDGDYYDSS GYYRPTLYNWLDPWGQGTRVTVSS	1771	DIVMTQSPGTLSLSPGERATLSCRASQ SVSSSYLAWYQQKPGQAPRLLIYGASS RATGIPDRFSGSGSGTDFTLTISRLEPE DFAVYYCQQYGSSPYTFGQGTKVEIK	IGHV1-2 (Human)	IGHJ5 (Human)	IGKV3-20 (Human)	IGKJ1 (Human)	2780	ARGDGDYYD SSGYYRPTLY NWLDP	3982	QQYGSSPY T	Philip Brouwer et al., 2020 (https://science.sciencemag.org/content/early/2020/06/15/science.abc5902)
COVA2-46	Ab	SARS-CoV2	SARS-CoV1		SARS-CoV1, SARS-CoV2	S; RBD	B-cells; SARS-CoV2 Human Patient	693	QVQLQESGPGLVKPSETLSLTCTASGGSI SSSSYYWGWIRQPPGKGLEWIGSIYYSG STYYNPSLKSRVTISVDTSKNQFSLKLSSV TAADTAVYYCARHPSGLYQLLNWGQGT LVTVSS	1772	AIRMTQSPSSLSASVGDRVTITCQASQ DISNYLNWYQQKPGKAPKLLIYDASNL ETGVPSRFSGSGSGTDFTFTISSLQPED IATYYCQQYDNLLSLTFGGGTKVEIK	IGHV4-39 (Human)	IGHJ4 (Human)	IGKV1-33 (Human)	IGKJ4 (Human)	2781	ARHPSGLYQL LN	3983	QQYDNLLS LT	Philip Brouwer et al., 2020 (https://science.sciencemag.org/content/early/2020/06/15/science.abc5902)
COVA2-47	Ab	SARS-CoV2	SARS-CoV1		SARS-CoV1, SARS-CoV2	S; non-RBD	B-cells; SARS-CoV2 Human Patient	694	EVQLVESGGGLVQPGRSLRLSCAASGFT FDDYAMHWVRQAPGKGLEWVSGISW NSGSIGYADSVKGRFTISRDSAKNSLYLQ MNSLRAEDTALYYCAKVATYYYDRSGYY YGGALDYWGQGTLVTVSS	1773	EIVLTQSPDSLAVSLGERATINCKSSQS VLYSSNNKNYLAWYQQKPGQPPKLLI YWASTRESGVPDRFSGSGSGTHFTLTI SSLQAEDVAVYYCQQYYSTPPLTFGGG TKVDIK	IGHV3-9 (Human)	IGHJ4 (Human)	IGKV4-1 (Human)	IGKJ4 (Human)	2782	AKVATYYYDR SGYYYGGALD Y	3984	QQYYSTPP LT	Philip Brouwer et al., 2020 (https://science.sciencemag.org/content/early/2020/06/15/science.abc5902)
COVA3-01	Ab	SARS-CoV1, SARS-CoV2			SARS-CoV1, SARS-CoV2	S; non-RBD	B-cells; SARS-CoV2 Human Patient	695	EVQLVESGPGLVKPSETLSLTCTVSGGSI SSYYWSWIRQPPGKGLEWIGYIYYSGST NYNPSLKSRVTISVDTSKNQFSLKLSSVTA ADTAVYYCARGPAATYYYYMDVWGKG TRVTVSS	1774	EIVMTQSPSSLSASVGDRVTITCRASQS MSSYLNWYQQKPGKAPKLLIYAASSL QSGVPSRFSGSGSGTDFTLTISSLQPED FATYYCQQSYSTLTFGGGTKVEIK	IGHV4-59 (Human)	IGHJ6 (Human)	IGKV1-39 (Human)	IGKJ4 (Human)	2783	ARGPAATYYY YMDV	3985	QQSYSTLT	Philip Brouwer et al., 2020 (https://science.sciencemag.org/content/early/2020/06/15/science.abc5902)
COVA3-03	Ab	SARS-CoV1, SARS-CoV2			SARS-CoV1, SARS-CoV2	S; non-RBD	B-cells; SARS-CoV2 Human Patient	696	EVQLVESGGGLVQPGGSLRLSCAASGFT FSSYAMSWVRQAPGKGLEWVSTISGSG GNTYYADSVKGRFTISRDNSKNTLYLQM NSLRAEDTAVYYCAKEIAVAGCFDYWG QGTLVTVSS	1775	QTVVTQPPSVSVSPGQTARITCSGDAL PKQYAYWYQQKPGQAPVLVIYKDSER PSGIPERFSGSSSGTTVTLTISGVQAED EADYYCQSADSSGTYRVFGGGTKLTVL	IGHV3-23 (Human)	IGHJ4 (Human)	IGLV3-25 (Human)	IGLJ3 (Human)	2784	AKEIAVAGCF DY	3986	QSADSSGT YRV	Philip Brouwer et al., 2020 (https://science.sciencemag.org/content/early/2020/06/15/science.abc5902)

COVA3-04	Ab	SARS-CoV2	SARS-CoV1		SARS-CoV1, SARS-CoV2	S; non-RBD	B-cells; SARS-CoV2 Human Patient	697	EVQLVESGGGVVQPGRSLRLSCAASGFTFSSYGMHWVRQAPGKGLEWVAVIWYDGSNKYYADSVKGRFTISRDNSKNTLYLQMNSLRAEDTAVYYCARVGSVKSTAGYDFWSGDPFDYWGQGTLVTVSS	1776	QPVLTQPPSVSVAPGQTARITCGGNNIGSKSVHWYQQKPGQAPVLVVYDDSDRPSGIPERFSGSNSGNTATLTISRVEAGDEADYYCQVWDSSSDHYVFGTGTKVTVL	IGHV3-33 (Human)	IGHJ4 (Human)	IGLV3-21 (Human)	IGLJ1 (Human)	2785	ARVGSVKSTAGYDFWSGDPFDY	3987	QVWDSSSDHYV	Philip Brouwer et al., 2020 (https://science.sciencemag.org/content/early/2020/06/15/science.abc5902)
COVA3-05	Ab	SARS-CoV2	SARS-CoV1		SARS-CoV1, SARS-CoV2	S; RBD	B-cells; SARS-CoV2 Human Patient	698	QVQLVQSGAEVKKPGASVKVSCKVSGYTLTELSMHWVRQAPGKGLEWMGGFDPEDGETIYAQKFQGRVTMTEDTSTDTAYMELSSLRSEDTAVYYCATAYSVDTAMVRGVGYWGQGTLVTVSS	1777	NFMLTQPPSASGTPGQRVTISCSGSSSNIGSNTVNWYQQLPGTAPKLLIYSNNQRPSGVPDRFSGSKSGTSASLAISGLQSEDEADYYCAAWDDSLNGPHWVFGGGTKLTVL	IGHV1-24 (Human)	IGHJ4 (Human)	IGLV1-44 (Human)	IGLJ3 (Human)	2786	ATAYSVDTAMVRGVGY	3988	AAWDDSLNGPHWV	Philip Brouwer et al., 2020 (https://science.sciencemag.org/content/early/2020/06/15/science.abc5902)
COVA3-06	Ab	SARS-CoV2	SARS-CoV1		SARS-CoV1, SARS-CoV2	S; RBD	B-cells; SARS-CoV2 Human Patient	699	QVQLVESRAEVKKPGSSVKVSCKASGGTFSSYAISWVRQAPGQGLEWMGRIIPILGITNYAQKFQGRVTITADKSTSTAYMELSSLRSEDTAVYYCARDAPDYYDSSGPTYFDYWGQGTLVTVSS	1778	DVVMTQSPDSLAVSLGERATINCKSSQSVLYSSNNKNYLAWYQQKPGQPPKLLIYWASTRESGVPDRFSGSGSGTDFTLTISSLQAEDVAVYYCQQYYSTPLTFGGGTKVDIK	IGHV1-69 (Human)	IGHJ4 (Human)	IGKV4-1 (Human)	IGKJ4 (Human)	2787	ARDAPDYYDSSGPTYFDY	3989	QQYYSTPLT	Philip Brouwer et al., 2020 (https://science.sciencemag.org/content/early/2020/06/15/science.abc5902)
COVA3-07	Ab	SARS-CoV2	SARS-CoV1		SARS-CoV1, SARS-CoV2	S; non-RBD	B-cells; SARS-CoV2 Human Patient	700	QVQLVESGGGLVQPGRSLRLSCAASGFTFDDYAMHWVRQAPGKGLEWVSGISWNSGSIGYADSVKGRFTISRDNAKNSLYLQMNSLRAEDTALYYCAKAEPEVGGYDYYMDVWGKGTMVTVSS	1779	EIVLTQSPGTLSLSPGERATLSCRASQSVSSSYLAWYQQKPGQAPRLLIYGASSRATGIPDRFSGSGSGTDFTLTISRLEPEDFAVYYCQQYGSSPFTFGPGTKLEIK	IGHV3-9 (Human)	IGHJ6 (Human)	IGKV3-20 (Human)	IGKJ3 (Human)	2788	AKMGPDPAHDYGRKNDAFDI	3990	QQYGSSPFT	Philip Brouwer et al., 2020 (https://science.sciencemag.org/content/early/2020/06/15/science.abc5902)
COVA3-08	Ab	SARS-CoV1, SARS-CoV2			SARS-CoV1, SARS-CoV2	S; non-RBD	B-cells; SARS-CoV2 Human Patient	701	EVQLVESGPGLVKPSETLSLTCTVSGGSISSYYWSWIRQPPGKGLEWIGYIYYSGSTNYNPSLKSRVTISVDTSKNQFSLRLSSVTAADTAVYYCARGPAATYYYYMDVWGKGTMVTVSS	1780	DIVMTQSPSSLSASVGDRVTITCRASQSISSYLNWYQQKPGKAPKLLIYAASSLQSGVPSRFSGSGSGTDFTLTISSLQPEDFATYYCQQSYSTPLTFGPGTKLEIK	IGHV4-59 (Human)	IGHJ6 (Human)	IGKV1-39 (Human)	IGKJ4 (Human)	2789	AKAEPEVGGYDYYMDV	3991	QQSYSTPLT	Philip Brouwer et al., 2020 (https://science.sciencemag.org/content/early/2020/06/15/science.abc5902)
COVA3-09	Ab	SARS-CoV2	SARS-CoV1		SARS-CoV1, SARS-CoV2	S; RBD	B-cells; SARS-CoV2 Human Patient	702	EVQLVESGGGLVQPGRSLRLSCAASGFTFDDYAMHWVRQAPGKGLEWVSGISWNSGSIGYADSVKGRFTISRDNAKNSLYLQMNSLRAEDTALYYCAKMGPDPAHDYGRKNDAFDIWGQGTMVTVSS	1781	DIVMTQSPSSLSASVGDRVTITCRASQSMSSYLNWYQQKPGKAPKLLIYAASSLQSGVPSRFSGSGSGTDFTLTISSLQPEDFATYYCQQSYSTLTFGGGTKLEIK	IGHV3-9 (Human)	IGHJ3 (Human)	IGKV1-39 (Human)	IGKJ4 (Human)	2790	ARGPAATYYYYMDV	3992	QQSYSTLT	Philip Brouwer et al., 2020 (https://science.sciencemag.org/content/early/2020/06/15/science.abc5902)
COVA3-10	Ab	SARS-CoV1, SARS-CoV2			SARS-CoV1, SARS-CoV2	S; RBD	B-cells; SARS-CoV2 Human Patient	703	EVQLVESRAEMKKPGESLKISCKGSGYTFTNHWIAWVRQMPGKGLEWMGIIYPGDSDTRYSPSFEGQVTISADKSISTAYLQWSSLKASDTAMYYCARRGYTYGADFYGLDVWGQGTRVTVSS	1782	DIVMTQSPDSLAVSLGERATINCKSSQSVLYSSNNKNYLAWYQQKPGQPPKLLIYWASTRESGVPDRFSGSGSGTDFTLTISSLQAEDVAVYYCQQYYSTPITFGQGTRLEIK	IGHV5-51 (Human)	IGHJ6 (Human)	IGKV4-1 (Human)	IGKJ5 (Human)	2791	ARRGYTYGADFYGLDV	3993	QQYYSTPIT	Philip Brouwer et al., 2020 (https://science.sciencemag.org/content/early/2020/06/15/science.abc5902)
CR3022	Ab	SARS-CoV1, SARS-CoV2		SARS-CoV1	SARS-CoV2	S; RBD	B-cells; SARS-CoV1 Human Patient	704	QMQLVQSGTEVKKPGESLKISCKGSGYGFITYWIGWVRQMPGKGLEWMGIIYPGDSETRYSPSFQGQVTISADKSINTAYLQWSSLKASDTAIYYCAGGSGISTPMDVWGQGTTVTVSS	1783	DIQLTQSPDSLAVSLGERATINCKSSQSVLYSSINKNYLAWYQQKPGQPPKLLIYWASTRESGVPDRFSGSGSGTDFTLTISSLQAEDVAVYYCQQYYSTPYTFGQGTKVEIK	IGHV5-51 (Human)	IGHJ6 (Human)	IGKV4-1 (Human)	IGKJ1 (Human)	2792	AGGSGISTPMDV	3994	QQYYSTPYT	Jan ter Meulen et al., 2006 (https://journals.plos.org/plosmedicine/article?id=10.1371/journal.pmed.0030237);Meng Yuan et al., 2020a (https://science.sciencemag.org/content/early/2020/04/02/science.abb7269);Meng Yuan et al., 2020b (https://www.biorxiv.org/content/10.1101/2020.06.08.141267v1)
CV-X1-126	Ab	SARS-CoV2	SARS-CoV1	SARS-CoV2		S; RBD	B-cells; SARS-CoV2 Human Patient		ND		ND	IGHV3-53 (Human)	IGHJ6 (Human)	ND	ND	2793	ARDLSEGGMDV	3995	QQANGFPPL	Jakob Kreye et al., 2020 (https://www.biorxiv.org/content/10.1101/2020.08.15.252320v1.full.pdf)
CV-X2-106	Ab	SARS-CoV2	SARS-CoV1	SARS-CoV2		S; RBD	B-cells; SARS-CoV2 Human Patient		ND		ND	IGHV1-69 (Human)	IGHJ6 (Human)	ND	ND	2794	ATRKETTVTTSLVYGMDV	3996	QQSYSTPYT	Jakob Kreye et al., 2020 (https://www.biorxiv.org/content/10.1101/2020.08.15.252320v1.full.pdf)
CV05-163	Ab	SARS-CoV2	SARS-CoV1	SARS-CoV2		S; RBD	B-cells; SARS-CoV2 Human Patient		ND		ND	IGHV1-2 (Human)	IGHJ6 (Human)	ND	ND	2795	AREVMVRGALPPYGMDV	3997	QQRSNWPPVT	Jakob Kreye et al., 2020 (https://www.biorxiv.org/content/10.1101/2020.08.15.252320v1.full.pdf)

CV07-200	Ab	SARS-CoV2	SARS-CoV1	SARS-CoV2		S; RBD	B-cells; SARS-CoV2 Human Patient		ND		ND	IGHV1-2 (Human)	IGHJ6 (Human)	ND	ND	2796	ARGPFYYDNS GTLGGLDV	3998	SSYTSSSTY V	Jakob Kreye et al., 2020 (https://www.biorxiv.org/content/10.1101/2020.08.15.252320v1.full.pdf)
CV07-209	Ab	SARS-CoV2	SARS-CoV1	SARS-CoV2		S; RBD	B-cells; SARS-CoV2 Human Patient		ND		ND	IGHV3-11 (Human)	IGHJ4 (Human)	ND	ND	2797	ARDGVIPPRF DY	3999	QQYDNLPL T	Jakob Kreye et al., 2020 (https://www.biorxiv.org/content/10.1101/2020.08.15.252320v1.full.pdf)
CV07-222	Ab	SARS-CoV2	SARS-CoV1	SARS-CoV2		S; RBD	B-cells; SARS-CoV2 Human Patient		ND		ND	IGHV1-2 (Human)	IGHJ3 (Human)	ND	ND	2798	ARGPYYYDSS GSLGAFDI	4000	CSYAGGST SYV	Jakob Kreye et al., 2020 (https://www.biorxiv.org/content/10.1101/2020.08.15.252320v1.full.pdf)
CV07-250	Ab	SARS-CoV2	SARS-CoV1	SARS-CoV2		S; RBD	B-cells; SARS-CoV2 Human Patient		ND		ND	IGHV1-18 (Human)	IGHJ6 (Human)	ND	ND	2799	AGSDNYGFPY NGMDV	4001	SSYAGNND FV	Jakob Kreye et al., 2020 (https://www.biorxiv.org/content/10.1101/2020.08.15.252320v1.full.pdf)
CV07-255	Ab	SARS-CoV2	SARS-CoV1	SARS-CoV2		S; RBD	B-cells; SARS-CoV2 Human Patient		ND		ND	IGHV1-2 (Human)	IGHJ4 (Human)	ND	ND	2800	ARDSRFSYVN GEFDY	4002	CSYAGHST WV	Jakob Kreye et al., 2020 (https://www.biorxiv.org/content/10.1101/2020.08.15.252320v1.full.pdf)
CV07-262	Ab	SARS-CoV2	SARS-CoV1	SARS-CoV2		S; RBD	B-cells; SARS-CoV2 Human Patient		ND		ND	IGHV1-2 (Human)	IGHJ6 (Human)	ND	ND	2801	ARVGWYDFG TPGDYYYYYG MDV	4003	CSYAGTST FV	Jakob Kreye et al., 2020 (https://www.biorxiv.org/content/10.1101/2020.08.15.252320v1.full.pdf)
CV07-270	Ab	SARS-CoV2	SARS-CoV1	SARS-CoV2		S; RBD	B-cells; SARS-CoV2 Human Patient		ND		ND	IGHV1-2 (Human)	IGHJ6 (Human)	ND	ND	2802	ARVFGPGLDC SSTSCYTYGM DV	4004	CSYAGSSS WV	Jakob Kreye et al., 2020 (https://www.biorxiv.org/content/10.1101/2020.08.15.252320v1.full.pdf)
CV07-283	Ab	SARS-CoV2	SARS-CoV1	SARS-CoV2		S; RBD	B-cells; SARS-CoV2 Human Patient		ND		ND	IGHV1-2 (Human)	IGHJ6 (Human)	ND	ND	2803	VRGPFYYDSS GPLGGMDV	4005	SSYTSSSTY V	Jakob Kreye et al., 2020 (https://www.biorxiv.org/content/10.1101/2020.08.15.252320v1.full.pdf)
CV07-287	Ab	SARS-CoV2	SARS-CoV1	SARS-CoV2		S; RBD	B-cells; SARS-CoV2 Human Patient		ND		ND	IGHV1-58 (Human)	IGHJ3 (Human)	ND	ND	2804	AAPYCSSTNC YDAFDI	4006	QQYYGSSP WT	Jakob Kreye et al., 2020 (https://www.biorxiv.org/content/10.1101/2020.08.15.252320v1.full.pdf)
CV07-315	Ab	SARS-CoV2	SARS-CoV1	SARS-CoV2		S; RBD	B-cells; SARS-CoV2 Human Patient		ND		ND	IGHV3-9 (Human)	IGHJ6 (Human)	ND	ND	2805	AKDFLWDLH PPRYYGMDV	4007	QQSYSTHA	Jakob Kreye et al., 2020 (https://www.biorxiv.org/content/10.1101/2020.08.15.252320v1.full.pdf)
CV1	Ab	SARS-CoV1, SARS-CoV2		SARS-CoV2		S; non-RBD	B-cells; SARS-CoV2 Human Patient	705	QVQLQESGPGLVKPSETLSLTCTVSGYSI SSGYYWGWIRQPPGKGLEWIGSIYHSG STYYNPSLKSRVTISVDTSKNQFSLKLSSV TAADTAVYYCARTPLSLRLRYNWYFDLW GRGTLVTVSS	1784	QSVLTQPPSASGTPGQRVTISCSGSSS NIGSNTVNWYQQLPGTAPKLLIYSNN QRPSGVPDRFSGSKSGTSASLAISGLQ SEDEADYYCAAWDDSLNGPVFGGGT KLTVL	IGHV4-38-2 (Human)	IGHJ2 (Human)	IGLV1-44 (Human)	IGLJ3 (Human)	2806	ARTPLSLRLRY NWYFDL	4008	AAWDDSL NGPV	Emilie Seydoux et al., 2020 (https://www.biorxiv.org/content/10.1101/2020.05.12.091298v1)
CV10	Ab	SARS-CoV1, SARS-CoV2			SARS-CoV2	S; non-RBD	B-cells; SARS-CoV2 Human Patient	706	QVQLQESGPGLVKPSETLSLTCNVSGGSI SSYYWSWIRQPPGKGLEWIGYIYYSGST NYNPSLKSRVTISVDTSKNQFSLKLSSVTA ADTAVYYCARGFDYWGQGTLVTVSS	1785	EIVLTQSPGTLSLSPGERATLSCRASQS VSSIYLAWYQQKPGQAPRLLIYGASSR ATGIPDRFSGSGSGTDFTLTISRLEPED FAVYYCQQYAGSPWTFGQGTKVEIK	IGHV4-59 (Human)	IGHJ4 (Human)	IGKV3-20 (Human)	IGKJ1 (Human)	2807	ARGFDY	4009	QQYAGSP WT	Emilie Seydoux et al., 2020 (https://www.biorxiv.org/content/10.1101/2020.05.12.091298v1)
CV11	Ab	SARS-CoV1, SARS-CoV2			SARS-CoV2	S; non-RBD	B-cells; SARS-CoV2 Human Patient	707	QVQLQESGPGLVKPSQTLSLTCTVSGGSI SSGGYYWSWIRQHPGKGLEWIGYIYYS GSTYYNPSLKSRVTISVDTSKNQFSLKLSS VTAADTAVYYCARETTGHFDYWGQGTL VTVSS	1786	EIVLTQSPATLSLSPGERATLSCRASQS VSSYLAWYQQKPGQAPRLLIYDASNR ATGIPARFSGSGSGTDFTLTISSLEPEDF AVYYCQQRSNWPPIFTFGPGTKVDIK	IGHV4-31 (Human)	IGHJ4 (Human)	IGKV3-11 (Human)	IGKJ3 (Human)	2808	ARETTGHFDY	4010	QQRSNWP PIFT	Emilie Seydoux et al., 2020 (https://www.biorxiv.org/content/10.1101/2020.05.12.091298v1)

CV12	Ab	SARS-CoV2	SARS-CoV1		SARS-CoV2	S; non-RBD	B-cells; SARS-CoV2 Human Patient	708	QVQLVESGGGVVQPGRSLRLSCAASGFNLSNYAMHWVRQASGKGLEWVSLISYDGSVKYYTDSVKGRFTVSGDNSKNTLFLQMNSLRPDDSALYYCVRGGVSGPNSFDMWGQGTTVTVSS	1787	DVVMTQSPLSLPVTLGQPATISCRSSQSLVYSDGNTYVNWFQQRPGQSPRRLIYQVSIRASGVPDRFSGSGSGTDFALKISRVEAEDVGVYYCMQGTHWPVTFGQGTKVEIK	IGHV3-30 (Human)	IGHJ4 (Human)	IGKV2-30 (Human)	IGKJ1 (Human)	2809	VRGGVSGPNSFDM	4011	MQGTHWPVT	Emilie Seydoux et al., 2020 (https://www.biorxiv.org/content/10.1101/2020.05.12.091298v1)
CV13	Ab	SARS-CoV1, SARS-CoV2			SARS-CoV2	S; non-RBD	B-cells; SARS-CoV2 Human Patient	709	QVQLVQSGSELKKPGASVKLSCQASGYSFTNHAMNWVRQAPGQGLEWMGWINTNTGNPTYAQGFTGRFVFSLDTSVSTTYLHISSLKAEDTAVYYCARASARPGVATNLDFWGQGTLVVVSS	1788	DIQMTQSPSSLSASVGDRVTITCRASQNIDNYLNWYQQKPGKAPKLLIYAASRLHSGVPSRFSGSGSGTDFTLIISSLQPEDLATYYCQQSYSNPLTFGPGTKVDIR	IGHV7-4-1 (Human)	IGHJ4 (Human)	IGKV1-39 (Human)	IGKJ3 (Human)	2810	ARASARPGVATNLDF	4012	QQSYSNPLT	Emilie Seydoux et al., 2020 (https://www.biorxiv.org/content/10.1101/2020.05.12.091298v1)
CV15	Ab	SARS-CoV2	SARS-CoV1		SARS-CoV2	S; non-RBD	B-cells; SARS-CoV2 Human Patient	710	EVQLVESGGGLVQPGGSLRLSCAASGFTFSSYWMSWVRQAPGKGLEWVANIKQDGSEKYYVDSVKGRFTISRDNAKNSLYLQMNSLRAEDTAVYYCARDFNSYQLLWYYYYGMDVWGQGTTVTVSS	1789	QSALTQPRSVSGSPGQSVTISCTGTSSDVGGYNYVSWYQQHPGKAPKLMIYDVSKRPSGVPDRFSGSKSGNTASLTISGLQAEDEADYYCCSYAGSYTWVFGGGTKLTVL	IGHV3-7 (Human)	IGHJ6 (Human)	IGLV2-11 (Human)	IGLJ3 (Human)	2811	ARDFNSYQLLWYYYYGMDV	4013	CSYAGSYTWV	Emilie Seydoux et al., 2020 (https://www.biorxiv.org/content/10.1101/2020.05.12.091298v1)
CV16	Ab	SARS-CoV2	SARS-CoV1		SARS-CoV2	S; non-RBD	B-cells; SARS-CoV2 Human Patient	711	EVQLVQSGAEVKKPGESLKISCKGSGYSFTSYWIGWVRQMPGKGLEWMGIIYPGDSDTRYSPSFQGQVTISADKSISTAYLQWSSLKASDTAMYYCARQSSFYSSGWYSYGMDVWGQGTTVTVSS	1790	EIVLTQSPGTLSLSPGERATLSCRASQSVSSSYLAWYQQKPGQAPRLLIYGASSRATGIPDRFSGSGSGTDFTLTISRLEPEDFAVYYCQQYGSSRGTFGQGTKVEIK	IGHV5-51 (Human)	IGHJ6 (Human)	IGKV3-20 (Human)	IGKJ1 (Human)	2812	ARQSSFYSSGWYSYGMDV	4014	QQYGSSRGT	Emilie Seydoux et al., 2020 (https://www.biorxiv.org/content/10.1101/2020.05.12.091298v1)
CV17	Ab	SARS-CoV2	SARS-CoV1		SARS-CoV2	S; non-RBD	B-cells; SARS-CoV2 Human Patient	712	QVQLVQSGAEVKKPGASVKVSCKASGYTFTGYYMHWVRQAPGQGLEWMGWINPNSGGTNYAQKFQGRVTMTRDTSISTAYMELSRLRSDDTAVYYCARVDYGSGSYGWGWFDPWGQGTLVTVSS	1791	QSALTQPASVSGSPGQSITISCTGTSSDVGSYNLVSWYQQHPGKAPKLMIYEGSKRPSGVSNRFSGSKSGNTASLTISGLQAEDEADYYCCSYAGSSTYVFGTGTKVTVL	IGHV1-2 (Human)	IGHJ5 (Human)	IGLV2-23 (Human)	IGLJ1 (Human)	2813	ARVDYGSGSYGWGWFDP	4015	CSYAGSSTYV	Emilie Seydoux et al., 2020 (https://www.biorxiv.org/content/10.1101/2020.05.12.091298v1)
CV18	Ab	SARS-CoV1, SARS-CoV2			SARS-CoV2	S; non-RBD	B-cells; SARS-CoV2 Human Patient	713	QVQLVQSGAEVKKPGASVKVSCKVSGYTLTELSMHWVRQAPGKGLEWMGGFDPEDGETIYAQKFQGRVTMTEDTSTDTAYMELSSLRSEDTAVYYCATTSPIVGAITWFDPWGQGTLVTVSS	1792	QSVLTQPPSVSAAPGQKVTISCSGSSSNIGNNYVSWYQQLPGTAPKLLIYDNNKRPSGIPDRFSGSKSGTSATLGITGLQTGDEADYYCGTWDSSLSAGPVFGGGTKLTVL	IGHV1-24 (Human)	IGHJ5 (Human)	IGLV1-51 (Human)	IGLJ3 (Human)	2814	ATTSPIVGAITWFDP	4016	GTWDSSLSAGPV	Emilie Seydoux et al., 2020 (https://www.biorxiv.org/content/10.1101/2020.05.12.091298v1)
CV19	Ab	SARS-CoV2	SARS-CoV1		SARS-CoV2	S; non-RBD	B-cells; SARS-CoV2 Human Patient	714	QVQLVQSGAEVKKPGASVKVSCKASGYTFTGYYMHWVRQAPGQGLEWMGWINPNSGGTNYAQKFQGRVTMTRDTSISTAYMELSRLRSDDTAVYYCAREYYYDSSVYPYYYYAMDVWGQGTTVTVSS	1793	EIVLTQSPGTLSLSPGERATLSCRASQSVSSSYLAWYQQKPGQAPRLLIYGASSRATGIPDRFSGSGSGTDFTLTISRLEPEDFAVYYCQQYGSSPPKYTFGQGTKLEIK	IGHV1-2 (Human)	IGHJ6 (Human)	IGKV3-20 (Human)	IGKJ2 (Human)	2815	AREYYYDSSVYPYYYYAMDV	4017	QQYGSSPPKYT	Emilie Seydoux et al., 2020 (https://www.biorxiv.org/content/10.1101/2020.05.12.091298v1)
CV2	Ab	SARS-CoV2	SARS-CoV1		SARS-CoV2	S; non-RBD	B-cells; SARS-CoV2 Human Patient	715	QVQLVESGGGVVQPGRSLRLSCAASGFTFSSYAMHWVRQAPGKGLEWVAVISYDGSNKYYADSVKGRFTISRDNSKNTLYLQMNSLRAEDTAVYYCARVRGSYYLFDYWGQGTLVTVSS	1794	EIVMTQSPATLSVSPGERATLSCRASQSVSSNLAWYQQKPGQAPRLLIYGASTRATGIPARFSGSGSGTEFTLTISSLQSEDFAVYYCQQYNNWPPSLTFGGGTKVEIK	IGHV3-30 (Human)	IGHJ4 (Human)	IGKV3-15 (Human)	IGKJ4 (Human)	2816	ARVRGSYYLFDY	4018	QQYNNWPPSLT	Emilie Seydoux et al., 2020 (https://www.biorxiv.org/content/10.1101/2020.05.12.091298v1)
CV21	Ab	SARS-CoV2	SARS-CoV1		SARS-CoV2	S; non-RBD	B-cells; SARS-CoV2 Human Patient	716	EVQLVESGGGLVKPGGSLRLSCAASGFTFSNAWMSWVRQAPGKGLEWVGRIKSKTDGGTTDYAAPVKGRFTISRDDSKNTLYLQMNSLKTEDTAVYYCTTDRVYDYIWGSYRYLDYWGQGTLVTVSS	1795	EIVLTQSPATLSLSPGERATLSCRASQSVSSYLAWYQQKPGQAPRLLIYDASNRATGIPARFSGSGSGTDFTLTISSLEPEDFAVYYCQQRSNWPLTFGGGTKVEIK	IGHV3-15 (Human)	IGHJ4 (Human)	IGKV3-11 (Human)	IGKJ4 (Human)	2817	TTDRVYDYIWGSYRYLDY	4019	QQRSNWPLT	Emilie Seydoux et al., 2020 (https://www.biorxiv.org/content/10.1101/2020.05.12.091298v1)
CV22	Ab	SARS-CoV1, SARS-CoV2			SARS-CoV2	S; non-RBD	B-cells; SARS-CoV2 Human Patient	717	EVQLVESGGGLVKPGGSLRLSCAASGFTFSSYSMNWVRQAPGKGLEWVSSISSSSSYIYYADSVKGRFTISRDNAKNSLYLQMNSLRAEDTAVYYCARDRESYDILTGYSMEGCFDYWGQGTLVTVSS	1796	QLVLTQSPSASASLGASVKLTCTLSSGHSSYAIAWHQQQPEKGPRYLMKLNSDGSHSKGDGIPDRFSGSSSGAERYLTISSLQSEDEADYYCQTWGTGIRVFGGGTKLTVL	IGHV3-21 (Human)	IGHJ4 (Human)	IGLV4-69 (Human)	IGLJ3 (Human)	2818	ARDRESYDILTGYSMEGCFDY	4020	QTWGTGIRV	Emilie Seydoux et al., 2020 (https://www.biorxiv.org/content/10.1101/2020.05.12.091298v1)
CV23	Ab	SARS-CoV2	SARS-CoV1		SARS-CoV2	S; non-RBD	B-cells; SARS-CoV2 Human Patient	718	QVQLVQSGAEVKKPGASVKVSCKASGYTFTSYAMHWVRQAPGQRLEWMGWINAGNGNTKYSQKFQGRVTITRDTSASTAYMELSSLRSEDTAVYYCARVWGYCSGGSCYVDAFDIWGQGTMVTVSS	1797	SYELTQPPSVSVSPGQTARITCSGDALPKQYAYWYQQKPGQAPVLVIYKDSERPSGIPERFSGSSSGTTVTLTISGVQAEDEADYYCQSADSSGTYVVFGGGTKLTVL	IGHV1-3 (Human)	IGHJ3 (Human)	IGLV3-25 (Human)	IGLJ3 (Human)	2819	ARVWGYCSGGSCYVDAFDI	4021	QSADSSGTYVV	Emilie Seydoux et al., 2020 (https://www.biorxiv.org/content/10.1101/2020.05.12.091298v1)
CV24	Ab	SARS-CoV2	SARS-CoV1		SARS-CoV2	S; non-RBD	B-cells; SARS-CoV2 Human Patient	719	QVQLVQSGAEVKKPGASVKVSCKVSGYTLTELSMHWVRQAPGKGLEWMGGFDPEDGETIYAQKFQGRVTMTEDTSTDTAYMELSSLRSEDTAVYYCATAPPYSPPSSWFDPWGQGTLVTVSS	1798	QSVLTQPPSVSAAPGQKVTISCSGSSSNIGNNYVSWYQQLPGTAPKLLIYDNNKRPSGIPDRFSGSKSGTSATLGITGLQTGDEADYYCGTWDSSLSASYVFGTGTKVTVL	IGHV1-24 (Human)	IGHJ5 (Human)	IGLV1-51 (Human)	IGLJ1 (Human)	2820	ATAPPYSPPSSWFDP	4022	GTWDSSLSASYV	Emilie Seydoux et al., 2020 (https://www.biorxiv.org/content/10.1101/2020.05.12.091298v1)
CV25	Ab	SARS-CoV2	SARS-CoV1		SARS-CoV2	S; non-RBD	B-cells; SARS-CoV2 Human Patient	720	QVQLQESGPGLVKPSQTLSLTCTVSGGSISSGDYYWSWIRQPPGKGLEWIGYIYYSGSTYYNPSLKSRVTISVDTSKNQFSLKLSSVTAADTAVYYCARDHHYDFWSGYSSYYYYGMDVWGQGTTVTVSS	1799	EIVMTQSPATLSVSPGERATLSCRASQSVSSNLAWYQQKPGQAPRLLIYGASTRATGIPARFSGSGSGTEFTLTISSLQSEDFAVYYCQQYNNWPYTFGQGTKLEIK	IGHV4-30-4 (Human)	IGHJ6 (Human)	IGKV3-15 (Human)	IGKJ2 (Human)	2821	ARDHHYDFWSGYSSYYYYGMDV	4023	QQYNNWPYT	Emilie Seydoux et al., 2020 (https://www.biorxiv.org/content/10.1101/2020.05.12.091298v1)

CV26	Ab	SARS-CoV1, SARS-CoV2			SARS-CoV2	S; non-RBD	B-cells; SARS-CoV2 Human Patient	721	QVQLVESGGGVVQPGRSLRLSCAASGF TFSSYAMHWVRQAPGKGLEWVAVISY DGSNKYYADSVKGRFTISRDNSKNTLYL QMNSLRAEDTAVYYCARDEAYYDILTGY INAPKNYYYYGMDVWGQGTTVTVSS	1800	DIQMTQSPSSLSASVGDRVTITCRASQ GIRNDLGWYQQKPGKAPKRLIYAASSL QSGVPSRFSGSGSGTEFTLTISSLQPED FATYYCLQHNSYPFTFGPGTKVDIK	IGHV3-30-3 (Human)	IGHJ6 (Human)	IGKV1-17 (Human)	IGKJ3 (Human)	2822	ARDEAYYDILT GYINAPKNYY YYGMDV	4024	LQHNSYPF T	Emilie Seydoux et al., 2020 (https://www.biorxiv.org/content/10.1101/2020.05.12.091298v1)
CV27	Ab	SARS-CoV2	SARS-CoV1		SARS-CoV2	S; non-RBD	B-cells; SARS-CoV2 Human Patient	722	QVQLVESGGGVVQPGRSLRLSCAASGF TFSSYAMHWVRQAPGKGLEWVALISYD GSNKYYADSVKGRFTISRDNSKNTLYLQ MNSLRAEDTAVYYCARSFGGSYYYGMD VWGQGTTVTVSS	1801	QSALTQPASVSGSPGQSITISCTGTSSD VGGYNYVSWYQQHPGKAPKLMIYDV SNRPSGVSNRFSGSKSGNTASLTISGL QAEDEADYYCSSYTSSSTPYVFGTGTK VTVL	IGHV3-30 (Human)	IGHJ6 (Human)	IGLV2-14 (Human)	IGLJ1 (Human)	2823	ARSFGGSYYY GMDV	4025	SSYTSSSTP YV	Emilie Seydoux et al., 2020 (https://www.biorxiv.org/content/10.1101/2020.05.12.091298v1)
CV3	Ab	SARS-CoV1, SARS-CoV2			SARS-CoV2	S; non-RBD	B-cells; SARS-CoV2 Human Patient	723	QVQLVQSGSELKKPGASVKLSCQASGYS FTNHAMNWVRQAPGQGLEWMGWIN TNTGNPTYAQGFTGRFVFSLDTSVSTTYL HISSLKAEDTAVYYCARASARPGVATNL DFWGQGTLVVVSS	1802	DIQMTQSPSSLSASVGDRVTITCRASQ NIDNYLNWYQQKPGKAPKLLIYAASRL HSGVPSRFSGSGSGTDFTLIISSLQPED LATYYCQQSYSNPLTFGPGTKVDIR	IGHV7-4-1 (Human)	IGHJ4 (Human)	IGKV1-39 (Human)	IGKJ3 (Human)	2824	ARASARPGVA TNLDF	4026	QQSYSNPL T	Emilie Seydoux et al., 2020 (https://www.biorxiv.org/content/10.1101/2020.05.12.091298v1)
CV30	Ab	SARS-CoV2	SARS-CoV1	SARS-CoV2		S; RBD	B-cells; SARS-CoV2 Human Patient	724	EVQLVESGGGLIQPGGSLRLSCAASGVI VSSNYMSWVRQAPGKGLEWVSVIYSG GSTYYADSVKGRFTISRDNSKNTLYLQM NSLRAEDTAVYYCARDLDVSGGMDVW GQGTTVTVSS	1803	EIVLTQSPGTLSLSPGERATLSCRASQS VSSSYLAWYQQKPGQAPRLLIYGASSR ATGIPDRFSGSGSGTDFTLTISRLEPED FAVYYCQQYGSSPQTFGQGTKLEIK	IGHV3-53 (Human)	IGHJ6 (Human)	IGKV3-20 (Human)	IGKJ2 (Human)	2825	ARDLDVSGG MDV	4027	QQYGSSP QT	Emilie Seydoux et al., 2020 (https://www.biorxiv.org/content/10.1101/2020.05.12.091298v1);Nicholas Hurlburt et al., 2020 (https://www.biorxiv.org/content/10.1101/2020.06.12.148692v1)
CV31	Ab	SARS-CoV1, SARS-CoV2			SARS-CoV2	S; non-RBD	B-cells; SARS-CoV2 Human Patient	725	QVQLVQSGAEVKKPGASVKVSCKVSGY TLTELSMHWVRQAPGKGLEWMGGFD PEDGETIYAQKFQGRVTMTEDTSTDTAY MELSSLRSEDTAVYYCATAPPYSPPSSWF DPWGQGTLVTVSS	1804	QSVLTQPPSVSAAPGQKVTISCSGSSS NIGNNYVSWYQQLPGTAPKLLIYDNN KRPSGIPDRFSGSKSGTSATLGITGLQT GDEADYYCGTWDSSLSASYVFGTGTK VTVL	IGHV1-24 (Human)	IGHJ5 (Human)	IGLV1-51 (Human)	IGLJ1 (Human)	2826	ATAPPYSPPSS WFDP	4028	GTWDSSLS ASYV	Emilie Seydoux et al., 2020 (https://www.biorxiv.org/content/10.1101/2020.05.12.091298v1)
CV32	Ab	SARS-CoV2	SARS-CoV1		SARS-CoV2	S; non-RBD	B-cells; SARS-CoV2 Human Patient	726	QVQLVQSGAEVKKPGASVKVSCKASGY TFTGYYMHWVRQAPGQGLEWMGWI NPNSDVTNYAQKFQGRVTMTRDTSIST AYMELSRLRSDDTAVYYCAREARDYYGS GSLDYWGQGTLVTVSS	1805	QSVLTQPPSVSAAPGQKVTISCSGSSS NIGNNYVSWYQQLPGTAPKLLIYDNN KRPSGIPDRFSGSKSGTSATLGITGLQT GDEADYYCGTWDSSLSAVVFGGGTKL TVL	IGHV1-2 (Human)	IGHJ4 (Human)	IGLV1-51 (Human)	IGLJ3 (Human)	2827	AREARDYYGS GSLDY	4029	GTWDSSLS AVV	Emilie Seydoux et al., 2020 (https://www.biorxiv.org/content/10.1101/2020.05.12.091298v1)
CV33	Ab	SARS-CoV2	SARS-CoV1		SARS-CoV2	S; non-RBD	B-cells; SARS-CoV2 Human Patient	727	QVQLVQSGAEVKKPGASVKVSCKASGY TFTSYDISWVRQAPGQGLEWMGWISA YNGNTNYAQKLQGRVTMTTDTSTSTAY MELRSLRSDDTAVYYCARDSVAGIYYYY GMDVWGQGTTVTVSS	1806	QSVLTQPPSVSGAPGQRVTISCTGSSS NIGAGYDVHWYQQLPGTAPKLLIYGN SNRPSGVPDRFSGSKSGTSASLAITGL QAEDEADYYCQSYDSSLSGPVVFGGG TKLTVL	IGHV1-18 (Human)	IGHJ6 (Human)	IGLV1-40 (Human)	IGLJ3 (Human)	2828	ARDSVAGIYY YYGMDV	4030	QSYDSSLS GPVV	Emilie Seydoux et al., 2020 (https://www.biorxiv.org/content/10.1101/2020.05.12.091298v1)
CV34	Ab	SARS-CoV2	SARS-CoV1		SARS-CoV2	S; non-RBD	B-cells; SARS-CoV2 Human Patient	728	QVQLVESGGGVVQPGRSLRLSCAASGF TFSSYAMHWVRQAPGKGLEWVALISYD GSNKYYADSVKGRFTISRDNSKNTLYL QMNSLRAEDTAVYYCARSYGGSYYYGM DVWGQGTTVTVSS	1807	SYELTQPHSVSVATAQMARITCGGNN IGSKAVHWYQQKPGQDPVLVIYSDSN RPSGIPERFSGSNPGNTATLTISRIEAG DEADYYCQVWDSSSDHVVFGGGTKL TVL	IGHV3-30-3 (Human)	IGHJ6 (Human)	IGLV3-12 (Human)	IGLJ3 (Human)	2829	ARSYGGSYYY GMDV	4031	QVWDSSS DHVV	Emilie Seydoux et al., 2020 (https://www.biorxiv.org/content/10.1101/2020.05.12.091298v1)
CV35	Ab	SARS-CoV2	SARS-CoV1		SARS-CoV2	S; non-RBD	B-cells; SARS-CoV2 Human Patient	729	QVQLQESGPGLVKPSETLSLTCTVSGYSI SSGYYWGWIRQPPGKGLEWIGSIYHSG STYYNPSLKSRVTISVDTSKNQFSLKLSSV TAADTAVYYCARTPLSLRLRYNWYFDLW GRGTLVTVSS	1808	QSVLTQPPSASGTPGQRVTISCSGSSS NIGSNTVNWYQQLPGTAPKLLIYSNN QRPSGVPDRFSGSKSGTSASLAISGLQ SEDEADYYCAAWDDSLNGPVFGGGT KLTVL	IGHV4-38 (Human)	IGHJ2 (Human)	IGLV1-44 (Human)	IGLJ3 (Human)	2830	ARTPLSLRLRY NWYFDL	4032	AAWDDSL NGPV	Emilie Seydoux et al., 2020 (https://www.biorxiv.org/content/10.1101/2020.05.12.091298v1)
CV36	Ab	SARS-CoV2	SARS-CoV1		SARS-CoV2	S; non-RBD	B-cells; SARS-CoV2 Human Patient	730	QVQLVQSGAEVKKPGASVKVSCKASGY TFTGYYMHWVRQAPGQGLEWMGWI NPNSGGTNYVQKFQGRVTMTRDTSIST AYMELNRLRSDDTAVYFCARDLTTTAGT DYYYGMDVWGQGTTVTVSS	1809	SYELTQPPSVSVSPGQTARITCSGDALP KQYAYWYQQKPGQAPVLVIYKDTERP SGIPERFSGSSSGTTVTLTISGVQAEDE ADYYCQSADSSGTYMIFGTGTKVTVL	IGHV1-2 (Human)	IGHJ6 (Human)	IGLV3-25 (Human)	IGLJ1 (Human)	2831	ARDLTTTAGT DYYYGMDV	4033	QSADSSGT YMI	Emilie Seydoux et al., 2020 (https://www.biorxiv.org/content/10.1101/2020.05.12.091298v1)
CV37	Ab	SARS-CoV1, SARS-CoV2			SARS-CoV2	S; non-RBD	B-cells; SARS-CoV2 Human Patient	731	QVQLVQSGAEVKKPGASVKVSCKASGY TFTSYGISWVRQAPGQGLEWMGWISA YNGNTNYAQKLQGRVTMTTDTSTSTAY MELRSLRSDDTAVYYCARARVAYDYIW GSYRYKAFDYWGQGTLVTVSS	1810	DIQMTQSPSSLSASVGDRVTITCQASQ DISNYLNWYQQKPGKAPKLLIYDASNL ETGVPSRFSGSGSGTDFTFTISSLQPED IATYYCQQYDNLPRFGPGTKVDIKR	IGHV1-18 (Human)	IGHJ4 (Human)	IGKV1-33 (Human)	IGKJ3 (Human)	2832	ARARVAYDYI WGSYRYKAF DY	4034	QQYDNLP R	Emilie Seydoux et al., 2020 (https://www.biorxiv.org/content/10.1101/2020.05.12.091298v1)
CV38	Ab	SARS-CoV1, SARS-CoV2			SARS-CoV2	S; non-RBD	B-cells; SARS-CoV2 Human Patient	732	QVQLVESGGGVVQPGRSLRLSCAASGF TFSSYAMHWVRQAPGKGLEWVAVISY DGSNKYYADSVKGRFTISRDNSKNTLYL QMNSLRAEDTAVYYCARAQTAHYSSSF DYWGQGTLVTVSS	1811	EIVLTQSPATLSLSPGERATLSCRASQS VSSYLAWYQQKPGQAPRLLIYDASNR ATGIPARFSGSGSGTDFTLTISSLEPEDF AVYYCQQRSNWPPITFGQGTRLEIK	IGHV3-30 (Human)	IGHJ4 (Human)	IGKV3-11 (Human)	IGKJ5 (Human)	2833	ARAQTAHYSS SFDY	4035	QQRSNWP PIT	Emilie Seydoux et al., 2020 (https://www.biorxiv.org/content/10.1101/2020.05.12.091298v1)
CV38-113	Ab	SARS-CoV2	SARS-CoV1	SARS-CoV2		S; RBD	B-cells; SARS-CoV2 Human Patient		ND		ND	IGHV3-53 (Human)	IGHJ4 (Human)	ND	ND	2834	ARGGRLADA AGDY	4036	QQYDNLPS WT	Jakob Kreye et al., 2020 (https://www.biorxiv.org/content/10.1101/2020.08.15.252320v1.full.pdf)

CV38-139	Ab	SARS-CoV2	SARS-CoV1	SARS-CoV2		S; RBD	B-cells; SARS-CoV2 Human Patient		ND		ND	IGHV3-53 (Human)	IGHJ4 (Human)	ND	ND	2835	ARGHYDLFDY	4037	QQLNSYPPGT	Jakob Kreye et al., 2020 (https://www.biorxiv.org/content/10.1101/2020.08.15.252320v1.full.pdf)
CV38-142	Ab	SARS-CoV1, SARS-CoV2		SARS-CoV2		S; RBD	B-cells; SARS-CoV2 Human Patient		ND		ND	IGHV5-51 (Human)	IGHJ4 (Human)	ND	ND	2836	ARIRGVYSSGWIGGDY	4038	QQSYSTPRQWT	Jakob Kreye et al., 2020 (https://www.biorxiv.org/content/10.1101/2020.08.15.252320v1.full.pdf)
CV38-183	Ab	SARS-CoV2	SARS-CoV1	SARS-CoV2		S; RBD	B-cells; SARS-CoV2 Human Patient		ND		ND	IGHV3-53 (Human)	IGHJ6 (Human)	ND	ND	2837	ARGDGWDNYYYGMDV	4039	QSYDSSLSGSV	Jakob Kreye et al., 2020 (https://www.biorxiv.org/content/10.1101/2020.08.15.252320v1.full.pdf)
CV38-221	Ab	SARS-CoV2	SARS-CoV1	SARS-CoV2		S; RBD	B-cells; SARS-CoV2 Human Patient		ND		ND	IGHV3-66 (Human)	IGHJ4 (Human)	ND	ND	2838	ARGFGDYYFDY	4040	QQLYT	Jakob Kreye et al., 2020 (https://www.biorxiv.org/content/10.1101/2020.08.15.252320v1.full.pdf)
CV39	Ab	SARS-CoV2	SARS-CoV1		SARS-CoV2	S; non-RBD	B-cells; SARS-CoV2 Human Patient	733	QVQLVESGGGVVQPGRSMRLSCAASGFNLSSYAMHWVRQASGKGLEWVSLISYDGSIKYYADSVKGRFTVSGDNSKNTLFLQMSSLRADDSALYYCVRGGVSGPNAFDIWGQGTTVTVSS	1812	DVVMTQSPLSLPVTLGQPASISCRSSQSLVYSDGNTYVNWFQQRPGQSPRRLIYKVSNRDSGVPDRFSGSGSGTDFALKISRVEAEDVGVYYCMQGTHWPVTFGQGTKVEIK	IGHV3-30 (Human)	IGHJ3 (Human)	IGKV2-30 (Human)	IGKJ1 (Human)	2839	VRGGVSGPNAFDI	4041	MQGTHWPVT	Emilie Seydoux et al., 2020 (https://www.biorxiv.org/content/10.1101/2020.05.12.091298v1)
CV4	Ab	SARS-CoV1, SARS-CoV2			SARS-CoV2	S; non-RBD	B-cells; SARS-CoV2 Human Patient	734	QVQLVESGGGVVQPGRSLRLSCAASGFTFSSYAMHWVRQAPGKGLEWVAVISYDGSNKYYADSVKGRFTISRDNSKNTLYLQMNSLRAEDTAVYYCARSISGSYLGAFDYWGQGTLVTVSS	1813	DIQMTQSPSTLSASVGDRVTITCRASQSISSWLAWYQQKPGKAPKLLIYKASSLESGVPSRFSGSGSGTEFTLTISSLQPDDFATYYCQQYNSYTFGQGTKLEIK	IGHV3-30 (Human)	IGHJ4 (Human)	IGKV1-5 (Human)	IGKJ2 (Human)	2840	ARSISGSYLGAFDY	4042	QQYNSYT	Emilie Seydoux et al., 2020 (https://www.biorxiv.org/content/10.1101/2020.05.12.091298v1)
CV40	Ab	SARS-CoV1, SARS-CoV2			SARS-CoV2	S; non-RBD	B-cells; SARS-CoV2 Human Patient	735	QVQLVQSGAEVKKPGASVKVSCKASGYTFSSYGISWVRQDPGQGLEWMGWISAYNGNTNYAQKLQGRVTMTTDTSTSTAYMELRSLRSDDTAVYYCARVGLWWLGHPDAFDIWGQGTMVTVSS	1814	DIQMTQSPSSLSASVGDRVTITCRASQGIRNDLGWYQQKPGKAPKRLIYAASSLQSGVPSRFSGSGSGTEFTLTISSLQPEDFATYYCLQHNSYPLTFGGGTKVEIK	IGHV1-18 (Human)	IGHJ3 (Human)	IGKV1-17 (Human)	IGKJ4 (Human)	2841	ARVGLWWLGHPDAFDI	4043	LQHNSYPLT	Emilie Seydoux et al., 2020 (https://www.biorxiv.org/content/10.1101/2020.05.12.091298v1)
CV41	Ab	SARS-CoV2	SARS-CoV1		SARS-CoV2	S; non-RBD	B-cells; SARS-CoV2 Human Patient	736	QVQLVESGGGVVQPGRSLRLSCAASGFTFSSYAMHWVRQAPGKGLEWVAVISYDGSNKYYADSVKGRFTISRDNSKNTLYLQMNSLRAEDTAVYYCARTKGGSYFAPFDYWGQGTLVTVSS	1815	EIVMTQSPATLSVSPGERATLSCRASQSVSSNLAWYQQKPGQAPRLLIYGASTRATGIPARFSGSGSGTEFTLTISSLQSEDFAVYYCQQYNNWPLTFGGGTKVEIK	IGHV3-30 (Human)	IGHJ4 (Human)	IGKV3-15 (Human)	IGKJ4 (Human)	2842	ARTKGGSYFAPFDY	4044	QQYNNWPLT	Emilie Seydoux et al., 2020 (https://www.biorxiv.org/content/10.1101/2020.05.12.091298v1)
CV42	Ab	SARS-CoV2	SARS-CoV1		SARS-CoV2	S; non-RBD	B-cells; SARS-CoV2 Human Patient	737	QVQLVQSGAEVKKPGASVKVSCKASGYTFTSYGISWVRQAPGQGLEWMGWISAYNGNTNYAQKVQGRVTMTTDTSTSTAYMELRSLRSDDTAVYYCARDRGYAATFGVFDYWGQGTLVTVSS	1816	DIQMTQSPSSLSASVGDRVTITCRASQSISSYLNWYQQKPGKAPKFLIYAASSLQSGVPSRFSGSGSGTDFTLTISSLQPEDFATYYCQQTYITAFTFGPGTKVDIK	IGHV1-18 (Human)	IGHJ4 (Human)	IGKV1-39 (Human)	IGKJ3 (Human)	2843	ARDRGYAATFGVFDY	4045	QQTYITAFT	Emilie Seydoux et al., 2020 (https://www.biorxiv.org/content/10.1101/2020.05.12.091298v1)
CV43	Ab	SARS-CoV2	SARS-CoV1		SARS-CoV2	S; RBD	B-cells; SARS-CoV2 Human Patient	738	QVQLVESGGGVVQPGRSLRLSCAASGFTFSSYAMHWVRQAPGKGLEWVAVISYDGSNKYYADSVKGRFTISRDNSKNTLYLQMNSLRAEDTAVYYCARVTVVHFDYWGQGTLVTVSS	1817	NFMLTQPHSVSESPGKTVTISCTGSSGSIASNYVQWYQQRPGSAPTTVIYEDNQRPSGVPDRFSGSIDSSSNSASLTISGLKTEDEADYYCQSYDSSNWVFGGGTKLTVL	IGHV3-30 (Human)	IGHJ4 (Human)	IGLV6-57 (Human)	IGLJ3 (Human)	2844	ARVTVVHFDY	4046	QSYDSSNWV	Emilie Seydoux et al., 2020 (https://www.biorxiv.org/content/10.1101/2020.05.12.091298v1)
CV44	Ab	SARS-CoV2	SARS-CoV1		SARS-CoV2	S; non-RBD	B-cells; SARS-CoV2 Human Patient	739	QVQLVQSGAEVKKPGASVKVSCKASGYTFTSYYMHWVRQAPGQGLEWMGIINPSGGSTSYAQKFQGRVTMTRDTSTSTVYMELSSLRSEDTAVYYCARDLTSTSSSPYSYYYGMDVWGQGTTVTVSS	1818	SYELTQPPSVSVSPGQTARITCSGDALPKQYAYWYQQKPGQAPVVVIYKDSERPSGIPERFSGSSSGTTVTLTISGVQAEDEADYYCQSADSSGTYVVFGGGTKLTVL	IGHV1-46 (Human)	IGHJ6 (Human)	IGLV3-25 (Human)	IGLJ3 (Human)	2845	ARDLTSTSSSPYSYYYGMDV	4047	QSADSSGTYVV	Emilie Seydoux et al., 2020 (https://www.biorxiv.org/content/10.1101/2020.05.12.091298v1)
CV45	Ab	SARS-CoV1, SARS-CoV2			SARS-CoV2	S; non-RBD	B-cells; SARS-CoV2 Human Patient	740	QVQLVQSGAEVKKPGASVKVSCKASGYTFTSYGISWVRQAPGQGLEWMGWISAYNGNTNYAQKLQGRVTMTTDTSTSTAYMELRSLRSDDTAVYYCARVTVEAIFGVVILPLKNWFDPWGQGTLVTVSS	1819	QSVLTQPPSVSGAPGQRVTISCTGSSSNIGAGYDVHWYQQLPGTAPKLLIYGNSNRPSGVPDRFSGSKSGTSASLAITGLQAEDEADYYCQSYDSSLTLYVFGTGTKVTVL	IGHV1-18 (Human)	IGHJ5 (Human)	IGLV1-40 (Human)	IGLJ1 (Human)	2846	ARVTVEAIFGVVILPLKNWFDP	4048	QSYDSSLTLYV	Emilie Seydoux et al., 2020 (https://www.biorxiv.org/content/10.1101/2020.05.12.091298v1)
CV46	Ab	SARS-CoV2	SARS-CoV1		SARS-CoV2	S; non-RBD	B-cells; SARS-CoV2 Human Patient	741	QVQLVESGGGVVQPGRSLRLSCAASGFNLSNYAMHWVRQASGKGLEWVSLISYDGSIKYYTDSVKGRFTVSGDNSKNTLFLQMNSLRPDDSALYYCVRGGVSGPNSFDMWGQGTTVTVSS	1820	DVVMTQSPLSLPVTLGQPASISCRSSQSLVYSDGNTYVNWFQQRPGQSPRRLIYQVSIRASGVPDRFSGSGSGTDFALKISRVEAEDVGVYYCMQGTHWPVTFGQGTKVEIK	IGHV3-30 (Human)	IGHJ4 (Human)	IGKV2-30 (Human)	IGKJ1 (Human)	2847	VRGGVSGPNSFDM	4049	MQGTHWPVT	Emilie Seydoux et al., 2020 (https://www.biorxiv.org/content/10.1101/2020.05.12.091298v1)

CV47	Ab	SARS-CoV2	SARS-CoV1		SARS-CoV2	S; non-RBD	B-cells; SARS-CoV2 Human Patient	742	QVQLVQSGAEVKKPGASVKVSCKASGY TFTSYGISWVRQAPGQGLEWMGWISA YSGNTNYAQKLQGRVTMTTDTSTSTAY MEVRSLRSDDTAVYYCARVGLWWLGH PDVFDIWGQGTMVTVSS	1821	DIQMTQSPSSLSASVGDRVTITCRASQ GIRNDLGWYQQKPGKAPKRLIYAASSL QSGVPSRFSGSGSGTEFTLTISSLQPED FATYYCLQHNSYPLTFGGGTKVEIK	IGHV1-18 (Human)	IGHJ3 (Human)	IGKV1-17 (Human)	IGKJ4 (Human)	2848	ARVGLWWL GHPDVFDI	4050	LQHNSYPL T	Emilie Seydoux et al., 2020 (https://www.biorxiv.org/content/10.1101/2020.05.12.091298v1)
CV48	Ab	SARS-CoV2			SARS-CoV2	S; non-RBD	B-cells; SARS-CoV2 Human Patient	743	QVQLVQSGAEVKKPGSSVKVSCKASGG TFSSYTINWVRQAPGQGLEWMGRIIPIL GIADYAQKFQGRVTITADKSTSTAYMEL SSLRSEDTAVYYCARDLVEDTAMVTGAA AGTWGQGTLVTVSS	1822	DVVMTQSPLSLPVTLGQPASISCRSSQ SLVYSDGNTYLNWFQQRPGQSPRRLI YKVSNRDSGVPDKFSGSGSGTDFTLKI SRVEAEDVGVYYCMQGTHWPPTFGQ GTKVEIK	IGHV1-69 (Human)	IGHJ4 (Human)	IGKV2-30 (Human)	IGKJ1 (Human)	2849	ARDLVEDTA MVTGAAAGT	4051	MQGTHW PPT	Emilie Seydoux et al., 2020 (https://www.biorxiv.org/content/10.1101/2020.05.12.091298v1)
CV5	Ab	SARS-CoV2	SARS-CoV1		SARS-CoV2	S; RBD	B-cells; SARS-CoV2 Human Patient	744	QVQLVQSGAEVKKPGASVKVTCKASGY TFTSYYLHWVRQAPGQGLEWMGIINPS GGTTSYAQKFQGRVTMTRDTSTSTVYM ELSSLRSEDTAVYYCARAGRRYSSSDDGA FDIWGQGTMVTVSS	1823	DIVMTQSPDSLAVSLGERATINCKSSQ NVLYSSNNKNYLAWYQQKPGQPPKLL IYWASTRESGVPDRFSGSGSGTDFTLTI SSLQAEDVAVYYCQQYYITPYTFGQGT KLEIK	IGHV1-46 (Human)	IGHJ3 (Human)	IGKV4-1 (Human)	IGKJ2 (Human)	2850	ARAGRRYSSS DDGAFDI	4052	QQYYITPYT	Emilie Seydoux et al., 2020 (https://www.biorxiv.org/content/10.1101/2020.05.12.091298v1)
CV50	Ab	SARS-CoV2			SARS-CoV2	S; non-RBD	B-cells; SARS-CoV2 Human Patient	745	QVQLVESGGGVVQPGRSLRLSCAASGF TFSSYGMHWVRQAPGKGLEWVAVIWY DGSNKYYADSVKGRFTISRDNSKNTLYL QMNSLRAEDTAVYYCARDIMFGDDWL QKQPDYWGQGTLVTVSS	1824	SYELTQPPSVSVSPGQTARITCSGDALP KKYAYWYQQKSGQAPVLVIYEDSKRP SGIPERFSGSSSGTMATLTISGAQVED EADYYCYSTDSSGNLYVFGTGTKVTVL	IGHV3-33 (Human)	IGHJ4 (Human)	IGLV3-10 (Human)	IGLJ1 (Human)	2851	ARDIMFGDD WLQKQPDY	4053	YSTDSSGN LYV	Emilie Seydoux et al., 2020 (https://www.biorxiv.org/content/10.1101/2020.05.12.091298v1)
CV7	Ab	SARS-CoV2	SARS-CoV1		SARS-CoV2	S; non-RBD	B-cells; SARS-CoV2 Human Patient	746	QVQLVESGGGVVQPGRSLRLSCAASGF TFSSYAMHWVRQAPGKGLEWVAVISY DGSNKYYADSVKGRFTISRDNSKNTLYL QMNSLRAEDTAVYYCARSISGSYLGAFD YWGQGTLVTVSS	1825	DIQMTQSPSTLSASVGDRVTITCRASQ SISSWLAWYQQKPGKAPKLLIYKASSL ESGVPSRFSGSGSGTEFTLTISSLQPDD FATYYCQQYNSYTFGQGTKLEIK	IGHV3-30 (Human)	IGHJ4 (Human)	IGKV1-5 (Human)	IGKJ2 (Human)	2852	ARSISGSYLGA FDY	4054	QQYNSYT	Emilie Seydoux et al., 2020 (https://www.biorxiv.org/content/10.1101/2020.05.12.091298v1)
CV8	Ab	SARS-CoV1, SARS-CoV2			SARS-CoV2	S; non-RBD	B-cells; SARS-CoV2 Human Patient	747	QVQLVQSGAEVKKPGASVKVSCKASGY TFTSYGISWVRQAPGQGLEWMGWISA YNGNTNYAQKLQGRVTMTTDTSTSTAY MELRSLRSDDTAVYYCARLVPTWASYYD FWSGYPGGYGMDVWGQGTTVTVSS	1826	EIVLTQSPGTLSLSPGERATLSCRASQS VSSSYLAWYQQKPGQAPRLLIYGASSR ATGIPDRFSGSGSGTDFTLTISRLEPED FAVYYCQQYGSSPGTFGQGTRLEIK	IGHV1-18 (Human)	IGHJ6 (Human)	IGKV3-20 (Human)	IGKJ5 (Human)	2853	ARLVPTWASY YDFWSGYPG GYGMDV	4055	QQYGSSP GT	Emilie Seydoux et al., 2020 (https://www.biorxiv.org/content/10.1101/2020.05.12.091298v1)
CV9	Ab	SARS-CoV1, SARS-CoV2			SARS-CoV2	S; non-RBD	B-cells; SARS-CoV2 Human Patient	748	QLQLQESGPGLVKPSETLSLTCTVSGGSI SSSSYYWGWIRQPPGKGLEWIGSIYYSG STYYNPSLKSRVTISVDTSKNQFSLKLSSV TAADTAVYYCATHIVVVTATPNWYFDL WGRGTLVTVSS	1827	QSALTQPASVSGSPGQSITISCTGTSSD VGGYNYVSWYQQHPGKAPKLMIYDV SNRPSGVSNRFSGSKSGNTASLTISGL QAEDEADYYCSSYTSISTWVFGGGTKL TVL	IGHV4-39 (Human)	IGHJ2 (Human)	IGLV2-14 (Human)	IGLJ3 (Human)	2854	ATHIVVVTAT PNWYFDL	4056	SSYTSISTW V	Emilie Seydoux et al., 2020 (https://www.biorxiv.org/content/10.1101/2020.05.12.091298v1)
EY6A	Ab	SARS-CoV2		SARS-CoV2		S; RBD	B-cells; SARS-CoV2 Human Patient	749	EVQLVESGGGVVQPGRSLRLSCAASAFT FSSYDMHWVRQAPGKGLEWVAVISYD GSNKYYADSVKGRFTISRDNSKNTLYLQ MNSLRAEDTAVYYCAKDGGKLWVYYFD YWGQGTLVTVSS	1828	DIQMTQSPSSLSASVGDRVTITCRASQ SISSYLNWYQQKPGKAPKLLIYAASSLQ SGVPSRFSGSGSGTDFTLTISSLQPEDF ATYYCQQSYSTLALTFGGGTKVEIK	IGHV3-30-3 (Human)	IGHJ4 (Human)	IGKV1-39 (Human)	IGKJ4 (Human)	2855	AKDGGKLWV YYFDY	4057	QQSYSTLA LT	Daming Zhou et al., 2020 (https://www.biorxiv.org/content/10.1101/2020.06.12.148387v1)
Fab 2-4	Ab	SARS-CoV2		SARS-CoV2		S; RBD	B-cells; SARS-CoV2 Human Patient	750	QVQLVQSGAEVKKPGASVKVSCKASGY TFTGYYMHWVRQAPGQGLEWMGWI NPNSGGTNYTQMFQGRVTMTRDTSIST AYMEVSRLRSDDTAVYYCARDRSWAVV YYYMDVWGKGTTVTVSS	1829	QSALTQPPSASGSPGQSVTISCTGTSS DVGGYNYVSWYQQHPGKAPKLMIYE VSKRPSGVPDRFSGSKSGNTASLTVSG LQAEDEADYYCSSYAGSNNLVFGGGT KLTVL	IGHV1-2 (Human)	IGHJ6 (Human)	IGLV2-8 (Human)	IGLJ3 (Human)	2856	ARDRSWAVV YYYMDV	4058	SSYAGSNN LV	David Ho et al., 2020 (https://www.biorxiv.org/content/10.1101/2020.06.17.153486v1)
FnC1t1p2_A5	Ab	SARS-CoV2		SARS-CoV2		S; S1 non-RBD	B-cells; SARS-CoV2 Human Patient	751	QVQLVQSGAEVKKPGASVKVSCKASGY TFTSYDINWVRQATGQGLEWMGWMN PNSGNTGYAQKFQGRVTMTRNTSISTA YMELSSLRSEDTAVYYCARATTDCSSTSC WSLDFWSGYYTGGREKIFDWGQGTLVT VSS	1830	EIVLTQSPGTLSLSPGERATLSCRASQS VSSSYLAWYQQKPGQAPRLLIYGASSR ATGIPDRFSGSGSGTDFTLTISRLEPED FAVYYCQQYGSSPGTFGQGTKVEIK	IGHV1-8 (Human)	IGHJ4 (Human)	IGKV3-20 (Human)	IGKJ1 (Human)	2857	ARATTDCSST SCWSLDFWS GYYTGGREKI FD	4059	QQYGSSP GT	Christoph Kreer et al., 2020 (https://doi.org/10.1016/j.cell.2020.06.044)
FnC1t2p1_D4	Ab	SARS-CoV2		SARS-CoV2		S; RBD	B-cells; SARS-CoV2 Human Patient	752	QVQLVQSGSELKKPGASVKVSCKASGYT FLRFAMNWLRQAPGQGLEWMGWIDT NTGTPTYAQGFTGRFVFSLDTSVSTAYL QISSLKAEDTAVYYCARSLRGANLVPWG QGTLVTVSS	1831	DIQMTQSPSSLSASVGDRVTITCQASQ DVSNYLNWYQQQPGKAPKLLIYDAFN LETGVPSRFSGSGSGTDFTFTISSLQPE DIATYYCQQQYDNLPLTFGGGTKVEIK	IGHV7-4-1 (Human)	IGHJ5 (Human)	IGKV1-33 (Human)	IGKJ4 (Human)	2858	ARSLRGANLV P	4060	QQYDNLPL T	Christoph Kreer et al., 2020 (https://doi.org/10.1016/j.cell.2020.06.044)
FnC1t2p1_G5	Ab	SARS-CoV2		SARS-CoV2		S; RBD	B-cells; SARS-CoV2 Human Patient	753	QVQLVQSGSELKKPGASVKVSCKASGYT FLRFAMNWLRQAPGQGLEWMGWIDT NTGTPTYAQGFTGRFVFSLDTSVSTAYL QISSLKAEDTAVYYCARSLRGANLVPWG QGTLVTVSS	1832	DIQMTQSPSSLSASVGDRVTITCQASQ DVSNYLNWYQQQPGKAPKLLIYDAFN LETGVPSRFSGSGSGTDFTFTISSLQPE DIATYYCQQYDNLPLTFGGGTKVEIK	IGHV7-4-1 (Human)	IGHJ5 (Human)	IGKV1-33 (Human)	IGKJ4 (Human)	2859	ARSLRGANLV P	4061	QQYDNLPL T	Christoph Kreer et al., 2020 (https://doi.org/10.1016/j.cell.2020.06.044)
H014	Ab	SARS-CoV1, SARS-CoV2		SARS-CoV1, SARS-CoV2		S; RBD	Immunised Humanised (hACE2) Mouse		ND		ND	ND	ND	ND		ND		ND	Zhe Lv et al., 2020 (https://www.biorxiv.org/content/10.1101/2020.06.02.129098v2)
H11-D4	Nb	SARS-CoV2		SARS-CoV2		S; RBD	Phage Display Library (Nanobody, non-immune)	754	QVQLVESGGGLMQAGGSLRLSCAVSGR TFSTAAMGWFRQAPGKEREFVAAIRWS GGSAYYADSVKGRFTISRDKAKNTVYLQ MNSLKYEDTAVYYCARTENVRSLLSDYA TWPYDYWGQGTQVTVSS		N/A	IGHV3-3 (Alpaca)	IGHJ4 (Alpaca)	N/A	N/A	2860	ARTENVRSLL SDYATWPYDY		N/A	Jiangdong Huo et al., 2020 (https://www.nature.com/articles/s41594-020-0469-6)

H11-H4	Nb	SARS-CoV2		SARS-CoV2		S; RBD	Phage Display Library (Nanobody, non-immune)	755	QVQLVESGGGLMQAGGSLRLSCAVSGR TFSTAAMGWFRQAPGKEREFVAAIRWS GGSAYYADSVKGRFTISRDKAKNTVYLQ MNSLKYEDTAVYYCAQTHYVSYLLSDYA TWPYDYWGQGTQVTVSS		N/A	IGHV3-3 (Alpaca)	IGHJ4 (Alpaca)	N/A	N/A	2861	AQTHYVSYLL SDYATWPYDY		N/A	Jiangdong Huo et al., 2020 (https://www.nature.com/articles/s41594-020-0469-6)
H4	Ab	SARS-CoV2		SARS-CoV2		S; RBD	B-cells; SARS-CoV2 Human Patient	756	QVQLVQSGAEVKKPGASVKVSCKASGY TFTGYYMHWVRQAPGQGLEWMGRIN PNSGGTNYAQKFQGRVTMTRDTSISTA YMELSRLRSDDTAVYYCARVPYCSSTSCH RDWYFDLWGRGTLVTVSS	1833	DIQMTQSPLSLPVTPGEPASISCRSSQS LLDSDDGNTYLDWYLQKPGQSPQLLIY TLSYRASGVPDRFSGSGSGTDFTLKISR VEAEDVGVYYCMQRIEFPLTFGGGTK VEIK	IGHV1-2 (Human)	IGHJ2 (Human)	IGKV2-40 (Human)	IGKJ4 (Human)	2862	ARVPYCSSTSC HRDWYFDL	4062	MQRIEFPL T	Yan Wu et al., 2020 (https://science.sciencemag.org/content/early/2020/05/12/science.abc2241)
HbnC2t1p2_D9	Ab	SARS-CoV2		SARS-CoV2		S; RBD	B-cells; SARS-CoV2 Human Patient	757	QVQLVESGGGVVQPGRSLRLSCAASGF TFSSYGMHWVRQAPGKGLEWVAVIWY DGRNKYYVDSVKGRFTISRDNSKNTLYL QISSLRAEDTAVYYCARAARRPVVTDTM AYYMDVWGKGTTVTVSS	1834	EIVLTQSPATLSLSPGERATLSCRASLSL SSYLAWYQQKPGQAPRLLIYDASNRA TGIPARFSGSGSGTDFTLTISSLEPEDFA VYYCQQRSNWPPTWTFGQGTKAEIK	IGHV3-33 (Human)	IGHJ6 (Human)	IGKV3-11 (Human)	IGKJ1 (Human)	2863	ARAARRPVVT DTMAYYMDV	4063	QQRSNWP PTWT	Christoph Kreer et al., 2020 (https://doi.org/10.1016/j.cell.2020.06.044)
HbnC3t1p1_C6	Ab	SARS-CoV2		SARS-CoV2		S; RBD	B-cells; SARS-CoV2 Human Patient	758	QMQLVQSGPEVKKPGTSVKVSCKASGF TFTSSAVQWVRQARGQRLEWIGWIVV GSGNTNYAQKFQERVTITRDMSTSTAY MELSSLRSEDTAVYYCAAPHCSSTICYDG FDIWGQGTMVTVSS	1835	EIVLTQSPGTLSLSPGERATLSCRASQS VSSSYLAWYQQKPGQAPRLLIYGASSR ATGIPDRFSGSGSGTDFTLTISRVEPED FAVYYCQQYGSSPWTFGQGTKVEIK	IGHV1-58 (Human)	IGHJ3 (Human)	IGKV3-20 (Human)	IGKJ1 (Human)	2864	AAPHCSSTICY DGFDI	4064	QQYGSSP WT	Christoph Kreer et al., 2020 (https://doi.org/10.1016/j.cell.2020.06.044)
HbnC3t1p1_F4	Ab	SARS-CoV2		SARS-CoV2		S; RBD	B-cells; SARS-CoV2 Human Patient	759	QVQLVESGGGVVQPGRSLRLSCAATGF TFRRYGMHWVRQAPGKGLEWVAGILF DGSNKYYVDSVKGRFTISRDSSRNTLYLQ LNSLRREDTAVYYCAKGGDYEWELLES WGQGTLVTVSS	1836	DIQMTQSPSTVSASVGDRVTITCRASQ SIDNWLAWYQEKPGKAPKVLIYKASSL ESGVPSRFSGRGSGTEFTLTISSLQPGD FATYYCQHYHSFPLTFGGGTKVDIK	IGHV3-30 (Human)	IGHJ5 (Human)	IGKV1-5 (Human)	IGKJ4 (Human)	2865	AKGGDYEWE LLES	4065	QHYHSFPL T	Christoph Kreer et al., 2020 (https://doi.org/10.1016/j.cell.2020.06.044)
HbnC3t1p1_G4	Ab	SARS-CoV2		SARS-CoV2		S; RBD	B-cells; SARS-CoV2 Human Patient	760	EVQLVESGGGLVQPGGSLRLSCAASGFT VSSNYMSWVRQAPGKGLEWVSVIYSG GSTFYADSVKGRFTISRDNSKNTLYLQM NSLRAEDTAVYYCARDFGDFFFDYWGQ GTLVTVSS	1837	EIVLTQSPGTLSLSPGERATLSCRASQS VSSYLAWYQQKPGQAPRLLIYGVSSRA TGIPDRFSGSGSGTDFTLTISRLEPEDF AVYYCQQYGSSPRTFGQGTKVEIK	IGHV3-66 (Human)	IGHJ4 (Human)	IGKV3-20 (Human)	IGKJ1 (Human)	2866	ARDFGDFFFD Y	4066	QQYGSSPR T	Christoph Kreer et al., 2020 (https://doi.org/10.1016/j.cell.2020.06.044)
HbnC3t1p2_B10	Ab	SARS-CoV2		SARS-CoV2		S; RBD	B-cells; SARS-CoV2 Human Patient	761	EVQLVESGGGLVQPGGSLRLSCAASGFI VSSNYMSWVRQAPGKGLEWVSVIYSG GSTFYADSVKGRFTISRDNSKNTLYLQM NSLRAEDTAVYYCARDYGDYFFDYWGQ GTLVTVSS	1838	EIVLTQSPGTLSLSPGERATLSCRASQS VSSYLAWYQQKPGQAPRLLISGASSRA AGIPDRFSGSGSGTDFTLTINRLEPEDF AVYYCQQYGSSPRTFGQGTKLEIK	IGHV3-66 (Human)	IGHJ4 (Human)	IGKV3-20 (Human)	IGKJ2 (Human)	2867	ARDYGDYFFD Y	4067	QQYGSSPR T	Christoph Kreer et al., 2020 (https://doi.org/10.1016/j.cell.2020.06.044)
HbnC3t1p2_C6	Ab	SARS-CoV2		SARS-CoV2		S; RBD	B-cells; SARS-CoV2 Human Patient	762	QMQLVQSGPEVKKPGTSVKVSCKASGF TFSSSAVQWVRQARGQRLEWIGWIVV GSGNTNYAQKFQGRVTITRDMSTRTAY MELSSLRSEDTAMYYCAAPYCSSTRCYD AFDIWGQGTMVTVSS	1839	EIVLTQSPGTLSLSPGERATLSCRASQS VSSSYLAWYQQKPGQAPRLLIYGASSR ATGIPDRFSGSGSGTDFTLTISRLEPED FAVYYCQQYGRSPWTFGQGTKVEI	IGHV1-58 (Human)	IGHJ3 (Human)	IGKV3-20 (Human)	IGKJ1 (Human)	2868	AAPYCSSTRC YDAFDI	4068	QQYGRSP WT	Christoph Kreer et al., 2020 (https://doi.org/10.1016/j.cell.2020.06.044)
HbnC4t1p1_D5	Ab	SARS-CoV2		SARS-CoV2		S; RBD	B-cells; SARS-CoV2 Human Patient	763	EVQLVESGGGLVQPGRSLRLSCAASGFT FDDYAMHWVRQAPGKGLEWVSGISW NSGSIGYADSVKGRFTISRDNAKNSLYLQ MNSLRAEDTGLYYCAKDINYDSGGYHK NYFDYWGQGTLVTVSS	1840	DIQMTQSPSSLSASVGDRATITCRASQ SISSYLNWYQEKPGKAPKLLIYAASSLQ SGVPSRFSGSGSGTDFTLTISSLQPEDF ATYYCQQSYSNPLTFGGGTKVEIK	IGHV3-9 (Human)	IGHJ4 (Human)	IGKV1-39 (Human)	IGKJ4 (Human)	2869	AKDINYDSGG YHKNYFDY	4069	QQSYSNPL T	Christoph Kreer et al., 2020 (https://doi.org/10.1016/j.cell.2020.06.044)
Ju et al., 2020	Ab	SARS-CoV2		SARS-CoV2	SARS-CoV2	S; Various	B-cells; SARS-CoV2 Human Patient		205		205	Various	Various	Various	Various		Various		Various	Bin Ju et al., 2020 (https://www.nature.com/articles/s41586-020-2380-z)
Kim et al., 2020	Ab	SARS-CoV2		SARS-CoV2		S; RBD	B-cells; SARS-CoV2 Human Patient		Various		Various	Various	Various	Various	Various		Various		Various	Sang Il Kim et al., 2020 (https://www.biorxiv.org/content/10.1101/2020.06.26.174557v2)
LR1	Nb	SARS-CoV2				S; RBD	Phage Display Library (Nanobody, non-immune)	764	QVQLVESGGGSVQAGGSLRLSCAASGSI SSITYLGWFRQAPGKEREGVAALITDSG RTYYADSVKGRFTVSLDNAKNTVYLQM NSLKPEDTALYYCAAAEWGYEWPLYYAS SWYWGQGTQVTVSS		N/A	IGHV3-3 (Alpaca)	IGHJ4 (Alpaca)	N/A	N/A	2870	AAAEWGYE WPLYYASSW Y		N/A	Tingting Li et al., 2020 (https://www.biorxiv.org/content/10.1101/2020.06.09.143438v1)
LR11	Nb	SARS-CoV2				S; RBD	Phage Display Library (Nanobody, non-immune)	765	QVQLVESGGGSVQAGGSLRLSCAASGSI SSITYLGWFRQAPGKEREGVAALITDSG RTYYADSVKGRFTVSLDNAKNTVYLQM NSLKPEDTALYYCAAAEWGYEWPLYYAS SWYWGQGTQVTVSS		N/A	IGHV3-3 (Alpaca)	IGHJ4 (Alpaca)	N/A	N/A	2871	AAAYWGWD WPLNSQDYW Y		N/A	Tingting Li et al., 2020 (https://www.biorxiv.org/content/10.1101/2020.06.09.143438v1)
LR15	Nb	SARS-CoV2				S; RBD	Phage Display Library (Nanobody, non-immune)	766	QVQLVESGGGSVQAGGSLRLSCAASGSI SSITYLGWFRQAPGKEREGVAALITDSG RTYYADSVKGRFTVSLDNAKNTVYLQM NSLKPEDTALYYCAAAEWGYEWPLYYAS SWYWGQGTQVTVSS		N/A	IGHV3-3 (Alpaca)	IGHJ4 (Alpaca)	N/A	N/A	2872	AAADWGYN WPLIREEYEY		N/A	Tingting Li et al., 2020 (https://www.biorxiv.org/content/10.1101/2020.06.09.143438v1)

LR16	Nb	SARS-CoV2				S; RBD	Phage Display Library (Nanobody, non-immune)	767	QVQLVESGGGSVQAGGSLRLSCAASGSI SSITYLGWFRQAPGKEREGVAALITDSG RTYYADSVKGRFTVSLDNAKNTVYLQM NSLKPEDTALYYCAAAEWGYEWPLYYAS SWYWGQGTQVTVSS		N/A	IGHV3-3 (Alpaca)	IGHJ4 (Alpaca)	N/A	N/A	2873	AAADWGYNI PLNITDYWY		N/A	Tingting Li et al., 2020 (https://www.biorxiv.org/content/10.1101/2020.06.09.143438v1)
LR2	Nb	SARS-CoV2				S; RBD	Phage Display Library (Nanobody, non-immune)	768	QVQLVESGGGSVQAGGSLRLSCAASGSI SSITYLGWFRQAPGKEREGVAALITDSG RTYYADSVKGRFTVSLDNAKNTVYLQM NSLKPEDTALYYCAAAEWGYEWPLYYAS SWYWGQGTQVTVSS		N/A	IGHV3-3 (Alpaca)	IGHJ4 (Alpaca)	N/A	N/A	2874	AAAMNGYNE PLYSYDYEY		N/A	Tingting Li et al., 2020 (https://www.biorxiv.org/content/10.1101/2020.06.09.143438v1)
LR3	Nb	SARS-CoV2				S; RBD	Phage Display Library (Nanobody, non-immune)	769	QVQLVESGGGSVQAGGSLRLSCAASGSI SSITYLGWFRQAPGKEREGVAALITDSG RTYYADSVKGRFTVSLDNAKNTVYLQM NSLKPEDTALYYCAAAEWGYEWPLYYAS SWYWGQGTQVTVSS		N/A	IGHV3-3 (Alpaca)	IGHJ4 (Alpaca)	N/A	N/A	2875	AAASWGYEW PLVYDDYWY		N/A	Tingting Li et al., 2020 (https://www.biorxiv.org/content/10.1101/2020.06.09.143438v1)
LR5	Nb	SARS-CoV2				S; RBD	Phage Display Library (Nanobody, non-immune)	770	QVQLVESGGGSVQAGGSLRLSCAASGSI SSITYLGWFRQAPGKEREGVAALITDSG RTYYADSVKGRFTVSLDNAKNTVYLQM NSLKPEDTALYYCAAAEWGYEWPLYYAS SWYWGQGTQVTVSS		N/A	IGHV3-3 (Alpaca)	IGHJ4 (Alpaca)	N/A	N/A	2876	AAATWGYH WPLGAWDY WY		N/A	Tingting Li et al., 2020 (https://www.biorxiv.org/content/10.1101/2020.06.09.143438v1)
LR6	Nb	SARS-CoV2				S; RBD	Phage Display Library (Nanobody, non-immune)	771	QVQLVESGGGSVQAGGSLRLSCAASGSI SSITYLGWFRQAPGKEREGVAALITDSG RTYYADSVKGRFTVSLDNAKNTVYLQM NSLKPEDTALYYCAAAEWGYEWPLYYAS SWYWGQGTQVTVSS		N/A	IGHV3-3 (Alpaca)	IGHJ4 (Alpaca)	N/A	N/A	2877	AAATWGYSW PLEHDEYWY		N/A	Tingting Li et al., 2020 (https://www.biorxiv.org/content/10.1101/2020.06.09.143438v1)
LR7	Nb	SARS-CoV2				S; RBD	Phage Display Library (Nanobody, non-immune)	772	QVQLVESGGGSVQAGGSLRLSCAASGSI SSITYLGWFRQAPGKEREGVAALITDSG RTYYADSVKGRFTVSLDNAKNTVYLQM NSLKPEDTALYYCAAAEWGYEWPLYYAS SWYWGQGTQVTVSS		N/A	IGHV3-3 (Alpaca)	IGHJ4 (Alpaca)	N/A	N/A	2878	AAAFHGEQY PLYTNKYHY		N/A	Tingting Li et al., 2020 (https://www.biorxiv.org/content/10.1101/2020.06.09.143438v1)
LR8	Nb	SARS-CoV2				S; RBD	Phage Display Library (Nanobody, non-immune)	773	QVQLVESGGGSVQAGGSLRLSCAASGSI SSITYLGWFRQAPGKEREGVAALITDSG RTYYADSVKGRFTVSLDNAKNTVYLQM NSLKPEDTALYYCAAAEWGYEWPLYYAS SWYWGQGTQVTVSS		N/A	IGHV3-3 (Alpaca)	IGHJ4 (Alpaca)	N/A	N/A	2879	AAANYGANF PLQANTYFY		N/A	Tingting Li et al., 2020 (https://www.biorxiv.org/content/10.1101/2020.06.09.143438v1)
mAb-1	Ab	SARS-CoV1, SARS-CoV2	229E, HKU1, NL63, OC43			S; Unk	B-cells; SARS-CoV1 Human Patient	774	QVQLVESGGGSVQAGGSLRLSCAASGSI SSITYLGWFRQAPGKEREGVAALITDSG RTYYADSVKGRFTVSLDNAKNTVYLQM NSLKPEDTALYYCAAAEWGYEWPLYYAS SWYWGQGTQVTVSS	1841	QPVLTQPPSVSGAPGQRITISCTGSSS NIGAGYDVHWYQQLPGTAPKLLIYGS SSRPSGVPDRFSGSKSGTSASLAITGLQ AEDEADYYCQSYDSSLSVLYVFGTGTK VTVL	IGHV3-21 (Human)	IGHJ4 (Human)	IGLV1-40 (Human)	IGLJ1 (Human)	2880	ARDFSGHTAV AGTGFEY	4070	QSYDSSLS VLYV	Anna Wec et al., 2020 (https://science.sciencemag.org/content/early/2020/06/15/science.abc7424)
mAb-10	Ab	SARS-CoV1, SARS-CoV2	229E, HKU1, NL63, OC43			S; Unk	B-cells; SARS-CoV1 Human Patient	775	QVQLVESGGGSVQAGGSLRLSCAASGSI SSITYLGWFRQAPGKEREGVAALITDSG RTYYADSVKGRFTVSLDNAKNTVYLQM NSLKPEDTALYYCAAAEWGYEWPLYYAS SWYWGQGTQVTVSS	1842	DIVLTQTPATLSVSPGEGATLSCRASQS VRSNLAWFQQRPGQVPRLLIYDASTR ATGVPARFTGSGSGTYFTLTISSLQSED FAVYYCQQYNSWPPLTFGGGTKLEIK	IGHV3-66 (Human)	IGHJ4 (Human)	IGKV3-15 (Human)	IGKJ4 (Human)	2881	VRASPPGGN TGWPFFED	4071	QQYNSWP PLT	Anna Wec et al., 2020 (https://science.sciencemag.org/content/early/2020/06/15/science.abc7424)
mAb-100	Ab	SARS-CoV2 (weak)	229E, HKU1, NL63, OC43, SARS-CoV1			S; Unk	B-cells; SARS-CoV1 Human Patient	776	QVQLVESGGGSVQAGGSLRLSCAASGSI SSITYLGWFRQAPGKEREGVAALITDSG RTYYADSVKGRFTVSLDNAKNTVYLQM NSLKPEDTALYYCAAAEWGYEWPLYYAS SWYWGQGTQVTVSS	1843	EIVMTQSPATLSVSPGETATLSCRASQ SVGRFMGWYQQKPGQAPRLLIFDAS NRVTGVPDRFRGSGSGTDFILTINSLEP EDSASYYCQRRGDGYNFGQGTKVEIK	IGHV3-30 (Human)	IGHJ4 (Human)	IGKV3-11 (Human)	IGKJ1 (Human)	2882	ARDNALQNA QIGYLDY	4072	QRRGDGY N	Anna Wec et al., 2020 (https://science.sciencemag.org/content/early/2020/06/15/science.abc7424)
mAb-101	Ab	SARS-CoV2 (weak)	229E, HKU1, NL63, OC43, SARS-CoV1			S; Unk	B-cells; SARS-CoV1 Human Patient	777	QVQLVESGGGSVQAGGSLRLSCAASGSI SSITYLGWFRQAPGKEREGVAALITDSG RTYYADSVKGRFTVSLDNAKNTVYLQM NSLKPEDTALYYCAAAEWGYEWPLYYAS SWYWGQGTQVTVSS	1844	ETTLTQSPLSLPVTLGQPASISCRSSQG LVHSDGNTYLNWFQQRPGQSPRRLIY KVSNRDSGVPDRFSGSGSGTDFTLKIS RVEAEDIGVYYCMQGTEWPRTFGQG TKVEIK	IGHV1-69 (Human)	IGHJ6 (Human)	IGKV2-30 (Human)	IGKJ1 (Human)	2883	VLDSDPYTAT FSHNHYWYA MDV	4073	MQGTEW PRT	Anna Wec et al., 2020 (https://science.sciencemag.org/content/early/2020/06/15/science.abc7424)
mAb-102	Ab	SARS-CoV2 (weak)	229E, HKU1, NL63, OC43, SARS-CoV1			S; Unk	B-cells; SARS-CoV1 Human Patient	778	QVQLVESGGGSVQAGGSLRLSCAASGSI SSITYLGWFRQAPGKEREGVAALITDSG RTYYADSVKGRFTVSLDNAKNTVYLQM NSLKPEDTALYYCAAAEWGYEWPLYYAS SWYWGQGTQVTVSS	1845	DIRVTQSPLSLPVTLGQPASISCRSSQRI VHTDGNTYLNWFLQRPGQSPRRLIYK VSNRDSGVPDRFSGSGSGTDFTLKISR VEAEDVGIYYCMQGTEWPRTFGQGT KVDIK	IGHV1-69 (Human)	IGHJ6 (Human)	IGKV2-30 (Human)	IGKJ3 (Human)	2884	ARDPSIHYTG NHHWYDLDI	4074	MQGTEW PRT	Anna Wec et al., 2020 (https://science.sciencemag.org/content/early/2020/06/15/science.abc7424)
mAb-103	Ab	SARS-CoV2 (weak)	229E, HKU1, NL63, OC43, SARS-CoV1			S; Unk	B-cells; SARS-CoV1 Human Patient	779	QVQLVESGGGSVQAGGSLRLSCAASGSI SSITYLGWFRQAPGKEREGVAALITDSG RTYYADSVKGRFTVSLDNAKNTVYLQM NSLKPEDTALYYCAAAEWGYEWPLYYAS SWYWGQGTQVTVSS	1846	EIVMTQSPSSLSASVGDRVTITCRAGH TISTYLNWYQQKPGKAPKILISGASSLQ SGVPSRFSGSGSGTDFTLTIGSLQPEDF ATYYCQQSYSTPYTFGQGTKVDIK	IGHV7-4-1 (Human)	IGHJ4 (Human)	IGKV1-39 (Human)	IGKJ3 (Human)	2885	AREEHYDFSS GYFRPAY	4075	QQSYSTPY T	Anna Wec et al., 2020 (https://science.sciencemag.org/content/early/2020/06/15/science.abc7424)
mAb-104	Ab	SARS-CoV2 (weak)	229E, HKU1, NL63, OC43, SARS-CoV1			S; Unk	B-cells; SARS-CoV1 Human Patient	780	QVQLVESGGGSVQAGGSLRLSCAASGSI SSITYLGWFRQAPGKEREGVAALITDSG RTYYADSVKGRFTVSLDNAKNTVYLQM NSLKPEDTALYYCAAAEWGYEWPLYYAS SWYWGQGTQVTVSS	1847	QPVLTQPASVSGSPGQSSTLSCSGTSS DVGSYDLVSWYQQHPGKAPKLMIYE GTKRPSGVSDRFSGSTSGNTASLTISGL QAEDEANYYCCSYAGSGTWIFGGGTK LTVL	IGHV4-34 (Human)	IGHJ4 (Human)	IGLV2-23 (Human)	IGLJ3 (Human)	2886	ARGMTSPVV HLYSSGRPSR WFDF	4076	CSYAGSGT WI	Anna Wec et al., 2020 (https://science.sciencemag.org/content/early/2020/06/15/science.abc7424)
mAb-105	Ab	SARS-CoV2 (weak)	229E, HKU1, NL63, OC43, SARS-CoV1			S; Unk	B-cells; SARS-CoV1 Human Patient	781	QVQLVESGGGSVQAGGSLRLSCAASGSI SSITYLGWFRQAPGKEREGVAALITDSG RTYYADSVKGRFTVSLDNAKNTVYLQM NSLKPEDTALYYCAAAEWGYEWPLYYAS SWYWGQGTQVTVSS	1848	EIVLTQSPGTLSLSPGDRVTLFCRASQN IANNHLAWYQQKPGQAPRVLIYGAST TATDIPDRFSGRVSGTDFTLTISRLDPE DFAVYYCHQYGSSPWTFGQGTKLEIK	IGHV4-4 (Human)	IGHJ6 (Human)	IGKV3-20 (Human)	IGKJ1 (Human)	2887	ARSFISFDSSG HPYYYYAMD V	4077	HQYGSSP WT	Anna Wec et al., 2020 (https://science.sciencemag.org/content/early/2020/06/15/science.abc7424)

mAb-106	Ab	SARS-CoV2 (weak)	229E, HKU1, NL63, OC43, SARS-CoV1			S; Unk	B-cells; SARS-CoV1 Human Patient	782	QVQLVESGGGSVQAGGSLRLSCAASGSI SSITYLGWFRQAPGKEREGVAALITDSG RTYYADSVKGRFTVSLDNAKNTVYLQM NSLKPEDTALYYCAAAEWGYEWPLYYAS SWYWGQGTQVTVSS	1849	ETTLTQSPATLSVSPGETATLSCRASQS VGRFMGWYQQKPGQAPRLLIFDASN RVTGVPDRFRGSGSGTDFILTINSLEPE DSASYYCQRRGDGYNFGQGTKVEIK	IGHV3-30 (Human)	IGHJ4 (Human)	IGKV3-11 (Human)	IGKJ1 (Human)	2888	ARDNALQNA QIGYLDY	4078	QRRGDGY N	Anna Wec et al., 2020 (https://science.sciencemag.org/content/early/2020/06/15/science.abc7424)
mAb-107	Ab	SARS-CoV1, SARS-CoV2 (weak)	229E, HKU1, NL63, OC43			S; Unk	B-cells; SARS-CoV1 Human Patient	783	QVQLVESGGGSVQAGGSLRLSCAASGSI SSITYLGWFRQAPGKEREGVAALITDSG RTYYADSVKGRFTVSLDNAKNTVYLQM NSLKPEDTALYYCAAAEWGYEWPLYYAS SWYWGQGTQVTVSS	1850	DIRMTQSPLSLPVDLGQSASISCRSSQ RVVHTNGNTYLHWFHQRPGQAPRRL IYKVSNRESGVPDRFSGSGSGTDFTLRI SRVEAEDVGVYYCMQATDWPRTFGQ GTKLEIK	IGHV1-69 (Human)	IGHJ6 (Human)	IGKV2-30 (Human)	IGKJ2 (Human)	2889	ARDPSILNTG NHHWYDLD M	4079	MQATDW PRT	Anna Wec et al., 2020 (https://science.sciencemag.org/content/early/2020/06/15/science.abc7424)
mAb-108	Ab	SARS-CoV2 (weak)	229E, HKU1, NL63, OC43, SARS-CoV1			S; Unk	B-cells; SARS-CoV1 Human Patient	784	QVQLVESGGGSVQAGGSLRLSCAASGSI SSITYLGWFRQAPGKEREGVAALITDSG RTYYADSVKGRFTVSLDNAKNTVYLQM NSLKPEDTALYYCAAAEWGYEWPLYYAS SWYWGQGTQVTVSS	1851	DIVMTQSPLSLSVTLGQAASISCTCSQT AVHSDGNTYLNWFHQRPGQSPRRLIY KVSNRDSGVPDRFSGSGSGTDFTLKIN RVEAEDVGIYYCMQTTDWPRTFGQG TKVEIK	IGHV1-69 (Human)	IGHJ6 (Human)	IGKV2-30 (Human)	IGKJ1 (Human)	2890	ARDPTFLNSG NHFWYDVDI	4080	MQTTDWP RT	Anna Wec et al., 2020 (https://science.sciencemag.org/content/early/2020/06/15/science.abc7424)
mAb-109	Ab	SARS-CoV1, SARS-CoV2 (weak)	229E, HKU1, NL63, OC43			S; Unk	B-cells; SARS-CoV1 Human Patient	785	QVQLVESGGGSVQAGGSLRLSCAASGSI SSITYLGWFRQAPGKEREGVAALITDSG RTYYADSVKGRFTVSLDNAKNTVYLQM NSLKPEDTALYYCAAAEWGYEWPLYYAS SWYWGQGTQVTVSS	1852	ETTLTQSPVTLPVTLGQPASISCTSSRW LVHTNGNTYLNWFHQRPGQSPRRLIY QVSNRDSGVPDRFSGSGSGTDFTLQIS RVEAEDVGVYYCMQGTEWPRTFGQ GTKLEIK	IGHV1-69 (Human)	IGHJ4 (Human)	IGKV2-30 (Human)	IGKJ2 (Human)	2891	ARDASFPNTG NHFWYDFDL	4081	MQGTEW PRT	Anna Wec et al., 2020 (https://science.sciencemag.org/content/early/2020/06/15/science.abc7424)
mAb-11	Ab	SARS-CoV1, SARS-CoV2	229E, HKU1, NL63, OC43			S; Unk	B-cells; SARS-CoV1 Human Patient	786	QVQLVESGGGSVQAGGSLRLSCAASGSI SSITYLGWFRQAPGKEREGVAALITDSG RTYYADSVKGRFTVSLDNAKNTVYLQM NSLKPEDTALYYCAAAEWGYEWPLYYAS SWYWGQGTQVTVSS	1853	EIVLTQSPSSLSASVGDRVTITCQASQD IRKCLNWYQHPGKAPKLLIHDASSLES GVPSRFSGSGSGTDFSFTINSLHPEDIA TYYCQQFEDLPITFGQGTRLEIK	IGHV3-30 (Human)	IGHJ4 (Human)	IGKV1-33 (Human)	IGKJ5 (Human)	2892	AKKGSPYCGV DCYKGYFDY	4082	QQFEDLPI T	Anna Wec et al., 2020 (https://science.sciencemag.org/content/early/2020/06/15/science.abc7424)
mAb-110	Ab	SARS-CoV1, SARS-CoV2 (weak)	229E, HKU1, NL63, OC43			S; Unk	B-cells; SARS-CoV1 Human Patient	787	EVQLVESGGGVVQPGRSLRLSCAASGFT FSSYGMHWVRQAPGKGLEWVAVIWY DGSNKYYADSVKGRFTISRDNSKNTLYL QMNSLRAEDTAVYYCARVGSGRVYWG QGTLVTVSS	1854	DIVMTQSPDSLAVSLGERATINCKSSQ SVLYSSNNKNYLAWYQQKPGQPPKLLI YWASTRESGVPDRFSGSGSGTDFTLTI SSLQAEDVAVYYCQQYYSTPYTFGQGT KVEIK	IGHV3-33 (Human)	IGHJ4 (Human)	IGKV4-1 (Human)	IGKJ1 (Human)	2893	ARVGSGRVY	4083	QQYYSTPY T	Anna Wec et al., 2020 (https://science.sciencemag.org/content/early/2020/06/15/science.abc7424)
mAb-111	Ab	229E (weak), SARS-CoV1, SARS-CoV2 (weak)	HKU1, NL63, OC43			S; Unk	B-cells; SARS-CoV1 Human Patient	788	QVQLVESGPGLVRPSGTLSVTCAVSGDS ISSDYWCTWVRQSPGKGLEWIGKISHS GSLNYNPSLKSRVTMSVDKSKNHFSLKL ASVTAADTAVYYCARVRIGASHHNFWS GYYTDAFDIWGQGTTVTVSS	1855	DIVVTQSPGTLSLSPGERAALSCRASQS VGNNYLAWYQQKPGQAPRLLIYGATS RATGIPDRFSGSGSGTDFTLTISRLEPE DFAVYYCQQYGTSPVYTFGQGTKVEIK	IGHV4-4 (Human)	IGHJ3 (Human)	IGKV3-20 (Human)	IGKJ1 (Human)	2894	ARVRIGASHH NFWSGYYTD AFDI	4084	QQYGTSPV YT	Anna Wec et al., 2020 (https://science.sciencemag.org/content/early/2020/06/15/science.abc7424)
mAb-112	Ab	229E (weak), HKU1 (weak), NL63, SARS-CoV1, SARS-CoV2 (weak)	OC43			S; Unk	B-cells; SARS-CoV1 Human Patient	789	QVQLVQSGAEVKKPGESLKISCKASGYS FTNYWVGWVRQMPAKGLEWMGIIWP DDSDTRYRPSFQGQVTISVDKSISTAYLH WNSLKASDNGMYFCARAPLASCSGGRC PTYNRFDLWGQGTLVTVSS	1856	QPVLTQPPSVSAAPGQKVTISCSGSSS NIENNYVSWYQQLPGAAPKLLIYDNN KRPSGIPDRFSGSKSGTSATLGITGLQT GDEADYYCGTWDFSLSAGVFGGGTKL TVL	IGHV5-51 (Human)	IGHJ4 (Human)	IGLV1-51 (Human)	IGLJ3 (Human)	2895	ARAPLASCSG GRCPTYNRFD L	4085	GTWDFSLS AGV	Anna Wec et al., 2020 (https://science.sciencemag.org/content/early/2020/06/15/science.abc7424)
mAb-113	Ab	229E, HKU1 (weak), NL63, SARS-CoV1, SARS-CoV2 (weak)	OC43			S; Unk	B-cells; SARS-CoV1 Human Patient	790	QVQLVQSGAEVKKPGSSMKVSCKASGV NFRSYSFSWVRQAPGQGLEWMGGVIP YFPTANYADKFRDRVTITADESTGTVYLD MSSLRSEDTAVYFCASEYFDGRSYHSFC GLDVWGQGTTVTVSS	1857	ETTLTQSPLSLPVTLGQPASISCRSSQG LVHTNGNLYLNWFHQRPGQSPRRLIY QVSNRDSGVPDRFSGSGSGTDFTLRIS RVEAEDVGIYYCMQGTEWPRTFGQG TKVEIK	IGHV1-69 (Human)	IGHJ6 (Human)	IGKV2-30 (Human)	IGKJ1 (Human)	2896	ASEYFDGRSY HSFCGLDV	4086	MQGTEW PRT	Anna Wec et al., 2020 (https://science.sciencemag.org/content/early/2020/06/15/science.abc7424)
mAb-114	Ab	229E, HKU1, NL63, SARS-CoV1, SARS-CoV2 (weak)	OC43			S; Unk	B-cells; SARS-CoV1 Human Patient	791	QVQLVESGGGLVQPGGSLRLSCAASGF TFSNYAMTWVRQAPGKGLKWVSGINP SGDATFYTDSVKGQFTISRDNSKNILYLQ MNRLRADDTAIYYCAKGLSFYGSGSDAF DVWGQGTTVTVSS	1858	DIQLTQSPSTLSASVGDSVTITCRASQSI SSWLAWYQQKPGKAPKLLIYKASSLET GVPSRFSGSGSGTEFTLTISSLQPDDFA TYYCQQYKSPLSFGGGTKVEIK	IGHV3-23 (Human)	IGHJ6 (Human)	IGKV1-5 (Human)	IGKJ4 (Human)	2897	AKGLSFYGSG SDAFDV	4087	QQYKSPLS	Anna Wec et al., 2020 (https://science.sciencemag.org/content/early/2020/06/15/science.abc7424)
mAb-115	Ab	229E, HKU1 (weak), NL63, SARS-CoV1, SARS-CoV2 (weak)	OC43			S; Unk	B-cells; SARS-CoV1 Human Patient	792	QVQLVQSGAEVKKPGASVKVSCKASGY TFTDYYVHWVRQVPGQGLEWMGWIS PDSGDTIRAQNFQGRVTMTRDTSMNT AYMEVNRLRTDDTAIYYCARDLISVIRGL GGGMDVWGQGTTVTVSS	1859	DIQVTQSPATLSLSPGERATLSCRASQS VSSYLAWYQQKPGQAPRLLIYDASKR ATGIPARFSGSGSGTDFTLTISSLEPEDF AVYYCQQRSDWHPITFGQGTRLEIK	IGHV1-2 (Human)	IGHJ6 (Human)	IGKV3-11 (Human)	IGKJ5 (Human)	2898	ARDLISVIRGL GGGMDV	4088	QQRSDWH PIT	Anna Wec et al., 2020 (https://science.sciencemag.org/content/early/2020/06/15/science.abc7424)
mAb-116	Ab	229E (weak), HKU1 (weak), NL63 (weak), SARS-CoV1, SARS-CoV2 (weak)	OC43			S; Unk	B-cells; SARS-CoV1 Human Patient	793	QVQLVQSGAEVKKPGASVKVSCKTSGY TFTGHYIHWVRQAPGQGLEWMGWIN PASGDTNYAQKFQGRVTKTRDTSITTAY MELNRLRSDDTAVYYCARGGPLPWSDL DIVGTFDYWGQGTLVTVSS	1860	DIQVTQSPSSLSASVGDRVTITCRASQS ISSSLNWYQQKPGKAPTLLIYTASNLQS GVPSRFSGSGSGTDFTLTITSLQPEDFA TYYCQQSYSTPGFGPGTKVDIK	IGHV1-2 (Human)	IGHJ4 (Human)	IGKV1-39 (Human)	IGKJ3 (Human)	2899	ARGGPLPWS DLDIVGTFDY	4089	QQSYSTPG	Anna Wec et al., 2020 (https://science.sciencemag.org/content/early/2020/06/15/science.abc7424)

WO 2022/067091
PCT/US2021/052040

mAb-117	Ab	229E, HKU1, NL63, SARS-CoV1, SARS-CoV2 (weak)	OC43			S; Unk	B-cells; SARS-CoV1 Human Patient	794	EVQLVESGGGVVQPGKSLRLSCVPSGFS FGTYGMHWVRQAPGKGPEWLAVMW YDGITQYYADSVKGRFTISRDNSKETLYL QMNSLTADDTGIYYCVKDQSSGDRLLYL GYFDLWGPGALVTVSS	1861	EIVMTQSPATLSLSPGERATLSCRASQS VSIYLAWYQQKPGQAPRLLIYDASNRA TGVPARFSGSGSGTDFTLTINNLEPED FAIYYCQQRAKWPPRVTFGPGTKVDIK	IGHV3-33 (Human)	IGHJ2 (Human)	IGKV3-11 (Human)	IGKJ3 (Human)	2900	VKDQSSGDRL LYLGYFDL	4090	QQRAKWP PRVT	Anna Wec et al., 2020 (https://science.sciencemag.org/content/early/2020/06/15/science.abc7424)
mAb-118	Ab	229E, HKU1 (weak), NL63 (weak), SARS-CoV1, SARS-CoV2 (weak)	OC43			S; Unk	B-cells; SARS-CoV1 Human Patient	795	QVQLVQSGGGVVQPGKSLRLSCVASGF SFGTYGMHWVRQAPGKGPEWLAVM WYDGITQYYADSVKGRFTISRDNSKETLY LQMNSLTADDTGVYYCVKDQSSGDRLL YLGYFDLWGPGTLVTVSS	1862	DIVLTQSPATLSLSPGERATLSCRASQS VSIYLAWYQQKPGQAPRLLIYDASNRA TGIPARFSGSGSGTDFTLTINNLEPEDF AIYYCQQRAKWPPRVIFGPGTKVEIK	IGHV3-33 (Human)	IGHJ2 (Human)	IGKV3-11 (Human)	IGKJ3 (Human)	2901	VKDQSSGDRL LYLGYFDL	4091	QQRAKWP PRVI	Anna Wec et al., 2020 (https://science.sciencemag.org/content/early/2020/06/15/science.abc7424)
mAb-119	Ab	229E, HKU1 (weak), NL63 (weak), SARS-CoV1, SARS-CoV2 (weak)	OC43			S; Unk	B-cells; SARS-CoV1 Human Patient	796	QVQLQESGPGLVKPSGTLSLTCAVSGAS VSSDHWWSWVRQSPGKGLEWIGEVY HSGSTNYNPSLKSRVTISLDQSNNQFSLK LTSVTAADTAIYYCATMWGGLCTASNCY GNPMDVWGQGTTVTVSS	1863	SYELTQPPSVSVSPGQTARITCSGDALP RRYAYWYQQRSGQAPVLVIYEDNKRP SGIPERFSAFSSGTMATLTISGAQVEDE ADYYCYSTDSTANYKVFGGGTKLTVL	IGHV4-4 (Human)	IGHJ6 (Human)	IGLV3-10 (Human)	IGLJ3 (Human)	2902	ATMWGGLCT ASNCYGNPM DV	4092	YSTDSTAN YKV	Anna Wec et al., 2020 (https://science.sciencemag.org/content/early/2020/06/15/science.abc7424)
mAb-12	Ab	SARS-CoV1, SARS-CoV2	229E, HKU1, NL63, OC43			S; Unk	B-cells; SARS-CoV1 Human Patient	797	QVQLVQSGAEVRKPGSSVKLSCKASGG TFSTHAISWVRQAPGQRPEWMGGIMP IFGESKDTQKFQGRVTFTADESTTTAYM ELRSLRSDDTAIYYCVRDSDPYTATVTSN HYWYAMDVWGQGTTVTVSS	1864	ETTLTQSPLSLPVTLGQPASISCRSSQG LVHSNGNTYVNWFHQRPGQSPRRLIY EVSNRDSGVPDRFSGSGSGTDFTLKIS RVEAEDIGVYYCMQGTEWPRTFGQG TKVDIK	IGHV1-69 (Human)	IGHJ6 (Human)	IGKV2-30 (Human)	IGKJ3 (Human)	2903	VRDSDPYTAT VTSNHYWYA MDV	4093	MQGTEW PRT	Anna Wec et al., 2020 (https://science.sciencemag.org/content/early/2020/06/15/science.abc7424)
mAb-120	Ab	229E (weak), HKU1 (weak), NL63 (weak), SARS-CoV1, SARS-CoV2 (weak)	OC43			S; Unk	B-cells; SARS-CoV1 Human Patient	798	QVQLQQWGAGVLKPSETLSLTCAVYGG SFRGFFWSWIRQPPGKGLEWIGQITHS GSTNYNSSLKSRLTISVDTSKNQFSLNLSS VTAADTAIYYCARGQGGYDLRRVGYGLT SWFDPWGQGILVTVSS	1865	QSVLIQPASVSGSPGQSITISCTGSSSD VGSYNLVSWYQQHPGKAPKLMIYEGY KRPSGVSNRFSGSKSGNTASLTISGLQ AEDEADYYCCSYAGSSAVVVVFGGGT KLTVL	IGHV4-34 (Human)	IGHJ5 (Human)	IGLV2-23 (Human)	IGLJ3 (Human)	2904	ARGQGGYDL RRVGYGLTS WFDP	4094	CSYAGSSA VVVV	Anna Wec et al., 2020 (https://science.sciencemag.org/content/early/2020/06/15/science.abc7424)
mAb-121	Ab	229E, HKU1 (weak), NL63 (weak), SARS-CoV1, SARS-CoV2 (weak)	OC43			S; Unk	B-cells; SARS-CoV1 Human Patient	799	QVQLVQSGAEVKKPGASVKVSCKASGY TFTSYYIHWVRQAPGQGLEWLGVIHPS GGSTTFAQKFQGRVTMTRDTSTSTVYM ELGSLRSDDTAVYYCARVLAGSSHEWQL THDAFDIWGQGTTVTVSS	1866	DIRVTQSPDSLAVSLGERATINCRTSQS VLYSSNNKNYLGWYQQKPGQPPKLLI YWASTRESGVPDRFSGSGSGTDFTLTI SSLQAEDVAVYYCQQYYSTPYTFGQGT KVDIK	IGHV1-46 (Human)	IGHJ3 (Human)	IGKV4-1 (Human)	IGKJ3 (Human)	2905	ARVLAGSSHE WQLTHDAFD I	4095	QQYYSTPY T	Anna Wec et al., 2020 (https://science.sciencemag.org/content/early/2020/06/15/science.abc7424)
mAb-122	Ab	229E (weak), HKU1 (weak), NL63 (weak), SARS-CoV1, SARS-CoV2 (weak)	OC43			S; Unk	B-cells; SARS-CoV1 Human Patient	800	EVQLVESGAEVKKPGASVILSCKASGYTV TNYYIHWVRQAPGQGLEWMGWIDPD SGVTNFAEKFQGRVTMTRDTSISTAYME LRWLESDDTAVYYCAKDLITVIRGLGGG MDVWGQGTTVTVSS	1867	EIVLTQSPATLSLSPGERATLSCRASQS VSTYLAWYQQKPGQAPRLLIYDASNR ATGIPARFSGSGSGTDFTLTISSLEPEDF ALYYCLQRSDWHPITFGQGTRLEIK	IGHV1-2 (Human)	IGHJ6 (Human)	IGKV3-11 (Human)	IGKJ5 (Human)	2906	AKDLITVIRGL GGGMDV	4096	LQRSDWH PIT	Anna Wec et al., 2020 (https://science.sciencemag.org/content/early/2020/06/15/science.abc7424)
mAb-123	Ab	229E (weak), HKU1 (weak), NL63 (weak), SARS-CoV1, SARS-CoV2 (weak)	NL63, OC43			S; Unk	B-cells; SARS-CoV1 Human Patient	801	EVQLLESGAEVKKPGSSVKVSCKASGGT FSSDAISWVRQAPGQGLEWMGGIIPIF GTTNYAQKFQGRVTITADESTNTAYMEL SSLRSEDTAVYYCARDGPYDSGGYHLNH WGQGTLVTVSS	1868	DIQLTQSPATLSLSPGERATLSCRANQS VSNFLAWYQQKPGQAPRHLIYDASNR ATGIPARFSGSGSGTDFTLTISSLEPEDF AVYYCQQRSNWPPRLTFGGGTKVEIK	IGHV1-69 (Human)	IGHJ1 (Human)	IGKV3-11 (Human)	IGKJ4 (Human)	2907	ARDGPYDSG GYHLNH	4097	QQRSNWP PRLT	Anna Wec et al., 2020 (https://science.sciencemag.org/content/early/2020/06/15/science.abc7424)
mAb-124	Ab	HKU1 (weak), SARS-CoV1, SARS-CoV2 (weak)	229E, NL63, OC43			S; Unk	B-cells; SARS-CoV1 Human Patient	802	EVQLLESGGGVVNPGGSMRLSCAGSGF TFSDHYMGWIRQAPGKGLEVISYISSSG SFIRDADSVKGRFTISRDNAKNSVYLQM NSLRAEDTAVYYCARMGPYGSGTFDYW GQGTLVTVSS	1869	DIVMTQTPGTLSVSPGERATLSCRASQ IINRSQLGWYQHKPGQPPRLLIFDSSK RATGTPDRFSASGSETDFTLTISGVEPE DSGVYYCLQYSLATTFGPGTKVEIK	IGHV3-11 (Human)	IGHJ4 (Human)	IGKV3-20 (Human)	IGKJ3 (Human)	2908	ARMGPYGSG TFDY	4098	LQYSLATT	Anna Wec et al., 2020 (https://science.sciencemag.org/content/early/2020/06/15/science.abc7424)

mAb-125	Ab	229E, HKU1 (weak), NL63 (weak), SARS-CoV1, SARS-CoV2 (weak)	OC43			S; Unk	B-cells; SARS-CoV1 Human Patient	803	EVQLVESGAEVRKPGSSVKVSCKATGGT FSSYGITWVRQAPGQGLEWMGRIIPTL GRTNYAQKFQGRVTITADKSTSTAHMEL SSLRSEDTAVYYCARDLSTLQPDAIVNFD YWGQGTLVTVSS	1870	QPVLTQSSSASASLGSSVKLTCTLSSGH SSYILAWHQQQPGKAPRFLMKFEVG GRYNKGSGVPDRFSGSSSGADRYLTIS NLQSEDEADYYCETWDSNLKGVFGG GTKVTVL	IGHV1-69 (Human)	IGHJ4 (Human)	IGLV4-60 (Human)	IGLJ6 (Human)	2909	ARDLSTLQPD AIVNFDY	4099	ETWDSNL KGV	Anna Wec et al., 2020 (https://science.sciencemag.org/content/early/2020/06/15/science.abc7424)
mAb-126	Ab	HKU1 (weak), SARS-CoV1, SARS-CoV2 (weak)	229E, NL63, OC43			S; Unk	B-cells; SARS-CoV1 Human Patient	804	QVQLVQSGAEVKKPGSSVKVSCKTSGG SFTSYVLSWVRQAPGQGLEWMGRIVP NLGVANYAQKFQDRVTITADKSTTTAYL ELRSLRSEDTAVYYCARDLYYDNGGYNY LDYWGPGTLVTVSS	1871	QPVLTQSSSASASLGSSVKLTCTLRSGH SSYIIAWHQQQPGKAPRFLMKVGHSG SYNKGSGVPDRFSGSRSGADHYLTISN LQPDDEADYYCEAWDNNNLGVFSGG TKVTVL	IGHV1-69 (Human)	IGHJ4 (Human)	IGLV4-60 (Human)	IGLJ6 (Human)	2910	ARDLYYDNG GYNYLDY	4100	EAWDNNN LGV	Anna Wec et al., 2020 (https://science.sciencemag.org/content/early/2020/06/15/science.abc7424)
mAb-127	Ab	229E (weak), HKU1 (weak), SARS-CoV1, SARS-CoV2 (weak)	NL63, OC43			S; Unk	B-cells; SARS-CoV1 Human Patient	805	QVQLVESGGGLVQPGGSLRLSCAASGF TFSNYNMVWVRQAPGKGLEWISYISSSS STIYYADSVKGRFIISRDNAKNSLHLQMN SLRDEDTAVYYCVRDYCNSVSCYTYYYIG MDVWGQGTTVTVSS	1872	DIQLTQSPSAMSASVGDRVTITCRASQ GINDNLAWFQQKPGKVPKRLIYAASN LQNGVPSRFSGSGSGTEFTLTISSLQPE DFATYYCLQHNSYPLTFGGGTKLEIK	IGHV3-48 (Human)	IGHJ6 (Human)	IGKV1-17 (Human)	IGKJ4 (Human)	2911	VRDYCNSVSC YTYYYIGMDV	4101	LQHNSYPL T	Anna Wec et al., 2020 (https://science.sciencemag.org/content/early/2020/06/15/science.abc7424)
mAb-128	Ab	229E (weak), HKU1, NL63 (weak), SARS-CoV1, SARS-CoV2 (weak)	OC43			S; Unk	B-cells; SARS-CoV1 Human Patient	806	EVQLVQSGAEVKKPGASVKVSCKASGYS STNYGFSWVRQAPGQGLEWMGWISV HSGNANFAQKFQGRITMTTDTSTTTAY MELRNLRSDDTATYYCATSASSYSRYYFG LDVWGQGTTVTVSS	1873	DIRMTQSPLSLPVTPGEPASISCRSSQS LLHSNGYNYLDWYLQKPGQSPQLLIYL GSNRASGVPDRFSGSGSGTDFTLKISR VEAEDVGVYYCMQALQTPGVTFGGG TKVDIK	IGHV1-18 (Human)	IGHJ6 (Human)	IGKV2-28 (Human)	IGKJ3 (Human)	2912	ATSASSYSRYY FGLDV	4102	MQALQTP GVT	Anna Wec et al., 2020 (https://science.sciencemag.org/content/early/2020/06/15/science.abc7424)
mAb-129	Ab	HKU1, SARS-CoV1 (weak), SARS-CoV2 (weak)	229E, NL63, OC43			S; Unk	B-cells; SARS-CoV1 Human Patient	807	EVQLLESGPGLVKPSQTLSLTCTVSNGFI SSGEYYWSWIRQSPGKGLEWIGYISHSG STYYNRSLKSRVTISLDTSRNQFSLNLSSV TAADTAVYYCARDLAKWSYGYYYSGMD VWGQGTTVTVSS	1874	QPVLTQPPSASGTPGQRVTISCSGSYS NIGTNPANWYQQLPGTAPKLLIYNND QRPSGVPDRFSGSKSGTSASLAISGLQ SEDETDYYCATWDDSLNGVVFGGGTK LTVL	IGHV4-31 (Human)	IGHJ6 (Human)	IGLV1-44 (Human)	IGLJ3 (Human)	2913	ARDLAKWSY GYYYSGMDV	4103	ATWDDSL NGVV	Anna Wec et al., 2020 (https://science.sciencemag.org/content/early/2020/06/15/science.abc7424)
mAb-13	Ab	SARS-CoV1, SARS-CoV2	229E, HKU1, NL63, OC43			S; Unk	B-cells; SARS-CoV1 Human Patient	808	QVQLVQSGAEVKKPGSSVKVSCKISGGT FKNSAFSWARQVPGQGFQWMGGIIP MFGVPHSVQMFQGRVTLTADESTSAVY MELSGLTSDDTAVYYCAREEYSGTVHNF FGMDVWGQGTTVTVSS	1875	DIRMTQSPLSLPVTRGQPASISCRSSH NVVHSDGKTYLNWFHQRPGQAPRRL IYQVSKRDSGVPDRFSGSGSGSDFTLTI SRVEAEDVGVYYCMQGTDWPRSFGG GTKVEIK	IGHV1-69 (Human)	IGHJ6 (Human)	IGKV2-30 (Human)	IGKJ4 (Human)	2914	AREEYSGTVH NFFGMDV	4104	MQGTDW PRS	Anna Wec et al., 2020 (https://science.sciencemag.org/content/early/2020/06/15/science.abc7424)
mAb-130	Ab	HKU1 (weak), NL63 (weak), SARS-CoV1 (weak), SARS-CoV2 (weak)	229E, OC43			S; Unk	B-cells; SARS-CoV1 Human Patient	809	EVQLVESGGGLVQPGRSLRLSCAASGFT FDDYAMHWVRQVPGRGLEWVSGISW NSGTINYADSVMGRFTISRDNAKNSLYL QMNSLRAEDTALYYCAKDGRYCSGISCR TGMDVWGQGTTVTVSS	1876	EIVLTQSPSSLSASVGDRVTITCRASRSI SSYLNWYQQKPGKAPNLLIYDASTLQS GVPSRFSGSGSGTDFSLTISSLQPEDFA TYYCLHTYTTPRTFGQGTKVEIK	IGHV3-9 (Human)	IGHJ6 (Human)	IGKV1-39 (Human)	IGKJ1 (Human)	2915	AKDGRYCSGI SCRTGMDV	4105	LHTYTTPRT	Anna Wec et al., 2020 (https://science.sciencemag.org/content/early/2020/06/15/science.abc7424)
mAb-131	Ab	229E (weak), HKU1 (weak), SARS-CoV1 (weak), SARS-CoV2 (weak)	NL63, OC43			S; Unk	B-cells; SARS-CoV1 Human Patient	810	EVQLVESGGGLVQPGESLRLSCAASGFN FSPYGMNWVRQAPGKGLEWIAYIISGS GTIYYADSVKGRFTISRDNAQSSLYLQM NSLRAEDTAVYYCARGLLDYLHDAFDIW GQGTMVTVSS	1877	EIVLTQSPATLSVSPGERITLSCRASHSV SSNLAWYQQKPGQVPRLLIYGASARA TGIPARFSGSGSGTEFTLTISSLQSEDFA VYYCQQYNYWPPLTFGGGTKVEIK	IGHV3-48 (Human)	IGHJ3 (Human)	IGKV3-15 (Human)	IGKJ4 (Human)	2916	ARGLLDYLHD AFDI	4106	QQYNYWP PLT	Anna Wec et al., 2020 (https://science.sciencemag.org/content/early/2020/06/15/science.abc7424)
mAb-132	Ab	229E, HKU1 (weak), NL63 (weak), SARS-CoV1 (weak), SARS-CoV2 (weak)	OC43			S; Unk	B-cells; SARS-CoV1 Human Patient	811	EVQLQESGPGLVKPSETLSLTCAVSGGS VSSDTDYWGWIRQPPGKGLEWIGSIHD SERTYYDPSLKSRVTISVDTSKNQFSLRLS SVTAADTALYFCASRHLDLLPIGSFDVW GRGTMVTVSS	1878	DIQMTQSPSSLSASVGDRVTITCRASQ SISTYLNWYQQKTGKAPELLIYVASSLQ SGVPSRFSGSGSGTDFTLTISSLQPEDF ATYYCQQSYRFPITFGQGTRLEIK	IGHV4-38-2 (Human)	IGHJ3 (Human)	IGKV1-39 (Human)	IGKJ5 (Human)	2917	ASRHLDLLPIG SFDV	4107	QQSYRFPI T	Anna Wec et al., 2020 (https://science.sciencemag.org/content/early/2020/06/15/science.abc7424)
mAb-133	Ab	HKU1 (weak), SARS-CoV1 (weak), SARS-CoV2 (weak)	229E, NL63, OC43			S; Unk	B-cells; SARS-CoV1 Human Patient	812	QVQLLESGGGLVQPGRSLRLSCTASGFR FGDYTMTWVRQAPGKGLEWVGFIRSIA YGGTTEHAASVEGRFIISRDDSKSIAYLQ MNSLKAEDTGVYFCTRGSGMFYGSSSG MDVWGQGTTVTVSS	1879	EIVLTQSPATLSLSPGERATLSCRASQS VGTYLAWYQQKHGQAPRLLISDVSKR ATGIPARFSGSGSGTDFTLTITSLEPEDF AVYYCQQRTNWPGATFGPGTKVDIK	IGHV3-49 (Human)	IGHJ6 (Human)	IGKV3-11 (Human)	IGKJ3 (Human)	2918	TRGSGMFYG SSSGMDV	4108	QQRTNWP GAT	Anna Wec et al., 2020 (https://science.sciencemag.org/content/early/2020/06/15/science.abc7424)

WO 2022/067091
PCT/US2021/052040

mAb-134	Ab	229E (weak), HKU1 (weak), SARS-CoV1 (weak), SARS-CoV2 (weak)	NL63, OC43			S; Unk	B-cells; SARS-CoV1 Human Patient	813	EVQLLESGAEVKKPGSSVKVSCKTSGGT FNSYTISWVRQAPGQGLEWMGGIIPIL DTPHYAQKFRGRVTITADKSTSTAFMDL SSLTSEDTAVYYCAIRRDYSDYRDFDYW GQGTLVTVSS	1880	QPVLTQSPSASASLGGSVKLTCTLTSG HSTYAIAWHQQQPEKGPRFLMKLNS DGSHNKGDGIPDRFSGSSSGAERYLTI SSLQSEDEADYYCHTWGTDIQVFGGG TKLTVL	IGHV1-69 (Human)	IGHJ4 (Human)	IGLV4-69 (Human)	IGLJ3 (Human)	2919	AIRRDYSDYR DFDY	4109	HTWGTDI QV	Anna Wec et al., 2020 (https://science.sciencemag.org/content/early/2020/06/15/science.abc7424)
mAb-135	Ab	HKU1 (weak), SARS-CoV1 (weak), SARS-CoV2 (weak)	229E, NL63, OC43			S; Unk	B-cells; SARS-CoV1 Human Patient	814	EVQLVESGPGLVKPSETLSLACTVSGGSI SNYYWNWVRQPPGKGLEWIGNIYYSGS TTFNPSLKSRVTISVDTSRNQFSLKLSSVT AADTAVYYCARQSSSWYNPYYFDQWG QGTLVTVSS	1881	NFMLTQPHSVSESPGKTVTISCTRSSG SIANNYVQWLQQRPGSSPTTIIYEDNQ RPSGVPDRFSGSIDASSNSASLTISGLK TEDEADYYCQSYDSSSQVFGGGTKVT VL	IGHV4-59 (Human)	IGHJ4 (Human)	IGLV6-57 (Human)	IGLJ6 (Human)	2920	ARQSSSWYN PYYFDQ	4110	QSYDSSSQ V	Anna Wec et al., 2020 (https://science.sciencemag.org/content/early/2020/06/15/science.abc7424)
mAb-136	Ab	HKU1, SARS-CoV1 (weak), SARS-CoV2 (weak)	229E, NL63, OC43			S; Unk	B-cells; SARS-CoV1 Human Patient	815	QVQLVQSGGGLVQPGESLRLSCAASGF NFSPYGMNWVRQAPGKGLEWIAYIISG SGTIYYADSVKGRFTISRDNAQSSLYLQM NSLRAEDTAVYYCARGLLDYLHDAFDIW GQGTMVTVSS	1882	DIVLTQSPATLSVSPGERITLSCRASHS VSSNLAWYQQKPGQVPRLLIYGASAR ATGIPARFSGSGSGTEFTLTISSLQSEDF AVYYCQQYNYWPPLTFGGGTKVEIK	IGHV3-48 (Human)	IGHJ3 (Human)	IGKV3-15 (Human)	IGKJ4 (Human)	2921	ARGLLDYLHD AFDI	4111	QQYNYWP PLT	Anna Wec et al., 2020 (https://science.sciencemag.org/content/early/2020/06/15/science.abc7424)
mAb-137	Ab	HKU1, SARS-CoV1 (weak), SARS-CoV2 (weak)	229E, NL63, OC43			S; Unk	B-cells; SARS-CoV1 Human Patient	816	EVQLVESGAEVKNPGSSVKISCKSSGGTL GDYAISWVRQAPGLGLEWLGGIMPLH GTTGYSQRFRPRLTITADESARTAYMELT ALSSEDSAIYYCARDPSILNTGNHHWYD LDLWGQGTEVTVSS	1883	ETTLTQSPLSLSVTLGQAASISCRPNLG LMHTDGNTYLNWFHQRPGQSPRRLI YKVSNRDSGVPDRFAGSGSGTHFTLEI SGVEADDVGVYYCMQGTEWPRTFG QGTKLEIK	IGHV1-69 (Human)	IGHJ4 (Human)	IGKV2-30 (Human)	IGKJ2 (Human)	2922	ARDPSILNTG NHHWYDLDL	4112	MQGTEW PRT	Anna Wec et al., 2020 (https://science.sciencemag.org/content/early/2020/06/15/science.abc7424)
mAb-138	Ab	HKU1 (weak), SARS-CoV1 (weak), SARS-CoV2 (weak)	229E, NL63, OC43			S; Unk	B-cells; SARS-CoV1 Human Patient	817	EVQLLESGGGVVQPGRSLRLSCAASGFT FNSYALFWVRQAPGKGLEWVAVVSYD GNNKYYADSVKGRFTISRDNSKNTLYLQ MNSLKTEDTSVYYCARPRSGSYRQAIDY WGLGTLVTVSS	1884	DIRMTQSPSTLSASVGDRVTITCRASQ TIGSWLAWYQQKPGKAPNLLIYKASSL ESGVPSRFSGSGSGTEFTLTISSLQPDD FATYYCQQYNSLYTFGQGTKLEIK	IGHV3-30 (Human)	IGHJ4 (Human)	IGKV1-5 (Human)	IGKJ2 (Human)	2923	ARPRSGSYRQ AIDY	4113	QQYNSLYT	Anna Wec et al., 2020 (https://science.sciencemag.org/content/early/2020/06/15/science.abc7424)
mAb-139	Ab	229E, HKU1 (weak), NL63, SARS-CoV1 (weak), SARS-CoV2 (weak)	OC43			S; Unk	B-cells; SARS-CoV1 Human Patient	818	QVQLVQSGGGLVQPGGSLRLSCAASGFI FSGHWMSWVRQAPGKGLEWVANIKQ DGREKHYVDSVKGRFTISRDNAKNSVSL QMNSLRAEDTAVYYCVRQNVAIQYYYY AMDVWGQGTTVTVSS	1885	ETTLTQSPGTLSVSPGERATLSCRASQS VISNLAWYQQKPGQAPRLLIYGASTRA TGVPARFSGSGSGTEFTLTIASLQSEDF AVYYCQQYHHWPPYTFGQGTKVDIK	IGHV3-7 (Human)	IGHJ6 (Human)	IGKV3-15 (Human)	IGKJ3 (Human)	2924	VRQNVAIQYY YYAMDV	4114	QQYHHWP PYT	Anna Wec et al., 2020 (https://science.sciencemag.org/content/early/2020/06/15/science.abc7424)
mAb-14	Ab	SARS-CoV1, SARS-CoV2	229E, HKU1, NL63, OC43			S; Unk	B-cells; SARS-CoV1 Human Patient	819	EVQLVESGGGVVQPGRSLRLSCAASGFT FSGYPMHWVRQAPGKGLEWVALISFD GDSKYYTDSVKARFAISRDNSKNTLFLQ MNSLRVADTALYYCARAKGGSYSNAFD YWGQGTLVTVSS	1886	EIVLTQSPDSLAVSLGERATINCKSSQS VLYSSNNENCLAWYQQKPGQPPKLLI YWASTRESGVPDRFSGSGSGTDFTLTI SSLQAEDVAVYYCQQYCSTPPYTFGQ GTKVDIK	IGHV3-30 (Human)	IGHJ4 (Human)	IGKV4-1 (Human)	IGKJ3 (Human)	2925	ARAKGGSYSN AFDY	4115	QQYCSTPP YT	Anna Wec et al., 2020 (https://science.sciencemag.org/content/early/2020/06/15/science.abc7424)
mAb-140	Ab	229E, HKU1 (weak), NL63, SARS-CoV1 (weak), SARS-CoV2 (weak)	OC43			S; Unk	B-cells; SARS-CoV1 Human Patient	820	QVQLVESGAEVKKPGSSVKVSCKASGGT LSDYAISWVRQAPGQGLEWMGGIMPI FGSPGYAEIFQGRVTITADESKSTVYMEL TSLRSEDTAVYYCARDPSILDTGNHHWY DLDIWGQGTMVTVSS	1887	EIVMTQSPLSLPVSLGQPASISCRSSQS VIHTDGNTYLNWYHQRPGQSPRRLIY KVSNRDSGVPDRFSGSGSGTDFTLKIS RVEAEDVGVYYCMQGTEWPRTFGQ GTKVEIK	IGHV1-69 (Human)	IGHJ3 (Human)	IGKV2-30 (Human)	IGKJ1 (Human)	2926	ARDPSILDTG NHHWYDLDI	4116	MQGTEW PRT	Anna Wec et al., 2020 (https://science.sciencemag.org/content/early/2020/06/15/science.abc7424)
mAb-141	Ab	229E, HKU1 (weak), NL63, SARS-CoV1 (weak), SARS-CoV2 (weak)	OC43			S; Unk	B-cells; SARS-CoV1 Human Patient	821	QVQLVQSGAEVKKPGSSVKVSCKTSGAT YKNSAFSWARQAPGQGFQWMGGIIPL FGVPHYVQMFQGRVTITADESTSAVYM ELSGLTSDDTAVYYCAREEYSGTVHNFF GMDVWGQGTTVTVSS	1888	DIVMTQSPLSLPVSRGQSASISCRSSHS VVHSDGKTYVNWFHQRPGQAPRRLI YQVSKRDSGVPDRFSGSGSGFDFTLKI SRVEAEDVGVYFCMQGTDWPRSFGG GTKVDIK	IGHV1-69 (Human)	IGHJ6 (Human)	IGKV2-30 (Human)	IGKJ3 (Human)	2927	AREEYSGTVH NFFGMDV	4117	MQGTDW PRS	Anna Wec et al., 2020 (https://science.sciencemag.org/content/early/2020/06/15/science.abc7424)
mAb-142	Ab	229E, HKU1 (weak), NL63, SARS-CoV1 (weak), SARS-CoV2 (weak)	OC43			S; Unk	B-cells; SARS-CoV1 Human Patient	822	EVQLVESGGGLVQPGGSLRLSCASEFT LRSHAMHWVRQAPGKGLEYVSGISTDG SGRFYADSVKGRFTISRDNSKNKLFLQM SSLRPEDTAVYYCVRDWGSSTHYDVFDL WGQGTMVTVSS	1889	DIVMTQSPSSLSASVGDRVTITCRASQ SINIYLNWYQQKPGKAPKLLIYAASSLQ SGVPSRFSGSGSGTDFTLTISSLQPEDF ATYYCQQSYSTPLITFGQGTRLEIK	IGHV3-64D (Human)	IGHJ3 (Human)	IGKV1-39 (Human)	IGKJ5 (Human)	2928	VRDWGSSTH YDVFDL	4118	QQSYSTPLI T	Anna Wec et al., 2020 (https://science.sciencemag.org/content/early/2020/06/15/science.abc7424)
mAb-143	Ab	229E, 229E (weak), HKU1 (weak), NL63 (weak), OC43 (weak), SARS-CoV1 (weak), SARS-CoV2 (weak)				S; Unk	B-cells; SARS-CoV1 Human Patient	823	QVQLVQSGAEVKKPGSSVKVSCKASGG TLADYAISWVRQAPGQGLEWMGGIKP LHGAAGYSQHFRGRLSITADESASTAYM ELTGLRSEDTAMYYCARDPSILNTGNHH WYDLDLWGQGTMVTVSS	1890	DIRLTQSPLSLPVTLGQAASISCKSSHFI VHTDGNTYLNWFHQRPGQSPRRLIYK VSNRDSGVPDRFSGSGSGTDFTLEISG VEAEDVGVYYCMQGTEWPRTFGQGT KVDIK	IGHV1-69 (Human)	IGHJ3 (Human)	IGKV2-30 (Human)	IGKJ3 (Human)	2929	ARDPSILNTG NHHWYDLDL	4119	MQGTEW PRT	Anna Wec et al., 2020 (https://science.sciencemag.org/content/early/2020/06/15/science.abc7424)

mAb-144	Ab	229E, HKU1, NL63, SARS-CoV1 (weak), SARS-CoV2 (weak)	OC43			S; Unk	B-cells; SARS-CoV1 Human Patient	824	QVQLVQSGAELKKPGSSVKVSCKASGG TFYNSAFSWLRHAPGQGPEWMGGITP SLGRVGYSERFLARLTITADESTSTVYME LTSLASEDTAVYYCARDASIVGTGNHLW YGLDFWGHGTTVTVSS	1891	ETTLTQSPLFLPVTLGQPASISCTSSVH VVHSDGNTYLNWFQQRPGQSPRRLIY KVSNRDSGVPDRFSGSGSGTYFTLKIS RVEAEDVGVYYCMQGTDWPRTFGQ GTKVDIK	IGHV1-69 (Human)	IGHJ6 (Human)	IGKV2-30 (Human)	IGKJ3 (Human)	2930	ARDASIVGTG NHLWYGLDF	4120	MQGTDW PRT	Anna Wec et al., 2020 (https://science.sciencemag.org/content/early/2020/06/15/science.abc7424)
mAb-145	Ab	229E, HKU1 (weak), NL63, SARS-CoV1 (weak), SARS-CoV2 (weak)	OC43			S; Unk	B-cells; SARS-CoV1 Human Patient	825	EVQLVESGGHVVLPGKSLRLSCAGSGFG FPLYAMQWVRRAPGKGLEWVALVSYD SSNIRYADSVKGRFTISRDNSQNTLYLQ MDSLRPEDTAMYYCARDNALQDGRPG YFDSWGQGTLVTVSS	1892	ETTLTQSPATLSLSPGERATLSCRASQSI NDYLGWYQHRPGQAPRLLIHDASTRA PGIPVRFSGSGSGTDFTLTISSLEPEDSA VYYCQQRFSWYNFGPGTKVEIK	IGHV3-30 (Human)	IGHJ5 (Human)	IGKV3-11 (Human)	IGKJ3 (Human)	2931	ARDNALQDG RPGYFDS	4121	QQRFSWY N	Anna Wec et al., 2020 (https://science.sciencemag.org/content/early/2020/06/15/science.abc7424)
mAb-146	Ab	229E, HKU1 (weak), NL63, SARS-CoV1 (weak), SARS-CoV2 (weak)	OC43			S; Unk	B-cells; SARS-CoV1 Human Patient	826	EVQLVESGGGLVKPGGSLRLSCAASGFIF SDYYMSWIRQAPGKGLEWVSYITGSGR TIHYADSVKGRFTISRDNAKNSVYLQMN SLRAEDTAVYYCARGHRFLEFPLNYFDP WGQGTLVTVSS	1893	QSVLTQPASVSGSPGQSITISCAVTSSD VGSYNLVSWHQQHPGKAPKLMIYEV NKRPSGVSNRFSGSKSGNTASLTISGL QAEDEAVYYCCSYGGRSTSVVFGGGT KLTVL	IGHV3-11 (Human)	IGHJ5 (Human)	IGLV2-23 (Human)	IGLJ3 (Human)	2932	ARGHRFLEFP LNYFDP	4122	CSYGGRST SVV	Anna Wec et al., 2020 (https://science.sciencemag.org/content/early/2020/06/15/science.abc7424)
mAb-147	Ab	229E, HKU1 (weak), NL63 (weak), SARS-CoV1 (weak), SARS-CoV2 (weak)	OC43			S; Unk	B-cells; SARS-CoV1 Human Patient	827	EVQLLESGGHVVLPGKSLRLSCAGSGFG FPLYAMQWVRRAPGKGLEWVALVSYD SSNIRYADSVKGRFTISRDNSQNTLYLQ MDSLRPEDTAMYYCARDNALQDGRPG YFDSWGQGTLVTVSS	1894	DIRLTQSPATLSLSPGERATLSCRASQSI NDYLGWYQHRPGQAPRLLIHDASTRA PGIPVRFSGSGSGTDFTLTISSLEPEDSA VYYCQQRFSWYNFGPGTKLEIK	IGHV3-30 (Human)	IGHJ5 (Human)	IGKV3-11 (Human)	IGKJ2 (Human)	2933	ARDNALQDG RPGYFDS	4123	QQRFSWY N	Anna Wec et al., 2020 (https://science.sciencemag.org/content/early/2020/06/15/science.abc7424)
mAb-148	Ab	229E, HKU1 (weak), NL63 (weak), SARS-CoV1 (weak), SARS-CoV2 (weak)	OC43			S; Unk	B-cells; SARS-CoV1 Human Patient	828	EVQLVESGGGVVQPGRSLRLSCAASGFT FSKFAMHWVRQAPGKGLEWVAIISYDG SHKNYADSVKGRFTISRDNSKNTVYLQV DSLRAEDTAVYYCALLYGSGSYYNFVFFG WKDGSDAWGPGTTVTVSS	1895	QPVLTQPASVSGSPGQSITISCTGTTSD VGGYDYVSWYQQRPGKAPKLIIYDVI NRPSGVSNRFSGSKSGNTASLTISGLQ ADDETDYYCSSYTSGGTLVFGTGTKLT VL	IGHV3-30 (Human)	IGHJ6 (Human)	IGLV2-14 (Human)	IGLJ3 (Human)	2934	ALLYGSGSYY NFVFFGWKD GSDA	4124	SSYTSGGTL V	Anna Wec et al., 2020 (https://science.sciencemag.org/content/early/2020/06/15/science.abc7424)
mAb-149	Ab	229E (weak), HKU1, NL63 (weak), SARS-CoV1 (weak), SARS-CoV2 (weak)	OC43			S; Unk	B-cells; SARS-CoV1 Human Patient	829	QVQLVQSGAEVKKPGSSVKVSCKASGG MFTDYAISWVRQAPGQRLEWMGGILP AFAASGSPGYAPIFRGRATFSADVSTSTA YLELTNLKPEDTAVYYCARDPSILNTGNH HWYDLDLWGQGTEVTVSS	1896	DIQMTQSPLSLPVGLGQSASISCRSSQ WVVHTDGNTYLNWFHQRPGQSPRR LIYKVSNRDSGVPDRFSGSGSGTDFTL RISRVEAEDVGVYYCMQATEWPRTFG QGTKVEIK	IGHV1-69 (Human)	IGHJ4 (Human)	IGKV2-30 (Human)	IGKJ1 (Human)	2935	ARDPSILNTG NHHWYDLDL	4125	MQATEWP RT	Anna Wec et al., 2020 (https://science.sciencemag.org/content/early/2020/06/15/science.abc7424)
mAb-15	Ab	SARS-CoV1, SARS-CoV2	229E, HKU1, NL63, OC43			S; Unk	B-cells; SARS-CoV1 Human Patient	830	QVQLVQSGAELKKPGSSVRVSCKAAGG TLTNYAISWVRQAPGQGFEWMGGIMP VSHTAGYAQKFQGRVTFTADESATTAY MDLTSLRPEDTAIYYCARDPSIHYTGNH HWYDLDIWGQGTMVTVSS	1897	DIRLTQSPLSLPVTLGQPASISCRSSQRI VHTDGNTYLNWFLQRPGQSPRRLIYK VSNRDSGVPDRFSGSGSGTDFTLKISR VEAEDVGIYYCMQGTEWPRTFGQGT KVDIK	IGHV1-69 (Human)	IGHJ3 (Human)	IGKV2-30 (Human)	IGKJ3 (Human)	2936	ARDPSIHYTG NHHWYDLDI	4126	MQGTEW PRT	Anna Wec et al., 2020 (https://science.sciencemag.org/content/early/2020/06/15/science.abc7424)
mAb-150	Ab	229E (weak), HKU1 (weak), NL63, SARS-CoV1 (weak), SARS-CoV2 (weak)	OC43			S; Unk	B-cells; SARS-CoV1 Human Patient	831	QVQLVQSGAELKKPGSSVRVSCKAAGG TLTNYAISWVRQAPGQGFEWMGGIMP VSHTAGYAQKFQGRVTFTADESATTAY MDLTSLRPEDTAIYYCARDPSIHYTGNH HWYDLDIWGQGTMVTVSS	1898	DIQLTQSPLSLPVTLGQPASISCRSSQRI VHTDGNTYLNWFLQRPGQSPRRLIYK VSNRDSGVPDRFSGSGSGTDFTLKISR VEAEDVGIYYCMQGTEWPRTFGQGT KVEIK	IGHV1-69 (Human)	IGHJ3 (Human)	IGKV2-30 (Human)	IGKJ1 (Human)	2937	ARDPSIHYTG NHHWYDLDI	4127	MQGTEW PRT	Anna Wec et al., 2020 (https://science.sciencemag.org/content/early/2020/06/15/science.abc7424)
mAb-151	Ab	229E (weak), HKU1 (weak), NL63 (weak), SARS-CoV1 (weak), SARS-CoV2 (weak)	OC43			S; Unk	B-cells; SARS-CoV1 Human Patient	832	QVQLVQSGAEVKKPGSSMRVSCRVSG GTFITHAMSWVRQAPGQGPEWMGGI VPLFGRASYAQPSQTRVQITADESTSTVY LEVPSLTSEDTAVYYCVRDSEPYTATRSQ NHYWYDMDVWGQGTTVTVSS	1899	ETTLTQSPLSLSVTLGQSASISCRASQT VVHSVDGNTYLNWFHQRPGQSPRRLI YKVSNRDSGVPDRFSGSGSGTDFTLRI SRVEAEDIGIYYCMQGTDWPRTFGQG TKVEIK	IGHV1-69 (Human)	IGHJ6 (Human)	IGKV2-30 (Human)	IGKJ1 (Human)	2938	VRDSEPYTAT RSQNHYWYD MDV	4128	MQGTDW PRT	Anna Wec et al., 2020 (https://science.sciencemag.org/content/early/2020/06/15/science.abc7424)

mAb-152	Ab	229E (weak), HKU1 (weak), NL63 (weak), SARS-CoV1 (weak), SARS-CoV2 (weak)	OC43			S; Unk	B-cells; SARS-CoV1 Human Patient	833	QVQLVQSGAELKKPGSSVRVSCKAAGG TLTNYAISWVRQAPGQGFEWMGGIMP VSHTAGYAQKFQGRVTFTADESATTAY MDLTSLRPEDTAIYYCARDPSIHYTGNH HWYDLDIWGQGTTVTVSS	1900	DIVMTQSPLSLPVTLGQPASISCRSSQR IVHTDGNTYLNWFLQRPGQSPRRLIYK VSNRDSGVPDRFSGSGSGTDFTLKISR VEAEDVGIYYCMQGTEWPRTFGQGT KVEIK	IGHV1-69 (Human)	IGHJ6 (Human)	IGKV2-30 (Human)	IGKJ1 (Human)	2939	ARDPSIHYTG NHHWYDLDI	4129	MQGTEW PRT	Anna Wec et al., 2020 (https://science.sciencemag.org/content/early/2020/06/15/science.abc7424)
mAb-153	Ab	229E (weak), HKU1 (weak), NL63 (weak), SARS-CoV1 (weak), SARS-CoV2 (weak)	OC43			S; Unk	B-cells; SARS-CoV1 Human Patient	834	QVQLVQSGAEVKKPGSSVKVSCKASGG TLSHYAISWVRQAPGQGLEWMGGIMP VSGTVGYAQKFQGRVKFTADEYASTAY MELTNLRSEDSAVYFCARDPSIVDSGPH HWYDLDIWGQGTMVTVSS	1901	DIRMTQSPLSLPVTLGQPASISCRSSQF VVHTDGNTYLNWFQQRPGQSPRRLIY KVSNRDSGVPDRFSGSGSGTDFTLKIS RVEAEDVGVYYCMQATEWPRTFGQG TKVDIK	IGHV1-69 (Human)	IGHJ3 (Human)	IGKV2-30 (Human)	IGKJ3 (Human)	2940	ARDPSIVDSG PHHWYDLDI	4130	MQATEWP RT	Anna Wec et al., 2020 (https://science.sciencemag.org/content/early/2020/06/15/science.abc7424)
mAb-154	Ab	229E (weak), HKU1 (weak), NL63 (weak), SARS-CoV1 (weak), SARS-CoV2 (weak)	OC43			S; Unk	B-cells; SARS-CoV1 Human Patient	835	QVQLVESGAEVKRPGASVKVSCKASGY AFSDYYMHWVRQAPGQGPEWMGWI NPNSGDTGYPQKFRGWVTMTRDTSVS TAYMELKRLKSDDTAVYYCASGPNYFDY WGQGTLVTVSS	1902	SYVLTQPPSVSVSPGQTARITCSADGL PKQYSYWYQQKPGQAPVMVIYKDTE RPSGIPERFSGSSSGTTATLTISGVQAE DEADYYCQSADSNDSSPVFGGGTQLT VL	IGHV1-2 (Human)	IGHJ4 (Human)	IGLV3-25 (Human)	IGLJ7 (Human)	2941	ASGPNYFDY	4131	QSADSNDS SPV	Anna Wec et al., 2020 (https://science.sciencemag.org/content/early/2020/06/15/science.abc7424)
mAb-155	Ab	229E (weak), HKU1 (weak), NL63 (weak), SARS-CoV1 (weak), SARS-CoV2 (weak)	OC43			S; Unk	B-cells; SARS-CoV1 Human Patient	836	EVQLLESGGGLVKPGGSLRLSCEASGFTF SNYNMNWVRQAPGKGLEWVSSISGSS SYISYADSVKGRFTISRDNAKNSLYLQMN SLRVEDTAVYYCARADRDYDFWSDPPLI DHWGQGTLVTVSS	1903	ETTLTQSPATLSLSPGEGATLSCRASQS VSSSLAWYQQKPGQAPRLLIYDASNR ATGIPARFSGSGSGTDYTLTISSLEPEDF AVYYCHQRSNWPYTFGQGTKVEIK	IGHV3-21 (Human)	IGHJ4 (Human)	IGKV3-11 (Human)	IGKJ1 (Human)	2942	ARADRDYDF WSDPPLIDH	4132	HQRSNWP YT	Anna Wec et al., 2020 (https://science.sciencemag.org/content/early/2020/06/15/science.abc7424)
mAb-156	Ab	229E (weak), HKU1 (weak), NL63 (weak), SARS-CoV1 (weak), SARS-CoV2 (weak)	NL63, OC43			S; Unk	B-cells; SARS-CoV1 Human Patient	837	EVQLVESGGGLIQPGGSLRLSCAASGFT VTDNYMSWVRQAPGKGLEWVSVLYSG GSTYYADAVQGRFSISRDNSKNALYLQM NSLRAEDTAVYYCARGFGNGWSYYFDY WGQGTLVTVSS	1904	DIVLTQTPSSLSASVGDRVTITCRASQTI ATYLSWYQQKPGKAPKLLIYAVSSLQS GVPSRFSGSGSGTDFTLTIGSLQPEDF ATYYCQQSYSIPWTFGQGTKVDIK	IGHV3-53 (Human)	IGHJ4 (Human)	IGKV1-39 (Human)	IGKJ1 (Human)	2943	ARGFGNGWS YYFDY	4133	QQSYSIPW T	Anna Wec et al., 2020 (https://science.sciencemag.org/content/early/2020/06/15/science.abc7424)
mAb-157	Ab	HKU1, SARS-CoV1 (weak), SARS-CoV2 (weak)	229E, NL63, OC43			S; Unk	B-cells; SARS-CoV1 Human Patient	838	EVQLVQSGGGLVQPGGSLRLSCAASGF TFSSYSMSWVRQAPGKGLEWVSYITRSS DNIYYAESVKGRFTISRDSAKNSLYLHMN SLRDEDTAVYYCARDPGLEYSGNYFSYYY YAMDVWGQGTTVTVSS	1905	EIVMTQSPSSLSASVGDRVTITCRASQS ISYYLNWYQQKPGKAPKLLIYAASSLQS GVPSRFSGSGSGTDFILTISSLQPEDIAT YYCQHSYSSPPLTFGGGTKVEIK	IGHV3-48 (Human)	IGHJ6 (Human)	IGKV1-39 (Human)	IGKJ4 (Human)	2944	ARDPGLEYSG NYFSYYYYAM DV	4134	QHSYSSPP LT	Anna Wec et al., 2020 (https://science.sciencemag.org/content/early/2020/06/15/science.abc7424)
mAb-158	Ab	HKU1, SARS-CoV1 (weak), SARS-CoV2 (weak)	229E, NL63, OC43			S; Unk	B-cells; SARS-CoV1 Human Patient	839	QVQLVQSGAEVKKPGSSVKVSCKASGG TFSTHAISWVRQAPGHGPEWMGGIIPL FGTSESAQRFQARVRFTADESTSTAYME LSSLTSEDTAVYYCVRDSDPYTATSRNNH YWYDMDVWGQGTTVTVSS	1906	ETTLTQSPLSLPVTLGQPASISCRSSQIV VHSDGNTYLNWFHQRPGQSPRRLIYK VSNRDSGVPDRFSGSGSGTDFTLKISR VEAEDIGVYYCMQGTDWPRTFGQGT KVDIK	IGHV1-69 (Human)	IGHJ6 (Human)	IGKV2-30 (Human)	IGKJ3 (Human)	2945	VRDSDPYTAT SRNNHYWYD MDV	4135	MQGTDW PRT	Anna Wec et al., 2020 (https://science.sciencemag.org/content/early/2020/06/15/science.abc7424)
mAb-159	Ab	HKU1, SARS-CoV1 (weak), SARS-CoV2 (weak)	229E, NL63, OC43			S; Unk	B-cells; SARS-CoV1 Human Patient	840	QVQLVQSGAEVKKPGSSVKVSCKVSGG RFSDYAISWLRQAPVKGLEWMGGIIPRL NRKGYSQDFQGRLTFTADESTSTAYMEL SGLTSEDTAVYYCARDPTFLNSGNHFWY AVDIWGQGTTVTVSS	1907	DIRLTQSPLSLSVTLGQAASISCTCSQT AVHSDGNTYLNWFHQRPGQSPRRLIY KVSNRDSGVPDRFSGSGSGTDFTLKIS RVEAEDVGIYYCMQTTDWPRTFGQG TKVEIK	IGHV1-69 (Human)	IGHJ6 (Human)	IGKV2-30 (Human)	IGKJ1 (Human)	2946	ARDPTFLNSG NHFWYAVDI	4136	MQTTDWP RT	Anna Wec et al., 2020 (https://science.sciencemag.org/content/early/2020/06/15/science.abc7424)
mAb-16	Ab	SARS-CoV1, SARS-CoV2	229E, HKU1, NL63, OC43			S; Unk	B-cells; SARS-CoV1 Human Patient	841	EVQLVESGAEVRTPGSSVKLSCKASGGT FSTHAFSWVRQAPGQRPEWMGGIIPIF GESKDTQKFQGRVTFTADESTTTVYMEL RSLKSDDTAIYYCVRDSDPYTATYRNNHY WYAMDVWGQGTTVTVSS	1908	EIVLTQSPLSLPVTLGQPASISCRSSLRL VHTDGNTYLNWFQQRPGQSPRRLIYK VSNRDSGVPDRFSGSGSGTDFTLKISR VEAEDIGVYYCMQGTEWPRTFGQGT KVDIK	IGHV1-69 (Human)	IGHJ6 (Human)	IGKV2-30 (Human)	IGKJ3 (Human)	2947	VRDSDPYTAT YRNNHYWYA MDV	4137	MQGTEW PRT	Anna Wec et al., 2020 (https://science.sciencemag.org/content/early/2020/06/15/science.abc7424)
mAb-160	Ab	HKU1, SARS-CoV1 (weak), SARS-CoV2 (weak)	229E, NL63, OC43			S; Unk	B-cells; SARS-CoV1 Human Patient	842	EVQLVESGGGVVKPGGSLRVSCVGSGF TFSDHYMSWIRQAPGKGLEIISYISTDGS YINDADSVKGRFINSRDNAKNSVYLQLN SLRAEDTAVYYCARMGPSGSGSLDYWG QGSLVTVSS	1909	DIVMTQSPGTLSLSPGERAALSCRASQ IVTRSQLAWYQHKPGQPPRLLIYDSSS RATGTPDRFSGSGSGTDFTLTISRLEPE DSAVYYCHQYSGSATFGPGTKVEIK	IGHV3-11 (Human)	IGHJ4 (Human)	IGKV3-20 (Human)	IGKJ3 (Human)	2948	ARMGPSGSG SLDY	4138	HQYSGSAT	Anna Wec et al., 2020 (https://science.sciencemag.org/content/early/2020/06/15/science.abc7424)

mAb-161	Ab	HKU1, SARS-CoV1 (weak), SARS-CoV2 (weak)	229E, NL63, OC43			S; Unk	B-cells; SARS-CoV1 Human Patient	843	EVQLVESGPTLVKPTQTLTLTCTFSGFSL NTRELGVGWIRQPPGKALEWLALIYWD DDKRYSPSLKSRLSITKDTSKNQVVLTLT NMDPGDTATYYCAHTSELPPRRPYAAF DFWGQGTLVTVSS	1910	SYELTQPPSVSGAPRQKVTISCSGSSAN IASNGVNWYQQLPGKAPKLLIYYDDL VSSGVSDRFSGSKSGTSASLAISGLQSE DEADYYCATWDDILNGPVFGGGTKLT VL	IGHV2-5 (Human)	IGHJ4 (Human)	IGLV1-36 (Human)	IGLJ3 (Human)	2949	AHTSELPPRR PYAAFDF	4139	ATWDDILN GPV	Anna Wec et al., 2020 (https://science.sciencemag.org/content/early/2020/06/15/science.abc7424)
mAb-162	Ab	HKU1 (weak), SARS-CoV1 (weak), SARS-CoV2 (weak)	229E, NL63, OC43			S; Unk	B-cells; SARS-CoV1 Human Patient	844	EVQLVESGGGVVQPGGSLRLSCVASGF PFGRYAMHWVRQAPGQGLEWLTLISF DSSNIEYSDSVQGRFTISRDNSRNTLFLQ MTSLRPEDTAVYFCARDLPPLDYWGQG TLVTVSS	1911	DIRMTQSPSSLSASVGDRVTITCRASQ GFGNKVAWYQQKPGTAPKLLIYETSTL QSGVPSRFSGSGSGTEFAFTISSLQPED GATYYCQKYNRAPWTFGQGTKVEIK	IGHV3-30 (Human)	IGHJ4 (Human)	IGKV1-27 (Human)	IGKJ1 (Human)	2950	ARDLPPLDY	4140	QKYNRAPWT	Anna Wec et al., 2020 (https://science.sciencemag.org/content/early/2020/06/15/science.abc7424)
mAb-163	Ab	HKU1 (weak), NL63 (weak), SARS-CoV1 (weak), SARS-CoV2 (weak)	229E, OC43			S; Unk	B-cells; SARS-CoV1 Human Patient	845	QVQLQQWGAGLLKPSETLSLTCAVNGG SFNNYYWSWIRQPPGKGPEWIGEVVHS GSTTYNPSLKSRVTISIDMSKNQFALKLN SVTAADTAVYYCARGFTFTYSDFLTGQRT FEYWGQGTLVTVSS	1912	QSALIQPASVSGSPGQSITISCTGTSSD VGRYNYVSWYQQHPGKAPKLMIYDV SNRPSGVSNRFSGSKSGNTASLTISGL QAEDEAAYYCSSYISDIKLVVFGGGTKL TVL	IGHV4-34 (Human)	IGHJ4 (Human)	IGLV2-14 (Human)	IGLJ3 (Human)	2951	ARGFTFTYSD FLTGQRTFEY	4141	SSYISDIKLV V	Anna Wec et al., 2020 (https://science.sciencemag.org/content/early/2020/06/15/science.abc7424)
mAb-164	Ab	HKU1 (weak), NL63 (weak), SARS-CoV1 (weak), SARS-CoV2 (weak)	229E, OC43			S; Unk	B-cells; SARS-CoV1 Human Patient	846	EVQLVESGGGVVQPGRSLRLSCAASGFT FSSYAMHWVRQAPGKGLEWVALISYD GDKKYYPDSVRGRFTISRDNSKNTLHLQ MNSLRLEDTAVYYCARSYGGSYSTVGY WGQGALVTVSS	1913	QSALIQPRSVSGSPGQSVTISCTGTSSD VGGSNYVSWYQQHPGKAPKLLVYDV TKRPSGVPDRFSGSKSGNTASLTISGL QAEDEADYYCCSYAGTYIFGTGTKLTV L	IGHV3-30 (Human)	IGHJ4 (Human)	IGLV2-11 (Human)	IGLJ1 (Human)	2952	ARSYGGSYST VGY	4142	CSYAGTYI	Anna Wec et al., 2020 (https://science.sciencemag.org/content/early/2020/06/15/science.abc7424)
mAb-165	Ab	HKU1 (weak), NL63 (weak), SARS-CoV1 (weak), SARS-CoV2 (weak)	229E, OC43			S; Unk	B-cells; SARS-CoV1 Human Patient	847	QVQLVQSGGDSVNPGGSLRLSCAGSGF SVRDVWMSWVRQAPGKGLEWIGRIKS EADGGSSDYRASLKDRFSIWRDASKNTL YLQVNGLQTEDTAIYFCSWNDVGWAFT FWGQGTLVTVSS	1914	QSVLTQPPSVSGSPGQSVSISCSGTSS DFGNYNRISWYQQTPGTAPKVIIYEVN SRPSGVPDRFSGSKSGNTASLTITGLQ AEDEADYYCCSYRSDNTYIFGGGTKVT VL	IGHV3-15 (Human)	IGHJ4 (Human)	IGLV2-18 (Human)	IGLJ1 (Human)	2953	SWNDVGWA FTF	4143	CSYRSDNT YI	Anna Wec et al., 2020 (https://science.sciencemag.org/content/early/2020/06/15/science.abc7424)
mAb-166	Ab	HKU1 (weak), SARS-CoV1 (weak), SARS-CoV2 (weak)	229E, NL63, OC43			S; Unk	B-cells; SARS-CoV1 Human Patient	848	QVQLVQSGAEVKKAGSSVKVSCKASGG PFSSFAISWVRQAPGQGLEWLGGIMTV FGPAHYAQKSRDRISITADESTSTSYLELS SLTSDDTAVYYCAAEERSGTNHNYYGLD VWGQGTTVTVSS	1915	ETTLTQSPLFLPVTLGQPASISCRSSQRL VHTNGNTYLNWFQQRPGHSPRRLIY QVSNRDSGVPDRFSGSGSGTDFTLKIS RVEAEDVGVYYCMQGTEWPRTFGG GTKLEIK	IGHV1-69 (Human)	IGHJ6 (Human)	IGKV2-30 (Human)	IGKJ4 (Human)	2954	AAEERSGTNH NYYGLDV	4144	MQGTEW PRT	Anna Wec et al., 2020 (https://science.sciencemag.org/content/early/2020/06/15/science.abc7424)
mAb-167	Ab	HKU1 (weak), SARS-CoV1 (weak), SARS-CoV2 (weak)	229E, NL63, OC43			S; Unk	B-cells; SARS-CoV1 Human Patient	849	EVQLVESGGGLIQPGGSLRLSCAASGFP FSGTYMTWVRQAPGKGLEWVSIIYSGG DTYYADSVKGRFTISRDNSKNTLFLQMN SLRVEDTAMYYCARDREMAIITERSYGL DVWGQGTMVTVSS	1916	QPVLTQPPSASGTPGQRVTISCSGGSS NIGSNSVNWYQQLPGTAPKLLIYSNSQ RPSGVPDRFSGSKSGTSASLAISGLQSE DEADYYCAAWDDSLNTFRYVFGTGTK VTVL	IGHV3-53 (Human)	IGHJ3 (Human)	IGLV1-44 (Human)	IGLJ1 (Human)	2955	ARDREMAIIT ERSYGLDV	4145	AAWDDSL NTFRYV	Anna Wec et al., 2020 (https://science.sciencemag.org/content/early/2020/06/15/science.abc7424)
mAb-168	Ab	HKU1 (weak), SARS-CoV1 (weak), SARS-CoV2 (weak)	229E, NL63, OC43			S; Unk	B-cells; SARS-CoV1 Human Patient	850	EVQLVESGGGLVQPGGSLRLSCGASGFT FSDYAMSWVRQAPGKGLEWVSTISGSG DKTYYADSLKGRFTNSRDNSKSTLYLQM TSLRAEDTAVYFCAKDRYCSGGSCFYDAF DIWGQGTTVTVSS	1917	ETTLTQSPSSLSASVGDRVNITCRASQS ISTYLTWYQQKPGKAPKLLIYGASSLHS GVPSRFTGVGSGTEFTLSISSLQPEDFA TYYCQQSYNTFFTFGGGTKVDIK	IGHV3-23 (Human)	IGHJ3 (Human)	IGKV1-39 (Human)	IGKJ3 (Human)	2956	AKDRYCSGGS CFYDAFDI	4146	QQSYNTFF T	Anna Wec et al., 2020 (https://science.sciencemag.org/content/early/2020/06/15/science.abc7424)
mAb-169	Ab	HKU1 (weak), SARS-CoV1 (weak), SARS-CoV2 (weak)	229E, NL63, OC43			S; Unk	B-cells; SARS-CoV1 Human Patient	851	EVQLVESGGGVVQPGRSLRLSCEASGFT FADYPMHWVRQAPGKGLEWVAVISSH GRSQGYAASVKGRFTFSRDNSQSSLFLQ LNSLRVEDTAVYFCAREAQSSGRAGCLD AWGQGTLVTVSS	1918	DIRLTQSPSSLSASVGDRVTITCRASQA IAGWLAWYQQKPGRAPKSLIYRASSL QSGVPSRFSGSGSGTDFSLTISNLQPE DSATYYCQHYDSYPTAFGQGTRLEIK	IGHV3-30 (Human)	IGHJ4 (Human)	IGKV1D-16 (Human)	IGKJ5 (Human)	2957	AREAQSSGRA GCLDA	4147	QHYDSYPT A	Anna Wec et al., 2020 (https://science.sciencemag.org/content/early/2020/06/15/science.abc7424)
mAb-17	Ab	SARS-CoV1, SARS-CoV2	229E, HKU1, NL63, OC43			S; Unk	B-cells; SARS-CoV1 Human Patient	852	QVQLVQSGAELKKPGSSVRVSCKAAGG TLTNYAISWVRQAPGQGFEWMGGIMP VSHTAGYAQKFQGRVTFTADESATTAY MDLTSLRPEDTAIYYCARDPSIHYTGNH HWYDLDIWGQGTMVTVSS	1919	ETGLTQIPFSLPVTFGQPASISCRFSQR LVHTDGNTNLNWFLQRPGQFPRGLIY KVFNRDSGVPDRFRGSGSGIDFTLKIS RVEVEDVGIYYGMQGTEWLGTFGQG TKVEIK	IGHV1-69 (Human)	IGHJ3 (Human)	IGKV2-30 (Human)	IGKJ1 (Human)	2958	ARDPSIHYTG NHHWYDLDI	4148	MQGTEWL GT	Anna Wec et al., 2020 (https://science.sciencemag.org/content/early/2020/06/15/science.abc7424)
mAb-170	Ab	HKU1 (weak), SARS-CoV1 (weak), SARS-CoV2 (weak)	229E, NL63, OC43			S; Unk	B-cells; SARS-CoV1 Human Patient	853	QVQLVQSGAEVREPGSSVKLSCKTSGGT FSTHAISWVRQAPGQRPEWMGGIMPI FGESKDTQKFQGRVTFTADESTTTAYME LRSLKSDDTAIYYCVRDSDPYTATVRSNH YWYAMDVWGQGTTVTVSS	1920	ETTLTQSPLSLAVTLGQPASISCRSSLGL VHTNGNTYLNWFQQRPGQSPRRLIYR VSNRDSGVPDRFSGSGSVTDFTLTISR VEAEDIGVYYCMQGTEWPRTFGQGT KVEIK	IGHV1-69 (Human)	IGHJ6 (Human)	IGKV2-30 (Human)	IGKJ1 (Human)	2959	VRDSDPYTAT VRSNHYWYA MDV	4149	MQGTEW PRT	Anna Wec et al., 2020 (https://science.sciencemag.org/content/early/2020/06/15/science.abc7424)
mAb-171	Ab	HKU1 (weak), SARS-CoV1 (weak), SARS-CoV2 (weak)	229E, NL63, OC43			S; Unk	B-cells; SARS-CoV1 Human Patient	854	EVQLVQSGAEVKKPGSSVKVSCKVSGG RFSDYAISWLRQAPVKGLEWMGGIIPRL NRKGYSQDFQGRLTFTADESTSTAYMEL SGLTSEDTAVYYCARDPTFLNSGNHFWY AVDIWGQGTTVTVSS	1921	ETTLTQSPLSLSVTLGQAASISCTCSQT AVHSDGNTYLNWFHQRPGQSPRRLIY KVSNRDSGVPDRFSGSGSGTDFTLKIS RVEAEDVGIYYCMQTTDWPRTFGQG TKVDIK	IGHV1-69 (Human)	IGHJ6 (Human)	IGKV2-30 (Human)	IGKJ3 (Human)	2960	ARDPTFLNSG NHFWYAVDI	4150	MQTTDWP RT	Anna Wec et al., 2020 (https://science.sciencemag.org/content/early/2020/06/15/science.abc7424)

mAb-172	Ab	HKU1 (weak), SARS-CoV1 (weak), SARS-CoV2 (weak)	229E, NL63, OC43			S; Unk	B-cells; SARS-CoV1 Human Patient	855	QVQLQESGRGLVKPSETLSLTCTVSGGSI TSSRYYWGWIRQPPGRNLEWIGSIHYS GTTSYNPSLWSRVAISVDTAQNQFSLRL NSVTAADTAVYYCAAPAPSNHESWSGT DWFDPWGQGILVTVSS	1922	EIVMTQSPASLSASVGDRVTITCRAGQ SISTNLCWYQQRQGKAPKLLIYAASSL RSGVPSRFSGSGSGTDFTLTISSLQPED FATYYCQQSYSTPPTFGGGTKVDIK	IGHV4-39 (Human)	IGHJ5 (Human)	IGKV1-39 (Human)	IGKJ3 (Human)	2961	AAPAPSNHES WSGTDWFDP	4151	QQSYSTPP T	Anna Wec et al., 2020 (https://science.sciencemag.org/content/early/2020/06/15/science.abc7424)
mAb-173	Ab	HKU1 (weak), SARS-CoV1 (weak), SARS-CoV2 (weak)	229E, NL63, OC43			S; Unk	B-cells; SARS-CoV1 Human Patient	856	QVQLVQSGAEVKGPGASVKVSCKVSGY SFITYDITWVRQAPGQGLEWMGWISTK SGDTRYAQNVQGRVTMTTDTSTNTAY MELRNLKSDDTALYYCARTTPRGWEQ WPVLEYWGQGTLVTVSS	1923	DIQVTQSPATLSVSPGERVTLSCRASQ SISNTLAWYQQKPGQAPRLLIYGASTR ATGIPARFSGSGSGTEFTLTISSLQSEDF AVYYCHQYNKWPPITFGGGTKVEIK	IGHV1-18 (Human)	IGHJ4 (Human)	IGKV3-15 (Human)	IGKJ4 (Human)	2962	ARTTPRGWE QWPVLEY	4152	HQYNKWP PIT	Anna Wec et al., 2020 (https://science.sciencemag.org/content/early/2020/06/15/science.abc7424)
mAb-174	Ab	HKU1 (weak), SARS-CoV1 (weak), SARS-CoV2 (weak)	229E, NL63, OC43			S; Unk	B-cells; SARS-CoV1 Human Patient	857	EVQLVESGGGLVQPGGSLRLSCEASGFN FNSYSMSWVRQAPGKGLEWLSYISSRSS TIKYASSVQGRFTVSRDNAKKSVYLQMN SLRDEDTAVYFCARELDSETYYNYNSLDV WGQGTTVTVSS	1924	DIQMTQSPSSLSASVGDRVTISCRASQ GISTFLAWFQQRPGKAPKSLIYAASKL QSGVPSRFSGSDSGPDFTLTIDNLRPE DSATYYCKQYNSYPYTFGQGTKLEIK	IGHV3-48 (Human)	IGHJ6 (Human)	IGKV1-16 (Human)	IGKJ2 (Human)	2963	ARELDSETYY NYNSLDV	4153	KQYNSYPY T	Anna Wec et al., 2020 (https://science.sciencemag.org/content/early/2020/06/15/science.abc7424)
mAb-175	Ab	HKU1 (weak), SARS-CoV1 (weak), SARS-CoV2 (weak)	229E, NL63, OC43			S; Unk	B-cells; SARS-CoV1 Human Patient	858	QVQLVESGGEVKKPGASVKVSCKASGY TLSSYPISWVRQAPGHGLEWMGWINT YNGRTNYEQMLQGRVTMTTDTSTSTAY MELRSLRSDDTAVYYCARVVFRHGQYD DSSGRLAFDIWGQGTMVTVSS	1925	EIVMTQSPSSLSASVGDSVTITCRASQS ISNYLNWYQDKPGKAPELLIYAASNLQ SGVPSRFSGSGSGTDFTLTISSLQPEDF ATYYCQQSYSDSWTFGQGTKVDIK	IGHV1-18 (Human)	IGHJ3 (Human)	IGKV1-39 (Human)	IGKJ1 (Human)	2964	ARVVFRHGQ YDDSSGRLAF DI	4154	QQSYSDS WT	Anna Wec et al., 2020 (https://science.sciencemag.org/content/early/2020/06/15/science.abc7424)
mAb-176	Ab	HKU1 (weak), SARS-CoV1 (weak), SARS-CoV2 (weak)	229E, NL63, OC43			S; Unk	B-cells; SARS-CoV1 Human Patient	859	QVQLVQSGAELKKPGSSVRVSCKAAGG TLTNYAISWVRQAPGQGFEWMGGIMP VSHTAGYAQKFQGRVTFTADESATTAY MDLTSLRPEDTAIYYCARDPSIHYTGNH HWYDLDIWGQGTMVTVSS	1926	ETTLTQSPLSLPVTLGQPASISCRSSQRI VHTDGNTYLNWFLQRPGQSPRRLIYK VSNRDSGVPDRFSGSGSGTDFTLKISR VEAEDVGIYYCMQGTEWPRTFGQGT KVEIK	IGHV1-69 (Human)	IGHJ3 (Human)	IGKV2-30 (Human)	IGKJ1 (Human)	2965	ARDPSIHYTG NHHWYDLDI	4155	MQGTEW PRT	Anna Wec et al., 2020 (https://science.sciencemag.org/content/early/2020/06/15/science.abc7424)
mAb-177	Ab	HKU1 (weak), SARS-CoV1 (weak), SARS-CoV2 (weak)	229E, NL63, OC43			S; Unk	B-cells; SARS-CoV1 Human Patient	860	EVQLLESGAEVKKPGSSVKVSCKTSGGT FSTHAISWVRQAPGQGPEWMGGIIPLF GTSEHAQRFQARVKFTADESTSTAYMEL SSLTPEDTAVYYCVRDSDPYTATSRNNH YWYGMDVWGQGTTVTVSS	1927	DIQMTQSPLSLPVTLGQPASISCRSSQS VVHSDGNTYLNWFHQRPGQSPRRLIY KVSNRDSGVPDRFSGSGSGTDFTLKIS RVEAEDIGVYYCMQGTDWPRTFGQG TKVDIK	IGHV1-69 (Human)	IGHJ6 (Human)	IGKV2-30 (Human)	IGKJ3 (Human)	2966	VRDSDPYTAT SRNNHYWYG MDV	4156	MQGTDW PRT	Anna Wec et al., 2020 (https://science.sciencemag.org/content/early/2020/06/15/science.abc7424)
mAb-178	Ab	SARS-CoV1 (weak), SARS-CoV2 (weak)	229E, HKU1, NL63, OC43			S; Unk	B-cells; SARS-CoV1 Human Patient	861	EVQLLESGGGVVQPGTSLRLSCAVSGF MFKNYAIHWVRQAPGKGLEWVAVISF DGSDISYTESVQGRFTISRDNSENMLYL QMNSLRAEDTAMYYCAREPDGIGAAGI SGYWGQGTLVTVSS	1928	GIVLTQSPDSLAVSVGERATINCKSSQT VLYSSKNKHYLAWYQQKPGQPPKLLT SSPSTREPGVPDRFSGSGSGTDFTLTIS SLQAEDVAVYYCQQYYTTPYTFGQGT KVDIK	IGHV3-30 (Human)	IGHJ4 (Human)	IGKV4-1 (Human)	IGKJ3 (Human)	2967	AREPDGIGAA GISGY	4157	QQYYTTPY T	Anna Wec et al., 2020 (https://science.sciencemag.org/content/early/2020/06/15/science.abc7424)
mAb-179	Ab	SARS-CoV1 (weak), SARS-CoV2 (weak)	229E, HKU1, NL63, OC43			S; Unk	B-cells; SARS-CoV1 Human Patient	862	EVQLVESGGGLVKPGGSLRLSCVASGFT FSDFYMSWIRQAPGKGLEWVSYISGSG DTIYYADSVKGRFTVSRDNAKNSLFLQM SSLGAEDTAMYYCAREMATSFGYYFVLD VWGQGTTVTVSS	1929	EIVMTQTPSSLSASVGDRVTITCRASQ SISNYVNWYQQKPGRAPNLLIYAASSL QSGVSSRFSGSGSGTDFTLTISSLQPED FATYYCQQTYSTPPEGPTFGPGTKVEIK	IGHV3-11 (Human)	IGHJ6 (Human)	IGKV1-39 (Human)	IGKJ3 (Human)	2968	AREMATSFGY YFVLDV	4158	QQTYSTPP EGPT	Anna Wec et al., 2020 (https://science.sciencemag.org/content/early/2020/06/15/science.abc7424)
mAb-18	Ab	SARS-CoV1, SARS-CoV2	229E, HKU1, NL63, OC43			S; Unk	B-cells; SARS-CoV1 Human Patient	863	QVQLQQWGAGLLKPSETLSLSCAVYGG SFSGFYWSWIRQPPGKGLEWIGEINHS GSANYNPSLMSRVTISMDTSKKQFSLQL RSVTAADTAVYYCARGQESPIVGVTGR WFDPWGQGTLVTVSS	1930	QPVLTQPASVSGSPGQSVTISCTGTSS DVGSYSDVGNYVSWYQHHPGKAPKL MIYEVRTRPSWVSTRFSGSKSGTTASL TISGLQAEDEADYYCCSYAGASPFVVF GGGTKLTVL	IGHV4-34 (Human)	IGHJ5 (Human)	IGLV2-23 (Human)	IGLJ3 (Human)	2969	ARGQESPIVG VTGRWFDP	4159	CSYAGASP FVV	Anna Wec et al., 2020 (https://science.sciencemag.org/content/early/2020/06/15/science.abc7424)
mAb-180	Ab	SARS-CoV1 (weak), SARS-CoV2 (weak)	229E, HKU1, NL63, OC43			S; Unk	B-cells; SARS-CoV1 Human Patient	864	EVQLVESGGGVVQPGRSLRLSCAASEFT FSTYAMHWVRQAPGKGLEWVALISYD GINKYYADSVKGRFAISRDNSKNTLYLQV NSLRADDTAVYYCVRPYSGSYTNWFDL WGQGTLVTVSS	1931	EIVMTQSPGTLSSSPGERATLSCRASQ SVSSRYLAWYQQKPGQAPRLLIYGTSN RATGIPDRFSGSGSGTDFTLTISRLEPE DFAVYYCQQYGSSYTFGPGTKLEIK	IGHV3-30 (Human)	IGHJ4 (Human)	IGKV3-20 (Human)	IGKJ2 (Human)	2970	VRPYSGSYTN WFDL	4160	QQYGSSYT	Anna Wec et al., 2020 (https://science.sciencemag.org/content/early/2020/06/15/science.abc7424)
mAb-181	Ab	SARS-CoV1 (weak), SARS-CoV2 (weak)	229E, HKU1, NL63, OC43			S; Unk	B-cells; SARS-CoV1 Human Patient	865	QVQLVQSGAEVKKPGSSVKVSCKASGG MLSDYAISWVRQAPGQRLEWMGGIM PAFGSPGYAQIFRGRATISADVSTSTAYL ELTSLKPEDTAVYYCARDPSILNTGNHH WYDLDIWGQGTMVTVSS	1932	DIVMTQSPLSLPVGLGQSASISCRSSQ RVVHTDGNTYLNWFHQRPGQSPRRLI YKVSNRDSGVPDRFSGSGSGTDFTLRI SRVEAEDVGVYYCMQATEWPRTFGQ GTKVEIK	IGHV1-69 (Human)	IGHJ3 (Human)	IGKV2-30 (Human)	IGKJ1 (Human)	2971	ARDPSILNTG NHHWYDLDI	4161	MQATEWP RT	Anna Wec et al., 2020 (https://science.sciencemag.org/content/early/2020/06/15/science.abc7424)
mAb-182	Ab	229E (weak), HKU1 (weak), SARS-CoV2 (weak)	NL63, OC43, SARS-CoV1			S; Unk	B-cells; SARS-CoV1 Human Patient	866	QVQLVQSGAEVKMPGSSVKVSCKVSG GRFSDYAISWLRQAPLEGLEWMGGIVP HLNRKGYSQKFQDRLTFTADDSTSTAYM ELSGLTSEDTAVYYCARDPTFLNTGNHF WYAVDIWGQGTTVTVSS	1933	DIRLTQSPLSLSVTLGQAASISCTCSQSA VHSDGTTYFNWFHQRPGQSPRRLIYK VSNRDSGVPDRFIGSGSGTHFTLKISR VEAEDVGVYYCMQTTDWPRTFGQGT KVEIK	IGHV1-69 (Human)	IGHJ6 (Human)	IGKV2-30 (Human)	IGKJ1 (Human)	2972	ARDPTFLNTG NHFWYAVDI	4162	MQTTDWP RT	Anna Wec et al., 2020 (https://science.sciencemag.org/content/early/2020/06/15/science.abc7424)
mAb-183	Ab	HKU1, SARS-CoV2 (weak)	229E, NL63, OC43, SARS-CoV1			S; Unk	B-cells; SARS-CoV1 Human Patient	867	QVQLVQSGAEVKKPGSSVKVSCKASGG TFSTHAISWVRQAPGHGPEWLGGILPLF GTSESAQRFQARVKITADESTSTAYMELS SLTSEDTAVYYCVRDSDPYTATSRNNHY WYAMDVWGQGTTVTVSS	1934	ETTLTQSPLSLPVTLGQPASISCRSSQS VVHSDGNTYLNWFHQRPGQSPRRLIY KVSNRDSGVPDRFSGSGSGTDFTLKIS RVEAEDIGVYYCMQGTDWPRTFGQG TKVEIK	IGHV1-69 (Human)	IGHJ6 (Human)	IGKV2-30 (Human)	IGKJ1 (Human)	2973	VRDSDPYTAT SRNNHYWYA MDV	4163	MQGTDW PRT	Anna Wec et al., 2020 (https://science.sciencemag.org/content/early/2020/06/15/science.abc7424)

mAb-184	Ab	HKU1 (weak), SARS-CoV2 (weak)	229E, NL63, OC43, SARS-CoV1			S; Unk	B-cells; SARS-CoV1 Human Patient	868	QVQLVQSGAEVKKPGSSVKVSCKVSGG TFSNYAISWLRQAPGQGPEWMGGIIPA LSRVGYVRKFQARLTISADELTTTAYMDL SSLTSEDTAVYYCARDPSFLNTGNHFWY DFDLWGQGTTVTVSS	1935	ETTLTQSPLSLPVTLGQPASISCTSSQTV VHTDRNTYLNWYHQRPGQSPRRLIYK VSNRDSGVPDRFSGSGSGSHFTLKISR VEAEDVGVYYCMQGTEWPRTFGQGT KLEIK	IGHV1-69 (Human)	IGHJ4 (Human)	IGKV2-30 (Human)	IGKJ2 (Human)	2974	ARDPSFLNTG NHFWYDFDL	4164	MQGTEW PRT	Anna Wec et al., 2020 (https://science.sciencemag.org/content/early/2020/06/15/science.abc7424)
mAb-185	Ab	SARS-CoV2 (weak)	229E, HKU1, NL63, OC43, SARS-CoV1			S; Unk	B-cells; SARS-CoV1 Human Patient	869	QVQLQQWGAGLLKPSETLSLTCAVYGG SFSGFYWTWIRQPPGKGLEWIGEINHS GSSNYDLSLKSRVTMSVDTSKNQFSLKLS SVTAADTAVYYCARGMISPRIPRTTRQR WFDTWGQGTLVTVSS	1936	QPGLTQPASVSGSPGQSITISCTGTSG DVGSDNLVSWYQRHPGKAPKLMIYE GSKRPSGVSHRFSGSNSGNTASLTISG LQAEDDADYYCCSYAGDDTVVFGGGT KLTVL	IGHV4-34 (Human)	IGHJ4 (Human)	IGLV2-23 (Human)	IGLJ3 (Human)	2975	ARGMISPRIP RTTRQRWFD T	4165	CSYAGDDT VV	Anna Wec et al., 2020 (https://science.sciencemag.org/content/early/2020/06/15/science.abc7424)
mAb-186	Ab	SARS-CoV2 (weak)	229E, HKU1, NL63, OC43, SARS-CoV1			S; Unk	B-cells; SARS-CoV1 Human Patient	870	QVQLQQWGAGLLKPSETLSLTCGVYGG SFSGYFWSWIRQSPGKGLEWIGEINHSR SMSYNPSLKSRITMSVDTSKNQFSLNLN SVTAADTAVYFCARGKAHRNDFWSGYY PHWFDPWGQGILVTVSS	1937	DIVLTQSPGTLSLSPGERVTLSCRASQSI SSNYLAWYQQKPGQAPRLLISDASSRA TGIPDRFSGSGSGADFTLIISRLEPEDFA VYFCHQYGGSPTTFGQGTKVEIK	IGHV4-34 (Human)	IGHJ5 (Human)	IGKV3-20 (Human)	IGKJ1 (Human)	2976	ARGKAHRND FWSGYYPHW FDP	4166	HQYGGSPT T	Anna Wec et al., 2020 (https://science.sciencemag.org/content/early/2020/06/15/science.abc7424)
mAb-187	Ab	SARS-CoV2 (weak)	229E, HKU1, NL63, OC43, SARS-CoV1			S; Unk	B-cells; SARS-CoV1 Human Patient	871	QVQLVQSGAEVKKPGSSVKISCKISGDTF STNAISWLRQAPGREPEWMGGIVPLVG PASYAQRPQGRLTITADEFTNTAYLELNS LRSEDTATYYCARDSDPYTATRRHNHYW YAMDVWGQGTTVTVSS	1938	ETTLTQSPLSLPVTLGQPASISCRSSQIA MHSDGNTYLSWFHQRPGQPPRRLIYK ISNRDSGVPDRFSGSGSGTDFTLKISRV EAEDIGTFYCMQGTDWPRTFGQGTK VEIK	IGHV1-69 (Human)	IGHJ6 (Human)	IGKV2-30 (Human)	IGKJ1 (Human)	2977	ARDSDPYTAT RRHNHYWYA MDV	4167	MQGTDW PRT	Anna Wec et al., 2020 (https://science.sciencemag.org/content/early/2020/06/15/science.abc7424)
mAb-188	Ab	SARS-CoV2 (weak)	229E, HKU1, NL63, OC43, SARS-CoV1			S; Unk	B-cells; SARS-CoV1 Human Patient	872	EVQLLESGPGLVKPSETLSLTCTVSGGSI NSQYWNWIRQSPGKGLEWIGYVYYSGS TNYNPSLKSRVTMSVDTSKNHFSLNLRS VTAADTAVYYCARGLVVRYFDGFPSGPII GAFDIWNQGTTVTVSS	1939	ETTLTQSPATLSLSPGERATLSCRASQS VSSYLAWYQQKPGQAPRLLIYDAFNR ATGVPARFSGSGSGTDFTLTISSLEPED FAVYYCQQRTSTLTFGGGTKVDIK	IGHV4-59 (Human)	IGHJ3 (Human)	IGKV3-11 (Human)	IGKJ4 (Human)	2978	ARGLVVRYFD GFPSGPIIGAF DI	4168	QQRTSTLT	Anna Wec et al., 2020 (https://science.sciencemag.org/content/early/2020/06/15/science.abc7424)
mAb-189	Ab	SARS-CoV2 (weak)	229E, HKU1, NL63, OC43, SARS-CoV1			S; Unk	B-cells; SARS-CoV1 Human Patient	873	QVQLVQSGAEVKKPGSSVKVSCKVSGG TFSSHAISWVRQAPGQRPEWMGGIMP IFGESKDTQKFQGRVTFTVDESTNTAYM ELTSLKSEDTAIYYCVRDPDPYTATVRHN HYWHGMDVWGQGTTVTVSS	1940	ETTLTQSPLSLPVTLGQAASISCRSSQA VVHSDGNTYLNWFQQRPGQPPRRLIY KVSNRDSGVPDRFSGSGSGTVFTLKIS RVEAEDIGVYYCMQGTEWPRTFGQG TKVEIK	IGHV1-69 (Human)	IGHJ6 (Human)	IGKV2-30 (Human)	IGKJ1 (Human)	2979	VRDPDPYTAT VRHNHYWH GMDV	4169	MQGTEW PRT	Anna Wec et al., 2020 (https://science.sciencemag.org/content/early/2020/06/15/science.abc7424)
mAb-19	Ab	OC43, SARS-CoV1, SARS-CoV2	229E, HKU1, NL63			S; Unk	B-cells; SARS-CoV1 Human Patient	874	QVQLQQWGAGLLKPSETLSLTCAVYGG SFSGFHWSWIRQPPGKGLEWIGEVNHS GSTKYNPSLKSRVTVSVDTSKNQFSLRLS SVTAADTAIYYCARGSLSREYDFLTAPQN GPWFDSWGQGALVTVSS	1941	QSVLTQPPSVSAAPGQKVTISCSGSSS NLGNNYVSWYQQLPGTAPKLLIYDNH KRPSGIPDRFSGSKSGTSATLGITGLQT GDEADYYCETWDSSLSVVVFGGGTKV TVL	IGHV4-34 (Human)	IGHJ5 (Human)	IGLV1-51 (Human)	IGLJ3 (Human)	2980	ARGSLSREYD FLTAPQNGP WFDS	4170	ETWDSSLS VVV	Anna Wec et al., 2020 (https://science.sciencemag.org/content/early/2020/06/15/science.abc7424)
mAb-190	Ab	SARS-CoV2 (weak)	229E, HKU1, NL63, OC43, SARS-CoV1			S; Unk	B-cells; SARS-CoV1 Human Patient	875	EVQLLESGPGLVKPSETLSLTCAVYGG SFSGFHWSWIRQPPGKGLEWIGEVNHS STYYNPSLKSRVIIPVDTSKDQFSLRLSSV TAADTAVYYCARHSQKDIVLIPAAQSPIF DYWGQGTLVTVSS	1942	QSVLTQPPSVSAAPGQKVTISCSGSSS NIGNNYVSWYQQLPGTAPKLLIYDNN KRPSGIPDRFSGSKSGTSATLGITGLQT GDEADYYCGTWDSRLSAVVFGGGTKL TVL	IGHV4-39 (Human)	IGHJ4 (Human)	IGLV1-51 (Human)	IGLJ3 (Human)	2981	ARHSQKDIVLI PAAQSPIFDY	4171	GTWDSRLS AVV	Anna Wec et al., 2020 (https://science.sciencemag.org/content/early/2020/06/15/science.abc7424)
mAb-191	Ab	SARS-CoV2 (weak)	229E, HKU1, NL63, OC43, SARS-CoV1			S; Unk	B-cells; SARS-CoV1 Human Patient	876	EVQLVESGGGLVQPGGSLRLSCASGFT FSRYAMHWVRQAPGKGLEYVSAINLNG DSTYYTDSVRGRFTISRDNSKNTLFLQMS NVRPEDTAFYYCVKDGGYYDSSGPGHW GQGTLVTVSS	1943	DIRVTQSPATLSLSPGERATLSCRASEN IAHYLAWYQQKPGQAPRLVIYDASSR ATGIPGRFSGSGAGTDFTLTINSLEPED FAVYYCQQRSNWPQNFGGGTKVDIK	IGHV3-64D (Human)	IGHJ1 (Human)	IGKV3-11 (Human)	IGKJ3 (Human)	2982	VKDGGYYDSS GPGH	4172	QQRSNWP QN	Anna Wec et al., 2020 (https://science.sciencemag.org/content/early/2020/06/15/science.abc7424)
mAb-192	Ab	SARS-CoV2 (weak)	229E, HKU1, NL63, OC43, SARS-CoV1			S; Unk	B-cells; SARS-CoV1 Human Patient	877	QVQLVQSGGGVVQPGGSLRLSCADSG NAFIANPMHWVRQAPGKGLEWLALIST DGNNRHYADSVKGRFTFSRDNSKNSLYL QMDSLRPEDTGVYYCARESRSSGRAGC FDSWGQGTLVTVSS	1944	DIRLTQSPSSLSASVGDRVTITCRASQD ISSWLAWYQQKSGKAPKSLIYAASSLQ NGVPSRFSGSRSGTDFTLTISSLQPEDL GTYYCQQQYDSYPVTFGQGTRLEIK	IGHV3-30 (Human)	IGHJ5 (Human)	IGKV1D-16 (Human)	IGKJ5 (Human)	2983	ARESRSSGRA GCFDS	4173	QQYDSYPV T	Anna Wec et al., 2020 (https://science.sciencemag.org/content/early/2020/06/15/science.abc7424)
mAb-193	Ab	SARS-CoV2 (weak)	229E, HKU1, NL63, OC43, SARS-CoV1			S; Unk	B-cells; SARS-CoV1 Human Patient	878	QVQLVESGGGVVQPGTSLRLSCAATGF TFTTYPMHWVRQAPGKGLEWVAVISY DGMNQYYADFLKGRFTISRDNSKNTLYL QMNSLRADDTAVYYCARAYGGNYQNH FDHWGQGTLVTVSS	1945	DIVLTQTPDSLAVSLGERATINCKSSQS VLYSSNNKNYLAWYQQKPGQPPKLLI YWASTRESGVPDRFSGSGSGTDFTLTI SSLQAEDVAVYYCQQYYTMWTFGQG TKVEIK	IGHV3-30 (Human)	IGHJ4 (Human)	IGKV4-1 (Human)	IGKJ1 (Human)	2984	ARAYGGNYQ NHFDH	4174	QQYYTMW T	Anna Wec et al., 2020 (https://science.sciencemag.org/content/early/2020/06/15/science.abc7424)
mAb-194	Ab	SARS-CoV2 (weak)	229E, HKU1, NL63, OC43, SARS-CoV1			S; Unk	B-cells; SARS-CoV1 Human Patient	879	EVQLVQWGAGLLKPSETLSLRCAVYGGS FNGFYWTWIRQAPGQGLEWIAEINHSG TTNYNPSLKSRVTISIDTSKKQFSLSLKSVT AADTAMYFCARGTISPIVGVPTPVVPRR GRSWFDPWGQGTLVTVSS	1946	QSVLTQPPSVSAAPGQKVTISCSGSSS NIGNDYVSWYQQLPGTAPKLLIYENYK RPSGIPDRFSGSKSGTSATLDITGLQTG DEADYYCGTWDSSLSVDNYVFGTGTK LTVL	IGHV4-34 (Human)	IGHJ5 (Human)	IGLV1-51 (Human)	IGLJ1 (Human)	2985	ARGTISPIVGV PTPVVPRRGR SWFDP	4175	GTWDSSLS VDNYV	Anna Wec et al., 2020 (https://science.sciencemag.org/content/early/2020/06/15/science.abc7424)
mAb-195	Ab	SARS-CoV2 (weak)	229E, HKU1, NL63, OC43, SARS-CoV1			S; Unk	B-cells; SARS-CoV1 Human Patient	880	QVQLVQSGAEVKKPGSSVKVSCKASGG TFSTHAISWVRQAPGHGPEWLGGIIPLF GTSESAQRFQARVKITADESTSTAYMELS SLTSEDTAVYYCVRDSDPYTATSRNNHY WYAMDVWGQGTTVTVSS	1947	DIVLTQSPLSLPVTLGQPASISCRSSQS VVHSDGNTYLNWFHQRPGQSPRRLIY KVSNRDSGVPDRFSGSGSGTDFTLKIS RVEAEDIGVYYCMQGTDWPRTFGQG TKVDIK	IGHV1-69 (Human)	IGHJ6 (Human)	IGKV2-30 (Human)	IGKJ3 (Human)	2986	VRDSDPYTAT SRNNHYWYA MDV	4176	MQGTDW PRT	Anna Wec et al., 2020 (https://science.sciencemag.org/content/early/2020/06/15/science.abc7424)

mAb-196	Ab	SARS-CoV2 (weak)	229E, HKU1, NL63, OC43, SARS-CoV1			S; Unk	B-cells; SARS-CoV1 Human Patient	881	QVQLVQSGAEVREPGSSVKLSCKTSGGP FSTHAFSWVRQAPGQRPEWMGGIMP VFGESKDTQKFKGRVTFTADASTTTTYM ELRSLKSDDTAIYYCVRDSDPYTATSSHN HYWYAMDVWGQGTTVTVSS	1948	ETTLTQSPLSLPVTLGQPASISCRSSQV LVHSDGNTYLNWFQQRPGQSPRRLIY KVSNRDSGVPDRFSGSGSGIDFTLKISR VEAEDIGVYYCMQGTEWPRTFGQGT KVDIK	IGHV1-69 (Human)	IGHJ6 (Human)	IGKV2-30 (Human)	IGKJ3 (Human)	2987	VRDSDPYTAT SSHNHYWYA MDV	4177	MQGTEW PRT	Anna Wec et al., 2020 (https://science.sciencemag.org/content/early/2020/06/15/science.abc7424)
mAb-197	Ab	SARS-CoV2 (weak)	229E, HKU1, NL63, OC43, SARS-CoV1			S; Unk	B-cells; SARS-CoV1 Human Patient	882	QVQLVESGGGLVKPGGSLRLSCAASGFT FSDYYMIWIRQAPGKGLEWLSYISHTAS TIYYADSVKGRFTISRDNAKNSLFLQMNS LTAEDTAVYYCARDRGSGVIDPWGQGT LVTVSS	1949	DIQLTQSPSSLSASVGDRVTITCRASQS ISHYLNWYQQKPGKAPKLLIYAASNLQ SGVPSRFSGNGSGTDFTLTISSLQPEDF ATYFCQQSYSTPLTFGGGTKVDIK	IGHV3-11 (Human)	IGHJ5 (Human)	IGKV1-39 (Human)	IGKJ4 (Human)	2988	ARDRGSGVID P	4178	QQSYSTPL T	Anna Wec et al., 2020 (https://science.sciencemag.org/content/early/2020/06/15/science.abc7424)
mAb-2	Ab	SARS-CoV1, SARS-CoV2	229E, HKU1, NL63, OC43			S; Unk	B-cells; SARS-CoV1 Human Patient	883	QVQLVESGGGLVQPGGSLRLSCSASGFT FSRFAMHWVRQAPGKGLEYVSAINLNG DSTYYTDSVRGRFTISRDNSKNTLYLQMS SVRPDDTAFYYCVKDGGYYDSSGPGHW GQGTLVTVSS	1950	EIVLTQSPATLSLSPGERATLSCRASENI AHYLAWYQQKPGQAPRLVIYDASSRA TGIPGRFSGSGAGTDFTLTINSLEPEDF AVYYCQQRSNWPQNFGGGTKVEIK	IGHV3-64D (Human)	IGHJ1 (Human)	IGKV3-11 (Human)	IGKJ4 (Human)	2989	VKDGGYYDSS GPGH	4179	QQRSNWP QN	Anna Wec et al., 2020 (https://science.sciencemag.org/content/early/2020/06/15/science.abc7424)
mAb-20	Ab	OC43, SARS-CoV1, SARS-CoV2	229E, HKU1, NL63			S; Unk	B-cells; SARS-CoV1 Human Patient	884	EVQLVESGPGLVKPSETLSLTCTVSGASV TAGSSYWGWIRQPPGKGLEWIGYMFSS GNTKYNPSLKSRVTISADTSKNQFSLRLS SVTAADTAVYFCARVGWVRYFDWSKPY YYFDLWGRGTLVTVSS	1951	QSVLTQPPSVSGAPGQRVTISCTGSSS NIGAGYYVHWYQQLPGTAPKLLIYDN NNRPSGVPDRFSGSRSGTSASLAITGL QAEDEGDYFCQSYDSSLSASFGGGTK VTVL	IGHV4-59 (Human)	IGHJ2 (Human)	IGLV1-40 (Human)	IGLJ6 (Human)	2990	ARVGWVRYF DWSKPYYYFD L	4180	QSYDSSLS AS	Anna Wec et al., 2020 (https://science.sciencemag.org/content/early/2020/06/15/science.abc7424)
mAb-21	Ab	SARS-CoV1, SARS-CoV2	229E, HKU1, NL63, OC43			S; Unk	B-cells; SARS-CoV1 Human Patient	885	EVQLVESGGGLVQPGGSLRLSCAASGFT FSTSAMSWVRQAPGKGLEWVSRIGGG GGRTKYADSVKGRFTISRDNSKNTLYLQ MNSLRADDTAVYYCAKCDLVRYFDWLG EENNWFDPWGQGTLVTVSS	1952	QSVLTQPPSVSGAPGQRVTISCTGSNS NIGAGYDVHWYQQLPETAPKLLIYAN GNRPSGVPDRFSGSKSGTSASLAITGL QAEDEADYYCQSYDSSLSGVLFGGGT KLTVL	IGHV3-23 (Human)	IGHJ5 (Human)	IGLV1-40 (Human)	IGLJ3 (Human)	2991	AKCDLVRYFD WLGEENNWF DP	4181	QSYDSSLS GVL	Anna Wec et al., 2020 (https://science.sciencemag.org/content/early/2020/06/15/science.abc7424)
mAb-22	Ab	SARS-CoV1, SARS-CoV2	229E, HKU1, NL63, OC43			S; Unk	B-cells; SARS-CoV1 Human Patient	886	QVQLVQSGAEVRKPGSSVKLSCKASGG TFSTHAISWVRQAPGQRPEWMGGIMP IFGESKDTQKFQGRVTFTADESTTTAYM ELRSLKSDDTAIYYCVRDSDPYTATVRNN HYWYALDVWGPGTMVTVSS	1953	DIQLTQSPLSLPVTLGQPASISCRSSQH LVHSDGNTYLNWFQQRPGQSPRRLIY KVSNRDSGVPDRFSGSGSGIDFTLKISR VEAEDIGVYYCMQGTEWPRTFGQGT KVEIK	IGHV1-69 (Human)	IGHJ3 (Human)	IGKV2-30 (Human)	IGKJ1 (Human)	2992	VRDSDPYTAT VRNNHYWYA LDV	4182	MQGTEW PRT	Anna Wec et al., 2020 (https://science.sciencemag.org/content/early/2020/06/15/science.abc7424)
mAb-23	Ab	SARS-CoV1, SARS-CoV2	229E, HKU1, NL63, OC43			S; Unk	B-cells; SARS-CoV1 Human Patient	887	EVQLVESGGGLSQPGGSLRLSCAASGFT VRTYCMNWVRQAPGKGLEWVSLVCG DNIDYYPDSVKGRFSISRDDSKNTLLLH MDSLRVEDTAVYYCARATPPGGGTGW PYFDFWGQGTLVTVSS	1954	DIQVTQSPATVSVSPGEGASLSCRASQ SVRSNLAWFQQKPGQAPRLLISDAST RASGVPARFTGSGFGTEFTLTISSLQSE DFAIYYCQQYNTWPPLTFGGGTKVEIK	IGHV3-66 (Human)	IGHJ4 (Human)	IGKV3-15 (Human)	IGKJ4 (Human)	2993	ARATPPGGG TGWPYFDF	4183	QQYNTWP PLT	Anna Wec et al., 2020 (https://science.sciencemag.org/content/early/2020/06/15/science.abc7424)
mAb-24	Ab	SARS-CoV1 (weak), SARS-CoV2	229E, HKU1, NL63, OC43			S; Unk	B-cells; SARS-CoV1 Human Patient	888	QVQLVQSGAEMRKPGSSVKVSCKASGG TFSRYCFSWVRQAPGQRLEWMGGIMS ILGAHYAQKFQGRVTFTADESTNTAYME LISLTSEDTAVYYCAREEPSGTYHNYYGL DVWGQGTTVTVSS	1955	DIRLTQSPLSLPVTLGQPASISCRSSQSL VHSNGNTYLNWFQQRPGQSPRRLIYE VSNRDSGVPDRFTGSGSGTDFTLKISR VEAEDVGVYYCMQGTHWPRSFGGG TKVEIK	IGHV1-69 (Human)	IGHJ6 (Human)	IGKV2-30 (Human)	IGKJ4 (Human)	2994	AREEPSGTYH NYYGLDV	4184	MQGTHW PRS	Anna Wec et al., 2020 (https://science.sciencemag.org/content/early/2020/06/15/science.abc7424)
mAb-25	Ab	SARS-CoV1, SARS-CoV2	229E, HKU1, NL63, OC43			S; Unk	B-cells; SARS-CoV1 Human Patient	889	QVQLQESGPGLVKPSGTLSLTCAVSGGS ISSSDWCSWVRQPPGKGPEWIAEISHS GSTNYNPSLKSRVTMSVDRSKNQFSLNL NSVTAADTAVYYCAARIRGATHYDFWS GFWAGPFDIWGQGTTVTVSS	1956	ETTLTQSPGTLSLSPGERATLSCRASQSI GSSYLAWYQQKPGQAPRLLIYGASSR ATGIPDRFSGSGSGTDFTLTISRLEPED FAVYYCQQYGSAPLYTFGQGTKVEIK	IGHV4-4 (Human)	IGHJ3 (Human)	IGKV3-20 (Human)	IGKJ1 (Human)	2995	AARIRGATHY DFWSGFWA GPFDI	4185	QQYGSAPL YT	Anna Wec et al., 2020 (https://science.sciencemag.org/content/early/2020/06/15/science.abc7424)
mAb-26	Ab	SARS-CoV1, SARS-CoV2	229E, HKU1, NL63, OC43			S; Unk	B-cells; SARS-CoV1 Human Patient	890	EVQLQESGPGLVKPSGTLSLTCGVSGVSI SSSSWWSWVRQPPGRGLEWIGEISPSG STSYNPSFRSRLTMSVDKSRNQLSLKLSS VTAADTAVYYCARTQSNDFWSGYYTAA FDLWGQGTMVTVSS	1957	EIVLTQSPGTLSLSPGERASLSCRASQS VSSSYLAWYQHRPGQAPRLLIYDASSR ATGIPDRFSGSGSGTDFTLTISRLESED FAVYYCQQYGNSPRTFGQGTKVDIK	IGHV4-4 (Human)	IGHJ3 (Human)	IGKV3-20 (Human)	IGKJ3 (Human)	2996	ARTQSNDFW SGYYTAAFDL	4186	QQYGNSP RT	Anna Wec et al., 2020 (https://science.sciencemag.org/content/early/2020/06/15/science.abc7424)
mAb-27	Ab	SARS-CoV1, SARS-CoV2	229E, HKU1, NL63, OC43			S; Unk	B-cells; SARS-CoV1 Human Patient	891	QVQLVQWGAGLLKPSETLSLTCAVYGG SFSGFHWSWIRQPPGKGLEWIGEINHS GSTKYNPSLKSRVTISVDTSKNQFSLRLRS VTAADTAIYYCARGSLSREYDFLTAPQN GPWFDSWGQGALVTVSS	1958	QPVLTQPPSVSAAPGQKVTISCSGSSS NIGDNYVSWYQQLPGTAPKLLIYDNN KRPSGIPDRFSGSKSGTSATLGITGLQT GDEADYYCETWDTSLSVVVFGGGTKL TVL	IGHV4-34 (Human)	IGHJ5 (Human)	IGLV1-51 (Human)	IGLJ3 (Human)	2997	ARGSLSREYD FLTAPQNGP WFDS	4187	ETWDTSLS VVV	Anna Wec et al., 2020 (https://science.sciencemag.org/content/early/2020/06/15/science.abc7424)
mAb-28	Ab	SARS-CoV1, SARS-CoV2	229E, HKU1, NL63, OC43			S; Unk	B-cells; SARS-CoV1 Human Patient	892	EVQLVESGPELKKPGSSVRVSCKASGGS FSNFAVSWVRQAPGQRLEWMGGVIPR FGRSEYVQKFQGRVTITVDEAASTAYME LSSLRSEDTAIYYCVLDTTSANPHNWYG MDVWGQGTTVTVSS	1959	DIVMTQTPLSLAVTLGQPASISCRSSH GLVHTNGNTYLNWFHQRPGQPPRRL IYKISNRDSGVPDRFSGSGSGTDFTLKI SRVEADDVGVYYCMQGTDWPRTFG QGTKVEIK	IGHV1-69 (Human)	IGHJ6 (Human)	IGKV2-30 (Human)	IGKJ1 (Human)	2998	VLDTTSANPH NWYGMDV	4188	MQGTDW PRT	Anna Wec et al., 2020 (https://science.sciencemag.org/content/early/2020/06/15/science.abc7424)
mAb-29	Ab	SARS-CoV1, SARS-CoV2	229E, HKU1, NL63, OC43			S; Unk	B-cells; SARS-CoV1 Human Patient	893	QVQLVQSGGGVVNPGGSLRLSCVGSGF TFSDYYMGWIRQAPGKGLEVISYISSTGS YIRDADSVKGRFTISRDNAENSVYLQMN SLRGEDTAVYYCARMGPYGSGSFDYWG LGTLVTVSS	1960	EIVLTQSPGTLSLSPGERATLSCRASQT VTRSQLAWYQHKPGQPPRLLIYDSSKR ATGSPDRFSASGSGTDFTLTISGLEPED TGIYYCLQYSDATTFGPGTKLEIK	IGHV3-11 (Human)	IGHJ4 (Human)	IGKV3-20 (Human)	IGKJ2 (Human)	2999	ARMGPYGSG SFDY	4189	LQYSDATT	Anna Wec et al., 2020 (https://science.sciencemag.org/content/early/2020/06/15/science.abc7424)
mAb-3	Ab	SARS-CoV1, SARS-CoV2	229E, HKU1, NL63, OC43			S; Unk	B-cells; SARS-CoV1 Human Patient	894	QVQLQESGPGLVRPSETLSLTCTVSGDS VSSSDYHWGWIRQPPGKGLEWIGSIYY GGRSHFNPSLKSRVAIFVDTSNNQFSLRL NSVTASDTAVYFCAGRHQELLPMGSFD MWAQGTTVTVSS	1961	EIVMTQSPSSLSASIGDRVTISCRASQN IGSYLNWYQQRPGKAPNLLIFVASSLQ SGVPSRFSGSGSGTDFTLTISSLQAEDF ATYYCQQSYTTPITFGQGTRLEIK	IGHV4-38-2 (Human)	IGHJ4 (Human)	IGKV1-39 (Human)	IGKJ5 (Human)	3000	AGRHQELLP MGSFDM	4190	QQSYTTPIT	Anna Wec et al., 2020 (https://science.sciencemag.org/content/early/2020/06/15/science.abc7424)

mAb-30	Ab	SARS-CoV2	229E, HKU1, NL63, OC43, SARS-CoV1			S; Unk	B-cells; SARS-CoV1 Human Patient	895	PGPACTVWAEVKKPGSSVKVSCKASGG MFSDYAISWVRQAPGQRLEWMGGIM PGLGSPGYAQIFRGRATISADVSTSTAYL ELTSLKPEDTAVYYCARDPSILNTGNHH WYDLDIWGQGTQVTVSS	1962	DIVMTQSPLSLPVGLGQSASISCRSSQ RVVHTDGNTYLNWFHQRPGQSPRRLI YKVSNRDSGVPDRFSGSGSGTDFTLRI SRVEAEDVGVYYCMQATEWPRTFGQ GTKVEIK	IGHV1-69 (Human)	IGHJ3 (Human)	IGKV2-30 (Human)	IGKJ1 (Human)	3001	ARDPSILNTG NHHWYDLDI	4191	MQATEWP RT	Anna Wec et al., 2020 (https://science.sciencemag.org/content/early/2020/06/15/science.abc7424)
mAb-31	Ab	SARS-CoV2	229E, HKU1, NL63, OC43, SARS-CoV1			S; Unk	B-cells; SARS-CoV1 Human Patient	896	QVQLVQSGAEVKKPGSSVKVSCKASGG TSSTHAISWVRQAPGQGLEWMGGIIPIF GTTNYAQKFQDRVTITADESTSTAYMEL SSLRSEDTAVYFCVRDGAYDSSGYYSTQ WGQGTLVTVSS	1963	EIVLTQSPATLSLSPGERATLSCRASQS VSNFLAWYQQKPGQPPRLLIYDASNR ASGIAARFSGRGSGTDFTLTISSLEPED FAVYYCQQRRNWPPMYTFGQGTKLEI K	IGHV1-69 (Human)	IGHJ4 (Human)	IGKV3-11 (Human)	IGKJ2 (Human)	3002	VRDGAYDSS GYYSTQ	4192	QQRRNWP PMYT	Anna Wec et al., 2020 (https://science.sciencemag.org/content/early/2020/06/15/science.abc7424)
mAb-32	Ab	SARS-CoV1, SARS-CoV2	229E, HKU1, NL63, OC43			S; Unk	B-cells; SARS-CoV1 Human Patient	897	EVQLVQSGAEVKKPGSSVKVSCKVSGG RFSDYAISWLRQAPVKGLEWMGGIIPRL NRKGYSQDFQGRLTFTADESTSTAYMEL SGLTSEDTAVYYCARDPTFLNSGNHFWY AVDIWGQGTTVTVSS	1964	EIVLTQSPLSLSVTLGQAASISCTCSQTA VHSDGNTYLNWFHQRPGQSPRRLIYK VSNRDSGVPDRFSGSGSGTDFTLKISR VEAEDVGIYYCMQTTDWPRTFGQGT KLEIK	IGHV1-69 (Human)	IGHJ6 (Human)	IGKV2-30 (Human)	IGKJ2 (Human)	3003	ARDPTFLNSG NHFWYAVDI	4193	MQTTDWP RT	Anna Wec et al., 2020 (https://science.sciencemag.org/content/early/2020/06/15/science.abc7424)
mAb-33	Ab	SARS-CoV1, SARS-CoV2	229E, HKU1, NL63, OC43			S; Unk	B-cells; SARS-CoV1 Human Patient	898	QVQLVQSGAEVKKPGSSVTVSCKVSGG RFSDYAISWLRQAPVEGLEWMGGIIPHL NKKGYSQKFQDRITFTADESTSTAYMEL SGLTSEDTAIYYCARDPTFLNTGNHFWY AVDIWGQGTTVTVSS	1965	ETTLTQSPLSLSVTLGQAASISCTCSQS AVHSDGNTYFNWFHQRPGQSPRRLIY KVSNRDSGVPERFSGSGSGTHFTLIISR VEAEDVGVYYCMQTTDWPRTFGQGT KVDIK	IGHV1-69 (Human)	IGHJ6 (Human)	IGKV2-30 (Human)	IGKJ3 (Human)	3004	ARDPTFLNTG NHFWYAVDI	4194	MQTTDWP RT	Anna Wec et al., 2020 (https://science.sciencemag.org/content/early/2020/06/15/science.abc7424)
mAb-34	Ab	SARS-CoV1, SARS-CoV2	229E, HKU1, NL63, OC43			S; Unk	B-cells; SARS-CoV1 Human Patient	899	QVQLVQSGAEVKKPGASVKVSCKASGY TFSLFHVHWVRQAPGQGLEWMGWIN PHNGDTTFAERFQGRVALTRDTSINTAY MELSRLTSDDTAVYFCARDFGVRYDDSR QLMKYCDSWGQGTLVTVSS	1966	NFMLTQPHSVSESPGKAVIISCTRSSG NIASNFVQWYQQRPGSSPTPVIYEDKL RPSGVPDRFSGSIDRSSNSASLTISGLK TEDEADYYCQSYDSGNLVVFGGGTKL TVL	IGHV1-2 (Human)	IGHJ5 (Human)	IGLV6-57 (Human)	IGLJ3 (Human)	3005	ARDFGVRYD DSRQLMKYC DS	4195	QSYDSGNL VV	Anna Wec et al., 2020 (https://science.sciencemag.org/content/early/2020/06/15/science.abc7424)
mAb-35	Ab	SARS-CoV1, SARS-CoV2	229E, HKU1, NL63, OC43			S; Unk	B-cells; SARS-CoV1 Human Patient	900	QVQLVQSGAEVKKPGSSVKVSCKASGG TLADYAISWVRQAPGQGLEWMGGIKP LHGAAGYSQLFRGRLSITADESASTAYM ELTGLTSDDTAMYYCARDPSILNTGNHH WYDLDLWGQGTTVTVSS	1967	DIQMTQSPLSLPVTLGQAASISCRSSQ PIPHTDGNTYLNWFHQRPGQSPRRLI HKVSNRDSGVPDRFSGSGSGLDFTLEI SGVEAEDVGIYYCMQGTEWPRTFGQ GTKVEIK	IGHV1-69 (Human)	IGHJ6 (Human)	IGKV2-30 (Human)	IGKJ1 (Human)	3006	ARDPSILNTG NHHWYDLDL	4196	MQGTEW PRT	Anna Wec et al., 2020 (https://science.sciencemag.org/content/early/2020/06/15/science.abc7424)
mAb-36	Ab	SARS-CoV1, SARS-CoV2	229E, HKU1, NL63, OC43			S; Unk	B-cells; SARS-CoV1 Human Patient	901	QVQLVQSGPELKKPGSSVRVSCKASGGS ISSYAISWVRQAPGQRLEWMGGVLPM MGRESPVQKFKDRVTIAADESTSTAYM ELRSLSAEDTAVYYCVVDTTMADPHNW YGLDVWGQGTTVTVSS	1968	EIVMTQTPLSLPVTLGQPASISCRSSHG LVHTNGNTYLNWFHQRPGQPPRRLIY QVSHRDSGVPDRFSGSGSGTDFTLKIS RVEADDVGVYYCMQGTDWPRTFGQ GTKVDIK	IGHV1-69 (Human)	IGHJ6 (Human)	IGKV2-30 (Human)	IGKJ3 (Human)	3007	VVDTTMADP HNWYGLDV	4197	MQGTDW PRT	Anna Wec et al., 2020 (https://science.sciencemag.org/content/early/2020/06/15/science.abc7424)
mAb-37	Ab	SARS-CoV1, SARS-CoV2	229E, HKU1, NL63, OC43			S; Unk	B-cells; SARS-CoV1 Human Patient	902	QVQLVQSGPGLVRPSGTLSLTCAVSGDS ISGDYWCTWVRQTPGKGLEWIGKISHS GSINYNPSLKSRITMSVDKSKNQFSLKLN SVTAADTAMYYCARVRVGASHHNFWS GYYTDAFDIWGQGTTVTVSS	1969	ETTLTQSPGTLSLSPGERATLSCRASQS VGNNYLAWYQQKPGQAPRLLIYGASS RATGIPDRFSGSGSGTDFTLTISRLEPE DFAVYYCQQYGTSPVYTFGQGTKVEIK	IGHV4-4 (Human)	IGHJ3 (Human)	IGKV3-20 (Human)	IGKJ1 (Human)	3008	ARVRVGASH HNFWSGYYT DAFDI	4198	QQYGTSPV YT	Anna Wec et al., 2020 (https://science.sciencemag.org/content/early/2020/06/15/science.abc7424)
mAb-38	Ab	SARS-CoV1, SARS-CoV2	229E, HKU1, NL63, OC43			S; Unk	B-cells; SARS-CoV1 Human Patient	903	QVQLVQSGAEVKKPGSSVKVSCKVSGG TFSNYAISWLRQAPGQGPEWMGGIIPA LSRVGYARKFQARLTISADELTTTAYMDL SSLTSEDTAVYYCARDPSFLNTGNHFWY DFDMWGQGTTVTVSS	1970	DIQLTQSPLSLPVTLGQPASISCTSSQN VVHTDGNTYLNWFHQRPGQSPRRLIY KVSNRDSGVPDRFSGSGSGHFTLKIS RVEAEDVGIYYCMQGTDWPRTFGQG TKVEIK	IGHV1-69 (Human)	IGHJ4 (Human)	IGKV2-30 (Human)	IGKJ1 (Human)	3009	ARDPSFLNTG NHFWYDFD M	4199	MQGTDW PRT	Anna Wec et al., 2020 (https://science.sciencemag.org/content/early/2020/06/15/science.abc7424)
mAb-39	Ab	SARS-CoV2	229E, HKU1, NL63, OC43, SARS-CoV1			S; Unk	B-cells; SARS-CoV1 Human Patient	904	EVQLQQSGAEVKKPGSSVKVSCKASGG TSSTHAISWVRQAPGQGLEWMGGIIPIF GTTNYAQKFQDRVTITADESTSTAYMEL SSLRSEDTAVYFCVRDGAYDSSGYYSTQ WGQGTLVTVSS	1971	DIVLTQTPATLSLSPGERATLSCRASQS VSNFLAWYQQKPGQPPRLLIYDASNR ASGIAARFSGRGSGTDFTLTISSLEPED FAVYYCQQRRNWPPMYTFGQGTKVE IK	IGHV1-69 (Human)	IGHJ4 (Human)	IGKV3-11 (Human)	IGKJ1 (Human)	3010	VRDGAYDSS GYYSTQ	4200	QQRRNWP PMYT	Anna Wec et al., 2020 (https://science.sciencemag.org/content/early/2020/06/15/science.abc7424)
mAb-4	Ab	SARS-CoV1, SARS-CoV2	229E, HKU1, NL63, OC43			S; Unk	B-cells; SARS-CoV1 Human Patient	905	EVQLVESGGGLVKPGGSLRLSCAASGFT FSDYYMNWVRQAPGKGLEWVSSISSSS YMYYADSMKGRFTISRDNAQNSLYLQM SSLRAEDTAVYYCARDFPGDTAVAGTGF NYWGQGTLVTVSS	1972	QSVLTQPPSVSGAPGQRVTISCTGSSS NIGAGYDVHWYQQVPGTAPKLLIYGN SNRPSGVPDRFSGSKSGTSASLAITGL QAEDEADYYCQSYDSSLSVLYVFGTGT KVTVL	IGHV3-21 (Human)	IGHJ4 (Human)	IGLV1-40 (Human)	IGLJ1 (Human)	3011	ARDFPGDTA VAGTGFNY	4201	QSYDSSLS VLYV	Anna Wec et al., 2020 (https://science.sciencemag.org/content/early/2020/06/15/science.abc7424)
mAb-40	Ab	SARS-CoV2	229E, HKU1, NL63, OC43, SARS-CoV1			S; Unk	B-cells; SARS-CoV1 Human Patient	906	QVQLVESGGDLVKPGRSLRLSCTASGFTI GDYAMTWFRQAPGKGLECVAVIRSRAF GGTTEYAASVKGRFIVSRDDSNSVAFLQ MNSLKTEDTAVYYCSRDLRRGYYDSNG HQQFDLWGQGTLVTVSS	1973	DIRLTQSPATLSLSPGERATLSCRASQSI GYYLAWFQQKPGQAPRLLIYDASKRA TGIPARFSGSGSGTDFTLTISSLEPEDFA VYYCQHRTNWPYTFGQGTKVEIK	IGHV3-49 (Human)	IGHJ4 (Human)	IGKV3-11 (Human)	IGKJ1 (Human)	3012	SRDLRRGYYD SNGHQQFDL	4202	QHRTNWP YT	Anna Wec et al., 2020 (https://science.sciencemag.org/content/early/2020/06/15/science.abc7424)
mAb-41	Ab	SARS-CoV2	229E, HKU1, NL63, OC43, SARS-CoV1			S; Unk	B-cells; SARS-CoV1 Human Patient	907	QVQLVESGGGVVQPGRSLRLSCAASGF TFSRYGMHWVRQAPGKGLEWVAVIYS DGRNEYYADSVKGRFTISRDNSKNTLHL QMNSLGAADTAVYYCARDPGPITFFDW SPDKSRKSYYDYNGMDVWGQGTTVTV SS	1974	QPGLTQEPSLTVSPGGTVTLTCGSSAG AVTSGHYPYWFQQKPGQAPRTLIYDT NNKYSWTPARFSGSLLGGKAALTLSG AQPEDEAEYFCFLSYRGAPPVFGGGT HLTVL	IGHV3-30 (Human)	IGHJ6 (Human)	IGLV7-46 (Human)	IGLJ3 (Human)	3013	ARDPGPITFF DWSPDKSRK SYYDYNGMD V	4203	FLSYRGAP PV	Anna Wec et al., 2020 (https://science.sciencemag.org/content/early/2020/06/15/science.abc7424)

mAb-42	Ab	SARS-CoV2	229E, HKU1, NL63, OC43, SARS-CoV1			S; Unk	B-cells; SARS-CoV1 Human Patient	908	EVQLLESGGGVVQPGTSLRLSCVASGFTFSTFAMHWVRQAPGKGLEWVALISFDSTNIRYANSVRGRFTISRDNSKNTLYLEVDSLRIEDTGVYYCARDLPPLDYWGQGTLVTVSS	1975	DIRMTQSPFSLSASVGDRVTITCRASQGFGNRLAWYQQKPGRAPKLLIYDASTLQSGVPSRFSGSGSETDFALTISSLQPEDVATYYCQKHDRDPWTFGQGTKVEIK	IGHV3-30 (Human)	IGHJ4 (Human)	IGKV1-27 (Human)	IGKJ1 (Human)	3014	ARDLPPLDY	4204	QKHDRDPWT	Anna Wec et al., 2020 (https://science.sciencemag.org/content/early/2020/06/15/science.abc7424)
mAb-43	Ab	SARS-CoV1, SARS-CoV2	229E, HKU1, NL63, OC43			S; Unk	B-cells; SARS-CoV1 Human Patient	909	QVQLVQSGAEVRKPGSSVKLSCKASGGTFSTHAISWVRQAPGQRPEWMGGIIPIFGESKDTQKFQGRVTFTADESTTTAYMELRSLRSDDTAIYYCVRDSDPYTTTFSHNHYWYAMDVWGQGTTVTVSS	1976	DIVMTQSPLSLPVTLGQPASISCRSSQRLVHSDGNTYLNWFQQRPGQSPRRLIYKVSNRDSGVPDRFSGSGSGTDFTLKISRVEAEDIGVYYCMQGTEWPRTFGQGTKVEIK	IGHV1-69 (Human)	IGHJ6 (Human)	IGKV2-30 (Human)	IGKJ1 (Human)	3015	VRDSDPYTTTFSHNHYWYAMDV	4205	MQGTEWPRT	Anna Wec et al., 2020 (https://science.sciencemag.org/content/early/2020/06/15/science.abc7424)
mAb-44	Ab	SARS-CoV1, SARS-CoV2	229E, HKU1, NL63, OC43			S; Unk	B-cells; SARS-CoV1 Human Patient	910	QVQLVQSGGGLVQPGGSLRVSCSASGFTFSSFAMHWVRQAPGKGLEYVAGISDNGHTTMYADSVKGRFTISRDNSKNTLYLQLSSLRPEDTAVYFCVKDNVILPGAIVRPQFDYWGQGTLVTVSS	1977	ETTLTQSPASVSASVGDRVTISCRASQGIGRWLAWYQQKPGRAPKLLIFSASSLQSGVPSRFSGSGSGTDFTLTISSLQPEDFATYYCQQAESFPFTFGGGTKVEIK	IGHV3-64D (Human)	IGHJ4 (Human)	IGKV1-12 (Human)	IGKJ4 (Human)	3016	VKDNVILPGAIVRPQFDY	4206	QQAESFPFT	Anna Wec et al., 2020 (https://science.sciencemag.org/content/early/2020/06/15/science.abc7424)
mAb-45	Ab	SARS-CoV2	229E, HKU1, NL63, OC43, SARS-CoV1			S; Unk	B-cells; SARS-CoV1 Human Patient	911	QVQLVQSGAEVKKPGSSVKVSCKVSGGMFSDYAISWVRQAPGQRLEWMGGIMPGLGSPAYAQIFRGRVTISADISTSTAYLEVTSLRPEDTAVYYCARDPSILNTGNHHWYDLDMWGQGTTVTVSS	1978	ETTLTQSPLSLPVDLGQSASISCRSSQRVVHTNGNTYLHWFHQRPGQAPRRLIYKVSNRESGVPDRFSGSGSGTDFTLRISRVEAEDVGVYYCMQATDWPRTFGQGTKVEIK	IGHV1-69 (Human)	IGHJ6 (Human)	IGKV2-30 (Human)	IGKJ1 (Human)	3017	ARDPSILNTGNHHWYDLDM	4207	MQATDWPRT	Anna Wec et al., 2020 (https://science.sciencemag.org/content/early/2020/06/15/science.abc7424)
mAb-46	Ab	SARS-CoV1, SARS-CoV2	229E, HKU1, NL63, OC43			S; Unk	B-cells; SARS-CoV1 Human Patient	912	EVQLVESGGGVVQPGRSLRLSCVASGFTLAPYGMQWVRQAPGKGLEWVAFLSHDGSHLGYVDSVKGRFTISRDNSKNTLYLEMNSLRAEDTATYYCARDNVVQQNADNVGYFDFWGQGSLVTVSS	1979	CIRLTQSPATLSLSPGERATLSCRASQSVTSYLAWYQQRPGQAPRLLIYDTSNRVTGVPVRFSGSGYGTDFTLTISSLEPEDFAVYYCQQRGNGYTFGPGTKVEIK	IGHV3-30 (Human)	IGHJ4 (Human)	IGKV3-11 (Human)	IGKJ3 (Human)	3018	ARDNVVQQNADNVGYFDF	4208	QQRGNGYT	Anna Wec et al., 2020 (https://science.sciencemag.org/content/early/2020/06/15/science.abc7424)
mAb-47	Ab	SARS-CoV1, SARS-CoV2	229E, HKU1, NL63, OC43			S; Unk	B-cells; SARS-CoV1 Human Patient	913	QVQLVQSGAEVKKPGSSVKVSCKASGGMFRDYAISWLRQAPGQRLEWMGGIMPAFGAPGYAQIFRGRATISADVSTTTAYLELTSLMPDDTAVYYCARDPSILNTGNHHWYDLDLWGQGTTVTVSS	1980	ETTLTQSPLSLPVGLGQSASISCRSSQRVVHTDGNTYLNWFHQRPGQSPRRLIYKVSNRDSGVPDRFSGSGSGTDFTLRISRVEAEDVGVYYCMQATEWPRTFGQGTKVDIK	IGHV1-69 (Human)	IGHJ6 (Human)	IGKV2-30 (Human)	IGKJ3 (Human)	3019	ARDPSILNTGNHHWYDLDL	4209	MQATEWPRT	Anna Wec et al., 2020 (https://science.sciencemag.org/content/early/2020/06/15/science.abc7424)
mAb-48	Ab	SARS-CoV1, SARS-CoV2	229E, HKU1, NL63, OC43			S; Unk	B-cells; SARS-CoV1 Human Patient	914	QVTLKESGAEVKKPGSSVKVSCKTSGGTFSTHAISWVRQAPGQGPEWMGGIIPLFGTSQHAQRFQARVKFTADESTNTAYMELSSLTPEDTAVYYCVRDSDPYTATSRNNHYWYGMDVWGHGTTVTVSS	1981	EIVMTQSPLSLPVTLGQPASISCRSSQSVVHSDGNTYLNWFHQRPGQSPRRLIYKVSNRDSGVPDRFSGSGSGTDFTLKISRVEAEDIGVYYCMQGTDWPRTFGQGTKLEIK	IGHV1-69 (Human)	IGHJ6 (Human)	IGKV2-30 (Human)	IGKJ2 (Human)	3020	VRDSDPYTATSRNNHYWYGMDV	4210	MQGTDWPRT	Anna Wec et al., 2020 (https://science.sciencemag.org/content/early/2020/06/15/science.abc7424)
mAb-49	Ab	SARS-CoV1, SARS-CoV2	229E, HKU1, NL63, OC43			S; Unk	B-cells; SARS-CoV1 Human Patient	915	QVQLVQSGAEVKKPGSSVKVSCKASGGMFSDYAISWVRQAPGQRLEWMGGIMPGLGSPAYAQSFGGRVTISADISTSTAYLEVTSLRPEDTAVYYCARDPSILNTGNHHWYDLDMWGQGTMVTVSS	1982	DIVMTQSPLSLPVDLGQSASISCRSSQTAVHTNGNTYLHWFHQRPGQAPRRLIYKVSNRESGVPDRFSGSGSGTDFTLRINRVEAEDVGVYYCMQATDWPRTFGQGTKLEIK	IGHV1-69 (Human)	IGHJ3 (Human)	IGKV2-30 (Human)	IGKJ2 (Human)	3021	ARDPSILNTGNHHWYDLDM	4211	MQATDWPRT	Anna Wec et al., 2020 (https://science.sciencemag.org/content/early/2020/06/15/science.abc7424)
mAb-5	Ab	SARS-CoV1, SARS-CoV2	229E, HKU1, NL63, OC43			S; Unk	B-cells; SARS-CoV1 Human Patient	916	EVQLVESGGGLVQPGRSLRLSCSASGFSFGDYAMSWFRQAPGKGLQWVGLIKTRAYGAATDYAASVQGRFIISRDDSKSIAYLQMNSLKTEDTAVYFCARETGTSLGYYYYYAMDVWGHGTTVTVSS	1983	DIVLTQTPSSLSASVGDRVTITCRASQTISYYLNWYQQKVGKAPQLLVYAASSLQSGVPSRFSGSGSGTDFTLTISSLQPEDFATYYCQQSYSVPLTLGQGTKVDIK	IGHV3-49 (Human)	IGHJ6 (Human)	IGKV1-39 (Human)	IGKJ3 (Human)	3022	AREGTSLGYYYYAMDV	4212	QQSYSVPLT	Anna Wec et al., 2020 (https://science.sciencemag.org/content/early/2020/06/15/science.abc7424)
mAb-50	Ab	SARS-CoV1, SARS-CoV2	229E, HKU1, NL63, OC43			S; Unk	B-cells; SARS-CoV1 Human Patient	917	QVQLVQSGAEVKKPGSSVKVSCKASGGMFSDYAISWVRQAPGQRLEWMGGIMPGLGSPAYAQIFRGRVTISADISTSTAYLEVTSLRPEDTAVYYCARDPSILNTGNHHWYDLDMWGQGTTVTVSS	1984	DIQMTQSPLSLPVDLGQSASISCRSSQRVVHTNGNTYLHWFHQRPGQAPRRLIYKVSNRESGVPDRFSGSGSGTDFTLRISRVEAEDVGVYYCMQATDWPRTFGQGTKVEIK	IGHV1-69 (Human)	IGHJ6 (Human)	IGKV2-30 (Human)	IGKJ1 (Human)	3023	ARDPSILNTGNHHWYDLDM	4213	MQATDWPRT	Anna Wec et al., 2020 (https://science.sciencemag.org/content/early/2020/06/15/science.abc7424)
mAb-51	Ab	SARS-CoV1, SARS-CoV2	229E, HKU1, NL63, OC43			S; Unk	B-cells; SARS-CoV1 Human Patient	918	EVQLVESGGGLVQPGGSLRLSCLTSGFSFSYWMIWVRQAPGKGLEWVANIEPDGNEEYYVDSVKGRFTISRDNAKNSLYLQMNSLRAEDTAVYYCARGPIRHFGLDAFDIWGQGTTVTVSS	1985	QPGLTQPASVSGSPGQSITISCTRTSGDVGDYNSVSWYVSWYQQHPGRAPKLMLYDVSNRPSGVSNRFSGSKLGDTASLTISELQAEDEADYYCSTYTSTSTIFGGGTKLTVL	IGHV3-7 (Human)	IGHJ3 (Human)	IGLV2-14 (Human)	IGLJ3 (Human)	3024	ARGPIRHFGLDAFDI	4214	STYTSTSTI	Anna Wec et al., 2020 (https://science.sciencemag.org/content/early/2020/06/15/science.abc7424)
mAb-52	Ab	SARS-CoV2	229E, HKU1, NL63, OC43, SARS-CoV1			S; Unk	B-cells; SARS-CoV1 Human Patient	919	QVQLVQSGDEMKKPGSSVKVSCKASGDTFSTHAISWVRQAPGQGPEWMGGIIPLFGTASYAQTSQSRVKITADESTSTAYMELSSLTSEDTAVYYCVRDSDPYTATSRNNHYWYGMDVWGQGTTVTVSS	1986	DIQMTQSPLSLPVTLGQPASISCRASQTVVHTNGNTYLNWFHQRPGQSPRRLIYEVSNRDSGVPDRFSGSGSGTDFTLSISRVEAEDIGVYYCMQGTDWPRTFGPGTKVEIK	IGHV1-69 (Human)	IGHJ6 (Human)	IGKV2-30 (Human)	IGKJ3 (Human)	3025	VRDSDPYTATSRNNHYWYGMDV	4215	MQGTDWPRT	Anna Wec et al., 2020 (https://science.sciencemag.org/content/early/2020/06/15/science.abc7424)
mAb-53	Ab	SARS-CoV1, SARS-CoV2	229E, HKU1, NL63, OC43			S; Unk	B-cells; SARS-CoV1 Human Patient	920	QVQLVQSGAEVKKPGSSVKVSCKASGGMFSDYAISWVRQAPGQRLEWMGGIMPGLGSPAYAQSFGGRVTISADISTSTAYLEVTSLRPEDTAVYYCARDPSILNTGNHHWYDLDMWGQGTMVTVSS	1987	DIRLTQSPLSLPVDLGQSASISCRSSQTVVHTNGNTYLHWFHQRPGQAPRRLIYKVSNRESGVPDRFSGSGSGTDFTLRISRVEAEDVGVYYCMQATDWPRTFGQGTKVDIK	IGHV1-69 (Human)	IGHJ3 (Human)	IGKV2-30 (Human)	IGKJ3 (Human)	3026	ARDPSILNTGNHHWYDLDM	4216	MQATDWPRT	Anna Wec et al., 2020 (https://science.sciencemag.org/content/early/2020/06/15/science.abc7424)

mAb-54	Ab	SARS-CoV1, SARS-CoV2	229E, HKU1, NL63, OC43			S; Unk	B-cells; SARS-CoV1 Human Patient	921	EVQLVESGGGLVQPGGSLRLSCSASGFT FSNYAMYWVRQAPGKRPEYVSGISSNG GITYYADSVEGRFTVSRDNSKKSLYLQM SSLRPEDTAVYYCVKDLGATVTYDVFDV WGQGTMVTVSS	1988	DIRVTQSPSSLSATVGDRVTITCRASQT ITKYLNWYQQKPGKAPKLLLYGASSLQ SGVPSRFSGSGSGTDFTLTISSLQPEDF ATYYCQQTYITPGTFGQGTRLEIK	IGHV3-64D (Human)	IGHJ3 (Human)	IGKV1-39 (Human)	IGKJ5 (Human)	3027	VKDLGATVTY DVFDV	4217	QQTYITPG T	Anna Wec et al., 2020 (https://science.sciencemag.org/content/early/2020/06/15/science.abc7424)
mAb-55	Ab	SARS-CoV2	229E, HKU1, NL63, OC43, SARS-CoV1			S; Unk	B-cells; SARS-CoV1 Human Patient	922	EVQLVESGGGLVQPGGSLRLSCAASGFT FSSYSMSWVRQAPGKGLEWVSGHDGG TTHYADSVKGRFTISRDDSMNTLSLQM NSLRAEDTAVYYCAKERDLPGRGGYFDH WGQGTLVTVSS	1989	DIRLTQSPDSLALSLGERATINCKSSQS VLFSSNNNNYLGWYQQKPGQPPKLLI YWASTRESGVPDRFSGSGSGTDFTLTI SSLQAEDVAVYYCQQYYLTPWTFGQG TKVDIK	IGHV3-23 (Human)	IGHJ4 (Human)	IGKV4-1 (Human)	IGKJ1 (Human)	3028	AKERDLPGRG GYFDH	4218	QQYYLTP WT	Anna Wec et al., 2020 (https://science.sciencemag.org/content/early/2020/06/15/science.abc7424)
mAb-56	Ab	SARS-CoV2	229E, HKU1, NL63, OC43, SARS-CoV1			S; Unk	B-cells; SARS-CoV1 Human Patient	923	QVQLQQWGAGLLKPSETLSLTCAVYGG SFRGFYWTWIRQPPGKGLEWIGEVSHS GETNYNPSLKSRVTISVDTSKNQFSLNLIS VTAADTSVYYCARGYTAPIIREVPITFRPR WFDPWGQGTPVTVSS	1990	QPVLTQPASVSGSPGQSITISCTGTSSD VGNYNVVSWYQQHPGKAPQLFIYED TKRPSGVSDRFSGSKSGITASLTISRLQ PEDEADYYCCSYAVSGTVLFGGGTKVT VL	IGHV4-34 (Human)	IGHJ5 (Human)	IGLV2-23 (Human)	IGLJ3 (Human)	3029	ARGYTAPIIRE VPITFRPRWF DP	4219	CSYAVSGT VL	Anna Wec et al., 2020 (https://science.sciencemag.org/content/early/2020/06/15/science.abc7424)
mAb-57	Ab	SARS-CoV1, SARS-CoV2	229E, HKU1, NL63, OC43			S; Unk	B-cells; SARS-CoV1 Human Patient	924	QVQLVQSGGGVVNPGGSMRLSCAGSG FTFSDHYMGWIRQAPGKGLEVISYISSS GSFIRDADSVKGRFTISRDNAKNSVYLQ MNSLRAEDTAVYYCARMGPYGSGTFDY WGQGTLVTVSS	1991	EIVLTQSPGTLSVSPGERATLSCRASQII NRSQLGWYQHKPGQAPRLLIFDSSKR ATGTPDRFSASGSETDFTLTISGVEPED SGVYYCLQYSLATTFGPGTKVDIK	IGHV3-11 (Human)	IGHJ4 (Human)	IGKV3-20 (Human)	IGKJ3 (Human)	3030	ARMGPYGSG TFDY	4220	LQYSLATT	Anna Wec et al., 2020 (https://science.sciencemag.org/content/early/2020/06/15/science.abc7424)
mAb-58	Ab	SARS-CoV1, SARS-CoV2	229E, HKU1, NL63, OC43			S; Unk	B-cells; SARS-CoV1 Human Patient	925	QVQLVQSGGNVVQPGGSLRLSCVGSEF SITFFAMQWVRRTPGKGLEWVALVSHD GSNIRYSDSVKGRFIISRDNAKNTLYLQL DSLTPEDTGIYYCARDHALQNGRPGYFD SWGQGSQVTVSS	1992	DIQLTQSPATLSLSPGERATLSCRASPS VFTFLAWYQQRPGQPPRLLIHDVSNR APGIPARFSGSGSGTDFTLIISSLEPDDS AVYFCQQRSDGYNFGPGTKVDIK	IGHV3-30 (Human)	IGHJ5 (Human)	IGKV3-11 (Human)	IGKJ3 (Human)	3031	ARDHALQNG RPGYFDS	4221	QQRSDGY N	Anna Wec et al., 2020 (https://science.sciencemag.org/content/early/2020/06/15/science.abc7424)
mAb-59	Ab	SARS-CoV1, SARS-CoV2	229E, HKU1, NL63, OC43			S; Unk	B-cells; SARS-CoV1 Human Patient	926	QVQLVQSGGGLVQPGGSLRLSCASGF TFNTYAMHWVRQAPGKRLEYVSSITRD GAGKFYADSVKGRFTISRDNSKNTLYQQ MSSLRPEDTAVYYCVREGQQWLGLYFD HWGQGALVTVSS	1993	DIRVTQSPSSLASVGDRVTITCRASQT INNYLNWYQQKPGKAPNLLIYAASTLQ NGVPSRFSGSGSGTDFTLTISSVQPED FATYYCQQTYITPTWTFGQGTKVEIK	IGHV3-64 (Human)	IGHJ4 (Human)	IGKV1-39 (Human)	IGKJ1 (Human)	3032	VREGQQWLG LYFDH	4222	QQTYITPT WT	Anna Wec et al., 2020 (https://science.sciencemag.org/content/early/2020/06/15/science.abc7424)
mAb-6	Ab	SARS-CoV1, SARS-CoV2	229E, HKU1, NL63, OC43			S; Unk	B-cells; SARS-CoV1 Human Patient	927	QVQLVQSGAEVKKPGASVKVSCRASGY TFSGYDINWVRQATGQGLEWMGWM NPNSGDTGYAHKFQGRVTMTRNSSIST AYMELSSLTSEDTAVYFCAREKKSFGPQY YYGSGEDWGQGTLVTVSS	1994	EIVMTQSPSSLSASVGDRVTITCRASQS ISNYLYWYQQKPGKAPKLLIYVASNLQ SGVPSRFSGSGSGTDFTLTISSLQPDD ATYYCQQSYSTPYNFGQGTKVDIK	IGHV1-8 (Human)	IGHJ4 (Human)	IGKV1-39 (Human)	IGKJ3 (Human)	3033	AREKKSFGPQ YYYGSGED	4223	QQSYSTPY N	Anna Wec et al., 2020 (https://science.sciencemag.org/content/early/2020/06/15/science.abc7424)
mAb-60	Ab	SARS-CoV1, SARS-CoV2	229E, HKU1, NL63, OC43			S; Unk	B-cells; SARS-CoV1 Human Patient	928	EVQLVQSGAEMKKPGESLKISCKGSGYS FPNYWIGWVRQMPGKGLEWMAIMW PSDSDTRYSPSFQGQVTISADTSTSTVYL QWGSLKASDTAMYYCVRQRYCSGGSCF LFEDAFEIWGQGTMVTVSS	1995	EIVLTQSPSTLSASVGDRVTITCRASQN VNNWLAWYQQKPGKAPKLLIYEASTL KSGVPSRFSGSGSGTEFTLTISSLQPDD FATYYCQQYNSQYTFGQGTKVDIK	IGHV5-51 (Human)	IGHJ3 (Human)	IGKV1-5 (Human)	IGKJ3 (Human)	3034	VRQRYCSGGS CFLFEDAFEI	4224	QQYNSQY T	Anna Wec et al., 2020 (https://science.sciencemag.org/content/early/2020/06/15/science.abc7424)
mAb-61	Ab	SARS-CoV2	229E, HKU1, NL63, OC43, SARS-CoV1			S; Unk	B-cells; SARS-CoV1 Human Patient	929	EVQLVESGGGLVQPGGSLRLSCAASGFI FKNEPMNWIRQFPGKGLEWISNIRDNG NDVYYADSVKGRFTVSRDNAKNSLYLQ MNSLRDDDTALYYCVRDTDWAFDSWG QGTLVTVSS	1996	QPVLTQPRSVSGSPGQSVTISCTGSSST FGTDNHISWYQQLPGKVPKLIIHAVSQ RPSVVPDRFSGSRSGNTASLTISGLQA EDEADYYCCSSPGTITWVFGGGTKVT VL	IGHV3-48 (Human)	IGHJ5 (Human)	IGLV2-11 (Human)	IGLJ3 (Human)	3035	VRDTDWAFD S	4225	CSSPGTIT WV	Anna Wec et al., 2020 (https://science.sciencemag.org/content/early/2020/06/15/science.abc7424)
mAb-62	Ab	SARS-CoV2	229E, HKU1, NL63, OC43, SARS-CoV1			S; Unk	B-cells; SARS-CoV1 Human Patient	930	EVQLVESGPTLVKPTQTLTLTCTFSGFSLT TRRQGVGWLRRPPGKALEWLALIYWD DDKRYSPSLKSRLTITKDTSKNHVVLSLT NVGPADTATYYCAHTSELPPRRPYAAFD FWGQGTLVTVSS	1997	QSVLTQPPSVSGVPRQKVTISCSGSTA NIASNGVNWYQLVPGKAPRLLISYDDL VPSGVSARFSGSKSGTSASLAISGLQAE DEADYYCATWDDILNGPVFGGGTKLT VL	IGHV2-5 (Human)	IGHJ4 (Human)	IGLV1-36 (Human)	IGLJ3 (Human)	3036	AHTSELPPRR PYAAFDF	4226	ATWDDILN GPV	Anna Wec et al., 2020 (https://science.sciencemag.org/content/early/2020/06/15/science.abc7424)
mAb-63	Ab	SARS-CoV2	229E, HKU1, NL63, OC43, SARS-CoV1			S; Unk	B-cells; SARS-CoV1 Human Patient	931	EVQLLESGGGLVQPGGSLRLSCAASGFP FSTDAMNWVRQAPGEGLEWVSTISDS GRDTYYAASVRGRFTISRDNSKNTVYLQ MNSLRVEDTAVYYCANTNFLDYWGQG TLVTVSS	1998	DIVLTQSPLSLPVTLGQSASISCRSSQG LVHSDGNIYLNWFQQRPGQSPRRLIY KVSNRDSGVPDRFSGSGSGTDFTLKIS RVEAEDVGLYYCMQATHWPRAFGQ GTKLEIK	IGHV3-23 (Human)	IGHJ4 (Human)	IGKV2-30 (Human)	IGKJ2 (Human)	3037	ANTNFLDY	4227	MQATHW PRA	Anna Wec et al., 2020 (https://science.sciencemag.org/content/early/2020/06/15/science.abc7424)
mAb-64	Ab	SARS-CoV1, SARS-CoV2	229E, HKU1, NL63, OC43			S; Unk	B-cells; SARS-CoV1 Human Patient	932	EVQLQESGPGLLKPSETLSLTCTVSGSPIA SNYWSWVRQPAGKGLEWIGRIDTSPTT DYNPSLKSRVIMSVDTSTSQFSLKMSSVT AADTAVYYCTRSFISFDSSGHPYYYYAMD VWGQGTTVTVSS	1999	EIVMTQSPGTLSLSPGERVTLSCRATQ SVSNNHLAWYQQKPGQAPRLLIYGAS TTATDIPDRFSGRVAGTDFTLTISRLDP EDFAVYYCHQYGSSPWTFGQGTKVEI K	IGHV4-4 (Human)	IGHJ6 (Human)	IGKV3-20 (Human)	IGKJ1 (Human)	3038	TRSFISFDSSG HPYYYYAMD V	4228	HQYGSSP WT	Anna Wec et al., 2020 (https://science.sciencemag.org/content/early/2020/06/15/science.abc7424)
mAb-65	Ab	SARS-CoV1, SARS-CoV2	229E, HKU1, NL63, OC43			S; Unk	B-cells; SARS-CoV1 Human Patient	933	QVQLVQSGAEVRKPGSSVKLSCRASGG TFHTYTVNWVRQAPGQGLEWLGGIIPIF GTPTYAQRFQGKVSITADSSTNTVFMEL TSLTSEDTAVYYCTRETGTDEFDFWGQG ALVTVSS	2000	DIRLTQSPATLSLSPGERATLSCRASQS VSSSLAWYQQKPGQAPRLLIYEASNRA TGVPARFSGSGSGTDFTLAISSLEPEDF AVYYCQHRSNWPPRYTFGQGTKVEIK	IGHV1-69 (Human)	IGHJ4 (Human)	IGKV3-11 (Human)	IGKJ1 (Human)	3039	TRETGTDEFD F	4229	QHRSNWP PRYT	Anna Wec et al., 2020 (https://science.sciencemag.org/content/early/2020/06/15/science.abc7424)
mAb-66	Ab	SARS-CoV2	229E, HKU1, NL63, OC43, SARS-CoV1			S; Unk	B-cells; SARS-CoV1 Human Patient	934	EVQLVESGPGLVKPSGTLSLTCAVSGAS VSSDHWWSWVRQSPGKGLEWIGEVY HSGSTNYNPSLKSRVTISLDQSNNQFSLK LTSVTAADTAIYYCATMWGGLCTASNCY GNPMDVWGQGTTVTVSS	2001	SYELTQPPSVSVSPGQTARITCSGDALP RRYAYWYQQRSGQAPVLVIYEDNKRP SGIPERFSAFSSGTRATLTISGAQVEDE ADYYCYSTDSTANYKVFGGGTKVTVL	IGHV4-4 (Human)	IGHJ6 (Human)	IGLV3-10 (Human)	IGLJ6 (Human)	3040	ATMWGGLCT ASNCYGNPM DV	4230	YSTDSTAN YKV	Anna Wec et al., 2020 (https://science.sciencemag.org/content/early/2020/06/15/science.abc7424)

mAb-67	Ab	SARS-CoV2	229E, HKU1, NL63, OC43, SARS-CoV1			S; Unk	B-cells; SARS-CoV1 Human Patient	935	EVQLVESGPGLVKPSGTLSLTCAVTGAS VSSDHWWSWVRQSPGKGLEWIGEVY HSGSTNYNPSLKSRVTISLDQSNNQFSLK LTSVTAADTAIYYCATMWGGLCTASNCY GNPMDVWGQGTTVTVSS	2002	SYELTQPPSVSVSPGQTARITCSGDALP RRYAYWYQQRSGQAPVLVIYEDNKRP SGIPERFSAFSSGTRATLTISGAQVEDE ADYYCYSTDSTANYKVFGGGTKLTVL	IGHV4-4 (Human)	IGHJ6 (Human)	IGLV3-10 (Human)	IGLJ3 (Human)	3041	ATMWGGLCT ASNCYGNPM DV	4231	YSTDSTAN YKV	Anna Wec et al., 2020 (https://science.sciencemag.org/content/early/2020/06/15/science.abc7424)
mAb-68	Ab	SARS-CoV1, SARS-CoV2	229E, HKU1, NL63, OC43			S; Unk	B-cells; SARS-CoV1 Human Patient	936	QVQLQESGPGLVKPSGTLSLTCAVSGAS VSSDHWWSWVRQSPGKGLEWIGEVY HSGSTNYNPSLKSRVTISLDQSNNQFSLK LTSVTAADTAIYYCATMWGGLCTASNCY GNPMDVWGQGTTVTVSS	2003	SYELTQPPSVSVSPGQTARITCSGDALP RRYAYWYQQRSGQAPVLVIYEDNKRP SGIPERFSAFSSGTRATLTISGAQVEDE ADYYCYSTDSTANYKVFGGGTKLTVL	IGHV4-4 (Human)	IGHJ6 (Human)	IGLV3-10 (Human)	IGLJ3 (Human)	3042	ATMWGGLCT ASNCYGNPM DV	4232	YSTDSTAN YKV	Anna Wec et al., 2020 (https://science.sciencemag.org/content/early/2020/06/15/science.abc7424)
mAb-69	Ab	SARS-CoV1, SARS-CoV2	229E, HKU1, NL63, OC43			S; Unk	B-cells; SARS-CoV1 Human Patient	937	QVQLQESGGGLVQPGGSLRLSCEASGF SFSDFVMHWVRQVPGKGLEWVSRISH DGSITSYVDSVKGRFTVSRDNGKKTLYL QMNSPRTEDTAVYYCARDLAWTFFDY WGHGTLVTVSS	2004	QSVLTQPSSLSASPGASASLTCTLHSGF NVGDHTINWYQQRPGSPPRYLLKYKS DSDKEQGSGVPIRFSGSKDASANAGFL LISGLRSEDEADYYCMIWHDNAVVFG GGTKLTVL	IGHV3-74 (Human)	IGHJ4 (Human)	IGLV5-45 (Human)	IGLJ3 (Human)	3043	ARDLAWTFF DY	4233	MIWHDNA VV	Anna Wec et al., 2020 (https://science.sciencemag.org/content/early/2020/06/15/science.abc7424)
mAb-7	Ab	SARS-CoV1, SARS-CoV2	229E, HKU1, NL63, OC43			S; Unk	B-cells; SARS-CoV1 Human Patient	938	EVQLLESGGGLSRPGGSLRLSCAASGFIA SRNCMQWVRQAPGKGLEWVSIICGDEI TYIRDSVKGRFTISRDDSKNTLHLEMNSL RADDTAVYYCARATPPGGTTGWPYIDL WGQGTLVTVSS	2005	EIVLTQSPATLSVSPGDGASLSCRASQS VGSNLAWYQQKPGQAPRLLISDASAR ATGVPARFTGSGSGTDFTLTISSLQSED FAVYYCHQYNTWPPLTFGGGTKLEIK	IGHV3-66 (Human)	IGHJ4 (Human)	IGKV3-15 (Human)	IGKJ4 (Human)	3044	ARATPPGGTT GWPYIDL	4234	HQYNTWP PLT	Anna Wec et al., 2020 (https://science.sciencemag.org/content/early/2020/06/15/science.abc7424)
mAb-70	Ab	229E, HKU1 (weak), NL63, SARS-CoV1 (weak), SARS-CoV2	OC43			S; Unk	B-cells; SARS-CoV1 Human Patient	939	EVQLLESGGGLVQPGGSLRLSCAASGFP FSTDAMNWVRQAPGEGLEWVSTISDT GRDTYYAASVKGRFTISRDNSKNTVYLQ MNSLRAEDTAVYYCANTNFLDYWGQG TLVTVSS	2006	EIVMTQSPLSLPVTLGQSASISCRSSQG LVHSDGNIYLNWFQQRPGQSPRRLIY KVSNRDSGVPDRFSGSGSGTDFTLKIS RVEAEDVGLYYCMQATHWPRAFGQ GTKVDIK	IGHV3-23 (Human)	IGHJ4 (Human)	IGKV2-30 (Human)	IGKJ3 (Human)	3045	ANTNFLDY	4235	MQATHW PRA	Anna Wec et al., 2020 (https://science.sciencemag.org/content/early/2020/06/15/science.abc7424)
mAb-71	Ab	SARS-CoV2	229E, HKU1, NL63, OC43, SARS-CoV1			S; Unk	B-cells; SARS-CoV1 Human Patient	940	EVQLVESGGGLVQPGRSLRLSCAASGFIL DDYAVHWVRLAPGKGLEWVSGITWNS GYLGYADSVKGRFTISRDNAKNSLYLQM NSLRPEDTALYYCAKLGTDHPIGVDVW GQGTTVTVSS	2007	DIVMTQSPLALSVTPGQPASISCKSSQ SLLHSDGKTYFYWYLQKPGQSPHLLIY EVSNRFSGVPDRFSGSGSGTDFTLKISR VEAEDVGVYYCMQSIQVPITFGGGTK LEIK	IGHV3-9 (Human)	IGHJ6 (Human)	IGKV2D-29 (Human)	IGKJ5 (Human)	3046	AKLGTDHPIG VDV	4236	MQSIQVPI T	Anna Wec et al., 2020 (https://science.sciencemag.org/content/early/2020/06/15/science.abc7424)
mAb-72	Ab	SARS-CoV2	229E, HKU1, NL63, OC43, SARS-CoV1			S; Unk	B-cells; SARS-CoV1 Human Patient	941	QVQLVQSGGGLVQPGGSLRLSCSASGF TFNTYTMHWVRQAPGKGLEYVSAISSN GVVTYYADSVKGRFTISRDNSKNTLYLQ MSSLRAEDTAVYYCVKALYSSSWCPFDY WGQGALVTVSS	2008	DIVMTQSPATLSVSPGERATLSCRASQ SVSSNLAWYQQKPGQAPRLLIYGAST RATNIPARFSGSGSGTEFTLTISSLQSE DFAVYYCQQYNLWPYTFGQGTKVDIK	IGHV3-64D (Human)	IGHJ4 (Human)	IGKV3-15 (Human)	IGKJ3 (Human)	3047	VKALYSSSWC PFDY	4237	QQYNLWP YT	Anna Wec et al., 2020 (https://science.sciencemag.org/content/early/2020/06/15/science.abc7424)
mAb-73	Ab	SARS-CoV2	229E, HKU1, NL63, OC43, SARS-CoV1			S; Unk	B-cells; SARS-CoV1 Human Patient	942	QVQLQQSGGGLVQPGGSLRLSCEASGF NFNSYSMSWVRQAPGKGLEWLSYISSR SSTIKYASSVQGRFTVSRDNAKKSVFLQ MNSLRDEDTAVYYCARELDSETYYNYNS LDVWGQGTTVTVSS	2009	EIVLTQSPSSLSASVGDRVTISCRASQGI STFLAWFQQRPGKAPKSLIYAASKLQS GVPSRFSGSDSGPDFTLTIDNLQPEDS ATYYCKQYNSYPYTFGQGTKLEIK	IGHV3-48 (Human)	IGHJ6 (Human)	IGKV1-16 (Human)	IGKJ2 (Human)	3048	ARELDSETYY NYNSLDV	4238	KQYNSYPY T	Anna Wec et al., 2020 (https://science.sciencemag.org/content/early/2020/06/15/science.abc7424)
mAb-74	Ab	SARS-CoV2	229E, HKU1, NL63, OC43, SARS-CoV1			S; Unk	B-cells; SARS-CoV1 Human Patient	943	QVQLQESGPGLVRPSETLSLTCTVSRGSI SSSYWSWIRQPPGKGLEWIGFMYYSGS TNYNPSLKSRVTISLDTSKNQFSLKLSSVT AADTAVYYCAKAQGIYYRGWSYWFDP WGQGTLVTVSS	2010	QSVVTQPPSVSAAPGQKVTISCSGSSS NIGNNYVSWYQQLPGTAPKLLIYDSD KRPSGIPERFSGSKSATSATLGITGLQT GDEADYYCETWDDSLSAVVFGGGTKL TVL	IGHV4-59 (Human)	IGHJ5 (Human)	IGLV1-51 (Human)	IGLJ3 (Human)	3049	AKAQGIYYRG WSYWFDP	4239	ETWDDSLS AVV	Anna Wec et al., 2020 (https://science.sciencemag.org/content/early/2020/06/15/science.abc7424)
mAb-75	Ab	229E, HKU1 (weak), NL63, SARS-CoV1 (weak), SARS-CoV2	OC43			S; Unk	B-cells; SARS-CoV1 Human Patient	944	EVQLVQSGAEVKKPGASVKISCKASGYA FRNNYINWIRQAPGQGLEWMGIINPSA GTSTYAQKFQGRVTMTRDTSTNTVYME ITSLRSEDTATYFCAREARRQVTQWFGE FWGPYNWFDPWGQGTLVTVSS	2011	DIVLTQSPLSLSVTPGQPASISCRSSQSL QHTDGKTYLYWYLQKPGQSPQLLIYEL FNRFSGVPERFSGSGSGTDFTLKISRVE AEDVGIYYCMQSIQTPITFGQGTRLEIK	IGHV1-46 (Human)	IGHJ5 (Human)	IGKV2D-29 (Human)	IGKJ5 (Human)	3050	AREARRQVT QWFGEFWG PYNWFDP	4240	MQSIQTPI T	Anna Wec et al., 2020 (https://science.sciencemag.org/content/early/2020/06/15/science.abc7424)
mAb-76	Ab	SARS-CoV1, SARS-CoV2	229E, HKU1, NL63, OC43			S; Unk	B-cells; SARS-CoV1 Human Patient	945	QVQLQQWGAGLLKPSETLSLTCGVYGV SFSDYYWSWIRQPPGKGLEWIGEINHS GITNYNPSLKSRVTISVDTSKNQFSLKLSS VTAADTAVYYCARGLISYTLWLRESYFDY WGQGTLVTVSS	2012	DIRVTQSPDSLAVSLGERATINCKSSQS VLYSSNNKNYLAWYQQKIGQPPKLLIY WASIRESGVPDRFTGSGSGTDFTLTISS LQAEDVAVYYCQQYYSTPPTFGGGTK LEIK	IGHV4-34 (Human)	IGHJ4 (Human)	IGKV4-1 (Human)	IGKJ4 (Human)	3051	ARGLISYTLW LRESYFDY	4241	QQYYSTPP T	Anna Wec et al., 2020 (https://science.sciencemag.org/content/early/2020/06/15/science.abc7424)
mAb-77	Ab	SARS-CoV1, SARS-CoV2	229E, HKU1, NL63, OC43			S; Unk	B-cells; SARS-CoV1 Human Patient	946	QVQLVQSGAEVKKPGSSVKVSCKASGG SLRDYAISWVRQAPGQGPEWMGGIMP IFGTAGYAQKFQGRVKFTADESATTAYM ELTGLRSEDSAVYFCARDPSILNTGNHH WYDLDIWGQGTTVTVSS	2013	EIVMTQTPLSLPVTLGQPASISCRSSQF VSHTDGNTYLNWFQQRPGQSPRRLIY KVSKRDSGVPDRFSGSGSGTDFTLTIS RVEAEDVGVYYCMQATEWPRTFGQG TKVEYQ	IGHV1-69 (Human)	IGHJ6 (Human)	IGKV2-30 (Human)	IGKJ1 (Human)	3052	ARDPSILNTG NHHWYDLDI	4242	MQATEWP RT	Anna Wec et al., 2020 (https://science.sciencemag.org/content/early/2020/06/15/science.abc7424)
mAb-78	Ab	SARS-CoV2	229E, HKU1, NL63, OC43, SARS-CoV1			S; Unk	B-cells; SARS-CoV1 Human Patient	947	QVQLVQSGAEVKKPGASVKVSCKASGY TFTNDGFVWVRQAPGQVPEWMGWIS VHTGDTIYAQRFQGRVTMTTDTSTRTSY MELMSLRSDDTAVYYCARDYGDGPPD HWGQGTLVTVSS	2014	DIVMTQSPDSLAVSLGERATINCKSSQ SVLFSSNNKNYLAWYQQKPGLPPKLLI YWASTRKSGVSDRFSGSGSGTDFTLTI SSLQAEDVAVYYCQQYYTTPLFTFGPG TKVDIK	IGHV1-18 (Human)	IGHJ4 (Human)	IGKV4-1 (Human)	IGKJ3 (Human)	3053	ARDYGDGPP DH	4243	QQYYTTPL FT	Anna Wec et al., 2020 (https://science.sciencemag.org/content/early/2020/06/15/science.abc7424)
mAb-79	Ab	SARS-CoV1, SARS-CoV2	229E, HKU1, NL63, OC43			S; Unk	B-cells; SARS-CoV1 Human Patient	948	QVQLVQSGPEVKKPGSSVRVSCKVSGG PFSSYGVSWARQAPEKGLEWMGGVLPI FGTVGYVHKFQGRVTITADESTSTVYMA LSSLRSEDTAVYYCVLDTTMSHPHNWY GMDVWGHGTTVTVSS	2015	DIVMTQSPLSLPVTLGQPASISCRSSHS LVHTNGNTYLNWFQQRPGQPPRRLIY QVSNRDSGVPDRFSGSGSGTDFTLKIS RVEADDVGIYYCMQGTDWPRTFGQG TKVDIK	IGHV1-69 (Human)	IGHJ6 (Human)	IGKV2-30 (Human)	IGKJ3 (Human)	3054	VLDTTMSHP HNWYGMDV	4244	MQGTDW PRT	Anna Wec et al., 2020 (https://science.sciencemag.org/content/early/2020/06/15/science.abc7424)

mAb-8	Ab	SARS-CoV1, SARS-CoV2	229E, HKU1, NL63, OC43			S; Unk	B-cells; SARS-CoV1 Human Patient	949	QVQLVQSGAEVKKPGSSMKLSCKASGI NFRSYSFSWVRQAPGQGLEWMGGVIP YFPTANYAEKFRGRVTATADESTGTVYLE MSSLRSEDTAVYYCASEYFDGRSYHSFC GLDVWGQGTLVTVSS	2016	ETTLTQSPLSLPVTLGQPASISCRSSQG LAHSNGNTYLNWFHQRPGQSPRRLIY QVSNRDSGVPDRFSGSGSGTDFTLKIS RVEAEDVGVYYCMQGTEWPRTFGQ GTKVEIK	IGHV1-69 (Human)	IGHJ4 (Human)	IGKV2-30 (Human)	IGKJ1 (Human)	3055	ASEYFDGRSY HSFCGLDV	4245	MQGTEW PRT	Anna Wec et al., 2020 (https://science.sciencemag.org/content/early/2020/06/15/science.abc7424)
mAb-80	Ab	229E, HKU1 (weak), NL63, SARS-CoV1 (weak), SARS-CoV2	OC43			S; Unk	B-cells; SARS-CoV1 Human Patient	950	QVQLVQSGAEVKKPGSSVKVSCKASGG TLSDYAISWVRQAPGQGLEWMGGIMP VFGSPGYAEIFQGRLTITADESRSTAYME LTSLRSEDTAVYYCARDPSILNTGPHHW YDLDIWGPGTTVTVSS	2017	DIVMTQSPLSLPVSLGQPASISCRSSQS VVHTDGNTYLNWYQQRPGQSPRRLIY KVSNRDSGVPDRFSGSGSVTDFTLKIS RVEAEDVAVYYCMQGTEWPRTFGQG TKVDIK	IGHV1-69 (Human)	IGHJ6 (Human)	IGKV2-30 (Human)	IGKJ3 (Human)	3056	ARDPSILNTG PHHWYDLDI	4246	MQGTEW PRT	Anna Wec et al., 2020 (https://science.sciencemag.org/content/early/2020/06/15/science.abc7424)
mAb-81	Ab	SARS-CoV2	229E, HKU1, NL63, OC43, SARS-CoV1			S; Unk	B-cells; SARS-CoV1 Human Patient	951	EVQLVQSGAEVKKPGSSMRVSCRVSGG TFITHAMSWVRQAPGQGPEWMGGIV PLFGRASYAQPSQTRVQITADESTSTVYL EVPSLTSEDTAVYYCVRDSEPYTATRSQN HYWYDMDVWGQGTTVTVSS	2018	DIQMTQSPLSLSVTLGQSASISCRASQT VVHSVDGNTYLNWFHQRPGQSPRRLI YKVSNRDSGVPDRFSGSGSGTDFTLRI SRVEAEDIGIYYCMQGTDWPRTFGQG TKVEIK	IGHV1-69 (Human)	IGHJ6 (Human)	IGKV2-30 (Human)	IGKJ1 (Human)	3057	VRDSEPYTAT RSQNHYWYD MDV	4247	MQGTDW PRT	Anna Wec et al., 2020 (https://science.sciencemag.org/content/early/2020/06/15/science.abc7424)
mAb-82	Ab	HKU1, SARS-CoV1, SARS-CoV2	229E, NL63, OC43			S; Unk	B-cells; SARS-CoV1 Human Patient	952	EVQLVESGPGLVKPSATLSLTCTVSGGSI NNYYWTWVRQSAGKGLEWIGRINTSG STNYNASLKSRVTMSIDTSKNEFSLRLSS VTAADTAVYYCAREFGVRFLDRSLFGAM DVWGHGATVTVSS	2019	QPVLTQPASVSGSPGQSITISCTGTSSD VGSFNYVSWYQQHPGKAPKLVIYDVY NRPSGVSNRFSGSKSGNTASLTISGLQ AEDEADYYCSSYTSSSTLYVFGTGTKVT VL	IGHV4-4 (Human)	IGHJ6 (Human)	IGLV2-14 (Human)	IGLJ1 (Human)	3058	AREFGVRFLD RSLFGAMDV	4248	SSYTSSSTL YV	Anna Wec et al., 2020 (https://science.sciencemag.org/content/early/2020/06/15/science.abc7424)
mAb-83	Ab	SARS-CoV2	229E, HKU1, NL63, OC43, SARS-CoV1			S; Unk	B-cells; SARS-CoV1 Human Patient	953	QVQLVESGGGVVQPGRSLRLSCAASGF TFSAFAMHWVRQAPGKGLEWVTIISYD GSNEYYADSVQGRFSISRDNSKNTLFLQ MSSLRTEDTAIYYCARAGGYLSAFDIWG QGTTVTVSS	2020	DIRLTQSPSTLSASVGDRVTITCRASQSI SSWLAWYQQKPGKAPNLLIYKASTLES GVPSRFSGSGSGTEFTLTISSLQPDDFA TYYCQQYNSGWTFGQGTKVEIK	IGHV3-30 (Human)	IGHJ3 (Human)	IGKV1-5 (Human)	IGKJ1 (Human)	3059	ARAGGYLSAF DI	4249	QQYNSGW T	Anna Wec et al., 2020 (https://science.sciencemag.org/content/early/2020/06/15/science.abc7424)
mAb-84	Ab	SARS-CoV1, SARS-CoV2	229E, HKU1, NL63, OC43			S; Unk	B-cells; SARS-CoV1 Human Patient	954	EVQLVQSGAEVKKPGSSVKVSCKVSGGT FSNYAISWLRQAPGQGPEWMGGIIPAL SKVGYAGKFQARLTFSADELKTTVYMDL SSLTSEDTAVYYCARDPSFLNAGNHFYYD FDVWGQGTMVTVSS	2021	DIRLTQSPLSLPVTLGQPASISCTSSQD VVHTDGNTYLNWFHQRPGQSPRRLIY KVSNRDSGVPDRFSGSGSGSHFTLKIS RVEAEDAGIYYCMQGTDWPRTFGQG TKVDIK	IGHV1-69 (Human)	IGHJ3 (Human)	IGKV2-30 (Human)	IGKJ3 (Human)	3060	ARDPSFLNAG NHFYYDFDV	4250	MQGTDW PRT	Anna Wec et al., 2020 (https://science.sciencemag.org/content/early/2020/06/15/science.abc7424)
mAb-85	Ab	SARS-CoV2	229E, HKU1, NL63, OC43, SARS-CoV1			S; Unk	B-cells; SARS-CoV1 Human Patient	955	QVQLQESGPGLVKPSGTLSLTCAVSGGS ITSRDWWSWVRQPPGKGLEWIGEVYH SGSTSYNPSLKSRVTISVDKSKNEFSLKLS SVTAADTAVYYCARAGNIVVMPAAQYY FDYWGQGTLVTVSS	2022	EIVLTQSPSSLSASVGDRVTITCRASQDI SNYLAWYQQKPGKAPKLLIYAASTLQS GVPLRFSGSGSGTDFTLTISSLQPEDFA TYYCLQLHNYSSFGGGTKVDIK	IGHV4-4 (Human)	IGHJ4 (Human)	IGKV1-9 (Human)	IGKJ3 (Human)	3061	ARAGNIVVM PAAQYYFDY	4251	LQLHNYSS	Anna Wec et al., 2020 (https://science.sciencemag.org/content/early/2020/06/15/science.abc7424)
mAb-86	Ab	SARS-CoV1, SARS-CoV2	229E, HKU1, NL63, OC43			S; Unk	B-cells; SARS-CoV1 Human Patient	956	EVQLVESGGSVVQPGTSLKLSCAGSAGL TITRYAMHWVRQAPGKGLEWVALVSH DGIHIGYSDSVRGRFTISRDNSRNTLYLQ MDGLRPEDTAVYYCVRDDVLQHSRPSG PGYFVSWGQGTLVTVSS	2023	EIVLTQSPATLSLSPGERATLSCRASQS VSTFLGWYQQRPGQPPRLLIYDASYR APDIPVRFSGSGSGTDFTLTINSLEPED SAVYYCQQRSDGYNFGPGTKLEIK	IGHV3-30 (Human)	IGHJ5 (Human)	IGKV3-11 (Human)	IGKJ2 (Human)	3062	VRDDVLQHS RPSGPGYFVS	4252	QQRSDGY N	Anna Wec et al., 2020 (https://science.sciencemag.org/content/early/2020/06/15/science.abc7424)
mAb-87	Ab	SARS-CoV2	229E, HKU1, NL63, OC43, SARS-CoV1			S; Unk	B-cells; SARS-CoV1 Human Patient	957	QVQLQESGPGLVKPSETLSLTCTVSGGS MNHYYWSWIRQPPGKGLEGIGYTYYSG STNYNPSLKSRVTISVDASKNQFSLRLSSV TAADTAVYYCARGSQIDLRGGLGATFFD YWGQGTLVTVSS	2024	QSVLTQPASVSGSPGQSITISCTGTSSD VGAYNYVSWYQQHPGKAPKLTVYDV RNRPSGVSNRFSGSKSGNTASLTISGL QAEDEAHYYCSSYTSTNTVFGGGTKLT VL	IGHV4-59 (Human)	IGHJ4 (Human)	IGLV2-14 (Human)	IGLJ3 (Human)	3063	ARGSQIDLRG GLGATFFDY	4253	SSYTSTNTV	Anna Wec et al., 2020 (https://science.sciencemag.org/content/early/2020/06/15/science.abc7424)
mAb-88	Ab	SARS-CoV2	229E, HKU1, NL63, OC43, SARS-CoV1			S; Unk	B-cells; SARS-CoV1 Human Patient	958	QVQLVESGAEVKKPGSSVKISCKISGDTF STNAISWLRQAPGREPEWMGGIVPLVG PASYAQRPQGRLTITADEFTNTAYLELNS LRSEDTATYYCARDSDPYTATRRHNHYW YAMDVWGQGTTVTVSS	2025	DIRLTQTPLSLPVTLGQPASISCRSSQIA MHSDGNTYLSWFHQRPGQPPRRLIYK ISNRDSGVPDRFSGSGSGTDFTLKISRV EAEDIGTFYCMQGTDWPRTFGQGTK VDIK	IGHV1-69 (Human)	IGHJ6 (Human)	IGKV2-24 (Human)	IGKJ3 (Human)	3064	ARDSDPYTAT RRHNHYWYA MDV	4254	MQGTDW PRT	Anna Wec et al., 2020 (https://science.sciencemag.org/content/early/2020/06/15/science.abc7424)
mAb-89	Ab	SARS-CoV1, SARS-CoV2	229E, HKU1, NL63, OC43			S; Unk	B-cells; SARS-CoV1 Human Patient	959	EVQLLESGGGLVQPGGSLRLSCAASGFIF KNEPMNWIRQFPGKGLEWISNIRDNG NDVYYADSVKGRFTVSRDNAKNSLYLQ MNSLRDDDTALYYCVRDTDWAFDSWG QGTLVTVSS	2026	QSALIQPRSVSGSPGQSVTISCTGSSST FGTDNHISWYQQLPGKVPKLIIHAVSQ RPSVVPDRFSGSRSGNTASLTISGLQA EDEADYYCCSSPGTITWVFGGGTKVT VL	IGHV3-48 (Human)	IGHJ5 (Human)	IGLV2-11 (Human)	IGLJ3 (Human)	3065	VRDTDWAFD S	4255	CSSPGTIT	Anna Wec et al., 2020 (https://science.sciencemag.org/content/early/2020/06/15/science.abc7424)
mAb-9	Ab	SARS-CoV1, SARS-CoV2	229E, HKU1, NL63, OC43			S; Unk	B-cells; SARS-CoV1 Human Patient	960	QVQLVQSGAEVKKPGASVKVSCKASGY TFSSYDINWVRQATGQGLEWMGWMS PNTGDTGYAHKFQGRVRMTSNTSISTA YMELNSLTSEDTAVYYCARRGNNFGYYY YYTVDVWGQGTTVTVSS	2027	DIRLTQSPSSLSASVGDRVTIACRASQS VSNYLNWYQQKPGKAPKLLIYAASSLQ NGVPSRFGGSGSGTDFTLTISSLQPED FATYYCQQCYSYPPTFGHGTKVEIK	IGHV1-8 (Human)	IGHJ6 (Human)	IGKV1-39 (Human)	IGKJ1 (Human)	3066	ARRGNNFGY YYYYTVDV	4256	QQCYSYPP T	Anna Wec et al., 2020 (https://science.sciencemag.org/content/early/2020/06/15/science.abc7424)
mAb-90	Ab	HKU1, SARS-CoV1, SARS-CoV2	229E, NL63, OC43			S; Unk	B-cells; SARS-CoV1 Human Patient	961	QVQLVQSGADVKKPGASVKVSCKASGY TFTSYYMHWVRQAPGQGLEWLGVIHP SGGSTTFAQKFQGRVTMTRDTSTSTVY MELSSLRSEDTAVYYCARVLAGSSHEW QLTHDAFDIWGQGTTVTVSS	2028	DIRMTQSPDSLAVSLGERATINCRTSQ SVLYSSNNKNYLGWYQQKPGQPPKLL IYWASTRESGVPDRFSGSGSGTDFTLTI SSLQAEDVAVYYCQQYYSTPYTFGQGT KVDIK	IGHV1-46 (Human)	IGHJ3 (Human)	IGKV4-1 (Human)	IGKJ3 (Human)	3067	ARVLAGSSHE WQLTHDAFD I	4257	QQYYSTPY T	Anna Wec et al., 2020 (https://science.sciencemag.org/content/early/2020/06/15/science.abc7424)

mAb-91	Ab	HKU1 (weak), SARS-CoV1 (weak), SARS-CoV2	229E, NL63, OC43			S; Unk	B-cells; SARS-CoV1 Human Patient	962	EVQLLESGGGLVQPGGSLRLSCAASGFT FSSYAMSWVRQAPGKGLEWVSGIDGG GGSSYYADSVRGRFTVSRDNSKNMLHL QMNSLRADDTAVYFCAKGDWIRYFDW SLPISFFDYWGQGALVTVSS	2029	QSALTQPASVSGSPGQSITISCTGTNSD ISNSYSVSWYQQYPGKAPKLVIFDVIN RPSGVSNRFSGSKSGNTASLTISGLQA DDEADYYCCSYTRTNTPVLFGGGTKLT VL	IGHV3-23 (Human)	IGHJ4 (Human)	IGLV2-14 (Human)	IGLJ3 (Human)	3068	AKGDWIRYF DWSLPISFFD Y	4258	CSYTRTNT PVL	Anna Wec et al., 2020 (https://science.sciencemag.org/content/early/2020/06/15/science.abc7424)
mAb-92	Ab	SARS-CoV1, SARS-CoV2	229E, HKU1, NL63, OC43			S; Unk	B-cells; SARS-CoV1 Human Patient	963	EVQLLESGPGLLKPSETLSLTCTVSGDSV SSGNFYWSWVRRPPGKALEWIAYSHYT GGTNSDPSFMGRVTMSIDPSRNQFSLR LTSVAAADTAVYYCARTTSPLTYSGHWP LFDYWGQGSLVTVSS	2030	DIQLTQSPATLSVSPGERATLSCRASQS VTKHLAWYQQKPGQAPRLLIYGASTR ATGVPARFSGSGSDTEFSLTISSLQSED FAVYYCQQYYSWPPLTFGGGTKLEIK	IGHV4-61 (Human)	IGHJ4 (Human)	IGKV3-15 (Human)	IGKJ4 (Human)	3069	ARTTSPLTYSG HWPLFDY	4259	QQYYSWP PLT	Anna Wec et al., 2020 (https://science.sciencemag.org/content/early/2020/06/15/science.abc7424)
mAb-93	Ab	SARS-CoV1, SARS-CoV2	229E, HKU1, NL63, OC43			S; Unk	B-cells; SARS-CoV1 Human Patient	964	QVQLVQSGDEMKKPGSSVKVSCKASGD TFSTHAISWVRQAPGQGPEWMGGIIPL FGTASYAQTSQSRVKITADESTSTAYMEL SSLTSEDTAVYYCVRDSDPYTATSRNNHY WYGMDVWGQGTTVTVSS	2031	DIVMTQTPLSLPVTLGQPASISCRASQ TVVHTNGNTYLNWFHQRPGQSPRRLI YEVSNRDSGVPDRFSGSGSGTDFTLSI SRVEAEDIGVYYCMQGTDWPRTFGP GTKVEIK	IGHV1-69 (Human)	IGHJ6 (Human)	IGKV2-30 (Human)	IGKJ3 (Human)	3070	VRDSDPYTAT SRNNHYWYG MDV	4260	MQGTDW PRT	Anna Wec et al., 2020 (https://science.sciencemag.org/content/early/2020/06/15/science.abc7424)
mAb-94	Ab	SARS-CoV2	229E, HKU1, NL63, OC43, SARS-CoV1			S; Unk	B-cells; SARS-CoV1 Human Patient	965	QVQLVQSGAEVKKPGSSVKVSCKASGG MFTDYAISWVRQAPGQRLEWMGGIM PGLGSPAYAQIFRDRATISADVSTSTAYL ELTSLKPEDTAVYYCARDPSILNTGNHH WYDLDIWGQGTTVTVSS	2032	DIQLTQSPLSLPVGLGQSASISCRSSQR VVHTDGNTYLNWYHQRPGQSPRRLIY KVSNRDSGVPDRFSGSGSGTDFTLRIS RVEAEDVGVYYCMQSTDWPRTFGQG TKLEIK	IGHV1-69 (Human)	IGHJ6 (Human)	IGKV2-30 (Human)	IGKJ2 (Human)	3071	ARDPSILNTG NHHWYDLDI	4261	MQSTDWP RT	Anna Wec et al., 2020 (https://science.sciencemag.org/content/early/2020/06/15/science.abc7424)
mAb-95	Ab	SARS-CoV1, SARS-CoV2	229E, HKU1, NL63, OC43			S; Unk	B-cells; SARS-CoV1 Human Patient	966	QVQLVQSGAEVKKPGSSVKVSCKASGG MFTDYAISWVRQAPGQRPEWMGGIM PGLGSPAYAQIFRGRATISADLSTSTAYLE LTSLKPEDTAVYYCARDPSILNTGNHHW YDLDIWGQGTMVTVSS	2033	DIVLTQSPLSLPVGLGQSASISCRSSQR VVHTDGNTYLHWFHQRPGQSPRRLIY KVSNRDSGVPDRFSGSGSGTDFTLRIS RVEAEDVGVYYCMQGTEWPRTFGQ GTKLEIK	IGHV1-69 (Human)	IGHJ3 (Human)	IGKV2-30 (Human)	IGKJ2 (Human)	3072	ARDPSILNTG NHHWYDLDI	4262	MQGTEW PRT	Anna Wec et al., 2020 (https://science.sciencemag.org/content/early/2020/06/15/science.abc7424)
mAb-96	Ab	SARS-CoV2	229E, HKU1, NL63, OC43, SARS-CoV1			S; Unk	B-cells; SARS-CoV1 Human Patient	967	QVTLKESGGGLVQPGGSLRLSCAASGFT VNSYGMSWVRQAPGKGLEWVSGFKSR SDRPDYAESVKGRFTISRDTSKNTVYLE MIGLRAEDTATYYCVRMDWMEWMKY YFDSWGQGALVTVSS	2034	ETTLTQSPVTLSVSPGERATLSCRASQS VISNLAWYQQKPGQAPRLLIFGASTRA TGVPARFSGSGSGTEFTLTISSLQSEDF AVYYCQQYNNWPSLTFGGGTKLEIK	IGHV3-66 (Human)	IGHJ5 (Human)	IGKV3-15 (Human)	IGKJ4 (Human)	3073	VRMDWME WMKYYFDS	4263	QQYNNWP SLT	Anna Wec et al., 2020 (https://science.sciencemag.org/content/early/2020/06/15/science.abc7424)
mAb-97	Ab	SARS-CoV1 (weak), SARS-CoV2	229E, HKU1, NL63, OC43			S; Unk	B-cells; SARS-CoV1 Human Patient	968	QVQLVQSGAEVKKPGSSVKVSCKASGG MISDYAISWVRQAPGQRLEWMGGIMP AFGSPGYAQIFRGRATISADVSTNTAYLE LTSLNPDDTAVYYCARDPSILNTGNHHW YDLDMWGQGTMVTVSS	2035	DIQVTQSPSLSPVGLGQSASISCRSSQR VVHTDGNTYLNWFHQRPGQSPRRLIY KVSNRDSGVPDRFSGSGSGTDFTLRIS RVEAEDVGVYYCMQATEWPRTFGQG TKVDIK	IGHV1-69 (Human)	IGHJ3 (Human)	IGKV2-30 (Human)	IGKJ3 (Human)	3074	ARDPSILNTG NHHWYDLD M	4264	MQATEWP RT	Anna Wec et al., 2020 (https://science.sciencemag.org/content/early/2020/06/15/science.abc7424)
mAb-98	Ab	SARS-CoV1, SARS-CoV2 (weak)	229E, HKU1, NL63, OC43			S; Unk	B-cells; SARS-CoV1 Human Patient	969	QVQLVESGGSVVQPGTSLKLSCAGSAGL TITRYAMHWVRQAPGKGLEWVALVSH DGIHIGYSDSVRGRFTISRDNSRNTLYLQ MDGLRPEDTAVYYCVRDDVLQHSRPSG PGYFVSWGQGTLVTVSS	2036	EIVMTQSPATLSLSPGERATLSCRASQS VSTFLGWYQQRPGQPPRLLIYDASYR APDIPVRFSGSGSGTDFTLTINSLEPED SAVYYCQQRSDGYNFGPGTKLEIK	IGHV3-30 (Human)	IGHJ5 (Human)	IGKV3-11 (Human)	IGKJ2 (Human)	3075	VRDDVLQHS RPSGPGYFVS	4265	QQRSDGY N	Anna Wec et al., 2020 (https://science.sciencemag.org/content/early/2020/06/15/science.abc7424)
mAb-99	Ab	SARS-CoV2 (weak)	229E, HKU1, NL63, OC43, SARS-CoV1			S; Unk	B-cells; SARS-CoV1 Human Patient	970	QVQLQESGPGLVKPSGTLSLTCAVSGAS VSSDHWWSWVRQSPGKGLEWIGEVY HSGSTNYNPSLKSRVTISLDQSNNQFSLK LTSVTAADTAIYYCATMWGGLCTASNCY GNPMDVWGQGTTVTVSS	2037	QPVLTQPPSVSVSPGQTARITCSGDAL PRRYAYWYQQRSGQAPVLVIYEDNKR PSGIPERFSAFSSGTRATLTISGAQVED QADYYCYSTDSTANYKVFGGGTKLTVL	IGHV4-4 (Human)	IGHJ6 (Human)	IGLV3-10 (Human)	IGLJ3 (Human)	3076	ATMWGGLCT ASNCYGNPM DV	4266	YSTDSTAN YKV	Anna Wec et al., 2020 (https://science.sciencemag.org/content/early/2020/06/15/science.abc7424)
mBG17	Ab	SARS-CoV1, SARS-CoV2, NL63 (weak)	229E			N	Immunised Mouse	971	EVKLEESGGGLVQPGGSMKFSCVASGF TFSDYWMNWVRQSPDKGLEWVAEIRL KSNNYATHYAASVKGRFTISRDDSKSSVY LQMNNLRAEDSGIYYCTRSAMDYWGQ GTSVTVSS	2038	DIVMSQSPSSLAVSVGEKITMSCKSSQ SLLYTSDQKNYLAWFQQKPGQSPKLLI FWASTRDSGVPDRFTGSGSGTDFTLTI SSVKAEDLAVYYCQQFYNYPRTFGGG TKLEIK	IGHV6-6 (Mouse)	IGHJ4 (Mouse)	IGKV8-30 (Mouse)	IGKJ1 (Mouse)	3077	TRSAMDY	4267	QQFYNYPR T	James Terry et al., 2020 (https://www.biorxiv.org/content/10.1101/2020.09.03.280370v1.full)
mBG21	Ab	SARS-CoV1, SARS-CoV2, NL63 (weak)	229E			N	Immunised Mouse	972	QIQLVQSGPELKKPGETVKISCKASGYTF TDYSMHWVKQAPGKGSKWMGWINTE TGEPTYADDFKGRFAFSLETSASTAYLQI NNLKNEDTATYFCALRRWGQGTLVTVS S	2039	IVMTQTPKFLLVSAGDRVTITCKASQS VSNDVAWFQQKPGQSPKKLLIYFASN RYTGVPDRFTGSGYGTDFTFTITTVQA EDLAVYFCQQDYSSPWTFGGGTKLEIK	IGHV9-2-1 (Mouse)	IGHJ3 (Mouse)	IGKV6-32 (Mouse)	IGKJ1 (Mouse)	3078	ALRR	4268	QQDYSSP	James Terry et al., 2020 (https://www.biorxiv.org/content/10.1101/2020.09.03.280370v1.full)
mBG22	Ab	SARS-CoV1, SARS-CoV2, NL63 (weak)	229E			N	Immunised Mouse	973	QIQLVQSGPELKKPGETVKISCKASGYTF TDYSMHWVKQAPGKGSKWMGWINTE TGEPTYADDFKGRFAFSLETSASTAYLQI NNLKNEDTATYFCALRRWGQGTLVTVS A	2040	IVMTQTPKFLLVSAGDRVTITCKASQS VSNDVAWFQQKPGQSPKLLIYFASNR YTGVPDRFTGSGYGTDFTFTITTVQAE DLAVYFCQQDYSSPWTFGGGTKLEIK	IGHV9-2-1 (Mouse)	IGHJ3 (Mouse)	IGKV6-32 (Mouse)	IGKJ1 (Mouse)	3079	ALRR	4269	QQDYSSP	James Terry et al., 2020 (https://www.biorxiv.org/content/10.1101/2020.09.03.280370v1.full)
mBG57	Ab	SARS-CoV1, SARS-CoV2, NL63 (weak)	229E			N	Immunised Mouse	974	QIQLVQSGPELKKPGETVKISCKASGYTF TDYSMHWVKQAPGKGSKWMGWINTE TGEPTYADDFKGRFAFSLETSASTAYLQI NNLKNEDTATYFCALRRWGQGTLVTVS A	2041	DIVMTQAAPSEPVTPGESVSISCGSSK SLLHSNDNTYLYWFLQRPGQSPQLLIY RMSNLASGVPDRFTGSGSGTAFTLRIS RVEAEDVGVYYCMQHLENPLGVRWR HQAGNQT	IGHV9-2-1 (Mouse)	IGHJ3 (Mouse)	IGKV2-137 (Mouse)	IGKJ5 (Mouse)	3080	ALRR	4270	MQHLENP LGVR	James Terry et al., 2020 (https://www.biorxiv.org/content/10.1101/2020.09.03.280370v1.full)

mBG67	Ab	SARS-CoV1, SARS-CoV2, NL63 (weak)	229E			N	Immunised Mouse	975	EVQLVESGGGLVQPGGSLKLSCAASGFT FSNYGMSWVRQTPDKRLELVATINRNG GSTYYLDSVKVRFTISRDNAKSTLFLQLSS LKSDDTAMYYCARIYDFDEDYFDVWGA GTTVTVSS	2042	QIVLTQSPAIMSASLGERVTMTCTASS SVSSSYLHWYQQKPGSSPKLWIYSTSN LASGVPARFSGSGSGTSYSLTISSMEAE DAATYYCLQYHRSPWTFGGGTKLEIK	IGHV5-6-3 (Mouse)	IGHJ1 (Mouse)	IGKV4-74 (Mouse)	IGKJ1 (Mouse)	3081	ARIYDFDEDY FDV	4271	LQYHRSP	James Terry et al., 2020 (https://www.biorxiv.org/content/10.1101/2020.09.03.280370v1.full)
MD17	Ab	SARS-CoV2		SARS-CoV2 (weak)		S; RBD	Phage Display Library (Antibody, human, immune - CoV2)		ND		ND	IGHV3-64 (Human)	ND	IGKV1-39 (Human)	ND	3082	VKDQDSSSW YDAFDI	4272	QQSYTTPL T	Tal Noy-Porat et al., 2020 (https://www.biorxiv.org/content/10.1101/2020.05.20.106609v2)
MD29	Ab	SARS-CoV2		SARS-CoV2 (weak)		S; RBD	Phage Display Library (Antibody, human, immune - CoV2)		ND		ND	IGHV3-64 (Human)	ND	IGKV1-39 (Human)	ND	3083	VKDQDSSSW YDAFDI	4273	HQTYTSPY T	Tal Noy-Porat et al., 2020 (https://www.biorxiv.org/content/10.1101/2020.05.20.106609v2)
MD45	Ab	SARS-CoV2		SARS-CoV2		S; RBD	Phage Display Library (Antibody, human, immune - CoV2)		ND		ND	IGHV3-53 (Human)	ND	IGKV3-20 (Human)	ND	3084	ARDLSVRGG MDV	4274	QQYGVSPE II	Tal Noy-Porat et al., 2020 (https://www.biorxiv.org/content/10.1101/2020.05.20.106609v2)
MD47	Ab	SARS-CoV2		SARS-CoV2 (weak)		S; RBD	Phage Display Library (Antibody, human, immune - CoV2)		ND		ND	IGHV3-23 (Human)	ND	IGLV3-21 (Human)	ND	3085	AKDLVTAPSY EAFDI	4275	QVWDSSS HHVV	Tal Noy-Porat et al., 2020 (https://www.biorxiv.org/content/10.1101/2020.05.20.106609v2)
MD62	Ab	SARS-CoV2		SARS-CoV2		S; RBD	Phage Display Library (Antibody, human, immune - CoV2)		ND		ND	IGHV3-53 (Human)	ND	IGKV1-12 (Human)	ND	3086	ARDLQYYGM DV	4276	QQANSFPL T	Tal Noy-Porat et al., 2020 (https://www.biorxiv.org/content/10.1101/2020.05.20.106609v2)
MD63	Ab	SARS-CoV2			SARS-CoV2	S; RBD	Phage Display Library (Antibody, human, immune - CoV2)		ND		ND	IGHV3-64 (Human)	ND	IGKV1-39 (Human)	ND	3087	VKDQDSNSW YDAFDI	4277	QQSYSTPY T	Tal Noy-Porat et al., 2020 (https://www.biorxiv.org/content/10.1101/2020.05.20.106609v2)
MD65	Ab	SARS-CoV2		SARS-CoV2		S; RBD	Phage Display Library (Antibody, human, immune - CoV2)		ND		ND	IGHV3-66 (Human)	ND	IGKV3-20 (Human)	ND	3088	ARDLAVAGAF DI	4278	QQYGSSPL T	Tal Noy-Porat et al., 2020 (https://www.biorxiv.org/content/10.1101/2020.05.20.106609v2)
MD67	Ab	SARS-CoV2		SARS-CoV2		S; RBD	Phage Display Library (Antibody, human, immune - CoV2)		ND		ND	IGHV3-53 (Human)	ND	IGKV3-20 (Human)	ND	3089	ARDLSVRGG MDV	4279	QQFGSSPL T	Tal Noy-Porat et al., 2020 (https://www.biorxiv.org/content/10.1101/2020.05.20.106609v2)
mNb6	Nb	SARS-CoV2		SARS-CoV2		S; RBD	Yeast Display Library (scFv, human)		ND		ND	ND	ND	ND	ND		ND		ND	Michael Schoof et al., 2020 (https://www.biorxiv.org/content/10.1101/2020.08.08.238469v1.full.pdf)
mNb6-tri	Nb	SARS-CoV2		SARS-CoV2		S; RBD	Yeast Display Library (scFv, human)		ND		ND	ND	ND	ND	ND		ND		ND	Michael Schoof et al., 2020 (https://www.biorxiv.org/content/10.1101/2020.08.08.238469v1.full.pdf)
MnC1t3p1_G9	Ab	SARS-CoV2		SARS-CoV2		S; RBD	B-cells; SARS-CoV2 Human Patient	976	EVQLLESGGGLVQPGGSLRLSCAASGFT FRNYAMTWVRQAPGKGLEWVSGISDS GDRTYNADSVKGRFSISRDNSKNTLHLQ MNSLRAEDTAVYYCALASGSYFGGANY WGQGTLVTVSS	2043	QAVVTQEPSLTVSPGGTVTLTCGSSTG PVTSDHYPYWFQQKPGQAPTTLIYDT NNKHSWTPARFSGSLLGGKAALTLSG AQPEDEAEYYCLLSYTGARVFGGGTKL TVL	IGHV3-23 (Human)	IGHJ4 (Human)	IGLV7-46 (Human)	IGLJ3 (Human)	3090	ALASGSYFGG ANY	4280	LLSYTGAR V	Christoph Kreer et al., 2020 (https://doi.org/10.1016/j.cell.2020.06.044)
MnC2t1p1_A3	Ab	SARS-CoV2		SARS-CoV2		S; RBD	B-cells; SARS-CoV2 Human Patient	977	EVQLVESGGGLVQPGGSLRLSCAASGFT VSSNYMSWVRQAPGRGLEWVSVIYSG GSTFYADSVKGRFTISRDNSKNTLYLQM NSLRPEDTAVYYCATGARFGESPFDYW GQGTLVTVSS	2044	DIQMTQSPSSVSASVGDRVTITCRASQ GISSWLAWYQQKPGKAPKLLIYAASSL QSGVPSRFSGSGSGTDFTLTISSLQPED FATYYCQQANSFPGTFGQGTKVEIK	IGHV3-66 (Human)	IGHJ4 (Human)	IGKV1D-12 (Human)	IGKJ1 (Human)	3091	ATGARFGESP FDY	4281	QQANSFP GT	Christoph Kreer et al., 2020 (https://doi.org/10.1016/j.cell.2020.06.044)
MnC2t1p1_C5	Ab	SARS-CoV2		SARS-CoV2		S; RBD	B-cells; SARS-CoV2 Human Patient	978	EVQLVESGGGLVQPGGSLRLSCAASGFT VSSNYMSWVRQAPGKGLEWVSVIYSG GSTYYADSVKGRFTISRDNSKNTLYLQM NSLRAEDTAVYYCATGARFGESPFDYW GQGTLVTVSS	2045	DIQMTQSPSSVSASVGDRVTITCRASQ GISSWLAWYQQKPGKAPKLLIYAASSL QSGVPSRFSGSGSGTDFTLTISSLQPED FATYYCQQANSFPGTFGQGTKVEIK	IGHV3-66 (Human)	IGHJ4 (Human)	IGKV1D-12 (Human)	IGKJ1 (Human)	3092	ATGARFGESP FDY	4282	QQANSFP GT	Christoph Kreer et al., 2020 (https://doi.org/10.1016/j.cell.2020.06.044)

MnC2t2p1_C11	Ab	SARS-CoV2		SARS-CoV2		S; RBD	B-cells; SARS-CoV2 Human Patient	979	QVQLVQSGAEVKKPGSSVKVSCKASGGTFSRYTIIWVRQAPGQGLEWMGRIIPILDIANYAQKFQGRVTITADKSTSTAYMELSSLRSEDTAVYYCAREGGLDYFGSRNSGWTYTWFDPWGQGTLVTVSS	2046	DIQMTQSPSSLSASVGDRVTITCRASQNISSYLNWYQQKPGKAPNLLIYAASSLQSGVPPRFSGSGSGTDFTLTISSLQPEDFATYYCQQSYSTLYSFGQGTKLEIK	IGHV1-69 (Human)	IGHJ5 (Human)	IGKV1-39 (Human)	IGKJ2 (Human)	3093	AREGGLDYFGSRNSGWTYTWFDP	4283	QQSYSTLYS	Christoph Kreer et al., 2020 (https://doi.org/10.1016/j.cell.2020.06.044)
MnC4t1p1_A10	Ab	SARS-CoV2		SARS-CoV2		S; RBD	B-cells; SARS-CoV2 Human Patient	980	QLQVQESGPGLVKPSETLSLTCTVSGASISSNHYFWGWIRQPPGKGLAWIGSMHYSGSTYYNPSLKSRVTISVDTSKNQLSLKLSSVTAADTAVYYCARGVNYYDRNGYYRNDGFDIRGQGTMVTVSS	2047	DIQMTQSPSSLSASVGDRVTITCRASQGIRNDLGWYEQKPGKAPKRLIYAASSLESGVPSRFSGSGSGTEFTLTISSLQPEDFATYYCLQHNTYPFTFGPGTRVDIK	IGHV4-39 (Human)	IGHJ3 (Human)	IGKV1-17 (Human)	IGKJ3 (Human)	3094	ARGVNYYDRNGYYRNDGFDI	4284	LQHNTYPFT	Christoph Kreer et al., 2020 (https://doi.org/10.1016/j.cell.2020.06.044)
MnC4t1p1_A11	Ab	SARS-CoV2		SARS-CoV2		S; RBD	B-cells; SARS-CoV2 Human Patient	981	EVQLVESGGGLVQPGGSLRLSCAASGFTFSSYSMNWVRQAPGKGLEWVSYISSSSNTRYYTDSVMGRFTISRDNAKNSLFLQMNSLRAEDTAVYYCASSKGFCSGGSCSDYWGQGTLVTVSS	2048	EIVLTQSPGTLSLSPGERATLSCRASQSVSSSYLAWYQQKPGQAPRLLIYGVSSRATGIPDRFSGSGSGTDFTLTISRLEPEDFVVYYCHQYGSSPWTFGQGTKVEIK	IGHV3-48 (Human)	IGHJ4 (Human)	IGKV3-20 (Human)	IGKJ1 (Human)	3095	ASSKGFCSGGSCSDY	4285	HQYGSSPWT	Christoph Kreer et al., 2020 (https://doi.org/10.1016/j.cell.2020.06.044)
MnC4t2p1_B3	Ab	SARS-CoV2		SARS-CoV2		S; RBD	B-cells; SARS-CoV2 Human Patient	982	EVQLVESGGHLVQPGRSLRLSCAASGFTFDDYAMHWVRQVPGKGLEWVSGISWNGGILDYADSVKGRFTISRDNAKNSLYLHMRSLRTDDTALYYCAKDLRRQDYYADWYFDLWGRGTLVTVSS	2049	DIQMIQSPSSVSASVGDRVTITCRASQGISSWLAWYQQKPGKAPKLLIYAASTLSAVPSRFSGSGSGTDFTLTISSLQPEDFATYYCQQGNSFPFTFGPGTIVDV	IGHV3-9 (Human)	IGHJ2 (Human)	IGKV1-12 (Human)	IGKJ3 (Human)	3096	AKDLRRQDYYADWYFDL	4286	QQGNSFPFT	Christoph Kreer et al., 2020 (https://doi.org/10.1016/j.cell.2020.06.044)
MnC4t2p1_D10	Ab	SARS-CoV2		SARS-CoV2		S; RBD	B-cells; SARS-CoV2 Human Patient	983	QLQVQESGPGLVKPSETLSLTCTVSGASISSNHYFWGWIRQPPGKGLAWIGSMHYSGSTYYNPSLKSRVTISVDTSKNQLSLKLSSVTAADTAVYYCARGVNYYDRNGYYRNDGFDIRGQGTMVTVSS	2050	DIQMTQSPSSLSASVGDRVTITCRASQGIRNDLGWYEQKPGKAPKRLIYAASSLESGVPSRFSGSGSGTEFTLTISSLQPEDFATYYCLQHNTYPFTFGPGTRVDIK	IGHV4-39 (Human)	IGHJ3 (Human)	IGKV1-17 (Human)	IGKJ3 (Human)	3097	ARGVNYYDRNGYYRNDGFDI	4287	LQHNTYPFT	Christoph Kreer et al., 2020 (https://doi.org/10.1016/j.cell.2020.06.044)
MnC4t2p1_E6	Ab	SARS-CoV2		SARS-CoV2		S; RBD	B-cells; SARS-CoV2 Human Patient	984	EVQLVESGGHLVQPGRSLRLSCAASGFTFDDYAMHWVRQVPGKGLEWVSGISWNGGILGYADSVKGRFTISRDNAKNSLYLQMRSLRTDDTALYYCAKDLRRQDYYADWYFDLWGRGTLVTVSS	2051	DIQMTQSPSSVSASVGDRVTITCRASQGISSWLAWYQQKPGKAPKLLIYAASTLLSAVPSRFSGSGSGTDFTLTISSLQPEDFATYYCQQGNSFPFTFGPGTKVDV	IGHV3-9 (Human)	IGHJ2 (Human)	IGKV1-12 (Human)	IGKJ3 (Human)	3098	AKDLRRQDYYADWYFDL	4288	QQGNSFPFT	Christoph Kreer et al., 2020 (https://doi.org/10.1016/j.cell.2020.06.044)
MnC4t2p1_F5	Ab	SARS-CoV2		SARS-CoV2		S; RBD	B-cells; SARS-CoV2 Human Patient	985	QLQVQESGPGLVKPSETLSLTCTVSGASISSNHYFWGWIRQPPGKGLAWIGSMHYSGSTYYNPSLKSRVTISVDTSKNQLSLKLSSVTAADTAVYYCARGVNYYDRNGYYRNDGFDIRGQGTMVTVSS	2052	DIQMTQSPSSLSASVGDRVTITCRASQGIRNDLGWYEQKPGKAPKRLIYAASSLESGVPSRFSGSGSGTEFTLTISSLQPEDFATYYCLQHNTYPFTFGPGTRVDIK	IGHV4-39 (Human)	IGHJ3 (Human)	IGKV1-17 (Human)	IGKJ3 (Human)	3099	ARGVNYYDRNGYYRNDGFDI	4289	LQHNTYPFT	Christoph Kreer et al., 2020 (https://doi.org/10.1016/j.cell.2020.06.044)
MnC4t2p2_A4	Ab	SARS-CoV2		SARS-CoV2		S; RBD	B-cells; SARS-CoV2 Human Patient	986	QVQLVQSGSELKKPGASVKISCKASGYIFINYAMNWVRQAPGQGLEWMGWINTNTGNPTYAQDFTGRFVFSLDTSLSTAYLQISSLEAEDTAVYYCAKIGSRNSLGVWGQGTLVTVSA	2053	EIVLTQSPGTLSLSPGERATLSCRASHSVDRSYLAWYQQKPGLAPRLLIYGASSRATGIPDRFSGSGSGTDFTLTISRLEPEDFALYYCQHFGTSSVTFGRGTRLEIK	IGHV7-4-1 (Human)	IGHJ4 (Human)	IGKV3-20 (Human)	IGKJ5 (Human)	3100	AKIGSRNSLGV	4290	QHFGTSSVT	Christoph Kreer et al., 2020 (https://doi.org/10.1016/j.cell.2020.06.044)
MnC5t2p1_G1	Ab	SARS-CoV2		SARS-CoV2		S; RBD	B-cells; SARS-CoV2 Human Patient	987	QMQLVQSGPEVKKPGTSVKVSCKASGFTFTSSAVQWVRQARGQRLEWIGWIVVGSGNTDYAQKFQERVTITRDVSTSTAYMELSSLRSEDTAVYYCAAPRCSGGSCYDGFDIWGQGTMVTVSS	2054	EIVLTQSPGTLSLSPGERATLSCRASQSVSSSYLAWYQHKPGQAPRLLICGASSRATGIPDRFSGSGSGTGFTLTISRLEPEDFAVYYCQQYGSSPWTFGQGTKVEIK	IGHV1-58 (Human)	IGHJ3 (Human)	IGKV3-20 (Human)	IGKJ1 (Human)	3101	AAPRCSGGSCYDGFDI	4291	QQYGSSPWT	Christoph Kreer et al., 2020 (https://doi.org/10.1016/j.cell.2020.06.044)
MR10	Nb	SARS-CoV2				S; RBD	Phage Display Library (Nanobody, non-immune)	988	QVQLVESGGGLVQAGGSLRLSCAASGFPVANTWMEWYRQAPGKEREWVAAITSYGYRTYYADSVKGRFTISRDNAKNTVYLQMNSLKPEDTAVYYCNVKDEGATTKVYDYWGQGTQVTVSS		N/A	IGHV3S53 (Alpaca)	IGHJ4 (Alpaca)	N/A	N/A	3102	NVKDEGATTKVYDY		N/A	Tingting Li et al., 2020 (https://www.biorxiv.org/content/10.1101/2020.06.09.143438v1)
MR14	Nb	SARS-CoV2				S; RBD	Phage Display Library (Nanobody, non-immune)	989	QVQLVESGGGLVQAGGSLRLSCAASGFPVMYTHMHWYRQAPGKEREWVAAIVSLGEYTTYADSVKGRFTISRDNAKNTVYLQMNSLKPEDTAVYYCNVKDWGAANKYYDYWGQGTQVTVSS		N/A	IGHV3S53 (Alpaca)	IGHJ4 (Alpaca)	N/A	N/A	3103	NVKDWGAANKYYDY		N/A	Tingting Li et al., 2020 (https://www.biorxiv.org/content/10.1101/2020.06.09.143438v1)
MR17	Nb	SARS-CoV2				S; RBD	Phage Display Library (Nanobody, non-immune)	990	QVQLVESGGGLVQAGGSLRLSCAASGFPVEVWRMEWYRQAPGKEREGVAAIESYGHGTRYADSVKGRFTISRDNAKNTVYLQMNSLKPEDTAVYYCNVKDDGQLAYHYDYWGQGTQVTVSS		N/A	IGHV3S53 (Alpaca)	IGHJ4 (Alpaca)	N/A	N/A	3104	NVKDDGQLAYHYDY		N/A	Tingting Li et al., 2020 (https://www.biorxiv.org/content/10.1101/2020.06.09.143438v1)
MR17_K56W	Nb	SARS-CoV2				S; RBD	Derived from MR17	991	QVQLVESGGGLVQAGGSLRLSCAASGFPVEVWRMEWYRQAPGKEREGVAAIESYGWGTRYADSVKGRFTISRDNAKNTVYLQMNSLKPEDTAVYYCNVKDDGQLAYHYDYWGQGTQVTVSS		N/A	IGHV3S53 (Alpaca)	IGHJ4 (Alpaca)	N/A	N/A	3105	NVKDDGQLAYHYDY		N/A	Tingting Li et al., 2020 (https://www.biorxiv.org/content/10.1101/2020.06.09.143438v1)
MR17_K99W	Nb	SARS-CoV2				S; RBD	Derived from MR17	992	QVQLVESGGGLVQAGGSLRLSCAASGFPVEVWRMEWYRQAPGKEREGVAAIESYGHGTRYADSVKGRFTISRDNAKNTVYLQMNSLKPEDTAVYYCNVWDDGQLAYHYDYWGQGTQVTVSS		N/A	IGHV3S53 (Alpaca)	IGHJ4 (Alpaca)	N/A	N/A	3106	NVWDDGQLAYHYDY		N/A	Tingting Li et al., 2020 (https://www.biorxiv.org/content/10.1101/2020.06.09.143438v1)

MR17_K99Y	Nb	SARS-CoV2				S; RBD	Derived from MR17	993	QVQLVESGGGLVQAGGSLRLSCAASGFPVEVWRMEWYRQAPGKEREGVAAIESYGHGTRYADSVKGRFTISRDNAKNTVYLQMNSLKPEDTAVYYCNVYDDGQLAYHYDYWGQGTQVTVSS		N/A	IGHV3S53 (Alpaca)	IGHJ4 (Alpaca)	N/A	N/A	3107	NVYDDGQLAYHYDY		N/A	Tingting Li et al., 2020 (https://www.biorxiv.org/content/10.1101/2020.06.09.143438v1)
MR2	Nb	SARS-CoV2				S; RBD	Phage Display Library (Nanobody, non-immune)	994	QVQLVESGGGLVQAGGSLRLSCAASGFPVYFSYMAWYRQAPGKEREWVAAINSEGDSTTYADSVKGRFTISRDNAKNTVYLQMNSLKPEDTAVYYCNVKDYGWYNSQYDYWGQGTQVTVSS		N/A	IGHV3S53 (Alpaca)	IGHJ4 (Alpaca)	N/A	N/A	3108	NVKDYGWYNSQYDY		N/A	Tingting Li et al., 2020 (https://www.biorxiv.org/content/10.1101/2020.06.09.143438v1)
MR3	Nb	SARS-CoV2				S; RBD	Phage Display Library (Nanobody, non-immune)	995	QVQLVESGGGLVQAGGSLRLSCAASGFPVNAHFMYWYRQAPGKEREWVAAIYSYGRTLYADSVKGRFTISRDNAKNTVYLQMNSLKPEDTAVYYCNVKDYGAASWEYDYWGQGTQVTVSS		N/A	IGHV3S53 (Alpaca)	IGHJ4 (Alpaca)	N/A	N/A	3109	NVKDYGAASWEYDY		N/A	Tingting Li et al., 2020 (https://www.biorxiv.org/content/10.1101/2020.06.09.143438v1)
MR4	Nb	SARS-CoV2				S; RBD	Phage Display Library (Nanobody, non-immune)	996	QVQLVESGGGLVQAGGSLRLSCAASGFPMYAWEMAWYRQAPGKEREWVAAIRSMGVHTHYSDSVKGRFTISRDNAKNTVYLQMNSLKPEDTAVYYCNVKDFGGHQAYYDYWGQGTQVTVSS		N/A	IGHV3S53 (Alpaca)	IGHJ4 (Alpaca)	N/A	N/A	3110	NVKDFGGHQAYYDY		N/A	Tingting Li et al., 2020 (https://www.biorxiv.org/content/10.1101/2020.06.09.143438v1)
MR6	Nb	SARS-CoV2				S; RBD	Phage Display Library (Nanobody, non-immune)	997	QVQLVESGGGLVQAGGSLRLSCAASGFPVEDTWMEWYRQAPGKEREWVAAITSWGFKTYYADSVKGRFTISRDNAKNTVYLQMNSLKPEDTAVYYCNVKDEGDTSASYDYWGQGTQVTVSS		N/A	IGHV3S53 (Alpaca)	IGHJ4 (Alpaca)	N/A	N/A	3111	NVKDEGDTSASYDY		N/A	Tingting Li et al., 2020 (https://www.biorxiv.org/content/10.1101/2020.06.09.143438v1)
MR7	Nb	SARS-CoV2				S; RBD	Phage Display Library (Nanobody, non-immune)	998	QVQLVESGGGLVQAGGSLRLSCAASGFPVNSWMEWYRQAPGKEREWVAAITSYGYKTYYADSVKGRFTISRDNAKNTVYLQMNSLKPEDTAVYYCNVKDEGYFSDEYDYWGQGTQVTVSS		N/A	IGHV3S53 (Alpaca)	IGHJ4 (Alpaca)	N/A	N/A	3112	NVKDEGYFSDEYDY		N/A	Tingting Li et al., 2020 (https://www.biorxiv.org/content/10.1101/2020.06.09.143438v1)
MR8	Nb	SARS-CoV2				S; RBD	Phage Display Library (Nanobody, non-immune)	999	QVQLVESGGGLVQAGGSLRLSCAASGFPVEWAHMHWYRQAPGKEREWVAAIVSAGHYTVYADSVKGRFTISRDNAKNTVYLQMNSLKPEDTAVYYCNVKDWGSSNQYYDYWGQGTQVTVSS		N/A	IGHV3S53 (Alpaca)	IGHJ4 (Alpaca)	N/A	N/A	3113	NVKDWGSSNQYYDY		N/A	Tingting Li et al., 2020 (https://www.biorxiv.org/content/10.1101/2020.06.09.143438v1)
Nb11	Nb	SARS-CoV2		SARS-CoV2		S; RBD	Yeast Display Library (scFv, human)		ND		ND	ND	ND	ND	ND		ND		ND	Michael Schoof et al., 2020 (https://www.biorxiv.org/content/10.1101/2020.08.08.238469v1.full.pdf)
Nb11-59	Nb	SARS-CoV1, SARS-CoV2		SARS-CoV1, SARS-CoV2		S; RBD	Phage Display (Immunised Camel)		ND		ND	ND	ND	ND	ND		ND		ND	Junwei Gai et al., 2020 (https://www.biorxiv.org/content/10.1101/2020.08.09.242867v1.full.pdf)
Nb3	Nb	SARS-CoV2		SARS-CoV2		S; RBD	Yeast Display Library (scFv, human)		ND		ND	ND	ND	ND	ND		ND		ND	Michael Schoof et al., 2020 (https://www.biorxiv.org/content/10.1101/2020.08.08.238469v1.full.pdf)
Nb3-bi	Nb	SARS-CoV2		SARS-CoV2		S; RBD	Yeast Display Library (scFv, human)		ND		ND	ND	ND	ND	ND		ND		ND	Michael Schoof et al., 2020 (https://www.biorxiv.org/content/10.1101/2020.08.08.238469v1.full.pdf)
Nb3-tri	Nb	SARS-CoV2		SARS-CoV2		S; RBD	Yeast Display Library (scFv, human)		ND		ND	ND	ND	ND	ND		ND		ND	Michael Schoof et al., 2020 (https://www.biorxiv.org/content/10.1101/2020.08.08.238469v1.full.pdf)
Nb4-43	Nb	SARS-CoV2	SARS-CoV1	SARS-CoV2	SARS-CoV1	S; RBD	Phage Display (Immunised Camel)		ND		ND	ND	ND	ND	ND		ND		ND	Junwei Gai et al., 2020 (https://www.biorxiv.org/content/10.1101/2020.08.09.242867v1.full.pdf)

Nb6	Nb	SARS-CoV2		SARS-CoV2		S; RBD	Yeast Display Library (scFv, human)		ND		ND	ND	ND	ND	ND		ND		ND	Michael Schoof et al., 2020 (https://www.biorxiv.org/content/10.1101/2020.08.08.238469v1.full.pdf)
Nb6-tri	Nb	SARS-CoV2		SARS-CoV2		S; RBD	Yeast Display Library (scFv, human)		ND		ND	ND	ND	ND	ND		ND		ND	Michael Schoof et al., 2020 (https://www.biorxiv.org/content/10.1101/2020.08.08.238469v1.full.pdf)
NIH-CoVnb-101	Nb	SARS-CoV2				S; RBD	Immunised Llama	1000	DVQLQESGGDLVQPGGSLRLSCAASGFTLDYYAIGWFRQAPGKEREGVSCISSSDGSTYYADSVKGRFTSSRDNAKNTVYLQMNSLKPEDTAVYYCAAVPSTYYNGSYYYTCHPGGMDYWGKGTQVTVSS		N/A	IGHV3-3 (Alpaca)	IGHJ7 (Alpaca)	N/A	N/A	3114	AAVPSTYYNGSYYYTCHPGGMDY		N/A	Thomas Esparza et al., 2020 (https://www.biorxiv.org/content/10.1101/2020.07.24.219857v1)
NIH-CoVnb-102	Nb	SARS-CoV2				S; RBD	Immunised Llama	1001	DVQLQESGGGLVQPGGSLRLSCAVSGFTLDYYAIGWFRQAPGKEREGVSCISSSDGSTYYADSVKGRFTSSRDNAKNTVYLQMNSLKPEDTAVYYCAAVPSTYYSGTYYYNCHPGGMDYWGKGTQVTVSS		N/A	IGHV3-3 (Alpaca)	IGHJ7 (Alpaca)	N/A	N/A	3115	AAVPSTYYSGTYYYNCHPGGMDY		N/A	Thomas Esparza et al., 2020 (https://www.biorxiv.org/content/10.1101/2020.07.24.219857v1)
NIH-CoVnb-103	Nb	SARS-CoV2				S; RBD	Immunised Llama	1002	DVQLQESGGGLVQPGGSLRLSCAASGLTLDYYTIGWFRQAPGKEREGVSCISSSDDSTYYADSVKGRFTISRDNAKNTVYLQMNSLKPEDTAVYYCATAPGTYYKGSYYPMCHYYGMDYWGKGTQVTVSS		N/A	IGHV3-3 (Alpaca)	IGHJ7 (Alpaca)	N/A	N/A	3116	ATAPGTYYKGSYYPMCHYYGMDY		N/A	Thomas Esparza et al., 2020 (https://www.biorxiv.org/content/10.1101/2020.07.24.219857v1)
NIH-CoVnb-104	Nb	SARS-CoV2				S; RBD	Immunised Llama	1003	DVQLQESGGGLVQPGGSLRLSCAVSGFTLDYYAIGWFRQAPGKEREGVACISSSDGTTYYADSVKGRFTISRDNAKNTVYLQMNSLKPEDTAVYYCATRPLTYYSGSYYTTCSDYGMDYWGKGTLVTVSS		N/A	IGHV3-3 (Alpaca)	IGHJ7 (Alpaca)	N/A	N/A	3117	ATRPLTYYSGSYYTTCSDYGMDY		N/A	Thomas Esparza et al., 2020 (https://www.biorxiv.org/content/10.1101/2020.07.24.219857v1)
NIH-CoVnb-105	Nb	SARS-CoV2				S; RBD	Immunised Llama	1004	DVQLQESGGGLVQPGGSLRLSCAASGFTLDYYAIGWFRQAPGKEREGVSCISNSDGSTYYADSVKGRFTTSRDNAKNTVYLQMNSLKPEDTAVYYCAAVPSTYYSGSYYYTCHPGGMDYWGKGTQVTVSS		N/A	IGHV3-3 (Alpaca)	IGHJ7 (Alpaca)	N/A	N/A	3118	AAVPSTYYSGSYYYTCHPGGMDY		N/A	Thomas Esparza et al., 2020 (https://www.biorxiv.org/content/10.1101/2020.07.24.219857v1)
NIH-CoVnb-106	Nb	SARS-CoV2				S; RBD	Immunised Llama	1005	DVQLQESGGGLVQSGGSLRLSCAASGFTLDYYAIGWFRQAPGKEREGVSCISNSDGSTYYADSVKGRFTTSRDNAKNTVYLQMNSLKPEDTAVYYCAAVPSTYYSGSYYYTCHPGGMDYWGKGTQVTVSS		N/A	IGHV3-3 (Alpaca)	IGHJ7 (Alpaca)	N/A	N/A	3119	AAVPSTYYSGSYYYTCHPGGMDY		N/A	Thomas Esparza et al., 2020 (https://www.biorxiv.org/content/10.1101/2020.07.24.219857v1)
NIH-CoVnb-107	Nb	SARS-CoV2				S; RBD	Immunised Llama	1006	DVQLQESGGGLVQPGGSLRLSCAASGFTLDYYAIGWFRQAPGKEREGVSCISNSDGSTYYADSVKGRFTTSRDNAKNTVYLQMNSLKPEDTAVYYCAAVPSTYYSGSYYYTCHPGGMDYWGKGTLVTVSS		N/A	IGHV3-3 (Alpaca)	IGHJ7 (Alpaca)	N/A	N/A	3120	AAVPSTYYSGSYYYTCHPGGMDY		N/A	Thomas Esparza et al., 2020 (https://www.biorxiv.org/content/10.1101/2020.07.24.219857v1)
NIH-CoVnb-108	Nb	SARS-CoV2				S; RBD	Immunised Llama	1007	DVQLQESGGGLVQPGGSLRLSCAASGFTLDYYAIGWFRQAPGKEREGVSCISNSGGSTYYADSVKGRFTTSRDNAKNTVYLQMNSLKPEDTAVYYCAAVPSTYYSGSYYYTCHPGGMDYWGKGTQVTVSS		N/A	IGHV3-3 (Alpaca)	IGHJ7 (Alpaca)	N/A	N/A	3121	AAVPSTYYSGSYYYTCHPGGMDY		N/A	Thomas Esparza et al., 2020 (https://www.biorxiv.org/content/10.1101/2020.07.24.219857v1)
NIH-CoVnb-109	Nb	SARS-CoV2				S; RBD	Immunised Llama	1008	DVQLQESGGGLVQSGGSLRLSCAASGFTLDYYAIGWFRQAPGKEREGVSCITNSDGSTYYADSVKGRFTTSRDNAKNTVYLQMNSLKPEDTAVYYCASFPSTYYSGSYYYTCHPGGMDYWGKGTQVTVSS		N/A	IGHV3-3 (Alpaca)	IGHJ7 (Alpaca)	N/A	N/A	3122	ASFPSTYYSGSYYYTCHPGGMDY		N/A	Thomas Esparza et al., 2020 (https://www.biorxiv.org/content/10.1101/2020.07.24.219857v1)
NIH-CoVnb-110	Nb	SARS-CoV2				S; RBD	Immunised Llama	1009	DVQLQESGGGLVQPGGSLRLSCAASGFTLDYYAIGWFRQAPGKEREGVSCISSSDGSTYYADSVKGRFTISRDNAKNTVYLQMNSLKPDDTAVYYCAAALSEGGYTIDGSSWCYHSVYGMDYWGKGTQVTVSS		N/A	IGHV3-3 (Alpaca)	IGHJ7 (Alpaca)	N/A	N/A	3123	AAVPSTYYSGTYYYNCHPGAMHY		N/A	Thomas Esparza et al., 2020 (https://www.biorxiv.org/content/10.1101/2020.07.24.219857v1)

NIH-CoVnb-111	Nb	SARS-CoV2				S; RBD	Immunised Llama	1010	DVQLQESGGGSVEAGGSLRLSCAASGV TLDYYAIGWFRQAPGKEREGVSCISSSD GSTYYADSVKGRFTTSRDNAKNTVYLQ MNSLKPEDTADYYCAAVPSTYYSGTYYY NCHPGAMHYWGKGTQVTVSS		N/A	IGHV3-3 (Alpaca)	IGHJ7 (Alpaca)	N/A	N/A	3124	AAVPSTYYSG TYYYNCHPGA MHY		N/A	Thomas Esparza et al., 2020 (https://www.biorxiv.org/content/10.1101/2020.07.24.219857v1)
NIH-CoVnb-112	Nb	SARS-CoV2				S; RBD	Immunised Llama	1011	DVQLQESGGGLVQPGGSLRLSCAASGL TLDYYAIGWFRQAPGKEREGVSCISSSD GSTYYADSVKGRFTTSRDNAKNTVYLQ MNSLKPEDTAVYYCAAVPSTYYSGTYYY TCHPGGMDYWGKGTQVTVSS		N/A	IGHV3-3 (Alpaca)	IGHJ7 (Alpaca)	N/A	N/A	3125	AAVPSTYYSG TYYYTCHPGG MDY		N/A	Thomas Esparza et al., 2020 (https://www.biorxiv.org/content/10.1101/2020.07.24.219857v1)
NIH-CoVnb-113	Nb	SARS-CoV2				S; RBD	Immunised Llama	1012	DVQLQESGGGLVQPGGSLRLSCAASGL TLDYYAIGWFRQAPGKEREGVSCISSSD GSTYYADSVKGRFTTSRDNAKNTVYLQ MNSLKPEDTAVYYCAAVPSTYYSGTYYY TCHPGGMDYWGKGTLVTVSS		N/A	IGHV3-3 (Alpaca)	IGHJ7 (Alpaca)	N/A	N/A	3126	AAVPSTYYSG TYYYTCHPGG MDY		N/A	Thomas Esparza et al., 2020 (https://www.biorxiv.org/content/10.1101/2020.07.24.219857v1)
P2B-2F6	Ab	SARS-CoV2	SARS-CoV1	SARS-CoV2		S; RBD	B-cells; SARS-CoV2 Human Patient	1013	QVQLQESGPGLVKPSETLSLTCTVSGYSI SSGYYWGWIRQPPGKGLEWIGSIYHSG STYYNPSLKTRVTISVDTSKNQFSLKLSSV TAADTAVYYCARAVVGIVVVPAAGRRAF DIWGQGTMVTVSS	2055	QSALTQPPSASGSPGQSVTISCTGTSS DVGGYNYVSWYQQHPGKAPKLMIYE VSKRPSGVPDRFSGSKSGNTASLTVSG LQAEDEADYYCSSYAGSNNLVFGGGT KLTVL	IGHV4-38-2 (Human)	IGHJ3 (Human)	IGLV2-8 (Human)	IGLJ3 (Human)	3127	ARAVVGIVVV PAAGRRAFDI	4292	SSYAGSNN LV	Bin Ju et al., 2020 (https://www.nature.com/articles/s41586-020-2380-z)
S110	Ab	SARS-CoV1, SARS-CoV2		SARS-CoV1		S; RBD+non-RBD	B-cells; SARS-CoV1 Human Patient		ND		ND	IGHV3-30 (Human)	ND	IGKV2-30 (Human)	ND	3128	AKDRFQFARS WYGDYFDY	4293	MQGTHW PPT	Dora Pinto et al., 2020 (https://www.nature.com/articles/s41586-020-2349-y)
S124	Ab	SARS-CoV1, SARS-CoV2		SARS-CoV1		S; RBD	B-cells; SARS-CoV1 Human Patient		ND		ND	IGHV2-26 (Human)	ND	IGKV1-39 (Human)	ND	3129	ARINTAAYDY DSTTFDI	4294	QQSYSTPP T	Dora Pinto et al., 2020 (https://www.nature.com/articles/s41586-020-2349-y)
S303	Ab	SARS-CoV1, SARS-CoV2		SARS-CoV1		S; RBD	B-cells; SARS-CoV1 Human Patient		ND		ND	IGHV3-23 (Human)	ND	IGKV1-5 (Human)	ND	3130	ARERDDIFPM GLNAFDI	4295	QQYDTYS WT	Dora Pinto et al., 2020 (https://www.nature.com/articles/s41586-020-2349-y)
S304	Ab	SARS-CoV1, SARS-CoV2		SARS-CoV1, SARS-CoV2 (weak)		S; RBD	B-cells; SARS-CoV1 Human Patient		ND		ND	IGHV3-13 (Human)	ND	IGKV1-39 (Human)	ND	3131	ARGDSSGYYY YFDY	4296	QQSYVSPT YT	Dora Pinto et al., 2020 (https://www.nature.com/articles/s41586-020-2349-y)
S306	Ab	SARS-CoV1, SARS-CoV2		SARS-CoV1	SARS-CoV2	S; non-RBD	B-cells; SARS-CoV1 Human Patient		ND		ND	IGHV1-18 (Human)	ND	IGKV3-11 (Human)	ND	3132	ASDYFDSSGY YHSFDY	4297	QQRSNWP PGCS	Dora Pinto et al., 2020 (https://www.nature.com/articles/s41586-020-2349-y)
S309	Ab	SARS-CoV1, SARS-CoV2		SARS-CoV2 and SARS-CoV1		S; RBD	B-cells; SARS-CoV1 Human Patient	1014	QVQLVQSGAEVKKPGASVKVSCKASGY PFTSYGISWVRQAPGQGLEWMGWIST YNGNTNYAQKFQGRVTMTTDTSTTTGY MELRRLRSDDTAVYYCARDYTRGAWFG ESLIGGFDNWGQGTLVTVSS	2056	EIVLTQSPGTLSLSPGERATLSCRASQT VSSTSLAWYQQKPGQAPRLLIYGASSR ATGIPDRFSGSGSGTDFTLTISRLEPED FAVYYCQQHDTSLTFGGGTKVEIK	IGHV1-18 (Human)	IGHJ4 (Human)	IGKV3-20 (Human)	IGKJ4 (Human)	3133	ARDYTRGAW FGESLIGGFD N	4298	QQHDTSLT	Dora Pinto et al., 2020 (https://www.nature.com/articles/s41586-020-2349-y)
S310	Ab	SARS-CoV1, SARS-CoV2		SARS-CoV1		S; non-RBD	B-cells; SARS-CoV1 Human Patient		ND		ND	IGHV1-69 (Human)	ND	IGLV2-23 (Human)	ND	3134	ATRTYDSSGY RPYYYGLDV	4299	CSYAGSDT VI	Dora Pinto et al., 2020 (https://www.nature.com/articles/s41586-020-2349-y)
S315	Ab	SARS-CoV1, SARS-CoV2		SARS-CoV2 and SARS-CoV1		S; RBD	B-cells; SARS-CoV1 Human Patient		ND		ND	IGHV3-7 (Human)	ND	IGLV3-25 (Human)	ND	3135	ARDLWWND QAHYYGMDV	4300	QSADSSGT V	Dora Pinto et al., 2020 (https://www.nature.com/articles/s41586-020-2349-y)
Sb#1	Nb	SARS-CoV2				S; RBD	Phage Display Library (Nanobody, non-immune)	1015	QVQLVESGGGLVQAGGSLRLSCAASGF PVRKANMHWYRQAPGKEREWVAAIM SKGEQTVYADSVEGRFTISRDNAKNTVY LQMNSLKPEDTAVYYCRVFVGWHYFG QGTQVTVS		N/A	IGHV3-3 (Alpaca)	IGHJ4 (Alpaca)	N/A	N/A	3136	RVFVGWHY		N/A	Justin Walter et al., 2020 (https://www.biorxiv.org/content/10.1101/2020.04.16.045419v2)
Sb#10	Nb	SARS-CoV2				S; RBD	Phage Display Library (Nanobody, non-immune)	1016	QVQLVESGGGLVQAGGSLRLSCAASGF PVQSHYMRWYRQAPGKEREWVAAIES TGHHTAYADSVKGRFTISRDNAKNTVYL QMNSLKPEDTAVYYCTVYVGYEYHGQG TQVTVS		N/A	IGHV3-3 (Alpaca)	IGHJ4 (Alpaca)	N/A	N/A	3137	TVYVGYEY		N/A	Justin Walter et al., 2020 (https://www.biorxiv.org/content/10.1101/2020.04.16.045419v2)
Sb#11	Nb	SARS-CoV2				S; RBD	Phage Display Library (Nanobody, non-immune)	1017	QVQLVESGGGLVQAGGSLRLSCAASGF PVETENMHWYRQAPGKEREWVAAIYS HGMWTAYADSVKGRFTISRDNTKNTVY LQMNSLKPEDTAVYYCEVEVGKWYFGQ GTQVTVS		N/A	IGHV3-3 (Alpaca)	IGHJ4 (Alpaca)	N/A	N/A	3138	EVEVGKWY		N/A	Justin Walter et al., 2020 (https://www.biorxiv.org/content/10.1101/2020.04.16.045419v2)
Sb#12	Nb	SARS-CoV2				S; RBD	Phage Display Library (Nanobody, non-immune)	1018	QVQLVESGGGLVQAGGSLRLSCAASGF PVKASRMYWYRQAPGKEREWVAAIQS FGEVTWYADSVKGRFTISRDNAKNTVYL QMNSLKPEDTAVYYCYVWVGQEYWG QGTQVTVS		N/A	IGHV3-3 (Alpaca)	IGHJ5 (Alpaca)	N/A	N/A	3139	YVWVGQEY		N/A	Justin Walter et al., 2020 (https://www.biorxiv.org/content/10.1101/2020.04.16.045419v2)

Sb#13	Nb	SARS-CoV2				S; RBD	Phage Display Library (Nanobody, non-immune)	1019	QVQLVESGGGLVQAGGSLRLSCAASGF PVYASNMHWYRQAPGKEREWVAAIES QGYMTAYADSVKGRFTISRDNAKNTVY LQMNSLKPEDTAVYYCWVIVGEYYVGQ GTQVTVS		N/A	IGHV3-3 (Alpaca)	IGHJ4 (Alpaca)	N/A	N/A	3140	WVIVGEYY		N/A	Justin Walter et al., 2020 (https://www.biorxiv.org/content/10.1101/2020.04.16.045419v2)
Sb#14	Nb	SARS-CoV2				S; RBD	Phage Display Library (Nanobody, non-immune)	1020	QVQLVESGGGLVQAGGSLRLSCAASGF PVQAREMEWYRQAPGKEREWVAAIKS TGTYTAYAYSVKGRFTISRDNAKNTVYLQ MNSLKPEDTAVYYCYVYVGSSYIGQGTQ VTVS		N/A	IGHV3-3 (Alpaca)	IGHJ4 (Alpaca)	N/A	N/A	3141	YVYVGSSY		N/A	Justin Walter et al., 2020 (https://www.biorxiv.org/content/10.1101/2020.04.16.045419v2)
Sb#15	Nb	SARS-CoV2				S; RBD	Phage Display Library (Nanobody, non-immune)	1021	QVQLVESGGGLVQAGGSLRLSCAASGF PVKNFEMEWYRKAPGKEREWVAAIQS GGVETYYADSVKGRFTISRDNAKNTVYL QMNSLKPEDTAVYYCFVYVGRSYIGQGT QVTVS		N/A	IGHV3-3 (Alpaca)	IGHJ4 (Alpaca)	N/A	N/A	3142	FVYVGRSY		N/A	Justin Walter et al., 2020 (https://www.biorxiv.org/content/10.1101/2020.04.16.045419v2)
Sb#16	Nb	SARS-CoV2				S; RBD	Phage Display Library (Nanobody, non-immune)	1022	QVQLVESGGGLVQAGGSLRLSCAASGF PVAYKTMWWYRQAPGKEREWVAAIES YGIKWTRYADSVKGRFTISRDNAKNTVY LQMNSLKPEDTAVYYCIVWVGAQYHG QGTQVTVS		N/A	IGHV3S53 (Alpaca)	IGHJ4 (Alpaca)	N/A	N/A	3143	IVWVGAQY		N/A	Justin Walter et al., 2020 (https://www.biorxiv.org/content/10.1101/2020.04.16.045419v2)
Sb#17	Nb	SARS-CoV2				S; RBD	Phage Display Library (Nanobody, non-immune)	1023	QVQLVESGGGLVQAGGSLRLSCAASGF PVAGRNMWWYRQAPGKEREWVAAIY SSGTYTEYADSVKGRFTISRDNAKNTVYL QMNSLKPEDTAVYYCHVWVGSLYKGQ GTQVTVS		N/A	IGHV3-3 (Alpaca)	IGHJ4 (Alpaca)	N/A	N/A	3144	HVWVGSLY		N/A	Justin Walter et al., 2020 (https://www.biorxiv.org/content/10.1101/2020.04.16.045419v2)
Sb#18	Nb	SARS-CoV2				S; RBD	Phage Display Library (Nanobody, non-immune)	1024	QVQLVESGGGLVQAGGSLRLSCAASGF PVKHARMWWYRQAPGKEREWVAAID SHGDTTWYADSVKGRFTISRDNAKNTV YLQMNSLKPEDTAVYYCYVYVGASYWG QGTQVTVS		N/A	IGHV3-3 (Alpaca)	IGHJ4 (Alpaca)	N/A	N/A	3145	YVYVGASY		N/A	Justin Walter et al., 2020 (https://www.biorxiv.org/content/10.1101/2020.04.16.045419v2)
Sb#19	Nb	SARS-CoV2				S; RBD	Phage Display Library (Nanobody, non-immune)	1025	QVQLVESGGGLVQAGGSLRLSCAASGF PVNSHEMTWYRQAPGKEREWVAAIQS TGTVTEYADSVKGRFTISRDNAKNTVYL QMNSLKPEDTAVYYCYVYVGSSYLGQG TQVTVS		N/A	IGHV3-3 (Alpaca)	IGHJ4 (Alpaca)	N/A	N/A	3146	YVYVGSSY		N/A	Justin Walter et al., 2020 (https://www.biorxiv.org/content/10.1101/2020.04.16.045419v2)
Sb#2	Nb	SARS-CoV2				S; RBD	Phage Display Library (Nanobody, non-immune)	1026	QVQLVESGGGLVQAGGSLRLSCATSGF PVYQANMHWYRQAPGKEREWVAAIQ SYGDGTHYADSVKGRFTISRDNAKNTVY LQMNSLKPEDTAVYYCRAVYVGMHYFG QGTQVTVS		N/A	IGHV3-3 (Alpaca)	IGHJ4 (Alpaca)	N/A	N/A	3147	RAVYVGMHY		N/A	Justin Walter et al., 2020 (https://www.biorxiv.org/content/10.1101/2020.04.16.045419v2)
Sb#20	Nb	SARS-CoV2				S; RBD	Phage Display Library (Nanobody, non-immune)	1027	QVQLVESGGGLVQAGGSLRLSCAASGF PVEQREMEWYRQAPGKEREWVAAIDS NGNYTFYADSVKGRFTISRDNAKNTVYL QMNSLKPEDTAVYYCVYVGKSYIGQGT QVTVS		N/A	IGHV3-3 (Alpaca)	IGHJ4 (Alpaca)	N/A	N/A	3148	YVYVGKSY		N/A	Justin Walter et al., 2020 (https://www.biorxiv.org/content/10.1101/2020.04.16.045419v2)
Sb#21	Nb	SARS-CoV2				S; RBD	Phage Display Library (Nanobody, non-immune)	1028	QVQLVESGGGLVQAGGSLRLSCAASGF PVKHHWMFWYRQAPGKEREWVAAIK SYGYGTEYADSVKGRFTISRDNAKNTVYL QMNSLKPEDTAVYYCFVGVGTHYAGQ GTQVTVS		N/A	IGHV3-3 (Alpaca)	IGHJ4 (Alpaca)	N/A	N/A	3149	FVGVGTHY		N/A	Justin Walter et al., 2020 (https://www.biorxiv.org/content/10.1101/2020.04.16.045419v2)
Sb#22	Nb	SARS-CoV2				S; RBD	Phage Display Library (Nanobody, non-immune)	1029	QVQLVESGGGLVQAGGSLRLSCAASGF PVYAAEMEWYRQAPGKEREWVAAISS QGTITYYADSVKGRFTISRDNAKNTVYLQ MNSLKPEDTAVYYCFVYVGKSYIGQGTQ VSVS		N/A	IGHV3-3 (Alpaca)	IGHJ4 (Alpaca)	N/A	N/A	3150	FVYVGKSY		N/A	Justin Walter et al., 2020 (https://www.biorxiv.org/content/10.1101/2020.04.16.045419v2)
Sb#23	Nb	SARS-CoV2				S; RBD	Phage Display Library (Nanobody, non-immune)	1030	QVQLVESGGGLVQAGGSLRLSCAASGF PVYAAEMEWYRQAPGKEREWVAAISS QGTITYYADSVKGRFTISRDNAKNTVYLQ MNSLKPEDTAVYYCFVYVGKSYIGQGTQ VSVS		N/A	IGHV3-3 (Alpaca)	IGHJ4 (Alpaca)	N/A	N/A	3151	FVYVGKSY		N/A	Justin Walter et al., 2020 (https://www.biorxiv.org/content/10.1101/2020.04.16.045419v2)
Sb#25	Nb	SARS-CoV2				S; RBD	Phage Display Library (Nanobody, non-immune)	1031	QVQLVESGGGLVQAGGSLRLSCAASGF PVHAWEMAWYRQAPGKEREWVAAIR SFGSSTHYADSVKGRFTISRDNAKNTVYL QMNSLKPEDTAVYYCNVKDFGTHHYAY DYWGQGTQVTVS		N/A	IGHV3S53 (Alpaca)	IGHJ4 (Alpaca)	N/A	N/A	3152	NVKDFGTHH YAYDY		N/A	Justin Walter et al., 2020 (https://www.biorxiv.org/content/10.1101/2020.04.16.045419v2)
Sb#26	Nb	SARS-CoV2				S; RBD	Phage Display Library (Nanobody, non-immune)	1032	QVQLVESGGGLVQAGGSLRLSCAASGF PVNTWWMHWYRQAPGKEREWVAAIT SWGFRTYYADSVKGRFTISRDNAKNTVY LQMNSLKPEDTAVYYCNVKDKGMAVQ WYDYWGQGTQVTVS		N/A	IGHV3S53 (Alpaca)	IGHJ4 (Alpaca)	N/A	N/A	3153	NVKDKGMAV QWYDY		N/A	Justin Walter et al., 2020 (https://www.biorxiv.org/content/10.1101/2020.04.16.045419v2)
Sb#27	Nb	SARS-CoV2				S; RBD	Phage Display Library (Nanobody, non-immune)	1033	QVQLVESGGGLVQAGGSLRLSCAASGF PVYNTWMEWYRQAPGKEREWVAAITS HGYKTYYADSVKGRFTISRDNAKNTVYL QMNSLKPEDTAVYYCNVKDEGDMFTA YDYWGQGTQVTVS		N/A	IGHV3S53 (Alpaca)	IGHJ4 (Alpaca)	N/A	N/A	3154	NVKDEGDMF TAYDY		N/A	Justin Walter et al., 2020 (https://www.biorxiv.org/content/10.1101/2020.04.16.045419v2)

Sb#28	Nb	SARS-CoV2				S; RBD	Phage Display Library (Nanobody, non-immune)	1034	QVQLVESGGGLVQAGGSLRLSCAASGF PVYHSTMFWYRQAPGKEREWVAAIYSS GQHTYYADSVKGRFTISRDNAKNTVYLQ MNSLKPEDTAVYYCNVKDSGQWRQEY DYWGQGTQVTVS		N/A	IGHV3-3 (Alpaca)	IGHJ4 (Alpaca)	N/A	N/A	3155	NVKDSGQWR QEYDY		N/A	Justin Walter et al., 2020 (https://www.biorxiv.org/content/10.1101/2020.04.16.045419v2)
Sb#29	Nb	SARS-CoV2				S; RBD	Phage Display Library (Nanobody, non-immune)	1035	QVQLVESGGGLVQAGGSLRLSCAASGF PVEHEMAWYRQAPGKEREWVAAIRS MGRKTLYADSVKGRFTISRDNAKNTVYL QMNSLKPEDTAVYYCNVKDFGYTWHEY DYWGQGTQVTVS		N/A	IGHV3S53 (Alpaca)	IGHJ4 (Alpaca)	N/A	N/A	3156	NVKDFGYTW HEYDY		N/A	Justin Walter et al., 2020 (https://www.biorxiv.org/content/10.1101/2020.04.16.045419v2)
Sb#3	Nb	SARS-CoV2				S; RBD	Phage Display Library (Nanobody, non-immune)	1036	QVQLVESGGGLVQAGGSLRLSCAASGF PVNYKTMWWYRQAPGKEREWVAAIW SYGHTTHYADSVKGRFTISRDNAKNTVY LQMNSLKPEDTAVYYCVVWVGHNYEG QGTQVTVS		N/A	IGHV3-3 (Alpaca)	IGHJ4 (Alpaca)	N/A	N/A	3157	VVWVGHNY		N/A	Justin Walter et al., 2020 (https://www.biorxiv.org/content/10.1101/2020.04.16.045419v2)
Sb#30	Nb	SARS-CoV2				S; RBD	Phage Display Library (Nanobody, non-immune)	1037	QVQLVESGGGLVQAGGSLRLSCAASGF PVTMAWMWWYRQAPGKEREWVAAI RSEGVRTYYADSVKGRFTISRDNAKNTV YLQMNSLKPEDTAVYYCNVKDYGQAHA YYDYWGQGTQVTVS		N/A	IGHV3-3 (Alpaca)	IGHJ4 (Alpaca)	N/A	N/A	3158	NVKDYGQAH AYYDY		N/A	Justin Walter et al., 2020 (https://www.biorxiv.org/content/10.1101/2020.04.16.045419v2)
Sb#31	Nb	SARS-CoV2				S; RBD	Phage Display Library (Nanobody, non-immune)	1038	QVQLVESGGGLVQAGGSLRLSCAASGF PVNSHFMEWYRQAPGKEREWVAAIQH SSGFHTYYADSVKGRFTISRDNAKNTVYL QMNSLKPEDTAVYYCNVKDTGTTEDYD YWGQGTQVTVS		N/A	IGHV3-3 (Alpaca)	IGHJ4 (Alpaca)	N/A	N/A	3159	NVKDTGTTED YDY		N/A	Justin Walter et al., 2020 (https://www.biorxiv.org/content/10.1101/2020.04.16.045419v2)
Sb#32	Nb	SARS-CoV2				S; RBD	Phage Display Library (Nanobody, non-immune)	1039	QVQLDESGGGLVQAGGSLRLSCAASGF PVYHAWMEWYRQAPGKEREWVAAITS SGRHTYYADSVKGRFTISRDNAKNTVYL QMNSLKPEDTAVYYCNVKDAGRVYNSY DYWGQGTQVTVS		N/A	IGHV3-3 (Alpaca)	IGHJ4 (Alpaca)	N/A	N/A	3160	NVKDAGRVY NSYDY		N/A	Justin Walter et al., 2020 (https://www.biorxiv.org/content/10.1101/2020.04.16.045419v2)
Sb#33	Nb	SARS-CoV2				S; RBD	Phage Display Library (Nanobody, non-immune)	1040	QVQLVESGGGLVQAGGSLRLSCAASGF PVAHAWMEWYRQAPGKEREWVAAIT SYGYKTYYADSVKGRFTISRDNAKNTVYL QMNSLKPEDTAVYYCNVKDTGTYRFYY DYWGQGTQVTVS		N/A	IGHV3S53 (Alpaca)	IGHJ4 (Alpaca)	N/A	N/A	3161	NVKDTGTYRF YYDY		N/A	Justin Walter et al., 2020 (https://www.biorxiv.org/content/10.1101/2020.04.16.045419v2)
Sb#34	Nb	SARS-CoV2				S; RBD	Phage Display Library (Nanobody, non-immune)	1041	QVQLVESGGGLVQAGGSLRLSCAASGF PVWNQTMVWYRQAPGKEREWVAAI WSMGHTYYADSVKGRFTISRDNAKNTV YLQMNSLKPEDTAVYYCNVKDAGVYNR YYDYWGQGTQVTVS		N/A	IGHV3S53 (Alpaca)	IGHJ4 (Alpaca)	N/A	N/A	3162	NVKDAGVYN RYYDY		N/A	Justin Walter et al., 2020 (https://www.biorxiv.org/content/10.1101/2020.04.16.045419v2)
Sb#35	Nb	SARS-CoV2				S; RBD	Phage Display Library (Nanobody, non-immune)	1042	QVQLVESGGGLVQAGGSLRLSCAASGF PVEHYWMEWYRQAPGKEREWVAAITS FGYRTYYADSVKGRFTISRDNAKNTVYL QMNSLKPEDTAVYYCNVKDWGFASHA YDYWGQGIQVTVS		N/A	IGHV3-3 (Alpaca)	IGHJ4 (Alpaca)	N/A	N/A	3163	NVKDWGFAS HAYDY		N/A	Justin Walter et al., 2020 (https://www.biorxiv.org/content/10.1101/2020.04.16.045419v2)
Sb#36	Nb	SARS-CoV2				S; RBD	Phage Display Library (Nanobody, non-immune)	1043	QVQLVESGGGLVQAGGSLRLSCAASGF PEIAWEMAWYRQAPGKEREWVAAIRS FGERTLYADSVKGRFTISRDNAKNTVYL QMNSLKPEDTAVYYCNVKDFGWQHQE YDYWGQGTQVTVS		N/A	IGHV3S53 (Alpaca)	IGHJ4 (Alpaca)	N/A	N/A	3164	NVKDFGWQ HQEYDY		N/A	Justin Walter et al., 2020 (https://www.biorxiv.org/content/10.1101/2020.04.16.045419v2)
Sb#37	Nb	SARS-CoV2				S; RBD	Phage Display Library (Nanobody, non-immune)	1044	QVQLVESGGGLVQAGGSLRLSCAASGF PVYHAYMEWYRQAPGKEREWVAAIYS NGEHTYYADSVKGRFTISRDNAKNTVYL QMNSLKPEDTAVYYCNVKDSGSFNQAY DYWGQGTQVTVS		N/A	IGHV3-3 (Alpaca)	IGHJ4 (Alpaca)	N/A	N/A	3165	NVKDSGSFN QAYDY		N/A	Justin Walter et al., 2020 (https://www.biorxiv.org/content/10.1101/2020.04.16.045419v2)
Sb#38	Nb	SARS-CoV2				S; RBD	Phage Display Library (Nanobody, non-immune)	1045	QVQLVESGGGLVQAGGSLRLSCAASGF PVEWSHMHWYRQAPGKEREWVAAIV SKGGYTLYADSVKGRFTISRDNAKNTVYL QMNSLKPEDTAVYYCNVKDYGVHFKRY DYWGQGTQVTVI		N/A	IGHV3S53 (Alpaca)	IGHJ4 (Alpaca)	N/A	N/A	3166	NVKDYGVHF KRYDY		N/A	Justin Walter et al., 2020 (https://www.biorxiv.org/content/10.1101/2020.04.16.045419v2)
Sb#39	Nb	SARS-CoV2				S; RBD	Phage Display Library (Nanobody, non-immune)	1046	QVQLVESGGGLVQAGGSLRLSCAASGF PVFHVWMEWYRQAPGKEREWVAAID SAGWHTYYADSVKGRFTISRDNAKNTV YLQMNSLKPEDTAVYYCNVKDAGNTTS AYDYWGQGTQVTVS		N/A	IGHV3-3 (Alpaca)	IGHJ4 (Alpaca)	N/A	N/A	3167	NVKDAGNTT SAYDY		N/A	Justin Walter et al., 2020 (https://www.biorxiv.org/content/10.1101/2020.04.16.045419v2)
Sb#4	Nb	SARS-CoV2				S; RBD	Phage Display Library (Nanobody, non-immune)	1047	QVQLVESGGGLVQAGGSLRLSCAASGF PVYAQNMHWYRQAPGKEREWVAAIYS HGYWTLYADSVKGRFTISRDNAKNTVYL QMNSLKPEDTAVYYCEVQVGAWYTGQ GTQVTVS		N/A	IGHV3-3 (Alpaca)	IGHJ4 (Alpaca)	N/A	N/A	3168	EVQVGAWY		N/A	Justin Walter et al., 2020 (https://www.biorxiv.org/content/10.1101/2020.04.16.045419v2)
Sb#40	Nb	SARS-CoV2				S; RBD	Phage Display Library (Nanobody, non-immune)	1048	QVQLVESGGGLVQAGGSLRLSCAASGF PVYYNWMEWYRQAPGKEREWVAAIH SNGDETFYADSVKGRFTISRDNAKNTVY LQMNSLKPEDTAVYYCNVKDIDAEAYAY DYWGQGTQVTVS		N/A	IGHV3S53 (Alpaca)	IGHJ4 (Alpaca)	N/A	N/A	3169	NVKDIDAEAY AYDY		N/A	Justin Walter et al., 2020 (https://www.biorxiv.org/content/10.1101/2020.04.16.045419v2)

Sb#41	Nb	SARS-CoV2				S; RBD	Phage Display Library (Nanobody, non-immune)	1049	QVQLVESGGGLVQAGGSLRLSCAASGFPVYHVWMEWYRQAPGKEREWVAAITSSGSHTYYADSVKGRFTISRDNAKNTVYLQMNSLKPEDTAVYYCNVKDSGQWRVQYDYWGQGTQVTVS		N/A	IGHV3-3 (Alpaca)	IGHJ4 (Alpaca)	N/A	N/A	3170	NVKDSGQWRVQYDY		N/A	Justin Walter et al., 2020 (https://www.biorxiv.org/content/10.1101/2020.04.16.045419v2)
Sb#42	Nb	SARS-CoV2				S; RBD	Phage Display Library (Nanobody, non-immune)	1050	QVQLVESGGGLVQAGGSLRLSCAASGFPVYWHHMHWYRQAPGKEREWVAAIISWGWYTTYADSVKGRFTISRDNAKNTVYLQMNSLKPEDTAVYYCNVKDHGAQNQMYDYWGQGTQVTVS		N/A	IGHV3S53 (Alpaca)	IGHJ4 (Alpaca)	N/A	N/A	3171	NVKDHGAQNQMYDY		N/A	Justin Walter et al., 2020 (https://www.biorxiv.org/content/10.1101/2020.04.16.045419v2)
Sb#45	Nb	SARS-CoV2				S; RBD	Phage Display Library (Nanobody, non-immune)	1051	QVQLVESGGGLVQAGGSLRLSCAASGFPVYRDRMAWYRQAPGKEREWVAAIYSAGQQTRYADSVKGRFTISRDNAKNTVYLQMNSLKPEDTAVYYCNVKDVGHHYEYYDYWGQGTQVTVS		N/A	IGHV3S53 (Alpaca)	IGHJ4 (Alpaca)	N/A	N/A	3172	NVKDVGHHYEYYDY		N/A	Justin Walter et al., 2020 (https://www.biorxiv.org/content/10.1101/2020.04.16.045419v2)
Sb#46	Nb	SARS-CoV2				S; RBD	Phage Display Library (Nanobody, non-immune)	1052	QVQLVESGGGLVQAGGSLRLSCAASGFPVDNGYMHWYRQAPGKEREWVAAIDSYGWHTIYADSVKGRFTISRDNAKNTVYLQMNSLKPEDTAVYYCNVKDKGQMRAAYDYWGQGTQVTVS		N/A	IGHV3S53 (Alpaca)	IGHJ4 (Alpaca)	N/A	N/A	3173	NVKDKGQMRAAYDY		N/A	Justin Walter et al., 2020 (https://www.biorxiv.org/content/10.1101/2020.04.16.045419v2)
Sb#47	Nb	SARS-CoV2				S; RBD	Phage Display Library (Nanobody, non-immune)	1053	QVQLVESGGGLVQAGGSLRLSCAASGFPVSWHSMYWYRQAPGKEREWVAAIFSEGDWTYYADSVKGRFTISRDNAKNTVYLQMNSLKPEDTAVYYCNVKDYGSSYYKYDYWGQGTQVTVS		N/A	IGHV3-3 (Alpaca)	IGHJ4 (Alpaca)	N/A	N/A	3174	NVKDYGSSYYKYDY		N/A	Justin Walter et al., 2020 (https://www.biorxiv.org/content/10.1101/2020.04.16.045419v2)
Sb#48	Nb	SARS-CoV2				S; RBD	Phage Display Library (Nanobody, non-immune)	1054	QVQLVESGGGLVQAGGSLRLSCAASGFPVSQSVMAWYRQAPGKEREWVAAIYSKGQYTHYADSVKGRFTISRDNAKNTVYLQMNSLKPEDTAVYYCNVKDAGSSYWDYDYWGQGTQVTVS		N/A	IGHV3S53 (Alpaca)	IGHJ4 (Alpaca)	N/A	N/A	3175	NVKDAGSSYWDYD		N/A	Justin Walter et al., 2020 (https://www.biorxiv.org/content/10.1101/2020.04.16.045419v2)
Sb#49	Nb	SARS-CoV2				S; RBD	Phage Display Library (Nanobody, non-immune)	1055	QVQLVESGGGSVQAGGSLRLSCAASGSIGQIEYLGWFRQAPGKEREGVAALNTWTGRTYYADSVKGRFTVSLDNAKNTVYLQMNSLKPEDTALYYCAAARWGRTKPLNTYYYSYWGQGTPVTVS		N/A	IGHV3-3 (Alpaca)	IGHJ4 (Alpaca)	N/A	N/A	3176	AAARWGRTKPLNTYYYSY		N/A	Justin Walter et al., 2020 (https://www.biorxiv.org/content/10.1101/2020.04.16.045419v2)
Sb#5	Nb	SARS-CoV2				S; RBD	Phage Display Library (Nanobody, non-immune)	1056	QVQLVESGGGLVQAGGSLRLSCAASGFPVFSGHMHWYRQAPGKEREWVAAILSNGDSTHYADSVKGRFTISRDNAKNTVYLQMNSLKPEDTAVYYCRVHVGAHYFGQGTQVTVS		N/A	IGHV3-3 (Alpaca)	IGHJ4 (Alpaca)	N/A	N/A	3177	RVHVGAHY		N/A	Justin Walter et al., 2020 (https://www.biorxiv.org/content/10.1101/2020.04.16.045419v2)
Sb#50	Nb	SARS-CoV2				S; RBD	Phage Display Library (Nanobody, non-immune)	1057	QVQLVESGGGSVQAGGSLRLSCAASGYIDKIVYLGWFRQAPGKEREGVAALYTLSGHTYYADSVKGRFTVSLDNAKNTVYLQMNSLKPEDTALYYCAAATEGHAHALYRLHYYWGQGTQVTVS		N/A	IGHV3-3 (Alpaca)	IGHJ4 (Alpaca)	N/A	N/A	3178	AAATEGHAHALYRLHYY		N/A	Justin Walter et al., 2020 (https://www.biorxiv.org/content/10.1101/2020.04.16.045419v2)
Sb#51	Nb	SARS-CoV2				S; RBD	Phage Display Library (Nanobody, non-immune)	1058	QVQLVESGGGLVQAGGSLRLSCAASGFPVYQGEMHWYRQAPGKEREWVAAIRSTGVQTWYADSVKGRFTISRDNAKNTVYLQMNSLKPEDTAVYYCRVWVGTHYFGQGTQVTVS		N/A	IGHV3-3 (Alpaca)	IGHJ4 (Alpaca)	N/A	N/A	3179	RVWVGTHY		N/A	Justin Walter et al., 2020 (https://www.biorxiv.org/content/10.1101/2020.04.16.045419v2)
Sb#52	Nb	SARS-CoV2				S; RBD	Phage Display Library (Nanobody, non-immune)	1059	QVQLVESGGGSVQAGGSLRLSCAASGNIQRIYYLGWFRQAPGKEREGVAALMTYTGHTYYADSVKGRFTVSLDNAKNTVYLQMNSLKPEDTALYYCAAAYVGAENPLPYSMYGYWGQGTQVTVS		N/A	IGHV3-3 (Alpaca)	IGHJ4 (Alpaca)	N/A	N/A	3180	AAAYVGAENPLPYSMYGY		N/A	Justin Walter et al., 2020 (https://www.biorxiv.org/content/10.1101/2020.04.16.045419v2)
Sb#53	Nb	SARS-CoV2				S; RBD	Phage Display Library (Nanobody, non-immune)	1060	QVQLVESGGGSVQAGGSLRLSCAASGQISHIKYLGWFRQAPGKEREGVAALITRWGQTYYADSVKGRFTVSLDNAKNTVYLQMNSLKPEDTALYYCAAADYGASDPLWFIHYLYWGQGTQVTVS		N/A	IGHV3-3 (Alpaca)	IGHJ4 (Alpaca)	N/A	N/A	3181	AAADYGASDPLWFIHYLY		N/A	Justin Walter et al., 2020 (https://www.biorxiv.org/content/10.1101/2020.04.16.045419v2)
Sb#55	Nb	SARS-CoV2				S; RBD	Phage Display Library (Nanobody, non-immune)	1061	QVQLVESGGGSVQAGGSLRLSCAASGKIWTIKYLGWFRQAPGKEREGVAALMTRWGYTYYADSVKGRFTVSLDNAKNTVYLQMNSLKPEDTALYYCAAANYGSNFPLAEEDYWYWGQGTQVTVS		N/A	IGHV3-3 (Alpaca)	IGHJ4 (Alpaca)	N/A	N/A	3182	AAANYGSNFPLAEEDYWY		N/A	Justin Walter et al., 2020 (https://www.biorxiv.org/content/10.1101/2020.04.16.045419v2)
Sb#56	Nb	SARS-CoV2				S; RBD	Phage Display Library (Nanobody, non-immune)	1062	QVQLVESGGGSVQAGGSLRLSCAASGNISQIHYLGWFRQAPGKEREGVAALNTDYGYTYYADSVKGRFTVSLDNAKNTVYLQMNSLKPEDTALYYCAAAYYFGDDIPLWWEAYSYWGQGTQVTVS		N/A	IGHV3-3 (Alpaca)	IGHJ4 (Alpaca)	N/A	N/A	3183	AAAYYFGDDIPLWWEAYSY		N/A	Justin Walter et al., 2020 (https://www.biorxiv.org/content/10.1101/2020.04.16.045419v2)
Sb#58	Nb	SARS-CoV2				S; RBD	Phage Display Library (Nanobody, non-immune)	1063	QVQLVESGGGSVQAGGSLRLSCAASGNISTIEYLGWFRQAPGKEREGVAALYTWHGQTYYADSVKGRFTVSLDNAKNTVYLQMNSLKPEDTALYYCAAARWGRHMPLSATEYSYWGQGTQVTVS		N/A	IGHV3-3 (Alpaca)	IGHJ4 (Alpaca)	N/A	N/A	3184	AAARWGRHMPLSATEYSY		N/A	Justin Walter et al., 2020 (https://www.biorxiv.org/content/10.1101/2020.04.16.045419v2)

Sb#59	Nb	SARS-CoV2				S; RBD	Phage Display Library (Nanobody, non-immune)	1064	QVQLVESGGGSVQAGGSLRLSCAASGN IESIYYLGWFRQAPGKEREGVAALWTG DGETYYADSVKGRFTVSLDNAKNTVYLQ MNSLKPEDTALYYCAAAAWGNSAPLTT YRYYYWGQGTQVTVS		N/A	IGHV3-3 (Alpaca)	IGHJ4 (Alpaca)	N/A	N/A	3185	AAAAWGNSA PLTTYRYYY		N/A	Justin Walter et al., 2020 (https://www.biorxiv.org/content/10.1101/2020.04.16.045419v2)
Sb#6	Nb	SARS-CoV2				S; RBD	Phage Display Library (Nanobody, non-immune)	1065	QVQLVESGGGLVQAGGSLRLSCAASGF PVEQGRMYWYRQAPGKEREWVAAIIS HGTVTVYADSVKGRFTISRDNAKNTVYL QMNSLKPEDTAVYYCYVYVGAQYWGQ GTQVTVS		N/A	IGHV3-3 (Alpaca)	IGHJ4 (Alpaca)	N/A	N/A	3186	YVYVGAQY		N/A	Justin Walter et al., 2020 (https://www.biorxiv.org/content/10.1101/2020.04.16.045419v2)
Sb#61	Nb	SARS-CoV2				S; RBD	Phage Display Library (Nanobody, non-immune)	1066	QVQLVESGGGSVQAGGSLRLSCAASGFI YGITYLGWFRQAPGKEREGVAALVTWN GQTYYADSVKGRFTVSLDNAKNTVYLQ MNSLKPEDTALYYCAAADWGYDWPLW DEWYWYWGQGTQVTVS		N/A	IGHV3-3 (Alpaca)	IGHJ4 (Alpaca)	N/A	N/A	3187	AAADWGYD WPLWDEWY WY		N/A	Justin Walter et al., 2020 (https://www.biorxiv.org/content/10.1101/2020.04.16.045419v2)
Sb#62	Nb	SARS-CoV2				S; RBD	Phage Display Library (Nanobody, non-immune)	1067	QVQLVESGGGSVQAGGSLRLSCAASGTI ADIKYLGWFRQAPGKEREGVAALMTR WGSTYYADSVKGRFTVSLDNAKNTVYL QMNSLKPEDTALYYCAAANYGANYPLYS QQYSYWGQGTQVTVS		N/A	IGHV3-3 (Alpaca)	IGHJ4 (Alpaca)	N/A	N/A	3188	AAANYGANY PLYSQQYSY		N/A	Justin Walter et al., 2020 (https://www.biorxiv.org/content/10.1101/2020.04.16.045419v2)
Sb#63	Nb	SARS-CoV2				S; RBD	Phage Display Library (Nanobody, non-immune)	1068	QVQLVESGGGSVQAGGSLRLSCAASGSI SSIKYLGWFRQAPGKEREGVAALMTRW GMTYYADSVKGRFTVSLDNAKNTVYLQ MNSLKPEDTALYYCAAANYGANEPLQY THYNYWGQGTQVTVS		N/A	IGHV3-3 (Alpaca)	IGHJ4 (Alpaca)	N/A	N/A	3189	AAANYGANE PLQYTHYNY		N/A	Justin Walter et al., 2020 (https://www.biorxiv.org/content/10.1101/2020.04.16.045419v2)
Sb#64	Nb	SARS-CoV2				S; RBD	Phage Display Library (Nanobody, non-immune)	1069	QVQLVESGGGSVQAGGSLRLSCAASGEI ESIFYLGWFRQAPGKEREGVAALYTYVG QTYYADSVKGRFTVSLDNAKNTVYLQM NSLKPEDTALYYCAAASYGAAHPLSIMR YYYWGQGTQVTVS		N/A	IGHV3-3 (Alpaca)	IGHJ4 (Alpaca)	N/A	N/A	3190	AAASYGAAHP LSIMRYYY		N/A	Justin Walter et al., 2020 (https://www.biorxiv.org/content/10.1101/2020.04.16.045419v2)
Sb#65	Nb	SARS-CoV2				S; RBD	Phage Display Library (Nanobody, non-immune)	1070	QVQLVESGGGSVQAGGSLRLSCAASGTI AHIKYLGWFRQAPGKEREGVAALMTK WGQTYYADSVKGRFTVSLDNAKNTVYL QMNSLKPEDTALYYCAAASYGANFPLKA SDYSYWGQGTQVTVS		N/A	IGHV3-3 (Alpaca)	IGHJ4 (Alpaca)	N/A	N/A	3191	AAASYGANFP LKASDYSY		N/A	Justin Walter et al., 2020 (https://www.biorxiv.org/content/10.1101/2020.04.16.045419v2)
Sb#66	Nb	SARS-CoV2				S; RBD	Phage Display Library (Nanobody, non-immune)	1071	QVQLVESGGGSVQAGGSLRLSCAASGSI QAITYLGWFRQAPGKEREGVAALVTW NGQTYYADSVKGRFTVSLDNAKNTVYL QMNSLKPEDTALYYCAAADWGYDWPL WDEWYWYWGQGTQVTVS		N/A	IGHV3-3 (Alpaca)	IGHJ4 (Alpaca)	N/A	N/A	3192	AAADWGYD WPLWDEWY WY		N/A	Justin Walter et al., 2020 (https://www.biorxiv.org/content/10.1101/2020.04.16.045419v2)
Sb#67	Nb	SARS-CoV2				S; RBD	Phage Display Library (Nanobody, non-immune)	1072	QVQLVESGGGSVQAGGSLRLSCAASGSI SSITYLGWFRQAPGKEREGVAALVTYSG NTYYADSVKGRFTVSLDNAKNTVYLQM NSLKPEDTALYYCAAATWGHSWPLYND EYWYWGQGSQVTVS		N/A	IGHV3-3 (Alpaca)	IGHJ4 (Alpaca)	N/A	N/A	3193	AAATWGHS WPLYNDEYW Y		N/A	Justin Walter et al., 2020 (https://www.biorxiv.org/content/10.1101/2020.04.16.045419v2)
Sb#68	Nb	SARS-CoV2				S; RBD	Phage Display Library (Nanobody, non-immune)	1073	QVQLVESGGGSVQAGGSLRLSCAASGSI SSITYLGWFRQAPGKEREGVAALITVNG HTYYADSVKGRFTVSLDNAKNTVYLQM NSLKPEDTALYYCAAAAWGYAWPLHQ DDYWYWGQGTQVTVS		N/A	IGHV3-3 (Alpaca)	IGHJ4 (Alpaca)	N/A	N/A	3194	AAAAWGYA WPLHQDDY WY		N/A	Justin Walter et al., 2020 (https://www.biorxiv.org/content/10.1101/2020.04.16.045419v2)
Sb#69	Nb	SARS-CoV2				S; RBD	Phage Display Library (Nanobody, non-immune)	1074	QVQLVESGGGSVQAGGSLRLSCAASGSI SSITYLGWFRQAPGKEREGVAALNTFNG TTYYADSVKGRFTVSLDNAKNTVYLQM NSLKPEDTALYYCAAATWGYSWPLIAEY NWYWGQGTQVTVS		N/A	IGHV3-3 (Alpaca)	IGHJ5 (Alpaca)	N/A	N/A	3195	AAATWGYSW PLIAEYNWY		N/A	Justin Walter et al., 2020 (https://www.biorxiv.org/content/10.1101/2020.04.16.045419v2)
Sb#7	Nb	SARS-CoV2				S; RBD	Phage Display Library (Nanobody, non-immune)	1075	QVQLVESGGGLVQAGGSLRLSCAASGF PVLFTYMHWYRQAPGKEREWVAAIWS SGNSTWYADSVKGRFTISRDNAKNTVYL QMNSLKPEDTAVYYCFVKVGNWYAGQ GTQVTVS		N/A	IGHV3-3 (Alpaca)	IGHJ4 (Alpaca)	N/A	N/A	3196	FVKVGNWY		N/A	Justin Walter et al., 2020 (https://www.biorxiv.org/content/10.1101/2020.04.16.045419v2)
Sb#71	Nb	SARS-CoV2				S; RBD	Phage Display Library (Nanobody, non-immune)	1076	QVQLVESGGGSVQAGGSLRLSCAASGSI SSITYLGWFRQAPGKEREGVAALKTQAG FTYYADSVKGRFTVSLDNAKNTVYLQM NSLKPEDTALYYCAAANWGYSWPLYEA DDWYWGQGTQVTVS		N/A	IGHV3-3 (Alpaca)	IGHJ4 (Alpaca)	N/A	N/A	3197	AAANWGYS WPLYEADDW Y		N/A	Justin Walter et al., 2020 (https://www.biorxiv.org/content/10.1101/2020.04.16.045419v2)
Sb#8	Nb	SARS-CoV2				S; RBD	Phage Display Library (Nanobody, non-immune)	1077	QVQLVESGGGLVQAGGSLRLSCAASGF PVNAGNMHWYRQAPGKEREWVAAIQ SYGRTTYYADSVKGRFTISRDNAKNTVYL QMNSLKPEDTAVYYCRVFVGMHYFGQ GTQVTVS		N/A	IGHV3-3 (Alpaca)	IGHJ4 (Alpaca)	N/A	N/A	3198	YVYVGGSY		N/A	Justin Walter et al., 2020 (https://www.biorxiv.org/content/10.1101/2020.04.16.045419v2)

Sb#9	Nb	SARS-CoV2				S; RBD	Phage Display Library (Nanobody, non-immune)	1078	QVQLVESGGGLVQAGGSLRLSCAASGF PVSSSTMTWYRQAPGKEREWVAAINSY GWETHYADSVKGRFTISRDNAKNTVYL QMNSLKPEDTAVYYCYVYVGGSYIGQG TQVTVS		N/A	IGHV3-3 (Alpaca)	IGHJ4 (Alpaca)	N/A	N/A	3199	RVFVGMHY		N/A	Justin Walter et al., 2020 (https://www.biorxiv.org/content/10.1101/2020.04.16.045419v2)
Sb100	Nb	SARS-CoV2		SARS-CoV2		S; RBD	Phage Display Library (Nanobody, non-immune)	1079	QVQLVESGGGSVQAGGSLRLSCAASGSI SSITYLGWFRQAPGKEREGVAALVTSDG RTYYADSVKGRFTVSLDNAKNTVYLQM NSLKPEDTALYYCAAANWGYSWPLYQT EYWYWGQGTQVTVSS		N/A	IGHV3-3 (Alpaca)	IGHJ4 (Alpaca)	N/A	N/A	3200	AAANWGYS WPLYQTEYW Y		N/A	Tania Custodia et al., 2020 (https://www.biorxiv.org/content/10.1101/2020.06.23.165415v1.full.pdf+html)
Sb12	Nb	SARS-CoV2		SARS-CoV2		S; RBD	Phage Display Library (Nanobody, non-immune)	1080	QVQLVESGGGLVQAGGSLRLSCAASGF PVQLYWMEWYRQAPGKEREWVAAITS DGDYTEYADSVKGRFTISRDNAKNTVYL QMNSLKPEDTAVYYCYVKVGEWYYGQ GTQVTVSS		N/A	IGHV3-3 (Alpaca)	IGHJ4 (Alpaca)	N/A	N/A	3201	YVKVGEWY		N/A	Tania Custodia et al., 2020 (https://www.biorxiv.org/content/10.1101/2020.06.23.165415v1.full.pdf+html)
Sb13	Nb	SARS-CoV2 (weak)				S; RBD	Phage Display Library (Nanobody, non-immune)	1081	QVQLVESGGGLVQAGGSLRLSCAASGF PVENYYMRWYRQAPGKEREWVAAIES SGAETRYADSVKGRFTISRDNAKNTVYL QMNSLKPEDTAVYYCYVVVGWGYAGQ GTQVTVSS		N/A	IGHV3-3 (Alpaca)	IGHJ4 (Alpaca)	N/A	N/A	3202	YVVVGWGY		N/A	Tania Custodia et al., 2020 (https://www.biorxiv.org/content/10.1101/2020.06.23.165415v1.full.pdf+html)
Sb15	Nb	SARS-CoV2				S; RBD	Phage Display Library (Nanobody, non-immune)	1082	QVQLVESGGGLVQAGGSLRLSCAASGF PVYEHYMRWYRQAPGKEREWVAAIQS HGNHTAYADSVKGRFTISRDNAKNTVYL QMNSLKPEDTAVYYCFVVVGNGYTGQ GTQVTVSS		N/A	IGHV3-3 (Alpaca)	IGHJ4 (Alpaca)	N/A	N/A	3203	FVVVGNGY		N/A	Tania Custodia et al., 2020 (https://www.biorxiv.org/content/10.1101/2020.06.23.165415v1.full.pdf+html)
Sb16	Nb	SARS-CoV2				S; RBD	Phage Display Library (Nanobody, non-immune)	1083	QVQLVESGGGLVRAGGSLRLSCAASGF PVASQEMTWYRQAPGKEREWVAAISSS GRQTEYADSVKGRFTISRDNAKNTVYLQ MNSLKPEDTAVYYCYVYVGGSYIGQGT QVTVSS		N/A	IGHV3-3 (Alpaca)	IGHJ4 (Alpaca)	N/A	N/A	3204	YVYVGGSY		N/A	Tania Custodia et al., 2020 (https://www.biorxiv.org/content/10.1101/2020.06.23.165415v1.full.pdf+html)
Sb17	Nb	SARS-CoV2		SARS-CoV2		S; RBD	Phage Display Library (Nanobody, non-immune)	1084	QVQLVESGGGLVQAGGSLRLSCAASGF PVKASEMEWYRQAPGKEREWVAAIASI GYNTYYADSVKGRFTISRDNAKNTVYLQ MNSLKPEDTAVYYCLVYVGATYIGQGTQ VTVSS		N/A	IGHV3-3 (Alpaca)	IGHJ4 (Alpaca)	N/A	N/A	3205	LVYVGATY		N/A	Tania Custodia et al., 2020 (https://www.biorxiv.org/content/10.1101/2020.06.23.165415v1.full.pdf+html)
Sb2	Nb	SARS-CoV2				S; RBD	Phage Display Library (Nanobody, non-immune)	1085	QVQLVESGGGLVQAGGSLRLSCAASGF PVSNEEMTWYRQAPGKEREWVAAIAS NGNQTEYADSVKGRFTISRDNAKNTVYL QMNSLKPEDTAVYYCYVYVGASYIGQG TQVTVSS		N/A	IGHV3-3 (Alpaca)	IGHJ4 (Alpaca)	N/A	N/A	3206	YVYVGASY		N/A	Tania Custodia et al., 2020 (https://www.biorxiv.org/content/10.1101/2020.06.23.165415v1.full.pdf+html)
Sb21	Nb	SARS-CoV2				S; RBD	Phage Display Library (Nanobody, non-immune)	1086	QVQLVESGGGLVQAGGSLRLSCAASGF PVKESEMTWYRQARGKEREWVAAINS HGMTTHYADSVKGRFTISRDNAKNTVY LQMNSLKPEDTAVYYCYVYVGGSYIGQ GTQVTVSS		N/A	IGHV3-3 (Alpaca)	IGHJ4 (Alpaca)	N/A	N/A	3207	YVYVGGSY		N/A	Tania Custodia et al., 2020 (https://www.biorxiv.org/content/10.1101/2020.06.23.165415v1.full.pdf+html)
Sb22	Nb	SARS-CoV2		SARS-CoV2		S; RBD	Phage Display Library (Nanobody, non-immune)	1087	QVQLVESGGGLVQAGGSLRLSCAASGF PVNHYEMEWYRQAPGREREWVAAIM DSTGYETAYADSVKGRFTISRDNAKNTV YLQMNSLKPEDTAVYYCYVYVGASYIGQ GTQVTVSS		N/A	IGHV3-3 (Alpaca)	IGHJ4 (Alpaca)	N/A	N/A	3208	YVYVGASY		N/A	Tania Custodia et al., 2020 (https://www.biorxiv.org/content/10.1101/2020.06.23.165415v1.full.pdf+html)
Sb23	Nb	SARS-CoV2		SARS-CoV2		S; RBD	Phage Display Library (Nanobody, non-immune)	1088	QVQLVESGGGLVQAGGSLRLSCAASGF PVESENMHWYRQAPGKEREWVAAIYS TGGWTLYADSVKGRFTISRDNAKNTVYL QMNSLKPEDTAVYYCAVQVGYWYEGQ GTQVTVSS		N/A	IGHV3-3 (Alpaca)	IGHJ4 (Alpaca)	N/A	N/A	3209	AVQVGYWY		N/A	Tania Custodia et al., 2020 (https://www.biorxiv.org/content/10.1101/2020.06.23.165415v1.full.pdf+html)
Sb25	Nb	SARS-CoV2				S; RBD	Phage Display Library (Nanobody, non-immune)	1089	QVQLVESGGGLVQAGGSLRLSCAASGF PVESTEMTWYRQAPGKEREWVAAIESE GHGTEYADSVKGRFTISRDNAKNTVYLQ MNSLKPEDTAVYYCYVYVGAGYIGQGT QVTVSS		N/A	IGHV3-3 (Alpaca)	IGHJ4 (Alpaca)	N/A	N/A	3210	YVYVGAGY		N/A	Tania Custodia et al., 2020 (https://www.biorxiv.org/content/10.1101/2020.06.23.165415v1.full.pdf+html)
Sb27	Nb	SARS-CoV2				S; RBD	Phage Display Library (Nanobody, non-immune)	1090	QVQLVESGGGLVQAGGSLRLSCAASGF PVKASEMVWYRQAPGKEREWVAAILS QGHATEYADSVKGRFTISRDNAKNTVYL QMNSLKPEDTAVYYCYVWVGRSYIGQG TQVTVSS		N/A	IGHV3-3 (Alpaca)	IGHJ4 (Alpaca)	N/A	N/A	3211	YVWVGRSY		N/A	Tania Custodia et al., 2020 (https://www.biorxiv.org/content/10.1101/2020.06.23.165415v1.full.pdf+html)

Sb28	Nb	SARS-CoV2				S; RBD	Phage Display Library (Nanobody, non-immune)	1091	QVQLVESGGGLVQAGGSLRLSCAASGF PVYSAEMEWYRQAPGKEREWVAAISSY GTNTYYADSVKGRFTISRDNAKNTVYLQ MNSLKPEDTAVYYCYVYVGSSYIGQGTQ VTVSS		N/A	IGHV3-3 (Alpaca)	IGHJ4 (Alpaca)	N/A	N/A	3212	YVYVGSSY		N/A	Tania Custodia et al., 2020 (https://www.biorxiv.org/content/10.1101/2020.06.23.165415v1.full.pdf+html)
Sb30	Nb	SARS-CoV2				S; RBD	Phage Display Library (Nanobody, non-immune)	1092	QVQLVESGGGLVQAGGSLRLSCAASGF PVWYKEMEWYRQAPGKEREWVAAITS AGHHTYYADSVKGRFTISRDNAKNTVYL QMNSLKPEDTAVYYCYVYVGESYIGQGT QVTVSS		N/A	IGHV3-3 (Alpaca)	IGHJ4 (Alpaca)	N/A	N/A	3213	YVYVGESY		N/A	Tania Custodia et al., 2020 (https://www.biorxiv.org/content/10.1101/2020.06.23.165415v1.full.pdf+html)
Sb32	Nb	SARS-CoV2				S; RBD	Phage Display Library (Nanobody, non-immune)	1093	QVQLVESGGGLVQAGGSLRLSCAASGF PVAHKSMWWYRQAPGKEREWVAAIES TGDTTRYADSVKGRFTISRDNAKNTVYL QMNSLKPEDTAVYYCVVWVGEVYRGQ GTQVTVSS		N/A	IGHV3-3 (Alpaca)	IGHJ4 (Alpaca)	N/A	N/A	3214	VVWVGEVY		N/A	Tania Custodia et al., 2020 (https://www.biorxiv.org/content/10.1101/2020.06.23.165415v1.full.pdf+html)
Sb37	Nb	SARS-CoV2 (weak)				S; RBD	Phage Display Library (Nanobody, non-immune)	1094	QVQLVESGGGLVQAGGSLRLSCAASGF PVYNTWMEWYRQAPGKEREWVAAITS YGFHTYYADSVKGRFTISRDNAKNTVYL QMNSLKPEDTAVYYCNVKDEGNTTAYY DYWGQGTQVTVSS		N/A	IGHV3S53 (Alpaca)	IGHJ4 (Alpaca)	N/A	N/A	3215	NVKDEGNTTAYYDY		N/A	Tania Custodia et al., 2020 (https://www.biorxiv.org/content/10.1101/2020.06.23.165415v1.full.pdf+html)
Sb38	Nb	SARS-CoV2				S; RBD	Phage Display Library (Nanobody, non-immune)	1095	QVQLVESGGGLVQAGGSLRLSCAASGF PVYWAHMTWYRQAPGKEREWVAAIV SSGAYTAYADSVKGRFTISRDNAKNTVYL QMNSLKPEDTAVYYCNVKDFGTQEHYY DYWGQGTQVTVSS		N/A	IGHV3S53 (Alpaca)	IGHJ4 (Alpaca)	N/A	N/A	3216	NVKDFGTQEHYYDY		N/A	Tania Custodia et al., 2020 (https://www.biorxiv.org/content/10.1101/2020.06.23.165415v1.full.pdf+html)
Sb39	Nb	SARS-CoV2				S; RBD	Phage Display Library (Nanobody, non-immune)	1096	QVQLVESGGGPVQAGGSLRLSCAASGF PVMWSHMHWYRQAPGKEREWVAAIV SYGAYTIYADSVKGRFTISRDNAKNTVYL QMNSLKPEDTAVYYCNVKDFGGYRYYY DYWGQGTQVTVSS		N/A	IGHV3S53 (Alpaca)	IGHJ4 (Alpaca)	N/A	N/A	3217	NVKDFGGYRYYYDY		N/A	Tania Custodia et al., 2020 (https://www.biorxiv.org/content/10.1101/2020.06.23.165415v1.full.pdf+html)
Sb40	Nb	SARS-CoV2				S; RBD	Phage Display Library (Nanobody, non-immune)	1097	QVQLVESGGGLVQAGGSLRLSCAASGF PVQGTWMEWYRQAPGKEREWVAAIT SVGYRTYYADSVKGRFTISRDNAKNTVYL QMNSLKPEDTAVYYCNVKDEGAIAKNY DYWGQGTQVTVSS		N/A	IGHV3S53 (Alpaca)	IGHJ4 (Alpaca)	N/A	N/A	3218	NVKDEGAIAKNYDY		N/A	Tania Custodia et al., 2020 (https://www.biorxiv.org/content/10.1101/2020.06.23.165415v1.full.pdf+html)
Sb42	Nb	SARS-CoV2		SARS-CoV2		S; RBD	Phage Display Library (Nanobody, non-immune)	1098	QVQLVESGGGLVQAGGSLRLSCAASGF PVYNTWMEWYRQAPGKEREWVAAITS WGFKTYYADSVKGRFTISRDNAKNTVYL QMNSLKPEDTAVYYCNVKDEGYTGYYY DYWGQGTQVTVSS		N/A	IGHV3S53 (Alpaca)	IGHJ4 (Alpaca)	N/A	N/A	3219	NVKDEGYTGYYYDY		N/A	Tania Custodia et al., 2020 (https://www.biorxiv.org/content/10.1101/2020.06.23.165415v1.full.pdf+html)
Sb43	Nb	SARS-CoV2		SARS-CoV2		S; RBD	Phage Display Library (Nanobody, non-immune)	1099	QVQLVESGGGLVQAGGSLRLSCAASGF PVEWTHMHWYRQAPGKEREWVAAIA SSGAYTVYADSVKGRFTISRDNAKNTVYL QMNSLKPEDTAVYYCNVKDWGSQDRY YDYWGQGTQVTVSS		N/A	IGHV3-3 (Alpaca)	IGHJ4 (Alpaca)	N/A	N/A	3220	NVKDWGSQDRYYDY		N/A	Tania Custodia et al., 2020 (https://www.biorxiv.org/content/10.1101/2020.06.23.165415v1.full.pdf+html)
Sb45	Nb	SARS-CoV2				S; RBD	Phage Display Library (Nanobody, non-immune)	1100	QVQLVESGGGLVQAGGSLRLSCAASGF PVAGTWMEWYRQAPGKEREWVAAITS YGYRTYYADSVKGRFTISRDNAKNTVYL QMNSLKPEDTAVYYCNVKDEGKSSQVY DYWGQGTQVTVSS		N/A	IGHV3S53 (Alpaca)	IGHJ4 (Alpaca)	N/A	N/A	3221	NVKDEGKSSQVYDY		N/A	Tania Custodia et al., 2020 (https://www.biorxiv.org/content/10.1101/2020.06.23.165415v1.full.pdf+html)
Sb46	Nb	SARS-CoV2		SARS-CoV2		S; RBD	Phage Display Library (Nanobody, non-immune)	1101	QVQLVESGGGLVQAGGSLRLSCAASGF PVNYTIMFWYRKAPGKEREWVAAIKSH GATTLYADSVKGRFTISRDNAKNTVYLQ MNSLKPEDTAVYYCNVKDVGNDQKSYD YWGQGTQVTVSS		N/A	IGHV3S53 (Alpaca)	IGHJ4 (Alpaca)	N/A	N/A	3222	NVKDVGNDQKSYDY		N/A	Tania Custodia et al., 2020 (https://www.biorxiv.org/content/10.1101/2020.06.23.165415v1.full.pdf+html)
Sb47	Nb	SARS-CoV2				S; RBD	Phage Display Library (Nanobody, non-immune)	1102	QVQLVESGGGLVQAGGSLRLSCAASGF PVVWAHMHWYRQAPGKEREWVAAIT SEGAHTIYADSVKGRFTISRDNAKNTVYL QMNSLKPEDTAVYYCNVKDWGTYSTYY DYWGQGTQVTVSS		N/A	IGHV3S53 (Alpaca)	IGHJ4 (Alpaca)	N/A	N/A	3223	NVKDWGTYSTYYDY		N/A	Tania Custodia et al., 2020 (https://www.biorxiv.org/content/10.1101/2020.06.23.165415v1.full.pdf+html)

WO 2022/067091 PCT/US2021/052040

Sb5	Nb	SARS-CoV2 (weak)				S; RBD	Phage Display Library (Nanobody, non-immune)	1103	QVQLVESGGGLVQAGGSLRLSCAASGF PVAQQEMTWYRQAPGKEREWVAAISS IGSITHYADSVKGRFTISRDNAKNTVYLQ MNSLKPEDTAVYYCYVYVGASYIGQGT QVTVSS		N/A	IGHV3-3 (Alpaca)	IGHJ4 (Alpaca)	N/A	N/A	3224	YVYVGASY		N/A	Tania Custodia et al., 2020 (https://www.biorxiv.org/content/10.1101/2020.06.23.165415v1.full.pdf+html)
Sb50	Nb	SARS-CoV2				S; RBD	Phage Display Library (Nanobody, non-immune)	1104	QVQLVESGGGLVQAGGSLRLSCAASGF PVQYEHMHWYRQAPGKEREWVAAIVS EGAYTHYADSVKGRFTISRDNAKNTVYL QMNSLKPEDTAVYYCNVKDWGWLAQY YDYWGQGTQVTVSS		N/A	IGHV3S53 (Alpaca)	IGHJ4 (Alpaca)	N/A	N/A	3225	NVKDWGWL AQYYDY		N/A	Tania Custodia et al., 2020 (https://www.biorxiv.org/content/10.1101/2020.06.23.165415v1.full.pdf+html)
Sb52	Nb	SARS-CoV2				S; RBD	Phage Display Library (Nanobody, non-immune)	1105	QVQLVESGGGLVQAGGSLRLSCAASGF PVNYNWMEWYRQAPGKEREWVAAIT SWGYKTYYADSVKGRFTISRDNAKNTVY LQMNSLKPEDTAVYYCNVKDEGMWQ HYYDYWGQGTQVTVSS		N/A	IGHV3S53 (Alpaca)	IGHJ4 (Alpaca)	N/A	N/A	3226	NVKDEGMW QHYYDY		N/A	Tania Custodia et al., 2020 (https://www.biorxiv.org/content/10.1101/2020.06.23.165415v1.full.pdf+html)
Sb54	Nb	SARS-CoV2				S; RBD	Phage Display Library (Nanobody, non-immune)	1106	QVQLVESGGGLVQAGGSLRLSCAASGF PVWNTWMEWYRQAPGKEREWVAAIT SYGFKTYYADSVKGRFTISRDNAKNTVYL QMNSLKPEDTAVYYCNVKDEGNSQSHY DYWGQGTQVTVSS		N/A	IGHV3S53 (Alpaca)	IGHJ4 (Alpaca)	N/A	N/A	3227	NVKDEGNSQ SHYDY		N/A	Tania Custodia et al., 2020 (https://www.biorxiv.org/content/10.1101/2020.06.23.165415v1.full.pdf+html)
Sb56	Nb	SARS-CoV2				S; RBD	Phage Display Library (Nanobody, non-immune)	1107	QVQLVESGGGLVQAGGSLRLSCAASGF PVEMWSMEWYRQAPGKEREWVAAI MSFGYQTWYADSVKGRFTISRDNAKNT VYLQMNSLKPEDTAVYYCNVKDAGNSK ALYDYWGQGTQVTVSS		N/A	IGHV3S53 (Alpaca)	IGHJ4 (Alpaca)	N/A	N/A	3228	NVKDAGNSK ALYDY		N/A	Tania Custodia et al., 2020 (https://www.biorxiv.org/content/10.1101/2020.06.23.165415v1.full.pdf+html)
Sb57	Nb	SARS-CoV2				S; RBD	Phage Display Library (Nanobody, non-immune)	1108	QVQLVESGGGLVQAGGSLRLSCAASGF PVEHDHMHWYRQAPGKEREWVAAIVS QGAYTVYADSVKGRFTISRDNAKNTVYL QMNSLKPEDTAVYYCNVKDWGRAGAR YDYWGQGTQVTVSS		N/A	IGHV3S53 (Alpaca)	IGHJ4 (Alpaca)	N/A	N/A	3229	NVKDWGRA GARYDY		N/A	Tania Custodia et al., 2020 (https://www.biorxiv.org/content/10.1101/2020.06.23.165415v1.full.pdf+html)
Sb58	Nb	SARS-CoV2 (weak)				S; RBD	Phage Display Library (Nanobody, non-immune)	1109	QVQLVESGGGLVQAGGSLRLSCAASGF PVDAAWMEWYRQAPGKEREWVAAIT SYGYRTYYADSVKGRFTISRDNAKNTVYL QMNSLKPEDTAVYYCNVKDMDRWRTT YDYWGQGTQVTVSS		N/A	IGHV3S53 (Alpaca)	IGHJ4 (Alpaca)	N/A	N/A	3230	NVKDMDRW RTTYDY		N/A	Tania Custodia et al., 2020 (https://www.biorxiv.org/content/10.1101/2020.06.23.165415v1.full.pdf+html)
Sb6	Nb	SARS-CoV2				S; RBD	Phage Display Library (Nanobody, non-immune)	1110	QVQLVESGGGLVQAGGSLRLSCAASGF PVNHTRMYWYRQAPGKEREWVAAIQS HGQNTFYADSVKGRFTISRDNAKNTVYL QMNSLKPEDTAVYYCYVWVGNQYWG QGTQVTVSS		N/A	IGHV3-3 (Alpaca)	IGHJ4 (Alpaca)	N/A	N/A	3231	YVWVGNQY		N/A	Tania Custodia et al., 2020 (https://www.biorxiv.org/content/10.1101/2020.06.23.165415v1.full.pdf+html)
Sb60	Nb	SARS-CoV2				S; RBD	Phage Display Library (Nanobody, non-immune)	1111	QVQLVESGGGLVQAGGSLRLSCAASGF PVVAWQMTWYRQAPGKEREWVAAIR SFGVSTHYADSVKGRFTISRDNAKNTVYL QMNSLKPEDTAVYYCNVKDWGYEYEG YDYWGQGTQVTVSS		N/A	IGHV3S53 (Alpaca)	IGHJ4 (Alpaca)	N/A	N/A	3232	NVKDWGYEY EGYDY		N/A	Tania Custodia et al., 2020 (https://www.biorxiv.org/content/10.1101/2020.06.23.165415v1.full.pdf+html)
Sb61	Nb	SARS-CoV2				S; RBD	Phage Display Library (Nanobody, non-immune)	1112	QVQLVESGGGLVQAGGSLRLSCAASGF PVQHEWMEWYRQAPGKEREWVAAIT SYGYRTYYADSVKGRFTISRDNAKNTVYL QMNSLKPEDTAVYYCNVKDTGTYQAW YDYWGQGTQVTVSS		N/A	IGHV3S53 (Alpaca)	IGHJ4 (Alpaca)	N/A	N/A	3233	NVKDTGTYQ AWYDY		N/A	Tania Custodia et al., 2020 (https://www.biorxiv.org/content/10.1101/2020.06.23.165415v1.full.pdf+html)
Sb62	Nb	SARS-CoV2		SARS-CoV2		S; RBD	Phage Display Library (Nanobody, non-immune)	1113	QVQLVESGGGLVQAGGSLRLSCAASGF PVEQEHMYWYRQASGKEREWVAAIVS EGAYTAYADSVKGRFTISRDNAKNTVYL QMNSLKPEDTAVYYCNVKDWGGYQW YYDYWGQGTQVTVSS		N/A	IGHV3S53 (Alpaca)	IGHJ4 (Alpaca)	N/A	N/A	3234	NVKDWGGY QWYYDY		N/A	Tania Custodia et al., 2020 (https://www.biorxiv.org/content/10.1101/2020.06.23.165415v1.full.pdf+html)
Sb63	Nb	SARS-CoV2				S; RBD	Phage Display Library (Nanobody, non-immune)	1114	QVQLVESGGGLVQAGGSLRLSCAASGF PVNAEIMFWYRQAPGKEREWVAAIKSA GTTTLYADSVKGRFTISRDNAKNTVYLQ MNSLKPEDTAVYYCNVKDYGAQAHYYD YWGQGTQVTVSS		N/A	IGHV3S53 (Alpaca)	IGHJ4 (Alpaca)	N/A	N/A	3235	NVKDYGAQA HYYDY		N/A	Tania Custodia et al., 2020 (https://www.biorxiv.org/content/10.1101/2020.06.23.165415v1.full.pdf+html)

Sb67	Nb	SARS-CoV2				S; RBD	Phage Display Library (Nanobody, non-immune)	1115	QVQLVESGGGLVQAGGSLRLSCAASGF PVMWAHMAWYRQAPGKEREWVAAI VSAGAYTHYADSVKGRFTISRDNAKNTV YLQMNSLKPEDTAVYYCNVKDWGTYNS YYDYWGQGTQVTVSS		N/A	IGHV3S5 3 (Alpaca)	IGHJ4 (Alpaca)	N/A	N/A	3236	NVKDWGTYN SYYDY		N/A	Tania Custodia et al., 2020 (https://www.biorxiv.org/content/10.1101/2020.06.23.165415v1.full.pdf+html)
Sb7	Nb	SARS-CoV2		SARS-CoV2		S; RBD	Phage Display Library (Nanobody, non-immune)	1116	QVQLVESGGGLVQAGGSLRLSCAASGF PVNAEEMEWYRQAPGKEREWVAAISS SGDWTYYADSVKGRFTISRDNAKNTVYL QMNSLKPEDTAVYYCLVYVGSTYIGQGT QVTVSS		N/A	IGHV3-3 (Alpaca)	IGHJ4 (Alpaca)	N/A	N/A	3237	LVYVGSTY		N/A	Tania Custodia et al., 2020 (https://www.biorxiv.org/content/10.1101/2020.06.23.165415v1.full.pdf+html)
Sb71	Nb	SARS-CoV2				S; RBD	Phage Display Library (Nanobody, non-immune)	1117	QVQLVESGGGSVQAGGSLRLSCAASGN IQHIKYLGWFRQAPGREREGVAALMTR YGQTYYADSVKGRFTVSLDNAKNTVYLQ MNSLKPEDTALYYCAAAHYGDNFPLAY QAYLYWGQGTQVTVSS		N/A	IGHV3-3 (Alpaca)	IGHJ4 (Alpaca)	N/A	N/A	3238	AAAHYGDNF PLAYQAYLY		N/A	Tania Custodia et al., 2020 (https://www.biorxiv.org/content/10.1101/2020.06.23.165415v1.full.pdf+html)
Sb75	Nb	SARS-CoV2				S; RBD	Phage Display Library (Nanobody, non-immune)	1118	QVQLVESGGGSVQAGGSLRLSCAASGYI NQIYYLGWFRQAPGKEREGVAALNTYQ GQTYYADSVKGRFTVSLDNAKNTVYLQ MNSLKPEDTALYYCAAARWGRDEPLYH YYYSYWGQGTQVTVSS		N/A	IGHV3-3 (Alpaca)	IGHJ4 (Alpaca)	N/A	N/A	3239	AAARWGRDE PLYHYYYSY		N/A	Tania Custodia et al., 2020 (https://www.biorxiv.org/content/10.1101/2020.06.23.165415v1.full.pdf+html)
Sb76	Nb	SARS-CoV2		SARS-CoV2		S; RBD	Phage Display Library (Nanobody, non-immune)	1119	QVQLVESGGGLVQAGGSLRLSCAASSFP VDTYHMAWYRQAPGKEREWVAAIVS WGWRTYYADSVKGRFTISRDNAKNTVY LQMNSLKPEDTAVYYCNVKDIGAQEVH YDYWGQGTQVTVSS		N/A	IGHV3-3 (Alpaca)	IGHJ4 (Alpaca)	N/A	N/A	3240	NVKDIGAQEV HYDY		N/A	Tania Custodia et al., 2020 (https://www.biorxiv.org/content/10.1101/2020.06.23.165415v1.full.pdf+html)
Sb78	Nb	SARS-CoV2				S; RBD	Phage Display Library (Nanobody, non-immune)	1120	QVQLVESGGGSVQAGGSLRLSCAASGYI KSIKYLGWFRQAPGKEREGVAALMTRY GETYYADSVKGRFTVSLDNAKNTVYLQ MNSLKPEDTALYYCAAANYGNNWPLTG VNYWYWGQGTQVTVSS		N/A	IGHV3-3 (Alpaca)	IGHJ4 (Alpaca)	N/A	N/A	3241	AAANYGNN WPLTGVNYW Y		N/A	Tania Custodia et al., 2020 (https://www.biorxiv.org/content/10.1101/2020.06.23.165415v1.full.pdf+html)
Sb8	Nb	SARS-CoV2				S; RBD	Phage Display Library (Nanobody, non-immune)	1121	QVQLVESGGGLVQAGGSLRLSCAASGF PVKSYEMEWYRQAPGKEREWVAAISSY GEYTEYADSVKGRFTISRDNAKNTVYLQ MNSLKPEDTAVYYCYVWVGDSYLGQGT QVTVSS		N/A	IGHV3-3 (Alpaca)	IGHJ4 (Alpaca)	N/A	N/A	3242	YVWVGDSY		N/A	Tania Custodia et al., 2020 (https://www.biorxiv.org/content/10.1101/2020.06.23.165415v1.full.pdf+html)
Sb83	Nb	SARS-CoV2				S; RBD	Phage Display Library (Nanobody, non-immune)	1122	QVQLVESGGGSVQAGGSLRLSCAASGG ITHIVYLGWFRQAPGKEREGVAALMTR WGTTYYADSVKGRFTVSLDNAKNTVYL QMNSLKPEDTALYYCAAAKYGQNFPLSY HAYRYWGQGTQVTVSS		N/A	IGHV3-3 (Alpaca)	IGHJ4 (Alpaca)	N/A	N/A	3243	AAAKYGQNF PLSYHAYRY		N/A	Tania Custodia et al., 2020 (https://www.biorxiv.org/content/10.1101/2020.06.23.165415v1.full.pdf+html)
Sb84	Nb	SARS-CoV2				S; RBD	Phage Display Library (Nanobody, non-immune)	1123	QVQLVESGGGSVQAGGSLRLSCAASGYI KHIEYLGWFRQAPGKEREGVAALKTSSG STYYADSVKGRFTVSLDNAKNTVYLQM NSLKPEDTALYYCAAARYGRSDPLHYHE YSYWGQGTQVTVSS		N/A	IGHV3-3 (Alpaca)	IGHJ4 (Alpaca)	N/A	N/A	3244	AAARYGRSDP LHYHEYSY		N/A	Tania Custodia et al., 2020 (https://www.biorxiv.org/content/10.1101/2020.06.23.165415v1.full.pdf+html)
Sb85	Nb	SARS-CoV2				S; RBD	Phage Display Library (Nanobody, non-immune)	1124	QVQLVESGGGSVQAGGSLRLSCAASGSI SSITYLGWFRQAPGKEREGVAALVTSRG KTYYADSVKGRFTVSLDNAKNTVYLQM NSLKPEDTALYYCAAASWGYTWPLYTYD YWYWGQGTQVTVSS		N/A	IGHV3-3 (Alpaca)	IGHJ4 (Alpaca)	N/A	N/A	3245	AAASWGYTW PLYTYDYWY		N/A	Tania Custodia et al., 2020 (https://www.biorxiv.org/content/10.1101/2020.06.23.165415v1.full.pdf+html)
Sb88	Nb	SARS-CoV2				S; RBD	Phage Display Library (Nanobody, non-immune)	1125	QVQLVESGGGLVQAGGSLRLSCAASGF PVWAHHMLWYRQAPGKEREWVAAIA SWGANTAYADSVKGRFTISRDNAKNTV YLQMNSLKPEDTAVYYCNVKDSGQYRE NYDYWGQGTQVTVSS		N/A	IGHV3S5 3 (Alpaca)	IGHJ4 (Alpaca)	N/A	N/A	3246	NVKDSGQYR ENYDY		N/A	Tania Custodia et al., 2020 (https://www.biorxiv.org/content/10.1101/2020.06.23.165415v1.full.pdf+html)
Sb9	Nb	SARS-CoV2				S; RBD	Phage Display Library (Nanobody, non-immune)	1126	QVQLVESGGGLVQAGGSLRLSCAASGF PVGQQHMYWYRQAPGKEREWVAAIYS YGHITKYADSVKGRFTISRDNAKNTVYLQ MNSLKPEDTAVYYCWVYVGDYYEGQG TQVTVSS		N/A	IGHV3-3 (Alpaca)	IGHJ4 (Alpaca)	N/A	N/A	3247	WVYVGDYY		N/A	Tania Custodia et al., 2020 (https://www.biorxiv.org/content/10.1101/2020.06.23.165415v1.full.pdf+html)

Sb90	Nb	SARS-CoV2				S; RBD	Phage Display Library (Nanobody, non-immune)	1127	QVQLVESGGGSVQAGGSLRLSCAASGA INQIYYLGWFRQAPGKEREGVAALSTKY GETYYADSVKGRFTVSLDNAKNTVYLQ MNSLKPEDTALYYCAAARWGRQYPLTF VYYSYWGQGTQVTVSS		N/A	IGHV3-3 (Alpaca)	IGHJ4 (Alpaca)	N/A	N/A	3248	AAARWGRQY PLTFVYYSY		N/A	Tania Custodia et al., 2020 (https://www.biorxiv.org/content/10.1101/2020.06.23.165415v1.full.pdf+html)
Sb93	Nb	SARS-CoV2				S; RBD	Phage Display Library (Nanobody, non-immune)	1128	QVQLVESGGGSVQAGGSLRLSCAASGH IAQIEYLGWFRQAPGKEREGVAALSTNQ GYTYYADSVKGRFTVSLDNAKNTVYLQ MNSLKPEDTALYYCAAARWGRTYPLSY MAYTYWGQGTQVTVSS		N/A	IGHV3-3 (Alpaca)	IGHJ4 (Alpaca)	N/A	N/A	3249	AAARWGRTY PLSYMAYTY		N/A	Tania Custodia et al., 2020 (https://www.biorxiv.org/content/10.1101/2020.06.23.165415v1.full.pdf+html)
Sb94	Nb	SARS-CoV2				S; RBD	Phage Display Library (Nanobody, non-immune)	1129	QVQLVESGGGSVQAGGSLRLSCAASGYI TMIEYLGWFRQAPGKEREGVAALNTHT GGTYYADSVKGRFTVSLDNAKNTVYLQ MNSLKPEDTALYYCAAARWGRYEPLHY AYYSYWGQGTQVTVSS		N/A	IGHV3-3 (Alpaca)	IGHJ4 (Alpaca)	N/A	N/A	3250	AAARWGRYE PLHYAYYSY		N/A	Tania Custodia et al., 2020 (https://www.biorxiv.org/content/10.1101/2020.06.23.165415v1.full.pdf+html)
Sb95	Nb	SARS-CoV2				S; RBD	Phage Display Library (Nanobody, non-immune)	1130	QVQLVESGGGSVQAGGSLRLSCAASGN IYNIKYLGWFRQAPGKEREGVAALMTRY GETYYADSVKGRFTVSLDNAKNTVYLQ MNSLKPEDTALYYCAAASYGANWPLVS AAYTYWGQGTQVTVSS		N/A	IGHV3-3 (Alpaca)	IGHJ4 (Alpaca)	N/A	N/A	3251	AAASYGANW PLVSAAYTY		N/A	Tania Custodia et al., 2020 (https://www.biorxiv.org/content/10.1101/2020.06.23.165415v1.full.pdf+html)
Sb97	Nb	SARS-CoV2				S; RBD	Phage Display Library (Nanobody, non-immune)	1131	QVQLVESGGGSVQAGGSLRLSCAASGA ISTIEYLGWFRQAPGREREGVAALYTER GYTYYADSVKGRFTVSLDNAKNTVYLQ MNSLKPEDTALYYCAAARYGHAQAPLH YFWYGYWGQGTQVTVSS		N/A	IGHV3-3 (Alpaca)	IGHJ4 (Alpaca)	N/A	N/A	3252	AAARYGHAQ APLHYFWYGY		N/A	Tania Custodia et al., 2020 (https://www.biorxiv.org/content/10.1101/2020.06.23.165415v1.full.pdf+html)
SR1	Nb	SARS-CoV2				S; RBD	Phage Display Library (Nanobody, non-immune)	1132	QVQLVESGGGLVQAGGSLRLSCAASGF PVAAYEMEWYRQAPGKEREWVAAINS MGDQTYYADSVKGRFTISRDNAKNTVY LQMNSLKPEDTAVYYCYVYVGFSYIGQG TQVTVSS		N/A	IGHV3-3 (Alpaca)	IGHJ4 (Alpaca)	N/A	N/A	3253	YVYVGFSY		N/A	Tingting Li et al., 2020 (https://www.biorxiv.org/content/10.1101/2020.06.09.143438v1)
SR13	Nb	SARS-CoV2				S; RBD	Phage Display Library (Nanobody, non-immune)	1133	QVQLVESGGGLVQAGGSLRLSCAASGF PVDYMEMEWFRQAPGKEREWVAAITS NGRETYYADSVKGRFTVSRDNAKNTVYL QMNSLKPEDTAVYYCYVYVGSSYIGQGT QVTVSS		N/A	IGHV3-3 (Alpaca)	IGHJ4 (Alpaca)	N/A	N/A	3254	YVYVGSSY		N/A	Tingting Li et al., 2020 (https://www.biorxiv.org/content/10.1101/2020.06.09.143438v1)
SR18	Nb	SARS-CoV2				S; RBD	Phage Display Library (Nanobody, non-immune)	1134	QVQLVESGGGLVQAGGSLRLSCAASGF PVWFQEMEWYRQAPGKEREWVAAISS QGTHTYYADSVKGRFTISRDNAKNTVYL QMNSLKPEDTAVYYCYVYVGASYLGQG TQVTVSS		N/A	IGHV3-3 (Alpaca)	IGHJ4 (Alpaca)	N/A	N/A	3255	YVYVGASY		N/A	Tingting Li et al., 2020 (https://www.biorxiv.org/content/10.1101/2020.06.09.143438v1)
SR31	Nb	SARS-CoV2				S; RBD	Phage Display Library (Nanobody, non-immune)	1135	QVQLVESGGGLVQAGGSLRLSCAASGF PVWQGEMAWYRQAPGKEREWVAAIS SMGYKTYYADSVKGRFTISRDNAKNTVY LQMNSLKPEDTAVYYCAVMVGFWYAG QGTQVTVSS		N/A	IGHV3-3 (Alpaca)	IGHJ4 (Alpaca)	N/A	N/A	3256	AVMVGFWY		N/A	Tingting Li et al., 2020 (https://www.biorxiv.org/content/10.1101/2020.06.09.143438v1)
SR34	Nb	SARS-CoV2				S; RBD	Phage Display Library (Nanobody, non-immune)	1136	QVQLVESGGGLVQAGGSLRLSCAAGGF PVKDHEMEWYRQAPGKEREWVAAITS SGWGTNTYYADSVKGRFTISRDNAKNT VYLQMNSLKPEDTAVYYCYVYVGSSYIG QGTQVTVSS		N/A	IGHV3-3 (Alpaca)	IGHJ4 (Alpaca)	N/A	N/A	3257	YVYVGSSY		N/A	Tingting Li et al., 2020 (https://www.biorxiv.org/content/10.1101/2020.06.09.143438v1)
SR38	Nb	SARS-CoV2				S; RBD	Phage Display Library (Nanobody, non-immune)	1137	QVQLVESGGGLVQAGGSLRLSCAASGF PVNQEEMEWYRQAPGKEREWVAAIKS WGTLTAYADSVKGRFTISRDNAKNTVYL QMNSLKPEDTAVYYCAVHVGQTYIGQG TQVTVSS		N/A	IGHV3-3 (Alpaca)	IGHJ4 (Alpaca)	N/A	N/A	3258	AVHVGQTY		N/A	Tingting Li et al., 2020 (https://www.biorxiv.org/content/10.1101/2020.06.09.143438v1)
SR4	Nb	SARS-CoV2				S; RBD	Phage Display Library (Nanobody, non-immune)	1138	QVQLVESGGGLVQAGGSLRLSCAASGF PVYSWNMWWYRQAPGKEREWVAAIE SHGDSTRYADSVKGRFTISRDNAKNTVY LQMNSLKPEDTAVYYCYVWVGHTYYG QGTQVTVSS		N/A	IGHV3-3 (Alpaca)	IGHJ4 (Alpaca)	N/A	N/A	3259	YVWVGHTY		N/A	Tingting Li et al., 2020 (https://www.biorxiv.org/content/10.1101/2020.06.09.143438v1)
SR5	Nb	SARS-CoV2				S; RBD	Phage Display Library (Nanobody, non-immune)	1139	QVQLVESGGGLVQAGGSLRLRCAASGF PVETTEMEWYRQAPGKEREWVAAISSY GSETYYADSVKGRFTISRDNAKNTVYLQ MNSLKPEDTAVYYCYVYVGTSYLGQGT QVTVSS		N/A	IGHV3-3 (Alpaca)	IGHJ4 (Alpaca)	N/A	N/A	3260	YVYVGTSY		N/A	Tingting Li et al., 2020 (https://www.biorxiv.org/content/10.1101/2020.06.09.143438v1)
SR7	Nb	SARS-CoV2				S; RBD	Phage Display Library (Nanobody, non-immune)	1140	QVQLVESGGGLVQAGGSLRLSCAASGF PVWSNEMEWYRQAPGKEREWVAAITS YGTTEYADSVKGRFTISRDNAKNTVYLQ MNSLKPEDTAVYYCYVYVGYSYIGQGTQ VTVSS		N/A	IGHV3S53 (Alpaca)	IGHJ4 (Alpaca)	N/A	N/A	3261	YVYVGYSY		N/A	Tingting Li et al., 2020 (https://www.biorxiv.org/content/10.1101/2020.06.09.143438v1)

Ty1	Nb	SARS-CoV2		SARS-CoV2		S; RBD	Immunised Alpaca	1141	QVQLVETGGGLVQPGGSLRLSCAASGF TFSSVYMNWVRQAPGKGPEWVSRISP NSGNIGYTDSVKGRFTISRDNAKNTLYL QMNNLKPEDTALYYCAIGLNLSSSSVRG QGTQVTVSS		N/A	IGHV3S1 (Alpaca)	IGHJ4 (Alpaca)	N/A	N/A	3262	AIGLNLSSSSV		N/A	Leo Hanke et al., 2020 (https://www.biorxiv.org/content/10.1101/2020.06.02.130161v1)
VH-Fc-B01	Nb	SARS-CoV2		SARS-CoV2		S; RBD	Phage Display (Human)		ND		ND	ND	ND	ND	ND		ND		ND	Colton J. Bracken et al., 2020 (https://www.biorxiv.org/content/10.1101/2020.08.08.242511v1.full.pdf)
VH2-A01-B01	Nb	SARS-CoV2		SARS-CoV2		S; RBD	Phage Display (Human)		ND		ND	ND	ND	ND	ND		ND		ND	Colton J. Bracken et al., 2020 (https://www.biorxiv.org/content/10.1101/2020.08.08.242511v1.full.pdf)
VH2-A01-B02	Nb	SARS-CoV2		SARS-CoV2		S; RBD	Phage Display (Human)		ND		ND	ND	ND	ND	ND		ND		ND	Colton J. Bracken et al., 2020 (https://www.biorxiv.org/content/10.1101/2020.08.08.242511v1.full.pdf)
VH3-B01	Nb	SARS-CoV2		SARS-CoV2		S; RBD	Phage Display (Human)		ND		ND	ND	ND	ND	ND		ND		ND	Colton J. Bracken et al., 2020 (https://www.biorxiv.org/content/10.1101/2020.08.08.242511v1.full.pdf)
VHH-72	Nb	SARS-CoV1, SARS-CoV2		SARS-CoV2 and SARS-CoV1		S; RBD	Immunised Llama	1142	QVQLQESGGGLVQAGGSLRLSCAASGR TFSEYAMGWFRQAPGKEREFVATISWS GGSTYYTDSVKGRFTISRDNAKNTVYLQ MNSLKPDDTAVYYCAAAGLGTVVSEW DYDYDYWGQGTQVTVSS		N/A	IGHV3-3 (Alpaca)	IGHJ4 (Alpaca)	N/A	N/A	3263	AAAGLGTVVS EWDYDYDY		N/A	Daniel Wrapp et al., 2020 (https://www.sciencedirect.com/science/article/pii/S0092867420304943)
W23UACh	Nb	SARS-CoV2				S; RBD	Immunised Alpaca	1143	QVQLVESGGGLVQPGESLRLSCAASGNI FGIAAVHWFRKAPGKEREFTAGFGSDG STNYANSVKGRFTISRDNAKNTTYLQMN SLKPEDTAVYYCHALIKNELGFLDYWGP GTQVTVSS		N/A	IGHV3S53 (Alpaca)	IGHJ4 (Alpaca)	N/A	N/A	3264	HALIKNELGFL DY		N/A	Guillermo Nieto et al., 2020 (https://www.biorxiv.org/content/10.1101/2020.06.09.137935v1)
W25UACh	Nb	SARS-CoV2				S; RBD	Immunised Alpaca	1144	QVQLVESGGGLVQPGESLRLSCAASGSI FGIYAVHWFRMAPGKEREFTAGFGSHG STNYAASVKGRFTMSRDNAKNTTYLQM NSLKPADTAVYYCHALIKNELGFLDYWG PGTQVTVSS		N/A	IGHV3S53 (Alpaca)	IGHJ4 (Alpaca)	N/A	N/A	3265	HALIKNELGFL DY		N/A	Guillermo Nieto et al., 2020 (https://www.biorxiv.org/content/10.1101/2020.06.09.137935v1)

All publications and patents mentioned in the present application are herein incorporated by reference. Various modification and variation of the described methods and compositions of the invention will be apparent to those skilled in the art without departing from the scope and spirit of the invention. Although the invention has been described in connection with specific preferred embodiments, it should be understood that the invention as claimed should not be unduly limited to such specific embodiments. Indeed, various modifications of the described modes for carrying out the invention that are obvious to those skilled in the relevant fields are intended to be within the scope of the following claims.

CLAIMS

We claim:

1. A method comprising:

a) administering a first composition to a subject, wherein said first composition comprises polycationic structures, and wherein said first composition is free, or essentially free, of nucleic acid molecules; and

b) administering a second composition to said subject after administering said first composition, wherein said second composition comprises a plurality of one or more non-viral expression vectors that encode at least one anti-SARS-CoV-2 antibody or antigen-binding portion thereof, and/or recombinant ACE2, and

wherein, as a result of said administering said first and second compositions, said at least one anti-SARS-CoV-2 antibody, or antigen-binding portion thereof, and/or said recombinant ACE2, is expressed in said subject.

2. The method of Claim 1, wherein:

A) said subject is infected with the SARS-CoV-2 virus, and wherein said at least one anti-SARS-CoV-2 antibody, or antigen-binding portion thereof, or recombinant ACE2 is expressed in said subject at an expression level sufficient to reduce: i) the SARS-CoV-2 viral load in said subject, and/or ii) at least one symptom in said subject caused by said SARS-CoV-2 infection; or

B) said subject is not infected with the SARS-CoV-2 virus, and wherein said at least one anti-SARS-CoV-2 antibody, or antigen-binding portion thereof, or recombinant ACE2 is expressed in said subject at an expression level sufficient to prevent said subject from being infected by the SARS-CoV-2 virus.

3. The method of Claim 2, wherein said expression level is maintained in said subject for at least two weeks without: i) any further, or only one, two, or three further repeat, of steps a) and b), and ii) any further administration of vectors encoding: said at least one anti-SARS-CoV-2 antibody or antigen-binding portion thereof, or said ACE2.

4. The method of Claim 2, wherein said expression level is maintained in said subject for at least one month without: i) any further, or only one, two, or three further repeat, of steps a) and b),

and ii) any further administration of vectors encoding: said at least one anti-SARS-CoV-2 antibody or antigen-binding portion thereof or said ACE2.

5. The method of Claim 2, wherein said expression level is maintained in said subject for at least one year without: i) any further, or only one, two, or three further repeat, of steps a) and b), and ii) any further administration of vectors encoding: said at least one anti-SARS-CoV-2 antibody or antigen-binding portion thereof or said ACE2.

6. The method of Claim 1, wherein said at least one anti-SARS-CoV-2 antibody, or antigen-binding portion thereof, is expressed in said subject at a level of: i) between 500ng/ml and 50ug/ml, or 10-20ug/ml, for at least 25 days, or ii) at least 250 ng/ml for at least 25 days.

7. The method of Claim 1, wherein said polycationic structures comprise cationic lipids.

8. The method of Claim 7, wherein said first composition comprises a plurality of liposomes, wherein at least some of said liposomes comprises said cationic lipids.

9. The method of Claim 7, wherein at least some of said liposomes comprise neutral lipids.

10. The method of Claim 9, wherein the ratio of said cationic lipids to said neutral lipids in said liposomes is 95:05 - 80:20 or about 1:1.

11. The method of Claim 10, wherein said cationic and neutral lipids are selected from the group consisting of: distearoyl phosphatidyl choline (DSPC); hydrogenated or non-hydrogenated soya phosphatidylcholine (HSPC); distearoylphosphatidylethanolamine (DSPE); egg phosphatidylcholine (EPC); 1,2-Distearoyl-sn-glycero-3-phospho-rac-glycerol (DSPG); dimyristoyl phosphatidylcholine (DMPC); 1,2-Dimyristoyl-sn-glycero-3-phosphoglycerol (DMPG); 1,2-Dipalmitoyl-sn-glycero-3-phosphate (DPPA); trimethylammonium propane lipids; DOTIM (1-[2-9(2)-octadecenoylloxy)ethyl]-2-(8(2)-heptadecenyl)-3-(2-hydroxyethyl) midizolinium chloride) lipids; and mixtures of two or more thereof.

12. The method of Claim 1, wherein said one or more non-viral expression vectors comprise plasmids, wherein said plasmids are not attached to, or encapsulated in, any delivery agent.

13. The method of Claim 1, wherein said one or more non-viral expression vectors comprise a first nucleic acid sequence encoding an antibody light chain variable region, and a second nucleic acid sequence encoding an antibody heavy chain variable region, and optionally, a third nucleic acid sequence encoding an antibody light chain variable region, and a fourth nucleic acid sequence encoding an antibody heavy chain variable region.

14. The method of Claim 1, wherein: A) said antigen-binding portion thereof is selected from the group consisting of: a Fab', F(ab)2, Fab, and a minibody, and/or B) said wherein said at least one anti-SARS-CoV-2 antibody, or antigen-binding portion thereof, is bi-specific for different SARS-CoV-2 antigens.

15. The method of Claim 1, wherein said anti-SARS-CoV-2 antibody is monoclonal antibody, or antigen-binding portion thereof, is selected from the group consisting of: REGN10933, REGN10987; VIR-7831; LY-CoV1404; LY3853113; Zost 2355K; CV07-209K; C121L; Zost 2504L; CV38-183L; COVA215K; RBD215; CV07-250L; C144L; COVA118L; C135K; and B38.

16. The method of Claim 1, wherein said anti-SARS-CoV-2 antibody, or antigen-binding portion thereof, comprises at least two, three, four, five, six, seven, eight, nine, ten, eleven, twelve, or more of any combination of the following: REGN10933, REGN10987; VIR-7831; LY-CoV1404; LY3853113; Zost 2355K; CV07-209K; C121L; Zost 2504L; CV38-183L; COVA215K; RBD215; CV07-250L; C144L; COVA118L; C135K; and B38.

17. The method of Claim 1, wherein said anti-SARS-CoV-2 antibody, or antigen binding portion thereof, is as described in Table 7.

18. The method of Claim 1, wherein said at least one anti-SARS-CoV-2 antibody, or antigen-binding portion thereof, comprises at least two anti-SARS-CoV-2 antibodies, and/or antigen-binding portions thereof, which are expressed in said subject at an expression level sufficient to reduce: i) the SARS-CoV-2 viral load in said subject, and/or ii) at least one symptom in said subject caused by said SARS-CoV-2 infection.

19. The method of Claim 1, wherein said at least one anti-SARS-CoV-2 antibody, or antigen-binding portion thereof, comprises at least four, or at least eight, or at least 11, anti-SARS-CoV-2 antibodies and/or antigen-binding portions thereof.

20. The method of Claim 1, wherein said at least one anti-SARS-CoV-2 antibody, or antigen-binding portion thereof, comprises at least four, or at least eight, or at least 11, anti-SARS-CoV-2 antibodies and/or antigen-binding portions thereof, and which are expressed in said subject at an expression level sufficient to reduce: i) the SARS-CoV-2 viral load in said subject, and/or ii) at least one symptom in said subject caused by said SARS-CoV-2 infection.

21. The method of Claim 1, wherein said administering comprises intravenous administering.

22. The method of Claim 1, wherein said second composition is administered: i) between 0.5 and 80 minutes after said first composition, or between about 1 and 20 minutes after said first composition.

23. The method of Claim 1, further comprising: c) administering an agent, in said first and/or second composition, or present in a third composition, wherein said agent: i) increases the level of expression of said at least one anti-SARS-CoV-2 antibody or antigen-binding portion thereof, and/or ii) and/or the length of time of said expression compared to when said agent is not administered to said subject.

24. The method of Claim 23, wherein said agent is present in said first composition.

25. The method of Claim 23, wherein said agent is present in said third composition, and is administered at least one hour prior to said first composition.

26. The method of Claim 23, wherein said agent is a dexamethasone fatty acid ester.

27. The method of Claim 26, wherein said dexamethasone fatty acid ester has the following Formula:

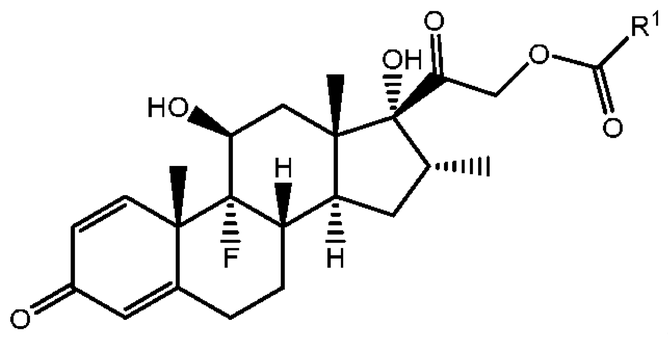

, wherein R^1 is C_5-C_{23} alkyl or C_5-C_{23} alkenyl.

28. The method of Claim 23, wherein said agent is present in said first, second, or third composition at a concentration of 0.01-35 mg/ml.

29. The method of Claim 1, wherein said subject has lung, cardiovascular, and/or multi-organ inflammation.

30. The method of Claim 1, wherein said subject is on a ventilator.

31. The method of Claim 1, wherein said first and/or second compositions further comprise a physiologically tolerable buffer or intravenous solution.

32. The method of Claim 1, wherein said first and/or second compositions further comprise lactated Ringer's solution or saline solution.

33. The method of Claim 1, wherein said first compositions comprise liposomes comprising said polycationic structures, wherein said liposomes further comprising one or more macrophage targeting moieties selected from the group consisting of: mannose moieties, maleimide moieties, a folate receptor ligand, folate, folate receptor antibody or fragment thereof, formyl peptide receptor ligands, N-formyl-Met-Leu-Phe, tetrapeptide Thr-Lys-Pro-Arg, galactose, and lactobionic acid.

34. The method of Claim 1, wherein said plurality of one or more non-viral expression vectors are not attached to, or encapsulated in, any delivery agent.

35. The method of Claim 1, wherein said subject is a human.

36. The method of Claim 1, wherein 0.05-60 mg/mL of said expression vectors are present in said second composition.

37. The method of Claim 1, wherein said polycationic structures comprise cationic liposomes which are present at a concentration of 0.5-100 mM in said first composition.

38. The method of Claim 1, wherein said subject is a human, wherein:

i) an amount of said first composition is administered such that said human receives a dosage of 2-50 mg/kg of said polycationic structures; and/or

ii) an amount of said second composition is administered such that said human receives a dosage of 0.05-60 mg/kg of said expression vectors.

39. The method of Claim 1, wherein said polycationic structures comprise cationic liposomes, wherein said cationic liposomes further comprise a lipid bi-layer integrating peptide and/or a target peptide.

40. The method of Claim 39, wherein: i) said lipid bi-layer integrating peptide is selected from the group consisting of: surfactant protein D (SPD), surfactant protein C (SPC), surfactant protein B (SPB), and surfactant protein A (SPA), and ii) said target peptide is selected from the group consisting of: microtubule-associated sequence (MTAS), nuclear localization signal (NLS), ER secretion peptide, ER retention peptide, and peroxisome peptide.

41. The method of Claim 1, wherein steps a) and b) are repeated between 1 and 60 days after the initial step b).

42. The method of Claim 1, wherein each of said non-viral expression vectors comprise between 5,500 and 30,000 nucleic acid base pairs.

43. The method of Claim 1, further comprising: administering an anti-viral agent to said subject.

44. The method of Claim 43, wherein said anti-viral agent comprises Remdesivir or a protein comprising at least part of the ACE2 receptor.

45. The method of Claim 1, further comprising: administering an anti-inflammatory and/or anticoagulant to said subject.

46. The method of Claim 1, wherein said one or more non-viral expression vectors are CPG-free or CPG-reduced.

47. A system comprising:

a) a first container;

b) a first composition inside said first container and comprising polycationic structures, wherein said first composition is free, or essentially free, of nucleic acid molecules;

c) a second container; and

d) a second composition inside said second container and comprising a plurality of one or more non-viral expression vectors that encode at least one anti-SARS-CoV-2 antibody or antigen-binding portion thereof, or an ACE2 protein.

48. The system of Claim 47, further comprising an agent that: i) increases the level of expression of said at least one anti-SARS-CoV-2 antibody or antigen-binding portion thereof, or said ACE2 protein, when administered to a subject, and/or ii) and/or the length of time of said expression; as compared to when said agent is not administered to said subject.

49. The system of Claim 48, wherein said agent is present in said first, second, or a third composition at a concentration of 0.01-35 mg/ml.

50. The system of Claim 48, wherein said agent is present in said first composition and/or said second composition.

51. The system of Claim 48, further comprising a third container, and wherein said agent is present in said third container.

52. A method of simultaneously expressing at least three different antibodies, or antigen binding portions thereof, in a subject comprising:

a) administering a first composition to a subject, wherein said first composition comprises polycationic structures, and wherein said first composition is free, or essentially free, of nucleic acid molecules; and

b) administering a second composition to said subject after administering said first composition, wherein said second composition comprises a plurality of one or more non-viral expression vectors that encode at least three different antibodies or antigen-binding portions thereof, and

wherein, as a result of said administering said first and second compositions, said at least three different antibodies, or antigen-binding portions thereof, are simultaneously expressed in said subject.

53. The method of Claim 52, wherein said at least three different antibodies or antigen-binding portions thereof, are each expressed in said subject at a level of at least 100 ng/ml.

54. The method of Claim 52, wherein said at least three different antibodies or antigen-binding portions thereof, are each expressed in said subject at a level of at least 100 ng/ml for at least 25 days.

55. The method of Claim 52, wherein said at least three different antibodies or antigen-binding portions thereof, are expressed in said subject at a level of at least 200 ng/ml.

56. The method of Claim 52, wherein said at least three different antibodies or antigen-binding portions thereof, are expressed in said subject at a level of at least 200 ng/ml for at least 25 days.

57. The method of Claim 52, wherein:

A) said expression level for each of said three different antibodies, or antigen binding portions thereof, is maintained in said subject for at least two weeks, or at least 3 weeks, without: i) any further, or only one further, repeat of steps a) and b), and ii) any further administration of vectors encoding said at least three different antibodies or antigen binding portions thereof;

B) repeating steps a) and b) at least once or at least twice.

58. The method of Claim 52, wherein said expression level is maintained in said subject for at least two weeks, or at least 3 weeks, without: i) any further, or only one or two further, repeats of steps a) and b), and ii) any further administration of vectors encoding said at least three different antibodies or antigen binding portions thereof.

59. The method of Claim 52, wherein said polycationic structures comprise cationic lipids.

60. The method of Claim 52, wherein said first composition comprises a plurality of liposomes, wherein at least some of said liposomes comprises said cationic lipids.

61. The method of Claim 60, wherein at least some of said liposomes comprise neutral lipids.

62. The method of Claim 60, wherein the ratio of said cationic lipids to said neutral lipids in said liposomes is 95:05 - 80:20 or about 1:1.

63. The method of Claim 61, wherein said cationic and neutral lipids are selected from the group consisting of: distearoyl phosphatidyl choline (DSPC); hydrogenated or non-hydrogenated soya phosphatidylcholine (HSPC); distearoylphosphatidylethanolamine (DSPE); egg phosphatidylcholine (EPC); 1,2-Distearoyl-sn-glycero-3-phospho-rac-glycerol (DSPG); dimyristoyl phosphatidylcholine (DMPC); 1,2-Dimyristoyl-sn-glycero-3-phosphoglycerol (DMPG); 1,2-Dipalmitoyl-sn-glycero-3-phosphate (DPPA); trimethylammonium propane lipids; DOTIM (1-[2-9(2)-octadecenoylloxy)ethyl]-2-(8(2)-heptadecenyl)-3-(2-hydroxyethyl) midizolinium chloride) lipids; and mixtures of two or more thereof.

64. The method of Claim 52, wherein said one or more non-viral expression vectors comprise plasmids or synthetic plasmids, wherein said plasmids and synthetic plasmids are not attached to, or encapsulated in, any delivery agent.

65. The method of Claim 52, wherein said one or more non-viral expression vectors comprise three non-viral expression vectors.

66. The method of Claim 65, wherein each of said three non-viral expression vector encodes a different antibody or antigen binding fragment thereof.

67. The method of Claim 52, wherein said one or more non-viral expression vectors comprise six non-viral expression vectors.

68. The method of Claim 67, wherein each of said six non-viral expression vectors encodes a different antibody light chain variable region, or heavy chain variable region.

69. The method of Claim 52, wherein said one or more non-viral expression vectors comprise first, second, and third nucleic acid sequences each encoding an antibody light chain variable region, and fourth, fifth, and sixth nucleic acid sequences each encoding an antibody heavy chain variable region.

70. The method of Claim 52, wherein said antigen-binding portions thereof are selected from the group consisting of: a Fab', F(ab)2, Fab, and a minibody.

71. The method of Claim 52, wherein: i) at least one of said at least three different antibodies or antigen-binding portions thereof is an anti-SARS-CoV-2 antibody or antigen binding portion thereof, or ii) at least one of said at least three different antibodies, or antigen binding portions thereof, is specific for SARS-CoV-2 and at least one is specific for influenza A, and/or at least one is specific for influenza B.

72. The method of Claim 52, wherein said at least three different antibodies, or antigen-binding portions thereof, at least two, three, four, five, six, seven, eight, nine, ten, eleven, or more of any combination of the following: REGN10933, REGN10987; VIR-7831; LY-CoV1404; LY3853113; Zost 2355K; CV07-209K; C121L; Zost 2504L; CV38-183L; COVA215K; RBD215; CV07-250L; C144L; COVA118L; C135K; 5J8, and B38.

73. The method of Claim 52, wherein said at least three different antibodies, or antigen-binding portions thereof, are each fully or substantially neutralizing for SARS-CoV-2.

74. The method of Claim 52, wherein said at least three different antibodies, or antigen-binding portions thereof, are each fully or substantially neutralizing for a virus selected from the group consisting of: HIV, influenza A, influenza B, and malaria.

75. The method of Claim 52, wherein at least one of said at least three different antibodies or antigen-binding portions thereof is an antibody or antigen binding portion thereof selected from Table 4, Table 5, and/or Table 7.

76. The method of Claim 52, wherein said at least three different antibodies or antigen-binding portions thereof comprise at least four different antibodies or antigen-binding portions thereof.

77. The method of Claim 52, wherein said at least three different antibodies or antigen-binding portions thereof comprise at least six different antibodies or antigen-binding portions thereof.

78. The method of Claim 52, wherein said at least three different antibodies or antigen-binding portions thereof comprise at least eleven different antibodies or antigen-binding portions thereof.

79. The method of Claim 52, wherein said administering comprises intravenous administering.

80. The method of Claim 52, wherein said second composition is administered: i) between 0.5 and 80 minutes after said first composition, or between about 1 and 20 minutes after said first composition.

81. The method of Claim 52, further comprising: c) administering an agent, in said first and/or second composition, or present in a third composition, wherein said agent: i) increases the level of expression of at least one of said at least three different antibodies or antigen-binding portions thereof, and/or ii) and/or the length of time of said expression of at least one of said three different antibodies, or antigen-binding portions thereof, compared to when said agent is not administered to said subject.

82. The method of Claim 81, wherein said agent is present in said first composition.

83. The method of Claim 81, wherein said agent is present in said third composition, and is administered at least one hour prior to said first composition.

84. The method of Claim 81, wherein said agent is a dexamethasone fatty acid ester.

85. The method of Claim 84, wherein said dexamethasone fatty acid ester has the following Formula:

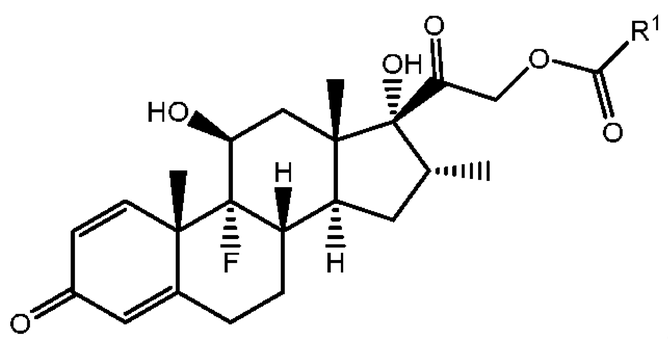

, wherein R^1 is C_5-C_{23} alkyl or C_5-C_{23} alkenyl.

86. The method of Claim 81, wherein said agent is present in said first, second, or third composition at a concentration of 0.01-35 mg/ml

87. The method of Claim 52, wherein said first and/or second compositions further comprise a physiologically tolerable buffer or intravenous solution.

88. The method of Claim 52, wherein said first and/or second compositions further comprise lactated Ringer's solution or saline solution.

89. The method of Claim 52, wherein said first composition comprises liposomes comprising said polycationic structures, wherein said liposomes further comprising one or more macrophage targeting moieties selected from the group consisting of: mannose moieties, maleimide moieties, a folate receptor ligand, folate, folate receptor antibody or fragment thereof, formyl peptide receptor ligands, N-formyl-Met-Leu-Phe, tetrapeptide Thr-Lys-Pro-Arg, galactose, and lactobionic acid.

90. The method of Claim 52, wherein said plurality of one or more non-viral expression vectors are not attached to, or encapsulated in, any delivery agent.

91. The method of Claim 52, wherein said subject is a human.

91. The method of Claim 52, wherein 0.05-60 mg/mL of said expression vectors are present in said second composition.

92. The method of Claim 52, wherein said polycationic structures comprise cationic liposomes which are present at a concentration of 0.5-100 mM in said first composition.

93. The method of Claim 52, wherein said subject is a human, wherein:

i) an amount of said first composition is administered such that said human receives a dosage of 2-50 mg/kg of said polycationic structures; and/or

ii) an amount of said second composition is administered such that said human receives a dosage of 0.05-60 mg/kg of said expression vectors.

94. The method of Claim 52, wherein said polycationic structures comprise cationic liposomes, wherein said cationic liposomes further comprise a lipid bi-layer integrating peptide and/or a target peptide.

95. The method of Claim 94, wherein: i) said lipid bi-layer integrating peptide is selected from the group consisting of: surfactant protein D (SPD), surfactant protein C (SPC), surfactant protein B (SPB), and surfactant protein A (SPA), and ii) said target peptide is selected from the group consisting of: microtubule-associated sequence (MTAS), nuclear localization signal (NLS), ER secretion peptide, ER retention peptide, and peroxisome peptide.

96. The method of Claim 52, wherein steps a) and b) are repeated at least once between 1 and 60 days after the initial step b).

97. The method of Claim 52, wherein each of said non-viral expression vectors comprise between 5,500 and 30,000 nucleic acid base pairs.

98. The method of Claim 52, wherein said one or more non-viral expression vectors are CPG-free or CPG-reduced.

99. A system comprising:

a) a first container;

b) a first composition inside said first container and comprising polycationic structures, wherein said first composition is free, or essentially free, of nucleic acid molecules;

c) a second container; and

d) a second composition inside said second container and comprising a plurality of one or more non-viral expression vectors that encode at least three different antibodies or antigen-binding portions thereof.

100. The system of Claim 99, further comprising an agent that: i) increases the level of expression of at least one of said at least three different antibodies or antigen-binding portions thereof when administered to a subject, and/or ii) and/or the length of time of said expression, as compared to when said agent is not administered to said subject.

101. The system of Claim 100, wherein said agent is present in said first, second, or a third composition at a concentration of 0.01-35 mg/ml.

102. The system of Claim 100, wherein said agent is present in said first composition and/or said second composition.

103. The system of Claim 100, further comprising a third container, and wherein said agent is present in said third container.

104. A method comprising:

a) administering a first composition to a subject, wherein said first composition comprises polycationic structures, and wherein said first composition is free, or essentially free, of nucleic acid molecules; and

b) administering a second composition to said subject after administering said first composition, wherein said second composition comprises a plurality of non-viral expression vectors that encode human growth hormone (hGH) and/or hGH linked to a half-life extending peptide (hGH-ext), and

wherein, as a result of said administering said first and second compositions, said hGH is expressed in said subject.

105. The method of Claim 104, wherein said hGH and/or hGH-ext is expressed in said subject at a serum expression level of at least 1 ng/ml.

106. The method of Claim 105, wherein said expression level is maintained in said subject for at least two weeks without: i) any further, or only one further repeat, of steps a) and b), and ii) any further administration of vectors encoding said hGH or hGH-ext.

107. The method of Claim 105, wherein said expression level is maintained in said subject for at least one month without: i) any further, or only one further repeat, of steps a) and b), and ii) any further administration of vectors encoding said hGH or hGH-ext.

108. The method of Claim 105, wherein said expression level is maintained in said subject for at least one year without: i) any further, or only one further repeat, of steps a) and b), and ii) any further administration of vectors encoding said hGH or hGH-ext.

109. The method of Claim 104, wherein said plurality of non-viral expression vectors encode said hGH-ext, and wherein said half-life extending peptide is selected from the group consisting of: an Fc region peptide, serum albumin, carboxy terminal peptide of human chorionic gonadotropin b-subunit (CTP), and XTEN (see, Schellenberger et al., Nat Biotechnol. 2009 Dec;27(12):1186-90).

110. The method of Claim 104, wherein said polycationic structures comprise cationic lipids.

111. The method of Claim 110, wherein said first composition comprises a plurality of liposomes, wherein at least some of said liposomes comprises said cationic lipids.

112. The method of Claim 110, wherein at least some of said liposomes comprise neutral lipids.

113. The method of Claim 112, wherein the ratio of said cationic lipids to said neutral lipids in said liposomes is 95:05 - 80:20 or about 1:1.

114. The method of Claim 112, wherein said cationic and neutral lipids are selected from the group consisting of: distearoyl phosphatidyl choline (DSPC); hydrogenated or non-hydrogenated soya phosphatidylcholine (HSPC); distearoylphosphatidylethanolamine (DSPE); egg phosphatidylcholine (EPC); 1,2-Distearoyl-sn-glycero-3-phospho-rac-glycerol (DSPG); dimyristoyl phosphatidylcholine (DMPC); 1,2-Dimyristoyl-sn-glycero-3-phosphoglycerol (DMPG); 1,2-Dipalmitoyl-sn-glycero-3-phosphate (DPPA); trimethylammonium propane lipids; DOTIM (1-[2-9(2)-octadecenoylloxy)ethyl]-2-(8(2)-heptadecenyl)-3-(2-hydroxyethyl) midizolinium chloride) lipids; and mixtures of two or more thereof.

115. The method of Claim 104, wherein said expression vectors comprise plasmids, wherein said plasmids are not attached to, or encapsulated in, any delivery agent.

116. The method of Claim 104, wherein said administering comprises intravenous administering.

117. The method of Claim 104, wherein said second composition is administered: i) between 0.5 and 80 minutes after said first composition, or between about 1 and 20 minutes after said first composition.

116. The method of Claim 104, further comprising: c) administering an agent, in said first and/or second composition, or present in a third composition, wherein said agent: i) increases the level of expression of said hGH and/or hGH-ext, and/or ii) and/or the length of time of said expression compared to when said agent is not administered to said subject.

117. The method of Claim 116, wherein said agent is present in said first composition.

118. The method of Claim 116, wherein said agent is present in said third composition, and is administered at least one hour prior to said first composition.

119. The method of Claim 117, wherein said agent is a dexamethasone fatty acid ester.

120. The method of Claim 119, wherein said dexamethasone fatty acid ester has the following Formula:

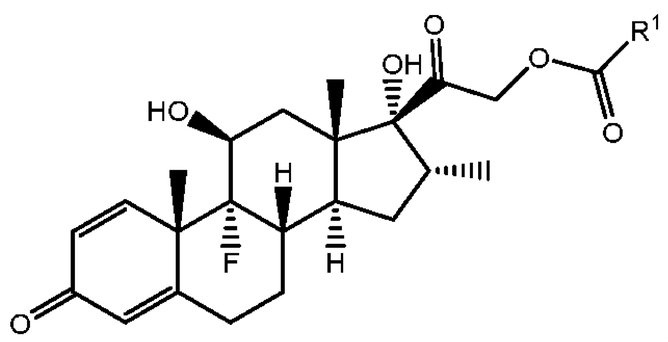

, wherein R^1 is C_5-C_{23} alkyl or C_5-C_{23} alkenyl.

121. The method of Claim 116, wherein said agent is present in said first, second, or third composition at a concentration of 0.01-35 mg/ml

122. The method of Claim 104, wherein said first and/or second compositions further comprise a physiologically tolerable buffer or intravenous solution.

123. The method of Claim 104, wherein said first and/or second compositions further comprise lactated Ringer's solution or saline solution.

124. The method of Claim 104, wherein said first compositions comprise liposomes comprising said polycationic structures, wherein said liposomes further comprising one or more macrophage targeting moieties selected from the group consisting of: mannose moieties, maleimide moieties, a folate receptor ligand, folate, folate receptor antibody or fragment thereof, formyl peptide receptor ligands, N-formyl-Met-Leu-Phe, tetrapeptide Thr-Lys-Pro-Arg, galactose, and lactobionic acid.

125. The method of Claim 104, wherein said plurality of non-viral expression vectors are not attached to, or encapsulated in, any delivery agent.

126. The method of Claim 104, wherein said subject is a human.

127. The method of Claim 104, wherein 0.05-60 mg/mL of said expression vectors are present in said second composition.

128. The method of Claim 104, wherein said polycationic structures comprise cationic liposomes which are present at a concentration of 0.5-100 mM in said first composition.

129. The method of Claim 104, wherein said subject is a human, wherein:

i) an amount of said first composition is administered such that said human receives a dosage of 2-50 mg/kg of said polycationic structures; and/or

ii) an amount of said second composition is administered such that said human receives a dosage of 0.05-60 mg/kg of said expression vectors.

130. The method of Claim 104, wherein said polycationic structures comprise cationic liposomes, wherein said cationic liposomes further comprise a lipid bi-layer integrating peptide and/or a target peptide.

131. The method of Claim 130, wherein: i) said lipid bi-layer integrating peptide is selected from the group consisting of: surfactant protein D (SPD), surfactant protein C (SPC), surfactant protein B (SPB), and surfactant protein A (SPA), and ii) said target peptide is selected from the group consisting of: microtubule-associated sequence (MTAS), nuclear localization signal (NLS), ER secretion peptide, ER retention peptide, and peroxisome peptide.

132. The method of Claim 104, wherein steps a) and b) are repeated between 1 and 60 days after the initial step b).

133. The method of Claim 104, wherein each of said non-viral expression vectors comprise between 5,500 and 30,000 nucleic acid base pairs.

134. The method of Claim 104, wherein said non-viral expression vectors are CPG-free or CPG-reduced.

135. A method comprising:

a) administering a first composition to an animal model, wherein said first composition comprises polycationic structures, and wherein said first composition is free, or essentially free, of nucleic acid molecules, and

wherein said animal model is infected with SARS-CoV-2; and

b) administering a second composition to said animal model after administering said first composition, wherein said second composition comprises a plurality of one or more non-viral expression vectors that encode first and second anti-SARS-CoV-2 antibodies or antigen-binding portion thereof, and

wherein, as a result of said administering said first and second compositions, said first and second candidate anti-SARS-CoV-2 antibodies or antigen-binding portions thereof, are expressed in said animal model; and

c) determining the extent to which said expression of said first and second candidate anti-SARS-CoV-2 antibodies, or antigen-binding portions thereof, i) reduce the SARS-CoV-2 viral load in said animal model, and/or ii) reduce at least one symptom in said animal model caused by said SARS-CoV-2 infection.

136. The method of Claim 135, wherein said plurality of one or more non-viral expression vectors further encode third, fourth, fifth, sixth, seventh, eight, ninth, tenth, or eleventh, candidate anti-SARS-CoV-2 antibodies or antigen-binding fragments thereof.

137. The method of Claim 135, wherein said animal model is selected from a: mouse, rat, hamster, Guinee pig, primate, monkey, chimpanzee, or rabbit.

138. The method of Claim 135, wherein said first and anti- SARS-CoV2 antibodies, or antigen binding portions thereof, are from Table 7.

139. The method of Claim 135, wherein said first and second anti- SARS-CoV2 antibodies, or antigen binding portions thereof, are selected from the group consisting of: REGN10933, REGN10987; VIR-7831; LY-CoV1404; LY3853113; Zost 2355K; CV07-209K; C121L; Zost 2504L; CV38-183L; COVA215K; RBD215; CV07-250L; C144L; COVA118L; C135K; and B38.

FIG. 1

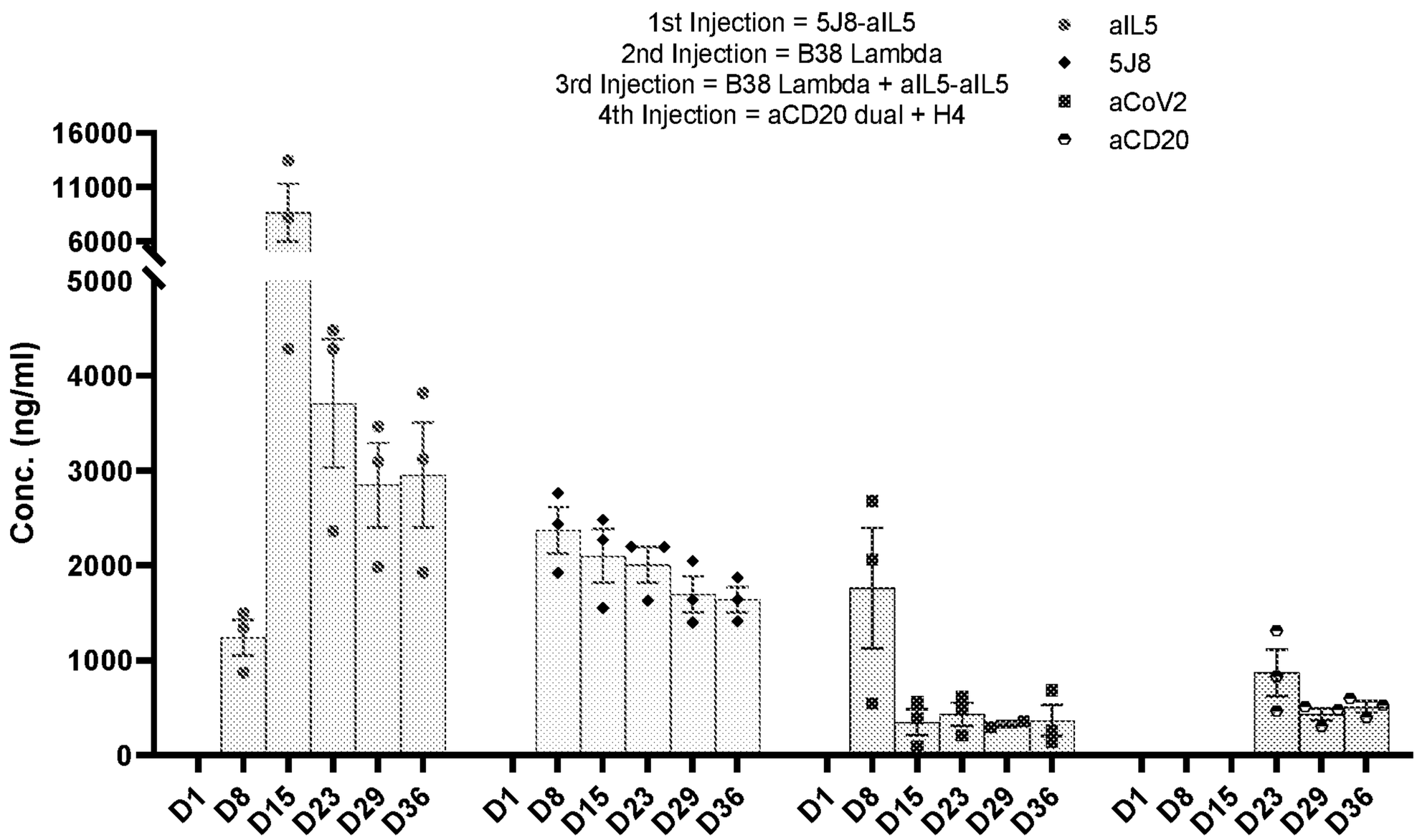
1st Injection = 5J8-aIL5
2nd Injection = B38 Lambda
3rd Injection = B38 Lambda + aIL5-aIL5
4th Injection = aCD20 dual + H4
aIL5
5J8
aCoV2
aCD20
Conc. (ng/ml)
16000
11000
6000
5000
4000
3000
2000
1000
0
D1 D8 D15 D23 D29 D36
Days after Injection

FIG. 2

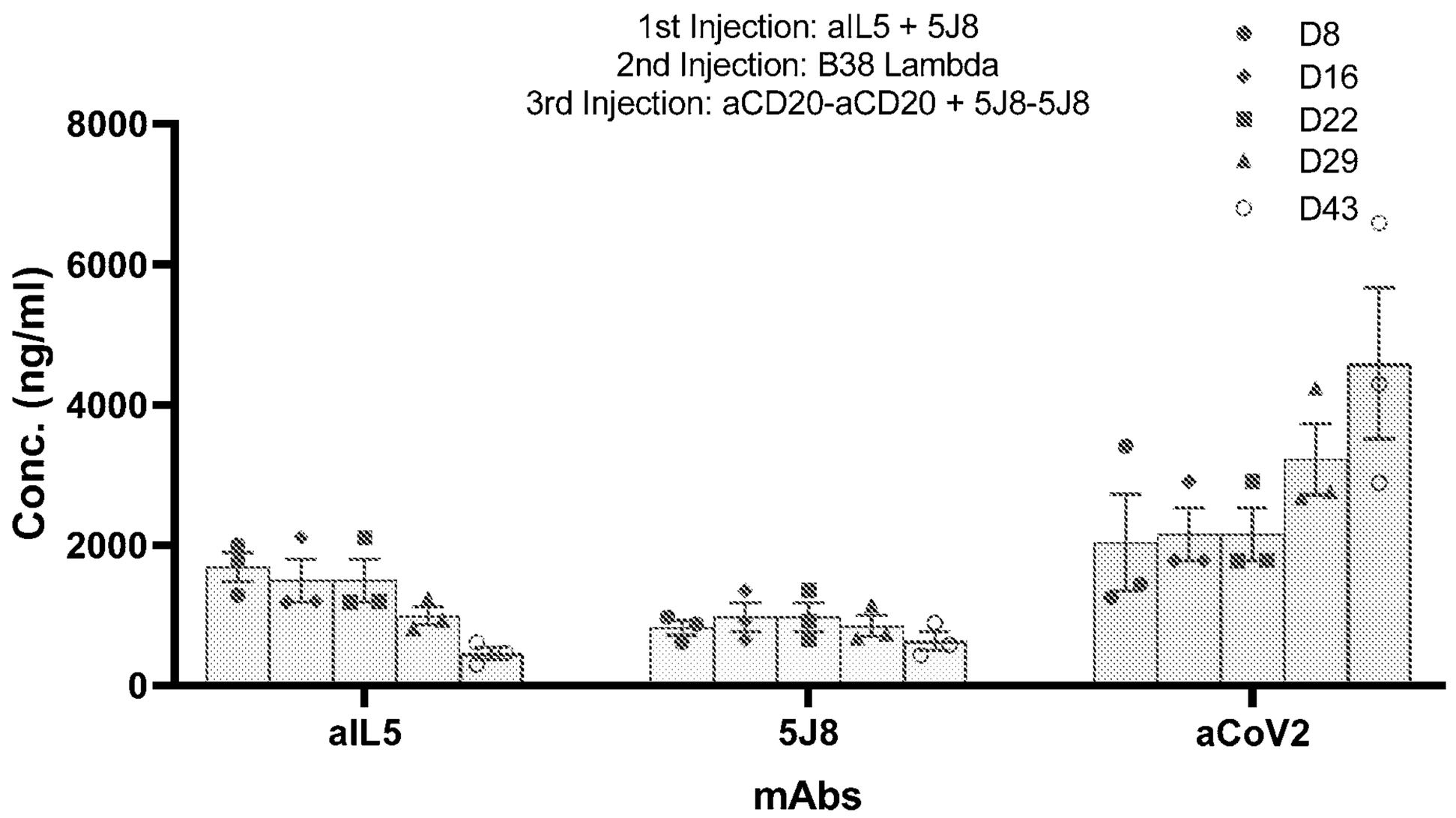
1st Injection: aIL5 + 5J8
2nd Injection: B38 Lambda
3rd Injection: aCD20-aCD20 + 5J8-5J8
D8
D16
D22
D29
D43
Conc. (ng/ml)
8000
6000
4000
2000
0
aIL5
5J8
aCoV2
mAbs

FIG. 3

A.

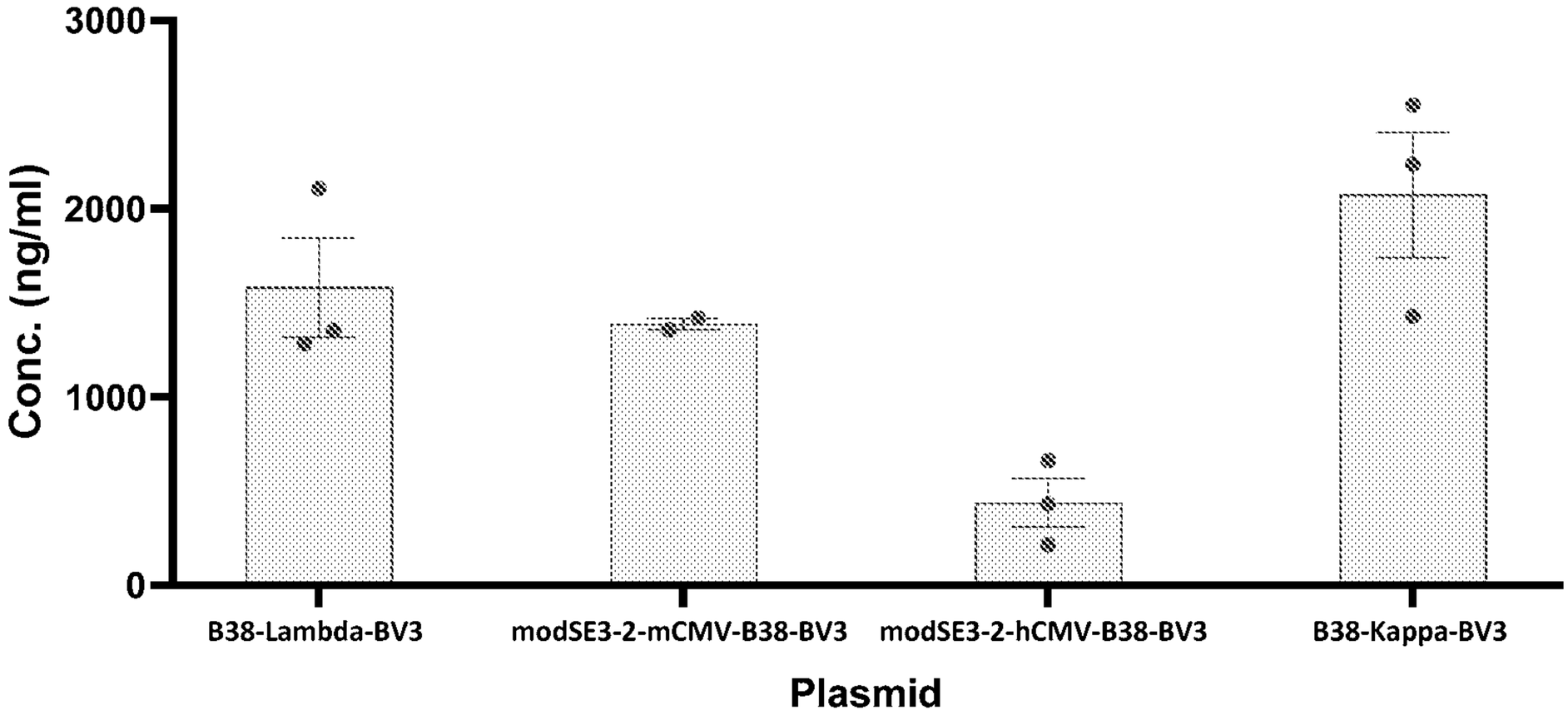
3000
2000
1000
0
Conc. (ng/ml)
B38-Lambda-BV3
modSE3-2-mCMV-B38-BV3
modSE3-2-hCMV-B38-BV3
B38-Kappa-BV3
Plasmid

B.

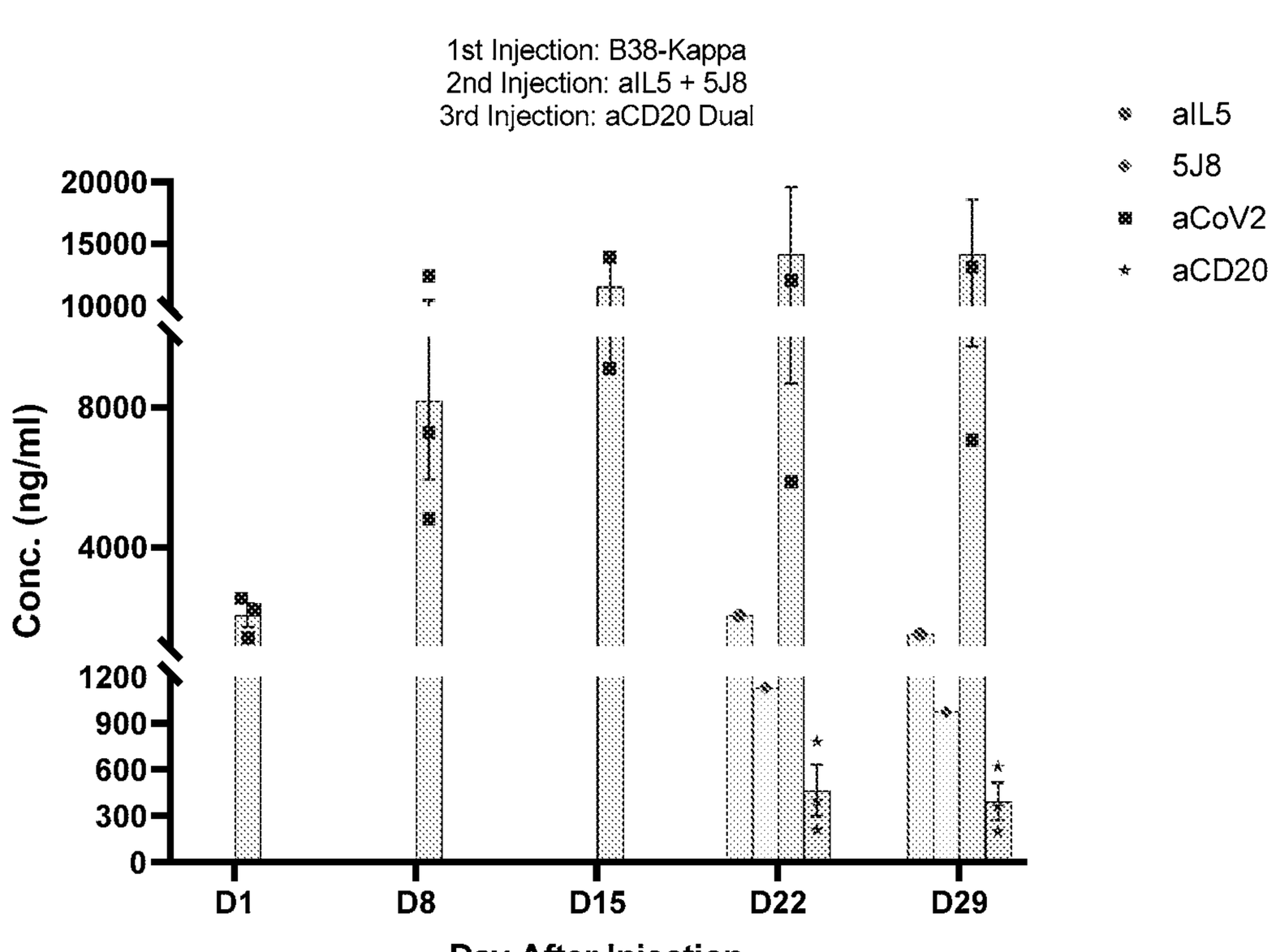
1st Injection: B38-Kappa
2nd Injection: aIL5 + 5J8
3rd Injection: aCD20 Dual
aIL5
5J8
aCoV2
aCD20
20000
15000
10000
8000
4000
1200
900
600
300
0
Conc. (ng/ml)
D1
D8
D15
D22
D29
Day After Injection

FIG. 4

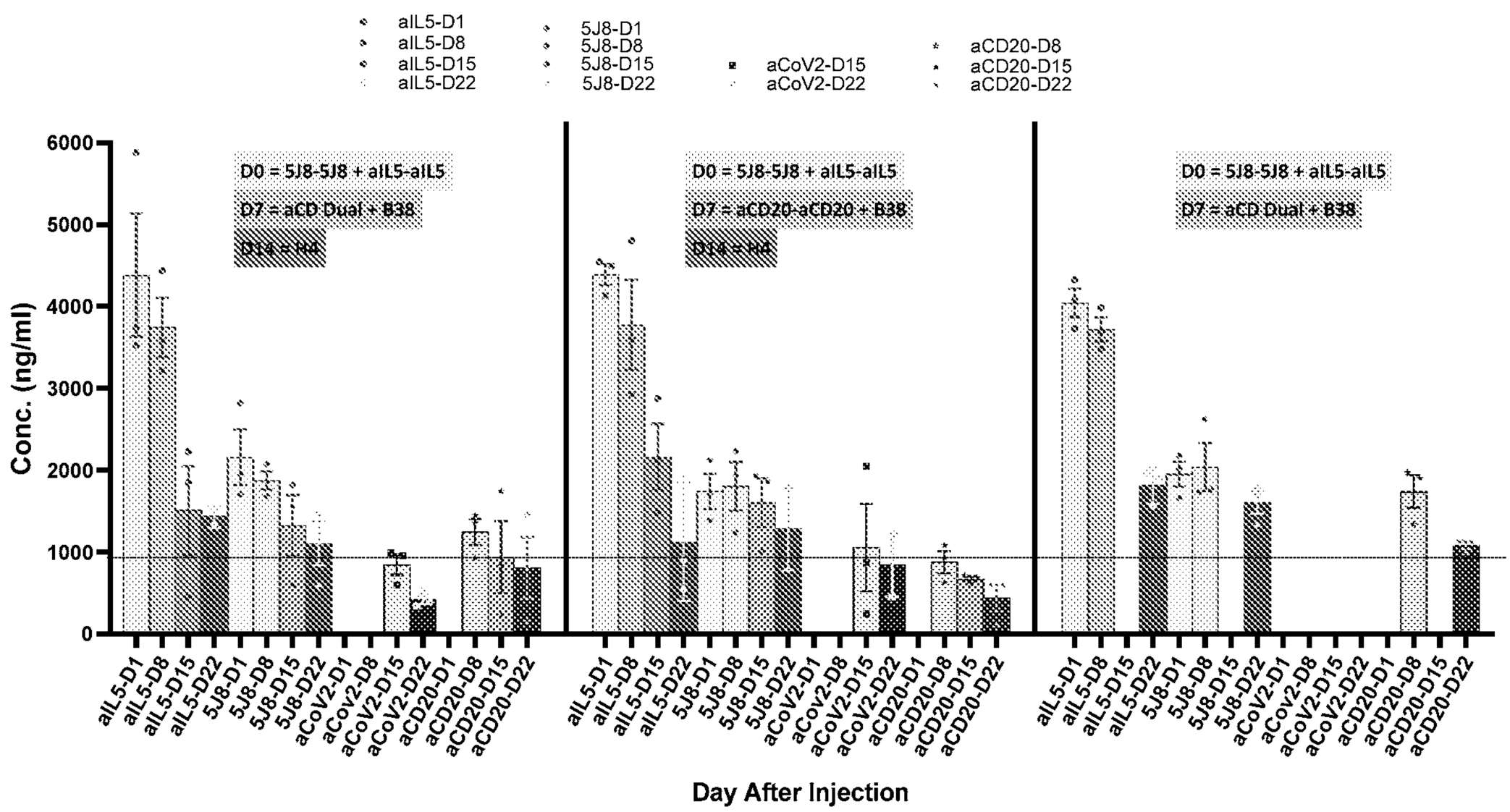
aIL5-D1
aIL5-D8
aIL5-D15
aIL5-D22
5J8-D1
5J8-D8
5J8-D15
5J8-D22
aCoV2-D15
aCoV2-D22
aCD20-D8
aCD20-D15
aCD20-D22
6000
5000
4000
3000
2000
1000
0
Conc. (ng/ml)
D0 = 5J8-5J8 + aIL5-aIL5
D7 = aCD Dual + B38
D14 = H4
D0 = 5J8-5J8 + aIL5-aIL5
D7 = aCD20-aCD20 + B38
D14 = H4
D0 = 5J8-5J8 + aIL5-aIL5
D7 = aCD Dual + B38
aIL5-D1
aIL5-D8
aIL5-D15
aIL5-D22
5J8-D1
5J8-D8
5J8-D15
5J8-D22
aCoV2-D1
aCoV2-D8
aCoV2-D15
aCoV2-D22
aCD20-D1
aCD20-D8
aCD20-D15
aCD20-D22
Day After Injection

FIG. 5

A.

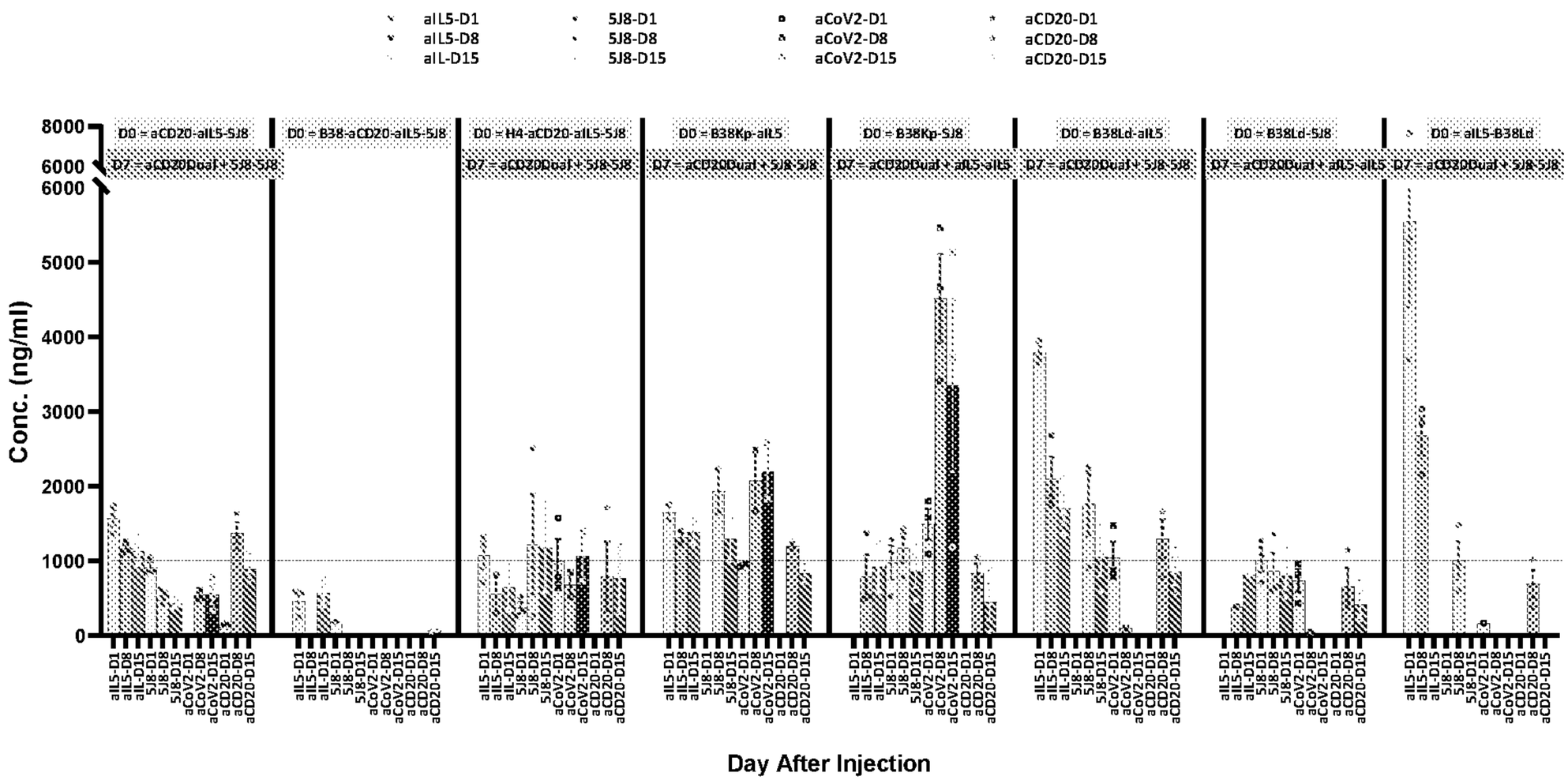
aIL5-D1
aIL5-D8
aIL-D15
5J8-D1
5J8-D8
5J8-D15
aCoV2-D1
aCoV2-D8
aCoV2-D15
aCD20-D1
aCD20-D8
aCD20-D15
D0 = aCD20-aIL5-5J8
D7 = aCD20Dual + 5J8-5J8
D0 = B38-aCD20-aIL5-5J8
D0 = H4-aCD20-aIL5-5J8
D7 = aCD20Dual + 5J8-5J8
D0 = B38Kp-aIL5
D7 = aCD20Dual + 5J8-5J8
D0 = B38Kp-5J8
D7 = aCD20Dual + aIL5-aIL5
D0 = B38Ld-aIL5
D7 = aCD20Dual + 5J8-5J8
D0 = B38Ld-5J8
D7 = aCD20Dual + aIL5-aIL5
D0 = aIL5-B38Ld
D7 = aCD20Dual + 5J8-5J8
Conc. (ng/ml)
8000
6000
6000
5000
4000
3000
2000
1000
0
Day After Injection

B.

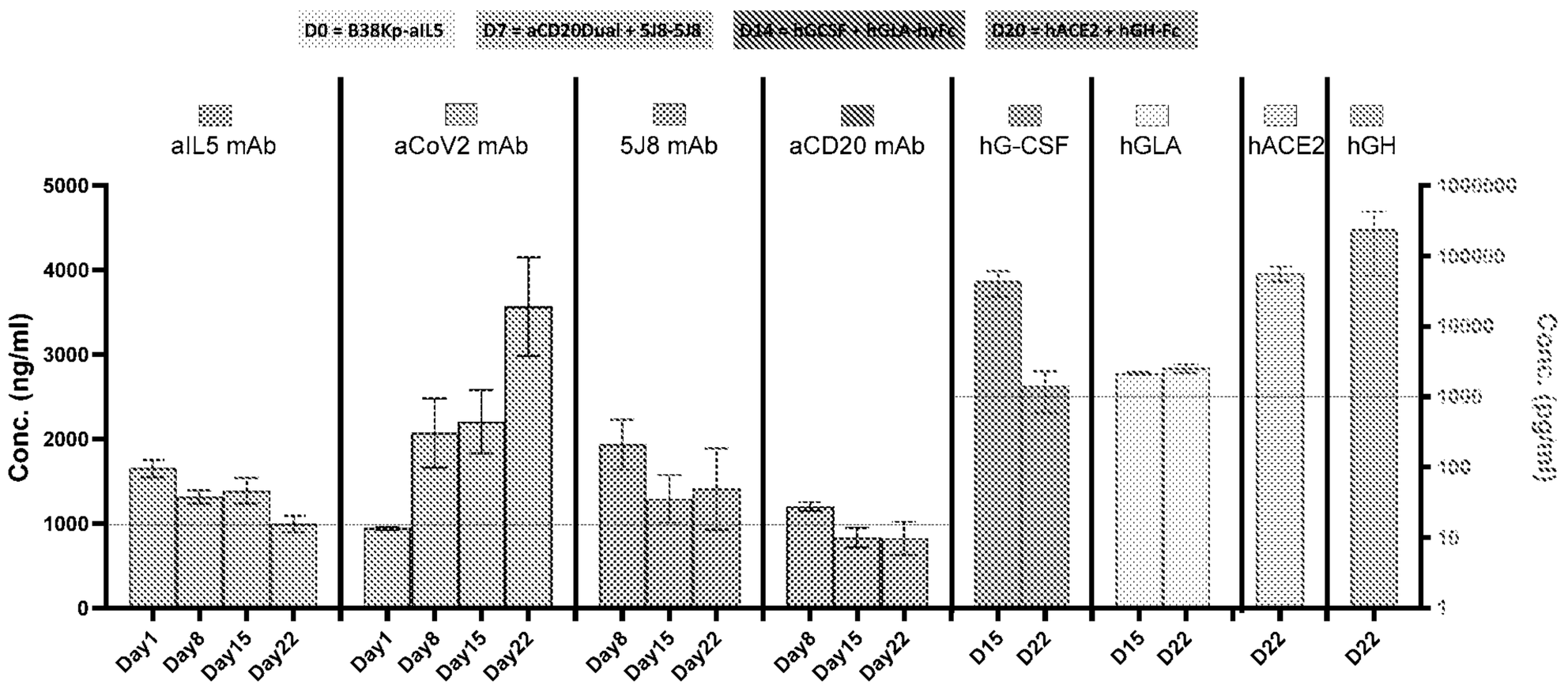
D0 = B38Kp-aIL5
D7 = aCD20Dual + 5J8-5J8
D14 = hGCSF + hGLA-hyFc
D20 = hACE2 + hGH-Fc
aIL5 mAb
aCoV2 mAb
5J8 mAb
aCD20 mAb
hG-CSF
hGLA
hACE2
hGH
Conc. (ng/ml)
5000
4000
3000
2000
1000
0
1000000
100000
10000
1000
100
10
1
Conc. (ng/ml)
Day1
Day8
Day15
Day22
D15
D22

FIG. 6

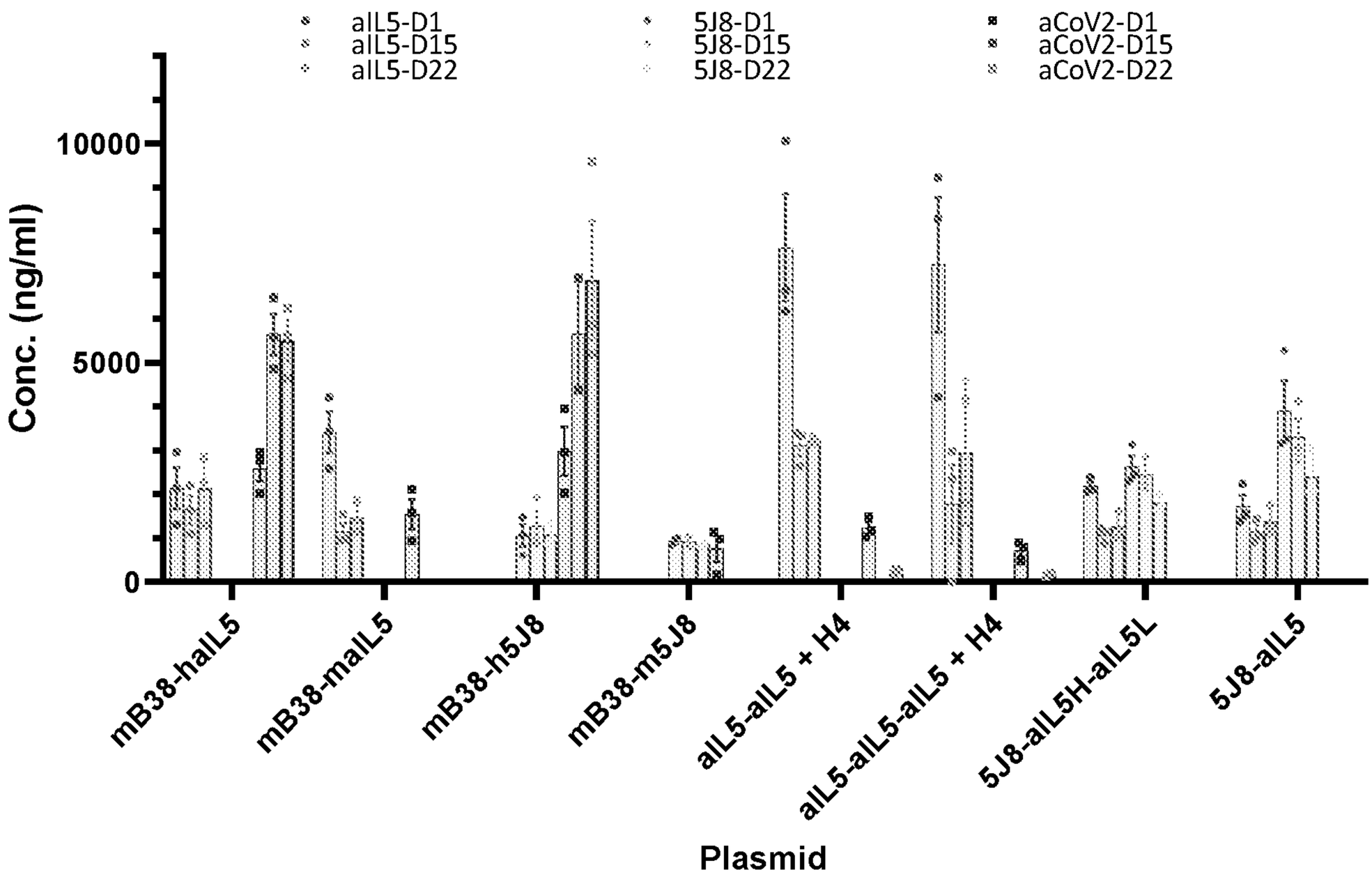
alL5-D1
alL5-D15
alL5-D22
5J8-D1
5J8-D15
5J8-D22
aCoV2-D1
aCoV2-D15
aCoV2-D22
Conc. (ng/ml)
10000
5000
0
mB38-halL5
mB38-malL5
mB38-h5J8
mB38-m5J8
alL5-alL5 + H4
alL5-alL5-alL5 + H4
5J8-alL5H-alL5L
5J8-alL5
Plasmid

FIG. 7

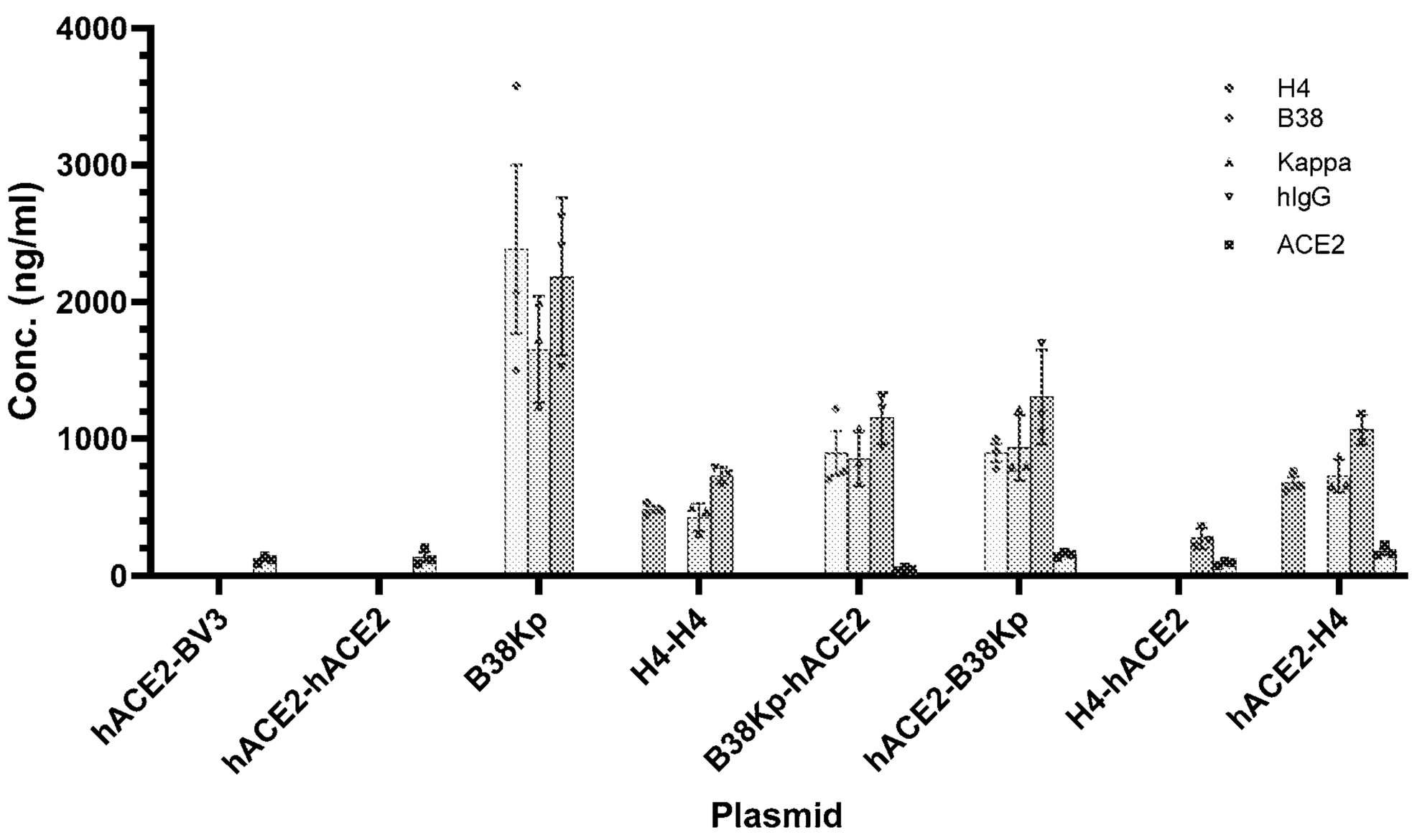
4000
3000
2000
1000
0
Conc. (ng/ml)
H4
B38
Kappa
hIgG
ACE2
hACE2-BV3
hACE2-hACE2
B38Kp
H4-H4
B38Kp-hACE2
hACE2-B38Kp
H4-hACE2
hACE2-H4
Plasmid

FIG. 8

A.

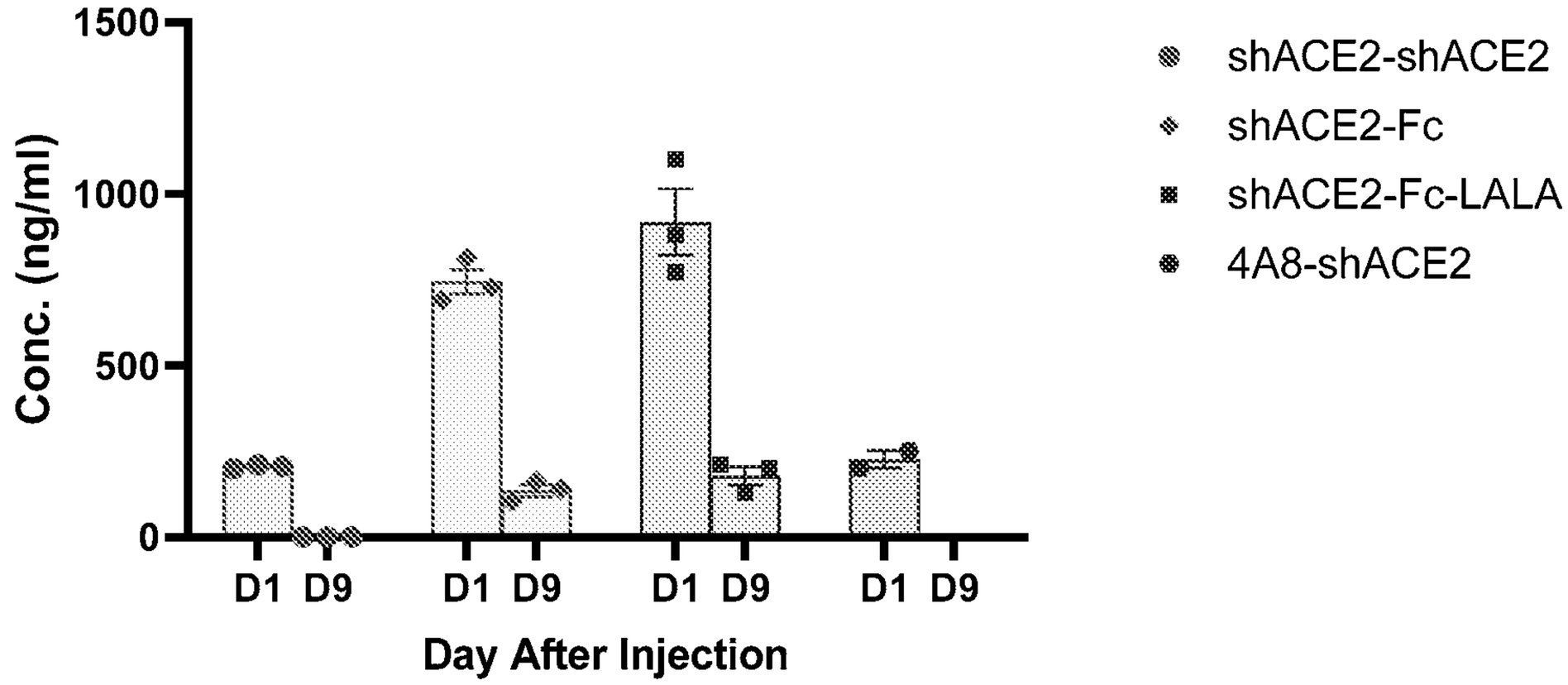
1500
1000
500
0
Conc. (ng/ml)
D1 D9 D1 D9 D1 D9 D1 D9
Day After Injection
shACE2-shACE2
shACE2-Fc
shACE2-Fc-LALA
4A8-shACE2

B.

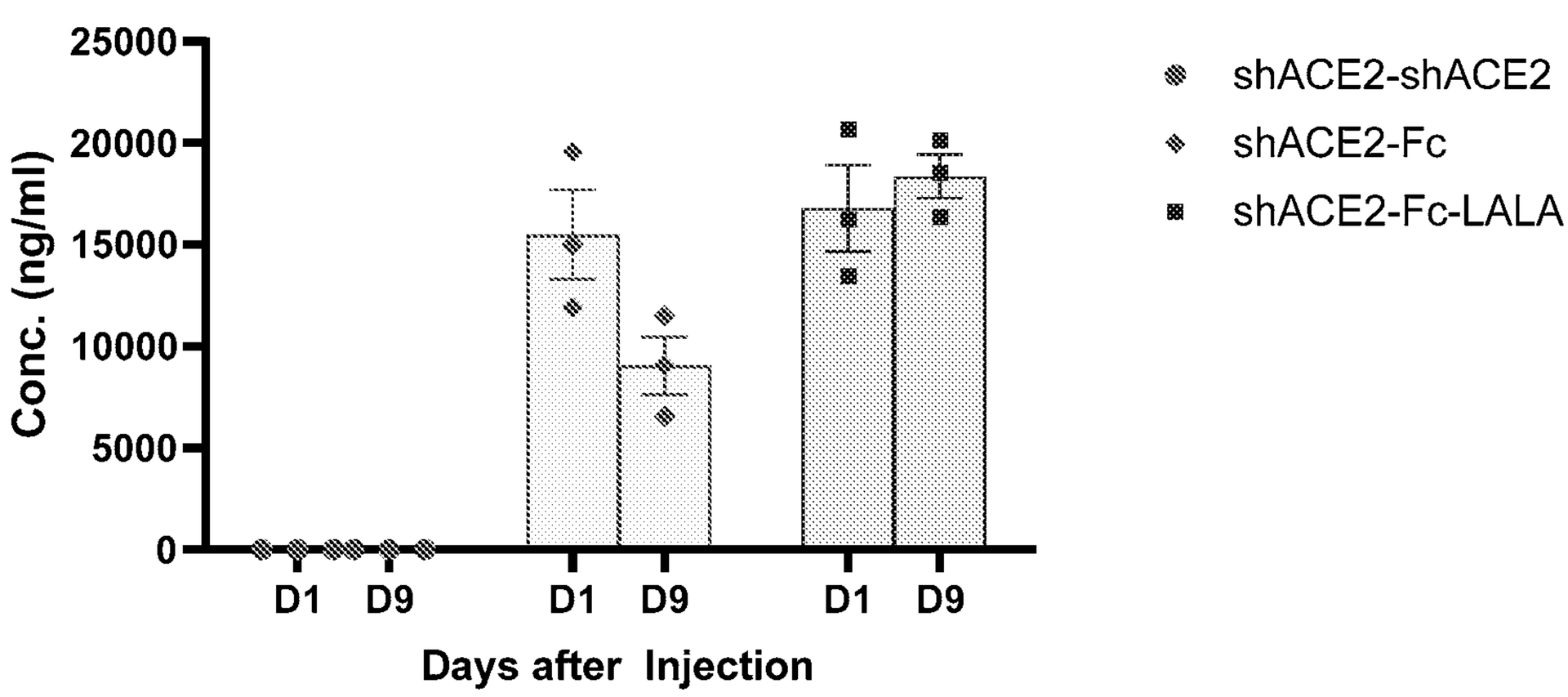
25000
20000
15000
10000
5000
0
Conc. (ng/ml)
D1 D9 D1 D9 D1 D9
Days after Injection
shACE2-shACE2
shACE2-Fc
shACE2-Fc-LALA

FIG. 9

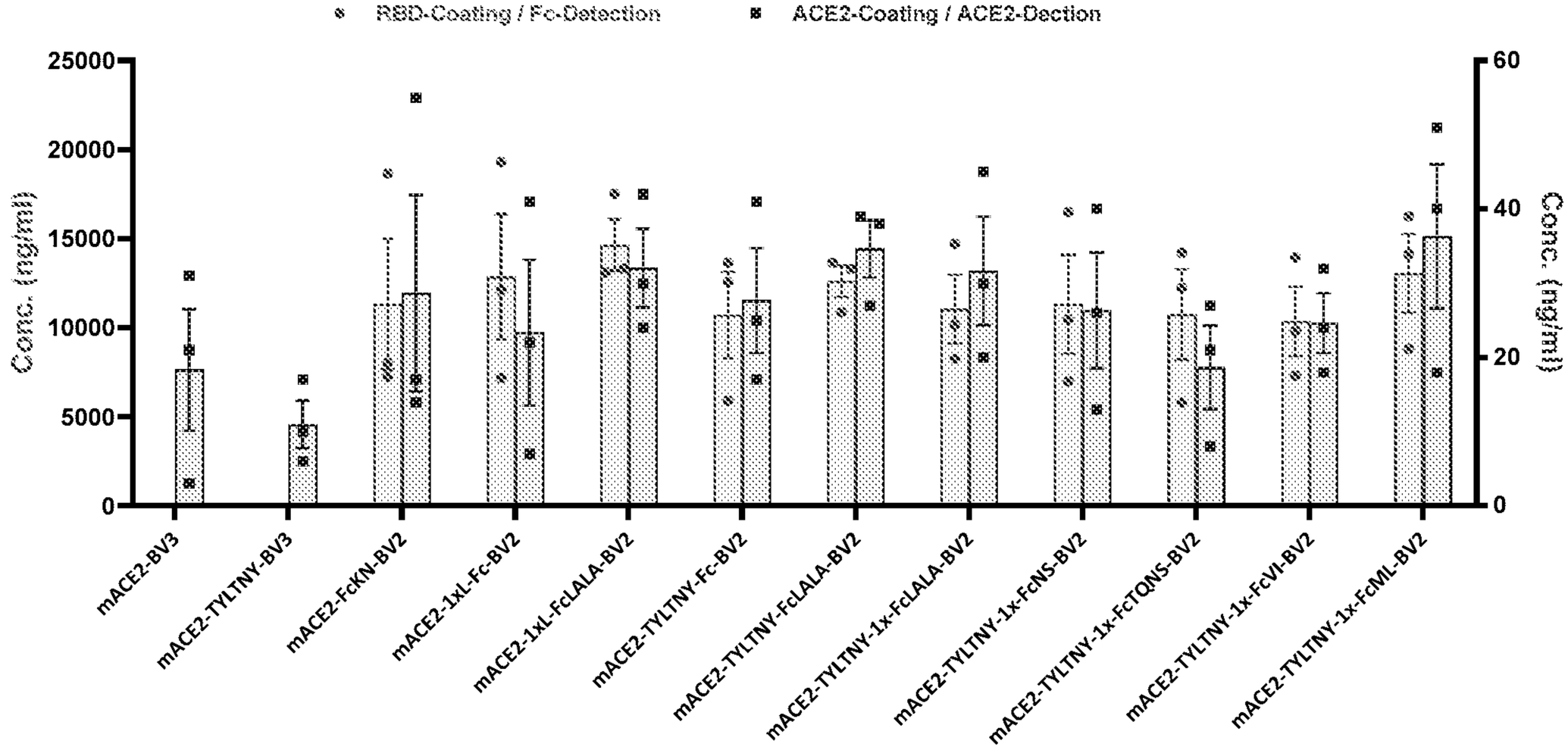

Plasmid

FIG. 10

070120 # 1 : B38-Lambda-BV3 (SEQ ID NO:10)

DraIII-βGlo BI-Nhe-mCMVΔEF1II26-BstEII -B38-Lambda-BglII-MazpA-IFNβ S/MAR-BV3

CACTATGTGTTAATTAAAATTATCTCTAAGGCATGTGAACTGGCTGTCTTGGTTTTCATCTGTACTTCATCTGCTACCTCTGTGACCTGAAACATATTTATAATTCCA
TTAAGCTGTGCATATGATAGATTTATCATATGTATTTTCCTTAAAGGATTTTTGTAAGAACTAATTGAATTGATACCTGTAAAGTCTTTATCACACTACCCAATAAA
TAATAAATCTCTTTGTTCAGCTCTCTGTTTCTATAAATATGTACCAGTTTTATTGTTTTTAGTGGTAGTGATTTTATTCTCTTTCTATATATATACACACACATGTGTG
CATTCATAAATATATACAATTTTTATGAATAAAAAATTATTAGCAATCAATATTGAAAACCACTGATTTTTGTTTATGTGAGCAAACAGCAGATTAAAAGGAATTT
GAATTCTCATAGCTAGCAGGAGTCAATGGGAAAAACCCATTGGAGCCAAGTACACTGACTCAATAGGGACTTTCCATTGGGTTTTGCCCAGTACATAAGGTCAA
TAGGGGGTGAGTCAACAGGAAAGTCCCATTGGAGCCAAGTACATTGAGTCAATAGGGACTTTCCAATGGGTTTTGCCCAGTACATAAGGTCAATGGGAGGTAA
GCCAATGGGTTTTTCCCATTACTGACATGTATACTGAGTCATTAGGGACTTTCCAATGGGTTTTGCCCAGTACATAAGGTCAATAGGGGTGAATCAACAGGAAA
GTCCCATTGGAGCCAAGTACACTGAGTCAATAGGGACTTTCCATTGGGTTTTGCCCAGTACAAAAGGTCAATAGGGGGTGAGTCAATGGGTTTTTCCCATTATTG
GCACATACATAAGGTCAATAGGGGTGACTAGTGGAGAAGAGCATGCTTGAGGGCTGAGTGCCCCTCAGTGGGCAGAGAGCACATGGCCCACAGTCCCTGAGA
AGTTGGGGGGAGGGGTGGGCAATTGAACTGGTGCCTAGAGAAGGTGGGGCTTGGGTAAACTGGGAAAGTGATGTGGTGTACTGGCTCCACCTTTTTCCCCAG
GGTGGGGGAGAACCATATATAAGTGCAGTAGTCTCTGTGAACATTCAAGCTTCTGCCTTCTCCCTCCTGTGAGTTTGGTAAGTCACTGACTGTCTATGCCTGGGA
AAGGGTGGGCAGGAGATGGGGCAGTGCAGGAAAAGTGGCACTATGAACCCTGCAGCCCTAGACAATTGTACTAACCTTCTTCTCTTTCCTCTCCTGACAGGTTG
GTAACCAAGCCACCATGGGATGGTCCCTGATCCTGCTGTTTCTGGTGGCTGTGGCCACCAGAGTGCTGTCTGAAGTGCAGCTGGTGGAAAGTGGTGGTGGCCT
GGTTCAGCCTGGTGGCTCTCTGAGACTGAGCTGTGCTGCCTCTGGCTTCATTGTGTCCAGCAACTACATGAGCTGGGTCAGACAGGCCCCTGGCAAAGGACTGG
AATGGGTGTCAGTGATCTACAGTGGTGGCAGCACCTACTATGCTGACTCTGTGAAGGGCAGATTCACCATCAGCAGACACAACAGCAAGAACACCCTGTACCTG
CAGATGAACAGCCTGAGAGCTGAGGACACTGCTGTGTACTACTGTGCCAGAGAAGCCTATGGCATGGATGTGTGGGGCCAGGGCACAACAGTGACTGTGTCCT
CTGCCAGCACAAAGGGCCCCTCTGTGTTTCCTCTGGCTCCCAGCAGCAAGAGCACCAGTGGTGGAACAGCTGCCCTGGGCTGTCTGGTCAAGGACTACTTTCCT
GAGCCTGTGACAGTGTCCTGGAACTCTGGGGCTCTGACATCTGGGGTGCACACATTCCCTGCAGTGCTGCAGTCCTCTGGCCTGTACAGCCTGTCCTCTGTGGTC
ACAGTGCCTAGCTCTAGCCTGGGCACCCAGACCTACATCTGCAATGTGAACCACAAGCCTAGCAACACCAAGGTGGACAAGAAGGCTGAGCCCAAGAGCTGTG
ACAAGACCCACACCTGTCCTCCATGTCCTGCTCCAGAGCTGCTTGGAGGACCATCAGTGTTTCTGTTCCCTCCAAAGCCTAAGGACACCCTGATGATCAGCAGAA
CCCCTGAAGTGACCTGTGTGGTGGTGGATGTGTCTCATGAGGACCCAGAAGTGAAGTTCAACTGGTATGTGGATGGTGTGGAGGTGCACAATGCCAAGACCAA
GCCTAGAGAGGAACAGTACAACTCCACCTACAGAGTGGTTTCTGTGCTGACAGTGCTCCACCAGGACTGGCTGAATGGCAAAGAGTACAAGTGCAAGGTGTCC
AACAAGGCCCTGCCTGCTCCTATTGAAAAGACCATCTCCAAGGCCAAGGGCCAGCCTAGGGAACCCCAGGTTTACACACTGCCACCTAGCAGGGATGAGCTGAC
CAAGAACCAGGTGTCCCTGACATGCCTGGTTAAGGGCTTCTACCCCTCTGACATTGCTGTGGAATGGGAGAGCAATGGCCAGCCAGAGAACAACTACAAGACA
ACCCCTCCTGTGCTGGACTCTGATGGCTCATTCTTCCTGTACTCCAAGCTGACTGTGGACAAGTCCAGATGGCAGCAGGGCAATGTCTTTAGCTGCTCTGTGATG
CATGAGGCCCTGCACAACCACTACACACAGAAGTCCCTGTCTCTGAGCCCTGGCAAG***AGAAAGAGAAGGAGTGGCTCTGGGGCCACCAACTTCAGCCTGCTGA***
AACAGGCTGGGGATGTTGAAGAGAACCCTGGACCTATGGCCTGGGCTCTGCTGCTTCTGGGACTGCTGTCTCACTGCACTGGCTCTGTGACAGACATTGTGAT
GACCCAGTCTCCATCCTTCCTGAGTGCCTCTGTGGGAGACAGAGTGACCATCACCTGTAGAGCCAGCCAGGGCATCAGCTCTTACCTGGCTTGGTATCAGCAAA
AGCCTGGCAAGGCCCCTAAGCTGCTGATCTATGCTGCCTCCACACTGCAGTCAGGGGTGCCCTCCAGATTTTCTGGCTCTGGATCTGGCACTGAGTTCACCCTGA
CCATCAGCTCCCTGCAGCCTGAGGACTTTGCCACCTACTACTGCCAGCAGCTGAACAGCTACCCTCCTTACACCTTTGGACAGGGCACCAAGCTGGAAATCAAGG
GAACAAAGCTGACAGTCCTGGGCCAGCCAAAGGCTGCTCCTTCTGTGACACTGTTCCCACCTAGCTCTGAGGAACTGCAGGCTAACAAGGCTACCCTTGTGTGC
CTGATCTCTGACTTCTACCCAGGGGCTGTGACTGTGGCTTGGAAGGCTGATAGCAGCCCTGTGAAGGCTGGGGTTGAGACAACCACACCTAGCAAGCAGAGCA
ACAACAAATATGCTGCCAGCTCCTACCTGAGTCTGACCCCTGAGCAGTGGAAGTCCCACAGATCCTACAGCTGCCAAGTGACCCATGAGGGCTCCACAGTGGAA
AAGACAGTGGCCCCAACAGAGTGCTCCTGAAGATCTACTTCTGTGCTAATAAAAGATCAGAGCTCTAGTGATCTGTGTTGGTTTTTTGTGTCTGCATTCTAGCA
AGTCAATATGTTCACCCCAAAAAAGCTGTTTGTTAACTTGTCAACCTCATTCTAAAATGTATATAGAAGCCCAAAAGACAATAACAAAAATATTCTTGTAGAACAA
AATGGGAAAGAATGTTCCACTAAATATCAAGATTTAGAGCAAAGCATGAGATGTGTGGGGATAGACAGTGAGGCTGATAAAATAGAGTAGAGCTCAGAAACA
GACCCATTGATATATGTAAGTGACCTATGAAAAAAATATGGCATTTTACAATGGGAAAATGATGGTCTTTTTCTTTTTTAGAAAAACAGGGAAATATATTTATATG
TAAAAAATAAAAGGGAACCCATATGTCATACCATACACACAAAAAAATTCCAGTGAATTATAAGTCTAAATGGAGAAGGCAAAACTTTAAATCTTTTAGAAAATA
ATATAGAAGCATGCCATCAAGACTTCAGTGTAGAGAAAAATTTCTTATGACTCAAAGTCCTAACCACAAAGAAAAGATTGTTAATTAGATTGCATGAATATTAAG
ACTTATTTTTAAAATTAAAAAACCATTAAGAAAAGTCAGGCCATAGAATGACAGAAAATATTTGCAACACCCCAGTAAAGAGAATTGTAATATGCAGATTATAAA
AAGAAGTCTTACAAATCAGTAAAAAATAAAACTAGACAAAAATTTGAACAGATGAAAGAGAAACTCTAAATAATCATTACACATGAGAAACTCAATCTCAGAAA
TCAGAGAACTATCATTGCATATACACTAAATTAGAGAAATATTAAAAGGCTAAGTAACATCTGTGGCTTAATTAACCTAGGTCTAGTGATCAGCAGTTCAACCTGT
TGATAGTATGTACTAAGCTCTCATGTTTAATGTACTAAGCTCTCATGTTTAATGAACTAAACCCTCATGGCTAATGTACTAAGCTCTCATGGCTAATGTACTAAGCT
CTCATGTTTCATGTACTAAGCTCTCATGTTTGAACAATAAAATTAATATAAATCAGCAACTTAAATAGCCTCTAAGGTTTTAAGTTTTATAAGAAAAAAAAGAATA
TATAAGGCTTTTAAAGGTTTTAAGGTTTCCTAGGTTATCCTCATATGAGCTCTTAGAAAAACTCATCCAGCATCAAATGAAACTGCAATTTATTCATATCAGGATT
ATCAATACCATATTTTTGAAAAAGTCTTTTCTGTAATGAAGGAGAAAACTCACCCAGGCAGTTCCATAGGATGGCAAGATCCTGGTATCTGTCTGCAATTCCAACT
CTTCCAACATCAATACAACCTATTAATTTCCCCTCATCAAAAATAAGGTTATCAAGTGAGAAATCACCATGAGTGACCACTGAATCTGGTGAGAATGGCAAAAGA
TTATGCATTTCTTTCCAGACTTGTTCAACAGGCCAGCCATTTCTCTCATCATCAAAATCACTGGCATCAACCAAACCATTATTCATTCTTGATTGGGCCTGAGCCAG
TCTAAATACTCTATCAGAGTTAAAAGGACAATTACAAACAGGAATGGAATGCAATCTTCTCAGGAACACTGCCAGGGCATCAACAATATTTTCACCTGAATCAGG
ATATTCTTCCAATACCTGGAATGCTGTTTTCCCTGGGATGGCAGTGGTGAGTAACCATGCATCATCAGGAGTTCTGATAAAATGCTTGATGGTTGGAAGAGGCAT
AAATTCAGTCAGCCAGTTTAGTCTGACCATCTCATCTGTAACATCATTGGCAACAGAACCTTTGCCATGTTTCAGAAACAACTCTGGGGCATCTGGCTTCCCATAC
AATCTATAGATTGTGGCACCTGATTGCCCAACATTATCTCTAGCCCATTTATACCCATATAAATCAGCATCCATGTTGGAATTTAATCTTGGCCTGGAGCAAGAGG
TTTCTCTTTGAATATGGCTCATACATGTGCACTCCTATAGTGAGTCGTATTATACTATGCAGATATACTATGCCAATGTTTAATTGTCAG

FIG. 11

070120 # 11 : B38H-B38L-BV3 : Dual (SEQ ID NO:11)

DraIII-βGlo BI-Nhe-[illegible]-CMVΔEF1II26-BstEII -B38H-BglII-MinpA-21q21 S/MAR-ΔhCMV -ΔEF1-RV-II26-BstEII-B38L -BglII-MinpA-IFNβ S/MAR-BV3

CACTATGTGTTAATTAAAATTATCTCTAAGGCATGTGAACTGGCTGTCTTGGTTTTCATCTGTACTTCATCTGCTACCTCTGTGACCTGAAACATATTTATAATTCCATTAAGCT
GTGCATATGATAGATTTATCATATGTATTTTCCTTAAAGGATTTTTGTAAGAACTAATTGAATTGATACCTGTAAAGTCTTTATCACACTACCCAATAAATAATAAATCTCTTT
GTTCAGCTCTCTGTTTCTATAAATATGTACCAGTTTTATTGTTTTTAGTGGTAGTGATTTTATTCTCTTTCTATATATATACACACACATGTGTGCATTCATAAATATATACAATT
TTTATGAATAAAAAATTATTAGCAATCAATATTGAAAACCACTGATTTTTGTTTATGTGAGCAAACAGCAGATTAAAAGGAATTTGAATTCTCATAGCTAGCAG[illegible]
[illegible]
[illegible]
[illegible]
[illegible]ACTAGTGGAGAAGAGCATGCTTGAGGGC
TGAGTGCCCCTCAGTGGGCAGAGAGCACATGGCCCACAGTCCCTGAGAAGTTGGGGGGAGGGGTGGGCAATTGAACTGGTGCCTAGAGAAGGTGGGGCTTGGGTAAAC
TGGGAAAGTGATGTGGTGTACTGGCTCCACCTTTTTCCCCAGGGTGGGGGAGAACCATATATAAGTGCAGTAGTCTCTGTGAACATTCAAGCTTCTGCCTTCTCCCTCCTGT
GAGTTTGGTAAGTCACTGACTGTCTATGCCTGGGAAAGGGTGGGCAGGAGATGGGGCAGTGCAGGAAAAGTGGCACTATGAACCCTGCAGCCCTAGACAATTGTACTAA
CCTTCTTCTCTTTCCTCTCCTGACAGGTTGGTAACC[illegible]ATGGGATGGTCCCTGATCCTGCTGTTTCTGGTGGCTGTGGCCACCAGAGTGCTGTCTGAAGTGCAGCTG
GTGGAAAGTGGTGGTGGCCTGGTTCAGCCTGGTGGCTCTCTGAGACTGAGCTGTGCTGCCTCTGGCTTCATTGTGTCCAGCAACTACATGAGCTGGGTCAGACAGGCCCCT
GGCAAAGGACTGGAATGGGTGTCAGTGATCTACAGTGGTGGCAGCACCTACTATGCTGACTCTGTGAAGGGCAGATTCACCATCAGCAGACACAACAGCAAGAACACCCT
GTACCTGCAGATGAACAGCCTGAGAGCTGAGGACACTGCTGTGTACTACTGTGCCAGAGAAGCCTATGGCATGGATGTGTGGGGCCAGGGCACAACAGTGACTGTGTCCT
CTGCCAGCACAAAGGGCCCCTCTGTGTTTCCTCTGGCTCCCAGCAGCAAGAGCACCAGTGGTGGAACAGCTGCCCTGGGCTGTCTGGTCAAGGACTACTTTCCTGAGCCTG
TGACAGTGTCCTGGAACTCTGGGGCTCTGACATCTGGGGTGCACACATTCCCTGCAGTGCTGCAGTCCTCTGGCCTGTACAGCCTGTCCTCTGTGGTCACAGTGCCTAGCTC
TAGCCTGGGCACCCAGACCTACATCTGCAATGTGAACCACAAGCCTAGCAACACCAAGGTGGACAAGAAGGCTGAGCCCAAGAGCTGTGACAAGACCCACACCTGTCCTC
CATGTCCT[illegible]
[illegible]
[illegible]
CCAAGGGCCAGCCTAGGGAACCCCAGGTTTACACACTGCCACCTAGCAGGGATGAGCTGACCAAGAACCAGGTGTCCCTGACATGCCTGGTTAAGGGCTTCTACCCCTCTG
ACATTGCTGTGGAATGGGAGAGCAATGGCCAGCCAGAGAACAACTACAAGACAACCCCTCCTGTGCTGGACTCTGATGGCTCATTCTTCCTGTACTCCAAGCTGACTGTGG
ACAAGTCCAGATGGCAGCAGGGCAATGTCTTTAGCTGCTCTGTGATGCATGAGGCCCTGCACAACCACTACACACAGAAGTCCCTGTCTCTGAGCCCTGGCAAGTGAAGAT
CTACTTCTGGCTAATAAAAGATCAGAGCTCTAGTGATCTGTGTGTTGGTTTTTTGTGTCTCTGCATTCTAGCAGAGCCCCACTGTGTTCATCTTACAGATGGAAATACTGACATT
CAGAGGAGTTAGTTAACTTGCCTAGGTGATTCAGCTAATAAGTGCAAGAAAGATTTCAATCCAAGGTGATTTGATTCTGAAGCCTGTGCTAATCACATTACACCAAGCTACA
ACTTCATTTATAAATAATAAGTCAGCTTTCAAGGGCCTTTCAGGTGTCCTGCACTTCTACAAGCTGTGCCATTTAGTGAACACAAAATGAGCCTTCTGATGAAGTAGTCTTTT
CATTATTTCAGATATTAGAACACTAAAATTCTTAGCTGCCAGCTGATTGAAGGCTGGGACAAAATTCAAACATGCATCTACAACAATATATATCTCAATGTTAGTCTCCAAAT
TCTATTGACTTCAACTCAAGAGAATATAAAGAGCTAGTCTTTATACACTCTTTAAGGTATGATATCATCTGGAAAGTAACAAAATTGATGCAAATTTGAATGAACTTTATCAT
GGTGTATTTACACAATGTGTTTCTTCTCCCTGCAATGTATTTCTTTCTCTAATTCCTTCCATTTGATCTTTCATACACAATCTGGTTCTGATGTATGTTTTTTGGATGCACTTTTC
AACTCCAAAAGACAGAGCTAGTTACTTTCTTCCTGGTGCTCCAAGCACTGTATTTGTATCTGTATTCAAGCCCTTTGCAATATTGTACTGGATCATTATTTCACCTCTAGGATG
GCTTCCCCAGGCAACTTGTGTTCACCCAGAGACTACATTTTGTATCTTGTTGACCTTTGAACTTCCACCAGTGTCTAAAAATAATATGTATGCAAAATTACTTGCTATGAGAAT
GTATAATTAAACAATATAAAAAGGAGAAGCAAGGAGAGAAACACAGGTGTGTATTTGTGTTTGTGTGCTTAAAAGGCAGTGTGGAAAAGGAAGAAATGCCATTTATAGTG
AGGAGACAAAGTTATATTACCTCTTATCTGGCTTTTAAGGAGATTTTGCTGAGCTAAAAATCCTATATTCATAGAAAAGCCTTACCTGAGTTGCCAATACCTCAATTCAGTCT
AGC**TGTTACATAACTTATGGTAAATGGCCTGCCTGGCTGACTGCCCAATGACCCCTGCCCAATGATGTCAATAATGATGTATGTTCCCATGTAATGCCAATAGGGACTTTC**
CATTGATGTCAATGGGTGGAGTATTTATGGTAACTGCCCACTTGGCAGTACATCAAGTGTATCATATGCCAAGTATGCCCCCTATTGATGTCAATGATGGTAAATGGCCT
GCCTGGCATTATGCCCAGTACATGACCTTATGGGACTTTCCTACTTGGCAGTACATCTATGTATTAGTCATTGCTATTACCATGGATTAGTGGAGAAGAGCATGCTTGAGG
GCTGAGTGCCCCTCAGTGGGCAGAGAGCACATGGCCCACAGTCCCTGAGAAGTTGGGGGGAGGGGTGGGCAATTGAACTGGTGCCTAGAGAAGGTGGGGCTTGGGTAA
ACTGGGAAAGTGATGTGGTGTACTGGCTCCACCTTTTTCCCCAGGGTGGGGGAGAACCATATATAAGTGCAGTAGTCTCTGTGAACATTCAAGCTTCTGCCTTCTCCCTCCT
GTGAGTTTGGATGCACCTACTAGATATCTTGGTAAGTCACTGACTGTCTATGCCTGGGAAAGGGTGGGCAGGAGGTGGGGCAGTGCAGGAAAAGTGGCACTGTGAACCC
TGCAGCCCTAGACAATTGTACTAACCTTCTTCTCTTTCCTCTCCTGACAGGTTGGTAACCAAG[illegible]
[illegible]ACAGACATTGTGATGACCCAGTCTCCATCCTTCCTGAGTGCCTCTGTGGGAGACAGAGTGACCATCACCTGTAGAGCCAGCCAGGGCATCAGCTCTTACCTG
GCTTGGTATCAGCAAAAGCCTGGCAAGGCCCCTAAGCTGCTGATCTATGCTGCCTCCACACTGCAGTCAGGGGTGCCCTCCAGATTTTCTGGCTCTGGATCTGGCACTGAGT
TCACCCTGACCATCAGCTCCCTGCAGCCTGAGGACTTTGCCACCTACTACTGCCAGCAGCTGAACAGCTACCCTCCTTACACCTTTGGACAGGGCACCAAGCTGGAAATCAA
GGGAACAAAGCTGACAGTCCTGGGCCAGCCAAAGGCTGCTCCTTCTGTGACACTGTTCCCACCTAGCTCTGAGGAACTGCAGGCTAACAAGGCTACCCTTGTGTGCCTGAT
CTCTGACTTCTACCCAGGGGCTGTGACTGTGGCTTGGAAGGCTGATAGCAGCCCTGTGAAGGCTGGGGTTGAGACAACCACACCTAGCAAGCAGAGCAACAACAAATATG
CTGCCAGCTCCTACCTGAGTCTGACCCCTGAGCAGTGGAAGTCCCACAGATCCTACAGCTGCCAAGTGACCCATGAGGGCTCCACAGTGGAAAAGACAGTGGCCCCAACA
GAGTGCTCCTGAAGATCT[illegible]AGTCAATATGTTCACCCCAAAAAAGCT
GTTTGTTAACTTGTCAACCTCATTCTAAAATGTATATAGAAGCCCAAAAGACAATAACAAAAATATTCTTGTAGAACAAAATGGGAAAGAATGTTCCACTAAATATCAAGAT
TTAGAGCAAAGCATGAGATGTGTGGGGATAGACAGTGAGGCTGATAAAATAGAGTAGAGCTCAGAAACAGACCCATTGATATATGTAAGTGACCTATGAAAAAAATATG
GCATTTTACAATGGGAAAATGATGGTCTTTTTCTTTTTTAGAAAAACAGGGAAATATATTTATATGTAAAAAATAAAAGGGAACCCATATGTCATACCATACACACAAAAAA
ATTCCAGTGAATTATAAGTCTAAATGGAGAAGGCAAAACTTTAAATCTTTTAGAAAATAATATAGAAGCATGCCATCAAGACTTCAGTGTAGAGAAAAATTTCTTATGACTC
AAAGTCCTAACCACAAAGAAAAGATTGTTAATTAGATTGCATGAATATTAAGACTTATTTTTAAAATTAAAAAACCATTAAGAAAAGTCAGGCCATAGAATGACAGAAAATA
TTTGCAACACCCCAGTAAAGAGAATTGTAATATGCAGATTATAAAAAGAAGTCTTACAAATCAGTAAAAAATAAAACTAGACAAAAATTTGAACAGATGAAAGAGAAACTC
TAAATAATCATTACACATGAGAAACTCAATCTCAGAAATCAGAGAACTATCATTGCATATACACTAAATTAGAGAAATATTAAAAGGCTAAGTAACATCTGTGGCTTAATTA
A[illegible]TCTAGTGATCAGCAGTTCAACCTGTTGATAGTATGTACTAAGCTCTCATGTTTAATGTACTAAGCTCTCATGTTTAATGAACTAAACCCTCATGGCTAATGTACTAA
GCTCTCATGGCTAATGTACTAAGCTCTCATGTTTCATGTACTAAGCTCTCATGTTTGAACAATAAAATTAATATAAATCAGCAACTTAAATAGCCTCTAAGGTTTTAAGTTTTA
TAAGAAAAAAAAGAATATATAAGGCTTTTAAAGGTTTTAAGGTTTCCTAGGTTATCCTCATATGAGCTCTTAGAAAAACTCATCCAGCATCAAATGAAACTGCAATTTATTCA
TATCAGGATTATCAATACCATATTTTTGAAAAAGTCTTTTCTGTAATGAAGGAGAAAACTCACCCAGGCAGTTCCATAGGATGGCAAGATCCTGGTATCTGTCTGCAATTCCA
ACTCTTCCAACATCAATACAACCTATTAATTTCCCCTCATCAAAAATAAGGTTATCAAGTGAGAAATCACCATGAGTGACCACTGAATCTGGTGAGAATGGCAAAAGATTAT
GCATTTCTTTCCAGACTTGTTCAACAGGCCAGCCATTTCTCTCATCATCAAAATCACTGGCATCAACCAAACCATTATTCATTCTTGATTGGGCCTGAGCCAGTCTAAATACTC
TATCAGAGTTAAAAGGACAATTACAAACAGGAATGGAATGCAATCTTCTCAGGAACACTGCCAGGGCATCAACAATATTTTCACCTGAATCAGGATATTCTTCCAATACCTG
GAATGCTGTTTTCCCTGGGATGGCAGTGGTGAGTAACCATGCATCATCAGGAGTTCTGATAAAATGCTTGATGGTTGGAAGAGGCATAAATTCAGTCAGCCAGTTTAGTCT
GACCATCTCATCTGTAACATCATTGGCAACAGAACCTTTGCCATGTTTCAGAAACAACTCTGGGGCATCTGGCTTCCCATACAATCTATAGATTGTGGCACCTGATTGCCCAA
CATTATCTCTAGCCCATTTATACCCATATAAATCAGCATCCATGTTGGAATTTAATCTTGGCCTGGAGCAAGAGGTTTCTCTTTGAATATGGCTCATACATGTGCA[illegible]
ACTGAGTTGTATTATACTATGCAGATATACTATGCCAATGTTTAATTGTCAG

FIG. 12

070320 # 4 : B38-Kappa-BV3 (SEQ ID NO:12)

DraIII-βGlo BI-Nhe-CMVΔEF1I126-BstEII -B38-Kappa-BglII-MinpA-IFNβ S/MAR-BV3

CACTATGTGTTAATTAAAATTATCTCTAAGGCATGTGAACTGGCTGTCTTGGTTTTCATCTGTACTTCATCTGCTACCTCTGTGACCTGAAACATATTTATAATTCCA
TTAAGCTGTGCATATGATAGATTTATCATATGTATTTTCCTTAAAGGATTTTTGTAAGAACTAATTGAATTGATACCTGTAAAGTCTTTATCACACTACCCAATAAA
TAATAAATCTCTTTGTTCAGCTCTCTGTTTCTATAAATATGTACCAGTTTTATTGTTTTTAGTGGTAGTGATTTTATTCTCTTTCTATATATATACACACACATGTGTG
CATTCATAAATATATACAATTTTTATGAATAAAAAATTATTAGCAATCAATATTGAAAACCACTGATTTTTGTTTATGTGAGCAAACAGCAGATTAAAAGGAATTT
GAATTCTCATAGCTAGCAGGAGTCAATGGGAAAAACCCATTGGAGCCAAGTACACTGACTCAATAGGGACTTTCCATTGGGTTTTGCCCAGTACATAAGGTCAA
TAGGGGGTGAGTCAACAGGAAAGTCCCATTGGAGCCAAGTACATTGAGTCAATAGGGACTTTCCAATGGGTTTTGCCCAGTACATAAGGTCAATGGGAGGTAA
GCCAATGGGTTTTTCCCATTACTGACATGTATACTGAGTCATTAGGGACTTTCCAATGGGTTTTGCCCAGTACATAAGGTCAATAGGGGTGAATCAACAGGAAA
GTCCCATTGGAGCCAAGTACACTGAGTCAATAGGGACTTTCCATTGGGTTTTGCCCAGTACAAAAGGTCAATAGGGGGTGAGTCAATGGGTTTTTCCCATTATTG
GCACATACATAAGGTCAATAGGGGTGACTAGTGGAGAAGAGCATGCTTGAGGGCTGAGTGCCCCTCAGTGGGCAGAGAGCACATGGCCCACAGTCCCTGAGA
AGTTGGGGGGAGGGGTGGGCAATTGAACTGGTGCCTAGAGAAGGTGGGGCTTGGGTAAACTGGGAAAGTGATGTGGTGTACTGGCTCCACCTTTTTCCCCAG
GGTGGGGGAGAACCATATATAAGTGCAGTAGTCTCTGTGAACATTCAAGCTTCTGCCTTCTCCCTCCTGTGAGTTTGGTAAGTCACTGACTGTCTATGCCTGGGA
AAGGGTGGGCAGGAGATGGGGCAGTGCAGGAAAAGTGGCACTATGAACCCTGCAGCCCTAGACAATTGTACTAACCTTCTTCTCTTTCCTCTCCTGACAGGTTG
GTAACCAAGCCACCATGGGATGGTCCCTGATCCTGCTGTTTCTGGTGGCTGTGGCCACCAGAGTGCTGTCTGAAGTGCAGCTGGTGGAAAGTGGTGGTGGCCT
GGTTCAGCCTGGTGGCTCTCTGAGACTGAGCTGTGCTGCCTCTGGCTTCATTGTGTCCAGCAACTACATGAGCTGGGTCAGACAGGCCCCTGGCAAAGGACTGG
AATGGGTGTCAGTGATCTACAGTGGTGGCAGCACCTACTATGCTGACTCTGTGAAGGGCAGATTCACCATCAGCAGACACAACAGCAAGAACACCCTGTACCTG
CAGATGAACAGCCTGAGAGCTGAGGACACTGCTGTGTACTACTGTGCCAGAGAAGCCTATGGCATGGATGTGTGGGGCCAGGGCACAACAGTGACTGTGTCCT
CTGCCAGCACAAAGGGCCCCTCTGTGTTTCCTCTGGCTCCCAGCAGCAAGAGCACCAGTGGTGGAACAGCTGCCCTGGGCTGTCTGGTCAAGGACTACTTTCCT
GAGCCTGTGACAGTGTCCTGGAACTCTGGGGCTCTGACATCTGGGGTGCACACATTCCCTGCAGTGCTGCAGTCCTCTGGCCTGTACAGCCTGTCCTCTGTGGTC
ACAGTGCCTAGCTCTAGCCTGGGCACCCAGACCTACATCTGCAATGTGAACCACAAGCCTAGCAACACCAAGGTGGACAAGAAGGCTGAGCCCAAGAGCTGTG
ACAAGACCCACACCTGTCCTCCATGTCCTGCTCCAGAGCTGCTTGGAGGACCATCAGTGTTTCTGTTCCCTCCAAAGCCTAAGGACACCCTGATGATCAGCAGAA
CCCCTGAAGTGACCTGTGTGGTGGTTGATGTGTCCCATGAGGACCCAGAAGTGAAGTTCAATTGGTATGTGGATGGTGTTGAGGTGCACAATGCCAAGACCAA
GCCTAGAGAGGAACAGTACAACTCCACCTACAGAGTGGTTTCTGTGCTGACAGTGCTCCACCAGGACTGGCTGAATGGCAAAGAGTACAAGTGCAAGGTGTCC
AACAAGGCCCTGCCTGCTCCTATTGAAAAGACCATCTCCAAGGCCAAGGGCCAGCCTAGGGAACCCCAGGTTTACACACTGCCACCTAGCAGGGATGAGCTGAC
CAAGAACCAGGTGTCCCTGACATGCCTGGTTAAGGGCTTCTACCCCTCTGACATTGCTGTGGAATGGGAGAGCAATGGCCAGCCAGAGAACAACTACAAGACA
ACCCCTCCTGTGCTGGACTCTGATGGCTCATTCTTCCTGTACTCCAAGCTGACTGTGGACAAGTCCAGATGGCAGCAGGGCAATGTCTTTAGCTGCTCTGTGATG
CATGAGGCCCTGCACAACCACTACACACAGAAGTCCCTGTCTCTGAGCCCTGGCAAG***AGAAAGAGAAGGAGTGGCTCTGGGGCCACCAACTTCAGCCTGCTGA***
AACAGGCTGGGGATGTTGAAGAGAACCCTGGACCTATGGACTTCCAGGTGCAGATCATCAGCTTTCTGCTTATCTCTGCCAGTGTGATCATGAGCAGGGGAGA
CATTGTGATGACCCAGTCTCCATCCTTCCTGAGTGCCTCTGTGGGAGACAGAGTGACCATCACCTGTAGAGCCAGCCAGGGCATCAGCTCTTACCTGGCTTGGTA
TCAGCAAAAGCCTGGCAAGGCCCCTAAGCTGCTGATCTATGCTGCCTCCACACTGCAGTCAGGGGTGCCCTCCAGATTTTCTGGCTCTGGATCTGGCACTGAGTT
CACCCTGACCATCAGCTCCCTGCAGCCTGAGGACTTTGCCACCTACTACTGCCAGCAGCTGAACAGCTACCCTCCTTACACCTTTGGACAGGGCACCAAGCTGGA
AATCAAGAGGACAGTGGCTGCTCCCTCTGTGTTCATCTTCCCACCATCAGATGAACAGCTGAAGAGTGGCACAGCCTCTGTTGTGTGCCTGCTGAACAACTTCTA
CCCTAGAGAAGCCAAGGTGCAGTGGAAAGTGGACAATGCCCTGCAGTCTGGCAACAGCCAAGAATCTGTGACTGAGCAGGACTCCAAGGACAGCACATACAG
CCTGAGCAGCACACTGACCCTGAGCAAGGCTGACTATGAGAAGCACAAAGTCTATGCCTGTGAAGTGACACACCAGGGCCTGTCTAGCCCAGTGACCAAGTCCT
TCAACAGGGGAGAGTGTTGAAGATCTACTTCTGGCTAATAAAAGATCAGAGCTCTAGTGATCTGTGTGTTGGTTTTTTGTGTCTGCATTCTAGCAAGTCAATATG
TTCACCCCAAAAAAGCTGTTTGTTAACTTGTCAACCTCATTCTAAAATGTATATAGAAGCCCAAAAGACAATAACAAAAATATTCTTGTAGAACAAAATGGGAAA
GAATGTTCCACTAAATATCAAGATTTAGAGCAAAGCATGAGATGTGTGGGGATAGACAGTGAGGCTGATAAAATAGAGTAGAGCTCAGAAACAGACCCATTGA
TATATGTAAGTGACCTATGAAAAAAATATGGCATTTTACAATGGGAAAATGATGGTCTTTTTCTTTTTTAGAAAAACAGGGAAATATATTTATATGTAAAAAATA
AAAGGGAACCCATATGTCATACCATACACACAAAAAAATTCCAGTGAATTATAAGTCTAAATGGAGAAGGCAAAACTTTAAATCTTTTAGAAAATAATATAGAA
GCATGCCATCAAGACTTCAGTGTAGAGAAAAATTTCTTATGACTCAAAGTCCTAACCACAAAGAAAAGATTGTTAATTAGATTGCATGAATATTAAGACTTATTTT
TAAAATTAAAAAACCATTAAGAAAAGTCAGGCCATAGAATGACAGAAAATATTTGCAACACCCCAGTAAAGAGAATTGTAATATGCAGATTATAAAAAGAAGTC
TTACAAATCAGTAAAAAATAAAACTAGACAAAAATTTGAACAGATGAAAGAGAAACTCTAAATAATCATTACACATGAGAAACTCAATCTCAGAAATCAGAGAA
CTATCATTGCATATACACTAAATTAGAGAAATATTAAAAGGCTAAGTAACATCTGTGGCTTAATTAACCTAGGTCTAGTGATCAGCAGTTCAACCTGTTGATAGTA
TGTACTAAGCTCTCATGTTTAATGTACTAAGCTCTCATGTTTAATGAACTAAACCCTCATGGCTAATGTACTAAGCTCTCATGGCTAATGTACTAAGCTCTCATGTT
TCATGTACTAAGCTCTCATGTTTGAACAATAAAATTAATATAAATCAGCAACTTAAATAGCCTCTAAGGTTTTAAGTTTTATAAGAAAAAAAAGAATATATAAGGC
TTTTAAAGGTTTTAAGGTTTCCTAGGTTATCCTCATATGAGCTCTTAGAAAAACTCATCCAGCATCAAATGAAACTGCAATTTATTCATATCAGGATTATCAATACC
ATATTTTTGAAAAAGTCTTTTCTGTAATGAAGGAGAAAACTCACCCAGGCAGTTCCATAGGATGGCAAGATCCTGGTATCTGTCTGCAATTCCAACTCTTCCAACA
TCAATACAACCTATTAATTTCCCCTCATCAAAAATAAGGTTATCAAGTGAGAAATCACCATGAGTGACCACTGAATCTGGTGAGAATGGCAAAAGATTATGCATT
TCTTTCCAGACTTGTTCAACAGGCCAGCCATTTCTCTCATCATCAAAATCACTGGCATCAACCAAACCATTATTCATTCTTGATTGGGCCTGAGCCAGTCTAAATAC
TCTATCAGAGTTAAAAGGACAATTACAAACAGGAATGGAATGCAATCTTCTCAGGAACACTGCCAGGGCATCAACAATATTTTCACCTGAATCAGGATATTCTTC
CAATACCTGGAATGCTGTTTTCCCTGGGATGGCAGTGGTGAGTAACCATGCATCATCAGGAGTTCTGATAAAATGCTTGATGGTTGGAAGAGGCATAAATTCAG
TCAGCCAGTTTAGTCTGACCATCTCATCTGTAACATCATTGGCAACAGAACCTTTGCCATGTTTCAGAAACAACTCTGGGGCATCTGGCTTCCCATACAATCTATA
GATTGTGGCACCTGATTGCCCAACATTATCTCTAGCCCATTTATACCCATATAAATCAGCATCCATGTTGGAATTTAATCTTGGCCTGGAGCAAGAGGTTTCTCTTT
GAATATGGCTCATACATGTGCACCTCCTATAGTGAGTTGTATTATACTATGCAGATATACTATGCCAATGTTTAATTGTCAG

FIG. 13

071320 # 3 : H4-Kappa-BV3 (SEQ ID NO:13)

DraIII-βGlo BI-Nhe-mCMVΔEF1Δ26-BstEII -H4-Kappa-BglII-MinpA-IFNβ S/MAR-BV3

CACTATGTGTTAATTAAAATTATCTCTAAGGCATGTGAACTGGCTGTCTTGGTTTTCATCTGTACTTCATCTGCTACCTCTGTGACCTGAAACATATTTATAATTCCA
TTAAGCTGTGCATATGATAGATTTATCATATGTATTTTCCTTAAAGGATTTTTGTAAGAACTAATTGAATTGATACCTGTAAAGTCTTTATCACACTACCCAATAAA
TAATAAATCTCTTTGTTCAGCTCTCTGTTTCTATAAATATGTACCAGTTTTATTGTTTTTAGTGGTAGTGATTTTATTCTCTTTCTATATATATACACACACATGTGTG
CATTCATAAATATATACAATTTTTATGAATAAAAAATTATTAGCAATCAATATTGAAAACCACTGATTTTTGTTTATGTGAGCAAACAGCAGATTAAAAGGAATTT
GAATTCTCATAGCTAGCAGGAGTCAATGGGAAAAACCCATTGGAGCCAAGTACACTGACTCAATAGGGACTTTCCATTGGGTTTTGCCCAGTACATAAGGTCAA
TAGGGGGTGAGTCAACAGGAAAGTCCCATTGGAGCCAAGTACATTGAGTCAATAGGGACTTTCCAATGGGTTTTGCCCAGTACATAAGGTCAATGGGAGGTAA
GCCAATGGGTTTTTCCCATTACTGACATGTATACTGAGTCATTAGGGACTTTCCAATGGGTTTTGCCCAGTACATAAGGTCAATAGGGGTGAATCAACAGGAAA
GTCCCATTGGAGCCAAGTACACTGAGTCAATAGGGACTTTCCATTGGGTTTTGCCCAGTACAAAAGGTCAATAGGGGGTGAGTCAATGGGTTTTTCCCATTATTG
GCACATACATAAGGTCAATAGGGGTGACTAGTGGAGAAGAGCATGCTTGAGGGCTGAGTGCCCCTCAGTGGGCAGAGAGCACATGGCCCACAGTCCCTGAGA
AGTTGGGGGGAGGGGTGGGCAATTGAACTGGTGCCTAGAGAAGGTGGGGCTTGGGTAAACTGGGAAAGTGATGTGGTGTACTGGCTCCACCTTTTTCCCCAG
GGTGGGGGAGAACCATATATAAGTGCAGTAGTCTCTGTGAACATTCAAGCTTCTGCCTTCTCCCTCCTGTGAGTTTGGTAAGTCACTGACTGTCTATGCCTGGGA
AAGGGTGGGCAGGAGATGGGGCAGTGCAGGAAAAGTGGCACTATGAACCCTGCAGCCCTAGACAATTGTACTAACCTTCTTCTCTTTCCTCTCCTGACAGGTTG
GTAACCAAGCCACCATGGGATGGTCCCTGATCCTGCTGTTTCTGGTGGCTGTGGCCACCAGAGTGCTGTCTCAGGTTCAGCTGGTGCAGTCTGGGGCTGAAGTG
AAGAAACCTGGGGCCTCTGTGAAGGTGTCCTGCAAGGCTTCTGGCTACACATTCACAGGCTACTACATGCACTGGGTCAGACAGGCCCCTGGACAGGGACTTG
AGTGGATGGGCAGAATCAACCCCAACAGTGGTGGCACCAACTATGCCCAGAAATTCCAGGGCAGAGTGACCATGACCAGAGACACCAGCATCAGCACAGCCTA
CATGGAACTGAGCAGGCTTAGGAGTGATGACACTGCTGTGTACTACTGTGCCAGAGTGCCCTACTGCAGCAGCACCTCTTGTCACAGAGACTGGTACTTTGACC
TGTGGGGCAGAGGCACCCTGGTCACAGTTAGCTCTGCCAGCACAAAGGGCCCCTCTGTGTTTCCTCTGGCTCCCAGCAGCAAGAGCACCAGTGGTGGAACAGC
TGCCCTGGGCTGTCTGGTCAAGGACTACTTTCCTGAGCCTGTGACAGTGTCCTGGAACTCTGGGGCTCTGACATCTGGGGTGCACACATTCCCTGCTGTGCTGCA
GTCCTCTGGCCTGTACAGCCTGTCCTCTGTGGTCACTGTGCCTAGCTCTAGCCTGGGCACCCAGACCTACATCTGCAATGTGAACCACAAGCCTAGCAACACCAA
GGTGGACAAGAAGGCTGAGCCCAAGAGCTGTGATAAGACCCACACCTGTCCTCCATGTCCTGCTCCAGAGCTGCTTGGAGGACCATCAGTGTTCCTGTTCCCTC
CAAAGCCTAAGGACACCCTGATGATCAGCAGAACTCCTGAAGTGACCTGTGTGGTGGTGGATGTGTCCCATGAGGACCCAGAAGTGAAGTTCAATTGGTATGT
GGATGGTGTTGAGGTGCACAATGCCAAGACCAAGCCTAGAGAGGAACAGTACAACAGCACCTACAGAGTGGTGTCTGTGCTGACAGTGCTGCACCAGGACTG
GCTGAATGGCAAAGAGTACAAGTGCAAGGTGTCCAACAAGGCCCTGCCTGCTCCTATTGAAAAGACCATCAGCAAGGCCAAGGGCCAGCCTAGGGAACCCCAA
GTGTATACCCTGCCTCCTAGCAGAGATGAGCTGACCAAGAACCAGGTGTCCCTGACATGCCTGGTTAAGGGCTTCTACCCCTCTGACATTGCTGTGGAATGGGA
GAGCAATGGCCAGCCTGAGAACAACTACAAGACCACACCTCCTGTGCTGGACTCTGATGGCTCATTCTTCCTGTACTCCAAGCTGACTGTGGACAAGTCCAGAT
GGCAGCAAGGCAATGTGTTCAGCTGCTCTGTGATGCATGAGGCCCTGCACAACCACTACACACAGAAGTCTCTGTCTCTGAGCCCTGGCAAG***AGAAAGAGAAG***
GAGTGGCTCTGGGGCCACCAACTTCAGCCTGCTGAAACAGGCTGGGGATGTTGAAGAGAACCCTGGACCTATGGACTTCCAGGTGCAGATCATCAGCTTCCTG
CTTATCTCTGCCAGTGTGATCATGAGCAGGGAGACATCCAGATGACACAGAGCCCTCTGAGCCTGCCAGTGACACCTGGGGAACCTGCCAGCATCTCTTGCAG
AAGCTCTCAGAGCCTCCTGGATTCTGATGATGGCAACACCTACCTGGACTGGTATCTGCAGAAGCCTGGCCAGTCTCCTCAGCTGCTGATCTACACCCTGAGCTA
CAGAGCCAGTGGGGTGCCAGACAGATTCTCTGGCTCTGGATCTGGCACTGACTTCACACTGAAGATTAGCAGAGTGGAAGCTGAGGATGTGGGAGTCTACTAC
TGTATGCAGAGGATTGAGTTCCCTCTGACTTTTGGTGGTGGTACAAAGGTGGAAATCAAGAGGACAGTGGCTGCTCCTTCTGTGTTCATCTTCCCACCATCTGAT
GAGCAGCTCAAGAGTGGCACAGCCTCTGTTGTGTGTCTGCTGAACAACTTCTACCCTAGGGAAGCCAAGGTGCAGTGGAAAGTGGACAATGCCCTCCAGTCTG
GCAACAGCCAAGAGAGTGTGACAGAACAGGACAGCAAGGACTCCACCTACAGCCTGAGCAGCACCCTGACACTGAGCAAGGCTGACTATGAGAAGCACAAAG
TCTATGCCTGTGAAGTGACACACCAGGGACTGAGCAGCCCTGTGACCAAGAGCTTCAACAGGGGAGAGTGCAGCTGAAGATCTACTTCTGGCTAATAAAAGAT
CAGAGCTCTAGTGATCTGTGTGTTGGTTTTTTGTGTCTGCATTCTAGCAAGTCAATATGTTCACCCCAAAAAAGCTGTTTGTTAACTTGTCAACCTCATTCTAAAAT
GTATATAGAAGCCCAAAAGACAATAACAAAAATATTCTTGTAGAACAAAATGGGAAAGAATGTTCCACTAAATATCAAGATTTAGAGCAAAGCATGAGATGTGT
GGGGATAGACAGTGAGGCTGATAAAATAGAGTAGAGCTCAGAAACAGACCCATTGATATATGTAAGTGACCTATGAAAAAAATATGGCATTTTACAATGGGAA
AATGATGGTCTTTTTCTTTTTTAGAAAAACAGGGAAATATATTTATATGTAAAAAATAAAAGGGAACCCATATGTCATACCATACACACAAAAAAATTCCAGTGA
ATTATAAGTCTAAATGGAGAAGGCAAAACTTTAAATCTTTTAGAAAATAATATAGAAGCATGCCATCAAGACTTCAGTGTAGAGAAAAATTTCTTATGACTCAAA
GTCCTAACCACAAAGAAAAGATTGTTAATTAGATTGCATGAATATTAAGACTTATTTTTAAAATTAAAAAACCATTAAGAAAAGTCAGGCCATAGAATGACAGAA
AATATTTGCAACACCCCAGTAAAGAGAATTGTAATATGCAGATTATAAAAAGAAGTCTTACAAATCAGTAAAAAATAAAACTAGACAAAAATTTGAACAGATGA
AAGAGAAACTCTAAATAATCATTACACATGAGAAACTCAATCTCAGAAATCAGAGAACTATCATTGCATATACACTAAATTAGAGAAATATTAAAAGGCTAAGTA
ACATCTGTGGCTTAATTAATCTAGCTCTAGTGATCAGCAGTTCAACCTGTTGATAGTATGTACTAAGCTCTCATGTTTAATGTACTAAGCTCTCATGTTTAATGAAC
TAAACCCTCATGGCTAATGTACTAAGCTCTCATGGCTAATGTACTAAGCTCTCATGTTTCATGTACTAAGCTCTCATGTTTGAACAATAAAATTAATATAAATCAGC
AACTTAAATAGCCTCTAAGGTTTTAAGTTTTATAAGAAAAAAAAGAATATATAAGGCTTTTAAAGGTTTTAAGGTTTCCTAGGTTATCCTCATATGAGCTCTTAGA
AAAACTCATCCAGCATCAAATGAAACTGCAATTTATTCATATCAGGATTATCAATACCATATTTTTGAAAAAGTCTTTTCTGTAATGAAGGAGAAAACTCACCCAG
GCAGTTCCATAGGATGGCAAGATCCTGGTATCTGTCTGCAATTCCAACTCTTCCAACATCAATACAACCTATTAATTTCCCCTCATCAAAAATAAGGTTATCAAGT
GAGAAATCACCATGAGTGACCACTGAATCTGGTGAGAATGGCAAAAGATTATGCATTTCTTTCCAGACTTGTTCAACAGGCCAGCCATTTCTCTCATCATCAAAA
TCACTGGCATCAACCAAACCATTATTCATTCTTGATTGGGCCTGAGCCAGTCTAAATACTCTATCAGAGTTAAAAGGACAATTACAAACAGGAATGGAATGCAAT
CTTCTCAGGAACACTGCCAGGGCATCAACAATATTTTCACCTGAATCAGGATATTCTTCCAATACCTGGAATGCTGTTTTCCCTGGGATGGCAGTGGTGAGTAAC
CATGCATCATCAGGAGTTCTGATAAAATGCTTGATGGTTGGAAGAGGCATAAATTCAGTCAGCCAGTTTAGTCTGACCATCTCATCTGTAACATCATTGGCAACA
GAACCTTTGCCATGTTTCAGAAACAACTCTGGGGCATCTGGCTTCCCATACAATCTATAGATTGTGGCACCTGATTGCCCAACATTATCTCTAGCCCATTTATACCC
ATATAAATCAGCATCCATGTTGGAATTTAATCTTGGCCTGGAGCAAGAGGTTTCTCTTTGAATATGGCTCATACATGTGCACCTCCTATAGTGAGTTGTATTATAC
TATGCAGATATACTATGCCAATGTTTAATTGTCAG

FIG. 14

080920 # 6 : H4-H4-Kappa-BV3 (SEQ ID NO:14)

DraIII-βGlo BI-Nhe--AmCMV&EF1I126-BstEII -H4-Kappa-BglII-MupA-**21q21**-AmCMV&EF1I126-BstEII -H4-Kappa-BglII-MupA-IFNβ S/MAR-BV3

CACTATGTGTTAATTAAAATTATCTCTAAGGCATGTGAACTGGCTGTCTTGGTTTTCATCTGTACTTCATCTGCTACCTCTGTGACCTGAAACATATTTATAATTCCATTAAGCTGTGCATATGATAGATTT
ATCATATGTATTTTCCTTAAAGGATTTTTGTAAGAACTAATTGAATTGATACCTGTAAAGTCTTTATCACACTACCCAATAAATAATAAATCTCTTTGTTCAGCTCTCTGTTTCTATAAATATGTACCAGTTT
TATTGTTTTTAGTGGTAGTGATTTTATTCTCTTTCTATATATATACACACACATGTGTGCATTCATAAATATATACAATTTTTATGAATAAAAAATTATTAGCAATCAATATTGAAAACCACTGATTTTTGTT
TATGTGAGCAAACAGCAGATTAAAAGG**AATTT**GAATTC**TCATA**GCTAGCAG[illegible]
[illegible]
[illegible]
[illegible]ACTACTGGCAGAAGACCATGCTTGAGGGCTGACTGCC
CCTCAGTGGGCAGAGAGCACATGGCCCACAGTCCCTGAGAAGTTGGGGGGAGGGGTGGGCAATTGAACTGGTGCCTAGAGAAGGTGGGGCTTGGGTAAACTGGGAAAGTGATGTGGTGTACTGGC
TCCACCTTTTCCCCAGGGTGGGGGAGAACCATATATAAGTGCAGTAGTCTCTGTGAACATTCAAGCCTTCTGCCTTCTCCCTCCTGTGAGTTTGGTAAGTCACTGACTGTCTATGCCTGGGAAAGGGTG
GGCAGGAGATGGGGCAGTGCAGGAAAAGTGGCACTATGAACCCTGCAGCCCTAGACAATTGTACTAACCTTCTTCTCTTTCCTCTCCTGACAGGTTGGTAACCAAGGCACCATGGGATGGTCCCTGAT
CCTGCTGTTTCTGGTGGCTGTGGCCACCAGAGTGCTGTCTCAGGTTCAGCTGGTGCAGTCTGGGGCTGAAGTGAAGAAACCTGGGGCCTCTGTGAAGGTGTCCTGCAAGGCTTCTGGCTACACATTCA
CAGGCTACTACATGCACTGGGTCAGACAGGCCCCTGGACAGGGACTTGAGTGGATGGGCAGAATCAACCCCAACAGTGGTGGCACCAACTATGCCCAGAAATTCCAGGGCAGAGTGACCATGACCA
GAGACACCAGCATCAGCACAGCCTACATGGAACTGAGCAGGCTTAGGAGTGATGACACTGCTGTGTACTACTGTGCCAGAGTGCCCTACTGCAGCAGCACCTCTTGTCACAGAGACTGGTACTTTGAC
CTGTGGGGCAGAGGCACCCTGGTCACAGTTAGCTCTGCCAGCACAAAGGGCCCCTCTGTGTTTCCTCTGGCTCCCAGCAGCAAGAGCACCAGTGGTGGAACAGCTGCCCTGGGCTGTCTGGTCAAGG
ACTACTTTCCTGAGCCTGTGACAGTGTCCTGGAACTCTGGGGCTCTGACATCTGGGGTGCACACATTCCCTGCTGTGCTGCAGTCCTCTGGCCTGTACAGCCTGTCCTCTGTGGTCACTGTGCCTAGCTC
TAGCCTGGGCACCCAGACCTACATCTGCAATGTGAACCACAAGCCTAGCAACACCAAGGTGGACAAGAAGGCTGAGCCCAAGAGCTGTGATAAGACCCACACCTGTCCTCCATGTCCT[illegible]
[illegible]
[illegible]
TACAAGTGCAAGGTGTCCAACAAGGCCCTGCCTGCCCCTATTGAAAAGACCATCAGCAAGGCCAAGGGCCAGCCTAGGGAACCCCAAGTGTATACCCTGCCTCCTAGCAGAGATGAGCTGACCAAGA
ACCAGGTGTCCCTGACATGCCTGGTTAAGGGCTTCTACCCCTCTGACATTGCTGTGGAATGGGAGAGCAATGGCCAGCCTGAGAACAACTACAAGACCACACCTCCTGTGCTGGACTCTGATGGCTCA
TTCTTCCTGTACTCCAAGCTGACTGTGGACAAGTCCAGATGGCAGCAAGGCAATGTGTTCAGCTGCTCTGTGATGCATGAGGCCCTGCACAACCACTACACACAGAAGTCTCTGTCTCTGAGCCCTGGC
AAC***AGAAAGAGAAGGAGTGGCTCTGGGGCCACCAACTTCAGCCTGCTGAAACAGGCTGGGGATGTTGAAGAGAACCCTGGACCT***[illegible]
[illegible]
[illegible]
[illegible]
[illegible]
[illegible]
[illegible]AGCTTCAACAGGGGAGAGTGCAGC**TGA**AGATCT[illegible]**AG**
AGCCCCACTGTGTTCATCTTACAGATGGAAATACTGACATTCAGAGGAGTTAGTTAACTTGCCTAGGTGATTCAGCTAATAAGTGCAAGAAAGATTTCAATCCAAGGTGATTTGATTCTGAAGCCTGTG
CTAATCACATTACACCAAGCTACAACTTCATTTATAAATAATAAGTCAGCTTTCAAGGGCCTTTCAGGTGTCCTGCACTTCTACAAGCTGTGCCATTTAGTGAACACAAAATGAGCCTTCTGATGAAGTA
GTCTTTTCATTATTTCAGATATTAGAACACTAAAATTCTTAGCTGCCAGCTGATTGAAGGCTGGGACAAAATTCAAACATGCATCTACAACAATATATATCTCAATGTTAGTCTCCAAATTCTATTGACTTC
AACTCAAGAGAATATAAAGAGCTAGTCTTTATACACTCTTTAAGGTATGATATCATCTGGAAAGTAACAAAATTGATGCAAATTTGAATGAACTTTATCATGGTGTATTTACACAATGTGTTTCTTCTCCC
TGCAATGTATTTCTTTCTCTAATTCCTTCCATTTGATCTTTCATACACAATCTGGTTCTGATGTATGTTTTTGGATGCACTTTTCAACTCCAAAAGACAGAGCTAGTTACTTTCTTCCTGGTGCTCCAAGCA
CTGTATTTGTATCTGTATTCAAGCCCTTTGCAATATTGTACTGGATCATTATTTCACCTCTAGGATGGCTTCCCCAGGCAACTTGTGTTCACCCAGAGACTACATTTTGTATCTTGTTGACCTTTGAACTTCC
ACCAGTGTCTAAAAAATAATATGTATGCAAAATTACTTGCTATGAGAATGTATAATTAAACAATATAAAAAGGAGAAGCAAGGAGAGAAACACAGGTGTGTATTTGTGTTTGTGTGCTTAAAAGGCAGT
GTGGAAAAGGAAGAAATGCCATTTATAGTGAGGAGACAAAGTTATATTACCTCTTATCTGGCTTTTAAGGAGATTTTGCTGAGCTAAAAATCCTATATTCATAGAAAAGCCTTACCTGAGTTGCCAATA
CC**TCAATTCAG**TCTAGCAG[illegible]
[illegible]
[illegible]
[illegible]ACTAGTGGAGAAGAGCATGCTTGAGGGCTGAGTGCCCCTCAGTGGGCAGAGAGCACATGGCCCACAGTCC
CTGAGAAGTTGGGGGGAGGGGTGGGCAATTGAACTGGTGCCTAGAGAAGGTGGGGCTTGGGTAAACTGGGAAAGTGATGTGGTGTACTGGCTCCACCTTTTTCCCCAGGGTGGGGGAGAACCATA
TATAAGTGCAGTAGTCTCTGTGAACATTCAAGCTTCTGCCTTCTCCCTCCTGTGAGTTTGGTAAGTCACTGACTGTCTATGCCTGGGAAAGGGTGGGCAGGAGATGGGGCAGTGCAGGAAAAGTGGCA
CTATGAACCCTGCAGCCCTAGACAATTGTACTAACCTTCTTCTCTTTCCTCTCCTGACAGGTTGGTAACCAAGGCACCATGGGATGGTCCCTGATCCTGCTGTTTCTGGTGGCTGTGGCCACCAGAGTGC
TGTCTCAGGTTCAGCTGGTGCAGTCTGGGGCTGAAGTGAAGAAACCTGGGGCCTCTGTGAAGGTGTCCTGCAAGGCTTCTGGCTACACATTCACAGGCTACTACATGCACTGGGTCAGACAGGCCCCT
GGACAGGGACTTGAGTGGATGGGCAGAATCAACCCCAACAGTGGTGGCACCAACTATGCCCAGAAATTCCAGGGCAGAGTGACCATGACCAGAGACACCAGCATCAGCACAGCCTACATGGAACTG
AGCAGGCTTAGGAGTGATGACACTGCTGTGTACTACTGTGCCAGAGTGCCCTACTGCAGCAGCACCTCTTGTCACAGAGACTGGTACTTTGACCTGTGGGGCAGAGGCACCCTGGTCACAGTTAGCTC
TGCCAGCACAAAGGGCCCCTCTGTGTTTCCTCTGGCTCCCAGCAGCAAGAGCACCAGTGGTGGAACAGCTGCCCTGGGCTGTCTGGTCAAGGACTACTTTCCTGAGCCTGTGACAGTGTCCTGGAACT
CTGGGGCTCTGACATCTGGGGTGCACACATTCCCTGCTGTGCTGCAGTCCTCTGGCCTGTACAGCCTGTCCTCTGTGGTCACTGTGCCTAGCTCTAGCCTGGGCACCCAGACCTACATCTGCAATGTGAA
CCACAAGCCTAGCAACACCAAGGTGGACAAGAAGGCTGAGCCCAAGAGCTGTGATAAGACCCACACCTGTCCTCCATGTCCT[illegible]
[illegible]
[illegible]
[illegible]CCCAAGTGTATACCCTGCCCTCCTAGCAGAGATGAGCTGACCAAGAACCAGGTGTCCCTGACATGCCTGGTTAAGGGCTTCT
ACCCCTCTGACATTGCTGTGGAATGGGAGAGCAATGGCCAGCCTGAGAACAACTACAAGACCACACCTCCTGTGCTGGACTCTGATGGCTCATTCTTCCTGTACTCCAAGCTGACTGTGGACAAGTCCA
GATGGCAGCAAGGCAATGTGTTCAGCTGCTCTGTGATGCATGAGGCCCTGCACAACCACTACACACAGAAGTCTCTGTCTCTGAGCCCTGGCAAC***AGAAAGAGAAGGAGTGGCTCTGGGGCCACCA***
ACTTCAGCCTGCTGAAACAGGCTGGGGATGTTGAAGAGAACCCTGGACCT[illegible]
[illegible]
[illegible]
[illegible]
[illegible]
[illegible]
GCCCAGAGTGCACC**TGA**AGATCT[illegible]AGTCAATATGTTCACCCCAAAAAAGCTGTTTGTTAACTT
GTCAACCTCATTCTAAAATGTATATAGAAGCCCAAAAGACAATAACAAAAATATTCTTGTAGAACAAAATGGGAAAGAATGTTCCACTAAATATCAAGATTTAGAGCAAAGCATGAGATGTGTGGGGA
TAGACAGTGAGGCTGATAAAATAGAGTAGAGCTCAGAAACAGACCCATTGATATATGTAAGTGACCTATGAAAAAAATATGGCATTTTACAATGGGAAAATGATGGTCTTTTTCTTTTTTAGAAAAACA
GGGAAATATATTTATATGTAAAAAATAAAAGGGAACCCATATGTCATACCATACACACAAAAAAATTCCAGTGAATTATAAGTCTAAATGGAGAAGGCAAAACTTTAAATCTTTTAGAAAATAATATAG
AAGCATGCCATCAAGACTTCAGTGTAGAGAAAAATTTCTTATGACTCAAAGTCCTAACCACAAAGAAAAGATTGTTAATTAGATTGCATGAATATTAAGACTTATTTTTAAAATTAAAAAACCATTAAGA
AAAGTCAGGCCATAGAATGACAGAAAATATTTGCAACACCCCAGTAAAGAGAATTGTAATATGCAGATTATAAAAAGAAGTCTTACAAATCAGTAAAAAATAAAACTAGACAAAAATTTGAACAGATG
AAAGAGAAACTCTAAATAATCATTACACATGAGAAACTCAATCTCAGAAATCAGAGAACTATCATTGCATATACACTAAATTAGAGAAATATTAAAAGGCTAAGTAACATCTGTGGC**TTAATTAA**[illegible]
[illegible]**TCTAGT**GATCAGCAGTTCAACCTGTTGATAGTATGTACTAAGCTCTCATGTTTAATGTACTAAGCTCTCATGTTTAATGAACTAAACCCTCATGGCTAATGTACTAAGCTCTCATGGCTAATGTACTAA
GCTCTCATGTTTCATGTACTAAGCTCTCATGTTTGAACAATAAAATTAATATAAATCAGCAACTTAAATAGCCTCTAAGGTTTTAAGTTTTATAAGAAAAAAAAGAATATATAAGGCTTTTAAAGGTTTTA
AGGTTTCCTAGGTTATCC**TCATATGAGCTC**TTAGAAAAACTCATCCAGCATCAAATGAAACTGCAATTTATTCATATCAGGATTATCAATACCATATTTTTGAAAAAGTCTTTTCTGTAATGAAGGAGAAA
ACTCACCCAGGCAGTTCCATAGGATGGCAAGATCCTGGTATCTGTCTGCAATTCCAACTCTTCCAACATCAATACAACCTATTAATTTCCCCTCATCAAAAATAAGGTTATCAAGTGAGAAATCACCATG
AGTGACCACTGAATCTGGTGAGAATGGCAAAAGATTATGCATTTCTTTCCAGACTTGTTCAACAGGCCAGCCATTTCTCTCATCATCAAAATCACTGGCATCAACCAAACCATTATTCATTCTTGATTGGG
CCTGAGCCAGTCTAAATACTCTATCAGAGTTAAAAGGACAATTACAAACAGGAATGGAATGCAATCTTCTCAGGAACACTGCCAGGGCATCAACAATATTTTCACCTGAATCAGGATATTCTTCCAATA
CCTGGAATGCTGTTTTCCCTGGGATGGCAGTGGTGAGTAACCATGCATCATCAGGAGTTCTGATAAAATGCTTGATGGTTGGAAGAGGCATAAATTCAGTCAGCCAGTTTAGTCTGACCATCTCATCTG
TAACATCATTGGCAACAGAACCTTTGCCATGTTTCAGAAACAACTCTGGGGCATCTGGCTTCCCATACAATCTATAGATTGTGGCACCTGATTGCCCAACATTATCTCTAGCCCATTTATACCCATATAAA
TCAGCATCCATGTTGGAATTTAATCTTGGCCTGGAGCAAGAGGTTTCTCTTTGAATATGGCTCAT**ACATGTGCA**[illegible]
CAG

FIG. 15

072620 # 5A : 4A8- BV3 (SEQ ID NO:15)

DraIII-**βGlo** RI-NheI-hCMVAEP31126-BstEII-**4A8**-BglII-BAIpA-**IFNβ S/MAR**-BV3

CACTATGTGTTAATTAAAATTATCTCTAAGGCATGTGAACTGGCTGTCTTGGTTTTCATCTGTACTTCATCTGCTACCTCTGTGACCTGAAACATATTTATAATTCCA
TTAAGCTGTGCATATGATAGATTTATCATATGTATTTTCCTTAAAGGATTTTTGTAAGAACTAATTGAATTGATACCTGTAAAGTCTTTATCACACTACCCAATAAA
TAATAAATCTCTTTGTTCAGCTCTCTGTTTCTATAAATATGTACCAGTTTTATTGTTTTTAGTGGTAGTGATTTTATTCTCTTTCTATATATATACACACACATGTGTG
CATTCATAAATATATACAATTTTTATGAATAAAAAATTATTAGCAATCAATATTGAAAACCACTGATTTTTGTTTATGTGAGCAAACAGCAGATTAAAAGGAATTT
GAATTCTCATAGCTAGCAGGAATTAATTCAGAAACTCATTGAGATTTTGCATTAAATTAAAAATAAATTTTCTGTTTTCT
TAGCGGTGAGTCAAGACGAAACTCCATTGGAGCAAGTACATTCACTCAATAGGAACTTTCAATGGTTTTGCCAGTACATAAGCTCAATGGCAGTAA
GCCAATGCATTTTTCCATTACTGACATCTATACTGAGTGATAGAACTTTCAACTGCATTTTGCCAGTACATAAGCTCAATGGCAGTTAATGAACAGTAAA
ATCCATTGGAGCCAAGTGACTGAGTAATAGGAATTTCAATTGGATTTTGCCAGTACATAAGCTTAATTCAATGGCAGTTTTTCCTATTATTG
CTAGTGGAAGAGCATGCTTGAGGGCTGAGTGCCCCTCAGTGGGCAGAGAGCACATGGCCCACAGTCCCTGAGA
AGTTGGGGGGAGGGGTGGGCAATTGAACTGGTGCCTAGAGAAGGTGGGGCTTGGGTAAACTGGGAAAGTGATGTGGTGTACTGGCTCCACCTTTTTCCCCAG
GGTGGGGGAGAACCATATATAAGTGCAGTAGTCTCTGTGAACATTCAAGCTTCTGCCTTCTCCCTCCTGTGAGTTTGGTAAGTCACTGACTGTCTATGCCTGGGA
AAGGGTGGGCAGGAGATGGGGCAGTGCAGGAAAAGTGGCACTATGAACCCTGCAGCCCTAGACAATTGTACTAACCTTCTTCTCTTTCCTCTCCTGACAGGTTG
GTAACCAAGTCACTCATGAACTTTGGCCTGAGCCTGATCTTCCTGGTGCTGATCCTGAAAGGGGTGCAGTGTGAAGTGCAGCTGGTGGAATCTGGGGCTGAAGT
GAAGAAACCTGGGGCCTCTGTGAAGGTGTCCTGCAAAGTGTCTGGCTACACCCTGACAGAGCTGAGCATGCACTGGGTCAGACAGGCCCCTGGCAAAGGCTT
GAATGGATGGGAGGCTTTGACCCTGAGGATGGGGAGACTATGTATGCCCAGAAATTCCAGGGCAGAGTGACCATGACAGAGGACACCAGCACAGACACAGCC
TACATGGAACTGAGCAGCCTTAGGAGTGAAGATACAGCTGTGTACTACTGTGCCACCAGCACTGCTGTGGCTGGCACCCCTGACCTGTTTGACTACTACTATGG
CATGGATGTGTGGGGCCAGGGCACCACAGTGACAGTCAGCTCTGCTTCCACAAAGGGCCCCTCTGTGTTCCCTCTGGCTCCTAGCAGCAAGAGCACCAGTGGTG
GAACAGCTGCCCTGGGCTGTCTGGTCAAGGACTACTTTCCTGAGCCAGTGACTGTGTCCTGGAACAGTGGGGCTCTGACATCTGGGGTGCACACATTCCCTGCT
GTGCTCCAGTCCTCTGGCCTGTACAGCCTCTCCTCTGTGGTCACTGTGCCAAGCTCTAGCCTGGGCACCCAGACCTACATCTGCAATGTGAACCACAAGCCTAGC
AACACCAAGGTGGACAAGAAGGCTGAGCCCAAGAGCTGTGACAAGACCCACACCTGTCCTCCATGTCCTTGCCTCCAGAAGCTGACTTGGAGGGATCTTCTGTCTTTCT
GTTCCCTCCTAAAGTCTAAGTGATACCCTCATGTCTCAGCCAGTGACCCTGGAAGTGACTTGTGTGGTGGATGTGTCTCATGAGGATCCAGAAGTGAAGTTCAA
GGTACGTGGATGGTGTTGAGGTGCACAATGCCAAGACCAAGCCTAGAGAGGAACAGTACAACAGCACCTACAGAGTGGTGTCAGTGCTGACAGTCCTGCACC
AGGACTGGCTGAATGGCAAGGAGTACAAGTGCAAGGTCTCCAACAAAGCCCTGCCTACTCCTATTGAGAAAACCATCAGCAAGGCCAGCCTAGGG
AACCCCAAGTGTATACCCTGCCACCTAGCAGAGATGAGCTGACCAAGAACCAGGTGTCCCTGACATGCCTGGTTAAGGGCTTCTACCCCTCTGACATTGCTGTG
GAATGGGAGAGCAATGGCCAGCCTGAGAACAACTACAAGACAACCCCTCCTGTGCTGGACTCTGATGGCTCATTCTTCCTGTACTCCAAGCTCACAGTGGACAA
GTCCAGATGGCAGCAAGGGAAATGTGTTCAGCTGCTCTGTGATGCATGAGGCCCTGCACAACCACTACACACAGAAGTCCCTGTCTCTGAGCCCTGGCAAGAGAA
AGAGAAGGAGTGGCTCTGGGGCCACCAACTTCAGCCTGCTGAAACAGGCTGGGGATGTTGAAGAGAACCCTGGACCTATGGAGACTGCCGTCGTTTTACAACGTC
GACTGACTGTCTCACTGCACAGGCTCTTGTGACAGAGATTGTGATGACACAGAGCCCTCTGTCTAGCCCTGTGACACTGGGACAGCCTGCCAGCATCAGCTGTAGA
AGCTCTCAGAGTCTGGTGCATTCTGATGGCAACACCTACCTGAGCTGGCTGCAACAGAGGCCTGGACAGCCACCTAGACTGCTGATCTACAAGATCAGCAACAG
GTTCTCTGGGGTCCCAGACAGATTCTCTGGAAGTGGTGCTGGCACAGACTTCACTCTGAAGATTAGCAGAGTGGAAGCTGAGGATGTTGGGGTTTACTATTGC
ACCCAGGGCTACACAGTTCCCTTACACCTTTGGCCAGGGAACAAAAGTGGAATCAAGGGCACCAAACTGACTGTTGCTGGGGCCAGCCAAAGGCTGCCCCTTCTGT
GACTCTGTTTCCACCTAGCTCTGAGGAACTCCAGGCTAACAAGGCCACACTTGTGTGCCTGATCTCTGACTTCTACCCTGGGGCTGTGACAGTGGCCTGGAAGGC
TGATAGCAGCCCAGTGAAGGCTGGGGTTGAGACAACCACACCTAGCAAGCAGAGCAACAACAAATATGCTGCCAGCAGCTACCTGAGTCTGACCCCTGAGCAG
TGGAAGTCCCACAGAACCTACAGCTGCCAAGTGACCCATGAGGGCTCTACAGTGGAAAAGACTGTGGCCCCAACAGAGTGCAGCTGAAGATCTACTTCTAGCTA
ATAAAAGATCAGAGCTCTAGTGATCTGTGTGTTGGTTTTTTGTGTGTCTGCATTCTAGCAAGTCAATATGTTCACCCCAAAAAAGCTGTTTGTTAACTTGTCAACCTC
ATTCTAAAATGTATATAGAAGCCCAAAAGACAATAACAAAAATATTCTTGTAGAACAAAATGGGAAAGAATGTTCCACTAAATATCAAGATTTAGAGCAAAGCA
TGAGATGTGTGGGGATAGACAGTGAGGCTGATAAAATAGAGTAGAGCTCAGAAACAGACCCATTGATATATGTAAGTGACCTATGAAAAAAATATGGCATTTT
ACAATGGGAAAATGATGGTCTTTTTCTTTTTTAGAAAAACAGGGAAATATATTTATATGTAAAAAATAAAAGGGAACCCATATGTCATACCATACACACAAAAAA
ATTCCAGTGAATTATAAGTCTAAATGGAGAAGGCAAAACTTTAAATCTTTTAGAAAATAATATAGAAGCATGCCATCAAGACTTCAGTGTAGAGAAAAATTTCTT
ATGACTCAAAGTCCTAACCACAAAGAAAAGATTGTTAATTAGATTGCATGAATATTAAGACTTATTTTTAAAATTAAAAAACCATTAAGAAAAGTCAGGCCATAG
AATGACAGAAAATATTTGCAACACCCCAGTAAAGAGAATTGTAATATGCAGATTATAAAAAGAAGTCTTACAAATCAGTAAAAAATAAAACTAGACAAAAATTT
GAACAGATGAAAGAGAAACTCTAAATAATCATTACACATGAGAAACTCAATCTCAGAAATCAGAGAACTATCATTGCATATACACTAAATTAGAGAAATATTAA
AAGGCTAAGTAACATCTGTGGCTTAATTAATCTAGTCTAGTGATCAGCAGTTCAACCTGTTGATAGTATGTACTAAGCTCTCATGTTTAATGTACTAAGCTCTCA
TGTTTAATGAACTAAACCCTCATGGCTAATGTACTAAGCTCTCATGGCTAATGTACTAAGCTCTCATGTTTCATGTACTAAGCTCTCATGTTTGAACAATAAAATTA
ATATAAATCAGCAACTTAAATAGCCTCTAAGGTTTTAAGTTTTATAAGAAAAAAAAGAATATATAAGGCTTTTAAAGGTTTTAAGGTTTCCTAGGTTATCCTCATA
TGAGCTCTTAGAAAAACTCATCCAGCATCAAATGAAACTGCAATTTATTCATATCAGGATTATCAATACCATATTTTTGAAAAAGTCTTTTCTGTAATGAAGGAGA
AAACTCACCCAGGCAGTTCCATAGGATGGCAAGATCCTGGTATCTGTCTGCAATTCCAACTCTTCCAACATCAATACAACCTATTAATTTCCCCTCATCAAAAATA
AGGTTATCAAGTGAGAAATCACCATGAGTGACCACTGAATCTGGTGAGAATGGCAAAAGATTATGCATTTCTTTCCAGACTTGTTCAACAGGCCAGCCATTTCTC
TCATCATCAAAATCACTGGCATCAACCAAACCATTATTCATTCTTGATTGGGCCTGAGCCAGTCTAAATACTCTATCAGAGTTAAAAGGACAATTACAAACAGGA
ATGGAATGCAATCTTCTCAGGAACACTGCCAGGGCATCAACAATATTTTCACCTGAATCAGGATATTCTTCCAATACCTGGAATGCTGTTTTCCCTGGGATGGCA
GTGGTGAGTAACCATGCATCATCAGGAGTTCTGATAAAATGCTTGATGGTTGGAAGAGGCATAAATTCAGTCAGCCAGTTTAGTCTGACCATCTCATCTGTAACA
TCATTGGCAACAGAACCTTTGCCATGTTTCAGAAACAACTCTGGGGCATCTGGCTTCCCATACAATCTATAGATTGTGGCACCTGATTGCCCAACATTATCTCTAG
CCCATTTATACCCATATAAATCAGCATCCATGTTGGAATTTAATCTTGGCCTGGAGCAAGAGGTTTCTCTTTGAATATGGCTCATACATGTGCACCTCCTATAGTG
AGTTGTATTATACTATGCAGATATACATCCGATGCTTTAATTGTCAG

FIG. 16

081820 # 2 : 4A8- 4A8-BV3 (SEQ ID NO:16)

DraIII-βGlo BI-Nhe--AmCMV&EF1126-BstEII -4A8-BglII--Mxp--**21q21**-AmCMV-&EF1126-BstEII – 4A8-BglII--Mxp--IFNβ S/MAR-BV3

CACTATGTGTTAATTAAAATTATCTCTAAGGCATGTGAACTGGCTGTCTTGGTTTTCATCTGTACTTCATCTGCTACCTCTGTGACCTGAAACATATTTATAATTCCATTAAGCTGTGCATATGATAGATTT
ATCATATGTATTTTCCTTAAAGGATTTTTGTAAGAACTAATTGAATTGATACCTGTAAAGTCTTTATCACACTACCCAATAAATAATAAATCTCTTTGTTCAGCTCTCTGTTTCTATAAATATGTACCAGTTT
TATTGTTTTTAGTGGTAGTGATTTTATTCTCTTTCTATATATATACACACACATGTGTGCATTCATAAATATATACAATTTTTATGAATAAAAAATTATTAGCAATCAATATTGAAAACCACTGATTTTTGTT
TATGTGAGCAAACAGCAGATTAAAAGG**AATTT**GAATTC**TCATA**GCTAGCAG[illegible]
[illegible]
[illegible]ACTAGTGGAGAAGAGCATGCTTGAGGGCTGAGTGCC
CCTCAGTGGGCAGAGAGCACATGGCCCACAGTCCCTGAGAAGTTGGGGGGAGGGGTGGGCAATTGAACTGGTGCCTAGAGAAGGTGGGGCTTGGGTAAACTGGGAAAGTGATGTGGTGTACTGGC
TCCACCTTTTTCCCCAGGGTGGGGGAGAACCATATATAAGTGCAGTAGTCTCTGTGAACATTCAAGCTTCTGCCTTCTCCCTCCTGTGAGTTTGGTAAGTCACTGACTGTCTATGCCTGGGAAAGGGTG
GGCAGGAGATGGGGCAGTGCAGGAAAAGTGGCACTATGAACCCTGCAGCCCTAGACAATTGTACTAACCTTCTTCTCTTTCCTCTCCTGACAGGTTGGTAACC[illegible]ATGAACTTTGGCCTGAGC
CTGATCTTCCTGGTGCTGATCCTGAAAGGCGTGCAGTGTGAAGTGCAGCTGGTGGAATCTGGGGCTGAAGTGAAGAAACCTGGGGCCTCTGTGAAGGTGTCCTGCAAAGTGTCTGGCTACACCCTGA
CAGAGCTGAGCATGCACTGGGTCAGACAGGCCCCTGGCAAAGGCCTTGAATGGATGGGAGGCTTTGACCCTGAGGATGGGGAGACTATGTATGCCCAGAAATTCCAGGGCAGAGTGACCATGACAG
AGGACACCAGCACAGACACAGCCTACATGGAACTGAGCAGCCTTAGGAGTGAAGATACAGCTGTGTACTACTGTGCCACCAGCACTGCTGTGGCTGGCACCCCTGACCTGTTTGACTACTACTATGGC
ATGGATGTGTGGGGCCAGGGCACCACAGTGACAGTCAGCTCTGCCTTCCACAAAGGGCCCCTCTGTGTTCCCTCTGGCTCCTAGCAGCAAGAGCACCAGTGGTGGAACAGCTGCCCTGGGCTGTCTGGT
CAAGGACTACTTTCCTGAGCCAGTGACTGTGTCCTGGAACAGTGGGGCTCTGACATCTGGGGTGCACACATTCCCTGCTGTGCTCCAGTCCTCTGGCCTGTACAGCCTCTCCTCTGTGGTCACTGTGCCA
AGCTCTAGCCTGGGCACCCAGACCTACATCTGCAATGTGAACCACAAGCCTAGCAACACCAAGGTGGACAAGAAGGCTGAGCCCAAGAGCTGTGACAAGACCCACACCTGTCCTCCATGTCCT[illegible]
[illegible]
[illegible]
[illegible]CAGCCTAGGGAACCCCAAGTGTATACCCTGCCACCTAGCAGAGATGAGCTGAC
CAAGAACCAGGTGTCCCTGACATGCCTGGTTAAGGGCTTCTACCCCTCTGACATTGCTGTGGAATGGGAGAGCAATGGCCAGCCTGAGAACAACTACAAGACAACCCCTCCTGTGCTGGACTCTGATG
GCTCATTCTTCCTGTACTCCAAGCTCACAGTGGACAAGTCCAGATGGCAGCAAGGCAATGTGTTCAGCTGCTCTGTGATGCATGAGGCCCTGCACAACCACTACACACAGAAGTCCCTGTCTCTGAGCC
CTGGCAAG***AGAAAGAGAAGGAGTGGCTCTGGGGCCACCAACTTCAGCCTGCTGAAACAGGCTGGGGATGTTGAAGAGAACCCTGGACCT***[illegible]
[illegible]
[illegible]
[illegible]
[illegible]
[illegible]
CAAGTGAGCCATGAGGGCTCTACAGTGGAAAAGACTGTGGCCCCAACAGAGTGCAGC**TGA**AGATCT[illegible]
CTAG**AGAGCCCCACTGTGTTCATCTTACAGATGGAAATACTGACATTCAGAGGAGTTAGTTAACTTGCCTAGGTGATTCAGCTAATAAGTGCAAGAAAGATTTCAATCCAAGGTGATTTGATTCTGAA**
GCCTGTGCTAATCACATTACACCAAGCTACAACTTCATTTATAAATAATAAGTCAGCTTTCAAGGGCCTTTCAGGTGTCCTGCACTTCTACAAGCTGTGCCATTTAGTGAACACAAAATGAGCCTTCTGAT
GAAGTAGTCTTTTCATTATTTCAGATATTAGAACACTAAAATTCTTAGCTGCCAGCTGATTGAAGGCTGGGACAAAATTCAAACATGCATCTACAACAATATATATCTCAATGTTAGTCTCCAAATTCTAT
TGACTTCAACTCAAGAGAATATAAAGAGCTAGTCTTTATACACTCTTTAAGGTATGATATCATCTGGAAAGTAACAAAATTGATGCAAATTTGAATGAACTTTATCATGGTGTATTTACACAATGTGTTTC
TTCTCCCTGCAATGTATTTCTTTCTCTAATTCCTTCCATTTGATCTTTCATACACAATCTGGTTCTGATGTATGTTTTTTGGATGCACTTTTCAACTCCAAAAGACAGAGCTAGTTACTTTCTTCCTGGTGCTC
CAAGCACTGTATTTGTATCTGTATTCAAGCCCTTTGCAATATTGTACTGGATCATTATTTCACCTCTAGGATGGCTTCCCCAGGCAACTTGTGTTCACCCAGAGACTACATTTTGTATCTTGTTGACCTTTG
AACTTCCACCAGTGTCTAAAAATAATATGTATGCAAAATTACTTGCTATGAGAATGTATAATTAAACAATATAAAAAGGAGAAGCAAGGAGAGAAACACAGGTGTGTATTTGTGTTTGTGTGCTTAAAA
GGCAGTGTGGAAAAGGAAGAAATGCCATTTATAGTGAGGAGACAAAGTTATATTACCTCTTATCTGGCTTTTAAGGAGATTTTGCTGAGCTAAAAATCCTATATTCATAGAAAAGCCTTACCTGAGTTG
CCAATACCTCAATTCAGTCTAGCAG[illegible]
[illegible]
[illegible]
[illegible]ACTAGTGGAGAAGAGCATGCTTGAGGGCTGAGTGCCCCTCAGTGGGCAGAGAGCACATGGCCC
ACAGTCCCTGAGAAGTTGGGGGGAGGGGTGGGCAATTGAACTGGTGCCTAGAGAAGGTGGGGCTTGGGTAAACTGGGAAAGTGATGTGGTGTACTGGCTCCACCTTTTTCCCCAGGGTGGGGGAG
AACCATATATAAGTGCAGTAGTCTCTGTGAACATTCAAGCTTCTGCCTTCTCCCTCCTGTGAGTTTGGTAAGTCACTGACTGTCTATGCCTGGGAAAGGGTGGGCAGGAGATGGGGCAGTGCAGGAAA
AGTGGCACTATGAACCCTGCAGCCCTAGACAATTGTACTAACCTTCTTCTCTTTCCTCTCCTGACAGGTTGGTAACC[illegible]ATGAACTTTGGCCTGAGCCTGATCTTCCTGGTGCTGATCCTGAAA
GGCGTGCAGTGTGAAGTGCAGCTGGTGGAATCTGGGGCTGAAGTGAAGAAACCTGGGGCCTCTGTGAAGGTGTCCTGCAAAGTGTCTGGCTACACCCTGACAGAGCTGAGCATGCACTGGGTCAGA
CAGGCCCCTGGCAAAGGCCTTGAATGGATGGGAGGCTTTGACCCTGAGGATGGGGAGACTATGTATGCCCAGAAATTCCAGGGCAGAGTGACCATGACAGAGGACACCAGCACAGACACAGCCTAC
ATGGAACTGAGCAGCCTTAGGAGTGAAGATACAGCTGTGTACTACTGTGCCACCAGCACTGCTGTGGCTGGCACCCCTGACCTGTTTGACTACTACTATGGCATGGATGTGTGGGGCCAGGGCACCAC
AGTGACAGTCAGCTCTGCCTTCCACAAAGGGCCCCTCTGTGTTCCCTCTGGCTCCTAGCAGCAAGAGCACCAGTGGTGGAACAGCTGCCCTGGGCTGTCTGGTCAAGGACTACTTTCCTGAGCCAGTGA
CTGTGTCCTGGAACAGTGGGGCTCTGACATCTGGGGTGCACACATTCCCTGCTGTGCTCCAGTCCTCTGGCCTGTACAGCCTCTCCTCTGTGGTCACTGTGCCAAGCTCTAGCCTGGGCACCCAGACCTA
CATCTGCAATGTGAACCACAAGCCTAGCAACACCAAGGTGGACAAGAAGGCTGAGCCCAAGAGCTGTGACAAGACCCACACCTGTCCTCCATGTCCT[illegible]
[illegible]
[illegible]
AAGGCCCTGCCTGCTCCCATTGAAAAGACCATCAGCAAGGCCAAGGGCCAGCCTAGGGAACCCCAAGTGTATACCCTGCCACCTAGCAGAGATGAGCTGACCAAGAACCAGGTGTCCCTGACATGCCT
GGTTAAGGGCTTCTACCCCTCTGACATTGCTGTGGAATGGGAGAGCAATGGCCAGCCTGAGAACAACTACAAGACAACCCCTCCTGTGCTGGACTCTGATGGCTCATTCTTCCTGTACTCCAAGCTCAC
AGTGGACAAGTCCAGATGGCAGCAAGGCAATGTGTTCAGCTGCTCTGTGATGCATGAGGCCCTGCACAACCACTACACACAGAAGTCCCTGTCTCTGAGCCCTGGCAAG***AGAAAGAGAAGGAGTGG***
CTCTGGGGCCACCAACTTCAGCCTGCTGAAACAGGCTGGGGATGTTGAAGAGAACCCTGGACCT[illegible]
[illegible]
[illegible]
[illegible]
[illegible]
[illegible]
GCAAAACACTGTGGCCCCAACAGAGTGCAGC**TGA**AGATCT[illegible]**AGTCAATATGTTCACCCCAA**
AAAAGCTGTTTGTTAACTTGTCAACCTCATTCTAAAATGTATATAGAAGCCCAAAAGACAATAACAAAAATATTCTTGTAGAACAAAATGGGAAAGAATGTTCCACTAAATATCAAGATTTAGAGCAAA
GCATGAGATGTGTGGGGATAGACAGTGAGGCTGATAAAATAGAGTAGAGCTCAGAAACAGACCCATTGATATATGTAAGTGACCTATGAAAAAAATATGGCATTTTACAATGGGAAAATGATGGTCT
TTTTCTTTTTAGAAAAACAGGGAAATATATTTATATGTAAAAAATAAAAGGGAACCCATATGTCATACCATACACACAAAAAAATTCCAGTGAATTATAAGTCTAAATGGAGAAGGCAAAACTTTAAA
TCTTTTAGAAAATAATATAGAAGCATGCCATCAAGACTTCAGTGTAGAGAAAAATTTCTTATGACTCAAAGTCCTAACCACAAAGAAAAGATTGTTAATTAGATTGCATGAATATTAAGACTTATTTTTA
AAATTAAAAAACCATTAAGAAAAGTCAGGCCATAGAATGACAGAAAATATTTGCAACACCCCAGTAAAGAGAATTGTAATATGCAGATTATAAAAAGAAGTCTTACAAATCAGTAAAAAATAAAACTA
GACAAAAATTTGAACAGATGAAAGAGAAACTCTAAATAATCATTACACATGAGAAACTCAATCTCAGAAATCAGAGAACTATCATTGCATATACACTAAATTAGAGAAATATTAAAAGGCTAAGTAAC
ATCTGTGGCTTAATTAA[illegible]**TCTAGTGATCAGCAGTTCAACCTGTTGATAGTATGTACTAAGCTCTCATGTTTAATGTACTAAGCTCTCATGTTTAATGAACTAAACCCTCATGGCTAATGTACTAAG**
CTCTCATGGCTAATGTACTAAGCTCTCATGTTTCATGTACTAAGCTCTCATGTTTGAACAATAAAATTAATATAAATCAGCAACTTAAATAGCCTCTAAGGTTTTAAGTTTTATAAGAAAAAAAAGAATAT
ATAAGGCTTTTAAAGCTTTTAAGGTTTCCTAGGTTATCCTCATATGAGCTCTTAGAAAAACTCATCCAGCATCAAATGAAACTGCAATTTATTCATATCAGGATTATCAATACCATATTTTTGAAAAAGTC
TTTTCTGTAATGAAGGAGAAAACTCACCCAGGCAGTTCCATAGGATGGCAAGATCCTGGTATCTGTCTGCAATTCCAACTCTTCCAACATCAATACAACCTATTAATTTCCCCTCATCAAAAATAAGGTTA
TCAAGTGAGAAATCACCATGAGTGACCACTGAATCTGGTGAGAATGGCAAAAGATTATGCATTTCTTTCCAGACTTGTTCAACAGGCCAGCCATTTCTCTCATCATCAAAATCACTGGCATCAACCAAAC
CATTATTCATTCTTGATTGGGCCTGAGCCAGTCTAAATACTCTATCAGAGTTAAAAGGACAATTACAAACAGGAATGGAATGCAATCTTCTCAGGAACACTGCCAGGGCATCAACAATATTTTCACCTGA
ATCAGGATATTCTTCCAATACCTGGAATGCTGTTTTCCCTGGGATGGCAGTGGTGAGTAACCATGCATCATCAGGAGTTCTGATAAAATGCTTGATGGTTGGAAGAGGCATAAATTCAGTCAGCCAGTT
TAGTCTGACCATCTCATCTGTAACATCATTGGCAACAGAACCTTTGCCATGTTTCAGAAACAACTCTGGGGCATCTGGCTTCCCATACAATCTATAGATTGTGGCACCTGATTGCCCAACATTATCTCTAG
CCCATTTATACCCATATAAATCAGCATCCATGTTGGAATTTAATCTTGGCCTGGAGCAAGAGGTTTCTCTTTGAATATGGCTCATACATGTGCA[illegible]
[illegible]

FIG. 17

081820 # 3 : 4A8- B38Kappa-BV3 (SEQ ID NO:17)

DraIII-βGlo RI-NheI-SmCBA/EF1126-BsrEII -4A8-BglII-MluI-SmCBA/EF1126-BsrEII -- B38kappa-BglII-MluI-IFNβ S/MAR-BV3

CACTATGTGTTAATTAAAAATTATCTCTAAGGCATGTGAACTGGCTGTCTTGGTTTTCATCTGTACTTCATCTGCTACCTCTGTGACCTGAAACATATTTATAATTCCATTAAGCTGTGCATATGATAGATTT
ATCATATGTATTTTCCTTAAAGGATTTTTGTAAGAACTAATTGAATTGATACCTGTAAAGTCTTTATCACACTACCCAATAAATAATAAATCTCTTTGTTCAGCTCTCTGTTTCTATAAATATGTACCAGTTT
TATTGTTTTTAGTGGTAGTGATTTTATTCTCTTTCTATATATATACACACACATGTGTGCATTCATAAATATATACAATTTTTATGAATAAAAAATTATTAGCAATCAATATTGAAAACCACTGATTTTTGTT
TATGTGAGCAAACAGCAGATTAAAAGGAATTTGAATTCTCATAGCTAGCAG[illegible]

ACTAGTGGAGAAGAGCATGCTTGAGGGCTGAGTGCCCTCAGTGGGCAGAGAGCACATGGCCCACAGTCCCTGAGAAGTT
GGGGGCGAGGGGTGGGCAATTGAACTGGTGCTAGAGAAGCTGGGGCTTGGGTAAACTGCGAAAGTGATGTGTGTACTGGCTCCACCTTTTTCCCCAGGGTGTGTGGAGAACCATATATAACTGCA
GTAGTCTCTGTGAACATTCAAGCTTCTGCCTTCTCCCTCCTGTGAGTTTGCTAAGTCACTGACTGTCTATGCCTGGGAAAGGGTGCGGCAGGAGATGTGGGCAGTGCAGGAAAAGTGGCACTATGAACCC
TGCAGCCCTAGACAATTGTACTAACCTTCTTCTCTTTCCTCTCCTGACAGGTTGCTAACCCATGGGATGGTCCTGATCCTGCTGTTTCTGGTGGCTGTGGCCACCAGATGTCCTGTTCTGAACTT
GCAGCTGGTGGAAAGTGGTGGTGGCCTGGTTCAGCCTGGTGGCTCTCTGAGACTGAGCTGTGCTGCCTCTGGCTTCATTGTCTCCAGCAACTACATGAGCTGGGTCAGACAGGCCCCTGGCAAAGGA
CTGGAATGGGTGTCAGTGATCTACAGTGGTGGCAGCACCTACTATGCTGACTCTGTGAAGGGCAGATTCACCATCAGCAGACACAACAGCAAGAACACCCTGTACCTGCAGATGAACAGCCTGAGAG
CTGAGGACACTGCTGTGTACTACTGTGCCAGAGAAGCCTATGGCAATGGATGTGTGGGGCCAGGGCACAACAGTGACTGTCTCCTCTGCCAGCACAAAGGGCCCATCTGTCTTTCCTCTGGCTCCCAGC
AGCAAGAGCACCAGTGGTGCAACAGCTGCCCTGGGCTGTCTGGTCAAGGACTACTTTCCTGAGCCTGTGACAGTGTCCTGGAACTCTGGGGCTCTGACATCTGGGGTGCACACATTCCCTGCAGTGCT
GCAGTCCTCTGGCCTGTACAGCCTGTCCTCTGTGGTCACAGTGCCCTAGCTCTAGCCTGGGCACCCAGACCTACATCTGCAATGTGAACCACAAGCCTAGCAACACCAAGGTGGACAAGAAGGCTGAGC
CCAAGAGCTGTGACAAGACCCACACCTGTCCTCCATGTCCT[illegible]

AGAGCCCAAGAGCTGTGACAAGACCCACACCTGTCCTCCATGTCCT

AGAAAGAGAAGGAGTGGCTCTGGGGCCACCAACTTCAGCCTGCTGAAACAGGCTGGGGATGTTGAAGAGAACCCTGGACCT

GAGCCCAAGAGCTGTGACAAGACCCACACCTGTCCTCCATGTCCT

GCTCTCATGTTTAATGAACTAAACCCTCATGGCTAATGTACTAAGCTCTCATGGCTAATGTACTAAGCTCTCATGTTTCATGTACTAAGCTCTCATGTTTGAACAATAAAATTAATATAAATCAGCAACTT
AAATAGCCTCTAAGGTTTTAAGTTTTATAAGAAAAAAAAGAATATATAAGGCTTTTAAAGGTTTTAAGGTTTCCTAGGTTATCCTCATATGAGCTCTTAGAAAAACTCATCCAGCATCAAATGAAACTGC
AATTTATTCATATCAGGATTATCAATACCATATTTTTGAAAAAGTCTTTTCTGTAATGAAGGAGAAAACTCACCCAGGCAGTTCCATAGGATGGCAAGATCCTGGTATCTGTCTGCCAATTCCAACTCTTCC
AACATCAATACAACCTATTAATTTCCCCTCGTCAAAAATAAGGTTATCAAGTGAGAAATCACCATGAGTGACCACTGAATCTGGTGAGAATGGCAAAAGATTATGCATTTCTTTCCAGACTTGTTCAACA
GGCCAGCCATTTCTCTCATCATCAAAATCACTGGCATCAACCAAACCATTATTCATTCTTGATTGGGCCTGAGCCAGTCTAAATACTCTATCAGAGTTAAAAGGACAATTACAAACAGGAATGGAATGCA
ATCTTCTCAGGAACACTGCCAGGGCATCAACAATATTTTCACCTGAATCAGGATATTCTTCCAATACCTGGAATGCTGTTTTCCCTGGGATGGCAGTGGTGAGTAACCATGCATCATCAGGAGTTCTGAT
AAAATGCTTGATGGTTGGAAGAGGCATAAATTCAGTCAGCCAGTTTAGTCTGACCATCTCATCTGTAACATCATTGGCAACAGAACCTTTGCCATGTTTCAGAAACAACTCTGGGGCATCTGGCTTCCCA
TACAATCTATAGATTGTGGCACCTGATTGCCCAACATTATCTCTAGCCCATTTATACCCATATAAATCAGCATCCATGTTGGAATTTAATCTTGGCCTGGAGCAAGAGGTTTCTCTTTGAATATGGCTCAT
ACATGTGCA[illegible]

FIG. 18

081820 # 4 : 4A8- H4-BV3 (SEQ ID NO:18)

DraIII-βGlo BI-Nhe--AmCMV&EF1I126-BstEII -4A8-BglII-Mxp--AmCMV&EF1I126-BstEII – H4-BglII-Mxp--IFNβ S/MAR-BV3

CACTATGTGTTAATTAAAATTATCTCTAAGGCATGTGAACTGGCTGTCTTGGTTTTCATCTGTACTTCATCTGCTACCTCTGTGACCTGAAACATATTTATAATTCCATTAAGCTGTGCATATGATAGATTT
ATCATATGTATTTTCCTTAAAGGATTTTTGTAAGAACTAATTGAATTGATACCTGTAAAGTCTTTATCACACTACCCAATAAATAATAAATCTCTTTGTTCAGCTCTCTGTTTCTATAAATATGTACCAGTTT
TATTGTTTTTAGTGGTAGTGATTTTATTCTCTTTCTATATATATACACACACATGTGTGCATTCATAAATATATACAATTTTTATGAATAAAAAATTATTAGCAATCAATATTGAAAACCACTGATTTTTGTT
TATGTGAGCAAACAGCAGATTAAAAGG**AATTT**GAATTC**TCATA**GCTAGCAG[illegible]
[illegible]
[illegible]
[illegible]ACTACTGGAGAAGACACCATGCTTGAGGGCTGACTGCC
CCTCAGTGGGCAGAGAGCACATGGCCCACAGTCCCTGAGAAGTTGGGGGGAGGGGTGGGCAATTGAACTGGTGCCTAGAGAAGGTGGGGCTTGGGTAAACTGGGAAAGTGATGTGGTGTACTGGC
TCCACCTTTTTCCCCAGGGTGGGGGAGAACCATATATAAGTGCAGTAGTCTCTGTGAACATTCAAGCTTCTGCCTTCTCCCTCCTGTGAGTTTGGTAAGTCACTGACTGTCTATGCCTGGGAAAGGGTG
GGCAGGAGATGGGGCAGTGCAGGAAAAGTGGCACTATGAACCCTGCAGCCCTAGACAATTGTACTAACCTTCTTCTCTTTCCTCTCCTGACAGGTTGGTAACC[illegible]ATGAACTTGGCCTGAGC
CTGATCTTCCTGGTGCCTGATCCTGAAAGGGCCTGCAGTGTGAAGTGCAGCTGGTGGAATCTGGGGCTGAAGTGAAGAAACCTGGGGCCTCTGTGAAGGTGTCCTGCAAAGTGTCTGGCTACACCCTGA
CAGAGCTGAGCATGCACTGGGTCAGACAGGCCCCTGGCAAAGGCCTTGAATGGATGGGAGGCTTTGACCCTGAGGATGGGGAGACTATGTATGCCCAGAAATTCCAGGGCAGAGTGACCATGACAG
AGGACACCAGCACAGACACAGCCTACATGGAACTGAGCAGCCTTAGGAGTGAAGATACAGCTGTGTACTACTGTGCCACCAGCACTGCTGTGGCTGGCACCCCTGACCTGTTTGACTACTACTATGGC
ATGGATGTGTGGGGCCAGGGCACCACAGTGACAGTCAGCTCTGCCTCCACAAAGGGCCCCTCTGTGTTCCCTCTGGCCTCCTAGCAGCAAGAGCACCAGTGGTGGAACAGCTGCCCTGGGCTGTCTGGT
CAAGGACTACTTTCCTGAGCCAGTGACTGTGTCCTGGAACAGTGGGGCTCTGACATCTGGGGTGCACACATTCCCTGCTGTGCTCCAGTCCTCTGGCCTGTACAGCCTCTCCTCTGTGGTCACTGTGCCA
AGCTCTAGCCTGGGCACCCAGACCTACATCTGCAATGTGAACCACAAGCCTAGCAACACCAAGGTGGACAAGAAGGCTGAGCCCAAGAGCTGTGACAAGACCCACACCTGTCCTCCATGTCCT[illegible]
[illegible]
[illegible]
[illegible]AGGGCCAGCCTAGGGAACCCCAAGTGTATACCCTGCCACCTAGCAGACATGAGCTGAC
CAAGAACCAGGTGTCCCTGACATGCCTGGTTAAGGGCTTCTACCCCTCTGACATTGCTGTGGAATGGGAGAGCAATGGCCAGCCTGAGAACAACTACAAGACAACCCCTCCTGTGCTGGACTCTGATG
GCTCATTCTTCCTGTACTCCAAGCTCACAGTGGACAAGTCCAGATGGCAGCAAGGCAATGTGTTCAGCTGCTCTGTGATGCATGAGGCCCTGCACAACCACTACACACAGAAGTCCCTGTCTCTGAGCC
CTGGCAAG*AGAAAGAGAAGGAGTGGCTCTGGGGCCACCAACTTCAGCCTGCTGAAACAGGCTGGGGATGTTGAAGAGAACCCTGGACCT*[illegible]
[illegible]
[illegible]
[illegible]
[illegible]
[illegible]
CAAGTGAGCCATGAGGGCCTCTACAGTGGAAAAGACTGTGGCCCCAACAGAGTGCAGC**TGA**AGATCT[illegible]
[illegible]
[illegible]
[illegible]
[illegible]ACTAGTGGAGAAGAGCATGCTTGAGGGCTGAGTGCCCCTCAGTGGGCAGAGAGCACATGGCCCACAGTCCCTGAGAAGTT
GGGGGGAGGGGTGGGCAATTGAACTGGTGCCTAGAGAAGGTGGGGCTTGGGTAAACTGGGAAAGTGATGTGGTGTACTGGCTCCACCTTTTTCCCCAGGGTGGGGGAGAACCATATATAAGTGCA
GTAGTCTCTGTGAACATTCAAGCTTCTGCCTTCTCCCTCCTGTGAGTTTGGTAAGTCACTGACTGTCTATGCCTGGGAAAGGGTGGGCAGGAGATGGGGCAGTGCAGGAAAAGTGGCACTATGAACCC
TGCAGCCCTAGACAATTGTACTAACCTTCTTCTCTTTCCTCTCCTGACAGGTTGGTAACC[illegible]ATGGGATGGTCCTGATCCTGCTGTTTCTGGTGGCTCTGGCCCACCAGAGTGCCTGTCTCAGGT
TCAGCTGGTGCAGTCTGGGGCTGAAGTGAAGAAACCTGGGGCCTCTGTGAAGGTGTCCTGCAAGGCTTCTGGCTACACATTCACAGGCTACTACATGCACTGGGTCAGACAGGCCCCTGGACAGGGA
CTTGAGTGGATGGGCAGAATCAACCCCAACAGTGGTGGCACCAACTATGCCCAGAAATTCCAGGGCAGAGTGACCATGACCAGAGACACCAGCATCAGCACAGCCTACATGGAACTGAGCAGGCTTA
GGAGTGATGACACTGCTGTGTACTACTGTGCCAGAGTGCCCTACTGCAGCAGCACCTCTTGTCACAGAGACTGGTACTTTGACCTCTGGGGCAGAGGCACCCTGGTCACAGTTAGCTCTGCCAGCACA
AAGGGCCCCTCTGTGTTCCCTCTGGCTCCCAGCAGCAAGAGCACCAGTGGTGGAACAGCTGCCCTGGGCTGTCTGGTCAAGGACTACTTTCCTGAGCCTGTGACAGTGTCCTGGAACTCTGGGGCTCT
GACATCTGGGGTGCACACATTCCCTGCTGTGCTGCAGTCCTCTGGCCTGTACAGCCTGTCCTCTGTGGTCACTGTGCCTAGCTCTAGCCTGGGCACCCAGACCTACATCTGCAATGTGAACCACAAGCCT
AGCAACACCAAGGTGGACAAGAAGGCTGAGCCCAAGAGCTGTGATAAGACCCACACCTGTCCTCCATGTCCT[illegible]
[illegible]
[illegible]
[illegible]AGCCCAGCCTAGGGAACCCCAAGTGTATACCCTGCCTCCTAGCAGAGATGAGCTGACCAAGAACCAGGTGTCCCTGACATGCCTGGTTAAGGGCTTCTACCCCTCTGAC
ATTGCTGTGGAATGGGAGAGCAATGGCCAGCCTGAGAACAACTACAAGACCACACCTCCTGTGCTGGACTCTGATGGCTCATTCTTCCTGTACTCCAAGCTGACTGTGGACAAGTCCAGATGGCAGCA
AGGCAATGTGTTCAGCTGCTCTGTGATGCATGAGGCCCTGCACAACCACTACACACAGAAGTCTCTGTCTCTGAGCCCTGGCAAG*AGAAAGAGAAGGAGTGGCTCTGGGGCCACCAACTTCAGCCTG*
CTGAAACAGGCTGGGGATGTTGAAGAGAACCCTGGACCT[illegible]
[illegible]
[illegible]
[illegible]
[illegible]
[illegible]
CAGC**TGA**AGATCT[illegible]AGTCAATATGTTCACCCCAAAAAAGCTGTTTGTTAACTTGTCAACCTCA
TTCTAAAATGTATATAGAAGCCCAAAAGACAATAACAAAAATATTCTTGTAGAACAAAATGGGAAAGAATGTTCCACTAAATATCAAGATTTAGAGCAAAGCATGAGATGTGTGGGGATAGACAGTG
AGGCTGATAAAATAGAGTAGAGCTCAGAAACAGACCCATTGATATATGTAAGTGACCTATGAAAAAAATATGGCATTTTACAATGGGAAAATGATGGTCTTTTTCTTTTTTAGAAAAACAGGGAAATAT
ATTTATATGTAAAAAATAAAAGGGAACCCATATGTCATACCATACACACAAAAAAATTCCAGTGAATTATAAGTCTAAATGGAGAAGGCAAAACTTTAAATCTTTTAGAAAATAATATAGAAGCATGCC
ATCAAGACTTCAGTGTAGAGAAAAATTTCTTATGACTCAAAGTCCTAACCACAAAGAAAAGATTGTTAATTAGATTGCATGAATATTAAGACTTATTTTTAAAATTAAAAAACCATTAAGAAAAGTCAGG
CCATAGAATGACAGAAAATATTTGCAACACCCCAGTAAAGAGAATTGTAATATGCAGATTATAAAAAGAAGTCTTACAAATCAGTAAAAAATAAAACTAGACAAAAATTTGAACAGATGAAAGAGAAA
CTCTAAATAATCATTACACATGAGAAACTCAATCTCAGAAATCAGAGAACTATCATTGCATATACACTAAATTAGAGAAATATTAAAAGGCTAAGTAACATCTGTGGC**TTAATTAA**[illegible]**TCTAGT**GA
TCAGCAGTTCAACCTGTTGATAGTATGTACTAAGCTCTCATGTTTAATGTACTAAGCTCTCATGTTTAATGAACTAAACCCTCATGGCTAATGTACTAAGCTCTCATGGCTAATGTACTAAGCTCTCATGT
TTCATGTACTAAGCTCTCATGTTTGAACAATAAAATTAATATAAATCAGCAACTTAAATAGCCTCTAAGGTTTTAAGTTTTATAAGAAAAAAAAGAATATATAAGGCTTTTAAAGGTTTTAAGGTTTCCTA
GGTTATCC**TCATATGAGCTC**TTAGAAAAACTCATCCAGCATCAAATGAAACTGCAATTTATTCATATCAGGATTATCAATACCATATTTTTGAAAAAGTCTTTCTGTAATGAAGGAGAAAACTCACCCAG
GCAGTTCCATAGGATGGCAAGATCCTGGTATCTGTCTGCAATTCCAACTCTTCCAACATCAATACAACCTATTAATTTCCCCTCATCAAAAATAAGGTTATCAAGTGAGAAATCACCATGAGTGACCACT
GAATCTGGTGAGAATGGCAAAAGATTATGCATTTCTTTCCAGACTTGTTCAACAGGCCAGCCATTTCTCTCATCATCAAAATCACTGGCATCAACCAAACCATTATTCATTCTTGATTGGGCCTGAGCCA
GTCTAAATACTCTATCAGAGTTAAAAGGACAATTACAAACAGGAATGGAATGCAATCTTCTCAGGAACACTGCCAGGGCATCAACAATATTTTCACCTGAATCAGGATATTCTTCCAATACCTGGAATG
CTGTTTTCCCTGGGATGGCAGTGGTGAGTAACCATGCATCATCAGGAGTTCTGATAAAATGCTTGATGGTTGGAAGAGGCATAAATTCAGTCAGCCAGTTTAGTCTGACCATCTCATCTGTAACATCAT
TGGCAACAGAACCTTTGCCATGTTTCAGAAACAACTCTGGGGCATCTGGCTTCCCATACAATCTATAGATTGTGGCACCTGATTGCCCAACATTATCTCTAGCCCATTTATACCCATATAAATCAGCATCC
ATGTTGGAATTTAATCTTGGCCTGGAGCAAGAGGTTTCTCTTTGAATATGGCTCAT**ACATGTGCA**[illegible]

FIG. 19

081820 # 5 : 4A8- shACE2-BV3 (SEQ ID NO:19)

DraIII-βGlo BI-Nhe--AmCMV&EF1I126-BstEII -4A8-BglII-Mlxp--AmCMV&EF1I126-BstEII – shACE2-BglII-MlxpA-IFNβ S/MAR-BV3

CACTATGTGTTAATTAAAATTATCTCTAAGGCATGTGAACTGGCTGTCTTGGTTTTCATCTGTACTTCATCTGCTACCTCTGTGACCTGAAACATATTTATAATTCCATTAAGCTGTGCATATGATAGATTT
ATCATATGTATTTTCCTTAAAGGATTTTTGTAAGAACTAATTGAATTGATACCTGTAAAGTCTTTATCACACTACCCAATAAATAATAAATCTCTTTGTTCAGCTCTCTGTTTCTATAAATATGTACCAGTTT
TATTGTTTTTAGTGGTAGTGATTTTATTCTCTTTCTATATATATACACACACATGTGTGCATTCATAAATATATACAATTTTTATGAATAAAAAATTATTAGCAATCAATATTGAAAACCACTGATTTTTGTT
TATGTGAGCAAACAGCAGATTAAAAGG**AATTT**GAATTC**TCATA**GCTAGCAG[illegible]
[illegible]
[illegible]
[illegible]ACTACTGGCAGAAGACCATGCTTGAGGGCTGACTGCC
CCTCAGTGGGCAGAGAGCACATGGCCCACAGTCCCTGAGAAGTTGGGGGGAGGGGTGGGCAATTGAACTGGTGCCTAGAGAAGGTGGGGCTTGGGTAAACTGGGAAAGTGATGTGGTGTACTGGC
TCCACCTTTTTCCCCAGGGTGGGGGAGAACCATATATAAGTGCAGTAGTCTCTGTGAACATTCAAGCTTCTGCCTTCTCCCTCCTGTGAGTTTGGTAAGTCACTGACTGTCTATGCCTGGGAAAGGGTG
GGCAGGAGATGGGGCAGTGCAGGAAAAGTGGCACTATGAACCCTGCAGCCCTAGACAATTGTACTAACCTTCTTCTCTTTCCTCTCCTGACAGGTTGGTAACC[illegible]ATGAACTTGGCCTGAGC
CTGATCTTCCTGGTGCCTGATCCTGAAAGGGCCTGCAGTGTGAAGTGCAGCTGGTGGAATCTGGGGCTGAAGTGAAGAAACCTGGGGCCTCTGTGAAGGTGTCCTGCAAAGTGTCTGGCTACACCCTGA
CAGAGCTGAGCATGCACTGGGTCAGACAGGCCCCTGGCAAAGGCCTTGAATGGATGGGAGGCTTTGACCCTGAGGATGGGGAGACTATGTATGCCCAGAAATTCCAGGGCAGAGTGACCATGACAG
AGGACACCAGCACAGACACAGCCTACATGGAACTGAGCAGCCTTAGGAGTGAAGATACAGCTGTGTACTACTGTGCCACCAGCACTGCTGTGGCTGGCACCCCTGACCTGTTTGACTACTACTATGGC
ATGGATGTGTGGGGCCAGGGCACCACAGTGACAGTCAGCTCTGCCTCCACAAAGGGCCCCTCTGTGTTCCCTCTGGCTCCTAGCAGCAAGAGCACCAGTGGTGGAACAGCTGCCCTGGGCTGTCTGGT
CAAGGACTACTTTCCTGAGCCAGTGACTGTGTCCTGGAACAGTGGGGCTCTGACATCTGGGGTGCACACATTCCCTGCTGTGCTCCAGTCCTCTGGCCTGTACAGCCTCTCCTCTGTGGTCACTGTGCCA
AGCTCTAGCCTGGGCACCCAGACCTACATCTGCAATGTGAACCACAAGCCTAGCAACACCAAGGTGGACAAGAAGCCTGAGCCCAAGAGCTGTGACAAGACCCACACCTGTCCTCCATGTCCT[illegible]
[illegible]
[illegible]
[illegible]AGGGCCAGCCTAGGGAACCCCAAGTGTATACCCTGCCACCTAGCAGACATGAGCTGAC
CAAGAACCAGGTGTCCCTGACATGCCTGGTTAAGGGCTTCTACCCCTCTGACATTGCTGTGGAATGGGAGAGCAATGGCCAGCCTGAGAACAACTACAAGACAACCCCTCCTGTGCTGGACTCTGATG
GCTCATTCTTCCTGTACTCCAAGCTCACAGTGGACAAGTCCAGATGGCAGCAAGGCAATGTGTTCAGCTGCTCTGTGATGCATGAGGCCCTGCACAACCACTACACACAGAAGTCCCTGTCTCTGAGCC
CTGGCAAG***AGAAAGAGAAGGAGTGGCTCTGGGGCCACCAACTTCAGCCTGCTGAAACAGGCTGGGGATGTTGAAGAGAACCCTGGACCT***[illegible]
[illegible]
[illegible]
[illegible]
[illegible]
CAAGTGAGCCATGAGGGCCTCTACAGTGGAAAAGACTGTGGCCCCAACAGAGTGCACC**TGA**AGATCTACT[illegible]
[illegible]
[illegible]
[illegible]
[illegible]ACTAGTGGAGAAGAGCATGCTTGAGGGCTGAGTGCCCCTCAGTGGGCAGAGAGCACATGGCCCACAGTCCCTGAGAAGTT
GGGGGGAGGGGTGGGCAATTGAACTGGTGCCTAGAGAAGGTGGGGCTTGGGTAAACTGGGAAAGTGATGTGGTGTACTGGCTCCACCTTTTTCCCCAGGGTGGGGGAGAACCATATATAAGTGCA
GTAGTCTCTGTGAACATTCAAGCTTCTGCCTTCTCCCTCCTGTGAGTTTGGTAAGTCACTGACTGTCTATGCCTGGGAAAGGGTGGGCAGGAGATGGGGCAGTGCAGGAAAAGTGGCACTATGAACCC
TGCAGCCCTAGACAATTGTACTAACCTTCTTCTCTTTCCTCTCCTGACAGGTTGGTAACC[illegible]
[illegible]
[illegible]
[illegible]
[illegible]
[illegible]
[illegible]
[illegible]
[illegible]
[illegible]
[illegible]
[illegible]
[illegible]
[illegible]
[illegible]**TAA**AGATCTAC
[illegible]AGTCAATATGTTCACCCCAAAAAAGCTGTTTGTTAACTTGTCAACCTCATTCTAAAATGTATAT
AGAAGCCCAAAAGACAATAACAAAAATATTCTTGTAGAACAAAATGGGAAAGAATGTTCCACTAAATATCAAGATTTAGAGCAAAGCATGAGATGTGTGGGGATAGACAGTGAGGCTGATAAAATAG
AGTAGAGCTCAGAAACAGACCCATTGATATATGTAAGTGACCTATGAAAAAAATATGGCATTTTACAATGGGAAAATGATGGTCTTTTTCTTTTTTAGAAAAACAGGGAAATATATTTATATGTAAAAA
ATAAAAGGGAACCCATATGTCATACCATACACACAAAAAAATTCCAGTGAATTATAAGTCTAAATGGAGAAGGCAAAACTTTAAATCTTTTAGAAAATAATATAGAAGCATGCCATCAAGACTTCAGTG
TAGAGAAAAATTTCTTATGACTCAAAGTCCTAACCACAAAGAAAAGATTGTTAATTAGATTGCATGAATATTAAGACTTATTTTTAAAATTAAAAAACCATTAAGAAAAGTCAGGCCATAGAATGACAG
AAAATATTTGCAACACCCCAGTAAAGAGAATTGTAATATGCAGATTATAAAAAGAAGTCTTACAAATCAGTAAAAAATAAAACTAGACAAAAATTTGAACAGATGAAAGAGAAACTCTAAATAATCAT
TACACATGAGAAACTCAATCTCAGAAATCAGAGAACTATCATTGCATATACACTAAATTAGAGAAATATTAAAAGGCTAAGTAACATCTGTGGC**TTAATTAA**[illegible]**TCTAGT**GATCAGCAGTTCAACC
TGTTGATAGTATGTACTAAGCTCTCATGTTTAATGTACTAAGCTCTCATGTTTAATGAACTAAACCCTCATGGCTAATGTACTAAGCTCTCATGGCTAATGTACTAAGCTCTCATGTTTCATGTACTAAGCT
CTCATGTTTGAACAATAAAATTAATATAAATCAGCAACTTAAATAGCCTCTAAGGTTTTAAGTTTTATAAGAAAAAAAAGAATATATAAGGCTTTTAAAGGTTTTAAGGTTTCCTAGGTTATCC**TCATATG**
AGCTCTTAGAAAAACTCATCCAGCATCAAATGAAACTGCAATTTATTCATATCAGGATTATCAATACCATATTTTTGAAAAAGTCTTTTCTGTAATGAAGGAGAAAACTCACCCAGGCAGTTCCATAGGA
TGGCAAGATCCTGGTATCTGTCTGCAATTCCAACTCTTCCAACATCAATACAACCTATTAATTTCCCCTCATCAAAAATAAGGTTATCAAGTGAGAAATCACCATGAGTGACCACTGAATCTGGTGAGAA
TGGCAAAAGATTATGCATTTCTTTCCAGACTTGTTCAACAGGCCAGCCATTTCTCTCATCATCAAAATCACTGGCATCAACCAAACCATTATTCATTCTTGATTGGGCCTGAGCCAGTCTAAATACTCTATC
AGAGTTAAAAGGACAATTACAAACAGGAATGGAATGCAATCTTCTCAGGAACACTGCCAGGGCATCAACAATATTTTCACCTGAATCAGGATATTCTTCCAATACCTGGAATGCTGTTTTCCCTGGGAT
GGCAGTGGTGAGTAACCATGCATCATCAGGAGTTCTGATAAAATGCTTGATGGTTGGAAGAGGCATAAATTCAGTCAGCCAGTTTAGTCTGACCATCTCATCTGTAACATCATTGGCAACAGAACCTTT
GCCATGTTTCAGAAACAACTCTGGGGCATCTGGCTTCCCATACAATCTATAGATTGTGGCACCTGATTGCCCAACATTATCTCTAGCCCATTTATACCCATATAAATCAGCATCCATGTTGGAATTTAATC
TTGGCCTGGAGCAAGAGGTTTCTCTTTGAATATGGCTCAT**ACATGTGCA**[illegible]

FIG. 20

080420 # 3 : shACE2- BV3 (SEQ ID NO:20)

DraIII-**βGlo** III-NheI-~~CMVAEP3I126~~-BstEII-**shACE2**-BglII-~~MfeI~~-**IFNβ S/MAR**-BV3

CACTATGTGTTAATTAAAATTATCTCTAAGGCATGTGAACTGGCTGTCTTGGTTTTCATCTGTACTTCATCTGCTACCTCTGTGACCTGAAACATATTTATAATTCCA
TTAAGCTGTGCATATGATAGATTTATCATATGTATTTTCCTTAAAGGATTTTTGTAAGAACTAATTGAATTGATACCTGTAAAGTCTTTATCACACTACCCAATAAA
TAATAAATCTCTTTGTTCAGCTCTCTGTTTCTATAAATATGTACCAGTTTTATTGTTTTTAGTGGTAGTGATTTTATTCTCTTTCTATATATATACACACACATGTGTG
CATTCATAAATATATACAATTTTTATGAATAAAAAATTATTAGCAATCAATATTGAAAACCACTGATTTTTGTTTATGTGAGCAAACAGCAGATTAAAAGGAATTT
GAATTCTCATAGCTAGCAGGAATTAATGCAAACCCATTGAACTAATAGCTCTGATTAACACAATTTCCTTGGTTTTGTTAATACATAAAGTCAA
TAGCGGTGAGTCAAGCAGAACTCCATTGGGGCAAGTCATTCATCAATGGGACTTTCCAATGGTTTTGCCAGTACATAAGCTCAATGGCACTTAA
GTCGACTGCATTTTTCCATTACTGACATCTATACTGAGTGATACGAACTTTCAACTGCATTTTGCCACGTACATAAGTCAATGGCATTGAATGACAGGAAA
ATTCTCATTGGAGCCACAGTGACTGAGTTAATAGGAATTTCATTGGATTTTGCTCAGTACATAAACGTTAATGGGAGTTGCTACTGGTTTTTCCTATTATTG
CTAGCAACAATAAGCTCAATAGCCTCTAGACTAGTGGAGAAGAGCATGCTTGAGGGCTGAGTGCCCCTCAGTGGGCAGAGAGCACATGGCCCACAGTCCCTGAGA
AGTTGGGGGGAGGGGTGGGCAATTGAACTGGTGCCTAGAGAAGGTGGGGCTTGGGTAAACTGGGAAAGTGATGTGGTGTACTGGCTCCACCTTTTTCCCCAG
GGTGGGGGAGAACCATATATAAGTGCAGTAGTCTCTGTGAACATTCAAGCTTCTGCCTTCTCCCTCCTGTGAGTTTGGTAAGTCACTGACTGTCTATGCCTGGGA
AAGGGTGGGCAGGAGATGGGGCAGTGCAGGAAAAGTGGCACTATGAACCCTGCAGCCCTAGACAATTGTACTAACCTTCTTCTCTTTCCTCTCCTGACAGGTTG
GTAACCAAGCCACCATGAGCAGCAGCTCTTGGCTGCTGCTGAGTCTGGTGGCTGTGACAGCTGCCCAGAGCACCATTGAGGAACAGGCCAAGACCTTCCTGGA
CAAGTTCAACCATGAGGCTGAGGACCTGTTCTACCAGAGCAGCCTGGCCAGCTGGAACTACAACACCAACATCACTGAAGAGAATGTGCAGAACATGAACAAT
GCTGGGGACAAGTGGAGTGCCTTCCTGAAAGAGCAGTCACTGGCCCAGATGTACCCTCTGCAAGAGATCCAGAACCTGACAGTGAAGCTCCAGCTCCAGGC
CTCTCCAGCAGAATGGCAGCTCTGTCTTGTCTGGAGACAAGAGCAAGAGACTGAACACCATCCTGAACACAATGAGCACCATCTACAGCACAGGCAAAGTGTG
CAACCCTGACAACCCTCAAGAGTGCCTGCTGCTGGAACCTGGCCTGAATGAGATCATGGCCAACAGCCTGGACTACAATGAGAGACTGTGGGCCTGGGAGTCT
TGGAGGAGTGAAGTGGGAAAGCAGCTGAGGCCCTGTATGAGGAATATGTGGTGCTGAAGAATGAGATGGCCAGGGCCAACCACTATGAGGACTATGGGGA
TTATTGGAGGGGAGACTATGAAGTGAATGGTGTTGATGGCTATGACTACAGCAGGGGCCAGCTGATTGAGGATGTGGAACACACCTTTGAGGAAATCAAGCCC
CTCTATGAGCACCTCCATGCCTATGTCAGAGCCAAGCTGATGAATGCTTACCCCAGCTACATCAGCCCCATTGGCTGCCTGCCTGCTGATCTGCTGGGAGACATG
TGGGGCAGATTCTGGACCAACCTGTACAGCCTGACTGTTGCCCTTTGGCCAGAAACCTAACATTGATGTGACAGATGCCATGGTGGATCAGGCCTGGGATGCCCA
GAGAATCTTCAAAGAGGCTGAGAAGTTCTTTGTGTCTGTGGGGCTGCCCAACATGACCCAAGGCTTTTGGGAGAACTCCATGCTGACAGACCCTGGCAATGTGC
AAAAGGCTGTGTGTCACCCACAGCCTGGGACCTTGGCAAGGGAGACTTCAGAATCTTGATGTGCACCAAAGTGACAATGGATGACTTTCTGACAGCTCACCAT
GAGATGGGCCACATCCAGTATGACATGGCTATGCTGCCCAGCCTTTCCTGCTGAGAAATGGGGCCAATGAGGGCTTCCATGAGGCAGTGGGAGAGATCATGA
GCCTGTCTGCTGCCACACCTAAGCACCTGAAGTCCATTGGCCTGCTGAGCCCTGACTTCCAAGAGGACAATGAGACAGAGATCAACTTCCTGCTCAAGCAGGCC
CTGACCATTGTGGGTACACTGCCCTTCACCTACATGCTGGAAAAGTGGAGATGGATGGTCTTTAAGGGAGAAATCCCAAGGACCAGTGGATGAAGAAATGCT
GGGAGATGAAGAGGGAAATTGTGGGAGTTGTGGAACCTGTGCCACATGATGAGACATACTGTGACCCTGCCAGCCTGTTCCATGTGTCCAATGACTACTCCTTC
ATTAGGTACTACACCAGGACACTGTACCAGTTCCAGTTTCAAGAGGCTCTGTGTCAGGCTGCTAAACATGAGGGCCCACTGCACAAGTGTGACATCAGCAACTC
CACAGAGGCTGGACAGAAACTGTTCAACATGCTGAGACTGGGCAAGTCTGAGCCTTGGACTCTGGCCCTGGAAAATGTTGTGGGAGCCAAGAATATGAATGTC
AGACCCCTGCTGAACTACTTTGAGCCCCTGTTCACCTGGCTGAAGGACCAGAACAAGAACAGCTTTGTTGGCTGGTCCACAGACTGGTCCCCATATGCTGACCA
GAGCATCAAAGTCAGAATCAGCCTGAAGAGTGCCCTGGGAGATAAGGCCTATGAGTGGAATGATAATGAGATGTACCTGTTCAGGTCCTCTGTGGCTTATGCT
ATGAGACAGTACTTTCTGAAAGTGAAGAACCAGATCCTGTTTGGAGAGGATGTCAGAGTGGCCAACCTGAAGCCTAGAATCAGCTTCAACTTCTTTGT
GACAGCCCCTAAGAATGTGTCTGACATCATCCCAGAACAGAGGTGGAAAGCCATCAGAATGAGCAGGTCCAGGATCAATGATGCCTTCAGGCTCAATGAC
AACTCCCTGGAATTTCTGGGCATTCAGCCCACACTGGGCCCTCCAAATCAGCCTCCTGTGTCCTAAGATCTACTTCTGGCTAATAAAAGATCAGAGCTCTAGTG
ATCTGTTGTGTTGTTTTTTGTGTCTGTTATTCTAGTAAGTCAATATGTTCACCCCAAAAAAGCTGTTTGTTAACTTGTCAACCTCATTCTAAAATGTATATAGAAGCC
CAAAAGACAATAACAAAAATATTCTTGTAGAACAAAATGGGAAAGAATGTTCCACTAAATATCAAGATTTAGAGCAAAGCATGAGATGTGTGGGGATAGACAG
TGAGGCTGATAAAATAGAGTAGAGCTCAGAAACAGACCCATTGATATATGTAAGTGACCTATGAAAAAAATATGGCATTTTACAATGGGAAAATGATGGTCTTT
TTCTTTTTTAGAAAAACAGGGAAATATATTTATATGTAAAAAATAAAAGGGAACCCATATGTCATACCATACACACAAAAAAATTCCAGTGAATTATAAGTCTAA
ATGGAGAAGGCAAAACTTTAAATCTTTTAGAAAATAATATAGAAGCATGCCATCAAGACTTCAGTGTAGAGAAAAATTTCTTATGACTCAAAGTCCTAACCACAA
AGAAAAGATTGTTAATTAGATTGCATGAATATTAAGACTTATTTTTAAAATTAAAAAACCATTAAGAAAAGTCAGGCCATAGAATGACAGAAAATATTTGCAACA
CCCCAGTAAAGAGAATTGTAATATGCAGATTATAAAAAGAAGTCTTACAAATCAGTAAAAAATAAAACTAGACAAAAATTTGAACAGATGAAAGAGAAACTCTA
AATAATCATTACACATGAGAAACTCAATCTCAGAAATCAGAGAACTATCATTGCATATACACTAAATTAGAGAAATATTAAAAGGCTAAGTAACATCTGTGGCTT
AATTAATCTAGTGATCAGCAGTTCAACCTGTTGATAGTATGTACTAAGCTCTCATGTTTAATGTACTAAGCTCTCATGTTTAATGAACTAAACCCTCATGG
CTAATGTACTAAGCTCTCATGGCTAATGTACTAAGCTCTCATGTTTCATGTACTAAGCTCTCATGTTTGAACAATAAAATTAATATAAATCAGCAACTTAAATAGCC
TCTAAGGTTTTAAGTTTTATAAGAAAAAAAAGAATATATAAGGCTTTTAAAGGTTTTAAGGTTTCCTAGGTTATCCTCATATGAGCTCTTAGAAAAACTCATCCAG
CATCAAATGAAACTGCAATTTATTCATATCAGGATTATCAATACCATATTTTTGAAAAAGTCTTTTCTGTAATGAAGGAGAAAACTCACCCAGGCAGTTCCATAGG
ATGGCAAGATCCTGGTATCTGTCTGCAATTCCAACTCTTCCAACATCAATACAACCTATTAATTTCCCCTCATCAAAAATAAGGTTATCAAGTGAGAAATCACCAT
GAGTGACCACTGAATCTGGTGAGAATGGCAAAAGATTATGCATTTCTTTCCAGACTTGTTCAACAGGCCAGCCATTTCTCTCATCATCAAAATCACTGGCATCAAC
CAAACCATTATTCATTCTTGATTGGGCCTGAGCCAGTCTAAATACTCTATCAGAGTTAAAAGGACAATTACAAACAGGAATGGAATGCAATCTTCTCAGGAACAC
TGCCAGGGCATCAACAATATTTTCACCTGAATCAGGATATTCTTCCAATACCTGGAATGCTGTTTTCCCTGGGATGGCAGTGGTGAGTAACCATGCATCATCAGG
AGTTCTGATAAAATGCTTGATGGTTGGAAGAGGCATAAATTCAGTCAGCCAGTTTAGTCTGACCATCTCATCTGTAACATCATTGGCAACAGAACCTTTGCCATG
TTTCAGAAACAACTCTGGGGCATCTGGCTTCCCATACAATCTATAGATTGTGGCACCTGATTGCCCAACATTATCTCTAGCCCATTTATACCCATATAAATCAGCAT
CCATGTTGGAATTTAATCTTGGCCTGGAGCAAGAGGTTTCTCTTTGAATATGGCTCATACATGTGCACCTCCTATAGTGAGTTGTATTATACTATTGCAGATACTACT
ATGCCAATGTTTAATTAGTCAG

FIG. 21

082020 # 1 : shACE2 TYLTNY- BV3 (SEQ ID NO:21)

DraIII-βGlo BI-Nhe-mCMVΔEF1I126-BstEII -shACE2 TYLTNY-BglII-MirpA-IFNβ S/MAR-BV3

CACTATGTGTTAATTAAAATTATCTCTAAGGCATGTGAACTGGCTGTCTTGGTTTTCATCTGTACTTCATCTGCTACCTCTGTGACCTGAAACATATTTATAATTCCA
TTAAGCTGTGCATATGATAGATTTATCATATGTATTTTCCTTAAAGGATTTTTGTAAGAACTAATTGAATTGATACCTGTAAAGTCTTTATCACACTACCCAATAAA
TAATAAATCTCTTTGTTCAGCTCTCTGTTTCTATAAATATGTACCAGTTTTATTGTTTTTAGTGGTAGTGATTTTATTCTCTTTCTATATATATACACACACATGTGTG
CATTCATAAATATATACAATTTTTATGAATAAAAAATTATTAGCAATCAATATTGAAAACCACTGATTTTTGTTTATGTGAGCAAACAGCAGATTAAAAGGAATTT
GAATTCTCATAGCTAGCAGGAGTCAATGGGAAAAACCCATTGGAGCCAAGTACACTGACTCAATAGGGACTTTCCATTGGGTTTTGCCCAGTACATAAGGTCAA
TAGGGGGTGAGTCAACAGGAAAGTCCCATTGGAGCCAAGTACATTGAGTCAATAGGGACTTTCCAATGGGTTTTGCCCAGTACATAAGGTCAATGGGAGGTAA
GCCAATGGGTTTTTCCCATTACTGGCACGTATACTGAGTCATTAGGGACTTTCCAATGGGTTTTGCCCAGTACATAAGGTCAATAGGGGTGAATCAACAGGAAA
GTCCCATTGGAGCCAAGTACACTGAGTCAATAGGGACTTTCCATTGGGTTTTGCCCAGTACAAAAGGTCAATAGGGGGTGAGTCAATGGGTTTTTCCCATTATTG
GCACATACATAAGGTCAATAGGGGTGACTAGTGGAGAAGAGCATGCTTGAGGGCTGAGTGCCCCTCAGTGGGCAGAGAGCACATGGCCCACAGTCCCTGAGA
AGTTGGGGGGAGGGGTGGGCAATTGAACTGGTGCCTAGAGAAGGTGGGGCTTGGGTAAACTGGGAAAGTGATGTGGTGTACTGGCTCCACCTTTTTCCCCAG
GGTGGGGGAGAACCATATATAAGTGCAGTAGTCTCTGTGAACATTCAAGCTTCTGCCTTCTCCCTCCTGTGAGTTTGGTAAGTCACTGACTGTCTATGCCTGGGA
AAGGGTGGGCAGGAGATGGGGCAGTGCAGGAAAAGTGGCACTATGAACCCTGCAGCCCTAGACAATTGTACTAACCTTCTTCTCTTTCCTCTCCTGACAGGTTG
GTAACCAAGCCACCATGAGCAGCAGCTCTTGGCTGCTGCTGAGTCTGGTGGCTGTGACAGCTGCCCAGAGCACCATTGAGGAACAGGCCAAG[illegible]TTCCTGGA
CAAGTTCAACCATGAGGCTGAGGACCTGTTCTACCAGAGCAGCCTGGCCAGCTGGAACTACAACACCAACATCACTGAAGAGAATGTGCAGAACATGAACAAT
GCTGGGGACAAGTGGAGTGCCTTCCTGAAAGAGCAGAGCACA[illegible]GCCCAGATGTACCCTCTGCAAGAGATCCAGAACCTGACAGTGAAGCTCCAGCTCCAGG
CTCTCCAGCAGAATGGCAGCTCTGTGCTGTCTGAGGACAAGAGCAAGAGACTGAACACCATCCTGAACACAATGAGCACCATCTACAGCACAGGCAAAGTGTG
CAACCCTGACAACCCTCAAGAGTGCCTGCTGCTGGAACCTGGCCTGAATGAGATCATGGCCAACAGCCTGGACTACAATGAGAGACTGTGGGCCTGGGAGTCT
TGGAGGAGTGAAGTGGGAAAGCAGCTGAGGCCCCTGTATGAGGAATATGTGGTGCTGAAGAATGAGATGGCCAGGGCCAACCACTATGAGGACTATGGGGA
TTATTGGAGGGGAGACTATGAAGTGAATGGTGTTGATGGCTATGACTACAGCAGGGGCCAGCTGATTGAGGATGTGGAACACACCTTTGAGGAAATCAAGCCC
CTCTATGAGCACCTCCATGCCTATGTCAGAGCCAAGCTGATGAATGCTTACCCCAGCTACATCAGCCCCATTGGCTGCCTGCCTGCTCATCTGCTGGGAGACATG
TGGGGCAGATTCTGGACCAACCTGTACAGCCTGACTGTGCCCTTTGGCCAGAAACCTAACATTGATGTGACAGATGCCATGGTGGATCAGGCCTGGGATGCCCA
GAGAATCTTCAAAGAGGCTGAGAAGTTCTTTGTGTCTGTGGGGCTGCCCAACATGACCCAAGGCTTTTGGGAG[illegible]TCCATGCTGACAGACCCTGGCAATGTGC
AAAAGGCTGTGTGTCACCCCACAGCCTGGGACCTTGGCAAGGGAGACTTCAGAATCCTGATGTGCACCAAAGTGACAATGGATGACTTTCTGACAGCTCACCAT
GAGATGGGCCACATCCAGTATGACATGGCCTATGCTGCCCAGCCTTTCCTGCTGAGAAATGGGGCCAATGAGGGCTTCCATGAGGCAGTGGGAGAGATCATGA
GCCTGTCTGCTGCCACACCTAAGCACCTGAAGTCCATTGGCCTGCTGAGCCCTGACTTCCAAGAGGACAATGAGACAGAGATCAACTTCCTGCTCAAGCAGGCC
CTGACCATTGTGGGCACACTGCCCTTCACCTACATGCTGGAAAAGTGGAGATGGATGGTCTTTAAGGGAGAAATCCCCAAGGACCAGTGGATGAAGAAATGGT
GGGAGATGAAGAGGGAAATTGTGGGAGTTGTGGAACCTGTGCCACATGATGAGACATACTGTGACCCTGCCAGCCTGTTCCATGTGTCCAATGACTACTCCTTC
ATTAGGTACTACACCAGGACACTGTACCAGTTCCAGTTTCAAGAGGCTCTGTGTCAGGCTGCTAAACATGAGGGCCCACTGCACAAGTGTGACATCAGCAACTC
CACAGAGGCTGGACAGAAACTGTTCAACATGCTGAGACTGGGCAAGTCTGAGCCTTGGACTCTGGCCCTGGAAAATGTTGTGGGAGCCAAGAATATGAATGTC
AGACCCCTGCTGAACTACTTTGAGCCCCTGTTCACCTGGCTGAAGGACCAGAACAAGAACAGCTTTGTTGGCTGGTCCACAGACTGGTCCCCATATGCTGACCA
GAGCATCAAAGTCAGAATCAGCCTGAAGAGTGCCCTGGGAGATAAGGCCTATGAGTGGAATGATAATGAGATGTACCTGTTCAGGTCCTCTGTGGCTTATGCT
ATGAGACAGTACTTTCTGAAAGTGAAGAACCAGATGATCCTGTTTGGAGAAGAGGATGTCAGAGTGGCCAACCTGAAGCCTAGAATCAGCTTCAACTTCTTTGT
GACAGCCCCTAAGAATGTGTCTGACATCATCCCCAGAACAGAGGTGGAAAAGGCCATCAGAATGAGCAGGTCCAGGATCAATGATGCCTTCAGGCTCAATGAC
AACTCCCTGGAATTTCTGGGCATTCAGCCCACACTGGGCCCTCCAAATCAGCCTCCTGTGTCCTAAAGATCTACTTCTGGCTAATAAAAGATCAGAGCTCTAGTG
ATCTGTGTGTTGGTTTTTTGTGTCTGCATTCTAGCAAGTCAATATGTTCACCCCAAAAAAGCTGTTTGTTAACTTGTCAACCTCATTCTAAAATGTATATAGAAGCC
CAAAAGACAATAACAAAAATATTCTTGTAGAACAAAATGGGAAAGAATGTTCCACTAAATATCAAGATTTAGAGCAAAGCATGAGATGTGTGGGGATAGACAG
TGAGGCTGATAAAATAGAGTAGAGCTCAGAAACAGACCCATTGATATATGTAAGTGACCTATGAAAAAAATATGGCATTTTACAATGGGAAAATGATGGTCTTT
TTCTTTTTTAGAAAAACAGGGAAATATATTTATATGTAAAAAATAAAAGGGAACCCATATGTCATACCATACACACAAAAAAATTCCAGTGAATTATAAGTCTAA
ATGGAGAAGGCAAAACTTTAAATCTTTTAGAAAATAATATAGAAGCATGCCATCAAGACTTCAGTGTAGAGAAAAATTTCTTATGACTCAAAGTCCTAACCACAA
AGAAAAGATTGTTAATTAGATTGCATGAATATTAAGACTTATTTTTAAAATTAAAAAACCATTAAGAAAAGTCAGGCCATAGAATGACAGAAAATATTTGCAACA
CCCCAGTAAAGAGAATTGTAATATGCAGATTATAAAAAGAAGTCTTACAAATCAGTAAAAAATAAAACTAGACAAAAATTTGAACAGATGAAAGAGAAACTCTA
AATAATCATTACACATGAGAAACTCAATCTCAGAAATCAGAGAACTATCATTGCATATACACTAAATTAGAGAAATATTAAAAGGCTAAGTAACATCTGTGGCTT
AATTAACCTAGGTCTAGTGATCAGCAGTTCAACCTGTTGATAGTATGTACTAAGCTCTCATGTTTAATGTACTAAGCTCTCATGTTTAATGAACTAAACCCTCATGG
CTAATGTACTAAGCTCTCATGGCTAATGTACTAAGCTCTCATGTTTCATGTACTAAGCTCTCATGTTTGAACAATAAAATTAATATAAATCAGCAACTTAAATAGCC
TCTAAGGTTTTAAGTTTTATAAGAAAAAAAAGAATATATAAGGCTTTTAAAGGTTTTAAGGTTTCCTAGGTTATCCTCATATGAGCTCTTAGAAAAACTCATCCAG
CATCAAATGAAACTGCAATTTATTCATATCAGGATTATCAATACCATATTTTTGAAAAAGTCTTTTCTGTAATGAAGGAGAAAACTCACCCAGGCAGTTCCATAGG
ATGGCAAGATCCTGGTATCTGTCTGCAATTCCAACTCTTCCAACATCAATACAACCTATTAATTTCCCCTCATCAAAAATAAGGTTATCAAGTGAGAAATCACCAT
GAGTGACCACTGAATCTGGTGAGAATGGCAAAAGATTATGCATTTCTTTCCAGACTTGTTCAACAGGCCAGCCATTTCTCTCATCATCAAAATCACTGGCATCAAC
CAAACCATTATTCATTCTTGATTGGGCCTGAGCCAGTCTAAATACTCTATCAGAGTTAAAAGGACAATTACAAACAGGAATGGAATGCAATCTTCTCAGGAACAC
TGCCAGGGCATCAACAATATTTTCACCTGAATCAGGATATTCTTCCAATACCTGGAATGCTGTTTTCCCTGGGATGGCAGTGGTGAGTAACCATGCATCATCAGG
AGTTCTGATAAAATGCTTGATGGTTGGAAGAGGCATAAATTCAGTCAGCCAGTTTAGTCTGACCATCTCATCTGTAACATCATTGGCAACAGAACCTTTGCCATG
TTTCAGAAACAACTCTGGGGCATCTGGCTTCCCATACAATCTATAGATTGTGGCACCTGATTGCCCAACATTATCTCTAGCCCATTTATACCCATATAAATCAGCAT
CCATGTTGGAATTTAATCTTGGCCTGGAGCAAGAGGTTTCTCTTTGAATATGGCTCATACATGTGCACCTCCTATAGTGAGTTGTATTATACTATGCAGATATACT
ATGCCAATGTTTAATTGTCAG

FIG. 22

081320 # 2A : shACE2-1xL-Fc- BV3 (SEQ ID NO:22)

DraIII-βGlo BI-Nhe-mCMVΔEF1I126-BstEII -shACE2-1xL-Fc-BglII-MinpA-IFNβ S/MAR-BV3

CACTATGTGTTAATTAAAATTATCTCTAAGGCATGTGAACTGGCTGTCTTGGTTTTCATCTGTACTTCATCTGCTACCTCTGTGACCTGAAACATATTTATAATTCCA
TTAAGCTGTGCATATGATAGATTTATCATATGTATTTTCCTTAAAGGATTTTTGTAAGAACTAATTGAATTGATACCTGTAAAGTCTTTATCACACTACCCAATAAA
TAATAAATCTCTTTGTTCAGCTCTCTGTTTCTATAAATATGTACCAGTTTTATTGTTTTTAGTGGTAGTGATTTTATTCTCTTTCTATATATATACACACACATGTGTG
CATTCATAAATATATACAATTTTTATGAATAAAAAATTATTAGCAATCAATATTGAAAACCACTGATTTTTGTTTATGTGAGCAAACAGCAGATTAAAAGG**AATTT**
GAATTC**TCATA**GCTAGCAGGAGTCAATGGGAAAAACCCATTGGAGCCAAGTACACTGACTCAATAGGGACTTTCCATTGGGTTTTGCCCAGTACATAAGGTCAA
TAGGGGGTGAGTCAACAGGAAAGTCCCATTGGAGCCAAGTACATTGAGTCAATAGGGACTTTCCAATGGGTTTTGCCCAGTACATAAGGTCAATGGGAGGTAA
GCCAATGGGTTTTTCCCATTACTGGCACGTATACTGAGTCATTAGGGACTTTCCAATGGGTTTTGCCCAGTACATAAGGTCAATAGGGGTGAATCAACAGGAAA
GTCCCATTGGAGCCAAGTACACTGAGTCAATAGGGACTTTCCATTGGGTTTTGCCCAGTACAAAAGGTCAATAGGGGGTGAGTCAATGGGTTTTTCCCATTATTG
GCACGTACATAAGGTCAATAGGGGTGACTAGTGGAGAAGAGCATGCTTGAGGGCTGAGTGCCCCTCAGTGGGCAGAGAGCACATGGCCCACAGTCCCTGAGA
AGTTGGGGGGAGGGGTGGGCAATTGAACTGGTGCCTAGAGAAGGTGGGGCTTGGGTAAACTGGGAAAGTGATGTGGTGTACTGGCTCCACCTTTTTCCCCAG
GGTGGGGGAGAACCATATATAAGTGCAGTAGTCTCTGTGAACATTCAAGCTTCTGCCTTCTCCCTCCTGTGAGTTTGGTAAGTCACTGACTGTCTATGCCTGGGA
AAGGGTGGGCAGGAGATGGGGCAGTGCAGGAAAAGTGGCACTATGAACCCTGCAGCCCTAGACAATTGTACTAACCTTCTTCTCTTTCCTCTCCTGACAGGTTG
GTAACCAAGCCACCATGAGCAGCAGCTCTTGGCTGCTGCTGAGTCTGGTGGCTGTGACAGCTGCCCAGAGCACCATTGAGGAACAGGCCAAGACCTTCCTGGA
CAAGTTCAACCATGAGGCTGAGGACCTGTTCTACCAGAGCAGCCTGGCCAGCTGGAACTACAACACCAACATCACTGAAGAGAATGTGCAGAACATGAACAAT
GCTGGGGACAAGTGGAGTGCCTTCCTGAAAGAGCAGAGCACACTGGCCCAGATGTACCCTCTGCAAGAGATCCAGAACCTGACAGTGAAGCTCCAGCTCCAGG
CTCTCCAGCAGAATGGCAGCTCTGTGCTGTCTGAGGACAAGAGCAAGAGACTGAACACCATCCTGAACACAATGAGCACCATCTACAGCACAGGCAAAGTGTG
CAACCCTGACAACCCTCAAGAGTGCCTGCTGCTGGAACCTGGCCTGAATGAGATCATGGCCAACAGCCTGGACTACAATGAGAGACTGTGGGCCTGGGAGTCT
TGGAGGAGTGAAGTGGGAAAGCAGCTGAGGCCCCTGTATGAGGAATATGTGGTGCTGAAGAATGAGATGGCCAGGGCCAACCACTATGAGGACTATGGGGA
TTATTGGAGGGGAGACTATGAAGTGAATGGTGTTGATGGCTATGACTACAGCAGGGGCCAGCTGATTGAGGATGTGGAACACACCTTTGAGGAAATCAAGCCC
CTCTATGAGCACCTCCATGCCTATGTCAGAGCCAAGCTGATGAATGCTTACCCCAGCTACATCAGCCCCATTGGCTGCCTGCCTGCTCATCTGCTGGGAGACATG
TGGGGCAGATTCTGGACCAACCTGTACAGCCTGACTGTGCCCTTTGGCCAGAAACCTAACATTGATGTGACAGATGCCATGGTGGATCAGGCCTGGGATGCCCA
GAGAATCTTCAAAGAGGCTGAGAAGTTCTTTGTGTCTGTGGGGCTGCCCAACATGACCCAAGGCTTTTGGGAGAACTCCATGCTGACAGACCCTGGCAATGTGC
AAAAGGCTGTGTGTCACCCCACAGCCTGGGACCTTGGCAAGGGAGACTTCAGAATCCTGATGTGCACCAAAGTGACAATGGATGACTTTCTGACAGCTCACCAT
GAGATGGGCCACATCCAGTATGACATGGCCTATGCTGCCCAGCCTTTCCTGCTGAGAAATGGGGCCAATGAGGGCTTCCATGAGGCAGTGGGAGAGATCATGA
GCCTGTCTGCTGCCACACCTAAGCACCTGAAGTCCATTGGCCTGCTGAGCCCTGACTTCCAAGAGGACAATGAGACAGAGATCAACTTCCTGCTCAAGCAGGCC
CTGACCATTGTGGGCACACTGCCCTTCACCTACATGCTGGAAAAGTGGAGATGGATGGTCTTTAAGGGAGAAATCCCCAAGGACCAGTGGATGAAGAAATGGT
GGGAGATGAAGAGGGAAATTGTGGGAGTTGTGGAACCTGTGCCACATGATGAGACATACTGTGACCCTGCCAGCCTGTTCCATGTGTCCAATGACTACTCCTTC
ATTAGGTACTACACCAGGACACTGTACCAGTTCCAGTTTCAAGAGGCTCTGTGTCAGGCTGCTAAACATGAGGGCCCACTGCACAAGTGTGACATCAGCAACTC
CACAGAGGCTGGACAGAAACTGTTCAACATGCTGAGACTGGGCAAGTCTGAGCCTTGGACTCTGGCCCTGGAAAATGTTGTGGGAGCCAAGAATATGAATGTC
AGACCCCTGCTGAACTACTTTGAGCCCCTGTTCACCTGGCTGAAGGACCAGAACAAGAACAGCTTTGTTGGCTGGTCCACAGACTGGTCCCCATATGCTGACCA
GAGCATCAAAGTCAGAATCAGCCTGAAGAGTGCCCTGGGAGATAAGGCCTATGAGTGGAATGATAATGAGATGTACCTGTTCAGGTCCTCTGTGGCTTATGCT
ATGAGACAGTACTTTCTGAAAGTGAAGAACCAGATGATCCTGTTTGGAGAAGAGGATGTCAGAGTGGCCAACCTGAAGCCTAGAATCAGCTTCAACTTCTTTGT
GACAGCCCCTAAGAATGTGTCTGACATCATCCCCAGAACAGAGGTGGAAAAGGCCATCAGAATGAGCAGGTCCAGGATCAATGATGCCTTCAGGCTCAATGAC
AACTCCCTGGAATTTCTGGGCATTCAGCCCACACTGGGCCCTCCAAATCAGCCTCCTGTGTCT**T**GGTGGAGGAGGTAGTGAGCCCAAGAGCTGTGACAAGACCCA
CACCTGTCCTCCATGTCCTGCTCCAGAGCTGCTTGGAGGACCTTCTGTGTTTCTGTTCCCTCCAAAGCCAAAGGACACCCTGATGATCAGCAGAACCCCTGAAGT
GACCTGTGTGGTGGTGGATGTGTCCCATGAGGACCCAGAAGTGAAGTTCAATTGGTATGTGGATGGTGTTGAGGTGCACAATGCCAAGACCAAGCCTAGAGA
GGAACAGTACAACAGCACCTACAGGGTTGTGTCAGTGCTGACTGTGCTGCACCAGGACTGGCTGAATGGCAAAGAGTACAAGTGCAAGGTGTCCAACAAGGCC
CTGCCTGCTCCTATTGAAAAGACCATCAGCAAGGCCAAGGGACAGCCTAGGGAACCCCAGGTGTACACACTGCCACCTAGCAGAGATGAGCTGACCAAGAATC
AGGTGTCCCTGACATGCCTTGTGAAGGGCTTCTACCCTTCTGACATTGCAGTGGAATGGGAGAGCAATGGCCAGCCTGAGAACAACTACAAGACAACCCCTCCT
GTGCTGGACTCTGATGGCTCATTCTTCCTGTACTCCAAGCTGACAGTGGACAAGTCCAGATGGCAGCAAGGCAATGTGTTCAGCTGCTCTGTGATGCATGAGGC
CCTGCACAACCACTACACACAGAAGTCCCTGTCTCTGAGCCCTGGCAAG**TGA**AGATCTACTTCTGGCTAATAAAAGATCAGAGCTCTAGTGATCTGTGTGTTGGT
TTTTTGTGTCTGCATTCTAGCAAGTCAATATGTTCACCCCAAAAAAGCTGTTTGTTAACTTGTCAACCTCATTCTAAAATGTATATAGAAGCCCAAAAGACAATAA
CAAAAATATTCTTGTAGAACAAAATGGGAAAGAATGTTCCACTAAATATCAAGATTTAGAGCAAAGCATGAGATGTGTGGGGATAGACAGTGAGGCTGATAAA
ATAGAGTAGAGCTCAGAAACAGACCCATTGATATATGTAAGTGACCTATGAAAAAAATATGGCATTTTACAATGGGAAAATGATGGTCTTTTTCTTTTTTAGAAA
AACAGGGAAATATATTTATATGTAAAAAATAAAAGGGAACCCATATGTCATACCATACACACAAAAAAATTCCAGTGAATTATAAGTCTAAATGGAGAAGGCAA
AACTTTAAATCTTTTAGAAAATAATATAGAAGCATGCCATCAAGACTTCAGTGTAGAGAAAAATTTCTTATGACTCAAAGTCCTAACCACAAAGAAAAGATTGTT
AATTAGATTGCATGAATATTAAGACTTATTTTTAAAATTAAAAAACCATTAAGAAAAGTCAGGCCATAGAATGACAGAAAATATTTGCAACACCCCAGTAAAGAG
AATTGTAATATGCAGATTATAAAAAGAAGTCTTACAAATCAGTAAAAAATAAAACTAGACAAAAATTTGAACAGATGAAAGAGAAACTCTAAATAATCATTACA
CATGAGAAACTCAATCTCAGAAATCAGAGAACTATCATTGCATATACACTAAATTAGAGAAATATTAAAAGGCTAAGTAACATCTGTGGC**TTAATTAA**TCTAGC**T**
CTAGTGATCAGCAGTTCAACCTGTTGATAGTATGTACTAAGCTCTCATGTTTAATGTACTAAGCTCTCATGTTTAATGAACTAAACCCTCATGGCTAATGTACTAA
GCTCTCATGGCTAATGTACTAAGCTCTCATGTTTCATGTACTAAGCTCTCATGTTTGAACAATAAAATTAATATAAATCAGCAACTTAAATAGCCTCTAAGGTTTTA
AGTTTTATAAGAAAAAAAAGAATATATAAGGCTTTTAAAGGTTTTAAGGTTTCCTAGGTTATCC**TCATATGAGCTC**TTAGAAAAACTCATCCAGCATCAAATGAA
ACTGCAATTTATTCATATCAGGATTATCAATACCATATTTTTGAAAAAGTCTTTTCTGTAATGAAGGAGAAAACTCACCCAGGCAGTTCCATAGGATGGCAAGATC
CTGGTATCTGTCTGCAATTCCAACTCTTCCAACATCAATACAACCTATTAATTTCCCCTCATCAAAAATAAGGTTATCAAGTGAGAAATCACCATGAGTGACCACT
GAATCTGGTGAGAATGGCAAAAGATTATGCATTTCTTTCCAGACTTGTTCAACAGGCCAGCCATTTCTCTCATCATCAAAATCACTGGCATCAACCAAACCATTAT
TCATTCTTGATTGGGCCTGAGCCAGTCTAAATACTCTATCAGAGTTAAAAGGACAATTACAAACAGGAATGGAATGCAATCTTCTCAGGAACACTGCCAGGGCA
TCAACAATATTTTCACCTGAATCAGGATATTCTTCCAATACCTGGAATGCTGTTTTCCCTGGGATGGCAGTGGTGAGTAACCATGCATCATCAGGAGTTCTGATAA
AATGCTTGATGGTTGGAAGAGGCATAAATTCAGTCAGCCAGTTTAGTCTGACCATCTCATCTGTAACATCATTGGCAACAGAACCTTTGCCATGTTTCAGAAACA
ACTCTGGGGCATCTGGCTTCCCATACAATCTATAGATTGTGGCACCTGATTGCCCAACATTATCTCTAGCCCATTTATACCCATATAAATCAGCATCCATGTTGGA
ATTTAATCTTGGCCTGGAGCAAGAGGTTTCTCTTTGAATATGGCTCAT**ACATGTGCA**CCTCCTATAGTGAGTCGTATTATACTATGCAGATATACTATGCCAATGT
TTAATTGTCAG

FIG. 23

081320 # 4A : shACE2-1xL-FcLALA- BV3 (SEQ ID NO:23)

DraIII-βGlo RI-NheI-hCMVAEP31126-BstEII-shACE2-1xL-FcLALA-BglII-MluI-pA-IFNβ S/MAR-BV3

CACTATGTGTTAATTAAAATTATCTCTAAGGCATGTGAACTGGCTGTCTTGGTTTTCATCTGTACTTCATCTGCTACCTCTGTGACCTGAAACATATTTATAATTCCA
TTAAGCTGTGCATATGATAGATTTATCATATGTATTTTCCTTAAAGGATTTTTGTAAGAACTAATTGAATTGATACCTGTAAAGTCTTTATCACACTACCCAATAAA
TAATAAATCTCTTTGTTCAGCTCTCTGTTTCTATAAATATGTACCAGTTTTATTGTTTTTAGTGGTAGTGATTTTATTCTCTTTCTATATATATACACACACATGTGTG
CATTCATAAATATATACAATTTTTATGAATAAAAAATTATTAGCAATCAATATTGAAAACCACTGATTTTTGTTTATGTGAGCAAACAGCAGATTAAAAGGAATTT
GAATTCTCATAGCTAGCAG[illegible]
[illegible]
[illegible]
[illegible]
[illegible]
[illegible]ACTAGTGGAGAAGAGCATGCTTGAGGGCTGAGTGCCCCTCAGTGGGCAGAGAGCACATGGCCCACAGTCCCTGAGA
AGTTGGGGGGAGAGGGTGGGCAATTGAACTGGTGCCTAGAGAAGGTGGGGCTTGGGTAAACTGGGAAAGTGATGTGGTGTACTGGCTCCACCTTTTTCCCCAG
GGTGGGGGAGAACCATATATAAGTGCAGTAGTCTCTGTGAACATTCAAGCTTCTGCCTTCTCCCTCCTGTGAGTTTGGTAAGTCACTGACTGTCTATGCCTGGGA
AAGGGTGGGCAGGAGATGGGGCAGTGCAGGAAAAGTGGCACTATGAACCCTGCAGCCCTAGACAATTGTACTAACCTTCTTCTCTTTCCTCTCCTGACAGGTTG
GTAACCAAGCCACCATGAGCAGCAGCTCTTGGCTGCTGCTGAGTCTGGTGGCTGTGACAGCTGCCCAGAGCACCATTGAGGAACAGGCCAAGACCTTCCTGGA
CAAGTTCAACCATGAGGCTGAGGACCTGTTCTACCAGAGCAGCCTGGCCAGCTGGAACTACAACACCAACATCACTGAAGAGAATGTGCAGAACATGAACAAT
GCTGGGGACAAGTGGAGTGCCTTCCTGAAAGAGCAGTCACTGGCCCAGATGTACCCTCTGCAAGAGATCCAGAACCTGACAGTGAAGCTCCAGCTCCAGGC
CTCTCCAGCAGAATGGCAGCTCTGTCTTGTCTTGTTGACAAGAGCAAGAGACTGAACACCATCCTGAACACAATGAGCAACCATCTACAGCAGCAGGCAAAGTGTG
CAACCCTGACAACCCTCAAGATGCCTGCTGCTGGAACCTGGCCTGAATGAGATCATGGCCAACAGCCTGGACTACAATGAGAGACTGTGGGCCTGGGAGTCT
TGGAGGAGTGAAGTGGGAAAGCAGCTGAGGCCCTGTATGAGGAATATGTGGTGCTGAAGAATGAGATGGCCAGGGCCAACCACTATGAGGACTATGGGGA
TTATTGGAGGGGAGACTATGAAGTGAATGGTGTTGATGGCTATGACTACAGCAGGGGCCAGCTGATTGAGGATGTGGAACACACTTTGAGGAAATCAAGCCC
CTCTATGAGCACCTCCATGCCTATGTCAGAGCCAAGCTGATGAATGCTTACCCCAGCTACATCAGCCCCATTGGCTGCCTGCCTGCTGATCTGCTGGGAGACATG
TGGGGCAGATTCTGGACCAACTGTACAGCCTGACTGTTGCCCTTTGGCCAGAAACCTAACATTGATGTGACAGATGCCATGGTGGATCAGGCCTGGGATGCCCA
GAGAATCTTCAAAGAGGCTGAGAAGTTCTTTGTGTCTGTGGGGCTGCCCAACATGACCCAAGGCTTTTGGGAGAACTCCATGCTGACAGACCCTGGCAATGTGC
AAAAGGCTGTGTGTCACCCACAGCCTGGGACCTTGGCAAGGGAGACTTCAGAATCTGATGTGCACCAAAGTGACAATGGATGACTTTCTGACAGCTCACCAT
GAGATGGGCCACATCCAGTATGACATGGCTATGCTGCCCAGCTTTCCTGCTGAGAAATGGGGCCAATGAGGGCTTCCATGAGGCAGTGGGAGAGATCATGA
GCCTGTCTGCTGCCACACCTAAGCACCTGAAGTCCATTGGCCTGCTGAGCCCTGACTTCCAAGAGGACAATGAGACAGAGATCAACTTCCTGCTCAAGCAGGCC
CTGACCATTGTGGGTACACTGCCCTTCACCTACATGCTGGAAAAGTGGAGATGGATGGTCTTTAAGGGAGAAATCCCAAAGGACCAGTGGATGAAGAAATGGT
GGGAGATGAAGAGGGAAATTGTGGGAGTTGTGGAACCTGTGCCACATGATGAGACATACTGTGACCCTGCCAGCCTGTTCCATGTGTCAATGACTACTCCTTC
ATTAGGTACTACACCAGGACACTGTACCAGTTCCAGTTTCAAGAGGCTCTGTGTCAGGCTGCTAAACATGAGGGCCCACTGCACAAGTGTGACATCAGCAACTC
CACAGAGGCTGGACAGAAACTGTTCAACATGCTGAGACTGGGCAAGTCTGAGCCTTGGACTCTGGCCCTGGAAAATGTTGTGGGAGCCAAGAATATGAATGTC
AGACCCCTGCTGAACTACTTTGAGCCCCTGTTCACCTGGCTGAAGGACCAGAACAAGAACAGCTTTGTTGGCTGGTCCACAGACTGGTCCCCATATGCTGACCA
GAGCATCAAAGTCAGAATCAGCCTGAAGAGTGCCCTGGGAGATAAGGCCTATGAGTGGAATGATAATGAGATGTACCTGTTCAGGTCCTCTGTGGCTTATGCT
ATGAGACAGTACTTTCTGAAAGTGAAGAACCAGATCCTGTTTGGAGAGGATGTCAGAGTGGCCAACCTGAAGCCTAGAATCAGCTTCAACTTCTTTGT
GACAGCCCTAAGATGTCTGACATCATCCCAGAACAGAGGTGGAAAAGGCCATCAGAATGAGCAGGTCCAGGATCAATGATGCCTTCAGGCTCAATGAC
AACTCCTGGAATTTCTGGCATTCAGCCCACACTGGCCCTCCAAATCAGCCTCCTGTGTCTGGTGGAGGAGGTAGTGAGCCCAAGAGCTGTGACAAGACCCA
CACCTGTCCTCCATGTCCTGCTCCAGAGGCTGCTGGAGGACCTTCTGTGTTTCTGTTCCCTCCAAAGCCAAAGGACACCCTGATGATCAGCAGAACCCCTGAAGT
GACCTGTGTGGTGGTGGATGTGTCCCATGAGGACCCAGAAGTGAAGTTCAATTGGTATGTGGATGGTGTTGAGGTGCACAATGCCAAGACCAAGCCTAGAGA
GGAACAGTACAACAGCACCTACAGGGTTGTGTCAGTGCTGACCGTGCTGCACCAGGACTGGCTGAATGGCAAAGAGTACAAGTGCAAGGTGTCCAACAAGGCC
CTGCCTGCTCCTATTGAAAAGACCATCAGCAAGGCCAAGGGACAGCCTAGGGAACCCCAGGTGTACACACTGCCACCTAGCAGAGATGAGCTGACCAAGAATC
AGGTGTCCCTGACATGCCTTGTGAAGGGCTTCTACCCTTCTGACATTGCAGTGGAATGGGAGAGCAATGGCCAGCCTGAGAACAACTACAAGACAACCCCTCCT
GTGCTGGACTCTGATGGCTCATTCTTCCTGTACTCCAAGCTGACAGTGGACAAGTCCAGATGGCAGCAAGGCAATGTGTTCAGCTGCTCTGTGATGCATGAGGC
CCTGCACAACCACTACACACAGAAGTCCCTGTCTCTGAGCCCTGGTAAGTGAAGATCTACTTCTGGCTAATAAAAGATCAGAGCTCTAGTGATCTGTTGTTGCT
TTTTGTGTCTGGATTCTAGCTAGTCAATATGTTCACCCCAAAAAAGCTGTTTGTTAACTTGTCAACCTCATTCTAAAATGTATATAGAAGCCCAAAAGACAATAA
CAAAAATATTCTTGTAGAACAAAATGGGAAAGAATGTTCCACTAAATATCAAGATTTAGAGCAAAGCATGAGATGTGTGGGGATAGACAGTGAGGCTGATAAA
ATAGAGTAGAGCTCAGAAACAGACCCATTGATATATGTAAGTGACCTATGAAAAAAATATGGCATTTTACAATGGGAAAATGATGGTCTTTTTCTTTTTTAGAAA
AACAGGGAAATATATTTATATGTAAAAAATAAAAGGGAACCCATATGTCATACCATACACACAAAAAAATTCCAGTGAATTATAAGTCTAAATGGAGAAGGCAA
AACTTTAAATCTTTTAGAAAATAATATAGAAGCATGCCATCAAGACTTCAGTGTAGAGAAAAATTTCTTATGACTCAAAGTCCTAACCACAAAGAAAAGATTGTT
AATTAGATTGCATGAATATTAAGACTTATTTTTAAAATTAAAAAACCATTAAGAAAAGTCAGGCCATAGAATGACAGAAAATATTTGCAACACCCCAGTAAAGAG
AATTGTAATATGCAGATTATAAAAAGAAGTCTTACAAATCAGTAAAAAATAAAACTAGACAAAAATTTGAACAGATGAAAGAGAAACTCTAAATAATCATTACA
CATGAGAAACTCAATCTCAGAAATCAGAGAACTATCATTGCATATACACTAAATTAGAGAAATATTAAAAGGCTAAGTAACATCTGTGGCTTAATTAA[illegible]CT
CTAGTGATCAGCAGTTCAACCTGTTGATAGTATGTACTAAGCTCTCATGTTTAATGTACTAAGCTCTCATGTTTAATGAACTAAACCCTCATGGCTAATGTACTAA
GCTCTCATGGCTAATGTACTAAGCTCTCATGTTTCATGTACTAAGCTCTCATGTTTGAACAATAAAATTAATATAAATCAGCAACTTAAATAGCCTCTAAGGTTTTA
AGTTTTATAAGAAAAAAAAGAATATATAAGGCTTTTAAAGGTTTTAAGGTTTCCTAGGTTATCCTCATATGAGCTCTTAGAAAAACTCATCCAGCATCAAATGAA
ACTGCAATTTATTCATATCAGGATTATCAATACCATATTTTTGAAAAAGTCTTTTCTGTAATGAAGGAGAAAACTCACCCAGGCAGTTCCATAGGATGGCAAGATC
CTGGTATCTGTCTGCAATTCCAACTCTTCCAACATCAATACAACCTATTAATTTCCCCTCATCAAAAATAAGGTTATCAAGTGAGAAATCACCATGAGTGACCACT
GAATCTGGTGAGAATGGCAAAAGATTATGCATTTCTTTCCAGACTTGTTCAACAGGCCAGCCATTTCTCTCATCATCAAAATCACTGGCATCAACCAAACCATTAT
TCATTCTTGATTGGGCCTGAGCCAGTCTAAATACTCTATCAGAGTTAAAAGGACAATTACAAACAGGAATGGAATGCAATCTTCTCAGGAACACTGCCAGGGCA
TCAACAATATTTTCACCTGAATCAGGATATTCTTCCAATACCTGGAATGCTGTTTTCCCTGGGATGGCAGTGGTGAGTAACCATGCATCATCAGGAGTTCTGATAA
AATGCTTGATGGTTGGAAGAGGCATAAATTCAGTCAGCCAGTTTAGTCTGACCATCTCATCTGTAACATCATTGGCAACAGAACCTTTGCCATGTTTCAGAAACA
ACTCTGGGGCATCTGGCTTCCCATACAATCTATAGATTGTGGCACCTGATTGCCCAACATTATCTCTAGCCCATTTATACCCATATAAATCAGCATCCATGTTGGA
ATTTAATCTTGGCCTGGAGCAAGAGGTTTCTCTTTGAATATGGCTCATACATGTGCA[illegible]
[illegible]

FIG. 24

082620 # 5A : shACE2 TYLTNY-1xL-FcLALA- BV3 (SEQ ID NO:24)

DraIII-βGlo BI-Nhe---CMVΔEF1II26-BstEII -shACE2 TYLTNY-1xL-FcLALA-BglII-MaxpA-IFNβ S/MAR-BV3

CACTATGTGTTAATTAAAATTATCTCTAAGGCATGTGAACTGGCTGTCTTGGTTTTCATCTGTACTTCATCTGCTACCTCTGTGACCTGAAACATATTTATAATTCCA
TTAAGCTGTGCATATGATAGATTTATCATATGTATTTTCCTTAAAGGATTTTTGTAAGAACTAATTGAATTGATACCTGTAAAGTCTTTATCACACTACCCAATAAA
TAATAAATCTCTTTGTTCAGCTCTCTGTTTCTATAAATATGTACCAGTTTTATTGTTTTTAGTGGTAGTGATTTTATTCTCTTTCTATATATATACACACACATGTGTG
CATTCATAAATATATACAATTTTTATGAATAAAAAATTATTAGCAATCAATATTGAAAACCACTGATTTTTGTTTATGTGAGCAAACAGCAGATTAAAAGGAATTT
GAATTCTCATAGCTAGCAGGAGTCAATGGGAAAAACCCATTGGAGCCAAGTACACTGACTCAATAGGGACTTTCCATTGGGTTTTGCCCAGTACATAAGGTCAA
TAGGGGGTGAGTCAACAGGAAAGTCCCATTGGAGCCAAGTACATTGAGTCAATAGGGACTTTCCAATGGGTTTTGCCCAGTACATAAGGTCAATGGGAGGTAA
GCCAATGGGTTTTTCCCATTACTGGCACGTATACTGAGTCATTAGGGACTTTCCAATGGGTTTTGCCCAGTACATAAGGTCAATAGGGGTGAATCAACAGGAAA
GTCCCATTGGAGCCAAGTACACTGAGTCAATAGGGACTTTCCATTGGGTTTTGCCCAGTACAAAAGGTCAATAGGGGGTGAGTCAATGGGTTTTTCCCATTATTG
GCACATACATAAGGTCAATAGGGGTGACTAGTGGAGAAGAGCATGCTTGAGGGCTGAGTGCCCCTCAGTGGGCAGAGAGCACATGGCCCACAGTCCCTGAGA
AGTTGGGGGGAGGGGTGGGCAATTGAACTGGTGCCTAGAGAAGGTGGGGCTTGGGTAAACTGGGAAAGTGATGTGGTGTACTGGCTCCACCTTTTTCCCCAG
GGTGGGGGAGAACCATATATAAGTGCAGTAGTCTCTGTGAACATTCAAGCTTCTGCCTTCTCCCTCCTGTGAGTTTGGTAAGTCACTGACTGTCTATGCCTGGGA
AAGGGTGGGCAGGAGATGGGGCAGTGCAGGAAAAGTGGCACTATGAACCCTGCAGCCCTAGACAATTGTACTAACCTTCTTCTCTTTCCTCTCCTGACAGGTTG
GTAACCAAGCCACCATGAGCAGCAGCTCTTGGCTGCTGCTGAGTCTGGTGGCTGTGACAGCTGCCCAGAGCACCATTGAGGAACAGGCCAAGTACTTCCTGGA
CAAGTTCAACCATGAGGCTGAGGACCTGTTCTACCAGAGCAGCCTGGCCAGCTGGAACTACAACACCAACATCACTGAAGAGAATGTGCAGAACATGAACAAT
GCTGGGGACAAGTGGAGTGCCTTCCTGAAAGAGCAGAGCACAACCGCCCAGATGTACCCTCTGCAAGAGATCCAGAACCTGACAGTGAAGCTCCAGCTCCAGG
CTCTCCAGCAGAATGGCAGCTCTGTGCTGTCTGAGGACAAGAGCAAGAGACTGAACACCATCCTGAACACAATGAGCACCATCTACAGCACAGGCAAAGTCTG
CAACCCTGACAACCCTCAAGAGTGCCTGCTGCTGGAACCTGGCCTGAATGAGATCATGGCCAACAGCCTGGACTACAATGAGAGACTGTGGGCCTGGGAGTCT
TGGAGGAGTGAAGTGGGAAAGCAGCTGAGGCCCCTGTATGAGGAATATGTGGTGCTGAAGAATGAGATGGCCAGGGCCAACCACTATGAGGACTATGGGGA
TTATTGGAGGGGAGACTATGAAGTGAATGGTGTTGATGGCTATGACTACAGCAGGGGCCAGCTGATTGAGGATGTGGAACACACCTTTGAGGAAATCAAGCCC
CTCTATGAGCACCTCCATGCCTATGTCAGAGCCAAGCTGATGAATGCTTACCCCAGCTACATCAGCCCCATTGGCTGCCTGCCTGCTCATCTGCTGGGAGACATG
TGGGGCAGATTCTGGACCAACCTGTACAGCCTGACTGTGCCCTTTGGCCAGAAACCTAACATTGATGTGACAGATGCCATGGTGGATCAGGCCTGGGATGCCCA
GAGAATCTTCAAAGAGGCTGAGAAGTTCTTTGTGTCTGTGGGGCTGCCCAACATGACCCAAGGCTTTTGGGAGTACTCCATGCTGACAGACCCTGGCAATGTGC
AAAAGGCTGTGTGTCACCCCACAGCCTGGGACCTTGGCAAGGGAGACTTCAGAATCCTGATGTGCACCAAAGTGACAATGGATGACTTTCTGACAGCTCACCAT
GAGATGGGCCACATCCAGTATGACATGGCCTATGCTGCCCAGCCTTTCCTGCTGAGAAATGGGGCCAATGAGGGCTTCCATGAGGCAGTGGGAGAGATCATGA
GCCTGTCTGCTGCCACACCTAAGCACCTGAAGTCCATTGGCCTGCTGAGCCCTGACTTCCAAGAGGACAATGAGACAGAGATCAACTTCCTGCTCAAGCAGGCC
CTGACCATTGTGGGCACACTGCCCTTCACCTACATGCTGGAAAAGTGGAGATGGATGGTCTTTAAGGGAGAAATCCCCAAGGACCAGTGGATGAAGAAATGGT
GGGAGATGAAGAGGGAAATTGTGGGAGTTGTGGAACCTGTGCCACATGATGAGACATACTGTGACCCTGCCAGCCTGTTCCATGTGTCCAATGACTACTCCTTC
ATTAGGTACTACACCAGGACACTGTACCAGTTCCAGTTTCAAGAGGCTCTGTGTCAGGCTGCTAAACATGAGGGCCCACTGCACAAGTGTGACATCAGCAACTC
CACAGAGGCTGGACAGAAACTGTTCAACATGCTGAGACTGGGCAAGTCTGAGCCTTGGACTCTGGCCCTGGAAAATGTTGTGGGAGCCAAGAATATGAATGTC
AGACCCCTGCTGAACTACTTTGAGCCCCTGTTCACCTGGCTGAAGGACCAGAACAAGAACAGCTTTGTTGGCTGGTCCACAGACTGGTCCCCATATGCTGACCA
GAGCATCAAAGTCAGAATCAGCCTGAAGAGTGCCCTGGGAGATAAGGCCTATGAGTGGAATGATAATGAGATGTACCTGTTCAGGTCCTCTGTGGCTTATGCT
ATGAGACAGTACTTTCTGAAAGTGAAGAACCAGATGATCCTGTTTGGAGAAGAGGATGTCAGAGTGGCCAACCTGAAGCCTAGAATCAGCTTCAACTTCTTTGT
GACAGCCCCTAAGAATGTGTCTGACATCATCCCCAGAACAGAGGTGGAAAAGGCCATCAGAATGAGCAGGTCCAGGATCAATGATGCCTTCAGGCTCAATGAC
AACTCCCTGGAATTTCTGGGCATTCAGCCCACACTGGGCCCTCCAAATCAGCCTCCTGTGTCTTGGTGGAGGAGGTAGTGAGCCCAAGAGCTGTGACAAGACCCA
CACCTGTCCTCCATGTCCTGCTCCAGAGGCTGCTGGAGGACCTTCTGTGTTTCTGTTCCCTCCAAAGCCAAAGGACACCCTGATGATCAGCAGAACCCCTGAAGT
GACCTGTGTGGTGGTGGATGTGTCCCATGAGGACCCAGAAGTGAAGTTCAATTGGTATGTGGATGGTGTTGAGGTGCACAATGCCAAGACCAAGCCTAGAGA
GGAACAGTACAACAGCACCTACAGGGTTGTGTCAGTGCTGACTGTGCTGCACCAGGACTGGCTGAATGGCAAAGAGTACAAGTGCAAGGTGTCCAACAAGGCC
CTGCCTGCTCCTATTGAAAAGACCATCAGCAAGGCCAAGGGACAGCCTAGGGAACCCCAGGTGTACACACTGCCACCTAGCAGAGATGAGCTGACCAAGAATC
AGGTGTCCCTGACATGCCTTGTGAAGGGCTTCTACCCTTCTGACATTGCAGTGGAATGGGAGAGCAATGGCCAGCCTGAGAACAACTACAAGACAACCCCTCCT
GTGCTGGACTCTGATGGCTCATTCTTCCTGTACTCCAAGCTGACAGTGGACAAGTCCAGATGGCAGCAAGGCAATGTGTTCAGCTGCTCTGTGATGCATGAGGC
CCTGCACAACCACTACACACAGAAGTCCCTGTCTCTGAGCCCTGGCAAGTGAAGATCTACCTTCTGGCTAATAAAAGATCAGAGCTCTAGTGATCTGTGTGTTGGT
TTTTTGTGTCTGCATTCTAGCAAGTCAATATGTTCACCCCAAAAAAGCTGTTTGTTAACTTGTCAACCTCATTCTAAAATGTATATAGAAGCCCAAAAGACAATAA
CAAAAATATTCTTGTAGAACAAAATGGGAAAGAATGTTCCACTAAATATCAAGATTTAGAGCAAAGCATGAGATGTGTGGGGATAGACAGTGAGGCTGATAAA
ATAGAGTAGAGCTCAGAAACAGACCCATTGATATATGTAAGTGACCTATGAAAAAAATATGGCATTTTACAATGGGAAAATGATGGTCTTTTTCTTTTTTAGAAA
AACAGGGAAATATATTTATATGTAAAAAATAAAAGGGAACCCATATGTCATACCATACACACAAAAAAATTCCAGTGAATTATAAGTCTAAATGGAGAAGGCAA
AACTTTAAATCTTTTAGAAAATAATATAGAAGCATGCCATCAAGACTTCAGTGTAGAGAAAAATTTCTTATGACTCAAAGTCCTAACCACAAAGAAAAGATTGTT
AATTAGATTGCATGAATATTAAGACTTATTTTTAAAATTAAAAAACCATTAAGAAAAGTCAGGCCATAGAATGACAGAAAATATTTGCAACACCCCAGTAAAGAG
AATTGTAATATGCAGATTATAAAAAGAAGTCTTACAAATCAGTAAAAAATAAAACTAGACAAAAATTTGAACAGATGAAAGAGAAACTCTAAATAATCATTACA
CATGAGAAACTCAATCTCAGAAATCAGAGAACTATCATTGCATATACACTAAATTAGAGAAATATTAAAAGGCTAAGTAACATCTGTGGCTTAATTAACCTAGCT
CTAGTGATCAGCAGTTCAACCTGTTGATAGTATGTACTAAGCTCTCATGTTTAATGTACTAAGCTCTCATGTTTAATGAACTAAACCCTCATGGCTAATGTACTAA
GCTCTCATGGCTAATGTACTAAGCTCTCATGTTTCATGTACTAAGCTCTCATGTTTGAACAATAAAATTAATATAAATCAGCAACTTAAATAGCCTCTAAGGTTTTA
AGTTTTATAAGAAAAAAAAGAATATATAAGGCTTTTAAAGGTTTTAAGGTTTCCTAGGTTATCCTCATATGAGCTCTTAGAAAAACTCATCCAGCATCAAATGAA
ACTGCAATTTATTCATATCAGGATTATCAATACCATATTTTTGAAAAAGTCTTTTCTGTAATGAAGGAGAAAACTCACCCAGGCAGTTCCATAGGATGGCAAGATC
CTGGTATCTGTCTGCAATTCCAACTCTTCCAACATCAATACAACCTATTAATTTCCCCTCATCAAAAATAAGGTTATCAAGTGAGAAATCACCATGAGTGACCACT
GAATCTGGTGAGAATGGCAAAAGATTATGCATTTCTTTCCAGACTTGTTCAACAGGCCAGCCATTTCTCTCATCATCAAAATCACTGGCATCAACCAAACCATTAT
TCATTCTTGATTGGGCCTGAGCCAGTCTAAATACTCTATCAGAGTTAAAAGGACAATTACAAACAGGAATGGAATGCAATCTTCTCAGGAACACTGCCAGGGCA
TCAACAATATTTTCACCTGAATCAGGATATTCTTCCAATACCTGGAATGCTGTTTTCCCTGGGATGGCAGTGGTGAGTAACCATGCATCATCAGGAGTTCTGATAA
AATGCTTGATGGTTGGAAGAGGCATAAATTCAGTCAGCCAGTTTAGTCTGACCATCTCATCTGTAACATCATTGGCAACAGAACCTTTGCCATGTTTCAGAAACA
ACTCTGGGGCATCTGGCTTCCCATACAATCTATAGATTGTGGCACCTGATTGCCCAACATTATCTCTAGCCCATTTATACCCATATAAATCAGCATCCATGTTGGA
ATTTAATCTTGGCCTGGAGCAAGAGGTTTCTCTTTGAATATGGCTCATACATGTGCACCTCCTATAGTGAGTTGTATTATACTATGCAGATATACTATGCCAATGT
TTAATTGTCAG

FIG. 25

080420 # 4 : shACE2- shACE2-BV3 (SEQ ID NO:25)

DraIII-**βGlo** BI-Nhe–AmCMV&EF1126-BstEII -**shACE2**-BglII-MaxpA-**21q21**-AmCMV-&EF1126-BstEII - **shACE2**-BglII-MaxpA-**IFNβ S/MAR**-BV3

CACTATGTGTTAATTAAAATTATCTCTAAGGCATGTGAACTGGCTGTCTTGGTTTTCATCTGTACTTCATCTGCTACCTCTGTGACCTGAAACATATTTATAATTCCATTAAGCTGTGCATATGATAGATTT
ATCATATGTATTTTCCTTAAAGGATTTTTGTAAGAACTAATTGAATTGATACCTGTAAAGTCTTTATCACACTACCCAATAAATAATAAATCTCTTTGTTCAGCTCTCTGTTTCTATAAATATGTACCAGTTT
TATTGTTTTTAGTGGTAGTGATTTTATTCTCTTTCTATATATATACACACACATGTGTGCATTCATAAATATATACAATTTTTATGAATAAAAAATTATTAGCAATCAATATTGAAAACCACTGATTTTTGTT
TATGTGAGCAAACAGCAGATTAAAAGG**AATTT**GAATTC**TCATA**GCTAGCAG[illegible]
[illegible]
CCTCAGTGGGCAGAGAGCACATGGCCCACAGTCCCTGAGAAGTTGGGGGGAGGGGTGGGCAATTGAACTGGTGCCTAGAGAAGGTGGGGCTTGGGTAAACTGGGAAAGTGATGTGGTGTACTGGC
TCCACCTTTTTCCCCAGGGTGGGGGAGAACCATATATAAGTGCAGTAGTCTCTGTGAACATTCAAGCTTCTGCCTTCTCCCTCCTGTGAGTTTGGTAAGTCACTGACTGTCTATGCCTGGGAAAGGGTG
GGCAGGAGATGGGGCAGTGCAGGAAAAGTGGCACTATGAACCCTGCAGCCCTAGACAATTGTACTAACCTTCTTCTCTTTCCTCTCCTGACAGGTTGGTAACC[illegible]
[illegible]
[illegible]**TAA**AGATCT[illegible]**AGAGCCCCACTGTGTTCAT**
CTTACAGATGGAAATACTGACATTCAGAGGAGTTAGTTAACTTGCCTAGGTGATTCAGCTAATAAGTGCAAGAAAGATTTCAATCCAAGGTGATTTGATTCTGAAGCCTGTGCTAATCACATTACACCA
AGCTACAACTTCATTTATAAATAATAAGTCAGCTTTCAAGGGCCCTTTCAGGTGTCCTGCACTTCTACAAGCTGTGCCATTTAGTGAACACAAAATGAGCCTTCTGATGAAGTAGTCTTTTCATTATTTCAG
ATATTAGAACACTAAAATTCTTAGCTGCCAGCTGATTGAAGGCTGGGACAAAATTCAAACATGCATCTACAACAATATATATCTCAATGTTAGTCTCCAAATTCTATTGACTTCAACTCAAGAGAATATA
AAGAGCTAGTCTTTATACACTCTTTAAGGTATGATATCATCTGGAAAGTAACAAAATTGATGCAAATTTGAATGAACTTTATCATGGTGTATTTACACAATGTGTTTCTTCTCCCTGCAATGTATTTCTTTC
TCTAATTCCTTCCATTTGATCTTTCATACACAATCTGGTTCTGATGTATGTTTTTTGGATGCACTTTTCAACTCCAAAAGACAGAGCTAGTTACTTTCTTCCTGGTGCTCCAAGCACTGTATTTGTATCTGTA
TTCAAGCCCTTTGCAATATTGTACTGGATCATTATTTCACCTCTAGGATGGCTTCCCCAGGCAACTTGTGTTCACCCAGAGACTACATTTTGTATCTTGTTGACCTTTGAACTTCCACCAGTGTCTAAAAAT
AATATGTATGCAAAATTACTTGCTATGAGAATGTATAATTAAACAATATAAAAAGGAGAAGCAAGGAGAGAAACACAGGTGTGTATTTGTGTTTGTGTGCTTAAAAGGCAGTGTGGAAAAGGAAGAA
ATGCCATTTATAGTGAGGAGACAAAGTTATATTACCTCTTATCTGGCTTTTAAGGAGATTTTGCTGAGCTAAAAATCCTATATTCATAGAAAAGCCTTACCTGAGTTGCCAATACCTCAATTCAGTCTAGC
[illegible]ACTAGTGGAGAAGAGCATGCTTGAGGCCTGAGTGCCCCTCAGTGGGCAGAGAGCACATGGCCCACAGTCCCTGAGAAGTTGGGGG
GAGGGGTGGGCAATTGAACTGGTGCCTAGAGAAGGTGGGGCTTGGGTAAACTGGGAAAGTGATGTGGTGTACTGGCCTCCACCTTTTTCCCCAGGGTGGGGGAGAACCATATATAAGTGCAGTAGTC
TCTGTGAACATTCAAGCTTCTGCCTTCTCCCTCCTGTGAGTTTGGTAAGTCACTGACTGTCTATGCCTGGGAAAGGGTGGGCAGGAGATGGGGCAGTGCAGGAAAAGTGGCACTATGAACCCTGCAGC
CCTAGACAATTGTACTAACCTTCTTCTCTTTCCTCTCCTGACAGGTTGGTAACC[illegible]
[illegible]**TAA**AGATCT[illegible]**AGTCAATATGTTCACCCCAAAAAAGCTGTTTGTTAACTTGTCAACCTCATTCTAAAATGTATATAGAAG**
CCCAAAAGACAATAACAAAAAATATTCTTGTAGAACAAAATGGGAAAGAATGTTCCACTAAATATCAAGATTTAGAGCAAAGCATGAGATGTGTGGGGATAGACAGTGAGGCTGATAAAATAGAGTAG
AGCTCAGAAACAGACCCATTGATATATGTAAGTGACCTATGAAAAAAATATGGCATTTTACAATGGGAAAATGATGGTCTTTTTCTTTTTTAGAAAAACAGGGAAATATATTTATATGTAAAAAATAAA
AGGGAACCCATATGTCATACCATACACACAAAAAAATTCCAGTGAATTATAAGTCTAAATGGAGAAGGCAAAACTTTAAATCTTTTAGAAAATAATATAGAAGCATGCCATCAAGACTTCAGTGTAGAG
AAAAATTTCTTATGACTCAAAGTCCTAACCACAAAGAAAAGATTGTTAATTAGATTGCATGAATATTAAGACTTATTTTTAAAATTAAAAAACCATTAAGAAAAGTCAGGCCATAGAATGACAGAAAAT
ATTTGCAACACCCCAGTAAAGAGAATTGTAATATGCAGATTATAAAAAGAAGTCTTACAAATCAGTAAAAAAATAAAACTAGACAAAAATTTGAACAGATGAAAGAGAAACTCTAAATAATCATTACAC
ATGAGAAACTCAATCTCAGAAATCAGAGAACTATCATTGCATATACACTAAATTAGAGAAATATTAAAAGGCTAAGTAACATCTGTGGCTTAATTAA[illegible]**TCTAGT**GATCAGCAGTTCAACCTGTTG
ATAGTATGTACTAAGCTCTCATGTTTAATGTACTAAGCTCTCATGTTTAATGAACTAAACCCTCATGGCTAATGTACTAAGCTCTCATGGCTAATGTACTAAGCTCTCATGTTTCATGTACTAAGCTCTCAT
GTTTGAACAATAAAATTAATATAAATCAGCAACTTAAATAGCCTCTAAGGTTTTAAGTTTTATAAGAAAAAAAAAGAATATATAAGGCTTTTAAAGGTTTTAAGGTTTCCTAGGTTATCC**TCATATGAGCT**
CTTAGAAAAACTCATCCAGCATCAAATGAAACTGCAATTTATTCATATCAGGATTATCAATACCATATTTTTGAAAAAGTCTTTTCTGTAATGAAGGAGAAAACTCACCCAGGCAGTTCCATAGGATGGC
AAGATCCTGGTATCTGTCTGCAATTCCAACTCTTCCAACATCAATACAACCTATTAATTTCCCCTCATCAAAAATAAGGTTATCAAGTGAGAAATCACCATGAGTGACCACTGAATCTGGTGAGAATGGC
AAAAGATTATGCATTTCTTTCCAGACTTGTTCAACAGGCCAGCCATTTCTCTCATCATCAAAATCACTGGCATCAACCAAACCATTATTCATTCTTGATTGGGCCTGAGCCAGTCTAAATACTCTATCAGA
GTTAAAAGGACAATTACAAACAGGAATGGAATGCAATCTTCTCAGGAACACTGCCAGGGCATCAACAATATTTTCACCTGAATCAGGATATTCTTCCAATACCTGGAATGCTGTTTTCCCTGGGATGGC
AGTGGTGAGTAACCATGCATCATCAGGAGTTCTGATAAAATGCTTGATGGTTGGAAGAGGCATAAATTCAGTCAGCCAGTTTAGTCTGACCATCTCATCTGTAACATCATTGGCAACAGAACCTTTGCC
ATGTTTCAGAAACAACTCTGGGGCATCTGGCTTCCCATACAATCTATAGATTGTGGCACCTGATTGCCCAACATTATCTCTAGCCCATTTATACCCATATAAATCAGCATCCATGTTGGAATTTAATCTTG
GCCTGGAGCAAGAGGTTTCTCTTTGAATATGGCTCAT**ACATGTGCA**[illegible]

FIG. 26

081120 # 1 : B38Kappa- shACE2-BV3 (SEQ ID NO:26)

DraIII-**βGlo** BI-Nhe--AmCMV&EF1126-BstEII **-B38Kappa**-BglII-MirpA-**21q21**-AmCMV&EF1126-BstEII **- shACE2**-BglII-Mirpa-**IFNβ S/MAR**-BV3

CACTATGTGTTAATTAAAATTATCTCTAAGGCATGTGAACTGGCTGTCTTGGTTTTCATCTGTACTTCATCTGCTACCTCTGTGACCTGAAACATATTTATAATTCCATTAAGCTGTGCATATGATAGATTT
ATCATATGTATTTTCCTTAAAGGATTTTTGTAAGAACTAATTGAATTGATACCTGTAAAGTCTTTATCACACTACCCAATAAATAATAAATCTCTTTGTTCAGCTCTCTGTTTCTATAAATATGTACCAGTTT
TATTGTTTTTAGTGGTAGTGATTTTATTCTCTTTCTATATATATACACACACATGTGTGCATTCATAAATATATACAATTTTTATGAATAAAAAATTATTAGCAATCAATATTGAAAACCACTGATTTTTGTT
TATGTGAGCAAACAGCAGATTAAAAGG**AATTT**GAATTC**TCATA**GCTAGCAG[illegible]
[illegible]
[illegible]
[illegible]ACTACTGGAGAAGAGCATGCTTGAGGGCTGAGTGCC
CCTCAGTGGGCAGAGAGCACATGGCCCACAGTCCCTGAGAAGTTGGGGGGAGGGGTGGGCAATTGAACTGGTGCCTAGAGAAGGTGGGGCTTGGGTAAACTGGGAAAGTGATGTGGTGTACTGGC
TCCACCTTTTTCCCCAGGGTGGGGGAGAACCATATATAAGTGCAGTAGTCTCTGTGAACATTCAAGCTTCTGCCTTCTCCCTCCTGTGAGTTTGGTAAGTCACTGACTGTCTATGCCTGGGAAAGGGTG
GGCAGGAGATGGGGCAGTGCAGGAAAAGTGGCACTATGAACCCTGCAGCCCTAGACAATTGTACTAACCTTCTTCTCTTTCCTCTCCTGACAGGTTGGTAACC[illegible]CATGGGATGGTGCCTGAT
CCTGCCTGTTTCTGCCTGGCCTGTGGCCACCAGACTGCTGTCTGAAGTGCAGCTGGTGGAAACTGGTGGTGGCCTGGTTCAGCCTGGTGGCTCTCTGAGACTGAGCTGTGCTGCCTCTGGCTTCATTGTGT
CCAGCAACTACATGAGCTGGGTCAGACAGGCCCCTGGCAAAGGACTGGAATGGGTGTCAGTGATCTACAGTGGTGGCAGCACCTACTATGCTGACTCTGTGAAGGGCAGATTCACCATCAGCAGACA
CAACAGCAAGAACACCCTGTACCTGCAGATGAACAGCCTGAGAGCTGAGGACACTGCTGTGTACTACTGTGCCAGAGAAGCCTATGGCATGGATGTGTGGGGCCAGGGCACAACAGTGACTGTGTCC
TCTGCCAGCACAAAGGGCCCCTCTGTCTTTCCTCTGGCTCCCAGCAGCAAGAGCACCAGTGCTGCAACAGCTGCCCTGGGCTGTCTGGTCAAGGACTACTTTCCTGAGCCTGTGACAGTGTCCTGGAA
CTCTGGGGCTCTGACATCTGGGGTGCACACATTCCCTGCAGTGCTGCAGTCCTCTGGCCTGTACAGCCTGTCCTCTGTGGTCACAGTGCCTAGCTCTAGCCTGGGCACCCAGACCTACATCTGCAATGT
GAACCACAAGCCTAGCAACACCAAGGTGGACAAGAAGGCTGAGCCCAAGAGCTGTGACAAGACCCACACCTGTCCTCCATGTCCT[illegible]
[illegible]
[illegible]
[illegible]
[illegible]
[illegible]CAGATGGCAGCAGGGCAATGTCTTTAGCTGCTCTGTGATGCATGAGGCCCTGCACAACCACTACACACAGAAGTCCCTGTCTCTGAGCCCTGGCAAG***AGAAAGAGAAGGAGTGGCTCTGGGGCCACC***
AACTTCAGCCTGCTGAAACAGGCTGGGGATGTTGAAGAGAACCCTGGACCT[illegible]
[illegible]
[illegible]
[illegible]
[illegible]
[illegible]**TGA**AGA
[illegible]AGAGCCCCACTGTGTTCATCTTACAGATGGAAATACTGACATTCAGAGGAGTTAGTTAA
CTTGCCTAGGTGATTCAGCTAATAAGTGCAAGAAAGATTTCAATCCAAGGTGATTTGATTCTGAAGCCTGTGCTAATCACATTACACCAAGCTACAACTTCATTTATAAATAATAAGTCAGCTTTCAAGG
GCCTTTCAGGTGTCCTGCACTTCTACAAGCTGTGCCATTTAGTGAACACAAAATGAGCCTTCTGATGAAGTAGTCTTTTCATTATTTCAGATATTAGAACACTAAAATTCTTAGCTGCCAGCTGATTGAAG
GCTGGGACAAAATTCAAACATGCATCTACAACAATATATATCTCAATGTTAGTCTCCAAATTCTATTGACTTCAACTCAAGAGAATATAAAGAGCTAGTCTTTATACACTCTTTAAGGTATGATATCATCT
GGAAAGTAACAAAATTGATGCAAATTTGAATGAACTTTATCATGGTGTATTTACACAATGTGTTTCTTCTCCCTGCAATGTATTTCTTTCTCTAATTCCTTCCATTTGATCTTTCATACACAATCTGGTTCTG
ATGTATGTTTTTTGGATGCACTTTTCAACTCCAAAAGACAGAGCTAGTTACTTTCTTCCTGGTGCTCCAAGCACTGTATTTGTATCTGTATTCAAGCCCTTTGCAATATTGTACTGGATCATTATTTCACCTC
TAGGATGGCTTCCCCAGGCAACTTGTGTTCACCCAGAGACTACATTTTGTATCTTGTTGACCTTTGAACTTCCACCAGTGTCTAAAAATAATATGTATGCAAAATTACTTGCTATGAGAATGTATAATTAA
ACAATATAAAAAGGAGAAGCAAGGAGAGAAACACAGGTGTGTATTTGTGTTTGTGTGCTTAAAAGGCAGTGTGGAAAAGGAAGAAATGCCATTTATAGTGAGGAGACAAAGTTATATTACCTCTTAT
CTGGCTTTTAAGGAGATTTTGCTGAGCTAAAAATCCTATATTCATAGAAAAGCCTTACCTGAGTTGCCAATACC**TCAATTCAG**TCTAGCAG[illegible]
[illegible]
[illegible]
[illegible]
[illegible]CACTAGTGGAGAAGAGCATGCTTGAGGGCTGAGTGCCCCTCAGTGGGCAGAGAGCACATGGCCCACAGTCCCTGAGAAGTTGGGGGGAGGGGTGGGCAATTGAACTGGTGCCTAGAGAAGGTGG
GGCTTGGGTAAACTGGGAAAGTGATGTGGTGTACTGGCTCCACCTTTTTCCCCAGGGTGGGGGAGAACCATATATAAGTGCAGTAGTCTCTGTGAACATTCAAGCTTCTGCCTTCTCCCTCCTGTGAGT
TTGGTAAGTCACTGACTGTCTATGCCTGGGAAAGGGTGGGCAGGAGATGGGGCAGTGCAGGAAAAGTGGCACTATGAACCCTGCAGCCCTAGACAATTGTACTAACCTTCTTCTCTTTCCTCTCCTGA
[illegible]
[illegible]**TAA**AGATCTACTTCT[illegible]
[illegible]AGTCAATATGTTCACCCCAAAAAAGCTGTTTGTTAACTTGTCAACCTCATTCTAAAATGTATATAGAAGCCCAAAAGACAATAACAAAAATATTCTTGTAGAACAAAATG
GGAAAGAATGTTCCACTAAATATCAAGATTTAGAGCAAAGCATGAGATGTGTGGGGATAGACAGTGAGGCTGATAAAATAGAGTAGAGCTCAGAAACAGACCCATTGATATATGTAAGTGACCTATG
AAAAAAATATGGCATTTTACAATGGGAAAATGATGGTCTTTTTCTTTTTTAGAAAAACAGGGAAATATATTTATATGTAAAAAATAAAAGGGAACCCATATGTCATACCATACACACAAAAAAATTCCA
GTGAATTATAAGTCTAAATGGAGAAGGCAAAACTTTAAATCTTTTAGAAAATAATATAGAAGCATGCCATCAAGACTTCAGTGTAGAGAAAAATTTCTTATGACTCAAAGTCCTAACCACAAAGAAAAG
ATTGTTAATTAGATTGCATGAATATTAAGACTTATTTTTAAAATTAAAAAACCATTAAGAAAAGTCAGGCCATAGAATGACAGAAAATATTTGCAACACCCCAGTAAAGAGAATTGTAATATGCAGATT
ATAAAAAGAAGTCTTACAAATCAGTAAAAAATAAAACTAGACAAAAATTTGAACAGATGAAAGAGAAACTCTAAATAATCATTACACATGAGAAACTCAATCTCAGAAATCAGAGAACTATCATTGCA
TATACACTAAATTAGAGAAATATTAAAAGGCTAAGTAACATCTGTGGC**TTAATTAA**[illegible]**TCTAGT**GATCAGCAGTTCAACCTGTTGATAGTATGTACTAAGCTCTCATGTTTAATGTACTAAGCTCTC
ATGTTTAATGAACTAAACCCTCATGGCTAATGTACTAAGCTCTCATGGCTAATGTACTAAGCTCTCATGTTTCATGTACTAAGCTCTCATGTTTGAACAATAAAATTAATATAAATCAGCAACTTAAATAG
CCTCTAAGGTTTTAAGTTTTATAAGAAAAAAAAGAATATATAAGGCTTTTAAAGGTTTTAAGGTTTCCTAGGTTATCC**TCATATGAGCTC**TTAGAAAAACTCATCCAGCATCAAATGAAACTGCAATTTAT
TCATATCAGGATTATCAATACCATATTTTTGAAAAAGTCTTTTCTGTAATGAAGGAGAAAACTCACCCAGGCAGTTCCATAGGATGGCAAGATCCTGGTATCTGTCTGCAATTCCAACTCTTCCAACATC
AATACAACCTATTAATTTCCCCTCATCAAAAATAAGGTTATCAAGTGAGAAATCACCATGAGTGACCACTGAATCTGGTGAGAATGGCAAAAGATTATGCATTTCTTTCCAGACTTGTTCAACAGGCCAG
CCATTTCTCTCATCATCAAAATCACTGGCATCAACCAAACCATTATTCATTCTTGATTGGGCCTGAGCCAGTCTAAATACTCTATCAGAGTTAAAAGGACAATTACAAACAGGAATGGAATGCAATCTTCT
CAGGAACACTGCCAGGGCATCAACAATATTTTCACCTGAATCAGGATATTCTTCCAATACCTGGAATGCTGTTTTCCCTGGGATGGCAGTGGTGAGTAACCATGCATCATCAGGAGTTCTGATAAAATG
CTTGATGGTTGGAAGAGGCATAAATTCAGTCAGCCAGTTTAGTCTGACCATCTCATCTGTAACATCATTGGCAACAGAACCTTTGCCATGTTTCAGAAACAACTCTGGGGCATCTGGCTTCCCATACAAT
CTATAGATTGTGGCACCTGATTGCCCAACATTATCTCTAGCCCATTTATACCCATATAAATCAGCATCCATGTTGGAATTTAATCTTGGCCTGGAGCAAGAGGTTTCTCTTTGAATATGGCTCAT**ACATGT**
GCA[illegible]

FIG. 27

081120 # 4 : shACE2-B38Kappa -BV3 (SEQ ID NO:27)

DraIII-βGlo BI-Nhe-AmCMV&EF1126-BstEII -shACE2-BglII-Mxpa-21q21-AmCMV-&EF1126-BstEII - B38Kappa -BglII-Mxpa-IFNβ S/MAR-BV3

CACTATGTGTTAATTAAAATTATCTCTAAGGCATGTGAACTGGCTGTCTTGGTTTTCATCTGTACTTCATCTGCTACCTCTGTGACCTGAAACATATTTATAATTCCATTAAGCTGTGCATATGATAGATTT
ATCATATGTATTTTCCTTAAAGGATTTTTGTAAGAACTAATTGAATTGATACCTGTAAAGTCTTTATCACACTACCCAATAAATAATAAATCTCTTTGTTCAGCTCTCTGTTTCTATAAATATGTACCAGTTT
TATTGTTTTTAGTGGTAGTGATTTTATTCTCTTTCTATATATATACACACACATGTGTGCATTCATAAATATATACAATTTTTATGAATAAAAAATTATTAGCAATCAATATTGAAAACCACTGATTTTTGTT
TATGTGAGCAAACAGCAGATTAAAAGG**AATTT**GAATTC**TCATA**GCTAGCAG[illegible]
[illegible]
CCTCAGTGGGCAGAGAGCACATGGCCCACAGTCCCTGAGAAGTTGGGGGGAGGGGTGGGCAATTGAACTGGTGCCTAGAGAAGGTGGGGCTTGGGTAAACTGGGAAAGTGATGTGGTGTACTGGC
TCCACCTTTTTCCCCAGGGTGGGGGAGAACCATATATAAGTGCAGTAGTCTCTGTGAACATTCAAGCTTCTGCCTTCTCCCTCCTGTGAGTTTGGTAAGTCACTGACTGTCTATGCCTGGGAAAGGGTG
GGCAGGAGATGGGGGCAGTGCAGGAAAAGTGGCACTATGAACCCTGCAGCCCTAGACAATTGTACTAACCTTCTTCTCTTTCCTCTCCTGACAGGTTGGTAACC[illegible]
[illegible]**TAA**AGATCT[illegible]**AGAGCCCCACTGTGTTCAT**
CTTACAGATGGAAATACTGACATTCAGAGGAGTTAGTTAACTTGCCTAGGTGATTCAGCTAATAAGTGCAAGAAAGATTTCAATCCAAGGTGATTTGATTCTGAAGCCTGTGCTAATCACATTACACCA
AGCTACAACTTCATTTATAAATAATAAGTCAGCTTTCAAGGGCCCTTTCAGGTGTCCTGCACTTCTACAAGCTGTGCCATTTAGTGAACACAAAATGAGCCTTCTGATGAACTAGTCTTTTCATTATTTCAG
ATATTAGAACACTAAAATTCTTAGCTGCCAGCTGATTGAAGGCTGGGACAAAATTCAAACATGCATCTACAACAATATATATCTCAATGTTAGTCTCCAAATTCTATTGACTTCAACTCAAGAGAATATA
AAGAGCTAGTCTTTATACACTCTTTAAGGTATGATATCATCTGGAAAGTAACAAAATTGATGCAAATTTGAATGAACTTTATCATGGTGTATTTACACAATGTGTTTCTTCTCCCTGCAATGTATTTCTTTC
TCTAATTCCTTCCATTTGATCTTTCATACACAATCTGGTTCTGATGTATGTTTTTTGGATGCACTTTTCAACTCCAAAAGACAGAGCTAGTTACTTTCTTCCTGGTGCTCCAAGCACTGTATTTGTATCTGTA
TTCAAGCCCTTTGCAATATTGTACTGGATCATTATTTCACCTCTAGGATGGCTTCCCCAGGCAACTTGTGTTCACCCAGAGACTACATTTTGTATCTTGTTGACCTTTGAACTTCCACCAGTGTCTAAAAAT
AATATGTATGCAAAATTACTTGCTATGAGAATGTATAATTAAACAATATAAAAAGGAGAAGCAAGGAGAGAAACACAGGTGTGTATTTGTGTTTGTGTGCTTAAAAGGCAGTGTGGAAAAGGAAGAA
ATGCCATTTATAGTGAGGAGACAAAGTTATATTACCTCTTATCTGGCTTTTAAGGAGATTTTGCTGAGCTAAAAATCCTATATTCATAGAAAAGCCTTACCTGAGTTGCCAATACC**TCAATTCAG**TCTAGC
[illegible]
[illegible]ACTAGTGGAGAAGAGCATGCTTGAGGGCTGAGTGCCCCTCAGTGGGCAGAGAGCACATGGCCCACAGTCCCTGAGAAGTTGGGGG
GAGGGGTGGGCAATTGAACTGGTGCCTAGAGAAGGTGGGGCTTGGGTAAACTGGGAAAGTGATGTGGTGTACTGGCCTCCACCTTTTTCCCCAGGGTGGGGGAGAACCATATATAAGTGCAGTAGTC
TCTGTGAACATTCAAGCTTCTGCCTTCTCCCTCCTGTGAGTTTGGTAAGTCACTGACTGTCTATGCCTGGGAAAGGGTGGGCAGGAGATGGGGCAGTGCAGGAAAAGTGGCACTATGAACCCTGCAGC
CCTAGACAATTGTACTAACCTTCTTCTCTTTCCTCTCCTGACAGGTTGGTAACC[illegible]ATGGCATGGCTCCCTGATCCTGCTGTTTCTGCTGGCCTGTGGCCACCAGACTGCTGTCTGAAGTGCAGCT
GGTGGAAAGTGGTGGTGGCCTGGTTCAGCCTGGTGGCTCTCTGAGACTGAGCTGTGCTGCCTCTGGCTTCATTGTGTCCAGCAACTACATGAGCTGGGTCAGACAGGCCCCTGGCAAAGGACTGGAA
TGGGTGTCAGTGATCTACAGTGGTGGCAGCACCTACTATGCTGACTCTGTGAAGGGCAGATTCACCATCAGCAGAGACAACAGCAAGAACACCCTGTACCTGCAGATGAACAGCCTGAGAGCTGAGG
ACACTGCTGTGTACTACTGTGCCAGAGAAGCCTATGGCATGGATGTCTGGGGCCAGGGCACAACAGTGACTGTGTCCTCTGCCAGCACAAAGGGCCCCTCTGTGTTTCCTCTGGCTCCCAGCAGCAAG
AGCACCAGTGGTGGAACAGCTGCCCTGGGCTGTCTGGTCAAGGACTACTTTCCTGAGCCTGTGACAGTGTCCTGGAACTCTGGGGCTCTGACATCTGGGGTGCACACATTCCCTGCAGTGCTGCAGTC
CTCTGGCCTGTACAGCCTGTCCTCTGTGGTCACAGTGCCTAGCTCTAGCCTGGGCACCCAGACCTACATCTGCAATGTGAACCACAAGCCTAGCAACACCAAGGTGGACAAGAAGGCTGAGCCCAAGA
GCTGTGACAAGACCCACACCTGTCCTCCATGTCCT[illegible]
[illegible]
[illegible]***AGAAAGAGAAGGAGTGGCTCTGGGGCCACCAACTTCAGCCTGCTGAAACAGGCTGGGGATGTTGAAGAGAACCCTGGA***
CCT[illegible]
[illegible]**TGA**[illegible]
[illegible]AGTCAATATGTTCACCCCAAAAAAGCTGTTTGTTAACTTGTCAACCTCATTCTAAAATGTATATAGAAGCCCAAAAGACAATAACAAAAATATTCTTGTAGAACAAAAT
GGGAAAGAATGTTCCACTAAATATCAAGATTTAGAGCAAAGCATGAGATGTGTGGGGATAGACAGTGAGGCTGATAAAATAGAGTAGAGCTCAGAAACAGACCCATTGATATATGTAAGTGACCTAT
GAAAAAAATATGGCATTTTACAATGGGAAAATGATGGTCTTTTTCTTTTTTAGAAAAACAGGGAAATATATTTATATGTAAAAAATAAAAGGGAACCCATATGTCATACCATACACACAAAAAAATTCC
AGTGAATTATAAGTCTAAATGGAGAAGGCAAAACTTTAAATCTTTTAGAAAATAATATAGAAGCATGCCATCAAGACTTCAGTGTAGAGAAAAATTTCTTATGACTCAAAGTCCTAACCACAAAGAAAA
GATTGTTAATTAGATTGCATGAATATTAAGACTTATTTTTAAAATTAAAAAACCATTAAGAAAAGTCAGGCCATAGAATGACAGAAAATATTTGCAACACCCCAGTAAAGAGAATTGTAATATGCAGAT
TATAAAAAGAAGTCTTACAAATCAGTAAAAAATAAAACTAGACAAAAAATTTGAACAGATGAAAGAGAAACTCTAAATAATCATTACACATGAGAAACTCAATCTCAGAAATCAGAGAACTATCATTGC
ATATACACTAAATTAGAGAAATATTAAAAGGCTAAGTAACATCTGTGGC**TTAATTAA**[illegible]**TCTAGT**GATCAGCAGTTCAACCTGTTGATAGTATGTACTAAGCTCTCATGTTTAATGTACTAAGCTCT
CATGTTTAATGAACTAAACCCTCATGGCTAATGTACTAAGCTCTCATGGCTAATGTACTAAGCTCTCATGTTTCATGTACTAAGCTCTCATGTTTGAACAATAAAATTAATATAAATCAGCAACTTAAATA
GCCTCTAAGGTTTTAAGTTTTATAAGAAAAAAAAGAATATATAAGGCTTTTAAAGGTTTTAAGGTTTCCTAGGTTATCC**TCATATGAGCTC**TTAGAAAAACTCATCCAGCATCAAATGAAACTGCAATTT
ATTCATATCAGGATTATCAATACCATATTTTTGAAAAAGTCTTTTCTGTAATGAAGGAGAAAACTCACCCAGGCAGTTCCATAGGATGGCAAGATCCTGGTATCTGTCTGCAATTCCAACTCTTCCAACAT
CAATACAACCTATTAATTTCCCCTCATCAAAAATAAGGTTATCAAGTGAGAAATCACCATGAGTGACCACTGAATCTGGTGAGAATGGCAAAAGATTATGCATTTCTTTCCAGACTTGTTCAACAGGCCA
GCCATTTCTCTCATCATCAAAATCACTGGCATCAACCAAACCATTATTCATTCTTGATTGGGCCTGAGCCAGTCTAAATACTCTATCAGAGTTAAAAGGACAATTACAAACAGGAATGGAATGCAATCTT
CTCAGGAACACTGCCAGGGCATCAACAATATTTTCACCTGAATCAGGATATTCTTCCAATACCTGGAATGCTGTTTTCCCTGGGATGGCAGTGGTGAGTAACCATGCATCATCAGGAGTTCTGATAAAA
TGCTTGATGGTTGGAAGAGGCATAAATTCAGTCAGCCAGTTTAGTCTGACCATCTCATCTGTAACATCATTGGCAACAGAACCTTTGCCATGTTTCAGAAACAACTCTGGGGCATCTGGCTTCCCATACA
ATCTATAGATTGTGGCACCTGATTGCCCAACATTATCTCTAGCCCATTTATACCCATATAAATCAGCATCCATGTTGGAATTTAATCTTGGCCTGGAGCAAGAGGTTTCTCTTTGAATATGGCTCAT**ACAT**
GTGCA[illegible]

FIG. 28

081120 # 2 : H4- shACE2-BV3 (SEQ ID NO:28)

DraIII-βGlo BI-Nhe–AmCMV&EF1I126-BstEII -H4-BglII-Mscp–**21q21**-AmCMV-AEF1I126-BstEII - shACE2-BglII-MiniA-IFNβ S/MAR-BV3

CACTATGTGTTAATTAAAATTATCTCTAAGGCATGTGAACTGGCTGTCTTGGTTTTCATCTGTACTTCATCTGCTACCTCTGTGACCTGAAACATATTTATAATTCCATTAAGCTGTGCATATGATAGATTT
ATCATATGTATTTTCCTTAAAGGATTTTTGTAAGAACTAATTGAATTGATACCTGTAAAGTCTTTATCACACTACCCAATAAATAATAAATCTCTTTGTTCAGCTCTCTGTTTCTATAAATATGTACCAGTTT
TATTGTTTTTAGTGGTAGTGATTTTATTCTCTTTCTATATATATATACACACACATGTGTGCATTCATAAATATATACAATTTTTATGAATAAAAAATTATTAGCAATCAATATTGAAAACCACTGATTTTTGTT
TATGTGAGCAAACAGCAGATTAAAAGG**AATTT**GAATTC**TCATA**GCTAGCAG[illegible]
[illegible]
[illegible]
[illegible]ACTACTGGCAGAAGACCATGCTTCAGGGCTGACTGCC
CCTCAGTGGGCAGAGAGCACATGGCCCACAGTCCCTGAGAAGTTGGGGGGAGGGGTGGGCAATTGAACTGGTGCCTAGAGAAGGTGGGGCTTGGGTAAACTGGGAAAGTGATGTGGTGTACTGGC
TCCACCTTTTTCCCCAGGGTGGGGGAGAACCATATATAAGTGCAGTAGTCTCTGTGAACATTCAAGCTTCTGCCTTCTCCCTCCTGTGAGTTTGGTAAGTCACTGACTGTCTATGCCTGGGAAAGGGTG
GGCAGGAGATGGGGCAGTGCAGGAAAAGTGGCACTATGAACCCTGCAGCCCTAGACAATTGTACTAACCTTCTTCTCTTTCCTCTCCTGACAGGTTGGTAACC[illegible]CATGGGATGGTGCCTGAT
CCTGCTGTTTCTGCCTGCCTGTGGCCACCAGACTGCTGTCTCAGGTTCAGCTGGTGCAGTCTGGGGCTGAAGTGAAGAAACCTGGGGCCTCTGTGAAGGTGTCCTGCAAGGCTTCTGGCTACACATTCA
CAGGCTACTACATGCACTGGGTCAGACAGGCCCCTGGACAGGGACTTGAGTGGATGGGCAGAATCAACCCCAACAGTGGTGGCACCAACTATGCCCAGAAATTCCAGGGCAGAGTGACCATGACCA
GAGACACCAGCATCAGCACAGCCTACATGGAACTGAGCAGGCTTAGGAGTGATGACACTGCTGTGTACTACTGTGCCAGAGTGCCCTACTGCAGCAGCACCTCTTGTCACAGAGACTGGTACTTTGAC
CTGTGGGGCAGAGGCACCCTGGTCACAGTTAGCTCTGCCAGCACAAAGGGCCCCTCTGTGTTTCCTCTGGCTCCCAGCAGCAAGAGCACCAGTGGTGGAACAGCTGCCCTGGGCTGTCTGGTCAAGG
ACTACTTTCCTGAGCCTGTGACAGTGTCCTGGAACTCTGGGGCTCTGACATCTGGGGTGCACACATTCCCTGCTGTGCTGCAGTCCTCTGGCCTGTACAGCCTGTCCTCTGTGGTCACTGTGCCTAGCTC
TAGCCTGGGCACCCAGACCTACATCTGCAATGTGAACCACAAGCCTAGCAACACCAAGGTGGACAAGAAGGCTGAGCCCAAGAGCTGTGATAAGACCCACACCTGTCCTCCATGTCCT[illegible]
[illegible]
[illegible]
[illegible]AAGGGCCAGCCTAGGGAACCCCAAGTGTATACCCTGCCTCCTAGCAGAGATGAGCTGACCAAGA
ACCAGGTGTCCCTGACATGCCTGGTTAAGGGCTTCTACCCCTCTGACATTGCTGTGGAATGGGAGAGCAATGGCCAGCCTGAGAACAACTACAAGACCACACCTCCTGTGCTGGACTCTGATGGCTCA
TTCTTCCTGTACTCCAAGCTGACTGTGGACAAGTCCAGATGGCAGCAAGGCAATGTGTTCAGCTGCTCTGTGATGCATGAGGCCCTGCACAACCACTACACACAGAAGTCTCTGTCTCTGAGCCCTGGC
AAC***AGAAAGAGAAGGAGTGGCTCTGGGGCCACCAACTTCAGCCTGCTGAAACAGGCTGGGGATGTTGAAGAGAACCCTGGACCT***[illegible]
[illegible]
[illegible]
[illegible]
[illegible]
[illegible]
[illegible]**TGA**AGATCT[illegible]**AG**
AGCCCCACTGTGTTCATCTTACAGATGGAAATACTGACATTCAGAGGAGTTAGTTAACTTGCCTAGGTGATTCAGCTAATAAGTGCAAGAAAGATTTCAATCCAAGGTGATTTGATTCTGAAGCCTGTG
CTAATCACATTACACCAAGCTACAACTTCATTTATAAATAATAAGTCAGCTTTCAAGGGCCTTTCAGGTGTCCTGCACTTCTACAAGCTGTGCCATTTAGTGAACACAAAATGAGCCTTCTGATGAAGTA
GTCTTTTCATTATTTCAGATATTAGAACACTAAAATTCTTAGCTGCCAGCTGATTGAAGGCTGGGACAAAATTCAAACATGCATCTACAACAATATATATCTCAATGTTAGTCTCCAAATTCTATTGACTTC
AACTCAAGAGAATATAAAGAGCTAGTCTTTATACACTCTTTAAGGTATGATATCATCTGGAAAGTAACAAAATTGATGCAAATTTGAATGAACTTTATCATGGTGTATTTACACAATGTGTTTCTTCTCCC
TGCAATGTATTTCTTTCTCTAATTCCTTCCATTTGATCTTTCATACACAATCTGGTTCTGATGTATGTTTTTGGATGCACTTTTCAACTCCAAAAGACAGAGCTAGTTACTTTCTTCCTGGTGCTCCAAGCA
CTGTATTTGTATCTGTATTCAAGCCCTTTGCAATATTGTACTGGATCATTATTTCACCTCTAGGATGGCTTCCCCAGGCAACTTGTGTTCACCCAGAGACTACATTTTGTATCTTGTTGACCTTTGAACTTCC
ACCAGTGTCTAAAAATAATATGTATGCAAAATTACTTGCTATGAGAATGTATAATTAAACAATATAAAAAGGAGAAGCAAGGAGAGAAACACAGGTGTGTATTTGTGTTTGTGTGCTTAAAAGGCAGT
GTGGAAAAGGAAGAAATGCCATTTATAGTGAGGAGACAAAGTTATATTACCTCTTATCTGGCTTTTAAGGAGATTTTGCTGAGCTAAAAATCCTATATTCATAGAAAAGCCTTACCTGAGTTGCCAATA
CC**TCAATTCAG**TCTAGCAG[illegible]
[illegible]
[illegible]
[illegible]ACTAGTGGAGAAGAGCATGCTTGAGGGCTGAGTGCCCCTCAGTGGGCAGAGAGCACATGGCCCACAGTCC
CTGAGAAGTTGGGGGGAGGGGTGGGCAATTGAACTGGTGCCTAGAGAAGGTGGGGCTTGGGTAAACTGGGAAAGTGATGTGGTGTACTGGCTCCACCTTTTTCCCCAGGGTGGGGGAGAACCATA
TATAAGTGCAGTAGTCTCTGTGAACATTCAAGCTTCTGCCTTCTCCCTCCTGTGAGTTTGGTAAGTCACTGACTGTCTATGCCTGGGAAAGGGTGGGCAGGAGATGGGGCAGTGCAGGAAAAGTGGCA
CTATGAACCCTGCAGCCCTAGACAATTGTACTAACCTTCTTCTCTTTCCTCTCCTGACAGGTTGGTAACC[illegible]
[illegible]
[illegible]
[illegible]
[illegible]
[illegible]
[illegible]
[illegible]
[illegible]
[illegible]
[illegible]
[illegible]
[illegible]
[illegible]
[illegible]
[illegible]
[illegible]
[illegible]
C**TAA**AGATCT[illegible]AGTCAATATGTTCACCCCAAAAAAGCTGTTTGTTAACTTGTCAACCTCATTC
TAAAATGTATATAGAAGCCCAAAAGACAATAACAAAAATATTCTTGTAGAACAAAATGGGAAAGAATGTTCCACTAAATATCAAGATTTAGAGCAAAGCATGAGATGTGTGGGGATAGACAGTGAGG
CTGATAAAATAGAGTAGAGCTCAGAAACAGACCCATTGATATATGTAAGTGACCTATGAAAAAAATATGGCATTTTACAATGGGAAAATGATGGTCTTTTTCTTTTTTAGAAAAACAGGGAAATATATT
TATATGTAAAAAATAAAAGGGAACCCATATGTCATACCATACACACAAAAAAATTCCAGTGAATTATAAGTCTAAATGGAGAAGGCAAAACTTTAAATCTTTTAGAAAATAATATAGAAGCATGCCATC
AAGACTTCAGTGTAGAGAAAAATTTCTTATGACTCAAAGTCCTAACCACAAAGAAAAGATTGTTAATTAGATTGCATGAATATTAAGACTTATTTTTAAAATTAAAAAACCATTAAGAAAAGTCAGGCC
ATAGAATGACAGAAAATATTTGCAACACCCCAGTAAAGAGAATTGTAATATGCAGATTATAAAAAGAAGTCTTACAAATCAGTAAAAAATAAAACTAGACAAAAATTTGAACAGATGAAAGAGAAACT
CTAAATAATCATTACACATGAGAAACTCAATCTCAGAAATCAGAGAACTATCATTGCATATACACTAAATTAGAGAAATATTAAAAGGCTAAGTAACATCTGTGGC**TTAATTAA**[illegible]**TCTAGT**GATC
AGCAGTTCAACCTGTTGATAGTATGTACTAAGCTCTCATGTTTAATGTACTAAGCTCTCATGTTTAATGAACTAAACCCTCATGGCTAATGTACTAAGCTCTCATGGCTAATGTACTAAGCTCTCATGTTT
CATGTACTAAGCTCTCATGTTTGAACAATAAAATTAATATAAATCAGCAACTTAAATAGCCTCTAAGGTTTTAAGTTTTATAAGAAAAAAAAGAATATATAAGGCTTTTAAAGGTTTTAAGGTTTCCTAG
GTTATCC**TCATATGAGCTC**TTAGAAAAACTCATCCAGCATCAAATGAAACTGCAATTTATTCATATCAGGATTATCAATACCATATTTTTGAAAAAGTCTTTTCTGTAATGAAGGAGAAAACTCACCCAGG
CAGTTCCATAGGATGGCAAGATCCTGGTATCTGTCTGCAATTCCAACTCTTCCAACATCAATACAACCTATTAATTTCCCCTCATCAAAAATAAGGTTATCAAGTGAGAAATCACCATGAGTGACCACTG
AATCTGGTGAGAATGGCAAAAGATTATGCATTTCTTTCCAGACTTGTTCAACAGGCCAGCCATTTCTCTCATCATCAAAATCACTGGCATCAACCAAACCATTATTCATTCTTGATTGGGCCTGAGCCAGT
CTAAATACTCTATCAGAGTTAAAAGGACAATTACAAACAGGAATGGAATGCAATCTTCTCAGGAACACTGCCAGGGCATCAACAATATTTTCACCTGAATCAGGATATTCTTCCAATACCTGGAATGCT
GTTTTCCCTGGGATGGCAGTGGTGAGTAACCATGCATCATCAGGAGTTCTGATAAAATGCTTGATGGTTGGAAGAGGCATAAATTCAGTCAGCCAGTTTAGTCTGACCATCTCATCTGTAACATCATTG
GCAACAGAACCTTTGCCATGTTTCAGAAACAACTCTGGGGCATCTGGCTTCCCATACAATCTATAGATTGTGGCACCTGATTGCCCAACATTATCTCTAGCCCATTTATACCCATATAAATCAGCATCCAT
GTTGGAATTTAATCTTGGCCTGGAGCAAGAGGTTTCTCTTTGAATATGGCTCAT**ACATGTGCA**[illegible]

FIG. 29

081120 # 5 : shACE2-H4 -BV3 (SEQ ID NO:29)

DraIII-βGlo BI-NheI-AmCMV/EF1126-BstEII -shACE2-BglII-Mlsp-**21q21**-AmCMV-EF1126-BstEII – H4-BglII-Mlsp-IFNβ S/MAR-BV3

CACTATGTGTTAATTAAAAATTATCTCTAAGGCATGTGAACTGGCTGTCTTGGTTTTCATCTGTACTTCATCTGCTACCTCTGTGACCTGAAACATATTTATAATTCCATTAAGCTGTGCATATGATAGATTT
ATCATATGTATTTTCCTTAAAGGATTTTTGTAAGAACTAATTGAATTGATACCTGTAAAGTCTTTATCACACTACCCAATAAATAATAAATCTCTTTGTTCAGCTCTCTGTTTCTATAAATATGTAGCAGTTT
TATTGTTTTTAGTGGTAGTGATTTTATTCTCTTTCTATATATATACACACACATGTGTGCATTCATAAATATATACAATTTTTATGAATAAAAAATTATTAGCAATCAATATTGAAAACCACTGATTTTTGTT
TATGTGAGCAAACAGCAGATTAAAAGGAATTTGAATTCTCATAGCTAGCAG[illegible]
[illegible]
CCATTGCCTTTTGCTCA-TACAAAGGTCAATAGTTATTGAATTCAAGGGTTTTTCCATTTTTCTTACATAAATAGCTCAATCTTTGTTACTAGTGGAGAAGAGCCATGCTTGAGGGCTGAGTGGCCCTCTCAGTGCGGCAGAGAGCACATGGCCCACAGTGCCTCAGAAGTTGGGGGG
CCTCAGTGGCCCAGAGAGCACATGGCTCACAGTCCCTGAGAAGTTGGGGGGAGGGGTGGGCAATTGAACTGGTGCCTAGAGAAGGTGGGGCCTGGGTAAACTGGGAAAGTGATGTGTGTACTGGC
TCCACCTTTTCCCCAGGGTGGGGGAGAACCATATATAAGTGCAGTAGTCTCTGTGAACATTCAAGCTTCTGCCTATCTGCTCCTGTGAGTTTGGTAAGTCACTGACTGTCTATGCCTGGGAAAGGGTG
GGCAGGAGATGGGGCAGTGCAGGAAAAGTGGCACTATGAACCCTGCAGCCCTAGACAATTGTACTAACCTTCTTCTCTTTCCTCTCCTGACAGGTTGGTAACCCCCCCCACCATGAGCTAGCAGCTCTTG
GCTCTTGCTTACTTCTGGTTGGCTTTTGACAGCTTGCCTAGTAGCGACCATTGAGCAACAGCCCAAGAGCTTCCTGGACAAGTTCAACGAGTACGGCCTGAGTTTCCAGCAGGTCCCTGACTACACCAG
CCCTAGCACCAACATCACTGAAGTAGAAAATGTCCAGCAAGCATGAACAATGCTTGGCCAGCAACTTGACTGCCTTTCCTCAAACAGCAGCAGCAGCACTCCCCCCACATGTAGCTTCTGCAAGAGACTCCAGCAACC
TGACAGTGAACGCTTCAGCTCCAGCCTCTCCAGCAGAATGCCAGCTCTGTCCTGTTCTGAGCACAAGAGCAAGAGACTGAACACTATCTTGAAGCAGATGAGCAGCATCTAGATGCACAGCCAAAGTGTG
CAACCCTGACAACATCCAAGATGTGCCTGCTTGTGGAACCTGGCCTGAATGAGATCATGCCCAACAGTTTGGACTACAATGAGAGACTATTGTGGCCTGCTGTATCTTTGAAGAGTGAAGTGCGAAAGCA
CCTGAGGCCCTTTGATGAGAATATGTTGGTGCTCAACAATGAGAGCCCAGGCCCAGCCACTATCAGCACTATGGGCATTATTGGAGGCCCAGACTATGAAGTGAATGGTTTGATGCTTATGACTA
CAGCAGGCCCAGCTGTATTGACCATGTGGAACCACCTTTGACCAAATCAAGCCCCTCTATGAGCACCTCCATGCCTATCTCCAGGCCAACCTGATGAATCCTTACCCCAGCTACATCAGCCCCATTG
GCTGCCTGCCTCATCTGCTGCCCATGATGTGGCCAGATTCTGGACCAACTGCTACAGCCTGACTTTGCCTTTGGCCAGAAACCTAACATTGATGTGACAGATGCCATGTTGCATCAGGCCTTG
GATTCCCAGATAACTCAAAGAGGCTGAGAATTCTTTGTTCTGTGGGCTGCCAACATGACCCAAGGCTTTTGGAGAACTCCATGCTGACAGACCCTGGCAATGTGCAAAAGGCTGTTGTGTCA
CCCACAGCCTCGGAACTTGCAAGGGAGCTTCAGAATCTGATGTCCACAAAGTGACAAGGATGATTTCTGACAGCTCACCATGAGATGGCTACATCCAGTATGACATGGCCTATGCTGCCC
AGCCTTTCGCTGCTCAGAAATGCCCCAAATGACGCCTTCAATGACGGCTCCTGCCTGGAGAAGATCAAGCAGTGTCAGGTCCAAGACCTTCAAGAGTCCATTGGCCTCCTGCAGGCTCAACTGAAACAG
GACAATGAGACAGAGATCAACTTCCTGCAAGCAGGCCTGAACCATTGTGGGCACACTGCTCTTCAGCTACATGCTGGAAAAGTGGAGATGGAGGGCTTTAATGGAGAAATTCCAAGGAGCAGT
CGATGAACAAATGGTGGAGATGAAGAGCGAAATTGTGGAATTCTGGAACCTGTCCCACATGATGACACATGTCTGAGCCTGCCAGGTCTTCATGTGTCCAATGACTACTCCTTCATTAGGTA
CTACAGCAGGAGACTGTACCATTTCCAGTTCAAGAGCTCTGTGTCAGGCTGCTAAACATGAGGGCCCCATGCACAAGTGTGACATCAGCAACTCCACAGAGGCTCTGGACAGAAACTGTTCAACATGC
TGAGACTGGGCCAGTCTGTGCCCTTCCTCAACTTCTCCCCTCTGAPAATCTTGTCCGGAGCCAACAPTATGAATCTCAGACCCCTCCTGTAPCTACTTTGAGCCCCTCTTCAACTCCCTGAAGCCACCAGAACAPG
AAGAGCTTTGTTGGCTTGTCCACAGACTGCTTCCCATATGCTGACCAGAGCATCAAAGTCAGAATCAGCCTGAAGAGTGCCTTGGGAGATAAGGCCTATGAGTGGAATGATAATGAGATGTACTTGTT
CATTGTCTCTTGTTGCCTTATGCTATGACACAGTACTTCTTGAAAG[illegible]
ACTAGTGGAGAAGAGCCATGCTTGAGGGCTGAGTGGCCCTCTCAGTGCGGCAGAGAGCACATGGCCCACAGTGCCTCAGAAGTTGGGGGG
GAGGGCTGGGCAATTGAACTGGTGCCTAGAGAAGGTGGGGCTTGGGTAAACTGGGAAAGTGATGTGGGTGTACTGGCTCCACCTTTTTCCCCAGGGTGTGGGGGAGAAGCATATATAAGTGCAGTAGTC
TCTGTGAACATTCAAGCTTCTGCCTATCTGCTCCTGTGAGTTTGGTAAGTCACTGACTGTCTATGCCTGGGAAAGGGTGGGGCAGGAGATGGGGCAGTGCAGGAAAAGTGGCACTATGAACCCTGCAGC
CCTAGACAATTGTACTAACCTTCTTCTCTTTCCTCTCCTGACAGCTTGGTAACCAAAAAATGCATGGCATGGTCCCTGATCCTGCTGTTTCTGGTGGCCGTGTGGCAGCAGAGCTGCTGTCTCAGGTTCAGCT
GGTGCAGTCTGGGGCTGAAGTGAAGAAACCTGGGGCCTCTGTGAAGGTGTCCTGCAAGGCTCTGGCTACACATTCACAGGCTACTACATGCACTGGGTCAGACAGGCCCCTGGACAGGGACTTGAG
TGGATGGGCAGAATCAACCCTAACAGTGGTGGCACCAACTATGCCCAGAAATTCCAGGGCAGAGTGACCATGACCAGAGACACCAGCATCAGCACAGCCTACATGGAACTGAGCAGGCTTAGGAGCT
GATGACACTGCCGTGTATTACTGTGCGAGAGTGCCCTACTGCAGCAGCACCTCTTGTCACAGAGACTGGTACTTTGACCTCTGGGGCCGCAGCACCCTGGTCACAGTTAGCTCTGCCAGCACAAAGGG
CCCCTCTGTGTTTCCTCTGGCTCCCAGCAGCAAGAGCACCAGTGGTGGAACAGCTGCCCTGGGCTGTCTGGTCAAGGACTACTTTCCTGAGCCTGTGACAGTGTCCTGGAACTCTGGGGCTCTGACATC
TGGGGTGCACACATTCCCTGCTGTGCTGCAGTCCTCTGGCCTGTACAGCCTCTCCTCTGTGGTCACTGTGCCTAGCTCTAGCCTGGGCACCCAGACCTACATCTGCAATGTGAACCACAAGCCTAGCAA
CACCAAGGTGGACAAGAAGGCTGAGCCCAAGAGCTGTGATAAGACCCACACCTGTCCTCCATGTCCT[illegible]
[illegible]
ATCAGTCAATATGTTCACCCCAAAAAAGCTGTTTGTTAACTTGTCAACCTCATTCTAAA
ATGTATATAGAAGCCCAAAAGACAATAACAAAAATATTCTTGTAGAACAAAATGGGAAAGAATGTTCCACTAAATATCAAGATTTAGAGCAAAGCATGAGATGTGTGGGGATAGACAGTGAGGCTGA
TAAAATAGAGTAGAGCTCAGAAACAGACCCATTGATATATGTAAGTGACCTATGAAAAAAATATGGCATTTTACAATGGGAAAATGATGGTCTTTTTCTTTTTTAGAAAAACAGGGAAATATATTTATA
TGTAAAAAATAAAAGGGAACCCATATGTCATACCATACACACAAAAAAATTCCAGTGAATTATAAGTCTAAATGGAGAAGGCAAAACTTTAAATCTTTTAGAAAATAATATAGAAGCATGCCATCAAGA
CTTCAGTGTAGAGAAAAATTTCTTATGACTCAAAGTCCTAACCACAAAGAAAAGATTGTTAATTAGATTGCATGAATATTAAGACTTATTTTTAAAATTAAAAAACCATTAAGAAAAGTCAGGCCATAGA
ATGACAGAAAATATTTGCAACACCCCAGTAAAGAGAATTGTAATATGCAGATTATAAAAAGAAGTCTTACAAATCAGTAAAAAATAAAACTAGACAAAAATTTGAACAGATGAAAGAGAAACTCTAAA
TAATCATTACACATGAGAAACTCAATCTCAGAAATCAGAGAACTATCATTGCATATACACTAAATTAGAGAAATATTAAAAGGCTAAGTAACATCTGTGGCTTAATTAATCTCTAGTGATCAGCAG
TTCAACCTGTTGATAGTATGTACTAAGCTCTCATGTTTAATGTACTAAGCTCTCATGTTTAATGAACTAAACCCTCATGGCTAATGTACTAAGCTCTCATGGCTAATGTACTAAGCTCTCATGTTTCATGTA
CTAAGCTCTCATGTTTGAACAATAAAATTAATATAAATCAGCAACTTAAATAGCCTCTAAGGTTTTAAGTTTTATAAGAAAAAAAAGAATATATAAGGCTTTTAAAGGTTTTAAGGTTTCCTAGGTTATCC
TCATATGAGCTCTTAGAAAAACTCATCCAGCATCAAATGAAACTGCAATTTATTCATATCAGGATTATCAATACCATATTTTTGAAAAAGTCTTTTCTGTAATGAAGGAGAAAACTCACCCAGGCAGTTCC
ATAGGATGGCAAGATCCTGGTATCTGTCTGCAATTCCAACTCTTCCAACATCAATACAACCTATTAATTTCCCCTCATCAAAAATAAGGTTATCAAGTGAGAAATCACCATGAGTGACCACTGAATCTGG
TGAGAATGGCAAAAGATTATGCATTTCTTTCCAGACTTGTTCAACAGGCCAGCCATTTCTCTCATCATCAAAATCACTGGCATCAACCAAACCATTATTCATTCTTGATTGGGCCTGAGCCAGTCTAAATA
CTCTATCAGAGTTAAAAGGACAATTACAAACAGGAATGGAATGCAATCTTCTCAGGAACACTGCCAGGGCATCAACAATATTTTCACCTGAATCAGGATATTCTTCCAATACCTGGAATGCTGTTTTCCC
TGGGATGGCAGTGGTGAGTAACCATGCATCATCAGGAGTTCTGATAAAATGCTTGATGGTTGGAAGAGGCATAAATTCAGTCAGCCAGTTTAGTCTGACCATCTCATCTGTAACATCATTGGCAACAG
AACCTTTGCCATGTTTCAGAAACAACTCTGGGGCATCTGGCTTCCCATACAATCTATAGATTGTGGCACCTGATTGCCCAACATTATCTCTAGCCCATTTATACCCATATAAATCAGCATCCATGTTGGAA
TTTAATCTTGGCCTGGAGCAAGAGGTTTCTCTTTGAATATGGCTCATACATGTGCA[illegible]

FIG. 30

072320 # 2 : H4-aCD20-aIL5-5J8-BV2 (SEQ ID NO:30)

DraIII- RI-Nhe-ΔmCMV/ΔEF1I1.26-BstEII H4-BglII-MαpA -ΔmCMV-ΔEF1I1.26-BstEII aCD20 -BglII-MαpA **-ΔhCMV**-RV-ΔEF1I126-BstEII -aIL5-BglII-MαpA -ΔmCMV-ΔEF1I1.26-BstEII-5J8 -BglII-MαpA-BV2

CACTATGTGAATTGGAATTCTCATAGCTAGCAG [illegible]

[illegible]

AGGTTCAGCTGGTGCAGTCTGGGGCTGAAGTGAAGAAACCTGGGGCCTCTGTGAAGGTGTCCTGCAAGGCTTCTGGCTACACATTCACAGGCTACTACATGCACTGGGTCAGACAGGCCCCTGGACAGGGACTTGAGTGGATGGGCAGAA

[illegible] GAGCCCAAGAGCTGTGATAAGACCCACACCTGTCCTCCATGTCCT [illegible]

[illegible] ***AGAAAGAGAAGGAGTGGCTCTGGGGCCACCAACTTCAGCCTGCTGAAACAGGCTGGGGATGTTGAAGAGAACCCTGGACCT*** [illegible]

[illegible] TGA [illegible]

[illegible] ***AGAAAGAGAAGGAGTGGAAGTGGAGCTACTAACTTCAGCCTGCTG AAGCAGGCTGGAGATGTGGAGGAGAACCCTGGACCT*** [illegible]

[illegible] TGA [illegible]

[illegible] **TGTTACATAACTTATGGTAAATGGCCTGCCTGGCTGACTGCCCAATGACCCCTGCCCAATGATGTCAATAATGATGTATGTTCCCATGT AATGCCAATAGGGACTTTCCATTGATGTCAATGGGTGGAGTATTTATGGTAACTGCCCACTTGGCAGTACATCAAGTGTATCATATGCCAAGTATGCCCCCTATTGATGTCAATGATGGTAAATGGCCTGCCTGGCATTATGCCCAGTAC ATGACCTTATGGGACTTTCCTACTTGGCAGTACATCTATGTATTAGTCATTGCTATTACCATGGA** [illegible]

[illegible] ***AGAAAGAGAAGGAGTGGCTCTGGGGCCACCAACTTTAGCCTGCTGAAACAGGCTGGGGATGTTGAAGAGAACCCTGGACCT*** [illegible]

[illegible] TGA [illegible]

[illegible] **TCTAGT**GATCAGCAGTTCAACCTGTTGATAGTATGTACTA
AGCTCTCATGTTTAATGTACTAAGCTCTCATGTTTAATGAACTAAACCCTCATGGCTAATGTACTAAGCTCTCATGGCTAATGTACTAAGCTCTCATGTTTCATGTACTAAGCTCTCATGTTTGAACAATAAAATTAATATAAATCAGCAACTTAA
ATAGCCTCTAAGGTTTTAAGTTTTATAAGAAAAAAAAGAATATATAAGGCTTTTAAAGGTTTTAAGGTTTCCTAGGTTATCC**TCATATGAGCTC**TTAGAAAAACTCATCCAGCATCAAATGAAACTGCAATTTATTCATATCAGGATTATCAATA
CCATATTTTTGAAAAAGTCTTTTCTGTAATGAAGGAGAAAACTCACCCAGGCAGTTCCATAGGATGGCAAGATCCTGGTATCTGTCTGCAATTCCAACTCTTCCAACATCAATACAACCTATTAATTTCCCCTCATCAAAAATAAGGTTATCAAG
TGAGAAATCACCATGAGTGACCACTGAATCTGGTGAGAATGGCAAAAGATTATGCATTTCTTTCCAGACTTGTTCAACAGGCCAGCCATTTCTCTCATCATCAAAATCACTGGCATCAACCAAACCATTATTCATTCTTGATTGGGCCTGAGCC
AGTCTAAATACTCTATCAGAGTTAAAAGGACAATTACAAACAGGAATGGAATGCAATCTTCTCAGGAACACTGCCAGGGCATCAACAATATTTTCACCTGAATCAGGATATTCTTCCAATACCTGGAATGCTGTTTTCCCTGGGATGGCAGTG
GTGAGTAACCATGCATCATCAGGAGTTCTGATAAAATGCTTGATGGTTGGAAGAGGCATAAATTCAGTCAGCCAGTTTAGTCTGACCATCTCATCTGTAACATCATTGGCAACAGAACCTTTGCCATGTTTCAGAAACAACTCTGGGGCATCT
GGCTTCCCATACAATCTATAGATTGTGGCACCTGATTGCCCAACATTATCTCTAGCCCATTTATACCCATATAAATCAGCATCCATGTTGGAATTTAATCTTGGCCTGGAGCAAGAGGTTTCTCTTTGAATATGGCTCAT**ACATGTGCA** [illegible]

[illegible]

FIG. 31

070620 # 2 : B38 Lambda-aCD20(Cys)-BV3 (SEQ ID NO:31)

DraIII-**βGlo** RI-Nhe-AmCMV-EF1I126-BstEII-B38 Lambda-BglII-MixpA-**21q21S/MAR**-AmCMV-EF1-I126-BstEII-**aCD20-N2A-L-Cys**-BglII-MixpA-**IFNβ S/MAR**-BV3

CACTATCTGTTAATTAAAAATTATCTCTAAGGCATGTGAACTGGCTGTCTTGGTTTTCATCTGTACTTCATCTGCTACCTCTGTGACCTGAAACATATTTATAATTCCATTAAGCTGTGCATATGATAGATTT
ATCATATGTATTTTCCTTAAAGGATTTTTGTAAGAACTAATTGAATTGATACCTGTAAAGTCTTTATCACACTACCCAATAAATAATAAATCTCTTTGTTCAGCTCTCTGTTTCTATAAATATGTACCAGTTT
TATTGTTTTTAGTGGTAGTGATTTTATTCTCTTTCTATATATATACACACACATGTGTGCATTCATAAATATATACAATTTTTATGAATAAAAAATTATTAGCAATCAATATTGAAAACCACTGATTTTTGTT
TATGTGAGCAAAACAGCAGATTAAAAGGAATTTGAATTCTCATAGCTATGCAG[illegible]ACTAGTGGAGAAGAGCATGCTTGAGGGCTGAGTGCC
CCTCAGTGGGCAGAGAGCACATGGCCCACAGTCCCTGAGAAGTTGGGGGGAGGGGTGGCAATTGAACTGTTGCCTAGAGAAGGTGGGGCCTTGGGTAAACTGGGAAAGTGATGTGGTGTACTGGC
TCCACCTTTTTCCCCAGGGTGTGGGGGACAACCATATATAAGTGCAGTAGTCTCTGTGAACATTCAAGCTTCTGCCTTCTCCCTCCTGTGAGTTTGGTAAGTCACTGACTGTCTATGCCTGGGAAAGGGTG
GGCAGGAGATGGGGCAGTGCACGAAAAGTGGCACTATGAACCCTGCAGCCCTAGACAATTGTACTAACCTTCTTCTCTTTCCTCTCCTGACAGGTTGGTAACCC[illegible]ATGGGATGTTCCTGAT
CCTGCTGTTCTGGTGGCTCCTGGCACCAGATGCTGTCTGAAGTGCAGCTGGTGGAAAGTGGTGGTGGCCTGGTTCAGCCTGGTGGCTCTCTGAGACTGAGCTGTGCTGCCTCTGGCTTCATTGTGT
CCAGCAACTACATGAGCTGGGTCAGACAGGCCCCTGGCAAAGGACTGGAATGGGTGTCAGTGATCTACAGTGGTGGCAGCACCTACTATGCTGACTCTGTGAAGGGCAGATTCACCATCAGCAGACA
CAACAGCAAGAACACCCTGTACCTGCAGATGAACAGCCTGAGAGCTGAGGACACTGCCTGTGTACTACTGTGCCAGAGAAGCCTATGGCATGGATGTGTGGGGCCAGGGCACAACAGTGACTGTGTCC
TCTGCCAGCACAAAGGGCCCCTCTGTGTTTCCTCTGGCTCCCAGCAGCAAGACCACCAGTGGTGGAACAGCTGCCCTGGGCTGTCTGGTCAAGGACTACTTTCCTGAGCCTGTGACAGTGTCCTGGAA
CTCTGGGGCTCTGACATCTGGGGTGCACACATTCCCTGCAGTGCTGCAGTCCTCTGGCCTGTACAGCCTGTCCTCTGTGGTCACAGTGCCTAGCTCTAGCCTGGGCACCCAGACCTACATCTGCAATGT
CAACCACAAGCCTAGCAACACCAAGGTGGACAAGAAGGTCGAGCCCAAGAGCTGTGACAAAACTCACACATGCCCACCGTGCCCAGCACCTGAACTCCTGGGGGGACCGTCAGTCTTCCTCTTCCCCCA
AAACCCAAGGACACCCTCATGATCTCCCGGACCCCTGAGGTCACATGCGTGGTGGTGGACGTGAGCCACGAAGACCCTGAGGTCAAGTTCAACTGGTACGTGGACGGCGTGGAGGTGCATAATGCCAAG
ACAAAGCCGCGGGAGGAGCAGTACAACAGCACGTACCGTGTGGTCAGCGTCCTCACCGTCCTGCACCAGGACTGGCTGAATGGCAAGGAGTACAAGTGCAAGGTCTCCAACAAAGCCCTCCCAGCCCC
CATCGAGAAAACCATCTCCAAAGCCAAAGGGCAGCCCCGAGAACCACAGGTGTACACCCTGCCCCCATCCCGGGATGAGCTGACCAAGAACCAGGTCAGCCTGACCTGCCTGGTCAAAGGCTTCTATCCC
AGCGACATCGCCGTGGAGTGGGAGAGCAATGGGCAGCCGGAGAACAACTACAAGACCACGCCTCCCGTGCTGGACTCCGACGGCTCCTTCTTCCTCTACAGCAAGCTCACCGTGGACAAGAGCAGGTGG
CAGCAGGGGAACGTCTTCTCATGCTCCGTGATGCATGAGGCTCTGCACAACCACTACACGCAGAAGAGCCTCTCCCTGTCTCCGGGTAAA**AGAAAGAGAAGGAGTGGCTCTGGGGCCACC**
AACTTCAGCCTGCTGAAACAGGCTGGGGATGTTGAAGAGAACCCTGGACCT[illegible]
ACGATCCTTGCTGAGTGCCTTCTGGGACACAGATGACCATCAGCTGTTACAGCCAGCCATGGCATCAGCTCTTACTTGCCTTCGTATCAGCAAAACGCTTGGCAAGGCGCTTAAGCTGTTGATCTATGC
TGCCTCCACACTGCAGTCAGGGGTGCCCTCTCGCTTCAGTGGATCTGGCACTGAGTTCACCCTTGACCATCAGCTCTCTGCAGCCTGATGACTTTGCCACTTACTACTGCCAGCAGCTGAACAGT
TACCCGTTCACGTTCGGCCAAGGGACCAAGGTGGAAATCAAAGGGGAACAAAAGCTGATCAGTGAAGAAGACCTGAACGGTGCCGCTGTGACCGACTCCGAGATGAAGGTGGCCCTGTTCGACAACCAG
AAGATCACCTACGTGGTGCTGTTCAACTTCGTGTCCATCATCCTGCCCGCCATCGGCCTGATCATGGGCGACGTGAAGCTGCAGGAGTCCGGCCCCGGCCTGGTGGCCCCCAGCCAGAGCCTGTCCGTG
ACCTGCACCGTGTCCGGCGTGTCCCTGCCCGACTACGGCGTGTCCTGGATCAGACAGCCCCCCAGAAAGGGCCTGGAGTGGCTGGGCGTGATCTGGGGCAGCGAGACCACCTACTACAACAGCGCCCT
GAAGTCCCGGCTGACCATCATCAAGGACAACAGCAAGAGCCAGGTGTTCCTGAAGATGAACAGCCTGCAGACCGACGACACCGCCATCTACTACTGCGCCAAGCACTACTACTACGGCGGCAGCTACGCC
ATGGACTACTGGGGCCAGGGCACCAGCGTGACCGTGTCCAGCGCCAAGACCACCCCCCCCAGCGTGTACCCCCTGGCCCCCGTGTGCGGCGACACCACCGGCAGCAGCGTGACCCTGGGCTGCCTGGTG
AAGGGCTACTTCCCCGAGCCCGTGACCCTGACCTGGAACAGCGGCAGCCTGAGCAGCGGCGTGCACACCTTCCCCGCCGTGCTGCAGAGCGACCTGTACACCCTGAGCAGCAGCGTGACCGTGCCCAGC
AGCACCTGGCCCAGCGAGACCGTGACCTGCAACGTGGCCCACCCCGCCAGCAGCACCAAGGTGGACAAGAAGATCGTGCCCAGGGACTGCGGCTGCAAGCCCTGCATCTGCACCGTGCCCGAGGTGTCC
AGCGTGTTCATCTTCCCCCCCAAGCCCAAGGACGTGCTGACCATCACCCTGACCCCCAAGGTGACCTGCGTGGTGGTGGACATCAGCAAGGACGACCCCGAGGTGCAGTTCAGCTGGTTCGTGGACGAC
CAGGAGGTGCAGACCGCCCACACCAAGCCCAGAGAGGAGCAGTTCAACAGCACCTTCCGGAGCGTGAGCGAGCTGCCCATCATGCACCAGGACTGGCTGAACGGCAAAGAGTTCAAGTGCAGAGTGAAC
AGCGCCGCCTTCCCCGCCCCCATCGAGAAAACCATCAGCAAAACCAAGGGCAGACCCAAGGCCCCACAGGTGTACACCATGCCCCCTAGCCGGGAGGAGATGACCAAGAACCAGGTGTCCCTGACCTGT
ATGGTCAAAGGCTTCTACCCCAGCGACATCGCCGTGGAGTGGGAGAGCAACGGCCAGCCCGAGAACAACTACAAGACCACCCCTCCCATGCTGGACAGCGACGGCAGCTTCTTCCTGTACAGCAAGCTG
ACCGTGGACAAGAGCCGGTGGCAGCAGGGCAACGTGTTCAGCTGCAGCGTGATGCACGAGGCCCTGCACAACCACTACACCCAGAAGAGCCTGAGCCTGTCCCCCGGCAAG**AGAAAGAGAAGGAGTGGAAGTGGAGCTACTAACTTCAGCCTGCTGAAGCAGGCTGGAGATGTGG**
AGGAGAACCCTGGACCT[illegible]
GGAAGAAATTGAGAAGAACCTGAAAGCCATGCTGCTGCTAGATCCAATTATCAACAGAATGTCCATAGAAGATGCTCATGCAGCAGGAAGCCAGCATCCTGTCTCAAGGTCTTA
ACTCTGATTCTCTGCACTCTGCATCTGCCACAACTACAGAGTGACTATACAGCAGTTGGAATCTCAGGATCTGTCACTTACTACTGTCAGCAGTGCAGAACAAATAGTTTCACCTTTGGCAGAGGCA
CCAAGCTGGAAATCAAGAGAACACTGGCTGCAGCCCTCTGTGTTCATCTTCCCACCGTCTGATGAGCAGCTGAAGTCTGGAACTGCCTCTGTTGTGTGCCTGCTGAATAACTTCTATCCCAGAGAGGCC
AAAGTACAGTGGAAGGTGGATAACGCCCTCCAATCGGGTAACTCCCAGGAGAGTGTCACAGAGCAGGACAGCAAGGACAGCACCTACAGCCTCAGCAGCACCCTGACGCTGAGCAAAGCAGACTACGAG
AAACACAAAGTCTACGCCTGCGAAGTCACCCATCAGGGCCTGAGCTCGCCCGTCACAAAGAGCTTCAACAGGGGAGAGTGT**TGA**AGATCT[illegible]
[illegible]AGTCAATATGTTCACCCCAAAAAAGCTGTTTGTTAACTTGTCAACCTCATTCTAAAATGTATATAGAAGCCCAAAAGACAATAACAAAAATATTCTTGTA
GAACAAAATGGGAAAGAATGTTCCACTAAATATCAAGATTTAGAGCAAAGCATGAGATGTGTGGGGATAGACAGTGAGGCTGATAAAATAGAGTAGAGCTCAGAAACAGACCCATTGATATATGTA
AGTGACCTATGAAAAAAATATGGCATTTTACAATGGGAAAATGATGGTCTTTTTCTTTTTTAGAAAAACAGGGAAATATATTTATATGTAAAAAATAAAAGGGAACCCATATGTCATACCATACACACA
AAAAAATTCCAGTGAATTATAAGTCTAAATGGAGAAGGCAAAACTTTAAATCTTTTAGAAAATAATATAGAAGCATGCCATCAAGACTTCAGTGTAGAGAAAAATTTCTTATGACTCAAAGTCCTAACC
ACAAAGAAAAGATTGTTAATTAGATTGCATGAATATTAAGACTTATTTTTAAAATTAAAAAACCATTAAGAAAAGTCAGGCCATAGAATGACAGAAAATATTTGCAACACCCAGTAAAGAGAATTGTA
ATATGCAGATTATAAAAAGAAGTCTTACAAATCAGTAAAAAATAAAACTAGACAAAAATTTGAACAGATGAAAGAGAAACTCTAAATAATCATTACACATGAGAAACTCAATCTCAGAAATCAGAGAA
CTATCATTGCATATACACTAAATTAGAGAAATATTAAAAGGCTAAGTAACATCTGTGGC**TTAATTAA**[illegible]**TCTAGT**GATCAGCAGTTCAACCTGTTGATAGTATGTACTAAGCTCTCATGTTTAATGT
ACTAAGCTCTCATGTTTAATGAACTAAACCCTCATGGCTAATGTACTAAGCTCTCATGGCTAATGTACTAAGCTCTCATGTTTCATGTACTAAGCTCTCATGTTTGAACAATAAAATTAATATAAATCAGC
AACTTAAATAGCCTCTAAGGTTTTAAGTTTTATAAGAAAAAAAAGAATATATAAGGCTTTTAAAGGTTTTAAGGTTTCCTAGGTTATCC**TCATATGAGCTC**TTAGAAAAACTCATCGAGCATCAAATGAA
ACTGCAATTTATTCATATCAGGATTATCAATACCATATTTTTGAAAAAGTCTTTTCTGTAATGAAGGAGAAAACTCACCCAGGCAGTTCCATAGGATGGCAAGATCCTGGTATCTGTCTGCCAATTCCAAC
TCTTCCAACATCAATACAACCTATTAATTTCCCCTCATCAAAAATAAGGTTATCAAGTGAGAAATCACCATGAGTGACCACTGAATCTGGTGAGAATGGCAAAAGATTATGCATTTCTTTCCAGACTTGTT
CAACAGGCCAGCCATTTCTCTCATCATCAAAATCACTGGCATCAACCAAACCATTATTCATTCTTGATTGGGCCTGAGCCAGTCTAAATACTCTATCAGAGTTAAAAGGACAATTACAAACAGGAATGGA
ATGCAATCTTCTCAGGAACACTGCCAGGGCATCAACAATATTTTCACCTGAATCAGGATATTCTTCCAATACCTGGAATGCTGTTTTCCCTGGGATGGCAGTGGTGAGTAACCATGCATCATCAGGAGTT
CTGATAAAATGCTTGATGGTTGGAAGAGGCATAAATTCAGTCAGCCAGTTTAGTCTGACCATCTCATCTGTAACATCATTGGCAACAGAACCTTTGCCATGTTTCAGAAACAACTCTGGGGCATCTGGC
TTCCCATACAATCTATAGATTGTGGCACCTGATTGCCCAACATTATCTCTAGCCCATTTATACCCATATAAATCAGCATCCATGTTGGAATTTAATCTTGGCCTGGAGCAAGAGGTTTCTCTTTGAATATG
GCTCATACATGTGCA[illegible]

FIG. 32

120717 # 1 : aCD20-aIL5-5J8-BV2 (SEQ ID NO:32)

DraIII- RI-NheI-SmCMV/AEF1126-BstEII-aCD20 -BglII-MAPP- **-ΔhCMV**-RV-AEF1126-BstEII **-aIL5**-BglII-MAPP- -SmCMV -AEF1126-BstEII-**5J8** -BglII-MAPP-**BV2**

CACTATGTGAATTGGAATTCTCATAGCTAGCAG

TGA

TGTTACATAACTTATGGTAAATGGCCTGCCTGGCTGACTGCCCAATGACCCCTGCCCAATG
ATGTCAATAATGATGTATGTTCCCATGTAATGCCAATAGGGACTTTCCATTGATGTCAATGGGTGGAGTATTTATGGTAACTGCCCACTTGGCAGTACATCAAGTGTATCATATGCCAAGTATGCCCCCTATTGATGT
CAATGATGGTAAATGGCCTGCCTGGCATTATGCCCAGTACATGACCTTATGGGACTTTCCTACTTGGCAGTACATCTATGTATTAGTCATTGCTATTACCATGGA

TTACTGGAAAGAGCATGCTTGAGGGCTGAGTGCCCCTCAGTGGGCAGAGAGCACATGGCCTCACAGTCCCTGAGAAGTTGGGGGGAGGGGTGGGCAATT
GAACTGCTGCCTAGAGAAGGTGGGGGCTTGGGTAAACTGGGAAAGTGATGTGGTGTACTGGCTCCACCTTTTTCCACCAGGGTGGGGGAGAACCATATATAAGTGCAGTAGTCTCTGTGAACATTTAAGCTTCTGCCTTCT
CCCTCCTGTGAGTTTGGTAAGTCACTGACTGTTCTATGCCTGGGAAGCCCTGGGCAGGAGATGGGGCAGTGCAGTGAAAAGTGGGCACTATGAACCCTCCAGCCCTAGACAATTGTACTAACCTTCTTCTCTTCCTCTCCT
GACAGGTTGGTAAGCCAACCCTATGGGATGCTCCACTGAGTCTTGTTTTCTGGTGGCTGTGGCAGCCAGATGTGCTGTCTGAAGTGCAGCCTGGTGGGAAGCCTGGGCCCTGGCCTGGTTAAGCCCTCTGACATCCTGAGCCT
GACCTGTGCTGTGTCTTGGCTACAGCATCAGCAGCAACTACTACTGGGGCTGGATCAGACAGCCTCCTGGCAAAGGCCTGGAATGGATTGGCAGCATCTATCACTCTTGGCTCCACCTACTACAAGCCAGCCTTGGAAAGC
AGACTGGGCATCTCTGTGGACACCAGCAAGAACCAGTTCAGCCTGAAGCTGAGCTTTGTGTCTGCTGCTGACACTGCTGTGTACTACTGTGCCAGACATGTTATGGACTGGCTACCCTGACACAGCCTACTACTTTGATAA
GTGGGGCCAGGGCACCCTGGTCACAGTGTCTGCTTCTACAAAGGGCCCATCTGTGTTCCCACTGGCTCTAGCAGCAAGAGCACCAGTGGTGGAACAGCTGCCCTGGGCTGTCTGGTCAAGGACTACTTTCCTGAGCCA
GTGACAGTGTCCTGGAACTCTGGGGCTCTGACTTCTGGGGTGCACACATTCCCTGCTGTCCTCCAGTCCTCTGGCCTGTACAGCCTGTCCTCTGTGGTCACTGTGCCAAGCTCTAGCCTGGGCACCCAGACCTACATCTG
CAATGTGAACCACAAGCCTAGCAACACCAAGGTGGACAAGAAGGTCGAGCCCAAGAGCTGTGACAAGACCCACACCTGTCCTCCATGTCCTGCTCCAGAGCTGCTTGGAGGACCTTCTGTGTTTCTGTTCCCTCCAAAG
CCAAAGGACACCCTGATGATCAGCAGAACCCCTGAAGTGACCTGTGTGGTGGTGGATGTGTCCCATGAGGACCCAGAAGTGAAGTTCAATTGGTATGTGGATGGTGTTGAGGTGCACAATGCCAAGACCAAGCCTAG
AGAGGAACAGTACAACAGCACCTACAGGGTTGTGTCAGTGCTGACTGTGCTGCACCAGGACTGGCTGAATGGCAAAGAGTACAAGTGCAAGGTGTCCAACAAGGCCCTGCCTGCTCCTATTGAAAAGACCATCAGCAA
GGCCAAGGGACAGCCTAGGGAACCCCAGGTGTACACACTGCCACCTAGCAGAGATGACCAAGAACCAGGTGTCCCTGACATGCCTTGTGAAGGGCTTCTACCCTTCTGACATTGCAGTGGAATGGGAGAGCAA
TGGCCAGCCTGAGAACAACTACAAGACAACCCCTCCTGTGCTGGACTCTGATGGCTCATTCTTCCTGTACTCCAAGCTGACAGTGGACAAGTCCAGATGGCAGCAAGGCAATGTGTTCAGCTGCTCTGTGATGCATGA
GGCCCTGCACAACCACTACACACAGAAGTCCCTGTCTCTGAGCCCTGGCAAG

TGA

AGATCTA

ACTAGTGGAGAAGAGCATGCTTGAGGGCTGAGTGCCCCTCAGTGGGCAGAGAGCACATGGCCTCACAGTCCCTGAGAAGTTGGGGGGAGGGGTGGGCAATT
GAACTGCTGCCTAGAGAAGGTGGGGGCTTGGGTAAACTGGGAAAGTGATGTGGTGTACTGGCTCCACCTTTTTCCACCAGGGTGGGGGAGAACCATATATAAGTGCAGTAGTCTCTGTGAACATTTAAGCTTCTGCCTTCT
CCCTCCTGTGAGTTTGGTAAGTCACTGACTGTTCTATGCCTGGGAAGCCCTGGGCAGGAGATGGGGCAGTGCAGTGAAAAGTGGGCACTATGAACCCTCCAGCCCTAGACAATTGTACTAACCTTCTTCTCTTCCTCTCCT
GACAGGTTGGTAAGCCAACCCTATGGGATGCTCCACTGAGTCTTGTTTTCTGGTGGCTGTGGCAGCCAGATGTGCTGTCTGAAGTGCAGCCTGGTGGGAAGCCTGGGCCCTGGCCTGGTTAAGCCCTCTGACATCCTGAGCCT
GACCTGTGCTGTGTCTTGGCTACAGCATCAGCAGCAACTACTACTGGGGCTGGATCAGACAGCCTCCTGGCAAAGGCCTGGAATGGATTGGCAGCATCTATCACTCTTGGCTCCACCTACTACAAGCCAGCCTTGGAAAGC
AGACTGGGCATCTCTGTGGACACCAGCAAGAACCAGTTCAGCCTGAAGCTGAGCTTTGTGTCTGCTGCTGACACTGCTGTGTACTACTGTGCCAGACATGTTATGGACTGGCTACCCTGACACAGCCTACTACTTTGATAA
GTGGGGCCAGGGCACCCTGGTCACAGTGTCTGCTTCTACAAAGGGCCCATCTGTGTTCCCACTGGCTCTAGCAGCAAGAGCACCAGTGGTGGAACAGCTGCCCTGGGCTGTCTGGTCAAGGACTACTTTCCTGAGCCA
GTGACAGTGTCCTGGAACTCTGGGGCTCTGACTTCTGGGGTGCACACATTCCCTGCTGTCCTCCAGTCCTCTGGCCTGTACAGCCTGTCCTCTGTGGTCACTGTGCCAAGCTCTAGCCTGGGCACCCAGACCTACATCTG
CAATGTGAACCACAAGCCTAGCAACACCAAGGTGGACAAGAAGGTCGAGCCCAAGAGCTGTGACAAGACCCACACCTGTCCTCCATGTCCTGCTCCAGAGCTGCTTGGAGGACCTTCTGTGTTTCTGTTCCCTCCAAAG
CCAAAGGACACCCTGATGATCAGCAGAACCCCTGAAGTGACCTGTGTGGTGGTGGATGTGTCCCATGAGGACCCAGAAGTGAAGTTCAATTGGTATGTGGATGGTGTTGAGGTGCACAATGCCAAGACCAAGCCTAG
AGAGGAACAGTACAACAGCACCTACAGGGTTGTGTCAGTGCTGACTGTGCTGCACCAGGACTGGCTGAATGGCAAAGAGTACAAGTGCAAGGTGTCCAACAAGGCCCTGCCTGCTCCTATTGAAAAGACCATCAGCAA
GGCCAAGGGACAGCCTAGGGAACCCCAGGTGTACACACTGCCACCTAGCAGAGATGACCAAGAACCAGGTGTCCCTGACATGCCTTGTGAAGGGCTTCTACCCTTCTGACATTGCAGTGGAATGGGAGAGCAA
TGGCCAGCCTGAGAACAACTACAAGACAACCCCTCCTGTGCTGGACTCTGATGGCTCATTCTTCCTGTACTCCAAGCTGACAGTGGACAAGTCCAGATGGCAGCAAGGCAATGTGTTCAGCTGCTCTGTGATGCATGA
GGCCCTGCACAACCACTACACACAGAAGTCCCTGTCTCTGAGCCCTGGCAAG

TGA

AGATCTA

TCTAGTGATCAGCAGTTCAACCTGTTGATAGTATGTACTAAGCTCTCATGTTTAATGTACT
AAGCTCTCATGTTTAATGAACTAAACCCTCATGGCTAATGTACTAAGCTCTCATGGCTAATGTACTAAGCTCTCATGTTTCATGTACTAAGCTCTCATGTTTGAACAATAAAATTAATATAAATCAGCAACTTAAATAGCCT
CTAAGGTTTTAAGTTTTATAAGAAAAAAAAGAATATATAAGGCTTTTAAAGGTTTTAAGGTTTCCTAGGTTATCCTCATATGAGCTCTTAGAAAAACTCATCCAGCATCAAATGAAACTGCAATTTATTCATATCAGGATT
ATCAATACCATATTTTTGAAAAAGTCTTTTCTGTAATGAAGGAGAAAACTCACCCAGGCAGTTCCATAGGATGGCAAGATCCTGGTATCTGTCTGCAATTCCAACTCTTCCAACATCAATACAACCTATTAATTTCCCCTCA
TCAAAAATAAGGTTATCAAGTGAGAAATCACCATGAGTGACGACTGAATCCGGTGAGAATGGCAAAAGATTATGCATTTCTTTCCAGACTTGTTCAACAGGCCAGCCATTTCTCTCATCATCAAAATCACTGGCATCAAC
CAAACCATTATTCATTCTTGATTGGGCCTGAGCCAGTCTAAATACTCTATCAGAGTTAAAAGGACAATTACAAACAGGAATGGAATGCAATCTTCTCAGGAACACTGCCAGGGCATCAACAATATTTTCACCTGAATCAG
GATATTCTTCCAATACCTGGAATGCTGTTTTCCCTGGGATGGCAGTGGTGAGTAACCATGCATCATCAGGAGTTCTGATAAAATGCTTGATGGTTGGAAGAGGCATAAATTCAGTCAGCCAGTTTAGTCTGACCATCTCA
TCTGTAACATCATTGGCAACAGAACCTTTGCCATGTTTCAGAAACAACTCTGGGGCATCTGGCTTCCCATACAATCTATAGATTGTGGCACCTGATTGCCCAACATTATCTCTAGCCCATTTATACCCATATAAATCAGCAT
CCATGTTGGAATTTAATCTTGGCCTGGAGCAAGAGGTTTCTCTTTGAATATGGCTCATACATGTGCA

FIG. 33

122019 # 2A: GLA-1xL-hyFc (SEQ ID NO:33)

DraIII-RINhe-AmCMV**ΔEF1I126**-BstEII-GLA-1xL/linker-hyFc-BglII-MixpA/BV2

CACTATGTGGACATGAATTCAATTGGCTAGCAG[illegible]
CTACATAAGCTCAATAGCGCTTGACTCAATAATGAAAGTCCATTGAACCAATCAATTGATGTCAATAATGGTTTCAATGCTTTTTGCTCACATGTATAAG
TCAATGATAGCTAATGGATTTTCCATTACTGATGTATCAATCAATATTGATGTCAATATCCTTTCAATGGTTTTGCTCACATGTATAAGTCAATGATAG
ATCATACTAGTAAGTCCTATTGGACTTTCCATTACTGATGTATCAATCAATATTGATGTCAATATCCTTTCAATGGTTTTGCTCACATGTATAAGTCAA
TTTTGCCATTACTGACGCAAATGGGCGGTAGGCGTGTACGGTGGGAGGTCTATATAAGCAGAGCTGGTTTAGTGAACCGTCAGATCGCCTGGAGACGC
CATCCACGCTGTTTTGACCTCCATAGAAGACACCGGGACCGATCCAGCCTCCGCGGCCGGGAACGGTGCATTGGAACGCGGATTCCCCGTGCCAAGAG
TGACGTAAGTACCGCCTATAGAGTCTATAGGCCCACAAAAATGCTTTCTTCTTTTAATATACTTTTTTGTTTATCTTATTTCTAATACTTTCCCTAAT
CTCTTTCTTTCAGGGCAATAATGATACAATGTATCATGCCTCTTTGCACCATTCTAAAGAATAACAGTGATAATTTCTGGGTTAAGGCAATAGCAATA
TCTCTGCATAAATATCTTTATTCTTCTGCAGTAACAACGTCAAGAGCAATAGCACATTCCAGAAATAAGATTTTATCCATGCACACATAAGGTCAATG
TCATCATGTGTAATCCCAGCAGCAGTTACAAACTCAAGAAGGTATATTGCTGTTGAGATGCATCACTTTGTCAACAAAATAATTTTCATCCATGCACG
CATTCCTCGAGGTCGACGGTATCGATAAGCTTGATATCGAATTCCACCATGGTGAGCAAGGGCGAGGAGCTGTTCACCGGGGTGGTGCCCATCCTGGT
CGAGCTGGACGGCGACGTAAACGGCCACAAGTTCAGCGTGTCCGGCGAGGGCGAGGGCGATGCCACCTACGGCAAGCTGACCCTGAAGTTCATCTGC
ACCACCGGCAAGCTGCCCGTGCCCTGGCCCACCCTCGTGACCACCCTGACCTACGGCGTGCAGTGCTTCAGCCGCTACCCCGACCACATGAAGCAGCA
CGACTTCTTCAAGTCCGCCATGCCCGAAGGCTACGTCCAGGAGCGCACCATCTTCTTCAAGGACGACGGCAACTACAAGACCCGCGCCGAGGTGAAGT
TCGAGGGCGACACCCTGGTGAACCGCATCGAGCTGAAGGGCATCGACTTCAAGGAGGACGGCAACATCCTGGGGCACAAGCTGGAGTACAACTACAAC
AGCCACAACGTCTATATCATGGCCGACAAGCAGAAGAACGGCATCAAGGTGAACTTCAAGATCCGCCACAACATCGAGGACGGCAGCGTGCAGCTCG
CCGACCACTACCAGCAGAACACCCCCATCGGCGACGGCCCCGTGCTGCTGCCCGACAACCACTACCTGAGCACCCAGTCCGCCCTGAGCAAAGACCC
CAACGAGAAGCGCGATCACATGGTCCTGCTGGAGTTCGTGACCGCCGCCGGGATCACTCTCGGCATGGACGAGCTGTACAAGTAAAGCGGCCGCGAC
TCTAGAGGATCCCCGGGTACCGAGCTCGAATTCACTGGCCGTCGTTTTACAACGTCGTGACTGGGAAAACCCTGGCGTTACCCAACTTAATCGCCTTG
CAGCACATCCCCCTTTCGCCAGCTGGCGTAATAGCGAAGAGGCCCGCACCGATCGCCCTTCCCAACAGTTGCGCAGCCTGAATGGCGAATGGGACGC
GCCCTGTAGCGGCGCATTAAGCGCGGCGGGTGTGGTGGTTACGCGCAGCGTGACCGCTACACTTGCCAGCGCCCTAGCGCCCGCTCCTTTCGCTTTC
TTCCCTTCCTTTCTCGCCACGTTCGCCGGCTTTCCCCGTCAAGCTCTAAATCGGGGGCTCCCTTTAGGGTTCCGATTTAGTGCTTTACGGCACCTCG
ACCCCAAAAAACTTGATTAGGGTGATGGTTCACGTAGTGGGCCATCGCCCTGATAGACGGTTTTTCGCCCTTTGACGTTGGAGTCCACGTTCTTTAAT
AGTGGACTCTTGTTCCAAACTGGAACAACACTCAACCCTATCTCGGTCTATTCTTTTGATTTATAAGGGATTTTGCCGATTTCGGCCTATTGGTTAAA
AAATGAGCTGATTTAACAAAAATTTAACGCGAATTTTAACAAAATATTAACGTTTACAATTTCAGGTGGCACTTTTCGGGGAAATGTGCGCGGAACCC
CTATTTGTTTATTTTTCTAAATACATTCAAATATGTATCCGCTCATGAGACAATAACCCTGATAAATGCTTCAATAATATTGAAAAAGGAAGAGTATGA
GCCATATTCAACGGGAAACGTCTTGCTCGAGGCCGCGATTAAATTCCAACATGGATGCTGATTTATATGGGTATAAATGGGCTCGCGATAATGTCGGG
CAATCAGGTGCGACAATCTATCGATTGTATGGGAAGCCCGATGCGCCAGAGTTGTTTCTGAAACATGGCAAAGGTAGCGTTGCCAATGATGTTACAG
ATGAGATGGTCAGACTAAACTGGCTGACGGAATTTATGCCTCTTCCGACCATCAAGCATTTTATCCGTACTCCTGATGATGCATGGTTACTCACCACT
GCGATCCCCGGGAAAACAGCATTCCAGGTATTAGAAGAATATCCTGATTCAGGTGAAAATATTGTTGATGCGCTGGCAGTGTTCCTGCGCCGGTTGC
ATTCGATTCCTGTTTGTAATTGTCCTTTTAACAGCGATCGCGTATTTCGTCTCGCTCAGGCGCAATCACGAATGAATAACGGTTTGGTTGATGCGAGT
GATTTTGATGACGAGCGTAATGGCTGGCCTGTTGAACAAGTCTGGAAAGAAATGCATAAACTTTTGCCATTCTACCTCTAGTTGCCAGAGACATTAT
TGTCTGATTCGTTACCAATTATGACAACTTGACGGCTACATCATTCACTTTTTCTTCACAACCGGCACGGAACTCGCTCGGGCTGGCCCCGGTGCATT
TTTTAAATACCCGCGAGAAATAGAGTTGATCGTCAAAACCAACATTGCGACCGACGGTGGCGATAGGCATCCGGGTGGTGCTCAACGAGTTCTTCTGA
GCGGGACTCTGGGGTTCGAAATGACCGACCAAGCGACGCCCAACCTGCCATCACGAGATTTCGATTCCACCGCCGCCTTCTATGAAAGGTTGGGCTTC
GGAATCGTTTTCCGGGACGCCGGCTGGATGATCCTCCAGCGCGGGGATCTCATGCTGGAGTTCTTCGCCCACCCCAACTTGTTTATTGCAGCTTATAA
TGGTTACAAATAAAGCAATAGCATCACAAATTTCACAAATAAAGCATTTTTTTCACTGCATTCTAGTTGTGGTTTGTCCAAACTCATCAATGTATCTT
ATCATGTCTGGATCGATCCTGCAGGCATGCAAGCTTGGCGTAATCATGGTCATAGCTGTTTCCTGTGTGAAATTGTTATCCGCTCACAATTCCACACA
ACATACGAGCCGGAAGCATAAAGTGTAAAGCCTGGGGTGCCTAATGAGTGAGCTAACTCACATTAATTGCGTTGCGCTCACTGCCCGCTTTCCAGTC
GGGAAACCTGTCGTGCCAGCTGCATTAATGAATCGGCCAACGCGCGGGGAGAGGCGGTTTGCGTATTGGGCGCTCTTCCGCTTCCTCGCTCACTGAC
TCGCTGCGCTCGGTCGTTCGGCTGCGGCGAGCGGTATCAGCTCACTCAAAGGCGGTAATACGGTTATCCACAGAATCAGGGGATAACGCAGGAAAGA
ACATGTGAGCAAAAGGCCAGCAAAAGGCCAGGAACCGTAAAAAGGCCGCGTTGCTGGCGTTTTTCCATAGGCTCCGCCCCCCTGACGAGCATCACAA
AAATCGACGCTCAAGTCAGAGGTGGCGAAACCCGACAGGACTATAAAGATACCAGGCGTTTCCCCCTGGAAGCTCCCTCGTGCGCTCTCCTGTTCCGA
CCCTGCCGCTTACCGGATACCTGTCCGCCTTTCTCCCTTCGGGAAGCGTGGCGCTTTCTCATAGCTCACGCTGTAGGTATCTCAGTTCGGTGTAGGT
CGTTCGCTCCAAGCTGGGCTGTGTGCACGAACCCCCCGTTCAGCCCGACCGCTGCGCCTTATCCGGTAACTATCGTCTTGAGTCCAACCCGGTAAGA
CACGACTTATCGCCACTGGCAGCAGCCACTGGTAACAGGATTAGCAGAGCGAGGTATGTAGGCGGTGCTACAGAGTTCTTGAAGTGGTGGCCTAACT
ACGGCTACACTAGAAGGACAGTATTTGGTATCTGCGCTCTGCTGAAGCCAGTTACCTTCGGAAAAAGAGTTGGTAGCTCTTGATCCGGCAAACAAAC
CACCGCTGGTAGCGGTGGTTTTTTTGTTTGCAAGCAGCAGATTACGCGCAGAAAAAAGGATCTCAAGAAGATCCTTTGATCTTTTCTACGGGGTCTG
ACGCTCAGTGGAACGAAAACTCACGTTAAGGGATTTTGGTCATGAGATTATCAAAAAGGATCTTCACCTAGATCCTTTTAAATTAAAAATGAAGTTTT
AAATCAATCTAAAGTATATATGAGTAAACTTGGTCTGACAGTTACCAATGCTTAATCAGTGAGGCACCTATCTCAGCGATCTGTCTATTTCGTTCATC
CATAGTTGCCTGACTCCCCGTCGTGTAGATAACTACGATACGGGAGGGCTTACCATCTGGCCCCAGTGCTGCAATGATACCGCGAGACCCACGCTCAC
CGGCTCCAGATTTATCAGCAATAAACCAGCCAGCCGGAAGGGCCGAGCGCAGAAGTGGTCCTGCAACTTTATCCGCCTCCATCCAGTCTATTAATTG
TTGCCGGGAAGCTAGAGTAAGTAGTTCGCCAGTTAATAGTTTGCGCAACGTTGTTGCCATTGCTACAGGCATCGTGGTGTCACGCTCGTCGTTTGGT
ATGGCTTCATTCAGCTCCGGTTCCCAACGATCAAGGCGAGTTACATGATCCCCCATGTTGTGCAAAAAAGCGGTTAGCTCCTTCGGTCCTCCGATCG
TTGTCAGAAGTAAGTTGGCCGCAGTGTTATCACTCATGGTTATGGCAGCACTGCATAATTCTCTTACTGTCATGCCATCCGTAAGATGCTTTTCTGTG
ACTGGTGAGTACTCAACCAAGTCATTCTGAGAATAGTGTATGCGGCGACCGAGTTGCTCTTGCCCGGCGTCAATACGGGATAATACCGCGCCACATAG
CAGAACTTTAAAAGTGCTCATCATTGGAAAACGTTCTTCGGGGCGAAAACTCTCAAGGATCTTACCGCTGTTGAGATCCAGTTCGATGTAACCCACTC
GTGCACCCAACTGATCTTCAGCATCTTTTACTTTCACCAGCGTTTCTGGGTGAGCAAAAACAGGAAGGCAAAATGCCGCAAAAAAGGGAATAAGGGC
GACACGGAAATGTTGAATACTCATACTCTTCCTTTTTCAATATTATTGAAGCATTTATCAGGGTTATTGTCTCATGAGCGGATACATATTTGAATGTA
TTTAGAAAAATAAACAAATAGGGGTTCCGCGCACATTTCCCCGAAAAGTGCCACCTGACGTCTAAGAAACCATTATTATCATGACATTAACCTATAAA
AATAGGCGTATCACGAGGCCCTTTCGTCTTCAAGAATTCGCCCTTAAGCTTGGTACCGAGCTCGGATCCACTAGTAACGGCCGCCAGTGTGCTGGAA
TTCGCCCTTCTAGAGTCGACCTGCAGAAGCTTGCCTCGAGCAGCGCTGCTCGAGAGATCTACGGGTGGCATCCCTGTGACCCCTCCCCAGTGCCTCT
CCTGGCCCTGGAAGTTGCCACTCCAGTGCCCACCAGCCTTGTCCTAATAAAATTAAGTTGCATCATTTTGTCTGACTAGGTGTCCTTCTATAATATT
ATGGGGTGGAGGGGGTGGTATGGAGCAAGGGGCAAGTTGGGAAGACAACCTGTAGGGCCTGCGGGGTCTATTGGGAACCAAGCTGGAGTGCAGTGGC
ACAATCTTGGCTCACTGCAATCTCCGCCTCCTGGGTTCAAGCGATTCTCCTGCCTCAGCCTCCCGAGTTGTTGGGATTCCAGGCATGCATGACCAGG
CTCAGCTAATTTTTGTTTTTTTGGTAGAGACGGGGTTTCACCATATTGGCCAGGCTGGTCTCCAACTCCTAATCTCAGGTGATCTACCCACCTTGGCC
TCCCAAATTGCTAGGATTACAGGCGTGAACCACTGCTCCCTTCCCTGTCCTTCTGATTTTGTAGGTAACCACGTGCGGACCGAGCGGCCGCAGGAAC
CCCTAGTGATGGAGTTGGCCACTCCCTCTCTGCGCGCTCGCTCGCTCACTGAGGCCGCCCGGGCAAAGCCCGGGCGTCGGGCGACCTTTGGTCGCCC
GGCCTCAGTGAGCGAGCGAGCGCGCAGAGAGGGAGTGGCCAACTCCATCACTAGGGGTTCCTTGTAGTTAATGATTAACCCGCCATGCTACTTATCT
ACGTAGCCATGCTCTAGAGATCTACTTCTGGCTAATAAAAGATCAGAGCTCTAGTGATCTGTGTGTTGGTTTTTTGTGTCTGCATTCTAGCTCTAGT
GATCAGCAGTTCAACCTGTTGATAGTATGTACTAAGCTCTCATGTTTAATGTACTAAGCTCTCATGTTTAATGAACTAAACCCTCATGGCTAATGTAC
TAAGCTCTCATGGCTAATGTACTAAGCTCTCATGTTTCATGTACTAAGCTCTCATGTTTTGAACAATAAAATTAATATAAATCAGCAACTTAAATAGC
CTCTAAGGTTTTAAGTTTTATAAGAAAAAAAAGAATATATAAGGCTTTTAAAGGTTTTAAGGTTTCCTAGGTTATCCTCATATGAGCTCTTAGAAAAA
CTCATCCAGCATCAAATGAAACTGCAATTTATTCATATCAGGATTATCAATACCATATTTTTGAAAAAGTCTTTTCTGTAATGAAGGAGAAAACTCAC
CCAGGCAGTTCCATAGGATGGCAAGATCCTGGTATCTGTCTGCAATTCCAACTCTTCCAACATCAATACAACCTATTAATTTCCCCTCATCAAAAATA
AGGTTATCAAGTGAGAAATCACCATGAGTGACCACTGAATCTGGTGAGAATGGCAAAAGATTATGCATTTCTTTCCAGACTTGTTCAACAGGCCAGCC
ATTTCTCTTCCAGACTTGTTCAACAGGCCAGCCATTTCTCTCATCATCAAAATCACTGGCATCAACCAAACCATTATTCATTCTTGATTGGGCCTGAG
CCAGTCTAAATACTCTATCAGAGTTAAAAGGACAATTACAAACAGGAATGGAATGCAATCTTCTCAGGAACACTGCCAGGGCATCAACAATATTTTCA
CCTGAATCAGGATATTCTTCCAATACCTGGAATGCTGTTTTCCCTGGGATGGCAGTGGTGAGTAACCATGCATCATCAGGAGTTCTGATAAAATGCTT
GATGGTTGGAAGAGGCATAAATTCAGTCAGCCAGTTTAGTCTGACCATCTCATCTGTAACATCATTGGCAACAGAACCTTTGCCATGTTTCAGAAACA
ACTCTGGGGCATCTGGCTTCCCATACAATCTATAGATTGTGGCACCTGATTGCCCAACATTATCTCTAGCCCATTTATACCCATATAAATCAGCATCCA
TGTTGGAATTTAATCTTGGCCTGGAGCAAGAGGTTTCTCTTTGAATATGGCTCATACATGTGCATCCTCCTCATATAGTGAGTTGTATTATACTAGTG
TCGTGTTTCCAAATGTTTAAATTGTCAG

FIG. 34

011215 # 7 : hGCSF-BV3 (SEQ ID NO:34)

DraIII-βGlo BI-Nhe-mCMVΔEF1II26-BstEII -hGCSF-BglII-mpA-IFNβ S/MAR-BV3

CACTATGTGTTAATTAAAATTATCTCTAAGGCATGTGAACTGGCTGTCTTGGTTTTCATCTGTACTTCATCTGCTACCTCTGTGACCTGAAACATATTTATAATTCCA
TTAAGCTGTGCATATGATAGATTTATCATATGTATTTTCCTTAAAGGATTTTTGTAAGAACTAATTGAATTGATACCTGTAAAGTCTTTATCACACTACCCAATAAA
TAATAAATCTCTTTGTTCAGCTCTCTGTTTCTATAAATATGTACCAGTTTTATTGTTTTTAGTGGTAGTGATTTTATTCTCTTTCTATATATATACACACACATGTGTG
CATTCATAAATATATACAATTTTTATGAATAAAAAATTATTAGCAATCAATATTGAAAACCACTGATTTTTGTTTATGTGAGCAAACAGCAGATTAAAAGGAATTT
GAATTCTCATAGCTAGCAGGAGTCAATGGGAAAAACCCATTGGAGCCAAGTACACTGACTCAATAGGGACTTTCCATTGGGTTTTGCCCAGTACATAAGGTCAA
TAGGGGGTGAGTCAACAGGAAAGTCCCATTGGAGCCAAGTACATTGAGTCAATAGGGACTTTCCAATGGGTTTTGCCCAGTACATAAGGTCAATGGGAGGTAA
GCCAATGGGTTTTTCCCATTACTGACATGTATACTGAGTCATTAGGGACTTTCCAATGGGTTTTGCCCAGTACATAAGGTCAATAGGGGTGAATCAACAGGAAA
GTCCCATTGGAGCCAAGTACACTGAGTCAATAGGGACTTTCCATTGGGTTTTGCCCAGTACAAAAGGTCAATAGGGGGTGAGTCAATGGGTTTTTCCCATTATTG
GCACATACATAAGGTCAATAGGGGTGACTAGTGGAGAAGAGCATGCTTGAGGGCTGAGTGCCCCTCAGTGGGCAGAGAGCACATGGCCCACAGTCCCTGAGA
AGTTGGGGGGAGGGGTGGGCAATTGAACTGGTGCCTAGAGAAGGTGGGGCTTGGGTAAACTGGGAAAGTGATGTGGTGTACTGGCTCCACCTTTTTCCCCAG
GGTGGGGGAGAACCATATATAAGTGCAGTAGTCTCTGTGAACATTCAAGCTTCTGCCTTCTCCCTCCTGTGAGTTTGGTAAGTCACTGACTGTCTATGCCTGGGA
AAGGGTGGGCAGGAGATGGGGCAGTGCAGGAAAAGTGGCACTATGAACCCTGCAGCCCTAGACAATTGTACTAACCTTCTTCTCTTTCCTCTCCTGACAGGTTG
GTAACCAAGCCACCATGGCTGGACCTGCCACCCAGAGCCCCATGAAGCTGATGGCCCTGCAGCTGCTGCTGTGGCACAGTGCACTCTGGACAGTGCAGGAAGC
CACCCCCCTGGGCCCTGCCAGCTCCCTGCCCCAGAGCTTCCTGCTCAAGTGCTTAGAGCAAGTGAGGAAGATCCAGGGCGATGGCGCAGCGCTCCAGGAGAAG
CTGTGTGCCACCTACAAGCTGTGCCACCCCGAGGAGCTGGTGCTGCTCGGACACTCTCTGGGCATCCCCTGGGCTCCCCTGAGCAGCTGCCCCAGCCAGGCCCT
GCAGCTGGCAGGCTGCTTGAGCCAACTCCATAGCGGCCTTTTCCTCTACCAGGGGCTCCTGCAGGCCCTGGAAGGGATCTCCCCCGAGTTGGGTCCCACCTTGG
ACACACTGCAGCTGGATGTTGCTGACTTTGCCACCACCATCTGGCAGCAGATGGAAGAACTGGGAATGGCCCCTGCCCTGCAGCCCACCCAGGGTGCCATGCCT
GCCTTTGCCTCTGCTTTCCAGAGAAGGGCAGGAGGGGTCCTGGTTGCCTCCCATCTGCAGAGCTTCCTGGAGGTGTCCTACAGAGTTCTAAGACACCTTGCCCA
GCCCTGATAGATCTACTTCTGGCTAATAAAAGATCAGAGCTCTAGTGATCTGTGTGTTGGTTTTTTGTGTCTGCATTCTAGCAAGTCAATATGTTCACCCCAAAAA
AGCTGTTTGTTAACTTGTCAACCTCATTCTAAAATGTATATAGAAGCCCAAAAGACAATAACAAAAATATTCTTGTAGAACAAAATGGGAAAGAATGTTCCACTA
AATATCAAGATTTAGAGCAAAGCATGAGATGTGTGGGGATAGACAGTGAGGCTGATAAAATAGAGTAGAGCTCAGAAACAGACCCATTGATATATGTAAGTGA
CCTATGAAAAAAATATGGCATTTTACAATGGGAAAATGATGGTCTTTTTCTTTTTTAGAAAAACAGGGAAATATATTTATATGTAAAAAATAAAAGGGAACCCAT
ATGTCATACCATACACACAAAAAAATTCCAGTGAATTATAAGTCTAAATGGAGAAGGCAAAACTTTAAATCTTTTAGAAAATAATATAGAAGCATGCCATCAAGA
CTTCAGTGTAGAGAAAAATTTCTTATGACTCAAAGTCCTAACCACAAAGAAAAGATTGTTAATTAGATTGCATGAATATTAAGACTTATTTTTAAAATTAAAAAAC
CATTAAGAAAAGTCAGGCCATAGAATGACAGAAAATATTTGCAACACCCCAGTAAAGAGAATTGTAATATGCAGATTATAAAAAGAAGTCTTACAAATCAGTAA
AAAATAAAACTAGACAAAAATTTGAACAGATGAAAGAGAAACTCTAAATAATCATTACACATGAGAAACTCAATCTCAGAAATCAGAGAACTATCATTGCATAT
ACACTAAATTAGAGAAATATTAAAAGGCTAAGTAACATCTGTGGCTTAATTAAGCTAGCTCTAGTGATCAGCAGTTCAACCTGTTGATAGTATGTACTAAGCTCTC
ATGTTTAATGTACTAAGCTCTCATGTTTAATGAACTAAACCCTCATGGCTAATGTACTAAGCTCTCATGGCTAATGTACTAAGCTCTCATGTTTCATGTACTAAGCT
CTCATGTTTGAACAATAAAATTAATATAAATCAGCAACTTAAATAGCCTCTAAGGTTTTAAGTTTTATAAGAAAAAAAAGAATATATAAGGCTTTTAAAGGTTTTA
AGGTTTCCTAGGTTATCCTCATATGAGCTCTTAGAAAAACTCATCCAGCATCAAATGAAACTGCAATTTATTCATATCAGGATTATCAATACCATATTTTTGAAAAA
GTCTTTTCTGTAATGAAGGAGAAAACTCACCCAGGCAGTTCCATAGGATGGCAAGATCCTGGTATCTGTCTGCAATTCCAACTCTTCCAACATCAATACAACCTAT
TAATTTCCCCTCATCAAAAATAAGGTTATCAAGTGAGAAATCACCATGAGTGACCACTGAATCTGGTGAGAATGGCAAAAGATTATGCATTTCTTTCCAGACTTG
TTCAACAGGCCAGCCATTTCTCTCATCATCAAAATCACTGGCATCAACCAAACCATTATTCATTCTTGATTGGGCCTGAGCCAGTCTAAATACTCTATCAGAGTTAA
AAGGACAATTACAAACAGGAATGGAATGCAATCTTCTCAGGAACACTGCCAGGGCATCAACAATATTTTCACCTGAATCAGGATATTCTTCCAATACCTGGAATG
CTGTTTTCCCTGGGATGGCAGTGGTGAGTAACCATGCATCATCAGGAGTTCTGATAAAATGCTTGATGGTTGGAAGAGGCATAAATTCAGTCAGCCAGTTTAGT
CTGACCATCTCATCTGTAACATCATTGGCAACAGAACCTTTGCCATGTTTCAGAAACAACTCTGGGGCATCTGGCTTCCCATACAATCTATAGATTGTGGCACCTG
ATTGCCCAACATTATCTCTAGCCCATTTATACCCATATAAATCAGCATCCATGTTGGAATTTAATCTTGGCCTGGAGCAAGAGGTTTCTCTTTGAATATGGCTCATA
CATGTGCACTCCCTATAGTGAGTCGTATTATACTATGCAGATATACTATGCCAATGTTTAATTGTCAG

FIG. 35

071816# 1: (SEQ ID NO:35)

DraIIRINhe ΔmCMVΔEP1126-BstEII-AaCD28H-BglII- MbspA **ΔhCMV**ΔEP1RV126-BstEII-AaCD28L-BglII- MbspA/ BV2

CACTATGTGGACATGAATTCAATTGGCTAGCAG[illegible]
[illegible]
TTATTGGCACATACTAAGTTCCCACTAGTGGAGAAGAGCATGCTTGAGGGCTGAGTGCCCCTCAGTGGGCAGAGAGCACATGGCC
CACAGTCCCTGAGAAGTTGGGGGGAGGGGTGGGCAATTGAACTGGTGCCTAGAGAAGGTGGGGCTTGGGTAAACTGGGAAAGTGATGTGGTGTACTGGCTC
CACCTTTTTCCCCAGGGTGGGGGAGAACCATATATAAGTGCAGTAGTCTCTGTGAACATTCAAGCTTCTGCCTTCTCCCTCCTGTGAGTTTGGTAAGTCACTGACT
GTCTATGCCTGGGAAAGGGTGGGCAGGAGATGGGGCAGTGCAGGAAAAGTGGCACTATGAACCCTGCAGCCCTAGACAATTGTACTAACCTTCTTCTCTTTCCT
CTCCTGACAGGTTGGTAACCAAGCC[illegible]ATGGCTGGTCCCTGATCCTGCTGTTCCTGCTGGCTGTGGCCACCAGAGTGCTGAGCCAGGTGCAGCTGCAGCAGC
CTGGGGCTGAGCTTGTGAAACCTGGGGCCTCTGTGAAGATGAGCTGCAAGGCCTCTGGCTACACCTTCACCAGCTACAACATGCACTGGGTCAAGCAGACCCCT
GGCAGAGGCCTGGAATGGATTGGAGCCATCTACCCTGGCAATGGGGACACCTCCTACAACCAGAAGTTCAAGGGCAAGGCCACCCTGACAGCTGACAAGAGC
AGCAGCACAGCCTACATGCAGCTGTCCAGCCTGACCTCTGAGGACTCTGCTGTGTACTACTGTGCCAGGTCCACCTACTATGGGGGAGACTGGTACTTCAATGT
GTGGGGAGCTGGCACCACAGTGACAGTGTCTGCTGCCAGCACCAAGGGCCCCTCTGTGTTTCCTCTGGCCCCCAGCAGCAAGAGCACCTCTGGGGGAACAGCT
GCCCTGGGCTGCCTTGTGAAGGACTACTTCCCTGAGCCTGTGACTGTGTCCTGGAACTCTGGGGCCCTGACATCTGGGGTGCACACCTTCCCTGCAGTGCTGCA
GTCCAGTGGCCTGTACTCCCTGTCCTCTGTTGTGACAGTGCCCAGCTCCAGCCTGGGCACCCAGACCTACATCTGCAATGTGAACCACAAGCCCAGCAACACCAA
GGTGGACAAGAAGGCTGAGCCCAAGAGCTGTGACAAGACCCACACCTGTCCCCCCTGTCCTGCCCCTGAACTGCTGGGAGGACCTTCTGTGTTCCTGTTCCCAC
CCAAGCCCAAGGATACCCTGATGATCAGCAGAACCCCTGAAGTGACCTGTGTGGTGGTGGATGTGTCCCATGAGGACCCAGAAGTGAAGTTCAATTGGTATGT
GGATGGGGTGGAAGTGCACAATGCCAAGACCAAGCCCAGAGAGGAACAGTACAACAGCACCTACAGAGTGGTGTCTGTGCTGACTGTGCTGCACCAGGACTG
GCTGAATGGCAAAGAGTACAAGTGCAAGGTGTCCAACAAGGCCCTGCCAGCCCCCATTGAGAAAACCATCAGCAAGGCCAAGGGCCAGCCTAGAGAACCCCA
GGTGTACACACTGCCCCCTAGCAGGGATGAGCTGACCAAGAACCAGGTGTCCCTGACATGCCTTGTGAAAGGCTTCTACCCCTCTGACATTGCTGTGGAATGGG
AGAGCAATGGACAGCCTGAGAACAACTACAAGACCACCCCCCCTGTGCTGGACTCTGATGGCTCATTCTTCCTGTACAGCAAGCTGACAGTGGACAAGTCCAGA
TGGCAGCAGGGCAATGTGTTCAGCTGCTCTGTGATGCATGAGGCCCTGCACAACCACTACACCCAGAAAAGCCTGTCCCTGTCCCCTGGCAAGTGAAGATCTAC
TTCTGGCTAATAAAGGATCACAGCTCTAGTGATCTGTGTGTTGATTTTTTGTGTCTGCATTCTAGC**TGTTACATAACTTATGGTAAATGGCCTGCCTGGCTGACT**
GCCCAATGACCCCTGCCCAATGATGTCAATAATGATGTATGTTCCCATGTAATGCCAATAGGGACTTTCCATTGATGTCAATGGGTGGAGTATTTATGGTAAC
TGCCCACTTGGCAGTACATCAAGTGTATCATATGCCAAGTATGCCCCCTATTGATGTCAATGATGGTAAATGGCCTGCCTGGCATTATGCCCAGTACATGACCT
TATGGGACTTTCCTACTTGGCAGTACATCTATGTATTAGTCATTGCTATTACCATGGATTAGTGGAGAAGAGCATGCTTGAGGGCTGAGTGCCCCTCAGTGGGC
AGAGAGCACATGGCCCACAGTCCCTGAGAAGTTGGGGGGAGGGGTGGGCAATTGAACTGGTGCCTAGAGAAGGTGGGGCTTGGGTAAACTGGGAAAGTGAT
GTGGTGTACTGGCTCCACCTTTTTCCCCAGGGTGGGGGAGAACCATATATAAGTGCAGTAGTCTCTGTGAACATTCAAGCTTCTGCCTTCTCCCTCCTGTGAGTTT
GGATATCGTAAGTCACTGACTGTCTATGCCTGGGAAAGGGTGGGCAGGAGATGGGGCAGTGCAGGAAAAGTGGCACTATGAACCCTGCAGCCCTAGACAATT
GTACTAACCTTCTTCTCTTTCCTCTCCTGACAGGTTGGTAACCAAGCCACCATGGACTTTCCAAGTGCAGATCATCAGCTTCCTGCTGATCTCTGCTCTGATCAT
GAGCAGAGGCAGATTGTGCTGAGCCAGTCTCCTGCATCCTGTCTGCAAGCCCTGGGGCAGAAAGTGACCATGACCTGCAGAGCCAGCAGCTCCGTGTCCTAC
ATTCACTGGTTCCAGCAGAAGCCTGGCAGCAGCCCCAAGCCTTGGATCTATGCCACCAGCAACCTGGCATCTGGAGTGCCAGTCAGATTCTCTGGCTCCGGATC
TGGCACCAGCTACAGCCTGACCATCAGCAGAGTGGAAGCTGAGGATGCTGCCACCTACTACTGCCAGCAGTGGACTAGCAATCCCCCACCTTTGGAGGGGGC
ACCAAGCTGGAAATCAAGAGAACAGTGGCTGCCCCATCTGTCTTCATCTTCCCACCCTCTGATGAGCAGCTGAAGTCTGGAACAGCCTCTGTTGTGTGCCTGCTG
AACAACTTCTACCCCAGAGAAGCCAAGGTGCAGTGGAAGGTGGACAATGCCCTGCAGTCTGGCAACTCCCAGGAATCTGTGACAGAGCAGGACAGCAAGGAC
TCCACCTACTCCCTGAGCAGCACCCTGACCCTGAGCAAGGCTGACTATGAGAAACACAAAGTGTATGCCTGTGAAGTGACCCACCAGGGCCTGTCGAGCCCTGT
CACAAGAGCTTCAACAGAGGCGAGAGCTGA**AGATCT**ACTTCTCGCCTAATAAAAGATCAGAGCTCTAGTGATCTGTGTGTTGATTTTTTGTGTCTGCATTCTAGC**TCTAG**
TCTAGTGATCAGCAGTTCAACCTGTTGATAGTATGTACTAAGCTCTCATGTTTAATGTACTAAGCTCTCATGTTTAATGAACTAAACCCTCATGGCTAATGTACTAA
GCTCTCATGGCTAATGTACTAAGCTCTCATGTTTCATGTACTAAGCTCTCATGTTTGAACAATAAAATTAATATAAATCAGCAACTTAAATAGCCTCTAAGGTTTTA
AGTTTTATAAGAAAAAAAAGAATATATAAGGCTTTTAAAGGTTTTAAGGTTTCCTAGGTTATCC**TCATATGAGCTC**TTAGAAAAACTCATCCAGCATCAAATGAA
ACTGCAATTTATTCATATCAGGATTATCAATACCATATTTTTGAAAAAGTCTTTTCTGTAATGAAGGAGAAAACTCACCCAGGCAGTTCCATAGGATGGCAAGATC
CTGGTATCTGTCTGCAATTCCAACTCTTCCAACATCAATACAACCTATTAATTTCCCCTCATCAAAAATAAGGTTATCAAGTGAGAAATCACCATGAGTGACCACT
GAATCTGGTGAGAATGGCAAAAGATTATGCATTTCTTTCCAGACTTGTTCAACAGGCCAGCCATTTCTCTCATCATCAAAATCACTGGCATCAACCAAACCATTAT
TCATTCTTGATTGGGCCTGAGCCAGTCTAAATACTCTATCAGAGTTAAAAGGACAATTACAAACAGGAATGGAATGCAATCTTCTCAGGAACACTGCCAGGGCA
TCAACAATATTTTCACCTGAATCAGGATATTCTTCCAATACCTGGAATGCTGTTTTCCCTGGGATGGCAGTGGTGAGTAACCATGCATCATCAGGAGTTCTGATAA
AATGCTTGATGGTTGGAAGAGGCATAAATTCAGTCAGCCAGTTTAGTCTGACCATCTCATCTGTAACATCATTGGCAACAGAACCTTTGCCATGTTTCAGAAACA
ACTCTGGGGCATCTGGCTTCCCATACAATCTATAGATTGTGGCACCTGATTGCCCAACATTATCTCTAGCCCATTTATACCCATATAAATCAGCATCCATGTTGGA
ATTTAATCTTGGCCTGGAGCAAGAGGTTTCTCTTTGAATATGGCTCATACATGTGCA[illegible]
TTAATTGTCAG

FIG. 36

072520 # 4: aCD20-aCD20 (SEQ ID NO:36)

DraIII-RINhe-**ΔhCMVΔEF1RVI126-8stEII-aCD20-8gIII-MixpA** Δ-hCMVΔEF1I126-8stEII-aCD20-8gIII-MixpA/BV2

CACTATGTGGACATGAATTCAATTGGCTAGCTGTTACATAACTTATGGTAAATGGCCTGCCTGGCTGACTGCCCAATGACCCCTGCCCAATGATGTCAATAATGATGTATG
TTCCCATGTAATGCCAATAGGGACTTTCCATTGATGTCAATGGGTGGAGTATTTATGGTAACTGCCCACTTGGCAGTACATCAAGTGTATCATATGCCAAGTATGCCCCCT
ATTGATGTCAATGATGGTAAATGGCCTGCCTGGCATTATGCCCAGTACATGACCTTATGGGACTTTCCTACTTGGCAGTACATCTATGTATTAGTCATTGCTATTACCATG
GATTACTGGAGAAGAGCATGCTTGAGGGCTGAGTGCCCCTCAGTGGGCAGAGAGCACATGGCCCACAGTCCCTGAGAAGTTGGGGGGAGGGGTGGGCAATTGAACTGG
TGCCTAGAGAAGGTGGGGCTTGGGTAAACTGGGAAAGTGATGTGGTGTACTGGCTCCACCTTTTTCCCCAGGGTGTGGGGGAGAACCATATATAAGTGCAGTAGTCTCTGTG
AACATTCAAGCTTCTGCCTTCTCCCTCCTGTGAGTTTGGTAAGTCACTGACTGTCTATGCCTGGGAAAGGGTGGGCAGGAGATGGGGCAGTGCAGGAAAAGTGGCACTATG
AACCCTGCAGCCCTAGACAATTGTACTAACCTTCTTCTCTTTCCTCTCCTGACAGGTTGGTAACCAACCACCATGGGCTGGTCCCTGATCCTGCTGTTCCTGGTGGCTGTG
GCCACCAGAAGTGCTGAGCCAGGTGCAGCTGCAGCAGCCTGGGGCTGAGCTTGTGAAACCTGGGGCCTCTGTGAAGATGAGCTGCAAGGCCTCTGGCTACACCTTCACC
AGCTACAACATGCACTGGGTCAAGCAGACCCCTGGCAGAGGCCTGGAATGGATTGGAGCCATCTACCCTGGCAATGGGGACACCTCCTACAACCAGAAGTTCAAGGGCAAG
GCCACCCTGACAGCTGACAAGAGCAGCAGCACAGCCTACATGCAGCTGTCCAGCCTGACCTCTGAGGACTCTGCTGTGTACTACTGTGCCAGGTCCACCTACTATGGGGGA
GACTGGTACTTCAATGTCTGGGGAGCTGGCACCACAGTGACAGTGTCTGCTGCCAGCACCAAGGGCCCCTCTGTGTTTCCTCTGGCCCCCAGCAGCAAGAGCACCTCTGGG
GGAACAGCTGCCCTGGGCTGCCTTGTGAAGGACTACTTCCCTGAGCCTGTGACTGTGTCCTGGAACTCTGGGGCCCTGACATCTGGGGTGCACACCTTCCCTGCAGTGCTG
CAGTCCAGTGGCCTGTACTCCCTGTCCTCTGTTGTGACAGTGCCCAGCTCCAGCCTGGGCACCCAGACCTACATCTGCAATGTGAACCACAAGCCCAGCAACACCAAGGTG
GACAAGAAGGCTGAGCCCAAGAGCTGTGACAAGACCCACACCTGTCCCCCTGTCCTGCCCCTGAACTGCTGGGAGGACCTTCTGTGTTCCTGTTCCCACCCAAGCCCAAG
GATACCCTGATGATCAGCAGAACCCCTGAAGTGACCTGTGTGGTGGTGGATGTGTCCCATGAGGACCCAGAAGTGAAGTTCAATTGGTATGTGGATGGGGTGGAAGTGCA
CAATGCCAAGACCAAGCCCAGAGAGGAACAGTACAACAGCACCTACAGAGTGGTGTCTGTGCTGACTGTGCTGCACCAGGACTGGCTGAATGGCAAAGAGTACAAGTGCA
AGGTGTCCAACAAGGCCCTGCCAGCCCCCATTGAGAAAACCATCAGCAAGGCCAAGGGCCAGCCTAGAGAACCCCAGGTGTACACACTGCCCCCTAGCAGGGATGAGCTG
ACCAAGAACCAGGTGTCCCTGACATGCCTTGTGAAAGGCTTCTACCCCTCTGACATTGCTGTGGAATGGGAGAGCAATGGACAGCCTGAGAACAACTACAAGACCACCCCC
CCTGTGCTGGACTCTGATGGCTCATTCTTCCTGTACAGCAAGCTGACAGTGGACAAGTCCAGATGGCAGCAGGGCAATGTGTTCAGCTGCTCTGTGATGCATGAGGCCCTG
CACAACCACTACACCCAGAAAAGCCTGTCCCTGTCCCCTGGCAAG***AGAAAGAGAAGGAGTGGAAGTGGAGCTACTAACTTCAGCCTGCTGAAGCAGGCTGGAGATGTGGAGGAGAACCCTGGACCT***ATGGACTTCCAGGTGCAGATTATCAGCTTCCTGCTAATCAGTGCTTCAGTCATAATGTCCAGAGGACAAATTGTTCTCACCCAGTCTCCAGCAATCATGTCTGCATCTCCAGGGGAGAAGGTCACCATGACCTGCAGTGCCAGCTCAAGTGTAAGTTACATGAACTGGTACCAGCAGAAGTCAGGCACTTCCCCCAAACTCTGGATTTATGACACATCCAAACTGGCTTCTGGAGTCCCTGCTCACTTCAGGGGCAGTGGGTCTGGGACCTCTTACTCTCTCACAATCAGCAGCATGGAGGCTGAAGATGCTGCCACTTATTACTGCCAGCAGTGGAGTAGTAACCCACTCACGTTCGGTGCTGGGACCAAGCTGGAGCTGAAACGGGCTGATGCTGCACCAACTGTATCCATCTTCCCACCATCCAGTGAGCAGTTAACATCTGGAGGTGCCTCAGTCGTGTGCTTCTTGAACAACTTCTACCCCAAAGACATCAATGTCAAGTGGAAGATTGATGGCAGTGAACGACAAAATGGCGTCCTGAACAGTTGGACTGATCAGGACAGCAAAGACAGCACCTACAGCATGAGCAGCACCCTCACGTTGACCAAGGACGAGTATGAACGACATAACAGCTATACCTGTGAGGCCACTCACAAGACATCAACTTCACCCATTGTCAAGAGCTTCAACAGGAATGAGTGTTAG

CACTAGTGGAGAAGAGCATGCTTGAGGGCTGAGTGCCCCTCAGTGGGCAGAGAGCACATGGCCCACAGTCCCTGAGAAGTTGGGGGGAGGGGTGGGCAATTGAACTGGTGCCTAGAGAAGGTGGGGCTTGGGTAAACTGGGAAAGTGATGTGGTGTACTGGCTCCACCTTTTTCCCCAGGGTGTGGGGGAGAACCATATATAAGTGCAGTAGTCTCTGTGAACATTCAAGCTTCTGCCTTCTCCCTCCTGTGAGTTTGGTAAGTCACTGACTGTCTATGCCTGGGAAAGGGTGGGCAGGAGATGGGGCAGTGCAGGAAAAGTGGCACTATGAACCCTGCAGCCCTAGACAATTGTACTAACCTTCTTCTCTTTCCTCTCCTGACAGGTTGGTAACCAACCACCATGGGCTGGTCCCTGATCCTGCTGTTCCTGGTGGCTGTGGCCACCAGAAGTGCTGAGCCAGGTGCAGCTGCAGCAGCCTGGGGCTGAGCTTGTGAAACCTGGGGCCTCTGTGAAGATGAGCTGCAAGGCCTCTGGCTACACCTTCACCAGCTACAACATGCACTGGGTCAAGCAGACCCCTGGCAGAGGCCTGGAATGGATTGGAGCCATCTACCCTGGCAATGGGGACACCTCCTACAACCAGAAGTTCAAGGGCAAGGCCACCCTGACAGCTGACAAGAGCAGCAGCACAGCCTACATGCAGCTGTCCAGCCTGACCTCTGAGGACTCTGCTGTGTACTACTGTGCCAGGTCCACCTACTATGGGGGAGACTGGTACTTCAATGTCTGGGGAGCTGGCACCACAGTGACAGTGTCTGCTGCCAGCACCAAGGGCCCCTCTGTGTTTCCTCTGGCCCCCAGCAGCAAGAGCACCTCTGGGGGAACAGCTGCCCTGGGCTGCCTTGTGAAGGACTACTTCCCTGAGCCTGTGACTGTGTCCTGGAACTCTGGGGCCCTGACATCTGGGGTGCACACCTTCCCTGCAGTGCTGCAGTCCAGTGGCCTGTACTCCCTGTCCTCTGTTGTGACAGTGCCCAGCTCCAGCCTGGGCACCCAGACCTACATCTGCAATGTGAACCACAAGCCCAGCAACACCAAGGTGGACAAGAAGGCTGAGCCCAAGAGCTGTGACAAGACCCACACCTGTCCCCCTGTCCTGCCCCTGAACTGCTGGGAGGACCTTCTGTGTTCCTGTTCCCACCCAAGCCCAAGGATACCCTGATGATCAGCAGAACCCCTGAAGTGACCTGTGTGGTGGTGGATGTGTCCCATGAGGACCCAGAAGTGAAGTTCAATTGGTATGTGGATGGGGTGGAAGTGCACAATGCCAAGACCAAGCCCAGAGAGGAACAGTACAACAGCACCTACAGAGTGGTGTCTGTGCTGACTGTGCTGCACCAGGACTGGCTGAATGGCAAAGAGTACAAGTGCAAGGTGTCCAACAAGGCCCTGCCAGCCCCCATTGAGAAAACCATCAGCAAGGCCAAGGGCCAGCCTAGAGAACCCCAGGTGTACACACTGCCCCCTAGCAGGGATGAGCTGACCAAGAACCAGGTGTCCCTGACATGCCTTGTGAAAGGCTTCTACCCCTCTGACATTGCTGTGGAATGGGAGAGCAATGGACAGCCTGAGAACAACTACAAGACCACCCCCCCTGTGCTGGACTCTGATGGCTCATTCTTCCTGTACAGCAAGCTGACAGTGGACAAGTCCAGATGGCAGCAGGGCAATGTGTTCAGCTGCTCTGTGATGCATGAGGCCCTGCACAACCACTACACCCAGAAAAGCCTGTCCCTGTCCCCTGGCAAG***AGAAAGAGAAGGAGTGGAAGTGGAGCTACTAACTTCAGCCTGCTGAAGCAGGCTGGAGATGTGGAGGAGAACCCTGGACCT***ATGGACTTCCAGGTGCAGATTATCAGCTTCCTGCTAATCAGTGCTTCAGTCATAATGTCCAGAGGACAAATTGTTCTCACCCAGTCTCCAGCAATCATGTCTGCATCTCCAGGGGAGAAGGTCACCATGACCTGCAGTGCCAGCTCAAGTGTAAGTTACATGAACTGGTACCAGCAGAAGTCAGGCACTTCCCCCAAACTCTGGATTTATGACACATCCAAACTGGCTTCTGGAGTCCCTGCTCACTTCAGGGGCAGTGGGTCTGGGACCTCTTACTCTCTCACAATCAGCAGCATGGAGGCTGAAGATGCTGCCACTTATTACTGCCAGCAGTGGAGTAGTAACCCACTCACGTTCGGTGCTGGGACCAAGCTGGAGCTGAAACGGGCTGATGCTGCACCAACTGTATCCATCTTCCCACCATCCAGTGAGCAGTTAACATCTGGAGGTGCCTCAGTCGTGTGCTTCTTGAACAACTTCTACCCCAAAGACATCAATGTCAAGTGGAAGATTGATGGCAGTGAACGACAAAATGGCGTCCTGAACAGTTGGACTGATCAGGACAGCAAAGACAGCACCTACAGCATGAGCAGCACCCTCACGTTGACCAAGGACGAGTATGAACGACATAACAGCTATACCTGTGAGGCCACTCACAAGACATCAACTTCACCCATTGTCAAGAGCTTCAACAGGAATGAGTGTTAG

CACTAGTGGAGAAGAGCATGCTTGAGGGCTGAGTGCCCCTCAGTGGGCAGAGAGCACATGGCCCACAGTCCCTGAGAAGTTGGGGGGAGGGGTGGGCAATTGAACTGGTGCCTAGAGAAGGTGGGGCTTGGGTAAACTGGGAAAGTGATGTGGTGTACTGGCTCCACCTTTTTCCCCAGGGTGTGGGGGAGAACCATATATAAGTGCAGTAGTCTCTGTGAACATTCAAGCTTCTGCCTTCTCCCTCCTGTGAGTTTGGTAAGTCACTGACTGTCTATGCCTGGGAAAGGGTGGGCAGGAGATGGGGCAGTGCAGGAAAAGTGGCACTATGAACCCTGCAGCCCTAGACAATTGTACTAACCTTCTTCTCTTTCCTCTCCTGACAGGTTGGTAACCAACCACCATGGGCTGGTCCCTGATCCTGCTGTTCCTGGTGGCTGTGGCCACCAGAAGTGCTGAGCCAGGTGCAGCTGCAGCAGCCTGGGGCTGAGCTTGTGAAACCTGGGGCCTCTGTGAAGATGAGCTGCAAGGCCTCTGGCTACACCTTCACCAGCTACAACATGCACTGGGTCAAGCAGACCCCTGGCAGAGGCCTGGAATGGATTGGAGCCATCTACCCTGGCAATGGGGACACCTCCTACAACCAGAAGTTCAAGGGCAAGGCCACCCTGACAGCTGACAAGAGCAGCAGCACAGCCTACATGCAGCTGTCCAGCCTGACCTCTGAGGACTCTGCTGTGTACTACTGTGCCAGGTCCACCTACTATGGGGGAGACTGGTACTTCAATGTCTGGGGAGCTGGCACCACAGTGACAGTGTCTGCTGCCAGCACCAAGGGCCCCTCTGTGTTTCCTCTGGCCCCCAGCAGCAAGAGCACCTCTGGGGGAACAGCTGCCCTGGGCTGCCTTGTGAAGGACTACTTCCCTGAGCCTGTGACTGTGTCCTGGAACTCTGGGGCCCTGACATCTGGGGTGCACACCTTCCCTGCAGTGCTGCAGTCCAGTGGCCTGTACTCCCTGTCCTCTGTTGTGACAGTGCCCAGCTCCAGCCTGGGCACCCAGACCTACATCTGCAATGTGAACCACAAGCCCAGCAACACCAAGGTGGACAAGAAGGCTGAGCCCAAGAGCTGTGACAAGACCCACACCTGTCCCCCTGTCCTGCCCCTGAACTGCTGGGAGGACCTTCTGTGTTCCTGTTCCCACCCAAGCCCAAGGATACCCTGATGATCAGCAGAACCCCTGAAGTGACCTGTGTGGTGGTGGATGTGTCCCATGAGGACCCAGAAGTGAAGTTCAATTGGTATGTGGATGGGGTGGAAGTGCACAATGCCAAGACCAAGCCCAGAGAGGAACAGTACAACAGCACCTACAGAGTGGTGTCTGTGCTGACTGTGCTGCACCAGGACTGGCTGAATGGCAAAGAGTACAAGTGCAAGGTGTCCAACAAGGCCCTGCCAGCCCCCATTGAGAAAACCATCAGCAAGGCCAAGGGCCAGCCTAGAGAACCCCAGGTGTACACACTGCCCCCTAGCAGGGATGAGCTGACCAAGAACCAGGTGTCCCTGACATGCCTTGTGAAAGGCTTCTACCCCTCTGACATTGCTGTGGAATGGGAGAGCAATGGACAGCCTGAGAACAACTACAAGACCACCCCCCCTGTGCTGGACTCTGATGGCTCATTCTTCCTGTACAGCAAGCTGACAGTGGACAAGTCCAGATGGCAGCAGGGCAATGTGTTCAGCTGCTCTGTGATGCATGAGGCCCTGCACAACCACTACACCCAGAAAAGCCTGTCCCTGTCCCCTGGCAAG***AGAAAGAGAAGGAGTGGAAGTGGAGCTACTAACTTCAGCCTGCTGAAGCAGGCTGGAGATGTGGAGGAGAACCCTGGACCT***ATGGACTTCCAGGTGCAGATTATCAGCTTCCTGCTAATCAGTGCTTCAGTCATAATGTCCAGAGGACAAATTGTTCTCACCCAGTCTCCAGCAATCATGTCTGCATCTCCAGGGGAGAAGGTCACCATGACCTGCAGTGCCAGCTCAAGTGTAAGTTACATGAACTGGTACCAGCAGAAGTCAGGCACTTCCCCCAAACTCTGGATTTATGACACATCCAAACTGGCTTCTGGAGTCCCTGCTCACTTCAGGGGCAGTGGGTCTGGGACCTCTTACTCTCTCACAATCAGCAGCATGGAGGCTGAAGATGCTGCCACTTATTACTGCCAGCAGTGGAGTAGTAACCCACTCACGTTCGGTGCTGGGACCAAGCTGGAGCTGAAACGGGCTGATGCTGCACCAACTGTATCCATCTTCCCACCATCCAGTGAGCAGTTAACATCTGGAGGTGCCTCAGTCGTGTGCTTCTTGAACAACTTCTACCCCAAAGACATCAATGTCAAGTGGAAGATTGATGGCAGTGAACGACAAAATGGCGTCCTGAACAGTTGGACTGATCAGGACAGCAAAGACAGCACCTACAGCATGAGCAGCACCCTCACGTTGACCAAGGACGAGTATGAACGACATAACAGCTATACCTGTGAGGCCACTCACAAGACATCAACTTCACCCATTGTCAAGAGCTTCAACAGGAATGAGTGTTAGTGAGTCTAGTGATCAGCAGTTCAACCTGTTGATAGTATGTACTAAGCTCTCATGTTTAATGTACTAAGCTCTCATGTTTAATGAACTAAACCCTCATGGCTAATGTACTAAGCTCTCATGGCTAATGTACTAAGCTCTCATGTTTCATGTACTAAGCTCTCATGTTTGAACAATAAAATTAATATAAATCAGCAACTTAAATAGCCTCTAAGGTTTTAAGTTTTATAAGAAAAAAAAGAATATATAAGGCTTTTAAAGGTTTTAAGGTTTCCTAGGTTATCCTCATATGAGCTCTTAGAAAAACTCATCCAGCATCAAATGAAACTGCAATTTATTCATATCAGGATTATCAATACCATATTTTTGAAAAAGTCTTTTCTGTAATGAAGGAGAAAACTCACCCAGGCAGTTCCATAGGATGGCAAGATCCTGGTATCTGTCTGCAATTCCAACTCTTCCAACATCAATACAACCTATTAATTTCCCCTCATCAAAAATAAGGTTATCAAGTGAGAAATCACCATGAGTGACCACTGAATCTGGTGAGAATGGCAAAAGATTATGCATTTCTTTCCAGACTTGTTCAACAGGCCAGCCATTTCTCTCATCATCAAAATCACTGGCATCAACCAAACCATTATTCATTCTTGATTGGGCCTGAGCCAGTCTAAATACTCTATCAGAGTTAAAAGGACAATTACAAACAGGAATGGAATGCAATCTTCTCAGGAACACTGCCAGGGCATCAACAATATTTTCACCTGAATCAGGATATTCTTCCAATACCTGGAATGCTGTTTTCCCTGGGATGGCAGTGGTGAGTAACCATGCATCATCAGGAGTTCTGATAAAATGCTTGATGGTTGGAAGAGGCATAAATTCAGTCAGCCAGTTTAGTCTGACCATCTCATCTGTAACATCATTGGCAACAGAACCTTTGCCATGTTTCAGAAACAACTCTGGGGCATCTGGCTTCCCATACAATCTATAGATTGTGGCACCTGATTGCCCAACATTATCTCTAGCCCATTTATACCCATATAAATCAGCATCCATGTTGGAATTTAATCTTGGCCTGGAGCAAGAGGTTTCTCTTTGAATATGGCTCATACATGTGCA

072520 # 4: aCD20-aCD20 (SEQ ID NO:36)

DraIII-RINhe-**ΔhCMVΔEF1RVI126-8stEII-aCD20-8gIII-MixpA** Δ-hCMVΔEF1I126-8stEII-aCD20-8gIII-MixpA/BV2

CACTATGTGGACATGAATTCAATTGGCTAGCTGTTACATAACTTATGGTAAATGGCCTGCCTGGCTGACTGCCCAATGACCCCTGCCCAATGATGTCAATAATGATGTATG
TTCCCATGTAATGCCAATAGGGACTTTCCATTGATGTCAATGGGTGGAGTATTTATGGTAACTGCCCACTTGGCAGTACATCAAGTGTATCATATGCCAAGTATGCCCCCT
ATTGATGTCAATGATGGTAAATGGCCTGCCTGGCATTATGCCCAGTACATGACCTTATGGGACTTTCCTACTTGGCAGTACATCTATGTATTAGTCATTGCTATTACCATG
GATTACTGGAGAAGAGCATGCTTGAGGGCTGAGTGCCCCTCAGTGGGCAGAGAGCACATGGCCCACAGTCCCTGAGAAGTTGGGGGGAGGGGTGGGCAATTGAACTGG
TGCCTAGAGAAGGTGGGGCTTGGGTAAACTGGGAAAGTGATGTGGTGTACTGGCTCCACCTTTTTCCCCAGGGTGTGGGGGAGAACCATATATAAGTGCAGTAGTCTCTGTG
AACATTCAAGCTTCTGCCTTCTCCCTCCTGTGAGTTTGGTAAGTCACTGACTGTCTATGCCTGGGAAAGGGTGGGCAGGAGATGGGGCAGTGCAGGAAAAGTGGCACTATG
AACCCTGCAGCCCTAGACAATTGTACTAACCTTCTTCTCTTTCCTCTCCTGACAGGTTGGTAACCAACCACCATGGGCTGGTCCCTGATCCTGCTGTTCCTGGTGGCTGTG
GCCACCAGAAGTGCTGAGCCAGGTGCAGCTGCAGCAGCCTGGGGCTGAGCTTGTGAAACCTGGGGCCTCTGTGAAGATGAGCTGCAAGGCCTCTGGCTACACCTTCACC
AGCTACAACATGCACTGGGTCAAGCAGACCCCTGGCAGAGGCCTGGAATGGATTGGAGCCATCTACCCTGGCAATGGGGACACCTCCTACAACCAGAAGTTCAAGGGCAAG
GCCACCCTGACAGCTGACAAGAGCAGCAGCACAGCCTACATGCAGCTGTCCAGCCTGACCTCTGAGGACTCTGCTGTGTACTACTGTGCCAGGTCCACCTACTATGGGGGA
GACTGGTACTTCAATGTCTGGGGAGCTGGCACCACAGTGACAGTGTCTGCTGCCAGCACCAAGGGCCCCTCTGTGTTTCCTCTGGCCCCCAGCAGCAAGAGCACCTCTGGG
GGAACAGCTGCCCTGGGCTGCCTTGTGAAGGACTACTTCCCTGAGCCTGTGACTGTGTCCTGGAACTCTGGGGCCCTGACATCTGGGGTGCACACCTTCCCTGCAGTGCTG
CAGTCCAGTGGCCTGTACTCCCTGTCCTCTGTTGTGACAGTGCCCAGCTCCAGCCTGGGCACCCAGACCTACATCTGCAATGTGAACCACAAGCCCAGCAACACCAAGGTG
GACAAGAAGGCTGAGCCCAAGAGCTGTGACAAGACCCACACCTGTCCCCCTGTCCTGCCCCTGAACTGCTGGGAGGACCTTCTGTGTTCCTGTTCCCACCCAAGCCCAAG
GATACCCTGATGATCAGCAGAACCCCTGAAGTGACCTGTGTGGTGGTGGATGTGTCCCATGAGGACCCAGAAGTGAAGTTCAATTGGTATGTGGATGGGGTGGAAGTGCA
CAATGCCAAGACCAAGCCCAGAGAGGAACAGTACAACAGCACCTACAGAGTGGTGTCTGTGCTGACTGTGCTGCACCAGGACTGGCTGAATGGCAAAGAGTACAAGTGCA
AGGTGTCCAACAAGGCCCTGCCAGCCCCCATTGAGAAAACCATCAGCAAGGCCAAGGGCCAGCCTAGAGAACCCCAGGTGTACACACTGCCCCCTAGCAGGGATGAGCTG
ACCAAGAACCAGGTGTCCCTGACATGCCTTGTGAAAGGCTTCTACCCCTCTGACATTGCTGTGGAATGGGAGAGCAATGGACAGCCTGAGAACAACTACAAGACCACCCCC
CCTGTGCTGGACTCTGATGGCTCATTCTTCCTGTACAGCAAGCTGACAGTGGACAAGTCCAGATGGCAGCAGGGCAATGTGTTCAGCTGCTCTGTGATGCATGAGGCCCTG
CACAACCACTACACCCAGAAAAGCCTGTCCCTGTCCCCTGGCAAG***AGAAAGAGAAGGAGTGGAAGTGGAGCTACTAACTTCAGCCTGCTGAAGCAGGCTGGAGATGTGGAGGAGAACCCTGGACCT***ATGGACTTCCAGGTGCAGATTATCAGCTTCCTGCTAATCAGTGCTTCAGTCATAATGTCCAGAGGACAAATTGTTCTCACCCAGTCTCCAGCAATCATGTCTGCATCTCCAGGGGAGAAGGTCACCATGACCTGCAGTGCCAGCTCAAGTGTAAGTTACATGAACTGGTACCAGCAGAAGTCAGGCACTTCCCCCAAACTCTGGATTTATGACACATCCAAACTGGCTTCTGGAGTCCCTGCTCACTTCAGGGGCAGTGGGTCTGGGACCTCTTACTCTCTCACAATCAGCAGCATGGAGGCTGAAGATGCTGCCACTTATTACTGCCAGCAGTGGAGTAGTAACCCACTCACGTTCGGTGCTGGGACCAAGCTGGAGCTGAAACGGGCTGATGCTGCACCAACTGTATCCATCTTCCCACCATCCAGTGAGCAGTTAACATCTGGAGGTGCCTCAGTCGTGTGCTTCTTGAACAACTTCTACCCCAAAGACATCAATGTCAAGTGGAAGATTGATGGCAGTGAACGACAAAATGGCGTCCTGAACAGTTGGACTGATCAGGACAGCAAAGACAGCACCTACAGCATGAGCAGCACCCTCACGTTGACCAAGGACGAGTATGAACGACATAACAGCTATACCTGTGAGGCCACTCACAAGACATCAACTTCACCCATTGTCAAGAGCTTCAACAGGAATGAGTGTTAG

CACTAGTGGAGAAGAGCATGCTTGAGGGCTGAGTGCCCCTCAGTGGGCAGAGAGCACATGGCCCACAGTCCCTGAGAAGTTGGGGGGAGGGGTGGGCAATTGAACTGGTGCCTAGAGAAGGTGGGGCTTGGGTAAACTGGGAAAGTGATGTGGTGTACTGGCTCCACCTTTTTCCCCAGGGTGTGGGGGAGAACCATATATAAGTGCAGTAGTCTCTGTGAACATTCAAGCTTCTGCCTTCTCCCTCCTGTGAGTTTGGTAAGTCACTGACTGTCTATGCCTGGGAAAGGGTGGGCAGGAGATGGGGCAGTGCAGGAAAAGTGGCACTATGAACCCTGCAGCCCTAGACAATTGTACTAACCTTCTTCTCTTTCCTCTCCTGACAGGTTGGTAACCAACCACCATGGGCTGGTCCCTGATCCTGCTGTTCCTGGTGGCTGTGGCCACCAGAAGTGCTGAGCCAGGTGCAGCTGCAGCAGCCTGGGGCTGAGCTTGTGAAACCTGGGGCCTCTGTGAAGATGAGCTGCAAGGCCTCTGGCTACACCTTCACCAGCTACAACATGCACTGGGTCAAGCAGACCCCTGGCAGAGGCCTGGAATGGATTGGAGCCATCTACCCTGGCAATGGGGACACCTCCTACAACCAGAAGTTCAAGGGCAAGGCCACCCTGACAGCTGACAAGAGCAGCAGCACAGCCTACATGCAGCTGTCCAGCCTGACCTCTGAGGACTCTGCTGTGTACTACTGTGCCAGGTCCACCTACTATGGGGGAGACTGGTACTTCAATGTCTGGGGAGCTGGCACCACAGTGACAGTGTCTGCTGCCAGCACCAAGGGCCCCTCTGTGTTTCCTCTGGCCCCCAGCAGCAAGAGCACCTCTGGGGGAACAGCTGCCCTGGGCTGCCTTGTGAAGGACTACTTCCCTGAGCCTGTGACTGTGTCCTGGAACTCTGGGGCCCTGACATCTGGGGTGCACACCTTCCCTGCAGTGCTGCAGTCCAGTGGCCTGTACTCCCTGTCCTCTGTTGTGACAGTGCCCAGCTCCAGCCTGGGCACCCAGACCTACATCTGCAATGTGAACCACAAGCCCAGCAACACCAAGGTGGACAAGAAGGCTGAGCCCAAGAGCTGTGACAAGACCCACACCTGTCCCCCTGTCCTGCCCCTGAACTGCTGGGAGGACCTTCTGTGTTCCTGTTCCCACCCAAGCCCAAGGATACCCTGATGATCAGCAGAACCCCTGAAGTGACCTGTGTGGTGGTGGATGTGTCCCATGAGGACCCAGAAGTGAAGTTCAATTGGTATGTGGATGGGGTGGAAGTGCACAATGCCAAGACCAAGCCCAGAGAGGAACAGTACAACAGCACCTACAGAGTGGTGTCTGTGCTGACTGTGCTGCACCAGGACTGGCTGAATGGCAAAGAGTACAAGTGCAAGGTGTCCAACAAGGCCCTGCCAGCCCCCATTGAGAAAACCATCAGCAAGGCCAAGGGCCAGCCTAGAGAACCCCAGGTGTACACACTGCCCCCTAGCAGGGATGAGCTGACCAAGAACCAGGTGTCCCTGACATGCCTTGTGAAAGGCTTCTACCCCTCTGACATTGCTGTGGAATGGGAGAGCAATGGACAGCCTGAGAACAACTACAAGACCACCCCCCCTGTGCTGGACTCTGATGGCTCATTCTTCCTGTACAGCAAGCTGACAGTGGACAAGTCCAGATGGCAGCAGGGCAATGTGTTCAGCTGCTCTGTGATGCATGAGGCCCTGCACAACCACTACACCCAGAAAAGCCTGTCCCTGTCCCCTGGCAAG***AGAAAGAGAAGGAGTGGAAGTGGAGCTACTAACTTCAGCCTGCTGAAGCAGGCTGGAGATGTGGAGGAGAACCCTGGACCT***ATGGACTTCCAGGTGCAGATTATCAGCTTCCTGCTAATCAGTGCTTCAGTCATAATGTCCAGAGGACAAATTGTTCTCACCCAGTCTCCAGCAATCATGTCTGCATCTCCAGGGGAGAAGGTCACCATGACCTGCAGTGCCAGCTCAAGTGTAAGTTACATGAACTGGTACCAGCAGAAGTCAGGCACTTCCCCCAAACTCTGGATTTATGACACATCCAAACTGGCTTCTGGAGTCCCTGCTCACTTCAGGGGCAGTGGGTCTGGGACCTCTTACTCTCTCACAATCAGCAGCATGGAGGCTGAAGATGCTGCCACTTATTACTGCCAGCAGTGGAGTAGTAACCCACTCACGTTCGGTGCTGGGACCAAGCTGGAGCTGAAACGGGCTGATGCTGCACCAACTGTATCCATCTTCCCACCATCCAGTGAGCAGTTAACATCTGGAGGTGCCTCAGTCGTGTGCTTCTTGAACAACTTCTACCCCAAAGACATCAATGTCAAGTGGAAGATTGATGGCAGTGAACGACAAAATGGCGTCCTGAACAGTTGGACTGATCAGGACAGCAAAGACAGCACCTACAGCATGAGCAGCACCCTCACGTTGACCAAGGACGAGTATGAACGACATAACAGCTATACCTGTGAGGCCACTCACAAGACATCAACTTCACCCATTGTCAAGAGCTTCAACAGGAATGAGTGTTAGTGAGTCTAGTGATCAGCAGTTCAACCTGTTGATAGTATGTACTAAGCTCTCATGTTTAATGTACTAAGCTCTCATGTTTAATGAACTAAACCCTCATGGCTAATGTACTAAGCTCTCATGGCTAATGTACTAAGCTCTCATGTTTCATGTACTAAGCTCTCATGTTTGAACAATAAAATTAATATAAATCAGCAACTTAAATAGCCTCTAAGGTTTTAAGTTTTATAAGAAAAAAAAGAATATATAAGGCTTTTAAAGGTTTTAAGGTTTCCTAGGTTATCCTCATATGAGCTCTTAGAAAAACTCATCCAGCATCAAATGAAACTGCAATTTATTCATATCAGGATTATCAATACCATATTTTTGAAAAAGTCTTTTCTGTAATGAAGGAGAAAACTCACCCAGGCAGTTCCATAGGATGGCAAGATCCTGGTATCTGTCTGCAATTCCAACTCTTCCAACATCAATACAACCTATTAATTTCCCCTCATCAAAAATAAGGTTATCAAGTGAGAAATCACCATGAGTGACCACTGAATCTGGTGAGAATGGCAAAAGATTATGCATTTCTTTCCAGACTTGTTCAACAGGCCAGCCATTTCTCTCATCATCAAAATCACTGGCATCAACCAAACCATTATTCATTCTTGATTGGGCCTGAGCCAGTCTAAATACTCTATCAGAGTTAAAAGGACAATTACAAACAGGAATGGAATGCAATCTTCTCAGGAACACTGCCAGGGCATCAACAATATTTTCACCTGAATCAGGATATTCTTCCAATACCTGGAATGCTGTTTTCCCTGGGATGGCAGTGGTGAGTAACCATGCATCATCAGGAGTTCTGATAAAATGCTTGATGGTTGGAAGAGGCATAAATTCAGTCAGCCAGTTTAGTCTGACCATCTCATCTGTAACATCATTGGCAACAGAACCTTTGCCATGTTTCAGAAACAACTCTGGGGCATCTGGCTTCCCATACAATCTATAGATTGTGGCACCTGATTGCCCAACATTATCTCTAGCCCATTTATACCCATATAAATCAGCATCCATGTTGGAATTTAATCTTGGCCTGGAGCAAGAGGTTTCTCTTTGAATATGGCTCATACATGTGCA

FIG. 37

111517 # 1 : 5J8-5J8: Double 2A (SEQ ID NO:37)

DraIII-βGlo III-NheI-MCMVAEP3I126-BstEII-5J8-BglII-MAPA-NotI-CMV-ΔEP3I126-BstEII-5J8-BglII-MAPA-IFNβ S/MAR-BV3

CACTATGTGTTAATTAAAAATTATCTCTAAGGCATGTGAACTGGCTGTCTTGGTTTTCATCTGTACTTCATCTGCTACCTCTGTGACCTGAAACATATTTATAATTCCATTAAGCTGTGCATATGATAGATTT
ATCATATGTATTTTCCTTAAAGGATTTTTGTAAGAACTAATTGAATTGATACCTGTAAAGTCTTTATCACACTACCCAATAAATAATAAATCTCTTTGTTCAGCTCTCTGTTTCTATAAATATGTAGCAGTTT
TATTGTTTTTAGTGGTAGTGATTTTATTCTCTTTCTATATATATACACACACATGTGTGCATTCATAAATATATACAATTTTTATGAATAAAAAATTATTAGCAATCAATATTGAAAACCACTGATTTTTGTT
TATGTGAGCAAACAGCAGATTAAAAGGAATTTGAATTCTCATAGCTAGCAG[illegible]ACTAGTGGAGAAGACCATGCTTGAGGGCTGAGTGCC
CCTCAGTGCCCAGAGAGCACATGGCTCACAGTCCCTGAGAAGTTGTGGGGGAGGGGTGGGCAATTGAACTGGTGCCTAGAGAAGGTGGGGCTTGGGTAAACTGGGAAAGTGATGTCGTGTACTGGC
TCCACCTTTTCCCCAGGGTGGGGGAGAACCATATATAAGTGCAGTAGTCTCTGTGAACATTCAAGCTTCTGCCTTCTCCCTCCTGTGAGTTTGGTAAGTCAGTGACTGTCTATGCCTGGGAAAGGGTG
GGCAGGAGATGGGGCAGTGCAGGAAAAGTGGCACTATGAACCCTGCAGCCCTAGACAATTGTACTAACCTTCTTCTCTTTCCTCTCCTGACAGGTTGGTAACCC[illegible]ATGGGATGGTCCCTGAT
CCTGCTGTTTCTGGTGGCTGTGGCCACCAGAGTGCTGTCTGAAGTGCAGCTGGTGGAATCTGGCCCTGGCCTGGTTAAGCCCTCTGACACTCCTGAGCCTGACCTGTGCTGTGTCTGGCTACAGCATCAG
CAGCAACTACTACTGGGGCTGGATCAGACAGCCTCCTGGCAAAGGCCTGGAATGGATTGGCAGCATCTACCACTCTGGCTCCACCTACTACAAGCCCAGCCTGGAAAGCAGACTGGGCATCTCTGTGG
ACACCAGCAAGAACCAGTTCAGCCTGAAGCTGAGCTTTGTGACTGCTGCTGACACTGCTGTGTACTACTGTGCCAGACATGTTAGGAGTGGCTACCC[illegible]AGGGCACCCTGGTCACAGTGTCTGCTTCTACAAAGGGCCCATCTGTGTTCCCACTGGCCCCTAGCAGCAAGAGCACCAGTGGTGGAACAGCTGGCCCTGGGCTGTCTGGTCAAGGACTACTTCCCTGAG
CCAGTGACAGTGTCCTGGAACTCTGGGGCTCTGACTCTGGGGTGCACACATTCCCTGCTGTGCTCCAGTCCTCTGGCCTGTACAGCCTGTCCTCTGTGGTCACTGTGCCAAGCTCTAGCCTGGGCACCC
AGACCTACATCTGCAATGTGAACCACAAGCCTAGCAACACCAAGGTGGACAAGAAGGCTGAGCCCAAGAGCTGTGACAAGACCCACACCTGTCCTCCATGTCCTGCTCCAGAGCTGCTTGGAGGACCT
TCTGTGTTTCTGTTCCCTCCAAAGCCAAAGGACACCCTGATGATCAGCAGAACCCCTGAAGTGACCTGTGTGGTGGTGGATGTGTCCCATGAGGACCCAGAAGTGAAGTTCAATTGGTATGTGGATGG
TGTTGAGGTGCACAATGCCAAGACCAAGCCTAGAGAGGAACAGTACAACAGCACCTACAGGGTTGTGTCAGTGCTGACTGTGCTGCACCAGGACTGGCTGAATGGCAAAGAGTACAAGTGCAAGGT
GTCCAACAAGGCCCTGCCTGCTCCTATTGAAAAGACCATCAGCAAGGCCAAGGGACAGCCTAGGGAACCCCAGGTGTACACACTGCCACCTAGCAGAGATGAGCTGACCAAGAATCAGGTGTCCCTG
ACATGCCTTGTGAAGGGCTTCTACCCTTCTGACATTGCAGTGGAATGGGAGAGCAATGGCCAGCCTGAGAACAACTACAAGACAACCCCTCCTGTGCTGGACTCTGATGGCTCATTCTTCCTGTACTCC
AAGCTGACAGTGGACAAGTCCAGATGGCAGCAAGGGAATGTGTTCAGCTGCTCTGTGATGCATGAGGCCCTGCACAACCACTACACACAGAAGTCCCTGTCTCTGAGCCCTGGCAAG[illegible]AAAAAGAAAA
GGAAGTGGATCTGGC*GCCACCAACTTCAGCCTGCTGAAACAGGCTGGGGATGTTGAAGAGAACCCTGGACCT*ATGCCCATCGGCTTGCTGCTCCTGGCAGCTGCCTTCGCAGTGGCAG
CCAGCTATGGCTGAGCAGGCTGCATGTGTGTGTGGCTCAGGGAGAGCAGCAGAATCAGCTGTGGCAACAACATTGGCAGAGGTCTGCGCCTGGTATCAGCAGAGCCCGGGAGCAGGC
ACCACTGCTGATGTTTATGAGGACTCTGACAGACCCTCTGGCATCCCTAGCAGGTTCTCTGGCAGCAACTCTGGGAACACGCCTACACTGACCATCTCGGGAACCCAGGCTATGGAGGCTGATT
ATTACTGTCAAGGTGGGAGCATCAGCAGCAGCCAGACTGTTGTTGGTGGTGGCACCAAGCTGACTGTCCTAGGCCAGCCCAAGGCTGCCCCCTCGGTCACTCTGTTCCCACCCTCCTCTGAGGAGCTTC
AAGCTAACAAAGCCACACTGGTGTGTCTCATAAGTGACTTCTACCCGGGAGCCGTGACAGTGGCCTGGAAGGCAGATAGCAGCCCCGTCAAGGCGGGAGTGGAGACCACCACACCCTCCAAACAAAGC
AACAACAAGTACGCGGCCAGCAGCTATCTGAGCCTGACGCCTGAGCAGTGGAAGTCCCACAGAAGCTACAGCTGCCAGGTCACGCATGAAGGGAGCACCGTGGAGAAGACAGTGGCCCCTACAGAATGCTCT
AGTCAATATGTTCACCCCAAAAAAGCTGTTTGTTAACTTGTCAACCTCATTCTAAAATGTATATAGAAGCCCAAAAGACAATAACAAAAATATTCTTGTAGAACAAAATGGGAAAGAATGTTCCACTAAATATC
AAGATTTAGAGCAAAGCATGAGATGTGTGGGGATAGACAGTGAGGCTGATAAAATAGAGTAGAGCTCAGAAACAGACCCATTGATATATGTAAGTGACCTATGAAAAAAATATGGCATTTTACAATGGGAAAA
TGATGGTCTTTTCTTTTTTAGAAAAACAGGGAAATATATTTATATGTAAAAAATAAAAGGGAACCCATATGTCATACCATACACACAAAAAAATTCCAGTGAATTATAAGTCTAAATGGAGAAGGCAAAACTTT
AAATCTTTAGAAAATAATATAGAAGCATGCCATCAAGACTTCAGTGTAGAGAAAAATTTCTTATGACTCAAAGTCCTAACCACAAAGAAAAGATTGTTAAATAGATTGCATGAATATTAAGACTTATTT
TTAAAATTAAAAAACCATTAAGAAAAGTCAGGCCATAGAATGACAGAAAATATTTGCAACACCCCAGTAAAGAGAATTGTAATATGCAGATTATAAAAAGAAGTCTTACAAATCAGTAAAAAATAAAA
CTAGACAAAAATTTGAACAGATGAAAGAGAAACTCTAAATAATCATTACACATGAGAAACTCAATCTCAGAAATCAGAGAACTATCATTGCATATACACTAAATTAGAGAAATATTAAAAGGCTAAGTA
ACATCTGTGGCTTAATTAA[illegible]TCTAGTGATCAGCAGTTCAACCTGTTGATAGTATGTACTAAGCTCTCATGTTTAATGTACTAAGCTCTCATGTTTAATGAACTAAACCCTCATGGCTAATGTACTA
AGCTCTCATGGCTAATGTACTAAGCTCTCATGTTTCATGTACTAAGCTCTCATGTTTGAACAATAAAATTAATATAAATCAGCAACTTAAATAGCCTCTAAGGTTTTAAGTTTTATAAGAAAAAAAAGAAT
ATATAAGGCTTTTAAAGGTTTTAAGGTTTCCTAGGTTATCCTCATATGAGCTCTTAGAAAAACTCATCCAGCATCAAATGAAACTGCAATTTATTCATATCAGGATTATCAATACCATATTTTTGAAAAAG
TCTTTTCTGTAATGAAGGAGAAAACTCACCCAGGCAGTTCCATAGGATGGCAAGATCCTGGTATCTGTCTGCAATTCCAACTCTTCCAACATCAATACAACCTATTAATTTCCCCTCATCAAAAATAAGGT
TATCAAGTGAGAAATCACCATGAGTGACCACTGAATCTGGTGAGAATGGCAAAAGATTATGCATTTCTTTCCAGACTTGTTCAACAGGCCAGCCATTTCTCTCATCATCAAAATCACTGGCATCAACCAA
ACCATTATTCATTCTTGATTGGGCCTGAGCCAGTCTAAATACTCTATCAGAGTTAAAAGGACAATTACAAACAGGAATGGAATGCAATCTTCTCAGGAACACTGCCAGGGCATCAACAATATTTTCACCT
GAATCAGGATATTCTTCCAATACCTGGAATGCTGTTTTCCCTGGGATGGCAGTGGTGAGTAACCATGCATCATCAGGAGTTCTGATAAAATGCTTGATGGTTGGAAGAGGCATAAATTCAGTCAGCCA
GTTTAGTCTGACCATCTCATCTGTAACATCATTGGCAACAGAACCTTTGCCATGTTTCAGAAACAACTCTGGGGCATCTGGCTTCCCATACAATCTATAGATTGTGGCACCTGATTGCCCAACATTATCTC
TAGCCCATTTATACCCATATAAATCAGCATCCATGTTGGAATTTAATCTTGGCCTGGAGCAAGAGGTTTCTCTTTGAATATGGCTCATACATGTGCA[illegible]

FIG. 38

111517 # 3 : aIL5-aIL5 : Double 2A (SEQ ID NO:38)

DraIII-βGlo BI-NheI-[illegible]-CMVAEP3I126-BstEII-aIL5-BglII-MfeI-[illegible]-AEP3I126-BstEII-aIL5-BglII-MfeI-pA-IFNβ S/MAR-BV3

CACTATGTGTTAATTAAAAATTATCTCTAAGGCATGTGAACTGGCTGTCTTGGTTTTCATCTGTACTTCATCTGCTACCTCTGTGACCTGAAACATATTTATAATTCCATTAAGCTGTGCATATGATAGATTT
ATCATATGTATTTTCCTTAAAGGATTTTTGTAAGAACTAATTGAATTGATACCTGTAAAGTCTTTATCACACTACCCAATAAATAATAAATCTCTTTGTTCAGCTCTCTGTTTCTATAAATATGTACCAGTTT
TATTGTTTTTAGTGGTAGTGATTTTATTCTCTTTCTATATATATACACACACATGTGTGCATTCATAAATATATACAATTTTTATGAATAAAAAATTATTAGCAATCAATATTGAAAACCACTGATTTTTGTT
TATGTGAGCAAACAGCAGATTAAAAGGAATTTGAATTCTCATAGCTAGCAG[illegible]

[illegible]ACTAGTGGAGAAGAGCATGCTTGAGGGCTGAGTGCCCTCAGTGTGGCAGAGAGCACATGGCCCACAGTCCCTGAGAAGTTGGGGGGAGGGGTGGGCAATTGAACTGGTGCCTAGAGAA
AGGTGGGGCTTGGGTAAACTGGGAAAGTGATGTCGTGTACTGGCTCCACCTTTTTCCCCAGGGTGGGGGAGAACCATATATAAGTGCAGTAGTCTCTGTGAACATTCAAGCTTCTGCCTTCTCCCTCCT
GTGAGTTTGGTAAGTCAGTGACTGTCTATGCCTGGGAAAGGGTGGGCAGGAGATGGGGCAGTGCAGGAAAAGTGGCACTATGAACCCTGCAGCCCTAGACAATTGTACTAACCTTCTTCTCTTTCCTC
TCCTGACAGGTTGCTAACCAA[illegible]TGTTCCTCAGACACAGGTGTTCATCAGCCTGCTCCTGTGGATCACTGCTGCCTATGGACAGGTCCAGCTGCAAGAGTCTGGCCCTGGACTTGTCAGACC
CAGCCAGACACTGAGCCTGACCTGTACAGTCTCTGGCTTCAGCCTGACCAGCTACTCTGTGCACTGGGTCAGACAGCCTCCAGGCAAGGGACTGGAATGGCTGGGAGTGATCTGGGCCAGTGGTGGC
ACAGACTACAACTCTGCCCTGATGAGCAGACTGAGCATCCTGAAGGACAACAGCAAGAACCAGGTGTCCCTGAGACTGTCCTCTGTGACAGCTGCTGATACAGCTGTGTACTTCTGTGCCAGAGATCC
TCCTAGCTCTCTGCTGAGACTGGACTACTGGGGCCAGGGCACAACAGTGACAGTGTCCAGTGCCAGCACAAAGGGCCCCTCTGTGTTTCCTCTGGCTCCCAGCAGCAAGAGCACCAGTGGTGGAACTG
CTGCCCTGGGCTGTCTGGTCAAGGACTACTTCCTGAGCCCTGTGACTGTGTCCTGGAACTCTGGGGCTCTGACATCTGGGGTGCACACATTCCCTGCTGTGCTGCAATCCTCTGGCCTGTACAGCCTCAG
CTCTGTGGTCACAGTGCCTAGCTCTAGCCTGGGCACCCAGACCTACATCTGCAATGTGAACCACAAGCCTAGCAACACCAAGGTGGACAAGAAGGCTGAGCCCAAGAGCTGTGACAAGACCCACACCT
GTCCTCCATGTCCTGCTCCAGAGCTGCTTGGAGGACCCAGTGTCTTCCTGTTTCCTCCAAAGCCAAAGGACACCCTGATGATCAGCAGAACCCCTGAAGTGACCTGTGTGGTGGTGGATGTGAGCCACG
AGGACCCTGAAGTCAAGTTCAATTGGTATGTGGATGGTGTTGAGGTGCACAATGCCAAGACCAAGCCTAGAGAGGAACAGTACAACAGCACCTACAGAGTGGTGTCAGTGCTGACAGTGCTGCACCA
GGACTGGCTGAATGGCAAAGAGTACAAGTGCAAGGTGTCCAACAAGGCCCTGCCTGCTCCTATTGAAAAGACCATCAGCAAGGCCAAGGGCCAGCCTAGGGAACCCCAGGTTTACACACTGCCACCT
AGCCAGAGATGAGCTGACCAAAAATCAGGTTTCCCTGACCTGCCTGGTTAAGGGCTTCTACCCCTCTGACATTGCTGTGGAATGGGAGAGCAATGGGCAGCCTGAGAACAACTACAAGACAACCCCTCC
TGTGCTGGACTCTGATGGCTCATTCTTCCTGTACTCCAAGCTGACTGTGGACAAAAGCAGATGGCAGCAAGGCAATGTGTTCAGCTGCTCTGTGATGCATGAGGCCCTGCACAACCACTACACCCAGAA
GTCCCTGTCTCTGAGCCCTGGCAAG*AGAAAGAGAAGGAGTGGCTCTGGGGCCACCAACTTTAGCCTGCTGAAACAGGCTGGGGATGTTGAAGAGAACCCTGGACCT*[illegible]

[illegible]TGAAGATCT[illegible]TCATATGAGCTCTTAGAAAAACTCATCCAGCATCAAATGAAACTGCAATTTATTCATATCAGGATTAT
CAATACCATATTTTTGAAAAAGTCTTTTCTGTAATGAAGGAGAAAACTCACCCAGGCAGTTCCATAGGATGGCAAGATCCTGGTATCTGTCTGCAATTCCAACTCTTCCAACATCAATACAACCTATTAAT
TTCCCCTCATCAAAAATAAGGTTATCAAGTGAGAAATCACCATGAGTGACCACTGAATCTGGTGAGAATGGCAAAAGATTATGCATTTCTTTCCAGACTTGTTCAACAGGCCAGCCATTTCTCTCATCAT
CAAAATCACTGGCATCAACCAAACCATTATTCATTCTTGATTGGGCCTGAGCCAGTCTAAATACTCTATCAGAGTTAAAAGGACAATTACAAACAGGAATGGAATGCAATCTTCTCAGGAACACTGCCA
GGGCATCAACAATATTTTCACCTGAATCAGGATATTCTTCCAATACCTGGAATGCTGTTTTCCCTGGGATGGCAGTGGTGAGTAACCATGCATCATCAGGAGTTCTGATAAAATGCTTGATGGTTGGAA
GAGGCATAAATTCAGTCAGCCAGTTTAGTCTGACCATCTCATCTGTAACATCATTGGCAACAGAACCTTTGCCATGTTTCAGAAACAACTCTGGGGCATCTGGCTTCCCATACAATCTATAGATTGTGGC
ACCTGATTGCCCAACATTATCTCTAGCCCATTTATACCCATATAAATCAGCATCCATGTTGGAATTTAATCTTGGCCTGGAGCAAGAGGTTTCTCTTTGAATATGGCTCATACATGTGCA[illegible]

FIG. 39

111517 # 19A : 5J8-aIL5 : Daul 2A (SEQ ID NO:39)

DraIII-βGlo RI-Nhe-[illegible]-CMVAEP31126-BstEII-5J8-BglII-MlupA-SmCBAV-AEP31126-BstEII-aIL5-BglII-MlupA-IFNβ S/MAR-BV3

CACTATGTGTTAATTAAAAATTATCTCTAAGGCATGTGAACTGGCTGTCTTGGTTTTCATCTGTACTTCATCTGCTACCTCTGTGACCTGAAACATATTTATAATTCCATTAAGCTGTGCATATGATAGATTT
ATCATATGTATTTTCCTTAAAGGATTTTTGTAAGAACTAATTGAATTGATACCTGTAAAGTCTTTATCACACTACCCAATAAATAATAAATCTCTTTGTTCAGCTCTCTGTTTCTATAAATATGTAGCAGTTT
TATTGTTTTTAGTGGTAGTGATTTTATTCTCTTTCTATATATATACACACACATGTGTGCATTCATAAATATATACAATTTTTATGAATAAAAAATTATTAGCAATCAATATTGAAAACCACTGATTTTTGTT
TATGTGAGCAAACAGCAGATTAAAAGGAATTTGAATTCTCATAGCTAGCAG[illegible]ACTAGTGGAGAAGACCATGCTTGAGGGCTGAGTGCC
CCTCAGTGCCCAGAGAGCACATGGCTCACAGTCCCTGAGAAGTTGTGGGGGAGGGGTGGGCAATTGAACTGGTGCCTAGAGAAGGTGGGGCTTGGGTAAACTGGGAAAGTGATGTGTGTACTGGC
TCCACCTTTTCCCCAGGGTGGGGGAGAACCATATATAAGTGCAGTAGTCTCTGTGAACATTCAAGCTTCTGCCTTCTCGCTGCTGTGAGTTTGGTAAGTCAGTGACTGTCTATGGCTGGGAAAGGGTG
GGCAGGAGATGGGGCAGTGCAGGAAAAGTGGCACTATGAACCCTGCAGCCCTAGACAATTGTACTAACCTTCTTCTCTTTCCTCTCCTGACAGGTTGGTAACCC[illegible]ATGGGATGGTCCTGAT
CCTGCTGTTTCTGGTGGCTGTGGCCACCAGAGTGCTGTCTGAAGTGCAGCTGGTGGAATCTGGCCCTGGCCTGGTTAAGCCCTCTGACACTCTGAGCCTGACCTGTGCTGTGTCTGGCTACAGCATCAG
CAGCAACTACTACTGGGGCTGGATCAGACAGCCTCCTGGCAAAGGCCTGGAATGGATTGGCAGCATCTACCACTCTGGCTCCACCTACTACAAGCCCAGCCTGGAAAGCAGACTGGGCATCTCTGTGG
ACACCAGCAAGAACCAGTTCAGCCTGAAGCTGAGCTTTGTGACTGCTGCTGACACTGCTGTGTACTACTGTGCCAGACATGTTAGGAGTGGCTACCCTGACACAGCCTACTACTTTGATAAGTGGGGCC
AGGGCACCCTGGTCACAGTGTCTGCTTCTACAAAGGGCCCATCTGTGTTCCCACTGGCCCCTAGCAGCAAGAGCACCAGTGGTGGAACAGCTGGCCCTGGGCTGTCTGGTCAAGGACTACTTTCCTGAG
CCAGTGACAGTGTCCTGGAACTCTGGGGCTCTGACTCTGGGGTGCACACATTCCCTGCTGTGCTCCAGTCCTCTGGCCTGTACAGCCTGTCCTCTGTGGTCACTGTGCCAAGCTCTAGCCTGGGCACCC
AGACCTACATCTGCAATGTGAACCACAAGCCTAGCAACACCAAGGTGGACAAGAAGGCTGAGCCCAAGAGCTGTGACAAGACCCACACCTGTCCTCCATGTCCTGCTCCAGAGCTGCTTGGAGGACCT
TCTGTGTTTCTGTTCCCTCCAAAGCCAAAGGACACCCTGATGATCAGCAGAACCCCTGAAGTGACCTGTGTGGTGGTGGATGTGTCCCATGAGGACCCAGAAGTGAAGTTCAATTGGTATGTGGATGG
TGTTGAGGTGCACAATGCCAAGACCAAGCCTAGAGAGGAACAGTACAACAGCACCTACAGGGTTGTGTCAGTGCTGACTGTGCTGCACCAGGACTGGCTGAATGGCAAAGAGTACAAGTGCAAGGT
GTCCAACAAGGCCCTGCCTGCTCCTATTGAAAAGACCATCAGCAAGGCCAAGGGACAGCCTAGGGAACCCCAGGTGTACACACTGCCACCTAGCAGAGATGAGCTGACCAAGAATCAGGTGTCCCTG
ACATGCCTTGTGAAGGGCTTCTACCCTTCTGACATTGCAGTGGAATGGGAGAGCAATGGCCAGCCTGAGAACAACTACAAGACAACCCCTCCTGTGCTGGACTCTGATGGCTCATTCTTCCTGTACTCC
AAGCTGACAGTGGACAAGTCCAGATGGCAGCAAGGCAATGTGTTCAGCTGCTCTGTGATGCATGAGGCCCTGCACAACCACTACACACAGAAGTCCCTGTCTCTGAGCCCTGGCAAG[illegible]
CGCACTGGATCTGGC*GCCACCAACTTCAGCCTGCTGAAACAGGCTGGGGATGTTGAAGAGAACCCTGGACCT*A[illegible]
CCAGCTATGTGCTGATGCAGCCTCATCTGTGTTGTGGCTTGAGGGTAGACAGCAGAATCAGCTTGGTGGCAACAACATTGGCAAAGGTTGTTGGCACTGTTATCAGCAGACTCCAGGACAGGC
ACCACTGCTGATGTTTATGATGACTTGAAAGCCTCTGCACTCCAGATGACTTTCTCTGGCAAGCAACTCTGGAAACACCCTAGACTGATGCTATCTGCAGTGTTGAAGTTGGATGATGAGGCTGATT
ACTACTGCAAGGTGTGGGATATCAGCAAAAGCAACGACTGTTTTGTGTTCGGCGGAGGCACCAAGCTGACTGTCCTAGGCCAGCCCAAAGCTGCCCCTTCTGTCACTCTGTTCCCACCCTCTAGCGAG
AGGCTAGCAAGCGCCACACTTGTTGTGTCTGATCTGCTTCTATCCAGGGCGCTGTGAACGTCGCCTGGAAGGCTGATAGCAGCCCCGTCAAGGCGGGAGTGGAGACCACCACACCCTCCAAACAAAGC
CGACAACAAGTATGCGGCCAGCAGCTACCTGAGCCTGACGCCTGAGCAGTGGAAGTCCCACAGAAGCTACAGCTGCCAGGTCACGCATGAAGGGAGCACCGTGGAGAAGACAGTGGCCCCTACAGAATGC
TGA[illegible]AGATCT[illegible]AGTCAA
TATGTTCACCCCAAAAAAGCTGTTTGTTAACTTGTCAACCTCATTCTAAAATGTATATAGAAGCCCAAAAGACAATAACAAAAATATTCTTGTAGAACAAAATGGGAAAGAATGTTCCACTAAATATCAA
GATTTAGAGCAAAGCATGAGATGTGTGGGGATAGACAGTGAGGCTGATAAAATAGAGTAGAGCTCAGAAACAGACCCATTGATATATGTAAGTGACCTATGAAAAAAATATGGCATTTTACAATGGG
AAAATGATGGTCTTTTTCTTTTTTAGAAAAACAGGGAAATATATTTATATGTAAAAAATAAAAGGGAACCCATATGTCATACCATACACACAAAAAAATTCCAGTGAATTATAAGTCTAAATGGAGAAG
GCAAAACTTTAAATCTTTAGAAAATAATATAGAAGCATGCCATCAAGACTTCAGTGTAGAGAAAAATTTCTTATGACTCAAAGTCCTAACCACAAAGAAAAGATTGTTAATTAGATTGCATGAATATTA
AGACTTATTTTAAAATTAAAAAACCATTAAGAAAAGTCAGGCCATAGAATGACAGAAAATATTTGCAACACCCCAGTAAAGACGAATTGTAATATGCAGATTATAAAAACGAAGTCTTACAAATCAGTAA
AAAATAAAACTAGACAAAAATTTGAACAGATGAAAGAGAAACTCTAAATAATCATTACACATGAGAAACTCAATCTCAGAAATCAGAGAACTATCATTGCATATACACTAAATTAGAGAAATATTAAAA
GGCTAAGTAACATCTGTGGCTTAATTAA[illegible]TCTAGTGATCAGCAGTTCAACCTGTTGATAGTATGTACTAAGCTCTCATGTTTAATGTACTAAGCTCTCATGTTTAATGAACTAAACCCTCATGGCT
AATGTACTAAGCTCTCATGGCTAATGTACTAAGCTCTCATGTTTCATGTACTAAGCTCTCATGTTTGAACAATAAAATTAATATAAATCAGCAACTTAAATAGCCTCTAAGGTTTTAAGTTTTATAAGAAA
AAAAAGAATATATAAGGCTTTTAAAGGTTTTAAGGTTTCCTAGGTTATCCTCATATGAGCTCTTAGAAAAACTCATCCAGCATCAAATGAAACTGCAATTTATTCATATCAGGATTATCAATACCATATTT
TTGAAAAAGTCTTTTCTGTAATGAAGGAGAAAACTCACCCAGGCAGTTCCATAGGATGGCAAGATCCTGGTATCTGTCTGCAATTCCAACTCTTCCAACATCAATACAACCTATTAATTTCCCCTCATCAA
AAATAAGGTTATCAAGTGAGAAATCACCATGAGTGACCACTGAATCTGGTGAGAATGGCAAAAGATTATGCATTTCTTTCCAGACTTGTTCAACAGGCCAGCCATTTCTCTCATCATCAAAATCACTGG
CATCAACCAAACCATTATTCATTCTTGATTGGGCCTGAGCCAGTCTAAATACTCTATCAGAGTTAAAAGGACAATTACAAACAGGAATGGAATGCAATCTTCTCAGGAACACTGCCAGGGCATCAACAA
TATTTTCACCTGAATCAGGATATTCTTCCAATACCTGGAATGCTGTTTTCCCTGGGATGGCAGTGGTGAGTAACCATGCATCATCAGGAGTTCTGATAAAATGCTTGATGGTTGGAAGAGGCATAAATT
CAGTCAGCCAGTTTAGTCTGACCATCTCATCTGTAACATCATTGGCAACAGAACCTTTGCCATGTTTCAGAAACAACTCTGGGGCATCTGGCTTCCCATACAATCTATAGATTGTGGCACCTGATTGCCC
AACATTATCTCTAGCCCATTTATACCCATATAAATCAGCATCCATGTTGGAATTTAATCTTGGCCTGGAGCAAGAGGTTTCTCTTTGAATATGGCTCATACATGTGCA[illegible]
ACTATCCAGAATATAATTATGCAAATGTTTAATTGTCP3

FIG. 40

A. Codon Optimized Human Growth Hormone (hGH1) cDNA (SEQ ID NO:40)

ATGGCTACAGGCAGCAGAACCTCTCTGCTGCTGGCTTTTGGCCTGCTGTGTCTGCCTTGGCTGCAAGAGGGCTCTGCTTTCCCTACAATCCCTCTGAGCAGGCTG
TTTGACAATGCCATGCTGAGAGCCCACAGACTGCACCAGCTGGCCTTTGACACCTACCAAGAGTTTGAAGAGGCTTACATCCCCAAAGAGCAGAAGTACAGCTT
CCTCCAGAATCCTCAGACCAGCCTGTGCTTCTCTGAGAGCATCCCCACACCTAGCAACAGAGAGGAAACCCAGCAGAAGTCCAACCTGGAACTGCTGAGAATCA
GCCTGCTGCTGATCCAGAGCTGGCTGGAACCTGTGCAGTTCCTGAGATCAGTGTTTGCCAACAGCCTGGTGTATGGGGCCTCTGACAGCAATGTGTATGACCTG
CTGAAGGACCTGGAAGAGGGCATCCAGACACTGATGGGCAGACTGGAAGATGGCAGCCCCAGAACAGGCCAGATTTTCAAGCAGACCTACAGCAAGTTTGACA
ACCAACAGCCACAATGATGATGCCCTGCTCAAGAACTATGGCCTGCTGTACTGCTTCAGAAAGGACATGGACAAGGTGGAAACCTTCCTGAGGATTGTGCAGT
GCAGAAGTGTGGAAGCAGCTGTGGCTTTGAGCCCAAGAGCTGTGACAAGACCCACACCTGTCCTCCATGTCCTGCTCCTGAAGCTGCTGGAGGACCCTCCTGTG
TTTCTGTTCCTCCCAAAGCCAAAGGACACCCTGATGATCAGCAGAACCCCTGAAGTGACCTGTGTGGTGGTGGACATGTCCCATGAGGACCCAGAAGTGAAGTT
CAATTGGTATGTGGATGGTGTGGAAGTGCACAATGCCAAGACCAAGCCTAGAGAGGAACAGTACAACAGCACCTACAGGGTTGTGTCAGTGCTGACCGTGCTGC
CACCAGGACTGGCTGAATGGCAAAGAGTACAAGTGCAAGGTGTCCAACAAGGCCCTGCCTGCTCCTATTGAAAAGACCATCAGCAAGGCCAAGGGACAGCCTAG
GGAACCCCAGGTGTACACACTGCCACCTAGCAGAGATGAGCTGACCAAGAATCAGGTGTCCCTGACATGCCTTGTGAAGGGCTTCTACCCTTCTGACATTGCAG
TGGAATGGGAGAGCAATGGCCAGCCTGAGAACAACTACAAGACAACCCCTCCTGTGCTGGACTCTGATGGCTCATTCTTCCTGTACTCCAAGCTGACAGTGGACA
AGTCCAGATGGCAGCAAGGCAATGTGTTCAGCTGCTCTGTGATGCATGAGGCCCTGCACAACCACTACACACAGAAGTCCCTGTCTCTGAGCCCTGGCAAGTGA

B. hGH1-Fc (SEQ ID NO:41)

ATGGCTACAGGCAGCAGAACCTCTCTGCTGCTGGCTTTTGGCCTGCTGTGTCTGCCTTGGCTGCAAGAGGGCTCTGCTTTCCCTACAATCCCTCTGAGCAGGCTG
TTTGACAATGCCATGCTGAGAGCCCACAGACTGCACCAGCTGGCCTTTGACACCTACCAAGAGTTTGAAGAGGCTTACATCCCCAAAGAGCAGAAGTACAGCTT
CCTCCAGAATCCTCAGACCAGCCTGTGCTTCTCTGAGAGCATCCCCACACCTAGCAACAGAGAGGAAACCCAGCAGAAGTCCAACCTGGAACTGCTGAGAATCA
GCCTGCTGCTGATCCAGAGCTGGCTGGAACCTGTGCAGTTCCTGAGATCAGTGTTTGCCAACAGCCTGGTGTATGGGGCCTCTGACAGCAATGTGTATGACCTG
CTGAAGGACCTGGAAGAGGGCATCCAGACACTGATGGGCAGACTGGAAGATGGCAGCCCCAGAACAGGCCAGATTTTCAAGCAGACCTACAGCAAGTTTGACA
ACCAACAGCCACAATGATGATGCCCTGCTCAAGAACTATGGCCTGCTGTACTGCTTCAGAAAGGACATGGACAAGGTGGAAACCTTCCTGAGGATTGTGCAGTC
GCAGAAGTGTGGAAGCAGCTGTGGCTTTGAGCCCAAGAGCTGTGACAAGACCCACACCTGTCCTCCATGTCCTGCTCCTGAAGCTGCTGGAGGACCCTCCTGTG
TTTCTGTTCCTCCCAAAGCCAAAGGACACCCTGATGATCAGCAGAACCCCTGAAGTGACCTGTGTGGTGGTGGACATGTCCCATGAGGACCCAGAAGTGAAGTT
CAATTGGTATGTGGATGGTGTGGAAGTGCACAATGCCAAGACCAAGCCTAGAGAGGAACAGTACAACAGCACCTACAGGGTTGTGTCAGTGCTGACCGTGCTGC
CACCAGGACTGGCTGAATGGCAAAGAGTACAAGTGCAAGGTGTCCAACAAGGCCCTGCCTGCTCCTATTGAAAAGACCATCAGCAAGGCCAAGGGACAGCCTAG
GGAACCCCAGGTGTACACACTGCCACCTAGCAGAGATGAGCTGACCAAGAATCAGGTGTCCCTGACATGCCTTGTGAAGGGCTTCTACCCTTCTGACATTGCAG
TGGAATGGGAGAGCAATGGCCAGCCTGAGAACAACTACAAGACAACCCCTCCTGTGCTGGACTCTGATGGCTCATTCTTCCTGTACTCCAAGCTGACAGTGGACA
AGTCCAGATGGCAGCAAGGCAATGTGTTCAGCTGCTCTGTGATGCATGAGGCCCTGCACAACCACTACACACAGAAGTCCCTGTCTCTGAGCCCTGGCAAGTGA

C. Linker GGGGS (SEQ ID NO:42)

1xLinker: GGTGGAGGAGGTAGT (SEQ ID NO:43)
2xLinker: GGTGGAGGAGGTAGTGGGGGTGGAGGTTCA (SEQ ID NO:44)
3xLinker: GGAGGAGGTGGATCAGGTGGAGGAGGTAGTGGGGGTGGAGGTTCA (SEQ ID NO:45)

D. Fc (SEQ ID NO:46)

GAGCCCAAGAGCTGTGACAAGACCCACACCTGTCCTCCATGTCCTGCTCCTGAAGCTGCTGGAGGACCCTCCTGTGTTTCTGTTCCTCCCAAAGCCAAAGGACACC
CTGATGATCAGCAGAACCCCTGAAGTGACCTGTGTGGTGGTGGACATGTCCCATGAGGACCCAGAAGTGAAGTTCAATTGGTATGTGGATGGTGTGGAAGTGCAC
AATGCCAAGACCAAGCCTAGAGAGGAACAGTACAACAGCACCTACAGGGTTGTGTCAGTGCTGACCGTGCTGCACCAGGACTGGCTGAATGGCAAAGAGTACAAG
TGCAAGGTGTCCAACAAGGCCCTGCCTGCTCCTATTGAAAAGACCATCAGCAAGGCCAAGGGACAGCCTAGGGAACCCCAGGTGTACACACTGCCACCTAGCAGA
GATGAGCTGACCAAGAATCAGGTGTCCCTGACATGCCTTGTGAAGGGCTTCTACCCTTCTGACATTGCAGTGGAATGGGAGAGCAATGGCCAGCCTGAGAACAAC
TACAAGACAACCCCTCCTGTGCTGGACTCTGATGGCTCATTCTTCCTGTACTCCAAGCTGACAGTGGACAAGTCCAGATGGCAGCAAGGCAATGTGTTCAGCTGC
TCTGTGATGCATGAGGCCCTGCACAACCACTACACACAGAAGTCCCTGTCTCTGAGCCCTGGCAAGTGA

E. Fc chainA (SEQ ID NO:47)

GAGCCCAAGAGCTGTGACAAGACCCACACCTGTCCTCCATGTCCTGCTCCTGAAGCTGCTGGAGGACCCTCCTGTGTTTCTGTTCCTCCCAAAGCCAAAGGACACC
CTGATGATCAGCAGAACCCCTGAAGTGACCTGTGTGGTGGTGGACATGTCCCATGAGGACCCAGAAGTGAAGTTCAATTGGTATGTGGATGGTGTGGAAGTGCAC
AATGCCAAGACCAAGCCTAGAGAGGAACAGTACAACAGCACCTACAGGGTTGTGTCAGTGCTGACCGTGCTGCACCAGGACTGGCTGAATGGCAAAGAGTACAAG
TGCAAGGTGTCCAACAAGGCCCTGCCTGCTCCTATTGAAAAGACCATCAGCAAGGCCAAGGGACAGCCTAGGGAACCCCAGGTGTACACACTGCCACCTTGCAGA
GATGAGCTGACCAAGAATCAGGTGTCCCTGGTGGTGCCTTGTGAAGGGCTTCTACCCTTCTGACATTGCAGTGGAATGGGAGAGCAATGGCCAGCCTGAGAACAAC
TACAAGACAACCCCTCCTGTGCTGGACTCTGATGGCTCATTCTTCCTGTACTCCAAGCTGACAGTGGACAAGTCCAGATGGCAGCAAGGCAATGTGTTCAGCTGC
TCTGTGATGCATGAGGCCCTGCACAACCACTACACACAGAAGTCCCTGTCTCTGAGCCCTGGCAAGTGA

F. Fc chainB (SEQ ID NO:48)

GAGCCCAAGAGCTGTGACAAGACCCACACCTGTCCTCCATGTCCTGCTCCTGAAGCTGCTTGGAGGACCCTCCTGTGTTTCTGTTCCTCCCAAAGCCAAAGGACACC
CTGATGATCAGCAGAACCCCTGAAGTGACCTGTGTGGTGGTGGACATGTCCCATGAGGACCCAGAAGTGAAGTTCAATTGGTATGTGGATGGTGTTGAAGTGCAC
ACAATGCCAAGACCAAGCCTAGAGAGGAACAGTACAACAGCACCTACAGGGTTGTGTCAGTGCTGACTGTGCTGCACCAGGACTGGCTGAATGGCAAAGAGTACAAG
TGCAAGGTGTCCAACAAGGCCCTGCCTGCTCCTATTGAAAAGACCATCAGCAAGGCCAAGGGACAGCCTAGGGAACCCCAGGTGTGCACACTGCCACCTAGCAGA
GATGAGCTGACCAAGAATCAGGTGTCCCTGTCATGTCTGTGAAGGGCTTCTACCCTTCTGACATTGCAGTGGAATGGGAGAGCAATGGCCAGCCTGAGAACAAC
TACAAGACAACCCCTCCTGTGCTGGACTCTGATGGCTCATTCTTCCTGTCTCCAAGCTGACAGTGGACAAGTCCAGATGGCAGCAAGGCAATGTGTTCAGCTGC
TCTGTGATGCATGAGGCCCTGCACAACCACTACACACAGAAGTCCCTGTCTCTGAGCCCTGGCAAGTGA

FIG. 41

A. Fc chainAB (SEQ ID NO:49)

GAGCCCAAGAGCTGTGACAAGACCCACACCTGTCCTCCATGTCCTGCTCCAGAGCTGCTTGGAGGACCTTCTGTGTTTCTGTTCCCTCCAAAGCCAAAGGACACC
CTGATGATCAGCAGAACCCCTGAAGTGACCTGTGTGGTGGTGGATGTGTCCCATGAGGACCCAGAAGTGAAGTTCAATTGGTATGTGGATGGTGTTGAGGTGC
ACAATGCCAAGACCAAGCCTAGAGAGGAACAGTACAACAGCACCTACAGGGTTGTGTCAGTGCTGACTGTGCTGCACCAGGACTGGCTGAATGGCAAAGAGTA
CAAGTGCAAGGTGTCCAACAAGGCCCTGCCTGCTCCTATTGAAAAGACCATCAGCAAGGCCAAGGGACAGCCTAGGGAACCCCAGGTGTGCACACTGCCACCT
TGCAGAGATGAGCTGACCAAGAATCAGGTGTCCCTGTCATGTGCTGTGAAGGGCTTCTACCCTTCTGACATTGCAGTGGAATGGGAGAGCAATGGCCAGCCTG
AGAACAACTACAAGACAACCCCTCCTGTGCTGGACTCTGATGGCTCATTCTTCCTGTCTCCAAGCTGACAGTGGACAAGTCCAGATGGCAGCAAGGCAATGTG
TTCAGCTGCTCTGTGATGCATGAGGCCCTGCACAACCACTACACACAGAAGTCCCTGTCTCTGAGCCCTGGCAAGTGA

B. Fc-IgG4 (SEQ ID NO:50)

GAAAGCAAATATGGCCCACCATGTCCTCCATGTCCAGCACCTGAACTCCTGGGGGACCGTCAGTCTTCCTCTTCCCCCAAAACCCAAGGACACCCTCATGATCT
CCCGGACCCCTGAGGTCACATGCGTGGTGGTGGACGTGAGCCACGAAGACCCTGAGGTCAAGTTCAACTGGTACGTGGACGGCGTGGAGGTGCATAATGCCAA
GACAAAGCCGCGGGAGGAGCAGTACAACAGCACGTACCGTGTGGTCAGCGTCCTCACCGTCCTGCACCAGGACTGGCTGAATGGCAAGGAGTACAAGTGCAAG
GTCTCCAACAAAGCCCTCCCAGCCCCCATCGAGAAAACCATCTCCAAAGCCAAAGGGCAGCCCCGAGAACCACAGGTGTACACCCTGCCCCCATCCCGGGAGG
AGATGACCAAGAACCAGGTCAGCCTGACCTGCCTGGTCAAAGGCTTCTATCCCAGCGACATCGCCGTGGAGTGGGAGAGCAATGGGCAGCCGGAGAACAACTA
CAAGACCACGCCTCCCGTGCTGGACTCCGACGGCTCCTTCTTCCTCTACAGCAAGCTCACCGTGGACAAGAGCAGGTGGCAGCAGGGGAACGTCTTCTCATGC
TCCGTGATGCATGAGGCTCTGCACAACCACTACACGCAGAAGAGCCTCTCCCTGTCTCTGGGTAAATGA

C. hyFc (SEQ ID NO:51)

AGAAACACAGGCAGAGGTGGAGAGGAAAAGAAGAAAGAGAAAGAAAAAGAGGAACAAGAGGAAAGGGAAACTAAGACCCCTGAGTGCCCCAGCCACACAC
AGCCTCTGGGAAGTTGTTCCTGTTTCCTCCAAAGCCAAAGGACACCCTGATGATCAGCAGAACCCCTGAAGTGACCTGTGTGGTGGTGGATGTGTCCCAAGAGGAC
CCAGAGGTGCAGTTCAATTGGTATGTGGATGGTGTTGAGGTGCACAATGCCAAGACCAAGCCTAGAGAGGAACAGTTCAACAGCACCTACAGAGTGGTGTCTG
TGCTGACAGTGCTGCACCAGGACTGGCTGAATGGCAAAGAGTACAAGTGCAAGGTGTCCAACAAGGGCCTGCCTAGCAGCATTGAAAAGACCATCAGCAAGG
CCAAGGGCCAGCCAAGAGAACCCCAGGTGTACACACTGCCCCCTAGCCAGGAAGAAATGACCAAGAACCAGGTGTCCCTGACCTGCCTGGTCAAGGGCTTCTA
CCCCTCTGACATTGCTGTGGAATGGGAGAGCAATGGCCAGCCTGAGAACAACTACAAGACCACACCTCCTGTGCTGGACTCTGATGGCTCATTCTTCCTGTACAG
CAAGCTGACCGTGGACAAGAGCAGATGGCAGCAGGGCAATGTGTTCAGCTGCTCCGTGATGCATGAGGCTCTGCACAACCACTACACCCAGAAGTCCCTGTCCCTG
CTGAGCCTGGGCAAATGA

D. mFc (SEQ ID NO:52)

CCTAGAGGCCCCACCATCAAGCCCTGTCCTCCATGCAAATGCCCTGCTCCTAACCTGCTTGGAGGCCCCTCTGTGTTCATCTTCCCACCTAAGATCAAGGATGTGC
TGATGATCTCTCTGAGCCCCATTGTGACCTGTGTGGTGGTGGATGTGTCTGAGGATGACCCAGATGTGCAGATTTCTTGGTTTGTGAACAATGTGGAAGTGCAC
ACAGCCCAGACTCAGACCCACAGAGAGGACTACAACAGCACACTGAGAGTGGTGTCTGCCCTGCCTATCCAGCACCAGGATTGGATGTCTGGCAAAGAGTTCA
AGTGCAAAGTGAACAACAAGGACCTGCCTGCTCCAATTGAGAGGACCATCTCCAAGCCAAAGGGCTCTGTCAGGGCCCCTCAAGTGTATGTGCTGCCTCCTCCA
GAGGAAGAGATGACCAAGAAGCAAGTCACCCTGACATGCATGGTCACAGACTTCATGCCAGAGGACATCTATGTGGAATGGACCAACAATGGCAAGACAGAG
CTGAACTACAAGAACACTGAGCCAGTGCTGGACTCTGATGGCAGCTACTTCATGTACAGCAAGCTGAGGGTTGAGAAGAAGAACTGGGTTGAGAGAAACAGCT
ACAGCTGCTCTGTGGTGCATGAGGGCCTGCACAATCACCACACCACCAAGAGCTTCAGCAGAACCCCTGGCAAGTGA

E. GAALIE (SEQ ID NO:53)

GAGCCCAAGAGCTGTGACAAGACCCACACCTGTCCTCCATGTCCTGCTCCAGAGCTGCTTGGAGGACCTTCTGTGTTTCTGTTCCCTCCAAAGCCAAAGGACACC
CTGATGATCAGCAGAACCCCTGAAGTGACCTGTGTGGTGGTGGATGTGTCCCATGAGGACCCAGAAGTGAAGTTCAATTGGTATGTGGATGGTGTTGAGGTGC
ACAATGCCAAGACCAAGCCTAGAGAGGAACAGTACAACAGCACCTACAGGGTTGTGTCAGTGCTGACTGTGCTGCACCAGGACTGGCTGAATGGCAAAGAGTA
CAAGTGCAAGGTGTCCAACAAGGCCCTGCCTGCTCCTATTGAAAAGACCATCAGCAAGGCCAAGGGACAGCCTAGGGAACCCCAGGTGTACACACTGCCACCT
AGCAGAGATGAGCTGACCAAGAATCAGGTGTCCCTGACATGCCTTGTGAAGGGCTTCTACCCTTCTGACATTGCAGTGGAATGGGAGAGCAATGGCCAGCCTG
AGAACAACTACAAGACAACCCCTCCTGTGCTGGACTCTGATGGCTCATTCTTCCTGTACTCCAAGCTGACAGTGGACAAGTCCAGATGGCAGCAAGGCAATGTG
TTCAGCTGCTCTGTGATGCATGAGGCCCTGCACAACCACTACACACAGAAGTCCCTGTCTCTGAGCCCTGGCAAGTGA

F. GAALIE-LS (SEQ ID NO:54)

GAGCCCAAGAGCTGTGACAAGACCCACACCTGTCCTCCATGTCCTGCTCCAGAGCTGCTTGGAGGACCTTCTGTGTTTCTGTTCCCTCCAAAGCCAAAGGACACC
CTGATGATCAGCAGAACCCCTGAAGTGACCTGTGTGGTGGTGGATGTGTCCCATGAGGACCCAGAAGTGAAGTTCAATTGGTATGTGGATGGTGTTGAGGTGC
ACAATGCCAAGACCAAGCCTAGAGAGGAACAGTACAACAGCACCTACAGGGTTGTGTCAGTGCTGACTGTGCTGCACCAGGACTGGCTGAATGGCAAAGAGTA
CAAGTGCAAGGTGTCCAACAAGGCCCTGCCTGCTCCTATTGAAAAGACCATCAGCAAGGCCAAGGGACAGCCTAGGGAACCCCAGGTGTACACACTGCCACCT
AGCAGAGATGAGCTGACCAAGAATCAGGTGTCCCTGACATGCCTTGTGAAGGGCTTCTACCCTTCTGACATTGCAGTGGAATGGGAGAGCAATGGCCAGCCTG
AGAACAACTACAAGACAACCCCTCCTGTGCTGGACTCTGATGGCTCATTCTTCCTGTACTCCAAGCTGACAGTGGACAAGTCCAGATGGCAGCAAGGCAATGTG
TTCAGCTGCTCTGTGATGCATGAGGCCCTGCACAACCACTACACACAGAAGTCCCTGTCTCTGAGCCCTGGCAAGTGA

FIG. 42

A. hGH1-HSA (SEQ ID NO:55)

ATGGCTACAGGCAGCAGAACCTCTCTGCTGCTGGCTTTTGGCCTGCTGTGTCTGCCTTGGCTGCAAGAGGGCTCTGCTTTCCCTACAATCCCTCTGAGCAGGCTG
TTTGACAATGCCATGCTCCAGGCCCACAGACTGCACCAGCTGGCCTTTGACACCTACCAAGAGTTTGAAGAGGCTTACATCCCCAAACAGCAGAAGTACAGC
TTCCTCCAGAATCCTCAGACCAGCCTGTGCTTCTCTGAGAGCATCCCCACACCTAGCAACAGAGAGGAAACCCAGCAGAAGTCCAACCTGGAACTGCTGAGA
ATCAGCCTGCTGCTGATCCAGAGCTGGCTGGAACCTGTGCAGTTCCTGAGATCAGTGTTTGCCAACAGCCTGGTGTATGGGGCCTCTGACAGCAATGTGTATG
ACCTGCTGAAGGACCTGGAAGAGGGCATCCAGACACTGATGGGCAGACTGGAAGATGGCAGCCCCAGAACAGGCCAGATTTTCAAGCAGACCTACAGCAA
GTTTGACACCAACAGCCACAATGATGATGCCCTGCTCAAGAACTATGGCCTGCTGTACTGCTTCAGAAAGGACATGGACAAGGTGGAAACCTTCCTGAGGAT
TGTGCAGTGCAGAAGTGTGGAAGGCAGCTGTGGCTTTGGTGGAGGAGGTACTGATGCCCACAAGTCTGAGGTGGCCCACAGATTCAAGGACCTGGGAGAA
GAGAACTTCAAGGCCTTGGTGCTGATTGCCTTTGCTCAGTACCTCCAGCAGTGCCCCTTTGAGGACCATGTGAAACTGGTCAATGAAGTGACAGAGTTTGCCA
AGACCTGTGTGGCTGATGAGTCTGCTGACAACTGTGACAAGAGCCTGCACACCCTGTTTGGAGACAAGCTGTGTACAGTGGCCACACTGAGAGAAACCTAT
GGAGAGATGGCTGACTGCTGTGCCAAGCAAGAACCTGAGAGGAATGAGTGCTTCCTCCAGCACAAGGATGACAACCCCAACCTGCCTAGACTTGTCAGACC
TGAAGTGGATGTGATGTGCACAGCCTTCCATGACAATGAGGAAACCTTCCTGAAGAAATACCTGTATGAGATTGCCAGAAGGCACCCCTACTTCTATGCCCCT
GAGCTGCTGTTCTTTGCTAAGAGATACAAGGCTGCCTTTACAGAGTGCTGCCAGGCTGCTGACAAAGCTGCCTGTCTGCTGCCCAAGCTGGATGAGCTGAGA
GATGAAGGCAAGGCCTCCTCTGCCAAGCAGAGACTGAAGTGTGCCAGCCTCCAGAAGTTTGGAGAGAGAGCCTTCAAGGCTTGGGCTGTTGCCAGACTGAG
CCAGAGATTCCCCAAGCTGAGTTTGCTGAGGTGTCCAAGCTGGTTACAGACCTGACCAAGGTGCACACTGAATGCTGCCATGGAGACCTGCTGGAATGTGC
TGATGACAGAGCTGACCTGGCCAAGTACATCTGTGAAAACCAGGACAGCATCAGCAGCAAGCTGAAAGAATGCTGTGAAAAGCCCCTCCTGGAAAAGAGCC
ACTGCATTGCAGAGGTCGAAAATGATGAGATGCCTGCTGATCTGCCCAGCCTTGCAGCTGACTTTGTGGAAAGCAAGGATGTGTGCAAGAACTATGCTGAG
GCCAAAGATGTGTTCCTGGGCATGTTCCTCTATGAGTATGCTAGAAGGCATCCTGACTACTCTGTGGTGCTGCTGCTGAGACTGGCTAAGACCTATGAGACAA
CACTGGAAAAGTGCTGTGCAGCTGCTGACCCTCATGAGTGCTATGCCAAAGTGTTTGATGAGTTCAAGCCTCTGGTGGAAGAACCCCAGAACCTGATCAAGC
AGAATTGTGAACTGTTTGAGCAGCTGGGAGAGTACAAGTTCCAGAATGCCCTGCTTGTCAGATACACCAAGAAAGTGCCCCAACTGTTCACAGTTGTCAAG
TTGAAGGTGCCAGAAATCTCGGCAAAGTGGGCAGCAAGTGCTGCAAGCACCCAGAGGCCAAGAGGATGCCATGTGCTGAGGACTACCTGTCAGTGGTGCTG
AACCAGCTGTGTGTCCTGCATGAGAAAACCCCTGTGTCTGACAGAGTGACAAAGTGTTGCACAGAGAGCCTGGTCAACAGAAGGCCTTGCTTCTCTGCCCTG
GAAGTTGATGAGACATATGTGCCCAAAGAGTTCAATGCTGAGACATTCACCTTCCATGCTGACATCTGCACCCTGTCTGAGAAAGAGAGGCAGATCAAGAAA
CAGACTGCCCTGGTGGAACTGGTCAAGCACAAGCCCAAGGCCACCAAAGAACAACTGAAGGCAGTGATGGATGACTTTGCTGCCTTTGTTGAGAAGTGCTG
TAAAGCAGATGACAAAGAGACATGCTTTGCTGAAGAGGGCAAAAACTGGTGGCTGCCTCTCAGGCTGCTCTGGGACTTTAA

B. HSA-K753P-Linker-GH1: (SEQ ID NO:56)

GGTAACCAAGCCACCATGAAATGGGTCACATTCATCAGCCTGCTGTTTCTGTTCAGCTCTGCCTACAGCAGGGGAGTGTTTCAGAAGAGATGCCCACAAGTCTGA
GGTGGCCCACAGATTCAAGGACCTGGGAGAAGAGAACTTCAAGGCCCTGGTGCTGATTGCCTTTGCTCAGTACCTCCAGCAGTGCCCCTTTGAGGACCATGT
GAAACTGGTCAATGAAGTGACAGAGTTTGCCAAGACCTGTGTGGCTGATGAGTCTGCTGACAACTGTGACAAGAGCCTGCACACCCTGTTTGGAGACAAGCT
GTGTACAGTGGCCACACTGAGAGAAACCTATGGAGAGATGGCTGACTGCTGTGCCAAGCAAGAACCTGAGAGGAATGAGTGCTTCCTCCAGCACAAGGAT
GACAACCCCAACCTGCCTAGACTTGTCAGACCTGAAGTGGATGTGATGTGCACAGCCTTCCATGACAATGAGGAAACCTTCCTGAAGAAATACCTGTATGAG
ATTGCCAGAAGGCACCCCTACTTCTATGCCCCTGAGCTGCTGTTCTTTGCTAAGAGATACAAGGCTGCCTTTACAGAGTGCTGCCAGGCTGCTGACAAAGCTG
CCTGTCTGCTGCCCAAGCTGGATGAGCTGAGAGATGAAGGCAAGGCCTCCTCTGCCAAGCAGAGACTGAAGTGTGCCAGCCTCCAGAAGTTTGGAGAGAGA
GCCTTCAAGGCTTGGGCTGTTGCCAGACTGAGCCAGAGATTCCCCAAGCTGAGTTTGCTGAGGTGTCCAAGCTGGTTACAGACCTGACCAAGGTGCACACT
GAATGCTGCCATGGAGACCTGCTGGAATGTGCTGATGACAGAGCTGACCTGGCCAAGTACATCTGTGAAAACCAGGACAGCATCAGCAGCAAGCTGAAAGA
ATGCTGTGAAAAGCCCCTCCTGGAAAAGAGCCACTGCATTGCAGAGGTGGAAAATGATGAGATGCCTGCTGATCTGCCCAGCCTTGCAGCTGACTTTGTGGA
AAGCAAGGATGTGTGCAAGAACTATGCTGAGGCCAAAGATGTGTTCCTGGGCATGTTCCTCTATGAGTATGCTAGAAGGCATCCTGACTACTCTGTGGTGCT
GCTGCTGAGACTGGCTAAGACCTATGAGACAACACTGGAAAAGTGCTGTGCAGCTGCTGACCCTCATGAGTGCTATGCCAAAGTGTTTGATGAGTTCAAGCC
TCTGGTGGAAGAACCCCAGAACCTGATCAAGCAGAATTGTGAACTGTTTGAGCAGCTGGGAGAGTACAAGTTCCAGAATGCCCTGCTTGTCAGATACACCAA
GAAAGTGCCCCAACTGTTCACAGTTGTCAAGTTGAAGGTGCCAGAAATCTCGGCAAAGTGGGCAGCAAGTGCTGCAAGCACCCAGAGGCCAAGAGGATGCC
ATGTGCTGAGGACTACCTGTCAGTGGTGCTGAACCAGCTGTGTGTCCTGCATGAGAAAACCCCTGTGTCTGACAGAGTGACAAAGTGTTGCACAGAGAGCC
TGGTCAACAGAAGGCCTTGCTTCTCTGCCCTGGAAGTTGATGAGACATATGTGCCCAAAGAGTTCAATGCTGAGACATTCACCTTCCATGCTGACATCTGCAC
CCTGTCTGAGAAAGAGAGGCAGATCAAGAAACAGACTGCCCTGGTGGAACTGGTCAAGCACAAGCCCAAGGCCACCAAAGAACAACTGAAGGCAGTGATG
GATGACTTTGCTGCCTTTGTTGAGAAGTGCTGTAAAGCAGATGACAAAGAGACATGCTTTGCTGAAGAGGGCAAAAACTGGTGGCTGCCTCTCAGGCTGCT
CTGGGACTTGGTGGAGGAGGTACTTCCCTACAATCCCTCTGAGCAGGCTGTTTGACAATGCCATGCTGAGAGCCCACAGACTGCACCAGCTGGCCTTTGACA
CCTACCAAGAGTTTGAAGAGGCTTACATCCCCAAAGAGCAGAAGTACAGCTTCCTCCAGAATCCTCAGACCAGCCTGTGCTTCTCTGAGAGCATCCCCACACC
TAGCAACAGAGAGGAAACCCAGCAGAAGTCCAACCTGGAACTGCTGAGAATCAGCCTGCTGCTGATCCAGAGCTGGCTGGAACCTGTGCAGTTCCTGAGAT
CAGTGTTTGCCAACAGCCTGGTGTATGGGGCCTCTGACAGCAATGTGTATGACCTGCTGAAGGACCTGGAAGAGGGCATCCAGACACTGATGGGCAGACTG
GAAGATGGCAGCCCCAGAACAGGCCAGATTTTCAAGCAGACCTACAGCAAGTTTGACACCAACAGCCACAATGATGATGCCCTGCTCAAGAACTATGGGCT
GCTGTACTGCTTCAGAAAGGACATGGACAAGGTGGAAACCTTCCTGAGGATTGTGCAGTGCAGAAGTGTGGAAGGCAGCTGTGGCTTCTGA

FIG. 43

A. hGH1-CTP (SEQ ID NO:57)

ATGGCTACAGGCAGCAGAACCTCTCTGCTGCTGGCTTTTGGCCTGCTGTGTCTGCCTTGGCTGCAAGAGGGCTCTGCCAGCTTCTAGCTCTAAGGCCCTTCACCT
TCTCTGCCATCTCCAAGCAGACTGCCTGGACCTTCTGACACCCTATCCTGCCTCAGTTCCCTACAATCCCTCTGAGCAGGCTGTTTGACAATGCCATGCTGAGAG
CCCACAGACTGCACCAGCTGGCCTTTGACACCTACCAAGAGTTTGAAGAGGCTTACATCCCCAAAGAGCAGAAGTACAGCTTCCTCCAGAATCCTCAGACCAGC
CTGTGCTTCTCTGAGAGCATCCCCACACCTAGCAACAGAGAGGAAACCCAGCAGAAGTCCAACCTGGAACTGCTGAGAATCAGCCTGCTGCTGATCCAGAGCTG
GCTGGAACCTGTGCAGTTCCTGAGATCAGTGTTTGCCAACAGCCTGGTGTATGGGGCCTCTGACAGCAATGTGTATGACCTGCTGAAGGACCTGGAAGAGGGCA
ATCCAGACACTGATGGGCAGACTGGAAGATGGCAGCCCCAGAACAGGCCAGATTTTCAAGCAGACCTACAGCAAGTTTGACACCAACAGCCACAATGATGATGC
CCTGCTCAAGAACTATGGGCTGCTGTACTGCTTCAGAAAGGACATGGACAAGGTGGAAACCTTCCTGAGGATTGTGCAGTGCAGAAGTGTGGAAGGCAGCTG
TGGCTTCTGA

B. CTP-hGH1-CTP (SEQ ID NO:58)

ATGGCTACAGGCAGCAGAACCTCTCTGCTGCTGGCTTTTGGCCTGCTGTGTCTGCCTTGGCTGCAAGAGGGCTCTGCCAGCTTCTAGCTCTAAGGCCCTTCACCT
TCTCTGCCATCTCCAAGCAGACTGCCTGGACCTTCTGACACCCTATCCTGCCTCAGTTCCCTACAATCCCTCTGAGCAGGCTGTTTGACAATGCCATGCTGAGAG
CCCACAGACTGCACCAGCTGGCCTTTGACACCTACCAAGAGTTTGAAGAGGCTTACATCCCCAAAGAGCAGAAGTACAGCTTCCTCCAGAATCCTCAGACCAGC
CTGTGCTTCTCTGAGAGCATCCCCACACCTAGCAACAGAGAGGAAACCCAGCAGAAGTCCAACCTGGAACTGCTGAGAATCAGCCTGCTGCTGATCCAGAGCTG
GCTGGAACCTGTGCAGTTCCTGAGATCAGTGTTTGCCAACAGCCTGGTGTATGGGGCCTCTGACAGCAATGTGTATGACCTGCTGAAGGACCTGGAAGAGGGCA
ATCCAGACACTGATGGGCAGACTGGAAGATGGCAGCCCCAGAACAGGCCAGATTTTCAAGCAGACCTACAGCAAGTTTGACACCAACAGCCACAATGATGATGC
CCTGCTCAAGAACTATGGGCTGCTGTACTGCTTCAGAAAGGACATGGACAAGGTGGAAACCTTCCTGAGGATTGTGCAGTGCAGAAGTGTGGAAGGCAGCTG
TGGCTTCTGA

C. CTP-hGH1 (SEQ ID NO:59)

ATGGCTACAGGCAGCAGAACCTCTCTGCTGCTGGCTTTTGGCCTGCTGTGTCTGCCTTGGCTGCAAGAGGGCTCTGCCAGCTTCTAGCTCTAAGGCCCTTCACCT
TCTCTGCCATCTCCAAGCAGACTGCCTGGACCTTCTGACACCCTATCCTGCCTCAGTTCCCTACAATCCCTCTGAGCAGGCTGTTTGACAATGCCATGCTGAGAG
CCCACAGACTGCACCAGCTGGCCTTTGACACCTACCAAGAGTTTGAAGAGGCTTACATCCCCAAAGAGCAGAAGTACAGCTTCCTCCAGAATCCTCAGACCAGC
CTGTGCTTCTCTGAGAGCATCCCCACACCTAGCAACAGAGAGGAAACCCAGCAGAAGTCCAACCTGGAACTGCTGAGAATCAGCCTGCTGCTGATCCAGAGCTG
GCTGGAACCTGTGCAGTTCCTGAGATCAGTGTTTGCCAACAGCCTGGTGTATGGGGCCTCTGACAGCAATGTGTATGACCTGCTGAAGGACCTGGAAGAGGGCA
ATCCAGACACTGATGGGCAGACTGGAAGATGGCAGCCCCAGAACAGGCCAGATTTTCAAGCAGACCTACAGCAAGTTTGACACCAACAGCCACAATGATGATGC
CCTGCTCAAGAACTATGGGCTGCTGTACTGCTTCAGAAAGGACATGGACAAGGTGGAAACCTTCCTGAGGATTGTGCAGTGCAGAAGTGTGGAAGGCAGCTG
TGGCTTCTGA

D. XTEN1-hGH1 (SEQ ID NO:60)

ATGGCCACAGGCAGCAGAACATCTCTGCTGCTGGCTTTTGGCCTGCTGTGCCTGCCTTGGCTGCAAGAGGGAAGTGCTGCTGAACCTGCTGGCAGCCCTACAAG
CACAGAAGAGGGAACACCTGGCTCTGGCACAGCTTCTTCTAGCCCTGGAAGCAGCACACCTTCTGGTGCTACAGGATCTCCTGGGGCCTCTCCTGGAACATCTTC
TACAGGTTCTCCAGGCAGCCCTGCTGGCTCTCCTACATCTACAGAGGAAGGCACCTCTGAGTCTGCCACACCTGAGTCTGGACCTGGCACCTCTACAGAGCCATC
TGAAGGATCTGCTCCAGGCTCACCAGCTGGCTCCCCAACTTCAACTGAAGAGGGCACAAGCACTGAACCCTCTGAGGGCTCTGCCCCTGGAACTTCAACAGAAC
CTTCAGAGGGATCAGCCCCAGGGACATCAGAGTCTGCTACTCCAGAATCTGGCCCAGGCTCTGAGCCAGCCACATCTGGATCTGAGACACCAGGATCAGAACCT
GCCACCTCTGGCTCTGAAACCCCTGGATCTCCAGCAGGCTCTCCCACTAGCACTGAGGAAGGGACATCTGAATCAGCAACCCCAGAGAGTGGCCCTGGCACCAG
TACTGAACCATCAGAAGGCTCAGCACCTGGGACCAGCACAGAACCATCTGAGGGTAGTGCTCCAGGTTCTCCTGCTGGAAGCCCAACCTCCACAGAAGAAGGT
ACTAGCACTGAGCCAAGTGAAGGCTCTGCCCCAGGCACATCAACTGAGCCATCAGAAGGATCTGCCCCTGGCACCTCTGAAAGTGCTACCCCTGAATCAGGACC
AGGGACCTCAACTGAACCTACTGAAGGATCAGCTCCTGGAACTTCTGAATCAGCCACTCCTGAATCAGGCCCTGGAAGTGAACCAGCTACTTCAGGATCTGAAA
CTCCAGGCACTTCCACAGAACCCTCAGAAGGCTCTGCTCCAGGGACTTCTACTGAACCATCTGAGGGATCAGCACCAGGCACCAGTGAATCTGCAACCCCAGAA
TCTGGACCTGGAACAAGTGAATCAGCTACCCCTGAGTCTGGCCCAGGATCACCAGCAGGATCACCTACCTCTACTGAAGAGGGAACCTCAGAAAGTGCCACTCC
AGAGAGTGGACCAGGATCTGAGCCAGCTACTTCAGGCTCAGAGACACCTGGCACATCTGAATCTGCTACACCAGAGTCAGGCCCTGGGACATCCACTGAGCCA
TCTGAAGGCAGTGCACCAGGCACCTCCACTGAACCATCTGAAGGCTCAGCCCCAGGCACTTCTACAGAACCCAGTGAAGGATCTGCACCAGGGACCAGTACTGA
ACCTTCTGAAGGATCTGCTCCTGGCACCAGCACAGAGCCAAGTGAAGGATCAGCACCTGGCACCTCAACTGAACCCTCTGAGGGAAGTGCTCCTGGCAGTCCTG
CTGGATCACCAACCAGCACTGAAGAGGGGACCTCTACAGAACCCTCTGAGGGATCTGCACCTGGGACCTCTGAGTCAGCAACACCAGAATCAGGTCCTGGCTCT
GAACCTGCTACTTCTGGTAGTGAAACCCCAGGGACCTCTGAAAGTGCAACACCAGAGTCTGGCCCTGGATCTGAACCAGCAACCAGTGGCTCTGAGACTCCTGG
TACTTCAGAGAGTGCAACACCTGAAAGTTGGCCCAGGGACCAGCACAGAGCCATCAGAAGGCTCTGCACCAGGCACATCTGAGTCTGCTACCCCTGAAAGTGGA
CCTGGCTCTCCTGCTGGGAGTCCCACAAGTACTGAAGAAGGTTCCCCAGCAGGGTCCCCAACATCCACTGAAGAAGGATCACCAGCTGGCAGCCCCACTTCCAC
AGAGGAAGGCACATCAGAATCAGCTACTCCAGAGTCTGGACCTGGTACTAGCACAGAACCATCAGAGGGAAGTGCCCCTGGAACATCTGAGAGTGCCACACCA
GAATCAGGACCTGGATCTGAGCCAGCCACCTCTGGTAGTGAAACTCCTGGTACTTCTGAGTCTGCAACCCCAGAGTCAGGCCCAGGATCAGAACCAGCTACTTC
TGGCAGTGAAACACCTGGCACCTCAGAATCAGCAACACCTGAATCTGGACCAGGCACTAGCACAGAACCATCTGAAGGATCAGCCCCTGGCTCTCCTGCTGGCT
CTCCAACTTCTACAGAAGAGGGAACTTCTGAAAGTGCAACTCCTGAATCTGGACCAGGATCTGAACCTGCAACTTCTGGATCAGAGACACCAGGGACCTCAGAG
AGTGCTACTCCTGAGTCAGGTCCTGGCAGCCCAGCTGGAAGCCCCACAAGTACAGAGGAAGGATCTCCTGCTGGGTCCCCTACCAGTACAGAAGAAGGCACTT
CTACTGAACCCTCAGAAGGATCAGCCCCTGGTACAAGTGAATCTGCCACTCCAGAGTCAGGACCAGGCACTTCAGAGTCAGCAACTCCTGAGAGTGGTCCAGGC
ACTTCAGAAAGTGCTACCCCAGAGTCTGGTCCAGGCAGTGAACCTGCTACAAGTGGCTCTGAAACACCAGGCTCTGAACCAGCTACTTCTGGCTCTGAGACTCCT
GGCTCACCAGCTGGCAGTCCTACCTCTACAGAAGAAGGGACTTCAACAGAACCATCTGAGGGCAGTGCACCTGGCACAAGCACAGAGCCATCTGAAGGATCTG
CACCTGGATCTGAACCAGCTACCTCTGGATCAGAAACCCCTGGAACCTCTGAATCAGCTACCCCAGAAAGTGGACCAGGCACATCCACAGAACCATCAGAGGGA
TCTGCACCAGGATTCCCTACAATCCCACTGAGCAGACTGTTTGACAATGCCATGCTGAGAGCCCACAGACTGCATCAGCTGGCCTTTGACACCTACCAAGAGTT
TGAAGAGGCTTACATCCCCAAAGAGCAGAAGTACAGCTTCCTGCAAAACCCACAGACCAGCCTGTGCTTCTCTGAGAGCATCCCCACACCTAGCAACAGAGA
GGAAACCCAGCAGAAGTCCAATCTGGAACTGCTGAGAATCTCACTGCTGCTGATCCAGTCTTGGCTGGAACCTGTGCAGTTCCTGAGATCAGTGTTTGCCAAC
AGCCTGGTGTATGGGGCTTCTGACAGCAATGTGTATGACCTGCTGAAAGACCTGGAAGAGGGCATCCAGACACCTGATGGGCAGACTGGAAGATGGCAGCCCC
TACAACAGGCCAGATTTTCAAGCAGACCTACAGCAAGTTTGACACCAACAGCCACAATGATGATGCCCTGCTCAAGAACTATGGGCTGCTGTACTGTTTCAG
AAAGGACATGGACAAGGTGGAAACCTTCCTGAGAATTGTGCAGTGCAGAAGTGTGGAAGGCAGCTGTGGCTTTTGA

FIG. 44

A. XTEN1-hGH1-XTEN2 (SEQ ID NO:61)

ATGGCCACAGGCAGCAGAACATCTCTGCTGCTGGCTTTTGGCCTGCTGTGCCTGCCTTGGCTGCAAGAGGGAAGTGCTTTGCTGAACCTGCTGGCAGCCCTACAAG
CACAGAAGACGGGAACACCTGGCTCTGGCACAGCTTCTTCTAGCCTGGAAGCAGCACACCTTCTGGTGCTACAGGATCTCCTGGGGCCTCTCCTGGAACATCTTC
TACAGGTTCTTCCAGGCAGCCCTGCTGGCTCTCCTACATCTACAGAGGAAGGCACCTCTGAGTCTGCCACACCTGAGTCTGGACCTGGCACCTCTACAGAGCCATC
TGAAGGATCTGCTCCAGGCTCACCAGCTGGCTCTCCAACTTCAACTGAAGAGGGCACAAGCACTGAACCCTCTGAGGGCTCTGCCCCTGGAACTTCAACAGAAC
CTTCAGAGGGATCAGCCCCAGGGACATCAGAGTCTGCTACTCCAGAATCTGGCTCAGGCTCTGAGCCAGCCACATCTGGATCTGAGACACCAGGATCAGAACCT
GCCACCTCTGGCTCTGAAACCCCTGGATCTCCAGCAGGCTCTCCCACTAGCACTGAGGAAGGGACATCTGAATCAGCAACCCCAGAGAGTGGCCCTGGCACCAG
TACTGAACCATCAGAAGGCTCAGCACCTGGGACCAGCACAGAACCATCTGAGGGTAGTGCTCCAGGTTCTCCTGCTGGAAGCCCAACCTCCACAGAAGAAGGT
ACTAGCACTGAGCCAAGTGAAGGCTCTGCCCCAGGCACATCAACTGAGCCATCAGAAGGATCTGCCCCTGGCACCTCTGAAAGTGCTACCCCTGAATCAGGACC
AGGGACCTCAACTGAACCTAGTGAAGGATCAGCTCCTGGAACTTCTGAATCAGCCACTCCTGAATCAGGCCCTGGAAGTGAACCAGCTACTTCAGGATCTGAAA
CTCCAGGGCACTTCCACAGAACCCTCAGAAGGCTCTGCTCCAGGGACTTCTACTGAACCATCTGAGGGATCAGCACCAGGCACCAGTGAATCTGCAACCCCAGAA
TCTGGACCTGGAACAAGTGAATCAGCTACCCCTGAGTCTGGCCCAGGATCACCAGCAGGATCACCTACCTCTACTGAAGAGGGAACCTCAGAAAGTGCCACTCC
AGAGAGTGGACCAGGATCTGAGCCAGCTACTTCAGGCTCAGAGACACCTGGCACATCTGAATCTGCTACACCAGAGTCAGGCCCTGGGGACATCCACTGAGCCA
TCTGAAGGCAGTGCACCAGGCACCTCCACTGAACCATCTGAAGGCTCAGCCCCAGGCACTTCTACAGAACCCAGTGAAGGATCTGCACCAGGGACCAGTACTGA
ACCTTCTGAAGGATCTGCTCCTGGCACCAGCACAGAGCCAAGTGAAGGATCAGCACCTGGCACCTCAACTGAACCCTCTGAGGGAAGTGCTCCTGGCAGTCCTG
CTGGATCACCAACCAGCACTGAAGAGGGGACCTCTACAGAACCCTCTGAGGGATCTGCACCTGGGACCTCTGAGTCAGCAACACCAGAATCAGGTCCTGGCTCT
GAACCTGCTACTTCTGGTAGTGAAACCCCAGGGACCTCTGAAAGTGCAACACCAGAGTCTGGCCCTGGATCTGAACCAGCAACCAGTGGRCTCTGAGACTCCTGG
TACTTCAGAGAGTGCAACACCTGAAAGTGGCCCAGGGACCAGCACAGAGCCATCAGAAGGCTCTGCACCAGGCACATCTGAGTCTGCTACCCCTGAAAGTGGA
CCTGGCTCTCCTGCTGGGAGTCCCACAAGTACTGAAGAAGGTTCCCCAGCAGGGTCCCAACATCCACTGAAGAAGGATCACCAGCTGGCAGCCCCACTTCCAC
AGAGGAAGGCACATCAGAATCAGCTACTCCAGAGTCTGGACCTGGTACTAGCACAGAACCATCAGAGGGAAGTGCCCCTGGAACATCTGAGAGTGCCACACCA
GAATCAGGACCTGGATCTGAGCCAGCCACCTCTGGTAGTGAAACTCCTGGTACTTCTGAGTCTGCAACCCCAGAGTCAGGCCCAGGATCAGAACCAGCTACTTC
TGGCAGTGAAACACCTGGCACCTCAGAATCAGCAACACCTGAATCTGGACCAGGCACTAGCACAGAACCATCTGAAGGATCAGCCCCTGGCTCTCCTGCTGGCT
CTCCAACTTCTACAGAAGAGGGAACTTCTGAAAGTGCAACTCCTGAATCTGGACCAGGATCTGAACCTGCAACTTCTGGATCAGAGACCAGGGACCTCAGAG
AGTGCTACTCCTGAGTCAGGTCCTGGCAGCCCAGCTGGAAGCCCCACAAGTACAGAAGGAAGGATCTCCTGCTGGGTCCCCTACCAGTACAGAAGAAGGCACTT
CTACTGAACCCTCAGAAGGATCAGCCCCTGGTACAAGTGAATCTGCCACTCCAGAGTCAGGACCAGGCACTTCAGAGTCAGCAACTCCTGAGAGTGGTCCAGGC
ACTTCAGAAAGTGCTACCCCAGAGTCTGGTCCAGGCAGTGAACCTGCTACAAGTGGCTCTGAAACACCAGGCTCTGAACCAGCTACTTCTGGCTCTGAGACTCCT
GGCTCACCAGCTGGCAGTCCTACCTCTACAGAAGAAGGGACTTCAACAGAACCATCTGAGGGCAGTGCACCTGGCACAAGCACAGAGCCATCTGAAGGATCTG
CACCTGGATCTGAACCAGCTACCTCTGGATCAGAAACCCCTGGAACCTCTGAATCAGCTACCCCAGAAAGTGGACCAGGCACATCCACAGAACCATCAGAGGGA

TGA

A

B. hGH1-XTEN2 (SEQ ID NO:62)

ATGGCCACAGGCAGCAGAACATCTCTGCTGCTGGCTTTTGGCCTGCTGTGCCTGCCTTGGCTGCAAGAGGGAAGTGCTTTGCTACAATCCCACTGAGCAGACT
GTTTGACAATGCCATGCTGAGAGCCCACAGACTGCATCAGCTGGCCTTTGACACCTACCAAGAGTTTGAAGAGGCTTACATCCCCAAAGAGCAGAAGTACAGC
CTTCTGCAAAACCCACAGACCAGCCTGTGCTTCTCTGAGAGCATCCCCACACCTAGCAACAGAGAGGAAACCCAGCAGAAGTCCAATCTGGAACTGCTGAG
AATCTCACTGCTGCTGATCCAGTCTTGGCTGGAACCTGTGCAGTTCCTGAGATCAGTGTTTGCCAACAGCTCTGGTGTATGGGGCTTCTGACAGCAATGTGTAT
GACCTGCTGAAAGACCTGGAAGAGGGCATCCAGACACTGATGGGCAGACTGGAAGATGGCTCCCCTAGAACAGGCCAGATTTTCAAGCAGACCTACAGCAAA
GTTTGACACCAACAGCCACAATGATGATGCCCTGCTCAAGAACTATGGGCTGCTGTACTGTTTCAGAAAGGACATGGACAAGGTGGAAACCTTCCTGAGAATT
GTGCAGTGCAGAAGTGTGGAAGGCAGCTGTGGCTTTGAGGAGAACTCAGAATCTGCCACTCCTGAGTCTGGCCTCAGGGACAAGTACAGAACCATCTGAGGGA

TGA

B

FIG. 45

A.

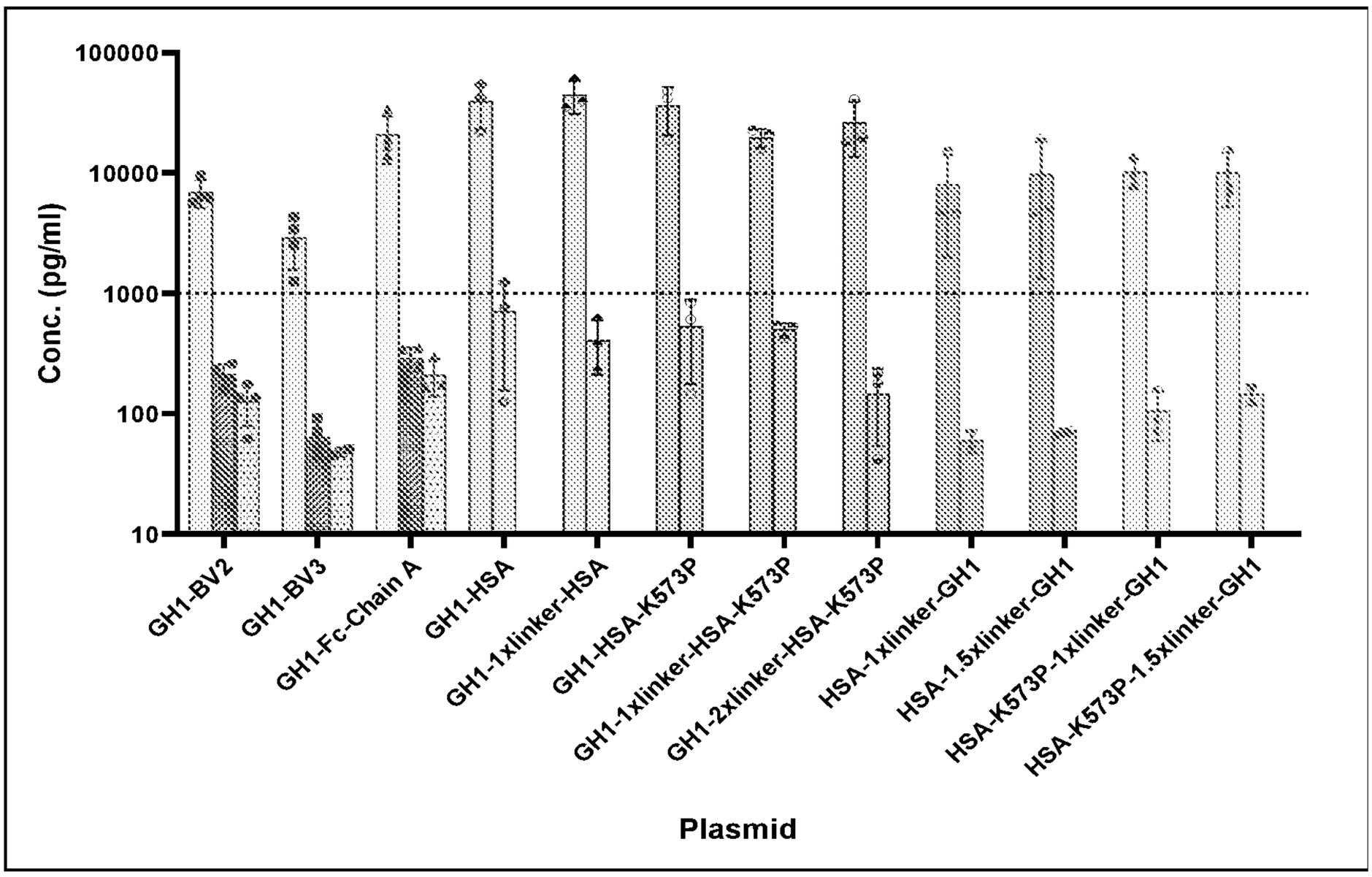
100000
10000
1000
100
10
Conc. (pg/ml)
GH1-BV2
GH1-BV3
GH1-Fc-Chain A
GH1-HSA
GH1-1xlinker-HSA
GH1-HSA-K573P
GH1-1xlinker-HSA-K573P
GH1-2xlinker-HSA-K573P
HSA-1xlinker-GH1
HSA-1.5xlinker-GH1
HSA-K573P-1xlinker-GH1
HSA-K573P-1.5xlinker-GH1
Plasmid

B.

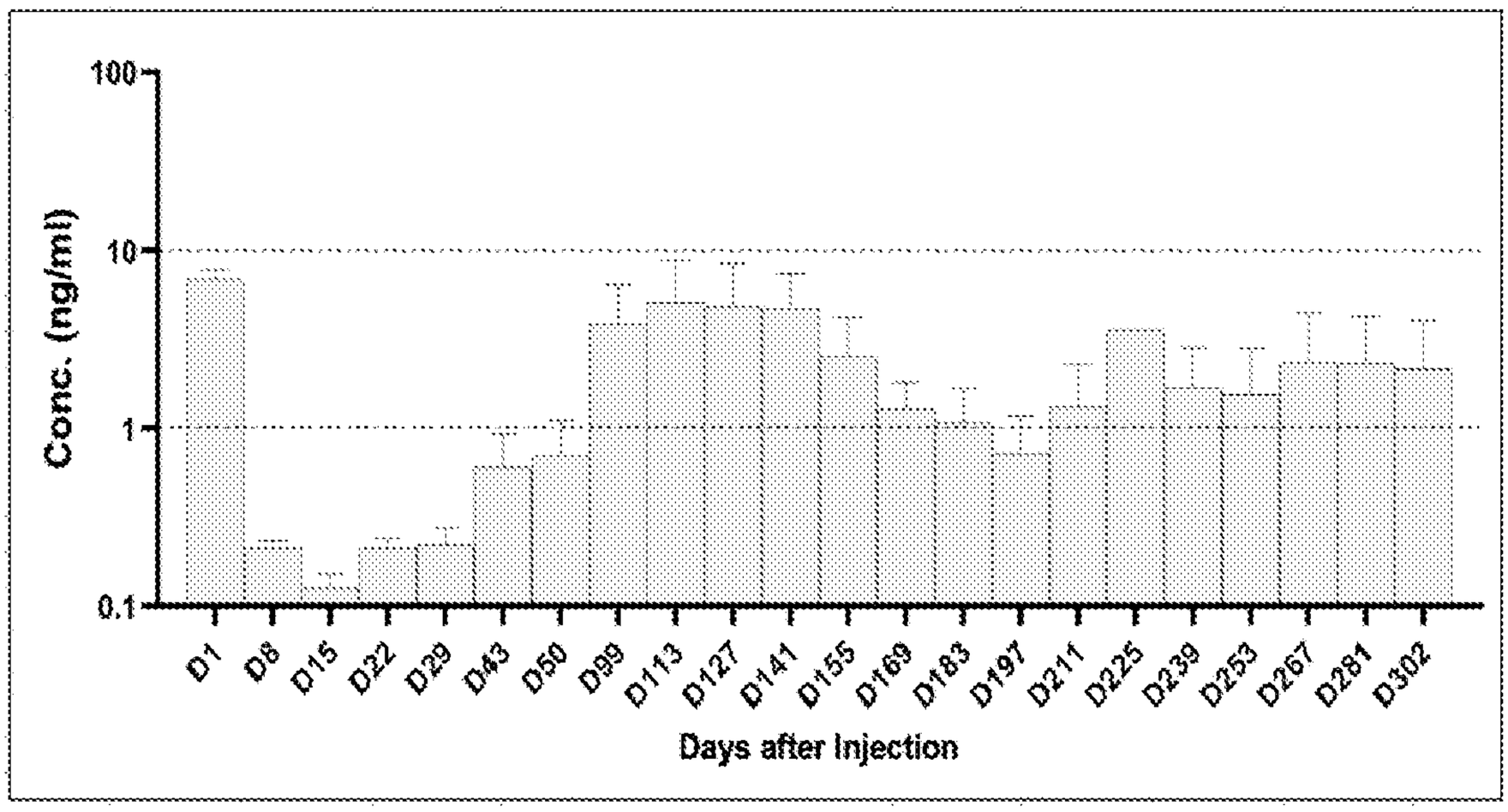
100
10
1
0.1
Conc. (ng/ml)
D1
D8
D15
D22
D29
D43
D50
D99
D113
D127
D141
D155
D169
D183
D197
D211
D225
D239
D253
D267
D281
D302
Days after Injection

FIG. 45 (cont.)

C.

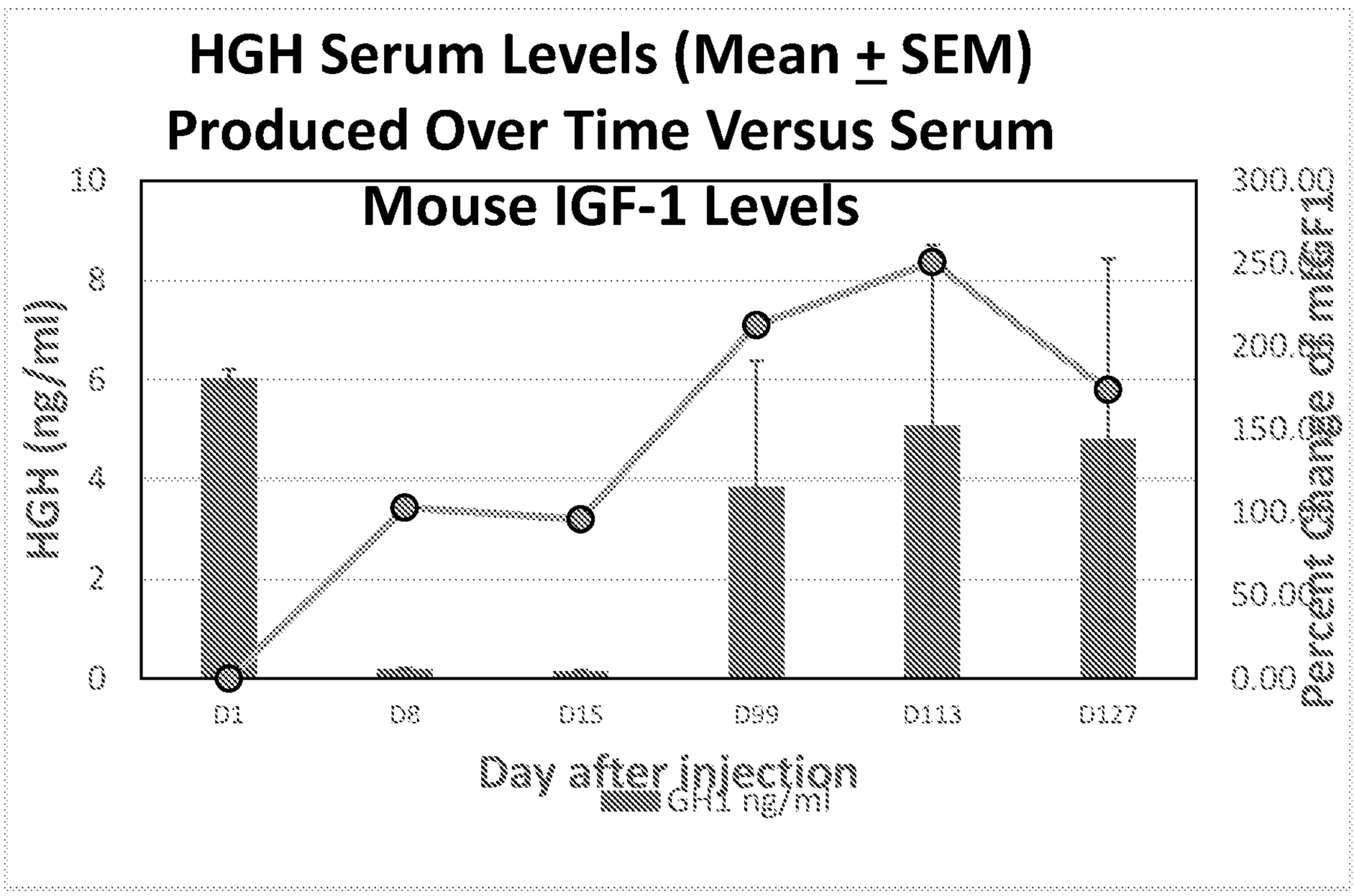
HGH Serum Levels (Mean ± SEM)
Produced Over Time Versus Serum
Mouse IGF-1 Levels
10
8
6
4
2
0
HGH (ng/ml)
300.00
250.00
200.00
150.00
100.00
50.00
0.00
Percent Change on mIGF1
D1
D8
D15
D99
D113
D127
Day after injection
GH1 ng/ml

FIG. 46

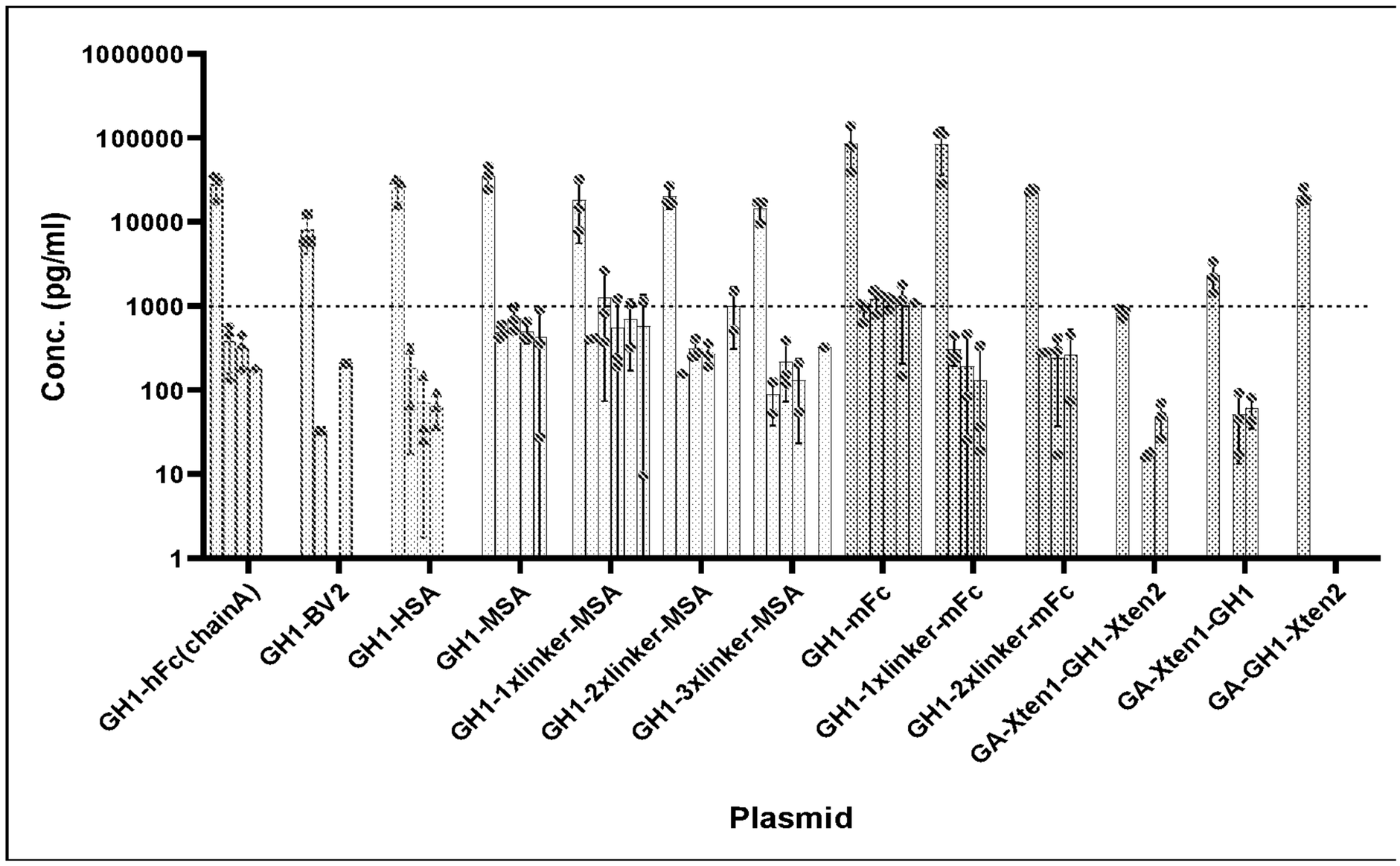
1000000
100000
10000
1000
100
10
1
Conc. (pg/ml)
GH1-hFc(chainA)
GH1-BV2
GH1-HSA
GH1-MSA
GH1-1xlinker-MSA
GH1-2xlinker-MSA
GH1-3xlinker-MSA
GH1-mFc
GH1-1xlinker-mFc
GH1-2xlinker-mFc
GA-Xten1-GH1-Xten2
GA-Xten1-GH1
GA-GH1-Xten2
Plasmid

FIG. 47

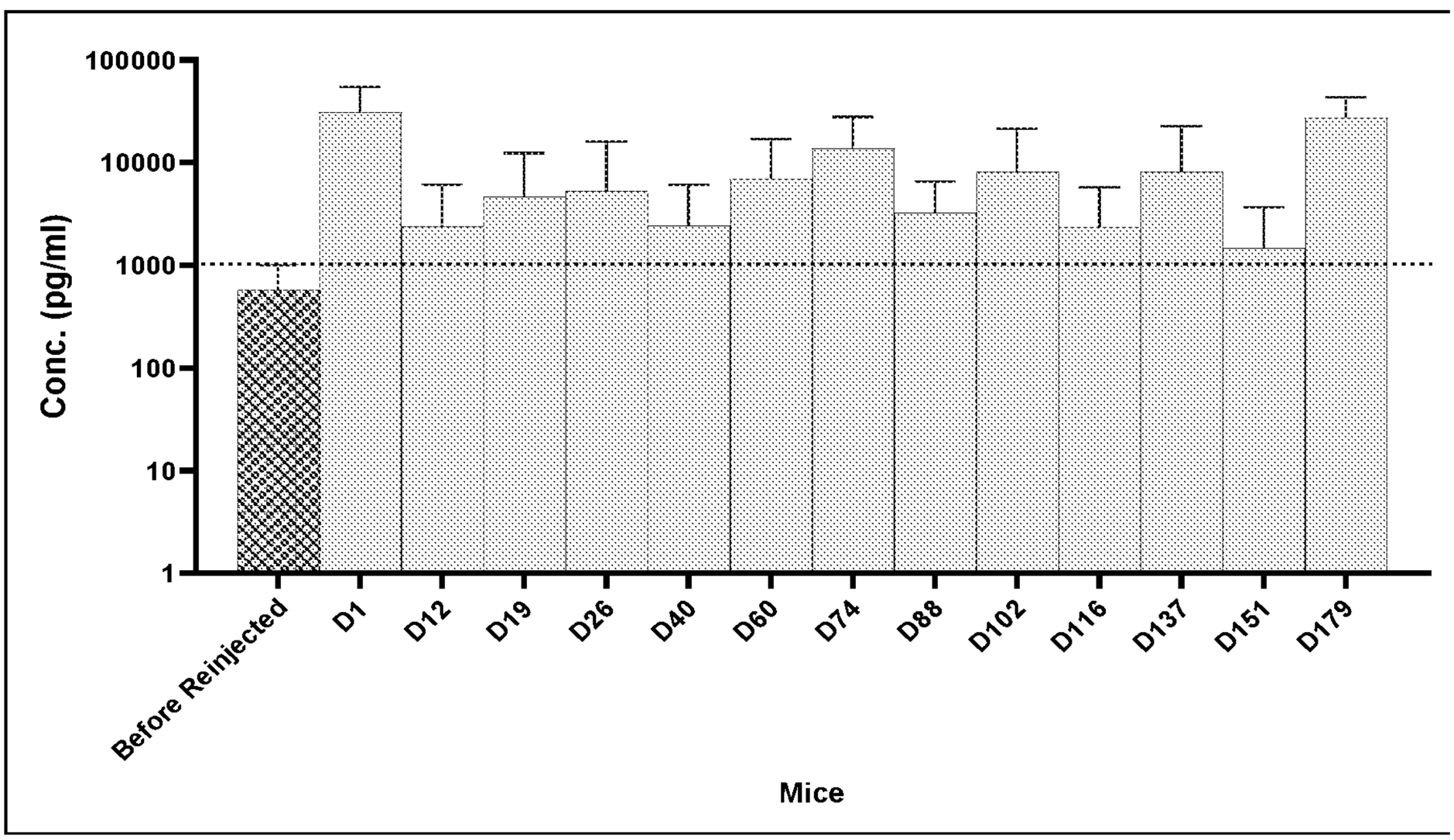
100000
10000
1000
100
10
1
Conc. (pg/ml)
Before Reinjected
D1
D12
D19
D26
D40
D60
D74
D88
D102
D116
D137
D151
D179
Mice

FIG. 48

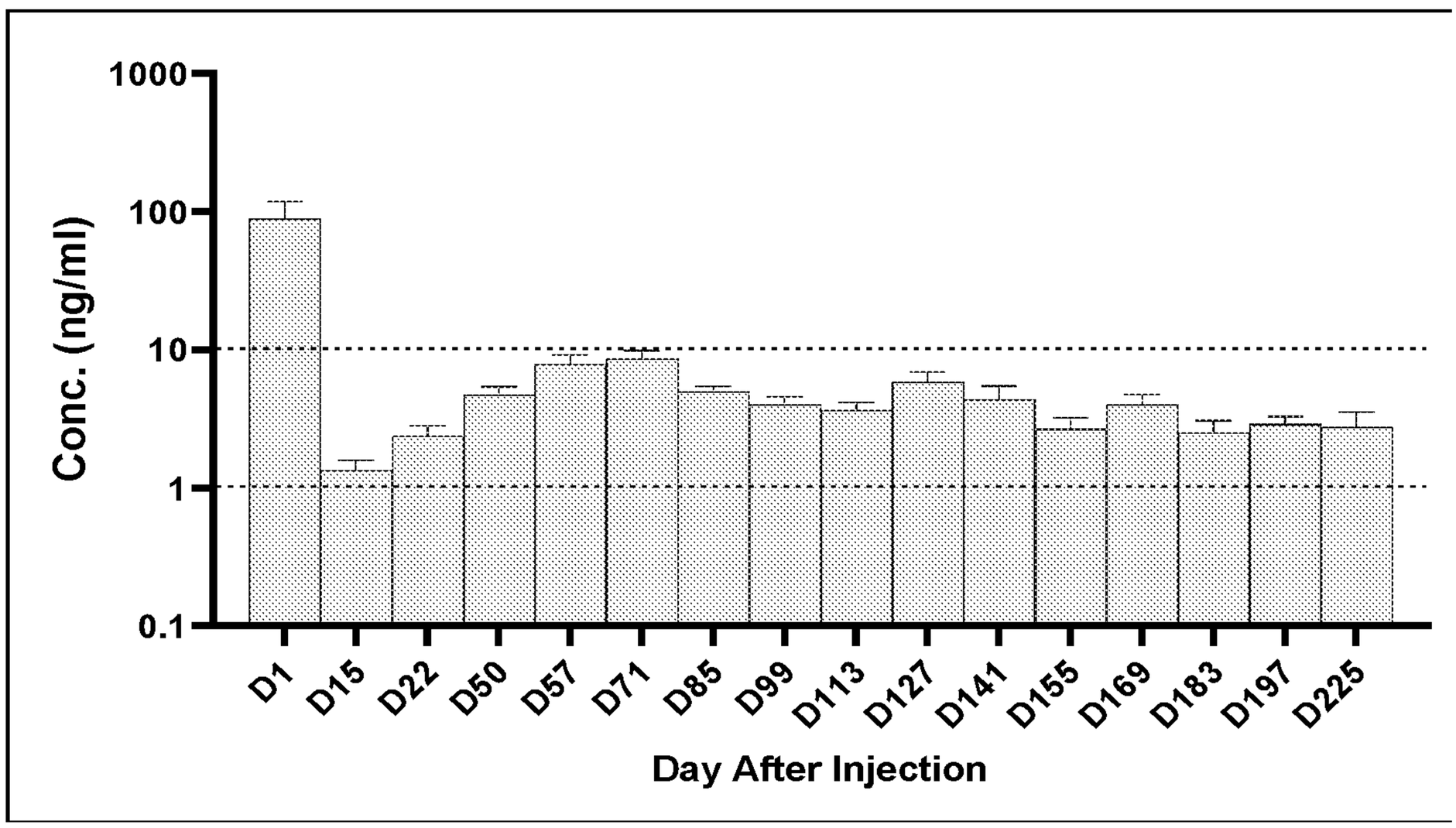
1000
100
10
1
0.1
Conc. (ng/ml)
D1
D15
D22
D50
D57
D71
D85
D99
D113
D127
D141
D155
D169
D183
D197
D225
Day After Injection

FIG. 49

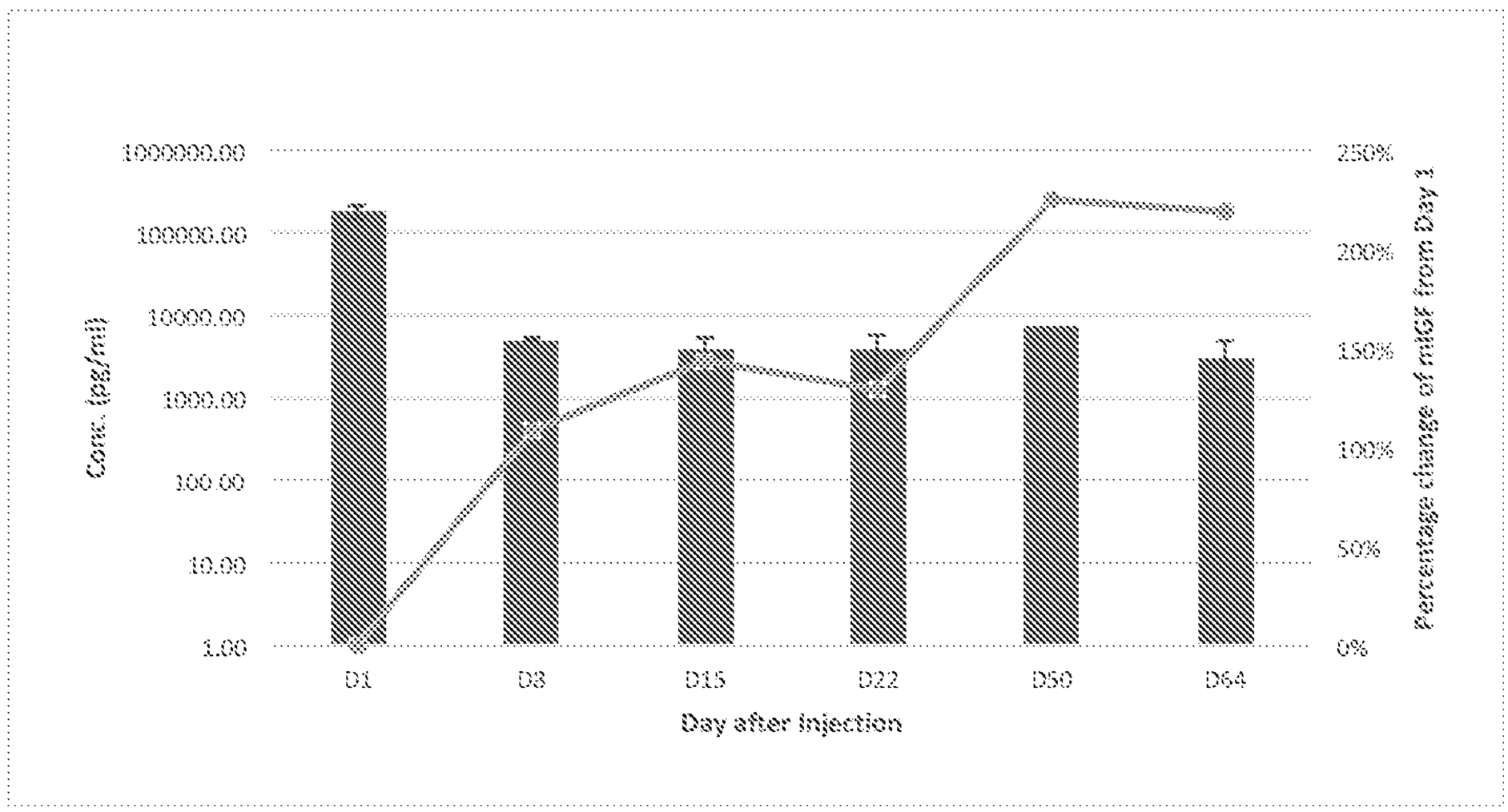
1000000.00
100000.00
10000.00
1000.00
100.00
10.00
1.00
Conc. (pg/ml)
250%
200%
150%
100%
50%
0%
Percentage change of mIGF from Day 1
D1
D8
D15
D22
D50
D64
Day after Injection

FIG. 50

A.

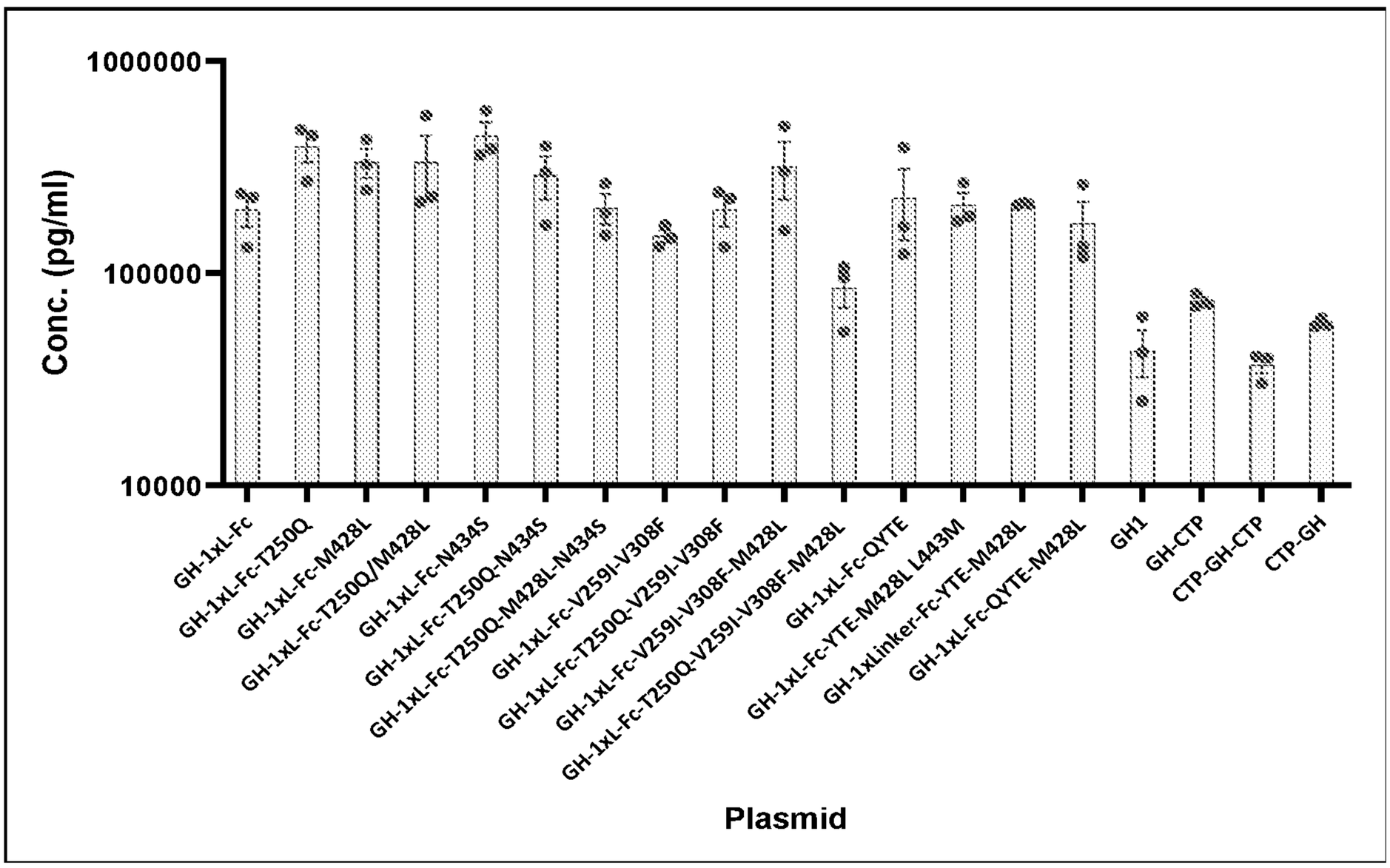
1000000
100000
10000
Conc. (pg/ml)
GH-1xL-Fc
GH-1xL-Fc-T250Q
GH-1xL-Fc-M428L
GH-1xL-Fc-T250Q/M428L
GH-1xL-Fc-N434S
GH-1xL-Fc-T250Q-N434S
GH-1xL-Fc-T250Q-M428L-N434S
GH-1xL-Fc-V259I-V308F
GH-1xL-Fc-T250Q-V259I-V308F
GH-1xL-Fc-V259I-V308F-M428L
GH-1xL-Fc-T250Q-V259I-V308F-M428L
GH-1xL-Fc-QYTE
GH-1xL-Fc-YTE-M428L L443M
GH-1xLinker-Fc-YTE-M428L
GH-1xL-Fc-QYTE-M428L
GH1
GH-CTP
CTP-GH-CTP
CTP-GH
Plasmid

B.

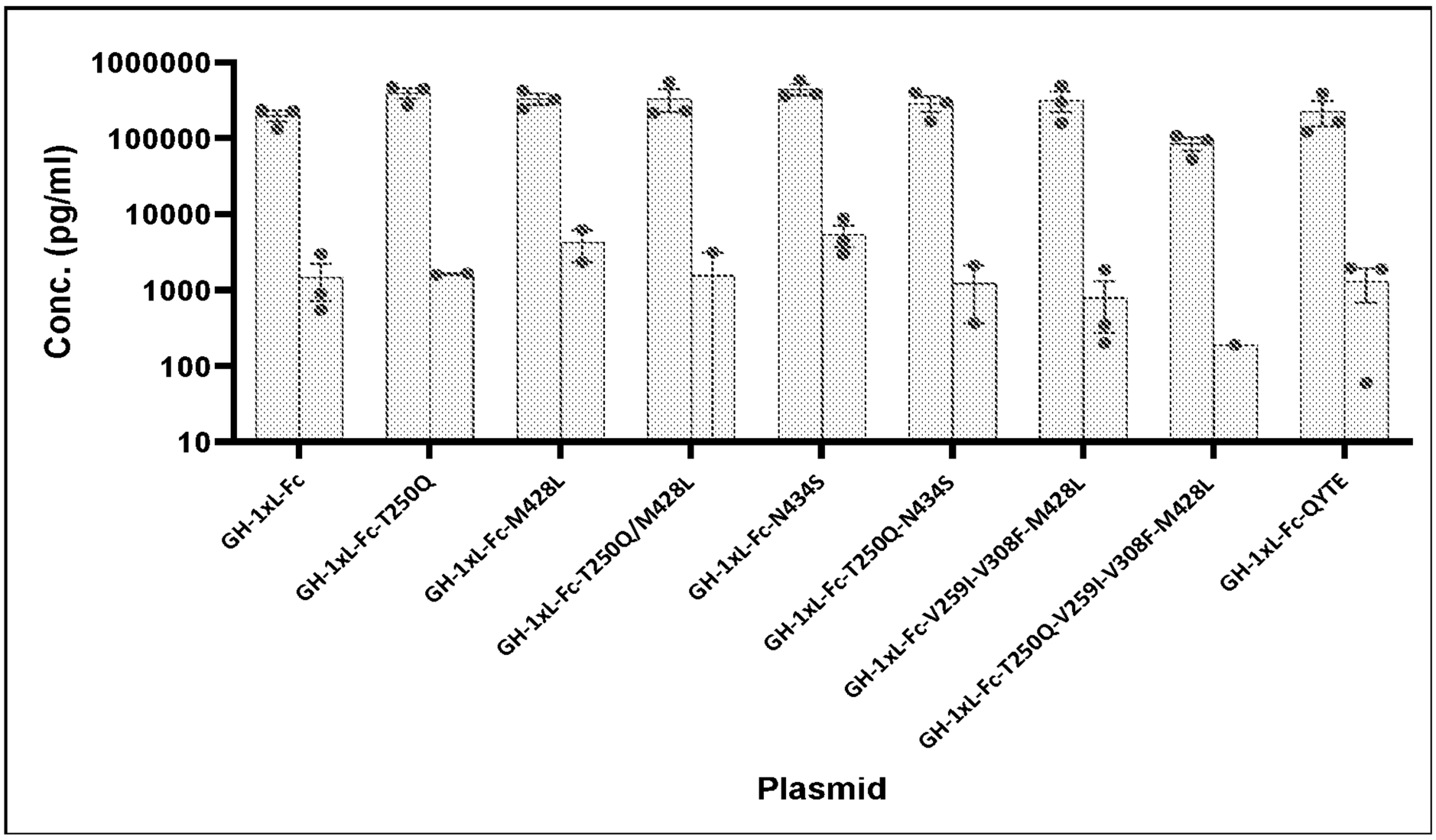
1000000
100000
10000
1000
100
10
Conc. (pg/ml)
GH-1xL-Fc
GH-1xL-Fc-T250Q
GH-1xL-Fc-M428L
GH-1xL-Fc-T250Q/M428L
GH-1xL-Fc-N434S
GH-1xL-Fc-T250Q-N434S
GH-1xL-Fc-V259I-V308F-M428L
GH-1xL-Fc-T250Q-V259I-V308F-M428L
GH-1xL-Fc-QYTE
Plasmid

FIG. 51

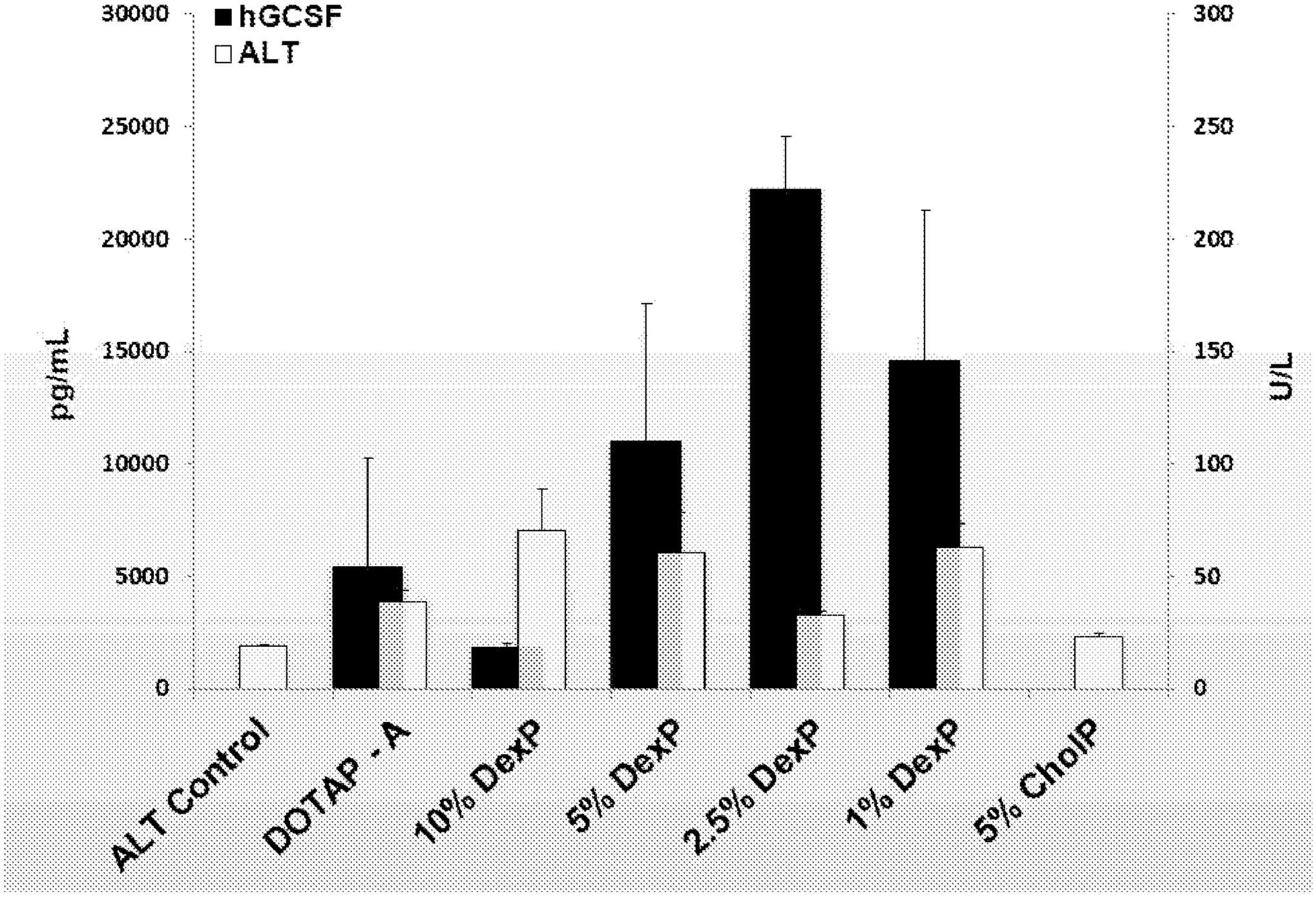
hGCSF
ALT
pg/mL
U/L
30000
25000
20000
15000
10000
5000
0
300
250
200
150
100
50
0
ALT Control
DOTAP - A
10% DexP
5% DexP
2.5% DexP
1% DexP
5% CholP

FIG. 52

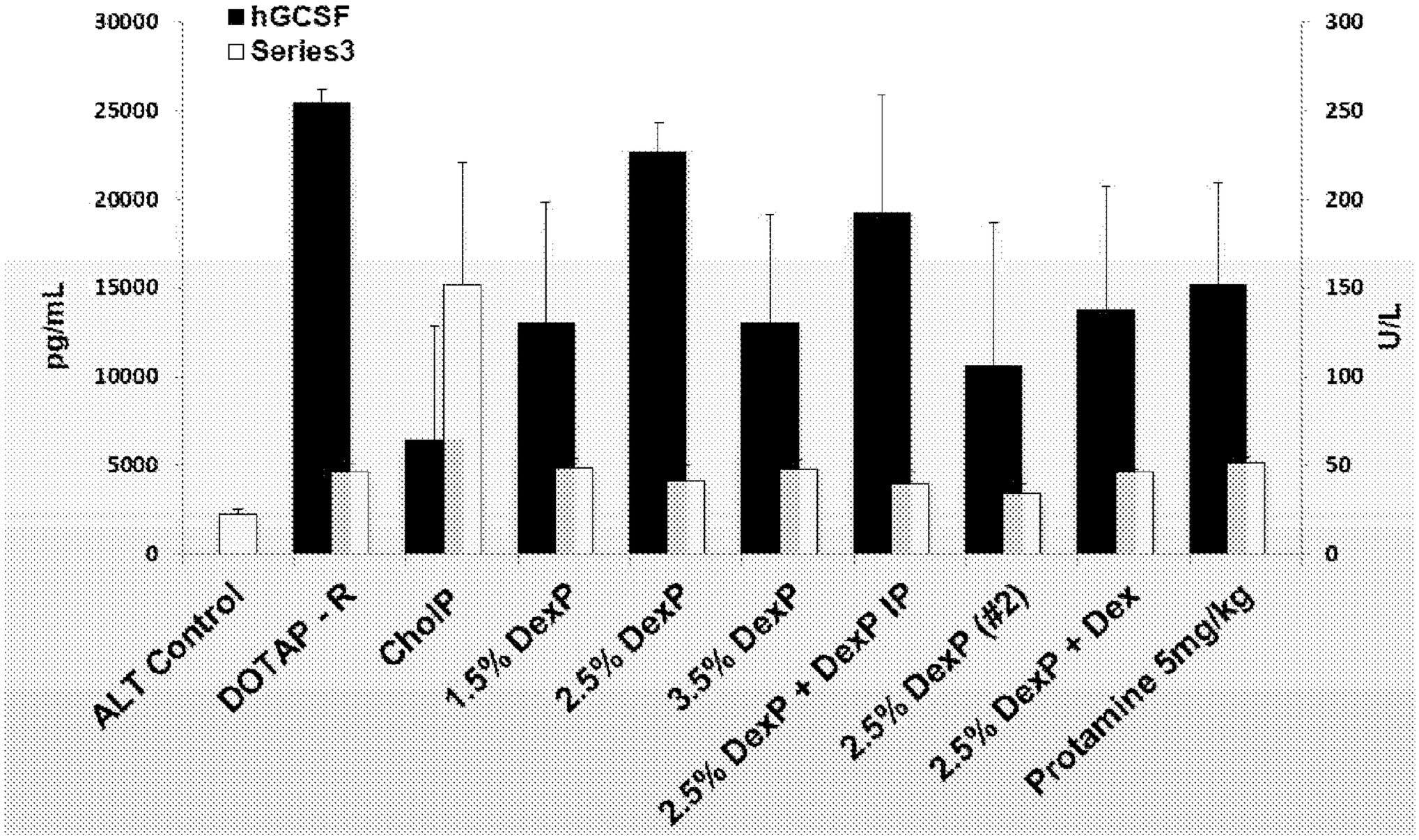
hGCSF
Series3
pg/mL
U/L
30000
25000
20000
15000
10000
5000
0
300
250
200
150
100
50
0
ALT Control
DOTAP - R
ChoIP
1.5% DexP
2.5% DexP
3.5% DexP
2.5% DexP + DexP IP
2.5% DexP (#2)
2.5% DexP + Dex
Protamine 5mg/kg

FIG. 53

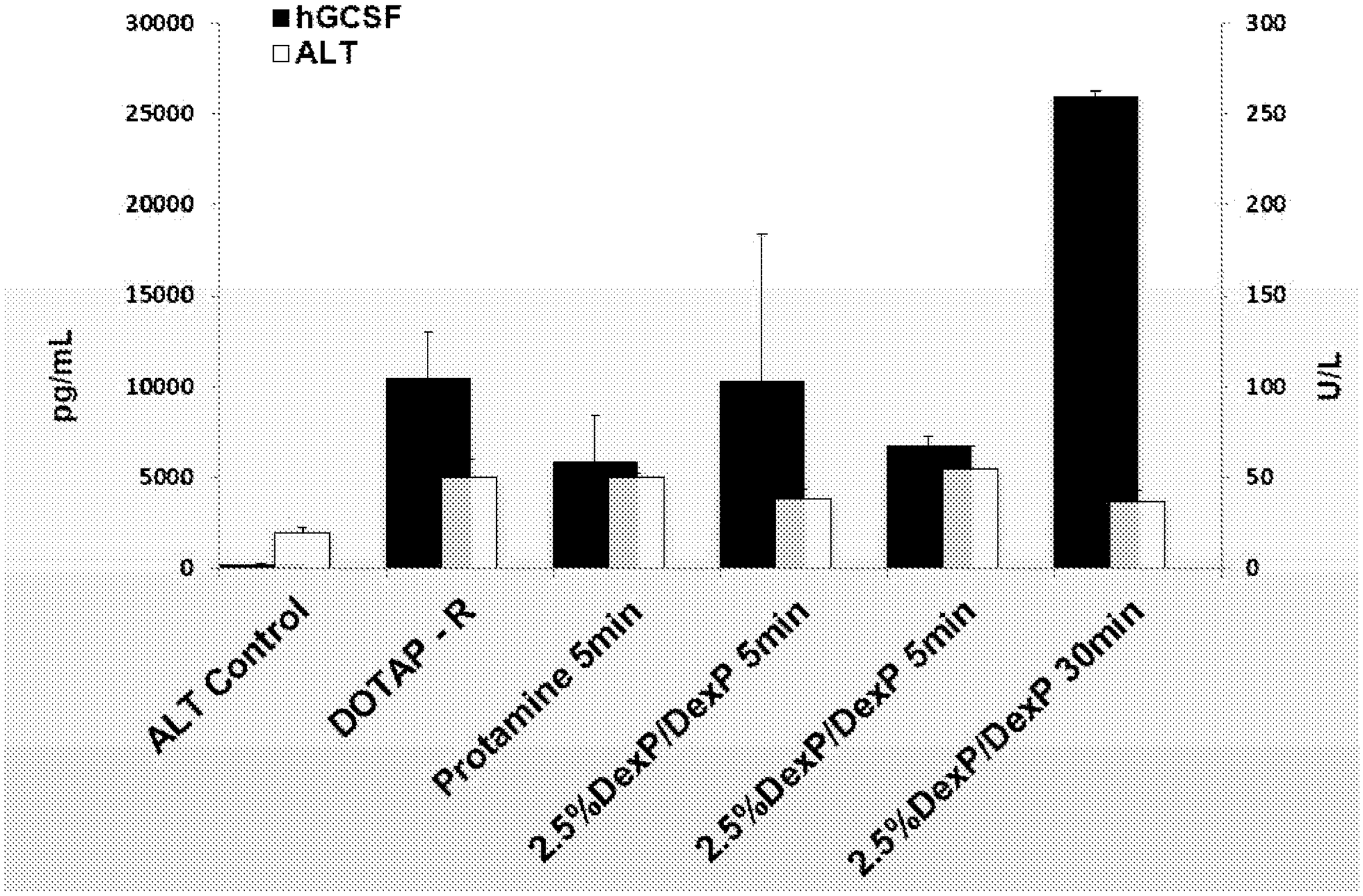
hGCSF
ALT
pg/mL
U/L
30000
25000
20000
15000
10000
5000
0
300
250
200
150
100
50
0
ALT Control
DOTAP - R
Protamine 5min
2.5%DexP/DexP 5min
2.5%DexP/DexP 5min
2.5%DexP/DexP 30min

FIG. 54

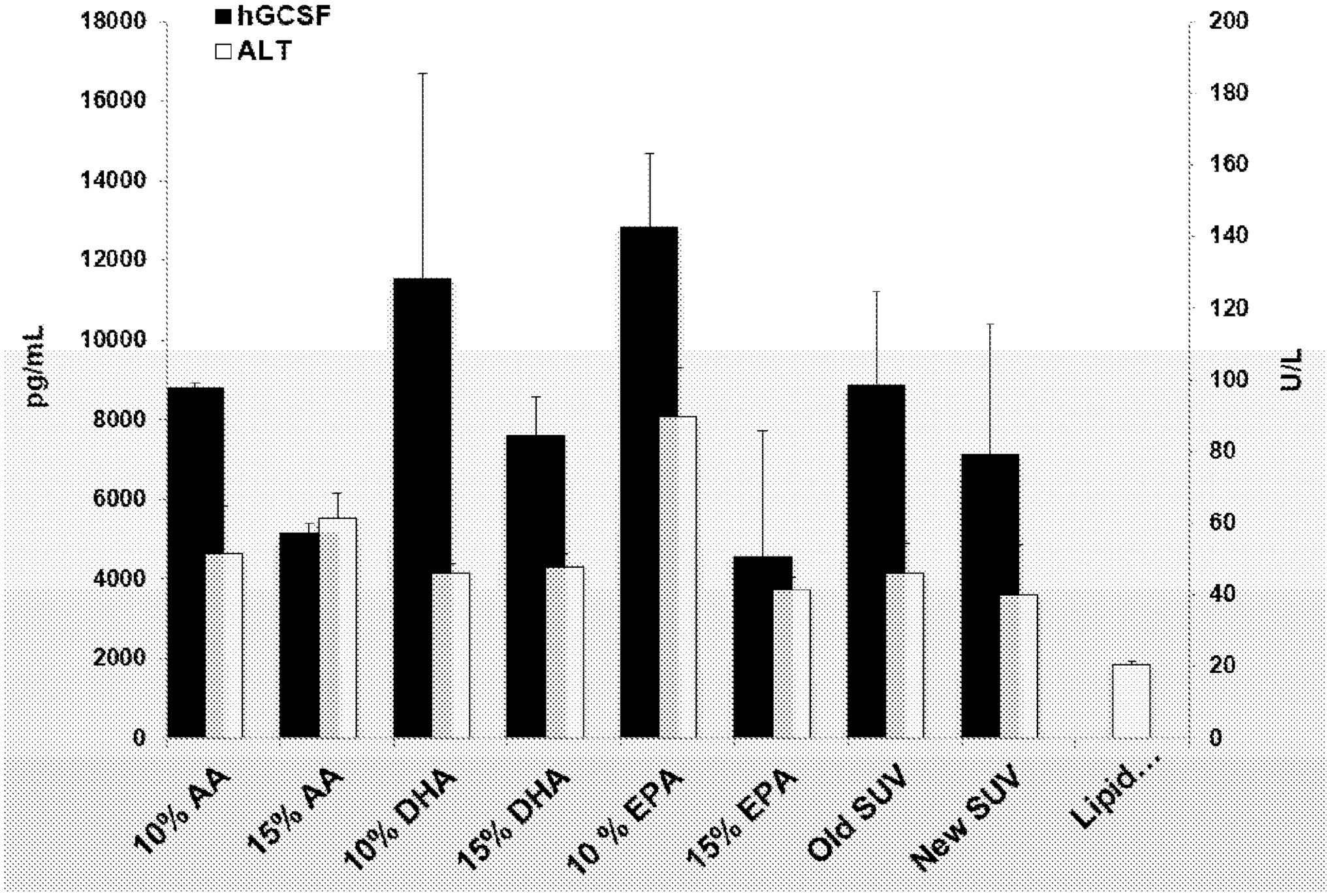
hGCSF
ALT
pg/mL
U/L
18000
16000
14000
12000
10000
8000
6000
4000
2000
0
200
180
160
140
120
100
80
60
40
20
0
10% AA
15% AA
10% DHA
15% DHA
10 % EPA
15% EPA
Old SUV
New SUV
Lipid...

FIG. 55

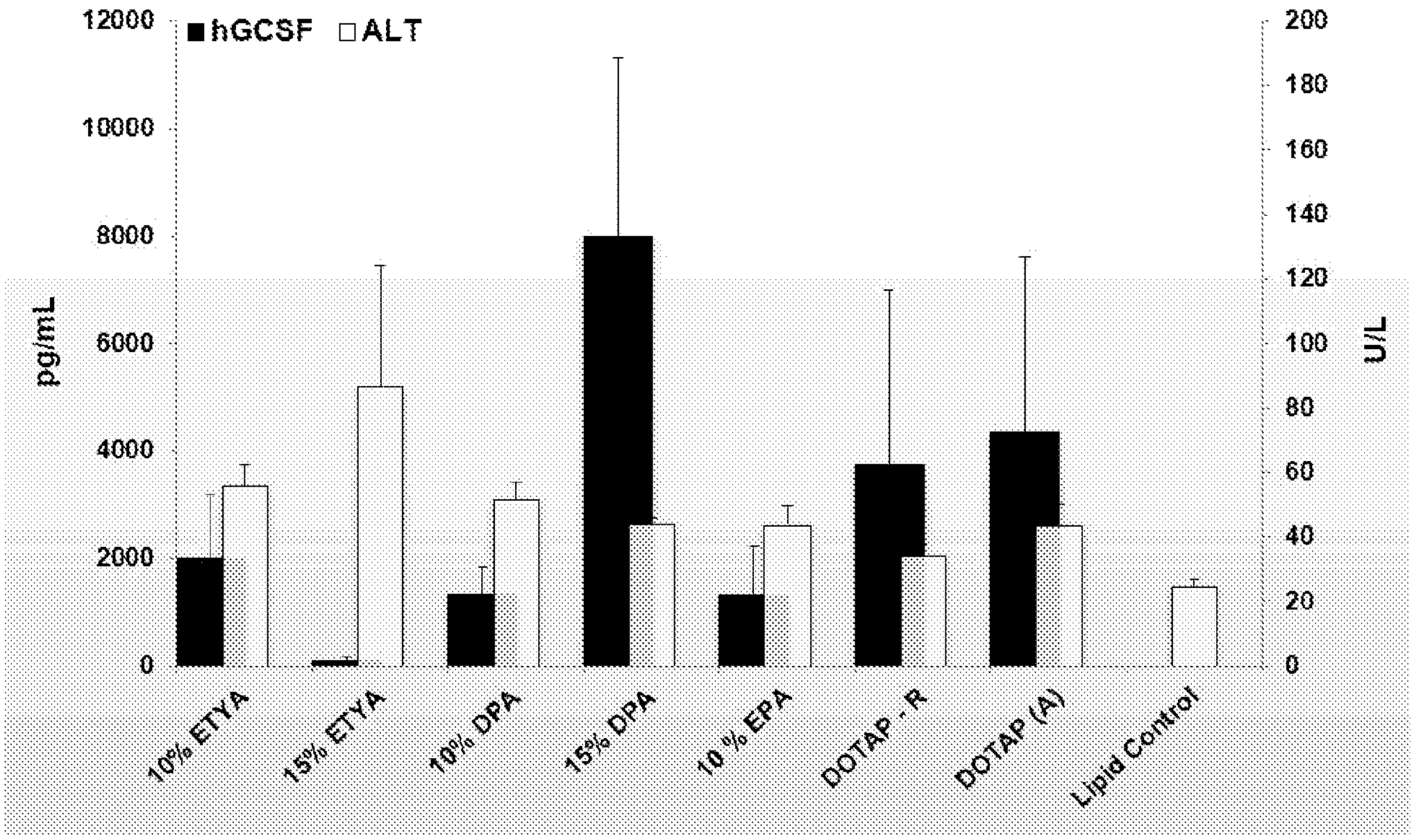
12000
10000
8000
6000
4000
2000
0
pg/mL
■hGCSF □ALT
200
180
160
140
120
100
80
60
40
20
0
U/L
10% ETYA
15% ETYA
10% DPA
15% DPA
10 % EPA
DOTAP - R
DOTAP (A)
Lipid Control

FIG. 56

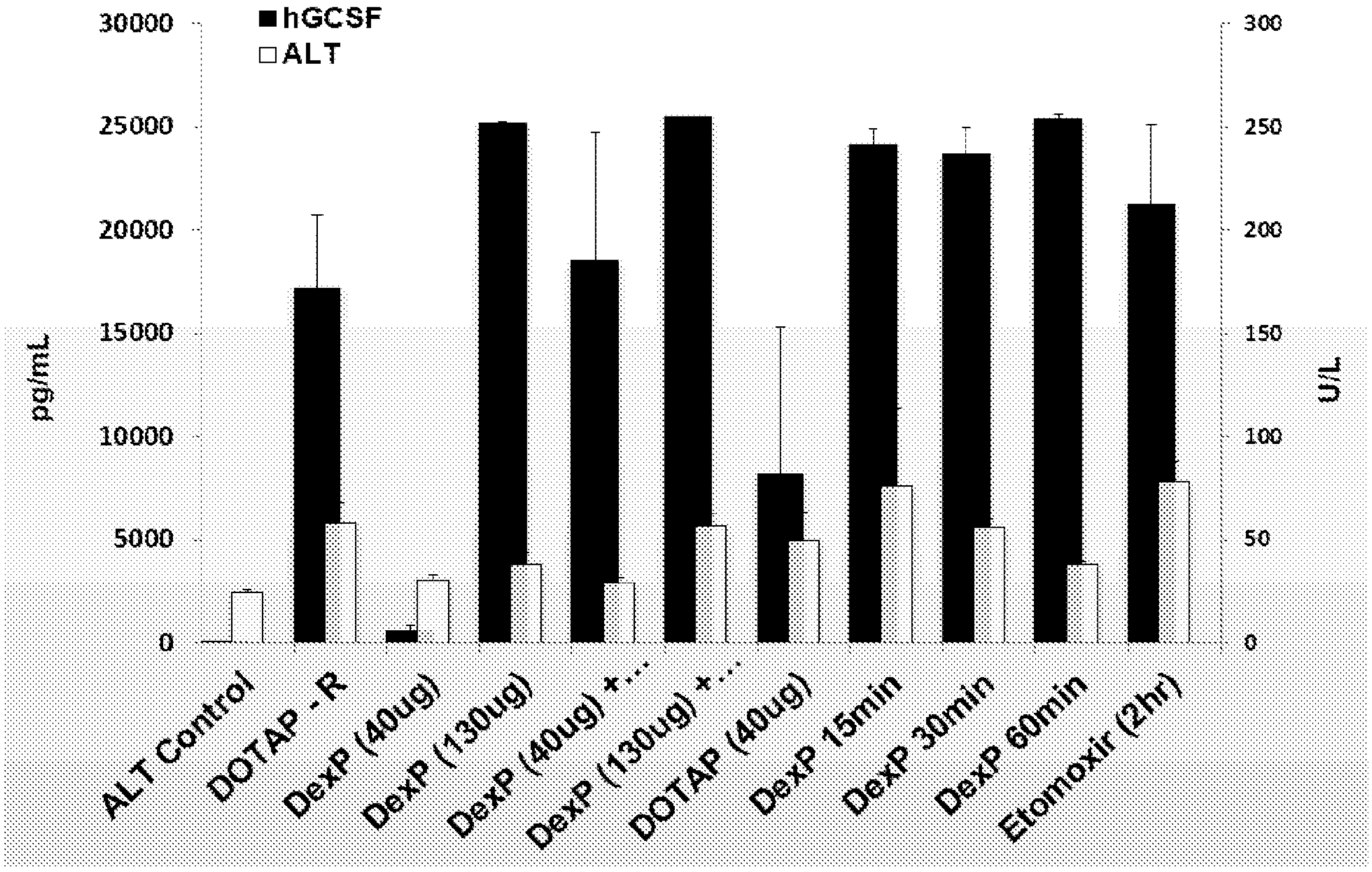
hGCSF
ALT
pg/mL
U/L
30000
25000
20000
15000
10000
5000
0
300
250
200
150
100
50
0
ALT Control
DOTAP - R
DexP (40ug)
DexP (130ug)
DexP (40ug) +...
DexP (130ug) +...
DOTAP (40ug)
DexP 15min
DexP 30min
DexP 60min
Etomoxir (2hr)

FIG. 57

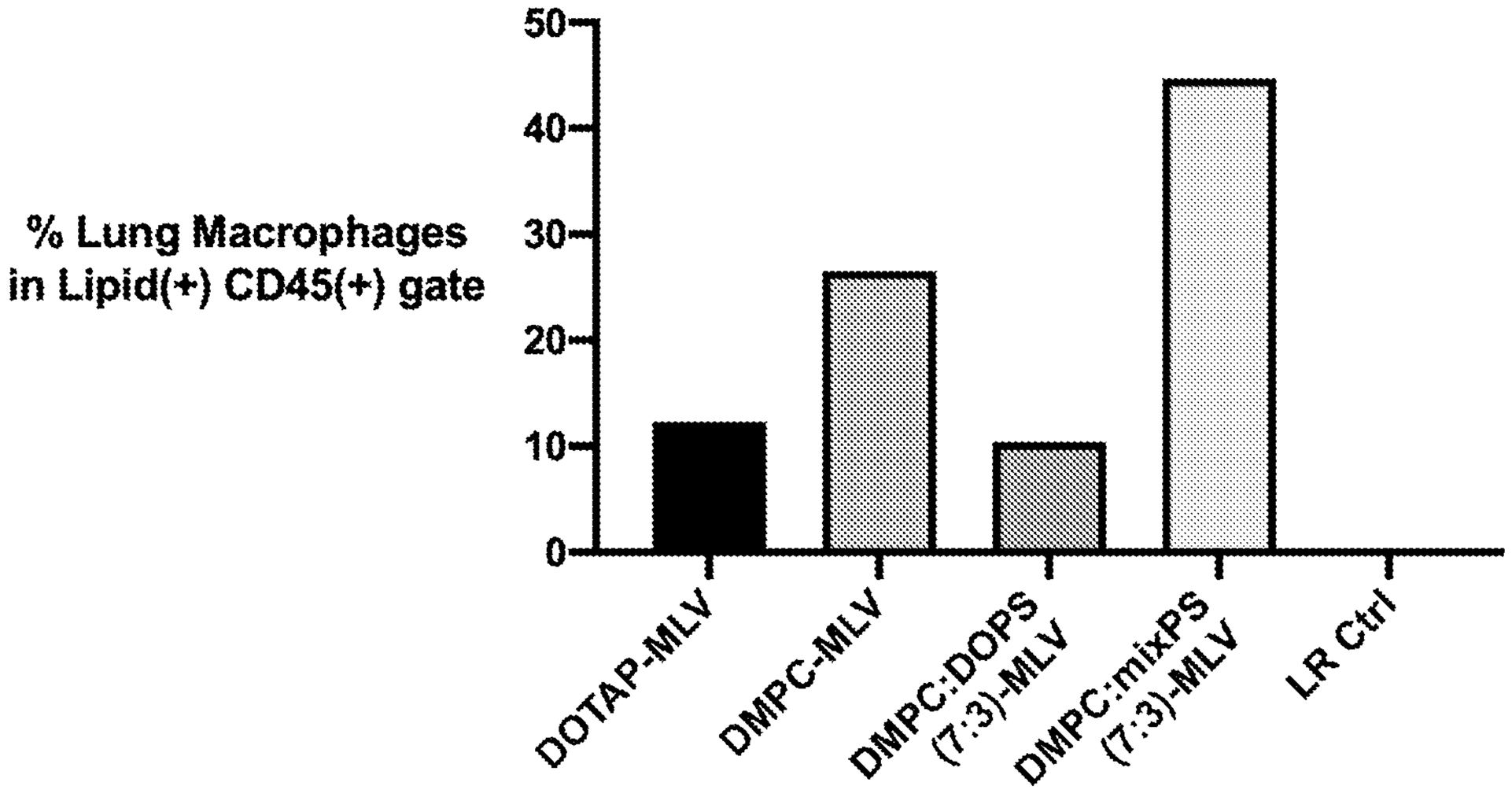
% Lung Macrophages
in Lipid(+) CD45(+) gate
50
40
30
20
10
0
DOTAP-MLV
DMPC-MLV
DMPC:DOPS
(7:3)-MLV
DMPC:mixPS
(7:3)-MLV
LR Ctrl

FIG. 58

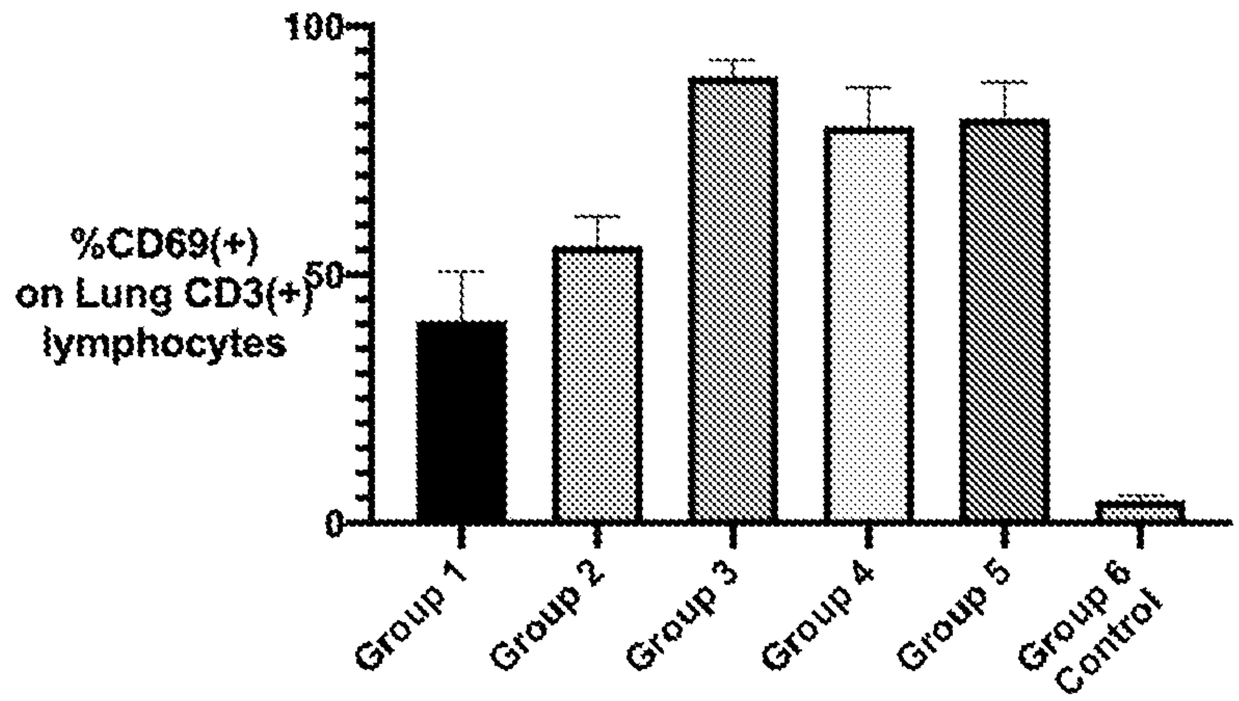
%CD69(+)
on Lung CD3(+)
lymphocytes
100
50
0
Group 1
Group 2
Group 3
Group 4
Group 5
Group 6
Control

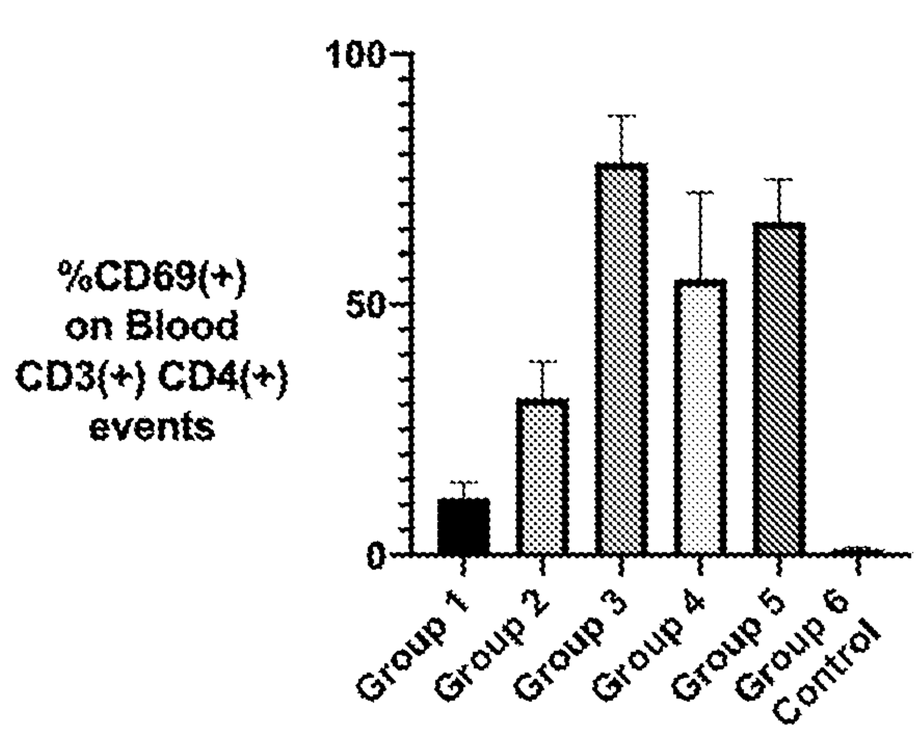
%CD69(+)
on Blood
CD3(+) CD4(+)
events
100
50
0
Group 1
Group 2
Group 3
Group 4
Group 5
Group 6
Control

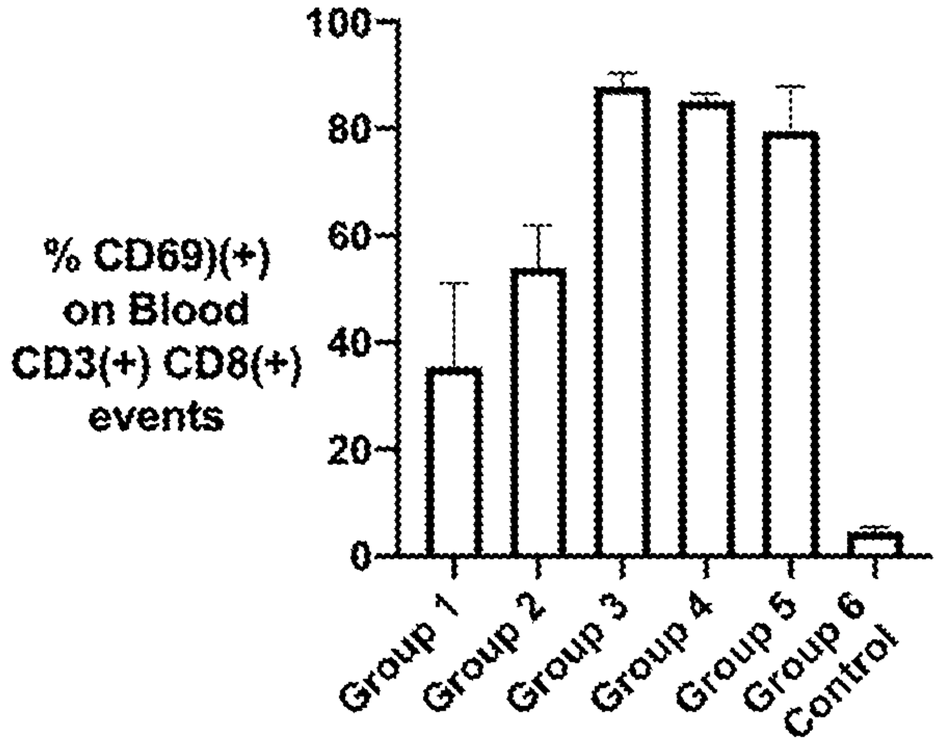
% CD69)(+)
on Blood
CD3(+) CD8(+)
events
100
80
60
40
20
0
Group 1
Group 2
Group 3
Group 4
Group 5
Group 6
Control

FIG. 59

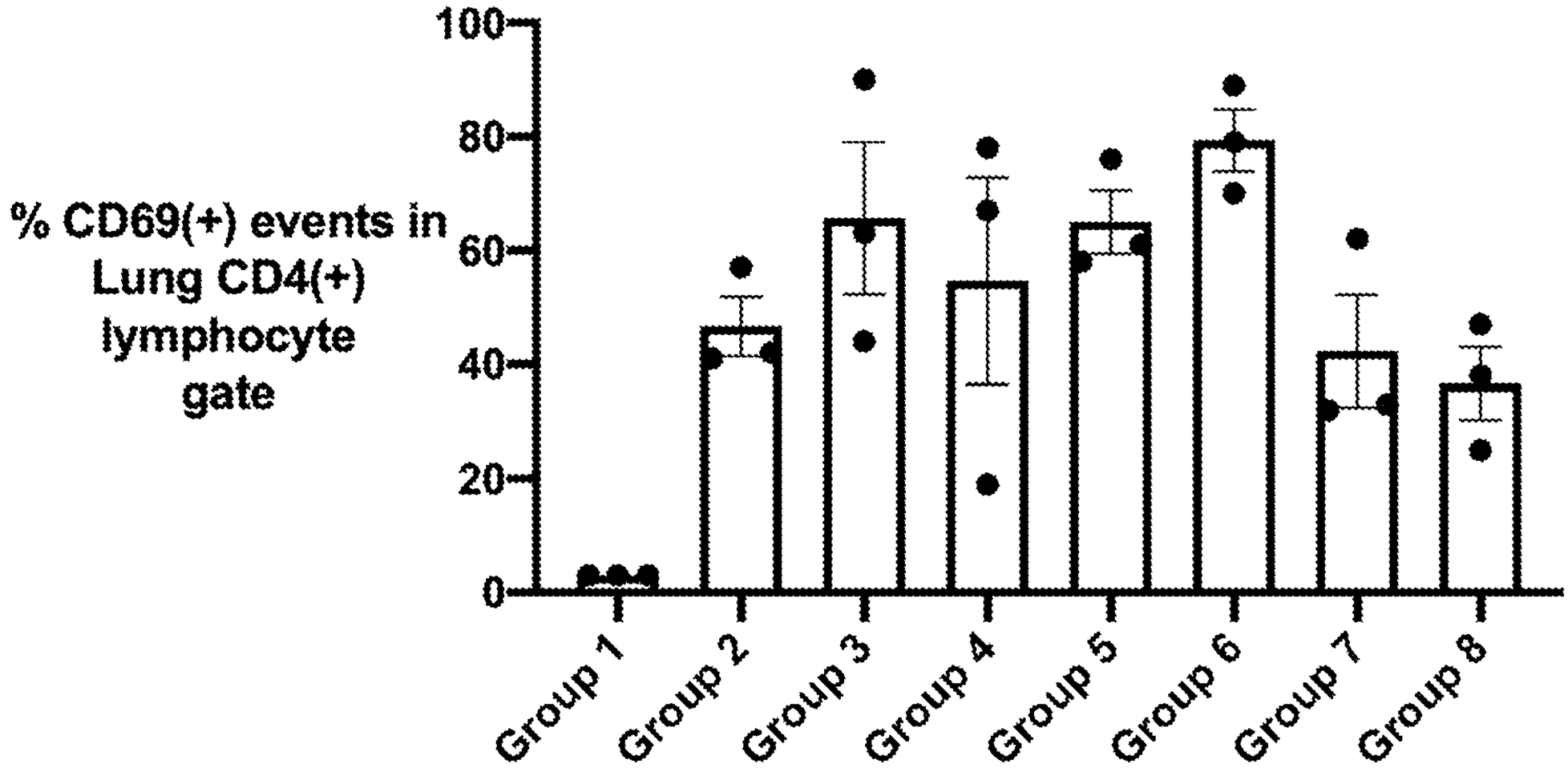
% CD69(+) events in Lung CD4(+) lymphocyte gate
100
80
60
40
20
0
Group 1
Group 2
Group 3
Group 4
Group 5
Group 6
Group 7
Group 8

FIG. 60

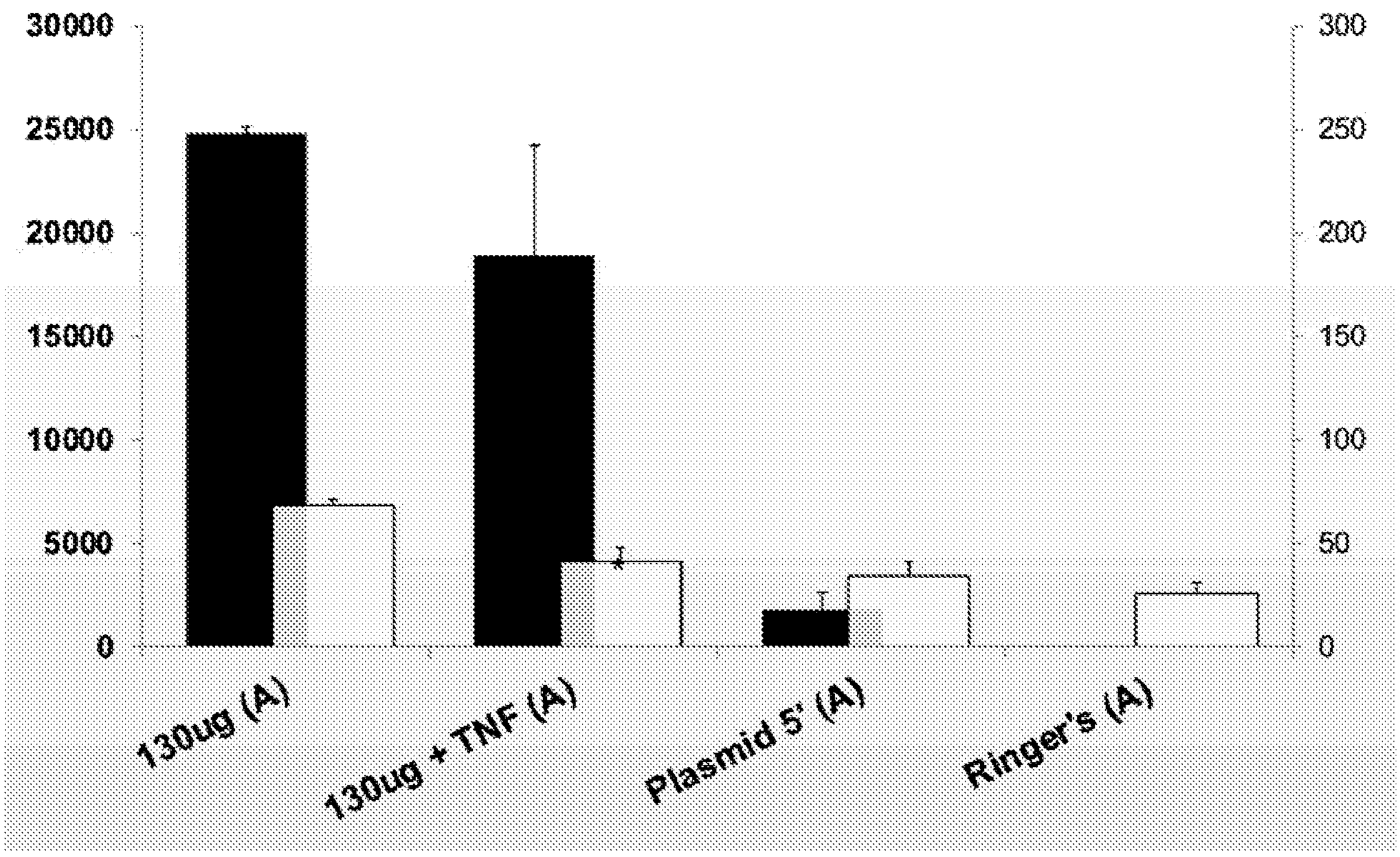
GCSF pg/mL
ALT U/L
30000
25000
20000
15000
10000
5000
0
300
250
200
150
100
50
0
130ug (A)
130ug + TNF (A)
Plasmid 5' (A)
Ringer's (A)

FIG. 61

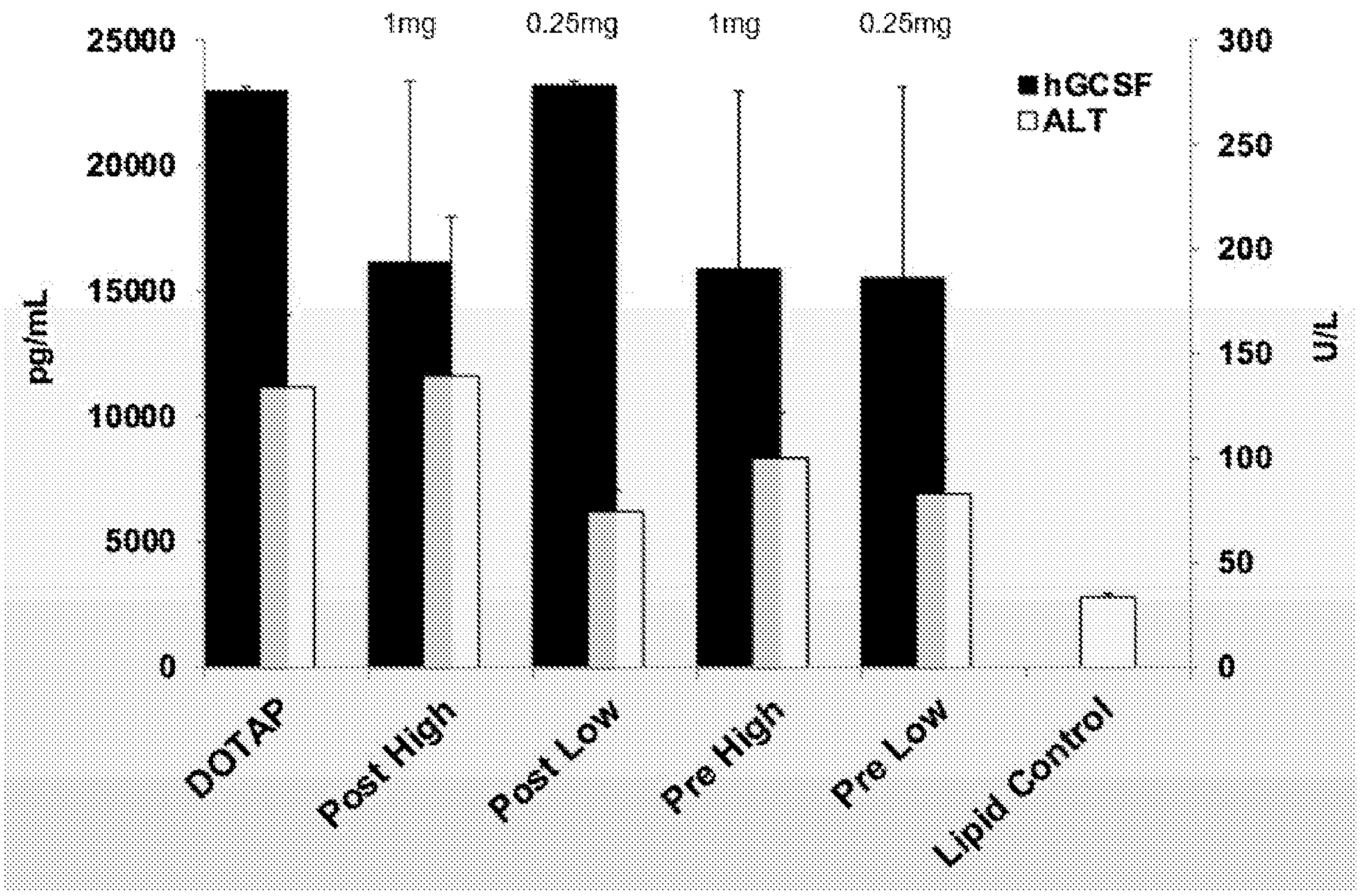
1mg
0.25mg
1mg
0.25mg
25000
20000
15000
10000
5000
0
pg/mL
hGCSF
ALT
300
250
200
150
100
50
0
U/L
DOTAP
Post High
Post Low
Pre High
Pre Low
Lipid Control

FIG. 62

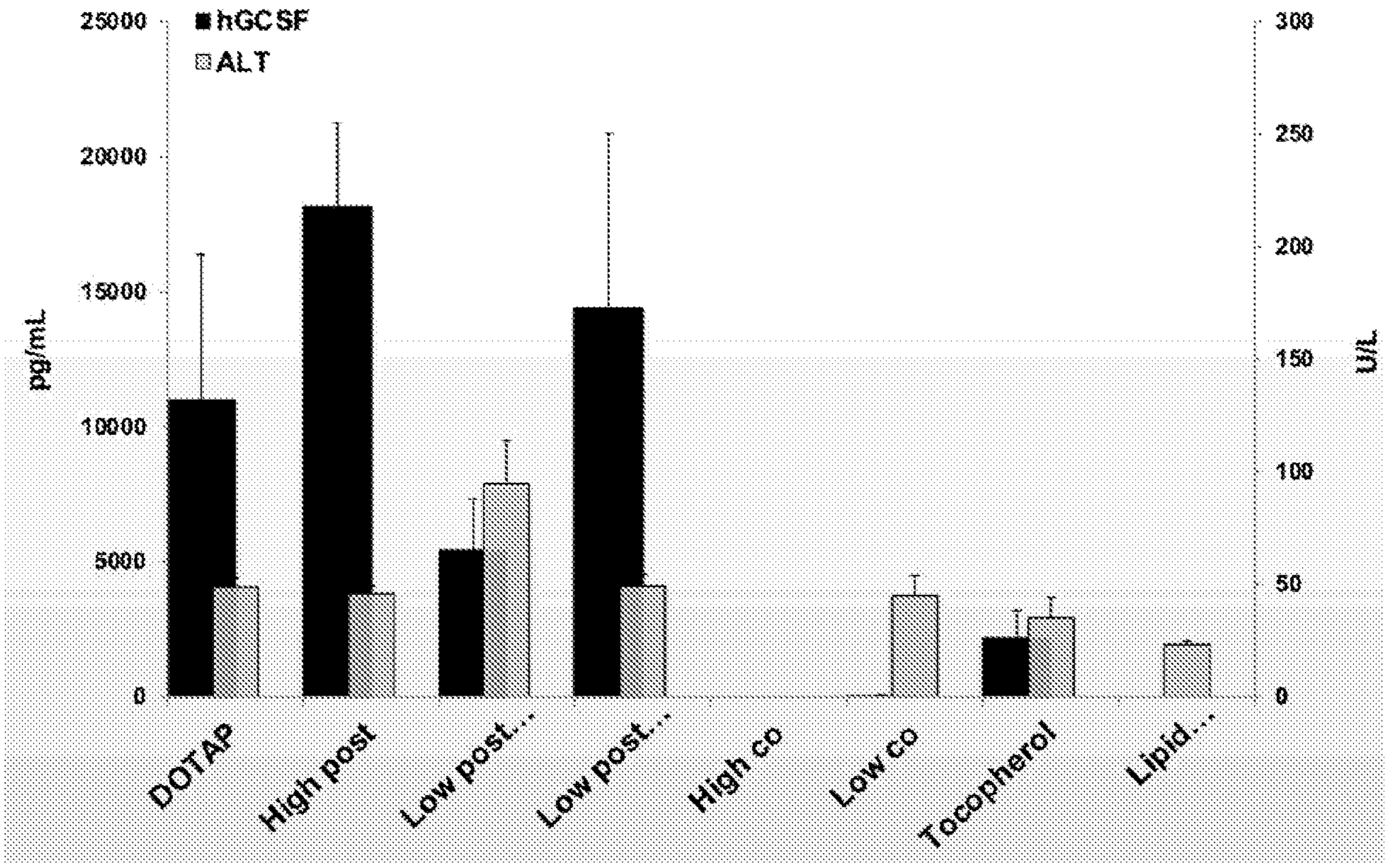
hGCSF
ALT
pg/mL
U/L
25000
20000
15000
10000
5000
0
300
250
200
150
100
50
0
DOTAP
High post
Low post...
Low post...
High co
Low co
Tocopherol
Lipid...

FIG. 63

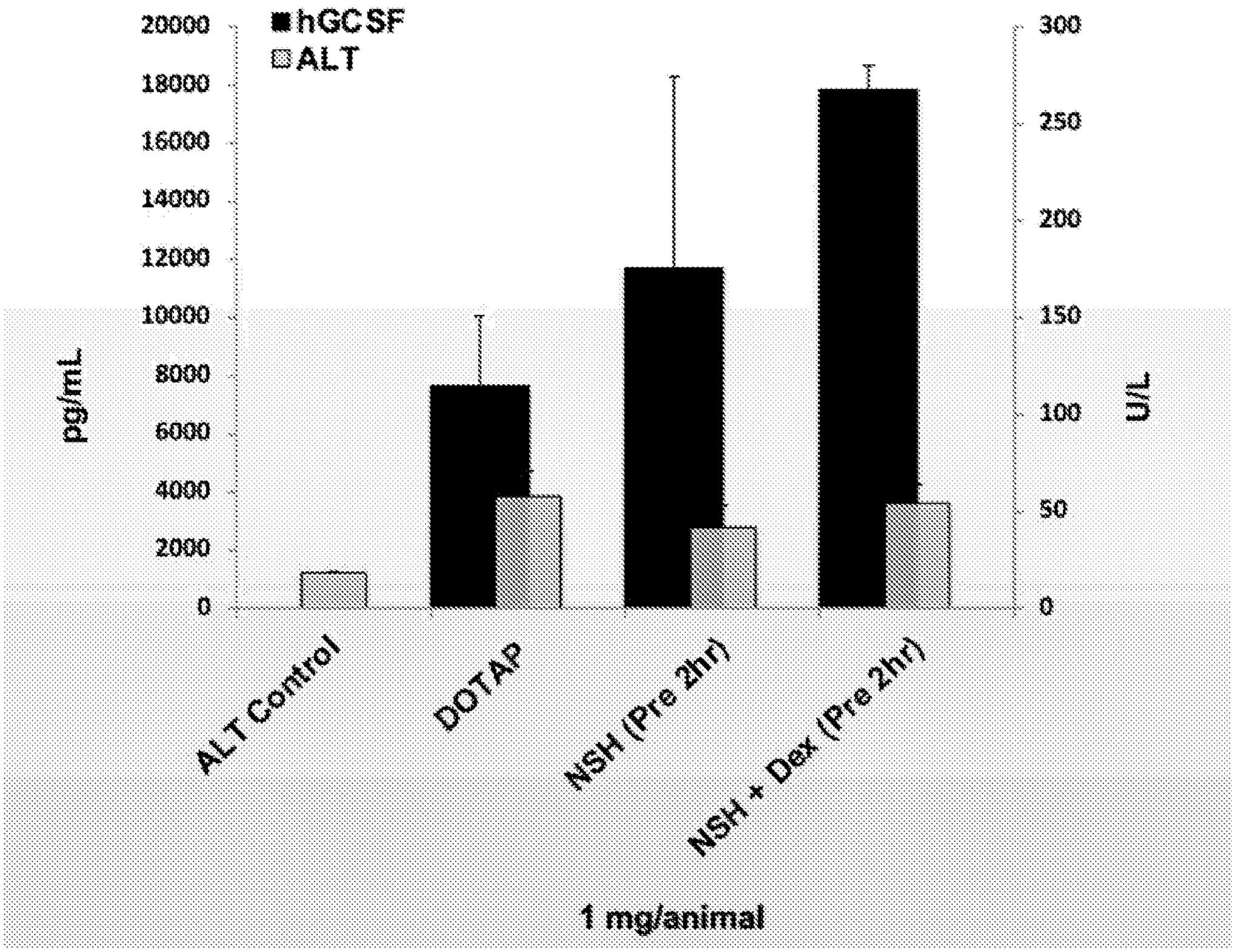
hGCSF
ALT
pg/mL
U/L
20000
18000
16000
14000
12000
10000
8000
6000
4000
2000
0
300
250
200
150
100
50
0
ALT Control
DOTAP
NSH (Pre 2hr)
NSH + Dex (Pre 2hr)
1 mg/animal

FIG. 64

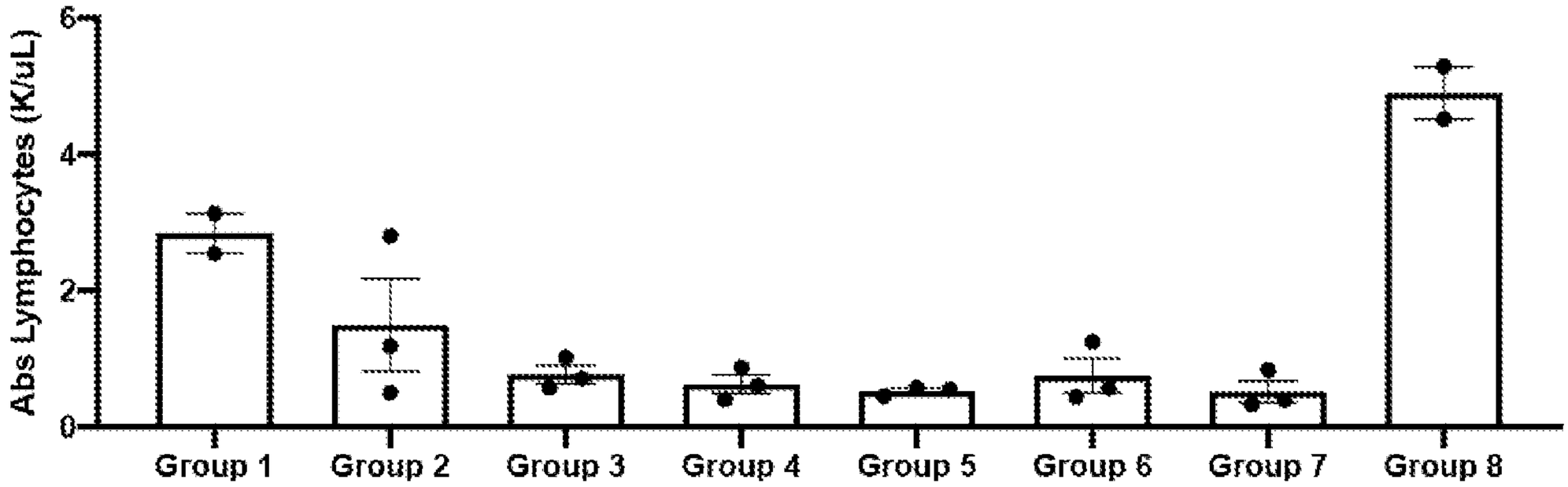
Abs Lymphocytes (K/uL)
0
2
4
6
Group 1
Group 2
Group 3
Group 4
Group 5
Group 6
Group 7
Group 8

FIG. 65

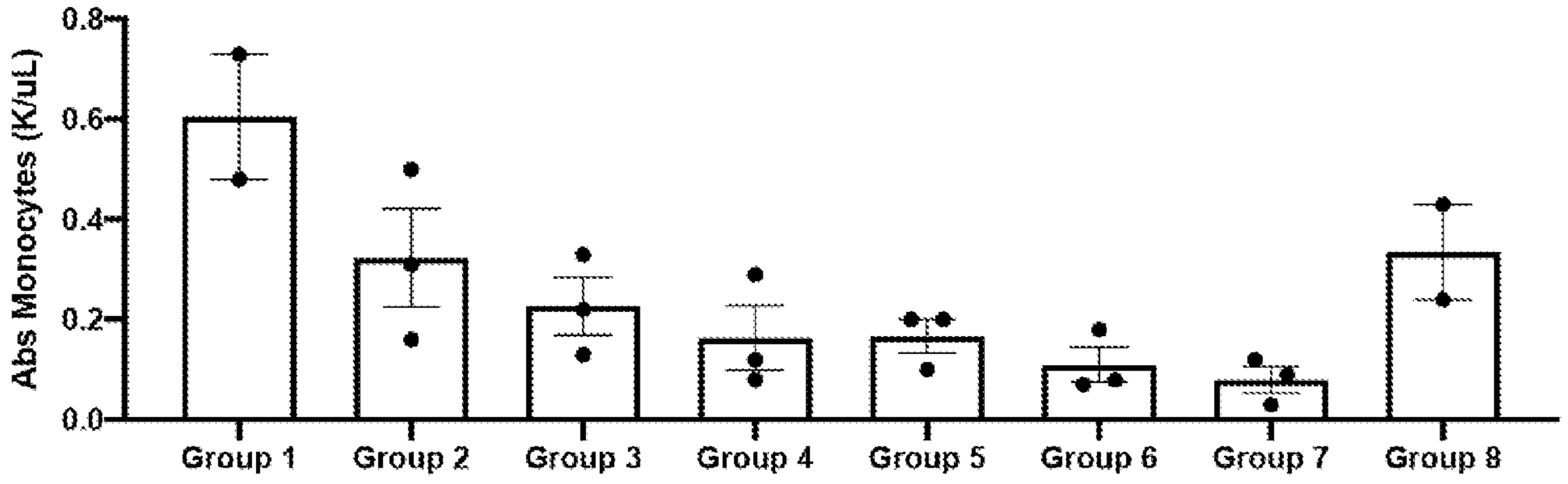
Abs Monocytes (K/uL)
0.0
0.2
0.4
0.6
0.8
Group 1
Group 2
Group 3
Group 4
Group 5
Group 6
Group 7
Group 8

FIG. 66

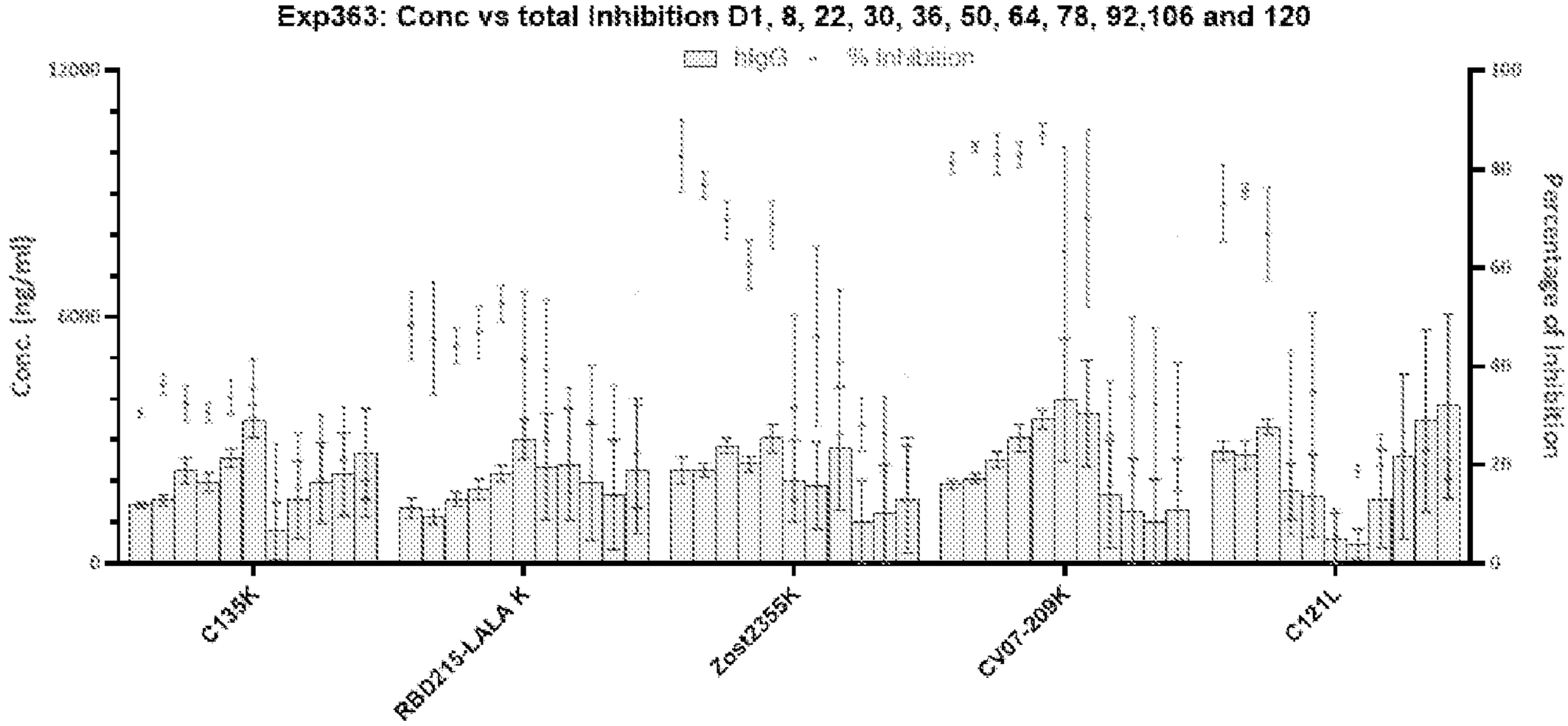
Exp363: Conc vs total inhibition D1, 8, 22, 30, 36, 50, 64, 78, 92,106 and 120
hIgG
% Inhibition
Conc. (ng/ml)
Percentage of Inhibition
C135K
RBD215-LALA K
Zost2355K
CV07-209K
C121L

FIG. 67

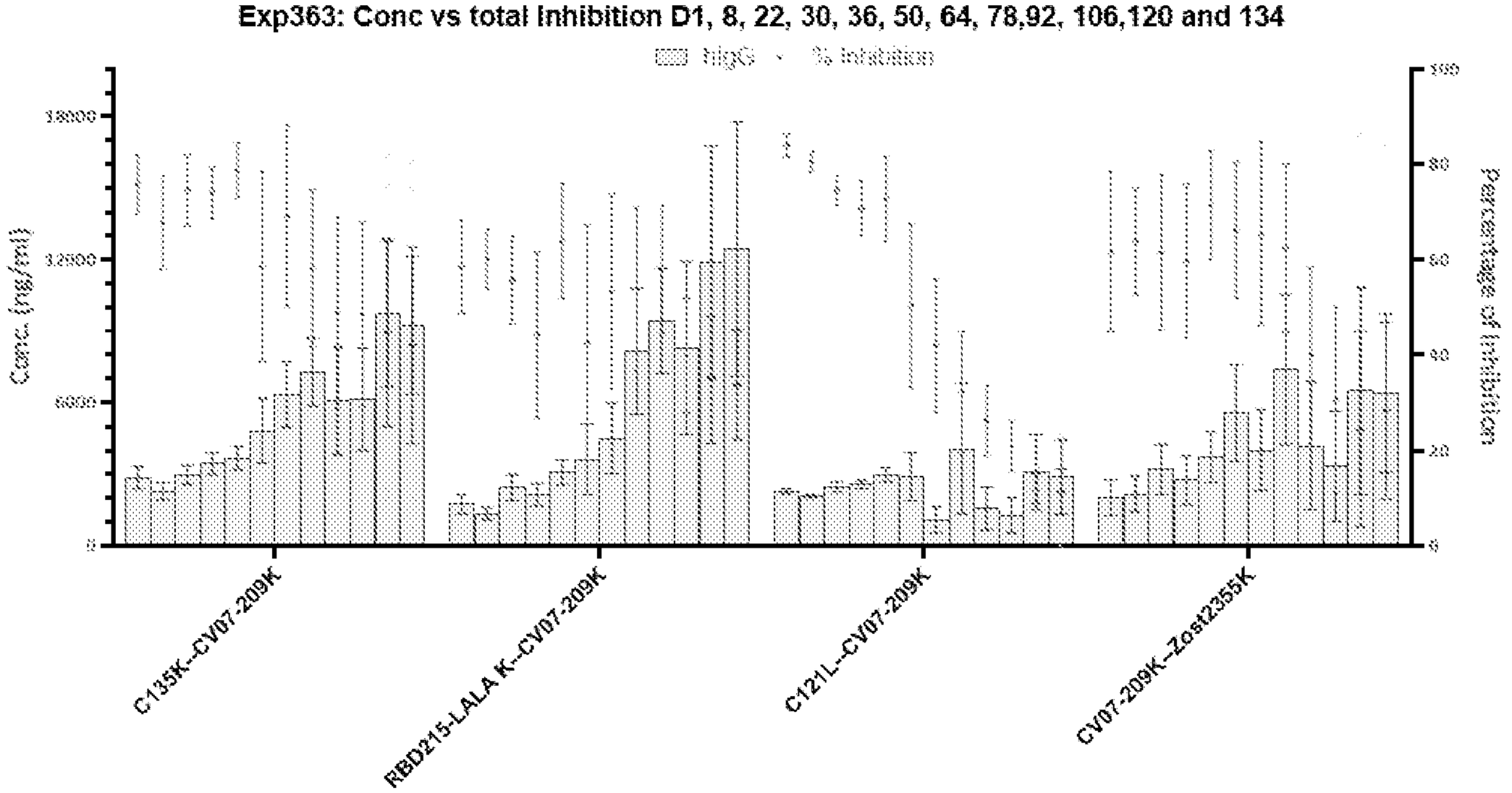
Exp363: Conc vs total Inhibition D1, 8, 22, 30, 36, 50, 64, 78,92, 106,120 and 134
hIgG
% Inhibition
Conc. (ng/ml)
Percentage of Inhibition
C135K-CV07-209K
RBD215-LALA K-CV07-209K
C121L-CV07-209K
CV07-209K-Zost2355K

FIG. 68

A.

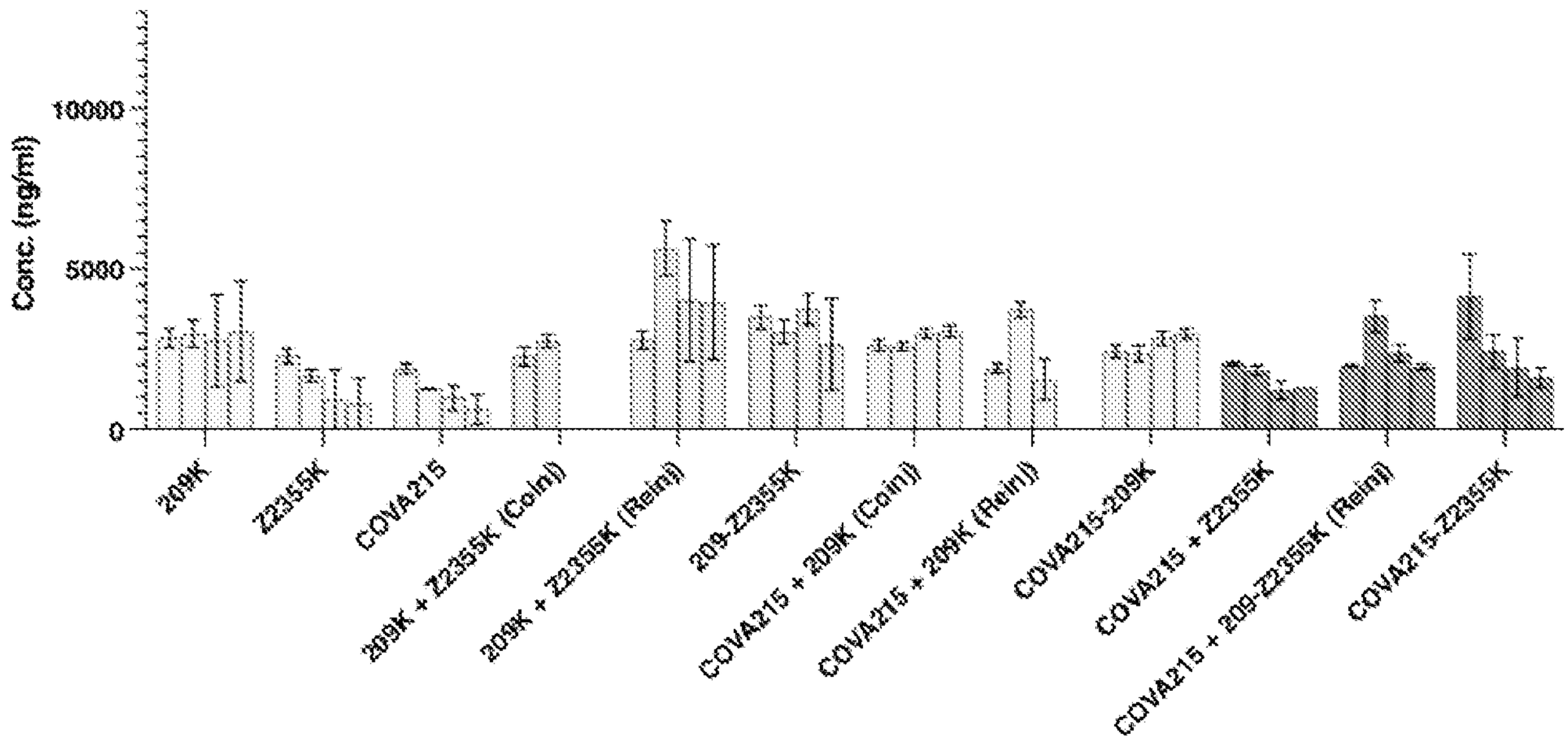
Conc. (ng/ml)
10000
5000
0
209K
Z2355K
COVA215
209K + Z2355K (Coinj)
209K + Z2355K (Reinj)
209-Z2355K
COVA215 + 209K (Coinj)
COVA215 + 209K (Reinj)
COVA215-209K
COVA215 + Z2355K
COVA215 + 209-Z2355K (Reinj)
COVA215-Z2355K

B.

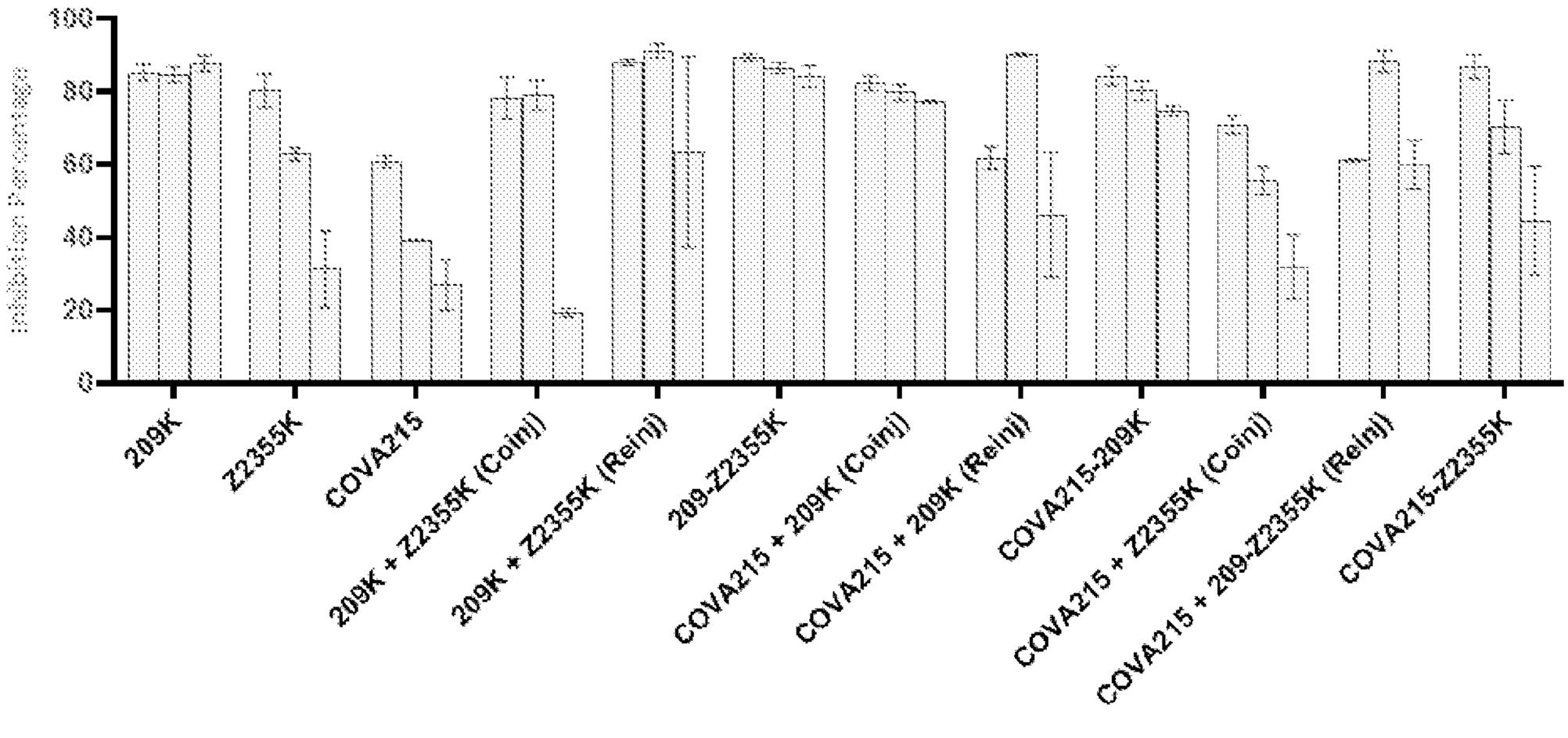
Inhibition Percentage
100
80
60
40
20
0
209K
Z2355K
COVA215
209K + Z2355K (Coinj)
209K + Z2355K (Reinj)
209-Z2355K
COVA215 + 209K (Coinj)
COVA215 + 209K (Reinj)
COVA215-209K
COVA215 + Z2355K (Coinj)
COVA215 + 209-Z2355K (Reinj)
COVA215-Z2355K

FIG. 69

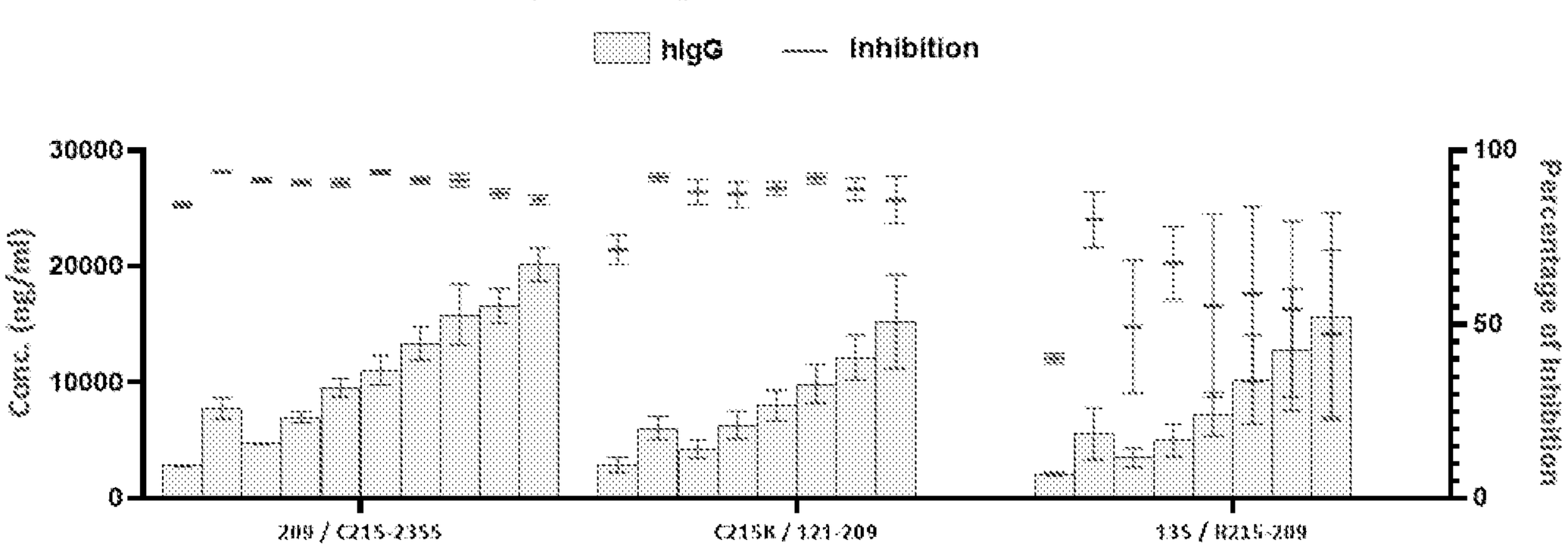
Exp 367: hIgG/Inhibition-3mAb-D1-120
hIgG
Inhibition
30000
20000
10000
0
Conc. (ng/ml)
100
50
0
percentage of inhibition
209 / C215-235S
C215K / 121-209
135 / R215-209

FIG. 70

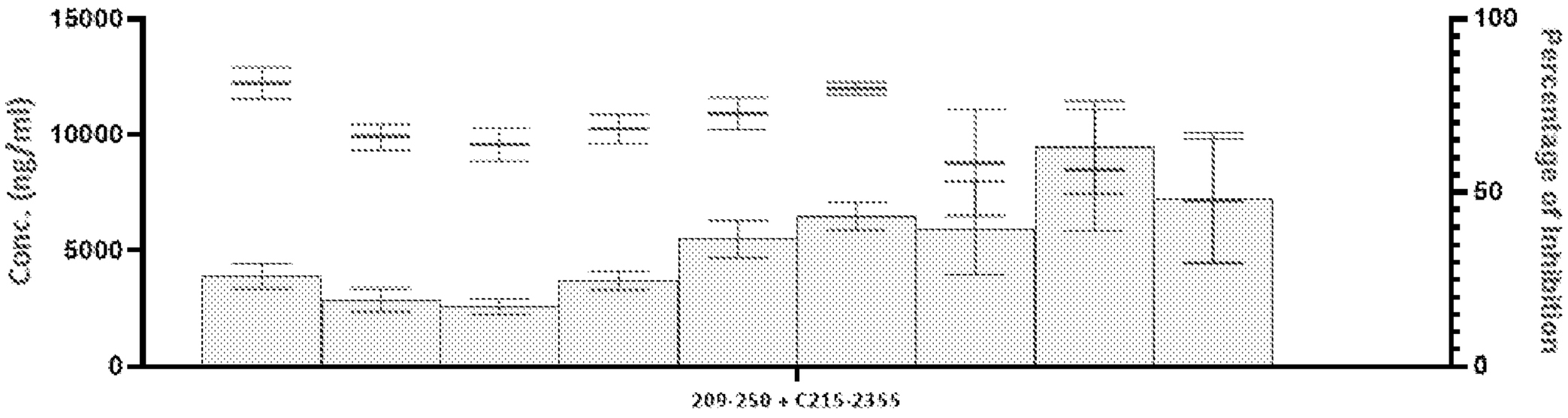
Exp 367: hIgG/Inhibition-4mAb single co-injection-D1-106
hIgG
Inhibition
15000
10000
5000
0
Conc. (ng/ml)
100
50
0
percentage of inhibition
209-250 + C215-2355

FIG. 71

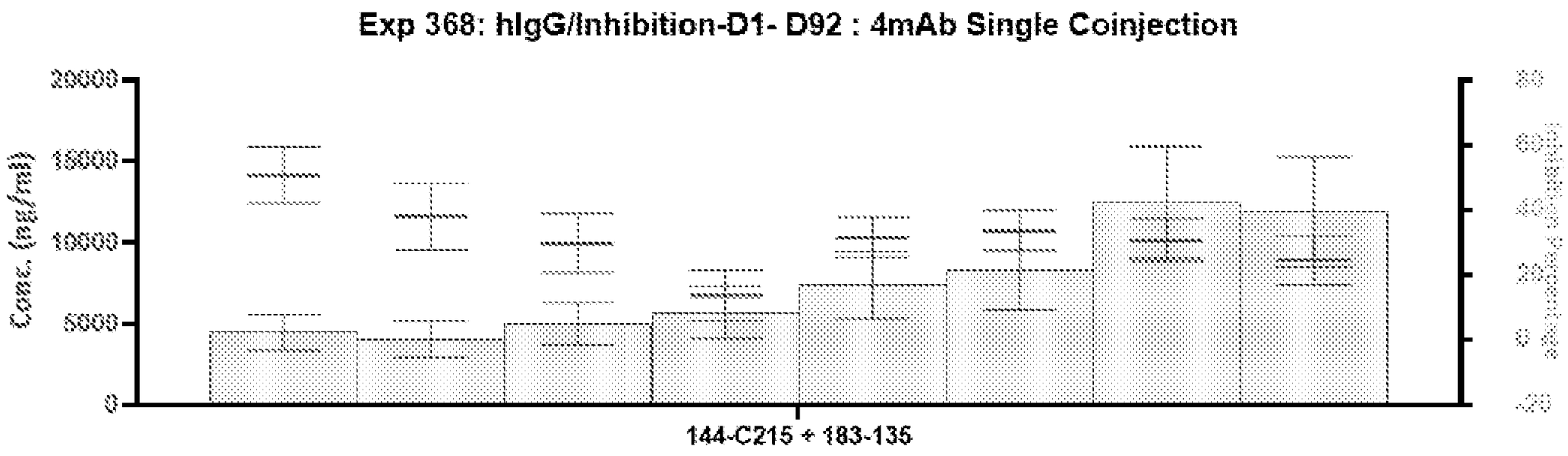
Exp 368: hIgG/Inhibition-D1- D92 : 4mAb Single Coinjection
Conc. (ug/ml)
20000
15000
10000
5000
0
Inhibition (%)
80
60
40
20
0
-20
144-C215 + 183-135

FIG. 72

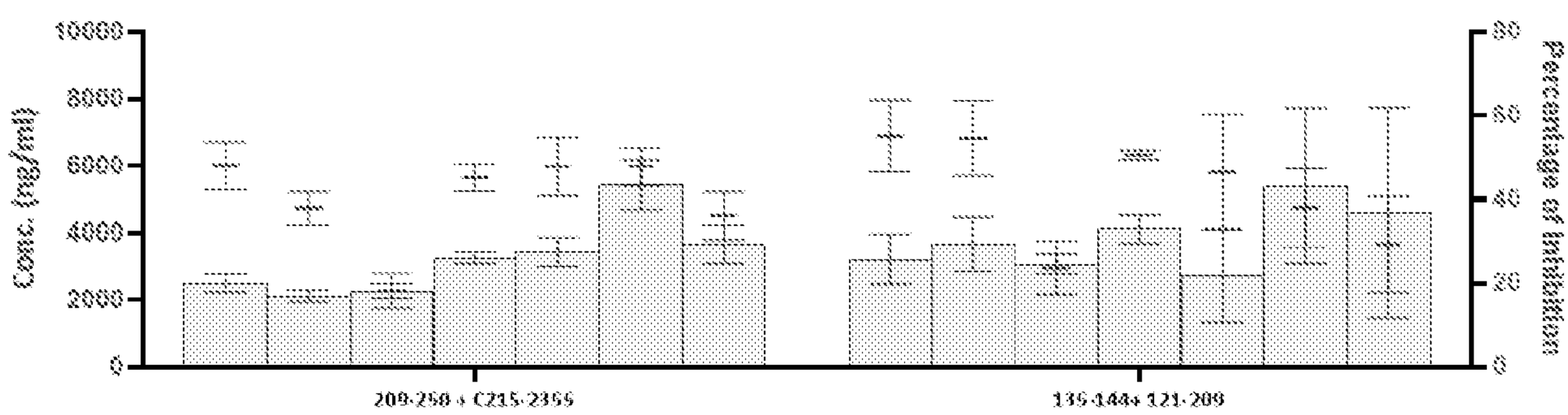
Exp370: hIgG/Inhibition-D1-99:4mab Single Coinjection
hIgG
Inhibition
Conc. (ng/ml)
10000
8000
6000
4000
2000
0
Percentage of Inhibition
80
60
40
20
0
209-258 + C215-2355
139-144+ 121-209

FIG. 73

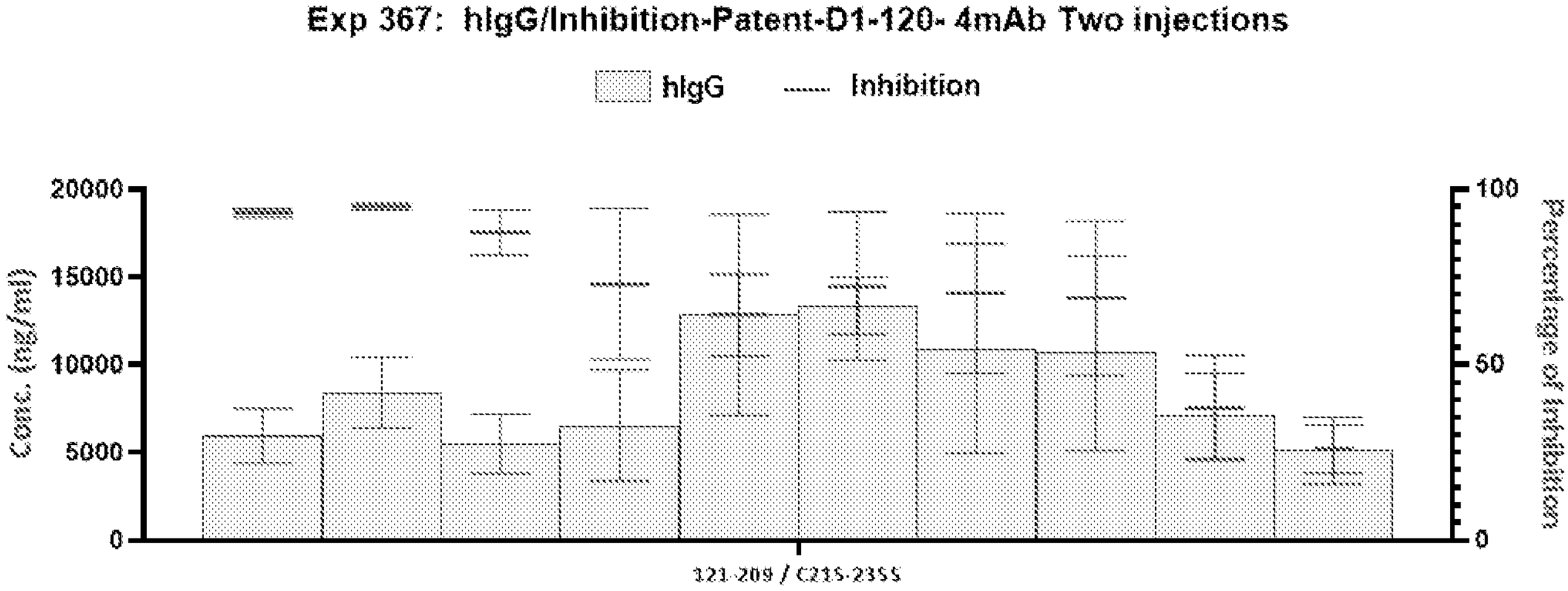
Exp 367: hIgG/Inhibition-Patent-D1-120- 4mAb Two injections
hIgG
Inhibition
Conc. (ng/ml)
20000
15000
10000
5000
0
Percentage of Inhibition
100
50
0
121-209 / C235-2355

FIG. 74

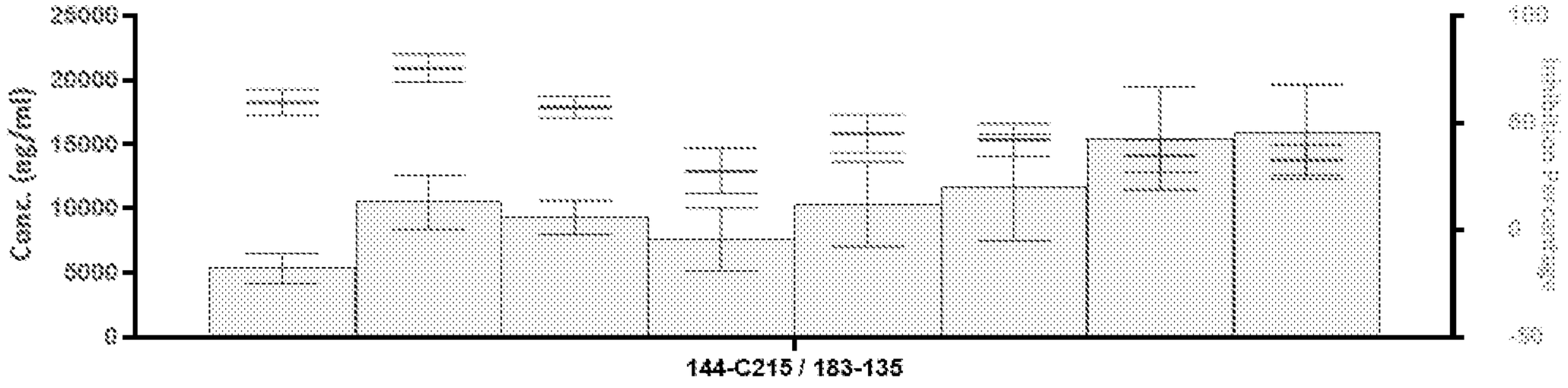
Exp 368: hIgG/Inhibition-D1- D92 : 4 mAb Two injection
Conc. (ug/ml)
25000
20000
15000
10000
5000
0
Inhibition Percentage
100
50
0
-50
144-C215 / 183-135

FIG. 75

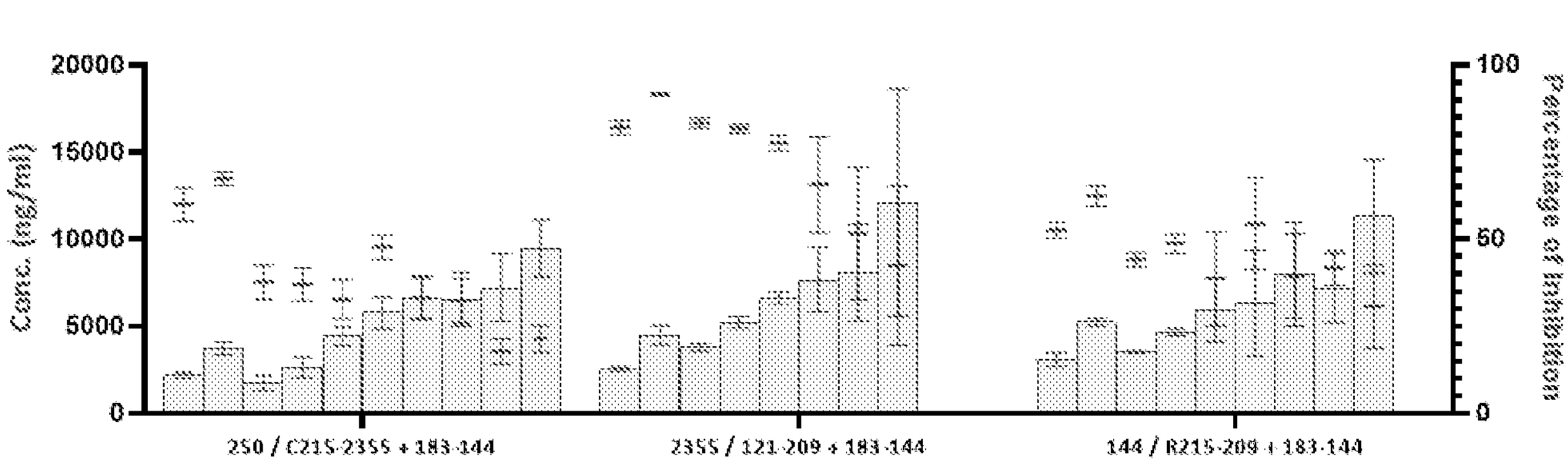
Exp 367: hIgG/Inhibition-Patent-D1-120- 5mAb
hIgG
Inhibition
Conc. (ng/ml)
20000
15000
10000
5000
0
100
50
0
Percentage of Inhibition
250 / C215-235S + 183-144
235S / 121-209 + 183-144
144 / R215-209 + 183-144

FIG. 76

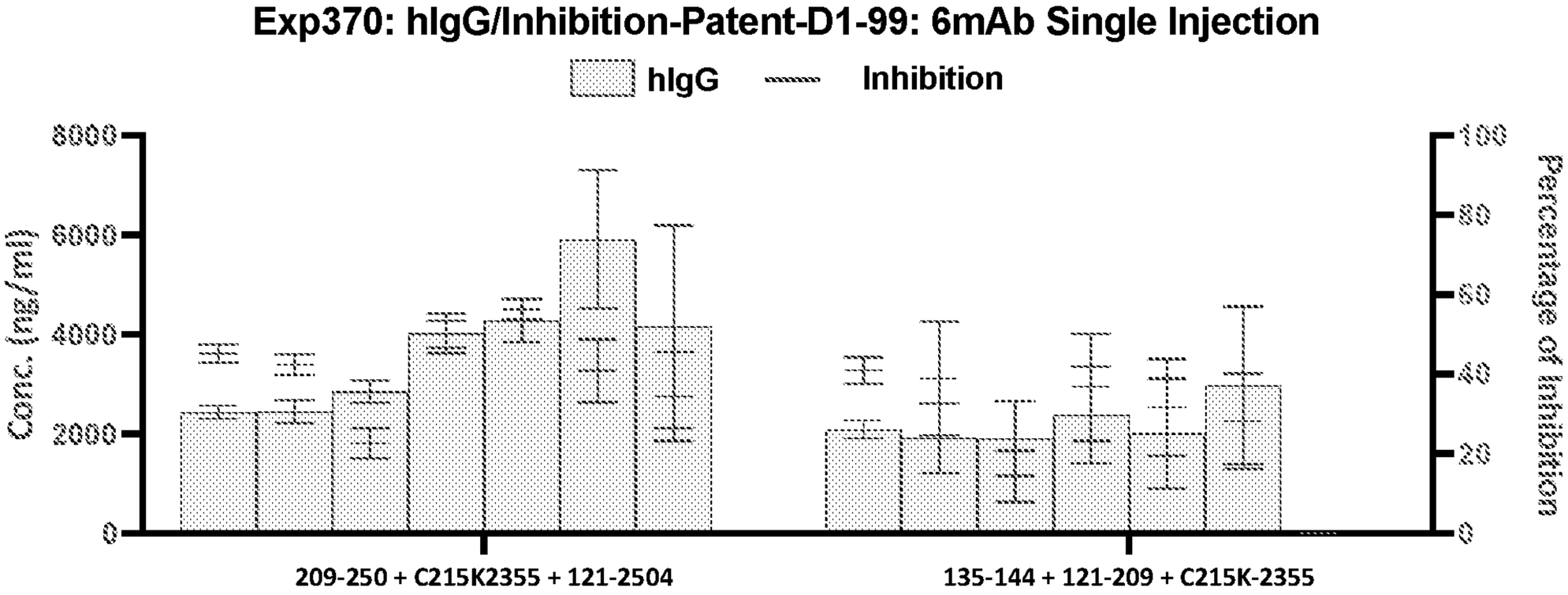
Exp370: hIgG/Inhibition-Patent-D1-99: 6mAb Single Injection
hIgG
Inhibition
Conc. (ng/ml)
8000
6000
4000
2000
0
Percentage of Inhibition
100
80
60
40
20
0
209-250 + C215K2355 + 121-2504
135-144 + 121-209 + C215K-2355

FIG. 77

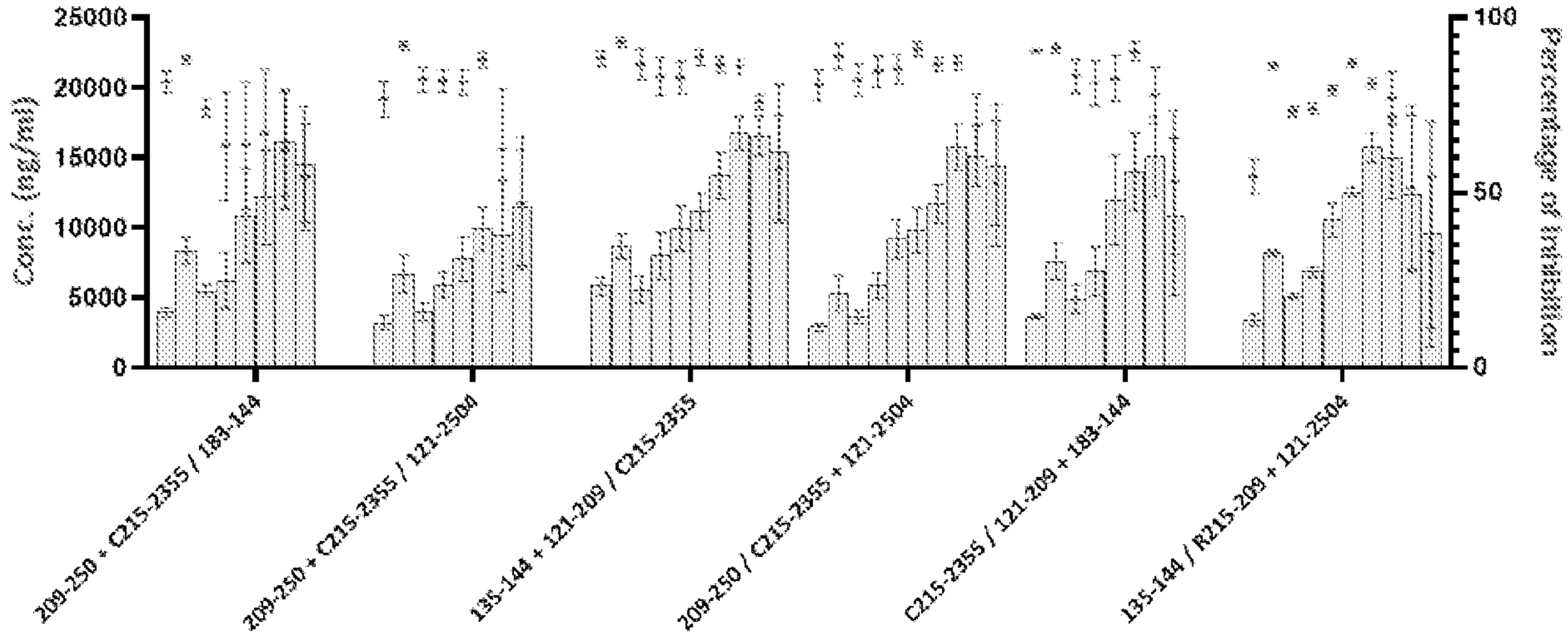
Exp 367: hIgG/Inhibition-Patent-D1-120- 6 mAb Two Injections
hIgG
Inhibition
Conc. (ug/ml)
25000
20000
15000
10000
5000
0
Percentage of Inhibition
100
50
0
209-250 + C215-2355 / 183-144
209-250 + C215-2355 / 121-2504
135-144 + 121-209 / C215-2355
209-250 / C215-2355 + 121-2504
C215-2355 / 121-209 + 183-144
135-144 / R215-209 + 121-2504

FIG. 78

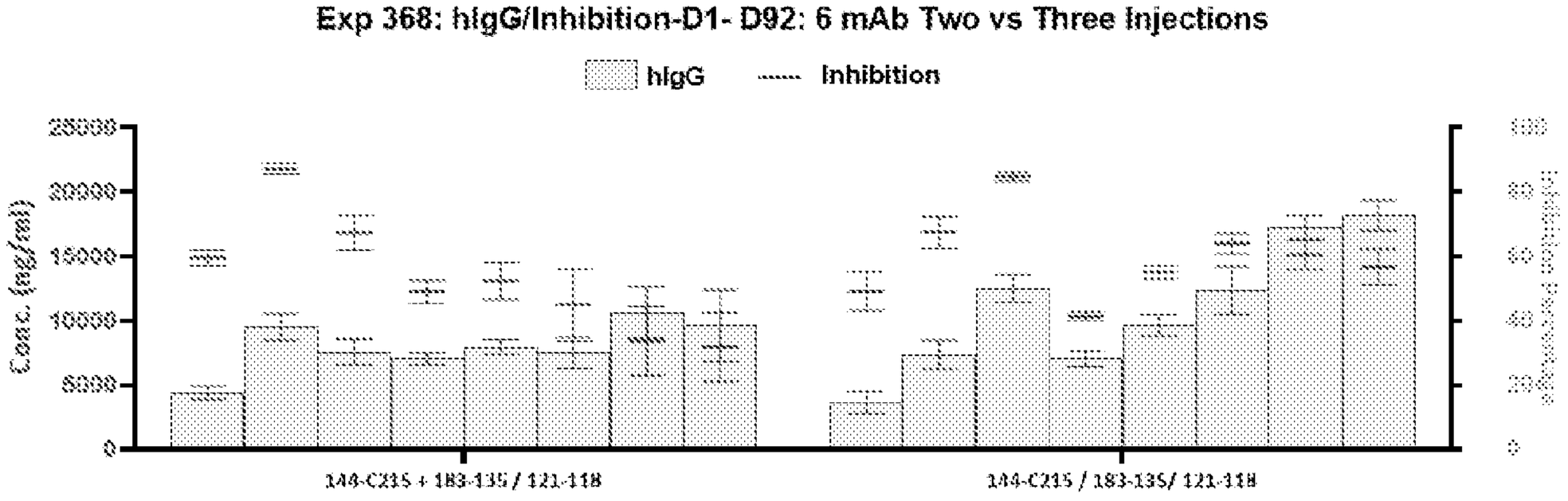
Exp 368: hIgG/Inhibition-D1- D92: 6 mAb Two vs Three Injections
hIgG
Inhibition
Conc. (ng/ml)
25000
20000
15000
10000
5000
0
100
80
60
40
20
0
Inhibition Percent
144-C215 + 183-135 / 121-118
144-C215 / 183-135/ 121-118

FIG. 79

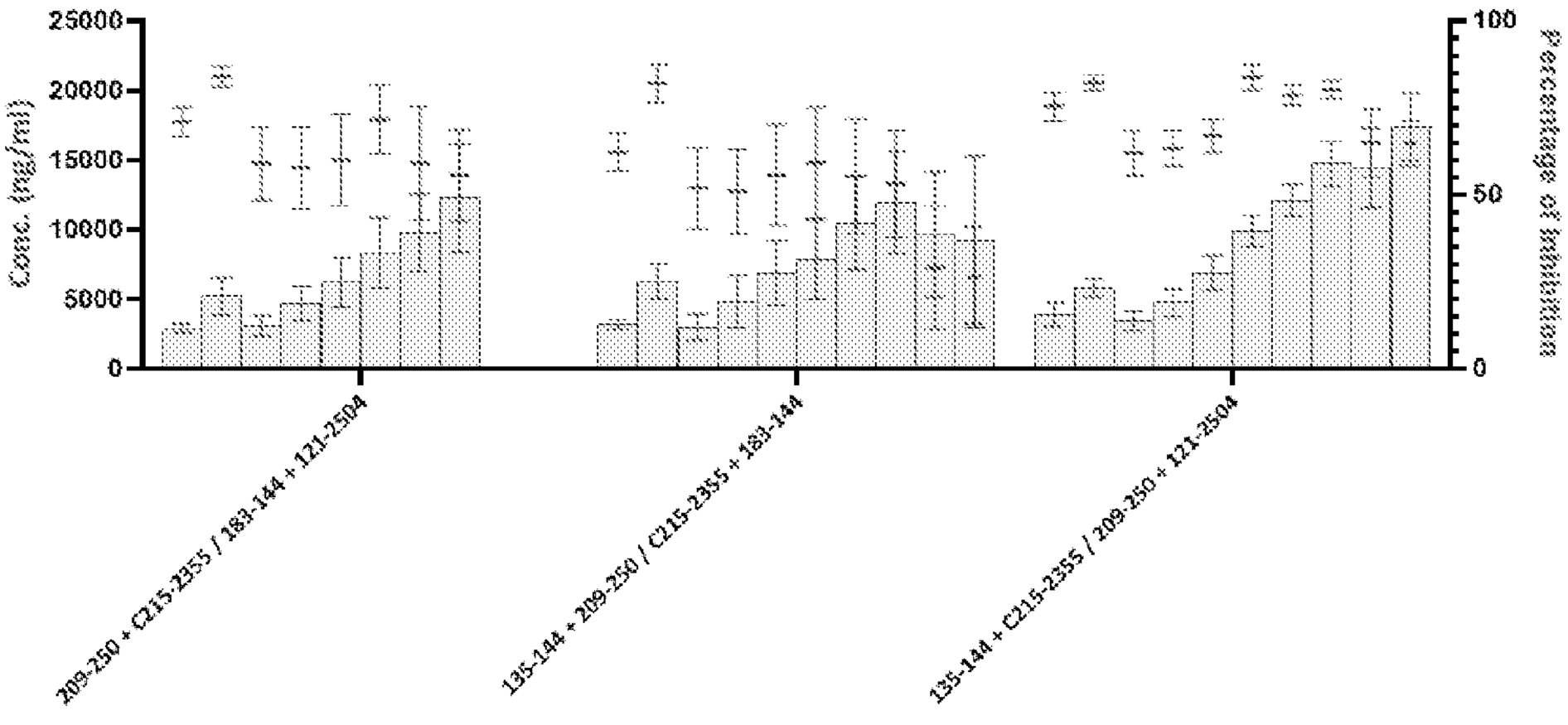
Exp 367: hIgG/Inhibition-Patent-D1-120- 8mAb: Two Injections
hIgG
Inhibition
Conc. (ng/ml)
25000
20000
15000
10000
5000
0
Percentage of Inhibition
100
50
0
209-250 + C215-2355 / 183-144 + 121-2504
135-144 + 209-250 / C215-2355 + 183-144
135-144 + C215-2355 / 209-250 + 121-2504

FIG. 80

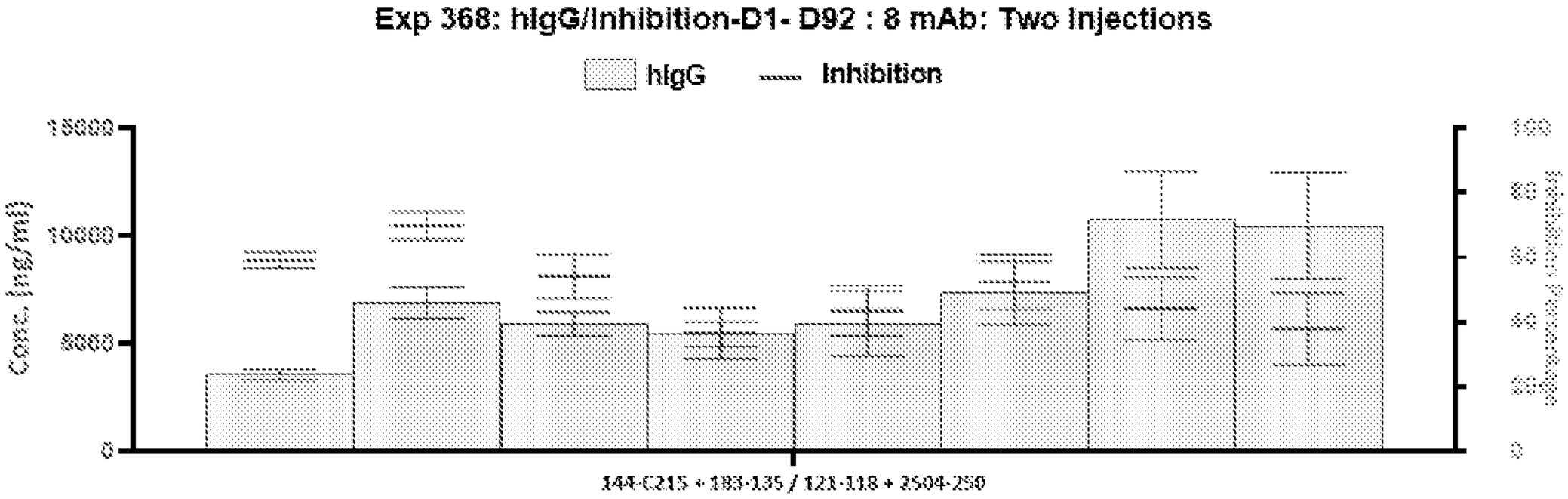
Exp 368: hIgG/Inhibition-D1- D92 : 8 mAb: Two Injections
hIgG
Inhibition
15000
10000
5000
0
Conc. (ng/ml)
100
80
60
40
20
0
Inhibition (%)
144-C215 + 183-135 / 121-118 + 2504-250

FIG. 81

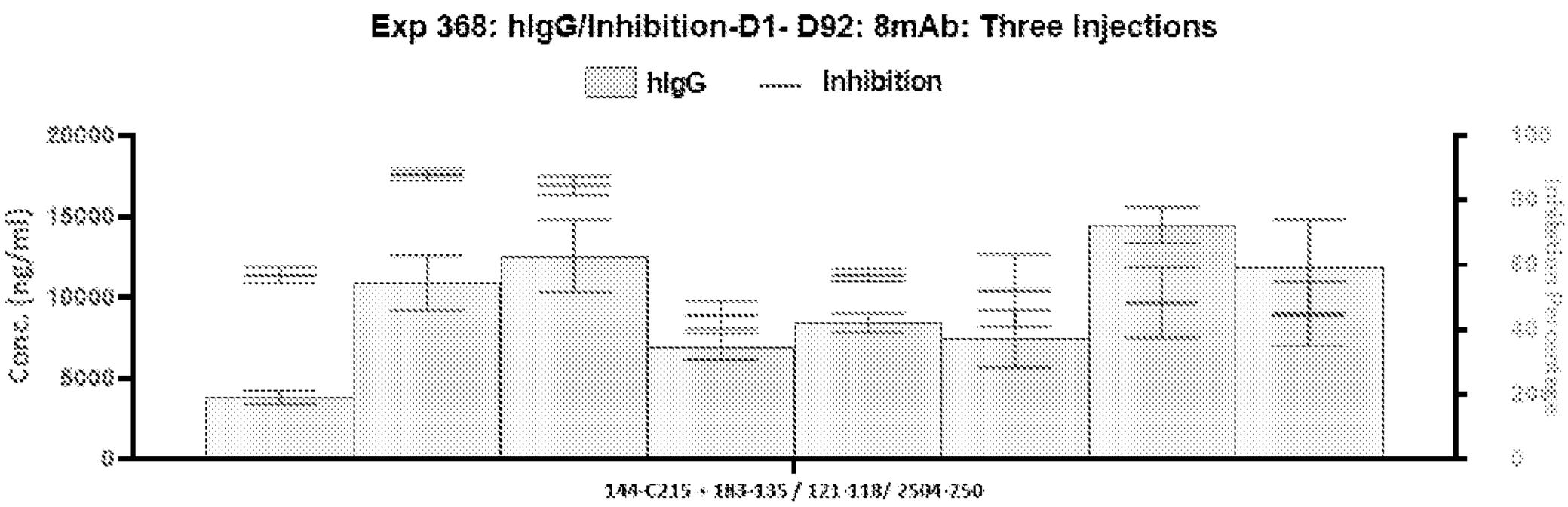
Exp 368: hIgG/Inhibition-D1- D92: 8mAb: Three Injections
hIgG
Inhibition
Conc. (ng/ml)
20000
15000
10000
5000
0
100
80
60
40
20
0
(Inhibition from zero)
144-C215 + 183-135 / 121-118/ 2584-250

FIG. 82

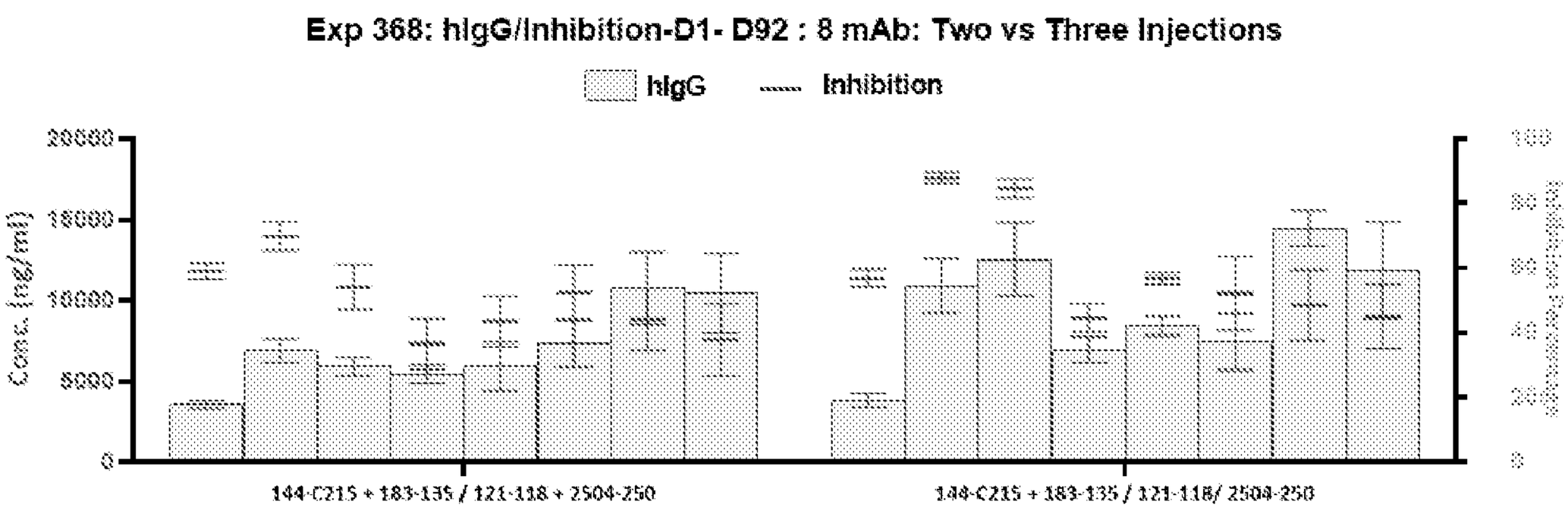
Exp 368: hIgG/Inhibition-D1- D92 : 8 mAb: Two vs Three Injections
hIgG
Inhibition
Conc. (ug/ml)
20000
15000
10000
5000
0
100
80
60
40
20
0
144-C215 + 183-135 / 121-118 + 2504-250
144-C215 + 183-135 / 121-118/ 2504-250

FIG. 83

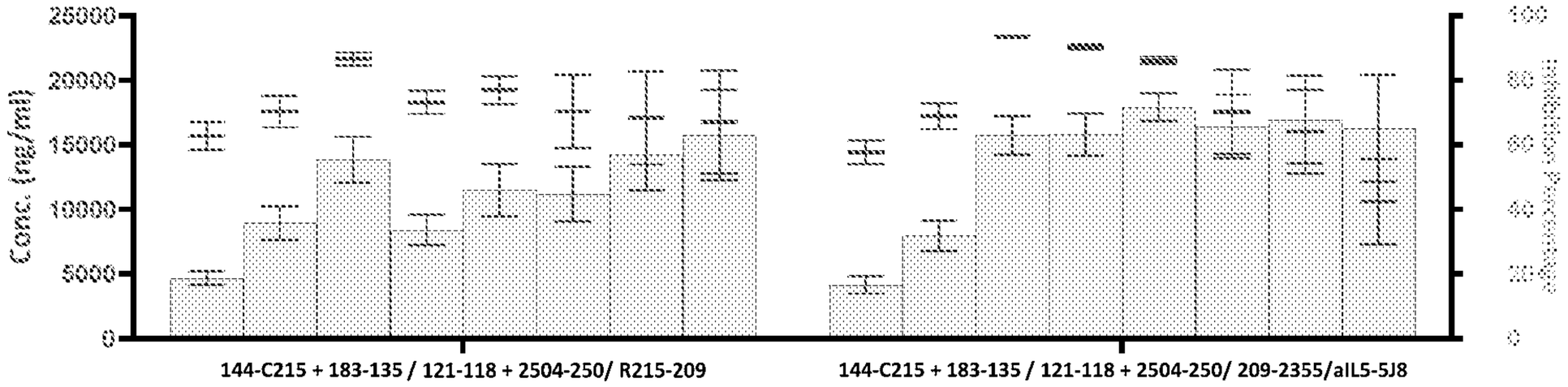
Exp 368: hIgG/Inhibition-D1- D92 : 10mAb Three and Four Injections
hIgG
Inhibition
Conc. (ng/ml)
25000
20000
15000
10000
5000
0
100
80
60
40
20
0
144-C215 + 183-135 / 121-118 + 2504-250/ R215-209
144-C215 + 183-135 / 121-118 + 2504-250/ 209-2355/aIL5-5J8

FIG. 84

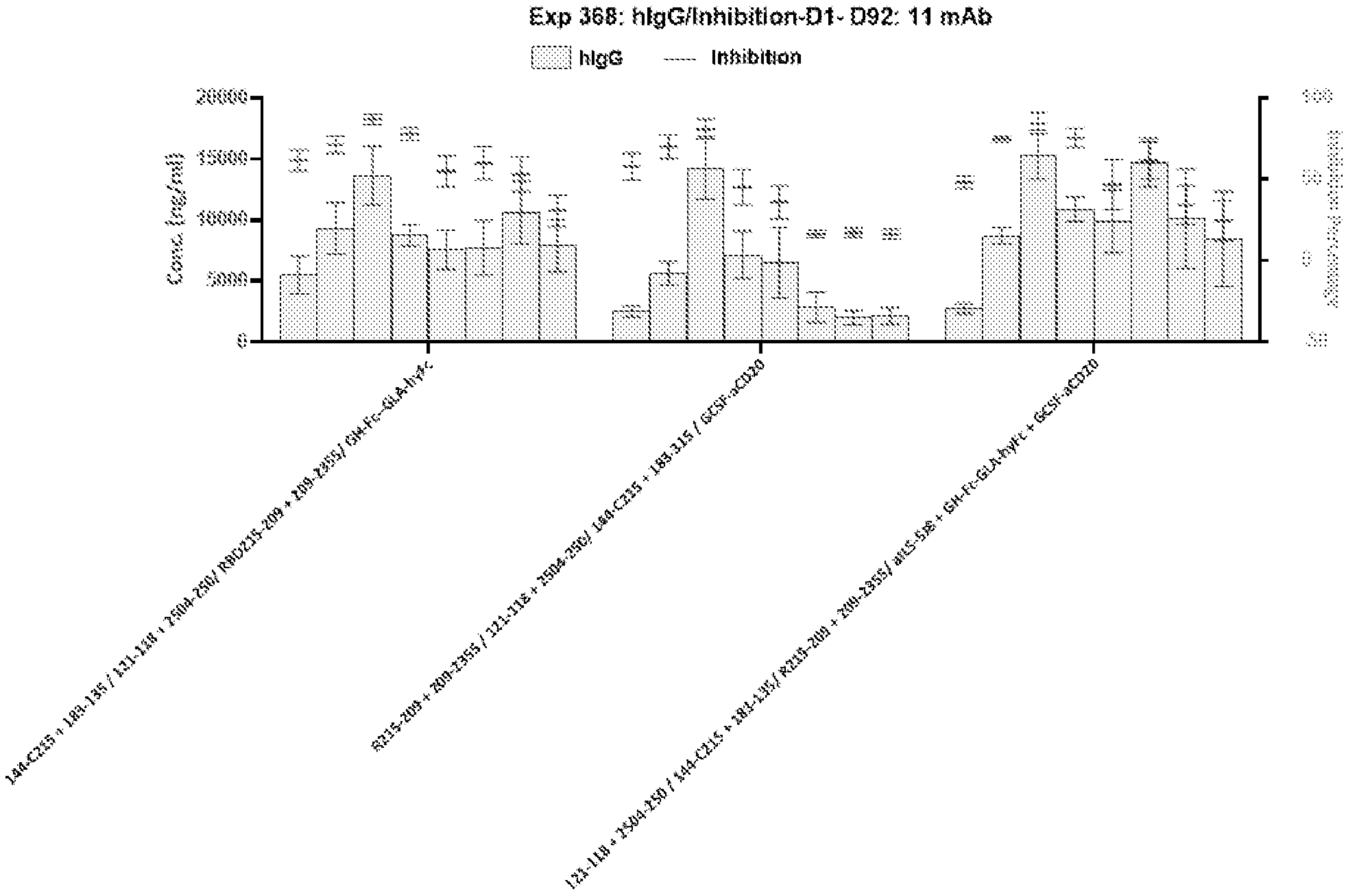
Exp 368: hIgG/Inhibition-D1- D92: 11 mAb
hIgG
Inhibition
Conc (ng/ml)
20000
15000
10000
5000
0
100
50
0
Inhibition percentage
148-C235 + 183-135 / 121-118 + 2504-250/ RBD235-209 + 209-2355/ GM-Fc-GLA-hyFc
R235-209 + 209-2355 / 121-118 + 2504-250/ 148-C235 + 183-135 / GCSF-aCD20
123-118 + 2504-250 / 144-C215 + 183-135/ R235-209 + 209-2355/ aIL-6R + GM-Fc-GLA-hyFc + GCSF-aCD20

FIG. 85

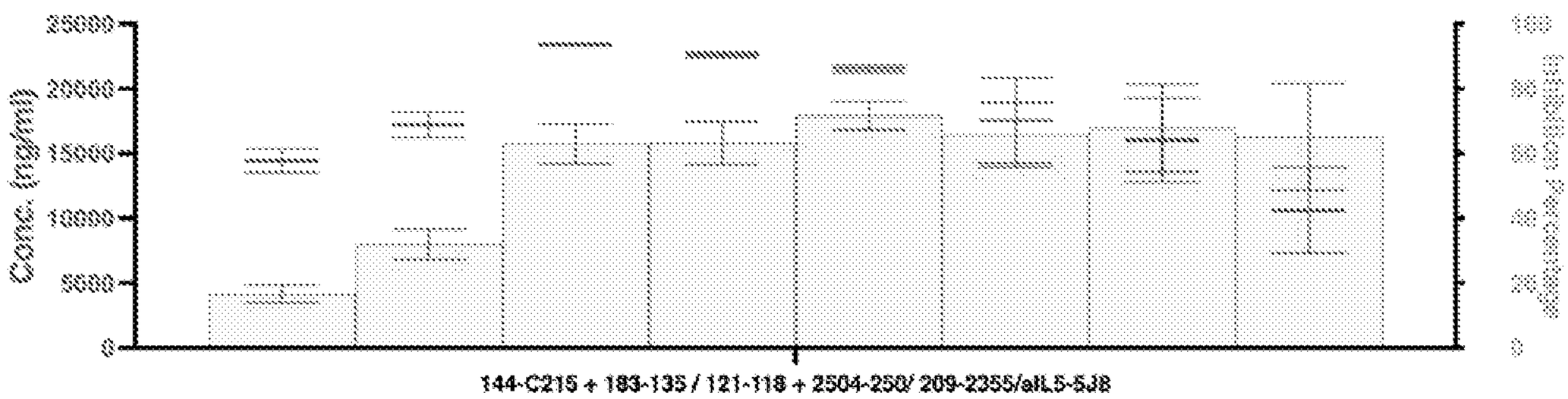
Exp 368: hIgG/Inhibition-D1- D92 : 10mAb Three Injections
hIgG
Inhibition
Conc. (ng/ml)
25000
20000
15000
10000
5000
0
Inhibition (%)
100
80
60
40
20
0
144-C215 + 183-135 / 121-118 + 2504-250/ 209-2355/aIL5-5J8

FIG. 86

A.

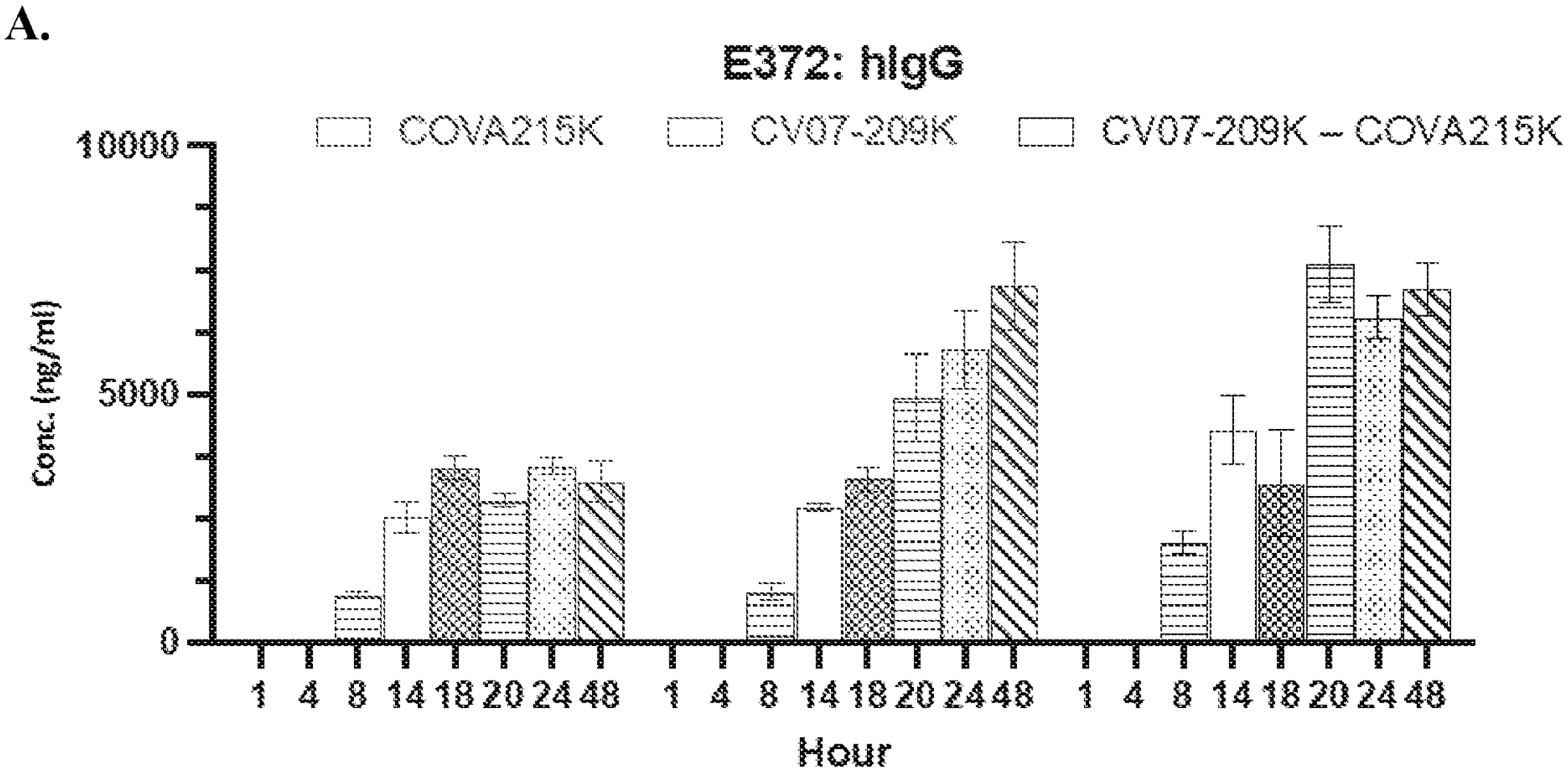
E372: hIgG
COVA215K
CV07-209K
CV07-209K – COVA215K
10000
5000
0
Conc. (ng/ml)
1 4 8 14 18 20 24 48 1 4 8 14 18 20 24 48 1 4 8 14 18 20 24 48
Hour

B.

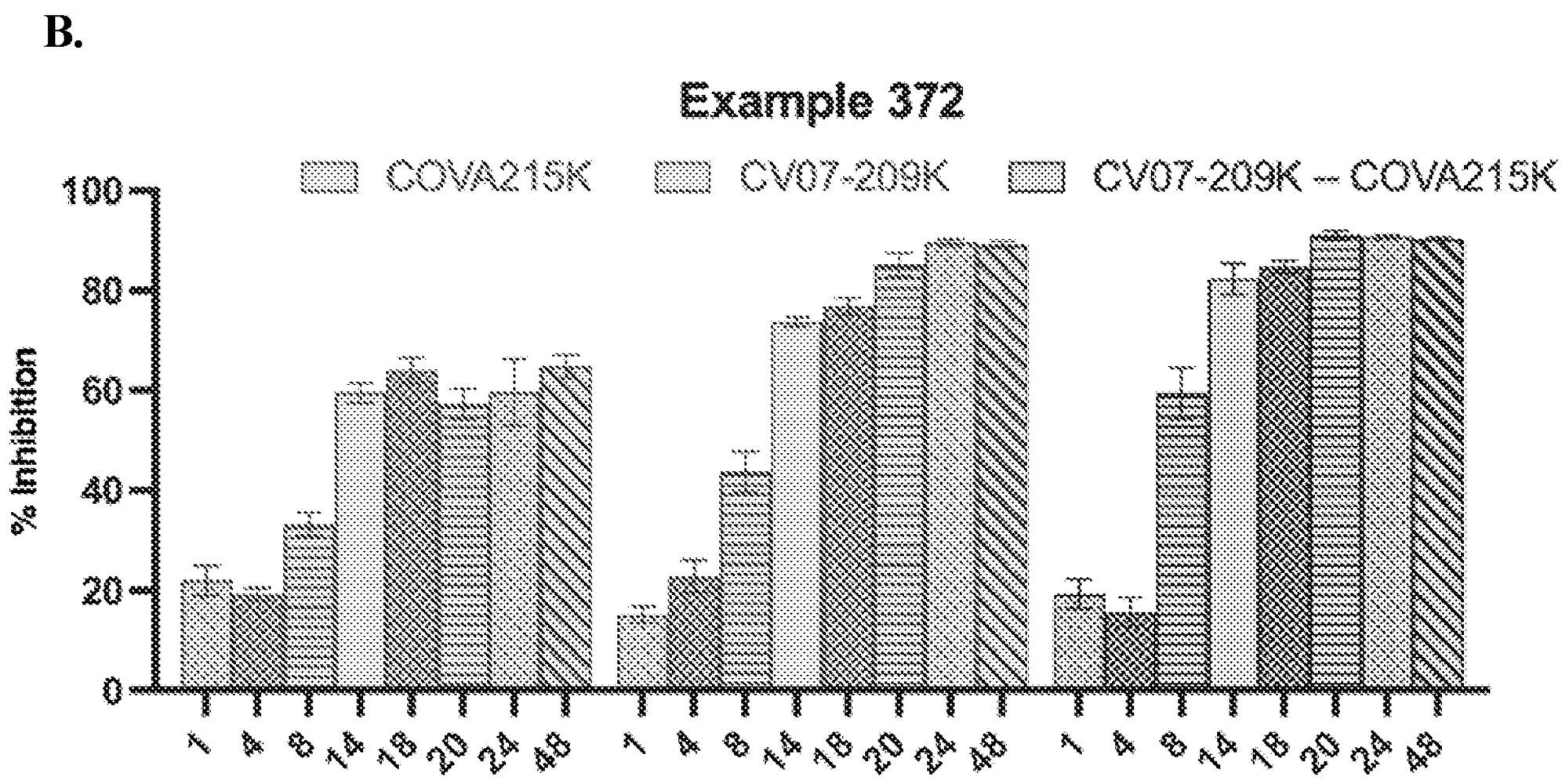
Example 372
COVA215K
CV07-209K
CV07-209K – COVA215K
100
80
60
40
20
0
% Inhibition
1 4 8 14 18 20 24 48 1 4 8 14 18 20 24 48 1 4 8 14 18 20 24 48

FIG. 87

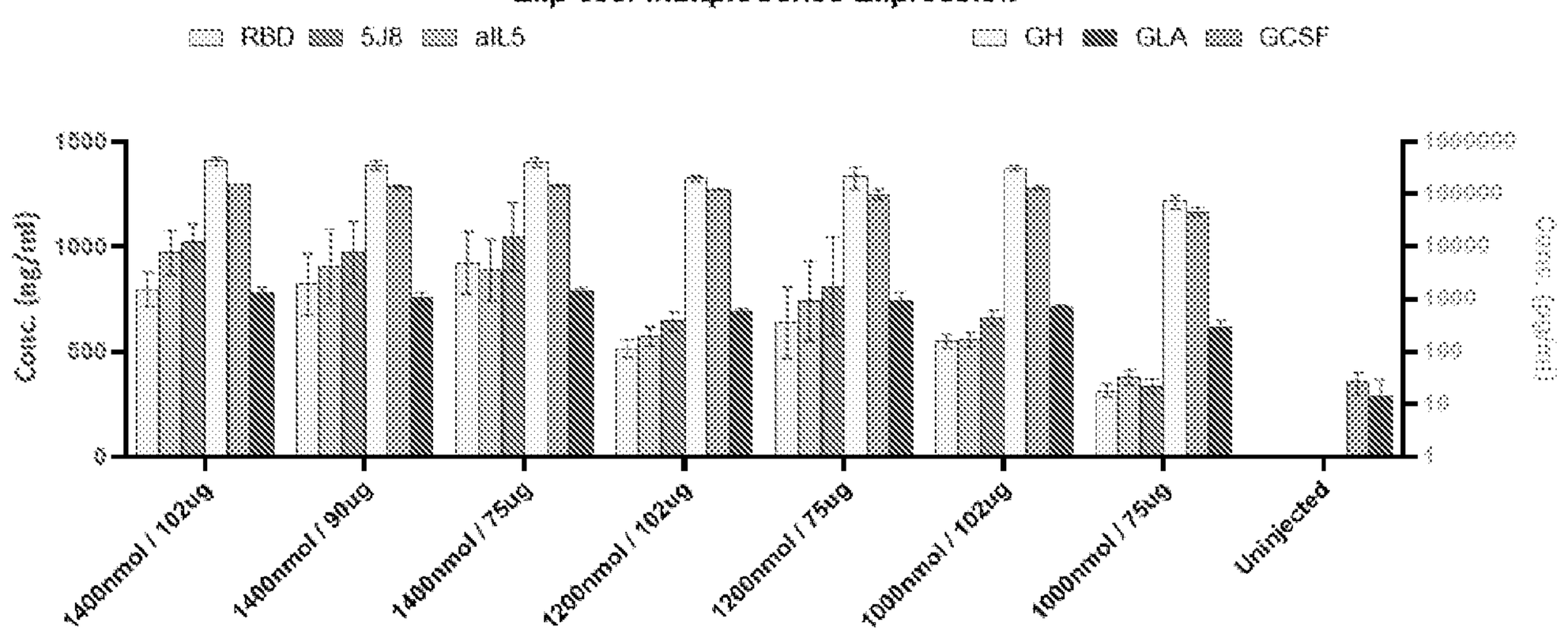
Exp 389: MultpleGenes Expression
RBD
5J8
aIL5
GH
GLA
GCSF
Conc. (ng/ml)
Copies / 100ng
1400nmol / 102ug
1400nmol / 90ug
1400nmol / 75ug
1200nmol / 102ug
1200nmol / 75ug
1000nmol / 102ug
1000nmol / 75ug
Uninjected

FIG. 88

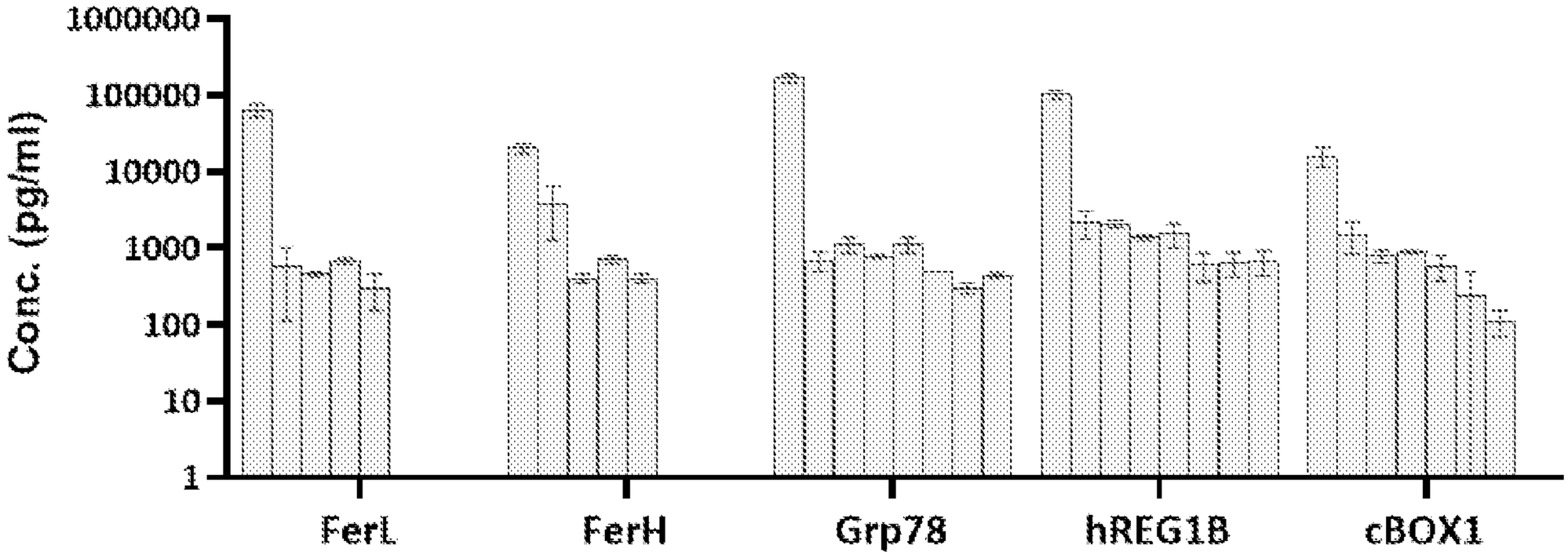
Human Growth Hormone expression under various promoter D1-120
Conc. (pg/ml)
1000000
100000
10000
1000
100
10
1
FerL
FerH
Grp78
hREG1B
cBOX1

FIG. 89

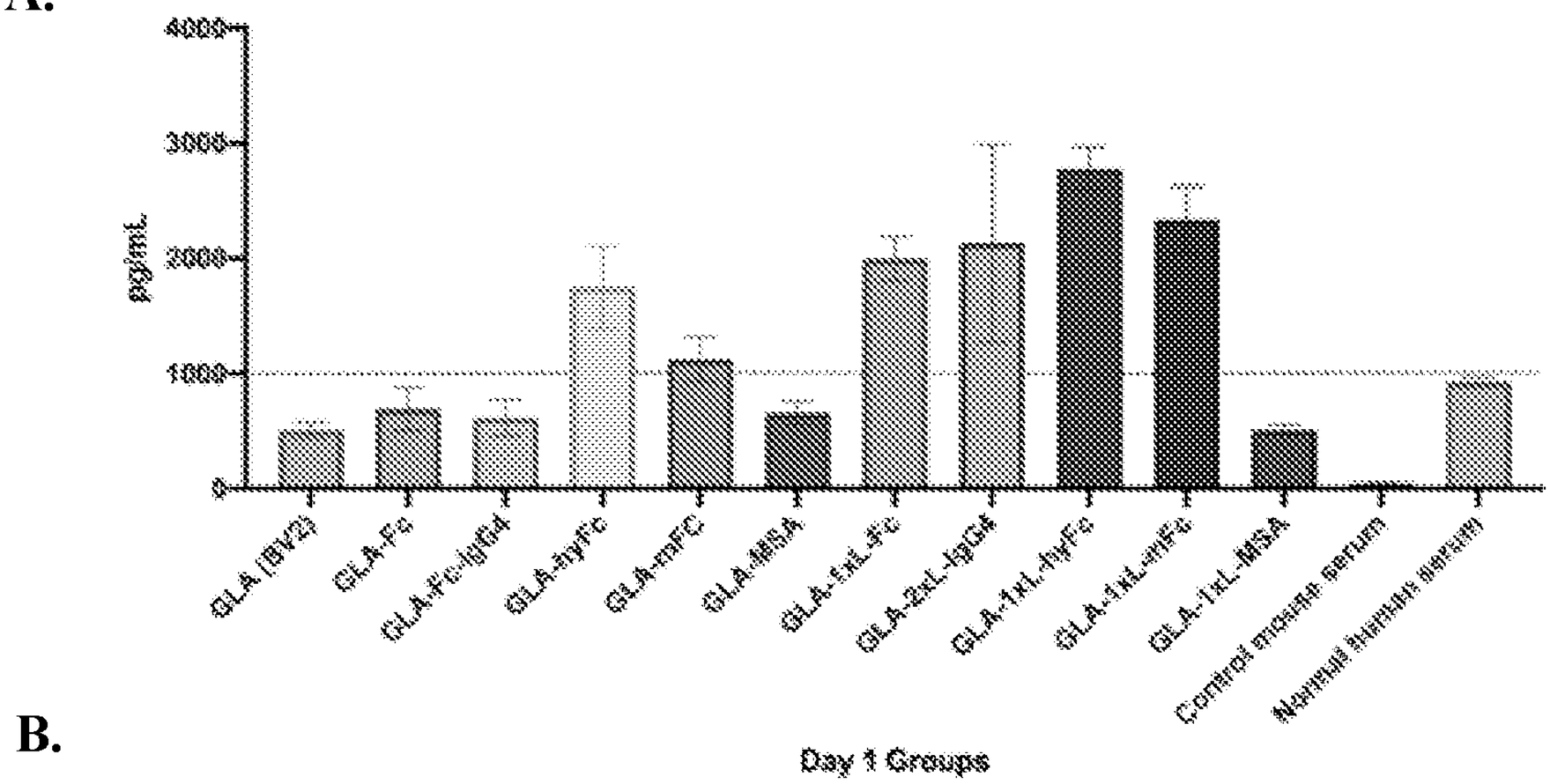
A.
pg/mL
0
1000
2000
3000
GLA (BV2)
GLA-Fc
GLA-Fc-IgG4
GLA-hyFc
GLA-mFC
GLA-MSA
GLA-1xL-Fc
GLA-2xL-IgG4
GLA-1xL-hyFc
GLA-1xL-mFc
GLA-1xL-MSA
Control mouse serum
Normal human serum
Day 1 Groups
B.
pg/mL
0
1000
2000
3000
4000
5000
Day after injection
GLA (BV2)
GLA-Fc
GLA-Fc-IgG4
GLA-hyFc
GLA-mFC
GLA-MSA
GLA-1xL-Fc
GLA-2xL-IgG4
GLA-1xL-hyFc
GLA-1xL-mFc
GLA-1xL-MSA
Control
Human

FIG. 90

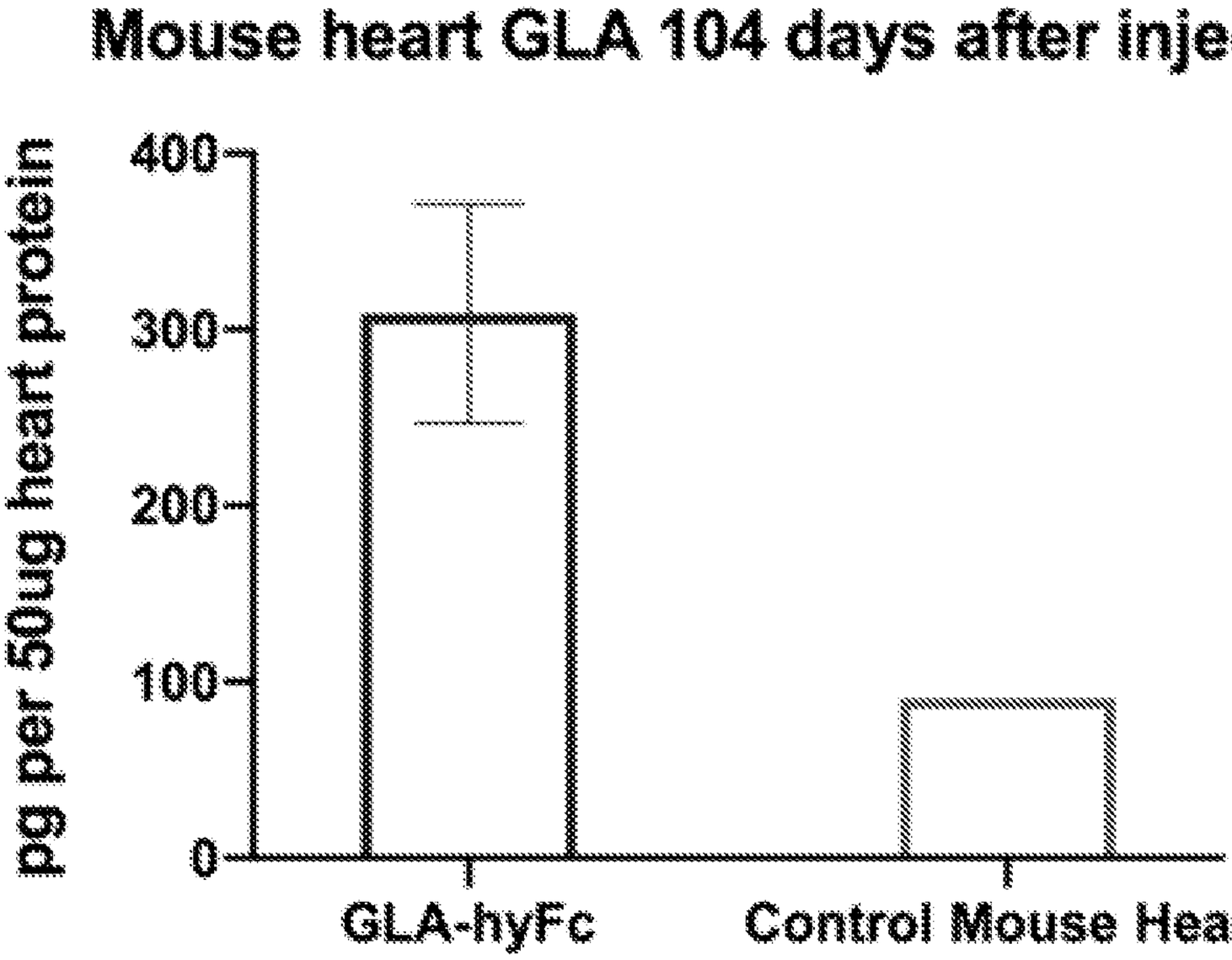
Mouse heart GLA 104 days after injection
pg per 50ug heart protein
400
300
200
100
0
GLA-hyFc
Control Mouse Heart

FIG. 91

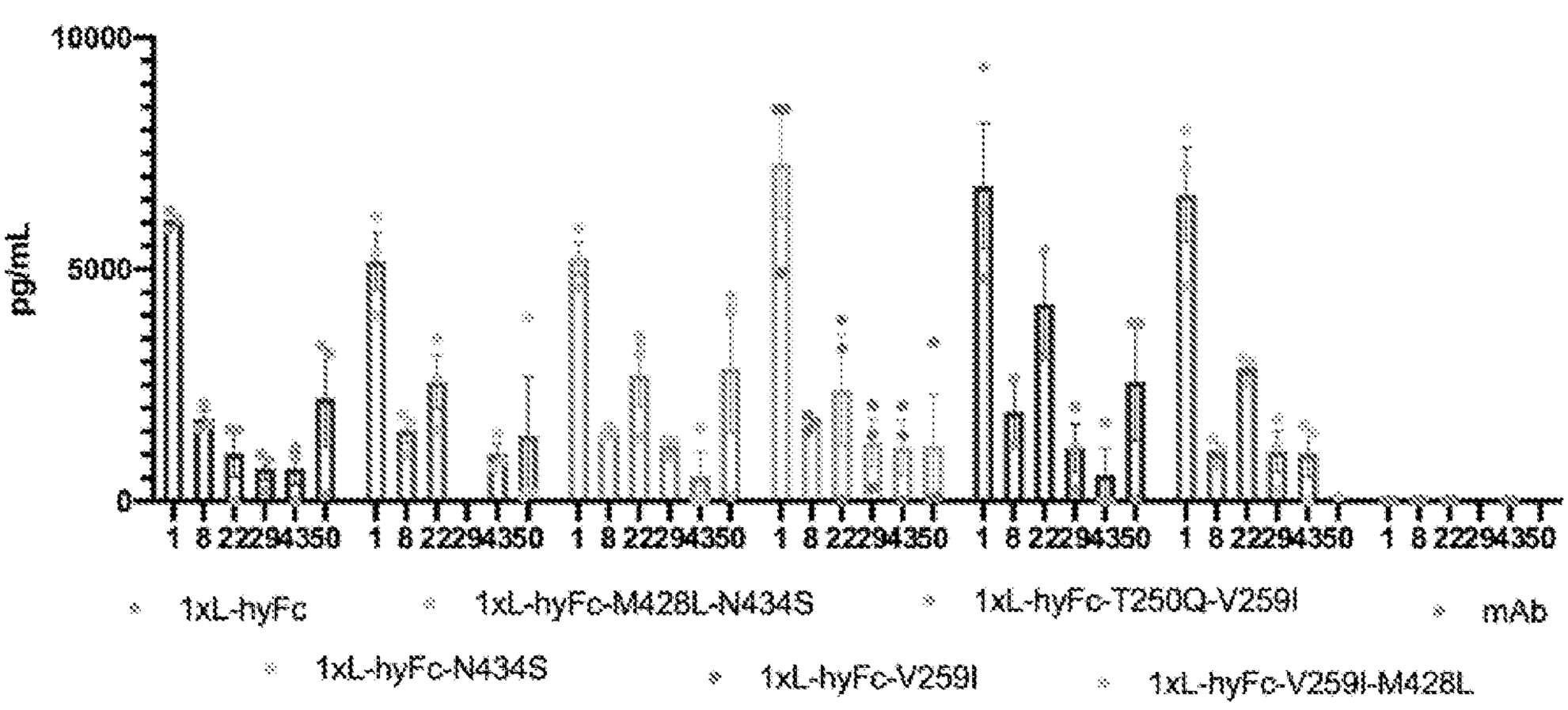
Exp326 Mutants - Reinject D21
pg/mL
10000
5000
0
1 8 22294350
1xL-hyFc
1xL-hyFc-M428L-N434S
1xL-hyFc-T250Q-V259I
mAb
1xL-hyFc-N434S
1xL-hyFc-V259I
1xL-hyFc-V259I-M428L

FIG. 92

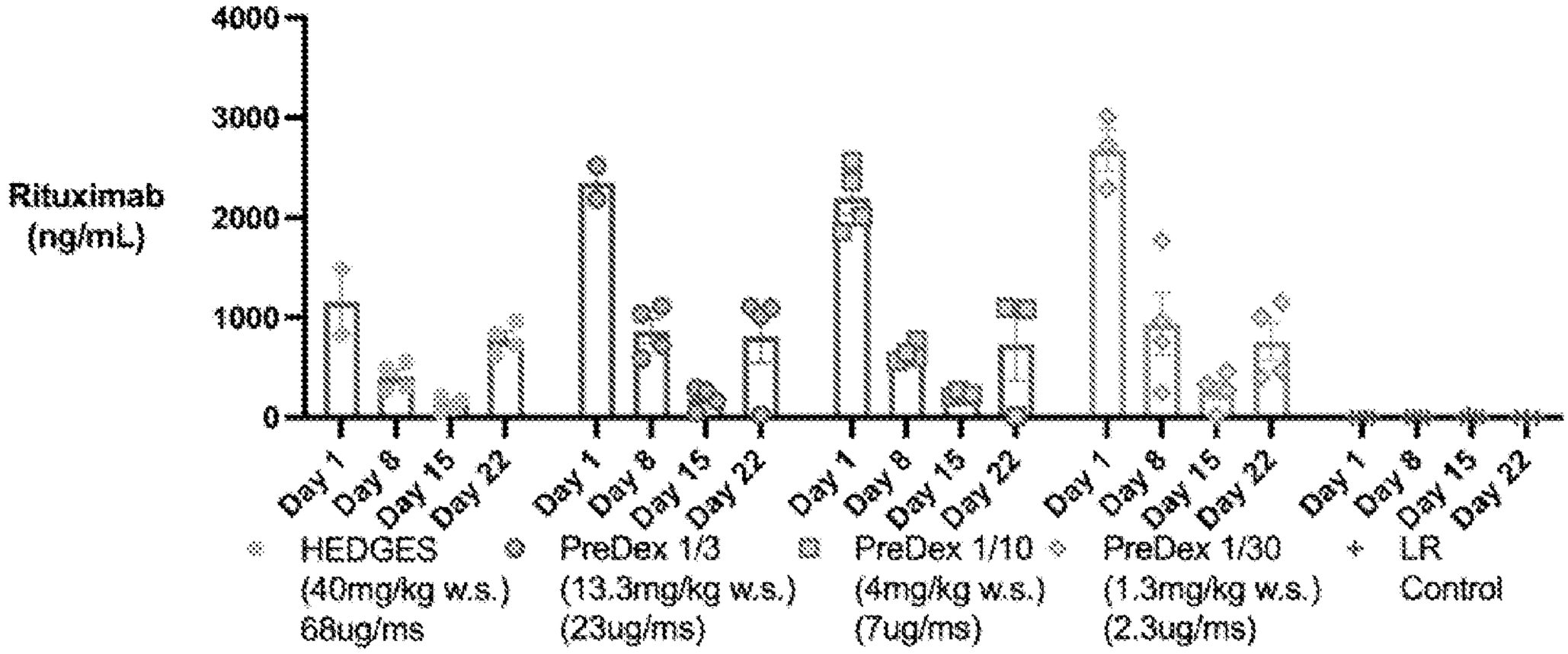
Rituximab (ng/mL)
4000
3000
2000
1000
0
Day 1
Day 8
Day 15
Day 22
HEDGES (40mg/kg w.s.) 68ug/ms
PreDex 1/3 (13.3mg/kg w.s.) (23ug/ms)
PreDex 1/10 (4mg/kg w.s.) (7ug/ms)
PreDex 1/30 (1.3mg/kg w.s.) (2.3ug/ms)
LR Control